



Moscow International Symposium on Magnetism

Dedicated to the centenary of E.I. Kondorskii birth

June 20-25, 2008

Book of Abstracts

M.V. Lomonosov State University, Faculty of Physics

Main Topics

Spintronics and Magnetotransport
Magnetophotonics
High Frequency Properties and Metamaterials
Diluted Magnetic Semiconductors and Oxides
Magnetic Nanostructures and Low Dimensional Magnetism
Magnetic Soft Matter
Soft and Hard Magnetic Materials
Shape-memory Alloys and Magnetocaloric Effect
Magnetism and Superconductivity
Biomagnetism
Miscellaneous

Editors: N.Perov
V. Samsonova
A. Semisalova

Moscow 2008

Moscow International Symposium on Magnetism (MISM),
20-25 June 2008, Moscow
Book of Abstracts

The text of abstracts is printed from original contributions without
editing.

Faculty of Physics M.V. Lomonosov MSU

Физический факультет МГУ имени М.В. Ломоносова

ISBN 978-5-8279-0072-6

© MISM 2008

Contributors to MISM 2008

Moscow International Symposium on Magnetism expresses its warmest appreciation on the following organizations for their generous support



Moscow State University



Russian Foundation for Basic Research



Dynasty Foundation (Moscow)



Institute for Theoretical and Applied
Electromagnetics of Russian Academy of
Sciences (ITAE RAS)



European Physical Society



Japanese Society for Promotion of
Science



Kapitza Institute for Physical Problems

Organizing Committee

Chairmen: A.Vedyayev

A.Granovsky

Secretary A.Radkovskaya

Program Committee

Chairman: A. Granovsky

O. Aktsipetrov	<i>Moscow</i>	Yu. Raikher	<i>Perm</i>
B. Aronzon	<i>Moscow</i>	A. Sarychev	<i>Moscow</i>
B. Aktas	<i>Gebze</i>	E. Shalygina	<i>Moscow</i>
M. Chetkin	<i>Moscow</i>	E. Shamonina	<i>Osnabrueck</i>
N. Garcia	<i>Madrid</i>	V. Shavrov	<i>Moscow</i>
E. Gan'shina	<i>Moscow</i>	A. Smirnov	<i>Moscow</i>
J. Inoue	<i>Nagoya</i>	P. Stetsenko	<i>Moscow</i>
V. Ivanov	<i>Moscow</i>	L. Tagirov	<i>Kazan</i>
O. Kazakova	<i>London</i>	N. Usov	<i>Moscow</i>
Cheol Gi Kim	<i>Daejon</i>	A. Vasil'ev	<i>Moscow</i>
K. Kugel	<i>Moscow</i>	V. Veselago	<i>Moscow</i>
X. Li	<i>Singapore</i>	A. Vinogradov	<i>Moscow</i>
L. Nikitin	<i>Moscow</i>	A. Zhukov	<i>San Sebastian</i>
L. Panina	<i>Plymouth</i>	V. Zubov	<i>Moscow</i>
A. Radkovskaya	<i>Moscow</i>		

Local Committee

Chairman: N. Perov

A. Batyrev	O. Kotel'nikova	N. Pugach	A. Semisalova
V. Belousova	A. Kudakov	A. Radkovskaya	P. Scherbak
Yu. Boriskina	V. Migunov	T. Rumyantseva	T. Shapaeva
S. Erokhin	E. Pan'kova	N. Ryzhanova	N. Strelkov
S. Granovsky	M. Prudnikova	V. Samsonova	A. Vinogradov

International Advisory Committee

P. Bruno	<i>Halle</i>	D. Khmel'nitskii	<i>Cambridge</i>
A. Buzdin	<i>Bordeaux</i>	N. Kioussis	<i>Northridge</i>
B. Dieny	<i>Grenoble</i>	C. Lacroix	<i>Grenoble</i>
D. Givord	<i>Grenoble</i>	S. Maekawa	<i>Sendai</i>
B. Hernando	<i>Oviedo</i>	D. Mapps	<i>Plymouth</i>
M. Farle	<i>Duisburg</i>	B.D. McCombe	<i>New York</i>
A. Fert	<i>Orsay</i>	S. Ovchinnikov	<i>Krasnoyarsk</i>
D. Fiorani	<i>Rome</i>	S. Parkin	<i>San Jose</i>
A. Freeman	<i>Evanstone</i>	H. Sato	<i>Tokyo</i>
J. Gonzalez	<i>San Sebastian</i>	H. Szymczak	<i>Warsaw</i>
B. Heinrich	<i>Burnaby</i>	V. Ustinov	<i>Ekaterinburg</i>
M. Inoue	<i>Toyohashi</i>	M. Vazquez	<i>Madrid</i>
D. Khomskii	<i>Koeln</i>		

National Advisory Committee

Chairman: V. Trukhin

V. Aksenov	P. Kashkarov	R. Pisarev	A. Sigov
N. Bebenin	A. Lagar'kov	L. Prozorova	N. Sysoev
Yu. Izyumov	S. Maleev	V. Prudnikov	A. Zvezdin

Contents

21 June	9
Plenary Lectures	9
Oral Session.....	13
Ultrafast Spin Dynamics.....	13
Magnetophotonics	19
Nanomagnetism and Nanostructures	25
Spintronics and Magnetotransport.....	35
X-ray MCD and Auger Spectroscopy.....	43
Multiferroics	47
Theory.....	53
Magnetic Materials.....	59
Application, Superconductivity and Miscellaneous	65
Poster Session.....	73
Magnetophotonics	73
High Frequency Properties, Metamaterials and Resonances.....	97
Biomagnetism and Miscellaneous	161
22 June	183
Plenary Lectures	183
Oral Session.....	187
Diluted Magnetic Semiconductors and Oxides	187
Nanomagnetism and Nanostructures	195
Magnetophotonics I	199
High Frequency Properties	207
Low Dimensional Magnetism.....	217
Soft Magnetic Matter.....	227
Magnetophotonics II	239
Magnetism and Superconductivity.....	247
Poster Session.....	255
Nanomagnetism and Nanostructures	255
23 June	351
Plenary Lectures	351
Oral Session.....	355
Magnetophotonics	355
Biomagnetism and Miscellaneous	361
Nanomagnetism and Nanostructures	367
Spintronics	373
Metamaterials	3739
High Frequency Properties	383
Magnetocaloric Effect and Shape Memory.....	389
Soft Magnetic Matter.....	397
Poster Session.....	411
Magnetism and Superconductivity.....	411
Soft Magnetic Matter.....	445
Spintronics and Magnetotransport.....	477
Theory.....	505
24 June	535
Plenary Lectures	535
Oral Session.....	539
Diluted Magnetic Semiconductors	539
Magnetic Oxides	545
Spintronics and Magnetotransport.....	551

Metamaterials	561
Magnetocaloric Effect	569
Theory.....	579
Poster Session	589
Diluted Magnetic Semiconductors	589
Magnetic Oxides	615
25 June	695
Oral Session.....	695
Diluted Magnetic Semiconductors	695
Amorphous and Nanocrystalline Materials	707
Nanomagnetism and Nanostructures	719
Theory.....	725
High Frequency Properties	731
Magnetic Oxides	735
Poster Session	741
Magnetic Materials.....	741
Magnetocaloric Effect and Shape Memory	809
Author Index	826

21 June Saturday

10:15-11:45

plenary lectures

21PL-A

21PL-A-1

CONTROLLING MAGNETISM WITH LIGHT

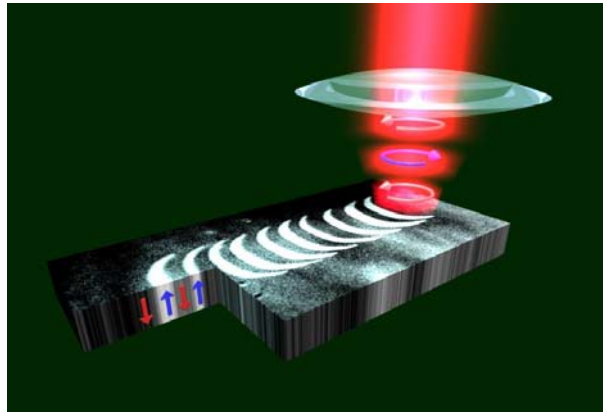
Rasing Th.

Institute for Molecules and Materials
Radboud University Nijmegen, The Netherlands

The interaction of light with magnetic matter is well known: magneto optical Faraday or Kerr effects are frequently used to probe the magnetic state of materials or manipulate the polarisation of light.

The inverse effects are less known but certainly as fascinating: with light one can manipulate or orient spins. Using femtosecond laser pulses we have recently demonstrated that one can thus generate ultrashort and very strong (\sim Tesla's) magnetic field pulses that provide unprecedented means for the generation, manipulation and coherent control of magnetic order on very short time scales, including the complete reversal of a magnet with a single 40 femtosecond laser pulse[1-3].

Demonstration of compact all-optical recording of magnetic bits by femtosecond laser pulses. This was achieved by scanning a circularly polarized laser beam across the sample and simultaneously modulating the polarization of the beam between left and right circular. White and black areas correspond to 'up' and 'down' magnetic domains, respectively.



[1] A.V.Kimel, A.Kirilyuk, P.A.Usachev, R.V.Pisarev, A.M.Balbashov and Th.Rasing, Ultrafast nonthermal control of magnetization by instantaneous photomagnetic pulses, **Nature** **435** (2005), 655-657

[2] C.D.Stanciu, F.Hansteen, A.V.Kimel, A.Kirilyuk, A.Tsukamoto, A.Itoh and Th.Rasing, All-optical Magnetic Recording with Circularly polarized Light, **Phys.Rev.Lett.****99**, 047601 (2007)

[3] A.Kalashnikova, A.V.Kimel, R.V.Pisarev, V.N.Gridnev, A.Kirilyuk and Th.Rasing, Impulsive Generation of Coherent Magnons by Linearly polarized Light in the Easy-Plane Antiferromagnet FeBO₃, **Phys.Rev.Lett.****99**, 167205 (2007)

21PL-A-2

PREPARATION AND MEDICAL APPLICATION OF MAGNETIC BEADS CONJUGATED WITH BIOACTIVE MOLECULES

Abe M.^{1, 2*}, Nishio N.³, Hatakeyama M.^{2, 3}, Hanyu N.⁴, Tanaka T.^{1, 5}, Tada M.¹, Nakagawa T.¹, Sandhu A.^{2, 6}, Handa H.^{2, 3}

¹Department of Physical Electronics, Tokyo Institute of Technology, Tokyo, Japan

²Integration Research Institute, Tokyo Institute of Technology, Tokyo, Japan

³Department of Life Science, Tokyo Institute of Technology, Yokohama, Japan

⁴Motortronics Laboratory, Tamagawa Seiki Co. Ltd. Iida, Japan

⁵Tokyo Bio R & D Center, Motortronics Laboratory,

Tamagawa Seiki Co. Ltd. Yokohama, Japan

⁶Quantum Nanoelectronics Research Center, Tokyo Institute of Technology, Tokyo, Japan

The unique properties of magnetic beads (MBs) are being exploited for medical diagnosis and cancer therapy with minimal side effects. Specific examples of the physical properties and applications of MBs include: magnetic manipulation for drug delivery systems (DDS); magnetically induced localized heating for anticancer magnetic hyperthermia; and electromagnetic/sonic response for NMR/sonography contrast enhancement. Here, we review the current and potential medical applications of MBs, especially cancer treatment based on our research on MBs.

The shape and size of magnetic beads for biomedical applications must be well defined and controllable. We have synthesized ferrite MBs with a **narrow size-distribution** by mixing seed ferrite crystals to an aqueous reaction solution and **obtained spherical shape**—which improves the homogeneity of bead surfaces and enhances water dispersibility—by adding a disaccharide to the reaction solution. The resulting MBs are shown in Fig.1.

Furthermore, the surfaces of MBs must facilitate conjugation with functional molecules for dispersion in water, efficient binding to target biomolecules, and incorporation MBs into cancer cells. We found proteins were **strongly conjugated** to ferrite beads **intermediated by proteins with specific amino acids compositions**. The amino acids had two carboxyl groups, which make chelate bonds onto ferrite surfaces (Fig.2) and they work as **adapter molecules** for stably conjugating specific biomolecules to ferrite beads.

We fabricated **monodisperse** (184 ± 9 nm in size) MBs, in which ferrite beads (40 nm in size) were encapsulated in a functional polymer (Fig.3(a)),

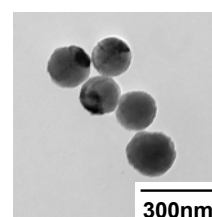


Fig.1 Monodisperse, spherical ferrite beads.

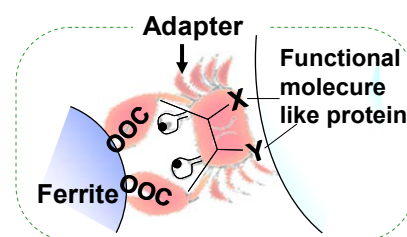


Fig.2 Adapter molecules strongly conjugate biomolecules onto ferrite surfaces via chelate bonds.

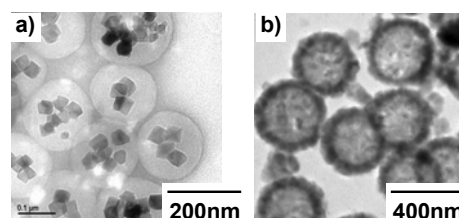


Fig.3 Monodisperse (a) polymer coated ferrite beads used for bioscreening and (b) ferrite hollow spheres for DDS and ultrasound contrast enhancement.

as carriers for a **high-throughput, automated bioscreening system** for affinity purification of target biomolecules. We also fabricated monodisperse, **hollow ferrite spheres** (Fig.3(b)) as DDS carriers and ultrasound contrast agents.

[1] K.Nishio et al., Colloids and Surfaces B, 54 (2007), 249.

21 June Saturday

12:15-13:45

oral session

21TL-A

21RP-A

**“Ultrafast Spin
Dynamics”**

21TL-A-1

ALL-OPTICAL ULTRAFAST MAGNETIZATION REVERSAL IN GdFeCo

Kirilyuk A.¹, Vahaplar K.¹, Kalashnikova A.M.¹, Kimel A.V.¹, Stanciu C.D.¹, Tsukamoto A.², Itoh A.², and Rasing Th.¹

¹ IMM, Radboud University Nijmegen, 6525 AJ Nijmegen, The Netherlands

² CST, Nihon University, 7-24-1 Funabashi, Chiba, Japan

In recent years the ultrafast manipulation of the magnetic state of matter by femtosecond laser pulses has emerged as one of the most intriguing issues of magnetism as well as a subject of importance for spintronics, information processing and magnetic recording. It has been shown that the speed of optically induced changes of magnetization may access timescales of sub-picoseconds [1]. However, the laser-induced magnetic changes come as the result of optical absorption followed by a rapid temperature increase. This thermal origin of spin excitation makes the effect non-reversible and considerably hampers potential applications because the repetition frequency is limited by the cooling time.

The solution is the direct *nonthermal* laser control of magnetism, when the spins are directly influenced by the electromagnetic field of the light wave. We have recently demonstrated that the magnetization can be fully controlled on a femtosecond time scale with circularly polarized laser pulses without any applied magnetic field, via the opto-magnetic inverse Faraday effect [1]. The effect of laser pulses on a magnetic system was found to be equivalent to the effect of equally short magnetic field pulses. It has been shown that such pulses can nonthermally excite and coherently control the magnetization in antiferromagnetic [1] and ferrimagnetic [2] materials, including metals [3]. Moreover, the direct all-optical recording was demonstrated [4].

In this talk I will consider the laser-induced magnetization dynamics in GdFeCo alloys, that are typical rare earth–3d transition metal (RE-TM) ferrimagnetic compounds. Depending on their composition, RE-TM ferrimagnets can exhibit a magnetization compensation temperature T_M where the magnetizations of the RE and TM sublattices cancel each other and similarly, an angular momentum compensation temperature T_A where the net angular momentum of the sublattices vanishes. At the latter point, the frequency of the homogeneous spin precession is expected to diverge, that should lead to an acceleration of the magnetization reversal.

We experimentally demonstrate that the magnetization can be reversed in a reproducible manner by a single 40 femtosecond circularly polarized laser pulse [4], without any applied magnetic field. This optically induced ultrafast magnetization reversal previously believed impossible is the combined result of femtosecond laser heating of the magnetic system to just below the Curie point and circularly polarized light simultaneously acting as a magnetic field with amplitudes of up to several Teslas. The direction of this opto-magnetic switching is determined only by the helicity of light.

In an alternative scheme, ultrafast heating of a ferrimagnet across its compensation points results in a subpicosecond magnetization reversal [5], initiated by crossing the magnetization compensation temperature, the short reversal time being related to the highly accelerated dynamics in the vicinity of T_A . These findings reveal an ultrafast and efficient pathway for writing magnetic bits at record-breaking speeds.

[1] A.V. Kimel et al, *Nature*, **435**, 655 (2005).

[2] F. Hansteen, A.V. Kimel, A. Kirilyuk, and Th. Rasing, *Phys. Rev. Lett.*, **95**, 047402 (2005).

[3] C.D. Stanciu et al., *Phys. Rev. Lett.* **98**, 207401 (2007).

[4] C.D. Stanciu et al., *Phys. Rev. Lett.* **99**, 047601 (2007).

[5] C.D. Stanciu et al., *Phys. Rev. Lett.* **99**, 217204 (2007).

21RP-A-2

IMPULSIVE EXCITATION OF COHERENT SPIN PRECESSION IN THE WEAK FERROMAGNET FeBO_3

*Kalashnikova A.M.^{1,2}, Kimel A.V.¹, Pisarev R.V.², Gridnev V.N.²,
Usachev P.A.², Kirilyuk A.¹, and Rasing Th.¹*

¹ IMM, Radboud University Nijmegen, 6525AJ Nijmegen, The Netherlands

² A. F. Ioffe Physico-Technical Institute of RAS, 194021 St. Petersburg, Russia

In recent years the ultrafast manipulation of the magnetic state of matter by femtosecond laser pulses has become one of most exciting topics in magnetism, spintronics and information processing and recording. Such a process requires fast and efficient channels for angular momentum transfer between external stimuli and spins, orbitals and phonons, while direct transfer of the momentum from photons to spins was shown to be insufficient for magnetization reorientation [1]. Circularly polarized pulses, possessing an angular momentum $L_z = \pm 1$, were shown to excite and control spin precession [2] and even to switch magnetization [3]. It was proposed that they can act on spins as a short effective magnetic field pulse directed along the propagation direction of light: $\mathbf{H}^{\text{eff}} = -\partial\Phi/\partial\mathbf{M}$, where Φ is the free energy describing the magneto-optical effects and \mathbf{M} is the magnetization.

In this paper we show that in the easy-plane weak ferromagnetic FeBO_3 spin precession can be excited by *linearly-polarized laser pulses, carrying no angular momentum*, more efficiently than by circularly polarized ones [4]. To describe this we extend the theory of impulsive stimulated Raman scattering [5] to the case of magnons and show that a crucial role in the process is played by the strong ellipticity of spin precession intrinsic to FeBO_3 . The angular momentum of light, in contrast, is not a decisive factor, since its transfer from photons to spins is not required in the process.

From the phenomenological point of view the spin precession excitation is described by the light-induced effective field $\mathbf{h}^{\text{eff}} = -\partial\Phi/\partial\mathbf{L}$, where \mathbf{L} is the antiferromagnetic vector. We show that this field has to be taken into account when dealing with a multi-sublattice magnetic medium.

Support by NanoNed (NanoSpintronics), NWO, RFBR, and INTAS is acknowledged.

- [1] B. Koopmans *et al.*, Phys. Rev. Lett. **85**, 884 (2000).
- [2] A. V. Kimel *et al.*, Nature **435**, 655 (2005).
- [3] C. D. Stanciu, *et al.*, Phys. Rev. Lett. **99**, 047601 (2007).
- [4] A. M. Kalashnikova *et al.*, Phys. Rev. Lett. **99**, 167205 (2007).
- [5] Y.-X. Yan, *et al.*, J. Chem. Phys. **83**, 5391 (1985).

21RP-A-3

THEORY FOR IMPULSIVE SPIN WAVE GENERATION THROUGH STIMULATED RAMAN SCATTERING

Gridnev V.N.

Ioffe Physico-Technical Institute, Russian Academy of Sciences, 194021 St. Petersburg, Russia

We present a phenomenological theory for generation of spin waves in transparent magnetic dielectrics through impulsive stimulated Raman scattering (ISRS). The work is motivated by recent experimental paper [1], where the excitation of spin waves by femtosecond laser pulses in the optically transparent antiferromagnet FeBO₃ was reported. It was shown that the mechanism of excitation is impulsive stimulated Raman scattering (ISRS).

The purpose of this work is to reveal the general properties of the spin wave generation through ISRS, in particular, to establish a connection between characteristics of equilibrium magnetic structure and the efficiency of the spin-wave excitation.

Consideration is given to a lattice which has an arbitrary number of localized spins in each magnetic unit cell. Our approach [2] is based on the Hamilton equations for the normal coordinate of the spin wave Q_α ,

$$\frac{dQ_\alpha}{dt} + i\Omega_\alpha Q_\alpha = -i \frac{\partial V}{\partial Q_\alpha^*}.$$

where Ω_α is the frequency of the spin wave of branch α and V is the interaction energy of light pulse with the spin system.

Using this equation, a general expression for the modulation of optical dielectric permittivity by light-induced spin waves is derived and its symmetry properties with respect to time reversal is analyzed. The modulation of the optical dielectric permittivity induced by the spin waves is straightforwardly related to optical effects detected by a probe pulse. The oscillating in time permittivity can be represented as a sum of cosine and sine contributions. The former depends on the magneto-optical constants and light polarization but is independent of the parameters of the spin precession, while the latter increases with the ellipticity of the spin precession. The ellipticity of the spin precession is inherent to major part of magnetic structures, but it is especially large for structures with easy plane type of magnetic anisotropy.

A simple cubic ferromagnet and a rutile-type structure antiferromagnet are treated as examples of application of the theory. In the former case the spin precession is circular while in the latter is elliptical. For this reason, in general, the impulsive spin wave generation by light is more efficient in antiferromagnets than in cubic ferromagnets.

Support by RFBR, INTAS and the program Spintronics of RAS is acknowledged.

[1] A.M. Kalasnikova *et al.*, *Phys. Rev. Lett.*, **99** (2007) 167205.

[2] V.N. Gridnev, *Phys. Rev.B*, **77** (2008) 094426.

21TL-A-4

ULTRAFAST DYNAMICS AT LANTHANIDE SURFACES: MICROSCOPIC INTERACTION OF THE CHARGE, LATTICE, AND SPIN SUBSYSTEMS

Melnikov A.¹, Radu I.^{2,3}, Povolotskiy A.⁴, Wehling T.⁵, Lichtenstein A.⁵, Bovensiepen U.¹

¹Fachbereich Physik, Freie Universität Berlin, Arnimallee 14, 14195 Berlin, Germany

²Institut für Experimentelle Physik, Universität Regensburg,
Universitätsstraße 31, 93040 Regensburg, Germany

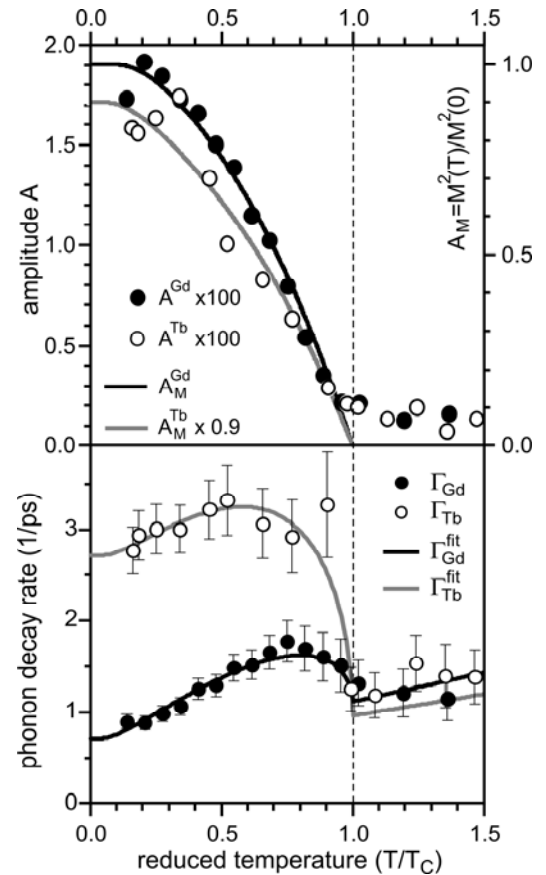
³BESSY GmbH, Albert-Einstein-Str. 15, 12489 Berlin, Germany

⁴St. Petersburg State University, Laser Research Institute, St. Petersburg, 198504 Russia

⁵Institut für Theoretische Physik, Universität Hamburg, Jungiusstrasse 9, 20355 Hamburg,
Germany

In solids the charge, lattice, and spin degrees of freedom are coupled and respective coupling strengths result in characteristic timescales on which excitations of one particular subsystem interact and equilibrate with the remaining subsystems. In ferromagnetic metals the respective elementary interaction processes occur on the pico- and femtosecond time scale. To elucidate these interaction mechanisms and the timescales we investigate the ultrafast dynamics of electrons, phonons, and spins excited by intense infrared optical pulse at Gd(0001) and Tb(0001) surfaces, employing complementary time-resolved methods of optical second harmonics generation and photoelectron spectroscopy. These surfaces exhibit rich dynamics including a collective response of the crystal lattice and the magnetization, manifested by a coupled coherent optical phonon-magnon mode at 3 THz [1]. Here we present new temperature- and fluence-dependent results of pump-probe experiments. The temperature dependence of the coherent phonon amplitude (Figure, top) shows that a spin and a charge driven excitation mechanism can be separated. The spin driven excitation dominates below the Curie temperature and scales accordingly to developed model with $M^2(T)$ (solid curves), where the magnetization M is calculated through Brillouin function. This behavior is in a good agreement with *ab initio* model calculations that establish a displacement of the surface plane equilibrium position upon a reduction of the surface spin polarization M_S induced by the pump pulse. A mechanism of ultrafast surface spin-flip leading to 50% reduction of M_S [1] is proposed.

Analysis of the temperature-dependent coherent phonon damping (Figure, bottom) shows an anomaly in the vicinity of the Curie temperature T_C that is for Gd well described (solid curve) by anharmonic phonon-magnon decay introduced in addition to anharmonic phonon-phonon decay and phonon-electron scattering discussed in [2]. In case of Tb an additional damping channel is required that could be related to local spin-flip excitations. Spin-dependent contribution to the coherent phonon damping in Tb is much larger



than in Gd, which is expected because of the considerably larger spin-orbit coupling in Tb (4f8, $L^{4f}=3$) compared to Gd (4f7, $L^{4f}=0$) leading to much stronger spin-lattice interaction.

[1] A. Melnikov *et al.*, *Phys. Rev. Lett.* **91** (2003) 77403.

[2] M. Hase *et al.*, *Phys. Rev. B* **71** (2005) 184301.

21 June Saturday

15:00-17:00

oral session

21TL-A

“Magnetophotonics”

21TL-A-5

FROM OPTICAL METAMAGNETICS TO ENGINEERED META-SPACE FOR LIGHT

Shalaev V.M., Kildishev A.V., Cai W., Yuan H.-K., Drachev V.P.
 Purdue University, Purdue, Sierra Leone
 e-mail: shalaev@ecn.purdue.edu

Artificial magnetic and negative-index structures in the optical range have been demonstrated. This new family of metamaterials enables a new paradigm for the science of light via transformation optics.

21TL-A-6

GYROTROPIC DEGENERATE BANDGAPS BY HIGH-ORDER WAVEGUIDE MODE COUPLING

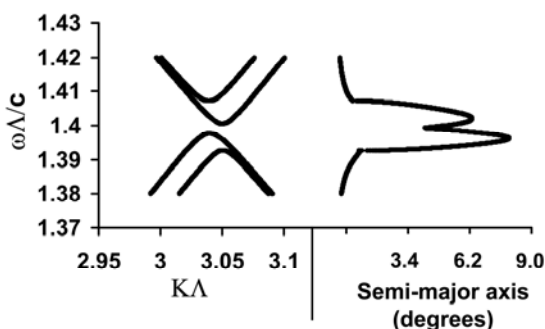
Levy M., Jalali A.A., Zhou Z., Dissanayake N.
 Physics Department, Michigan Technological University, Houghton, MI 49931, U.S.A.

The formation of gyrotropic degenerate bandgaps has recently been predicted for non-uniform elliptically birefringent magnetophotonic crystals.[1,2] Elliptical birefringence refers to the difference in refractive index between elliptically polarized local normal modes. These bandgaps open up inside the Brillouin zone as a result of spatial variations in the polarization state of the modes, and are of interest because the polarization response and transmittance of the system in and around these gaps can be made tunable by the application of a magnetic field.

Elliptical birefringence occurs naturally in planar magnetophotonic crystal waveguides. Hence these structures present a model system for the study of the gyrotropic degenerate bandgap. Moreover, the possibility to excite different waveguide modes lends added richness to the class of phenomena that can be probed in such systems. Recent work by some of the present authors has shown that different waveguide modes can be coupled together in one-dimensional magnetophotonic crystals fabricated in bismuth-substituted iron garnet films.[3] In particular, bandgaps have been observed where the Bragg reflection mechanism links forward-going

fundamental waveguide modes to high-order backscattered ones.

The present talk will discuss the consequences of such coupling between different waveguide modes travelling in opposite directions upon the properties of the gyrotropic degenerate bandgap and its polarization response. In particular, we predict the formation of much wider bandgaps than contemplated in prior work on these systems, and present an explanation for the significant polarization rotation observed near the band edges



in high-order backscattering waveguide magnetophotonic crystals. The figure shown here plots the calculated band structure for a stack model system with different modes travelling in opposite directions. Two nearly overlapping gyrotropic degenerate bandgaps corresponding to different Bloch states of the photonic crystal are visible. Also plotted in the figure is the

polarization response in the forward direction, parameterized by the angular orientation (absolute value) of the semi-major axis of the polarization ellipse relative to the input (linear) polarization. It is clear from the figure that the selective suppression of one or another of the Bloch states by the overlapping bandgaps leads to largely enhanced polarization rotations.

Support by the NSF through grants ECCS-0520814 and DMR-0709669 is acknowledged. Some of the samples used for this work were fabricated by R. Li and X. Huang.

[1] Amir A. Jalali and Miguel Levy, *J. Opt. Soc. Am. B*, **25** (2008) 119.

[2] A.M. Merzlikin, A.P. Vinogradov, A.V. Dorofeenko, M. Inoue, M. Levy and A.B. Granovsky, *Physica B: Condensed Matter*, **394** (2007) 277.

[3] M. Levy and R. Li, *Appl. Phys. Lett.*, **89** (2006) 121113.

21TL-A-7

ULTRAFAST MAGNETIC AND OPTICAL PHENOMENA IN RARE EARTH ORTHOFERRITES

Pisarev R.V.

Ioffe Physico-Technical Institute, Russian Academy of Sciences,
194021 St. Petersburg, Russia

Rare earth orthoferrites $R\text{FeO}_3$ are a well known group of magnetically ordered materials. They crystallize in the distorted perovskite-type orthorhombic structure and the unit cell contains four molecular units. Four magnetic sublattices of Fe^{3+} ions are coupled antiferromagnetically. However the Dzyaloshinsky's interaction leads to canting of antiferromagnetic sublattices which results in the weak ferromagnetic moment. One of the interesting features of orthoferrites is the presence in many of them spontaneous orientation phase transitions. Review of their magnetic, acoustic, optical, magneto-optical and other properties can be found in [1].

In the present talk we are going to discuss magnetic and optical phenomena in orthoferrites which have been studied during the recent 2-3 years with the use of titanium-sapphire pulse lasers with pulse duration typically 150 fs and the repetition rate 1 kHz. The measurements were performed at photon energy 1.55 eV where, on the one hand, orthoferrites have a transparency window, and, on the other hand, possess high magneto-optical Faraday rotation. This rotation, or in some cases the magnetic linear birefringence (MLB), were used for monitoring the pump-induced changes of magnetization and its subsequent relaxation.

We discuss the laser-induced spin reorientation in TmFeO_3 [2]. This process occurs via two second-order phase transitions in the temperature range from 80 to 92 K. We have proved that using short laser pulses the spins of TmFeO_3 can indeed be manipulated on a timescale of a few picoseconds, in contrast to the hundreds picoseconds in ferromagnets. No dependence on polarization of light was found which allowed us to assign these phenomena to ultrafast heating of samples by laser light. However the *thermal* origin of spin excitation considerably limits potential applications because the repetition frequency is limited by the cooling time.

Another phenomenon was observed in DyFeO_3 [3]. We demonstrated that circularly polarized femtosecond laser pulses can be used to *non-thermally* excite and coherently control the spin dynamics by way of the inverse Faraday effect. Such nonlinear interaction of light with magnetic media is instantaneous and is limited in time by the laser pulse duration used for pumping.

In the two previous orthoferrites the orientation phase transitions occurs when the weak ferromagnetic moment and the antiferromagnetic vector rotates in the xz plane. In the case of HoFeO_3 orientation transitions go via more complicated pathway and a first order phase

transition occurs at about 52 K. We found [4] that the phase transition caused by the laser-induced magnetic field occurs at much shorter time scale of several picoseconds, whereas the same phase transition but due to thermal heating occurs on much longer time scale of several hundreds of picoseconds. Important conclusion from this study was the observation that in antiferromagnets *inertia-driven* picoseconds spin dynamics can be realized.

This work is supported by RFBR, NWO, and INTAS.

[1] Landolt-Boernstein, *New Series, Group III*, Vol. 27f (Springer, Berlin, 1996).

[2] A.V. Kimel, A. Kirilyuk, A. Tsvetkov, R.V. Pisarev, and Th. Rasing, *Nature* **429**, 850 (2004).

[3] A.V. Kimel, A. Kirilyuk, P.A. Usachev, R.V. Pisarev, A. M. Balbashov, and Th. Rasing, *Nature* **435**, 655 (2005).

[4] A.V. Kimel, B. A. Ivanov, R.V. Pisarev, P. A. Usachev, A. Kirilyuk, and Th. Rasing (submitted).

21TL-A-8

NONLINEAR OPTICS OF MAGNETOPHOTONIC CRYSTALS

Murzina T.V.¹, Razdolski I.E.¹, Aksamitov O.A.¹, Grishin A.M.², Khartsev S.I.², Inoue M.³

¹Department of Physics, Moscow State University, 119991 Moscow, Russia

²Condensed Matter Physics, Royal Institute of Technology, 164 40 Stockholm-Kista, Sweden

³Toyohashi University of Technology, 441-8580 Toyohashi, Japan

It has been demonstrated recently that a strong enhancement of optical and nonlinear optical effects can be achieved in photonic crystals (PCs) composed of dielectric, liquid crystalline and semiconductor materials. For nonlinear-optical effects, the increase of local fields due to the photon trapping and redistribution of light within inhomogeneous PC structure and parametric enhancement due to the phase-matching are responsible for the observed phenomena. In the case of magnetophotonic crystals, e.g. PC structures formed, at least partially, by magnetic materials, similar enhancement mechanisms can result in an amplification of linear and nonlinear magneto-optical effects.

In this paper, the results of recent observation and studies of second- and third-order nonlinear optical effects in magnetophotonic crystals (MPCs) are discussed [1,2].

Nonlinear magneto-optical effects are studied in two types of magnetophotonic structures: magnetophotonic microcavities (MPMCs) and MPCs. Two types of structures of different composition were studied: (1) polycrystalline (Bi:YIG/SiO₂)⁵ MPC, each layer being quarter-wavelength thick, and MPMC of the composition (Ta₂O₃/SiO₂)⁵/(Bi:YIG)/(Ta₂O₃/SiO₂)⁵, formed by nonmagnetic Bragg mirrors and a half-wavelength thick magnetic microcavity spacer, and (2) all-garnet heteroepitaxial MPMC composed of alternating quarter-wavelength magnetic bismuth iron-garnet (Bi₃Fe₅O₁₂) and nonmagnetic gadolinium gallium garnet (Gd₃Ga₅O₁₂) layers, the microcavity spacer consisting of half-wavelength thick Bi₃Fe₅O₁₂ layer [3].

The following main results are discussed: (i) high values of the second-order nonlinear magneto-optical Kerr (Faraday) effects in MPC and MPMC, the magnetization-induced rotation of the polarization plane being up to 140 degrees, magnetic contrast in the intensity of second harmonic generation up to 0.9; (ii) observation of the magnetization-induced effect in third harmonic generation via transversal nonlinear-optical Kerr effect; (iii) experimental observation of the third-order nonlinear-optical self-action effects in photonic-crystal microcavities, including polarization self-action effect, which demonstrate a considerable defocusing and rotation of polarization plane of the laser radiation resonant to the microcavity mode.

The experimental methods which were exploited are based on magnetization-induced optical second- and third harmonics generation, including magnetization-induced changes in harmonics' polarization, intensity and phase, and polarization-sensitive Z-scan technique for the case of the third-order self-focusing effects. The role of the following mechanisms, responsible for the enhancement of the magnetization-induced nonlinear-optical effects, such as the spatial localization of the fundamental light within the microcavity mode, fulfillment of the phase-matching conditions for second- and third-harmonics generation at the spectral edge of the photonic band gap, and nonlinear birefringence expected in the microcavity layer, are discussed.

- [1] M. Inoue, R. Fujikawa, A. Baryshev, et. al., *J. Phys. D: Appl. Phys.*, **39**, (2006) R151.
- [2] I.E. Razdolsky, T.V. Murzina, O.A. Aktsipetrov, M. Inoue. *JETP Lett.*, **84**, (2006) 451.
- [3] S.I. Khartsev, A.M. Grishin, *Appl. Phys. Lett.*, **87**, (2005) 122504.

21 June Saturday

12:15-13:45

15:00-17:00

oral session

21TL-B

21RP-B

**“Nanomagnetism
and Nanostructures”**

21TL-B-1

A MICROSCOPIC UNDERSTANDING OF EXCHANGE ANISOTROPY IN Fe/MnF₂ BILAYERS

Krivorotov I.N.¹, Leighton C.², Nogues J.³, Schuller I.K.⁴, and Dahlberg E.D.¹

¹Physics Department, University of Minnesota, Minneapolis, MN 55455, USA

²Department of Chem. E and Mat. Sci., U of Minnesota, Minneapolis, MN 55455, USA

³Department de Fisica, Universitat Autònoma de Barcelona, 08193 Bellaterra, Spain

⁴Physics Department, UC San Diego, La Jolla, CA 92093, USA

A microscopic understanding of the Ferromagnetic/Antiferromagnetic (F/AF) direct exchange coupling or exchange biasing has been elusive for the over 50 years since it was discovered. In part, the almost exclusive use of hysteresis loops to study the phenomenon has limited our understanding. A new experimental technique was developed to study the exchange coupling between a ferromagnet and antiferromagnet [1]. This new technique has enjoyed considerable success in explaining many general exchange bias features using Co/CoO as a model system [2, 3, 4].

We will review the models of exchange bias and then apply them to our work on Fe/MnF₂ bilayers. In this work we used variations of the AMR technique to study the angular dependence of the exchange anisotropy in Fe/MnF₂ bilayers. We were able to phenomenologically describe the anisotropy energy as a combination of unidirectional, uniaxial, threefold and fourfold components [5, 6] and thus explain the anomalous magnetization reversal asymmetry discovered in this system [7]. In our efforts we have been able to explain the phenomenological energy terms [5] using a microscopic model which sums over all lattice sites in both the ferromagnet and antiferromagnet [6]. The microscopic model includes terms for the interfacial exchange coupling, uncompensated spin density in the AF, the AF spin-canting energy, and domain walls in both the F and AF. Application of the model to the Fe/MnF₂ bilayer experimental data allows one to separately determine the fraction of uncompensated interfacial spins in the AF layer and the interfacial exchange coupling energy for the first time. An understanding of the spatial distribution of the microscopic energies allows for a simplification of the energy in which the physics is transparent.

This work supported by the University of Minnesota MRSEC

[1] B.H. Miller and E. Dan Dahlberg, *Appl. Phys. Lett.*, **69** (1996) 3932-3934.

[2] T. Gredig, I.N. Krivorotov, C. Merton, A.M. Goldman, and E.D. Dahlberg, *J. Appl. Phys.*, **87** (2000) 6418-20.

[3] I. N. Krivorotov, T. Gredig, K. R. Nikolaev, A. M. Goldman, and E. Dan Dahlberg, *Phys. Rev. B*, **65**(RC) (2002) 180406-10.

[4] T. Gredig, I. N. Krivorotov, and E. Dan Dahlberg, *Physical Review B*, **74**, e094431 (2006).

[5] I. N. Krivorotov, C. Leighton, J. Nogues, I. K. Schuller, and E. D. Dahlberg *Phys. Rev. B*, **65**(RC) (2002) 100402.

[6] I. N. Krivorotov, C. Leighton, J. Nogues, Ivan K. Schuller, and E. Dan Dahlberg *Physical Review B*, **68** (RC) (2003) 54430-1.

[7] M. R. Fitzsimmons, P. Yashar, C. Leighton, Ivan K. Schuller, J. Nogues, C. F. Majkrzak, and J. A. Dura, *Phys. Rev. Lett.*, **84** (2000) 3986.

21TL-B-2

TILTED MEDIA FOR PERPENDICULAR RECORDING

Varvaro G., Agostinelli E., Laureti S., Testa A.M., and Fiorani D.
ISM-CNR, Research Area Roma1, 00016 Monterotondo Scalo (RM), Italy

Magnetic recording is the dominant information storage technology and the hard disk, due to its versatility, high capacity and low cost, is the most diffuse device not only for applications in computers but also in consumer electronics. In response to an ever increasing demand for stored information, the hard disk drive manufacturers have come forward with spectacular increase in storage capacities and densities over the last decade. Further progress, will require major breakthroughs and novel technologies. The search for new media for ultrahigh density recording, beyond 1 Tbit/in², needs to address key issues for making them feasible, i.e. the trade off among thermal stability, write-ability and signal to noise ratio (the so called recording *trilemma*) and, at the same time, to develop simple, low cost and high throughput media fabrication methods suitable for mass production.

The proposed new media for ultra-high recording density will be reviewed with special emphasis on tilted media for perpendicular recording. They present some advantages with respect to current perpendicular media: lower noise (due to much smaller sensitivity of switching fields to the easy axis distribution), better write-ability (due to a much smaller switching field, well below current state of write head field) still maintaining large thermal stability, higher data transfer rate (due to much faster switching) and simpler deposition processes.

The magnetic properties of L1₀ CoPt (111)/ Pt (111)/ MgO (100) films, grown by PLD, exhibiting 4 tilted easy axes (36° out-of-plane with orthogonal in-plane projections) will be discussed. They were investigated by measuring the angular dependence of the remanent magnetization, using a VSM vectorial magnetometer, and by MFM measurements

21TL-B-3

SPIN CURRENT AND TWO MAGNON SCATTERING IN NANOSCALE SYSTEMS

Heinrich B.¹, Woltersdorf G.², Kardasz B.¹, Mosendz O.¹, Freeman M.³, and Back Ch.²

¹Physics Department, Simon Fraser University, Burnaby, BC, Canada

²Physics Department, University of Regensburg, Germany

³Physics Department, University of Alberta, Edmonton, Canada

Research interest in magnetic nanostructures and spintronics has shifted increasingly from the static to dynamic properties of magnetic nanostructures. This is motivated by the fact that the switching time of magnetic hybrid multilayers used in mass data storage devices and magnetic random access memories (MRAM) is a real technological issue. The crystalline Fe/Au,Pd/Fe/Au (001) nano-structures were prepared by Molecular Beam Epitaxy (MBE) technique using 4x6 reconstructed GaAs(001) substrates. A gyrating magnetic moment creates a spin current in surrounding normal metal layers and leads to non-local interface spin damping. The precessing magnetization acts as a peristaltic spin pump, which transports the spin momentum and allows one to establish a transfer of information between the magnetic layers separated over thick nonmagnetic metallic spacers. Modified Landau-Lifshitz-Gilbert (LLG) equations of motion are modified by spin pumping and spin sink effects. Time Resolved

Magneto-Optical Kerr effect (TRMOKE) is an ideal tool to investigate propagation of spin currents. The stroboscopic time-resolved measurements (with the time resolution of 1 ps and sub micron spatial resolution) were carried out using a slotted transmission line with repetitive ps magnetic pulses. Spin currents generated by spin pumping at the Au/Fe interface were investigated from the ballistic to spin diffusion limits by using the Fe/Au interface as a spin detector.

The Pd lattice has a large lattice mismatch with respect to Fe. The lattice strain is partially released by a self-assembled rectangular network of misfit dislocations. It will be shown that the nano-network of misfit dislocations leads to a strong extrinsic magnetic damping. This system provides an ideal opportunity to investigate the role of two magnon scattering in a wide range of microwave frequencies. FMR measurements were carried out from 4 GHz to 73 GHz. The contribution to the FMR linewidth from this two magnon scattering is strongly anisotropic and follows the rectangular symmetry of the glide planes of the misfit dislocation network. The angular dependence of the FMR linewidth is a consequence of channeling of the scattered spinwaves along the misfit dislocation glide planes.

21TL-B-4

MAGNETIC ORDERING AND SWITCHING OF FE-PORPHYRIN MOLECULES MEDIATED BY FERROMAGNETIC SURFACES

Wende H.¹, Bernien M.², Luo J.², Weis C.¹, Ponpandian N.², Kurde J.², Miguel J.², Piantek M.², Xu X.², Eckhold Ph.², Srivastava P.¹, Kuch W.², Baberschke K.², Panchmatia P.M.³, Sanyal B.³, Oppeneer P.M.³, Eriksson O.³

¹Universität Duisburg-Essen, Fachbereich Physik, Experimentalphysik, Lotharstr. 1, D-47048 Duisburg, Germany

²Institut für Experimentalphysik, Freie Universität Berlin, Arnimallee 14, D-14195 Berlin-Dahlem, Germany

³Department of Physics, Uppsala University, Box 530, S-751 21 Uppsala, Sweden

A class of materials particularly promising as building blocks in molecular nano-electronics are the paramagnetic porphyrin molecules in contact with a metallic substrate. These biologically significant molecules are candidates for various applications, e.g., in information storage, as optical switches and in non-linear optics. The study of the structural orientation and the magnetic coupling of in-situ sublimated Fe-porphyrin molecules on ferromagnetic Ni and Co films which are epitaxially grown on Cu(100) is presented. These studies utilize near edge X-ray absorption fine structure spectroscopy (NEXAFS) at the C and N K-edges, and X-ray magnetic circular dichroism (XMCD) at the Fe, Co and Ni L_{2,3}-edges, which provide element specific magnetic properties [1]. In a combined experimental-computational study we demonstrate that due to an indirect super exchange interaction between Fe atoms in the molecules and atoms of the substrate (Co or Ni) the paramagnetic molecules can be made to order ferromagnetically. By means of temperature-dependent XMCD investigations we determine different coupling strengths for the Fe atoms in the molecule to the two magnetic substrates, being weaker in the case of Ni [2]. The Fe magnetic moment can be rotated along directions in-plane as well as out-of-plane by a magnetization reversal of the substrate, thereby opening up an avenue for spin-dependent molecular electronics. Supported by BMBF (05 KS4 KEB 5) and DFG (SFB 658, Heisenberg-Programm).

- [1] H. Wende, M. Bernien, J. Luo, C. Sorg, N. Ponpandian, J. Kurde, J. Miguel, M. Piantek, X. Xu, Ph. Eckhold, W. Kuch, K. Baberschke, P.M. Panchmatia, B. Sanyal, P.M. Oppeneer and O. Eriksson, *Nature Materials* **6**, 516 (2007).
- [2] M. Bernien, X. Xu, J. Miguel, M. Piantek, Ph. Eckhold, J. Luo, J. Kurde, W. Kuch, K. Baberschke, H. Wende and P. Srivastava, *Phys. Rev. B* **76**, 214406 (2007).

21TL-B-5

LARGE SCALE AB INITIO SIMULATIONS OF MULTIPLY TWINNED TRANSITION METAL NANOPARTICLES

Gruner M.E.

Department of Physics, University of Duisburg-Essen, 47048 Duisburg, Germany

Arrays of $L1_0$ ordered nanoparticles of near-stoichiometric Fe-Pt and Co-Pt with diameters down to 4 nm are considered as promising material for future ultra-high density recording media. However, with decreasing particle size, also so-called multiply twinned morphologies as decahedra and icosahedra are frequently encountered in experiment (e.g., [1,2]). The occurrence of multiple twinned morphologies is related to the competition between the energy contribution of the surfaces on the one hand and internal strain and interfaces on the other.

Multiply twinned structures, however, will not possess the required hard magnetic properties due to the different crystallographic orientations of the individual twins. The close interrelation of electronic structure and morphology in these materials requires a quantum-mechanical description in the framework of density functional theory (DFT) combining the necessary accuracy while providing the scalability to the interesting system sizes on contemporary supercomputers. Previous large scale ab initio structure optimizations with up to 641 atoms have been successfully carried out on the IBM Blue Gene/L installation at Forschungszentrum Jülich to explain the size dependent evolution of morphologies in elemental Fe nanoparticles [3]. For the case of binary near-stoichiometric Fe-Pt alloys, also ordering and segregation tendencies have to be considered. Here, several morphologies with up to ~ 2.5 nm in diameter (561 atoms) have been compared, showing that ordered multiply twinned structures are energetically preferred over $L1_0$ cuboctahedra in this size range [4].



The current investigation is concerned with the classification of chemical trends for the structural stability of the $L1_0$ phase, as alloying may help to control the occurrence of multiply twinned morphologies. The impact on the electronic structure, magnetic properties and the energetic order of the morphologies has been monitored by a systematic variation of the $3d$ and the $5d$ element. Significant effects are encountered when the $3d$ element Fe is replaced by Mn or

Co. For Co-Pt particles, segregated and twinned morphologies are favored. For Mn-Pt, these structures are suppressed at the expense of a strong preference for an antiferromagnetic spin arrangement.

- [1] D. Sudfeld *et al.*, Mater. Res. Soc. Symp. Proc. **998E** (2007) 0998-J01-06.
 [2] R. M. Wang *et al.*, *Phys Rev. Lett.* **100** (2008) 017205.
 [3] G. Rollmann, M. E. Gruner, A. Hucht, R. Meyer, P. Entel, M. L. Tiago, and J. R. Chelikowsky, *Phys. Rev. Lett.* **99** (2007) 083402.
 [4] M. E. Gruner, G. Rollmann, P. Entel, and M. Farle, *Phys. Rev. Lett.* **100** (2008) 087203.

21RP-B-6

DOMAIN FORMATION AND TRANSFORMATION IN ANTIFERROMAGNETICALLY COUPLED MULTILAYERS: REFLECTOMETRY AND MONTE CARLO SIMULATION

*Nagy D.L.¹, Bottyan L.¹, Chumakov A.I.², Deak L.¹, Harth E.¹, Khaidukov Yu.N.³,
Major M.¹, Nikitenko Yu.V.³, Petrenko A.V.³, Proglyado V.V.³, Rueffer R.², Szilagyi E.¹,
Tancziko F.¹, Visontai D.¹*

¹KFKI Research Institute for Particle and Nuclear Physics,
H-1525 Budapest, P.O.B. 49, Hungary

²European Synchrotron Radiation Facility, BP 220, F-38043 Grenoble, France

³Frank Laboratory of Neutron Physics, Joint Institute for Nuclear Research,
141 980 Dubna, Moscow Region, Russia

Antiferromagnetically (AF) coupled metallic multilayers (ML) have received much attention in recent years due to their relevance in fundamental science and magnetic recording technology alike. The performance of magnetoresistive devices is strongly affected by the ML domain structure [1]. We will present studies of the magnetic-field-history-dependent formation and transformation of magnetic domains in strongly AF-coupled epitaxial MLs by two closely related nuclear scattering techniques, viz. synchrotron Moessbauer reflectometry (SMR) and polarized neutron reflectometry (PNR). One of the observed transformations will be described by a Monte Carlo simulation.

An epitaxial MgO(001)/[⁵⁷Fe(2.6 nm)/Cr(1.3 nm)]₂₀ ML was fabricated by MBE technique. The saturation field of the ML was found to be $H_S = 0.85$ T and 1.05 T along the easy and hard axes, respectively. A bulk-spin-flop (BSF) transition took place when a magnetic field of 14 mT was applied along the easy axis in which the layer magnetizations actually lay as evidenced from SMR [2], PNR [3] and Moessbauer polarimetry experiments. The size ξ of the AF domains was taken from the q_x -scan width Δq_x of diffuse SMR and PNR maps at the AF Bragg peak as $\xi = 1/\Delta q_x$. Native domains differing from each other in the sense of rotation of the magnetization of layers of the same (i.e. odd or even) parity were formed when the decreasing magnetic field leaved the saturation region. The native domain size proved to be $\xi = 370$ nm and did not change down to 200 mT. The domain size increased spontaneously and irreversibly to $\xi = 800$ nm between 200 and 100 mT and did not change further down to remanence. We ascribe this *domain ripening* to the excess domain-wall energy limited by coercivity. The BSF transition induced a further, explosion-like increase of the domain size up to ca. 100 μm (*domain coarsening*) [3].

We describe domain ripening in terms of a *Monte Carlo simulation* based on a *cellular automaton* algorithm. Lattice points of the cellular automaton consist of about 10^8 strongly cou-

pled spins of the ML stack; the whole simulation includes about 10^4 lattice points. The cellular automaton rule is to minimize the total energy of the lattice in monotonically changing external magnetic field. The Hamiltonian contains a nearest-neighbor domain-wall energy term as well as a dissipative penalty term, the latter describing the hysteresis loss that belongs to the change of sense of rotation of the layer magnetizations of a lattice point. Further terms of the Hamiltonian, i.e., the Zeeman energy and the bilinear layer-layer interaction of random lateral distribution are replaced by a logical condition since these terms are independent of the sense of rotation. The model fairly well reproduces all details of domain ripening only by adjusting the ratio of the domain-wall coupling constant to the coercive field of the ferromagnetic layers.

- [1] H.T. Hardner, M.B. Weissmann, S.S.P. Parkin, *Appl. Phys. Lett.*, **67** (1995) 1938.
- [2] L. Bottyan et al., *J. Magn. Magn. Mat.*, **240** (2002) 514.
- [3] D.L. Nagy et al., *Phys. Rev. Lett.*, **88** (2002) 157202.

21TL-B-7

POWER-LAW SCALING BEHAVIOR OF BARKHAUSEN AVALANCHES IN 2D FERROMAGNETS

Shin S.-C.¹, Ryu K.-S.¹, Kim D.-H.², Im M.-Y.^{1,3}, Lee S.-H.¹, and Akinaga H.⁴

¹Department of Physics and Center for Nanospinics of Spintronic Materials, KAIST,
Daejeon 305-701, Korea

²Department of Physics, Chungbuk National University, Chungbuk, Korea

³Center for X-ray Optics, Lawrence Berkeley National Laboratory, Berkeley, CA94720, USA

⁴Nanotechnology Research Institute, NAIST, Tsukuba, Ibaraki 305-8562, Japan

The magnetization under an applied field around the coercivity reverses with a sequence of discrete and jerky jumps, known as the Barkhausen effect. Recently, interest in the Barkhausen effect has grown as it is a good example exhibiting dynamical critical scaling behavior, evidenced by experimental observation of a power-law distribution of the Barkhausen jump size. So far, most studies have been carried out on 3D bulk samples by a classical inductive technique and very few experiments have been done on 2D systems mainly due to the low signal intensity of the inductive method. In this talk, we will present critical scaling behavior of Barkhausen avalanches of various 2D ferromagnetic thin films investigated via time-resolved magneto-optical microscopy, enabling to directly image Barkhausen avalanches at criticality [1]. A statistical analysis of the fluctuating size of Barkhausen jumps from numerous repetitive experiments shows a power-law scaling behavior in the 2D ferromagnetic systems. In 2D Co films, the critical exponent is found to be ~ 1.33 independent of a film thickness from 5-50 nm. Strikingly, the power-law distribution in 2D MnAs films is found that the critical exponent varies continuously from 1.32 to 1.04 as the temperature increases [2]. This is the first time to observe that the scaling behavior of the Barkhausen criticality of a given ferromagnetic film is experimentally tuneable by varying the temperature (not dimensionality). We also report a universal scaling behavior of the first arrival time of a traveling magnetic domain wall into a finite space-time observation window, which can be explained by the random-walking model [3].

- [1] S-C Shin, et al. *J. Appl. Phys.*(invited) **103**, 07D907 (2008).
- [2] K-S Ryu, et al. *Nature Physics* **3**, 547 (2007).
- [3] M.-Y. Im, et al. *Phys. Rev. Lett.*, in press (2008).

21RP-B-8

SQUID SENSOR APPLICATION FOR SMALL METALLIC PARTICLE DETECTION

Tanaka S.¹, Hatsukade Y.¹, and Ohtani T.², Suzuki Sh.²

¹Toyohashi University of Technology, 1-1 Tempaku-cho Toyohashi Aichi, 441-8580, Japan

²Advance Food Tech Co., Ltd., Toyohashi, Aichi 441-8113, Japan

High-Tc superconducting quantum interference device (SQUID) system for detection of magnetic foreign matters in industrial products was developed. There is a possibility that ultra-small metallic foreign matters have been accidentally mixed with industrial products such as lithium ion batteries. If it happens, the manufacture of the product suffers a large amount of loss to recall for the products. Outer dimension of metallic particles less than 100 micron can not be detected by an X-ray imaging, which is commonly used as the inspection. Therefore a high sensitive detection system for small foreign matters is required. We developed a detection system based on high-Tc SQUID microscope with a high performance magnetic shield. Two sets of a SQUID microscope with a 0.5 mm-thick vacuum window which separates the SQUID and atmosphere were employed. This design enables the SQUID to approach an object to be measured as close as 1 mm. Since intensity of magnetic field from the object is inversely proportional to cube of the distance, making the object closer to the SQUID is very important to enhance the signal. The minimal detectable size of the foreign matter is also highly dependent on the shielding factor of a magnetic shield. Therefore, we carefully designed a double-layered cylindrical magnetic shield with a new technology. We adopted a magnetic shield with ducts, which shielding factor SF was 1/3850 in z-component. This value is extremely high as compared with the SF we obtained before. As a result, we could successfully measure small iron particles less than 100 micron as shown in Fig.1. This detection level was hard to be achieved by a conventional X-ray detection method.

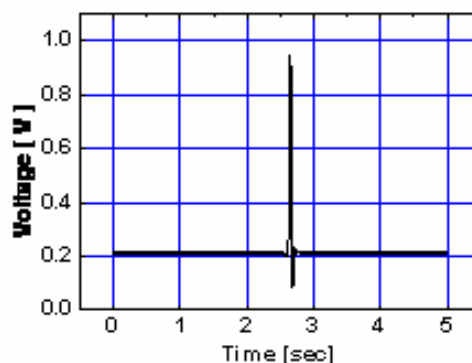


Fig.1 Time trace of the SQUID output signal for the test objects.

[1] S. Tanaka, M. Natsume, T. Matsuda, Z. Aspanut and M. Uchida: Supercond. Science and Technol. 17, pp. 620-623 (2004).

[2] M. Bick, K. Leslie, R. Binks, D. Tilbrook, S. Lam, R. Gnanarajan, Supercond. Sci. Technol. Vol. 18, pp.346-351 (2005).

[3] G.B. Donaldson, A. Cochran and D. McKirdy, "Fundamentals and Applications" ed. Weinstock H, Kluwer Academic Publishers, pp. 599 (1996).

[4] H.J. Krause, G.I. Panaitov, N. Wolter, D. Lomparski, W. Zander, Y. Zhang, E. Oberdoerffer, D. Wollersheim and W. Wilke: IEEE Trans. Appl. Supercond. Vol. 15, pp. 729-732 (2005).

[5] S. Tanaka, H. Fujita, Y. Hatsukade, T. Nagaishi, K. Nishi, H. Ota, T. Otani and S. Suzuki, "A food contaminant detection system based on high-Tc SQUIDS", Supercond. Sci. Technol. Vol. 19, pp. S280-S283 (2006).

21RP-B-9

MAGNETIC AND ELECTRICAL PROPERTIES OF MAGNETIC NANO-DEVICES FABRICATED BY ATOMIC FORCE MICROSCOPE

Takemura Y.¹, Shirakashi J.²

¹Yokohama National University, Yokohama 240-8501, Japan

²Tokyo University of Agriculture and Technology, Tokyo 184-8588, Japan

Lithography techniques using scanning probe microscopes (SPM) have attracted much interest as novel tools for fabricating electron devices with well-defined nanostructures. It has been reported that surfaces of metal and semiconductor thin films are selectively oxidized by applying a bias on the SPM tip. As this anodic oxidation process does not require any pretreatments such as resist coating, it is a useful tool for fabricating nanostructure materials devices. We have demonstrated fabrications of magnetic nanostructures using this technique [1]. In this paper, magnetic and electrical properties of magnetic nanostructures and magnetic nano-devices fabricated by atomic force microscope (AFM) local oxidation are discussed.

As nanostructures of oxide fabricated by the AFM local oxidation exhibited insulating properties, planar-type ferromagnetic tunnel junctions were fabricated using this technique. We have observed diode characteristics in current-voltage measurements from the fabricated Ni- and Co-based tunnel junctions. The single electron conduction due to the charging effect of the Coulomb blockade was also obtained in nano-scale Ni-based double tunnel junction [2].

The surface of the planar-type junction suffers exposure to air and humidity, which degrades stability of the device performance. In order to protect the surface, we have developed the AFM local oxidation process for metal thin films covered with insulating cap layers [3]. The AFM local oxidation of Al-oxide/NiFe thin films and fabrication of the planar-type NiFe/NiFe-oxide/NiFe tunnel junction covered with the Al-oxide layer were studied. After patterning the NiFe film to a stripe shape by photolithography and dry etching processes, the film was covered by an Al-oxide layer. This insulating layer of Al-oxide was obtained by oxidation of the deposited Al thin layer in air. The fabricated tunnel junction exhibited a rectifying characteristic in the current-voltage measurement. It was indicated that the NiFe was oxidized through the capped Al-oxide layer by the AFM local oxidation. The equivalent values for barrier height of 1.75 eV and the barrier width of 1.5 nm were determined by fitting with the calculation using the Simmons formula.

Surfaces of patterned NiFe strip-shaped thin films of 15-30 nm thickness were modified by nano-wires of NiFe oxide fabricated by the local oxidation. The anisotropy magnetoresistance was measured in order to study the effect of the nano-wires in magnetization reversal process. The domain wall was pinned at the nano-wires of NiFe oxide. It was indicated that the propagation of domain wall could be controlled by the AFM nano-lithography. Direct modification of magnetic domain wall structures [4] and magnetization reversal of magnetic nanostructures fabricated by the AFM lithography are also discussed.

[1] Y. Takemura and J. Shirakashi, *Jpn. J. Appl. Phys.*, 39, 1292 (2000).

[2] J. Shirakashi and Y. Takemura, *IEEE Trans. Magn.* 40, 2640 (2004).

[3] Y. Takemura, Y. Shimada, G. Watanabe, T. Yamada, J. Shirakashi, *J. Phys.* 61, 1147 (2007).

[4] Y. Takemura, S. Hayashi, N. Okazaki, T. Yamada and J. Shirakashi, *Jpn. J. Appl. Phys.* 44 L285 (2005).

21 June Saturday

12:15-13:45

15:00-17:00

oral session

21TL-C

**“Spintronics and
Magnetotransport”**

21TL-C-1

MAGNETO-OPTICAL STUDY OF FERROMAGNETIC SEMICONDUCTORS

Ando K., Saito H., Zayets V., and Debnath M.C.

National Institute of Advanced Industrial Science and Technology (AIST),
Nanoelectronics Research Institute,
Tsukuba Central 2, Umezono 1-1-1, Tsukuba, Ibaraki 305-8568, Japan

Ferromagnetic semiconductors are now attracting much attention because they are expected to play key roles in a variety of future spintronics devices. The essentially important character of the ferromagnetic semiconductors is the mutual interaction between magnetic properties (supported by the d electrons of the magnetic ions) and the semiconductor properties (supported by the s and p electrons) [1,2]. With this s , p - d exchange interaction, one can combine magnetic and electrical properties without using the classical electromagnetic coil. If magnetic properties and semiconductor properties existed independently of each other, ferromagnetic semiconductors would have no value for device applications. Therefore, investigation of a spin-polarized band structure (Zeeman splitting) should be the starting point of the ferromagnetic semiconductor research.

The Zeeman splitting of a semiconductor band can be easily detected as a magnetic circular dichroism (MCD) because the quantum mechanical selection rules for optical absorption by the spin-polarized band inevitably induces the different optical absorption for clockwise-polarized and counterclockwise-polarized light [1-3].

In this talk, we will discuss the electronic structures of a variety of ferromagnetic semiconductors probed by the MCD spectroscopy [1, 4-9].

Support by Grant-in-Aid for Scientific Research (B) (20360013) is acknowledged.

- [1] K. Ando, *Science* 312, 1883 (2006).
- [2] K. Ando, in *Magneto-Optics*, edited by S. Sugano and N. Kojima, Springer Series in Solid-State Sciences Vol. 128 (Springer-Verlag, Berlin, 2000), p. 211.
- [3] K. Ando, H. Saito, M. C. Debnath, V. Zayets, and A. K. Bhattacharjee, *Phys. Rev. B* 77, 125123 (2008).
- [4] K. Ando and H. Munekata, *J. Magn. Magn. Mater.* 272–276, 2004 (2004).
- [5] K. Ando, T. Hayashi, M. Tanaka, and A. Twardowski, *J. Appl. Phys.* 83, 6548 (1998).
- [6] K. Ando, H. Saito, K. C. Agarwal, M. C. Debnath, and V. Zayets, *Phys. Rev. Lett.*, 100, 067204 (2008).
- [7] H. Saito, V. Zayets, S. Yamagata, and K. Ando, *Phys. Rev. Lett.* 90, 207202 (2003).
- [8] K. Ando, *Appl. Phys. Lett.* 82, 100 (2003).
- [9] K. Ando, H. Saito, V. Zayets, and M. C. Debnath, *J. Phys. Condens. Matter* 16, S5541 (2004).

21TL-C-2

DENSITY FUNCTIONAL THEORY FOR SPIN-TRANSPORT

Sanvito S.

School of Physics and CRANN, Trinity College, Dublin 2, Ireland

Density functional theory has revolutionized our way to do materials science and it is now a fundamental asset for research in Physics, Chemistry, Biology and Nanoscience. This is mainly due to a combination of conceptual simplicity, rigorous theoretical foundation and efficient numerical algorithms. The *Smeagol* [1,2] project (www.smeagol.tcd.ie) has the ambitious goal of setting the same revolution in the field of *ab initio* quantum transport. *Smeagol* combines density functional theory with the non-equilibrium Green's function method for quantum transport and it has been specifically designed for dealing with spin-transport properties.

In this talk I will present our recent results for the bias-dependent transport of various spin-devices. I will first start from Fe/MgO (001) tunnel junctions and demonstrate how the magnetoresistance depends on the presence of resonant tunneling through surface states, how it is affected by bias and how it is reduced by FeO allowing at the interfaces. I will then move to discuss spin-effects in organic materials, and demonstrate that molecules offer the unique possibility to engineer the magneto-transport response of spin-valves. Finally I will present some very recent results on electron transport across Mn_{12} magnetic molecules and demonstrate that the magnetic state of the molecule can be inferred by a detailed analysis of the *I-V* characteristics.

This work is supported by Science Foundation of Ireland.

[1] *Towards Molecular Spintronics*, Alexandre Reily Rocha, Victor Garcia-Suarez, Steve W. Bailey, Colin J. Lambert, Jaime Ferrer and Stefano Sanvito, *Nature Materials* 4, 335 (2005).

[2] *Spin and Molecular Electronics in Atomically-Generated Orbital Landscapes*, Alexandre Reily Rocha, Victor Garcia-Suarez, Steve W. Bailey, Colin J. Lambert, Jaime Ferrer and Stefano Sanvito, *Phys. Rev. B.* 73, 085414 (2006).

21TL-C-3

SPIN HALL EFFECT IN METALS AND SUPERCONDUCTORS

Takahashi S.

Institute for Materials Research, Tohoku University, Sendai 980-8577, Japan

Spin Hall effect (SHE) is caused by spin-asymmetric scattering of conduction electrons in the presence of spin-orbit interaction in nonmagnetic conductors. Up-spin electrons are deflected preferentially in one direction, and down-spin electrons are in the opposite direction. As a consequence, charge current flowing in a nonmagnetic conductor generates spin current in the transverse direction (direct SHE) due to the spin-orbit scattering of conducting electrons by nonmagnetic impurities. Inversely, spin current flowing in a nonmagnetic conductor generates charge current in the transverse direction (inverse SHE). Thus, SHE enables us to convert the spin (charge) degrees of freedom to charge (spin) degrees of freedom.

Spin injection techniques makes it possible to observe the direct and inverse SHE using a nonlocal spin Hall device with a ferromagnetic metal (F) and a nonmagnetic metal (N). Recently, the direct and inverse SHE have been observed in nano-structured nonlocal devices of CoFe/Al [1], Py/Cu/Pt [2], and FePt/Au [3]. In this article, a theoretical description of SHE based on a diffusive transport in a nonlocal spin-injection device is presented [4], and discuss SHE in terms of side jump and skew scattering mechanisms. We show that the theoretically expected values of the nonlocal spin Hall signal are consistent with recent experiments, and obtain information about the spin-orbit coupling in N. We extend the result to a nonlocal spin Hall device with a superconductor (S), and examine SHE induced by quasiparticle spin current in S. It is found that the calculated spin Hall signal is greatly enhanced by the opening of the superconducting gap in the superconducting state.

[1] S.O. Valenzuela, M. Tinkham, *Nature* **442** (2006) 176.

[2] T. Kimura, Y. Otani, T. Sato, S. Takahashi, S. Maekawa, *Phys. Rev. Lett.* **98** (2007) 156601.

[3] T. Seki, Y. Hasegawa, S. Mitani, S. Takahashi, H. Imamura, S. Maekawa, J. Nitta, K. Takasani, *Nature Materials* **7** (2008) 125.

[4] S. Takahashi, S. Maekawa, *Phys. Rev. Lett.* **88** (2002) 116601; *Physica C* **437-438** (2006) 309; *Sci. Technol. Adv. Mater.* **9** (2008) 014105.

21TL-C-4

ANOMALOUS HALL EFFECT IN ULTRA-THIN IRON FILMS

Jin X.

Department of Physics, Fudan University, Shanghai 200433, China

The anomalous Hall effect is investigated in ultra-thin films of iron. Through the manipulation of thickness and temperature, we have proved experimentally that the extrinsic skew scattering effect does not change with temperature-induced resistivity. An intrinsic contribution to anomalous Hall effect is found to be dominant for films above 4 nm. The intrinsic contribution decreases below 4 nm with decreasing thickness and reverses its sign around 1.4 nm, while the extrinsic part increases monotonically. The reduction and sign reversal in ultra-thin range provide a new challenge for various theories.

21TL-C-5

GIANT SPIN HALL EFFECT IN PERPENDICULARLY SPIN-POLARIZED FePt/Au SYSTEMS

Takanashi K.¹, Seki T.¹, Hasegawa Y.¹, Mitani S.¹, Takahashi S.^{1,4}, Imamura H.^{2,4},
Maekawa S.^{1,4} and Nitta J.³

¹Institute for Materials Research, Tohoku University, 980-8577 Japan

²National Institute of Advanced Industrial Science and Technology, Tsukuba 305-8568, Japan

³Graduate School of Engineering, Tohoku University, Sendai 980-8579, Japan

⁴CREST, Japan Science and Technology Agency, Tokyo 102-0075, Japan

The generation and detection of spin current are important issues for the further development of spintronics. Spin Hall effect (SHE) makes the conversion between charge current and pure spin current in nonmagnetic semiconductors or metals, which enables us to generate or detect spin current without ferromagnetic materials. Thus, it is expected that SHE provides a new functionality of materials for spintronic devices. The theoretical predictions of SHE have stimulated scientific interests, and the optical detection of SHE was demonstrated in nonmagnetic semiconductors. Recently the electrical detection of SHE was also reported in nonmagnetic metals such as Al[1] and Pt[2,3]. However, complicated device structures or sophisticated measurement techniques were required to detect SHE, and the small magnitudes of SHE signals limit the possibility of device applications.

In this paper, we present the electrical detection of giant SHE at room temperature in perpendicularly spin-polarized FePt/Au systems[4]. We fabricated a multi-terminal device with a nano-sized Au Hall cross and a FePt perpendicular spin injector through the use of electron beam lithography and Ar ion etching. Perpendicularly magnetized FePt generates or detects the perpendicularly polarized spin current without external magnetic field, which allows us to simplify the device structure.

A non-local spin injection technique has been employed to detect the direct and inverse SHE signals. In the case of inverse SHE, the spin polarized electric current is injected from FePt to Au; the spin current flows in Au due to the spin accumulation, and the non-local Hall voltage induced by SHE is detected by the Au Hall cross. For the direct SHE, on the other hand, the electric current flows in the Au cross; the spin current is generated by SHE, and the generated spin current is detected by the FePt spin injector. An important point is that the SHE is detected even at zero applied field owing to the perpendicular magnetization of FePt.

Non-local Hall voltages were successfully observed in both direct and inverse SHE geometries, and show clear hysteresis loops resulting from the magnetization reversal of FePt. The magnitudes of SHE signals at room temperature are significantly larger than those in previous reports[1-3]. The spin Hall angle α_H , which is the ratio of the spin Hall conductivity to the electric conductivity, has been evaluated to be 0.113. This large α_H in Au is explained from the mechanism of skew scattering. α_H shows the weak temperature dependence, which is consistent with the dominant contribution of skew scattering in the present Au. We believe that the giant SHE opens a way of new techniques for spintronic devices.

This work was partially supported by Industrial Technology Research Grant Program in 2005 from NEDO.

[1] S. Valenzuela and M. Tinkham, *Nature* **442**, 176 (2006).

[2] E. Saito *et al.*, *Appl. Phys. Lett.* **88**, 182509 (2006).

[3] T. Kimura *et al.*, *Phys. Rev. Lett.* **98**, 156601 (2007).

[4] T. Seki *et al.*, *Nature Materials* **7**, 125 (2008)

21TL-C-6

MICROWAVE EMISSION AT ZERO FIELD AND PHASE LOCKING EXPERIMENTS IN SPIN TRANSFER NANO-OSCILLATORS

Cros V.¹, Georges B.¹, Boulle O.¹, Grollier J.¹, Darques M.¹, Marcilhac B.¹, Deranlot C.¹,
Faini G.², Barnaś J.³, Fert A.¹

¹Unité Mixte de Physique CNRS/Thales and Université Paris Sud 11, RD 128,
91767 Palaiseau, France

²Phynano team, Laboratoire de Photonique et de Nanostructures LPN-CNRS, route de Nozay,
91460 Marcoussis, France

³Department of Physics, Adam Mickiewicz University, Umultowska 85, 61-614 Poznań, Poland

The Spin Transfer Nano Oscillators (STNOs) are non-linear oscillators [1,2] that will certainly have important applications in the technology of telecommunications for the generation of oscillations in the microwave frequency range. They have interesting advantages, in particular the easy and fast control (agility) of the frequency by tuning a DC current and also in terms of integration. Up to recently, they had the disadvantage of needing an applied field but we have recently conceived and operated a special type of STO working at zero field [3]. An other key problem is that the microwave power of the STOs is still too small (typically less than 1 nW) for applications. Synchronizing an array of STOs to increase this power is now the crucial challenge before developing practical devices. should result in an increase the output power and a decrease the linewidth of the emitted signals [4,5,6]. We have recently proposed a scheme for synchronization of several STOs by connecting them in series or parallel [6]. Furthermore, in order to investigate the prerequisites to lock-in of large networks of STOs, we have studied the phase locking of a single STO with an external microwave source in various conditions of applied field and dc current. From the analysis, we can correlate the locking efficiency with the intrinsic characteristics of the STO : linewidth, emitted power, agility of the free-running oscillations. The collected informations allow us to propose some optimized conditions needed for successful synchronization through the stimulated microwave current of a large amount of STOs [7].

This work was partly supported by the French National Agency of Research ANR through the PNANO program (NANOMASER PNANO-06-067-04) and the EU network SPINSWITCH (MRTN-CT-2006-035327)

[1] W.H. Rippard *et al* Phys. Rev. B 70, 100406(R) (2004)

[2] S.I. Kiselev *et al.*, Phys. Rev. B 72, 064430 (2005)

[3] O. Boulle *et al*, Nature Physics, 3, 492 (2007)

[4] W.H. Rippard *et al*, Phys Rev. Lett. 95, 067203 (2005)

[5] S. Kaka *et al.*, Nature 437, 389 (2005); F.B. Mancoff *et al*, Nature 437, 393 (2005)

[6] J. Grollier, V. Cros, A. Fert, Phys. Rev. B 73, 060409 R (2006)

[7] B. Georges *et al*, cond-mat/0802.4162

21TL-C-7

SPIN AND FUNCTIONAL-OXIDE ELECTRONICS AS BEYOND CMOS CANDIDATES

Akinaga H.^{1,2}, Takano F.¹, Shima H.^{1,2}, Suemasu T.³

¹Nanotechnology Research Institute (NRI), National Institute of Advanced Industrial Science and Technology (AIST), Tsukuba, Ibaraki 305-8568, Japan

²JST, CREST, Tsukuba, Ibaraki 305-8568, Japan

³Graduate School of Pure and Applied Sciences, University of Tsukuba, Tsukuba, Ibaraki 305-8573, Japan

To promote uniting of spintronic materials and functional oxides in the silicon technology, we are now focusing on (1) the development of silicon-based ferromagnets, (2) the fabrication of ferromagnetic-metal / silicon heterostructures, and (3) the development of functional-oxides / silicon heterostructures. We will show the recent achievements in the symposium.

(1) Synthesis of a silicon carbide (SiC)-based ferromagnet:

The synthesis of the SiC-based ferromagnetic semiconductor has been attempted using the thermal diffusion and the ion implantation methods. In this study, 4H (hexagonal) and 3C (cubic) poly-types of homo-epitaxial SiC wafers have been employed as hosts. We have made use of manganese (Mn) as a magnetic element incorporated into the SiC host. A good possibility that these systems show the ferromagnetic behavior was theoretically predicted in a previous report.

For the 4H-SiC host, we obtained the result that the majority of Mn atoms were incorporated into the interstitial site in the host lattice and no ferromagnetic behavior was detected [1]. When employing the 3C poly-type, on the other hand, the possibility that a Si atom in the 3C-SiC lattice was substituted with Mn atom was experimentally confirmed.

(2) Fabrication of Fe₃Si/CaF₂/Fe₃Si heterostructure:

We succeeded in the optimization of the growth condition to obtain a very flat Fe₃Si surface by employing the low temperature MBE growth followed by the post-anneal process at 250 °C, though the ruggedness of the Fe₃Si surface was not able to be suppressed before this research project was started. At the same time, this result enabled us to fabricate the magnetic tunnel junction (MTJ) having an epitaxial heterostructure of Fe₃Si/CaF₂/Fe₃Si on Si [2]. Actually, step-like behavior in the magnetization curve (vs. magnetic field) reflecting the formation of an effective MTJ structure was observed. Recently, we also developed a selective dry etching process for Fe₃Si / CaF₂.

(3) Nonvolatile change of Schottky barrier between Pt and TiO_x

The Pt/ TiO_x / Pt trilayer with electrically asymmetrical interface have been synthesized by means of the reactive sputtering technique followed by the oxygen annealing. The initial current-voltage characteristics in the Pt/ TiO_x / Pt trilayer cell have rectifying behavior originated from the Schottky junction formed between TiO_x and the Pt top electrode layer [3]. In the symposium, we will demonstrate the non-volatile change of rectifying current-voltage curvature, operated by an electric pulse.

The works of (1) and (2) were supported partly by a Grant-in-Aid for Scientific Research in Priority Area, Creation and Control of Spin Current, MEXT, Japan.

[1] W. H. Wang, F. Takano, H. Ofuchi, and H. Akinaga, *Phys. Rev. B* **75**, 165323 (2007).

[2] T. Harianto, K. Kobayashi, T. Suemasu, and H. Akinaga, *Jpn. J. Appl. Phys.* **46**, L904 (2007).

[3] H. Shima, F. Takano, H. Muramatsu, H. Akinaga, I.H. Inoue, and H. Takagi, *Appl. Phys. Lett.* **92**, 043510 (2008).

21 June Saturday

12:15-13:45

oral session

21TL-D

**“X-ray MCD and
Auger Spectroscopy”**

21TL-D-1

ATOMIC MAGNETISM AT SURFACES*Carbone C.*Istituto di Struttura della Materia, Consiglio Nazionale delle Ricerche
Trieste, Italy

Advanced synchrotron radiation techniques are able to provide high sensitivity to the study of very diluted magnetic systems, unveiling thus novel properties hardly accessible by other experimental techniques. X-ray circular dichroism, in particular, has been successfully used to track the evolution of the magnetic properties in nanostructures constructed at surfaces, from finite-sized particles to isolated adatoms. This presentation will illustrate how x-ray circular magnetic dichroism carried out in high magnetic fields and cryogenic conditions can be employed to simultaneously measure the valence state and magnetic moment of individual atoms on surfaces. The results show how Hund rule magnetic moments of a free atom change upon adsorption on a surface, the appearance of magnetic anisotropy, the dependence of the magnetic and electronic configuration on the substrate interaction and the atomic coordination.

21TL-D-2

**HARD X-RAY MAGNETIC CIRCULAR DICHROISM:
APPLICATION TO SPINTRONICS MATERIALS***Rogalev A., Wilhelm F., Smekhova A., Goulon J.*European Synchrotron Radiation Facility (E.S.R.F.) 6, rue Jules Horowitz 38000,
Grenoble, France

Recent developments in the synchrotron radiation instrumentation have made possible the production of high flux of hard X-ray photons (2 - 15 keV) with flexible polarization [1]. Magnetic circular dichroism (MCD), the difference in the absorption or reflection of magnetic samples using left- and right-handed circularly polarized light has been widely exploited in the visible and soft X-ray spectral regions to provide useful information on the electronic and magnetic properties of magnetically ordered systems [2].

This talk reviews the recent advances in magnetic circular dichroism experiments in the hard X-ray energy range which covers K-edges of transition metals, L-edges of rare-earths, L-edges of 4d and 5d metals and M-edges of actinides. After giving a short introduction to the principles of X-ray MCD spectroscopy, we shall focus on the experimental aspects and the main strengths of this technique. These are quantitative determination of the element and orbital selective magnetic moments and their anisotropies using magneto-optical sum rules [3]. Hard X-ray MCD measurements, that have been performed at the ESRF beamline ID12 on a wide variety of magnetic systems promising for spintronics applications, have contributed to a deeper understanding of the microscopic origin of magnetism in these materials. This includes the study of the layer-by-layer magnetic structure in ferromagnets and antiferromagnets, induced magnetism at interfaces, local magnetic moments and their interactions in ferromagnetic semiconductors and half-metallic double perovskites. Finally, determination of the origin of magnetism in diluted magnetic semiconductors is shown as an example of great potentialities of hard X-ray MCD.

- [1] J. Goulon et al, *J. Synch. Rad.*, 5 (1998) 232.
[2] *Magnetism and Synchrotron Radiation*, eds. by E. Beaurepaire, F.Scheurer, G. Krill and J.-P. Kappler, Springer-Verlag, Berlin, 2001.
[3] P. Carra *et al*, *Phys. Rev. Lett.*, **70** (1993) 694.

21TL-D-3

SPIN POLARIZED AUGER ELECTRON SPECTROSCOPY

Petrov V.N.

St. Petersburg State Polytechnical University, 29 Polytechnicheskaya st.,
195251 St. Petersburg, Russia

One of the most powerful methods for the analysis of local surface magnetic properties is spin polarized Auger electron spectroscopy (SPAES). In term of analyzing power this method is approaching the technique of x-ray magnetic circular dichroism. However, it does not require the application of synchrotron radiation and can be performed under laboratory conditions. SPAES is not widely used since the suitable energy analyzers and electron polarization detectors were not available.

First, the physical idea of spin polarized Auger electron spectroscopy is discussed. Then the, relevant parameters for SPAES are discussed. In the third part of the talk the design and performance of the high transmission cylindrical mirror analyzer [1] coupled to a high efficient compact classical spin detector (Mott detector) [2] are considered. In the fourth part the performance of the system is discussed with measurements on FeNi₃, Fe₃O₄, FeNi₃-V and Fe₃O₄-Bi.

[1] V.N. Petrov, A.S. Kamochkin, *Rev. Sci. Instrum.*, **75(5)** (2004) 1274

[2] V.N. Petrov, V.V. Grebenshikov, A.N. Andronov, P.G. Gabdullin, A.V. Maslevtcov, *Rev. Sci. Instrum.*, **78(2)** (2007) 025102

21 June Saturday

15:00-17:00

oral session

21TL-D

21RP-D

“Multiferroics”

21TL-D-4

MULTIFUNCTIONAL MATERIALS

Grössinger R., Sato Turtelli R., Mehmood N.

Inst. Of Solid State Physics, Techn. Univ. Vienna; Wiedner Hauptstr. 8-10; A-1040 Austria

Multifunctional materials are sensitive to different environmental properties (such as temperature, magnetic field, electric field etc.) which can be used for technical applications. This sensitivity can be achieved in single phase but more often in multiphase materials. Modern material science tries to use new ways of sample production to optimize such materials. Here especially wet chemical methods are often favourable. Within the here presented work examples of multifunctional materials which can be used in industry are given. Especially in composites the microstructure (grain size, interfacing) plays a very important role. The properties of magnetic materials are very sensitive to the grain size. In the last years it was shown that the magnetic properties (such as magnetization, losses, stored energy etc.) of soft magnetic as well as hard magnetic nanocrystalline materials were improved remarkable (see e.g. 1,2,3). Two steps were important for the improvement: i) reduction of the grain size to nanometers and ii) addition of a second phase with favourable properties. This leads to a remanence enhancement for hard magnetic materials but also to a remarkable improvement of soft magnetic properties (such as permeability etc.).

Also in materials with high magnetostriction these steps can improve the behaviour. Producing these materials in a multiphase nanocrystalline state causes a drastic reduction of the anisotropy, however a high magnetostriction still remains. Interesting candidates are here RFe_2 compounds ($R = Tb, Sm$).

The combination of magnetic and piezo-electric properties in one material leads to so-called magnetoelectric systems. These materials exhibit an electric charge applying a magnetic field or a magnetic moment applying an electric field. There exist only few single phase materials, which are called multiferroic, which exhibit such a behaviour, however generally only at low temperatures. The conditions as well as the state of art of suitable multiferroic composites will be shown. Also here a nanocrystalline state is favourable for achieving a high magneto-electric coefficient. The application of magneto-electric composites which exhibit such a behaviour at room temperature may be in new sensors.

Beside this exist also other families of multifunctional materials which should be mentioned. These are magnetocaloric materials which can be used in refrigerator systems. These are in competition with thermoelectric systems which may also be used to cool devices. Both material families were not used for large scale applications because of material problems – as will be discussed.

21TL-D-5

NATURE OF UNUSUAL SPONTANEOUS AND FIELD INDUCED PHASE TRANSITIONS IN MULTIFEROICS RMn_2O_5

Pyatakov A.P.^{1,2}, Kadomtseva A.M.¹, Vorob'ev G.P.¹, Popov Yu.F.¹, Lukina M.M.¹, Zvezdin A.K.²

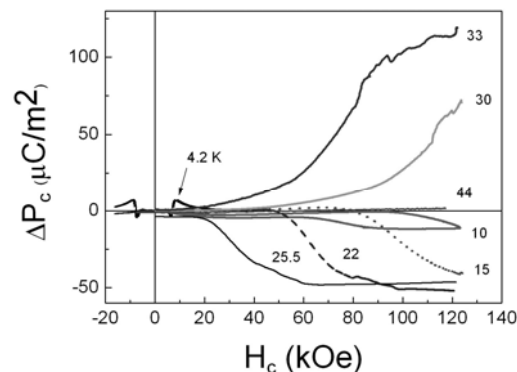
¹M.V. Lomonosov Moscow State University, Leninskie gory, MSU, Russia, 119992

²A.M. Prokhorov General Physics Institute, 38, Vavilova st., Russia, 119991

Orthorhombic manganites RMn_2O_5 being representative example of the so-called spiral multiferroics [1] demonstrates a plenty of various spontaneous phase transitions below the Neel temperature $T_N=44$ K. For example in TmMn_2O_5 , in accordance with neutron data [2], at 35K the incommensurate-commensurate (IC-C) phase transition takes place followed at further cooling by reverse phase transition into another incommensurate state at 25K (low temperature incommensurate phase) and finally the phase transition associated with rare-earth ordering occurs at $T < T_{N2}=4.8$ K.

Complex magnetic, magnetoelectric and magnetoelastic studies were done in high magnetic field up to 250kOe in the temperature range 4.2-100 K. In accordance with [3] from magnetization curve measurement it follows that rare earth is ordered along c-axis at $T < 4.8$ K. The longitudinal magnetoelastic (magnetoelastic) dependences along a and b axis demonstrated the jumps of polarization (magnetostriction) induced by the field ~ 150 kOe near phase transition temperatures 35K and 25K. These anomalies can be attributed to the influence of magnetic field on the conditions of IC-C phase transition at 35K and the reverse one at 25K. In b-axis dependences the magnetic field induced spin-reorientation phase transition was also observed below 20K. On the figure c-axis longitudinal dependence of magnetoelectric effect is shown. The anomalies at incommensurate-commensurate phase transitions at 35K and 25 K are clearly seen. The jumps of polarization are opposite in sign reflecting the opposite changes of wave number at these two phase transitions [2]. Below the temperature of rare earth subsystem ordering in accordance with [3] the magnetoelectric anomaly associated with metamagnetic transition is observed at relatively small critical fields of 5kOe. The magnetoelastic dependence along c-axis demonstrates good correlation with magnetoelastic one. The influence of magnetic field directed along c-axis on magnetic phase transitions evidences for small deflection of Mn^{3+} spins from ab-plane.

The variety of spontaneous and induced phase transitions in RMn_2O_5 stems from the interplay of three magnetic subsystems: Mn^{3+} , Mn^{4+} , R^{3+} . The comparison with YMn_2O_5 [4] highlights the role of rare earth in low temperature region (metamagnetic and spin reorientation phase transitions), while the phase transition at higher temperatures between incommensurate and commensurate phases should be ascribed to the different temperature dependences of Mn^{3+} and Mn^{4+} ions. The strong correlation of magnetoelastic and magnetoelectric properties observed in the whole class of RMn_2O_5 (the results of this work and [4]) highlights their multiferroic nature.



Support by RFBR #07-02-00580 and “Progetto Lagrange-Fondazione CRT” is acknowledged.

- [1] H. Kimura Y.Kamada, Y. Noda, K. Kaneko, N. Metoki, K. Kohn, JPSJ, **75** (2006) 113701
- [2] S. Kobayashi, H. Kimura, Y. Noda, K. Kohn, JPSJ, **74** (2005) 468
- [3] M. Uga, N. Iwata, K. Kohn, Ferroelectrics, **219** (1998) 55
- [4] A.M. Kadomtseva, et al, Low Temp. Phys., **32** (2006) 709

21TL-D-6

SPIN-DRIVEN FERROELECTRICITY IN THE MULTIFERROIC COMPOUNDS OF RMn_2O_5

Kimura H.¹, Noda Y.¹, Kohn K.²

¹Institute of Multidisciplinary Research for Advanced Materials, Tohoku University, Japan

²Department of Physics, Waseda University, Japan

Recent progress on the studies of macroscopic dielectric properties as well as microscopic magnetic properties for the multiferroic materials of RMn_2O_5 ($R = \text{rare earth, Bi, Y}$) is reviewed. A series of RMn_2O_5 is well known as showing multiferroic properties, where dielectric and magnetic orders coexist and their order parameters mutually couple. This material has attracted much attention for showing a colossal magnetoelectric effect, which is the induction of electric polarization by magnetic field, or inversely the induction of magnetization by electric field. Complex network composed by Mn^{3+} , Mn^{4+} , and R^{3+} spins in this material causes geometrical magnetic frustration. This magnetic frustration results in yielding multiple magnetic orders with a long wavelength such as incommensurate order. In this situation, an external perturbation such as magnetic field can easily induce various magnetic phase transitions because of the competition among multiple magnetic ground states within a small energy scale.

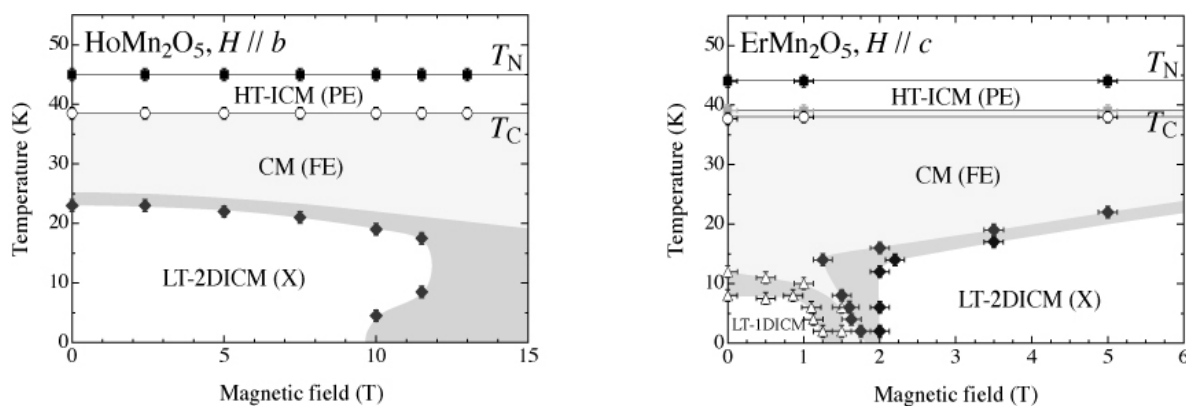
In the present study, we have conducted neutron diffraction studies of $HoMn_2O_5$ and $ErMn_2O_5$ under magnetic field to elucidate the field response of microscopic magnetism and their relevance with the field response of dielectric properties. Figure shows magnetic field (H) - temperature (T) magnetic phase diagrams for both the materials[1], where H - T dielectric phase diagram obtained by Higashiyama *et al.*[2] is also displayed. There exists one-to-one correspondence between the field response of magnetic property and that of dielectric property, which establishes that the ferroelectricity is magnetically induced. It is also interesting that the commensurate phase at zero field is robust against the applied magnetic field while the low-temperature incommensurate phase at zero field becomes sensitive as magnetic field is applied.

The microscopic origin of these field responses will be discussed on the basis of magnetic structure obtained by our single crystal structure analyses [3].

[1] H. Kimura *et al.*, *J. Phys. Soc. Jpn.*, **75** (2006) 113701., *J. Korean Phys. Soc.*, **51** (2007) 870.

[2] D. Higashiyama *et al.*, *Phys. Rev. B*, **72** (2005) 064421.

[3] H. Kimura *et al.*, *J. Phys. Soc. Jpn.*, **76** (2007) 074706.



Figure; Dielectric and magnetic phase diagrams as functions of temperature and magnetic field for $HoMn_2O_5$ and $ErMn_2O_5$. Data for dielectric phase was taken by Higashiyama *et al.*[2] Abbreviations; PE: paraelectric, FE: ferroelectric, X: unidentified phase, PM: paramagnetic, HT-ICM: high temperature incommensurate magnetic, CM: commensurate magnetic, LT-2DICM: 2-dimensionally modulated incommensurate magnetic, LT-1DICM: 1-dimensionally modulated incommensurate magnetic

21RP-D-7

ULTRALOW FREQUENCY MAGNETOELECTRIC INTERACTION IN FERROMAGNETIC-PIEZOELECTRIC LAYERED STRUCTURES

Fetisov Y.K. and Kamentsev K.E.

Moscow State Institute of Radio Engineering, Electronics and Automation
Pr. Vernadskogo 78, 119454 Moscow, Russia

There has been considerable interest in recent years on magnetoelectric (ME) interactions in composite structures consisting of ferromagnetic and piezoelectric layers [1]. When the structure is subjected to a slow varying magnetic field $H(t)$, strain due to magnetostriction results in an induced polarization $P(t)$ due to piezoelectric effect. The voltage $U(t)$ generated across the structure thickness is a function of H and frequency f of the field variation [2].

This work describes specific features of ultralow frequency ME interaction in different layered structures. The first structure consisted of 20 alternate layers of 18 μm thick NiZn ferrite and lead zirconium titanate (PZT) of dimensions $4 \times 4 \times 0.36 \text{ mm}^3$. It was fabricated using thick film ceramic method. The second one consisted of two 0.2 mm thick Ni and PZT layers with dimensions of $4 \times 5 \text{ mm}^2$ bonded to each other with epoxy glue. The third structure consisted of a 0.5 mm thick $\text{Ga}_{0.2}\text{Fe}_{0.8}$ magnetostrictive layer bonded with a 0.5 mm thick PZT layer. The field and frequency dependences of ME interaction efficiency have been measured in different regimes under H amplitudes up to 1 kOe and over the frequency range of $f = 10^{-3} - 10 \text{ Hz}$.

Figure 1 shows time profiles of the field $H(t)$ with $f = 0.03 \text{ Hz}$ applied to the Ni-PZT structure, the ME voltage $U(t)$ measured under open-circuit condition, and the ME current $I(t)$ measured under short-circuit condition. The dependences of the ME voltage and current as functions of the field variation frequency f at $H = 1 \text{ kOe}$ are shown in Fig.2. One can see a doubling in the frequency of generated voltage and current as well as a saw-like distortion in the time profile of the current. Amplitude of the voltage is nearly frequency independent, while the current is going down as the frequency decreases. Measured efficiency of the ME interaction reached values of $\sim 0.1 - 1 \text{ mV/Oe cm}$ for the structures investigated.

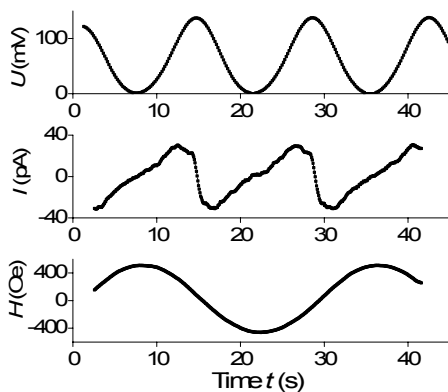


Fig.1. Time profiles of the applied field $H(t)$, generated voltage $U(t)$ and current $I(t)$.

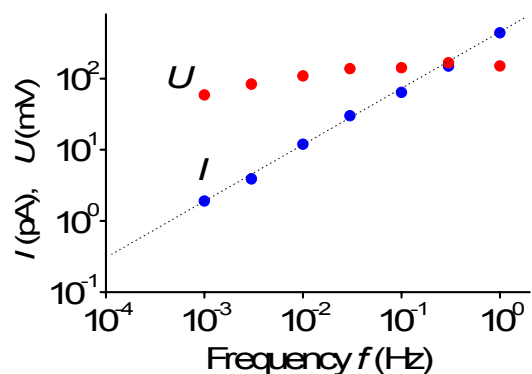


Fig.2. Amplitudes of the ME voltage U and current I as functions of the field frequency f for $H = 1 \text{ kOe}$.

The research was supported by grants from the Ministry of High Education and Science of Russia and the Russian Fund for Basic Research.

[1] M. Fiebig, J. Phys. D. 38 (2005) R1.

[2] K.E. Kamentsev, Y.K. Fetisov, and G. Srinivasan, APL, 89 (2006) 142510.

21RP-D-8

LOW FREQUENCY MAGNETOELECTRIC EFFECTS IN FERRITE-PIEZOELECTRIC NANOSTRUCTURES

Bichurin M.I.¹, Petrov V.M.¹, Srinivasan G.²

¹Novgorod State University, 41, B. St.-Petrburgskaya, Veliky Novgorod 173003, Russia

²Oakland University, Rochester MI, 48309, USA

A material is termed a magnetoelectric (ME) multiferroic if ferromagnetism and ferroelectricity occur simultaneously and allow coupling between the two. In general, known single-phase ME materials manifest weak ME coupling. Considerably stronger ME interactions, on the other hand, have been obtained in layered composites consisting of piezoelectric and magnetostrictive components. The ME effect in a composite is related to the interaction between the magnetostrictive and piezoelectric subsystems through the mechanical deformation [1].

Investigations on the ME effect in nanostructures in the shape of wires, pillars and films are important for increased functionality in miniature devices. This work is focused on modeling the ME effect in magnetostrictive-piezoelectric nanostructures. We have chosen nickel ferrite (NFO) - lead zirconate titanate (PZT) as the model system for numerical estimations. We consider nanostructures grown on MgO substrates or templates. MgO is experimentally attractive because of its good lattice match with the ferroelectric and ferromagnetic oxides. Additionally, vertical arrays of single-crystalline MgO nanowires can be readily grown using a simple vapor deposition technique, which can be used as a template to produce the nanowire ME structures.

For the estimation of ME voltage coefficient α_E it is assumed that the piezoelectric phase is electrically poled in a dc field E and that the composite is subjected to a bias field and an ac magnetic field, giving rise to a piezomagnetic deformation. We solve the electrostatic, magnetostatic and elastostatic equations taking into account constitutive equations, Hooke's law, lattice mismatch effect and boundary conditions. Variation in piezoelectric and piezomagnetic coefficients, permeability and permittivity of components due to lattice mismatch is taken into account by using the classical Landau-Ginsburg-Devonshire phenomenological thermodynamic theory. The ME voltage coefficient which is the ratio of ME susceptibility and permittivity of bilayer is calculated. The ME voltage coefficients α_E have been estimated for field orientations corresponding to minimum demagnetizing fields and maximum α_E . The effect of substrate or template clamping has been described in terms of dependence of α_E on substrate/template dimensions or volume fraction.

Calculations for bilayers show that the coupling strength decreases with increasing substrate clamping. For increasing volume of MgO substrate in a bilayer (i) the ME coefficient drops exponentially and (ii) the PZT volume required for maximum ME effects increases. For nanopillars of NFO in PZT matrix on MgO, the substrate pinning effects are negligible only when the length of the pillar is much greater than its radius. In the case of NFO-PZT nanowires grown on a MgO nanowire template, the ME coefficient is predicted to decrease from a maximum to approaching zero as the radius of the template layer is increased.

The model can be used to estimate the ME couplings from known material parameters (piezoelectric coefficients, magnetostriction, stiffness, etc.) or data on ME coupling can be used to extract composite parameters.

Support by RFBR (project 06-08-00896-a) is acknowledged.

[1] M. I. Bichurin, V. M. Petrov, and G. Srinivasan, Phys. Rev. B **68**, 054402 (2003).

21 June Saturday

12:15-13:45

15:00-17:00

oral session

21TL-E

“Theory”

21TL-E-1

CUBIC HELIMAGNETS IN MAGNETIC FIELD AND AT PRESSURE

Maleyev S.V.

Petersburg Nuclear Physics Institute, Gatchina, St. Petersburg 188300, Russia

Cubic helimagnets with non-centrosymmetric B20 structure (MnSi etc.) display unusual behavior under external actions such as magnetic field and pressure. In particular at very weak field the helix wave-vector \mathbf{k} rotates toward the field and then transition to the ferromagnetic state occurs. At pressure the quantum phase transition to the partly disordered state takes place. All these phenomena are discussed from single point of view. Following interactions are involved: ferromagnetic exchange, Dzyaloshinskii interaction responsible for the helix structure, anisotropic exchange and cubic anisotropy, magneto-elastic interaction (MEI) and Zeeman energy. Neglecting MEI in the linear spin-wave theory one obtains gapless spin-wave spectrum [1,2] and transition to ferromagnetic state at $H_c = Ak^2$ where A is the spin-wave stiffness at $q \gg k$ [1]. However in this approximation the spin-wave spectrum becomes unstable in infinitesimal field perpendicular to vector \mathbf{k} and assumed helical structure has to fail in contradiction with experiment. The magnon-magnon interaction leads to the spin-wave gap Δ which saves the structure and the ground state energy in magnetic field is given by

$$E = -\frac{SH_{\parallel}^2}{2H_c} - \frac{SH_{\perp}^2\Delta^2}{H_c(\Delta^2 - H_{\perp}^2/\sqrt{2})} + L(\mathbf{k}),$$

where H_{\parallel} and H_{\perp} are the field components along and perpendicular to \mathbf{k} and L is a cubic invariant which depends on \mathbf{k} direction relative the crystal axes. Behavior of MnSi and compounds $\text{Fe}_{1-x}\text{Co}_x\text{Si}$ in magnetic field was studied by small-angle polarized neutron scattering [3] and above equation was verified. In particular was found that for MnSi the gap $\Delta = 13\mu\text{eV}$.

The magneto-elastic interaction is responsible for i) negative contribution to the square of the spin-wave gap Δ , ii) $2\mathbf{k}$ modulation of the lattice, iii) change of the magnetic anisotropy. It is suggested that competition between positive contribution to Δ^2 which stems from magnon-magnon interaction and its negative magneto-elastic part leads to the quantum phase transition observed at high pressure in MnSi and FeGe. This transition has to occur when $\Delta^2 = 0$. For MnSi from rough estimations at ambient pressure we obtain that $\Delta_{ME} \sim \Delta/3$ where Δ is the experimentally observed gap. Observation of the lattice modulation allows determine the strength of anisotropic part of the magneto-elastic interaction responsible for this negative contribution to Δ^2 and the lattice chirality.

[1] S.V. Maleyev, *Phys. Rev. B* **73**, (2006) 174402.

[2] D. Belitz, T.R. Kirpatrick, A. Rosch, *Phys. Rev. B* **72**, (2006) 054401.

[3] S.V. Grigoriev et al., *Phys. Rev. B* **74**, (2006) 214414; *Phys. Rev. B* **76**, (2007) 224424.

21TL-E-2

MAGNETO-OPTICAL PHENOMENA IN SUPERCONDUCTORS WITH TIME REVERSAL BREAKING

Mineev V. P.

Commissariat a l'Energie Atomique, INAC/SPSMS, 38054 Grenoble, France

We derive the current response to the linearly polarized electromagnetic field with finite frequency and wave vector incident normally on the specular surface of a clean nonconventional superconductor. The result includes the usual part known from the theory of conventional superconductivity and as well the magneto-optical term typical for the superconductors with spontaneous time reversal breaking. As an application of the basic current-field relation we consider the Kerr effect for the rotation of polarization of infrared light reflected from the superconductor surface.

21TL-E-3

GENERALIZED ONSAGER CAVITY FIELD METHOD FOR MAGNETS WITH LOCAL SPIN FLUCTUATIONS

Wysocki A.L., Glasbrenner J.K., Belashchenko K.D.

Department of Physics and Astronomy and Nebraska Center for Materials and Nanoscience,
University of Nebraska-Lincoln, Lincoln, Nebraska 68588-0111, USA

Using an expansion around the atomic limit, we extend the Onsager cavity field method to magnets with local spin fluctuations. We find that *both* the interatomic exchange coupling and the on-site interaction are renormalized by magnetic short-range order. In the localized (Heisenberg) limit Onsager's approximation is recovered in the paramagnetic state, but in itinerant systems it is essential to include both corrections. This method is applied to a classical spin fluctuation model which interpolates between the limits of localized and itinerant magnetism and captures the qualitative features of itinerant thermodynamics. In this model both the orientation and the magnitude of the local magnetic moments fluctuate. The results are compared with Monte Carlo simulations. For close-packed lattices with nearest-neighbor exchange interaction the generalized Onsager method yields a very accurate Curie temperature for any degree of itinerancy. Interestingly, magnetic short-range order is found to be essentially independent on the degree of itinerancy (both in Monte Carlo and from the generalized Onsager method). A similar formulation of the method for correlated quantum systems with local spin or charge fluctuations is indicated within the dynamical mean-field theory, where magnetic short-range order *dynamically* renormalizes both the kinetic coupling to the lattice and the on-site interaction (*e.g.* Hubbard U). In general, the generalized Onsager method is applicable to any lattice model where local dynamical spin or charge fluctuations are important.

21TL-E-4

ELECTRON-PHONON INTERACTION AND SUPERCONDUCTIVITY IN CARBIDES AND NITRIDES UNDER HIGH PRESSURE

Maksimov E.G.¹, Wang S.Q.², Magnitskaya M.V.³, Karakozov A.E.³, Ebert S.V.¹

¹P.N. Lebedev Physical Institute, Leninskii prosp. 53, Moscow 119991, Russia

²SYNL, Institute of Metal Research, 72 Wenhua Rd., Shenyang 110016, P.R. China

³Institute for High Pressure Physics, Troitsk, Moscow Region 142190, Russia

We present density-functional linear-response calculations of the phonon spectra, the electron-phonon interaction (EPI) and related properties for several transition metal carbides and

nitrides in a NaCl-type structure at normal and high pressures. Calculated kinetic, optical, and superconducting properties (see [1]) are found to well agree with the experiment. Transition metal compounds with light elements have long been considered as candidates to superconductors with rather high critical temperature T_c . In fact, in most of the cubic compounds under consideration, observed T_c values are considerably lower than, say, in MgB_2 , where superconductivity is primarily due to the coupling between optical vibrations and the electrons localized at B sites. In this talk, factors accounting for relatively low T_c values in cubic monocarbides and mononitrides are analyzed.

We show that in most of the compounds under study the coupling of light-element electrons with high-energy optical phonons is rather weak because of a low partial C (or N) electron density of states at the Fermi level $N_{\text{C(N)}}(E_F)$, a typical example offered by cubic niobium carbide NbC. However, in compounds with high $N_{\text{C(N)}}(E_F)$, exemplified by hypothetical cubic yttrium carbide YC, the critical temperature is found rather low, too. Unlike the case of NbC, the coupling of carbon electrons with optical phonons in YC is weak because the electron states near E_F are almost pure unhybridized carbon p -states, which results in a small EPI matrix element. The hybridization of the C(N) p -states with either s -states or transition-metal d -states is most likely to occur in complex compounds rather than in monocarbides and mononitrides.

Pressure dependence of the phonon spectra, the EPI and T_c is studied in detail for cubic nitrides ZrN и HfN. Our calculated phonon densities of states are in reasonable qualitative agreement with Raman spectra measured at various pressures in the range up to 32 GPa [2]. The theoretical pressure derivative of critical temperature $\partial T_c / \partial p$ well agrees with available experimental data. An observed decrease in T_c with pressure is mainly due to an increase in phonon frequencies. At $p > 10$ GPa, the pressure dependence of T_c becomes non-linear, with decreasing $\partial T_c / \partial p$.

Support by Leading Scientific Schools Program, RAS, RFBR (grants nos. 06-02-16978, 07-02-00280, 08-02-00757), and RFBR–GFEN (grant no. 05-02-39012) is acknowledged.

[1] E.G. Maksimov, S.V. Ebert, M.V. Magnitskaya, A.E. Karakozov, *ZhETF*, **132** (2007) 731 [*JETP*, **105** (2007) 642].

[2] X.-J. Chen, V.V. Struzhkin, S.Kung, *et al.*, *Phys. Rev. B* **70** (2004) 014501.

21TL-E-5

ASTROID CURVES OF TWO MAGNETIC PARTICLES

Forrester D.M.¹, Kovacs E.^{1,2}, Kuerten K.E.^{1,2} and Kusmartsev F.V.¹

¹Department of Physics, Loughborough University, LE11 3TU, UK

²Faculty of Physics, University of Vienna, 5, Boltzmannngasse, A-1090 Vienna, Austria

The various types of magnetic random access memory are now well established, practically realized and highly beneficial for society. There are many examples of their usage within current technology and it is certain that its non-volatile properties will continue to be exploited for future memory and logic devices. Here we have determined astroids for a stack of two magnetic particles, which the particles depending on the value of show the regions in the magnetic field plane where stable or metastable states of the system may exist. We argue that the finding of these astroids is crucial for modeling stable information storage devices made of pairs of small magnetic particles. We found that at any magnetic anisotropy of particles the astroid curves consists of two elements: the first element is similar to the conventional four cusped hypocycloid curve having the shape exactly as the Stoner-Wohlfarth (SF) astroid[1], the

second element is a closed curve, which shape changes with the anisotropy constant. It has a shape of nearly ideal circle at very small anisotropy, then slightly deformed circle or the convex oval when the anisotropy increases. When the constant of the anisotropy increases further, the oval shape transforms first to a peanut shape, and then further to the squeezed "8"-shaped or then, even to over-squeezed form, which arises at very large anisotropy constants. At small anisotropy the two particles astroid represent a set of two four cusped closed hypocycloid curves with their centers located on the axes symmetrically around the zero field. And they are first inside the circle or the oval. The form of these two hypocycloids are very similar to the Stoner-Wohlfarth astroid[1] although the position in the magnetic field plane is very different.

When the anisotropy constant increases further (that may correspond to the case when the shape of particles is getting more elongated) the size of these two four cusped hypocycloids increases and at some values of anisotropy larger than the critical one they will be crossing the "peanut"-shaped closed curve of the outer circle. There will be the parts of these two hypocycloids, which are now located outside of the "peanut" curve. In the regions associated with these parts there are exist two minima associated with the collinear ferromagnetic and antiferromagnetic states, respectively. Inside the "peanut"-shaped curve the classifications remains the same, ie inside the hypocycloids there are three minima, while outside the hypocycloids there are two minima associated with two ferromagnetic states. At large anisotropy constant the "peanut shape" is transformed into the "8"-shape. In this moment also the inner parts of the two hypocycloids vanishes. The size of their outer parts increases further. When the anisotropy constant will be larger then the critical value associated with this "8"-shape, the "8"-shape will be over-squeezed and there in the central region on the magnetic field plane a new area arises. In this new region there exist four different minima associated with two ferromagnetic states and with two counted states. which are double degenerate.

Support by EPSRC is acknowledged.

[1] E M Lifshitz, L D Landau, L. P. Pitaevskii, *Electrodynamics of Continuous Media*, Pergamon Press, NY, V.8, Ch.5 (1984)

21TL-E-6

THE EXCHANGE COUPLING IN MAGNETS

Antropov V.

Ames Laboratory, Ames, IA, 50011, USA

Starting from the general principles of magnetic exchange concept, we analyse the connection between the inverse susceptibility approach and the widely used long-wave approximation. A smallness parameter that controls the validity of latter approach is discussed. By combining the inverse susceptibility approach and the multiple scattering techniques we derive expression of exchange suitable for the first principles calculations beyond the long-wave approximation. Application of the formulism is presented and it is shown to enhance the short-range exchange and provide a better description of the short-range order effects. A generalized scheme of the exchange coupling construction where the direct exchange, superexchange, RKKY interaction and others can be obtained in some limiting cases is described. A classification of different magnets based on criteria of locality is introduced and the connection with the character of the exchange coupling is discussed. The numerous applications of the proposed scheme for real magnets with different degree of localization are shown.

21TL-E-7

FIRST-PRINCIPLES STUDY OF THE CURIE TEMPERATURE OF THE HALF-METALLIC FERROMAGNETIC SYSTEMS

Sandratskii L.M.

Max-Planck Institute of Microstructure Physics, Weinberg 2, D-06120 Halle, Germany

The half-metallicity is an interesting state of the magnetic systems where the electronic structure of one of the spin subsystems is metallic whereas the other is semiconducting. Since the half-metallic materials are characterized by a 100% spin polarization of the electronic states at the Fermi level they are important constituents of the spintronics devices utilizing the spin degree of freedom by means of creating and registering the spin polarized current.

To the materials most promising for the spintronics applications belong the diluted magnetic semiconductors and Heusler alloys. Since the spintronics devices should be operative at the room temperature it is important that the Curie temperature of the corresponding systems exceeds the room temperature considerably. Therefore the understanding of the mechanisms of the exchange interactions in the half-metallic systems is of primary importance for both fundamental physics and applications.

In the talk I will report on our intensive studies of the exchange interactions and Curie temperature in diluted magnetic semiconductors and Heusler alloys. Since these two types of half-metallic systems are very different the physical mechanisms leading to the ferromagnetism are also different. In the diluted magnetic semiconductors the primary role is played by the presence and properties of the holes in the valence band. There are two mutually compromising properties of the holes that are essential for the strong interatomic exchange interaction. To mediate the exchange interaction between atomic moments of the magnetic impurities the hole states must, first, be strongly exchange coupled to the impurity moments and, second, to be strongly delocalised from the impurity to efficiently mediate the exchange interaction between distant moments. We study how these properties vary from system to system and how they are influenced by the on-site electron-electron correlations. We analyse the exchange interactions in terms of the competition between ferromagnetic double exchange and antiferromagnetic superexchange.

The origin of the half-metallicity in the Heusler alloys is essentially different from the origin of the half-metallicity in diluted magnetic semiconductors. We calculate the exchange interactions and the Curie temperature in a number of Heusler alloys and discuss the influence of the half-metallicity on the character of longitudinal and transversal magnetic fluctuations.

21 June Saturday

12:15-13:45

oral session

21TL-F

21RP-F

“Magnetic Materials”

21TL-F-1

MAGNETIC PROPERTIES OF DISORDERED FERRITE AND ILMENITE-HEMATITE THIN FILMS

Tanaka K.

Department of Material Chemistry, Graduate School of Engineering, Kyoto University,
Nishikyo-ku, Kyoto 615-8510, Japan

Ferro- or ferrimagnetic oxide thin films are promising materials for the applications in the fields of magneto-optics, photomagnetism, and spintronics. The author's research group has synthesized thin films of disordered zinc ferrite (ZnFe_2O_4) and ilmenite-hematite solid solution ($\text{FeTiO}_3\text{-Fe}_2\text{O}_3$), the former and the latter are interesting from a point of view of magneto-optics and spintronics, respectively, by utilizing sputtering and pulsed laser deposition (PLD) methods, and has explored their magnetic, magneto-optical, and electrical properties. Although the ZnFe_2O_4 possesses a normal spinel structure as its stable phase, some of the Fe^{3+} ions occupy the tetrahedral as well as the octahedral sites in ZnFe_2O_4 of which the sputtered thin film is composed. As a result, the as-deposited thin film manifests high magnetization even at room temperature as shown in Fig.1(a) although the magnetic phase transition temperature of the stable phase of ZnFe_2O_4 is as low as 10 K. Figure 1(b) shows the temperature dependence of magnetization for the as-deposited thin film. Both field cooling and zero field cooling were performed for the measurements, and the thin film exhibits cluster spin glass transition, the temperature of which is as high as 325 K. At the cluster spin glass transition temperature, a broad peak of the nonlinear component of magnetization is also observed. Furthermore, the as-deposited ZnFe_2O_4 thin film exhibits large Faraday effect at the wavelength of 400 nm or so.

The ilmenite-hematite solid solution is one of the ferrimagnetic semiconductors. Most of the compositions possess Curie temperature higher than room temperature, and the type of carrier can be tuned only by changing the composition. By using the PLD method, the author's research group has succeeded in synthesizing single crystal-like solid-solution thin films of various compositions grown epitaxially on the sapphire substrate with (0001) plane, and has shown that indeed the thin films are ferrimagnetic semiconductors. The thin films may be promising materials for the spintronics devices.

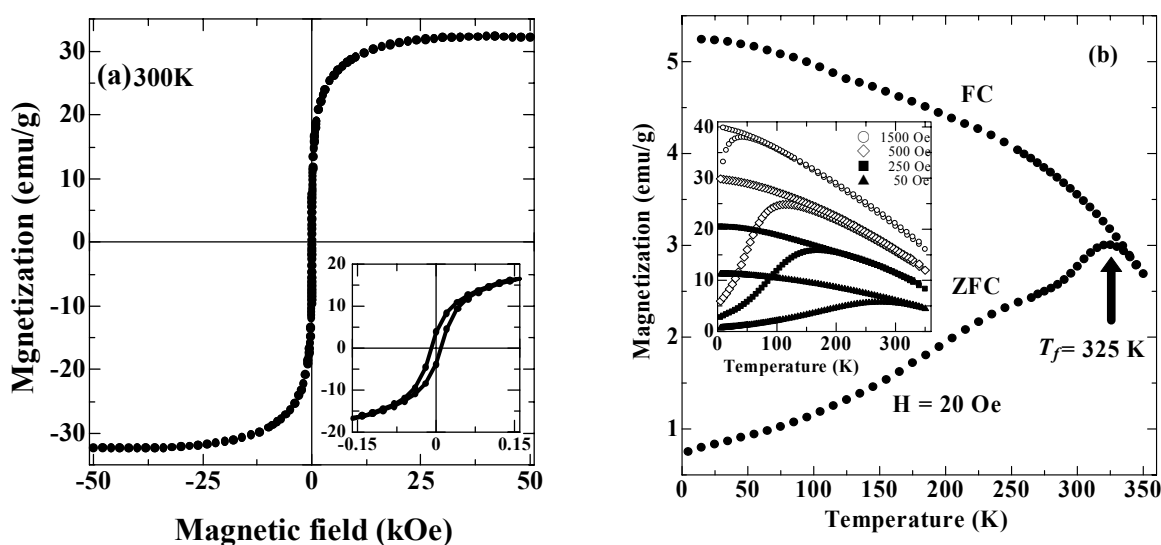


Fig.1 (a) The magnetic field dependence of magnetization at 300 K and (b) the temperature dependence of magnetization for disordered ZnFe_2O_4 thin film prepared by using the sputtering method. The field cooling and zero field cooling were performed in (b).

21RP-F-2

POSITIVE MAGNETISATION IN CARBON NANOCCLUSERS

Rode A.V.¹, Arcon D.^{2,3}, Christy A.G.¹

¹The Australian National University, Canberra, ACT 0200, Australia

²Institute Jozef Stefan, Jamova 39, 1000 Ljubljana, Slovenia

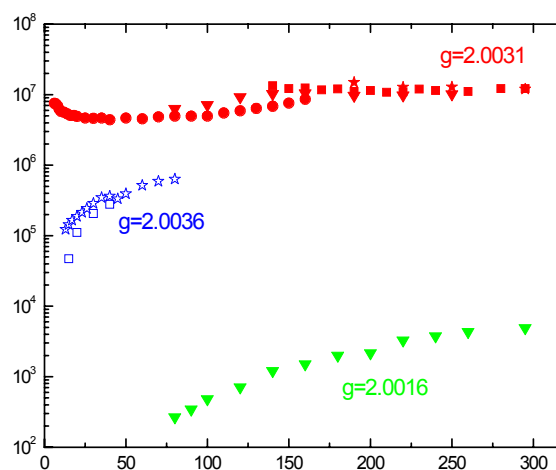
³Faculty of Mathematics and Physics, University of Ljubljana, Jadranska 19, Slovenia

Carbon nanoclusters produced by high-repetition-rate laser ablation of graphite and glassy carbon in Ar exhibits paramagnetic, superparamagnetic, and ferromagnetic behaviour [1,2]. The results show that the degree of remanent order is strongly dependent on the magnetic history, i.e. whether the samples were cooled under zero-field or field conditions. Such behaviour is typical for a spin glass structure where the system can exist in many different roughly equivalent spin configurations. The spin-freezing temperature is unusually high (50 - 300 K) compared with ≤ 15 K for typical spin glasses. The maximum in the zero-field magnetic susceptibility experiments and their field dependence indicate that there is competition between ferromagnetic and antiferromagnetic exchange pathways, accounting for the spin glass behavior and/or a low-dimensionality of the system. Magnetic inhomogeneity is supported by detailed EPR studies, where we recognized three different types of centre with significantly different relaxation times, from very long one of the order of 1 ms, down to 100 ns. Preliminary results on NMR will also be presented.

These carbon nanoclusters may find biomedical applications such as target drug delivery, non-viral vectors for gene delivery, and as a contrast agent for in vivo Magnetic Resonance Imaging.

Support by the Australian Research Council through the Discovery Program is gratefully acknowledged.

Fig. 1. Temperature dependence of the electron spin-lattice relaxation times measured in different carbon nanofoam samples and different signals. Here (∇) stands for experiments on 2 Torr sample, (\square) for 10 Torr, (\oplus) for 50 Torr, and squares for 200 Torr experiments.



- [1] A. V. Rode, E. G. Gamaly, A. G. Christy, J. D. Fitz Gerald, S. T. Hyde, R. G. Elliman, B. Luther-Davies, A. I. Veinger, J. Androulakis, J. Giapintzakis, *Phys. Rev. B* **70**, 054407 (2004).
 [2] D. Arcon, Z. Jagličič, A. Zorko, A. V. Rode, A. G. Christy, N. R. Madsen, E. G. Gamaly, B. Luther-Davies, *Phys Rev B* **74**, 014438 (2006).

21RP-F-3

ANISOTROPIC Nd-Fe-B THICK FILM MAGNETS WITH Ga ADDITIVE

Nakano M.¹, Takeda H.¹, Yanai T.¹, Yamashita F.², Fukunaga H.¹

¹Nagasaki University, Bunkyo-machi 1-14, Nagasaki 852-8521, Japan

²Matsushita Electric Industrial Co., Ltd., Osaka 574-0044, Japan

In order to advance a size-reduction in electronic devices such as milli-size motors and microactuators, thick film magnets are strongly required. Nd-Fe-B film magnets thicker than 10 μm have been prepared by the sputtering method, and recently Uehara reported the superior magnetic properties of a Nd-Fe-B/Ta multilayered thick film. (H_{CJ} : 1210 kA/m, J_r : 1.24 T, $(BH)_{\text{max}}$: 279 kJ/m³) [1]. On the other hand, we have already reported anisotropic Nd-Fe-B thick films by the high-speed PLD (Pulsed Laser Deposition) method, and the coercivity, remanence and $(BH)_{\text{max}}$ values were approximately 500 kA/m, 0.75 T, and 75 kJ/m³, respectively [2]. In this study, an investigation on the effect of Ga additive was carried out in the anisotropic PLD-made films.

A target with the composition of Nd_{2.6}Fe₁₄B+Ga was ablated with a Nd-YAG pulse laser ($\lambda = 355 \text{ nm}$) at the repetition rate of 30 Hz, and the distance between a target and a Ta substrate was fixed at 10 mm. Before the ablation, the chamber was evacuated down to approximately 10⁻⁴ Pa with a molecular turbo pump. A Ti sublimation pump was used as an auxiliary pump during the deposition. Figure 1 shows a diagram of a substrate heating system which was made of Ta sheet. Electric current flowed through the Ta sheet, and a sample on a substrate was annealed by Joule heat during deposition. The substrate temperature was fixed at 873 K [2]. The analyses of crystal structure were carried out with an X-ray diffractometer.

The coercivity (H_{CJ}), remanence (J_r) and $(BH)_{\text{max}}$ of a film magnet prepared from a target with Ga additive were approximately 843 kA/m, 0.94 T and 153 kJ/m³, respectively. These values were improved compared with those for the anisotropic PLD-made thick films [1]. We also confirmed that the peak intensities of a X-ray diffraction pattern corresponding to c-plane such as (004), (006) and (008) for the film prepared in this study were stronger than those for the above-mentioned anisotropic film [1]. It was clarified that use of a target with Ga additive is effective to improve the magnetic properties in an anisotropic Nd-Fe-B film magnet.

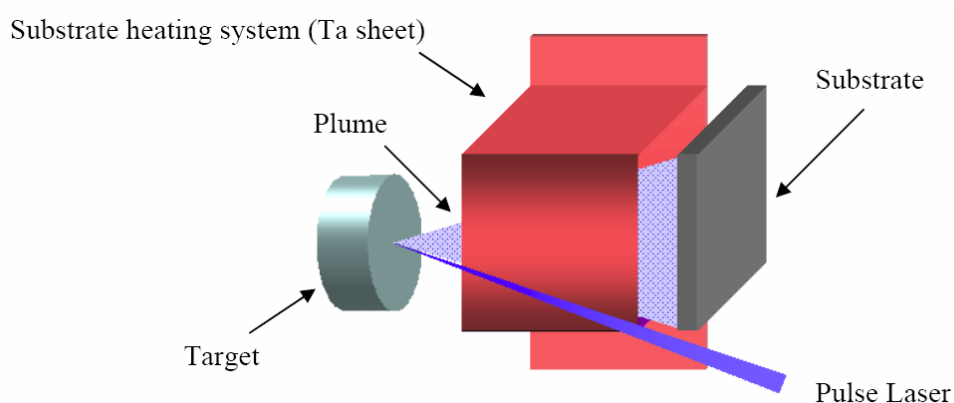


Fig. 1. Diagram of PLD method with a substrate heating system. Electric current flowed through the Ta sheet, and a sample on a substrate was annealed by Joule heat during deposition.

[1]M. Uehara, J. Magn. Soc. Japan, **28**(2004)1043. (in Japanese)

[2]M. Nakano *et al.*, J. Magn. Mater. **303**(2006)e375.

21RP-F-4

MAGNETIC PROPERTIES OF THE Fe SUBLATTICE IN $R_2Fe_{14}Si_3$

Andreev A.V.

Institute of Physics, Academy of Sciences, Na Slovance 2, 18221 Prague, Czech Republic

A study of polycrystalline $R_2Fe_{14}Si_3$ (R is a rare-earth metal) compounds [1], Si solid solutions in the well-known group of R_2Fe_{17} intermetallics, has shown a strong modification of both the intra- and inter-sublattice interactions compared to R_2Fe_{17} . The effect is rather complicated, because the Fe-sublattice moment is weakened by dilution with the non-magnetic Si whereas the Fe-Fe exchange interaction is simultaneously enhanced (the Curie temperature is higher in $R_2Fe_{14}Si_3$ than in R_2Fe_{17}). Studies of compounds with non-magnetic R give information on the contribution of Fe sublattice to the total properties and allow to separate the R-sublattice contribution. Since the compounds have large magnetic anisotropy, single crystals are strongly needed for a detailed study of magnetism.

In the present work, single crystals of $R_2Fe_{14}Si_3$, with the non-magnetic R = Y and Lu as well as with presumably non-magnetic Ce in this type of compounds, have been grown by the modified Czochralski method in a tri-arc furnace. A detailed investigation of the magnetization from 5 to 600 K was performed in fields applied along the main crystallographic axes.

All compounds studied are ferromagnets and exhibit a moderate magnetic anisotropy of the easy-plane type. The results of the work are summarized in Table 1. Despite of structure modifications (the Ce compound has the rhombohedral structure, whereas the compounds with Y and Lu are hexagonal) and different atomic radii and valence of R, the magnetic properties of all three compounds are rather similar. The Fe sublattice in $R_2Fe_{14}Si_3$ has K_1 of -1 MJ m^{-3} , decreasing with temperature as M_s^3 and negligible K_2 .

Table 1. Structural and magnetic properties of $R_2Fe_{14}Si_3$ compounds. a and c are the lattice parameters; V is the unit-cell volume; T_C is the Curie temperature; M_s is the spontaneous magnetic moment per formula unit at 5 K; H_a is the anisotropy field at 5 K; K_1 is the first anisotropy constant at 5 K.

R	a (pm)	c (pm)	V (nm ³)	c/a	T_C (K)	M_s (μ_B /f.u.)	$\mu_0 H_a$ (T)	K_1 (MJ m ⁻³)
Y	841.6	828.6	0.5083	0.9846	483	26.1	1.92	-0.93
Ce	845.0	1244.3 (829.5)*	0.7694 (0.5130)*	1.4725 (0.9817)*	447	25.6	1.95	-0.90
Lu	836.1	825.9	0.5000	0.9878	475	25.0	2.15	-0.98

* These values of c , V and c/a for $Ce_2Fe_{14}Si_3$ have been reduced by a factor of 1.5 to enable comparison with the other compounds.

This work is a part of the research project AVOZ10100520 and has been supported by grant GACR 202/06/0185.

[1] B.G. Shen, B. Liang, Z.H. Cheng, T.Y. Gong, H. Tang, F.R. de Boer, K.H.J. Buschow, *Solid State Commun.*, **103** (1997) 71.

21RP-F-5

GRAPHENE IN MULTILAYERED CPP SPIN VALVES*Mohiuddin T.M.G.^{1,3}, Zhukov A.A.^{1,3}, Hill E.W.^{2,3}, Elias D.^{1,3}, Novoselov K.S.^{1,3}, Geim A.K.^{1,3}*¹School of Physics and Astronomy, University of Manchester, Manchester, M13 9PL, UK²School of Computer Science, University of Manchester, Manchester, M13 9PL, UK³Center for Mesoscience and Nanotechnology, University of Manchester, Manchester, M13 9PL, UK

Graphene is a flat monolayer of carbon atoms arranged laterally in a two dimensional honeycomb benzene ring like structure and represents a basic building block for all other graphitic materials. It is the thinnest well ordered material layer known so far. For a long time graphene was a focal object in a number of theoretical investigations but only recently it was experimentally shown to exist in a free state [1]. Graphene is a zero gap semiconductor, where the charge carriers have a linear dispersion relation near the Dirac point. The ambipolar electric field effect in graphene makes it possible to control continuously density of electrons and holes in a wide range with carrier concentrations up to 10^{13} cm^{-2} . Room temperature carrier mobilities of $\sim 2 \cdot 10^4 \text{ cm}^2/\text{Vs}$ are routinely observed. The charge carriers in graphene were found to behave like a 2-D gas of massless Dirac fermions, and the quantum Hall effect was observed at room temperature [2]. These outstanding electronic qualities not only position graphene as a novel material for electronics but also open new perspective for spintronics research. The opportunity to control charge carriers in graphene along with their spin by an applied gate voltage makes it very appealing for application in spintronics.

Graphene has been shown to support spin polarized current in the plane (CIP) of the film [3]. However, no study has been done yet to employ graphene in devices where the current is perpendicular to plane (CPP). Here we look into the use of graphene as a non-magnetic spacer layer, in multilayer spin-valve devices. Doing this we were able to successfully sandwich for the first time a mono-atomic thick film between metallic/magnetic thin films.

Graphene flakes were prepared by exfoliation method [1] on a wafer with an array of pre-patterned bottom permalloy electrode lines. After identifying a graphene flake above one of these electrodes another step of e-beam lithography is carried out to design the top layer. Optical images of the graphene flake and adjacent alignment marks make it possible to easily locate and accurately position the top electrode design without exposing graphene to electron irradiation. The last lithography step also involves producing contacts to the upper and lower electrodes for measurement purposes. A reference device without graphene is in addition fabricated for a comparison.

Our measurement results show that the graphene (Gr) layer efficiently constrains the exchange coupling between the magnetic electrodes. A significant anisotropy was observed in the magnetoresistance for the cross electrode geometry employed. In this case CIP and CPP contributions qualitatively differ by a sign in the arising voltage. For a NiFe/Au/Gr/NiFe stack Gr layer channels the spin current perpendicular to the plane and produces an enhanced (by a factor ~ 5) magnetoresistance effect compared to a simple stack without a graphene layer.

[1] K. S. Novoselov *et al.*, *Science*, **306** (2004) 666.

[2] A. K. Geim and K. S. Novoselov, *Nature Materials*, **6** (2007) 183.

[3] E.W. Hill *et al.*, *IEEE Trans. Magn.*, 42 (2006) 2694, N. Tombros *et al.*, *Nature*, **448** (2007) 571.

21 June Saturday

15:00-17:00

oral session

21TL-F

21RP-F

**“Application,
Superconductivity
and Miscellaneous”**

21TL-F-6

PERPENDICULAR MAGNETIC RECORDING FOR HARD DISK DRIVE APPLICATION

Muraoka H.

Tohoku University, Sendai 980-8577, Japan

Areal density of hard disk drives (HDD) is continuously growing. Current target density is 1 Tbits/inch², in which one bit corresponds to a square of only 25.4 nm on a side. Even higher density is being investigated. Magnetic recording can attain a high areal density greater than any other information storage devices. The technology is a good example of nano-sized magnetism and nano-technology. Outline of high density magnetic recording technology is first presented.

A recent topic in magnetic recording for the HDD is the commercialization of perpendicular magnetic recording [1] from 2005. A rapid transition from longitudinal to perpendicular recording is taking place.

For high density recording demagnetization field is a major factor. In contrast to conventional longitudinal recording, demagnetization field in perpendicular magnetization becomes minimum at magnetization transitions. Due to this intrinsic advantage, perpendicular recording was originally proposed to avoid extremely thin media thickness [1].

Another notable advantage was granular nature of the first Co-Cr perpendicular recording medium [2]. The recording layer of the media consists of magnetically isolated fine grains, which design concept has not been changed. To understand recording characteristics, the granular nature is essential. Fig 1 schematically indicates the magnetic transition structure in the granular media. Any written magnetization transitions cannot be ideally straight, but they follow the boundaries of the grains. Due to this random fluctuation of the transition, the position of resultant read back pulse is randomly shifted around the ideal transition position. This random pulse shift is a major noise source of current perpendicular media, which is referred to as transition jitter or simply 'jitter'. The jitter and resultant media noise are obviously proportional to grain size. However, the recorded bit stability is also governed by a ratio of magnetic energy of $K_u V$ to thermal energy of $k_B T$. Herein, K_u , V , k_B , and T are magnetic anisotropy energy, grain volume, Boltzmann constant and temperature, respectively. It is required for a practical disks that the $K_u V/k_B T$ is greater than 60 or so. Minimum grain volume must be larger than this criteria. The dilemma between jitter and thermal stability is the issue.

In order to increase areal density beyond this limitation, we have to abandon the assumed scheme for media, i.e., non-granular structure or high K_u with small switching field. The future strategy for high areal density is discussed for the candidates, such as bit patterned media, energy assisted recording, exchange coupled media, etc.

This work is supported in part by "Research and Development for Next-Generation Information Technology" from MEXT, Japanese Government.

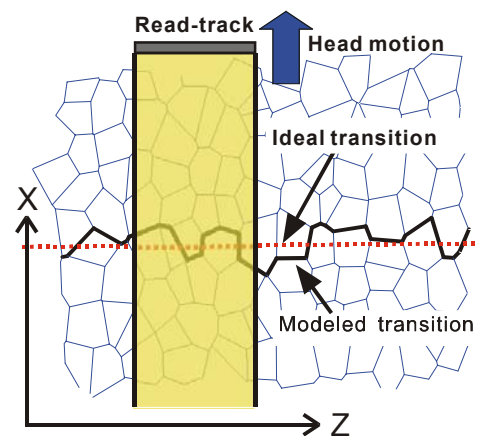


Fig. 1 Granular structure model with Voronoi cells and magnetization transition.

- [1] S. Iwasaki, Y. Nakamura, *IEEE Trans. Magn.*, **13** (1977) 1272.
 [2] S. Iwasaki, K. Ouchi, *IEEE Trans. Magn.*, **14** (1978) 849.

21TL-F-7

EXPLOSIVE INSTABILITY AND LOCALIZATION OF THREE- PHONON PARAMETRICALLY COUPLED EXCITATION IN MAGNETS

Preobrazhensky V.^{1,2}, Pernod P.², Bou Matar O.²

Joint European Laboratory LEMAC:

¹Wave Research Center, A.M. Prokhorov General Physics Institute RAS, 38 Vavilov str.,
 Moscow 119991, Russia

²Institut d'Electronique, de Micro-Electronique et de Nanotechnologie (IEMN-DOAE-UMR
 CNRS 8520), Ecole Centrale de Lille, 59651 Villeneuve d'Ascq, France

The results of experimental observation and theoretical studies of a new parametric phenomenon in the coupled spin- phonon system of magnets are reported. Supercritical parametric excitation of phonon pairs in magnetic media is well known and successfully used in modern ultrasonics for wave front reversal of acoustic waves. Strong nonlinearity of magnetic subsystem and magnetoelastic interaction in solids favours the multi-phonon coupling. Three-phonon coupling generated by the transversal magnetic pumping was recently observed for the first time [1] in “easy plane” antiferromagnet (EPAF) α -Fe₂O₃ known as a model crystal for nonlinear magnetoacoustics. Energy and momentum conservation law for the three-phonon coupling is :

$$\Omega_P = \omega_1 + \omega_2 + \omega_3 ; \mathbf{k}_1 + \mathbf{k}_2 + \mathbf{k}_3 = 0.$$

where Ω_P is the magnetic pumping frequency. Unlike the case of phonon pair generation, the characteristic feature of phonon triad excitations is the formation of a singularity of acoustic field within a finite time of pumping, that is an indication of the explosive instability. The time of explosion τ_e is defined by the relaxation time of phonons τ_{ph} and supercriticality parameter Γ :

$$\tau_e = \tau_{ph} \ln \left(\frac{\Gamma}{\Gamma - 1} \right)$$

The theoretical analysis show that three- phonon supercritical parametric coupling of travelling waves (fig.1) in EPAF is accompanied by the space-time “peaking and localization” of the acoustic field (fig.2). Mechanisms of stabilisation of the singularities and applications of the three-phonon coupling in magnets are discussed.

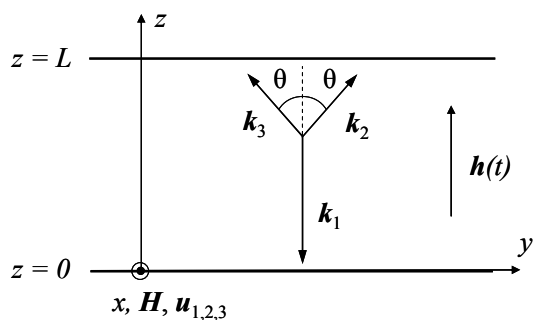


Fig.1 Three-phonon parametric excitation geometry

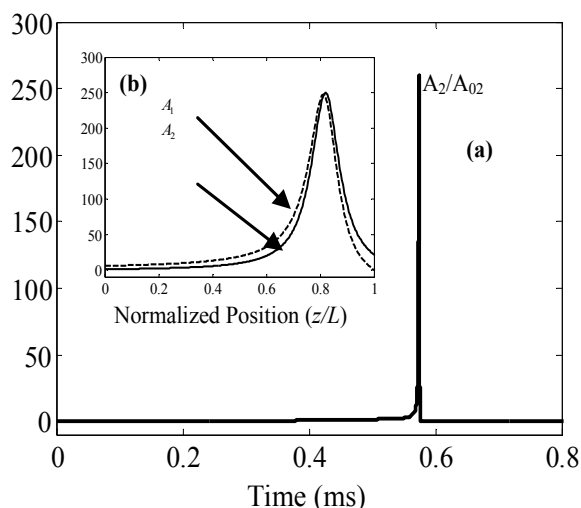


Fig.2 «Peaking and localization» of the acoustic field

Support by the program “Coherent acoustic fields and signals” RAS and by the Russian Federal Program of Support for Leading Scientific Schools (NSH-2099.2008) are acknowledged.

[1] V.Preobrazhensky, V.Rudenko, P.Pernod, V.Ozhogin, *JETP Letter.*, **86** (2007) 348.

21RP-F-8

NON-CONTACT ENERGY TRANSMISSION SYSTEM FOR ARTIFICIAL ORGANS

Matsuki H., Sato F.

Dept. of Elect. Eng., Tohoku Univ., 6-6-05 Aoba Sendai, 980-8579 Japan

Non-contact energy transmission system ranging from 1mW to 30kW have been developed.

We applied the system to implanted medical devices. In this paper we discussed the system for artificial heart and artificial sphincter.

1) for implanted artificial heart

Heart transplantation is currently the best treatment for end-stage heart failure. There is a large disparity between the number of available donor hearts and the number of people who need them. Total artificial heart and ventricular assist devices have been developed as alternatives to the transplantation. We have developed transcutaneous energy transmission system for the undulation pump ventricular assist device. Our system has thin ferrite cores, which increase the magnetic coupling factor and self-inductance. In addition MOSFET synchronous rectifier can reduce forward voltage drops.

The inverter consists of full-bridged MOSFETs and drives the primary coil at the fixed frequency of 160kHz. The rectifier board was designed to achieve a balance between thermal radiation and reduction of eddy-current losses.

The maximum efficiency and output power for various coil distance were measured. The output voltage is stable at the gap of 10mm, while output voltage decrease drastically at the gap of 0mm because of increase of internal impedance. The maximum efficiency at the gap of 5mm was of 93.4%, the maximum efficiency of the transformer increases as the coupling factor

increasing. In this measurement the efficiency involves the switching loss, resistance of MOSFET and diodes' forward drop during transition periods.

We evaluated the system *in vivo*, the internal unit was implanted to the goat and a load characteristics were measured. Maximum efficiency was the same value as the value of *in vitro* measurement 93.4%.

2) for artificial sphincter

Patients relying on artificial anuses can have independent evacuation disorders, because artificial anuses have no corresponding mechanism to sphincter externus of actual anuses. We have developed artificial sphincters utilizing shape memory alloy (SMA) and thermosensitive transformer. We designed a prototype of thermosensitive transformer for evaluations and tested it to confirm the temperature controllability.

Since an artificial sphincter is used implanted inside a body, there must be a mechanism that monitor the ambient temperature and that control the output heating power by itself. We used the transformer with a thermosensitive ferrite core as a temperature sensor at the same time as a power controlling device.

The prototype transformer was prepared in the way that it can be placed on the SMA plate. We did a heating experiment to confirm the temperature controllability of SMA with the thermosensitive transformer. In the beginning, the heater was fed the power of 5 watts. Small overshoot was observed and then it was confirmed the temperature control was realized.

21RP-F-9

MAGNETIC TRANSITIONS IN 3d-METAL OXIDES UNDER SUPER HIGH PRESSURES

Lyubutin I.S.¹, Gavriiliuk A.G.^{1,2}, Struzhkin V.V.³

¹Institute of Crystallography, RAS, Leninsky av. 59, Moscow 119333, Russia

²Institute for High Pressure Physics, RAS, 142190, Troitsk, Moscow region, Russia

³Geophysical Laboratory, Carnegie Institution of Washington, Washington DC 20015, USA

Transition metal oxides constitute a very large class of materials of considerable importance for both fundamental science and practical applications. They include high temperature superconductors, manganites with colossal magneto-resistance, multiferroics, materials for spintronic and optoelectronic applications. Moreover, mixed iron oxides and perovskites are very important for geophysics. The properties and behavior of transition metal oxides are mainly governed by strong electron-electron correlations. In magnetic systems with strong electronic correlations, many theories predict the pressure-induced insulator-metal phase transition which is accompanied by a collapse of the localized magnetic moment and a structural phase transition. However, until recently such scenario was not observed experimentally, since the expected values of necessary pressures exceed 2 Megabar.

Here we report on the complex studies performed at super high pressures up to 200 GPa in diamond anvil cells using several experimental methods: Moessbauer transmission spectroscopy and Moessbauer synchrotron spectroscopy (Nuclear Resonance Forward Scattering – NFS), x-ray diffraction and synchrotron high resolution x-ray emission Fe-K β spectroscopy (XES), optical absorption spectroscopy and direct measurements of electric resistance. The materials with different crystal structures, such as nickel monoxide NiO and magnesiowustite (Mg,Fe)O, iron oxide Fe₂O₃, rare-earth orthoferrites RFeO₃ (R = Nd, Lu, Y), yttrium iron garnet Y₃Fe₅O₁₂, iron borates FeBO₃ and GdFe₃(BO₃)₄, multiferroic BiFeO₃ and manganites LaMnO₃ and MnFeO₄ have been studied.

The transitions from the magnetic to a nonmagnetic state (magnetic collapse) was discovered in all crystals at pressures of about 40-55 GPa. The magnetic collapse is accompanied by a transformation of electronic and spin structures due to the spin crossover in $3d$ electron system at the transition of Fe^{3+} ions from the high-spin $S = 5/2$ (HS) to the low-spin $S = 1/2$ (LS) state. At the same pressures, the structural phase transitions with a sharp drop of the unit cell volume were found in those crystals. We have established that the metallization process is very complicated. In the pressure region of the HS-LS spin crossover, many crystals are transformed from the dielectric to a semiconducting state. The direct insulator-metal transition (IMT) was found in $\text{Y}_3\text{Fe}_5\text{O}_{12}$ and BiFeO_3 crystals. These effects are explained by the Mott-Hubbard type transitions with the extensive suppression of strong $d-d$ electronic correlations.

A new mechanism of the insulator-metal transition in Mott-Hubbard insulators was found. This new mechanism can be initiated by high pressure and it is driven by the spin-crossover of d^5 ions from HS to LS state. The spin-crossover suppresses the Coulomb correlation energy U_{eff} down to the value enabling the insulator-metal transition according to the Mott mechanism $U_{\text{eff}}/W \approx 1$ (W is the half bandwidth). Such type of Mott metallization was observed experimentally in multiferroic BiFeO_3 . We call the new IMT mechanism as the "Hubbard energy control" mechanism in addition to the known "band-width control" mechanism.

Supports by RFBR (Grants № 08-02-00897a and № 07-02-00490-a) and by the RAS Program "Strongly correlated electronic systems" are acknowledged.

21RP-F-10

MAGNETISM IN π ELECTRON SYSTEM

Hwang Ch.¹

Korea Research Institute of Standards and Science,
P.O.Box 102 Yuseong Daejeon, Republic of Korea

Ever since the first report on magnetism in solid C_{60} , there have been a lot of reports on magnetism in carbon. Even though this first report was withdrawn, the existence of ferromagnetic order in graphite is reproducible. However, the origin of the long-range ferromagnetic order in this system is not fully understood. In the mean time, this topic is still controversial since Fe impurity is not avoidable when we use the graphite. Even considering this impurity level of tens of ppm, the existence of the long range ferromagnetic order at this concentration cannot be justified. We employed several experimental techniques combined with the first principles calculation to study the origin of the carbon magnetism and the effect of the Fe impurity. Topics that will be covered in this talk are as follows.

- 1) MCD : possible clue for the origin of FM order
- 2) Impurity effect : How to get rid of the impurity in ppb level
- 3) Surface Magnetism : Conclusive proof of carbon magnetism
- 4) Possible configuration of atomic arrangement : STM and 1st principles calculation
- 5) Electronic structure of magnetic carbon

Based on the above results, we will give the conclusive results on carbon magnetism.

Support by KRISS is acknowledged. This work is in collaboration with Dr. W. Kim, Dr. D. Lee, Y. S. Kim at KRISS, Prof. C. G. Kim at CNU, Prof. J. S. Hong at PNU, Dr. M. Venkatesan, Prof. M. Coey at Trinity College.

[1] T. L. Makarova, B. Sundqvist, R. Hohne, P. Esquinazi, Y. Kopelevich, P. Scharff, V. Davydov, L. S. Kashevarova, & A. V. Rakhmania, Magnetic carbon. *Nature* 413, 716-718(2001). This paper has been retracted. *Nature* 440, 707 (2006).

21RP-F-11

TAILORED JOSEPHSON PHASE BY PLANAR AND STEPPED FERROMAGNETIC INTERLAYERS

Weides M.¹, Bannykh A.¹, Peralagu U.¹, Pfeiffer J.², Koelle D.², Kleiner R.² and Goldobin E.²

¹Institute for Solid State Research, Research Centre Juelich, Germany

²Physikalisches Institut-Experimentalphysik II, Universität Tübingen, Germany

In superconducting/ferromagnet (S/F) systems the superconducting order parameter may leak to the ferromagnet and display damped oscillations as function of SF interface distance d_F . This results in novel and interesting physics, such as a non-monotonic critical current density j_c dependence on d_F and the realization of so-called π coupled Josephson junctions (JJs). These SFS/SIFS-type junctions (I: tunnel barrier) are characterized by a phase-shift of π in the ground state of current-phase relation.

We have fabricated SIFS Josephson junctions based on Nb/Al₂O₃/F/Nb multilayers, using either Ni_{0.6}Cu_{0.4} or Ni as magnetic interlayer. Depending on the F-layer thickness the junctions were in the 0 or π coupled ground state. The Al₂O₃ tunnel barrier allows achieving low damping of Josephson oscillations and to observe dynamics properties in the IVC [1].

Using a ferromagnetic layer with a *stepped* thickness we obtain a so-called 0- π Josephson junction with identical critical currents density amplitudes of 0 and π parts [2,3,4]. The ground state of 0- π junctions has a spontaneous vortex of supercurrent, which is pinned at the phase discontinuity. Its magnetic field corresponds to some fraction of the magnetic flux quantum Φ_0 [5]. The ground state is double degenerate, i.e. it has either positive or negative spontaneously formed fractional flux (clockwise or counter clockwise circulation of supercurrent) and can be considered as two states (up and down) of a macroscopic spin.

Our SIFS 0- π JJ is the first underdamped tunnel 0- π junction based on low- T_c superconductors. It can be measured using standard setups due to the rather high characteristic voltage V_c . Dynamic properties of its IVC such as Fiske steps and integer and semi-integer zero field steps were measured. Multi-stepped (0- π -0 etc.) and 0- π junctions in short to long limit were investigated by experiment and simulation.

The possibility to fabricate 0, π , and 0- π JJs within the same process opens perspectives for application of SIFS technology in complimentary logic circuits, in RSFQ logic with active π junctions, in π qubits, as well as for the investigation of fractional magnetic flux quanta.

Support by DFG is acknowledged

[1] M. Weides, M. Kemmler, H. Kohlstedt, A. Buzdin, E. Goldobin, D. Koelle, and R. Kleiner, *Appl. Phys. Lett.* **89**, 122511-122513 (2006).

[2] M. Weides, H. Kohlstedt, R. Waser, M. Kemmler, J. Pfeiffer, D. Koelle, R. Kleiner, and E. Goldobin, *Appl. Phys. A* **89**, 613-617 (2007).

[3] M. Weides, M. Kemmler, H. Kohlstedt, R. Waser, D. Koelle, R. Kleiner, and E. Goldobin, *Phys. Rev. Lett.* **97**, 247001-247004 (2006).

[4] M. Weides, C. Schindler, and H. Kohlstedt, *J. Appl. Phys.* **101**, 63902-63908 (2007).

[5] E. Goldobin, D. Koelle and R. Kleiner, *Phys. Rev. B* **66**, 100508 (2002).

21RP-F-12

THE COMBINED METHOD FOR THE REALIZATION OF φ -JOSEPHSON JUNCTIONS

Pugach N.G., Vedyayev A.V.

Faculty of Physics, M. V. Lomonosov Moscow State University, Leninskie Gory, 119992,
Moscow, Russia

An interest to Josephson junction devices having ferromagnetic layers in a weak link region is continuously increasing in the last few years. The critical current of a junction with a ferromagnetic (F) spacer exhibits damping oscillations as a function of F-layer thickness and the order parameter phase difference between the superconducting banks φ could be equal by 0 or π in the ground state. Today the technological achievements open the way for fabrication not only 0 or π -junctions, but also long Josephson contacts having the alternating 0 and π -regions. Mints and Buzdin [1,2] have considered theoretically the periodic structure composed of small alternating 0- and π - Josephson junctions. The length of each region not exceeded the Josephson penetrating length λ_J . It was shown that after the rapid oscillating phase averaging the slowly changing phase difference of the order parameters between the superconducting banks could have arbitrary value $0 < |\varphi| < \pi$ in the ground state. Then so-called φ -junction could be realized. This φ -junction has to exhibit very unusual properties: the current-phase relation of unusual form, the behavior in the external magnetic field, the existence of fractional magnetic vortices and so on. All of these properties connect to the large enough second harmonic in the current-phase relation originated due to the rapid oscillations averaging under some conditions.

In this work based on the developed method we have found that if the 0- and π -Josephson junctions forming the structure have the intrinsic second harmonic in the current-phase relation: $J = J_{c1} \sin \varphi + J_{c2} \sin 2\varphi$, it creates new conditions for existence of φ -junction. First, it weakens the existed condition if $J_{c2} < 0$, second it creates one new condition, but it is difficult to realize. The possibility of the necessary second harmonic is also analyzed basing on present theories [3]. It is not so exotic for the Josephson junctions with weak link containing ferromagnet. The second harmonic of these junctions was even measured experimentally [4]. Non-sinusoidal current-phase relation is peculiar to pure SFS junctions [5] also taking into account s-d scattering in the ferromagnet [6], to the structure in the "dirty" limit in the presence of parallel spin-flip scattering in F-layer [7]. It could be realized by introducing of a thin dielectric spacer into the junction with the certain transparency of S/F interface [8]. The intrinsic second harmonic J_{c2} in every case can be not large enough to form the ground state with the arbitrary phase difference, but combination of these junctions into a long 0- π junction with the alternating regions increases the possibility to create the φ -junction and extend the probability of its experimental discovery.

This work was supported by the RFBR (grant 07-02-00918-a).

- [1] R. G. Mints, *Phys. Rev.* **B 57** (1998) R3221.
- [2] A.I. Buzdin, A.E. Koshelev, *Phys. Rev.* **B 67** (2003) 220504.
- [3] A.A. Golubov, M.Yu.Kupriyanov, E. Il'ichev, *Rev. Mod. Phys.* **76** (2004) 411.
- [4] S.M. Frolov, D.J. Van Harlingen, V.A. Oboznov, et.al., *Phys. Rev.* **B 70** (2004) 144505.
- [5] Z. Radovic, L. Dobrosavljevic-Grujic, B. Vujicic, *Phys. Rev.* **B 63** (2001) 214512.
- [6] A.V. Vedyayev, N. Ryzhanova, N. Pugach, *J. Magn. Magn. Mat.* **305** (2006) 53.
- [7] A.I. Buzdin, *Phys. Rev.* **B 72** (2005) 100501(R).
- [8] A.A. Golubov, M.Yu.Kupriyanov, *Pis'ma v ZhETF* **81** (2005) 419.

21 June Saturday

17:00-19:00

poster session

21PO-2

“Magnetophotonics”

21PO-2-1

ULTRAFAST NON-THERMODYNAMIC PATHWAY FOR A MAGNETIC FIRST-ORDER PHASE TRANSITION IN HoFeO_3

*Kimel A.V.¹, Ivanov B.A.², Pisarev R.V.³
Usachev P.A.³, Kirilyuk A.¹, Rasing Th.¹*

¹IMM, Radboud University Nijmegen, 6525 ED Nijmegen, The Netherlands

²Institute of Magnetism, NASU, 03142 Kiev, Ukraine

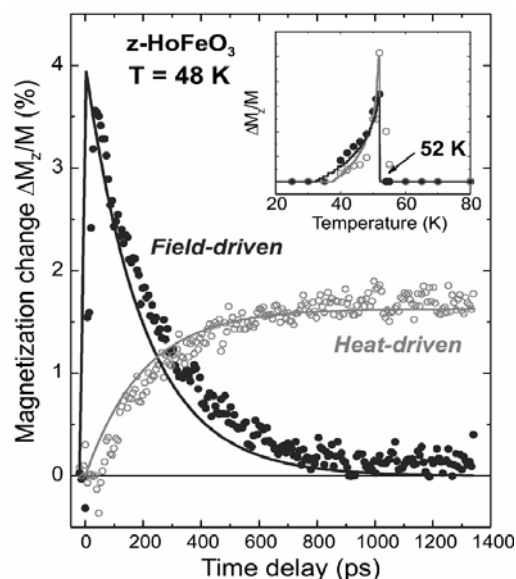
³A.F. Ioffe Physico-Technical Institute of RAS, 194021 St.-Petersburg, Russia

First-order phase transitions are very well known phenomena. However, on time scales pertinent to atomic, orbital and spin motion the kinetics of first-order phase transitions is still poorly understood. This is a particularly interesting problem in magnetism, where, in addition to be of purely fundamental interest, ultrafast phase transitions may potentially have impact on technological applications such as spintronics, ultrafast processing and recording of information

The dynamic response of magnetically ordered materials to femtosecond laser excitation has been intensively studied over the last 10 years [1-4], but the studies of magnetic first-order phase transitions are scarce. Moreover, in all these cases the observed phase transformations were the result of ultrafast laser heating [3]. In [4] was demonstrated that a 100 fs circularly polarized laser pulse may act on spins as a similarly short magnetic field pulse up to 1 T. In magnetically ordered materials such a strong field is a stimulus that on itself can efficiently induce a first-order phase transition and in contrast to heat-driven phase transitions, it is not associated with an increase of entropy and thus expected to have different kinetics.

We investigate the difference in kinetics of first-order magnetic phase transition in HoFeO_3 induced by magnetic field and heating pulses and demonstrate that a laser-generated effective magnetic field of 100 fs provides a novel and ultrafast pathway for the first order magnetic phase transition. The transition occurs within 3 ps, which is about two orders of magnitude faster than via laser-induced heating. In contrast to the slow thermodynamic scenario, a 100 fs magnetic field pulse brings the spins into a strongly nonequilibrium state, so that the following relaxation from this state results in an ultrafast phase transformation.

On figure: Ultrafast first order phase transition from Γ_{12} to Γ_{24} driven by laser heating (open circles) and laser-generated magnetic field (solid circles). Inset shows temperature dependencies of the efficiencies of the phase transition from Γ_{12} to Γ_{24} . Lines show calculated efficiencies of the phase transitions.



This work was partially supported by INTAS, RFBR, NWO, FOM as well as the Dutch nanotechnology initiative NanoNed.

- [1] E. Beaurepaire, J.-C. Merle, A. Daunois, and J.-Y. Bigot, *Phys. Rev. Lett.* **76**, 4250 (1996)
 [2] A. Scholl, L. Baumgarten, R. Jacquemin, and W. Eberhardt, *Phys. Rev. Lett.* **79**, 5164 (1997)
 [3] A.V. Kimel, A. Kirilyuk, A. Tsvetkov, R.V. Pisarev, and Th. Rasing, *Nature* **429**, 850 (2004)

- [4]. A. V. Kimel, A. Kirilyuk, P.A. Usachev, R.V. Pisarev, A.M. Balbashov, and Th. Rasing, Nature **435**, 655 (2005).

21PO-2-2

SPIN-WAVE EXCITATIONS OF 2D RHOMBIC MAGNONIC CRYSTAL

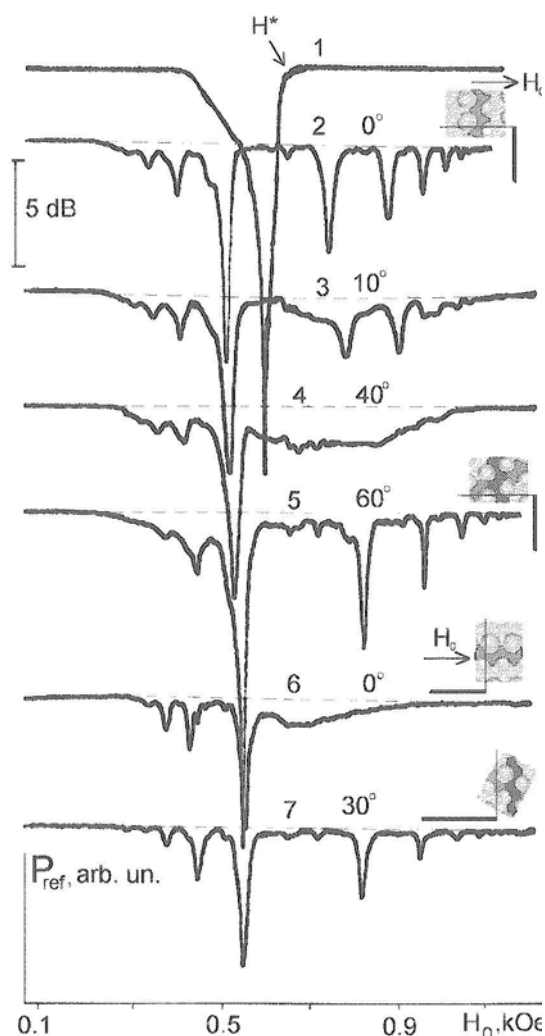
Vysotsky S.L.¹, Pavlov A.I.¹, Nikitov S.A.², Filimonov Yu.A.¹

¹Saratov branch of IRE RAS, Zelenaya str., 38, Saratov, 410019, Russia

²IRE RAS, Mokhovaya 11-7, Moscow, 125009, Russia

The paper presents the detail investigation of eigen spin-wave spectra (SWS) of 2D magnonic crystal (MC) consist of rhombic array of 4-4,5 μm depth chemically etching holes based on 5 μm yttrium iron garnet (YIG) film reported in [1]. There the dependencies of power P_{ref} reflected from a microstrip transducer placed onto both the YIG film (curve 1) and MC surface (curve 2-5) on bias tangentially directed magnetic field H_0 at $f=3,5$ GHz were described. There was found that SWS of MC include two sets of absorption peaks: "low-field" and "high-field" comprising to long-wave boundary value H^* of magnetostatic surface waves (MSSW) in YIG film (see curve 1). It was shown that "low-field" peaks could be observed at any value of angle φ between the array's axis and excited wave vector without significant changes. In contrast "high-field" peaks was observed at φ values in the vicinity of $0^\circ \pm n\pi/3$ (0° corresponds to array's axis) and transformed to broadband excitation region at other φ values so they were associated with the excitation determined by the array's symmetry (see curves 2-5).

In the presented paper the eigen SWS of MC both in MSSW (curves 2-5) and in backward volume MSW (curves 6,7) geometry are compared. In the last case the "high-field" peaks could be observed at $\varphi=30^\circ \pm n\pi/3$ so in both geometries they are associated with spin waves excited in perpendicularly magnetized elementary parts of MC topology (see inserts to curves 2,5,7). The possibility of representing of MC topology by a periodic system of coupled narrow ferrite waveguide and the influence of edge modes on SWS are discussed.



Support by RFBR grants No. 06-07-89341-a and No. 08-02-00785-a is acknowledged.

- [1] S.A. Nikitov, S.L. Vysotsky, E.S. Pavlov, Yu.A. Filimonov "Eigen spin-waves excitations in 2D magnon crystals". Abstracts of International Symposium "Spin waves 2007", Saint Petersburg, Russia, June 16-21, 2007, p.17.

21PO-2-3

PROBING THE DOMAIN MICROSTRUCTURE AND MAGNETIZATION DYNAMICS OF Fe/Cr FILMS WITH BIAXIAL IN-PLANE MAGNETIC ANISOTROPY BY SECOND HARMONIC GENERATION

Rzhevsky A.A.^{1,2}, Krichevtsov B.B.¹, Bürgler D.E.², Schneider C.M.²

¹Ioffe Physico-Technical Institute of RAS, 194021 St.-Petersburg, Russia

²Institut für Festkörperforschung IFF-9 “Elektronische Eigenschaften”,
Forschungszentrum Jülich GmbH, D-52425 Jülich, Germany

The magnetic microstructure of single-crystalline Fe(001) thin films has been studied by magnetic second harmonic generation and conventional magneto-optical Kerr effect methods. The layers were grown on GaAs/Fe/Ag(100) substrates, capped by a Cr overlayer, and displayed a four-fold in-plane magnetic anisotropy. We observe the formation of a multi-domain structure at magnetic fields $|H| \leq 0.5$ kOe, when the field is applied in a narrow range of azimuthal angles close to the hard axis direction ($|\Delta\xi| \leq 1^\circ$). The domains are characterized by the same longitudinal magnetization component M_x and transversal components M_y of opposite signs. We developed an approach to extract the change of the relative contributions of domains with different magnetization directions during magnetization reversal from the experimental data. The formation of a domain structure can be explained by taking into account the lateral fluctuations of the magnetic anisotropy energy caused by defects and stress at the interfaces and the role of the biquadratic exchange coupling between interfacial Fe and Cr magnetic moments.

The interface and bulk magnetization dynamics of single-crystalline Fe(001) thin films with Cr cap layers have been studied by measuring transient second harmonic generation (TrSHG) and transient Kerr effect (TrMOKE) by means of an all-photon pump-probe technique. Experiments have been carried out in longitudinal geometry with orientation of the hard axis close ($\Delta\xi \approx 1.5^\circ$) to the magnetic field $H=0.5$ kOe. TrSHG was measured for the PP polarization combination. The frequency f and damping of TrSHG oscillations is the same as for oscillations observed by TrMOKE. The phase of the TrMOKE oscillations is shifted by 90° as compared to TrSHG, proving that the TrSHG and TrMOKE oscillations are related to the temporal variation of different components of the elliptically precessing magnetization \mathbf{M} . TrMOKE is associated with the out-of-plane component M_z and TrSHG with in-plane component M_y perpendicular to the light incidence plane. Additionally, weak oscillations of TrMOKE and TrSHG at doubled frequency $2f$ were detected. The $2f$ -oscillations are related to contributions of terms quadratic in the in-plane magnetization components. By comparison of static SHG variations caused by an external magnetic field and the amplitude of SHG oscillations induced by the ultra-fast optical pulse we evaluate the amplitude of the in-plane interface magnetization oscillations $\Delta\zeta \approx 13^\circ$, where $\Delta\zeta$ is the angle between the magnetization orientation in equilibrium and after the photon pump pulse. This large amplitude of the in-plane magnetization oscillations shows that the system is close to the validity limit of the linearised LLG equations. Therefore, non-linear effects in magnetization dynamics may be expected.

21PO-2-4

MAGNETOPLASMONIC EFFECTS IN 2D AND 3D METALLIC MAGNETOPHOTONIC CRYSTALS

*Zhdanov A.¹, Grunin A.¹, Tsema B.¹, Ezhov A.¹, Dolgova T.¹, Napol'sky K.², Tsirlina G.²,
Ganshina E.¹, Fedyanin A.¹*

¹Faculty of Physics M.V. Lomonosov Moscow State University, Moscow, Russia

²Chemical faculty M.V. Lomonosov Moscow State University, Moscow, Russia

Photonic crystals have been in the center of attention within the latest few years due to the unique ability of light propagation control they provide. Periodic structures at the nanometer scale with magnetic properties are often called magnetophotonic crystals [1]. Magneto-optical response can be efficiently enhanced in metal structures. However due to significant optical absorption in metals the specific design of such structures is required [2].

Various designs of metal submicrostructures are considered in the current work. First type of structures represent themselves 3D inverted opals. 500 nm silica spheres are self-assembled in fcc-lattice on the golden substrate and form up to 20 layers of the structure. Then free space between spheres is filled by nickel and spheres are etched out. Such structures exhibit at the same time typical traits of conventional photonic crystals such as *photonic-band-gap* and also peculiar magneto-optical properties. Experimental results of spectroscopy at various angles of incidence prove the presence of photonic-band-gap. Angular spectroscopy at fixed wavelength ($\lambda=532$ nm) gives the period of the structure ~ 506 nm. Both AFM and MFM characterization of the samples is carried out. AFM results prove high-uniformity of inverted opal structure at the scale up-to $3 \times 3 \text{ mm}^2$. Magnetic properties of the samples were obtained using vibrating sample magnetometer technique in the range of magnetic fields up to 7kOe. Measurements of magneto-optical Kerr effect in transversal geometry demonstrate striking difference in magneto-optical spectra of inverted Ni opals in comparison with bulk Ni which indicates on the role of diffraction in magneto-optical response.

Another type of samples is fabricated by method of nanosphere lithography (NSL) [3]. The samples represent themselves 2D arrays of metallic islands on metallic surface. The first step of NSL for fabricating plasmon-active metallic nanoislands on metallic substrate is vacuum sputtering of Au or Ni thin film with thickness about 150-200 nm onto the silicon substrate. The second step is formation of a monolayer of polystyrene spheres metallic film by tilted or convective evaporation methods. The third step of NSL is vacuum sputtering of metal film with thickness about 50 nm onto the substrate using monolayer as a shadow mask. Then, polystyrene spheres are removed in ethanol solution in ultrasonic bath. As result of these steps well-ordered gold or nickel nanohills on gold-silicon or nickel-silicon substrate are formed. Optical and magneto-optical properties of such 2D structures in comparison with 3D inverted opals are considered. Detailed characterization of these structures utilizing AFM and MFM measurements show high uniformity of the structure.

The work is supported by grant of RFBR #07-02-012337-a.

[1]A. A. Fedyanin, O. A. Aktsipetrov, D. Kobayashi, K. Nishimura, H.Uchida, M. Inoue, *J. Magn. Magn. Mater.* **282** (2004) 256.

[2]V.I. Belotelov and A.K. Zvezdin, *J. Opt. Soc. Am. B* **22** (2005) 286.

[3]J. C. Hulteen and R. P. Van Duyne, *J. Vac. Sci. Technol. A* **13** (1995) 1553.

21PO-2-5

THERMODYNAMIC AND SPECTROSCOPIC STUDY OF RARE-EARTH CHROMIUM BORATES $\text{RCr}_3(\text{BO}_3)_4$ WITH $\text{R}=\text{Sm}, \text{Ho}, \text{AND Dy}$

*Popova E.A.¹, Vasiliev A.N.¹, Leonyuk N.I.¹, Boldyrev K.N.², Popova M.N.², Chukalina E.P.²,
Tristan N.³, Klingeler R.³, Büchner B.³*

¹Moscow State University, 119992 Moscow, Russia

²Institute of Spectroscopy RAS, 142190 Troitsk, Moscow region, Russia

³Leibniz-Institute for Solid State and Materials Research IFW Dresden,
01171 Dresden, Germany

Borates with the general formula $\text{RM}_3(\text{BO}_3)_4$ ($\text{R} = \text{Y}, \text{La} - \text{Lu}; \text{M} = \text{Al}, \text{Ga}, \text{Sc}, \text{Fe}, \text{Cr}$) have a trigonal structure of the natural mineral huntite. Recent studies of the rare-earth iron borates $\text{RFe}_3(\text{BO}_3)_4$ have shown that these compounds exhibit a variety of phase transitions. Their magnetic properties are governed by the presence of two interacting magnetic subsystems, i.e. the Fe^{3+} and the R^{3+} ones. It turns out that the magnetic structure of $\text{RFe}_3(\text{BO}_3)_4$ changes as a function of temperature, external magnetic field and substitutions in the rare-earth subsystem. Interestingly, at least two compounds belonging to the family of rare-earth iron borates, namely $\text{GdFe}_3(\text{BO}_3)_4$ and $\text{NdFe}_3(\text{BO}_3)_4$, display a considerable magnetoelectric coupling and their electric (magnetic) properties can be controlled by the magnetic (electric) field. This is a promising finding in view of possible device applications. Up to now, only little was known about the properties of the rare-earth borates $\text{RCr}_3(\text{BO}_3)_4$ with another magnetic ion, i.e. chromium. The first results on thermodynamic and optical properties $\text{NdCr}_3(\text{BO}_3)_4$ have been presented in a recent paper [1].

In this work, we have undertaken the first investigation of the thermal, magnetic, and optical properties of $\text{SmCr}_3(\text{BO}_3)_4$, $\text{HoCr}_3(\text{BO}_3)_4$ and of the optical properties of $\text{DyCr}_3(\text{BO}_3)_4$. $\text{SmCr}_3(\text{BO}_3)_4$ demonstrates peculiarities on the temperature dependences of the specific heat and of the spectral line shifts at the three temperatures, $T_1 = 8.2$ K, $T_2 = 6.7$ K, and $T_3 = 4.5$ K. The shift of the spectral line below $T_1 = 8.2$ K, is probably connected with the splitting of the Sm^{3+} Kramers doublets in the internal magnetic field that appears due to the magnetic phase transition. The nature of the specific heat peculiarity at $T_2 = 6.7$ K is not clear at the moment. An abrupt additional splitting and narrowing of spectral lines at $T_3 = 4.5$ K, accompanied by a sharp strong peak in specific heat suggests the first order spin-reorientation phase transition together with ordering of samarium magnetic moments. From the optical data, we have determined the upper limit of the ground-state splitting of Sm^{3+} ions. For $\text{HoCr}_3(\text{BO}_3)_4$, we have performed identification of Stark levels of Ho^{3+} . We observed peculiarities on the specific heat and optical line shifts at $T_1 = 8.8$ K and $T_2 = 6.7$ K. We assume that the phase transition at $T_1 = 8.8$ K corresponds to the antiferromagnetic ordering while the first-order phase transition at $T_2 = 6.7$ K is the spin reorientation. According to optical data, $\text{DyCr}_3(\text{BO}_3)_4$ undergoes two second-order phase transitions (at $T_1 = 8.9$ K and $T_2 = 7.3$ K) and the first-order phase transition at $T_3 = 5.0$ K. We discuss the physical nature of the observed phase transitions.

This work was supported by the Russian Foundation for Basic Research, Grants Nos. 07-02-01185, 04-05-64709, and 05-05-08021 and by the Russian Academy of Sciences under the Programs for Basic Research. The authors acknowledge funding by the Deutsche Forschungsgemeinschaft through Contracts Nos. HE-3439/6 and 436 RUS 113/864/0-1.

[1] E.A.Popova, N.I.Leonyuk, M.N.Popova, E.P.Chukalina, K.N.Boldyrev, Tristan N., Klingeler R., and Büchner B., Thermodynamic and optical properties of $\text{NdCr}_3(\text{BO}_3)_4$, Phys. Rev. B, **76** (2007).

21PO-2-6

EFFICIENT APPROACH TO THE COMPUTER MODELING OF MAGNETOOPTICAL AND TOROIDAL NANOSTRUCTURES

Kalish A.N.^{1,2}, Belotelov V.I.^{1,2}, Zvezdin A.K.^{2,3}

¹M.V. Lomonosov Moscow State University, 119992, Moscow

²A.M. Prokhorov General Physics Institute of RAS, 119991, Moscow

³Fondazione ISI, 10133, Torino, Italy

Magnetic nanostructured media offer a number of possibilities for applications due to significant improvement of optical and magneto-optical effects in comparison with uniform media. Recently materials with toroidal magnetic ordering have also become an object of interest and nanostructured toroidal media are of great interest as well [1]. An example of such nanostructured medium is a periodic grating. Thus a number of theoretical and experimental problems dealing with magnetic and toroidal gratings arise such as investigation of magnetic or toroidal material parameters influence on grating optical response or experimental optical determination of these material parameters and so on.

The most common method for determination of periodic gratings optical properties is based on rigorous coupled-waves analysis (RCWA) [2]. In this work we present a modified RCWA method that becomes more efficient for solving problems related with magnetic and toroidal gratings.

In this method the magneto-optical and toroidal parameters of the material are considered as perturbations due to their small values in comparison with dielectric permittivity. This approach allows to perform calculations much faster than using common RCWA method.

The essential point of common RCWA method is solving of matrix equation of the kind

$$\begin{pmatrix} \mathbf{J} \\ \mathbf{R} \end{pmatrix} = \mathbf{C}^{-1}(z_0) \left(\prod_{k=0}^{S-1} \mathbf{P}_k e^{-d_k \mathbf{D}_k} \mathbf{P}_k^{-1} \right) \mathbf{C}(z_s) \begin{pmatrix} \mathbf{T} \\ \mathbf{0} \end{pmatrix},$$

where S is the number of layers in the grating (d_k is the k -th layer's thickness), and the column vectors \mathbf{R} and \mathbf{T} are to be found. The matrices \mathbf{P}_k and \mathbf{D}_k depend on the k -th layer's material parameters and are found by means of solving an eigenvalue problem.

In our method the matrix $e^{-d_k \mathbf{D}_k}$ is replaced by $\mathbf{\Omega}_k = \int_{z_k}^{z_{k+1}} e^{-(z-z_k) \mathbf{D}_k} \mathbf{P}_k^{-1} \left(\frac{1}{d_k} \mathbf{I} - \mathbf{M}_k^{(1)} \right) \mathbf{P}_k e^{-(z_{k+1}-z) \mathbf{D}_k} dz$ where the matrix $\mathbf{M}_k^{(1)}$ is defined by the magnetic and toroidal material parameters. It makes the matrices \mathbf{P}_k and \mathbf{D}_k depend only on refractive indices. The principal advantage of this approach over the common RCWA method comes from the latter and is that while considering different materials with close values of refractive indices the corresponding eigenvalue problem is solved only once which makes computational resources to be used more efficiently.

The results of calculations presented in this work demonstrate the validity of the developed approach.

Support by RFBR (07-02-91588, 07-02-92183, 08-02-00717), "Progetto Lagrange-Fondazione CRT" and Russian foundation "Dynasty" is acknowledged.

[1] N. Kida, et al., *Phys. Rev. Lett.*, **96** (2006) 167202.

[2] N. Chateau, J.-P. Hugonin, *J. Opt. Soc. Am. A*, **11** (1994) 1321.

21PO-2-7

BAND GAP MAGNETOOPTICAL MATERIALS WITH LEFT-HANDED CONSTITUENTS

Yershova E.A.¹, Belotelov V.I.^{1,2}, Kalish A.N.^{1,2}, Zvezdin A.K.^{2,3}

¹M.V. Lomonosov Moscow State University, 119992, Moscow

²A.M. Prokhorov General Physics Institute of Russian Academy of Science, 119991, Moscow

³Fondazione ISI, 10133, Torino, Italy

Media with negative refractive index - left handed materials (LHM), attract particular attention due to their unusual properties. The main reason for such interest was the practical realization of these media from split ring resonators, that gives the opportunity to make a material with negative permeability and metal strips which are responsible for negative permittivity. The LHM can be interesting when they are combined with gyrotropy [1] and particularly as the constituents of band-gap magneto-optical materials.

In this work we investigate two kinds of the periodic multilayered magnetic structures (one-dimensional magnetophotonic crystals) with LHM constituents.

The first considered structure consists of two kinds of alternating layers. One of these layers is both gyrotropic and LHM. So its permittivity and permeability tensors have two non-diagonal components and negative diagonal components. Another kind of layers is a non-magnetic dielectric medium, and so non-diagonal elements in both its tensors equal zero.

The second magnetophotonic structure consists similarly of two different alternating layers, but in this case the first layer is magnetized, i. e. there are non-diagonal components, but diagonal elements have the positive values. The second one is left-handed but non-magnetic media, so that its permittivity and permeability tensors have zero non-diagonal components and negative diagonal components.

On the basis of the electro-dynamics transfer matrices method [2] spectra of optical reflection and transmission and Faraday rotation angle (in the reflected and transmitted light) were calculated. We have found that the magneto-optical properties of such structures acquire some additional peculiarities with respect to the case of conventional magnetophotonic crystals. These are Faraday rotation positive and negative resonances, pronounced transmission and reflection dependences on the magnetization. Obtained results demonstrate the potential of the gyrotropic LHM for creation of new functional materials.

As the LHM consists of complex structure of split rings and strips using of RCWA method is of interest. We have considered perspectives of the use of modified RCWA method described in [3]. This method is valid when the characteristic size of the structure is much less than the wavelength of the electromagnetic radiation, which is the case for the LHM. Comparison of the results obtained with the modified RCWA and transfer matrices method is conducted.

Finally, we analyze and discuss the role of time and spatial inversion symmetries break in the context of the considered magneto-optical effects.

This work is supported by RFBR (06-02-16801, 06-02-17507, 07-02-01445), "Progetto Lagrange-Fondazione CRT" and Russian foundation "Dynasty".

[1] Ivanov A.V., Kotelnikova O.A., Ivanov V.A., *JMMM* **300**, e67 (2006).

[2] Belotelov V.I., Zvezdin A.K., *JOSA B* **22**, 286 (2005).

[3] Kalish A.N., et. al, Efficient approach to the computer modeling of magneto-optical and toroidal nanostructures, *MISM 2008*.

21PO-2-8

TRANSIENT INVERSE FARADAY EFFECT AND ULTRAFAST SWITCHING OF MAGNETIZATION IN MAGNETIC MATERIALS

Kurkin M.I.¹, Bakulina N.B.¹, and Pisarev R.V.²

¹Institute of Metal Physics, Ural Division of RAS, 620041 Ekaterinburg, Russia

²Ioffe Physical Technical Institute of RAS, 194021 St. Petersburg, Russia

The processes of light-induced ultrafast demagnetization, switching of magnetization, phase transitions, and other phenomena have attracted a lot of attention during last decade. However the nature of microscopic mechanisms involved in these processes remains an issue of controversial debates. In this talk we present theoretical results on transient inverse Faraday effect and its possible involvement into the process of switching of magnetization. “Static” inverse Faraday effect (SIFE) is a nonlinear magneto-optical phenomenon observed when materials are excited with circularly polarized light pulses whose duration exceed orbital-lattice and spin-lattice relaxation times. Typically this effect in solids is observed with nanosecond laser pulses and the light-induced magnetization is measured with the use of the pick-up coils. In the pump-probe experiments with femtosecond laser pulses the pick-up coils are inefficient and the Faraday (Kerr) magneto-optical effects are used for monitoring changes of magnetic properties. We call these non-equilibrium changes as transient inverse Faraday effect (TIFE). By contrast to the SIFE which is defined exclusively by the equilibrium spin magnetization, the TIFE may contain orbital and spin contributions both of which are functions of time.

We propose a model in which optical transitions induced by circularly polarized femtosecond laser pulses transfer the orbital momentum $\pm\mathbf{L}$ to the magnetic medium. In the optical range direct coupling of light with spins via magnetic-dipole transitions is inefficient but it may become important in the infrared region nearby magnetic resonances. The electric-dipole processes result in a non-equilibrium orbital state but the spin moments \mathbf{S} remain unaffected. However they are coupled with the non-equilibrium orbital momentum L^{ne} by the spin-orbit interaction $V_{SL} = -\lambda L^{ne} S$. However we found that the direct transfer of non-equilibrium orbital momentum L^{ne} to the spin system cannot explain the reorientation of spins. In view of that we propose the following process of spin coupling with phonons (Ph):

$$S - V_{SL} - L^{ne} - V_{cf} - Ph, \quad (1)$$

where V_{cf} is the interaction of orbital momentum L^{ne} with the crystal field H_{cf} . We have to emphasize that the role of non-equilibrium orbital momentum L^{ne} is not to transfer the angular momentum to the spin system, but create necessary conditions for spin reorientation with participation of phonons. The latter can be regarded as an unlimited reservoir of angular momentum. Mathematically the conditions for these processes can be expressed in a form of an effective orbital field H_L which acts on spins due to spin orbit interaction V_{SL} :

$$H_L = -\frac{\partial V_{SL}}{\partial M_S} = -\frac{1}{2\mu_B} \frac{\partial V_{SL}}{\partial S} = \frac{\lambda}{2\mu_B} L, \quad (2)$$

where $M_S = 2\mu_B S$ is the spin magnetic moment and the direction of the vector \mathbf{H}_L (and \mathbf{L}^{ne}) is given by the chirality of the pump light. The field \mathbf{H}_L can induce the reorientation of \mathbf{M}_S due to lowering of the energy. However this process requires the transfer of the angular momentum to phonons that can be realized according to the process (1) when the interaction with phonons makes the vector \mathbf{L} to relax along the direction of the crystal field H_{cf} and the interaction V_{SL} makes dynamics of the spin system irreversible providing orientation of M_S along the field (2) during the relaxation time τ_S . However the interaction V_{cf} contains a part responsible for the quenching of the orbital magnetism during the life-time τ_L of L^{ne} . Finally the spin reorientation may occur if $\tau_L > \tau_S$. The question arises in what systems and how this criterion can be fulfilled.

This work is supported in part by the RFBR Projects #08-02-00904 and #06-02-17030.

21PO-2-9

REFLECTANCE SPECTRA OF PHOTONIC CRYSTALS, FILLED BY FERRITES

Gorelik V.S.¹, Gryasnov V.V.¹, Samoilovich M.I.², Yurasov N.I.¹

¹P.N. Lebedev Physical Institute of Russian Academy of Sciences, Moscow, Leninsky prosp.,53, 119991, Russia, e-mail: gorelik@sci.lebedev.ru

²OAO CNII Tehnomash, Moscow, I.Franko, 4

Optical properties of globular photonic crystals – artificial opals, consisting from monosized silica globules [1], have been investigated. Sizes of globules depended on conditions of 3D-photonic crystals growth and were 200-400 nm. Pores occupied 26 percent of total volume of photonic crystal. Such pores were filled by ferrites: Fe-Ni and Fe-Co. Reflectance spectra of prepared samples of 3D-photonic crystals in visible region have been investigated. Halogen lamp has been used as a source of light. Reflectances spectra have been obtained with the help of fiber optic technique and have been recorded by minispectrometer. Parameters of dispersion laws were calculated from reflectance spectra, revealing the forbidden zone in visible region. An approximation of one-dimensional photonic crystal dispersion law has been used. Such approximation described the dispersion law for [111] direction of three dimensional photonic crystal. The influence of ferrites presence inside porous of photonic crystals has been established. For the second photonic band, corresponding to visible or ultraviolet region in our photonic crystals, the refraction index becomes negative; besides, for this band the effective mass of photons is negative at small impulse value and positive with impulse increase. We have analyzed the influence of magnetic field on reflectance spectra of investigated photonic crystals. Conditions of Faraday and Cotton-Mutson effects observation have been established.

Support by Russian Foundation for Basic Research. Project Numbers: 07-02-00106, 07-02-12027 and 08-02-00114.

[1] V.S. Gorelik. Bound and dark photonic states in globular photonic crystals. *Acta Phys. Hung. B* 26/1-2 (2006) 37-46.

21PO-2-10

EXPERIMENTAL DEMONSTRATION OF OPTICAL TAMM STATES IN ONE-DIMENSIONAL MAGNETOPHOTONIC CRYSTALS

Goto T.¹, Dorofeenko A.V.², Merzlikin A.M.², Baryshev A.V.^{1,}, Vinogradov A.P.², Inoue M.¹, Lisyansky A.A.³, Granovsky A.B.⁴*

¹Toyohashi University of Technology, Toyohashi 441-8580, Japan

²Institute for Theoretical and Applied Electromagnetics, Moscow 125412, Russia

³Queens College of the City University of New York, Flushing, NY 11367

⁴Moscow State University, Moscow 119992, Russia

We experimentally demonstrate a new type of one-dimensional magnetophotonic crystals (1D MPCs). A localized surface state, the so-called optical Tamm state predicted theoretically in [1], was observed at the internal interface of a 1D MPC. Such a state provides a sharp transmission peak within the photonic band gap of the MPC and a significant enhancement of Faraday rotation for the corresponding wavelength.

The experimental samples were composed of two photonic crystals [nonmagnetic photonic crystal (PC1) and magnetic photonic crystal (PC2)] and had the following structure, a quartz substrate/ $\text{Ta}_2\text{O}_5/(\text{SiO}_2/\text{Ta}_2\text{O}_5)^5/(\text{Bi:YIG}/\text{SiO}_2)^5$ multilayer. These were designed to exhibit optical Tamm states at the interface between PC1 and PC2 for light of a chosen wavelength. The samples were fabricated by ion beam sputtering. Experimental transmission spectra of PC1, PC2 and 1D MPC (joint PC1 and PC2) are shown in Fig. 1. One can see photonic band gaps of PC1 and PC2 in the spectral range of 650 to 1000 nm and a transmission peak inside the photonic band gap of the MPC at 800 nm; transmissivity was $\approx 37\%$. Significant enhancement of the Faraday rotation (θ_F) was observed at the wavelength of 800 nm. If compared with θ_F of the magnetic PC2, the Faraday rotation of the MPC was ≈ 8 times larger.

It is worth noting that structures exhibiting optical Tamm states can be useful for localizing light within any active material used as the constitutive layers of PCs or introduced at the interface between two PCs.

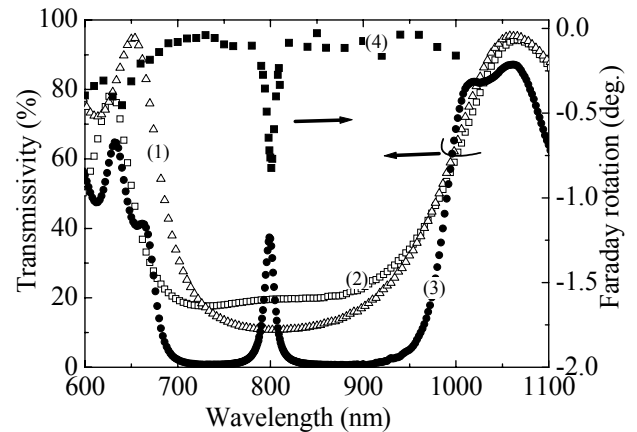


Fig. 1 Transmission spectra of PC1 (1), PC2 (2) and the 1D MPC (3). Faraday rotation spectrum of the 1D MPC (4).

[1] A.P. Vinogradov, A.V. Dorofeenko, S.G. Erokhin, M. Inoue, A.A. Lisyansky, A.M. Merzlikin, A.B. Granovsky, *Phys. Rev. B* **74**, 045128 (2006).

21PO-2-11

MAGNETOSTATIC WAVES IN PHOTON-MAGNETIC CRYSTAL BRILLOUIN ZONE

Annenkov A.Yu., Gerus S.V.

Institute of Radio Engineering and Electronics (Fryazino Branch),
Russian Academy of Sciences,
sq. Vvedenskogo 1, Fryazino, Moscow oblast, 141190 Russia

Propagation of electromagnetic waves in periodic artificial media (photonic crystals) [1] has attracted much attention in recent years. It is assumed that the period of a crystal is comparable with the radiation wavelength. In this case, transverse electromagnetic waves (polaritons) play the same role as electrons in conventional crystals. The difference between the Maxwell equations and the Schrödinger equation leads to some specificity of photonic crystals; however, there is a close analogy between them and electronic crystals: gaps are observed in photonic crystals, as well as defect and surface states. In this study, we consider the case where

magnetostatic spin waves are an analog of electrons. Such a magnetic photonic crystal is implemented on the basis of an yttrium iron garnet (YIG) film magnetized to saturation in a uniform bias field. Surface magnetostatic spin waves can propagate through such a film. To form a photonic crystal, a spatially periodic magnetic structure is imposed on a film. The magnetic field of this structure, penetrating the YIG film, modulates its magnetic permeability, thus forming a magnetic photonic crystal [2]. We used a high-coercivity ($H_C = 1000$ Oe) magnetic tape with a recorded sinusoidal signal to form a one-dimensional magnetic crystal.

Waves in a YIG film are excited by a microwave current passing through a thin wire (antenna), which is pressed against the film surface. The transmitted wave is detected by a similar receiving antenna. Wave vector of a surface magnetostatic spin wave is oriented perpendicularly to the direction of the bias field, which lies in the YIG film plane [2], and the reverse vector of the recorded signal is perpendicular to the bias field.

In the pan mode, a dip is observed in the amplitude–frequency characteristic of the measuring device, which corresponds to the band gap [1]. Obviously, a wave penetrates the magnetic photonic crystal at band gap frequencies; however, its exponential (on average) decay, related to the imaginary part of the Bloch wave vector (Lyapunov index), is observed. In this study, we experimentally measured the frequency dependence of the Lyapunov index. To this end, the signal amplitude was measured at a specified frequency, with a displacement of the receiving antenna along the propagation direction of the surface magnetostatic spin wave. Frequency dependence of the Lyapunov index for the Brillouin zone is shown on Fig. 1. It can be seen that this dependence has a characteristic bell-shaped form.

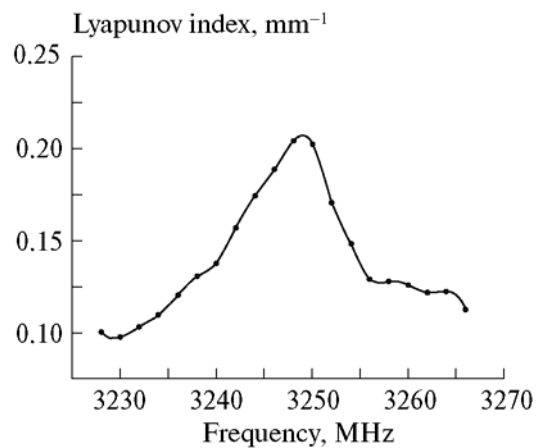


Fig. 1. Lyapunov index for a surface magnetostatic spin wave of a magnetic crystal in the band gap region.

This work is supported by RFFR pr. №07-02-00233a.

[1] J. D. Joannopoulos, R. D. Meade, J. N. Winn, *Photonic Crystals: Molding the Flow of Light*, Princeton: Princeton Univ. Press, 1995.

[2] A. V. Voronenko, S. V. Gerus, and V. D. Kharitonov, *Izv. Vyssh. Uchebn. Zaved., Fiz.*, 1988, no. 11, p. 76.

21PO-2-12

MAGNETOSTATIC WAVE PATTERN VISUALIZATION IN PHOTON-MAGNETIC CRYSTAL

Annenkov A.Yu., Gerus S.V.

Institute of Radio Engineering and Electronics (Fryazino Branch),
Russian Academy of Sciences,
sq. Vvedenskogo 1, Fryazino, Moscow oblast, 141190 Russia

The distribution of the magnetostatic surface waves in the artificial magnetic crystals is studied. As it is known, magnetostatic waves are excited in the ferrite media magnetized by a bias field. As a ferrite the YIG film which was tangentially magnetized to saturation by a magnetic field of 500 Oe was used. The magnetic crystal was created by sine signal written to a magnetic recorder tape. The magnetic field of the tape created in YIG film spatially - periodic modulation of the magnetic permeability. The designed in this way media can be considered as magnetic analogue of an one-dimensional photon crystal. Coercitivity of a recorder tape was higher than 1000 Oe, and because of this it did not demagnetized in a bias field. For excitation and receiving of magnetostatic waves the single wire transducers were used. Transducers were putted down to YIG film under some angle to a bias field that corresponded to excitation of magnetostatic surface waves (MSSW).

In Fig. 1 the mutual positioning of transducers and a recorder tape in relation to the bias field are schematically represented. Vector network analyzer was used in the experiments.

The excited MSSW passed through a region with the induced magnetic crystal and then it was received by the output transducer. On the amplitude-frequency characteristic the rejection corresponding to reflection of MSSW at the edge of Brillouin zone was observed. The scanning of a surface of YIG film has been carried out for studying the interaction of MSSW and magnetic crystal. It has allowed getting two-dimensional distribution of MSSW amplitude on the film surface that is represented in the Fig. 2. The received data allow to see and study the reflection MSSW caused by the magnetic crystal.

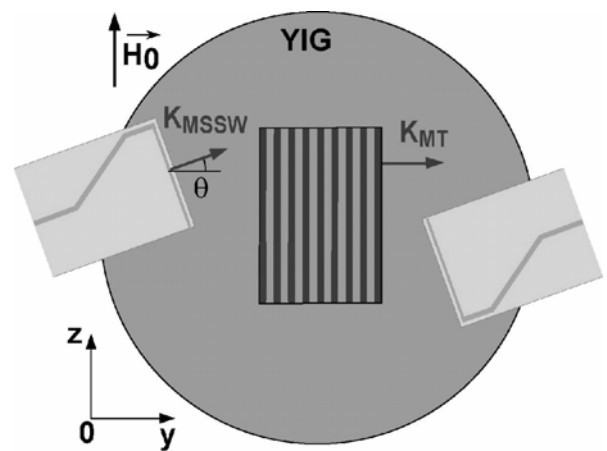


Fig. 1

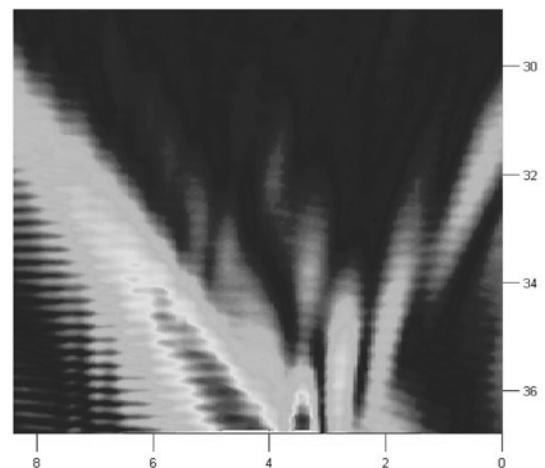


Fig. 2

This work is supported by RFFR pr. №07-02-00233a.

21PO-2-13

PUMP-PROBE MAGNETO-OPTICAL SPECTROSCOPY OF ULTRAFAST SPIN DYNAMICS IN TbFeCo THIN FILMS

Gofman M.S.^{1,2}, Ashitkov S.I.¹, Agranat M.B.¹, Granovsky A.B.²

¹Joint Institute for High Temperatures, RAS, Moscow 125412, Russia

²Faculty of Physics, Moscow State University, Moscow 119991, Russia

Development of ultrafast information magnetic storage, THz spintronics, magnetic holography, ultrafast modulators of light, all-optical magnetization reversal requires femtosecond spin manipulation and control. The physical processes that govern the spin dynamics in ferromagnets on nanosecond and picosecond timescale was studied by magneto-optical technique for the first time in 1984 [1] and are still under debate. During timescales comparable or even shorter than the characteristic response times of the magnetic system the validity of conventional thermodynamic concepts for describing a magnetic system become questionable.

We have performed time-resolved magneto-optical Faraday effect measurements of magnetization dynamics in TbFeCo thin films with femtosecond ($\approx 10^{-13}$ s) resolution in a pump-probe experiment using a 100 fs pulsed laser ($\lambda=780$ nm). In comparison with our previous study of spin dynamics in these films [2] we improve both temporal and spatial resolution as well as significantly increase a power of laser pulses. The films were heated to the Curie temperature in the amorphous state and to the crystallization temperature. It is shown that the spin subsystem is heated to the Curie temperature about 10 ps after the end of the laser pulse.

[1] M.B. Agranat, S.I. Ashitkov, A.D. Granovsky, et al. JETP **86** (1984) 1376.

[2] M.B. Agranat, S.I. Ashitkov, A.V. Kirillin, et al. JETP Lett. **67** (1998) 953.

21PO-2-14

THREE-DIMENSIONAL MAGNETOPHOTONIC HETEROSTRUCTURES: FABRICATION AND MAGNETO-OPTICAL RESPONSE

Dokukin M.E.^{1,2}, Khanikaev A.B.¹, Baryshev A.V.^{1,3}, Inoue M.¹

¹Toyohashi University of Technology, Toyohashi, Aichi 441-8580, Japan

²Faculty of Physics, Moscow State University, Leninskie gory, 119992, Moscow, Russia

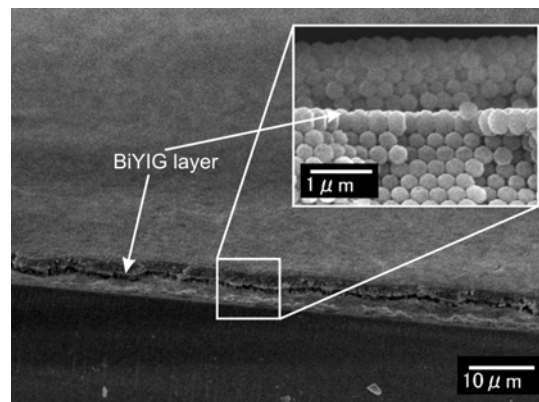
³Ioffe Physico-Technical Institute, St. Petersburg 194021, Russia

Photonic crystals with embedded magneto-optically active constituents, magnetophotonic crystals (MPCs), are shown to exhibit unique optical and magneto-optical (MO) properties [1]. These structures are of great interest due to the possibility to control light flow by magnetic field.

In the present work we have studied optical and MO properties of three-dimensional MPC heterostructures. These heterostructures composed of a Bi:YIG layer sandwiched in between two thin high quality opal films were fabricated by an improved vertical deposition method. The fabrication steps were as follows. The quartz substrates were introduced into the colloidal suspension of monodisperse SiO₂ spheres 290 nm in diameter (Nippon Shokubai Co.) with the concentration of 0.05 wt.%. In the atmosphere with the humidity of 80% and at the temperature of 80°C, SiO₂ spherical particles were deposited onto the substrates forming the first opal film (a sequence of the two-dimensional hexagonal (111) layers [2]). The Bi:YIG layer was formed atop of the first opal film using the ion-beam sputtering technique. The second opal film

was deposited on the top of the Bi:YIG at the same conditions as for the first layer. The as-deposited heterostructures were subjected to annealing at 750°C to crystallize Bi:YIG layer and to harden the opal structure.

The properties of the 3D MPCs were evaluated using the field emission scanning electron microscope (FESEM, Jeol JSM-6700), spectrophotometer (Shimadzu UV-3100PC) and magneto-optical set-up (Neo Ark BH-M600VIR-FKR-TU). The cross-section of the structure under study is shown in the figure. Angle- and polarization-dependent transmission spectra of the heterostructures exhibit Fabri-Perot resonant peaks within the stop-band region of the opal films. For light with the wavelengths of transmission resonance, the significant enhancement of Faraday rotation was found. It is worth noting that these 3D MPCs act in the similar way as their 1D counterparts [1, 3], but possess richer properties. For example, 3D MPCs exhibit various stop bands due to diffraction from the fcc lattice, the regime of multiple Bragg diffraction. It was also found that diffraction from the 2D periodicity of the textured Bi:YIG layer has significant impact on the optical response of the structures. We found that the heterostructure with the 140-nm-thick Bi:YIG film exhibited a specific regime where polarization rotation changes from 1.5 to -1.5 deg. in the narrow spectral range of 10 nm.



The cross-section of a 3D MPC: a Bi:YIG defect layer is sandwiched in between two opal films.

- [1] M. Inoue, R. Fujikawa, A. Baryshev, et al., *J. Phys. D: Appl. Phys.*, **39** (2006) R151.
 [2] P. Jiang, J. F. Bertone, K. S. Hwang, and V. L. Colvin, *Chem. Mater.*, **11** (1999) 2132.
 [3] A. Khanikaev, A. Baryshev, R. Fujikawa, P. B. Lim, M. Inoue, A. B. Granovsky, *Proc. SPIE*, **6182** (2006) 61820M.

21PO-2-15

FEATURES OF DC ELECTRIC FIELD IN POLARITON DYNAMICS OF ONE-DIMENSIONAL MAGNETIC PHOTONIC CRYSTAL

Kulagin D.¹, Kotov V.², Shavrov V.², Savchenko A.¹, Tarasenko S.¹

¹Donetsk Institute for Physics and Engineering of NASU, Donetsk, Ukraine

²Institute of Radioengineering and Electronics of RAS, Moscow, Russia

In contexts of methods of transfer matrix and effective medium, features of polariton dynamics of semi-bounded magnetic photonic crystal (MPC) are investigated. One-dimensional superlattice of “easy-axis ferromagnet – nonmagnetic dielectric” type is chosen as a basis for photonic crystal. The MPC is in external dc electric field. Two types of interlayer exchange of tangentially magnetized layers are considered: ferro- and antiferromagnetic. The conditions are determined for a one-dimensional MPC, under which square-low magneto-optical interaction leads to a number of anomalies upon propagation and localization of bulk waves of TE and TM types. Electromagnetic wave falls from without on a surface of superlattice.

In particular, in a case of ferromagnetic interlayer exchange for thin layer MPC, it is shown:

1) Independent existence of normal magnetic polaritons of TE and TM types is possible only in a case $\mathbf{k} \in XY$ (\mathbf{k} – wave vector of an electromagnetic wave). But for all that the formation of a surface wave is possible only TE type.

2) In presence external dc field even in model of unbounded MPC, the spectrum of bulk magnetic TE polariton is nonreciprocal ($\omega(\mathbf{k}) \neq \omega(-\mathbf{k})$) relatively inversion of wave line along an unit vector $[\mathbf{E}_0 \mathbf{M}_0] / [|\mathbf{E}_0 \mathbf{M}_0|]$.

3) Conditions of distribution and localization of bulk TE polaritons on a border “MPC - nonmagnetic dielectric” type essentially being dependent on what ordered vector triple (left or right) form positive directions of vectors \mathbf{k}_x , \mathbf{M}_0 and \mathbf{E}_0 .

4) In conditions of total reflection, inhomogeneous polaritonic TE wave can decrease deep into photonic crystal either monotonously or with oscillation, depending on size and orientation of an external dc electric field.

5) Abnormal modes of refraction of bulk magnetic TE polariton induced by external dc field are possible.

In a case of antiferromagnetic interlayer exchange for thin layer MPC, it is shown: (thicknesses of magnetic layers are equal):

1) If thicknesses of magnetic layers are equal then photonic crystal is nongyrotropic.

2) Independent existence of normal magnetic polaritons of TE and TM types are possible both in a case $\mathbf{k} \in XY$, and in a case $\mathbf{k} \in YZ$. But for all that formation of surface TE mode is possible at $\mathbf{k} \in XY$, and surface TM mode is possible at $\mathbf{k} \in YZ$.

3) The view of spectrum of surface TE or TM polaritons essentially being dependent on the sign of projection of an external dc electric field on a direction normal line to boundary of magnetic and nonmagnetic media.

21PO-2-16

MAGNETO-OPTICAL EFFECTS IN EXCITONIC ONE-DIMENSIONAL STRUCTURES

Erokhin S.¹, Deych L.², Lisyansky A.², and Granovsky A.¹

¹Faculty of Physics, M.V.Lomonosov Moscow State University, Leninskie Gory,
Moscow 119991, Russia

²Queens College of the City University of New York, 65-30 Kissena Blvd., Flushing,
New York, 11367, USA

Giant Zeeman-splitting of excitonic states in low Curie temperature diluted magnetics semiconductors, for example in GdMnTe, provides record values of magneto-optical effects but only at low temperatures. Quantum confinement effects in a quantum well significantly modify properties of excitons resulting in increased binding energies and oscillator strengths. As a result, the exciton related effects even in III-V semiconductor compounds could be observed at room temperature. Besides, recently developed diluted magnetic semiconductors and oxides with high Curie temperatures make excitonic magneto-optics promising for various magnetophotonic applications.

We present theoretical investigation of excitonic magneto-optical effects in one-dimensional magnetophotonic crystals [1] with Fabry-Perot resonator structure. The most prominent feature of the crystal in our case is that it is based on quantum well system. Such materials belong to the class of so-called resonant photonic crystals. Light propagates through such structures in the form of polaritons and the optical properties of such structures are very sensitive to the excitonic characteristics of constituting materials [2].

In this work we used the approach developed by Ivchenko et al [3] to take into account a non-local character of interaction of light with excitons and transfer matrix approach to numerically calculate the magneto-optical response of Fabry-Perot exciton resonator structure in the case of normal incidence of light. Obtained results show that Faraday rotation can be increased up to 5 times in magnetophotonic crystals based on quantum well in comparison with non-resonant structures. The developed algorithm can be also applied to magneto-optics in multiple quantum wells periodical structures.

Support by the Russian Foundation for Basic Research and Dynasty Foundation is acknowledged.

- [1] M.Inoue, R.Fujikawa, A.Baryshev, A. Khanikaev, P.B.Lim, H. Uchida, O. Aktsipetrov, A. Fedyanin, T. Murzina, A. Granovsky, Magnetophotonic crystals, *J. Phys. D: Appl. Phys.*, **39** (2006) R151.
 [2] E.L Ivchenko, M.M. Voronov, M.E. Erementchouk, L.I. Deych, A.A. Lisiansky, *Phys. Rev. B.*, **70** (2004) 195106.
 [3] E.L. Ivchenko, A.V. Kavokin, V.P. Kochereshko, et al. , *Phys. Rev. B.*, **46** (1992) 7713.

21PO-2-17

NONLINEAR OPTICAL STUDIES OF MAGNETIC GARNET FILMS

Maydykovskiy A.I.¹, Dubrovina N.V.¹, Razdolski I.E.¹, Aktsipetrov O.A.¹, Levy M.²

¹Department of Physics, Moscow State University, 119991 Moscow, Russia

²Departments of Physics and Materials Science and Engineering, Michigan Technological University, Houghton, Michigan 49931

Magneto-optical garnet films are a well-known material which is currently used in various types of optoelectronic devices and are potential for the applications in nonreciprocal devices, such as optical isolators and circulators. This high applicability of garnets originates from their unique magneto-optical properties, which combine high Faraday rotation with low optical losses in the near-infrared region, which is of high interest for the optical communication through glass fiber. At the same time, a task remains to figure out the technological parameters of the composition and fabrication of garnets, that are responsible for the achievement of high values of magneto-optical activity and for a good crystalline quality as well. One of the possible ways to realize such films is to introduce epitaxial stress in thin garnet films.

In this paper, thin epitaxial garnet films are fabricated on gallium gadolinium garnet (GGG) substrates and their crystallographic structure and magneto-optical response are studied using the nonlinear-optical probe of second harmonic generation (SHG).

Garnet films of the thickness of 400÷900 nm were epitaxially grown by RF-Magnetron sputtering method on (111) GGG substrate. The following parameters of the deposition procedure were varied: base pressure, sputtering time, flow rate of oxygen and argon.

SHG experiments are performed using the output of the Ti-sapphire laser (at 800 nm wavelength, pulse duration of 80fs) as a fundamental radiation. For the magneto-optical characterization of the films the geometry of the transversal nonlinear magneto-optical Kerr effect (NOMOKE) is used.

Strong influence of the deposition parameters on azimuthal SHG dependencies from the samples fabricated under different conditions is observed. Namely, we obtain that the annealing in O₂ atmosphere results in a breaking of crystallographic structure of a subsurface layer. Figure 1 shows the SHG azimuthal patterns measured for the p-in, p-out and p-in, s-out

combinations of polarizations for the samples (fig1(a) shows pattern for film prepared without oxygen, fig(b) with oxygen.). We observed that SHG effectiveness strongly depends on growth parameters.

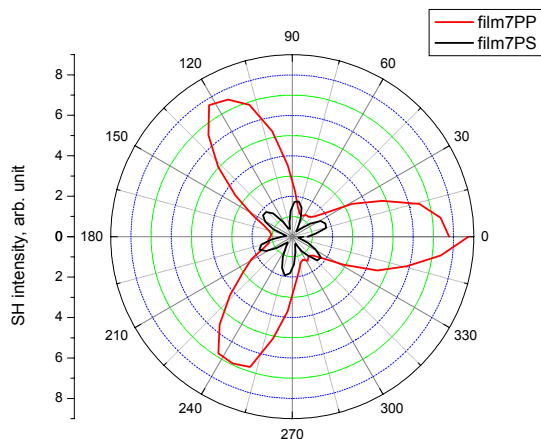


Fig 1(a)

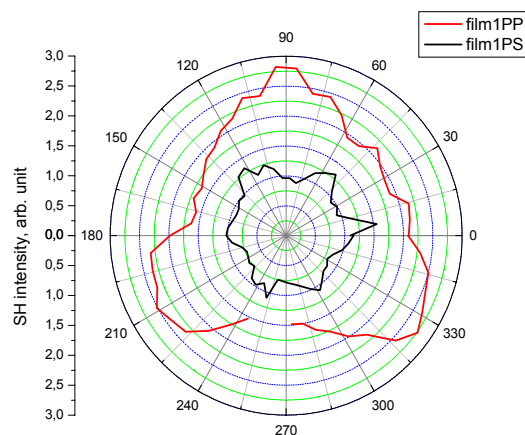


Fig1 (b)

- [1] M. Inoue, R. Fujikawa, A. Baryshev, et. al., *J. Phys. D: Appl. Phys.*, **39**, (2006) R151.
 [2] I.E. Razdolsky, T.V. Murzina, O.A. Aktsipetrov, M. Inoue. *JETP Lett.*, **84**, (2006) 451.

21PO-2-18

NONLINEAR OPTICS OF MAGNETIC NANOPARTICLES

Kolmychek I.A.¹, Murzina T.V.¹, Fourier S.², Wouters J.², Verbiest T.², Aktsipetrov O.A.¹

¹Department of Physics, Moscow State University, 119991 Moscow, Russia

²Institute for Nanoscale Physics and Chemistry (INPAC), Molecular and Nanomaterials, Katholieke Universiteit Leuven, Celestijnenlaan 200 D, B-3001 Leuven, Belgium

Optical and nonlinear optical properties of nanostructures are the subject of intensive investigations during the last few decades. Previous studies of them have been focused mostly on noble-metal nanoparticles which display resonances in the optical-absorption spectrum dependent on the particles' size, shape, and inter-particle spacing. Magneto-optically active nanoparticles are very perspective as they could have applications in the emerging field of nanophotonics, data storage, or sensing [1]. In this work, magnetization-induced second harmonic generation (SHG) is applied for the studies of the nonlinear magneto-optical properties of magnetic nanoparticles. Magnetization-induced SHG is an extremely sensitive probe of magnetism of surfaces and nanostructures.

Two types of magnetic nanoparticles are studied: Fe₃O₄ (magnetite) nanoparticles embedded in polymethylmethacrylate (PMMA) matrix and plasmonic core(shell) γ -Fe₂O₃(Au), both deposited on glass substrate. Core-shell nanoparticles consist of Fe₂O₃ core 20-25 nm in diameter, and the Au shell of the thickness about 2-4 nm. These structures demonstrate the plasmon resonance at the wavelength of about 550 nm. Magnetite nanoparticles in PMMA have the average diameter about 20-25 nm. The size distribution of nanoparticles is very narrow.

For the nonlinear magneto-optical experiments, the 0.5 MW/cm² 10 ns pulses of 1064 nm YAG: Nd³⁺ laser were used. The second harmonic radiation generated in transmission through the samples at the angle of incidence of 45° was detected by a photomultiplier and gated

electronics. The transversal magnetic field up to 4 kOe was applied to the samples. The measure of the magnetization-induced SHG is the magnetic contrast: $\rho_{2\omega} = (I_{2\omega}(\uparrow) - I_{2\omega}(\downarrow)) / (I_{2\omega}(\uparrow) + I_{2\omega}(\downarrow))$, where $I_{2\omega}(\uparrow)$ and $I_{2\omega}(\downarrow)$ are the SHG intensities measured for the opposite directions of the applied magnetic field. The value of the SHG magnetic contrast characterizes the ratio of the magnetic to the nonmagnetic components of the second order susceptibility tensor [2].

The SHG generated by the samples was diffuse and depolarized, that are the intrinsic features of the hyper-Rayleigh scattering. This type of the nonlinear-optical response is attributed to incoherent response of nanoparticles, the averaged SHG intensity is proportional to the number of the nonlinear scatterers (nanoparticles). The value of $\rho_{2\omega}$ is determined by the ratio of the magnetic to nonmagnetic components of the hyperpolarizability of a *single* nanoparticle and can serve for the characterization of its magnetic properties.

The dependencies of the SHG magnetic contrast on the value of the applied *dc* magnetic field were measured for the both types of samples. For the core(shell) nanoparticles the value of $\rho_{2\omega}$ increases continuously with the increase of the magnetic field, and reaches the value of about 25% at the field 3.3 kOe. For the magnetite nanoparticles in PMMA such dependence is close to a linear function of the magnetic field and saturates in the fields of about 2.5~3 kOe. These values correspond to the saturating values of the magnetization of magnetite nanoparticles obtained for the magnetization loops measurements. One can evaluate the ratio of the magnetic to nonmagnetic components of the hyperpolarizability of a single nanoparticle, $\gamma^M/\gamma^0 \sim 0.4$ for both types of nanoparticles in the field about 3 kOe.

[1] D. A. Smith, Yu. A. Barnakov, B. L. Scott, S. A. White and K. L. Stokes, "Magneto-optical spectra of closely spaced magnetite nanoparticles", J. Appl. Phys. **97**, 10M504 (2005).

21PO-2-19

MAGNETO-OPTICAL SPECTROSCOPY OF Tm^{3+} AND Yb^{3+} IONS IN HUNTITE STRUCTURE

Malakhovskii A.V., Sokolov A.E., Sukhachev A.L., Temerov V.L., Edelman I.S.

L.V. Kirensky Institute of Physics Siberian Branch Russian Academy of Sciences ,
660036 Krasnoyarsk, Russia

Present work is devoted to investigation of absorption and magnetic circular dichroism (MCD) spectra of $\text{Yb}_x\text{Tm}_{1-x}\text{Al}_3(\text{BO}_3)_4$ crystals ($x=0, 0.1, 0.2, 1.0$). These crystals are of interest from view point of laser generation.

They have huntite type structure with the space group R32. Trivalent rare-earth (RE) ions occupy only one type positions with the local symmetry D_3 at room temperature. Ions Yb^{3+} and Tm^{3+} have half integer and integer total moment, respectively. This difference substantially influences interpretation of optical and magneto-optical properties of the corresponding crystals.

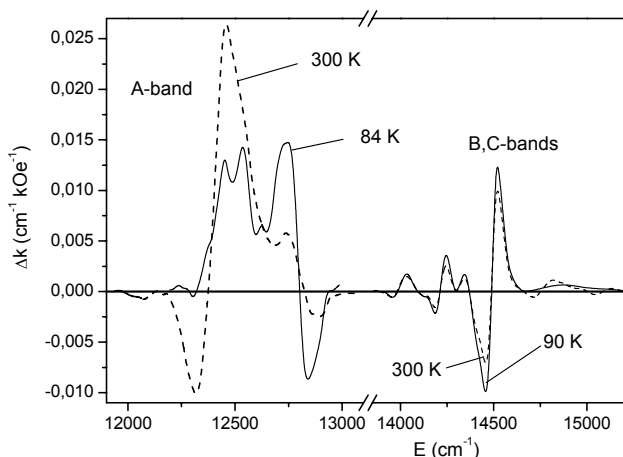


Fig. 1. MCD of ${}^3\text{H}_6\text{-}{}^3\text{H}_4$ (A) and ${}^3\text{H}_6\text{-}{}^3\text{F}_3, {}^3\text{F}_2$ (B,C) transitions of Tm^{3+}

We have studied temperature dependence of absorption and MCD of the transition ${}^2F_{7/2-}$ ${}^2F_{5/2}$ in Yb^{3+} ion and of the transitions ${}^3H_6 \rightarrow {}^3H_4$ (*A*-band) and ${}^3H_6 \rightarrow {}^3F_3, {}^3F_2$ (*B, C*-bands) in Tm^{3+} ion. As a consequence, we have obtained temperature dependences of paramagnetic magneto-optical activity (MOA) of enumerated transitions (the ratio of the zero moments of MCD and absorption bands). Spectra MCD in Tm^{3+} ion are shown in Fig. 1. MOA of the transition in Yb^{3+} at room temperature is $A_{\text{exp}}=1.46$ in the units of $\mu_B H/kT$. MOA of the transitions in Tm^{3+} are 2.0 and 0.24, respectively. Yb^{3+} ion has half-integer total moment. Therefore, in any CF all states are at least doubly degenerated and have magnetic moment. Consequently, temperature dependent MCD (*C*-term) will exist. This effect is usually much larger than the mixing effect. The trigonal CF splits states of Tm^{3+} ion with an integer total moment into states with a less than threefold degeneracy. These states do not have a magnetic moment. Accordingly, there should be no a paramagnetic term *C* of the MCD. However, if the splitting of states in the trigonal crystal field is small, the components of this splitting exhibit a strong *B*-type paramagnetic effect equal in magnitude but opposite in sign with a magneto-optical activity of the order of $\mu_B H/\Delta$, where Δ is the splitting in the trigonal CF. If these effects originate from the splitting of the ground state, the band-integrated effect may be different from zero because of the difference in the population of the splitting components of the ground state in the trigonal CF. As a result, the integrated MOA will be of the order of the product: $(\mu_B H/\Delta) * (\Delta/kT) = \mu_B H/kT$. Thus, the magnetic circular dichroism of *B, C*-band is predominantly due to the splitting of the excited state, whereas the magnetic circular dichroism of *A*-band is governed primarily by the splitting of the ground state in the trigonal crystal field. Maximum possible MOA of all transitions were estimated in the framework of the model presented in [1]. Temperature dependences of MOA do not follow the Curie law, and this is discussed.

Support by RFBR grant No 07-02-704 is acknowledged.

[1] A.V. Malakhovskii, V.A. Isachenko, A.L. Sukhachev, A.M. Potseluyko, V.N. Zabluda, T.V. Zarubina, I.S. Edelman, Phys. Solid State, **49** (2007) 701-707.

21PO-2-20

ANALYSIS OF MAGNETOREFRACTIVE EFFECT IN Fe/Cr/Fe/Cr/Fe STRUCTURE

Yurasov A.N.¹, Granovsky A.B.², Sukhorukov Yu.P.³

¹Moscow State Institute of Radioengineering, Electronics and Automation (Technical Univesity),
Moscow 119454, Russia

²Faculty of Physics, Moscow State University, Moscow 119991, Russia

³Institute of Metal Physics, Ural Division of RAS, Ekaterinburg 620041, Russia

The magnetorefractive effect (MRE) is a high frequency analogy of magnetoresistance (MC) and consists in variations of the coefficients of reflection, transmission and absorption of electromagnetic waves of samples with GMR, TMR or CMR under magnetization (see [1,2] and references therein). In spite of success in a qualitative explanation of MRE in multilayers, all-metallic granular alloys, nanocomposites, and manganites there is still a misunderstanding of a lot of experimental data [1,2]. Recently, the magnetotransmission and magnetoreflexion of light for Fe/Cr/Fe/Cr/Fe structure have been studied from 70 to 300 K in a wide spectral range in a magnetic field up to 8 kOe [3]. Since this multilayer Fe/Cr/Fe/Cr/Fe has the intermediate Fe layer thinner than the outer Fe layers, and therefore it is a pseudo-valve structure and exhibits GMR up to 10%, one can expect that its magnetotransmission and magnetoreflexion both are

due to MRE. But some of obtained experimental data are in a strong disagreement with developed theories for MRE in multilayers. We analyzed numerically MRE for Fe/Cr/Fe/Cr/Fe structure in the framework of the self-averaged limit [4]. It was shown that the sign, magnitude, frequency dependencies of MRE in reflection and transmission modes are very sensitive to the model parameters and a sample thickness. We obtained an overall qualitative agreement with the experimental data but failed to explain the frequency dependencies of magnetotransmission at 0.8-2 μm and temperature dependences of magnetotransmission. It was proposed that the peculiarities of magnetotransmission at 0.8-2 μm are not due to MRE but originates from the change of interband optical transitions under magnetization. Besides, the theory does not take into account that s-like electrons responsible for magnetoresistance and MRE but both s- and d-like electrons are responsible for optical properties. That is a possible reason for the quantitative disagreement and invalidity of the strict correlation between MRE and magnetoresistance.

This work was supported by the Russian Foundation for Basic Research.

[1]. A.B. Granovsky, E.A. Ganshina, A.N. Yurasov, et al. J. Commun. Technol. Electron. **52** (2007) 1065

[2] A.B. Granovsky, M. Inoue J. Magn. Mater, 272-276, Suppl.1, (2004) E1601.

[3] A.V. Telegin, et al. Books of Abstracts, MISM-2008

[4] J.C. Jacquet, T.Valet Mater. Res.Soc.Symp.Proc. **384** (1995) 477

21PO-2-21

SECOND HARMONIC GENERATION IN ALL-GARNET MAGNETOPHOTONIC MICROCAVITY

Razdolski I.E.¹, Murzina T.V.¹, Aktsipetrov O.A.¹, Grishin A.M.² Khartsev S.I.²

¹Department of Physics, Moscow State University, 119991, Moscow, Russia

²Condensed Matter Physics, Royal Institute of Technology, 164 40 Stockholm-Kista, Sweden

Magnetophotonic crystals (MPCs) have appeared recently to be an object of great interest due to their remarkable optical and magneto-optical properties. Since the works of M. Inoue *et al.* [1] several possible MPC configurations have been suggested, most of them been based on rare-earth garnets as materials which possess high magneto-optical response in the visible range.

Here we report on the nonlinear-optical studies of all-garnet magnetophotonic microcavity (MPMC). The sample was similar to the one described in [2]. The structure of the sample is given by $[\text{BIG}/\text{SGG}]^5/[\text{BIG}]^2/[\text{SGG}/\text{BIG}]^5/\text{GGG}[001]$ with the thicknesses of layers as large as 73.6 nm and 99.5 nm for BIG and SGG, respectively, with BIG ($\text{Bi}_3\text{Fe}_5\text{O}_{12}$) and SGG ($\text{Sm}_3\text{Ga}_5\text{O}_{12}$) heteroepitaxial multilayers grown on to the GGG ($\text{Gd}_3\text{Ga}_5\text{O}_{12}$)[001] single crystal by rf-magnetron sputtering. Film synthesis was finalized with *in situ* postannealing at 550 $^\circ\text{C}$ for 10 min at 500 Torr in oxygen atmosphere. The microcavity (MC) has been designed and fabricated for the resonance wavelength of 779 nm.

Giant second harmonic generation (SHG) in MPMC and other nonlinear optical and magneto-optical effects are attributed to the localization of the electromagnetic field within the microcavity. The distribution of the fundamental radiation inside the structure in the vicinity of the MC mode was calculated using the transfer matrix method, which shows a strong localization of the electromagnetic field in the MC layer. In the case of all-garnet MPMCs, nonlinear-optical response originates not only from the MC layer, but from distributed Bragg reflectors (DBR) as

well. The calculated spectrum of the SHG intensity confirms that the SH signal from DBR should be definitely taken into consideration, as its intensity is of the same order of magnitude as the SHG signal from the MC.

The sharp peak at 779 nm in the transmission spectrum of the sample corresponds to the MC mode. The Faraday rotation magnitude in the vicinity of the MC mode is as large as 10° , which corresponds to the specific rotation of $11.4^\circ/\mu\text{m}$. The SHG experiments were performed with the tunable Ti:Sapphire laser setup with 80 fs pulsewidth, 82 MHz repetition rate and average power of 150 mW. The SHG spectra reveal localization of the nonlinear-optical response in the spectral vicinity of the MC mode. Nonlinear magneto-optical properties of MPMC were studied for the transversal magneto-optical Kerr effect. The SHG magnetic contrast of approximately 0.5 was observed for the *p*-in geometry, noticeably decreasing with increasing angle of incidence. For the *s*-polarized fundamental beam, the dependence of the SHG magnetic contrast on the angle of incidence is not so strong, while the similar trend has also been observed. For the longitudinal Kerr effect, the magnetization-induced rotation of the SH polarization plane of 85° was obtained. The possible mechanisms of the observed effects are discussed.

[1] M. Inoue, K. Arai, T. Fujii, M. Abe, *J. Appl. Phys.*, **85**, 5768 (1999).

[2] S.I. Khartsev, A.M. Grishin, *J. Appl. Phys.*, **101**, 053906 (2007).

21PO-2-22

THE AMPLIFICATION OF EVANESCENT ACOUSTIC WAVE BY MEANS OF 1D MAGNETIC PHOTONIC CRYSTALS

Laptyeva T.V.¹, Tarasenko O.S.¹, Tarasenko S.V.¹, Yurchenko V.M.¹, Shavrov V.G.², Kotov V.A.²

¹Donetsk Institute for Physics&Engineering, 72, R. Luxemburg str., Donetsk, 83114, Ukraine

²Institute of Radioengineering&Electronics, 11-7, Mokhovaya str., Moscow, 125009, Russia

Until now the most of theoretical and experimental papers are devoted to a detailed study the electromagnetic wave propagation and localization in the magnetic photonic crystals (MPC) [1], however in most cases the MPC are the acoustic continuous media. As a result, for case of the elastic waves propagating we can consider MPC as the magnetic phonon crystal. This approach allowed us to investigate the acoustical analogies of the well known peculiarities of 1D MPC polariton dynamics for the radically different frequency band. Furthermore, in that case the condition of a magnetic photonic crystal transparency in the optical band are not required, so that a range of the possible structural component parts of such MPC can extend. Finally, in such composite magnetic media it is possible to control the elastic wave propagation by means of external parameters (pressure, magnetic or electric fields, wave angle).

In this paper by using transfer matrix method the influence of magnetoelastic interaction on the normal SH modes transmission through the interface between the 1D MPC and the nonmagnetic elastic isotropic medium has been analyzed. As an example of 1D MPC the two-component magnetic superlattice with the ferro- or antiferromagnetic ordered adjacent layers (similar to “easy axis ferromagnetic – nonmagnetic dielectric” or “easy axis antiferromagnetic – ideal superconductor”) was studied. We assume that the elastic properties of magnetic and nonmagnetic components of the MPC are identical. In particular it is shown:

1) the criterion of nonreflection transmission of shear bulk elastic wave through the finite 1D MPC has been formulated;

2) the collective shear surface acoustic wave spectrum and the condition of nonreflection transmission can have a nonreciprocity relative to the inversion of the direction of SH-wave propagation along the MPC surface;

3) under the above mentioned criterion the requirement of translational ordering along the normal to the layers interface are not necessarily for the case of composite magnetic materials composed out of two-component structure like the “easy axis antiferromagnetic – ideal diamagnetic” type.

[1] I.L. Lyubchanskii, N.N. Dadoenkova, M.I. Lyubchanskii, E.A. Shapovalov, Th. Rasing, *J. Phys. D: Appl. Phys.*, **36** (2003) R277 – R287.

21PO-2-23

MAGNETIZATION OF Fe-14Al-2Cr ALLOY DEPENDING ON TEMPERATURE AND STRUCTURE

Valeev I.¹, Almukhametov R.², Mulyukov Kh.¹

¹Institute for Metals Superplasticity Problems, St.Khalturina str. 39, Ufa, Russia

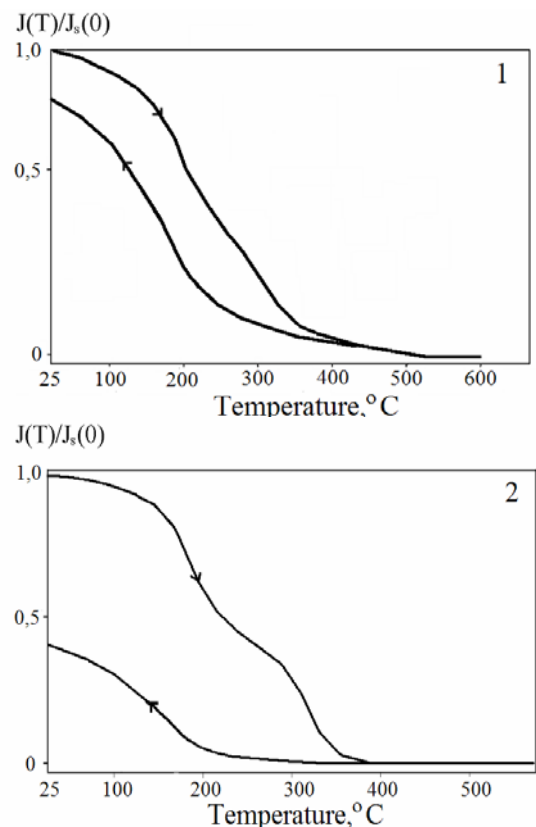
²Bashkir State University, Frunze str.32, Ufa, Russia

Fe-Al alloys are characterized by high strength and rust-resistance, however, because of their low deformability their practical application is restricted. One of the methods for increasing deformability is alloying of such alloys by different chemical elements. Until now detailed investigations of their physical properties depending on structural conditions have not been carried out.

The present paper considers temperature dependence of magnetization for Fe-14Al-2Cr alloy in three structural conditions: a) after hardening from 1300 K, b) after annealing of hardened specimen at 673 K for 10 min and c) after deformation of hardened specimen by 50 %.

Fig.1 shows curves of temperature dependences of magnetization for coarse-grained hardened specimens at heating and cooling. It is seen that the curve has a bend at 200°C. One can assume that this bend may be caused by the presence of two phases with different Curie points. However, the performed investigations have shown that this change is attributed to structure ordering beginning in the hardened disordered alloy at 200°C. The temperature dependence of magnetization for the hardened alloy at cooling has not any bend. Note that a value of magnetization of the hardened sample is higher than the annealed one. Evidently, this fact is connected with the presence of a small amount of Cr in the alloy composition.

The curves $J(T)/J_s(0)$ corresponding to the deformed specimen are of much interest (fig.2) too. In this case the bend is more distinct and a value of magnetization after cooling of the specimen amounts less than half the value for the deformed



state. The observed difference in magnetization values before heating and after cooling might be connected with refinement of a granular structure during deformation that results in much structure ordering.

So, the obtained results have revealed an essential structure dependence of magnetic properties of the studied alloy.

This work was financially supported by a Grant of the Russian Fond for Basic Researches № 06-02-16984a.

21 June Saturday

17:00-19:00

poster session

21PO-16

**“High Frequency
Properties,
Metamaterials
and Resonances”**

21PO-16-1

CALCULATION OF AVERAGE FIELD AND RELAXATION SPECTRA COMPOSITE (FERROMAGNETIC-DIELECTRIC) MATERIALS

Asadullin F.F.¹, Kotov L.N.², Golchevsky Yu.V.¹, Poleshchikov S.M.¹, Asadullina N.S.¹

¹Syktvykar Forest Institute, Physics dept., Lenina 39, Syktvykar, 167000, Russia

²Syktvykar State Univ., Radiophysics dept., Oktyabrsky Pr. 55, Syktvykar 167001, Russia

Recently great attention has been paid to the development of radio absorption and reflecting materials on the basis of various structure composite materials that assumes the knowledge of dynamic magnetic characteristics of ferrite. One of the basic characteristics describing absorption and reflection of electromagnetic waves in magnetic materials is complex magnetic permeability $\mu = \mu' - i\mu''$. Dynamic frequency properties of radio-frequency devices with the use of composite materials are determined by the dependence of the average magnetic permeability module on the frequency $\langle |\mu(f)| \rangle$ where $\langle |\mu| \rangle = \sqrt{\langle \mu' \rangle^2 + \langle \mu'' \rangle^2}$, thus averaging is carried out on the sample's whole.

In the given work the calculation method of the composite material average field consisting from ferromagnetic and dielectric areas in the absence of an external constant magnetic field is reported. The average field $\langle H \rangle$ is determined by the magnetization of saturation M_S , constant anisotropy K_1 (or the field of anisotropy H_A) and the frequencies distribution function of natural ferromagnetic resonance in composite materials magnetic granules $\varphi(f_0) = A \cdot \exp(-(f_0 - f_{0\min})^2 / B_1^2)$, where f_0 - natural resonance frequency in granules composite materials, $f_{0\min} = \gamma' \cdot H_A$ - minimal resonance frequency, γ' - gyromagnetic ratio. The frequencies dispersion B_1 can be determined by the relation:

$$B_1 = 6\pi M_S \gamma' \beta \frac{p}{1+p} + \gamma' 2K_1 / M_S (1 + \alpha),$$

where β - exchange interaction constant between ferromagnetic granules, α - dissipation parameter, p - specific volume of dielectric. This calculation method of the average field value, maximal values of the magnetic permeability components $\mu', \mu'', |\mu|$ and the relaxation width Δf_R does not take much time. Knowing the average field value it is possible to estimate the components of the spectrum maximal magnetic permeability $\langle |\mu| \rangle_{MAX}$, the width of the relaxation area Δf_R and to construct the relaxation magnetic spectrum.

Support by RFBR (grant 06-02-17302).

21PO-16-2

MSSW PROPAGATION IN 1D MAGNONIC CRYSTAL

Filimonov Yu.A.¹, Nikitov S.A.², Novitskii N.N.³, Pavlov E.S.¹, Stognij A.I.³, Vysotsky S.L.¹

¹Saratov branch of IRE RAS, Zelenaya str., 38, Saratov, 410019, Russia

²IRE RAS, Mokhovaya 11-7, Moscow, 125009, Russia

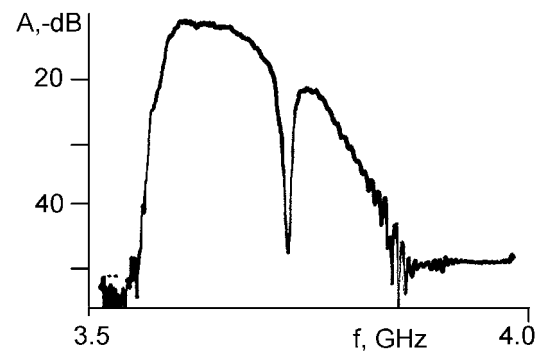
³Scientific-Practical Materials Research Centre of NAS of Belarus, 19 P, Brovki Street, Minsk, 220072, Belarus

MSSW propagation in magnonic crystal (MC) including two-dimensional (2D) etched holes periodic structure in yttrium iron garnet (YIG) single-crystal films was reported in [1]. The forbidden gap found in the frequency spectra was attributable to Bragg reflection of the MSW from the surface periodic structures. So the MC can be used as a tunable rejected microwave filter.

In the same time the 1D structure consist of periodic gratings carved on the surface of YIG film by a high-precision dicing saw was reported [2]. Using of 50 mkm deep gratings with width and spacing of 100 mkm on the surface of 97 mkm thick YIG film both band-stop and bandpass filters were designed. The bandpass filter's characteristics were as follows: inserted loss of 5 dB and -3 dB bandwidth of 150 MHz. The reported rejection of band-stop filter reached 40 dB with low information about bandwidth. It should be noted that the used in [2] technology is complex enough.

The structures actually represent 1D MC can be made by chemical etching, ion-beam milling and ion implantation (see citation in [2]) but filters using such structures haven't good characteristics.

The paper reports the results of investigation of 1D MC consist of 70 mkm width 0.66 mkm deep grooves separated by 30 mkm lands was etched in 3 mkm thick YIG film. The MC was placed in microstrip delay line. The figure demonstrates the amplitude-response characteristic obtained at tangential bias magnetic field of 650 Oe directed along the grooves. The distance between microstrip transducers was 3 mm. One can see that the rejection is about 30 dB and 3 dB bandwidth reach 4 MHz corresponding quality factor about 900. The rejection frequency could be tuned by bias magnetic field in at least 2 - 4 GHz region without significant change of filter characteristics. Note that the characteristics can be improved by optimization of MC's topology.



Support by RFBR grants No. 06-07-89341-a and No. 08-02-00785-a is acknowledged.

[1] Yu. V. Gulyaev, S. A. Nikitov et al., *JETP Lett.*, **77** (2003) 567.

[2] A. Maeda and M. Susaki, *IEEE Trans. on Magn.*, **42** (2006) 3096.

21PO-16-3

FERROMAGNETIC RESONANCE INVESTIGATIONS OF TWO SERIES OF $(\text{Co}_{45}\text{Fe}_{45}\text{Zr}_{10})_x(\text{Al}_2\text{O}_3)_{1-x}$ THIN FILMS

Kotov L.N.¹, Efimets Yu.Yu.¹, Petrakov A.P.¹, Turkov V.K.¹, Kalinin Yu.E.², Sitnikov A.V.²

¹Syktyvkar State Univ., Radiophysics dept., Oktyabrsky Pr. 55, Syktyvkar 167001, Russia

²State Technical Univ., Physics of Solids, Moskovsky Pr. 14, Voronezh 394026, Russia

This work is devoted to the research on magnetic and relaxation properties two series of the films with the composition of $(\text{Co}_{45}\text{Fe}_{45}\text{Zr}_{10})_x(\text{Al}_2\text{O}_3)_{1-x}$ ($0,25 < x < 0,64$) and revealing their relationship with the nanostructure characteristics. The films with thicknesses 2÷6 microns were deposited on substrates of polycrystalline glass by the ion-beam sputtering method using compound targets of ferromagnetic and dielectric substances as previously described [1]. The films were received in an atmosphere of argon with pressure $P_{\text{Ar}} \approx 4 \cdot 10^{-2}$ Pa (the first series) and with addition of oxygen with $P_{\text{O}} \approx 3 \cdot 10^{-6}$ Pa (the second series). Initial films and films after annealing were studied.

The nanostructure of films, the size of metal and dielectric areas and degree of their crystallization were studied with using X-ray diffractometer DRON-2 [2]. Nonlinear dependences of the sizes of metal and dielectric areas on concentration x have been found. Division into metal and dielectric phases, increasing of the sizes of metal inclusions and changing of their form after annealing are found out.

The magnetic and relaxation properties of films have been characterized by means of ferromagnetic resonance (FMR). The FMR spectra were obtained by an electron paramagnetic spectrometer at 9.45GHz using a standard modulation index meter. The FMR spectra were used to investigate the dependences of the resonant fields, FMR line widths and magnetization relaxation on concentration x in films [3,4]. The FMR line width and the specific resistance are strongly correlated to the metal phase percentage for films two series. The films of two series had the differing magnetic and relaxation properties. Significant changes in the shape of the FMR spectra lines are connected to nanostructural transformations in the ferromagnetic granules topology and sizes of metal alloy crystallites.

Support by RFBR (grant 06-02-17302).

[1] Y.E. Kalinin et al., *Phys. and Chem. of Processing of Materials*, (2001) 14.

[2] A.P. Petrakov, *GTP*, **73** (2003) 129.

[3] L.N. Kotov et al. *JMMM*, **316** (2007) 20.

[4] L.N. Kotov et al., *Mat. Sc. and Eng.*, **442** (2006) 352.

21PO-16-4

MINIMIZING THE EFFECT OF NOISE IN HIGH-SPEED REVERSAL OF A MAGNETIC DIPOLE

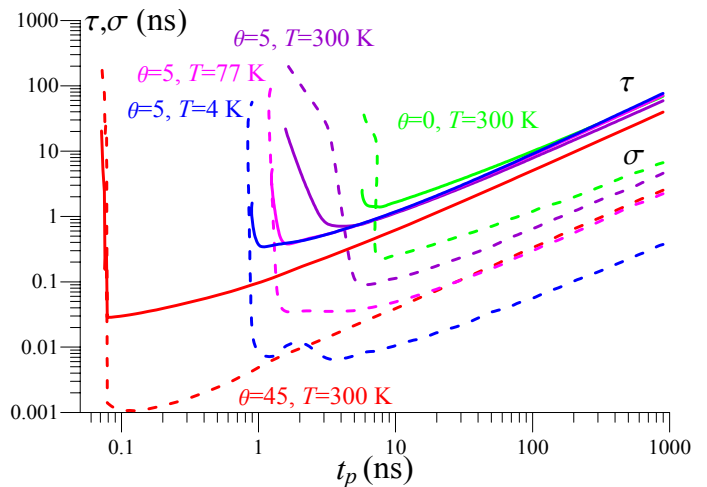
Pankratov A.L., Vdovichev S.N., Nefedov I.M., Adamchik D.A.

Institute for Physics of Microstructures of RAS, GSP-105, Nizhny Novgorod, 603950, Russia

The effect of noise on the reversal of a magnetic dipole is investigated on the basis of computer simulation of the Landau-Lifshits equation. It is demonstrated that at the reversal by the pulse with sinusoidal shape, there exists the optimal duration, which minimizes the mean reversal time (MRT) and the standard deviation (SD, jitter). Both the MRT and the jitter significantly depend on the angle θ between the reversal magnetic field and the anisotropy axis. At the optimal angle the MRT can be decreased by a factor of 7 for damping $\alpha=1$ and up to 2 orders of magnitude for $\alpha=0.01$, and the jitter can be decreased from 1 to 3 orders of magnitude in comparison with the uniaxial symmetry case. It has been demonstrated that fluctuations can not only decrease the reversal time, as it has been known before for the magnetic systems and is correct for small angles only, but it can also significantly increase the reversal time - the effect which can be avoided by proper choice of pulse duration.

In the figure the MRT τ (solid curves) and SD σ (dashed curves) are presented versus pulse duration t_p for three different values of angles $\theta=0^\circ, 5^\circ, 45^\circ$ for $T=300\text{K}$ and three different temperatures for $\theta=5^\circ$. The parameters are typical for the magnetic recording media with $\alpha=0.1$. It is seen that all curves have minima, so there exists the optimal pulse duration, which

minimizes the mean reversal time and the standard deviation. First, let us focus on the curves for $\theta=5^\circ$. In spite that at large t_p one can see little decrease of MRT with increase of the temperature, at small t_p around minimum the opposite effect of noise delayed switching is clearly visible, quite similar to the one observed before for Josephson junctions [1]. Besides, here the SD behaves as $\sigma \sim T^{1/2}$, see [1]. Second, from the figure it is obvious that for $\theta=45^\circ$ the reversal is faster and more stable than for $\theta=0^\circ, 5^\circ$ at all other equal conditions. Besides, the difference



between MRT for the angles $\theta=0^\circ$ and $\theta=5^\circ$ is two times, while the difference of SD is about three times. For the cases $\theta=5^\circ$ and $\theta=45^\circ$ the gain is even larger, more than one order for MRT and almost two orders for SD (for $\alpha=0.1$). This means that the reversal process principally depends on the precession of the magnetic dipole, and can not be described by a simple two-state model. This result gives the quantitative substantiation for the idea to use the tilted magnetic field to speed up the reversal process [2], and also to use additional weak perpendicular magnetic field for the same purpose [3], which actually leads to the tilt of the aggregate magnetic field.

Support by RFBR-Povolzhie (project 08-02-97033) is acknowledged.

[1] A.L. Pankratov and B. Spagnolo, *Phys.Rev.Lett.*, **93** (2004) 177001; A.V. Gordeeva and A.L. Pankratov, *Appl. Phys. Lett.*, **88** (2006) 022505.

[2] Y.Y. Zou, J.P. Wang, C.H. Hee, and T.C. Chong, *Appl. Phys. Lett.*, **82** (2003) 2473.

[3] R.L. Stamps and B. Hillebrands, *Appl. Phys. Lett.*, **75** (1999) 1143.

21PO-16-5

HIGH FREQUENCY MAGNETIC REVERSAL IN THE ONE-DOMAIN PARTICLES AND THIN FILMS

Nosov L.S.¹, Kotov L.N.¹, Ustugov V.A.¹, Asadullin F.F.²

¹Syktyvkar State University, Syktyvkar, Oktiabrsky pr., 55, Russia

²Syktyvkar Forrest Institute, Syktyvkar, Lenina st., 39, Russia

The investigation of nonlinear high frequency magnetization dynamics is one of the most popular fields of research in connection with generation of the new methods of writing and reading of information and with generation of the new magnetic data storages [1-3]. From this point of view, we propose to use one-domain particle array as data storage, based on frequency principle of reading and writing. Such technique data storage creation have been suggested in the case of non-interacting particle array [2,3].

Magnetic reversal of one-domain ferromagnetic particles and thin films excited by rf magnetic field are studied by means of computer simulation. It is shown that the phenomenon of the rf magnetic reversal has a bound character. The particle magnetic reversal leads to the magnetic texture changing, which results in a bound character as well. Bound dependences from different parameters such as damping constant, neighbor dipole-dipole field and others, are presented.

The nonlinear magnetization dynamics of one-domain particles and thin films can result in the texture changing. This phenomenon has a bound character. The bound frequency dependence has a minimum. All the bound frequency dependences are similar to the nonlinear ferromagnetic resonance bound frequency dependence [4]. The texture of the particle array determinate magnetic spectrum, and one can conclude that the texture change causes magnetic spectrum change. Thus, in the case of interacting particles, the phenomenon of texture changing can be used for new data storage creation, based on frequency principle of reading and writing [5]. In the case of thin film the magnetic reversal may result from inhomogeneous oscillations of the magnetization.

Support by Russian Foundation for Basic Research (grant №06-02-17302).

[1] D.A. Thompson, J.S. Best. *IBM J. Res. and Dev* **44** (2000) 311.

[2] L.N. Kotov, L.S. Nosov. *Tech. Phys. Lett.* **29** (2003) 853.

[3] L.N. Kotov, L.S. Nosov. *Tech. Phys.* **50** (2005) 1305.

[4] J.A. Monosov. *Nonlinear ferromagnetic resonance*. (Science, Moscow. 1971)

[5] L.N. Kotov, L.S. Nosov, F.F. Asadullin. *Tech. Phys.* **53** (2008)

21PO-16-6

CHANGE OF THE MAGNETIC STRUCTURE OF FERROMAGNETIC THIN FILMS BY HIGH-FREQUENCY EXTERNAL FIELD

Golov A.V., Kotov L.N., Nosov L.S.

Syktvyvkar State Univ., Radiophysics dept., Oktyabrsky Pr. 55, Syktvyvkar 167001, Russia

Studying the reversal mechanism of magnetization in magnetic material start at beginning of XX century. It is connected with phenomenon of the magnetization and the reversal mechanism in ferromagnetic and ferrite thin films and small particles is broadly used for record media [1]. Under influence of the external magnetic field the magnetic structure thin film changes, but after cessation of the influence structure gradually returns to its initial position. Only under greater amplitude of the external variable magnetic field possible change the magnetic structure in sample. This result can be used for writing data, for instance, on thin ferrite film.

With leaving the frequency of the field from frequency of the linear ferromagnetic resonance (FMR), for change the structure of the film necessary to put the field vastly greater, than at frequency linear FMR, since influence of the external field on the magnetic structure is significant low for this case. The phenomenon of the changing the magnetic structure in film has threshold character. Similarly that, as this is made for the phenomenon of the reorientations single domain particles [1] can be determined threshold amplitude of the change the magnetic structure of the ferromagnetic film. In given work observed the phenomenon of reorientations in multidomain film: is determined threshold amplitude of the variable external field at miscellaneous damp parameter.

On result of the simulation of the magnetic structure dynamics with using the Gilbert equation and standard methods of micromagnetic modeling [2] is built dependence of the threshold amplitude from frequencies for different damp parameter. As a result received that least amplitude of the field exists on frequency linear FMR, after which initial condition of the magnetic structure decays. Under small leaving the frequency of the field from resonance frequency, the amplitude of the variable field, required for change the magnetic structure of the thin films, sharply increases. At frequency of the field, in two times exceeding frequency linear FMR, exists the area of the minimum on dependence.

The character of curve form of dependency threshold amplitudes from frequency of excitement powerfully changes with increase the damp parameter. Threshold amplitude of the change the magnetic structure first grows with growing of the value magnetization saturation, but afterwards at achievement of a certain critical importance sharply falls short of zero. The studies show that at low magnetization saturation, there is only one minimum on dependencies on frequency linear FMR. The reduction and growing of importance threshold amplitudes in this minimum after occurs more smooth, than under greater importance.

The phenomenon of the change the magnetic structure by influences pulse variable magnetic field can be used for making new microelectronics device, but in the same way drives to information, founded on frequency principle record-sensing.

Support by RFBR (grant 06-02-17302).

[1]. L.N. Kotov at al. *J.Appl. Ph.*, **75** (2005) 55.

[2]. Josef Fidler at al. *J. Phys. D: Appl. Phys.*, **33** (2000) 135.

21PO-16-7

MICROWAVE LOGIC GATES BASED ON NONLINEAR SPIN WAVE INTERFEROMETER

Ustinov A.B., Kalinikos B.A.

Department of Physical Electronics and Technology, St.Petersburg Electrotechnical University, St.Petersburg, Russia, 197376

Recently the logic gates based on the *linear* spin waves were proposed [1,2]. Logical functions, such as NOT and XOR, were performed using an external control signal. The purpose of the present work is to develop the logic gates based on the *nonlinear* spin waves. A distinguishing feature of the proposed device is that no control signal is necessary for the logic gate operation.

A circuit structure of the logic gate is shown in Fig. 1(a). The device had two input and one output ports. The main part of the device is a nonlinear spin wave interferometer (NSWI) based on a yttrium iron garnet (YIG) film. The interferometer had a two-arm structure similar to that described in [3]. A 5.2 μm thick, 2 mm wide, and 4 mm long YIG film was utilized in the device. A 50 μm wide and 2 mm long short-circuited microstrip transducers separated by 5 mm were used to excite the nonlinear spin waves in the YIG film. A saturation magnetization of the film was 1750 G. An external magnetic field of 2910 Oe was applied perpendicular to the film plane. Microwave signals in the form of rectangular pulses (see Fig. 1(b)) were supplied to the input ports of the logic gate. A carrier frequency of the pulses was 3374 MHz. A width of the pulses was 20 μs .

Figs. 1(b) and (c) demonstrate typical oscilloscope traces of the detected input and output signals. It is seen that the logic gate performs XOR function. Also, it was possible to achieve the device operation as NAND gate if the carrier frequency was changed to 3371.5 MHz. In conclusion, the use of the nonlinear spin waves is a powerful approach for development of the microwave logic gates of different types.

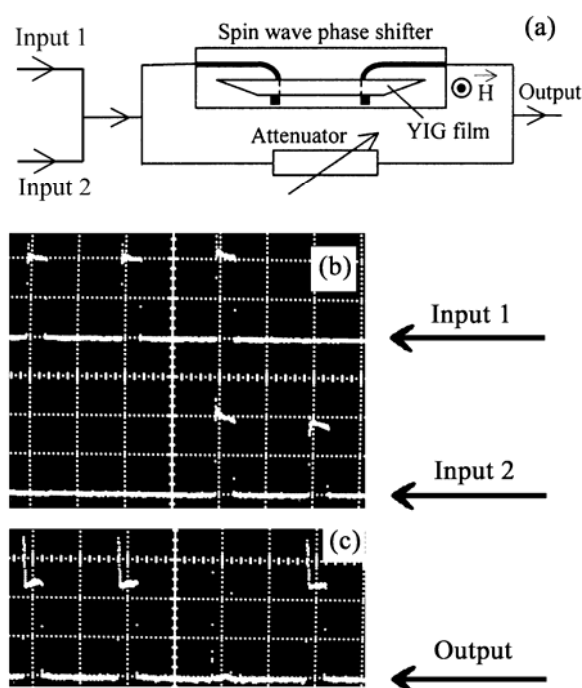


Fig. 1.

This work was supported in part by Russian Foundation for Basic Research, Grant No. 08-02-00959, Russian Federal Agency for Education, Projects RNP/2.1.1.1382, NSh-2124.2008.2, and MK-2804.2008.8.

[1] M. P. Kostylev, A. A. Serga, T. Schneider, B. Leven, and B. Hillebrands, *Appl. Phys. Lett.*, **87** (2005) 153501.

[2] T. Schneider, A. A. Serga, B. Leven, B. Hillebrands, R. L. Stamps, and M. P. Kostylev, *Appl. Phys. Lett.*, **92** (2008) 022505.

[3] A. B. Ustinov and B. A. Kalinikos, *Appl. Phys. Lett.*, **90** (2007) 252510.

21PO-16-8

FERRITE-FERROELECTRIC ACTIVE RING FILTER*Ustinov A.B.¹, Kalinikos B.A.¹, Srinivasan G.²*¹Department of Physical Electronics and Technology, St.Petersburg Electrotechnical University, St.Petersburg, Russia, 197376²Department of Physics, Oakland University, Rochester, MI 48309, USA

A combination of ferrite and ferroelectric materials in a layered structure provides the possibility of simultaneous “magnetic” and “electric” tuning of its microwave characteristics [1]. Different microwave devices could be designed using such layered structures (see e.g. [2,3]).

The purpose of this paper is to report on the creation of the dual-tunable active ring filter based on the ferrite-ferroelectric layered structure. The filter had a circuit structure of the ring resonator. The main elements of the resonator were a ferrite-ferroelectric delay line and a microwave amplifier in the feedback loop. The ferrite-ferroelectric structure utilized in the delay line was composed of a 5.7 μm thick, 2 mm wide and 40 mm long single-crystal yttrium-iron garnet (YIG) film and a 500 μm thick, 10 mm wide and 5 mm long ceramic barium strontium titanate (BST) slab. One surface of the BST slab was covered by 50 nm thick chromium electrode. A copper electrode of thickness 5 μm covered the other surface of the slab.

Two 50 μm wide and 2 mm long short circuited microstrip antennas were used to excite and receive waves in the layered structure. The distance between the antennas was taken to be 8 mm. The YIG-BST delay line was placed between the poles of an electromagnet. The bias magnetic field of 2010 Oe was applied parallel to the plane of the YIG film and to the antennas. Electric field in the range of 0-18 kV/cm was produced in the BST slab through application of voltage to the metal electrodes.

The experimental results show that for the ring gain ranging from -3.5 dB to -1 dB the effective Q-factor of the resonator was varied from 10000 to 50000 at 8 GHz. Application of the electric field led to the shift in the resonant frequencies. The maximum shift of about 5 MHz was obtained for the lowest mode of the ring. At the same time, a frequency shift for the mode having the maximum Q-factor of about 50000 was 2.9 MHz. Thus, the proposed active ring filter had a pass-band of approximately 0.2 MHz at ~ 8 GHz and allowed electric tuning of ~ 3 MHz, i.e. over 15 pass-bands.

In conclusion, an active ring filter based on an YIG-BST layered structure has been designed and characterized. The performance characteristics of the filter compare favorably with the existing dual-tunable narrow-band microwave filters.

This work was supported in part by Russian Foundation for Basic Research, Grant No. 08-02-00959, Russian Federal Agency for Education, Projects RNP/2.1.1.1382, NSh-2124.2008.2, and MK-2804.2008.8.

[1] V. E. Demidov, B. A. Kalinikos, S. F. Karmanenko, A. A. Semenov, and P. Edenhofer, *IEEE Trans. MTT*, **51** (2003) 2090.

[2] A. A. Semenov, S. F. Karmanenko, B. A. Kalinikos, G. Srinivasan, A. N. Slavin, and J. V. Mantese, *Electron. Lett.*, **42** (2006) 641.

[3] A. B. Ustinov, G. Srinivasan, B. A. Kalinikos, *Appl. Phys. Lett.*, **90** (2007) 031913.

21PO-16-9

CHAOTIC SIGNAL GENERATOR BASED ON FERRITE FILMS

Kondrashov A.V.¹, Ustinov A.B.¹, Stemler T.², Kalinikos B.A.¹, Wu M.³, and Benner H.²

¹St. Petersburg Electrotechnical University, St. Petersburg, 197376 Russian Federation

²Institute for Solid State Physics, Darmstadt University of Technology, Darmstadt, Germany

³Department of Physics, Colorado State University, Fort Collins, Colorado, USA

The generators fabricated in the form of magnetic film active feedback rings have been investigated for the frequencies where both three- and four-wave processes are possible and interacted to allow for the self-generation of chaotic spin wave signals [1,2]. The aim of the present work is to study chaotic signal generators where only four-wave processes are responsible for nonlinear dynamics. The experiments have been performed for surface spin wave configurations. With increasing the ring gain, one observed changing of the generation regimes. Thus, in the frequency domain, the development of the power-frequency spectrum from a single mode to a comb-like spectrum, a multiple frequency comb, and a broadband chaotic spectrum have been subsequently observed. The recorded chaotic signals show typical signatures of deterministic chaos. The generator consists of a 6.8 μm -thick yttrium iron garnet film strip with input and output microstrip transducers, a broadband microwave amplifier, and an adjustable attenuator for gain control. Detailed information on the experimental setup is given in [3]. A static magnetic field of 1200 Oe was applied in the film plane and perpendicular to spin wave propagation direction. The ring signals were measured through a directional coupler and then analyzed with a fast oscilloscope and a spectrum analyzer. The experimental results show that the generation of the broadband chaotic signals took place for the ring gain G above 11 dB. In order to prove the deterministic origin of the observed chaotic signals, we recorded the corresponding time-series data. A quantitative measure of the strength of deterministic chaos is obtained by evaluating the largest Lyapunov exponent. The evaluation was done with the standard time series analysis program TISEAN [4]. We obtained the following values for the largest Lyapunov exponent: $\lambda = 0.0028 \pm 0.0004$, $\lambda = 0.0039 \pm 0.0003$, and $\lambda = 0.0032 \pm 0.0002$ for $G = 11$ dB, $G = 15$ dB, and $G = 22$ dB, respectively. These values result in a time limit of about 2 μs for reasonable predictions of the system dynamics. Also we calculated the embedding dimension and fractal dimension using the usual methods [5]. We obtained a fractal dimension of about 1.7 and an embedding dimension of about 7 for $G = 11$ dB. The calculated data clearly proved the deterministic origin of the observed dynamic behavior. The obtained results may have applications to wideband data transmission systems for secure and high-speed communications, for example, spread spectrum communications [6].

This work was supported in part by Russian FBR, Grant 08-02-00959, Russian Federal Agency for Education, Project RNP/2.1.1.1382, NSc-2124.2008.2, MK-2804.2008.8, the U. S. NSF, Grant ECCS-0725386, and Deutsche Forschungsgemeinschaft, Grant 436 RUS 113/644/0-2.

M. Wu, B. A. Kalinikos, L. D. Carr, and C. E. Patton, Phys. Rev. Lett. 96, 187202 (2006).

V. E. Demidov and N. G. Kovshikov, JETP Lett. 66 (4), 261 (1997).

M. Wu, B. A. Kalinikos, and C. E. Patton, Phys. Rev. Lett. 95, 237202 (2005).

R. Hegger, H. Kantz, and T. Schreiber, Chaos 9, 413 (1999).

H. Schuster, Deterministic Chaos, Physic-Verlag, 1984

Yu. V. Gulayev et al, J. Communication Technology and Electronics 48, 1063 (2003).

21PO-16-10

INVESTIGATION OF DIPOLE-EXCHANGE SPECTRUM OF VOLUME SPIN WAVES IN TANGENTIALLY MAGNETIZED FERROMAGNETIC FILM WITH PERIODIC METALLIC GRATING

Grigorieva N.Yu.

St. Petersburg Electrotechnical University, St. Petersburg, 197376 Russian Federation

Recently we have elaborated a theory, which describes the dipole-exchange spectrum of spin waves propagating in thin-film ferromagnetic periodic structures. The aim of this work is to present a detailed numerical analysis of the dispersion characteristics of backward volume spin-waves in ferromagnetic film with periodic metallic grating based on the elaborated theory.

The investigation is carried out for the different values of the surface spin-pinning parameter η , distance between the film surface and metallic grating b , the period of the metallic grating T , and the filling factor of the grating f .

It is shown that the width and the position of the frequency "gaps" in the dipole-exchange spin wave spectrum are influenced by geometric parameters of the structure (b , T , f) as well as by spin-pinning conditions on the film surfaces (η). Also, it is shown that the filling factor of the metallic grating influence the width of the first three "gaps" very differently (Fig.1). All the dispersion curves have one or more maxima, and their shape depends crucially on the period of the structure. One can see from Fig.1 that the "gaps" labeled 2 and 3 practically collapse at some values of the grating filling factor; thus, at these points the allowed pass-bands merge.

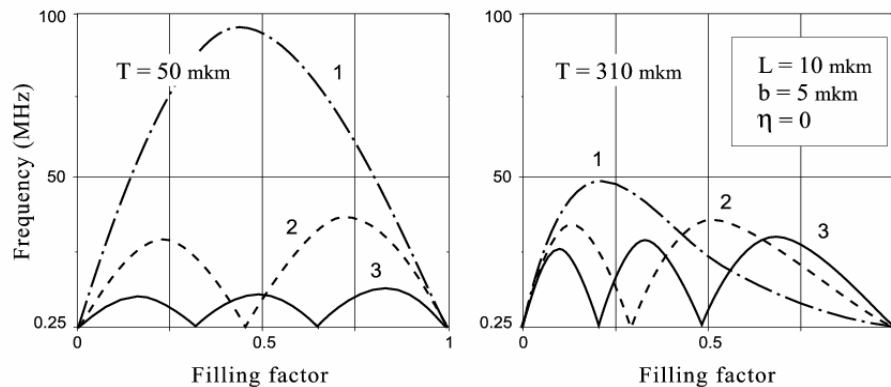


Fig. 1 Width of the first three "gaps" (1, 2, 3) versus filling factor of the metallic grating.

While investigating the relation between the surface spins pinning conditions and the width of the stop bands, it was established that in the ferromagnetic film with free surface spins ($\eta=0$) the "gaps" are much wider than in the film with pinned surface spins ($\eta=100$) and the position of the "gap" center lays higher in frequency for larger values of the spin-pinning parameter than for its smaller values. It was also demonstrated that the distance between the magnetic film and the metallic grating influenced mostly on the width of the "gaps", and only slightly shifts their central frequencies.

Thus, in this work we demonstrate that the shape of the dipole-exchange spin-wave spectrum depends not only on the geometry of the magnetic periodic structure, but also is strongly influenced by the surface anisotropy of the ferromagnetic film.

This work was supported in part by Russian Foundation for Basic Research, Grant No. 08-02-00959, Russian Federal Agency for Education, Projects RNP/2.1.1.1382 and NSh-2124.2008.2.

21PO-16-11

NONLINEAR MAGNETOELASTIC HIGH - FREQUENCY DYNAMICS IN FERRITE FILM

Vlasov V.S.¹, Kotov L.N.¹, Asadullin F.F.², Sheglov V.I.³, Shavrov V.G.³

¹Syktyvkar State University, 167001 Syktyvkar, Russia

²Syktyvkar Forest Institute, 167000 Syktyvkar, Russia

³Institute of Radioengineering and Electronics of RAS, 125009 Moscow, Russia

The magnetoelastic nonlinear oscillations dynamics in the thin ferrite film close to the elastic resonance (ER) is investigated theoretically. We consider the case of alternating field transversal pumping of a thin monocrystal ferrite film which is in dc field higher the saturation field. Let the condition of the ferromagnetic resonance (FMR) be fulfilled. The first order parametric decay processes can be avoided by exciting the precession under the FMR frequency, which conforms the floor of spin wave spectrum [1]. We consider the magnetization precession angles smaller than thresholds of the second order parametric processes. Only homogeneous oscillations of magnetization are paid attention to. Boundary conditions for mechanical displacement are taken into account due to the absence of the mechanical stresses on the film surface [2]. To describe magnetoelastic film oscillations we use the Gilbert equation and the equation for components of the mechanical displacement vector [1, 2]. Averaging the effective magnetoelastic field accordingly to coordinate inside the film and consider only first mode of mechanical displacement we'll get the system of non-linear differential equations. We consider only transversal elastic oscillations. The solving of the system is found by the 7 order Runge-Kutta method. The magnetoelastic relaxation time dependences on the magnitudes of saturation magnetization, second magnetoelastic constant, magnitude of the magnetic and elastic subsystems relaxation times ratio, other material parameters are obtained. The area of the magnetic dissipation parameter magnitudes, in which the fastest saturation of elastic oscillations is observed, is defined. The regime of the relaxation type magnetoelastic autooscillations is observed if there is relative detuning of the elastic eigenfrequency from FMR frequency in certain intervals of values of the alternating field amplitude during its action. The period of these autooscillations is much more than the period of the oscillations of the alternating field and is equal magnetoelastic relaxation time approximately. The dependences of the autooscillations excitation bound on the dc magnetic field magnitude, saturation magnetization, second magnetoelastic constant, magnitude of the magnetic and elastic subsystems relaxation times ratio and other material parameters are investigated. After the action of the alternating field impulse 2 regimes of magnetoelastic relaxation were discovered. The character of relaxation in first regime is near to elastic character and the 2-d regime is near to magnetic in character. The relaxation time dependences of nonlinear magnetoelastic oscillations after alternating field impulses on the magnetic dissipation parameter, saturation magnetization, alternating field amplitude and the second magnetoelastic constant were investigated.

The work was supported by RFBR grant 06-02-17302

[1] A.G. Gurevich, G.A. Melkov. Magnetic oscillations and waves (Nauka, Moscow, 1994).

[2] B.A. Goldin, L.N. Kotov, L.K. Zarembo, S.N. Karpachev. Spin-phonon interactions in the crystals (ferrites) (Nauka, Leningrad, 1991).

21PO-16-12

MAGNETIC HYSTERESIS IN MONOCRYSTALLINE SAMPLES OF UNIAXIAL HEXAFERRITES

Kostenko V.I., Chevnyuk L.V., Chamor T.G., Sorochnik A.M., Romanyuk V.F.
National Taras Shevchenko University of Kyiv,
Kyiv, Volodymyrska str., 64, Radiophysics faculty, Ukraine

Experimental researches of high-frequency and static processes of reversal magnetization are continued in the suggested article in the uniaxial hexaferrites.

In the article [1] hysteresis of the frequency-field dependences of ferromagnetic resonance (FMR) was discovered and it is experimentally explored in the epitaxial films and bulk single-crystal samples of barium hexaferrites for the first time. In future we conducted researches and on the samples of magnetoplumbite ($\text{PbFe}_{12}\text{O}_{19}$) and also strontium hexaferrite ($\text{SrFe}_{12}\text{O}_{19}$). The good agreement of dynamic and static magnetic characteristics has been obtained at the transition of samples from homogeneous state in the heterogeneous (Fig.1).

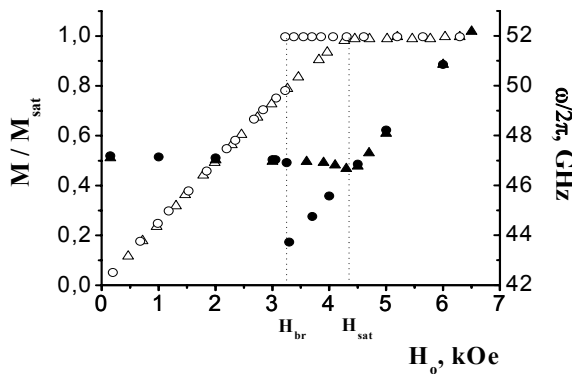


Figure 1.

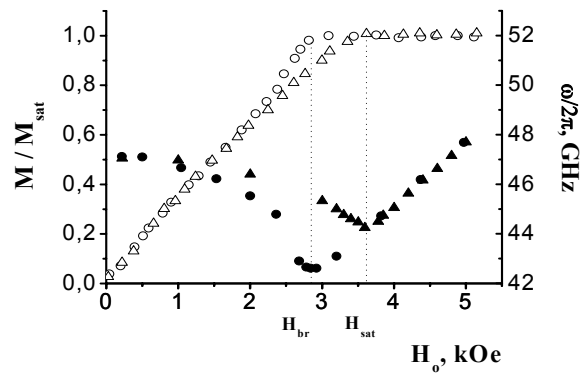


Figure 2.

Such parameters of the hysteresis are observed for all high-quality samples of the uniaxial hexaferrites with the narrow FMR linewidth. In specimens with the defects of crystallography structure and significantly broadening of FMR linewidth, the reverse branches of hysteresis in area of transition from saturated to domain state differ from parameters of hysteresis in the high-quality structures (Fig.2).

Consequently it was shown that the transition in the high-frequency specimens of monocrystalline hexaferrites to the unsaturated state occurred spasmodically and his parameters substantially depend on quality of specimens and anisotropy field H_a . For specimens with the broadening of FMR linewidth description of transition are differed substantially. The spasmodically transition from saturated to domain state is explained the delay of generation and growth of magnetic reversal center.

[1] I.V. Zavislyak, V.I. Kostenko, T.G. Chamor, L.V. Chevnyuk, *Jour Tech. Phys.*, **75**, No. 4 (2005) 128 (in Russian).

[2] V.I. Kostenko, T.G. Chamor, L.V. Chevnyuk, A.F. Lozenko, A.M. Sorochnik, *The Sixth international Kharkov symposium on physics and engineering of microwaves, millimeter and submillimeter waves and workshop on terahertz technology*. Kharkov (Ukraine), **2** (2007) 791.

21PO-16-13

HYBRID OSCILLATIONS IN THE COMPOSITE SOLID-STATE RESONATORS IN THE SATURATION AREA

Chamor T.G., Chevnyuk L.V., Kostenko V.I., Gorpynyuk A.Yu.
National Taras Shevchenko University of Kyiv,
Kyiv, Volodymyrska str., 64, Radiophysics faculty, Ukraine

Coupled oscillations are theoretically and experimentally investigated in the composite solid-state resonators. The experiments have conducted for barium ferrite ($\text{BaFe}_{12}\text{O}_{19}$) and $\text{SrGa}_{12}\text{O}_{19}$ platelets in the saturation area.

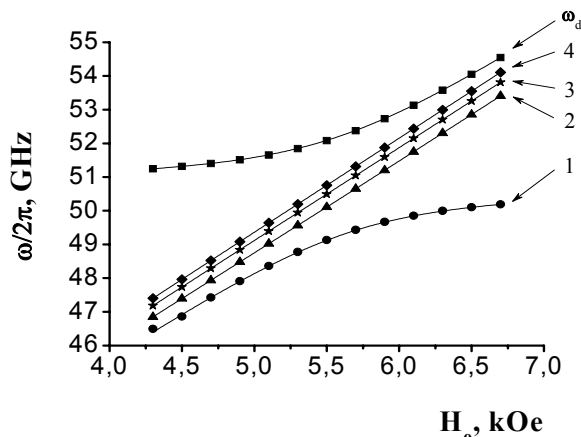
Uniaxial hexaferrites such as $\text{BaFe}_{12}\text{O}_{19}$ and $\text{SrFe}_{12}\text{O}_{19}$ are used the main materials in the creation for spin-wave UHF devices of millimeter range.

Theoretical and experimental investigation of effect in electromagnetic and magnetostatic oscillations and waves [1,2] give potential possibilities to improve resonance and frequency – field characteristics of composite ferrite-dielectric structures.

In the proposed article phenomenon of oscillations hybridization in the composite rectangular ferrite-dielectric resonator in the saturation area is investigated theoretically and experimentally. The $\text{SrGa}_{12}\text{O}_{19}$ platelet is used as dielectric resonator. Frequency ω_d for this platelet is evaluated for the base oscillation mode $H_{11\delta}$ as in the work [3]. Frequencies of magnetostatic oscillations ω_f in rectangular normally magnetized resonator based on $\text{BaFe}_{12}\text{O}_{19}$ ($a=1,81$ mm; $b=2,31$ mm, $t=17$ μm [4]) are carried out for the first four modes (0, 1,1), (0,1,3), (0,3,1), (0,3,3) (on the Fig. 1,2,3,4 – accordingly). Experiment is conducted of magnetic spectrums method on the panoramic display.

To perform calculations for interaction of electromagnetic and magnetostatic oscillations was used the theory in [5] in linear approximation in other words at the same coupling coefficients.

The theory [5] is considered with linear approximation that is with the same coupling coefficients for all magnetostatic modes, which is absolutely correct taking into account its small magnitude ($K \times B = 0,01$).



Experiment and calculation has demonstrated that in the case of the same coupling coefficient for dielectric mode with anyone of magnetostatic modes (for its small values) hybridization taken place only for the main modes (0,1,1) and $H_{11\delta}$. Consequently, the higher magnetostatic modes almost doesn't interact with electromagnetic mode of dielectric resonator.

[1] V.E. Demidov, B.A. Kalinikos, *J. Appl. Phys.*, **91**, No. 12 (2002) 10007.

[2] T.G. Chamor, A.Yu. Gorpynyuk, V.I. Kostenko, L.V. Chevnyuk, Proc. of the 17th International Crimean Conference "Microwave & Telecommunication Technology". – Sevastopol (Ukraine) **II**. (2007) 562.

[3] M.E. Ilchenko, S.N. Basenko, *Radiotekhnika and Electronics* (1986) 15.

[4] V.I. Kostenko, M.A. Sigal, *Fizika Tverdogo Tela.*, – **29**, No. 4 (1987). – c. 1217.

[5] B. A. Auld, *J. Appl. Phys.*, No.6 (1963) 1629.

21PO-16-14

SOLITARY WAVES AND NONLINEAR DYNAMIC COHERENT STRUCTURES IN MAGNETIC METAMATERIALS

Tankev A.P., Smagin V.V., Borich M.A.

Institute of Metal Physics of the Ural Division of Russian Academy of Sciences,
18 Sofia Kovalevskaya Str., Ekaterinburg 620041, Russia

The magnetic metamaterials are the man-made compositions possessing a set of the unexpected properties which are missing in natural materials and are not intrinsic to constituent elements of compositions. The real representatives of such compositions are the well-known layered ferromagnet-dielectric-metal structures. It has been established that spectra of both the volume magnetostatic waves, and the surface waves are nonmonotone functions of the wave vector in such structures. As a rule, the dispersion laws of these waves include both the frequency regions with the negative group velocity (anomalous dispersion), and the regions where the space dispersion of the group velocity is lacking ("zero-dispersion" point). The latter takes place in the vicinity of the inflection point in the dispersion law. The long-range magnetic dipole-dipole interaction, the presence of the external steady-state magnetic field and the size effects give rise to such features. The phase and group velocities of the wave packet are directed towards inside the region of the anomalous dispersion. These circumstances are the cause of the new and unexpected features in the linear and nonlinear regimes of wave propagation. The negative wave refraction inherent in the wave with the negative group velocity, the inverse Vavilov-Cherenkov effect etc[1] are among these effects. The lack of space dispersion of the group velocity in the vicinity of the "zero-dispersion" point affects essentially the a formation and propagation of solitary waves of the magnetization in such materials. The nonlinear dynamic models taking into account the noted features of the spectrum of the magnetostatic waves, size effects, and higher order linear and nonlinear dispersions have been constructed earlier [2]. The correlation between the marked features of the spectrum of the carrier wave and a kind of the incipient solitary waves has been established. Analytical and numerical algorithms for analysis of scenarios of emergence and evolution of quasi-solitons, as well as the processes of their interaction, transformation, and decay under the action of external monochromatic radiation, have been developed [3].

The exact solutions of an extended non-linear Schrodinger equation (the equation of quasi-solitons evolution) and the results of an investigation of the conditions for the formation and a propagation of the coherent breather structures (two-soliton states) in the system ferromagnetic-dielectric-metal are presented in this report. It is shown that the formation of breather lattices is possible inside the frequency region of the linear spectrum where the existence conditions of the "light" quasi-solitons are fulfilled. The similar lattices are not formed inside the frequency region where the existence conditions of the "dark" quasi-solitons are fulfilled; and instead of them, the structures composed from the kinks of the opposite polarity (the composite quasi-solitons) are formed. The stability criterion and the conditions of experimental observing of the above-mentioned breather states and composite quasi-solitons are discussed in detail.

The work was done within the framework of Program of Basic Researches of the Presidium of RAS "Mathematical methods in the nonlinear dynamics".

[1] V.M Agranovich , Yu.N. Gartstein, *Usp.Fiz.Nauk*, 2006, **176** (2006) 1051.

[2] M.A Borich , V.V.Smagin, A.P.Tankev , *Bull.of the RAS: Phys.*, **71** (2007),1571.

[3] M.A Borich, V.V.Smagin, A.P.Tankeyev, *The Phys.of Met.and Metallography*,103(2007), 118.

21PO-16-15

METAMATERIALS FROM AMORPHOUS FERROMAGNETIC MICROWIRES: INTERACTION BETWEEN MICROWIRES

Ivanov A.V.¹, Shalygin A.N.^{1,2}, Galkin V.Yu.², Vedyayev A.V.¹, Ivanov V.A.³

¹Faculty of Physics, Moscow State University, Moscow, 119992 Russia

²R&P VICHEL (High-Frequency Systems), Moscow, 119991 Russia

³N. S. Kurnakov Institute of General and Inorganic Chemistry of the RAS, Moscow, 119991 Russia

For a few recent years, new developments in artificially structured materials giving rise to negative refractive index $n = \sqrt{\epsilon(\omega) \cdot \mu(\omega)} < 0$ with simultaneously negative real parts of frequency dependent permittivity $\epsilon(\omega)$ and permeability $\mu(\omega)$ in some frequency ranges have been attracting much attention. They are named left-handed materials [1], negative-index mediums, negative phase-velocity mediums (NPVM), backward wave mediums or even double negative media. Recently developed *homogeneous NPVM* have been paid much attention in journals and press. For NPVM anomalous effects such as negative refraction, Doppler shift, Cherenkov-Vavilov radiation, light pressure, invisibility effect have been discovered in different frequency ranges. For them the gyrotropic phenomena are possible as well [2-4]. But other electromagnetic effects such as optical Magnus effects are given by a circular polarization of propagating waves and ∇n . Are they anomalous in *inhomogeneous NPVM* and is it possible to realize them per se? In this presentation the optical circular polarized effects are calculated for inhomogeneous mediums and they are anomalous in NPVM with respect to right-handed materials. The proposed metamaterials fabricated from glass coated amorphous ferromagnetic Co-Fe-Cr-B-Si microwires [5] are shown theoretically [6] and experimentally to exhibit a negative refractive index for electromagnetic waves over scale of GHz frequencies. The magnetostatic interaction between microwires has been taking into account. Optical properties of such metamaterials are tunable by an external magnetic field and mechanical stress.

This work is partially supported by RFBR Project 08-02-00830-a.

[1] V.G. Veselago, *Soviet Physics - Uspekhi* **10** (1968) 509 [*Uspekhi Fizicheskikh Nauk* **92** (1967) 517 (*in Russian*)]; *ZhETF* **52** (1966) 1025.

[2] I.V. Lindell, S.A. Tretyakov, K.I. Nikoskinen et al., *Microwave and Opt. Tech. Lett.* **31** (2001)129.

[3] T.G. Mackay, A. Lakhtakia, *Phys. Rev. E* **69** (2004) 026602.

[4] A.V. Ivanov, O.A. Kotelnikova, A.V. Vedyayev et al., *JMMM* **300** (2006) e67; *Vestnik Moskovskogo universiteta. Fizika. (in Russian)* (Moscow University Physics Bulletin (Allerton Press, Inc.)) No **4** (2006) 25.

[5] V.V. Molokanov, P.P. Umnov, N.V. Kurakova et al., *Perspektivnye materialy (in Russian) (Journal of Advanced Materials)* No **2** (2006) 5.

[6] A.V. Ivanov, A.N. Shalygin, A.V. Vedyayev et al., *JETP Lett.* **85** (2007) 565

[7] A.V. Ivanov, A.N. Shalygin, V.Yu. Galkin, A.V. Vedyayev et al., *Proceedings of Metamaterials 2007 – Rome 22-26 October 2007.*

21PO-16-16

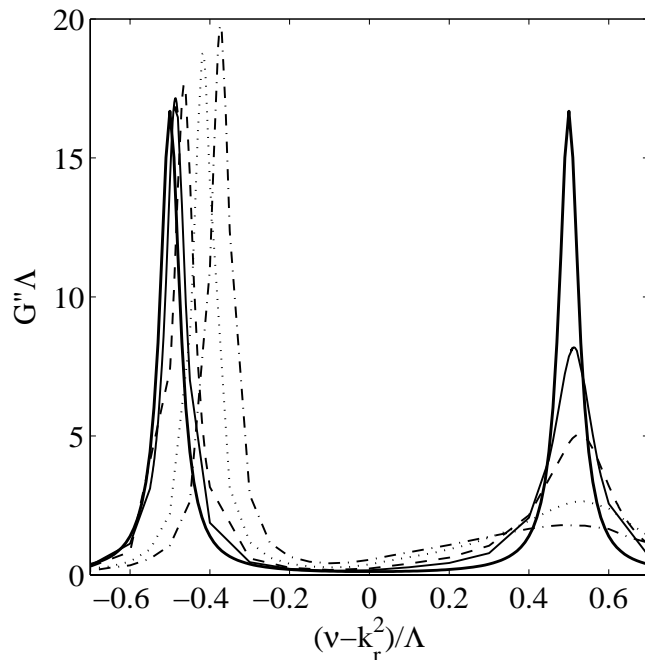
HIGH-FREQUENCY SUSEPTIBILITY OF SUPERLATTICES WITH TWO-DIMENSIONAL INHOMOGENEITIES

Ignatchenko V.A.¹, Mankov Yu.I.^{1,2}, Tsikalov D.S.²

¹Kirensky Institute of Physics, Akademgorodok, 660036 Krasnoayrsk, Russia

²Siberian Federal University, 660062 Krasnoayrsk, Russia

The high-frequency susceptibility (Green's function) of the initially sinusoidal superlattice with two-dimensional (2D) phase inhomogeneities which model deformations of the interfaces of the superlattice is investigated. We consider a ferromagnet in which the parameter of the anisotropy is periodic along the z axis in the initial superlattice but in a superlattice with inhomogeneities it depends on all three coordinates: $\beta(\mathbf{x}) = \beta + \Delta\beta\rho(\mathbf{x})$, where β is the mean value of the parameter of anisotropy, $\Delta\beta$ is its rms deviation, $\mathbf{x} = \{x, y, z\}$, $\rho(\mathbf{x}) = \sqrt{2} \cos[qz + u_2(\mathbf{x}_\perp) + \psi]$, $u_2(\mathbf{x}_\perp)$ and ψ are inhomogeneous and homogeneous random



phases, respectively $\mathbf{x}_\perp = \{x, y\}$; $q = 2\pi/l$, l is the period of the superlattice. The correlation function of the superlattice is derived and suitable approximation is found for it which allows to calculate the averaged Green's function. It is shown that is the essential distinction between the peaks the imaginary part G'' of the Green's function corresponding to the different edges of the forbidden zone in the spectrum of waves. The peak corresponding to the edge with the smaller frequency remains practically invariable at the increase of rms fluctuations of 2D inhomogeneities γ_2 , while the peak corresponding to the edge with the greater frequency broadens and sharply decreases in height before its full

disappearance (see Fig.). Here $\nu = (\omega - \omega_0)/\alpha g M_0$, $\Lambda = \sqrt{2}\Delta\beta/\alpha$, where ω is the frequency, ω_0 is the frequency of the ferromagnetic resonance, g is the gyromagnetic ratio, α is the exchange parameter, and M_0 is the magnetization; $k_r = q/2$ is the boundary of the first Brillouin zone of the superlattice. Such behavior of the peaks corresponds to the mechanism of the forbidden zone closing that is distinct from the traditional, typical for 1D and 3D inhomogeneities (peaks symmetrically decrease and become closer to each other until they merge into one peak). These effects are explained by the peculiarity of the energy conservation law of the falling and scattering waves for 2D inhomogeneities in an one-dimensional superlattice

$$k_{sx}^2 + k_{sy}^2 = \nu - k_r^2, \quad (1)$$

where \mathbf{k}_s is the wave vector of the scattering wave. If the inequality $\nu - k_r^2 < 0$ is fulfilled, the equality (1) breaks down and the scattering becomes impossible. The effect of asymmetry of peaks of the high-frequency susceptibility can be used practically at studying inhomogeneities in

a superlattice by spectral methods. The experimental observation of this effect would testify the presence of the 2D inhomogeneities in the superlattice.

This work was partially supported by the Grant of the RF President, SS – 3818.2008.3.

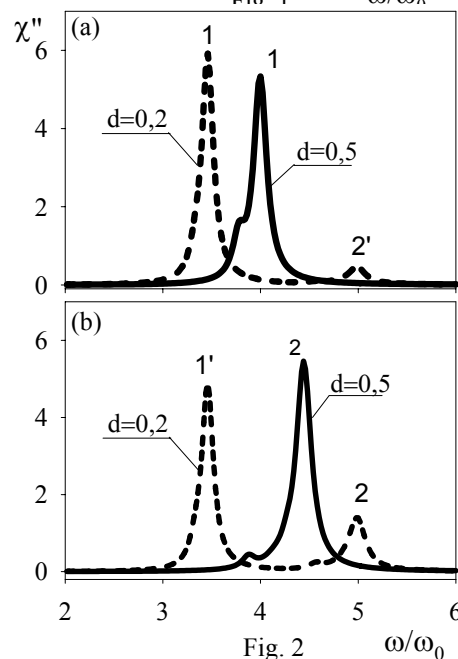
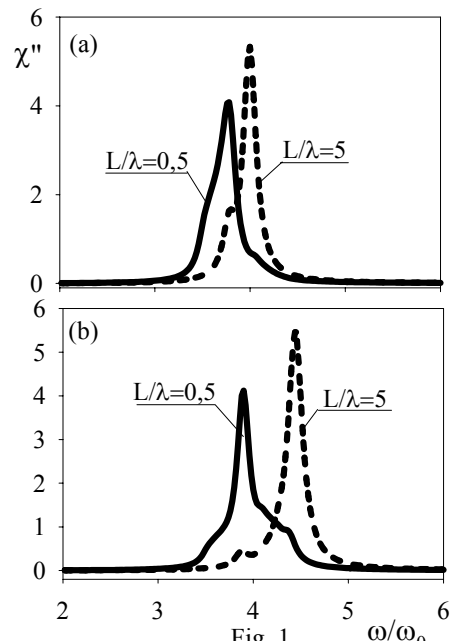
21PO-16-17

THE FERROMAGNETIC RESONANCE IN THE PLATE WITH STRIPE DOMAIN STRUCTURE TAKING INTO ACCOUNT NONUNIFORMITY OF THE DEMAGNETIZING FIELD

Shul'ga N.V., Doroshenko R.A., Mal'ginova S.D.

Institute of Molecular and Crystal Physics, Academy of Sciences, 151, October Prospect, Ufa, 450057, Russia

Computation of the ferromagnetic resonance in the absence of an external magnetic field in a plate with the high factor of quality has been carried out. The domain structure with Bloch domain walls was studied. The dependences of an imaginary part of a scalar dynamic susceptibility χ'' upon the reduced frequency ω/ω_0 for the sample with quality factor $Q=4$ are given in Fig. 1 and 2; (a) the weak alternating magnetic field is directed perpendicularly to domain wall (low-frequency mode); (b) it is directed parallel to domain wall (high-frequency mode). The account of nonuniformity of the demagnetizing field results in appearance of additional peaks in FMR spectrum. In Fig. 1 resonance curve change is shown at change of the relation of a thickness of plate L to a period of domain structure λ . One can see that with reduction of a thickness of a plate there is a bias of peaks of a resonance curve in the low-frequency region. In Fig. 2 change of a resonance curve with change of the relative size of the left domain in a period d is shown. The growth of the size of one of domains at the expense of another leads to increase of amplitude of a susceptibility of a low-frequency mode of the ferromagnetic resonance (it's denoted 1) and it shift in the low-frequency region. Accordingly the amplitude of a susceptibility of a high-frequency mode (it's denoted 2) decreases and there is its shift in the high-frequency region. In addition, at a resonance in a plate with unequal domains the peak of the resonance curve corresponding to a high-frequency mode is observed also in the weak alternating magnetic field directed perpendicularly to domain wall (it's denoted 1'), and low-frequency mode is observed in the weak alternating magnetic field directed parallel to domain wall (it's denoted 2'). The found out features of a resonance curve are explained by respective changes of the nonuniform demagnetizing field.



21PO-16-18

THE STIMULATION AND SPREADING OF NONLINEAR LOCALIZED SOLITARY BENDING WAVE IN DRIVING DOMAIN WALLS IN MAGNETICS WITH LOCAL INHOMOGENEITIES

Ekomasov E., Shabalin M., Azamatov Sh., Murtazin R.

Bashkir State University, Ufa, Frunze str. 32, Russia

In different physical appendices the large concern introduces nature of dissipation of mobile excitation, including solitons and kinks, on local heterogeneities of parameters of a stuff, which one model defects in studied medium [1]. The case is specially interesting, when the size of a magnetic nonhomogeneity and the size describing a nonhomogeneity of parameters of a stuff are of the same order, then the form of a magnetic nonhomogeneity should undergo strong changes at transit through an inhomogeneous area [2]. The experimental works have also appeared [3,4], demonstrating that the presence of defects in rare earth orthoferrites (REO), can result in a nonhomogeneity of a constant of a magnetic anisotropy (NCMA). With the help of the theory of a perturbation earlier the nonlinear bending waves of domain walls (DW) in orthoferrites were theoretically investigated [5]. The solutions in the shape of solitary non – linear waves were obtained, and a supposition that the cause of their excitation in the process of DW motion can be local nonhomogeneities was made. In experimental work [6] the modification of the DW structure was studied at intersection of a defect in a thin plate orthoferrites of yttrium. In this work with the help of numerical methods the nonlinear dynamic of DW intersecting two-dimensional magnetic defect, leading to the nonhomogeneity of NCMA, was investigated. The process of engendering and evolution of solitary bending wave was studied. The dependence of solitary wave velocity \tilde{v} on DW velocity value \tilde{u} , near to the well-know law $\tilde{u}^2 + \tilde{v}^2 = c^2$ was found. The dependence of solitary wave amplitude on the domain wall velocity value was found. Considering the passing of the DW through the region with two similar NCMA, one can study the interaction of acquired bending waves. In the region of their interaction, one can observe deviations that are the kink sine - Gordon equation (fig. 1).

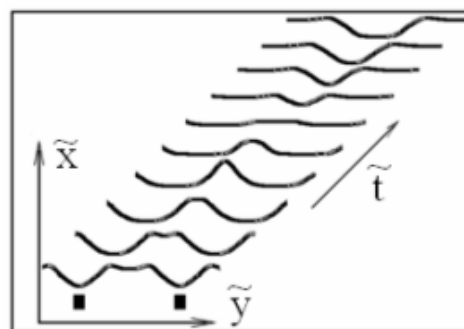


Fig. 1 Position of center DW dependence on coordinates (\tilde{x}, \tilde{y}) in different instants. The black rectangle – is NCMA placing.

- [1] A.M. Kosevich, A.S. Kovalev. Leading in nonlinear physics mechanics. Kiev, Naukova dumka, 1989.
- [2] A. Hubert. Theory of domain walls in clustered environment, Moskow, World, 1977.
- [3] A.M. Balbashov, A.V. Zaleskij, V.G.Krivenko, E.V. Sinicin. Pis'ma Zh. Tech. Fiz. 14 (1988) 293.
- [4] M.V. Chetkin, A.P.Kuz'menko, A.V. Kaminskiy, V.N. Filatov Sol.State Phys. 40 (1998) 1656.
- [5] A.K. Zvezdin, A.F. Popkov, Pis'ma Zh. Exp.Teor. Fiz. 39 8 (1984) 348.
- [6] M.V. Chetkin, Yu.N. Kurbatova Fiz. Tverd. Tela 43 (2001) 1503.

21PO-16-19

THE STUDY OF THE ORIGIN AND EVOLUTION OF THE MAGNETIC INHOMOGENEITY OF BREAZER AND PULSON TYPES IN REAL MAGNETICS

Ekomasov E., Azamatov Sh., Murtazin R., Gumerov A.
Bashkir State University, Ufa, Frunze str. 32, Russia

It is known that in real magnetics the appearance of magnetic parameters local changes happens due to structural and chemical non-homogeneities and local influence (mechanical, thermal or solar). As it is usually difficult to make a precise (microscopic) calculation, one is to model the functions, which describe the parameters of a non-homogeneous material [1]. The case is especially interesting, when the size of a magnetic non-homogeneity and the size, describing a non-homogeneity of parameters of a stuff, are of the same order. It results in considerable complication of Landau-Lifshitz equation for the magnetization. Although the task of excitation and distribution of the magnetization waves, under certain conditions, is reduced to the studies of the modified sine-Gordon equation with floating factor [2]. The investigation of big perturbations influence on the solution of modified sine-Gordon equation in general case can be investigated only with the help of numerical methods [3]. In dynamic, when in the area of such non-homogeneities (or defects) a temporally or spatial non-homogeneous perturbation acts, under certain conditions, a strongly non-linear waves of magnetic character can be aroused. Such waves are weakly investigated.

In the research a non-linear dynamic of domain walls (DW) (sine-Gordon equation kinks) for the case of 1D and 2D non-homogeneity of the material parameters (for example, magnetic anisotropy and exchange constant) was investigated with the help of numerical methods. We use method of iteration for the explicit scheme [4]. For the 1D case we have studied the origin and evolution of the structure of fading breazer types of magnetic non-homogeneous appearing in anisotropy non-homogeneity region. The value areas for the parameters governing the possibility of their existence, the amplitude formed by pulson slowly decreased with time. The dependence of breazer oscillation frequency from the parameters of the material inhomogeneity is discovered. For the 2D case we have investigated the dynamic of solitary bending waves, which appear on the DW crossing of defect region, and the origin and evolution of the magnetic non-homogeneities of pulson type, localized in this region. The amplitude formed pulson slowly decreases with time.

[1] *Paul D.I.* // *J.Phys.C: Solid State Phys*, **12**, 585 (1979).

[2] *Ekomasov E.G., Shabalin M.A.* // *Physics of Metals and Metallography*, **101**, Suppl. 1, S48 (2006).

[3] *Ekomasov E.G., Shabalin M.A., Azamatov Sh.A., Buharmetov A.F.* // *Functional Materials*, **13**, 443 (2006).

[4] *Ekomasov E.G., Azamatov Sh.A., Murtazin R.R.* // *Physics of Metals and Metallography*, **105**, 341 (2008).

21PO-16-20

SWR IN THREE - LAYER NiFe/Cu/ NiFe FILMS AND MULTILAYERED Co/Pd FILMS

Iskhakov R.S.¹, Shepeta N.A.³, Stolyar S.V.^{1,2}, Yakovchuk V.Yu.¹, Chekanova L.A.¹

¹Kirenski Institute of Physics, Siberian Division, Russian Academy of Sciences, Krasnoyarsk, 660036 Russia

²Siberian Federal University, Krasnoyarsk, 660041 Russia

³Siberian State Air Space University, Krasnoyarsk, 660014 Russia

Spin-wave resonance and ferromagnetic resonance were used to study the magnetic parameters of multilayers Co/Pd films and NiFe/Cu/NiFe sandwiches. The Co/Pd multilayered films with a total thickness of 150 nm were chemically deposited on cover glasses. Sandwich layers were formed by evaporation.

For Co/Pd multilayers films, united spin-wave resonance spectra have also been observed at thickness of the paramagnetic palladium layer up to $d_{Pd} < 3$ nm. The partial exchange stiffness has been calculated for a spin wave propagating across the Pd layer $A_{Pd} = 0.1 \times 10^{-6}$ erg/cm.

It is established by SWR technique that interlayer coupling in trilayers "NiFe(950E)/Cu/NiFe(950E)" initially are exchange and then it is substituted for magnetostatic with increasing of diamagnetic spacer thickness (fig.1). The following increasing of diamagnetic spacer thickness is result in restoring exchange coupling (fig.2) and then for the Cu thickness is more than 70E magnetostatic coupling is established finally(fig.3).

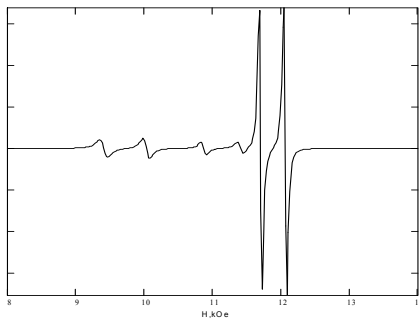


fig. 1. SWR in NiFe/Cu(42Å)/NiFe,

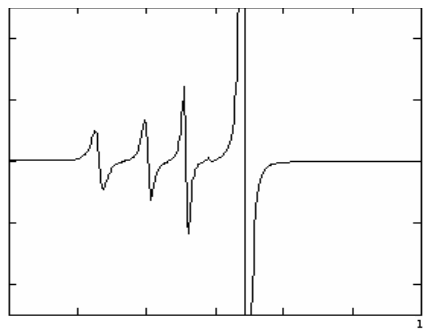


fig. 2. SWR in NiFe/Cu(55Å)/NiFe,

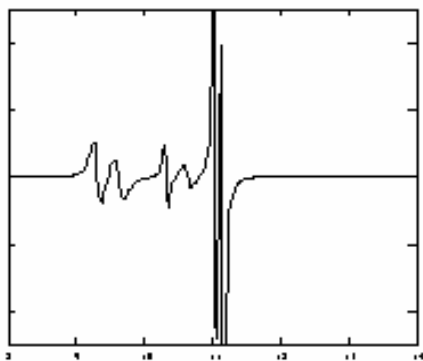


fig. 3. SWR in NiFe/Cu(75Å)/NiFe,

Support by RFBR, project no. 07-02-01172-a is acknowledged.

21PO-16-21

NON-LINEAR DYNAMICS OF A 360-DEGREE DOMAIN WALL IN A BIAxIAL FERROMAGNET IN THE MAGNETIC FIELD

Nazarov V.N.¹, Shamsutdinov M.A.²

¹Institute of Molecular and Crystal Physics, Ufa, 151, Pr. Oktyabrya, 450075, Russia

²Bashkir State University, Ufa, 32, Frunze St., 450074, Russia

The paper [1] showed a possibility of a motion of the two 180-degree domain walls in a uniaxial ferromagnet relative to the stationary centre of the 360-degree wall formed by the two ones above. This paper presents the results of an investigation of the dynamics of a wall with the structure determined by the following expression:

$$\text{ctg}^2(\theta/2) = (\Omega + \tilde{Q}^{-1} \sin^2 \varphi)(\Omega - 1)^{-1} \text{sh}^2(\sqrt{1 - \Omega} \cdot \xi), \quad (1)$$

in the biaxial ferromagnet placed in the external magnetic field H with due account taken of dissipation. Here, $\tilde{Q} = K_u / (2\pi M_s^2 + K_p)$, K_u is the uniaxial anisotropy constant; K_p is the rhombic anisotropy constant; $0 \leq \theta \leq 2\pi$ is the angle of magnetization rotation; $\varphi = \varphi(t)$ characterizes the change in the structure of the

180-degree wall [2], $-\infty < \Omega(t) < -\tilde{Q}^{-1} \sin^2 \varphi$.

The numerical solution of the system for φ and Ω demonstrates the existence of an oscillatory motion of the two strongly interacting 180-degree walls of opposing polarities relative to the centre of the 360-degree wall formed by them. Such a motion of the walls is accompanied by a continuous change of their structure from the Bloch one ($\varphi = 0$) to the Neel ($\varphi = \pi/2$) one and back (See Fig.). The nature of the structure transformation with no dissipation present is strongly affected by the initial condition of the 360-degree wall and the external magnetic field.

At small values of initial amplitudes the oscillation frequency of two 180-degree walls is expressed by the following equation:

$$\omega_0 = \frac{2\gamma}{M_s} \left[(K_p + 2\pi M_s^2) M_s H \right]^{1/2}, \quad (2)$$

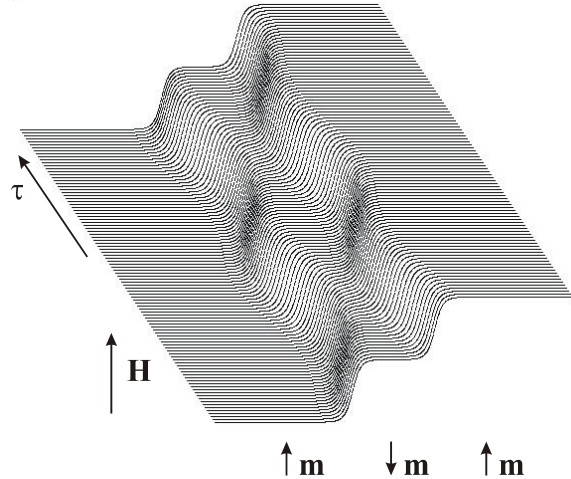
where γ is the gyromagnetic ratio. As the initial amplitude rises, according to computational modeling, the value of the frequency became lower than (2), and the significant deviation from the harmonic will be observed. Taking into account the dissipation α the frequency of the small-amplitude oscillations is expressed as follows:

$$\omega = \sqrt{\omega_0^2 - \delta^2}, \quad \delta = \frac{\alpha\gamma}{M_s} (K_p + 2\pi M_s^2 + M_s H).$$

Such dependence conditions the existence of a critical field that delineates the modes of the walls' fading motion of the periodic and aperiodic nature.

[1] N.V. Ostrovskaya, A.F. Popkov, and V.P. Romanov, *Fiz. Met. Metalloved.* **73** (1992) 24.

[2] M.A. Shamsutdinov, V.N. Nazarov, and I.Yu. Lomakina, *Fiz. Met. Metalloved.* **101** (2006) 309.



21PO-16-22

AUTORESONANCE EXCITATION OF NONLINEAR OSCILLATIONS OF DOMAIN WALLS

Shamsutdinov M.A.¹, Kalyakin L.A.², Sukhonosov A.L.¹, Khalfina A.A.¹

¹Bashkir State University, 450074, Ufa, Frunze str., 32, Russia

²Institute of Mathematics with Computing Centre, Ufa Scientific Center, Russian Academy of Sciences, 450077, Ufa, Chernyshevskogo str., 112, Russia

The paper presents the results of investigating small nonlinear oscillations of domain walls within the lattice of striped domains, these oscillations excited by a low-amplitude alternating field. In the case of small nonlinear oscillations, the equation of the domain wall motion [1] can be reduced to the form:

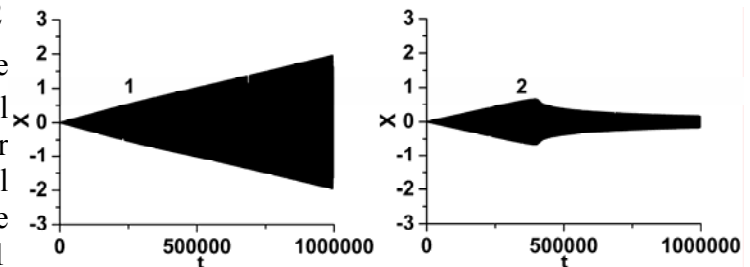
$$x_{tt} + 2\lambda x_t + x + \gamma x^3 = \varepsilon h_0(t) \cos \Phi \quad (1)$$

Here, x is the domain wall movement, λ is the attenuation parameters, and γ is the small parameter of nonlinearity. The distinguishing feature of this paper lies in the fact that both frequency and amplitude are presumed to be dependent on time. The frequency and amplitude of the external field are assumed as slowly changing with time following the law $\omega(\theta) = \frac{d\Phi}{dt} = 1 + \alpha \varepsilon^{2/3} \theta^n$, $h_0(\theta) = h_0(1 + p\theta)$, where $0 < \alpha \ll 1$ and $p > 0$ are the parameters

that determine the speed of variation of the external field's frequency and amplitude, $\theta = \varepsilon^{2/3} t$ is slow time. The equations of the main resonance of the system (1) are thoroughly investigated, and it has been shown that in the case of zero dissipation ($\lambda = 0$) and with constant amplitude of the external field ($p = 0$), capturing the oscillations into autoresonance is possible if the variation of frequency takes place sufficiently slowly, when the pump amplitude exceeds a certain threshold value h_{0p} , at $n = 2$ $h_{0p} = 2\sqrt{8\alpha/(3\gamma)}$ [2]. This frequency "capture" maintained for a considerable length of time brings about a substantial increase of the domain wall oscillation amplitude at the low pump amplitude h_0 .

For the case when dissipation was taken into account ($\lambda \neq 0$), the condition of slowness of the pump frequency variation turned out to be insufficient to capture the oscillations into autoresonance. Solutions with the increasing amplitude may arise when both the frequency and the amplitude of the external alternating field vary to the appropriate degree. An analysis of the main resonance equations shows that to make up for the attenuation effect one should assume $p > p_k$, where in the case of $n = 2$

$p_k = \lambda / \varepsilon^{2/3}$. If these conditions are met, the amplitude of the domain wall oscillations may increase to greater values. The figure presents numerical solutions of equation (1) for the parameters $n = 2$, $\lambda = 0.01$



$\varepsilon = 0.001$, $h_0 = 0,0040 > h_{0p} \approx 0.0038$, $\gamma = 0.074$, $\alpha = 10^{-7}$. Curve 1 corresponds to the case of $p = 1.1 > p_k$, while Curve 2 – to the one of $p = 0.9 < p_k$, where $p_k = 1.0$.

[1] M.M. Solov'ev, B. N. Filippov, Technical Physics, 45, (2000) 1566

[2] L.A. Kalyakin, Doklady Mathematics, 67, (2003) 107

21PO-16-23

EXCITATION OF A MAGNETIC BREATHER BY A FIELD OF AN ACOUSTIC WAVE

Kharisov A.T.¹, Shamsutdinov M.A.¹, Kalyakin L.A.²

¹Bashkir State University, Ufa, 450074, Russia

²Institute of Mathematics with Computing Center, Ufa, 450077, Russia

e-mail: Khantaf@mail.ru

As is known, an elastic wave can be used to parametrically excite linear magnetic waves [1, 2]. This paper investigates parametric excitation of a low-amplitude magnetic inhomogeneity in the form of a breather by the field of an elastic wave. Non-linear dynamics of magnetization in dimensionless variables is described by the perturbed sin-Gordon equation:

$$u_{tt} - u_{xx} + \sin u = -2h_0 \sin \frac{u}{2} - \beta u_t + b \frac{\partial e_x}{\partial x} \sin u, \quad (1)$$

where $h_0 = \mu t$ is the magnetic field strength slowly increasing with time; β is the attenuation parameter; b is the magnetoelastic constant; $e_x = e_0 \sin(kx - \omega t)$ is the longitudinal acoustic wave. Having taken the low-amplitude breather of the unperturbed sin-Gordon equation as a solution of equation (1), and following the logic of papers [3, 4], the equations of the main resonance can be obtained:

$$\begin{aligned} \frac{dR}{d\tau} &= R \left[-\frac{2\beta}{\varepsilon} + \frac{h_1}{\varepsilon} \sin \Psi \right], \\ \frac{d\Psi}{d\tau} &= -R + \frac{h_1}{2\varepsilon} \cos \Psi + \frac{\mu}{\varepsilon^2} \tau, \end{aligned} \quad (2)$$

where $\tau = \varepsilon t$, $0 < \varepsilon \ll 1$, $h_1 = kbe_0$. An analysis shows that at $h_1 > 2\beta$ there exists a solution of the system of equations (2) with the amplitude R increasing at $\tau \rightarrow \infty$ within the specific range of initial values of amplitudes R_0 and phases Ψ_0 [3, 4]. The amplitude of the elastic wave should satisfy the condition $e_0 > e_{cr} = 2\beta/(kb)$. In dimensional variables, the threshold value of the amplitude of the elastic wave of pumping will be written as

$$a_{cr} = \frac{\alpha VM}{2\gamma B},$$

where α is Gilbert's attenuation parameter; V is the acoustic wave speed; M is saturation magnetization; B is the magnetoelastic constant; γ is the gyromagnetic ratio.

Thus, parametric excitation of a magnetic breather is possible by an elastic wave with a frequency two times greater than that of ferromagnet resonance as the resonance field slowly increases with time.

Support by Academy of Science of Republic Bashkortostan is acknowledged.

[1] A.G. Gurevich, G.A. Melkov, *Magnitnye kolebaniya i volny* (Fizmatlit, Moscow, Russia 1994).

[2] H. Matthews, F.R. Morgenthaler, *Phys. Rev. Lett.* **13** (1964) 614.

[3] L.A. Kalyakin et al., *The Physics of Metals and Metallography* **104** (2007) 107.

[4] M.A. Shamsutdinov et al.: *Ferro- i antiferromagnitodinamika. Nelineinye kolebaniya, volny i solitony* (Gilem, Ufa, Russia 2007).

21PO-16-24

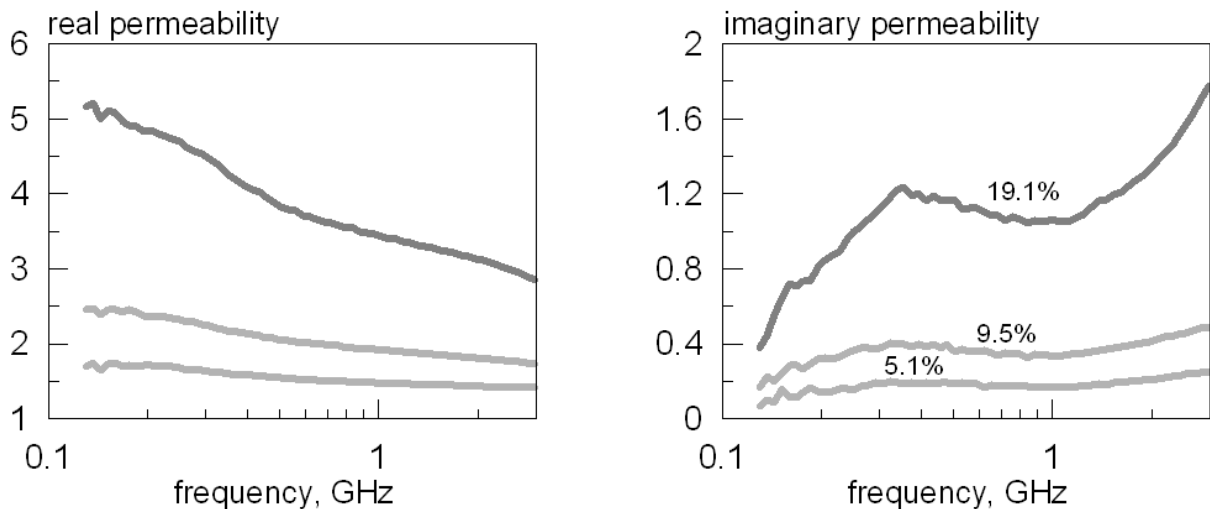
A MICROWAVE STUDY OF INTRINSIC PERMEABILITY OF MECHANICALLY ACTIVATED FE AND FE-SI POWDERS

Petrov D.A.¹, Yelsukov E.P.², Rozanov K.N.¹, Lomayeva S.F.², Osipov A.V.¹, Shuravin A.S.², Starostenko S.N.¹, Chulkina A.A.², Konygin G.N.²

¹Institute for Theoretical and Applied Electromagnetics RAS, Moscow, Russia

²Physical-Technical Institute UrB RAS, Izhevsk, Russia

We study microwave properties of composites comprising either Fe or Fe-Si powder inclusions and paraffin matrix. The powders are produced by milling under different milling conditions. The microwave permeability and permittivity of the composites are measured with a HP8753A vector network analyzer and coaxial measurement cell in the frequency range of 100 MHz to 3 GHz. The figure shows the measured microwave frequency dependence of permeability of composites with different concentrations of Fe₈₇Si₁₃ powder milled in a heptane solution of oleic acid. Volume concentrations of inclusions are given in the figure. We measure the permeability and permittivity as a function of the concentration of inclusions and calculate intrinsic permeability of inclusions with the use of the Maxwell Garnett (MG) approximation and the Ghosh-Fuchs (GF) theory [1]. After that we restore the intrinsic permeability of inclusions for different concentrations to analyze which approximation provides better agreement. The GF theory is found to provide better agreement with the measured permittivity and permeability of the composites than the MG theory. We demonstrate the effect of shape of powder particles on the microwave properties of the composites. The anisotropy of the samples is observed to depend on manufacturing process.



The study is partially supported by RFBR projects nos. 06-08-00788 and 07-08-92111.

[1]K. N. Rozanov, A. V. Osipov, D. A. Petrov, S. N. Starostenko, E. P. Yelsukov, Reconstruction of intrinsic permeability of inclusions from the measured permeability of a composite, Proc. of Symposium R: Electromagnetic Materials, 4th Int. Conf. on Materials for Advanced Technologies (ICMAT 2007), 1–6 July 2007, Sing., pp. 59–66.

21PO-16-25

AUTORESONANT EXCITATION OF NONLINEAR FMR IN SMALL PARTICLES

Shamsutdinov M.A.¹, Kalyakin L.A.²

¹Bashkir State University, Ufa, 450074, Russia

²Institute of Mathematics with Computing Center, Ufa, 450077, Russia

e-mail: ShamsutdinovMA@bsu.bashedu.ru

The paper attempts at investigating a possibility of exciting nonlinear FMR in single-domain particles with uniaxial anisotropy by alternate fields \mathbf{H}_1 of sufficiently small amplitudes. Both the frequency and the amplitude of the excitation field are considered as slowly-varying functions of time t . Due to the autoresonance effect, there is a possibility that processing magnetization \mathbf{M} may deflect by sufficiently great angles in low-amplitude fields. Autoresonance is usually understood as a phenomenon that involves a non-linear dynamic system automatically adjusting the frequency of its own oscillations to match the frequency of the external influence. For the case of small nonlinear variations of magnetization, the Landau-Lifshits equation, by introducing the complex field $(M_x + iM_y) \approx \varepsilon^{1/3}UM_0 \exp(i\Phi)$ may be written as [1]

$$iU_\tau + (\mu_\omega \tau^n + i\alpha \varepsilon^{-2/3} - k |U|^2)U = h_1(\tau) / \varepsilon. \quad (0 < \varepsilon \ll 1) \quad (1)$$

Here, $n = 1, 2$. $\Phi = \int \omega(t) dt$ – is the phase, and $\omega(t) = \omega_0(1 - \mu_\omega \varepsilon^{2/3} \tau^n)$, is the frequency of the transverse circularly polarized field, $\tau = t \omega_0 \varepsilon^{2/3}$, ω_0 is the frequency of linear FMR, $0 < \mu_\omega \ll 1$ is the parameter which characterizes the frequency variation, $0 < \alpha \ll 1$ is the damping constant, $0 < k \leq 1/2$ is the parameter that depends on the longitudinal field and effective anisotropy, $h_1(t) = \gamma_e H_1(\tau) / \omega_0$, γ_e is the gyromagnetic ratio. In the case of $\alpha = 0$, the equation (1) turns into a model equation of autoresonant excitation of oscillations with a substantially great amplitude under the influence of disturbances no matter how weak they can be ($h_1 \ll 1$). The mathematical fundamentals of this phenomenon at $h_1 = \text{const}$ are defined in detail [2]. Due to damping that brings about a decrease of the precession angle, in the case of small amplitudes of the alternating field, these amplitudes also invariable in time, the autoresonance phenomenon in ferromagnets is impossible. In this paper, the autoresonance phenomenon is studied as the amplitude of the alternating field slowly builds up following the law $h_1 = h_{10}(1 + \mu_h \tau)$. An analysis shows that if

$$n = 2, \quad h_{10} > \varepsilon \sqrt{\mu_\omega / k}, \quad \mu_h > \alpha / \varepsilon^{2/3},$$

hold, autoresonant excitation of nonlinear FMR may take place. The former condition means that the amplitude of the excitation field should be greater than a certain threshold value necessary to switch the system in the mode of nonlinear variations of magnetization. The latter condition means that the amplitude of pumping should be increased sufficiently fast not to allow the magnetization precession angle to decrease thus upsetting the resonant condition due to dissipation.

Support by Academy of Science of Republic Bashkortostan is acknowledged.

[1] M.A. Shamsutdinov et. al.: *Ferro- i antiferromagnitodynamika. Nelineinye kolebaniya, volny i solitony* (Gilem, Ufa, Russia 2007).

[2] L.A. Kalyakin: *Sovremennaya matematika i eyo prilozheniya* Vol 5 (2003), p. 79

21PO-16-26

INFLUENCE OF ELASTIC STRESS ON MAGNITOIMPEDANCE OF AMORPHOUS FOILS WITH LOW MAGNETOSTRICTION CONSTANT

Semirov A.V.¹, Gavriliuk A.A.², Bukreev D.A.¹, Kudryavcev V.O.¹, Moiseev A.A.¹

¹Irkutsk state teachers training university, Irkutsk, 664011 Russia

²Irkutsk state university, Irkutsk, 664003 Russia

The influence of elastic stress on magnetoimpedance of ribbons, which cut out from amorphous of a tape of structure Vitrovac 6025Z is investigated.

The impedance of samples was measured at frequencies f from 0.5 MHz to 10 MHz at amplitude of HF-current 30 mA. The elastic stress were enclosed along length of the sample and varied in range from 0 MPa up to 255 MPa. The maximal intensity of external magnetic field enclosed along the length of the sample was 3.6 kA/m.

Researched samples had length of 10 mm, width of 1 mm and thickness 25 microns. The induction of saturation was equal 0.55 T, magnetostriction constant was equal $-3 \cdot 10^{-7}$. The axis of easy magnetization of the ribbons had orientation perpendicularly to their length.

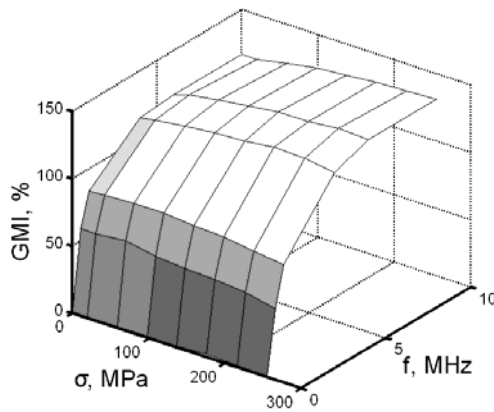


Fig. 1

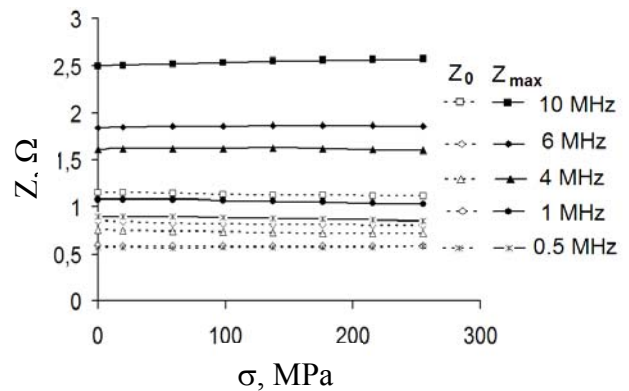


Fig. 2

During researches the field and frequency dependences of impedance of ribbons were received at various values of elastic stress σ . At frequencies is lower 4 MHz with increasing of elastic stress the weak decreasing of GMI-effect and its increasing at frequencies is higher 4 MHz is observed (fig. 1). The given character of frequency dependences of GMI-effect from elastic stress is caused in the basic behavior Z_{\max} (the maximal impedance in external magnetic field). It is illustrated by dependences of initial impedance Z_0 and Z_{\max} from elastic stress for various frequencies of HF-current (fig. 2). In all frequency range the elastic stress weak influence on Z_{\max} and Z_0 . It will be coordinated to model of behavior of magnetization under influence of elastic stress in materials with a negative magnetostriction constant and influence of mutual orientation of magnetization, external magnetic field and axis of HF-current on value of the impedance. However it is necessary to note, at frequencies less than 4 MHz with increasing of elastic stress, weak decreasing of Z_{\max} is observed, Z_0 practically did not change. At frequencies is higher than 4 MHz with increasing of elastic stress, increasing of Z_{\max} and weak decreasing of Z_0 is observed.

This research was supported by Russian Foundation for Basic Research (05-08-18063-a).

21PO-16-27

TEMPERATURE DEPENDANCE OF MAGNITOIMPEDANCE OF FeCoMoSiB FOILS

Semirov A.V.¹, Gavriiliuk A.A.², Bukreev D.A.¹, Kudryavcew V.O.¹, Moiseev A.A.¹

¹Irkutsk state teachers training university, Irkutsk, 664011 Russia

²Irkutsk state university, Irkutsk, 664003 Russia

The temperature researches of samples impedance of amorphous $\text{Fe}_4\text{Co}_{67}\text{Mo}_{1,5}\text{Si}_{16,5}\text{B}_{11}$ foils are carried out.

The researches was spent in temperature range from $t = 20\text{ }^\circ\text{C}$ to $220\text{ }^\circ\text{C}$. The impedance of samples was measured at frequencies from 0.5 to 10 MHz. The amplitude of HF-current was 30 mA. The maximal intensity of external magnetic field enclosed along the length of the sample was 3.6 kA/m.

Samples parameters: length – 10 mm, width – 1 mm, thickness – 25 μm , saturation induction – 0,55 T, magnetostriction constant $-3 \cdot 10^{-7}$. The axis of easy magnetization of the ribbons had orientation perpendicularly to their length.

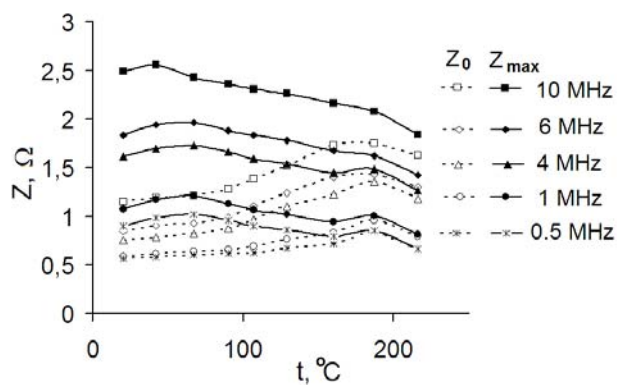


Fig. 1

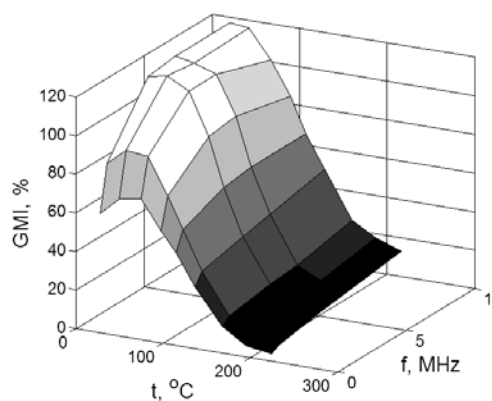


Fig. 2

It has been found, in whole frequency range with increasing the temperature from $20\text{ }^\circ\text{C}$ to $190\text{ }^\circ\text{C}$, value of initial impedance Z_0 (sample impedance in zero magnetic field) was increasing (fig.1). With further temperature increasing, initial ribbons impedance was decreasing. The temperature dependence of maximal impedance Z_{max} in external magnetic field depends on frequency of HF-current flowing through the sample. In a frequency range of (6 ÷ 10) MHz with increasing the temperature, insignificant increasing Z_{max} and then decreasing Z_{max} is observed. For the frequencies lower than 6 MHz after initial increase of Z_{max} its reduction up to temperatures about $160\text{ }^\circ\text{C}$ is observed. Next with increasing the temperature up to $190\text{ }^\circ\text{C}$ the increasing of Z_{max} , and then its decreasing is observed. With increasing the temperature the displacement of maximum on field dependences of impedance towards the smaller magnetic fields is observed. The temperature-frequency dependences of GMI-effect are represented on the figure 2. The value of GMI-effect was determined as $\frac{(Z_{\text{max}} - Z_0)}{Z_0} \cdot 100\%$. The temperature

dependences of GMI-effect for the different frequencies of HF-current have some differences. For the frequencies from 6 MHz to 10 MHz the decreasing of GMI-effect with increasing the temperature is observed. For the frequencies below 6 MHz the insignificant increasing of GMI and then its sharp reduction is observed.

This research was supported by Russian Foundation for Basic Research (05-08-18063-a).

21PO-16-28

EFFICIENCY OF COMPOSITES WITH METAL AND GRAPHITE FILLING IN ULTRAHIGH FREQUENCY

Fediy A.A., Bychkov I.V., Buchelnikov V.D.
Chelyabinsk State University, 454021, Chelyabinsk, Russia
E-mail: fediiaa@is74.ru

Electromagnetic radiation reflection and transmission coefficient of composite materials depends upon their content and geometry. Metal, carbon, soot, graphite, ferrites or ferrite mixture powder, or their mixture are most frequent fillings for the composite materials [1, 2]. Multilayer absorbents are proving materials because it will be easier to obtain an absorber with characteristics needed if some layers electrodynamic characteristics are changed.

In this work, we show the results of experiments with dependence of an efficient dielectric penetrability of dielectric matrix upon fine-dispersed Al content and flaked graphite content and dependence of reflection coefficient. CaSO_4 powder, $\text{CaSO}_4 \cdot 2\text{H}_2\text{O}$ and epoxy resin were used as dielectric matrixes. It was found that fine-dispersed Al has stronger influence upon ϵ' . If Al concentration in epoxy resin rises from 2 to 10%, ϵ' rises from 4 to 15.5. Reflection coefficient of semi-infinite sample was changing from -10.5 up to -3.5 dB. Such a strong dependence may be explained with percolation absence.

Graphite powder additions entail a very strong concentration dependence of ϵ'' . In CaSO_4 powder with coefficient equal to 0.5 and graphite filling increasing from 0 to 10% with respect to CaSO_4 leads to ϵ' change from 2.2 up to 3.5 and ϵ'' from 0.02 up to 0.6. Indistinguishable samples of $\text{CaSO}_4 \cdot 2\text{H}_2\text{O}$ show change of ϵ'' several times. Reflection coefficient of semi-infinite sample was changing from -12 up to -6.5 dB when graphite concentration was changed from 0 to 12%.

Thus, changing the graphite filing content and Al in the composite, we can obtain a material with defined characteristics ϵ' and ϵ'' to produce an optimal low-reflective absorber.

The work was financed by a grant RFFI – Ural 07-02-96030.

- [1] V.S.Pirumov, A.G.Alexeev, B.V.Aizikovich “New radio-absorbing materials and layers”.// Foreign Radioelectronics”, 1994, No 6, p. 2-9.
- [2] N.E.Kazantseva, N.G. Ryvkina, I.A.Chmutin “Good materials for absorbents of electromagnetic waves in superhigh frequency “.// Radio devices and electronics , 2003, vol.48, No2, p.196-209.

21PO-16-29

BIAS CURRENT EFFECT ON NONLINEAR MAGNETOIMPEDANCE RESPONSE IN AMORPHOUS WIRES WITH CIRCULAR ANISOTROPY

Buznikov N.A.¹, Antonov A.S.², Rakhmanov A.A.²

¹Scientific-Research Institute of Natural Gases and Gas Technologies – VNIIGAZ,
142717 Razvilka, Leninsky District, Moscow Region, Russia

²Institute for Theoretical and Applied Electrodynamics, Russian Academy of Sciences,
125412 Moscow, Russia

The giant magnetoimpedance (GMI) is one of the most promising magnetotransport effects due to its application in highly sensitive magnetic-field sensors. The GMI effect implies a large change in the impedance of a magnetic conductor in the presence of a static magnetic field and has been observed in different soft magnetic materials. The majority of the GMI studies are carried out at sufficiently low amplitudes of the exciting current, when the output voltage is proportional to the sample impedance.

The nonlinear voltage response occurs, when the magnetic field induced by the current is of the order of the anisotropy field. The appearance of higher harmonics in the magnetoimpedance response has been detected in electroplated wires [1] and Co-based amorphous wires [2–4]. This mode is often referred to as the nonlinear magnetoimpedance. The behavior of the nonlinear voltage response has been analyzed in the framework of quasi-static models [2,4]. Odd harmonics are always present in the nonlinear magnetoimpedance, whereas even harmonics occur in the presence of helical anisotropy in a wire, where there is an asymmetry in the magnetization curve. Although the first harmonic is dominant one in the voltage signal, the relatively low second harmonic has higher field sensitivity [3,4].

Another mechanism leading to the appearance of even harmonics in the voltage across the wire is related to the application of bias current. In this work, we study the bias current effect on the nonlinear magnetoimpedance in amorphous wires with a circular anisotropy. The rotational model to calculate the voltage response in the case of a weak skin effect is proposed. The appearance of alternating longitudinal magnetic field inside the wire due to the cross-magnetization process is taken into account. It is assumed that the alternating field distribution coincides with that obtained for the case of low current amplitudes [5]. In this approximation, expression for the voltage across the wire is obtained. It is shown that the appearance of higher harmonics in the voltage can be ascribed to the magnetization reversal process in the wire. The frequency spectra of the voltage are analyzed as a function of the external magnetic field, current amplitude and the value of the bias current. It is demonstrated that the application of the bias current may result in significant increase of the second harmonic amplitude. The conditions of maximum field sensitivity of the second harmonic are found. The results obtained may be of importance for a design of weak magnetic field sensors.

[1] G.V. Kurlyandskaya, H. Yakabchuk, E. Kisker, N.G. Bebenin, H. Garcia-Miquel, M. Vazquez, V.O. Vas'kovskiy, *J. Appl. Phys.*, **90** (2001) 6280.

[2] C. Gomez-Polo, M. Knobel, K.R. Pirota, M. Vazquez, *Physica B*, **299** (2001) 322.

[3] J.G.S. Duque, A.E.P. de Araujo, M. Knobel, A. Yelon, P. Ciureanu, *Appl. Phys. Lett.*, **83** (2003) 99.

[4] D. Seddaoui, D. Menard, P. Ciureanu, A. Yelon, *J. Appl. Phys.*, **101** (2007) 093907.

[5] D.P. Makhnovskiy, L.V. Panina, D.J. Mapps, *Phys. Rev. B*, **63** (2001) 144424.

21PO-16-30

ON Fe BASED GLASS COATED MICROWIRE'S ABSORPTION PROPERTIES

Garcia K.L.¹, Yamaguchi M.¹, Baranov S.A.², Vazquez M.³

¹Graduate School of Engineering, Tohoku University 980-8579 Sendai, Japan.

²Institute of Applied Physics AS RM, 5 Academy str. MD-2028, Chisinau, Republic of Moldova.
Dnester University, Tiraspol.

³Instituto de Ciencia de Materiales, CSIC. Campus Cantoblanco, 28049 Madrid. Spain.

The actual tendency to work at high and super-high frequencies in microdevices as led to problems such as noise and signal interference between miniaturized components. As a result of this there is an ongoing search for materials with outstanding high frequency properties that could be considered as successful candidates to fulfilled two aims: suppress the signal interference and meet the specific needs of industry (small size, near field absorption, specific frequency range). As there are not publications (that we know of) on noise suppressors based on cast amorphous microwires, in this work we will take the opportunity to size the probability of success for this materials to be used as noise suppressors.

The radio absorption properties of cast amorphous microwires (produced by Ulitovskiy-Taylor method) appear around the natural ferromagnetic resonance frequency, in the range of **1 - 12 GHz** (see [1-3]). The absorption of electromagnetic waves absorption in microwires is governed by the following expression:

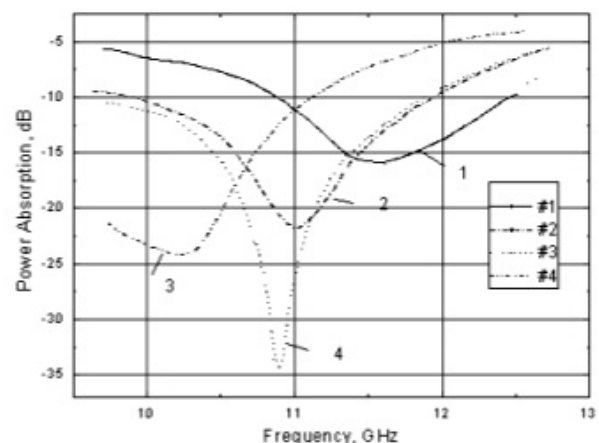
$$(f_{\text{res}}/\gamma)^2 = (H_a + H_b + 4\pi M)(H_a + H_b),$$

where f_{res} (Hz) is frequency of natural ferromagnetic resonance, $\gamma = 2.8$ MHz/Oe is the gyromagnetic ratio, H_a is the magnetization field inside the wire, H_b is the anisotropy field, which is proportional to effective residual stresses and magnetostriction and M is magnetization of the as-cast microwire. Experimental measurements of the radio absorption properties of glass-coated microwires in a suitable polymeric matrix were conducted in free space using standard technique of the TRL calibration (Trough-Reflection-Line) (see [3]).

As can be seen on figure 1, Fe-base microwires with large and positive magnetostriction exhibit outstanding radio absorption in the frequency range from 8 to 10 GHz.

FIGURE –1) In this figure, the power absorption of a composite with microwire inclusions is represented with an angular dependence respect to the h-component of the applied electromagnetic field. Line 1 is parallel to h, 2, 3, 4 correspond to in plane rotation angles of 90°, 180° and 270° respectively.

Optimum results of resonant absorption were obtained for microwires of length $L = 1 \div 4$ mm with a nucleus diameter of $2 \div 5$ μm . A detailed analysis of this behavior is presented.



[1] S.A. Baranov. *Technical physics letters*. Vol. 24, No 7, pp. 549-550. 1998

[2] S.A. Baranov. *Journal of Communications Technology and Electronics*. Vol.48. No2. P. 226-228. 2003.

[3] G.H. Bryant. "Principles of Microwave Measurements". *IEE Electrical Measurement Series*. No5. 1993; ISBN 0-86341-296-3

21PO-16-31

MODELLING OF INHOMOGENEOUS COATING WITH DEFINED MICROWAVE PROPERTIES

Yemets V.N., Bychkov I.V., Buchelnikov V.D.

Chelyabinsk State University, Br. Kashirinykh Str. 129, 454021 Chelyabinsk, Russia

The problem of synthesis of nonuniform on a thickness of magnetic dielectric coats with the defined reflection $R(\lambda)$ and transmission $T(\lambda)$ coefficients of electromagnetic waves is considered. Such problem is an incorrect inverse problem. In an operational view the problem is defined as $\hat{R}(\lambda, \mu, d) = R(\lambda)$. Permeability μ and permittivity ε is searched in the form of $\mu(z) = \sum_{i=1}^M a_i \varphi_i(z)$, where $\varphi_i(z)$ - a known set of basic functions. In this case the problem is reduced to search of unknown coefficients a_i . Method Levenberg-Marquardt [1] is used for definition a_i .

Operators of reflection \hat{R} and transmission \hat{T} of electromagnetic waves are calculated from the solution of a direct problem which is solved Galerkin method [2]. The direct problem of definition $R(\lambda)$ and $T(\lambda)$ on known $\mu(z)$ for normally incident TE wave is described by the wave equation $\frac{d^2 E}{dz^2} - \frac{d \ln \mu(z)}{dz} \frac{dE}{dz} + k^2 \varepsilon(z) \mu(z) = 0$. By means of Galerkin methods the wave equation with boundary conditions is reduced to system of the linear algebraic equations $M(\lambda, \mu) \vec{x} = \vec{b}(\lambda, \mu)$, $\vec{x} = [r, t, \vec{u}]^T$, where \vec{u} - wave amplitude within the coating, r and t - amplitudes of the reflected and transmitted wave outside the coating. The carried out calculations have shown possibility of modelling of the nonuniform coats with the given microwave properties.

Support by the Grant of RFBR-Ural № 07-02-96030 is acknowledged.

[1] D. Marquardt, *J. Appl. Math.*, **11** (1963) 431.

[2] C.A.J. Fletcher Computational Galerkin methods, Springer-Verlag, NY (1984)

21PO-16-32

ABSORPTION OF THE ELECTROMAGNETIC WAVE IN STRUCTURE OF METAL-FERROMAGNETIC

Butko L.N., Buchelnikov V.D., Bychkov I.V.

Chelyabinsk State University, 454021 Chelyabinsk, Russia

In this paper the absorption coefficient of normally incident plane electromagnetic wave $h_x = h_0 \exp(-i\omega t + ikz)$ for the structure from metal and ferromagnetic layers is theoretical studied.

It is assumed, that the magnetization of ferromagnetic layer is a constant value and it guide along y-axis. The axis z is directed along the normal \mathbf{n} to surface. The constant external magnetic field \mathbf{H}_0 coincides with direction of magnetization.

The investigation of the absorption coefficient is carried out by help the method based on the solution of coupled system of Maxwell and Landau-Lifshits equations together with boundary conditions on an electromagnetic field and magnetization [1].

The frequency dependences of absorption coefficient of electromagnetic waves were obtained. These dependences were analyzed at various layer's thickness. It is shown, that the absorption coefficient have resonant features in the areas of the frequencies between the ferromagnetic resonance and magnetostatic resonance ($\omega = 4\pi g M_s$) in ferromagnetic layers, i.e. when $|\mu_{fm}| \gg |\varepsilon'_{fm} + i\varepsilon''_{fm}|$. With certain ratio between the thickness and conductance of metal layer and also at certain parameters of ferromagnetic layer such structure efficiently absorbs the electromagnetic waves in broad bands. This phenomenon has the bigger value near a point of orientational phase transition. It can have the practical interest at designing of the broad band electromagnetic waves absorbers.

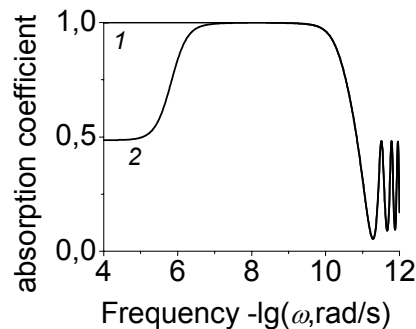


Fig.1. The frequency dependence of absorption coefficient for metal-ferromagnet layer structure. 1 – the ferromagnetic layer is in the point of orientational phase transition; 2 - the ferromagnetic layer is near the point of orientational phase transition.

Support by the Grant of RFRR-Ural № 07-02-96030 is acknowledged.

[1] V.D.Buchelnikov, A.V. Babushkin, I.V.Bychkov. FTT **45**, 4, (2003), 663.

21PO-16-33

ELECTROMAGNETIC WAVE PROPAGATION IN LAYER STRUCTURE WITH MAGNETOELECTRIC INTERACTION

Bychkov I.V., Selivanova E.M., Buchelnikov V.D.

Chelyabinsk State University, Br. Kashirinykh Str. 129, 454021 Chelyabinsk, Russia

Last years interest to layered periodic structures on the basis of thin films of metals, semiconductors and dielectrics has raised. The given layered periodic structures can be considered as new type of artificial materials with the new physical properties. These properties can be operated effectively by means of external physical influences (temperature, elastic pressure, magnetic and electric fields). Reaction of layered periodic structures on the electromagnetic radiation depends on the electric and magnetic parameters and a thickness of layers. In electric and magnetic materials parameters of each layer are the tensors of electrical conductivity, dielectric permittivity and magnetic permeability. At account of the

magnetolectric interaction we need to consider the tensor of magnetolectric permeability in Maxwell equations. Influence of magnetolectric interaction on dynamic properties semi-infinite antiferromagnetic has been studied in work [1].

In the given work we studied the layered periodic structure of gyrotropic semiconductor – tetragonal antiferromagnet with magnetolectric interaction. The propagation of electromagnetic wave through layered structure is described by a method of transmission matrix. The amplitude factors of reflection and absorption are directly expressed through components of the transmission matrix. The results of numerical calculations of frequency dependence of reflection, transmission and absorption factors at normal falling of electromagnetic wave on the surface of structure are presented. The influence of number of layers, of magnetic relaxation, of constant of magnetolectric interaction on the reflection, transmission and absorption factors was investigated. Faraday effect for such structure was also calculated.

It is shown, that the increase of number of layers at a constant magnitude of relaxation leads to increase of reflection and absorption factors of electromagnetic wave in resonance regions. At increase of parameter of magnetolectric interaction the reflection factor in the region of spin wave frequency is increased. The value of Faraday effect for layered structure depend on the magnitude of an external magnetic field and from the thickness of dielectric and antiferromagnetic layers.

Support by the Grant of RFBR-Ural № 07-02-96030 is acknowledged.

[1] V.D. Buchelnikov, V.V. Rive, JETP Letters, 84(2006) 395

21PO-16-34

SHEAR THICKNESS MODES IN A PRESENCE OF MAGNETOELASTIC WAVES PARALLEL TO A SURFACE GUIDED BY FERROMAGNETIC FILM

Gareeva Z.V., Doroshenko R.A.

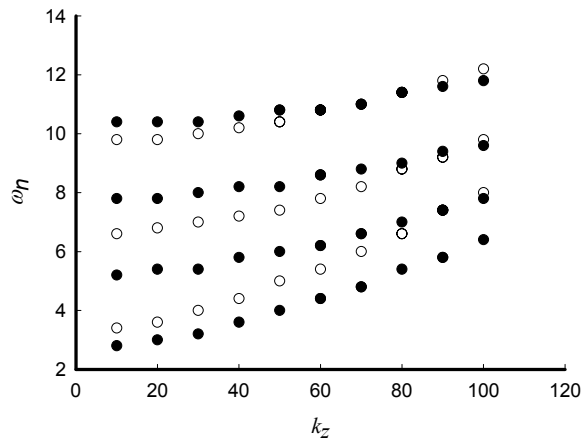
Institute of Molecular and Crystal Physics, prospect Octyabrya 151, 450075 Ufa, Russia

Thickness shear modes of magnetoelastic waves (MEW) in the ferromagnetic plate are studied. Coupled vibrations of magnetization and shear elastic deformations excited simultaneously by a variable magnetic field propagate in two mutually perpendicular directions: parallel and normal to a surface. For parameters characteristic of isotropic ferromagnet with the sample magnetization and Zeeman field parallel to the surface, resonant frequencies of shear modes are computed and their dispersion law is examined.

Plots illustrating dependences of resonant frequencies of thickness shear modes upon wave vector k_z of ME wave traveling in a surface plane are presented in Fig. The family of dispersion curves shown in Fig. is identified with the main harmonics of dimensional resonances frequencies. The cases corresponding to two values of C_{11} are depicted. Family 1 (black points) corresponds to the lower C_{11} ($C_{11}=16.9 \cdot 10^{11}$ erg/cm³) value, family 2 (white points) corresponds to the higher C_{11} ($C_{11}=26.9 \cdot 10^{11}$ erg/cm³) value. Material parameters are chosen as follows $C_{44}=8.06 \cdot 10^{11}$ erg/cm³, $B=6.67 \cdot 10^6$ erg/cm³, $H=1000$ Oe, $K_A=1 \cdot 10^4$ erg/cm³, $M_0=140$ G, $\gamma=1.76 \cdot 10^7$ (Oe·s)⁻¹, $\rho=5.2$ g/cm³.

Let us note the principal features of the represented plots.

The resonant frequencies of thickness shear modes appear to be dependent on the wave



number k_z of a ME wave traveling parallel to the surface. The quantity of this effect depends on the elasticity module C_{11} , material density and thickness of a plate d . Spectrum $\omega_n(k_z)$ changes with the change of enumerated parameters in a following way: (i) With increasing of C_{11} value the dependence $\omega_n(k_z)$ becomes stronger, with decreasing of C_{11} value the dependence $\omega_n(k_z)$ becomes weaker, (ii) With increasing of material density the dependence $\omega_n(k_z)$ weakened, (iii) $\omega_n(k_z)$ curves weakly depend on the change of C_{44} , B , K_A , H .

We can conclude that thickness modes frequencies are determined not only by transverse dimensions (thickness of a plate) but also by longitudinal dimensions (length of a plate). The frequency of resonant excitation of the thickness vibrations can be changed by change of wave number k_z and length of a plate connected with this parameter. That points out to the assertion that multimode thickness vibrations can occur in real samples possessing with scattering in lengths values. In the paper [1] it is shown the presence of multimode character of standing ME waves in samples. The physical origin of multimode standing waves can be various. One of the possible reasons can be interaction between MEW propagating parallel and normal to a surface in a confined structure.

[1] I.V. Pleshakov, *Fiz.Tverd.Tela* **47** (2005) 1629.

21PO-16-35

PENETRATION AND TRANSMISSION OF MICROWAVE RADIATION THROUGH METALLIC POWDER COMPOSITE

Anzulevich A.P.¹, Buchelnikov V.D.¹, Bychkov I.V.¹, Lousguine-Luzgin D.V.², Yoshikawa N.³, Sato M.⁴, Inoue A.²

¹Chelyabinsk State University, Chelyabinsk 454021, Russia

²WPI Advanced Institute for Materials Research, Tohoku University, Sendai, 980-8577, Japan

³Graduate School of Environmental Studies, Tohoku University Sendai, 980-8579, Japan

⁴National Institute for Fusion Science, 322-6 Oroshi, Toki, Gifu, 509-5292 Japan

It is known that bulk metals reflect microwaves (MWs) and can hardly be heated. They can undergo only surface heating. Recently MW heating has been successfully applied to powdered metals. The present work shows a direct experimental evidence of penetration of a layer of metallic powder by MW radiation and contains theoretical explanation of such behavior. For theoretical explanation of powder heating we considered a problem about transmission of MWs through a plate from composite conductive material. We divide our problem onto three parts: the region from left side of the plate, the plate and area between right side of the plate and fully reflected medium. Using the transition matrix method [1] we can find the expressions for the amplitudes of electric and magnetic fields in each region.

In the plate the fields depends on a real and imaginary parts of dielectric permittivity and magnetic permeability. Thus, in case when the plate consists of spherical metallic powder particles (R_1, ε_1) with dielectric shells (R_2, ε_2) it is necessary to know the effective values of

dielectric permittivity and magnetic permeability of such a composite medium. For calculations of effective permittivity and permeability we use the effective medium approximation [2]

$$p\zeta \frac{\varepsilon_2[3\varepsilon_1 + (\zeta - 1)(\varepsilon_1 + 2\varepsilon_2)] - \varepsilon_{eff}[3\varepsilon_2 + (\zeta - 1)(\varepsilon_1 + 2\varepsilon_2)]}{2\alpha\varepsilon_{eff} + \beta\varepsilon_2} + (1 - p\zeta) \frac{\varepsilon_g - \varepsilon_{eff}}{\varepsilon_g + 2\varepsilon_{eff}} = 0, \quad (1)$$

where p is the volume fraction of metal in effective medium, $\zeta = (R_2 / R_1)^3 = (1 + l)^3$, $l = (R_2 - R_1) / R_1$, $\alpha = (\zeta - 1)\varepsilon_1 + (2\zeta + 1)\varepsilon_2$, $\beta = (2 + \zeta)\varepsilon_1 + 2(\zeta - 1)\varepsilon_2$, $\varepsilon_g = 1$.

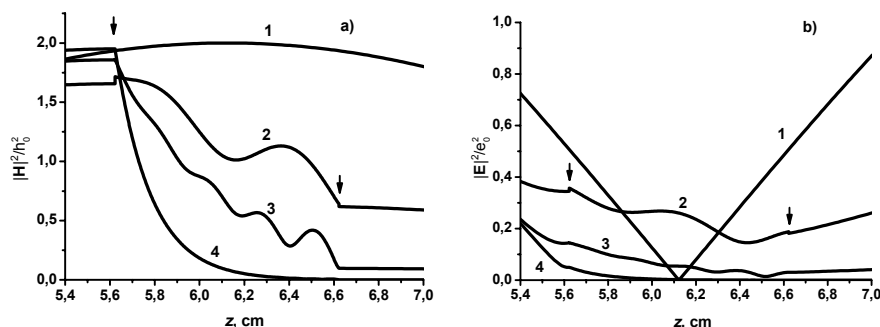


Fig.1. The distribution of square modulus of magnetic a) and electric b) fields inside the plate from core-shell powder for different relative thickness of shell: 1) the fields without plate; 2) $l = 0.02$; 3) $l = 0.002$; 4) $l = 0.0002$. The thickness of plate is 1 cm, it sides shown by arrows.

The theoretical evaluation indicates that really powdered metallic samples can be penetrated by MW radiation.

Support by the grant RFBR-Ural 07-02-96030 is acknowledged.

[1] M. Born, E. Wolf, Principles of optics, Pergamon, New York, 1986

[2] D.A.G. Bruggeman, *Ann. Phys. (Leipzig)* **416**, 636 (1935).

21PO-16-36

DEVELOPMENT OF COMPOSITE MAGNETIC MATERIALS ON A BASE OF NANOCRYSTALLINE SOFT-MAGNETIC ALLOYS FOR EFFICIENT ELECTROMAGNETIC PROTECTION SYSTEM APPLICATIONS

Kuznetsov P.A., Askinazi A.Yu., Farmakovskiy B.V.

Central Research Institute of Structural Materials «Prometey»,
Saint-Petersburg, Russia

In the work the researches of nanocrystalline conditions on magnetic properties of powder composite materials made of soft-magnetic alloy of a FINEMET type are given. The powders were received by a high energy mechanical activation in disintegrator from initial amorphous ribbon and divided into three types of fractions. The thermal processing was carried out at temperature range 430 - 570 C and time of isothermal duration with in 30 minutes. The composites contained 80 wt % of the powder. The measurements were carried out in frequencies range 100 – 1000 MHz. It was shown that nonmonotonic function of permeability versus thermal processing temperature is observed.

Developed electromagnetic protection systems were shown that at a transition of amorphous alloy in nanocrystalline condition twice extends a frequencies range in which a

reflectance less than minus 10 ÷ 15 dB can be supplied. The received data demonstrate an availability of manufacturing electromagnetic protection systems.

21PO-16-37

DOMAIN WALL DYNAMICS IN A DOUBLE LAYER MAGNETIC FILM WITH DIFFERENT UNIAXIAL ANISOTROPY THE LAYERS

Randoshkin V.V., Sysoev N.N., Mastin A.A.

M.V. Lomonosov Moscow State University, 119899 Moscow, Russia

Magnetouniaxial single crystal ferrite-garnet films, which are used in memory storage devices based on cylindrical magnetic domains in a variety of magneto-optics devices, are grown by the method of liquid-phase epitaxy from a supercooled solution-melt on non-magnetic-garnet substrates. A major particular quality of the liquid-phase epitaxy is that the initial stage of the epitaxial growth is a non-stationary process. This gives rise to formation of a transition surface layer at the surface-substrate interface, which differ from the bulk of the film in composition and magnetic parameters [1]. In other words, all real SCFGFs have, at least, two-layers. The domain wall (DW) dynamic in such films deserves special attention because the combination of layer parameters (intensity of magnetization, gyromagnetic ratio, anisotropy, layer thickness) may reveal new effects in DW dynamic unachievable in uniform films. For example, unlimited increasing of field of disruption of the steady-state motion of DW is possible in two layered films with opposite sign of layer gyromagnetic ratio. The DW dynamic in materials with high quality factor is well described by Slonczewski equation [2].

In this work we investigated by numerical simulation the DW dynamics in two layered films with different layer uniaxial anisotropy. We assumed free boundary conditions at film surfaces and continuity of DW profile at the layer interfaces due to high exchange bounding of layers. The stray field was assumed in static approximation.

We investigated the dependences of DW velocity from magnetic field in films with different layer anisotropy and thickness and dependences of films field and velocity of disruption steady-state motion of DW from layer anisotropy and thickness and get, that:

1) The dependences DW velocity from magnetic field contains a series velocity peak that relies on steady motion of Bloch lines across film, in DW unsteady motion regime. The DW velocity in such cases can't be simply increased by increasing magnetic field and limited by some volume.

2) The field of disruption of DW state steady motion is decreased when anisotropy of layers became equal. The velocity of disruption of DW state steady motion is decreased when we increased anisotropy of first layer.

3) The field and velocity of disruption of DW state steady motion is decreased when we increased a layer thickness.

[1] V. V. Randoshkin and A. Ya. Chervonenkis, Applied Magneto-optics [in Russian], Moscow, Energoatomizdat (1990).

[2] A. P. Malozemoff and J. Slonczewski, Magnetic Domain Walls in Bubble Materials, Applied Solid State Science, Academic, New York (1979).

21PO-16-38

3-D CHARACTER OF DOMAIN STRUCTURE OF THE YTTRIUM IRON GARNET FILMS WITH HIGH UNIAXIAL ANISOTROPY FIELD.

Lock E.H., Shcheglov V.I., Temiryazeva M.P., Vashkovsky A.V.

Institute of the Radio Engineering and Electronics of Russian Academy of Science,
Vvedensii square 1, Fryazino 141190, Moscow region, Russia

As it is known [1], epitaxial yttrium iron garnet (YIG) (111)-grown films may be divided in two groups, that differ in nonsaturation state by the parameters of domain structure (DS). Theoretic and experimental investigation of the DS for the first group of the YIG films, having uniaxial anisotropy field H_a higher than ~ 120 Oe but considerably smaller than film's saturation magnetization $4\pi M_0$, are reported below. During investigation of DS of these tangentially magnetized films by both optical microscope and atomic force microscope (magnetic mode) "NT-MDT", there was found that DS has extraordinary character: pictures, obtained from these microscopes, differ each from other radically. Although linear symmetric stripe DS was observed in both microscopes but the boundaries of DS, observed by optical microscope, were parallel to the vector of external uniform magnetic field \mathbf{H}_0 whereas the boundaries of DS, observed by magnetic microscope, were declined from the \mathbf{H}_0 vector on the some angle φ . While the value H_0 was about 0 the value of the angle φ was about 90° and when the value H_0 was increased, the value φ was decreased to $\sim 20^\circ - 30^\circ$. Thus, since the atomic microscope, scanning surface magnetic fields, senses only thin near-surface DS and the optical microscope shows the integrate DS picture, determined mainly by the DS from the film volume, we can suppose, that YIG film's DS has 3-D character: there are three layers – two thin near-surface layers and one layer, representing main film volume – with various DS in each adjacent layers.

To explain 3-D character of YIG film's DS theoretical study of nonsaturated ferrite films was carried out for the case $H_a \ll 4\pi M_0$. Distribution of magnetization in domains of different layers was investigated. The density of the domain wall energy is calculated also by net method, basing on the micro-magnetic study of magnetization distribution inside of domain wall for the different orientations of this wall respect to the crystallographic anisotropy axis and respect to the film plane. The study of the domain stray fields, formed by the exit of magnetization vector on film surface, is based on the model of infinite thin domain wall. Magnetic dipoles, arising on the film surface and on the domain wall surface, are considered to calculate these stray fields by the net method for different kinds of opened and closed DS and for the case of transition from opened to closed DS. It is shown that there may exist a phase transition in the film from the whole closed DS to the half-opened DS, having the width of the closed domain smaller than the width of the main (volume) domain. It is found that two types of closed DS can exist in the film: magnetization vectors in adjacent closed domains are lied in the film plane and are oriented oppositely in the first type of DS; in the second type of DS these vectors are co-directional. As a kind of the second DS type there can exist the near-surface DS, walls of which are oriented normally to the walls of the main (volume) DS.

It is the near-surface DS that was observed in experimental study by the atomic force microscope for small in-plane external values of magnetic field H_0 .

This work is supported by RFFR pr. №07-02-00233a. Support of RSP pr. № 2.1.1.4639 is acknowledged by Lock E.H.

[1] Vashkovsky A.V., Lock E.H., Shcheglov V.I. *Solid State Phys.*, **41** (1999) 1868.

21PO-16-39

METAMATERIALS FABRICATED OF AMORPHOUS FERROMAGNETIC MICROWIRES: NEGATIVE MICROWAVE PERMEABILITY

Ivanov A.V.¹, Galkin V.Yu.², Ivanov V.A.^{2,3}, Petrov D.A.⁴, Rozanov K.N.⁴, Shalygin A.N.^{1,2}, Starostenko S.N.⁴

¹Faculty of Physics, Moscow State University, 119992 Moscow, Russia

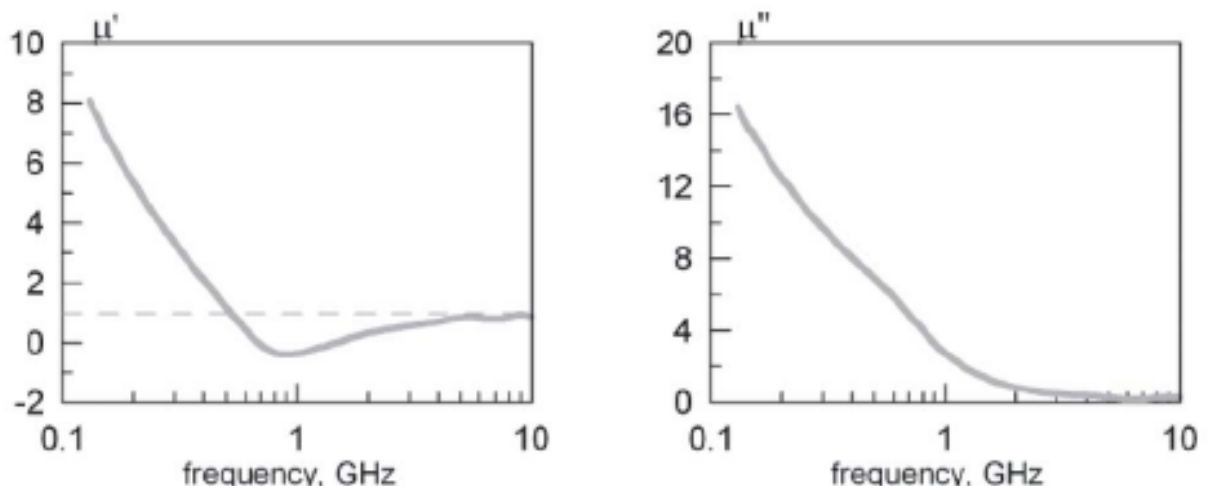
²R&P VICHEL (High-Frequency Systems), 119991 Moscow, Russia

³N.S. Kurnakov Institute of General and Inorganic Chemistry of the RAS, 119991 Moscow, Russia

⁴Inst. for theoretical and applied electromagnetics, 13 Izhorskaya ul., 125412 Moscow, Russia

Metamaterials with negative refraction index attract great attention recently, mostly because of multitude of promising applications proposed for these materials. The conventional design of a metamaterial combines long conductive wires and split-ring resonators. Other opportunities to develop metamaterials are also of great interest, such as that based on exploitation of negative permeability appearing at frequencies above the ferromagnetic resonance frequencies in magnetic materials, particularly, amorphous magnetic microwires. In arrays of microwires, negative permittivity arises due to inherent inductance of the wire. Therefore, arrays of crossed microwires seem to be an excellent candidate to metamaterial, because of simple design, isotropic in-plane performance, and possible tunability of microwave material parameters by application of external magnetic bias.

The study deals with measured effective permeability of microwire-based composites. Glass-coated microwires being of 12 μm in diameter of metal core and 20 μm in diameter of glass shell and possessing weak negative magnetostriction are wound to compose a 7/3 washer-shaped sample, the permeability of which is measured in a standard coaxial measurement cell in the frequency range of 0.1 to 10 GHz. In the figure, the measured permeability is plotted against frequency for a sample comprising 10% of magnetic constituent. It is seen that the effective permeability of the sample is negative within the frequency range of approximately 0.7 to 1.5 GHz, with the permeability attaining the value as low as -0.4 . Therefore, the use of microwire-based composites is a promising approach to developing metamaterials. However, for feasible metamaterial to be made of microwire arrays, the wires have to exhibit higher magnitude of the ferromagnetic resonance, higher quality factor, and higher resonance frequency.



The study is supported by RFBR according to agreement # 08-02-00830.

21PO-16-40

MICROWAVE HEATING OF METALLIC POWDERS

Buchelnikov V.¹, Louzguine-Luzgin D.², Bychkov I.¹, Anzulevich A.¹

¹Chelyabinsk State University, Br. Kashirinykh Str. 129, 454021 Chelyabinsk, Russia

²WPI Advanced Institute for Materials Research, Tohoku University, Sendai, 980-8577, Japan

Owing to so-called skin-effect bulk metals reflect microwaves and can hardly be heated at room temperature. They can undergo only surface heating due to limited penetration of the microwave radiation. However, recently microwave heating has been successfully applied to powdered metals and fully sintered samples were obtained in 1999 in a multimode cavity [1].

In the present work we provide theoretical explanation of microwave (MW) heating of metallic powders.

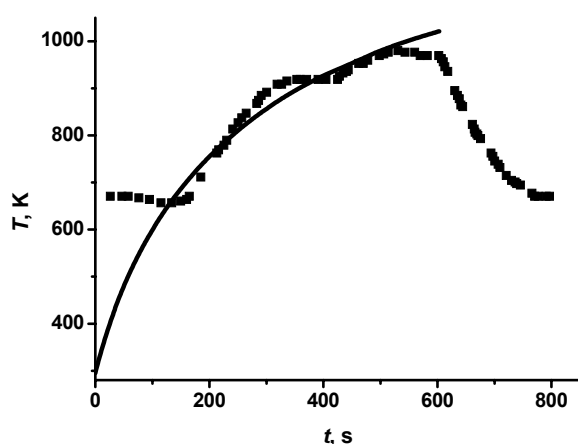


Fig.1. The time dependence of temperature for iron powder. Solid line is simulation, black square is the experimental data.

For explanation of experimental results we considered a problem about transmission of electromagnetic wave through a plate from composite conductive material and reflection from ideal (fully reflected) massive conductive medium behind of the plate. If the plate is absent then in the problem there is a standing wave only. In this case we can find the positions of maximums of electric (E-) and magnetic (H-) fields in the standing wave. Knowledge of these positions will allow us to place the plate either in maximum of E-field or H-field. For the calculation of the electromagnetic fields in the problem we used the transition matrix method [2].

It is known, that a heat density Q_{eh} absorbed in the plate from the external electromagnetic wave in one second is a sum of electric Q_e and magnetic Q_h parts of heat and it is expressed as

$$Q_{eh} = Q_e + Q_h = \frac{\omega}{8\pi} (\epsilon'' |\mathbf{E}|^2 + \mu'' |\mathbf{H}|^2) = . \quad (1)$$

From equations (1) it is follows that the absorbed heat and the modulus of amplitudes of electric and magnetic fields in the plate depends on a real and imaginary parts of dielectric permittivity and magnetic permeability. So, in case when the plate consists of powder of metallic particles with dielectric shells (core-shell composite) it is necessary to know the effective values of dielectric permittivity and magnetic permeability of such composite medium. For calculations of effective dielectric permittivity, magnetic permeability and also electric conductivity we used the effective medium approximation [3]. After calculations of the effective dielectric permittivity and magnetic permeability we solved the one-dimensional heat conduction equation in which as a source of the external heat was used the heat density Q_{eh} (1). In the heat conduction equation we also taken into account the radiation and convection heats. The results of computer simulations of time dependence of temperature for iron powder are presented on Fig.1. It is seen that theoretical results are in good agreement with experimental data.

[1] N. Yoshikawa, E. Ishizuka, S. Taniguchi, *Materials Transactions*, **47** (2006) 898.

[2] M. Born, E. Wolf, *Principles of optics*, Cambridge University Press, Cambridge, 1999.

[3] D.A.G. Bruggeman, *Ann. Phys. (Leipzig)* **416**, 636 (1935).

21PO-16-41

ANALYSIS OF NONLINEAR MAGNETIZATION OSCILLATIONS FOLLOWING PROCESS OF 90° PULSE MAGNETIZATION IN FERRITE-GARNET FILMS WITH EASY PLANE ANIZOTROPY

Kolotov O.S., Matyunin A.V., Polyakov P.A., Rusakov A.E.
Moscow State University, 119991, Vorob'evy Gory, Moscow, Russia

Nonlinear magnetization oscillations following process of 90° pulse magnetization in ferrite-garnet films with easy plane anisotropy were first investigated in [1,2]. An interesting feature of the oscillations has been found: they are reliably observed when duration of magnetizing pulse front τ_f exceeds up to 3 and more times oscillation period $T_k \sim 2$ ns. One makes an assumption that the oscillations have magnetostatic nature, and weak dependence of their intensity on the pulse front duration can be explained by the presence of a biaxial anisotropy in the plane of real films. The last circumstance leads to effect of transient process delayed acceleration which can occur when amplitude of the magnetizing field exceeds a threshold field H_0 ($\sim 14-20$ Oe) of a coherent rotation. It is observed as a rapid increase of magnetization rotation rate after overcoming of some critical angle $\varphi \approx 25^\circ$ (in time $\approx \tau_f$): the magnetization vector turns through angle $\varphi \approx 60^\circ$ in time $\Delta t \leq 1$ ns.

A theoretical analysis of magnetization behaviour is necessary for confirmation of above assumption. An analysis of Landau-Lifshitz equation numerical solutions is presented here. Solutions in a form of longitudinal and transverse signals which are determined by the change of magnetization components parallel and perpendicular to magnetizing field H_p , respectively, have been obtained. The main results consist in the following. The effect of delayed magnetization acceleration, which causes magnetostatic oscillations with period T_k close to the experimental values, should be observed in discussed films at finite duration of the front. At the same time the calculated and experimental signals considerably differ as a whole. In particular, one can see the oscillation amplitude of the calculated signal decreases slower than the amplitude of the experimental one. This difference is especially essential at the initial stage of transient process. It can be explained that the value of Landau-Lifshitz parameter λ depends on the oscillation amplitude [3].

- [1] E.I. Il'yashenko, O.S. Kolotov, O.A. Mironets, *Physics of the Solid State*, **48**, №2 (1999) 297.
- [2] E.I. Il'yashenko, O.S. Kolotov, A.V. Matyunin, V.A. Pogozhev, *Izvestiya RAN. Seriya fizicheskaya*, **71**, №11(2007) 1570.
- [3] E.M. Gyorgy, *in Magnetism*, **III**, Academic Press, New York (1963) 525.

21PO-16-42

MAGNETIC RESONANCE PHENOMENA IN 3D-NANOCOMPOSITE WITH Ni-Zn-Fe SPINEL NANOPARTICLES

Rinkevich A.B.¹, Ustinov V.V.¹, Samoilovich M.I.², Klesheva S.M.², Kuznetsov E.A.³

¹Institute of Metal Physics, the Ural Division of the Russian Academy of Sciences, 18, S. Kovalevskaya St, GSP - 170 Ekaterinburg 620041 Russia,

²Central Research Technological Institute "TECHNOMASH",
4, I. Franko St, Moscow 121108 Russia

³Nizhny Tagil State Socially - Pedagogical Academy 57, Krasnogvardejskaya St,
Nizhny Tagil 622031 Russia

Magnetically doped 3D-nanocomposites can become the basic material for a new class of magnetic field-driven devices of centimeter and millimeter wavebands. The double magnetic-dielectric nanocomposites have been investigated based on the cubic packages of the SiO₂ nano-spheres that are called as opal matrices or magnetic photonic crystals. They are exemplified by island-type filling of the inter-sphere voids, and the magnetic inclusions are isolated from each other. The opal matrices have been doped with nickel-zinc ferrite in this work.

Sintering of the opal matrices with the diameter of SiO₂ nano-spheres about 250 nm have been carried out. The difference of the nanospheres in diameter does not exceed 5%. The particles of the introduced phases are sized from 5 to 50 nm. Concentration of the phases introduced does not exceed 5 volume percent. Magnetic properties of the 3D-nanocomposites have been measured at room temperature in magnetic fields up to 30 kOe. It can be concluded from the view of magnetization curves that Ni-Zn ferrite-doped nanocomposite has ferro- or ferrimagnetic ordering along with superparamagnetic nanoparticles.

Electromagnetic waves penetration and reflection were studied in the frequency range from 26 to 38 GHz. The sample was placed in the cross section of convenient rectangular waveguide operating on TE₁₀ mode. The thickness of the sample was about 1 mm. The transmission D and reflection R coefficient modules were measured as well as their relative variations. The steady external magnetic field was applied along the narrow walls of the waveguide, so the external field H lied perpendicular to the microwave magnetic field H_{ω} . The magnetic field dependency of transmission coefficient module is resonant in shape and the resonance field shifts to the higher fields as the frequency rises. Comparing the frequency and the field of magnetic resonance one can restore the magnetic resonance spectrum. The magnitude of the field variations reached 45%. Keeping in mind to increase the effectiveness of interaction of the nanocomposite with the electromagnetic wave, the number of experiments was carried out where the sample was placed in the rectangular resonator. If the sample was placed near the point where the electric or magnetic microwave fields have maximums, the microwave field intensity is much higher than the same in the waveguide. The field dependence of the transmission coefficient module is resonant and the module sharply diminished near the resonance field. In these experiments, variations up to 70% were reached.

This work is partly supported by the grant № NSh-3257.2008.2 and the "Quantum macrophysics" program of the Russian Academy of Sciences.

21PO-16-43

MICROWAVE ABSORPTION IN THE TETRAGONAL SINGLET PARAMAGNETS $\text{HoBa}_2\text{Cu}_3\text{O}_x$ ($x = 6.0, 6.3$) IN HIGH PULSED MAGNETIC FIELDS

Goiran M.¹, Kazei Z.A.², Snegirev V.V.², Kozeva L.P.³, Kameneva M.Yu.³

¹Laboratoire National des Champs Magnetiques Pulses, 31432 Toulouse, Cedex 4, France

²Moscow State University, 119992 Moscow, Russia

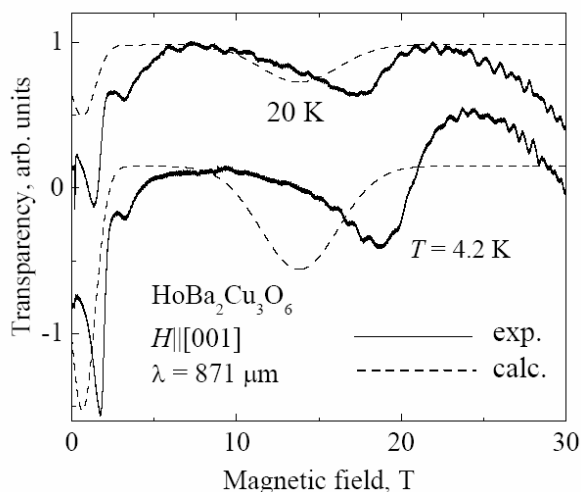
³Nikolaev Institute of Inorganic Chemistry RAS, 630090 Novosibirsk, Russia

In $\text{RBa}_2\text{Cu}_3\text{O}_x$ compounds (R is a rare-earth, RE, ion), RE ions are arranged in the structure sufficiently close to CuO_2 ‘superconducting planes’ and can act as a probe sensitive to the local symmetry of their environment and charge density distribution, whose changes affect the crystal field (CF) forming the electron structure of the RE ion. Magnetic behavior of singlet paramagnets is expected to be the most sensitive to the CF variation on the oxygen content x . Studies of microwave absorption spectra under a high magnetic field provide direct information about the electron structure of the R^{3+} ion: energy spacings, value and anisotropy of g-factors, matrix elements of corresponding operators.

Single crystals of $\text{HoBa}_2\text{Cu}_3\text{O}_x$ were grown by the flux method; then the crystals were additionally annealed and quenched quickly to room temperature in air or vacuum in order to reduce the oxygen content to $x = 6.0$ and 6.3 , respectively. The iodometric titration method was used to determine the oxygen content. Microwave absorption spectra in the Faraday geometry at the wave length 871, 406, 305 and 118 μm were studied in magnetic fields up to 40 T and temperatures ranging from 4.2 to 60 K. Calculations within the CF formalism with the known CF and interaction parameters were carried out to interpret the experimental spectra.

In the tetragonal crystal with $x = 6.0$ for a magnetic field along the tetragonal crystal axis, a number of resonance absorption lines are observed at the wavelengths 871 (full curves in Fig.), 406, 306 and 118 μm resulting from transitions between the ground and low lying energy levels of the Ho^{3+} ion split in the CF. The positions and intensities of the observed resonance lines are described adequately within the CF formalism with the known CF parameters [1] (dashed curves in Fig.).

To the contrary, for the tetragonal $\text{HoBa}_2\text{Cu}_3\text{O}_x$ crystal with $x = 6.3$, microwave absorption spectra under a high magnetic field reveal a more complicated behavior. Non resonance absorption dominates and broad resonance absorption lines are observed for which the positions and intensities do not agree with the known electron structure of the Ho^{3+} ion. The effects of the low symmetry (orthorhombic, monoclinic) and inhomogeneous CF components on the magnetic properties and microwave absorption spectra are analyzed and discussed. The low symmetry interactions, namely the second-order term of the orthorhombic and monoclinic CF as well as molecular field are found to change the microwave absorption spectra and magnetic properties closer to the experimental ones. These terms are absent for the ideal crystal and magnetic structures but might arise due to some disorder in the oxygen subsystem or deviation of the Cu^{2+} magnetic moments from the simple collinear structure for crystals with $x > 6.0$.



Support by RFBR (project no. 07-02-0104) and EuroMagNet Foundation is acknowledged.

[1] U. Staub, J. Mesot, M. Guillaume, et al., *Phys. Rev. B*, **50** (1994) 4068.

21PO-16-44

PROPERTIES OF FeCoBSi THIN FILMS PREPARED ON THIN FLEXIBLE SUBSTRATES

Lu Haipeng, Cui Jingjing, Deng Longjiang

State Key Laboratory of Electronic Thin Films and Integrated Devices, University of Electronic Science and Technology of China, Chengdu 610054, P.R.China

Materials with high microwave permeability are of practical importance for a number of applications. As ferromagnetic films with in-plane anisotropy are able to overcome the Snoek's limits, they might obtain larger values of microwave permeability than bulk magnets [1]. So a lot of research has been carried out to develop ferromagnetic thin films for the use in high frequency devices such as high-frequency micro inductors or micro transformers.

However, more and more new applications such as flexible EMI suppressors require flexible samples which under a suitable form [2]. This was the motivation for the experimental study of thin films deposited on thin flexible substrates.

Iron-based films are known with high saturation magnetization. Alloying iron with cobalt, boron and silicon may result in the materials with high saturation magnetization and appropriate anisotropy or resistivity. Such films may have high permeability at frequencies of several GHz.

Fe₆₆Co₁₇B₁₆Si₁ thin films were produced on flexible 11.5 μm thick mylar substrates by DC magnetron sputtering. The hysteresis loops were obtained by vibrating sample magnetometer measurements. The permeability has been measured from 500 MHz up to 18 GHz using a coaxial technique described elsewhere [3]. The technique implies winding a film into a roll sample that adapts to the geometry of the coaxial line cavity.

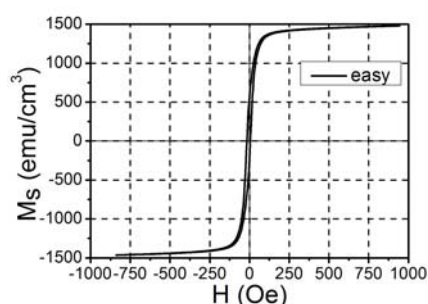


Fig. 1 Hysteresis loop along the easy axis of a FeCoBSi thin film deposited on mylar substrate

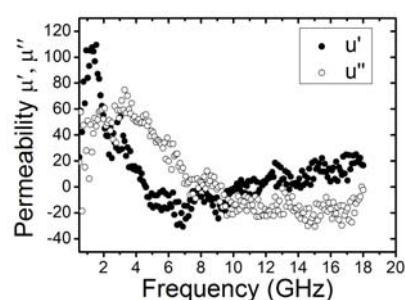


Fig. 2 Complex permeability of a 610nm thick FeCoBSi thin film deposited on mylar substrate

Fe₆₆Co₁₇B₁₆Si₁ films prepared on thin flexible substrates are shown as an amorphous structure. The static and dynamic magnetic properties of FeCoBSi film are given in Fig. 1 and Fig. 2. High saturation magnetization is observed from hysteresis loop of Fe₆₆Co₁₇B₁₆Si₁ thin films. It is the key point for obtaining high microwave permeability. At GHz frequencies characteristic permeability dependence with a resonance frequency f_r at about 3.2 GHz was observed. It somewhat disagrees with the parameter of the magnetic spectra which were predicted by the Landau-Lifshitz equation. Potential causations will be discussed.

Support by the Natural Science Foundation of China (Grant No.50601005) and the 2008-2009 NSFC-RFBR (Russian Foundation for Basic Research).

- [1] I.T. Iakubov, A.N. Lagarkov, et al., *J. Magn. Magn. Mater.*, **300** (2006) e74.
 [2] O. Valls, D. Damiani, et al., *Digests of the Intermag Conference*, (2002) FD07.
 [3] O. Acher, J.L. Vermeulen, et al., *J. Magn. Magn. Mater.*, **136** (1994) 269.

21PO-16-45

MICROWAVE PROPERTIES OF SANDWICH STRUCTURE BASED ON IRON AND BARIUM NANOPARTICLES

Babushkin A.V.¹, Bychkov I.V.², Buchel'nikov V.D.²

¹FSUE "RFNC – VNIITF", 13, Vasilyev Street, Snezhinsk, 456770, Russia

²Chelyabinsk State University, 129, Brat'ev Kashirinykh Street, Chelyabinsk, 454021, Russia

Along with the wide-range application of electromagnetic wave (EMW), serious electromagnetic interference (EMI) problem have recently become apparent. Using electromagnetic wave absorbers is an effective way to reduce EMI.

The granular materials representing a composite in which nanocrystalline iron and barium ferrite are located in a nonmagnetic matrix are very promising microwave absorption materials because of their high saturation magnetization, high Curie temperature, and large magnetic permeability at microwave frequencies (e.g. see [1, 2]).

Many studies were carried out to investigate the absorption properties of single-layer microwave absorbers employing indicated above particles, but the single-layer absorbers cannot realize the low reflection in wide band. Meanwhile, it is known that the microwave absorbers with multi-layer structure has wider

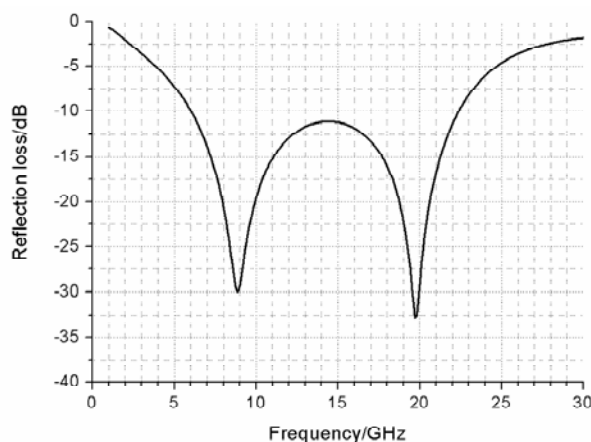


Fig. 2. The reflection loss of the sandwich microwave absorber. First layer: iron/epoxy, $f_{Fe} = 0.2$, $\alpha_{Fe} = 0.5$, $d_1 = 1.5$ mm. Second layer: insulator, $\epsilon_{Ins} = 2.0$, $d_2 = 2.0$ mm. Third layer: barium/epoxy, $f_{Ba} = 0.3$, $\alpha_{Ba} = 0.5$, $d_3 = 0.75$ mm.

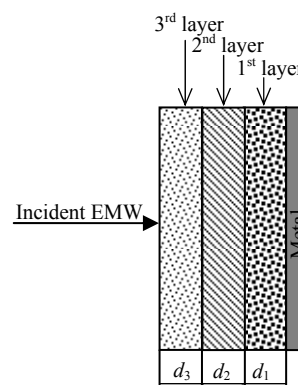


Fig. 1. Structure of proposed microwave absorber.

absorption bandwidth and lower reflection loss than the single-layer absorber.

In the present work, based on the Landau-Lifshitz-Gilbert equation, extended Bruggeman's effective medium theory with the consideration of the skin effect [3] and transmission-line theory, electromagnetic and microwave-absorbing properties were theoretically studied for sandwich structure (see Fig. 1) consisting of the composites with iron (1st layer) and barium ferrite (3rd layer) single-domain particles separated by the insulator layer (2nd layer) with isotropic permittivity $\epsilon_{Ins} = 2$.

It was found that the microwave properties of the composites were influenced by many material properties, such as damping parameter (α), volume fractions (f)

and particles size (d).

Finally, a microwave absorber having excellent absorbing properties was achieved (Fig. 2), and the bandwidth of the reflection loss less than -10 dB can reach 16 GHz in the range of 6-22 GHz with the total thickness 4.25 mm.

- [1] V.B. Bregar, *IEEE Trans. Magn.*, **40** (2004) 1679.
- [2] J. Qiu, H. Shen, M. Gu, *Powder Technology*, **154** (2005) 116.
- [3] A.K. Sarychev, R.C. McPhedran, V.M. Shalaev, *Phys. Rev. B*, **62** (2000) 8531.

21PO-16-46

THE POLAR KERR EFFECT AND MIRROR SPECTRAL CROSSOVER

Yurasov N.I.

BMSTU, 107005 Moscow, 2-ya Baumanskaya 5, Russia

We report results of theoretical investigations of the polar Kerr effect analytically in microwave and infrared ranges for ferromagnetic metals, semimetals and semiconductors. We have supposed that the polar Kerr effect and negative reflection index are roughly connected. Therefore Kerr rotation angle α_K is function of Z_{\pm} and $Z_{\pm} = n_{\pm} / \varepsilon_{\pm}$ where Z_{\pm} , n_{\pm} , ε_{\pm} are impedances, reflection indexes and dielectric permittabilities of the waves with circular polarizations (nonresonance and resonance polarizations in ferromagnetic resonance (FMR) range) correspondingly. Our theoretical model consists of two main elements: two-current model [1], [2] and two magnetic subsystems [3]. These systems own of the ordinary and extraordinary Hall effects and magnetoresistance. We consider that the Kerr rotation angle α_K is function of electromagnetic field frequency and static magnetic field both.

It was found that a zero Kerr rotation and FMR are connected but correlation between it was different in microwave and infrared ranges. We have shown that resonance attenuation is the most important in infrared range but is the dispersion of reflection index is more important in microwave range. The frequency dependence of resistance is not important in microwave range but it is very important in infrared range. It's shown that the magnetic moments of subsystems are rotating as whole in microwave range but we have more complete picture in infrared range.

These results follow from the frequency dependence of the magnetic permeability. It's determined by interactions of magnetic subsystems which consist of spin and orbital magnetic moments. The size of magnetic subsystems elements are approximately 1 nm.

Another part of theoretical model is connected with electron and hole currents [1, 2]. Spin orbital interaction in both carrier systems is important element of two-current model. We have considered limit of dirty metal also. We have shown that the magnetoresistance may be negative or positive or equal zero.

We have found that the sign of Kerr rotation and the sign of refraction index change together. Negative refraction index is connected with the mirror spectral crossover [3]. The theory predicts connection between the polar Kerr effect and the mirror spectral crossover.

- [1] A. Fert, I.A. Campbell, *Phys. Rev. Lett.* **21**, (1968), 1190.
- [2] N.I. Yurasov, *Vestnik MGTU, Estestvennye Nauki*, N4 (2005), 26.
- [3] N.I. Yurasov, L.A. Yurasova, A.Y. Shenkarenko, *The physics of metals and metallography*, **92** (2001), S143.

21PO-16-47

RESONANTLY ENHANCED STRIPE LINE TECHNIQUE FOR MEASUREMENT OF MICROWAVE PERMEABILITY OF THIN FILMS

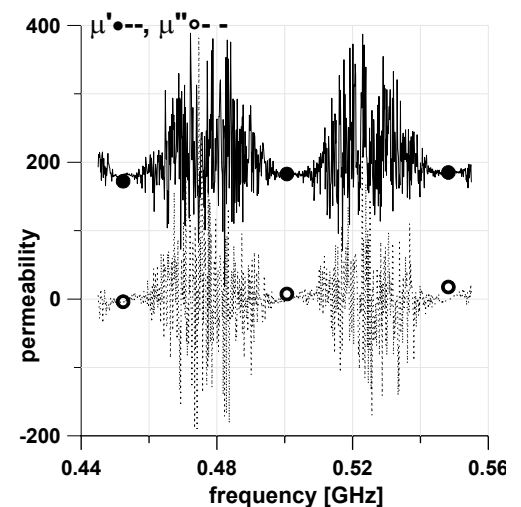
Starostenko S.N., Rozanov K.N., Osipov A.V.

Institute for Theoretical and Applied Electromagnetics, Moscow, RUSSIA

Conventional measurements of permittivity and permeability at microwaves (MW) [1] need large samples and are ill suited for conductive films. A broadband stripe-line technique developed to measure the permeability of sheet samples [2-4] is not sensitive enough for metal films with thickness limited at MW by eddy currents. The sensitivity (the product of permeability μ and cross-section area of the sample S) $\mu \times S$ of experimental setup [4] is limited by the accuracy of reflectivity measurements, and is about 5mm^2 at 20% error level for measurements with standard vector network analyzers (VNA). We increase the setup sensitivity at a discrete set of resonance frequencies f where the dependence of reflectivity $R(f)$ on $\mu \times S$ becomes approximately Q -times steeper, where Q is the resonance quality factor. We assemble the multimode coaxial-stripe-line resonator by connecting the measurement cell [2,4] to a VNA through an impedance discontinuity and a long section of coaxial line. The longer is the coaxial section, the higher is the number of modes and the number of resonance frequencies. As the field structure inside the stripe cell is not uniform and the transmission line includes a coaxial-to-stripe connection with unknown S -parameters, the experimental setup is to be calibrated. The calibration procedure [4] includes reflectivity measurements of both the empty cell and the cell with a reference sample with known $\mu \times S$.

The complex permeability may be calculated via two procedures. The first one is based on the numerical fitting of Q -factor, resonance frequency, and amplitude that describe the Lorentzian shape of the reflectivity curve $R(f)$ in the vicinity of resonance. The second one is based on the numerical solution of Fresnel's equation for complex reflectivity and approximate account for ϵ [4]. The first procedure is less accurate as it neglects the electrical size of strip-line section with the sample, but it treats the scalar reflectivity data that can be measured by a simple SWR-meter.

The measured permeability data of Fe-based film of $25 \times 8 \times 0.00025\text{mm}$ in size are shown in Fig.1. Dots show the data obtained from the fitted parameters of the Lorentzian reflectivity curves, lines present μ calculated from Fresnel's equation. It is clearly seen that for the second procedure the reliable permeability data are grouped around resonance frequencies where the measurement error is minimal. The calculating procedures both produce close results, with the difference arising because the procedures are approximate and based on different assumptions. The sensitivity gain is illustrated in Fig.1 by the noise levels close and far from the resonance frequencies. The noise level far from the resonance frequencies (0.452, 0.500, 0.548 GHz) corresponds to measurement error of non-enhanced technique [4].



- [1] A.R. Von Hippel, Dielectric Materials and Applications, Artech House, 1995.
- [2] V. Bekker, K. Seemann, H. Leiste, *J. Mag. Magn. Mater.*, **270** (2004) 327
- [3] P. Queffelec, Marcel Le Floch, Philippe Gelin, *IEEE Trans. Instr. Meas.*, **47** (1998) 956
- [4] S. N. Starostenko, K. N. Rozanov, A. V. Osipov, *J. Appl. Phys.*, **103** (2008) 07E914.

21PO-16-48

MAGNETIC POLARITONS ON THE INTERFACE OF SUPERCONDUCTOR AND FERROMAGNETIC

Sannikov D.G.², Sementsov D.I.¹, Zhirnov S.V.¹

¹Ulyanovsk State University, 432970 Ulyanovsk, L.Tolstoy str., 42, Russia

²Ulyanovsk Branch of Radio Engineering and Electronics Engineering Institute of the Russian Academy of Science, 43211 Ulyanovsk, Goncharov str., 48, Russia

Surface polaritons on the media interface have been for many years an object of theoretical and experimental investigations. The surface waves on the interface of a superconductor (SC) and ferromagnetic (FM) (for example, on the basis of yttrium iron garnet YIG/YBCO [1]) are of special interest. It is known, that the high-temperature SC possess significant anisotropy of both optical properties and depth of a magnetic field penetration which should be considered at modeling of a SC dielectric permeability. For these purposes the model of two-component plasma can be, as a rule, is used according to which at temperature below critical the electronic subsystem is presented as an ensemble of "normal" (experiencing collisions) and "superconducting" (moving without collisions) electrons which concentration has various temperature dependence.

In the report the results of surface polariton study in "FM-anisotropic SC" structure will be presented. Dielectric permeability of a SC in the context of two-liquid model in a low temperatures limit $\varepsilon_\alpha = \varepsilon_{0\alpha} - \omega_{0\alpha}^2 / \omega^2$, where $\varepsilon_{0\alpha}$ and $\omega_{0\alpha}$ - static dielectric permeability and plasma frequency for corresponding crystallographic directions $\alpha = a, b, c$. FM is magnetized along the axis y ($\vec{B} \uparrow \uparrow \vec{M} \uparrow \uparrow y$) and its high-frequency properties are defined by the magnetic permeability tensor, diagonal and non-diagonal components μ and ν of which are frequency-dependent ones. The dispersive equation achieved for a case when crystallographic axis a coincides with the axis z and a wave propagates along crystallographic axis b (in parallel with axis x), and looks like:

$$\sqrt{k^2 - \kappa_0^2 \varepsilon_2 \mu_\perp} - (\nu / \mu)k + \mu_\perp \sqrt{k^2 - \kappa_0^2 \varepsilon_c} = 0 \quad (1)$$

In Fig.1 the dispersive curves 1-5 are presented plotted on the basis of (1) for the values of plasma frequency $\omega_{0c} = (50; 10; 1; 0.6; 10^{-3}) \cdot 10^{11} \text{ s}^{-1}$. Calculations were made for following parameters of FM and SC: $4\pi M_0 = 1670 \text{ G}$, $H_0 = 180 \text{ Oe}$, $\varepsilon_2 = 15$, $\varepsilon_{0c} = 11.3$. It is necessary to note the fact of non-reciprocity according to which the dispersion character for the opposite directed surface waves is distinguished. Dispersive dependences are limited on frequency by conditions $k^2 - \kappa_0^2 \varepsilon_2 \mu_\perp = 0$ and $k^2 - \kappa_0^2 \varepsilon_c = 0$. The analysis is developed also for other orientations of crystallographic axes.

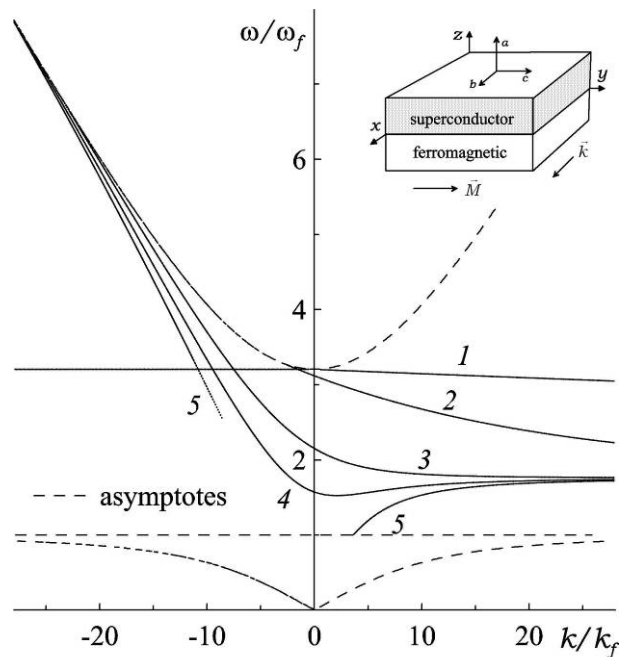


Fig.1. Dispersion curves for magnetic polaritons

21PO-16-49

FERRITE FILM WITH NONSYMMETRIC STRIPE DOMAIN STRUCTURE IS A NATURAL MAGNONIC CRYSTAL FOR MAGNETOSTATIC WAVE.

Lock E.H., Shcheglov V.I., Vashkovsky A.V.

Institute of the Radio Engineering and Electronics of Russian Academy of Science,
Vvedensii square 1, Fryazino 141190, Moscow region, Russia.

Tangentially magnetized epitaxial yttrium iron garnet (YIG) (111)-grown films may be divided in two groups, that differ in nonsaturation state by parameters of domain structure (DS) and characteristics of magnetostatic waves (MSW) [1]. For the first group of the YIG films, having uniaxial anisotropy field H_a higher than ~ 120 Oe, magnetization vectors of domains, as a rule, are significantly declined from the film plane and the period of the DS is considerably smaller than MSW length λ , which usually lies in limits $50 \mu\text{m} < \lambda < 5 \text{ mm}$. For the second group of the YIG films, which have $H_a < \sim 120$ Oe, magnetization vectors of domains are oriented near the film plane and period of the DS may exceed the low limit of variation of MSW length λ . We have realized experimentally situation, where domain width $d = \lambda/2$ and, thus, YIG film represented natural magnonic crystal.

YIG film, used in this experiment, had the next parameters: thickness $s = 17.9 \mu\text{m}$, $2\Delta H = 0.54$ Oe, saturation magnetization $4\pi M_0 = 1920$ Gs, uniaxial anisotropy field $H_a = 108$ Oe, external field, magnetizing film to saturation along easy axis (along direction, perpendicular to the projection of [111]-axis on the film plane) $H_{sat}^e = 19.1$ Oe, external field, magnetizing film to saturation along hard axis (along projection of [111]-axis on the film plane) $H_{sat}^h = 33.5$ Oe.

When external uniform magnetic field \mathbf{H}_0 , applied along easy axis, was increased up to 10 Oe, there was transformation of symmetric stripe DS, having period $T_{sds} = 21 \mu\text{m}$, into nonsymmetric stripe DS, period of which T_{nds} was grew up to $\sim 160 \mu\text{m}$ during the H_0 value was increased to H_{sat}^e (the width d of wide domains grew up mainly and the width of narrow domains wasn't changed practically). Such significant increase of value T_{nds} led to appearance of magnonic crystal for surface MSW, propagated perpendicular

to the boundaries of DS: for MSW, whose wavelength λ was about $2d$, there was the dip on amplitude frequency characteristic (AFC) of transmission coefficient from excited to received MSW transducers, disposed each from other at a distance 15 mm (Fig.1). The dip on AFC corresponds to the wave numbers, lying within interval $190 \text{ cm}^{-1} < k < 230 \text{ cm}^{-1}$ (i.e. $270 \mu\text{m} < \lambda < 330 \mu\text{m}$). Mention must be made, that for $H_0 > 16$ Oe (i.e. when H_0 values lied near value H_{sat}^e) it was impossible to observe DS by optical microscope because of very low contrast of DS, so we have judge about parameters of DS for $H_0 > 16$ Oe by graphical extrapolation.

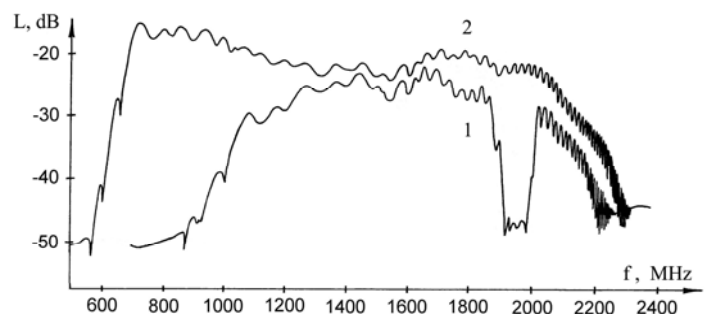


Fig. 1. AFC of transmission coefficient of MSW for unsaturated film (1) at $H_0 = 18.4$ Oe and for saturated film (2) at $H_0 = H_{sat}^e = 19.1$ Oe.

This work is supported by RFFR pr. №07-02-00233a. Support of RSP pr. № 2.1.1.4639 is acknowledged by Lock E.H.

[1] Vashkovsky A.V., Lock E.H., Shcheglov V.I. *Solid State Phys.*, **41** (1999) 1868.

21PO-16-50

PHENOMENOLOGICAL MODELLING OF MAGNETORESONANCE RESPONSE FROM GMI GRANULAR NANOSTRUCTURE IN EHF-BAND

Bagmut T., Khodzitskiy M., Nedukh S., Tarapov S.

Institute of Radiophysics and Electronics NAS of Ukraine; 12 Ac. Proskura St., Kharkov, 61085, Ukraine, e-mail: bagmut@ire.kharkov.ua

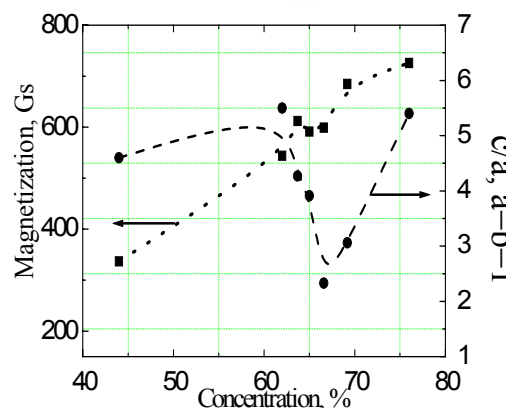
The primary goal of the given work is the simulation of processes of Electron Spin Resonance (ESR) in magnetic nanostructures. Such nanostructures, demonstrating the spin-dependent magnetoresistance are of great interest as a base to design the high-sensitivity electronic devices of Extra High Frequency (EHF) band.

The magnetic properties of thin-film granulated nanostructure $\text{Co}_x(\text{NbLiO}_3)_{100-x}$ [1] with various concentration of ferromagnetic ($x=44\%$; 52% ; 62% ; 63.7% ; 65% ; 66.6% ; 69.25% ; 76%) were investigated. Nanocomposite under study was formed by the nanosized amorphous structure of cobalt clusters, randomly distributed in the segnetoelectric amorphous matrix LiNbO_3 .

The ESR response (which should called correctly the electron magnetoresonance response) had been detected and analyzed at frequency range of 38-43 GHz. The magnetization of saturation M_S was determined on the basis of experimentally obtained ESR peaks.

The abnormal behavior of the magnetization of saturation as a function of the metal phase concentration (δx), reveals itself as a sharp dip for $\delta x = 63.7\% - 69.25\%$. Note that this dip is observed in the area of percolation concentrations, namely in the same concentration area, where the Giant Magnetic Impedance/Resistance (GMI/GMR) [2] magnitude takes place. The dip on the magnetization curve can be attributed most likely to that fact that in the percolation area the change of the mechanism of conductivity takes place [1]. This leads to the appearance of the strong interaction between granules. This, in turn, leads to the essential reorganization of magnetic structure of granulated system, which results in formation of dividing barriers between structural granules are possible to explain this failure.

The phenomenological model [3], supposing formation of magnetic clusters under influence of external magnetic field, is applied to describe ESR-peak shape and their position. Magnetic clusters can be approximated initially [3] as ellipsoids. The model had allowed to determine their shape (the ratio between ellipsoid axis) in the given nanostructure. It was shown, that the shape of magnetic clusters depends on the concentration of the ferromagnetic component of nanostructure, and correlates satisfactorily with the magnetization of saturation magnitude. Besides, in the area of the abnormal behavior of magnetization (δx), the shapes of magnetic clusters approximates to the spherical ones. This can be explained most likely by the appearance of dividing barriers between granules.



Authors are grateful to Prof. Kalinin E.V. for the specimens providing. Researches are supported partially by STCU Project #3727.

[1] V.A. Vyzulin, V.E. Buravcova, V.S. Guschin, et al., *Izvestiya RAN. Seriya fizicheskaya*, **70** №7 (2006) 949-952.

[2] Baibich M.N., Broto J.M., Fert A., et. al. *Phis. Rev. Let*, 61 (1988) №21 2472-2475.

[3] T.V.Bagmut, S.V.Nedukh, S.T.Roschenko, et.al, *JMMM*, **302** (2006) 334-339.

21PO-16-51

BASES OF GENERALISED ELECTRODYNAMICS

Tomilin A.K.

East-Kazakhstan State Technical University,
Ust-Kamenogorsk, Republic of Kazakhstan

In modern electrodynamics \vec{A} vector potential is used as auxiliary function. Its features are assigned by additional conditions (calibrations), which are entered from mathematical considerations formally. In particular, in magnetostatics curly nature is prefixed to the field of the vector \vec{A} . This is confirmed at study of magnetic fields of currents' the most simplest deskside: rectilinear endless current and separate closed sidebar. However it is possible to show [1], for instance, that system of two sidebars with current, creates magnetic field, for description of which, potential component of the vector \vec{A} is required, except curly. This points to insufficiency of traditional magnetostatics (and electrodynamics in general). In this article features of electrodynamic potential with provision for curly and potential components are researched. It is shown that in the aggregate with scalar potential φ , it forms the four-dimensional vector (\vec{A}, φ) , which is offered to take as main feature of the electromagnetic field. Under such approach magnetic field is described by four-dimensional vector (\vec{H}, H^*) , where H^* - scalar function connected with potential component of the vector \vec{A} . Existence of the scalar magnetic field (SMF) is confirmed experimental in research works of Nikolaev G.V. and Tomilin A.K.. It is shown that at interaction of the current with SMF longitudinal electromagnetic power appears, acting on direction of the current or against it depending on sign of the H^* function. Analogue of the law of electromagnetic induction is theoretically motivated and experimentally confirmed: it is shown that under longitudinal moving of conductor in the SMF, EMF of induction appears in it. System of differential equations of generalized electrodynamics is written, based on the worked out research. These equations take into account vector and scalar components of the magnetic field. These equations describe the generation and spreading of the electromagnetic field, created by any complex deskside of electric sidebars. It is shown that except transverse EH -waves, longitudinal electromagnetic E -waves exist, spreading towards potential forming of vector. Experimental facts, confirming real existence of longitudinal E -waves, are provided. Thereby, Maxwell's electrodynamics does not allow us to research the fields of complex electrodynamic systems to the full, because incorporated calibrations exclude one of real existing component of the magnetic field. Generalized electrodynamics is a section, linking Maxwell's theory and four-dimensional quantum electrodynamics. Consideration of electrodynamic phenomena on quantum level without use of the artificial calibrations will allow us to work out the most general electromagnetic theory.

21PO-16-52

FEM ANALYSIS OF CONDUCTION NOISE ATTENUATION BY MAGNETIC THIN FILMS ON MICROSTRIP LILE

Ryu Gi-Bong, Kim Sun-Hong, and Kim Sung-Soo

Department of Materials Engineering, Chungbuk National University
Cheongju 361-763, Korea

Granular or amorphous magnetic thin films with high magnetic loss have been proposed to suppress the unnecessary high-frequency electromagnetic noise in highly integrated electronic devices. Microstrip or coplanar lines are typically used to determine their noise absorbing capability by measuring reflection and transmission parameters (S_{11} and S_{21} , respectively). In this study, noise absorbing properties of the magnetic thin films have been analyzed by using electromagnetic field simulator (HFSS 9.0 Ansoft Co.) which employs finite element method (FEM) and adaptive meshing. With a simulation model of microstrip line attached by $\text{Fe}_{55}\text{Al}_{18}\text{O}_{27}$ thin film of high magnetic loss [1], the S parameters and power absorption are calculated in the frequency range of available material parameters (0.1–1.5 GHz). It is demonstrated that the S parameters and power absorption are dominantly controlled by the electrical properties of the thin film. Although the film has a large value of magnetic loss due to ferromagnetic resonance in the frequency range, it is predicted that the power dissipation by magnetic loss is negligibly small. Simulation under assumption of high electrical resistivity reveals that both S_{11} and S_{21} values approach to the value of original microstrip line. Another simulation of sheet resistance effect by film thickness control (in the range of 0.4–10 μm) shows that higher value of power absorption is predicted in the films of small thickness. It is found that S_{11} parameter is more strongly influenced by the sheet resistance. The smaller the sheet resistance of the film (with increase of film thickness), the higher the wave reflection in the microstrip line due to impedance mismatch at the boundary of thin film suppressor. For the conductive and magnetic $\text{Fe}_{55}\text{Al}_{18}\text{O}_{27}$ thin film, it can be suggested that the dominant power loss mechanism is eddy current loss for magnetic field or ohmic loss for electric field around the strip conductor in the frequency range investigated.

[1] S. Yoshida, H. Ono, S. Ando, F. Tsuda, T. Ito, Y. Shimada, M. Yamaguchi, K. Arai, S. Ohnuma, and T. Masumoto, IEEE Trans. Mag. vol. 37, pp. 2401-2403 (2001).

21PO-16-53

THE MAGNETOSTATIC WAVES IN STRUCTURE FERRITE - DIELECTRIC - METAL GRATING BIASED BY NONUNIFORM MAGNETIC FIELD

Shcheglov V.I., Zubkov V.I.

Institute of Radioengineering and Electronics of RAS, 125009, Moscow, Russia

The investigation of forward and backward electromagnetic waves propagating in composite media is very interesting [1]. The important example of these waves are forward and backward magnetostatic surface waves (MSSW) propagating in ferrite yttrium iron garnet films and structures containing these films. The paper [2] is devoted to investigation of MSSW in structure ferrite-dielectric-metal grating (FDG). The interpretation of observed phenomena in [2] was based on the model simultaneously negative permittivity and permeability [3,4], which

unfortunately is insufficient. In paper [5] we suggest the alternative interpretation based on the model of partial percolation of electromagnetic wave energy through metal grating. The effectiveness of this percolation depends on the wave number and increase when the wave number of MSSW is increased. For the quantitative description of observed phenomenon we introduce the grating screen parameter, which obvious appearance is determined through the MSSW wave number. Using this model we described the MSSW propagation in FDG structure biased by linear nonuniform field. Then we consider the MSSW propagation in FDG structure biased by quadratic nonuniform field in the shape of "valley": $H_z = H_0 (a z^2 + b z + c)$, where a, b, c - constants. The MSSW dispersion relation for this case has the form [5]: $[\beta - 1 - 2\mu\alpha \operatorname{cth}(k d \alpha)] + g(\beta + 1 + 2\nu\delta) \exp(-2k p) = 0$, where the designations are the

same as [5]. The grating screen parameter: $g = \left[\frac{1}{1 - W_B} + W_B \cdot A_N \cdot (k d)^N \right]^{-1}$, where W_B - the relation of window width to the metal grating period, N - whole number, k - wave number, d - ferrite film thickness, A_N - number coefficient. When $g = 0$ this relation correspond to ferrite film having free surfaces. When $g = 1$ this relation correspond to ferrite-dielectric-metal structure. We have shown, that in interval $4 \leq N \leq 8$ the grating screen parameter dependence explains all observed experimental curves.

In linear field the MSSW paths have V-formed character and strive towards the regions where bias field is increased. When the dependence of grating screen parameter from wave number is described by first degree, the MSSW paths always place between the paths corresponded by the ferrite layer with free surfaces and ferrite-dielectric-metal structure. When the degree of this dependence is two or more, the distortion tendency of paths is increased and some paths leave region between above paths and pass outside this region. In quadratic nonuniform magnetic field in the shape of "valley" the paths of MSSW have V-formed or S-formed character and strive towards the regions where bias field is increased. The transition between these two kinds of paths take place by critical value of MSSW frequency. When this frequency is fixed the transition may be produced by changing of bias field or grating screen parameter.

This work is supported by RFFR, Grant 07-02-00233-a.

- [1] J.B.Pendry, A.J.Holden, W.J.Stewart, I.Youngs, *Phys.Rev.Lett.*, **76** (1996) 4773.
- [2] A.V.Vashkovsky, E.H.Lock, *Rad. and El.(Rus.)*, **48** (2003) 169.
- [3] V.G.Veselago, *UFN (Rus.)*, **92** (1967) 571.
- [4] I.V.Lindell, S.A.Tretyakov, K.I.Nikoskinen, S.Ilvonen, *Micr.Opt.Tech. Lett.*, **31** (2001) 129.
- [5] V.I.Zubkov, V.I.Shcheglov, *Proc. XIII Int. Conf. on Spin-Electronics and Gyrovector Electrodynamics*, Moscow (2004) 167.

21PO-16-54

THE DISPERSION OF FORWARD AND BACKWARD MAGNETOSTATIC WAVES PROPAGATING IN BIISOTROPIC MAGNETODIELECTRIC RESONANCE MEDIUM

Shcheglov V.I., Zubkov V.I.

Institute of Radioengineering and Electronics of RAS, 125009, Moscow, Russia

The investigations of electromagnetic waves propagation in composite biisotropic, bianisotropic and chiral media are in current interest [1,2]. In this work we consider the media with arbitrary dependence electric and magnetic inductions simultaneous from electric and magnetic fields: $\vec{D} = \varepsilon \vec{E} + \xi \vec{H}$, $\vec{B} = \eta \vec{E} + \mu \vec{H}$. We have shown that the electromagnetic waves propagation in these media may be described by the system of two connected wave equations. We solved this system for the case of straight propagate plane waves, found the dispersion relation:

$$k^4 - \frac{\omega^2}{c^2} \left[2\varepsilon\mu - (\xi^2 + \eta^2) \right] k^2 + \frac{\omega^4}{c^4} (\varepsilon\mu - \xi\eta)^2 = 0.$$

If ε , μ , ξ , η depend only from frequency ω , but do not depend from wave number k , the dispersion relation may be resolved from k :

$$k^2 = \frac{\omega^2}{c^2} \left\{ \varepsilon\mu + \frac{1}{2} \left[-(\xi^2 + \eta^2) \pm (\xi - \eta) \sqrt{-4\varepsilon\mu + (\xi + \eta)^2} \right] \right\},$$

We showed that the necessary condition for propagation of continuous waves is equality each other of "cross" permittivity and permeability ξ and η , which determine the dependencies electric induction from magnetic field and magnetic induction from electric field. If this equality does not able, in media can propagate only waves, which amplitude is decreasing or increasing according to exponential law. For the continuous waves we have found the condition which connects the ordinary permittivity and permeability ε and μ with "cross" permittivity and permeability ξ and η . We have investigate the waves propagation conditions in medium where ordinary permittivity and permeability depend from frequency by resonance law and "cross" permittivity and permeability are equal and constant. As a basis preliminary we considered the case when "cross" permittivity and permeability are equal to zero. When electric and magnetic resonance frequencies are equal or near to each other there are two frequency regions of forward waves and between its lies the frequency region of backward waves. When these resonance frequencies are very different there are three frequency regions of forward waves and backward waves are absent. Then we considered the case when "cross" permittivity and permeability are not equal to zero. We have shown that in this case in medium also is possible the forward and backward waves propagation. The wave propagation frequency regions in dependence on "cross" permittivity and permeability are stripe-formed and its width is decreased when permittivity and permeability are increased. In ordinary medium at the same time may be only two these stripes. The stripe having lower frequency correspond to forward waves in all the cases, the stripe having upper frequency may be corresponded to backward waves in some conditions.

This work is supported by RFFR, Grant 07-02-00233-a.

- [1] I.V.Lindell, A.H.Sihvola, S.A.Tretyakov, A.J.Viitanen, *Electromagnetic Waves in Chiral and Bi-Isotropic Media*, L.: Artech House (1994).
 [2] I.V.Lindell, S.A.Tretyakov, K.I.Nikoskinen, S.Ilvonen, *Micr.Opt.Tech.Lett.*, **31** (2001) 129.

21PO-16-55

THE MAGNETOSTATIC WAVES IN FERROMAGNETIC WITH MOVING PERIODICAL DOMAIN STRUCTURE

Vilkov E.

Ul'yanovsk Branch of Institute of Radio Engineering and Electronics of Russian Academy of Sciences, Goncharova 48/2, 432011, Ul'yanovsk, Russia

Although a large number of theoretical works have been devoted to the investigation of magnetostatic waves in magnetic materials with a periodic domain structure, all these studies have been concerned with a static domain structure [1,2]. However, it is known that domain walls can move in a crystal under an external control action. In this respect, it is of theoretical interest to investigate the behaviour of magnetostatic waves in crystal with a moving periodic domain structure. The evaluation of the ability of magnetostatic waves to be transformed by a system of moving domain walls is particularly important, for example, for developing new methods intended for transmitting and transforming signals.

It should be noted that, since moving domain walls are the objects of investigation, the problem under consideration belongs to those solved in the framework of magnetodynamics [3,4]. However, in magnetodynamics, primary attention is focused on the determination of the conditions providing stable motion of domain walls and on the description of perturbations that developed in domain walls along different internal (structural) degrees of freedom and in the magnetic material itself, as is the case with solving the problem of spin generation. The purpose of magnetodynamic investigations is to reveal the conditions under which the excitation of spin waves is absent and the motion of the domain walls (in specific velocity ranges) occurs without a substantial change in its structure. In this case, domain walls can be considered to be geometric and structureless and the motion of a periodic system of domain walls can be treated as specified. In this work, the influence of uniform motion of a superlattice formed by domain walls on the spectral properties of magnetostatic waves is analysed without regard for the structural sensitivity of the domain walls to external control actions.

It is demonstrated that the Doppler frequency shift caused by the domain-wall motion leads to the splitting of the spectrum of each magnetostatic wave mode into two dispersion branches, namely, into high-frequency branches. It is established that the larger the mode number, the larger the separation between these branches with respect to the mode spectrum in the presence of the static domain structure. It is also stated, that the motions induces a nonreciprocity in the propagation of waves belonging to the magnetostatic wave spectrum.

[1] G.A. Vugal'ter and I.A. Gilinskiy, *Izv. Vysh. Uchebn. Zaved., Radioviz.* **32** (1989) 1187

[2] I.A. Gilinskiy, R.G. Mints, *Zh Eksp. Teor Fiz.* **59** (1970), 673.

[3] M.A. Sigal, *Zh. Tekh. Fiz.* **59** (1989), 1173.

[4] J.M. Winter, *Phys. Rev.* **124** (1961), 452.

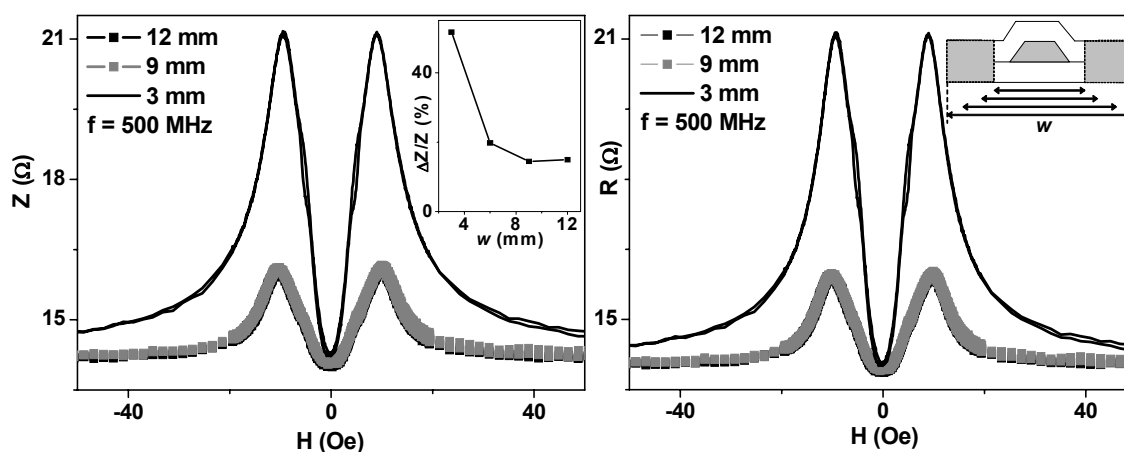
21PO-16-56

HIGH FREQUENCY MAGNETOIMPEDANCE OF FeNi/Cu/FeNi SENSITIVE ELEMENTS WITH DIFFERENT GEOMETRIES

Volchkov S.O., Svalov A.V., Kurlyandskaya G.V.

Ural State University named under A.M.Gorky, Dept. Magnetism and Magnetic Nanomaterials, Lenin Ave. 51, 620083, Ekaterinburg, Russian Federation

Magnetoimpedance (MI) is the change of the impedance of a soft ferromagnet under application external magnetic field [1]. Mathematical MI description requires analytical solution of the Maxwell's equations that can be done only for simplest geometries and using approximations [2]. For example, analytical solution is impossible in case of MI sandwiched structure ferromagnet/conductor/ferromagnet. The finite elements method (FEM) was proposed as useful numerical method for complex geometry of MI sensitive elements [3]. In this work MI behaviour was studied for Fe₁₉Ni₈₁(175 nm)/Cu(350 nm)/Fe₁₉Ni₈₁(175 nm) sensitive elements deposited onto glass substrates at room temperature by rf-sputtering. A constant magnetic field was applied in plane of the sandwiches during deposition perpendicular to the Cu-lead in order to induce a magnetic anisotropy. MI elements had following dimensions: 1 mm × 8 mm for copper part; lengths of magnetic parts was kept constant being of 8 mm. Sandwiches with different width (*w*) of FeNi parts were obtained: *w* = 12, 9, 6 or 3 mm. The complex impedance of the samples (absolute value of the total impedance (*Z*), real (*R*) and imaginary (*X*) components) was measured as a function of the external magnetic field for a frequency (*f*) range of 1 MHz to 990 MHz for MI elements with all above mentioned geometries. MI ratio was defined as follow: $\Delta Z/Z = (Z(H) - Z(H = 0))/Z(H = 0)$. Figure shows selected *Z*(*H*), *R*(*H*) responses and $\Delta Z/Z(H)$ experimental dependence. Frequency dependencies of experimental MI ratios are comparatively analysed with FEM numerical calculations data. The obtained results can be useful for optimization of the design of miniaturized MI detectors.



Supports by Grant RNP.2.1.1.6945 (Russian Federation Program of High School Science Potential Development), and № GP09r/07 by the FASIE (Russian Federation) are acknowledged.

[1] A. Antonov, S. Gadetsky, A. Granovsky, A. Diachkov, M. Sedova, N. Perov, T. Furmanova, A. Lagarkov, *Physica A*, **241** (1997) 414.

[2] L.V. Panina, K. Mohri, *Sens. and Act. A*, **81** (2000) 71.

[3] G.V. Kurlyandskaya, J.L. Muñoz, J.M. Barandiaran, A. García-Arribas, A.V. Svalov, V.O. Vas'kovskiy, *J. Magn. Magn. Mater.*, **242-245** (2002) 291.

21PO-16-57

ELECTRON SPIN RESONANCE AND MAGNETIC POLARONS IN EuB_6 Semenov A.V.¹, Glushkov V.V.¹, Bogach A.V.¹, Sluchanko N.E.¹, Dukhnenko A.V.², Fillippov V.B.², Shitsevalova N.Yu.², Demishev S.V.¹¹A.M.Prokhorov General Physics Institute of RAS, 38, Vavilov str., Moscow 119991, Russia²Institute for Problems of Materials Science of NASU, 03680 Kiev, Ukraine

Strongly correlated magnet EuB_6 attracts attention as a material with complicated ferromagnetic ordering, which nature still remains subject of debates. It is believed that unusual transport properties of this material like giant temperature dependent effective mass renormalization [1] are caused by the magnetic polaron (MP) and magnetic phase separation (MPS) effects. In recent publications [2,3] it was supposed that MP formation and MPS strongly affects the electron spin resonance (ESR) at low temperatures leading to a complicated spectrum consisting of several lines. Moreover, in the available literature there is no agreement about

either the ESR line width or temperature dependence of this parameter. In order to elucidate these problems we have carried out cavity measurements of a high frequency (60 GHz) ESR for a single crystal of EuB_6 at temperatures 4.2-50K in magnetic field up to 7 T. It is found that in conditions of a homogeneous magnetic field in the sample the ESR spectrum in EuB_6 is formed by a single line at all temperatures studied including the ferromagnetic ordering region $T_C \sim 15$ K, whereas the presence of the gradient of the magnetic field in the samples induces double peak ESR structure at low temperatures. The developed procedure of the baseline subtraction and absolute calibration of the ESR data has allowed obtaining

resonant magnetoabsorption in the units of the magnetic permeability (fig. 1). For the quantitative description of the ESR line shape we suggested a new analytical approach applicable for the cavity measurements of a metal with an arbitrary magnetic permeability including strongly magnetic case and obtained full set of the resonant microscopic parameters, namely the oscillating magnetization M_0 , g -factor and the line width. Our analysis has explained the visible resonance line shift and revealed a coincidence of the oscillating magnetization defining the resonance amplitude with the static magnetization. The anomaly consisting in the low temperature growth of the line width below Curie temperature $T_C \sim 15$ K is discovered. We argue that the ESR in EuB_6 is not seriously affected by either interaction with the MP or the MPS and reflects merely the oscillation of the Eu^{2+} localized magnetic moments, which can be well understood within mean field approximation. However some minor features of the magnetic resonance like small temperature variation of the g -factor may be attributed to the MP effect.

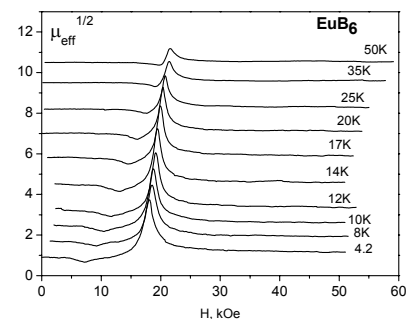


Fig.1. The ESR spectrum in EuB_6 for [001] direction.

Support from the RFBR grants 07-02-00243, 05-08-33463 and Program of Russian Academy of Sciences “Strongly Correlated Electrons” is acknowledged.

[1] V.V. Glushkov, A.V. Bogach, et al., *JETP*, **105** (2007) 132

[2] V.V. Glushkov, A.V. Semenov, et al., *Physica B*, **403** (2008) 932

[3] T. Altshuler, Y. Goryunov, et al., in *Modern Development of Magnetic Resonance, Abstracts of the International Conference, 2007*, p. 138-139

21PO-16-58

MAGNETIC RESONANCE AND NATURE OF MAGNETISM IN CeB₆

*Demishev S.V.¹, Semeno A.V.¹, Bogach A.V.¹, Samarina N.A.¹, Ohta H.²,
Okubo S.², Shitsevalova N.Yu.³, Sluchanko N.E.¹*

¹A.M.Prokhorov General Physics Institute of RAS, 38, Vavilov str., Moscow 119991, Russia

²Kobe University, 1-1 Rokkodai, Nada, Kobe 657-8501, Japan

³Institute for Problems of Materials Science of NASU, 3, Krzhyzhanovskiy Str.,
Kiev 03680, Ukraine

The strongly correlated heavy fermion metal CeB₆ is considered as an archetypical dense Kondo system and is often referred as a model object especially in view of the establishing of the transition from the Kondo-impurity to the Kondo-lattice in a row of the solid solutions Ce_xLa_{1-x}B₆. Additional interest to CeB₆ is caused by peculiar magnetic phase diagram originating, as believed, from the interplay between the spin and orbital degrees of freedom. As a result the orbital ordering at T_Q is achieved preceding antiferromagnetic ordering of the localized magnetic moments (LMM) of Ce³⁺ ions with lowering temperature. Some recent magnetic and transport measurements of CeB₆ and Ce_xLa_{1-x}B₆ system have raised questions concerning the validity of this interpretation [1,2] and here we consider this problem in view of the magnetic resonance study in CeB₆.

We have carried out high frequency (up to 360 GHz) electron spin resonance (ESR) measurements on high quality CeB₆ single crystals along different crystallographic directions in the temperature range 1.8-300 K in magnetic field B up to 30 T. The data obtained were compared with the anisotropy of the static susceptibility and magnetization, which led us to the following conclusions. (1) In the paramagnetic phase ($T > T_Q(B)$) the ESR is not observed and free LMM are totally screened due to formation of the spin polarons in the vicinity of the Ce³⁺ ions. (2) For $T < T_Q(B)$ (i.e. in the supposed orbital ordering region) the magnetization of CeB₆ consists of several contributions, only one of which is responsible for magnetic resonance. (3) The oscillating magnetic contribution can be interpreted as a set of quasi-free magnetic dipoles with the magnitude $\mu = (0.8-0.9)\mu_B$ and quantum number $J = 1/2$, which develop on each Ce³⁺ ion below $T_Q(B)$. (4) The standard Kondo-lattice and orbital ordering models [3] completely fail in description of the observed oscillating magnetic moments even in the exotic case, when magnetic octupole contribution [3] oscillates in the orbitally ordered phase. (5) The distinguished character of the EPR data for the [111] direction corresponding to the strongest g -factor shift indicates the importance of spin fluctuations between the Ce³⁺ and B₆ sites in the genesis of the observed magnetic resonance. (6) The appearance for $T < T_Q(B)$ of the oscillating magnetic moments may be understood in the model [1,2] assuming that at $T_Q(B)$ the spin density wave in CeB₆ is formed on the heavy quasi-particles (spin polarons) and related spin density spatial redistribution leads to “release” of the pseudo free Ce³⁺ magnetic moments responsible for the observed ESR.

Summarizing, we present the ESR evidence that the standard Kondo model based explanation of the CeB₆ physical properties fails or at least faces serious difficulties, whereas a consistent description of the oscillating phenomena can be reached within spin polaron approach [1,2].

Support from the RFBR grant 07-02-00243 and Program of Russian Academy of Sciences “Strongly Correlated Electrons” is acknowledged.

[1] N.E.Sluchanko et al., *JETP*, **104** (2007) 120

[2] N.E.Sluchanko et al., *Physica B*, **403** (2008) 1393

[3] M.Sera, Y.Kobayashi, *J. Phys. Soc. Jpn.*, **68**, (1999)1664

21PO-16-59

INFLUENCE OF GLASS COATING THICKNESS ON MAGNETOIMPEDANCE RATIO IN Co-BASED AMORPHOUS MICROWIRES

Antonov A.S.¹, Buznikov N.A.², D'yachkov A.L.¹, Rakhmanov A.A.¹, Samsonova V.V.^{1,3}

¹Institute for Theoretical and Applied Electrodynamics, Russian Academy of Sciences,
125412 Moscow, Russia

²Scientific-Research Institute of Natural Gases and Gas Technologies – VNIIGAZ,
142717 Razvilka, Leninsky District, Moscow Region, Russia

³Faculty of Physics, M.V. Lomonosov Moscow State University, 119992 Moscow, Russia

Glass-coated amorphous microwires fabricated by Taylor–Ulitsky technique are novel materials having unique magnetic properties and promising for sensor applications. Magnetic behavior of such microwires is determined by thermoelastic stresses arising in amorphous metal during manufacturing process due to the difference in the expansion coefficients of metal and glass [1]. The stress distribution results in the formation of a specific domain structure in glass-coated Co-based microwires with negative magnetostriction, which consists of outer shell with azimuthal or helical anisotropy and inner core with longitudinal or radial easy axis direction. It was shown that the shell occupies practically the entire volume of the microwire [2,3]. The glass removal causes a decrease of the stresses and a change in the easy axes distribution within the microwire [1]. This may result in a further improvement of magnetic softness as well as an increase of the giant magnetoimpedance (GMI). The later effect consists in large changes in the impedance of a soft magnetic conductor in the presence of a static external magnetic field.

In this work, the influence of etching of the glass layer on the GMI in CoFeSiB amorphous microwires was studied. The microwires had the metal core diameter of 18 μm , and the glass coating thickness was 3.5 μm . In order to change the glass thickness, the studied microwire was etched in hydrofluoric acid solution. The field dependence of the impedance was measured for the obtained samples with different glass thickness. The frequency of the excited current was varied from 0.5 to 25 MHz, and the measurements were carried out in the external magnetic field, which was changed from -36 to 36 Oe. It was observed that the value of the external magnetic field corresponding to the maximum of the impedance decreased with the thickness of the glass layer. This fact may be attributed to improvement of magnetic softness of the microwire. However, contrary to expectations, with an increase of the etching time, the magnetoimpedance ratio did not change significantly and even dropped at high frequencies.

The experimental results are interpreted in terms of a core–shell model. It is assumed that before etching the microwire has a helical anisotropy, with the exception of a small region near the sample axis. The etching of the glass layer leads to a relaxation of the internal stresses. As a result, the size of the longitudinally magnetized core increases, and the anisotropy axis angle in the shell deviates from the azimuthal direction. The field distribution within the microwire and the magnetoimpedance are found analytically by means of a simultaneous solution of Maxwell equations and the Landau–Lifshitz equation for the magnetization motion. The results obtained allow one to explain qualitatively the evolution of the GMI with the etching time observed in the experiment and do not contradict magnetostatic data.

[1] H. Chiriac, T.A. Ovari, *Prog. Mat. Sci.*, **40** (1996) 333.

[2] H. Chiriac, T.A. Ovari, Gh. Pop, *Phys. Rev. B*, **52** (1995) 10104.

[3] A.S. Antonov, V.T. Borisov, O.V. Borisov, A.F. Prokoshin, N.A. Usov, *J. Phys. D*, **33** (2000) 1161.

21PO-16-60

CIRCULAR MAGNETIZATION PROCESSES IN CoFeNi ELECTROPLATED WIRES

García-Miquel H.¹, García-Chocano V.M.¹, Kurlyandskaya G.V.²

¹Dpto. Ing. Electrónica, E.T.S.I.T, Universidad Politécnica de Valencia, Camino de Vera, s/n,
46022 Valencia, Spain

²Ural State University named under A.M.Gorky , Dept. Magnetism and Magnetic Nanomaterials,
Lenin Ave. 51, 620083, Ekaterinburg, Russian Federation

Magnetization processes in electroplated wires consisting of highly conductive cylindrical central part and a ferromagnetic cover layer were actively studied in recent years [1]. One of the research topics which up to now were not sufficiently studied in these materials is circular magnetization processes. For rapidly quenched wires some difficulties of the determination of M_ϕ - H_ϕ curves are caused by inhomogeneity of the H_ϕ field created by the flowing current [2-3]. In electroplated wires the changes of this field over the thickness of the magnetic layer can be neglected. In this work the longitudinal and circular magnetization processes in $\text{Cu}_{98}\text{Be}_2/\text{Co}_{16}\text{Fe}_{20}\text{Ni}_{64}$ were studied using an experimental set-up similar to that one designed by A.Hernando et al [3]. The diameter of non-magnetic CuBe was 60 μm and CoFeNi magnetic layer was 1 μm thick. The longitudinal hysteresis loops, M_z - H_z , were measured by inductive technique in a frequency range of 10 to 70 Hz. The M_ϕ - H_ϕ curves were measured for frequencies of 50 and 100 kHz in the H_ϕ field up to 1500 A/m for different values of the axial external field of 0 to 500 A/m (Fig.1). The longitudinal and circular magnetization curves are comparatively analyzed, as well as the relationship between the magnetization processes with the non linear magnetoinductive effect at MHz frequencies.

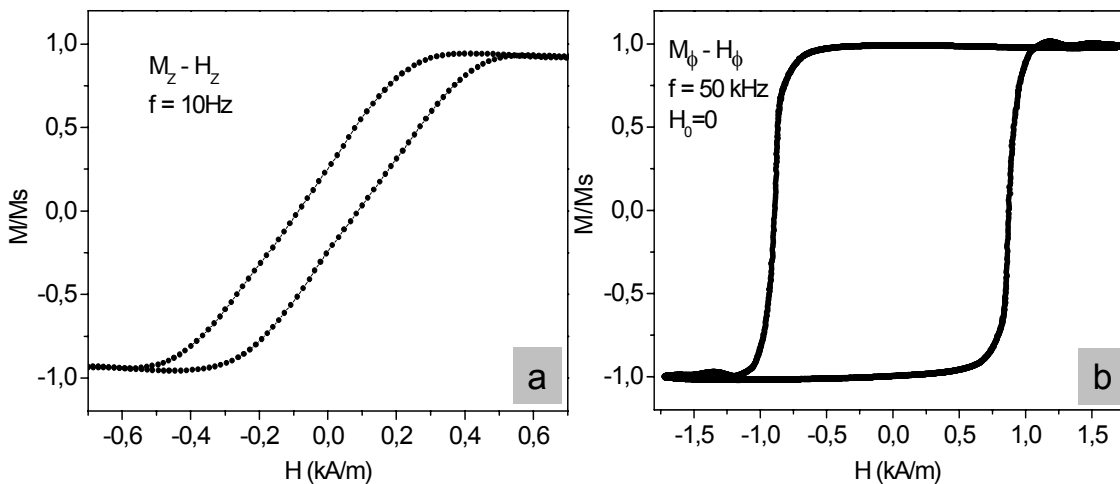


Fig.1: Hysteresis loops (a) Axial M_z - H_z (b) Circular M_ϕ - H_ϕ

Supports by Generalitat Valenciana and RNP.2.1.1.6945 Grant of Russian Federation Program of High School Science Potential Development are acknowledged.

[1] G.V. Kurlyandskaya, H. García-Miquel, M. Vazquez, A.V. Svalov, V.O. Vas'kovskiy, *J. Magn. Magn. Mater.*, **242-245** (2002) 291.

[2] K. Mohri, L.V. Panina, T. Uchiyama, K. Bushida, M. Noda, *IEEE Trans. Magn.*, **31** (1995) 1266.

[3] A. Hernando, J.M. Barandiaran, *J. Phys. D.: Appl. Phys.*, **11** (1978) 1539.

21PO-16-61

INVESTIGATION OF MAGNETIC AND MAGNETOELASTIC PROPERTIES OF A CAST MICROWIRE IN GLASS COVER WITH THE USE OF FERROMAGNETIC RESONANCE

Baranov S.A.¹, Tarapov S.I.², von Gratovsky S.V.³

¹MD 2005, Institute of Applied Physics Moldavian Academy of Sciences, 5 Academiei Kishinev (Chisinau), Moldova., e-mail: stbaranov27@araxinfo.com

²Institute of Radiophysics and Electronics of NASU 12 Ac. Proskury str., 61085.Kharkov, Ukraine+380577203463

³Institute of Radio Engineering and Electronics, Fryazino Branch, Russian Academy of Sciences, IRE RAS, Vvedenski sq.1, Fryazino, Moscow region, 141190 Russia

Existence of natural ferromagnetic resonance (NFMR) in an amorphous microwire make ferromagnetic resonance (FMR) to standard method of investigation of microwire. A shift in the resonant field due to the core deformation of the microwire associated with fusing the glass and core at the temperature of microwire formation was then observed. Both this shift and the FMR line width are of interest; these characterize, in particular, the structural parameters. Since the penetration depth of the microwave field in the metallic wire is small relative to the wire diameter (on account of the skin effect), the resonant frequency in FMR may be determined by Kittel formula for a thin film magnetized parallel to the surface, taking account of the magnetoelastic stress field. The radio absorption properties of cast amorphous microwire (produced by Ulitovsky-Taylor method) appear around the frequency of NFMR, in the range of 1 - 12 GHz [1-5]. We can obtain for NFMR in these microwire shaped nanostructures: $(\Omega/\gamma)^2 = (H_a + H_b + 4\pi M) \cdot (H_a + H_b)$, where Ω is frequency of natural ferromagnetic resonance; $\gamma=2\pi \cdot 2,8$ MHz/Oe (the gyromagnetic ratio); H_a is internal magnetization field; H_b is the deformation anisotropy field, which is proportional to effective residual tensing and magnetostriction; M is the magnetization of cast microwire [4,5]. The FMR and NFMR spectra of cast amorphous microwire in glass insulation have been investigated experimentally and theoretically. General theoretical equations reveal a shift in the FMR resonant field on account of residual stress in the microwire. The formulas are compared with experimental data in the case where the NFMR resonant frequency depends on X . The FMR line width is determined, and the magnetic permeability of the microwire is estimated.

This research received support from RFFI – Moldova grant

- [1] S.A. Baranov.” Use of microconductor with natural ferromagnetic resonance for radio-absorbing materials” Technical physics letters. Vol. 24, No 7, pp. 549-550. 1998.
- [2] S.A. Baranov.” Magnetic properties of an amorphous microconductor in microwave range ” Technical physics. Vol. 43, No 1, pp. 122-123.. 1998.
- [3] S.A. Baranov “Permeability of an amorphous microwire in the Microwave band “ Journal of Communications Technology and Electronics. Vol.48. No2. P. 226-228. 2003.
- [4] S.A. Baranov, V. S. Larin. , A.V Torkunov, A Zhukov and M. Vazquez, ” Magnetic properties of glass insulated amorphous microwires” in “Nanostructured & non Crystalline Materials”. Ed. M.Vazquez and A.Hernando (World Scientific, Singapore), pp. 567-571. 1995.
- [5] S.A. Baranov, V.N. Berzhanski, S.K. Zotov, V.L. Kokoz, V.S. Larin and A. Torkunov, ” Ferromagnetic resonance in amorphous magnetic microwires” Fiz. Met. Metalloved. Vol. 67. No 1, pp. 73 – 78. 1989

21PO-16-62

STUDY OF MAGNETIC PERMEABILITY OF NICKEL FILLED ION TRACK MEMBRANES IN MICROWAVE AND MILLIMETER WAVE FREQUENCY RANGE

Baranov S.A.¹, Kumar S.², Meriakri V.V.³, von Gratovsky S.V.³

¹MD 2005, Institute of Applied Physics Moldavian Academy of Sciences, 5 Academiei Kishinev (Chisinau), Moldova, e-mail: stbaranov27@araxinfo.com

²University College of Engineering, Punjabi University, Patiala, INDIA - 147002

³Institute of Radio Engineering and Electronics, Fryazino Branch, Russian Academy of Sciences, IRE RAS, Vvedenski sq.1, Fryazino, Moscow region, 141190 Russia

Study of magnetic dynamic properties of magnetic nanostructures is of great interest last time. Magnetic dynamic of magnetic metallic nanowire arrays in microwave and millimetre wave frequency range reveals many interesting effects like giant magnetoresistance, giant magnetoimpedance, ferromagnetic resonance, spin-polarized transport, photonic band gap properties etc. [1-4]. Many information about magnetic high frequency dynamic gives study of magnetic permeability in microwave and millimetre wave frequency range. In this report we have investigate samples of polycarbonate ion track membranes polycarbonate filled with nickel and copper. Incident ions with suitably high energies competent of crossing the detector sheet entirely leads to the creation of through tracks, which become see-through channels in the detector sheets. These act as ion track membranes (ITMs) or nuclear track filters (NTFs). Under controlled etching conditions, these see-through channels can be enlarged to preferred size and shape. 15 μm thick polycarbonate foils (Makrofol N, Bayer Leverkusen) were irradiated with heavy ions 58Ni (sp. energy 11.4MeV per nucleon) at normal incidence using UNILAC facility at GSI. Fluence of 107 ions/cm² was applied. The obtained samples have sizes of the order of 1 cm square and metallic wires have diameters in the range 100 nm. The measurements were carried out on an R2-69 network analyzer operating in the 54-78 GHz range. During all experiments external magnetic field was lined in plane of sample. The samples were fixed between the feed and receiving horns, so that wave vector of incident electromagnetic wave was perpendicular to the sample plane. The measurements were carried out in 3 different configurations: the E polarization (when the polarization vectors of the feed and receiving horns are parallel to the external magnetic field), the H-polarization (when high frequency magnetic field are parallel to the external magnetic field), and the cross-polarized configuration. In every configuration it was observed large reflection. For interpretation of experimental results the models of ferromagnetic resonance and also some other models of magnetic dynamics of metallic magnetic nanowire were used.

[1] G. Goglio, S. Pignard, A. Radulescu, L. Piraux, I. Huynen, D. Vanhoenacker, A. Vander Vorst "Microwave properties of metallic nanowires". Appl. Phys. Lett. V. 75, N. 12. p. 1769. 1999.

[2] U. Ebels, J. -L. Duvail, P. E. Wigen, L. Piraux, L. D. Buda, K. Ounadjela „Ferromagnetic resonance studies of Ni nanowire arrays" Phys. Rev. B, V. 64, p. 144421. 2001.

[3] A. Saib, D. Vanhoenacker-Janvier, I. Huynen, A. Encinas, L. Piraux, E. Ferain R. Legras. «Magnetic photonic band-gap material at microwave frequencies based on ferromagnetic nanowires". Appl. Phys. Lett. V. 83, N.12. 22. p. 2378. 2003.

[4] Hiroshi Koshikawaa, , Yasunari Maekawaa and Hiroaki Usui. "Formation of composite films of ion-track membranes embedded with oblique Cu nanowires for anisotropic infrared absorption" Radiation Physics and Chemistry V. 77, N 4, p. 453-455. April 2008.

21PO-16-63

PULSED LASER DEPOSITED $\text{Y}_3\text{Fe}_5\text{O}_{12}$ FILM MAGNETOSTATIC BAND PASS FILTERS

Manuilov S.A., Fors R., Khartsev S.I., Grishin A.M.

Department of Condensed Matter Physics, Royal Institute of Technology,
SE-164 40 Stockholm-Kista, SWEDEN

Commercial magnetostatic wave (MSW) devices use 20-100 μm thick $\text{Y}_3\text{Fe}_5\text{O}_{12}$ (YIG) films grown by liquid phase epitaxy (LPE) on $\text{Gd}_3\text{Ga}_5\text{O}_{12}$ (GGG) substrates. In these films uniaxial anisotropy is negligible since film-to-substrate mismatch strain is released through the nucleation of misfit dislocations so the most part of the film is a cubic YIG crystal. Also, YIG-to-GGG interdiffusion in LPE films grown at high temperatures additionally facilitates strain release hence a strong reduction of uniaxial anisotropy. Contrary to LPE growth, methods of physical vapor deposition performed at moderate temperatures eliminate interdiffusion and enable achievement of sharp film-to-substrate and layer-to-layer interfaces. We fabricated and tested magnetostatic surface wave (MSSW) filters based on pulsed laser deposited YIG/GGG(111) films. Processing conditions were optimized to obtain 220 nm thick films with 9 GHz ferromagnetic resonance (FMR) linewidth as narrow as 1.3 Oe and coercive field ~ 40 mOe. Due to submicron thickness and sharp film-to-substrate interface YIG films remain strained hence demonstrate lattice mismatch induced uniaxial anisotropy characterized by anisotropy field $H_u = -880$ Oe and typical value of cubic anisotropy $H_k = -62$ Oe. Unusually high magnetic anisotropy results in high FMR frequency that was utilized for MSSW band pass filters of two different designs: traditional *hybrid*-type - YIG film laid on transducers alumina board and *integrated* - short-circuited microwave stripe transducers lithographically defined directly on YIG surface. Also, the filters with different effective antennas areal size of 2 and 1 mm^2 were fabricated and tested. The quality factor $Q = f_{\text{res}}/\Delta f_{-3\text{dB}}$ and out of band rejection in dB for all the devices at 2.6 and 6.7 GHz are presented in the Table. We consider micromachined fully integrated electrostatically- or piezo-tunable MSW Si-based filters as an ultimate solution for future RF front-end modules.

Filter type	Size	Frequency	
		2.6 GHz	6.7 GHz
<i>Hybrid</i>	2 mm^2	260 / 36 dB	614 / 33 dB
	1 mm^2	185 / 29 dB	565 / 24 dB
<i>Integrated</i>	2 mm^2	162 / 33 dB	400 / 29 dB
	1 mm^2	59 / 25 dB	338 / 26 dB

21 June Saturday

17:00-19:00

poster session

21PO-21

**“Biomagnetism
and Miscellaneous”**

21PO-21-1

LOW OF BULK ELASTICITY IN MAGNETISM

Poljakov P.I.

Mining Processes Physics Institute of the National Academy of Sciences of Ukraine, str. R.
Luxembourg, 72, Donetsk, 83114, Ukraine

Physical processes in magnet-containing media determine the regularities of evolution of states, properties and phenomena. The development of the more sensitive methods of investigations led to the specialization of studies in the narrower areas, as a result the possibility to observe and to generalize laws of physical processes was lost. The analysis of the wide spectrum of results about well studied galvanomagnetic phenomena into magnetodielectrics, semiconductors and metals makes it possible to reveal the generality of the effects of temperature, magnetic field and pressure (T, H, P).

In the present work we consider the mechanism of elastic strains and stresses as the main controlling factor of structure change under the influence of temperature, magnetic field, hydrostatic pressure. We should take into account that the energy of elastic deformation is commensurate to the energy of electric interactions and that is much higher than the rest of the bonds of lower energy value. Besides, the energy elastic stresses are of long range, so it forms the linearity in magnetization and bulk change. These regularities requires a fundamental understanding of the laws of interaction with respect to accepted interpretation of quantum mechanical forces of short range that are attributes of magnetism formation.

From existing thermodynamic parameters the high pressure proved to be that most important parameter, which allowed us to establish the role of the elastic stresses. Allowance method for high pressure is described in a separate chapter. Developed devices permitted us to combine the studies under varied temperature, magnetic field and hydrostatic pressure [1,2].

The estimations of the parameters of the structure of a single-crystal magneto-dielectric under hydrostatic pressure were performed. The fact of irregular evolution of the structure parameters and anisotropy of elasticity was established.

Due to the high sensitivity of electronic and resonance properties with respect to small changes of the structure, we were able to define the direct relation between elastic stresses and field-frequency dependences, as well as to analyze the evolution of the dynamics of phase transitions and phase states. A cycle of studies of the influence of hydrostatic pressure on the resonance properties are presented also. The analysis of the effect of magnetic, magneto-elastic and elastic energy allowed us to define the combinations of magnetoelastic interactions.

The results of investigations of magnetic semiconductors and their electronic properties revealed the linear dependence of T-P-H influence that confirmed the role of elastic stresses in the structure changes. The same regularity was established in magnetization and magnetostriction features in single crystals. The explanation of the heating and cooling effects of the pressure and magnetic field is presented. The secondary signs of the structural phase transition of the second order are singled out from the correspondences of the maxima of baric, magnetic and resistive effects.

The role of elastic stresses in the linear changes of the magnetostriction, magnetization, magnetoelasticity of single-crystal magnetic semiconductors is described in details. We suggest also the explanation of the colossal magnetoresistance as a consequence of the elasticity laws. Here we state the results of the causal action of the elastic stresses that control the evolution of the structure and the properties and form the phase transformations in magnetic dielectrics and metals.

[1] P.I. Polyakov, S.S. Kucherenko JMMM 278(2004) 138-155.

[2] P.I. Poyakov, S.S. Kucherenko JMMM 248(2002) p. 396 – 401.

21PO-21-2

COMPARATIVE INVESTIGATIONS OF STRUCTURE AND ABSORPTIVE CAPACITY OF NANO- AND MICROSIZED MAGNETIC-OPERATED PARTICLES FOR THEIR APPLICATION IN MEDICINE AND BIOLOGY

Yanovsky Yu.G.¹, Komissarova L.Kh.², Danilin A.N.¹, Zaraysky E.I.¹

¹Institute of Applied Mechanics, RAS, Leninsky prosp., 32A, 119991, Moscow, Russia

²N.M. Emanuel Institute of Biochemical Physics, RAS, Kosygin str., 4, 11977, Moscow, Russia

For the first time the comparative investigations of structure and sorption efficiency of nano- and microsized magnetic-operated particles (ferromagnetics) in respect to both the antigens and viruses (e.g. hepatitis B) also to the substance-markers (low-, middle- and highmolecular substances) were carried out.

By using the optical interference microscope the structures, form and sizes of magnetic particles have been investigated. It has been shown that the aggregation processes of Fe_3O_4 and CoFe_2O_4 particles grained to nano-dimensions and stabilized in a saline solution after drying up occur. The aggregates had relatively smooth structure of surfaces and therefore very bad sorption efficiency to low-, middle - and highmolecular weight substances. The sorption efficiency of magnetic particles to the substances of different molecular masses was evaluated in vitro experiments. As low-, middle- and highmolecular substances have been used methylene-blue cyancobalamin and human hemoglobin respectively. Before adsorption suspension of particles in distillate water was subjected to ultrasonic waves and incubated with the substance-markers. We defined an amount of adsorbed substances using a spectrophotometer.

This part of work has been dedicated to study adsorption virus of hepatitis B and antigen of virus hepatitis B (HBs Ag) by magnetic particles of Fe_3O_4 and CoFe_2O_4 . For this the "sandwich"-immunoferment analyze of the positive to HBs-antigenes samples has been made. The above mentioned magnetic particles have good sorption capacity to antigen and virus hepatitis B. Besides, Fe_3O_4 particles demonstrate the best adsorption. It is probably accounted for by merged dipole interactions between polar molecules of magnetite, on the one hand, and antigens and viruses on the other.

In the work the absorptive capacity of magnetic microsized composites of ferrocarrbon (FC) has also been investigated. We have studied ultradispersed powders of ferrocarrbon prepared by plasma-chemical technology from iron and carbon, and biocomposites on their base, when particles were covered by albumin. It has been shown that magnetic particles of composites with 40-50% carbon content are optimum in terms of chemical content. They have the saturation magnetization 50-70 emu/g. It allows conducting their magnetic separation by magnetic field with intensity 100-150 mTl. Besides, such kinds of composites have shown high sorption efficiency.

To investigate the sorption efficiency of FC composites, the screening of different samples of FC to substance-markers of different molecular masses has been undertaken. The high absorptive capacity to low- and highmolecular substances (methylene-blue and hemoglobin, respectively) has been observed for FC covered with albumin. Besides, the sorption capacity of FC and their biocomposites to highmolecular components, is much more in comparison with mere carbon sorbents. The consideration of these results give us an opportunity to use the above mentioned magnetic sensitive nano- and microsized particles in medicine, in particular, for apparatus of extracorporeal detoxication of biological fluids.

21PO-21-3

MAGNETIC PROPERTIES OF THE THERMODYNAMICAL SYSTEM IN THE EQUILIBRIUM STATE

Urusova B.I., Uzdenova F.A., Laipanov U.M.

Karachaevo - Cherkessk State University, 369202, Karachaevsk, Russia

Problem of the magnetic properties of the thermodynamic systems in the equilibrium state was considered. We suggest that it is an ensemble of the super – paramagnetic systems (grains) of ore. To obtain exact solution of this problem the statistical sum was computed:

$$Z = \sum \exp\left(\frac{\chi}{kT}\right), \quad (1)$$

where Σ - means the summation with respect to all possible system states;

χ - magnetic susceptibility of the grains; k - Boltzmann's constants;

T - thermo dynamical temperature.

For ensemble of N identical uniaxial oriented particles we wrote:

$$\chi = -\frac{1}{2} \sum_{i \neq j} \mu_0 m_i H_{ij} - \sum_i \mu_0 m_i H = -\frac{1}{2} \sum_{i \neq j} U_{ij} \sigma_i \sigma_j - \mu_0 m H \sum_i \sigma_i \quad (2)$$

where $U_{ij} = \frac{\mu_0 m^2 (3 \cos^2 \theta_{ij} - 1)}{4\pi r_{ij}^3}$ - dipole – dipole (bidipol) interaction potential;

$H_{ij} = \frac{U_{ij} \sigma_i}{\mu_0 m}$, $m_i = m \sigma_i$, $\sigma_i = \pm 1$; r_{ij} - from i to j grains distances; θ_{ij} - from \vec{r}_{ij} to \vec{l} ,

angle, where $\vec{l} \parallel \vec{H}$ and by forming of residual magnetization- I_{rt} we can set a limit approximation where an interaction efficient field is \vec{H} - projection to the light axis of the particle; μ_0 - magnetic permeability of vacuum; m_i - i - particle mass.

We got that «phase transition» really exists in the molecular field approach.

The point T_g is a «freezing point», a lower temperatures its particles magnetic moments are as though «freeze» in some, random direction for each particle.

Thus, using the molecular field theory, one can analyze ferro-antiferro as well as ferromagnetic systems.

21PO-21-4

GAUGE THEORY OF FERROELECTRIC-ELASTIC INTERACTION IN UNIAXIAL FERROELECTRIC WITH STRIP DOMAIN STRUCTURE

Kharrasov M.Kh.¹, Kizirgulov I.R.², Khusainov A.T.¹

¹Baskir state university, Ufa, 450074

²Sterlitamak state pedagogical academy, Sterlitamak, 453434

At present methods of a gauge field theory are considered to be among the strongest ways of describing phenomena either in physics of elementary particles, or in solid state physics. They are successfully used for describing elastic and magnetoelastic media with continuously distributed dislocatoin and diclinatoin [1].

In this work the expansion of bound segnetoelastic waves in thick plate of uniaxial segnetoelectric with a large constant of polarization anisotropy is described with the help of given method. As a rule strip domain structure exists at the finite thickness of crystals, at the large thickness domain distribution can be considered to be continuous. Thus it can be interpreted as a result of homogeneous operation of translation group $T(3)$.

In the work it is shown that the existance of continuous distributed domains in the medium leads to the necessity to consider elastic and segnetoelectric freedom degrees of medium. Gauge fiels, describing strip domain structure ensure invariant of lagrangian of the medium according to local homogeneous rotations and in homogeneous translations of grate. Lagrangian of the medium has the folloving form:

$$L = T_y + T_p - [\rho_0 U(\eta_{ij}, \mu_i^*, \theta_i^*, K_{ij}) + L_\varphi + L_\theta],$$

where T_y – kinetic energy of elastic subsystem, L_φ , L_θ – langrangians of gauge fields, T_p kinetic energy of segnetoelectric subsystem.

Equations for displacement for gauge fields and polarization are got by variant method, supposing that the modulus of the last one is not changed:

$$\partial_b Z_i^b = 0, \quad \partial_b R_j^{bc} = \frac{1}{2} Z_j^c, \quad \varepsilon^{kpi} \delta_{pr} \mu^r [-\partial_l Z_k^{(P)l} + \Xi_k^{(P)}] = 0, \quad \partial_b Q_j^{bc} = \frac{1}{2} M_j^c, \quad (1)$$

where index b and c are changed from 1 to 4, but the rest – Latin and Greek – from 1 to 3.

Equations (1) must satisfy conditions of integrability:

$$dZ = 0, \quad dM = 0.$$

Dispersion dependence of bound segnetoelastic waves is found if domain fields exist. It has been found out, than in this case additional mode of bound waves segnetoelectric and elastic subsystems appear in comparison with an ideal crystal. Their emergence is conditioned by interaction of polarization vector and domain fields.

If domain structure in the medium is absent, the results we have can become simple theory of segnetoelastic interaction.

[1] V.V. Menshenin, *FTT*, **33** (1991) 1518.

21PO-21-5

AN EMI IMMUNITY STUDY OF TMR HEADS IN QUASI-STATIC TESTER DUE TO THE DIRECTION OF SWEEPING FREQUENCY

Siritaratiwat A.^{1,2}, Kruesubthaworn A.¹, Ungvichian V.³*

¹Department of Electrical Engineering, Khonkaen University, Khon Kaen, 40002, Thailand

²Industry/University Cooperation Research Center in HDD Component, Faculty of Engineering, Khon Kaen, 40002, Thailand

³EMI Laboratory, Department of Electrical Engineering, Florida Atlantic University, Boca Raton, FL 33431-0991, USA

* e-mail: apirat@kku.ac.th

The electromagnetic interference effect on recording head has been recently concerned but no effective result in production line has been published [1] This report aims to investigate a comparative EMI effect on recording heads due to sweeping directions of low-to-high and high-to-low frequencies. Four Quasi-Static Tester (QST) parameters; MR resistance, Asymmetry, Barkhausen noise change and Hysteresis, are used for monitoring the EMI effect on Head Gimbal Assembly (HGA). It is undoubtedly found that the Asymmetry and Hysteresis parameters provide insufficient indication of EMI effect for both sweeping frequency directions.

On the other hand, it is discovered that the sweeping direction of the low-to-high frequency is more effective to two test parameters; MR resistance and Barkhausen noise, than the other direction. The dramatic energy accumulation is possibly explained this phenomenon but this energy level is not high enough to cause the Hysteresis change. The different transfer curves confirm this assumption.

This research is funded by the Industry/University Cooperative Research Center in HDD Component (I/U CRC in HDD Component), Khon Kaen University, and the National Electronics and Computer Technology Center (NECTEC) under the National Science and Technology Development Agency (NSTDA), Thailand. Authors would like to acknowledge this work to staff of Western Digital Company (BangPa-In), Thailand, for their provision of samples, facilities and technical discussion.

[1] Kraz V and Wallash A, *J. Electrostat.*, **54** (2002) 39.

21PO-21-6

COUPLED ELECTROMAGNETIC-THERMAL FIELD INVESTIGATION IN INDUCTION HEATING DEVICE

Iatcheva I.¹, Stancheva R.¹, Tahrilov H.², Lilianova I.²

¹Technical University of Sofia, 8, Kl. Ohridski Blvd., Sofia, Bulgaria

²Technical University of Varna, 1, Studentska Str., Varna, Bulgaria

The aim of the work is precise coupled field analysis (electromagnetic-temperature) by finite element method of an induction heating system. Presented example is referred to real induction heating system. The principal geometry of the system is shown in Fig. 1. It consists of multisectional disc-type inductor and heated detail. Heated details after plastic deformation and hardening are used for producing instruments.

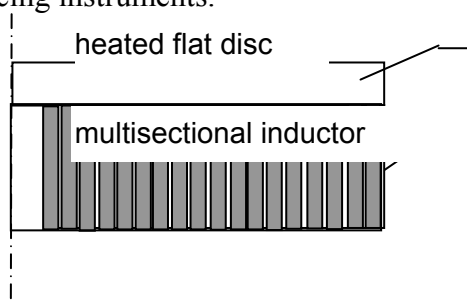


Fig. 1. Principal geometry of the induction system

The problem was solved as nonlinear, transient, axisymmetrical, coupled electromagnetic and temperature field. The numerical model of the coupled electromagnetic and temperature fields is based on the finite element method and electromagnetic and temperature distribution has been obtained using COMSOL 3.3 software package.

The temperature distribution in the heated disc in radial direction at different moments of the heating process is shown in Fig.2.

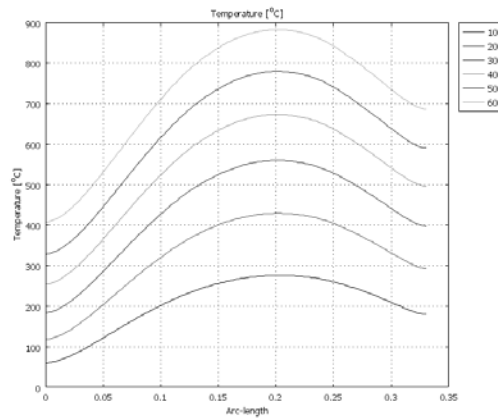


Fig. 2. Temperature distribution in the heated disc in radial direction in different moments of heating process

The presented numerical model can be used in optimization tasks in order to satisfy special requirements for temperature distribution in the heated detail.

21PO-21-7

3D MAGNETIC FIELD MODELLING AND FORCE COMPUTATION OF A PERMANENT MAGNET LINEAR ACTUATOR

Yatchev I., Hinov K., Gueorgiev V.

Technical University of Sofia, 8, Kl. Ohridski Blvd, 1000 Sofia, Bulgaria

Rare earth permanent magnets have been increasingly used in numerous electromagnetic applications [1], [2]. One of them is application of the rare earth magnets in linear electromagnetic actuators. Permanent magnet actuators feature increased energy efficiency compared with actuators driven by neutral electromagnets is the.

In the present paper, three-dimensional finite element modelling of a construction of recently developed permanent magnet linear actuator is presented and its static force characteristic is obtained when varying different factors.

The principal construction of the actuator is shown in Fig. 1. The actuator consists of several cores placed on a common yoke. There are also coils placed on each core. The mover is brick-type rare earth permanent magnet. The specific requirements to the actuator are that the mover has to be able to stay at four stable positions when there is no supply to the coils and to maintain minimum static force over the stroke.

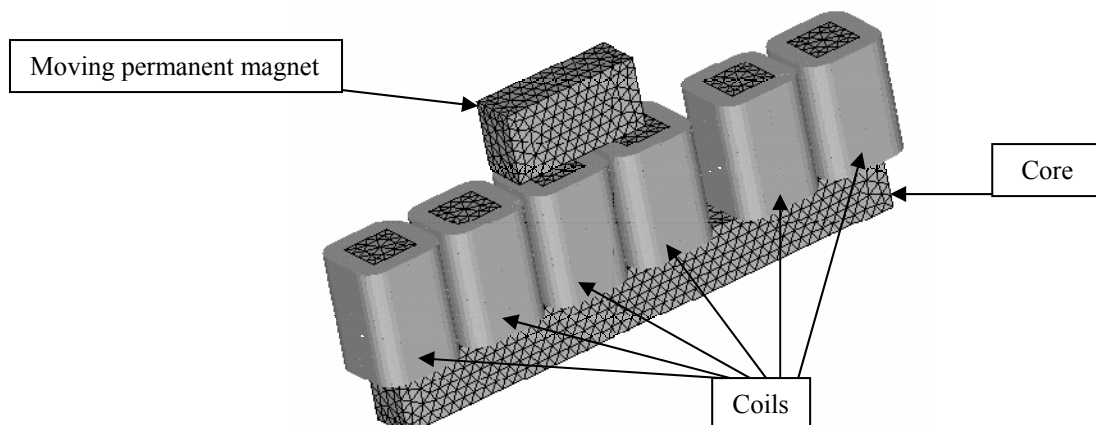


Fig. 1. Principal construction of the actuator with finite element mesh.

Three-dimensional finite element method has been employed for modelling of the magnetic field of the actuator and computation of the electromagnetic force on the mover. Two formulations are used – reduced magnetic scalar potential nodal formulation and magnetic vector potential edge formulation. In Fig. 1, the finite element mesh of the core and the permanent magnet for the reduced magnetic scalar potential formulation is shown.

The electromagnetic force and the static force-stroke characteristics are obtained for the single and double sided constructions when varying different factors – dimensions of the magnet, dimensions of the cores and magnetomotive force of the coils. For obtaining force in the right direction at each position, suitable coils supply is chosen.

The obtained results will give the opportunity for further design optimization and for estimation of dynamic behaviour of the actuator.

The present work was supported by the National Science Fund of Bulgarian Ministry of Education and Science, Project No. VU-EEC-306/2007.

[1] P. Campbell, *Permanent magnet materials and their application*, Cambridge University Press, 1994.

[2] E. Furlani, E. Kodak, *Permanent Magnet and Electromechanical Devices*, Academic Press, San Diego, London, 2001.

21PO-21-8

COMPUTER SIMULATION OF MAGNETIC PHASE TRANSITIONS IN Re-Tb AMORPHOUS ALLOYS

Bondarev A.V., Bataronov I.L., Ozherelyev V.V., Barmin Yu.V., Dorovscoy Yu.V.
Voronezh State Technical University, 14 Moskovski prospect, Voronezh 394026, Russia

Using the Monte Carlo method in the frame of the Heisenberg model we carried out simulation of magnetic properties of pure amorphous Tb and $\text{Re}_{100-x}\text{Tb}_x$ ($x=5, 8, 10, 13, 20, 29, 49, 59$ and 91 at. %) amorphous alloys. The model Hamiltonian contains the terms describing exchange interaction between nearest neighboring Tb atoms and random anisotropy which is essential for formation of the spin-glass state in the rare-earth alloys:

$$H = -\frac{1}{2} J \sum_{i,j} (\vec{S}_i \cdot \vec{S}_j) - D \sum_i (n_i \cdot S_i)^2,$$

where J is exchange interaction constant between the pairs of Tb ions; D is anisotropy constant; \vec{S}_i is classical Heisenberg spin placed in each site of the model amorphous structure; \vec{n}_i is unit vector determining the direction of the local anisotropy axes.

We calculated the temperature dependence of spontaneous magnetization, Edwards–Anderson order parameter and magnetic susceptibility. In all the models the transition to the spin-glass state was observed except of $\text{Re}_{95}\text{Tb}_5$ amorphous alloy where paramagnetic phase exists in the entire temperature region up to 1 K. Magnetization at low temperatures for all compositions did not exceed 0.1. The temperature of the spin-glass transition was determined as position of maximums on temperature dependencies of magnetic susceptibility. With increasing concentration of Tb atoms the transition temperature linearly increases, this linear dependence qualitatively agrees with the experimental results.

21PO-21-9

EMR SPECTRA OF IRON-BASED NANOPARTICLES PRODUCED BY DASSIMILATORY BACTERIA

*Koksharov Yu.A.¹, Chistyakova N.I.¹, Zavarzina D.G.²
Treninkov I.A.¹, Polyakov S.N.¹, Rusakov V.S.¹*

¹Faculty of Physics, M.V.Lomonosov Moscow State University, 119991 Moscow, Russia

²Institute of Microbiology RAS, Prospect 60-letiya Oktyabrya 7/2, 117312, Moscow, Russia

Pathways to biomineralization, the production of inorganic phases by living organisms, are rather complex and not clearly understood [1]. Intracellular biosynthesis and transformation of various iron oxides are biochemical processes used widely by bacteria. We have studied magnetic nanoparticles produced by some new iron-reducing bacteria by the electron magnetic resonance (EMR) spectroscopy. This method is very sensitive and informative in studying of biogenic magnetite [2] and, in general, of iron-based nanoparticles [3].

The substrate (control sample) for bacteria iron-reducing and products of bacteria activity were studied depending on the temperature and aging time. The details of the samples have been described in [4]. The parameters of EMR signal of as-prepared control sample is close to those of superparamagnetic non-interacted iron-oxide amorphous nanoparticles [3,5]. The shape of the room-temperature EMR signal is close to Lorentzian; the g-value is about 2.0; there is also the weak additional line with $g \approx 3.8$. This weak line is usually assigned to isolated Fe^{3+} ions situated at a highly distorted low-symmetry site. Similar to EMR spectra of iron-based nanoparticles embedded in polyethylene matrixes [3] the signal can be presented as a sum of two Lorentzians.

The as-prepared samples containing biogenic iron-oxide has demonstrated the EMR signal with effective g-value near 2.13 and can be related to magnetite phase in nanoparticles [2]. The two-line fitting analysis has showed that EMR spectra of these samples contains the Lorentzian which resembles the EMR signal in the control sample and the Gaussian with $g = 2.13$. Therefore, the first signal can be attributed to residual magnetic fractions which have not been treated by bacteria; the second signal can be considered as magnetite nanoparticles obtaining due to bacterial activity. Besides, biologically induced superparamagnetic nanoparticles of magnetite often reveal Gaussian line shape of the EMR spectra (or superposition of Gaussians) [2].

After long open-air storage the samples were investigated repeatedly. In all samples the EPR spectra have shifted to lower magnetic field region and became narrower. In case of EMR in superparamagnetic nanoparticle the shift of the spectra to lower magnetic fields can be related to increasing of particle magnetization [3]. The latter could be due to crystal structure transformation, which can change magnetic structure.

The EMR spectra change very little after cooling, the resonance lines slightly shifted to lower magnetic fields. Probably, this indicates very small sizes of nanoparticles which remained superparamagnetic at liquid nitrogen temperatures.

[1] A. Navrotsky, PNAS, 101 (2004) 12096

[2] B.P. Weiss et al., Earth and Planetary Science Letters 224 (2004) 73

[3] Yu.A. Koksharov et al., J. Appl. Phys., 88 (2000) 1587.

[4] N.I. Chistyakova et al., International Conference on the Application of the Mössbauer Effect, Kanpur, India, 2007, Abstracts, p.19.

21PO-21-10

MRI MONITORING OF TARGETING, ACTIVATION, AND HYPER THERMAL HEATING OF MAGNETIC SENSITIVE ANTICANCER DRUGS

Brusentsov N.¹, Pirogov Yu.², Lichinicer M.¹, Uchevatkin A.², Ivanov A.¹, Polianski V.³,
Kupriyanov D.², Nikitin P.⁴, Brusentsova T.⁴, Nikitin M.⁴, Anashkin O.⁵

¹N. N. Blokhin SE Russian Cancer Research Center RAMS, Moscow, 115478, Russia

²Research Center for Magnetic Tomography and Spectroscopy, M.V. Lomonosov Moscow State University, Leninskie gory 1-73, Moscow 119991, Russia

³Institute of Mechanics, M.V. Lomonosov Moscow State University, Michurinskiy Prospect 1, Moscow 119192, Russia

⁴Natural Science Center of General Physics Institute, Russian Academy of Sciences, Vavilov Str. 38, Moscow 119991, Russia

⁵Kurchatov Institute, Russian Research Center, Kurchatov square 1, Moscow 123182, Russia

It is proposed to realize magnetic hyperthermia by the method [1] in combination with monitoring by magnetic resonance imaging (MRI). The method [1] consists in magnetically sensitive sol (MS) containing magnetic active nanocapsules of anticancer drug. An example of such sol is for instance a suspension of dextran-ferrite nanocapsules – Fe₂O₃ particles in dextran shells. For containment of injected to tumor MS, it is applied a non uniform constant magnetic field coagulating nanocapsules into macroparticles and not allowing to extract MS from tumor by fluid flows (blood, lymph, etc.). Constructed by this way MS macroparticles are heated by variable magnetic field in an inductive magnetic coil of high frequency (about 1 MHz) generator and hyperthermally destruct tumor tissues. The magnetic hyperthermia experiments were carried out on small animals – mice and rats – with MRI control of MS injection to tumor, drug magnetic activation (immobilization) and hyperthermal heating. As a MRI scanner, the specialized bio-spectrometer of CMTS MSU – Bruker BioSpec 70/30 URS with 30-cm warm aperture and 7 T magnetic field. The constant SmCo₅ and NdFeB magnets, magnetic applicators-bandages [2] with 0.5 T field, resistive and super-conducting magnets with the field from 0.7 up to 7 T are used for coagulation of MS particles by non uniform constant magnetic field. The magnetic bandages and super-conducting coils with magnetic flux concentrators were the most effective during creation of high non uniform magnetic field. With changing of sizes and shape of applicators, one can change in wide limits magnitudes and spatial distribution of immobilized magnetic fields. Mobile applicators are used as well for navigation of magnetic catheters and other devices inside blood vessels. Measuring of MS parameters in experiments *in vitro* and *in vivo* (on small animals) was realized by before developed BioMag technique [3]. Mobile applicators as indicators of magnetic field disturbances and MRI scanner BioSpec 70/30 URS are applied for visualization of MS localization zones.

The carried out experiments demonstrate unique possibilities of MRI visualization of magnetic controlled drug targeting and activation with following realization of tumor hyperthermia with help of variable magnetic field.

The work was supported by RFBR, No. 08-01-00026, 07-01-00026, 96 WFA0100119, 07-04-92001-HHC_a.

[1] N.A. Brusentsov, T.N. Brusentsova, et al., *J. Magn. Magn. Mat.*, **311** (2007) 176.

[2] U.O. Hafeli, K. Gilmour, A. Zhou, S. Lee, M.E. Hayden, *J. Magn. Magn. Mat.*, **311** (2007) 323.

[3] P.I. Nikitin, P.M. Vetoshko, T.I. Ksenevich, *J. Magn. Magn. Mat.*, **311** (2007) 445.

21PO-21-11

CROSSOVER FROM VALENCE PHASE TRANSITION TO KONDO BEHAVIOR IN $\text{Yb}_{1-x}\text{Ce}_x\text{InCu}_4$ AS PROBED BY ^{63}Cu NQR

Gippius A.A.^{1,2}, Okhotnikov K.S.¹, Anferova P.A.¹, Mushnikov N.V.³, Vasiliev A.N.¹

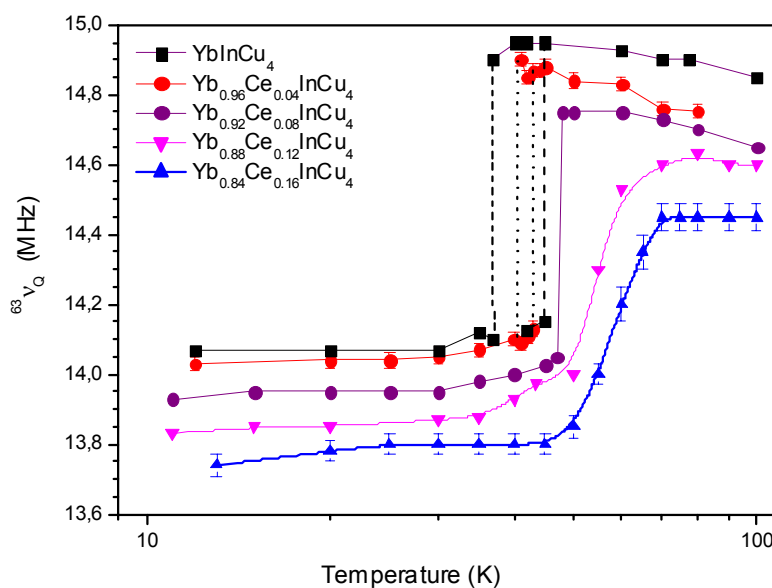
¹Faculty of Physics, Moscow State University, Moscow, Russia

²Shubnikov Institute of Crystallography, Moscow, Russia

³Institute of Metal Physics, RAS, Ekaterinburg, Russia

YbInCu_4 is the only intermetallic ternary compound which exhibits isostructural 1-st order valence phase transition at ambient pressure [1-2]. The transition at $T_v \sim 40$ K is accompanied by abrupt changes in the lattice volume, electrical resistivity, specific heat, magnetic susceptibility and other physical properties [2-4]. We report the results of detailed NQR study the influence of cerium substitution on the valence phase transition in $\text{Yb}_{1-x}\text{Ce}_x\text{InCu}_4$ system.

The temperature dependences of ^{63}Cu NQR frequencies for $\text{Yb}_{1-x}\text{Ce}_x\text{InCu}_4$ compounds with $x = 0, 0.04, 0.08, 0.12$ and 0.16 are presented in the Figure. As seen from this figure, at low Ce concentration $x < 0.08$ the $\text{Yb}_{1-x}\text{Ce}_x\text{InCu}_4$ exhibits a discontinuous transition characterized by the presence of both Yb^{3+} and $\text{Yb}^{2.9+}$ valence state phases in the finite temperature range around the phase transition temperature. This is evidenced by simultaneous observation of two ^{63}Cu NQR lines in this region. This intermediate temperature range is the widest for pure YbInCu_4 where two ^{63}Cu NQR lines coexist in the temperature range 37 – 45 K (dashed lines). This feature is rather unique for the systems exhibiting the first order phase transition. It is interesting to mention that, to our knowledge, NQR is the only experimental technique which is able to observe the coexistence of the LT and HT phases.



For $\text{Yb}_{0.96}\text{Ce}_{0.04}\text{InCu}_4$ the phase coexistence interval becomes more narrow 41 – 43 K (dot lines) and finally shrinks into almost one point for $\text{Yb}_{0.92}\text{Ce}_{0.08}\text{InCu}_4$. With increasing Ce concentration ($x > 0.08$) the transition shifts to higher temperatures and becomes more gradual with only one ^{63}Cu NQR line observable at each temperature point in the entire temperature range. Therefore we can conclude that in the vicinity of Ce concentration $x = 0.08$ there is a crossover from the 1-st order valence phase transition to a behavior characteristic for concentrated Kondo systems with a unique energy scale [4].

Support by Russian Science Support Foundation is acknowledged.

[1] I. Felner., I. Nowik, *Phys. Rev. B* **33** (1986) 617.

[2] N.V. Mushnikov et al., *J. Phys.: Condens. Matter* **16** (2004) 2395.

[3] J.L. Sarrao et al., *Phys. Rev. B* **58** (1998) 409.

[4] T. N. Voloshok et al, *Phys. Rev. B* **76** (1998) 172408.

21PO-21-12

SOME NOTEWORTHY PHENOMENA REVEALED IN ANISOTROPIC MAGNETIC FILMS BY POLARIZED NEUTRON SCATTERING

Kovalev A.V.

Petersburg Nuclear Physics Institute of the Russian Academy of Science,
188300 Gatchina, Leningrad region, Russia

The Co–Fe films manufactured by magnetron sputtering exhibits a strong magnetic in-plane anisotropy and the remanent magnetization. Such samples are the objects of our intense study in connection with the origin of the induced magnetic anisotropy. In attempts to explain the nature of this phenomenon we used the hypotheses [1] demanding detailed and scrupulous examination. It turns out that a technique based on polarized neutron reflectometry is the most convenient for such work.

The measurements were carried out at the small-angle polarized neutron setup VECTOR (WWR-M reactor, Gatchina). The angular distributions of intensities, such as depicted in Fig. 1 (non-spin-flip) and Fig. 2 (spin-flip), were measured for reflected and refracted neutrons. The research approaches to the above-mentioned problem and a great deal of experimental evidences are submitted in the article [2] where one can find the necessary details and references.

The pattern of specular and non-specular reflections allows us to obtain a unique information about the magnetic texture of the sample. For example, the curves shown in figures correspond to the initial stage of transformation of unidirectional texture (\bullet , 1) into uniaxial (\circ , 2) one. Strong distinctions in spin-flip neutron reflectivity $J(-, +)$ measured with another sample were found for opposite magnetization states. Non-trivial conclusions from these investigations will be discussed.

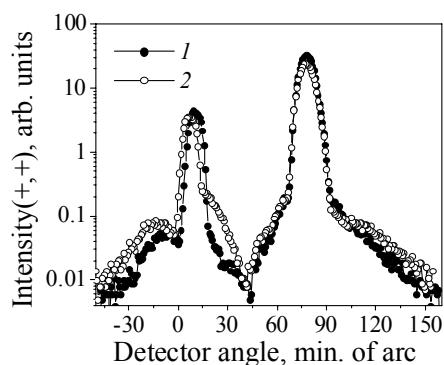


Fig. 1.

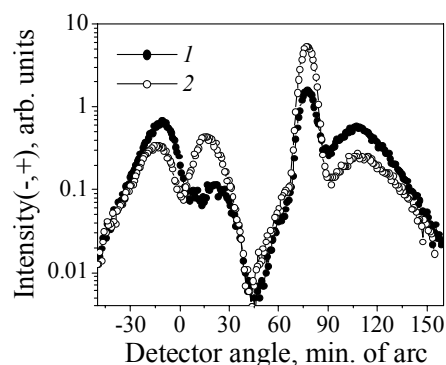


Fig. 2.

The work is partly supported by grant RFBR – 07-02-00290.

[1] A.V. Kovalev. *Journ. Magn. Magn. Mater.* **300**. 2006. P. e550.

[2] A.V. Kovalev. <http://zhurnal.ape.relarn.ru/articles/2007/036.pdf>

21PO-21-13

MULTI-CHANNEL HIGH-TC SQUID SYSTEM FOR BIO-APPLICATIONS

Hatsukade Y., Noda K., Masaki S., Yoshida S., Tanaka S.

Toyohashi University of Technology, 1-1 Hibarigaoka, Tenpaku-cho, Toyohashi, Aichi 441-8580, Japan

Regenerative medicine using incubated cells has lately drawn considerable attention. In order to monitor the activities of such cells noninvasively, we have studied bio-magnetic measurement system utilizing small high-Tc SQUIDs. Since high-Tc SQUIDs have uncontested magnetic sensitivity, there is possibility that only SQUIDs could detect small magnetic signals from the activities of incubated cells. So far, we fabricated small high-Tc SQUID magnetometers with size of 0.1 mm^2 for a high spatial resolution multi-channel high-Tc SQUID system. However, the magnetic field sensitivity of the SQUID was about $10 \text{ pT/Hz}^{1/2}$ and not enough. In this study, we designed directly-coupled-type high-Tc SQUID magnetometers with pick-up coil size of 1.5 mm^2 , which was comparable with the system lift-off distance of 1 to 1.5 mm. Figure 1 (a) shows the design of the three-channel high-Tc SQUID magnetometers. In order to improve the magnetic field sensitivity, the hole size of the SQUID ring was optimized as $80 \mu\text{m} \times 3.5 \mu\text{m}$. To increase the coupling factor between input coil and the SQUID ring, two slits were introduced on the SQUID ring as shown in the Fig. 1 (b). We fabricated the three-channel high-Tc SQUID magnetometers with $\text{YBa}_2\text{Cu}_3\text{O}_{7-x}$ thin film of about 200-nm thickness on bicrystal SrTiO_3 substrate with mis-orientation angle of 30 degree. The magnetic field noise level of the SQUID magnetometer in a magnetically shielded room was about $700 \text{ fT/Hz}^{1/2}$ as shown in Fig. 2. We installed the three-channel high-Tc SQUID magnetometers on the multi-channel high-Tc SQUID system. With the system, MCG of a normal 21-day-old rat was measured to evaluate the system performance. We could successfully measure the magnetic field distribution of QRST waves in the MCG above the rat heart by averaging the MCG signals about 100 to 130 times.

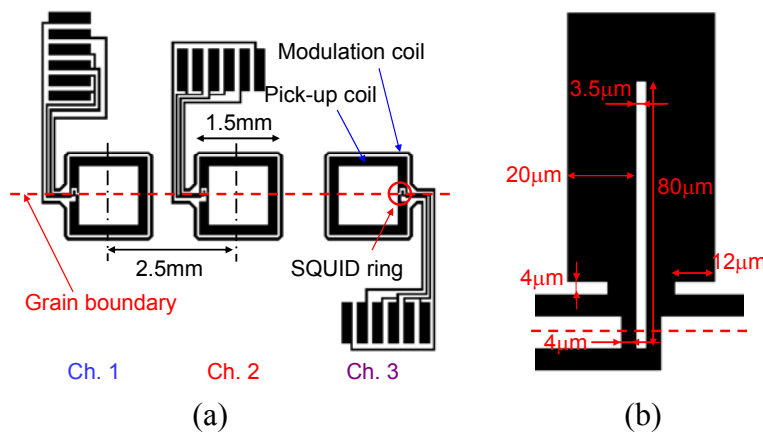


Fig. 1 Three-channel high-Tc SQUID magnetometers designed for bicrystal STO substrate. (a) Three-channel design. (b) Magnified view around the SQUID ring, which is directly coupled to pick-up coil.

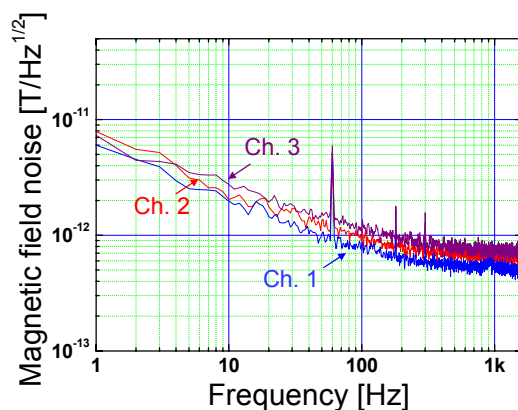


Fig. 2 Magnetic field noise spectra of three-channel high-Tc SQUID magnetometers. The averaged white noise level of these SQUID is about $700 \text{ fT/Hz}^{1/2}$.

21PO-21-14

INFLUENCE OF MAN-CAUSED FACTORS TO MAGNETIC PHASE MINERALIZATION IN BEE ONTHOGENESIS

Lomaev G.V., Bondareva N.V., Baykova E.N.

Izhevsk State Techic University, Studencheskaja st., 7, Izhevsk, 426069 Russia

A ponderomotive method of magnetic moment determination of an individual bee is developed. The method is as sensitive as SQUID- magnetometry. By means of the method and a device the bees growing under the conditions of hypo- and hypermagnetic fields and the increased Fe admission with feed were examined.

Under natural conditions, ferromagnetic phase in bee onthogenesis is registered at prepupa stage (10-11th day from the moment of eggs laying). Under the conditions of increased Fe admission with feed, the mineralization of ferromagnetic material starts at larva stage (8-9th day). Hyper-geomagnetic fields do not influence noticeably to the beginning of magnetic material formation in bee organism. For bees growing under hypo-geomagnetic field, the appearance of ferromagnetic phase is registered at pupa stage (12th day from the moment of eggs laying).

21PO-21-15

MODELLING PROCESSES OF REVERSE MAGNETIZATION OF REAL CRYSTALS

Vakhitov R.M.¹, Gareyeva Ye.R.¹, Vakhitova M.M.², Yumaguzin A.R.²

¹Bashkir State University, 450074, Ufa, ul. Frunze 32, Russia

²Ufa Institute of Russian State of Trade and Economics,
450086, Ufa, ul. Mendeleyeva 177/3, Russia

The processes of magnetization and reverse magnetization of magnetic materials are known to substantially influence the presence in them of defects of various kinds. Magnetic inhomogeneities originate on the defects, these inhomogeneities lingering on the defects during the sample's reverse magnetization and, ultimately, making a contribution to the value of its coercive force. In spite of the fact that certain notions of these processes have been established in the research community active in this area, many of its aspects are yet to be investigated, specifically, the behaviour of magnetic inhomogeneities localized on defects in variable magnetic fields.

The paper investigates the structure and propoerties of magnetic inhomogeneities originating upon defects in cubic ferromagnets of finite dimensions. It is assumed that the sample is a (011)-oriented slab with uniaxial anisotropy induced along [011]. A theoretical analysis of the domain structure in these slabs has shown [2], that in the vicinity of the spin-reorientational phase transition (SRPT) there arise solutions of the relevant Euler-Lagrange equations corresponding to 0-degree domain walls (0°DWs). The solutions thus obtained largely correspond to the distribution of magnetization in the area of the defects of the slab-like magnetic inclusion type which enables one to describe the nucleation processes on defects at SRPT of the 1st kind which agree well with the experimental data [3]. Similar solutions arise when a magnetic field is present which gives one ground for modelling reverse magnetization processes of the defect-containing crystals under study. The calculations involved the variational

approach which used the solutions of the 0°DW type as trial functions that describe the reverse-magnetization domains fixed upon the defects. Correspondingly, the functional, which represents the total energy of magnetic inhomogeneities of the (011) slab, is minimized with due account taken of the slab's demagnetizing fields and of the presence of defects therein. It follows from the results of the numerical realization of the variational problem that 0°DW s as stable formations can originate in the defect area only at certain values of the parameters of the slab, defect and external field. The stability area of 0°DW s as far as the field is concerned is limited by their two critical values: at certain values 0°DW s diffuse, while collapse at others. The sample's coercive force was obtained from the analysis of the critical fields of 0°DW existence. The dependence of the coercive force on the defect parameters agrees well with similar results obtained in other models [4]. The calculations show however, that the model under consideration possesses certain advantages over others since it allows taking into account the sample's geometric dimensions and, in particular, determining the dependence of coercive force on the slab thickness.

- [1] S. Tikadzumi, Fizika ferromagnetizma. Magntinye kharakteristiki i prakticheskiye primeneniya. M.: Mir, (1987) 419 s.
- [2] R.M. Vakhitov, Ye.R. Gareyeva, M.M. Vakhitova, FNT, Vol. 84, 1 (2006) 277.
- [3] V.K. Vlasko-Vlasov, M.V. Indenbom, ZhETF, **86** (1984) 1084.
- [4] H. Kronmuller, Phys.Stat.Sol, **144** (1987) 385.

21PO-21-16

HEATING IN AN ALTERNATING MAGNETIC FIELD DUE TO NON-EQUILIBRIUM MAGNETIZATION

Polyanskiy V.A., Tyatyushkin A.N.

Institute of Mechanics, Moscow State University, Michurinskiy Pr., 1, Moscow 119192, Russia

The interest to investigation of heating of magnetizable media in alternating magnetic fields is caused by the possibility of using the magnetic hyperthermia as a method of cancer treatment [1]–[2]. In treating with this method, magnetic particles dispersed in a liquid (i.e., magnetic fluid) are introduced into a treated carcinoma, and the latter is affected by an alternating magnetic field. The carcinoma saturated with magnetic particles is magnetized and, since the magnetization is non-equilibrium, heated. As the result, the temperature of the carcinoma increases up to the value at which the cancer cells perish.

When the temperature of the magnetic particles reaches some critical value (Curie point), the state of the particles changes from ferromagnetic or ferrimagnetic to paramagnetic. As the result, the spontaneous magnetization of the particles becomes equal to zero. Transition to the paramagnetic state is proposed to use for self-regulation of the magnetic hyperthermia [3]–[5]. Heating in the alternating field is implied to stop immediately when the transition is accomplished. Consequently, if the particles of the magnetic fluid used for magnetic hyperthermia have the critical temperature optimal for hyperthermia (42–45°C), then there is no necessity of additional equipment for maintaining the constant temperature.

However, the magnetic relaxation (due to which the magnetization is non-equilibrium) and, consequently, heating take place within paramagnetic particles too [6]. Besides, if paramagnetic particles are not spherical, then the Brownian magnetic relaxation takes place within a dispersion of those particles in a viscous liquid.

The goal of the present work is to study the influence of the transition to the paramagnetic state on the heating in alternating magnetic fields and, in particular, to investigate

the influence of the weak heating due to non-equilibrium magnetization of the dispersion of paramagnetic particles.

We model the magnetic hyperthermia using the equations describing heating of a magnetizable spherical body (carcinoma saturated with magnetic particles) surrounded by an unbounded medium (healthy tissue) with a given temperature at infinity in an applied alternating uniform magnetic field. The magnetic susceptibility and magnetic relaxation time depend on the temperature. The heat generation power density due to non-equilibrium magnetization in an alternating magnetic field of a given frequency decreases with the temperature, and there is some critical temperature at which the heat generation power density is small, and its rate of decrease experiences a jump. The frequency of the magnetic field oscillation and electric conductivity are regarded as so small that the heating due to eddy currents and non-equilibrium electric polarization can be neglected and the ferrohydrodynamic approximation [7] is valid. The influence of the induced magnetic field is neglected. The dependence of the heat generation power density on the temperature is approximated by a piecewise linear function with a fracture at the critical point. The steady temperature distribution within and outside the sphere is found.

The present work is supported by the RFBR grants 08-01-00026 and 07-01-00026.

- [1] R.E. Rosensweig, *J. Magn. Magn. Mat.*, **252** (2002) 370.
- [2] W. Andra et al., *J. Magn. Magn. Mat.*, **194** (1999), 197.
- [3] M.B. Lilly, I.A. Brezovich and W.J. Atkinson, *Radiology*, **154** (1985) 243.
- [4] A.A. Kuznetsov et al., *Eur. Cells Mater.*, **3** Suppl. 2 (2002) 75.
- [5] M. Bettge, J. Chatterjee and Y. Haik, *BioMagnetic Research and Technology*, **2** (2004) 4.
- [6] S.V. Vonsovsky, *Magnetism* (John Wiley, New York, 1974), Vol. 1.
- [7] R.E. Rosensweig, *Ferrohydrodynamics* (Cambridge University Press, Cambridge, 1985).

21PO-21-17

MESSBAUER STUDY OF IRON MINERALS FORMED BY DISSIMILATORY BACTERIUM

*Chistyakova N.I.¹, Rusakov V.S.¹, Koksharov Yu.A.¹,
Zavarzina D.G.², Greneche J.-M.³*

¹Faculty of Physics, M.V. Lomonosov Moscow State University,
Leninskie gory, 119991 Moscow, Russia

²Institute of Microbiology, Russian Academy of Sciences, Prospect
60-letiya Oktyabrya 7/2, 117312 Moscow, Russia

³Laboratoire de Physique de l'Etat Condense, UMR CNRS 6087
Universite du Maine F72085 Le Mans Cedex 9, France

A microbiological pathway of mineral formation has been intensively studied last years. One of the possible ways of iron-bearing mineral formation is their extracellular precipitation induced by dissimilatory iron-reducing bacteria. Thermophilic anaerobic iron-reducing bacterium (strain Z-0001) was isolated from the ferric sediments of hot springs Stolbovskie (T = 60 – 65°C and pH = 6.8 – 7.0), Kunashir Island. Bacterium used amorphous Fe(III)-hydroxide as an electron acceptor, and acetate (CH₃COO⁻) as an electron donor for the anaerobic growth.

The kinetics of iron mineral formation by strain Z-0001 was investigated earlier by Moessbauer spectrometry at room temperature [1-2]. Both the values of pH and redox reaction potential Eh of the medium were taken into account in our studies as well as X-ray analysis and

electron microscopy data. The electron paramagnetic resonance (EPR) measurements were also performed.

For more detailed study of bacterium synthesis the measurements of some samples at low temperature (77 K and 4.2 K) and at 10 K in presence of an external magnetic field (6 T) were carried out. Moessbauer spectra of some obtained samples recorded at 77 K are shown in Fig. 1. We have found that magnetic structure of investigated amorphous Fe(III)-hydroxide (AFH) can be described as two rather randomly oriented and antiparallel magnetic lattices, suggesting that AFH sample consists of either a disordered packing of Fe tetrahedral and octahedral units as an amorphous, or a random packing of small ferrimagnetic clusters. Moessbauer spectra of samples obtained in exponential phase of bacterium growing are consistent with the presence of superparamagnetic nanoparticles. Room temperature Mossbauer study has shown that after 5 days from beginning of the experiment the relative content of magneto-ordered phase (a mixture of magnesioferrite $MgFe_2O_4$ and magnetite Fe_3O_4) was 100 % and did not change in stationary phase of strain growth in future.

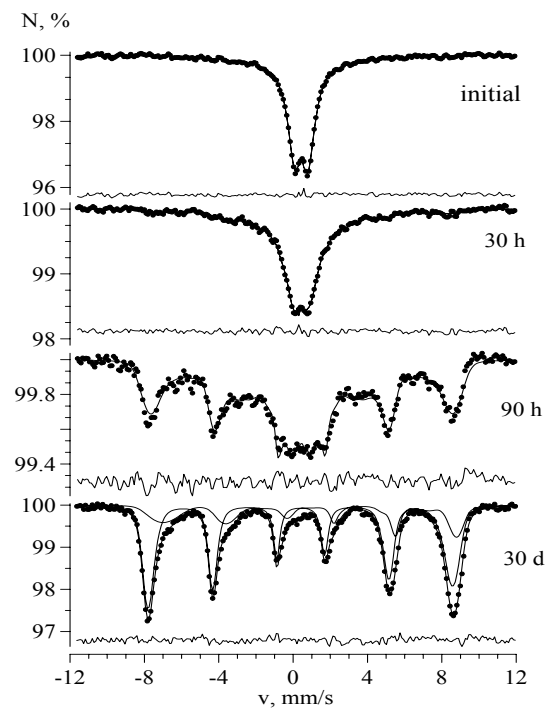


Fig. 1. Moessbauer spectra recorded at 77 K of the samples formed by strain Z-0001 under different incubation time.

[1] N.I. Chistyakova, V.S. Rusakov, D.G. Zavarzina, S.V. Kozerenko, *The Physics of Metals and Metallography* **92** (2001) S138.

[2] N.I. Chistyakova, V.S. Rusakov, D.G. Zavarzina, A.I Slobodkin., T.V. Gorohova, *Czechoslovak J. of Physics* **50** (2005) 781.

21PO-21-18

EXPERIMENTAL STUDY ON THE HEMOLYTIC EFFECT OF MAGNETIC AND ELECTROMAGNETIC EXPOSURE IN ANIMAL BLOOD – ACUTE AND CHRONIC EXPOSURES

Nadejde C., Creanga D.E., Comaniciu E., Tufescu F.M.

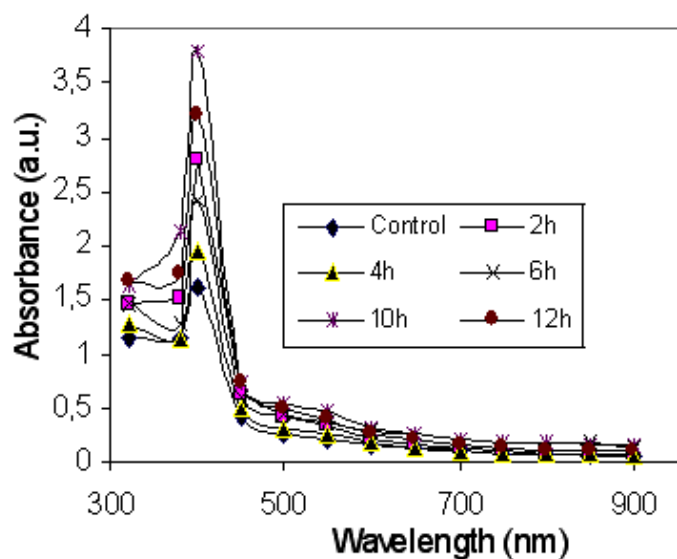
Al. I. Cuza University, Faculty of Physics, 11A Carol I Blvd., RO-700506, Iasi, Romania

Considering the risk of biological effects caused by enhanced electromagnetic pollution, even the human exposure is not always intense or/and continuous, it seems to be of actual interest to get any new data regarding the putative effects of electromagnetic exposure [1-3].

The purpose of the study was to investigate comparatively the influence of non thermal microwaves and static magnetic field upon red blood cells. Spectral assay was carried out to evidence the hemolytic effect induced following different types of *in vitro* electromagnetic and respectively magnetic exposures in animal blood samples (horse and bovine). Acute exposures to microwaves were carried out for 2-4-6-8-10-12 hours, using laboratory generator based on horn antenna (10.75 GHz/ 1.0 mW/cm²) while chronic exposures of 30 min duration with 30 min

break totalizing 2-4-6-8 hours were also carried out in the same controlled environmental conditions of temperature, humidity and illumination.

Similarly, in the case of magnetic exposure, permanent magnets of about 20 mT (as measured with Hall probe magnetometer) were used for the same time durations. The hemoglobin spectra were used to measure the hemolysis extent in the experimental blood serum samples, prepared by 30 min incubation at 37°C within a water bath and further centrifugation at 3,500 cycle/min for 10 min. Complementary data were provided by measurements of total protein content in blood serum. Statistic significance of the spectrophotometric investigation was ensured by repeated measurements and ANOVA statistic analysis.



In all exposed samples the hemoglobin level was found higher than in the control samples, probably following the increasing of free radical concentration, able to induce molecular damage in the erythrocyte membrane that can further result in hemolysis phenomenon. The differences noticed between the four types of blood serum samples were discussed accordingly to literature reports. The biomedical significance of free radical detection in living tissues under various external constraints is directly related to their role in the impeding of the human system development, in maturation delay and enhancing leukemia incidence.

In all exposed samples the hemoglobin level was found higher than in the control samples, probably following the increasing of free radical concentration, able to induce molecular damage in the erythrocyte membrane that can further result in hemolysis phenomenon. The differences noticed between the four types of blood serum samples were discussed accordingly to literature reports. The biomedical significance of free radical detection in living tissues under various external constraints is directly related to their role in the impeding of the human system development, in maturation delay and enhancing leukemia incidence.

[1] K. Kinoshita, T.Y. Tsong, *Proc. Natl. Acad. Sci. USA, Biochemistry*, **5(74)** (1977) 1923.

[2] St. F. Cleary, L.M. Liu, F. Garber, *Bioelectromagnetics*, **6(3)** (1985) 313.

[3] S.L. Tsui, A.K. Lee, S.K. Lui, R.T. Poon, S.T. Fan, *Hepatogastroenterology*, **50** (2003) 526.

21PO-21-19

MAGNETIC PROPERTIES OF BACTERIA-PRODUCED Fe-S NANOPOWDERS

Gordeev S.N.¹, Watson J.H.P.², de Groot P.A.J.³

¹Department of Physics, University of Bath, Bath, UK

²School of Physics and Astronomy, University of Southampton, Southampton, UK

Magnetic nanoparticles are the subject of increasing interest due to their unique properties as well as their technological applications. However, difficulties in a large-scale fabrication of such fine powders hamper the utilisation of nanoparticle magnetism in technical applications. Recently a low cost and technologically simple technique of producing nanoscale magnetic particles using sulfate-reducing magnetic bacteria was proposed [1]. This new material was found to be strongly magnetic at room temperatures and an excellent adsorbent for many toxic and radioactive materials, and heavy metals. Individual nanoparticles have the size in the range of 35-130nm and consist of greigite Fe₃S₄ and mackinawite Fe_{1+x}S. We have performed

magnetisation studies of bacteria produced Fe-S materials in the temperature range of 4.2-300K at fields up to 12T using SQUID and Vibration Sample magnetometers. It was found that their magnetic properties can be described as a sum of two contributions, one of which is ferromagnetic and the other is superparamagnetic. The first contribution apparently originates from individual nanoparticles and small clusters (<0.5 μm) and the other one from clusters of larger size. The supermagnetic nanoparticles have a wide distribution in size; their magnetisation cannot be described in terms of Neel-Brown model. Relaxation of magnetisation was found to be weak and governed by thermal processes. Freeze-dried powders demonstrated good stability of their magnetic characteristics for at least 1 month. These properties of the Fe-S powders in conjunction with the simple technological process and low-production costs make them very attractive for a wide range of applications, including cleaning up of contaminated water and soil, recovery of precious metals and many others.

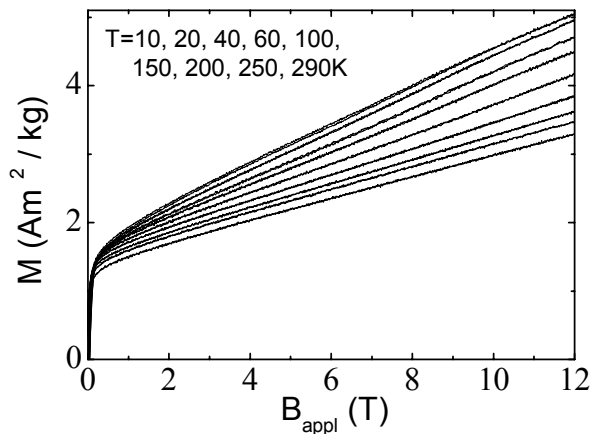


Fig. 1. Field dependence of magnetisation for different temperatures.

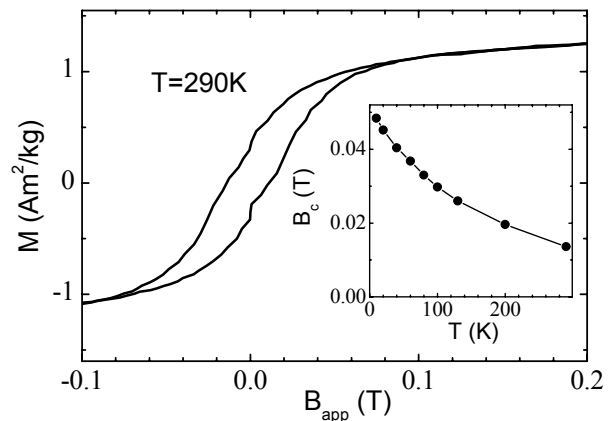


Fig. 2. Hysteresis loop and temperature dependence of the coercive field (inset).

[1] J.H.P. Watson, D.C. Ellwood, C.J. Duggleby, *Miner. Eng.* **9** (1996) 973.

21PO-21-20

DOMAIN STRUCTURE REVERSIBLE RECONSTRUCTION OF AMORPHOUS FERROMAGNETIC BY WATER MOLECULES WEAK ADSORPTION

Zubov V.E., Kudakov A.D., Levsyin N.L., Mezenkov N.A.

Faculty of Physics, M.V.Lomonosov Moscow State University, Leninskie Gory, Moscow, 119992, Russia

Influence of water molecules reversible adsorption on domain structure and domain wall structure in amorphous Fe-rich ferromagnetic samples is investigated by magneto-optical micro-magnetometer at room temperature. The investigated samples of composition $\text{Fe}_{76,5}\text{Cu}_1\text{Nb}_3\text{Si}_{13,5}\text{B}_6$ were obtained by spinning technique. Before amorphization, the melt was

subjected to a special time-temperature treatment to obtain a uniform distribution of doping elements and, as a result, an improvement of the soft magnetic properties of the alloy. The samples were 30 μm thick, 0.55 mm wide, and 15-20 mm long. Initial magnetic structure consisted of two domains divided by 180-degree domain wall, which was parallel to the long side of the samples. The efficient domain wall width at the surface and the coercive force of the domain wall were determined using magneto-optical technique and appeared to be equal to ~ 10 μm and 1 A/m, respectively. Magnetic saturation induction of the samples measured by vibration sample magnetometer was 1,2 T. Two series of samples were used. Series 1 was kept in desiccator at low humidity, series 2 was kept in open vessel. Investigation shows that domain structure of the samples of series 1 and 2 is distinguished in vacuum. Domain structure of the series 1 samples is invariable in vacuum and in atmosphere of water vapor. Domain wall width is invariable too. Magnetic susceptibility of the sample becomes 30% less after flooding of water vapor into the vacuum cell with the sample up the pressure $0.5p_s$ (p_s - the pressure of saturated vapor). This effect we observed earlier [1]. The new effect is found during investigation of the series 2 samples. Domain structure of the samples significantly changes in vacuum: instead one 180-degree domain wall several domain walls appear which are oriented with angle 45° to the long side of the sample. This effect is completely reversible. Flooding of water vapor into the vacuum cell with the sample leads to reconstruction of initial domain structure.

Another new effect is found during direct measuring domain wall width by magneto-optical method on the surface of the series 2 samples: domain wall width in vacuum is 35% bigger (13.5 μm) than in atmosphere of water vapor (10 μm).

Our model of discovered effects predicts the appearance of surface perpendicular magnetic anisotropy due to desorption of water molecules for series 2 samples in vacuum. In order to control this suggestion the investigation of magneto-optical polar Kerr effect on the surface of amorphous samples is conducted. Polar Kerr effect is proportional the normal component of magnetization on the sample surface. Polar Kerr effect was not detected. Valuation shows that sensitivity of magneto-optical measuring must be greater by order for registration of polar Kerr effect.

This work was supported by the Russian Foudation for Basic Research (grant № 07-02-00892).

[1]. V.E.Zubov, A.D.Kudakov, N.L.Levsyin, T.S.Fedulova. Sensors and Actuators A 91 (2001) 214-217.

21PO-21-21

DEPENDENCE OF FOS CAPACITANCE ON HBM-ESD AFFECTED TMR HEAD

Jutong N.¹, Sompongse D.², Rakpongsiri P.² and Siritaratiwat A.^{1,3}*

¹Department of Electrical Engineering, Khonkaen University, Khon Kaen, 40002, Thailand

²Western Digital Company, BangPa-In Industrial Estate, Ayuthaya, 13160, Thailand

³Industry/University Cooperation Research Center in HDD Component,
Faculty of Engineering, Khon Kaen, 40002, Thailand

* e-mail: apirat@kku.ac.th

Electrostatic discharge (ESD) effect on GMR recording heads have been reported for the major cause of head failure [1]. Since the information density in hard-disk drive has dramatically increased, the GMR head will be no longer in use [2]. The tunneling magnetoresistive (TMR)

read heads are initially introduced for a 100 Gbit/in² density or more. Although the failure mechanism of ESD in GMR recording head has not been explicitly understood in detail, the study to protect this effect has to be undergone. As far as the TMR head has been commercially started, the ESD effect is closely aware.

This is the first report on the TMR equivalent circuit in order to evaluate the ESD effect. A standard human body model (HBM) is discharged across R+ and R- pads where the capacitance of flex on suspension (FOS) are varied. It is intriguingly found that electrical characteristic of TMR head during discharge period depends on discharge position. This may be explained in term of asymmetry impedance of TMR by analyzing adapted Thevenin's theory. The effect of FOS component on TMR recording head is also discussed.

This research is funded by the Industry/University Cooperative Research Center in HDD Component (I/U CRC in HDD Component), Khon Kaen University, and the National Electronics and Computer Technology Center (NECTEC) under the National Science and Technology Development Agency (NSTDA), Thailand. Authors would like to acknowledge this work to staff of Western Digital Company (BangPa-In), Thailand, for their provision of samples, facilities and technical discussion.

- [1] A. Siritaratiwat, N. Jutong and C. Puprichitkul, *J Magn Magn Mater.*, **272-276** (2004) 2307.
 [2] F. Lui and et al. *IEEE Trans Magn.*, **42** (2006)

21PO-21-22

ESD AFFECTED GMR HEAD DETECTION BY USING MACHINE MODEL: WAVELET TRANSFORM TECHNIQUE APPROACH

Suwannata N.¹, Sompongse D.², Rakpongsiri P.² and Siritaratiwat A.^{1,3}*

¹Department of Electrical Engineering, Khonkaen University, Khon Kaen, 40002, Thailand

²Western Digital Company, BangPa-In Industrial Estate, Ayuthaya, 13160, Thailand

³Industry/University Cooperation Research Center in HDD Component,
 Faculty of Engineering, Khon Kaen, 40002, Thailand

*e-mail: apirat@kku.ac.th

A common electrical signal of defective recording head is normally captured by commercial instrument but an occurrence of undesired glitch on this signal is impossibly understood. Moreover, it is difficultly detected due to its short duration. It represents instability of recording head characteristic and it can cause an ESD event which degrades the head performance [1]. This report is originally proposed the wavelet transform technique using the 4th Daubechies order to detect the glitch on a magnetic recording head signal in time-domain [2]. It is found that the glitch is occurred when the ESD level of machine model (MM) on giant magnetoresistive (GMR) heads in ranges of 6-9 V. The electrical test parameter and scanning electron microscope (SEM) photo of recording heads show no change in reader sensor. However, the parameter and SEM results are clearly found the visible GMR damage when the MM-VESD is 10 V. The glitch in magnetic response signal of GMR head is occurred when the ESD voltage (VESD) is increased. Therefore, the wavelet transform technique can be a novel instrument to forecast the GMR degradation due to Machine-Model ESD effect.

This research is funded by Thailand Research Fund, Grant No. RMU4880033. Many constructive suggestion and facility provision are sincerely dedicated to Western Digital (Bangpa-In), Co. Ltd., Thailand.

- [1] Mizoh Y, Nakano T, Tagashira K, Nakamura K and Tatsuya Suzuki, *J. Electrostatics.*, **64** (2006) 72.
- [2] Suwannata N and Siritaratiwat A, *Proc. of the 22nd Int. Conf. on Circuits/System, Computer and Communications (ITC-CSCC), Busan, Korea, 8-11 July 2007*, vol. 2 pp 909.

21PO-21-23

CONFINED - CHALCOGENIDE PHASE - CHANGE MEMORY WITH THIN METAL INTERLAYER FOR LOW RESET CURRENT BY FINITE ELEMENT MODELING

Harnsoongnoen S.¹, Siritaratiwat A.^{1,2} and Sa-ngiamsak C.^{1,2}*

¹Department of Electrical Engineering, Khon Kaen University, Khonkaen, 40002, Thailand

²Industry/University Cooperation Research Center in HDD Component, Faculty of Engineering, Khonkaen, 40002, Thailand

* e-mail : chiranut@kku.ac.th

Phase-change random access memory (PRAM) is a promising candidate for the next generation of Non-volatile memory (NVM) due to its fast write speed, non-destructive readout, superb scalability, and great compatibility with current silicon-base mass fabrication [1]. Nevertheless, the setback of PRAM is a high reset-current, typically higher than 1mA [2]. One of most important solutions for reset-current reduction is to optimize the structure of PRAM cell, edge contact cell and μ -trench architecture. However, the fabrication of these memory cells is much complicated and the area of these cells is larger than that of the corresponding normal-bottom-contact (NBC) cell. This is the first time report on the confined-chalcogenide phase-change memory with thin metal interlayer (CC-TMI) for low reset-current and less complicated fabrication. The comparison of conventional normal-bottom-contact with thin metal interlayer (NBC-TMI) [3] and proposed CC-TMI PRAM cells is studied by using 2-D Finite Element Modeling. It is intriguingly found that the reset operation current of the CC-TMI cell is much lower than that of the traditional NBC-TMI cell in an order of $>100 \mu\text{A}$. This may be explained that a CC-TMI programming volume is smaller than that of NBC-TMI cell. The effect of quench speed on the memory cell is also discussed.

This project is financially funded by I/U CRC in HDD Component, Khon Kaen University and the National Electronics and Computer Technology Center in an association with the Thailand Microelectronics Center (TMEC).

- [1] Kim Y, Kim H and Yoon S, *Appl.Phys.Lett.*, **89**, (2006) 102.
- [2] Lai S, *Proc. of IEEE International Electron Device Meeting (IIDEM)*, Washington D.C., USA, 8-10 December 2003, 10.1.1.
- [3] Yi J and et al, *Proc. of IEEE International Electron Device Meeting (IIDEM)*, Washington D.C., USA, 8-10 December 2003, 37.3.1.

22 June Sunday

10:00-11:30

plenary lectures

22PL-A

22PL-A-1

ORIGIN OF FERROMAGNETISM IN MAGNETICALLY DOPED SEMICONDUCTORS

Dietl T.

Institute of Physics, Polish Academy of Sciences, PL 02 668 Warsaw, Poland

Institute of Theoretical Physics, University of Warsaw, PL 00681 Warsaw, Poland

The demonstrated and foreseen functionalities of ferromagnetic semiconductors such as (Ga,Mn)As and p-(Cd,Mn)Te [1], have stimulated a considerable effort to develop semiconductor systems in which spontaneous magnetization would persist to above room temperature. Indeed, high temperature ferromagnetic features have been found in a number of semiconductors and oxides doped with various transition metals and rare earth elements or even in materials nominally undoped with magnetic elements. At the same time, it is becoming clear that the adequate characterization of these systems requires the application of advanced space-resolved and element-specific tools. On the theoretical side, it has been appreciated that conceptual difficulties of charge transfer insulators and strongly correlated disordered metals are combined in these materials with intricate aspects of heavily doped semiconductors and semiconductor alloys, such as Anderson-Mott localization, defect formation by self-compensation mechanisms, spinodal decomposition, and the breakdown of the virtual crystal approximation [2].

In this talk, after presenting the p-d Zener model that describes successfully (Ga,Mn)As and related systems, the progress in the understanding of the origin of high apparent Curie temperatures in diluted magnetic semiconductors and oxides will be described [3-6]. It will be shown that doping above the solubility limit allows one to fabricate a variety of magnetic nanocrystals embedded coherently into the semiconductor host. Importantly, shape and dimension, and thus blocking temperature of the magnetic particles, can be controlled by co-doping with shallow dopants and through growth parameters. Appealing functionalities of these multicomponent systems will be presented together with prospects for their applications.

[1] see, e.g., T. Dietl, H. Ohno, F. Matsukura, IEEE—Trans. Electr. Dev. **54** (2007) 945.

[2] see, e.g., T. Dietl, J. Phys. Soc. Jpn. **77** (2008) 031005, and references therein.

[3] T. Dietl, Nature Mat. **5** (2006) 673.

[4] H. Katayama-Yoshida, K. Sato, T. Fukushima, M. Toyoda, H. Kizaki, V. A. Dinh, P. H. Dederichs, phys. stat. solidi (a) **204** (2007) 15.

[5] S. Kuroda, N. Nishizawa, K. Takita, M. Mitome, Y. Bando, K. Osuch, and T. Dietl, Nature Mat. **6** (2007) 440.

[6] T. Dietl, J. Appl. Phys. **103** (2008) 07D111.

22PL-A-2

FERROMAGNETIC ORDERING IN DILUTE MAGNETIC MATERIALS WITHOUT FREE CARRIERS

Kikoin K.

School of Physics and Astronomy, Tel-Aviv University, Tel-Aviv 69978, Israel

The available experimental information and existing theoretical considerations about the nature of ferromagnetic ordering in dilute magnetic dielectrics (DMD) (mostly, oxides doped with transition metal ions) clearly demonstrate essential differences between these wide-gap materials and dilute magnetic semiconductors (DMS). This review summarizes the inherent features of DMD, which allow treating these materials as a separate family of dilute magnetic materials.

Unlike DMS, in the most of DMD with high Curie temperature T_C , the room-temperature ferromagnetism is apparently not related to high concentration of free carriers. These materials are characterized by extreme sensitivity to the growth and annealing conditions, and practically in all cases one may conclude that the indirect exchange between magnetic transition metal ions is mediated by complex defects involving oxygen vacancies, shallow impurities or other imperfections.

We review the experimental situation with materials, in which the role of magnetic inclusions is ruled out (II-VI oxides, TiO_2 , CeO_2 etc diluted with 3d impurities of iron group) and discuss in some details possible mechanisms of indirect ferromagnetic exchange specific for the wide gap materials. Among possible complex defects, which may mediate indirect ferromagnetic exchange between transition metal impurities in oxides, one may mention oxygen vacancies (both free and bound with impurities), defect magnetic polarons and bound excitons

22 June Sunday

12:00-13:30

15:00-17:00

oral session

22TL-A

22RP-A

**“Diluted Magnetic
Semiconductors
and Oxides”**

22TL-A-1

MAGNETIC EXCITATIONS IN FERROMAGNETIC SEMICONDUCTORS

Furdyna J.K.

University of Notre Dame, Department of Physics, Notre Dame, IN 46556, USA

The study of magnetic excitations in ferromagnetic (FM) semiconductors can tell us a great deal about spin dynamics in these new systems. For specificity we will describe experiments carried out on FM semiconductor GaMnAs as representative examples. Magnetic excitations in GaMnAs have been studied by two complementary approaches -- by frequency-domain techniques, such as ferromagnetic resonance (FMR) [1]; and by optical real time techniques, such as time-resolved magneto-optical Kerr effect (MOKE)[2,3]. Using the FMR approach, multi-mode spin wave spectra have been observed, whose analysis provides new information on magnetic anisotropy (including surface anisotropy), distribution of magnetization in the GaMnAs film, dynamic surface spin pinning (derived from the surface anisotropy), and the value of the exchange stiffness constant D -- a quantity that is not accessible by other techniques. A very different approach to the problem of spin dynamics (and, it should be emphasized, to the *manipulation of magnetic phase transition* in GaMnAs [4]) is the study of photoinduced collective magnetization precession using time-resolved MOKE. Here the observed coherent oscillations provide a measure of *ultrafast* changes in the in-plane orientation of magnetization in a given ferromagnetic domain due to laser induced transient changes of the magnetic anisotropy of GaMnAs. This approach provides real-time confirmation of the properties of spin excitations observed by the frequency-domain FMR-like measurements already mentioned. What is especially exciting about these real-time studies is that the photo-induced magnetization changes are extraordinarily fast, with speeds that are characteristic of semiconductor processes, thus illustrating a combination of magnetism and semiconductor physics that is unique to magnetic semiconductors.

[1] X. Liu, Y. Y. Zhou and J.K. Furdyna, *Phys. Rev. B* **75** (2007) 195220 (2007).

[2] D. M. Wang, Y. H. Ren, X. Liu, J. K. Furdyna, M. Grinsditch and R. Merlin, *Phys. Rev. B* **75** (2007) 233308

[3] J. Qi, Y. Xu, N. H. Tolk, X. Liu, J. K. Furdyna and I. E. Perakis, *Appl. Phys. Lett.* **91** (2007) 112506.

[4] J. Wang, I. Cotoros, K. M. Dani, X. Liu, J. K. Furdyna and D. S. Chemla, *Phys. Rev. Lett.* **98** (2007) 217401.

22TL-A-2

MANGANESE IN GERMANIUM

*Ing-Song Yu*¹, *Devillers T.*¹, *Tardif S.*², *Barski A.*¹, *Bayle-Guillemaud P.*¹,
*Bellet-Amalric E.*¹, *Cherifi S.*², *Cibert J.*², *Jamet M.*¹,

¹INAC, CEA Grenoble, 17 avenue des Martyrs, 38054 Grenoble Cedex, France

²Institut Neel, CNRS-UJF, BP166, 38042 Grenoble, France

Making ferromagnetic a semiconductor compatible with mainstream Silicon technology, like Germanium, is highly desirable. Following early reports on Ge_{1-x}Mn_x as a homogeneous diluted magnetic semiconductor [1], recent reports have focused on a strongly inhomogeneous

incorporation of Mn in Germanium. A dramatic example is that of Mn-rich self-organized nanocolumns. These nanocolumns may run throughout the Germanium layer, with a structure matching that of the matrix. They feature a large ferromagnetic interaction, and strongly influence the magneto-transport properties of the whole layer, with *e.g.* a strong anomalous Hall effect (Hall angle as high as 0.6 rad at low temperature) persisting up to above room temperature [2].

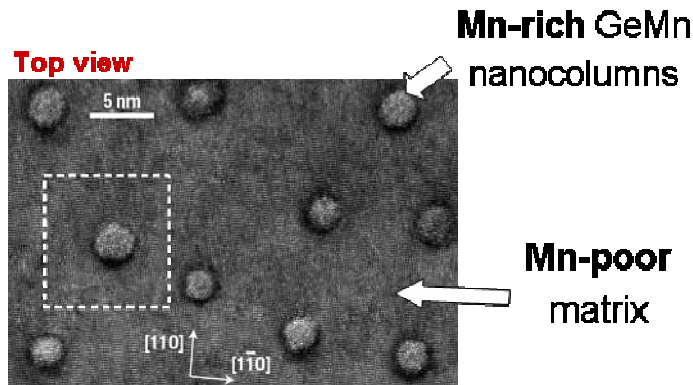


Fig.: Transmission Electron Microscopy image of a 80 nm-thick $\text{Ge}_{0.94}\text{Mn}_{0.06}$ epitaxial layer - High resolution plane view along [001].

In this talk we will discuss the influence of the growth conditions (growth temperature, Mn concentration, substrate morphology...) on the nature of the Mn rich inclusions (nanocolumns vs. Ge_3Mn_5 clusters) and on the morphology of the Mn rich nanocolumns. We will show how structural properties of our GeMn layers strongly influence their electronic and magnetic properties. Moreover we will discuss the role of a very thin Mn oxide layer which can be deposited - intentionally or not - on the surface of our GeMn material.

[1] Y. D. Park *et al.*, Science **295**, 651-654 (2002).

[2] M. Jamet *et al.*, Nature Materials **5**, 653 (2006).

22TL-A-3

ISOTOPICALLY ENGINEERED SI AND GE FOR SPINTRONICS AND QUANTUM COMPUTATION

Shlimak I.

Jack and Pearl Resnick Institute of Advanced Technology, Physics Department, Bar-Ilan University, Ramat Gan 52900, Israel

Si, Ge as well as SiGe structures are the most promising semiconductor materials for Spintronics and Quantum Computation due to the fact that in both crystals only one isotope (^{29}Si among three stable Si isotopes and ^{73}Ge among five stable Ge isotopes) has nuclear spin. As a result, isotopic engineering of Si and Ge permits to control the density of nuclear spins and vary the spin coherence time, a crucial parameter in spintronics and quantum computing where nuclear spin is used as a qubit.

The first part of the talk is devoted to the nuclear magnetic resonance study of ^{73}Ge nuclear spin decoherence in Ge single crystals with different abundance of the ^{73}Ge isotope. It

was observed that the slow component of the dephasing process is elongated with depletion of Ge crystal with isotope ^{73}Ge which is encouraging for application of this material in Ge- and SiGe-based structures for a nuclear spin-based quantum computers (NSQC). The second part of the talk is devoted to the development of a well-known model of NSQC based on using the nuclear spin of ^{31}P impurity atoms in a ^{28}Si matrix as qubits. We discuss a new method of placing ^{31}P atoms in a ^{28}Si layer with nanoscale precision which is based on neutron-transmutation-doping of isotopically engineered Si and Ge. In the proposed structure, interqubit entanglement is due to indirect interaction of ^{31}P nuclear spins with electrons localized in a ^{28}Si quasi-one-dimensional nanowire which allows one to control the coupling between distant qubits. The proposed method enables one to fabricate Ge- and Si-based structures for spintronics on the basis of the present-day nanolithography.

22TL-A-4

MAGNETO-GYROTROPIC PHOTOGALVANIC EFFECTS IN SEMICONDUCTOR QUANTUM WELLS

Ganichev S.D.

Terahertz Center, University of Regensburg, 93040 Regensburg, Germany

We present experimental and theoretical studies of photocurrents induced by intrasubband and intersubband optical transitions in semiconductor quantum well structures in the presence of an in-plane magnetic field. We discuss spin-related mechanisms of these magneto-gyrotropic photogalvanic effects (MGE) [1] comprising the spin-galvanic effect [1] induced by the Larmor precession and the photocurrent caused by the zero-bias spin separation [2]. Microscopic mechanisms of these phenomena are based on the spin-orbit coupling which provides a versatile tool to generate and to manipulate the spin degree of freedom in low-dimensional semiconductor structures. We show that the photocurrent is caused by the asymmetry of photoexcitation and/or relaxation processes. In general both the zero-bias spin separation and the spin-galvanic effect do not require an application of an external magnetic effect and for some mechanisms even light. However, they have been demonstrated and are most intensively studied applying MGE technique. Magneto-gyrotropic photogalvanic effects are observed in GaAs, InAs, SiGe and GaN low dimensional structures at free-carrier absorption of terahertz radiation as well as at intersubband absorption of the mid-infrared light. The results are well described by the phenomenological description based on the symmetry. Several applications of MGE will also be discussed, in particular, we analyze spin splitting of subbands in k-space due to bulk inversion asymmetry (BIA) and structural inversion asymmetry (SIA) in QWs of various crystallographic orientations.

Support by the DFG is acknowledged.

[1] S.D. Ganichev and W. Prettl, *Intense Terahertz Excitation of Semiconductors* (Oxford University Press, Oxford 2006).

[2] S.D. Ganichev, V.V. Bel'kov, S.A. Tarasenko, et al., *Nature Physics* **2**, 609 (2006).

22TL-A-5

PURE SPIN PHOTOCURRENTS IN SEMICONDUCTOR STRUCTURES

Tarasenko S.A.

A.F. Ioffe Physico-Technical Institute, 194021 St. Petersburg, Russia

The pure spin current of free carriers, electrons or holes, can be considered as a counterflow of the spin-up and spin-down particles. The pure spin current is accompanied by no charge current, because electric currents contributed by the spin-up and spin-down particles cancel each other, but leads to the spatial spin separation and, in particular, to the accumulation of opposite spins at the opposite edges of the sample.

Here, we show that pure spin currents can readily be injected in semiconductor structures by optical excitation with linearly polarized or even unpolarized light. We present the microscopic description of the effect for (i) interband optical transitions in undoped quantum wells as well as for (ii) direct intersubband and (iii) indirect intrasubband (Drude-like) transitions in n -doped quantum well structures [1]. We also demonstrate that pure spin currents emerge in quantum wells as soon as the electron gas is simply driven out of thermal equilibrium with the crystal lattice. The theoretical results are compared with recent experimental observations.

The pure spin currents injected in semiconductor quantum wells by direct interband or intersubband optical pumping are contributed by two microscopic mechanisms of different origins. The first mechanism is linked to the spin-sensitive selection rules for the optical transitions together with the spin splitting of the energy spectrum, which is linear in the wave vector \mathbf{k} . The second contribution comes from linear-in- \mathbf{k} terms in the matrix elements of the optical transitions. The above mechanisms lead to different polarization and spectral dependencies of the pure spin currents allowing one to distinguish between them in experiments. Under the intrasubband excitation, the dominant contribution to the pure spin photocurrent comes from spin-dependent asymmetry of the electron scattering by phonons or static defects accompanying the free-carrier absorption.

Experimentally, the spatial separation of electron spins caused by the spin photocurrent was first observed in (110)-oriented GaAs quantum well structures at room temperature by using the spatially resolved pump-probe technique [2]. The pure spin current caused by the free-carrier absorption can also be revealed by the conversion into a measurable electric current applying an external magnetic field, which polarizes electron spins and lifts the cancellation of the partial electron fluxes in the spin-up and spin-down subbands [3].

In addition to the spin, free carriers in solid states can be characterized by another internal property, e.g., by a valley index in multi-valley semiconductors. Thus, one can consider pure valley-orbit currents where the role of spin-up and spin-down states is replaced by the valley index. In pure valley-orbit currents, electrons in different valleys travel in different directions so that the net charge current vanishes.

[1] S.A. Tarasenko and E.L. Ivchenko, *JETP Lett.* **81** (2005) 231; arXiv:0803.3282.

[2] H. Zhao, X. Pan, A.L. Smirl et al., *Phys. Rev. B* **72** (2005) 201302.

[3] S.D. Ganichev, V.V. Bel'kov, S.A. Tarasenko et al., *Nature Phys.* **2** (2006) 609.

22TL-A-6

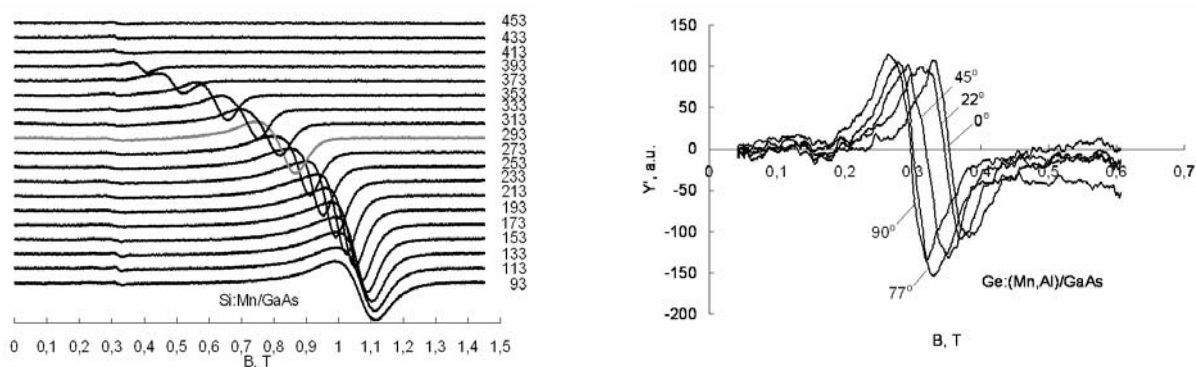
NANOSIZED LASER DEPOSITED LAYERS OF HIGH TEMPERATURE FERROMAGNETICS BASED ON SILICON AND GERMANIUM DOPED BY MANGANESE OR IRON IMPURITIES

Demidov E.S.¹, Podolskii V.V.¹, Lesnikov V.P.¹, Sapozhnikov M.V.², Karzanov V.V.¹, Gribkov B.A.², Druzhnov D.M.¹, Gusev S.N.¹, Levchuk S.A.¹

¹Nizhni Novgorod State University, Nizhni Novgorod 603950, Russia

²Institute for Physics of Microstructures, RAS, Nizhni Novgorod 603950, Russia

Coexistence of magnetism and semiconducting properties in diluted magnetic semiconductors (DMS) increases functionalities of spin-electronics. The possibility of a laser synthesis of thin 30-200 nm layers of DMS GaSb:Mn and InSb:Mn with the Curie temperature T_c above 500 K and Ge:Mn, Si:Mn, Si:Fe with T_c up to 400, 500, 250 K respectively was earlier demonstrated [1]. The DMS layers based on Ge and Si represent special interest for the spintronics, compatible with the most widespread silicon technology. This report represents results of research of magnetic Si and Ge layers grown at wider temperature range. $T_g=20-550$ eC. Difficulties of removal thermally steady natural silicon oxide were overcome. The variants of random digital alloys, introduction of additional "not magnetic" shallow acceptor Al impurity and influence of the additional subsequent pulse laser annealing were studied. The ferromagnetism of layers was controlled by results of ferromagnetic resonance (FMR), magneto-optical Kerr effect (MOKE), anomalous Hall effect (AHE), negative magnetoresistance (NMR) measurements. The surface profile and distribution of magnetization were determined by atomic and magnetic force microcopies. As against variant of GaSb:Mn the magnetic layers on basis Si and Ge are strongly different on magnetic and electric properties for random and discrete 3d-doping. In the case Si:Mn/GaAs the increase of T_g from 300eC up to 400eC allows to achieve for smaller contents of manganese more uniform distribution of magnetization, single line FMR (left fig.), higher magnetization, AHE and hysteretic MOKE at 293K. The opportunity of low temperature at $T_g \approx 20$ eC laser synthesis of ferromagnetic layers Ge: (Mn, Al)/GaAs or Ge (Mn, Al)/Si with $T_c > 300$ K is established. Such layers differ by abnormal angular dependence of FMR (right fig.) with strengthening instead of weakening of magnetization at the normal orientation of magnetic field. Nature of ferromagnetism in the nanosized DMS layers deposited from laser plasma depending on conditions of synthesis is discussed.



This work is supported by RFBR (05-02-17362, 08-02-01222), ISTC (G1335), carried out in collaboration with Kurchatov institute under contract with Federal Agency on Science and Innovations № 02.513.11.3176 (2007-3-1.3-07-07-098).

[1] E.S. Demidov, V.V. Podolskii, V.P. Lesnikov et al., *JETP*, **106** (2008) 110.

22RP-A-7

ORIGIN OF FERROMAGNETISM IN Mn (Co) – IMPLANTED Si: IMPURITIES OR DEFECTS?

*Orlov A.F.¹, Balagurov L.A.¹, Granovsky A.B.², Perov N.S.², Semisalova A.S.², Agafonov Yu.A.³,
Zinenko V.I.³, Bublik V.T.⁴, Scherbachev K.D.⁴, Vdovin V.I.⁵, Kartavych A.V.⁵, Saraikin V.V.⁶,
Andreev B.A.⁷, Sapelkin A.⁸, Rogalev A.⁹, Smekhova A.⁹*

¹State Institute for Rare Metals, Moscow, Russia.

²Moscow State University, Dept. of Physics, Moscow, Russia

³Institute of Microelectronics Technology and High Purity Materials RAS,
Chernogolovka, Russia

⁴Moscow Institute of Steel and Alloys, Moscow, Russia

⁵Institute for Chemical Problems of Microelectronics, Moscow, Russia

⁶Lukin State Research Institute of Physical Problems, Zelenograd, Russia

⁷Institute for Physics of Microstructures RAS, Nizhny Novgorod, Russia

⁸Queen Mary University of London, London, UK

⁹European Synchrotron Radiation Facility, Grenoble Cedex, France.

Semiconductor silicon wafers both *n*- and *p*-type conductivity with the carriers concentration in the range from $9 \cdot 10^{14}$ up to $2 \cdot 10^{19}$ cm⁻³, keeping a ferromagnetic ordering at above room temperature have been prepared by implantation with Mn (Co) impurities at fluxes density of $1 \times 10^{15} - 5 \times 10^{16}$ cm⁻². The crystalline and electron structure, magnetic and transport properties, as well as the state of impurities in these materials have been investigated. We used the techniques of XRD, SIMS, TEM, XPS, EXAFS, DLTS, FL, MCD, SQUID, VSM, and Spreading Resistance Probe. Measurements were made both at room temperature and in temperature range 77-400K. Impurities of Mn were found to generate silicide nanoparticles in Si wafer with the crystalline structure of B20. The post implantation pulse anneal at 850 °C leads to creation of Si layer with reduced lattice parameter. DLTS and FL –spectroscopies show that Mn-impurity gives the addition levels in the electron spectrum of Si. Mn in Si reveals the amphoteric behaviour and compensates donors (acceptors) in Si of electron (hole) – conductivity type. Ferromagnetic ordering in Si:Mn (Co) was observed at least up to 400 K. In Mn-implanted Si the magneto optic Faraday effect was manifested in the spectral region 1-6 μm at temperatures up to 305 K. However we did not observe any regular dependence of Si:Mn (Co) magnetization on the character of impurity (Mn or Co), conductivity type, the charge carriers concentration, and post implantation annealing. The value of saturation magnetization increases slightly along with augmentation of the implantation flux. The value of saturation magnetization is comparable with that due to the structural defects in Si. The XMCD technique did not discover any magnetic moment on Mn atoms in Si. Apparently, the total magnetization of Mn (Co) – implanted Si can be caused by the defects of Si crystalline structure arising during the implantation.

22RP-A-8

ION-BEAM SYNTHESIS OF FERROMAGNETIC SEMICONDUCTOR BY COBALT IMPLANTATION OF SINGLE-CRYSTALLINE RUTILE (TiO₂)

Khaibullin R.¹, Tagirov L.^{1,2}, Bazarov V.¹, Ibragimov Sh.², Achkeev A.A.², Faizrakhmanov I.¹, Akdoğan N.³, Nefedov A.³, Zabel H.³, Mackova A.^{4,5}, Hnatowicz V.⁴

¹Kazan Physical-Technical Institute of RAS, Sibirsky Trakt 10/7, 420029 Kazan, Russia

²Kazan State University, Kremlevskaya 18, 420008 Kazan, Russia

³Ruhr-Universität Bochum, D-44780 Bochum, Germany

⁴Nuclear Physics Institute, 250 68 Rez, Czech Republic

⁵J.E. Purkinje University Department of Physics, Faculty of Science, Ceske mladeze 8, 400 96 Usti nad Labem, Czech Republic

We report on synthesis of ferromagnetic semiconducting material based on rutile – a wide-band n-type oxide semiconductor. The homogeneously-doped samples of the ferromagnetic material were obtained by implantation with 40 keV cobalt ions into single-crystalline rutile plates along the *c* axis (i.e. [001] crystallographic direction) to fluence of $(1-2) \times 10^{17}$ ions/cm². The rutile substrates were kept at 900 K upon the implantation process. The magnetic properties of the material are as follows: the ferromagnetic ordering temperature is about 850K, the saturation magnetic moment is 0.5-1.2 Bohr magnetons per cobalt ion, the remanence-to-saturation magnetic moment ratio as large as 0.2-0.6, and the coercive field is about 10-50 mT at room temperature. The room-temperature resistivity of the material varies in the range 1-100 Ohm*cm depending on the implantation parameters such as the ion flux and fluence. Implantation of the [100] oriented surface of single crystalline rutile results in anisotropic ferromagnetism due to nucleation and growth of cobalt nanoparticles in the irradiated samples. The implant diffusion during the irradiation process was studied theoretically and applied to the experimental data. The implantation regimes issue, sample characterization and physical properties are discussed in details.

The work was supported by RFBR, grants 07-02-00559-a and 04-02-97505-r_ofi.

22 June Sunday

12:00-13:30

oral session

22TL-B

**“Nanomagnetism
and Nanostructures”**

22TL-B-1

MAGNETIC AND CRYSTALLINE STRUCTURE OF FePt NANOPARTICLES

Farle M.

Universität Duisburg-Essen, Fachbereich Physik, Lotharstr. 1, 47048 Duisburg, Germany

E-mail: farle@uni-due.de

Element-specific magnetism and interface properties inside a nanoparticle can be studied by combining superparamagnetic resonance and different x-ray absorption spectroscopies [1]. Different shapes and structures of nanoparticles are obtained by different organometallic synthesis routes or by enhancing diffusion processes during the formation of particles in gas-phase condensation methods [2]. Using the magnetic alloy FePt as an example the possibilities will be discussed. In ligand and oxide free $\text{Fe}_x\text{Pt}_{1-x}$ icosahedral particles (6 nm), which have been annealed to 800 K, we find enhanced (330 %) orbital magnetism at the Fe site [1,2] and a reduced orbital magnetism at the Pt site. Modifications of the magnon excitation spectrum due to size effects in FePt nanocubes [3] lead to changes of the temperature dependence of the magnetization and can be experimentally determined. The special importance of correlating experimental structural and magnetic findings with ab-initio calculations will be demonstrated by showing experimentally resolved surface reconstructions of few percent [4] and theoretical results confirming that below 3 nm diameter the formation of fct L10 chemically ordered FePt nanoparticles is energetically not favored [5].

Supported by National Center of Electron Microscopy, Berkeley, Deutsche Forschungsgemeinschaft SFB 445, and EU network "Syntorbmag".

[1] C. Antoniak et al, Phys. Rev. Lett. **97** (2006) 117201

[2] O. Dmitrieva, et al. Phys. Rev. B **76** (2007) 064414

[3] O. Margeat, et al. Phys. Rev. B **75** (2007) 134410

[4] Rongming Wang, et al, Phys. Rev. Lett. **100** (2008) 017205

[5] M. E. Gruner, et al, Phys. Rev. Lett. **100** (2008) 087203

22TL-B-2

EFFECTS OF DIMENSIONALITY ON MAGNETIC PROPERTIES OF GROUP-IV SEMICONDUCTORS

Kazakova O.¹, Morgunov R.², Kulkarni J.³, Holmes J.³, Ottaviano L.⁴, and Farle M.⁵

¹National Physical Laboratory, Teddington, United Kingdom

²Institute of Problems of Chemical Physics, Chernogolovka, Russia

³University Collage Cork, Cork, Ireland

⁴Università dell'Aquila, Coppito L'Aquila, Italy

⁵Universität Duisburg-Essen, Duisburg, Germany

Modern electronics vastly relies on semiconductor heterostructures and rapidly develops towards high-speed digital circuits, novel material approaches and ever diminishing transistor's size. One of the emerging material solutions is to use diluted magnetic semiconductors (DMS). The search for an ideal DMS material with tunable ferromagnetic behavior is being actively

pursued for realization of spintronics devices. In such materials a Curie temperature, T_c , far in excess of 300 K is essential for practical spintronic applications. Besides they should be compatible with conventional silicon technology. From this point of view, magnetically doped group-IV semiconductors (Ge and Si) would be ideal candidates. Germanium is an especially attractive material with high carrier mobility and, hence, ideally suitable for ultra-high-speed electronics. The unhindered development of nanoelectronics requires systematic reductions in feature sizes and the corresponding increases in integration densities. These trends force us to focus on exploring nanoscale device elements, including semiconductor nanowires (NWs). Room-temperature ferromagnetism in $\text{Ge}_{1-x}\text{Mn}_x$ [1] and $\text{Si}_{1-x}\text{Mn}_x$ [2] nanowires and nanocolumns [3] was recently demonstrated and a perfect dilution of Mn ions in the host has been proven [1]. It was also shown that Ge:Mn films are ferromagnetic with $T_c \approx 270$ K [4].

In this work effects of dimensionality and the role of defects in magnetic ordering of 1D and 2D GeMn systems are investigated by means of ESR and SQUID magnetometry techniques. In magnetically homogeneous $\text{Ge}_{1-x}\text{Mn}_x$ nanowires, all observed electron spin resonances are related to absorption on individual magnetic centres (Mn^{3+} , Mn^{2+} ions and polarized charge carriers) in a broad temperature range, $T=5$ -300 K. On the other hand, in strongly inhomogeneous 2D Ge:Mn films a collective spin excitation, the spin wave resonance, is observed at low temperatures, $T=5$ -60 K, see Figure. This signifies the presence of long-range spin states and a cooperative magnetic response originating from crystalline precipitates and diluted Mn ions. Additionally, a strong negative background was attributed to the microwave magnetoresistance of the Ge:Mn thin films. The absence of the magnetoresistance in the $\text{Ge}_{1-x}\text{Mn}_x$ nanowires indicates that the scattering of charge carriers is determined by dimensions of the nanostructure. Overall, our analysis of magnetic resonance phenomena reveals a significant difference between 1D and 2D magnetic semiconductors. It emphasizes the important role of dimensionality as well as the type and distribution of magnetic defects in spin-dependent scattering and dynamic magnetic properties of group-IV semiconductors.

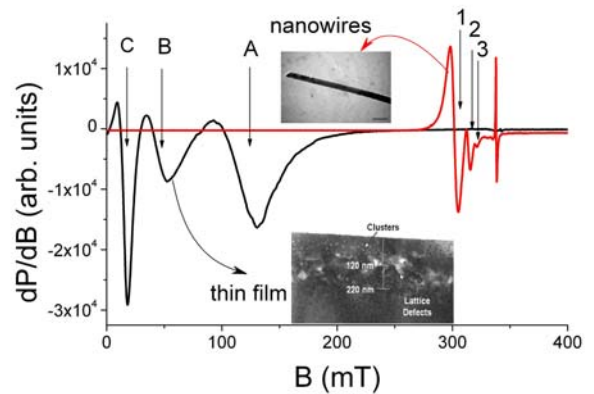


Figure. Typical ESR spectra of Ge:Mn thin film ($x=4\%$) and NW ($x=1\%$) samples at $T=15$ K. Insets show TEM images of a NW (top) and thin film (bottom).

- [1] O. Kazakova, et al., *Phys.Rev. B*, **72**, (2005) 094415.
- [2] M. Jamet, et al., *Nature Materials*, **5**, (2006) 653.
- [3] H. W. Wu, et al. *Appl. Phys. Lett.*, **90**, (2007) 043121.
- [4] M. Passacantando, et al., *Phys.Rev.B*, **73**, (2006) 195207.

22TL-B-3

Fe₃O₄ NANOPARTICLES WITH BULK MAGNETIC PROPERTIES

Pérez N.¹, Guardia P.¹, Roca A.G.², Morales M.P.², Serna C.J.², Bartolomé F.³, García L.M.³,
Batolomé J.³, Cezar J.C.⁴, Labarta A.¹, Batlle X.¹

¹Dept. Física Fonamental and Insitut de Nanociència i Nanotecnologia IN2UB, U.
Barcelona, Martí i Franqués 1, 08028 Barcelona, Catalonia, Spain

²ICMM CSIC, Sor Juana Inés de la Cruz 3, Cantoblanco 28049, Madrid, Spain

³Dept. Física de la Materia Condensada, U. Zaragoza and ICMA CSIC, Pedro Cerbuna 12,
50009 Zaragoza, Spain

⁴ESRF, 6 rue Jules Horowitz, 38000 Grenoble, France

Nowadays, fine magnetic particles are used in many technological applications and are considered promising materials for biomedicine. Consequently, the study of their magnetic properties has attracted many efforts in recent times, in particular because considerable deviations from bulk behavior have been widely reported for particle sizes below about 100 nanometers [1]. Fe₃O₄ nanoparticles (NP) in the 5-20 nm range were synthesized by the high temperature decomposition of an organic Fe precursor in the presence of a variety of coatings (oleic acid, PVA, TMAOH, dextrane...). The use of decanoic acid as coating agent leads to 8-75 nm particles with controlled shape from cubic to cube-octahedral, thus opening a new range of sizes not reachable before. All the foregoing materials show polydispersity below 20% high crystallinity with an inverse spinel structure and lattice parameters similar to those of magnetite, as revealed by X-ray diffraction, transmission electron microscopy (TEM), and high resolution TEM. Surprisingly enough, saturation magnetization M_s almost reaches the expected value for bulk magnetite at low temperature, being highest in those NP with surfactant covalently bonded to their surface. A variety of colloidal suspensions of quasi non-interacting Fe₃O₄ NP with oleic acid covalently bonded to their surface and mean diameter $\langle d \rangle = 5$ nm, has been subject of a deeper study on individual particle properties. In particular, on the subject of surface related issues that affect the switching of the magnetic moment, still under debate in literature, we have developed an analytical model to account for the effective surface contribution to the effective energy barrier distribution. This model enables us to transform the volume anisotropy distribution into the effective energy barrier distribution for anisotropy obtained with the $T \ln(t/t_0)$ scaling method [2,3]. Finally, X-ray absorption spectra (XAS) in the L_{2,3} edges suggest charge transfer to the surfactant due to covalent bond. X-ray magnetic circular dichroism (XMCD) confirms the dependence of the magnetic moment on the surface bond suggesting that the orbital momentum is more effectively quenched in covalently bonded NP and, in this case, giving a value of $\langle S_z \rangle = 3.54-3.63 \mu_B/\text{f.u.}$ that is very close to the values for bulk samples measured with the same technique. The funding from the Spanish MEC, and from the Catalan DURSI is acknowledged.

[1] For example, see the review paper, X. Batlle and A. Labarta, *J. Phys D* **35**, R15, (2002).

[2] A. Labarta, O. Iglesias, LI. Balcells, F. Badia, *Phys. Rev. B*, **48**, 10240, (1993).

[3] N. Pérez, P. Guardia, A.G. Roca, M.P. Morales, C.J. Serna, F. Bartolomé, L.M. García, A. Labarta and X. Batlle, 'Surface anisotropy broadening of the energy barrier distribution in magnetic nanoparticles', submitted.

22 June Sunday

15:00-17:00

oral session

22TL-B

22RP-B

“Magnetophotonics I”

22TL-B-4

OPTICAL STUDY OF THREE-DIMENSIONAL MAGNETIC PHOTONIC CRYSTALS OPAL/Fe₃O₄

*Pavlov V.V.¹, Usachev P.A.¹, Pisarev R.V.¹, Kurdyukov D.A.¹, Kaplan S.F.¹,
Kimel A.V.², Kirilyuk A.², and Rasing Th.²*

¹A.F. Ioffe Physico-Technical Institute, RAS, 194021 St. Petersburg, Russia

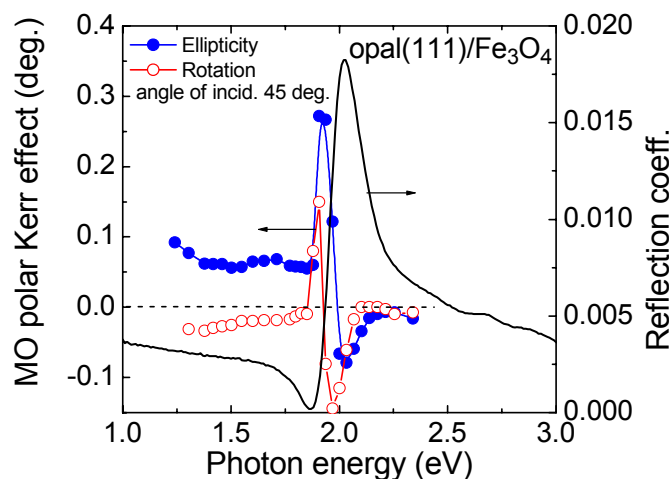
²Institute for Molecules and Materials, RUN, 6525 ED Nijmegen, the Netherlands

Photonic crystals (PCs) are n -dimensional ($n=1-3$) space-modulated structures where the modulation period is comparable to the light wavelength [1]. Interference phenomena in PCs are responsible for specific photonic bands with the high-transparency and high-reflectance regions. A construction of PCs from magnetic materials or an impregnation of PCs with a magnetic material produces a formation of so-called magnetic photonic crystals (MPCs) [2, 3]. PCs possess unique optical properties and tuneable parameters enabling their use for applications in near-infrared and visible wave ranges. An external magnetic field can effectively change the magnetic state of MPCs that in combination with enhanced optical phenomena allows a new degree of freedom for the manipulation of optical characteristics.

We present experimental results on optical and magneto-optical phenomena in new three-dimensional MPCs, based on opal PCs with magnetite Fe₃O₄ inside pores. Artificial opal was chosen as a volumetric matrix formed from submicron silica spheres with effective diameter of 290 nm. These spheres had the compact packing of face-centred cubic type. Opal thin film samples having (111)-orientation with the thickness of 5 μm were impregnated with magnetite Fe₃O₄. Magnetite is a half-metal with the high Curie temperature $T_C = 858$ K, that makes MPCs opal/Fe₃O₄ very interesting from fundamental and applied points of view.

A formation of the photonic band-gap in the spectral range of 1.6-2.0 eV was proved by the optical transmission and reflection (see Figure) techniques. All measurements were done at the room temperature. A strong enhancement of the polar Kerr effect (see Figure) and a modification of the Faraday effect have been found near the photonic band-gap due to the localization of light electromagnetic field.

The magnetic circularly dichroism as a function of an external magnetic field was studied for different photon energies. Unusual shapes of hysteresis curves and their dependence on photon energy have been revealed in the spectral region where the magneto-optical effect reverses its sign. This phenomenon has been modelled and explained to be due to two types of magnetite particles inside the opal matrix having different coercive fields and spectral behaviours of the magnetic circularly dichroism.



Financial supports by RFBR, NWO-RFBR, INTAS, and the Program on Spintronics of RAS are acknowledged.

[1] K. Sakoda, *Optical Properties of Photonic Crystals* (Springer-Verlag, New York, 2001).

[2] I. L. Lyubchanskii *et al.*, *J. Phys. D: Appl. Phys.* **36** (2003) R277.

[3] M. Inoue, *et al.*, *J. Phys. D: Appl. Phys.* **39** (2006) R151.

22RP-B-5

MAGNETO-PHOTONIC CRYSTALS WITH VARIOUS DESIGNS: CONTROL OF THE DIRECTION AND STATE OF POLARIZATION

Baryshev A.V.^{1,}, Goto T.¹, Dokukin M.E.^{1,3}, Merzlikin A.M.², Vinogradov A.P.²,
Khanikaev A.B.¹, Granovsky A.B.³, Inoue M.¹*

¹Toyohashi University of Technology, Toyohashi, Aichi 441-8580, Japan

²Institute of Theoretical and Applied Electromagnetism, Moscow 125412, Russia

³Moscow State University, Moscow 119992, Russia

Artificial structures composed of alternating dielectric materials with different refractive indices, known as photonic crystals (PCs), have been shown to affect the propagation of light, providing a new mechanism to control and manipulate the flow of light [1–3]. For magnetophotonic crystals (MPCs), in which the constitutive elements are magnetic (or even only a defect introduced into the periodic structure is magnetic), there exists an additional degree of freedom to operate the photonic band structure, diffraction patterns, and the state of polarization of light, i.e., these characteristics can be influenced by the external magnetic field [4–6].

In this work we present a new type of MPCs composed of two 1D PCs, namely, magnetic and non-magnetic Bragg mirrors with slightly different photonic properties. Fabricated MPCs of this type exhibited the resonant transmission and were experimentally shown to enhance the magneto-optical response of known materials. The surface state, so-called the Tamm state [6], is originated by the interface between two 1D PCs, and supports multiple propagation (localization) of light within magnetic layers. When magnetic field is applied, the difference of the wave vectors for left- and right-circular polarized localized Tamm modes, multiple propagation of these modes within the magnetic layer and the nonreciprocal character of the Faraday effect result in an enhancement of the polarization rotation by one order of magnitude.

3D magneto-photonic structures composed of thin opal and Bi:YIG films were fabricated and studied. Heterostructures with opal/garnet/opal structure were shown to exhibit enhancement of Faraday rotation, since they act as their 1D counterpart [4]. We have found that opal/Bi:YIG heterostructures provide rich possibilities to control the state of polarization of light beams as resonant light is trapped in their structure due to 2D and 3D diffraction. The interplay of the Faraday rotation and the anisotropy of polarized light propagation [7] in these 3D MPCs strongly influence characteristics of emerging beams.

*Permanent address: Ioffe Physico-Technical Institute, St. Petersburg 194021, Russia.

[1] J.D. Joannopoulos, R. Meade, J. Winn, *Photonic Crystals*. Princeton University Press, Princeton (1995).

[2] C. Lopes, *Adv. Mater.* **15**, (2003) 1679.

[3] J.-M. Lourtioz, H. Benisty, V. Berger, et al., *Photonic Crystals: Towards Nanoscale Photonic Devices*, Springer, Berlin (2005).

[4] M. Inoue, R. Fujikawa, A. Baryshev, et al., *J. Phys. D: Appl. Phys.* **39**, (2006) R151.

[5] A.B. Khanikaev, A.V. Baryshev, M. Inoue, et al., *Phys. Rev. B* **72**, (2005) 035123.

[6] A.P. Vinogradov, A.V. Dorofeenko, S.G. Erokhin, et al., *Phys. Rev. B* **74**, (2006) 045128.

[7] A.V. Baryshev, A.B. Khanikaev, H. Uchida, M. Inoue, M.F. Limonov, *Phys. Rev. B* **73**, (2006) 033103.

22RP-B-6

STUDIES ON ARTIFICIAL NANOSTRUCTURES WITH LARGE MAGNETO-OPTICAL RESPONSES

Fujikawa R.¹, Baryshev A.V.^{1,2}, Khanikaev A.B.¹, Kim J.¹, Uchida H.¹, Inoue M.¹

¹Toyohashi University of Technology, 1-1 Hibari-Ga-Oka, Toyohashi, Aichi 441-8580, Japan

²Ioffe Physico-Technical Institute, St. Petersburg 194021, Russia

We have studied optical and magneto-optical properties of artificial magnetophotonic nanostructures. Experimental samples comprising bismuth-substituted yttrium iron garnet (Bi:YIG) films in combination with thin opal films (3D photonic crystals) or Au nanoparticles (composites supporting localized surface plasmon resonances) have been found to provide larger magneto-optical (MO) responses.

In the last decade, we have utilized the idea of photonic crystals (PCs) to enhance the MO responses of known magneto-optical materials by constructing structures called magnetophotonic crystals (MPCs). The simplest MPC composed of magneto-optical film sandwiched between two one-dimensional PCs (Bragg reflectors) is demonstrated in [1]. In this work, we present a new magneto-photonic structure in which one of the constituents is the thin opal film. Provided that 3D PCs exhibit richer optical properties (various stop bands, the regime of multiple Bragg diffraction), fabrication and studies on light coupling to 3D MPCs are of our interest.

The fabrication procedure of such a new type of MPCs was as follows. Bi:YIG film was deposited by magnetron sputtering system on the dielectric Bragg mirror (1D PCs) and was annealed at 750 °C. Finally, an opal film was deposited atop of Bi:YIG film. The opal film was composed of close-packed SiO₂ spheres with the diameter of 260 nm; the vertical deposition method was used [2]. Transmission spectra of the fabricated samples showed a peak of the resonant transmission (the localized mode) within in the (111) photonic stop band overlapping with the stop band of the 1D PC. The Faraday rotation of the sample at the wavelength corresponding to the peak was enhanced as compared with that of the structure without the opal film. Our calculations for optical and MO responses of the sample are in excellent agreement with the experimental data.

The interplay between the effect of the bulk plasma resonance and the Kerr effect, which provides enhancement of the MO response, is demonstrated for planar structures [3]. Another approach to influence the MO response is demonstrated for the structures supporting localized surface plasmon resonances (LSPRs) [4]. We have recently fabricated Bi:YIG films impregnated with Au nanoparticles and demonstrated their Faraday rotation. The experimental sample was a 90-nm-thick Bi:YIG films deposited onto a quartz substrate using a magnetron sputtering system. Next, a 5 nm-thin Au film was deposited onto the Bi:YIG film using a quick coater, and then this two-component structure was subjected to annealing at 750 °C in air. Such treatment allowed to get the crystalline phase of Bi:YIG and form a planar array of Au nanoparticles atop the Bi:YIG film. For such noble metal/garnet nanocomposites, we have found a significant enhancement of Faraday rotation for the wavelengths corresponding to LSPRs.

[1] M. Inoue, K. Arai, T. Fujii, M. Abe, *J. Appl. Phys.*, **83** (1998) 6768.

[2] R. Fujikawa, A. V. Baryshev, H. Uchida, P. B. Lim, and M. Inoue, *J. Porous Mater.*, **13** (2006) 287.

[3] T. Katayama, H. Awano, and Y. Nishihara, *J. Phys. Soc. Jpn.*, **55** (1986) 2539.

[4] S. Tomita, T. Kato, S. Tsunashima, S. Iwata, M. Fujii, and S. Hayashi, *Phys. Rev. Lett.*, **96** (2006) 167402.

22TL-B-7

MAGNETO - PHOTONIC PROPERTIES OF INVERTED MAGNETIC METALLIC OPALS

Semin S.¹, Kuznetsov M.¹, Ivanov M.¹, Valdner V.¹, Mishina E.¹
Napol'skiy K.², Tsirlina G.², van Etteger A.³, Rasing Th.³

¹Moscow State Institute of Radioengineering, Electronics and Automation, Prosp.
Vernadskogo 78, 119454 Moscow, Russia

²Department of Chemistry, Moscow State University, Moscow 119991, Russia

³Institute for Molecules and Materials, Radboud University Nijmegen, Toernooiveld 1,
6525ED Nijmegen, The Netherlands

Metallic photonic crystals (PhCs) have recently attracted considerable attention due to their potential new properties in comparison with dielectric and semiconductor PhCs. Metallic PhCs possess unique optical absorption and reflectivity, which may be used for filters (including terahertz filters), thermally stimulated emission and nanoplasmonic behavior [1]. Using magnetic metals they may form a new class of magneto-photonic crystals which presently consist mostly out of magnetic garnet PhCs [2]. However no magneto-optical properties were reported for magnetic metallic opals so far.

In this work we report the results of the fabrication and characterization of magnetic metallic inverted opals fabricated by electrodeposition of Ni inside the voids of a polystyrene opal, which is chemically dissolved afterwards. Linear and nonlinear magneto-optical studies were performed using a femtosecond Ti:sapphire laser. Fig. 1 (a) shows reflectivity spectra for two samples, PhC1 and PhC2, with the following parameters: hole diameters of 450 and 380nm and periods of 520 and 430nm, respectively. The reflectivity minima correspond to the cutoff frequency of the PhCs. In the same spectral range the second harmonic generation (SHG) spectrum is shown, with the maxima matching the reflectivity minima. Fig.1(b) shows reflectivity and Kerr rotation in the “blue” spectral range which possesses analogous behavior: the increase of Kerr rotation matches the minimum of reflectivity. Thus, analogously to other

magneto-photonic crystals, a strong enhancement is observed for SHG and Kerr rotation for nickel inverted opals.

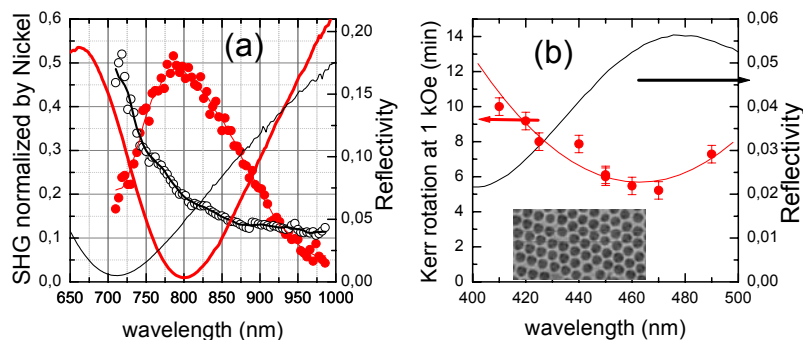


Fig. 1. (a) “Red range” reflectivity (left scale) and SHG intensity normalized by the SHG signal from nickel film for PhC1 (solid circles, thick line) and PhC2 (open circle, thin line); (b) “Blue range” reflectivity (right scale) and Kerr rotation for PhC1. Inset: microscopic image of PhC1

This work is supported by the Nederlandse Organisatie voor Wetenschappelijk Onderzoek (NWO), RFBR and the Ministry of Science and Education of RF.

[1] X. Yu, Yun-Ju Lee, R. Furstenberg, J. O. White, P.V. Braun, *Adv. Mater.* **19** (2007) 1689.

[2] M. Inoue, R. Fujikawa, A.

Baryshev, A. Khanikaev, P.B. Lim, H. Uchida, O. Aktsipetrov, A. Fedyanin, T. Murzina, A. Granovsky, *J. Phys. D: Appl. Phys.* **39** (2006) R151.

22RP-B-8

OPTICAL TWEEZERS FOR MAGNETIC MICRO- AND NANOPARTICLES DIAGNOSTICS

Zhdanov A.G., Khokhlova M.D., Lyubin E.V., Soboleva I.V., and Fedyanin A.A.
Faculty of Physics, Lomonosov Moscow State University, Moscow 119991, Russia

This work is devoted to diagnostics of single magnetic particles of submicrometer scale utilizing optical tweezers' technique. Optical tweezers have been proved to be an efficient tool for micro-objects manipulating and has found lots of applications mainly in biology [1,2]. However applications of this unique method both in solid state physics are not so wide-spread. The main idea of optical tweezing lies in trapping of microobjects utilizing forces of optical pressure. If the trapped particle is transparent this method turns out to be non-disturbing way of diagnostics of single objects of micrometer scale. Microparticle is usually placed into cavity with liquid and is trapped by strongly focused beam. Physical properties of single magnetic micro- and nanoparticles can differ significantly from the properties of both bulk samples and thin films, and at the same time are of the greatest interest in the whole range of applications connected with novel micromagnetic devices. It makes the problem of single microparticles diagnostics really challenging.

The scheme of experimental setup is the following. Light from continuous 100 mW Nd:YAG laser is expanded by two-lens system and after that is reflected from multilayered mirror to the microscope objective with high (NA=1.25) numeric aperture. The cavity with studied particles is placed in front of microscope objective in the region of beam waist. The image of trapped particles is formed using conventional microscope scheme. The position of studied objects is controlled by micromanipulators. Magnetic modification of optical tweezers includes permanent magnets placed near the experimental samples. Magnetic fields applied to the sample are approximately 1 kOe. The important characteristic of optical trap is statistics of microparticle's motion in the trap. Quadrant photodiode (QPD) is used to detect such motion. Light diffracted and scattered from the studied particle falls on the input window of QPD which is divided into four sectors. Depending on the displacement of the particle corresponding sectors of QPD are illuminated. The displacement of the particle is obtained measuring the difference of the signals from different QPD sectors. Such method affords the opportunity to measure statistics of the particle's motion in the trap and its reaction on the magnetic field in the case of magnetic particles. It gives a key to investigating of magnetic properties of single microparticles analyzing the signal from QPD in the presence of external magnetic field. The examples of studied nanoparticles are series of ferromagnetic particles ($\text{Fe}_2\text{O}_3:\text{SiO}_2$ and $\text{La}_{0.8}\text{Ag}_{1.5}\text{MnO}_3$) with size ranging from 300 to 700 nm. Statistics of their motion is measured and analyzed. The ability of magnetic field manipulation of the trapped particles is demonstrated. Moreover dielectric microparticles with metal core of various thicknesses are investigated. The ways of optical torque translation from input radiation to the trapped particles is considered. The ability of magnetic phase transitions in single micro- and nanoparticles is also demonstrated. Finally, the advantages of dual-beam optical tweezers allowing independent trapping of two individual magnetic nanoparticles are demonstrated.

[1] P.L. Biancaniello, A.J. Kim, J.C. Crocker, *Phys. Rev. Lett.*, **94**, (2005) 058302.

[2] D.G. Grier, *Nature* **22**, (2006) 424.

22RP-B-9

MAGNETOPLASMONICS OF METALLIC NANOSTRUCTURES WITH EMBEDDED MAGNETO-OPTICAL MATERIALS

Khanikaev A.¹, Baryshev A.¹, Granovsky A.², and Inoue M.^{1,2}

¹Toyohashi University of Technology, 1-1 Hibari-Ga-Oka, Toyohashi, 441-8580 Japan

²Faculty of Physics, Moscow State University, Leninskie gory, 119992, Moscow, Russia

The necessity of an optical analogue of electronic integrated circuits capable of routing, controlling and processing optical signals is evident because of rather limited performance of electronic circuits. Photonics offers an effective solution to this problem by implementing optical communication systems based on optical fibers and photonic circuits. However, scaling down optical devices to nanometric dimensions and their integration in photonic circuits requires *novel approaches to light manipulation*. One of possible approaches is application of optically active magneto-optic components which, when acting on optical field, give rise to nontrivial **polarization and/or phase evolution**.

When the constitutive materials of the metallo/dielectric nanostructure are magnetic, it starts to exhibit unique optical and magneto-optical properties. The strong photon confinement in the vicinity of the magnetic materials due to plasmon and spoof-plasmon resonances results in a large enhancement in the magneto-optical response of the media. Novel effects such as magnetically controllable and non-reciprocal extraordinary optical transmission were theoretically predicted. It was realized that magnetic materials can be utilized to control electromagnetic energy flows at infrared and optical frequency ranges, provided that light coupling to magneto-optic constituents is enhanced by appropriate nanoscale design of optical elements. These ideas are coming now to the forefront of plasmonics and near-field optics and it is only a matter of time till the potential of **polarization/phase engineering**, addressed in this talk, will be fully engaged in exciting research and applications of nanophotonics worldwide.

22 June Sunday

12:00-13:30

15:00-17:00

oral session

22TL-C

22RP-C

**“High Frequency
Properties”**

22TL-C-1

HIGH FREQUENCY PERMEABILITY OF SOFT MAGNETIC MATERIALS AND ITS APPLICATION TO ICT DEVICES

Yamaguchi M., Endo Y., Shimada Y.

Department of Electrical and Communication Engineering, Tohoku University
6-6-05 Aoba, Aramaki, Aoba-ku, Sendai 980-8579, Japan

This paper discusses applications of soft magnetic films associated with the ferromagnetic resonance (FMR). By measuring frequency dependent complex permeability profile [1], it is found that there are number of outstanding candidates for these applications, including metal alloy, granular, nano-particulate composite, etc.

It is popular that the real part permeability turns into negative beyond the FMR frequency. Material with negative permeability is useful to suppress skin effect in conductors [2]. Suppose an alternately multilayered structure of metal/magnetic thin film with thickness of each layer as t_N and t_F , respectively. Then the volume average of relative permeability, $\mu_{rav} = (1/t_N + \mu_r/t_F)/(t_N+t_F)$ (1), can be set zero if μ_r is negative. We have reported that the 0.3 μm -thick Al film and the 0.1 μm -thick NiFe film were sputter-deposited in turn to the total thickness of 6 μm on a glass substrate, and the measured resistance exhibits decrease monotonically from the top level of 3.2 Ω at 13 GHz to the bottom level of 1.9 Ω at 17 GHz [3]. In detail, the signal line is 1000 μm long and 36 μm wide. The signal-to-ground gap is 11 μm . For the NiFe layer, $4\pi M_s = 10.0$ kG, $H_k = 10$ Oe (nominally, before microfabrication) and $\rho = 16.7$ $\mu\Omega\text{cm}$. Easy axis direction is along the length direction of the coplanar line. The existence of a frequency range where resistance monotonically decreases is the first experimental verification of the skin effect suppression. This never happens in the case of normal metal. Such a frequency range linearly shifted toward higher frequency range with the applied external field.

Extensive discussion is on the actual thickness of each layer. Detailed electromagnetic field simulation by FEM (Ansoft Co., HFSS Ver. 11) clarified the resistance monotonically decreases with thinning the layer, keeping the relation show in eq. (1) until the thickness equals to the half of the skin depth. Right now this is only phenomenological understanding and physical analysis should follow soon. Anyway this idea may open a new high-Q application of the permeability at just below the anti-resonance frequency.

It is also well known that the FMR is associated with the losses. Such a magnetic film is useful as a frequency-selective loss generator. Therefore the 1.0 μm -thick soft magnetic $\text{Co}_{85}\text{Zr}_3\text{Nb}_{12}$ film, and 100 μm -thick polymer-embedded Fe/permalloy composite nanoparticles were integrated onto the bare LSI chip. Magnetic field above the chip has been evaluated by a planar shielded-loop probe we developed before. In addition to published paper [4], we analyzed the harmonic peaks one by one and found that the nano-composite film exhibited attenuation of 3.0~6.7dB throughout 40 MHz ~ 2.0 GHz (maximum at 774 MHz) whereas the CoZrNb film attenuated the field in the 100 MHz ~ 2.1 GHz range with the maximum of 11.5 dB at 401 MHz, which demonstrate potentials for practical applications.

Supports by JST, SCOPE are acknowledged.

- [1] M. Yamaguchi, et al., "A New 1MHz-9GHz Thin-Film Permeameter Using a Side-Open TEM Cell and a Planar Shielded-Loop Coil," Trans. Magnetics Society of Japan, **3**, (2003), 137.
[2] Behzad Rejaei, et al., "Suppression of skin effect in metal/ferromagnet superlattice conductors," JOURNAL OF APPLIED PHYSICS, **96**, (2004), 6863-6868.

- [3] S. Shiozawa, et al., “Experimental Verification of Skin Effect Suppression in Multilayer Thin-Film Conductor Taking Advantage of Negative Permeability of Magnetic Film beyond FMR frequency,” Intermag2008, FF-04 (Madrid, 2008).
- [4] Fukushima, et al., “Evaluation of RF Magnetic Thin Film Noise Suppressor Integrated onto an Operating LSI Chip”, Trans. Magnetics Society of Japan, **30**, (2006), 531.

22TL-C-2

BOSE-EINSTEIN CONDENSATION OF MAGNONS AT ROOM TEMPERATURE

Demokritov S.O.¹, Demidov V.E.¹, Dzyapko O.¹, Melkov G.A.², Slavin A.N.³

¹Institute for Applied Physics, University Münster, 48149, Münster, Germany

²Department of Radiophysics, National Taras Shevchenko University of Kiev, Kiev, Ukraine.

³Department of Physics, Oakland University, Rochester, MI, USA.

Magnons, which are quanta of magnetic excitations of a magnetically ordered ensemble of magnetic moments, are bosons. In the thermal equilibrium they can be described by Bose-Einstein statistics with zero chemical potential, and a temperature dependent density. In the experiments presented here we show that by using a technique of microwave pumping it is possible to excite additional magnons and to create a system of quasi-equilibrium magnons with a non-zero chemical potential. With increasing pumping intensity the chemical potential of the magnons reaches the energy of the lowest magnon state, and a Bose-condensate of magnons is formed [1].

The experiments have been performed in films of yttrium-iron-garnet (YIG). YIG films comprise a very suitable medium for experimental investigation of the magnon BEC transition. First, the well-known process of parametric pumping offers an effective way to feed energy into the low-frequency part of the magnon spectrum, which then can relax into magnons with the minimum frequency, where BEC should take place. Second, YIG films provide a very long spin-lattice relaxation above 200 ns. In contrast, the magnon-magnon thermalization time due to the two- and four-magnon scattering mechanisms can be as low as 10 – 20 ns [2]. Since both scattering mechanisms keep the number of magnons constant, a quasi-equilibrium state for the magnon system can be realized with a nonzero chemical potential.

The magnon distribution over the spectrum was experimentally studied using Mandelstam-Brillouin light scattering spectroscopy. Mapping the magnon distribution one can see that for relatively smaller numbers it can be described by the Bose-Einstein statistics. At higher numbers of pumped magnons a narrow peak of magnon population close to the bottom of the magnon spectrum appears on the top of the broad magnon distribution corresponding to the Bose-Einstein statistics. The widths of the peak both in the frequency and the k-vector-space are determined. The measured frequency width of the peak is six orders of magnitude smaller than that expected for the thermal distribution. We associate this effect with Bose-Einstein condensation of magnons, with the narrow peak reflecting the formation of the condensate.

Experimental evidence for spontaneous coherence of the condensate is found [3].

Support by Support by the Deutsche Forschungsgemeinschaft, US Army Research Office (MURI Grant No.W911NF-04-1-0247), and by the Science & Technology Center of Ukraine is gratefully acknowledged

[1] S.O. Demokritov et al., *Nature*, **443** (2006) 430.

[2] V.E. Demidov et al., *Phys. Rev. Lett.* **99** (2007) 037205.

[3] V.E. Demidov et al., *Phys. Rev. Lett.* **100** (2008) 047205.

22TL-C-3

CHALLENGE OF ULTRA HIGH FREQUENCY LIMIT OF PERMEABILITY FOR MAGNETIC NANOPARTICLE ASSEMBLY WITH ORGANIC POLYMER

~APPLICATION OF SUPERPARAMAGNETISM ~

Takahashi M.¹, Hasegawa D.², and Ogawa T.³

¹New Industry Creation Hatchery Center, Tohoku University, 6-6-05, Aoba, Sendai, Japan

²Department of Electronic Engineering, Tohoku University, 6-6-05, Aoba, Sendai, Japan

³Center for Research Strategy & Support, Tohoku University, 6-6-05, Aoba, Sendai, Japan

The magnetic material to high frequency device application above GHz range requires the high anisotropic and/or isotropic permeability, low loss, and high resonance frequency, which determines upper applicable limitation of devices. To realize above mentioned physical items, magneto-dielectric hybrid material embedding monodispersed metallic superparamagnetic nanoparticles (NPs), which have no hysteresis loss and isotropic permeability, into an organic polymer matrix is proposed.

For the permeability of general ferromagnetic NP assembly in ultra high frequency over GHz range, the intrinsic ferromagnetic resonance frequency (f_r^{int}) originating from the anisotropy field of NP determines its physical limit. Under superparamagnetic state, the 3-dimensionally fluctuating thermal field (H_t) and the magnetic dipole interaction field act on the magnetic moment of NP as the real effective field and affect on the magnetic resonance phenomena. Therefore, increasing H_t with decreasing the size of NP is expected to enhance the blocking resonance frequency (f_b) originating from superparamagnetic to ferromagnetic transition.

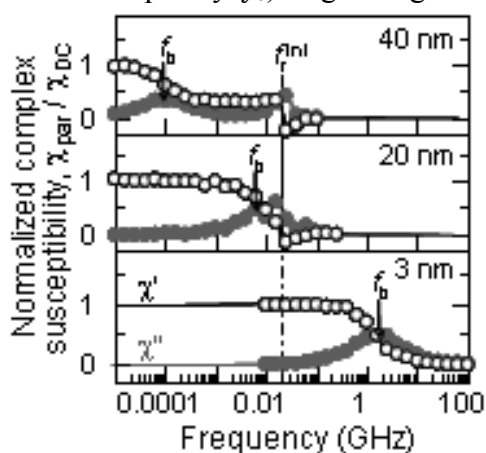


Fig. 1 Calculated frequency dependence of complex susceptibility normalized by DC susceptibility at 300 K. Saturation magnetization, anisotropy field, and damping constant of nanoparticle are assumed 1000emu/cm³, 10Oe, 0.1, and 300K, respectively.

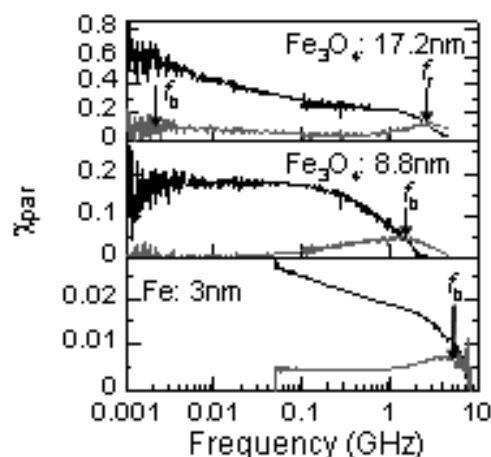


Fig. 2 Measured frequency dependence of complex susceptibility for Fe₃O₄ and Fe nanoparticle assemblies.

Fig. 1 shows LLG calculation results of frequency dependence of susceptibility (χ_{par}) normalized by DC susceptibility (χ_{DC}) for NP assembly without any interactions (size dependence). f_b increases with decreasing NP size. Especially, in the case of 3nm, ferromagnetic resonance is not appeared anymore at f_r^{int} . This means that superparamagnetic behavior is

maintained over f_r^{int} . This calculated result is supported by experiments of Fe_3O_4 and Fe NP assemblies with various sizes (Fig. 2). In particular, 3nm Fe NP assembly has a resonance at 5GHz which is higher than f_r^{int} of about 1.5GHz for Fe NP.

Within the frame work of the present paper, the magnetic resonances which originate from the intrinsic anisotropy field and the fields due to the thermal and the interaction for superparamagnetic NP assembly will be widely discussed in connection with high frequency devices using the magneto-dielectric hybrid material.

22TL-C-4

MICROWAVE PERMITTIVITY AND PERMEABILITY PROPERTIES OF FE NANOPARTICLES COATED WITH CARBON (INVITED)

Deng Longjiang, Han Mangui, Ou Yu, Tang Wu

State Key Laboratory of Electronic Thin Films and Integrated Devices, University of Electronic Science and Technology of China, Chengdu, 610054, P. R. of China.

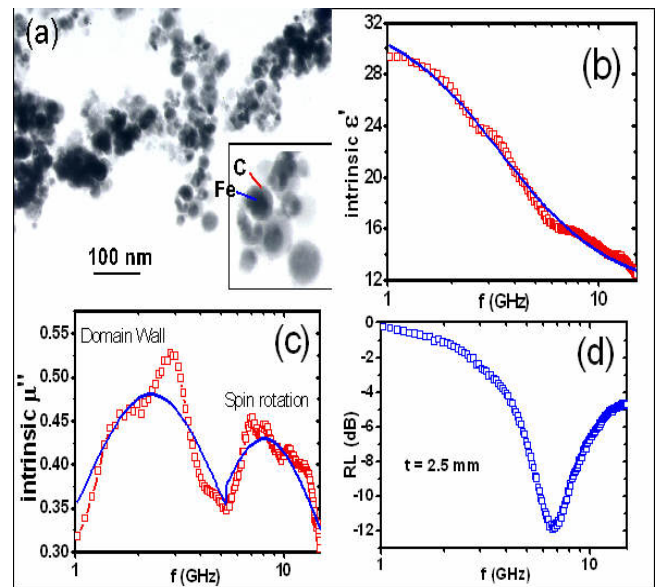
Ferrites are often used in the high frequency areas [1], but they suffer from lower saturation magnetization (M_s) values and bad temperature stability. However, if nano scale ferromagnetic materials were used, these shortcomings can be overcome. The microwave permeability of ferromagnetic submicrometer sized particles ($\text{Co}_{65}\text{Ni}_{35}$) had been studied by Acher et al [2]. To avoid the oxidation problem of ferromagnetic nanoparticles, they are often been coated with SiO_2 , carbon and gold. In this contribution, we report the studies on the microwave permittivity and permeability properties of nano-sized Fe particles coated with carbon (denoted as Fe-C). The transmission electron microscopy of Fe-C nanoparticles is shown in Fig. 1(a).

The coercivity of Fe-C nanoparticles is found about 325 Oe. The Law of Approach to Saturation has been used to explain the origin of large coercivity. Within the frequency range of 1 GHz – 15 GHz, the intrinsic permeability and permittivity values have been extracted from the experimental values using the Bruggeman's effective medium theory. The intrinsic permittivity (ϵ') dispersion spectra have been fitted with the Cole-Cole dispersion law [3]:

$$\epsilon' = \epsilon_{r\infty} + (\epsilon_{rs} - \epsilon_{r\infty}) \frac{1 + (\omega\tau)^{-\beta} \sin(\tau\beta/2)}{1 + 2(\omega\tau)^{-\beta} \sin(\tau\beta/2) + (\omega\tau)^{2(1-\beta)}},$$

where ϵ_{rs} is the static permittivity, $\epsilon_{r\infty}$ is the

permittivity at extremely large frequency, τ is the relaxation time in second (s), β is the distribution of relaxation time ($0 \leq \beta \leq 1$). Smaller β value implies narrow distribution of relaxation time. The fitting results for ϵ_{rs} , $\epsilon_{r\infty}$, τ and β are 32.97, 10.87, 4.66×10^{-11} s, 0.079 respectively. The fitting of intrinsic $\epsilon' - f$ behaviors is shown by the solid line in Fig. 1(b). The intrinsic permeability (μ'') dispersion behaviors, as shown in Fig. 1(c), have been fitted based on the dispersion mechanisms due to the domain wall movements and spin rotation. For the one due to domain wall movement, the permeability dispersion can be described by the Debye's dispersion law: $\mu'' = \chi_{d0} \times (f/f_{dw}) / [1 + (f/f_{dw})^2]$, where χ_{d0} is the static susceptibility, f_{dw} is the



peak frequency of dispersion due to the domain wall. For the one due to the spin rotation, the following equation can be used [4]: $\mu_s'' = \frac{\chi_{s0}\omega_s\omega\alpha[\omega_s^2 + \omega^2(1 + \alpha^2)]}{[\omega_s^2 - \omega^2(1 + \alpha^2)]^2 + 4\omega^2\omega_s^2\alpha^2}$. Using the above two equations, we have separately fitted each peak in the $\mu'' - f$ spectrum, as indicated by the solid lines in Fig. 1(c). For fitting, we have obtained the following values for χ_{d0} , f_{dw} , χ_{s0} , f_s ($f_s = \omega_s/2\pi$) and α (damping coefficient) respectively: 0.96, 2.3 GHz, 0.751, 16.57 GHz and 1.795. Also, our results reveal that Fe-C nano particles can be used for microwave absorption application, as shown in Fig. 1(d), where t is the thickness of absorber. When t is 2.5 mm, the minimum reflection loss (RL) is about -12 dB at $f = 6.63$ GHz.

We want to thank the financial support from the Natural Science Foundation of China (Grant No.50601005) and the 2008-2009 NSFC-RFBR.

- [1] K. N. Rozanov, Z. W. Li, L. F. Chen, M. Y. Koledintseva, *J. Appl. Phys.* **97** (2005) 013905.
 [2] P. Toneguzzo, O. Acher, et al, *J. Appl. Phys.* **81** (1997) 5546.
 [3] Longjiang Deng, Mangui Han, *Appl. Phys. Letter.* **91** (2007) 023119.
 [4] Mangui Han, Difei Liang, Longjiang Deng, *Appl. Phys. Letter.* **90** (2007) 192507.

22TL-C-5

MAGNETIZATION DYNAMICS OF MAGNETIC HETEROSTRUCTURES

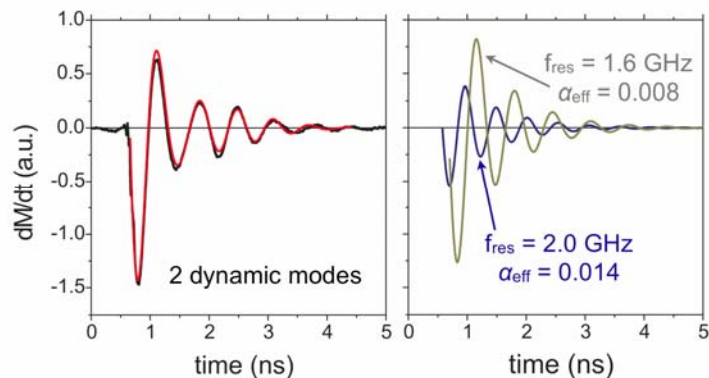
McCord J.

IFW Dresden, Institute for Metallic Materials, Postfach 270116, 01171 Dresden, Germany

The understanding of the high-frequency (hf) performance of soft-magnetic thin films for hf applications is critical for e.g. achieving good quality factors. The selection of the magnetic materials is usually based on the analysis of the full film magnetization dynamics like precessional frequency f_{res} and effective damping parameter α . For most practical applications, patterned magnetic films are used, introducing shape anisotropy and leading to multi-domain formation and thus altering the hf response. On the other hand, the use of magnetic multilayers can also strongly influence the dynamic magnetic properties.

In the presentation it is demonstrated how the internal microstructure of thin films as well as regular structuring in patterned magnetic elements can be used to alter the dynamic magnetic response of ferromagnetic thin films. For instance, by magnetic property patterning a coupled micromagnetic system with GHz oscillation frequency similar to that of coupled pendulums is generated (the time-domain step response of the magnetic system and the analysis of the two precessional modes is illustrated on the right).

This multi-mode response is compared to similar dynamic behavior as exhibited in regularly patterned structures, films with perpendicular anisotropy, amorphous films with nanometer crystallites, and partially exchange biased structures of different ferromagnetic materials. In one case the occurrence of the coupled magnetic modes is associated with



domain branching at the element's edges and dynamic mode-to-mode energy transfer results in a precessional decay-time exceeding the natural ferromagnetic material's relaxation time. In another example it will be shown how antiferromagnetic layers can be used to tailor the magnetization dynamics of ferromagnetic thin films even without the occurrence of exchange bias.

Special emphasis will be given to the comparison of the influence of static magnetic properties on the dynamic properties like precessional frequency and magnetic damping.

Support by BMBF project "MIMAK" and the German Science Foundation DFG is highly acknowledged. Special thanks go to J. Fassbender, A. Gerber, R. Kaltoven, R. Mattheis, A. Neudert, E. Quandt, U. Queitsch, R. Schäfer, L. Schultz and all other contributors.

- [1] J. Fassbender, J. McCord, JMMM 320, 579-596 (2008)
- [2] J. McCord, R. Kaltoven, T. Gemming, et al., Phys. Rev. B 75, 134418 (2007)
- [3] A. Gerber, J. McCord, C. Schmutz, et al., IEEE Trans. Magn. 43, 2624 (2007)
- [4] U. Queitsch, J. McCord, A. Neudert et al., J. Appl. Phys. 100, 93911 (2006)
- [5] J. McCord, T. Gemming, L. Schultz et al., Appl. Phys. Lett. 86 162502 (2005)
- [6] J. McCord, J. Paul, IEEE Trans. Magn. 39, 2359 (2003)

22TL-C-6

HIGH-FREQUENCY MAGNETIC PROPERTIES AND ATTENUATION CHARACTERISTICS OF BARIUM-FERRITE/EPOXY COMPOSITES

Li W., Lin G.Q., Wu Y.P. and Kong L.B.

Temasek Laboratories, National University of Singapore

This is a comprehensive report on high-frequency magnetic properties and attenuation characteristics for barium-ferrite/epoxy composites, based on work on Temasek Laboratories of National University of Singapore in the recent years.

Electromagnetic (EM) materials or composites, consisting of magnetic fillers and polymer, are widely applied in industry, commerce and defence, because the composites can strongly attenuate the EM energy that propagates into the material, thus achieving reflection deduction in the boundary between the material and free space.

Ferrites with soft magnetic properties are ideal fillers for the EM materials, due to their unique characteristics, such as relatively small permittivity, high resonance frequency, high resistivity, low density and good chemical stability. Most of spinel ferrites with large initial permeability and low loss are of wide applications in electric and electronic technology at low or radio frequency. The garnet ferrites have high gyromagnetic property, very low magnetic and dielectric loss. Hence, they are very useful in microwave non-reciprocal devices. However, the two ferrites are not suitable for use as EM materials at GHz frequency, due to their significantly low resonance frequency. On the other hand, barium ferrites with c-plane anisotropy are essentially soft magnetic materials, which have relatively large μ' and μ'' , and, at the same time, have significantly high anisotropy fields due to the low crystal symmetry, which lead to a high resonance frequency. Therefore, the barium ferrite composites have attracted much attention and been extensively studied.

The paper is divided into two parts. (1) To achieve low reflectivity and broad bandwidth at microwave frequency of 2-18 GHz, EM composites should have large μ' matching with relatively large ϵ' , large imaginary permeability μ''_{\max} to significantly attenuate the incident EM

wave, and the appropriate resonance frequency f_R . The methods for increasing μ' and μ'' and controlling f_R are introduced, including ion substitution, doping of small amount of oxides, modification of particle size and shape. (2) The barium ferrites are classified into different types, such as W-, Y-, Z- and M-type, according to the crystal structures. The high-frequency magnetic and dielectric properties and the typical dispersion characteristics have been comprehensively studied for the W-, Y-, Z- and M-type barium ferrite composites. The corresponding attenuation properties are calculated and the results show that the composites are potential candidates for use as EM attenuation materials with low reflectivity and broad bandwidth at 2-18 GHz.

22RP-C-7

MICROWAVE PROPERTIES OF FERROMAGNETIC NANOWIRES AND APPLICATIONS TO TUNABLE DEVICES

Spiegel J.¹, de la Torre J.², Darques M.², Piraux L.² and Huynen I.¹

¹Université Catholique de Louvain, Microwave Laboratory, B-1348 Louvain-la-neuve, Belgium,

E-mail : judith.spiegel@uclouvain.be

²Université Catholique de Louvain, PCPM Laboratory, B-1348 Louvain-la-neuve, Belgium

Microwave devices as filters, couplers and circulators demand nowadays small size and broad bandwidth. Ferromagnetic nanowired substrates (Fig. 1) are ideal candidates for this purpose due to their excellent material properties, the ability to build tunable or non-reciprocal planar devices for this frequency range. The applications of those composite materials are Electronic Bandgap filters, due to the occurrence of ferromagnetic resonance and circulators and isolators due to the anisotropy in the material. All these applications work without applying an external magnetic DC field, which is of great interest for the industry. Other advantages of such materials compared to classical ferrites are a higher operation frequency, a higher saturation magnetization and a higher resonant frequency.

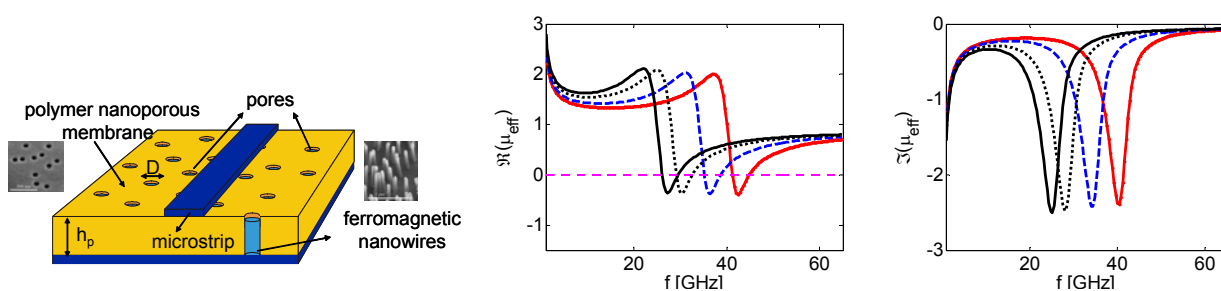


Fig 1.: (a) Microstrip line on ferromagnetic nanowired substrate used for FMR determination and as microwave circuit (b) real and (c) imaginary part of effective permeability, as a function of external applied DC magnetic field.

The “nanowired substrate” consists of a porous insulating membrane filled with ferromagnetic nanowires by electrodeposition. The effective permittivity of the material is a scalar and depends on the porosity and the height of the nanowires [1]. The effective permeability, noted μ_{eff} , can be deduced from the susceptibility tensor, containing κ and μ . We developed a variational model for this purpose [2, 3], which is able to predict the influence of ferromagnetic content and external applied DC field on the effective permeability. Figure 1(bc) shows that, besides the nonreciprocity induced by non zero off-diagonal term κ , the ferromagnetic “nanowired” substrate achieves several functionalities: stopband filters exploiting strong absorption at FMR frequency, single negative metamaterials in the frequency range where

μ_{eff} is negative, and frequency-tunable devices or magnetic sensors, due to the high sensitivity to external DC magnetic field. All these concepts will be illustrated by the practical applications listed at the top the abstract.

Support by the European Union under projects EU-NoE METAMORPHOSE and EU-STREPS-NANOTEMPLATES, and by the Research Science Foundation, Belgium, is acknowledged.

- [1] J. Spiegel, J. de la Torre, M. Darques, L. Piraux, I. Huynen, *IEEE MWCL*, vol. 17, no. 7 (2007)
 [2] A. Berk, *IEEE Transactions on Antennas and Propagation*, 4 (1956) 104-111.
 [3] J. Spiegel, L. Piraux, I. Huynen, 37th EuMC, 8-12 October 2007, Munich, Germany.

22RP-C-8

HIGH FREQUENCY MAGNETIC PROPERTIES OF Co_2MnGe HEUSLER THIN FILMS

Belmeguenai M.^{1,2}, Zighem F.², Martin T.¹, Woltersdorf G.¹, Rousigné Y.², Chérif S-M.², Westerholt K.³ and Bayreuther G.¹

¹Institut für Experimentelle Physik, Universität Regensburg, Universitätsstraße 31, 93040 Regensburg, Germany

²LPMTM, CNRS, Université Paris 13, 99 Av. J-B. Clément 93430 Villetaneuse, France

³Ruhr-Universität Bochum, 44780 Bochum, Germany

Heusler alloys like Co_2MnGe and Co_2MnSn are considered as excellent candidates for spintronic applications, since the Curie temperature is high (905 K) and there is a good lattice matching with the GaAs semiconductor family [1]. We have therefore studied the magnetic anisotropy and the dynamic properties of Co_2MnGe thin films with ferromagnetic resonance (FMR) and micro-stripe line FMR spectroscopy (MS-FMR).

Co_2MnGe films of 30, 50 and 75 nm in thickness were grown by RF-sputtering at an Ar pressure of 5×10^{-3} mbar on Al_2O_3 a-plane substrates at a growth temperature of 470°C. Before deposition of the Heusler film, a seed layer of V, 4 nm thick, was deposited and a final protective overlayer of gold, 4 nm thick, was grown on top of the film [2].

The study of spin wave frequencies in dependence of the in-plane sample orientation allows for the determination of anisotropy constants of thin magnetic films while the out-of-plane angular dependence gives the effective magnetization. This in-plane angular dependency of the resonance frequency (at 130 Oe) and the dispersion relation of the uniform precession and the first perpendicular standing spin wave (PSSW) for the 50-nm-thick sample are represented on Fig.1a and Fig.1b, respectively. The sample exhibits a clear predominant four-fold magnetic anisotropy beside a uniaxial anisotropy along (110). This uniaxial anisotropy is most probably induced by the growth condition (Vanadium seed layer) as far as the Co_2MnGe films are fcc. For each sample, from the in-plane and the out-of-plane resonance field values, the effective magnetization ($4\pi M_{\text{eff}}$) and the g-factor are calculated ($g=2.17$). These values are then used to fit both the in-plane angular- and the field-dependence of the resonance frequency (Fig. 1b) of the uniform and PSSW mode to determine the uniaxial ($H_u=2K_u/M_s$), the fourfold ($H_2=4K_4/M_s$) anisotropy fields and the exchange stiffness constant. More details about the obtained results and analysis will be presented.

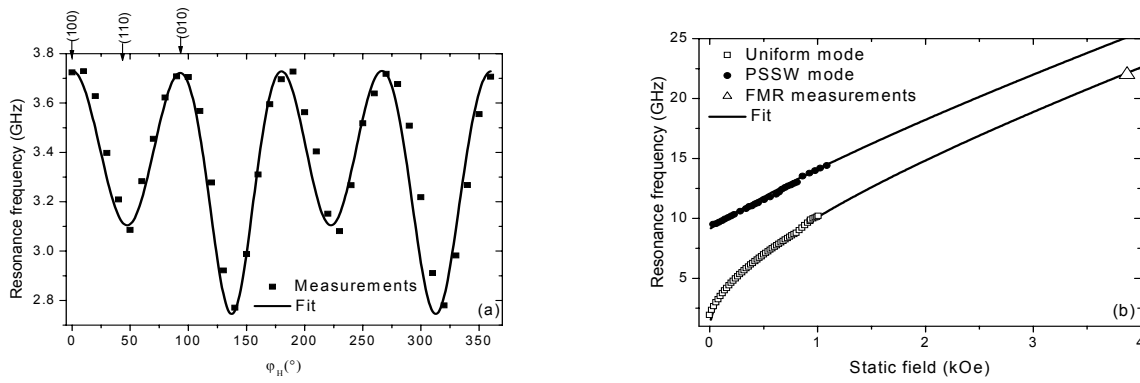


Figure 1: (a) MS-FMR in-plane angular-dependence, and (b) resonance frequency of the uniform and the first PSSW modes as a function of the in-plane field (parallel to [100] direction) of 50-nm-thick Co_2MnGe Heusler.

- [1] S. Picozzi, A. Continenza, and A. J. Freeman, *J. Phys. Chem. Solids* 64, 1697 (2003).
 [2] U. Geiersbach, K. Westerholt and H. Bach *J. Magn. Magn. Mater.* 240 (2002), p. 546

22 June Sunday

12:00-13:30

15:00-17:00

oral session

22TL-D

22RP-D

**“Low Dimensional
Magnetism”**

22TL-D-1

ANOMALOUS LOW ENERGY EXCITATIONS IN ONE DIMENSIONAL CUPRATES

Buchner B.

Institute for Solid State Research, IFW Dresden, Germany

The low energy excitations in several quasi one-dimensional $S=1/2$ antiferromagnets, such as SrCuO_2 , Sr_2CuO_3 and $\text{Li}_2\text{ZrCuO}_4$, were investigated using a broad spectrum of experimental techniques. While the magnetic susceptibility and the specific heat of the Sr cuprates, which contain corner sharing CuO_4 plaquettes with a large antiferromagnetic coupling between the Cu spins, are in a fair agreement with predictions based on a simple Heisenberg model, the measurements of the Cu-NMR yields very surprising results. In particular, the data signal the development of magnetically different Cu sites below 100K, i.e. well above the transition to a static magnetic order. In the same temperature range an anomalous behaviour is found for the dielectric constant pointing to a strange coupling between electronic and magnetic degrees of freedom which is not expected in the framework of a Heisenberg model for $S=1/2$ antiferromagnetic chains.

A strange magnetoelectric coupling is also found in $\text{Li}_2\text{ZrCuO}_4$, whose magnetic properties are determined by competing nearest neighbour and next nearest neighbour interactions characteristic for chains built by edge sharing CuO_4 plaquettes. This magnetic frustration causes very unusual magnetic and thermodynamic properties which we have analysed in a J_1 - J_2 model¹. In addition, our recent NMR and ESR data suggest that the mobility and/or the position of Li ions are important for the magnetic properties of the Cu ions. This leads to a novel mechanism for a “multiferroic coupling” which is also revealed from the measurements of the temperature dependence of the dielectric constant.

[1] S.L.Drechsler et al., *Phys. Rev. Lett.* **98** (2007) 077202

22TL-D-2

VISUALIZING HEAT TRANSPORT IN QUANTUM MAGNETS

van Loosdrecht P.H.M.¹, Otter M.¹, Pchenichnikov M.S.¹, Krasnikov V.¹, Revcolevschi A.²

¹Zernike Institute for Advanced Materials, University of Groningen, The Netherlands

²Laboratoire de Physico-chimie de l'Etat Solide, Universite Paris XI, France

Low dimensional quantum magnets show an unusually high thermal conductivity originating from the magnetic excitations in these compounds.[1] The conductivity is highly anisotropic and dwarfs the usual phonon contribution, making low dimensional quantum magnets highly relevant for heat management in electronic devices. The present work focuses on optical methods to study and control the heat conduction in magnetically low dimensional cuprate systems as for instance found in the magnetic chain compounds SrCuO_2 and Sr_2CuO_3 , and the so-called telephone number ladder compounds $(\text{La,Sr,Ca})_{14}\text{Cu}_{24}\text{O}_{41}$. It will be shown that luminescence microscopy techniques yield direct information on both the magnitude and the anisotropy of the heat diffusion in these materials. This can be achieved either by direct imaging (see figure 1), or by a ‘time-of-flight’ technique which studies the propagation of a heat pulse through the materials. This contribution presents and discusses results obtained using thermal

imaging and ‘time-of-flight’ experiments. In addition, it will address the potential use of these materials in technological applications, as well as the possibilities to control the heat transport for advanced thermal management schemes.

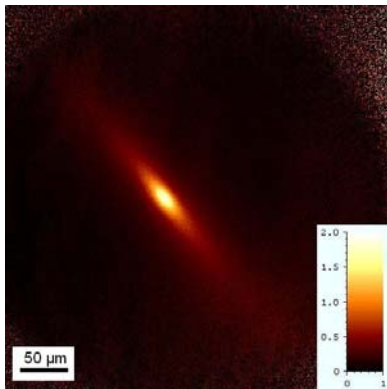


Figure 1. Thermal image of the *ac*-plane of $\text{La}_5\text{Ca}_9\text{Cu}_{24}\text{O}_{41}$ generated by a localized heat pulse in the center of the image. It shows a highly anisotropic pattern due to the high thermal conductivity in the (diagonal) *c*-direction.

This work is supported by the NOV MAG EU-FP6 project (proj. nr. 032980, www.novmag.eu)

[1] C. Hess, C. Baumann, U. Ammerahl, B. Buchner, F. Heidrich-Meisner, W. Brenig, A. Revcolevschi, *Phys. Rev. B*, **64** (2001) 184305.

22TL-D-3

NEUTRON SCATTERING STUDY OF MASSIVE MAGNONS IN QUASI-1D: SPIN LADDERS AND TUBES

Zheludev A.

Oak Ridge National Laboratory, Oak Ridge, TN 37831, USA.

Quasi-one-dimensional quantum spin liquids, such as weakly coupled even-legged $S=1/2$ spin ladders or spin tubes, have a singlet non-magnetic ground state and gap in the excitation spectrum. Their low-temperature properties can be described in terms of triplet massive quasiparticles.

These magnons possess some unique features due to the peculiar topology of one dimension. For example, two-particle interactions totally destroy single-particle states for certain energy and momentum transfers, resulting in a so-called termination of the magnon spectrum. At a finite temperature collisions between quasiparticles lead to totally universal renormalization of their masses and lifetimes. At high magnetic fields the quasiparticles may condense in the ground state producing a "quantum spin solid" phase. In that exotic state "conventional" magnetic order co-exists with excitations that are totally outside conventional spin wave theory. Depending on the details of the spin Hamiltonian, the transition itself can be fully equivalent to Bose-Einstein condensation, yet can also be of a chiral universality class.

These diverse phenomena are best probed by neutron scattering experiments that directly measure the spin correlation functions and excitation spectra. In the talk I will review recent experimental results on two specific model compounds: the spin-ladder material IPA-CuCl_3 [1,2,4] and the 4-leg spin-tube compound $\text{Sul-Cu}_2\text{Cl}_4$ [3,4].

[1] T. Masuda *et al.*, *Phys. Rev. Lett.* **96**, 047210 (2006).

[2] V. O. Garlea *et al.*, *Phys. Rev. Lett.* **98**, 167202 (2007); A. Zheludev *et al.*, *Phys. Rev. B* **76**, 054450 (2007).

[3] V. O. Garlea *et al.*, Phys. Rev. Lett. **100**, 037206 (2008).

[4] A. Zheludev *et al.*, Phys. Rev. Lett., accepted (2008); arXiv:0711.4094.

22TL-D-4

ORIGIN OF MAGNETIC ANISOTROPY OF GEOMETRICALLY FRUSTRATED KAGOME STAIRCASE LATTICES

Szymczak R.¹, Aleshkevych P.¹, Adams C.P.^{2,4}, Barilo S.N.³, Berlinsky A.J.^{2,5}, Clancy J.P.², Fink-Finowicki J.¹, Gaulin B.D.^{2,5}, Ramazanoglu M.², Shiryayev S.V.³, Yamani Z.⁶, Szymczak H.¹

¹Institute of Physics, Polish Academy of Sciences, 02-668 Warsaw, Poland

²Department of Physics and Astronomy, McMaster University, Hamilton, Ontario, Canada

³Institute of Solid State and Semiconductor Physics, NAS, Minsk, Belarus

⁴Department of Physics, St. Francis Xavier University, Antigonish, NS, Canada

⁵Canadian Institute for Advanced Research, Toronto, Ontario, Canada

⁶Canadian Neutron Beam Centre, NRC, Chalk River, Ontario, Canada

Frustrated magnetic materials have recently attracted much interest, both theoretically and experimentally. This interest is stimulated by attempts to find new fundamental effects such as the magnetization plateaus and the magnetization jumps which represent a genuine macroscopic quantum effect. Of particular interest has been magnetism on the two-dimensional kagome- staircase $M_3V_2O_8$ ($M = Ni, Co$) lattice having highly frustrated nature and an interplay with the strong quantum fluctuations [1]. This system displays a rich, highly anisotropic, phase diagram. This phase diagram is expected to be determined by anisotropic exchange interactions as well as by crystal field interactions (magnetocrystalline anisotropy).

To gain insights into the magnetic interactions in kagome staircase $M_3V_2O_8$ oxides, we decided to investigate mechanisms responsible for their magnetic anisotropy. Following methods have been used:

- Inelastic neutron scattering measurements on single crystal $Co_3V_2O_8$
- Low temperature high field magnetization (field induced phase transitions) and high temperature susceptibility measurements of single crystals $Co_3V_2O_8$, $Ni_3V_2O_8$, $Ni_{3-3x}Co_xV_2O_8$ ($x = 0.03$) and $Co_{3-3x}Mg_xV_2O_8$ ($x = 0.05, 0.1$)
- EPR of Co^{2+} ions in kagome staircase $Mg_3V_2O_8$ single crystals

The single-ion anisotropy Hamiltonian was used to analyze experimental results. It was shown that the magnetic anisotropy in kagome staircase $M_3V_2O_8$ oxides has single-ion origin. Magnetocrystalline anisotropy is significantly weaker in $Ni_3V_2O_8$ than in $Co_3V_2O_8$ crystals. Cobalt doping increases considerably crystal field parameters in $Ni_3V_2O_8$ and induces change of an easy axis direction. This reorientation is due to presence of Ising- like Co^{2+} ions strongly coupled to the kagome lattice. The same effect is also responsible for the anisotropy of the paramagnetic Curie temperatures, which increases with Co ions doping.

The work was supported in part by the Ministry of Science (Poland) under the project N202 057 32/1201.

[1] R. Szymczak, M. Baran, R. Diduszko, J. Fink-Finowicki, M. Gutowska, A. Szewczyk, and H. Szymczak, *Phys. Rev. B* **73**, (2006) 094425.

22TL-D-5

FERROELECTRICITY IN AN ISING CHAIN MAGNET*Kiryukhin V., Choi Y.J., Yi H.T., Lee S., Cheong S-W.*

Dept. Physics and Astronomy, Rutgers University, Piscataway, NJ 08854, USA

The concept of magnetism-driven ferroelectricity has recently drawn a significant attention [1]. Magnetically-driven ferroelectrics exhibit intrinsically large magnetoelectric coupling, which gives rise to dramatic magnetoelectric effects. This opens up a possibility for controlling electric properties (e.g. electric polarization) by a magnetic field, and vice versa. These effects may find applications in novel devices, for example, in spintronics. Two microscopic mechanisms of magnetoelectric coupling have been extensively discussed in application to the recently-discovered magnetoelectrics: inverse Dzyaloshinskii-Moriya (DM) interaction in spiral magnets, and exchange striction in (nearly) collinear chain magnets. Most of the actual compounds were found to belong to the first class. However, unlike the DM interaction, exchange striction is associated with symmetric superexchange, and therefore is, generally, a much stronger effect. Thus, magnetic ferroelectrics driven by exchange striction hold significant promise as candidate materials with enhanced functional properties.

In this talk, we briefly review the magnetoelectric coupling mechanisms described above, and present a discovery [2] of a conceptually simple experimental system of the exchange-striction type. The compound in question, $\text{Ca}_3(\text{Co,Mn})_2\text{O}_6$, consists of frustrated quasi-one-dimensional Ising chains assembled on a triangular lattice. Due to magnetic frustration, the up-up-down-down magnetic order is realized. Combined with the Co/Mn ionic order, it breaks inversion symmetry and gives rise to a ferroelectric moment. Thus, $\text{Ca}_3(\text{Co,Mn})_2\text{O}_6$ is a clean realization of a simple exchange-driven model magnetoelectric that was previously discussed theoretically [1]. We also discuss interesting effects associated with interchain geometrical frustration (magnetoelectric freezing).

Support by the US DOE, and KOSEF is acknowledged.

[1] S.-W. Cheong and M. Mostovoy, *Nature Materials* **6**, 13 (2007).

[2] Y.J. Choi, H.T. Yi, S. Lee, Q. Huang, V. Kiryukhin, and S.-W. Cheong, *Phys. Rev. Lett.* **100**, 047601 (2008).

22TL-D-6

TWO-MAGNON DECAYS IN NONCOLLINEAR ANTIFERROMAGNETS*Zhitomirsky M.E.*

CEA, INAC, SPSMS, 38054 Grenoble, France

Quantum many-body system with a non-conserved number of particles may have cubic vertices, which describe interaction between one- and two-particle states. Two well-known examples are phonons in crystals, where cubic anharmonicities are responsible for a finite thermal conductivity, and quasiparticles in superfluid ^4He , where single-particle branch disappears completely at high energies due to two-roton decays. Two-magnon decay processes are also present in *noncollinear* quantum spin systems such as an antiferromagnet on a frustrated triangular lattice [1] and a square lattice antiferromagnet in an applied magnetic field [2]. Using the anharmonic spin-wave theory I discuss effect of quantum fluctuations on the dynamics

of the above two magnetic systems. The spontaneous ($T=0$) decays produce various peculiarities in the magnon spectra. In particular, they can lead to a logarithmic divergence of the decay rate near special lines (points) in the Brillouin zone.

[1] A. L. Chernyshev and M. E. Zhitomirsky, *Phys. Rev. Lett.* **97**, 207202 (2006).

[2] M. E. Zhitomirsky and A. L. Chernyshev, *Phys. Rev. Lett.* **82**, 4536 (1999).

22RP-D-7

MAGNETIC RESONANCE OF THE SPIN-GAP MAGNET $\text{NiCl}_2\text{-4SC}(\text{NH}_2)_2$ IN THE FIELD-INDUCED ORDERED PHASE

Smirnov A.I.¹, Zvyagin S.A.², Wosnitza J.², Kolezhuk A.K.³, Zapf V.S.⁴, Jaime M.⁴,
Paduan-Filho A.⁵, Glazkov V.N.¹, Sosin S.S.¹

¹P.L.Kapitza Institute for Physical Problems RAS, 119334 Moscow, Russia

²HMFL, Forschungszentrum Dresden - Rossendorf, 01314 Dresden, Germany

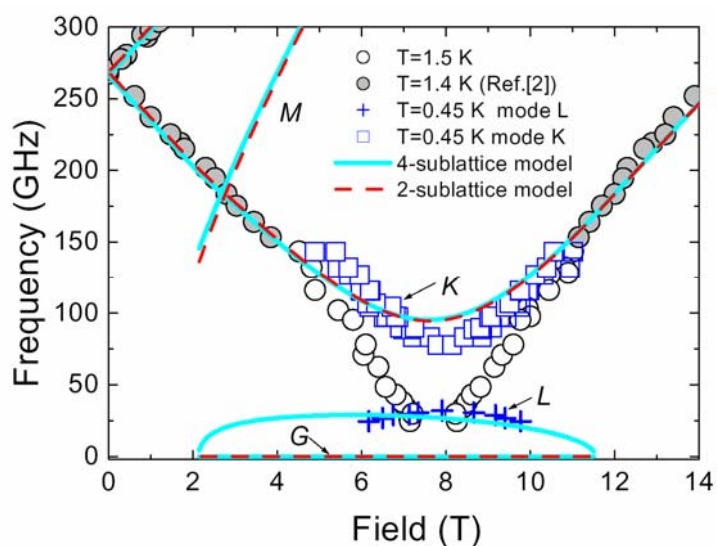
³Institut für Theoretische Physik C, RWTH Aachen, 52056 Aachen, Germany

⁴National High Magnetic Field Laboratory, LANL, MS-E536, Los Alamos, NM 87545, USA

⁵Instituto de Física, Universidade de Sao Paulo, 05315-970 Sao Paulo, Brazil

$\text{NiCl}_2\text{-4SC}(\text{NH}_2)_2$ (known as DTN) is a $S=1$ spin-chain material with a strong single-ion uniaxial anisotropy. The spin-gap of a quantum disordered singlet phase is located at the wave vector $q=\pi/a$. This gap may be closed by a magnetic field $H_{c1}=2$ T. In the magnetic field above H_{c1} and at the temperature below 1 K there is a field-induced antiferromagnetic phase, interpreted in terms of Bose-Einstein condensation (BEC) of magnons [1]. According to BEC scenario, for a conventional two-sublattice ordering, the excitation spectrum should have a Goldstone (gapless) mode and an upper gapped mode (see the dashed line on the Figure). We performed a study of the low-energy excitation spectrum of DTN by means of high-field electron spin resonance measurements, both above and below the ordering temperature. At cooling through $T=1$ K, the most efficient change of the magnetic resonance frequency occurs in the vicinity of the magnetic field $H_0=8$ T, closing the gap of $q=0$ excitations. Surprisingly, below $T=1$ K, we have found two gapped modes (K and L on the Figure).

Two gapped modes could be explained by crystal lattice distortions, breaking the uniaxial symmetry. This explanation, however, is not consistent with several features of the observed spectrum. The observed two-gap spectrum can be consistently interpreted within a four-sublattice model with a weak interaction between two tetragonal two-sublattice subsystems and unbroken axial symmetry (solid lines on the Figure). In this model, a gapless Goldstone mode G exists along with two gapped modes. The four sublattice spin structure in form of two weakly interacting tetragonal subsystems is natural for the body-centered tetragonal crystal lattice of DTN.



- [1] V. S. Zapf *et al.*, *Phys. Rev. Lett.* **96** (2006) 077204.
 [2] S. A. Zvyagin *et al.*, *Phys. Rev. Lett.* **98** (2007) 047205.

22RP-D-8

MAGNETIC AND ELECTRONIC PROPERTIES OF DOPED OXIDE NANOTUBES

Klingeler R.¹, Hellmann I.¹, Popa A.¹, Kataev V.¹, Vavilova E.^{1,2}, Arango Y.¹, Täschner C.¹, Knapfer M.¹, Masquelier C.³, Klauss H.-H.⁴, Zakharova G.S.⁵ and Büchner B.¹

¹Leibniz-Institute for Solid State and Materials Research IFW Dresden, Germany

²Kazan Physical Technical Institute, RAS, Kazan, Russia

³Laboratoire de Réactivité et de Chimie des Solides, Amiens, France

⁴Department of Physics, Technical University of Dresden, Germany

⁵Institute of Solid State Chemistry, RAS, Yekaterinburg, Russia

We present studies on a new class of nanoscale low-dimensional magnets based on mixed valent transition metal oxides. The low dimensional structure and the large surface allows to change the valency of the metal ions electrochemically e.g. by Li intercalation or to introduce magnetic ions (Fe,Cr,Co,Mn,Ni) which both strongly affects the electronic and magnetic properties of the nanostructures. Here, we present data on VO_x, MnO₂, MoO₃, and Fe₂O₃ nanostructures, among them optical, photoemission, and electron energy-loss spectroscopy as well as static magnetization, ESR, μ SR and NMR studies.

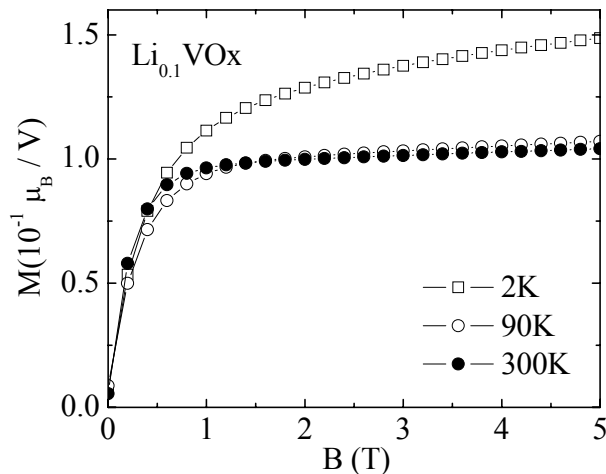


Fig.: Magnetization of electrochemically doped Vanadiumoxide-Nanotubes.

In the example of vanadium oxide multiwall nanotubes (VO_x-NTs), we find an averaged vanadium valency of about 4.4⁺ in the undoped case [1]. Our data imply that, in the structurally well-defined vanadium-spin chains in the walls, owing to an inhomogeneous charge distribution, antiferromagnetic dimers and trimers occur. We find a spin gap of the order of 700 K [2]. Upon electron doping of VO_x-NTs, our spectroscopic data confirm a higher number of magnetic V⁴⁺ sites [3]. Interestingly, room temperature ferromagnetism evolves after electrochemical intercalation of Li making VO_x-NTs a novel type of self-assembled nanoscaled ferromagnets (see Fig.). This finding is corroborated by recent μ SR data.

- [1] X. Liu *et al.*, *Phys. Rev. B* **72**, 115407 (2005)
 [2] E. Vavilova *et al.*, *Phys. Rev. B* **73**, 144417 (2006)
 [3] I. Hellmann *et al.*, *submitted* (2008)

Support by the DFG through GZ436Rus17/90/06 and KL 1824/2 is acknowledged.

22RP-D-9

MAGNETIC RESONANCE STUDY OF THE FRUSTRATED ANTIFERROMAGNET ZnCr_2O_4

Glazkov V.N.¹, Farutin A.M.¹, Tsurkan V.^{2,3}, Krug von Nidda H.-A.², Loidl A.²

¹P.L. Kapitza Institute for Physical Problems RAS, Kosygin str.2, 119334 Moscow, Russia

²Experimental Physics V, EKM, University of Augsburg, 86135 Augsburg, Germany

³Institute of Applied Physics, Academy of Sciences, MD-2028 Chisinau, R. Moldova

Exchange interaction is the conventional driving force for the formation of magnetic order. However, in the case of geometrically frustrated magnets, due to the geometry of the exchange bonds, the exchange interaction alone cannot establish a unique ordered ground state. Thus, in exchange approximation the classical antiferromagnet should remain in the disordered macroscopically degenerate state down to $T=0$. This degeneration could be lifted by weaker interactions (dipolar, relativistic or further neighbour exchange) or by fluctuations. The choice of the ordered state is governed by the subtle interplay of numerous weak interactions that could result in exotic magnetically ordered phases and in complicated magnetic phase diagrams.

The spinel ZnCr_2O_4 is a model system to study geometric frustration [1]. The magnetic Cr^{3+} ions form a pyrochlore lattice (lattice of corner sharing tetrahedra). Despite of the strong exchange interaction (Curie-Weiss temperature Θ is about -390K) it remains disordered down to $T_N=12.5\text{K}$ ($\Theta/T_N \approx 30$). The magnetic phase transition is coupled with a structural transition: lattice deformation reduces the lattice symmetry and removes the frustration of the magnetic subsystem. The transition is of first order. The structure of the magnetically ordered phase is not deciphered completely yet [2].

Magnetic resonance provides a tool to probe the low-energy dynamics of a magnet and, thus, to obtain information on the structure of the ordered phase. We have observed an antiferromagnetic resonance signal below T_N . It demonstrates nonlinear frequency-field dependence with several branches, zero-field gaps of 20, 25 and 115 GHz, and softening of certain modes indicating a spin-reorientation transition. The observed frequency-field dependences correspond to a noncollinear magnetic structure and can be described within framework of exchange symmetry theory. We have found that several types of magnetic and structural domains are present and that some of these domains can be suppressed by field cooling. The analysis of the experimental data indicates that the lattice symmetry below the transition is not tetragonal, as was reported before, but orthorhombic.

Support by RFBR (project 07-02-00725), Russian Science Support Foundation, and DFG via SFB 484 is acknowledged.

[1] S.-H.Lee, C.Broholm, W.Ratcliff et al., *Nature* **418**, 856 (2002)

[2] S.-H.Lee, G.Gasparovich, C.Broholm et al, *J.Phys.:Condens.Matter* **19**, 145259 (2007)

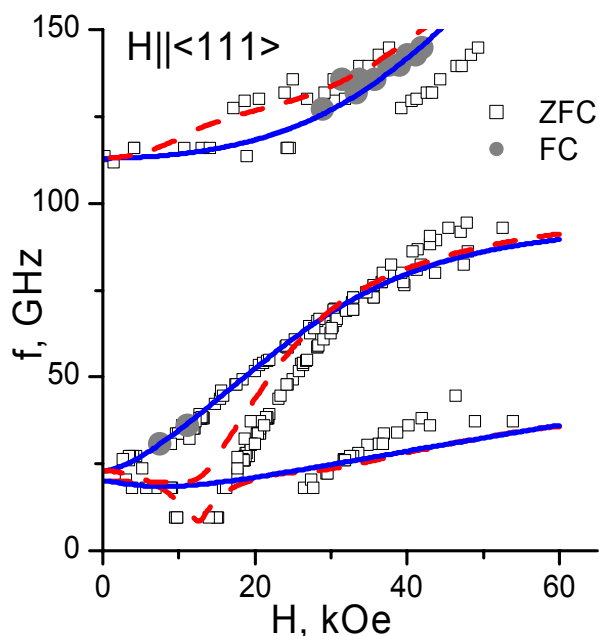


Figure 1. $f(H)$ dependence. Solid and dashed curves correspond to the different orthorhombic domains' resonance modes.

22RP-D-10

**SPIN-MODULATED QUASI-ONE DIMENSIONAL
ANTIFERROMAGNET LiCuVO_4**

Svistov L.E.¹, Büttgen N.², Prozorova L.A.¹

¹P.L. Kapitza Institute for Physical Problems RAS, 119334
Moscow, Russia

²Center for Electronic Correlations and Magnetism EKM,
Experimentalphysik V, Universität Augsburg, D-86135 Augsburg, Germany

The quasi-one dimensionality of the spin system in LiCuVO_4 is provided by the magnetic ions of Cu^{2+} ($3d^9$ configuration, $S=1/2$). Lithium and copper ions share the octahedral sites in the orthorhombically distorted spinel structure in a way that the copper ions are arranged along the chains separated by the nonmagnetic ions of lithium, vanadium and oxygen. The temperature dependence of the magnetic susceptibility exhibits a broad maximum at around $T=28$ K, typical for low-dimensional antiferromagnets, and a sharp anomaly at $T=2.3$ K, which is associated with the establishing of three dimensional magnetic order. Elastic neutron diffraction experiments [1] on single crystals of LiCuVO_4 revealed that the 3D ordered phase exhibits an incommensurate, noncollinear magnetic structure. According to that work, the wave vector of this magnetic structure is directed along the copper chains $\mathbf{k}_{ic} \parallel \mathbf{b}$ and the value of the ordered magnetic moments of the Cu^{2+} ions amounts to $0.31\mu_B$, lying within the ab -planes. At the presence of static magnetic fields two spin-reorientational transitions were observed. One at magnetic field $H_{c1} \approx 25$ kOe applied within the crystallographical ab -plane, and the second one at $H_{c2} \approx 75$ kOe [2,3]. Spectra of ^7Li nuclear magnetic resonance show [3] that, within the magnetically ordered phase of LiCuVO_4 in the low-field range $H < H_{c1}$, a planar spiral spin structure is realized with the spins lying in the ab -plane in agreement with neutron scattering studies [1]. Based on nuclear magnetic resonance spectra simulations, the transition at H_{c1} can well be described as a spin-flop transition, where the spin plane of the magnetically ordered spiral structure rotates to be perpendicular to the direction of the applied magnetic field.

In the present work possible magnetic structures of LiCuVO_4 in the high field range $H > H_{c2}$ are discussed. We performed the ^7Li and ^{51}V NMR spectra simulations for different magnetic structures and compare these with spectra obtained in experiments. From the form of ^{51}V nuclear magnetic resonance spectra it is concluded, that high-field phase exhibits a modulation of the spin projections along the direction of the applied magnetic field H for all field orientations. The amplitude of this modulation is near $0.3 \mu_B$. The best fit of ^7Li nuclear magnetic resonance spectra can be obtained by assumption of spin-modulated structure with modulation along the field direction, with magnetic disorder in c -direction.

[1] B.J. Gibson et al.: *Physica B* **350**, (2004) 253 .

[2] M.G. Banks et al.: *J.Phys.:Condens.Matter* **19**, (2007) 145227.

[3] N. Büttgen et al.: *Phys.Rev. B* **76**, 014440, (2007)

22 June Sunday

12:00-13:30

15:00-17:00

oral session

22TL-E

22RP-E

**“Soft Magnetic
Matter”**

22TL-E-1

FLEXIBLE FERROMAGNETIC FILAMENTS AND THE INTERFACE WITH BIOLOGY

Ērglis K., Belovs M., Cēbers A.
University of Latvia, Zēļļu 8, Latvia

Flexible ferromagnetic filaments may be produced artificially and exist in the living world – magnetotactic bacteria use them for the navigation purposes [1,2]. Ferromagnetic filaments investigated in the present work are synthesized by linking functionalized core-shell ferromagnetic particles with 1000 bp long biotinized DNA fragments. Their flexibility is illustrated by the anomalous orientation of the filament in the AC magnetic field H with a frequency ω , which is high enough. Its energy reads [3] (\vec{h}, \vec{n} are the unit vectors along the field and axis of a filament respectively) $E = 2ACm^2 \chi_1 (\vec{h} \cdot \vec{n})^2 / L$. Here

$Cm = MHL^2 / A$ is the magnetoelastic number, A is a bending modulus, M is the magnetization per unit length, $2L$ is the length of filament. Magnetic susceptibility χ_1 depends on $\omega\tau$ (τ is the elastic relaxation time) [3]. Kinetics of the filament orientation at different field strengths is shown in Fig.1. Estimate of the magnetic moment of core-shell particle $m = 6 \cdot 10^{-13}$ emu and dependence of the relaxation rate on the field strength for the bending modulus gives the value $A = 9 \cdot 10^{-13}$ erg·cm. This value for 31 μm long filament in the field 28 Oe gives $Cm \cong 11$, which is in good agreement with the value of the magnetoelastic number obtained from dynamics of U and S like deformation modes of the filament at magnetic field inversion. Basing on these results magnetic twisting cytometry for the study of the properties of cytoskeleton of the magnetotactic bacterium is proposed and investigated experimentally.

Rich behaviour of ferromagnetic filaments in the viscous fluid is predicted under the action of twist. Phase diagram in the plane (Cm, χ) ($Cm = \pm MHL^2 / A$; $\chi = C\Omega_3 L / A$, Ω_3 is twist, C is twist modulus) as obtained numerically by a linear stability analysis of the filament with free and

unclamped ends is shown in Fig.2. Solid lines correspond to the neutral curves of buckled filaments. On the curves shown by dashed lines the complex eigenvalues arise, which correspond to the rotational modes of the filaments with the broken mirror symmetry. For large values of applied twist beautiful shapes of the filaments, as shown in Fig.3, are found. The finding of rotational modes allows one to create magnetic microdevices of new types.

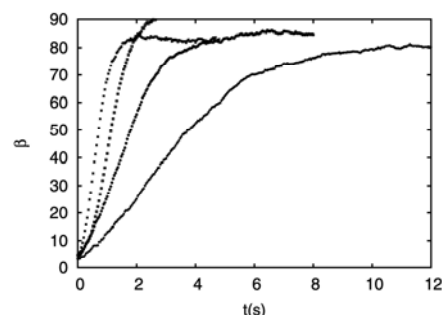


Fig.1. Orientation angle as a function of time for $H = 14; 21; 28; 35$ Oe.

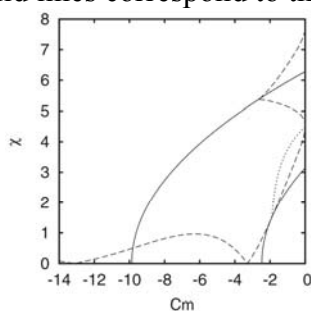


Fig.2. Phase diagram of twisted filament.

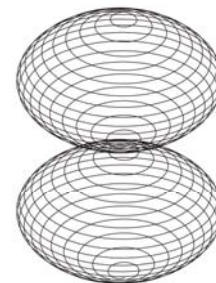


Fig. 3. Neutral shape of twisted filament $\chi = 2\pi + 250$.

- [1] A.Scheffel et al, *Nature*, **440** (2006) 110.
[2] K.Ērglis et al, *Biophysical Journal*, **93** (2007) 1402.
[3] M.Belovs, A.Cēbers, *Phys.Rev.E*, **73** (2006) 051503.

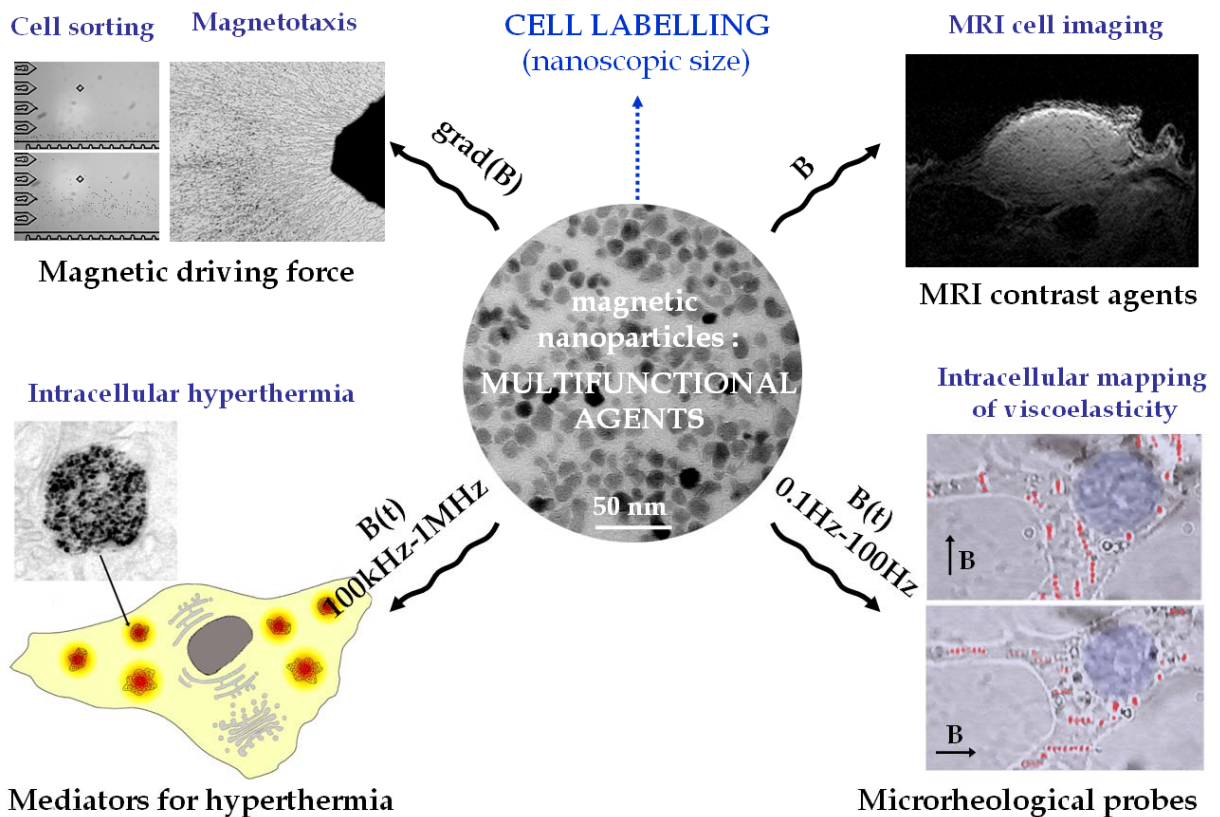
22TL-E-2

MAGNETIC NANOPARTICLES FOR BIOMEDICAL STRATEGIES

Wilhelm C. and Gazeau F.

Laboratoire Matière et Systèmes Complexes,
CNRS & University Paris 7, Paris, France

Labeling living cells with magnetic nanoparticles has received increasing interest for the last ten years, mainly because of the emerging method of MRI cell imaging. A few years ago, we proposed the use of anionic maghemite nanoparticles as efficient agents for cell internalisation. Since this date, we achieved, with these nanoparticles, the magnetic labelling of a large variety of cells, demonstrating that this magnetic cell labelling procedure was ubiquitous and biologically innocuous. Conferring magnetic properties to cells has allowed high sensitive and non invasive MR detection of a specific cell population in living organisms. Beyond imaging, the concept of “magnetic cells” opens new possibilities for cell manipulation by non-contact constraints. Magnetic forces at a distance could be used to control the movement of flowing cells (with application in cell sorting), but also to influence the organization and the migration of cells on a substrate (cell magnetotaxis). Inside the cells, the nanoparticles concentrate in pre-existing intracellular membrane-bound vesicles known as endosomes. This renders these compartments magnetic, and allows them to be manipulated within the intracellular environment by applying an external rotating magnetic field in order to explore the local mechanical properties of the cell interior. Finally magnetic nanoparticles can be used as heat sources for magnetic hyperthermia. Under the influence of an alternating high frequency magnetic field, they generate heat through relaxation processes. Intracellular magnetic endosomes localise the source of heat in the internal volume of the cell, with direct application for tumour cell therapies.



22RP-E-3

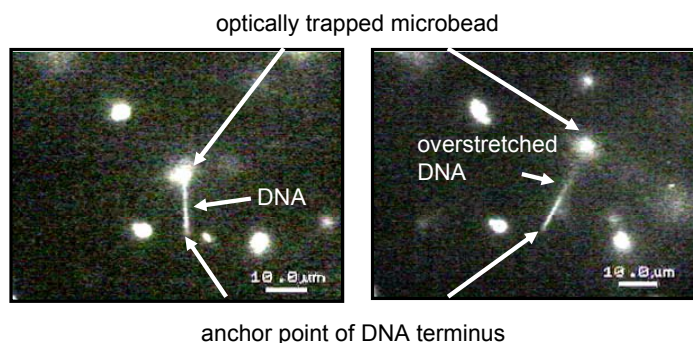
PHYSICAL MANIPULATION OF SINGLE-MOLECULE DNA USING MICROBEAD AND ITS APPLICATION TO DNA-PROTEIN INTERACTION

Kurita H.¹, Yasuda H.¹, Takashima K.¹, Katsura Sh.², and Mizuno A.¹

¹Department of Ecological Engineering, Toyohashi University of Technology,
1-1 Tempaku-cho, Toyohashi, Aichi 441-8580, Japan

²Department of Chemical and Environmental Engineering, Gunma University,
1-5-1 Tenjin-cho, Kiryu, Gunma 376-8515, Japan

Single-molecule imaging and single-molecule detection techniques have been investigated to analyze various DNA-protein interactions. Real-time fluorescent observations are particularly helpful for understanding single-molecule phenomena since the positions of individual protein or DNA molecules can be directly detected by fluorescent labeling. In this field, single-molecule DNA manipulation is a crucial technique, too. Because the form of DNA molecules always changes in solution by Brownian motion, a “physical form control” technique is required to measure the length of individual fluorescent-stained DNA and position of fluorescent-labeled proteins. DNA manipulation methods using a flow solution or electrostatic force are widely used [1]. Optical trapping and magnetic trapping of a microbead are also a powerful technique in single-molecule studies [1, 2]. In this study, we carried out single-molecule DNA manipulation using optical trapping and modification of glass surface for one-end immobilization of DNA molecule. One end of lambda DNA (48.5 kbp, linear) modified with thiol group was immobilized on a glass surface that was modified with dichlorodimethylsilane. The other end of the lambda DNA was modified with biotin. The biotinylated end of the DNA was attached on a streptavidin-coated polystyrene bead. Single-molecule DNA was manipulated by trapping a polystyrene bead that was attached to the DNA molecule (see figure). We controlled the form of an individual DNA molecule by moving the focal point of IR laser. In addition, we applied this method to analyze DNA hydrolysis. We also used microchannel for single-molecule observation of DNA hydrolysis. The shortening of DNA in length caused by enzymatic hydrolysis was observed in real time. Single-molecule DNA manipulation should contribute to elucidate detailed mechanisms of DNA-protein interactions.



- [1] J.H. Kim, V.R. Dukkipati, S.W. Pang and R.G. Larson, *Nanoscale Research Letters*, **2**, (2007) pp.185-201.
[2] H. Kurita, K. Inaishi, K. Torii, M. Urisu, M. Nakano, S. Katsura and A. Mizuno, *J. Biomol. Struct. Dyn.*, **25**, (2008) pp.473-480.

22RP-E-4

EXTERNAL FIELD-RESPONSIVE ORGANIC-INORGANIC HYBRID CAPSULES FABRICATED VIA LAYER-BY-LAYER ASSEMBLY

Matsuda A.¹, Katagiri K.², Koumoto K.²

¹Department of Materials Science, Toyohashi University of Technology,
1-1 Hibarigaoka, Tempaku-cho, Toyohashi 441-8580, Japan

²Graduate School of Engineering, Nagoya University,
Furo-cho, Chikusa-ku, Nagoya 484-8503, Japan

Microcapsules have attracted widespread interest because of their potential applications in the areas of drug delivery, agriculture, and the food and cosmetics industries. A versatile method that affords microcapsules with control over their size, stability, loading, and release properties is the layer-by-layer (LbL) assembly technique. This process involves the successive deposition of various materials, assembled alternately through complementary interactions (e.g., electrostatics, H-bonding, covalent bonding), onto colloidal particles, followed by particle removal. Recent studies have focused on the development of “smart capsules” with stimuli-responsive behavior [1]. In this study, two types of organic-inorganic hybrid capsules were developed for stimuli-responsive hollow capsules as candidates of delivery vehicles.

UV-responsive capsules were firstly designed by a combination of LbL assembly and sol-gel methods. TiO₂ was selected as the UV-responsive component since it can decompose organic materials by photocatalytic reaction. Such a reaction was used to trigger rupturing of the polymer capsule walls, releasing the encapsulated matters. The hybrid capsules can be successfully obtained by formation of the polyelectrolyte hollows and subsequently sol-gel coating. On demand release of the encapsulated dyes upon UV irradiation can be confirmed for the capsules formed with TiO₂. The capsules without TiO₂ were unaffected by UV irradiation. Hence, the UV-induced release is attributed to the photocatalytic activity of the TiO₂ component to decompose polyelectrolytes, which causes the capsules to rupture.

Next, we have designed magnetic field-responsive capsules. There are some difficulties in the application of UV-responsive capsules for the medical field since UV light is toxic for the body. On the other hand, the magnetic field is not toxic for the body and has already been applied for the cancer therapy using the hyperthermia effects. Here, we have chosen Fe₃O₄ as an inorganic component. Fe₃O₄ nanoparticles heat when an alternative magnetic field is applied. Therefore, the hollow capsules composed of Fe₃O₄ and thermoresponsive organic matters can work as magnetic field-responsive delivery vehicles. Fe₃O₄ was obtained by aqueous process with Pd catalysts. Selective deposition of Fe₃O₄ can be controlled by surface charge condition of LbL polyelectrolyte films since Pd catalyst particles were deposited only strongly charged surface of polycations. Therefore, homogeneous coating of Fe₃O₄ on the polyelectrolyte multilayer coated core particles can be achieved when the Pd catalysts are deposited on the well-defined LbL film with a polycation outmost layer.

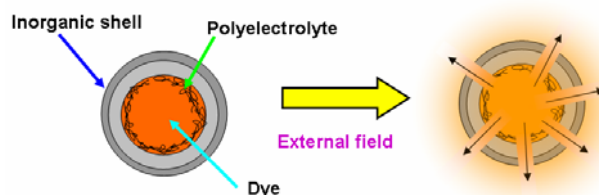


Fig. 1. Schematic representation of external field responsive organic-inorganic hybrid

[1] A. S. Angelatos, K. Katagiri, F Caruso, *Soft Matter*, **2** (2006) 18.

22TL-E-5

SELF-ORGANIZED CORE-SHELL COACERVATES OF MAGNETIC NANOPARTICLES AND DI-BLOCK COPOLYMERS

Frka-Petesic B.¹, Fresnais J.², Berret J.-F.², Dupuis V.¹, Perzynski R.¹ and Sandre O.¹

¹Université Pierre et Marie Curie Paris-VI, LI2C UMR 7612 CNRS-UPMC-ESPCI, 4 place Jussieu, F-75252 Paris Cedex 05 France

²Laboratoire Matière et Systèmes Complexes, UMR 7057 Bâtiment Condorcet 10 rue Alice Domon et Léonie Duquet, 75205 Paris Cedex 13

The complexation between nanocolloids and oppositely charged polymers is currently the subject of intense theoretical and experimental investigations [1,2,3]. We synthesize here by electrostatic interactions, stabilized core-shell clusters, on the scale of 50 – 200 nm, based on self-assembled magnetic nanoparticles and polymers, that could be useful for biomedicine applications [2]. In order to synthesize these core-shell clusters, we use γ -Fe₂O₃ maghemite nanoparticles (lognormal size distribution $d_0 = 8.5$ nm, $\sigma = 0.29$) dispersed in aqueous media thanks to a citrate ligand coating which provides strong electrostatic repulsion (Zeta potential = -30mV, [Na₃Cit] = 10mM, pH \approx 7) and di-block co-polymers of Poly-(Trimethylammonium Ethyl Acrylate) –*b*– Poly-(Acrylamid) (PTEA–*b*–PAM) to stabilize our clusters. PTEA blocks are positively charged in solution whereas PAM blocks are neutral, so we expect that positively charged PTEA blocks would adsorb on the surface of the negatively charged nanoparticles and make the nanoparticles aggregate, while the neutral PAM blocks provide a steric repulsion limiting the cluster to a finite size and stabilizing it in the solution.

We develop here a complementary approach using static and dynamic measurements to probe the size, shape and structure of the core-shell colloids we synthesize. Dynamic Light Scattering, Small Angle Neutron and X-ray Scattering are coupled to Transmission Electron Microscopy. The magnetic properties of the clusters are also probed by magneto-optical measurements involving static and dynamic birefringence.

Support by ANR blanche “ITC-nanoprobe” and by ECO-NET program n°6274QL is acknowledged.

[1] K. Yokota, M. Morvan, JF Berret and J. Oberdisse, *Europhys. Lett.* **69** (2005) 284-290

[2] J.F. Berret, N. Schonbeck, F. Gazeau, D. El Kharrat, O. Sandre, A. Vacher and M. Airiau, *J. Am. Chem. Soc.* **128** (2006) 1755-1761

[3] J.F. Berret, A. Seghal, M. Morvan, O. Sandre, A. Vacher and M. Airiau, *J. Coll. Int. Sci.* **303** (2006) 315-318

22RP-E-6

NEUTRON REFLECTIVITY ON POLYMER MULTIPLAYERS DOPED WITH MAGNETIC NANOPARTICLES

*Frka-Petesic B.¹, Douadi-Masrouki S.¹, Sandre O.¹, Cousin F.²,
Dupuis V.¹, Perzynski R.¹ et Cabuil V.¹*

¹Universite Pierre et Marie Curie Paris-VI, LI2C UMR 7612 CNRS-UPMC-ESPCI, 4 place Jussieu, F-75252 Paris Cedex 05 France

²Laboratoire Leon Brillouin (LLB) - CEA/Saclay, 91191 GIF sur YVETTE Cedex France

We have probed using neutron reflectivity an original system made of di-block copolymer layers [1,2] doped with magnetic nanoparticles, and deposited on a silicon substrate. It combines the multilayer self-organization properties of a di-block copolymer matrix of poly(*n*-butyl methacrylate)-*b*-poly(styrene) (Pn-BMA-*b*-PS) [3], and the magnetic properties of magnetic nanoparticles (MNPs) of maghemite (γ -Fe₂O₃) when a magnetic field is applied. Confinement of the MNPs in the PS layers of the previous matrix is obtained by coating the MNPs with a “grafting from” polymerization of PS on their surface. The multilayer organized films are obtained by spin-coating on a silicon substrate, which are then heated beyond the copolymer glass transition temperature T_g . This multilayer organization is responsible of the holes or islands that appear on the upper layer [3,4] (fig. 1).

To probe the multilayer organization of the copolymer film, we use complementary techniques such as reflective interferential optic microscopy, atomic force microscopy (AFM), ellipsometry and neutron reflectivity which we performed in Laboratoire Leon Brillouin (LLB, Saclay – France) on the time-of-flight reflectometer EROS. Ellipsometric measurements give us the global thickness of the film while neutron reflectivity gives us the number and the thickness of the individual layers. We fit the reflectivity spectra by suggesting a neutron scattering length density profile through the film, which is related to the chemical components of the layers (fig. 2).

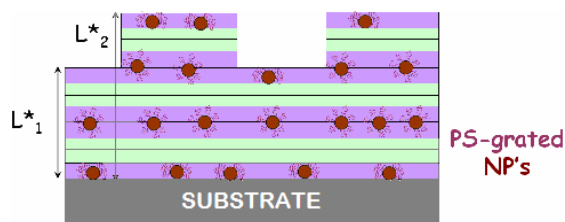


Fig. 1: Scheme of the Pn-BMA-*b*-PS multilayers doped with MNPs.

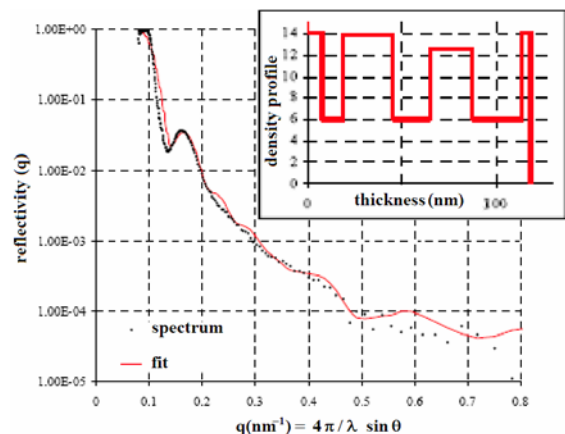


Fig. 2: reflectivity spectrum with fit.
In insert: scattering length density profile

- [1] G. Vignaud, A. Gibaud, G. Grubel, S. Joly, D. Ausserre, J-F. Legrand, Y. Gallot, Physica B 248 (1998) 250
- [2] B. Toperverg, V. Lauter-Pasyuk, H. Lauter, O. Nokonov, D. Aussere, Y. Gallot, Physica B 283 (2000) 60
- [3] M. Save, B. Charleux, S. Douadi, O. Sandre, V. Cabuil, B. Hamdoun, Polymer Preprints (2005), *46*(2), 440-441.
- [4] G. Coulon, B. Collin, D. Chatenay, Y. Gallot, J. Phys. II France 3 (1993) 697

22RP-E-7

MAGNETIC MICROSTRUCTURE OF MAGNETITE DOPED ELASTOMERS INVESTIGATED BY SANS AND SAXS

Balasoiu M.^{1,2}, Craus M.L.^{1,3}, Haramus V.⁴, Plestil J.⁵, Kuklin A.I.¹, Erhan R.¹, Anitas E.M.¹, Schreyer A.⁴, Lozovan M.³, Tripadus V.², Bica I.⁶

¹Joint Institute of Nuclear Research, Dubna, Russia

²¹National Institute of Physics and Nuclear Engineering, Bucharest, Romania

³National Institute of Research and Development for Technical Physics, Iasi, Romania

⁴GKSS Forschungszentrum, Geesthacht, Germany

⁵Institute of Macromolecular Chemistry, Academy of Sciences of the Czech Republic, Prague

⁶The West University of Timisoara, Department of Electricity and Magnetism, Timisoara, Romania

The combination of polymers with magnetic materials displays novel properties compared to the traditional materials. They open new possibilities for technological applications. Combination of magnetic and elastic properties leads to different phenomena which are exhibited in different magnetic fields [1, 2]. Such composites are quite new and understanding of the behavior of these materials depending on the composition, external conditions, and the synthesis processes is intensively under investigation [3].

The present work analyses the results of SANS and SAXS investigations of magnetite doped elastomers polymerized in magnetic field and without. The magnetic elastomers sample were prepared at the West University of Timisoara, Department of Electricity and Magnetism by embedding in the polymer matrix of a magnetite magnetic liquid produced at the Magnetic Fluid Laboratory of the Romanian Academy Section of Timisoara [4].

The SAXS measurements were performed at the Institute of Macromolecular Chemistry, Academy of Sciences of the Czech Republic, Prague. The SANS experiments were realized at GKSS Forschungszentrum, Geesthacht, Germany.

The SANS and SAXS experiments performed on investigated materials allowed us to obtain information concerning the presence of aggregates and their changing due to the magnetite doping. The presence of magnetic field during the preparation process influences the ordering of the aggregates.

Support by JINR, Grant of Romanian Plenipotentiary is acknowledged.

[1] Yu.L.Raikher, O.V.Stolbov, *Letter to JTF*, **26**, Issue 4 (2000) 47 (Rus.)

[2] S. Abramchuk, E. Kramarenko, G. Stepanov, L. V. Nikitin, G. Filipcsei, A. R. Khokhlov, M. Zrínyi, *Polymers for Advanced Technologies* **18**, Issue 11 (2007) 883

[3] E.M.Anitas, A.Kh.Islamov, M.Balasoiu, C.Muresan, I.Bica, Yu.S.Kovalev, O.L.Orelovich, A.I.Kuklin, *Journal of Optoelectronics and Advanced Materials* (2008) (accepted).

[4] Vekas L., Bica D., Avdeev M.V., *China Particuology*, **5** (2007) 43

22RP-E-8

STRUCTURAL ASPECTS OF STABILIZATION OF MAGNETIC FLUIDS BY MONOCARBOXYLIC ACIDS

Avdeev M.V.^{1,2}, Bica D.³, Vekas L.³, Aksenov V.L.^{2,1}, Rosta L.⁴, Garamus V.M.⁵, Willumeit R.⁵

¹Joint Institute for Nuclear Research, Dubna, Russia

²Russian Research Center "Kurchatov Institute", Moscow, Russia

³Center for Fundamental and Advanced Technical Research, Timisoara, Romania

⁴Research Institute for Solid State Physics and Optics, Budapest, Hungary

⁵GKSS Research Centre, Geesthacht, Germany

Colloidal stability of magnetic fluids, especially at a high volume fraction of magnetic nanoparticles, is a complex issue connected to the synthesis procedure, including the nature of surfactant(s) and carrier liquids used. In this work we report our recent results on structural studies of stabilization factors in magnetic fluids based on non-polar organic carriers.

It is well known that one of the best molecules for stabilizing magnetite nanoparticles in organic non-polar liquids is oleic acid [1], a non-saturated mono-carboxylic (fatty) acid, which has a C₁₈-tail with a double bond kink in the middle. Despite wide use of this surfactant in stabilization procedures of magnetic fluids, still there is no full understanding what factors responsible for the resulting stabilization distinguish oleic acid from its saturated analogue, stearic acid, which is always considered as a poor stabilizer. Here, we investigate the structure of magnetic fluids based on decahydronaphtalene and stabilized by various chain length molecules from a series of saturated fatty acids, namely lauric (LA), myristic (MA), palmitic (PA) and stearic (SA) acids with C₁₂, C₁₄, C₁₆, C₁₈- tails, respectively, and compared them with the classical fluid stabilized by oleic acid (OA). This work is a continuation of experiments started in [2]. The structure of stabilized magnetic particles is obtained by small-angle neutron (SANS) performed for H- and D-carriers. It is shown that for all saturated acids magnetite is dispersed in the carrier approximately with the same particle size distribution whose mean value and width are significantly less than in the OA case. Along with it, these acids exhibit different initial dispersing efficiency. A dependence of the thickness of the stabilizing shell around magnetite on the surfactant type was observed, which is discussed with respect to stabilizing properties of saturated fatty acids.

The work is done in the frame of the project RFBR-Helmholtz (HRJRG-016).

This research project has been also supported by the European Commission under the 6th Framework Program through the Key Action: Strengthening the European Research Area, Research Infrastructures. Contract nr: RII3-CT-2003-505925, GKSS, Germany, as well as by the CEEX research program of the Romanian Ministry of Education and Research, contract NanoMagneFluidSeal nr.83/2006.

[1] Rosensweig R E Ferrohydrodynamics (Cambridge University Press, 1985)

[2] M.V.Avdeev, D.Bica, L.Vékás, et al., J. Mag. Mag. Mater. 2007 V. 311 P. 6-9.

22RP-E-9

COMPUTER SIMULATION AND THEORETICAL MODELLING OF THE STRUCTURE FACTOR OF MAGNETIC FLUIDS

Camp P.J.¹, Cerda J.J.², Elfimova E.A.³, Holm C.², Ivanov A.O.³, Krutikova E.V.³

¹School of Chemistry, University of Edinburgh,

West Mains Road, Edinburgh EH9 3JJ, United Kingdom

²Frankfurt Institute for Advanced Studies, Johann Wolfgang Goethe Universitat,

Max-von-Laue Strasse 1, D-60438 Frankfurt am Main, Germany

³Department of Mathematical Physics, Urals State University,

Lenin Avenue 51, Ekaterinburg 620083, Russia

The interparticle correlations and the structure factor of monodisperse ferrofluids are investigated with and without the presence of an external magnetic field. We consider ferrofluids with weak to moderate dipole-dipole interparticle interactions, meaning that chain-like aggregates are absent. Results are obtained using computer simulations (Monte Carlo and molecular dynamics) and a thermodynamic perturbation theory based on a virial expansion in terms of the ferroparticle volume concentration. Both the radial distribution function $g(r)$ and its Fourier transform, the structure factor $S(q)$, are investigated. A detailed comparison is performed between the results from theory and from computer simulations.

The structure factor is studied for different values of ferroparticle concentration and the dipolar coupling constant (which measures the strength of the dipole-dipole interparticle interactions as compared to the thermal energy $k_B T$). Increasing the ferroparticle concentration leads to an increase in the degree of structural correlations in the system. The low-wavevector (low- q) region is of particular significance because it signals the nature of the most important interparticle interactions. With a moderate dipolar coupling constant the structure factor at low q exhibits a decreasing parabolic dependence. This means that attractive forces dominate in the ferrofluid system. Increasing the ferroparticle concentration transforms the decreasing parabolic dependence in to an increasing parabolic dependence, reflecting the growing influence of the short-range repulsive interactions. The theoretical results compare well against the results from computer simulations.

In the case of zero fields the ferrofluid structure is rotationally invariant and the structure factor it is not dependent on the direction of the wavevector \mathbf{q} . The application of an external magnetic field induces anisotropic correlations in the system; the structure factors parallel and perpendicular to the field are then different from one another. Anisotropic correlations become significant when the interaction energy between the dipoles and the magnetic field exceeds $k_B T$. Anisotropic structure factors are presented for different combinations of ferroparticle concentration, dipolar coupling constant, and intensity of the external magnetic field.

This research was carried out under the financial support of CDRF Grant No. PG07-005-02, RFBR Grant No 08-02-00647-a and joint RFBR-DFG Grant Nos. 06-02-04019 and HO 1108/12-1

22RP-E-10

GROUND STATE STRUCTURES IN FERROFLUID MONOLAYERS: THEORY AND SIMULATIONS

Kantorovich S.^{1,2}, Danilov V.¹, Prokopieva T.¹, Holm C.^{2,3}

¹Ural State University, Ekaterinburg, Russia

²Max-Planck-Institute for Polymer Research, Mainz, Germany

³Frankfurt Institute for Advanced Studies, Frankfurt, Germany

Recently, the method of in situ cryo-TEM imaging and ferroparticle cluster analysis was presented in [1] for ferrofluids (suspensions of magnetic nanoparticles in magnetopassive carriers) in monolayers (particles trapped in one plane with their moments free to rotate in 3D). To analyse the influence of geometric constraints on the cluster formation in ferrofluids the combination of molecular dynamic simulations and density functional theory was used [2]. This study drove to the main question of the present work: “What is the ground state microstructure of a ferrofluid monolayer?” Any ground state study of a many-body system is unavoidably accompanied by the difficulties: in theory we have to cope with interparticle interactions, in simulations annealing is extremely time-taking. Some ground state analysis was presented in [3], [4], but no universal solution to the above mentioned problems has been obtained yet. Here we decided to approach the subject differently and divided our work into several steps.

First of all we used Monte Carlo (MC) simulations to anneal the system of n identical interacting magnetic hard spheres in a monolayer. Several “most frequently observed” structures at 0 K were obtained: a ring, a chain, two embedded rings and two rings side-by-side. Different cluster structures were also observed in our simulations, but they were indeed seldom. The next step was to idealise these 4 ground state structure “candidates”. For that, the energy of a ring and a chain was minimised analytically at 0 K. It was predictably shown, that the chain has to be a rod with particle magnetic moments strictly aligned in a head-to-tail position to fulfil the energy minimum, and the ring has to be based on a regular polygon with moments aligned tangentially. These limitations are extremely useful, because they make it possible to perform an analytical exact calculation of the energies for the idealised candidates in which each particle interacts with each! So, the last step of this investigation was to calculate the energies of an ideal n -particle chain, ideal n -particle ring, two ideal embedded rings and two ideal rings side-by-side. For the pairs of rings the energy was also minimised with respect to mutual orientations of moments in the rings and with respect to the mutual spatial rotation of rings. In order to check the analytical calculations MC simulations were carried. An excellent agreement was found when the theoretical predictions were compared to the MC data.

It was shown that the ground state energy of a ring is lower than the one of a chain. We found that once the embedded rings are formed in a system, they would hardly collapse into a single ring in any simulations, as there is an energetic barrier when the number of particles in an inner ring goes to 3. However, the energy of two rings in any configuration is higher than the energy of a single ring. Therewith we conclude that the ground state structure of n magnetic hard spheres in an infinite monolayer is an ideal ring.

The research was carried out with the financial support of DFG Grant No. HO 1108/12-1, and a stipend to SK coming from the MPG. One of the authors (SK) was supported by CRDF Grant Y3-P-05-11 and President RF Grant MK-412.2008.2.

[1] Klokkenburg M. et al, *Phys. Rev. L*, **96** (2006) 037203.

[2] Kantorovich S., et al, *PCCP*, **10** (2008) 1883.

[3] Clarke A. S. and Patey G. N., *J.Chem.Phys.*, **100** (1994) 2213.

[4] Jund P. et al, *Phys. Rev. L*, **74** (1995) 3049.

22RP-E-11

Q2D-FERROFLUID MONOLAYERS IN MAGNETIC FIELDS: THEORY AND SIMULATION

Cerdà J.J.¹, Holm C.^{1,2}, and Kantorovich S.^{2,3}

¹Frankfurt Institute for Advanced Studies, Frankfurt, Germany

²Max-Planck Institute for Polymer Research, Mainz, Germany

³Department of Mathematical Physics, Urals State University, Ekaterinburg, Russia

The morphology of the magnetic equilibrium structures in ferrofluid monolayers in absence of an external field has been recently addressed in experimental [1] and theory-simulation studies [2]. Those studies have provided a valuable insight on the physics of monolayers at zero-field. In contrast, the structural transitions induced in ferrofluid monolayers by an external magnetic field are only partially understood. The topic is of substantial relevance because magnetic colloids in external fields are an integral part of many applications and biomedicine. In recent zero field studies [2], it has been proved that the Quasi two dimensional geometry (Q2D) [particles in-plane, dipoles freely rotate in 3D] exhibits a physics different from pure 2D or 3D systems. Thus, previous field-studies in pure 2D or 3D systems could not be the most suitable frameworks to get insight about the behaviour of ferrofluid monolayers under external fields. Recent in situ cryogenic transmission electron microscopy experiments [3] have reported the existence of in-plane field-induced columnar phases which locally exhibit distorted hexagonal symmetry although it was not possible to clearly establish neither the mechanism that produces the columns of a certain width nor the regular spacing between the columns. In the present work, Q2D ferrofluid monolayers under an external field are thoroughly examined using a combination of Density Functional Theory and Molecular Dynamics simulations. The effects of the orientation of the external field on the morphology of the formed structures is also reviewed. The study focuses in both monodisperse and bidisperse ferrofluids. A comparison to the recent experimental results in [3] will be also presented.

Support of DFG Grant No. HO 1108/12-1, and a stipend to SK coming from the MPG is acknowledged. SK thanks also the CRDF Grant Y3-P-05-11, and L'Oreal-Unesco Stipend.

[1] M. Klokkenburg, R.P.A. Dullens, W.K. Kegel, B.H. Ern , A.P. Philipse, *PRL*, **96**, 037203, (2006).

[2] S. Kantorovich, J.J. Cerd , and C. Holm, *PCCP*, DOI: 10.1039/b719460a

[3] M. Klokkenburg, B.H. Ern , J.D. Meeldijk, A. Wiedenmann, *PRL*, **97**, 185702, (2006).

22 June Sunday

12:00-13:30

oral session

22TL-F

22RP-F

“Magnetophotonics II”

22RP-F-1

DEGENERATE BAND GAP IN 1D PHOTONIC CRYSTAL

Merzlikin A.M.¹, Vinogradov A.P.¹, Levy M.² and Granovskiy A.B.³

¹Institute for Theoretical and Applied Electromagnetics of Russian Academy of Sciences,
Izhorskaya 13/19, Moscow 125412, Russia

²Department of Physics, Michigan Technological University, 1400 Townsend Drive Houghton,
Michigan 49931-1295, USA

³Faculty of Physics, Moscow State University, Leninskie Gory, Moscow 119992, Russia

Almost all applications of the photonic crystal are mostly connected with the existence of the band gap in their transmission spectra. That is why a lot of attention is focused on the conditions at which band gaps appears or disappears (so-called “gap closing” or “zero-width band gaps”) [1, 2].

In this communication we report the results of an investigation of the 1D anisotropic magneto-photonic crystals. It is shown the possibilities to control the appearance or disappearance of the band gap in such crystals by means of magnetic field. In particular it is shown the existence of the special type of the band gaps - gyrotropic degenerate band gap [3, 4], which appears due to applying of the magnetic field. Peculiarities of degenerate band gaps such as polarization degeneracy, Bormann effect, interconnection of degenerate band gaps with the concept of Degenerate Band Edge [5] and distinction of this type of gaps from common one are discussed.

[1] I. Nusinsky, A.A. Hardy, *Phys. Rev. B*, **73** (2006) 125104

[2] S. Zouhdi, A.V. Dorofeenko, A.M. Merzlikin, A.P. Vinogradov, *Phys. Rev. B*, **75** (2007) 035125

[3] A.M. Merzlikin, A.P. Vinogradov, A.V. Dorofeenko, M. Inoue, M. Levy, A. B. Granovsky, *Physica B*, **394** (2007) 277

[4] A.A. Jalali, M. Levy, *JOSA B*, **25** (2008) 119

[5] A. Figotin, I. Vitebskiy, *Phys. Rev. E*, **74** (2006) 066613

22RP-F-2

SLOW LIGHT PHENOMENON AND EXTRAORDINARY MAGNETOOPTICAL EFFECTS IN PERIODIC NANOSTRUCTURED MEDIA

Belotelov V.I.^{1,2}, Kalish A.N.^{1,2}, Kotov V.A.^{1,3}, Zvezdin A.K.^{1,4}

¹A.M. Prokhorov General Physics Institute of RAScience, 119991, Moscow

²M.V. Lomonosov Moscow State University, 119992, Moscow

³Institute of Radio-engineering and Electronics RAS, 125009, Moscow

⁴Fondazione ISI, 10133, Torino, Italy

We investigate physical nature of the magneto-optical effects enhancement in periodic nanostructured media: magnetic photonic crystals and plasmonic materials. The correlation between group velocity and the Faraday rotation peaks is found. The Faraday rotation gets its maximum values at vanishing group velocity. At this efficiency of light - magnetic-matter

interaction increases significantly. Thus, the increase of the magneto-optical effects in magnetic periodic systems is related to the slow wave phenomenon.

Optical properties of periodic nanostructured media: magnetic photonic crystals and plasmonic metal-dielectric materials, are shown to have some peculiarities leading to new optical effects like the effect of the extraordinary optical transmission. At the same time, it was revealed, that magneto-optical properties of such systems also demonstrate rather interesting behavior at the resonance frequencies. For example, the Faraday effects enhancement by an order of magnitude was reported recently.

In this work we investigate physical nature of the magneto-optical effects enhancement in periodic nanostructured media: magnetic photonic crystals and plasmonic materials. The correlation between group velocity and the Faraday rotation peaks is found. The Faraday rotation gets its maximum values at vanishing group velocity. It is shown that in the vicinity of the photonic band gap the Faraday angle is inversely proportional to the group velocity and directly proportional to the magneto-optical parameter Q averaged along the period of the structure. At this efficiency of light - magnetic-matter interaction increases significantly. Thus, the increase of the magneto-optical effects in magnetic periodic systems is related to the slow wave phenomenon.

It is important to note that since the averaging of the magneto-optical parameter is taken with the complex amplitudes of the corresponding Bloch waves, the Faraday effect in the periodic materials becomes dependent on the distribution of the electromagnetic wave amplitude along the structure, which is directly demonstrated for the case of one-dimensional magnetic photonic crystals.

This work is supported by RFBR (06-02-17507, 07-02-01445), "Progetto Lagrange-Fondazione CRT" and Russian foundation "Dynasty".

22RP-F-3

ENHANCEMENT OF THE FARADAY ROTATION IN MULTILAYER STRUCTURES

Dorofeenko A.V.¹, Vinogradov A.P.¹, Merzlikin A.M.¹, Granovsky A.B.², Lisyansky A.A.³

¹Institute for Theoretical and Applied Electromagnetics of Russian Academy of Sciences, 13 Izhorskaya St., Moscow, 125412, Russia

²Faculty of Physics, Moscow State University, Leninskie Gori, Moscow, 119992, Russia

³Department of Physics, Queens College of the City University of New York, Flushing, NY 11367

Due to infinitesimality of magneto-optical (MO) effects numerous attempts are made to enhance a MO response. It has been suggested to enhance the MO effects by employing magnetophotonic crystals (MPC) with defect-mode [1] or Tamm surface state [2]. The enhancement is proportional to Q factor of the corresponding Fabry-Perot resonator. Unfortunately, an increase in the Faraday rotation is accompanied by a decrease in transmission [3]. This problem can be resolved by addition of the second defect [3], but such a scheme is very sensitive to parameters deviation. Inevitable technological fluctuations should kill the effect. Hence, two-defect scheme is hardly realizable.

Other expectations are connected with plasmon resonance in multilayer system. Due to selectivity of surface plasmon resonance with respect to polarization one can achieve the enhancement of the Kerr rotation [4, 5]. By passing a metal layer, due to plasmon resonance a TM-wave may increase, whereas the TE-wave always decreases. The key-moment is that if the TE-polarized wave is chosen as incident it excites TM-wave in the magneto-optical layers. The

formed TM wave is then amplified by surface plasmon resonance [4]. The amplitudes of the excited and reflected TM waves are proportional to optical thickness of MO layer. The transmitted wave is an evanescent one, and the Faraday effect is hardly observed.

We suggest a scheme that is analogous to the one suggested in [4], but modified for observation of the Faraday effect. In the suggested scheme the resonance with surface wave at PC/PC boundary is used instead of resonance with plasmon on the surface metal/vacuum. Absence of metal layers significantly decreases absorption, which makes the scheme suitable for application. Really, this scheme works as a converter changing the polarization from TE to TM. The effective angle of rotation is equal to 90° .

Comparative analysis of the two methods is carried out.

- [1] M.Inoue, T.Fujii, *J. Appl. Phys.*, **81** (1997) 5659
- [2] A. P. Vinogradov, A. V. Dorofeenko, S.G. Erokhin et al. *Phys. Rev. B* **74** (2006) 045128.
- [3] M. J. Steel, M. Levy, and R. M. Osgood, *J. Lightwave Technol.*, **18** (2000) 1297
- [4] V.I. Safarov, V.A. Kosobukin, C. Herman, et al. *Phys. Rev. Lett.* **73** (1994) 3574
- [5] N. Richard, A. Dereux, E. Bourillot, et al. *J. Appl. Phys.* **88** (2000) 2541

22RP-F-4

TAMM STATES IN ONE-DIMENSIONAL MAGNETOPHOTONIC CRYSTALS IN EHF FREQUENCY BAND

*Chernovtsev S.V.¹, Khodzitskiy M.¹, Tarapov S.I.¹, Belosorov D.²,
Merzlikin A.M.³, Vinogradov A.P.³ and Granovskiyy A.B.⁴*

¹Institute of Radiophysics and Electronics NAS of Ukraine; 12 Ac. Proskura St., Kharkov, 61085, Ukraine, e-mail: tarapov@ire.kharkov.ua

²Akhiezer Institute for Theoretical Physics National Science Center “Kharkov Institute of Physics & Technology” NAS of Ukraine; 1 Akademicheskaja St., Kharkov, 61108, Ukraine.

³Institute for Theoretical and Applied Electromagnetics of Russian Academy of Sciences, Izhorskaya 13/19, Moscow 125412, Russia

⁴Faculty of Physics, Moscow State University, Leninskie Gory, Moscow 119992, Russia

The existence of the optical Tamm state, namely, the state localized at the interface of two adjoining 1D photonic crystals, was theoretically predicted in [1]. The amplitude of this state decreases exponentially with a distance from the interface. Later, the presence of optical Tamm states was experimentally demonstrated for optical frequencies [2]. The direct field distribution measurements at optical frequencies are quite complicated due to a small thickness of a structure. Therefore the existence of Tamm states was shown by the observation of the associated with Tamm states effects, such as a narrow peak in transmission spectra and enhancement of Faraday rotation.

In this communication we report the results of an experimental and theoretical investigation of the optical Tamm state in EHF band, namely at GHz frequencies. The structure under investigation consists of two adjoining 1D photonic crystals. The primitive cell of the first photonic crystal consists of ferrite and vacuum layers. In the second photonic crystal the ferrites layers are substituted by polystyrene or quartz layers.

We experimentally studied the distribution of the electrical field in this system. The theoretically predicted frequency of the Tamm state is located inside the intersection of the band gaps of adjoining photonic crystals. At this frequency the maximum of the electrical field is observed near the interface of these photonic crystals. It can be considered as the direct observation of the Tamm localized state at the interface because at other frequencies the field

exponentially decays deep into the system. The frequency of Tamm states in photonic crystals based on ferrites depends on an applied magnetic field and it makes possible to develop tunable by magnetic field EHF devices.

This work was supported by the Russian Foundation for Basic Research and ISTC and Science and Technology Center of Ukraine (Project #3727).

[1] A.P. Vinogradov, A.V. Dorofeenko, S.G.Erokhin, M. Inoue, A.A.Lisyansky, A.M.Merzlikin, A.B.Granovsky, Phys.Rev B **74**, 045128 (2006).

[2] T. Goto, A.V. Dorofeenko, A.M. Merzlikin, A.V. Baryshev, A.P. Vinogradov, M. Inoue, A.A. Lisyansky, A.B. Granovsky, arXiv:0802.3192v1 [cond-mat.other] 21 Feb 2008

22RP-F-5

OPTICAL AND MAGNETO-OPTICAL PROPERTIES OF FERROMAGNETIC ROOM-TEMPERATURE In(Ga)MnAs LAYERS, DEPOSITED BY PULSE LASER ABLATION

Gan'shina E.A.¹, Golik L.L.², Kovalev V.I.², Kunkova Z.E.², Zvonkov B.N.³, Vinogradov A.N.¹

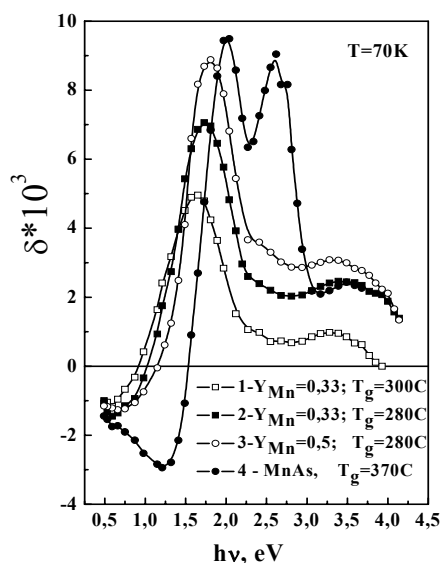
¹Department of Physics, Moscow State University, 119991 Moscow, Russia

²Institute of Radioengineering and Electronics, RAS, 141190 Fryazino, Russia

³Nizhny Novgorod State University, 603950 Nizhny Novgorod, Russia

In this work we present the results of researches of spectral dependences of the refraction and absorption indices (n and k) and also transversal Kerr effect (TKE) of In(Ga)MnAs and MnAs layers, deposited by pulse laser ablation on GaAs(001) substrates. The sputtering time ratio of Mn and In(Ga)As ($Y_{Mn} = t_{Mn}/t_{Mn} + t_{In(Ga)As}$) and temperature of the substrate (T_g) were varied during growth of the In(Ga)MnAs layers. The In(Ga)MnAs layers were ferromagnetic at room temperature, they demonstrated semiconducting behaviour of the temperature dependence conductivity and anomalous Hall effect was observed for a series of the samples. Presence of inclusions of MnAs hexagonal phase was revealed too [1,2].

Spectra of the diagonal component of the dielectric permittivity tensor (DPT) of the



layers $\epsilon_1(h\nu) = \epsilon_1(h\nu) - i\epsilon_2(h\nu)$ have been calculated from ellipsometry data. The feature, which is characteristic for InAs ($E_1, E_1 + \Delta_1$ -transitions), is observed in spectra $\epsilon_2(h\nu)$ of the InMnAs layers. This feature becomes less pronounced and its spectral position is changed as Mn content increases. Changes in the TKE spectra $\delta(h\nu)$ with composition of the InMnAs layers are shown in figure (curves 1-3). In these spectra two bands with maxima at $h\nu_1 \approx 1.6-1.8$ eV and $h\nu_2 \approx 3.2-3.5$ eV are well pronounced, the low-energy band being shifted to higher energy with increasing Mn content. Spectrum $\delta(h\nu)$ of MnAs layer (curve 4) differs from the spectra 1-3 on presence of the third band at $h\nu_3 \approx 2.6$ eV. At $T=50$ K the TKE spectra of the GaMnAs layers were similar to the spectra 1-3, but at $T=293$ K they were similar to the spectrum $\delta(h\nu)$ of MnAs at room temperature.

We used the optical and magneto-optical data to determine the spectral dependences of the off-diagonal component $\epsilon'(h\nu)$ of DPT and interband

state density of the studied layers. Comparison of the dependences $\delta(h\nu)$, $\varepsilon'(h\nu)$ and $\varepsilon'' \times (h\nu)^2$ of the In(Ga)MnAs layers with those of MnAs and with magnetic circular dichroism spectra of $\text{In}_{1-x}(\text{Ga}_{1-x})\text{Mn}_x\text{As}$ layers [3] leads one to associate the features in the spectra of the In(Ga)MnAs layers with a competition of contributions of $\text{In}_{1-x}\text{Mn}_x\text{As}$ host and MnAs inclusions. The received results allow drawing a conclusion about intrinsic ferromagnetism at room temperature in semiconducting $\text{In}_{1-x}\text{Mn}_x\text{As}$ layers deposited by pulse laser ablation.

This work was supported by the RFBR 06-0216604a, 08-0200548.

[1] O.V. Vihrova, Yu.A. Danilov et al. *Izvestiya RAN, ser. Phys.*, **71** (2007) 137.

[2] O.V. Vihrova, Yu.A. Danilov et al *Phys. State Solid*, **50** (2008) 50.

[3] P.T. Chiu, B.W. Wessels, *Phys. Rev.*, **B 76** (2007) 165201.

22RP-F-6

TRANSMITTIVITY IN ONE-DIMENSIONAL MAGNETIC PHOTONIC CRYSTAL WITH TWO DIFFERENT DEFECT LAYERS: EFFECTS OF OPTICAL BISTABILITY

Lyubchanskii I.L.¹, Dadoenkova N.N.¹, Zabolotin A.E.¹, Lee Y.P.², and Rasing Th.³

¹Donetsk Physical & Technical Institute of the National Academy of Sciences of Ukraine,
83114, Donetsk, Ukraine

²q-Psi and Department of Physics, Hanyang University, 17 Haengdang-Dong, Sungdong-Ku,
Seoul, 133-791, Korea

³Institute for Molecules and Materials, Radboud University Nijmegen, 6525 ED,
Nijmegen, the Netherlands

Magnetic photonic crystals (MPCs) are very promising for applications in modern photonics as they possess an additional degree of freedom [1]. Linear and nonlinear optical properties of MPCs were already investigated in numerous publications [1, 2]. An intriguing issue is the effect of optical bistability, which is well studied for non-magnetic photonic crystals [3] and for which preliminary results were obtained for an MPC with one defect layer [4].

In this report we present detailed results of a theoretical investigation on optical bistability in an MPC with two different (magnetic and non-magnetic) defect layers. These defect layers lead to so-called defect modes inside the photonic band gap. Taking into account the nonlinear optical susceptibility, we investigated analytically and numerically the nonlinear optical response of a two-defect MPC upon intensive optical radiation in the polar and transversal magneto-optical configurations for normal incidence of light. Similarly to our previous investigation for MPCs with two magnetic defect layers [5, 6], the intensity dependences of different defect modes as well as the sign of the nonlinear part of the refractive index are explained.

Support by INTAS under grant No.03-51-3784 and MOST/KOSEF through q-Psi is acknowledged.

[1] I.L. Lyubchanskii, N.N. Dadoenkova, M.I. Lyubchanskii, E.A. Shapovalov, and Th.Rasing. *J.Phys. D: Appl. Phys.* **36** (2003) R277.

[2] M. Inoue, B. Fujikawa, A. Baryshev, A. Khanikaev, P.B. Lim, H. Ushida, O. Aktsipetrov, A. Fedyanin, T. Murzina, and A. Granovskii. *J. Phys. D: Appl. Phys.* **39** (2006) R151.

- [3] M. Soljacic and J.D. Joannopoulos. *Nature Materials*. **3** (2004) 211.
- [4] F. Jonsson and C. Flytzanis. *Phys. Rev. Lett.* **96** (2006) No.063902.
- [5] I.L. Lyubchanskii , N.N. Dadoenkova, M.I. Lyubchanskii, E.A. Shapovalov, A.E. Zabolotin, Y.P. Lee, and Th. Rasing. *J. Appl. Phys.* **100** (2006) No.096110.
- [6] I.L. Lyubchanskii , N.N. Dadoenkova, A.E. Zabolotin, Y.P.Lee, and Th.Rasing., *J. Appl. Phys.* **103** (2008) No.07B321.

22 June Sunday

15:00-17:00

oral session

22TL-F

22RP-F

**“Magnetism and
Superconductivity”**

22TL-F-7

EFFECTS OF GEOMETRICAL FRUSTRATION REVEALED BY FINE-TUNING QUANTUM MAGNETS AT HIGH MAGNETIC FIELDS

Jaime M.

National High Magnetic Field Laboratory
Los Alamos National Laboratory
Los Alamos, NM 87544

With advancements in the way very high magnetic fields are produced in the laboratory, a new class of physical phenomena has attracted attention into an area of condensed matter physics seldom visited: the physics of magnetic elemental excitations that are created and live in quantum paramagnets. These excitations, known as triplons, behave in ways that can be described with identical formalism to that used for neutral atoms that form condensates or electron-pairs that superconduct. While the thermodynamic phase transition that leads into these states has been studied in excruciating detail in liquid He (including gravity-less experiments carried out in the NASA Space Shuttle), the quantum phase transition had to wait for longer since it is hard to change the chemical potential continuously in an atomic gas. In the case of triplons, instead, high magnetic fields can be used to induce a quantum phase transition by chemical potential, i.e. controlling the concentration of particles in a reversible way at temperature near the absolute zero. In these conditions, when the host material is highly symmetric, the magnetic phase transition into a XY-AFM state is mathematically indistinguishable from a Bose-Einstein condensation. On the other hand, if the underlying crystal symmetry is complex the resulting magnetic frustration has dramatic effects and creates ideal conditions for the observation of dimensional reduction such as first observed in the ancient Chinese pigment BaCuSi₂O₆, [1-3] and magnetic texture with similar origin to that of Quantum Hall Effect in the Shastry-Sutherland compound SrCu₂(BO₃)₂. [4] In my seminar I will discuss recent experiments conducted at the National High Magnetic Field Laboratory in the above and other compounds [5], as well as some theoretical efforts to model our results.

Work done in collaboration with Neil Harrison, Suchitra Sebastian, Vivien Zapf, Eric Samulon, Ian Fisher, Yosimitsu Kohama, Oscar Ayala-Valenzuela, Pinaki Sengupta and Cristian Batista, among several others.

[1]M. Jaime et al., Phys. Rev. Lett. 93, 087203 (2004).

[2]S. Sebastian et al., Phys. Rev. B 72, 100404 (2005).

[3]S. Sebastian et al., Nature 441, 617 (2006).

[4]S. Sebastian et al., arXiv:0707.2075v1 [cond-mat.str-el]

[5]V.S. Zapf et al., Phys. Rev. Lett. 96, 077204 (2006).

22RP-F-8

SYMMETRY LOWERING IN Mo₃Sb₇ WITH SPIN FLUCTUATIONS AND SUPERCONDUCTIVITY

Nakamura H.¹, Koyama T.², Yamashita H.², Kohara T.², Takahashi Y.², Tabata Y.¹

¹Department of Materials Science and Engineering, Kyoto University, Kyoto 606-8501, Japan

²Graduate School of Material Science, University of Hyogo, Kamigori, Hyogo 651-0084, Japan

Recently Candolfi et al., reported that the superconductivity and spin fluctuations coexist in a relatively simple intermetallic compound Mo_3Sb_7 with the cubic Ir_3Ge_7 type structure. In this structure Mo-Mo dumbbells forms a quite attractive three-dimensional network. The characteristic energy of spin fluctuations is approximately 200 K and the superconducting transition temperature is 2.2 K.

We have performed Sb nuclear quadrupole resonance (NQR) experiments of Mo_3Sb_7 , and found the divergence of the nuclear spin-lattice relaxation rate, $1/T_1$, at around 50 K. Below the temperature, the NQR spectrum tunes to be complicated, indicating apparent symmetry lowering. These results are consistent with anomalies found very recently in specific heat, susceptibility and resistivity, reported by Tran and Miiller [2].

Our low-temperature x-ray diffraction and thermal expansion experiments showed a clear structural transition from cubic to tetragonal at ~ 50 K and thermal expansion anomaly below the temperature. The symmetry lowering accompanied by the spin singlet formation seems to be the necessary condition for the appearance of superconductivity. We will discuss the origin of the symmetry lowering in terms of the characteristic structure of the Mo sublattice, in which antiferromagnetic interaction is weakly frustrated by taking account of nearest and next-nearest neighbor interactions.

[1] C.Candolfi et al., *Phys. Rev. Lett.*, **99** (2007) 037006.

[2] V.H.Tran and W.Miiller, *Phys. Rev. Lett.*, **100** (2008) 137004.

22RP-F-9

DOUBLY SUPPRESSED RE-ENTRANT SUPERCONDUCTIVITY IN SUPERCONDUCTOR/FERROMAGNET BILAYERS

Tagirov L.R.¹, Zdravkov V.², Morari R.², Kehrle J.³, Obermeier G.³, Gsell S.³, Schreck M.³, Muller C.³, Ryazanov V.V.⁴, Horn S.³, Sidorenko A.², Tidecks R.³

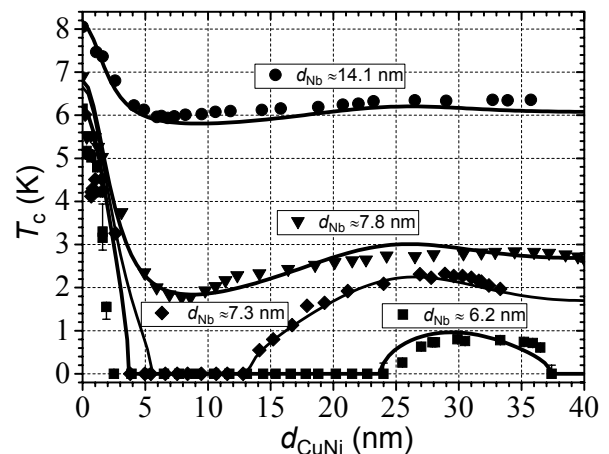
¹Solid State Physics Department, Kazan State University, Kazan, 420008, Russia

²Institute of Electronic Engineering and Industrial Technologies ASM, Kishinev, MD2028, Moldova

³Institut für Physik, Universität Augsburg, Augsburg, D-86159, Germany

⁴Institute of Solid State Physics, Russian Academy of Sciences, Chernogolovka, 142432, Russia

In superconductor-ferromagnetic metal (S/F) contacts the superconducting condensate penetrates through the S/F interface into a F-layer, and the pairing wave function not only decays into the deep of F metal, but simultaneously oscillates. Based on these oscillations a variety of new physical effects were predicted (see reviews [1] and references therein), and some of them were observed experimentally: non-monotonous superconducting T_c behavior as a function of the F-layer thickness, Josephson junctions with the intrinsic π shift across the junction, capped differential I-V characteristics. In this work we report on the first experimental observation of spectacular re-entrant and doubly suppressed superconductivity in



Nb/Cu_{1-x}Ni_x bilayers as a function of the ferromagnetic layer thickness d_{CuNi} . The superconducting T_c drops sharply with increasing d_{CuNi} till total suppression of superconductivity at $d_{\text{CuNi}} \approx 2.5\text{-}5$ nm. At further increase of the Cu_{1-x}Ni_x layer thickness, the superconductivity restores at $d_{\text{CuNi}} \approx 13$ nm for the re-entrant behavior ($d_{\text{Nb}} \approx 7.3$ nm) [2], and $d_{\text{CuNi}} \approx 24$ nm for the doubly suppressed re-entrant behavior ($d_{\text{Nb}} \approx 6.2$ nm) [3]. Then, with the subsequent increase of d_{CuNi} the superconductivity either saturates ($d_{\text{Nb}} \approx 7.3$ nm) [2] or vanishes again at $d_{\text{CuNi}} \approx 38$ nm ($d_{\text{Nb}} \approx 6.2$ nm) [3]. Our experiments give evidence for the realization of the quasi-one dimensional Fulde-Ferrell-Larkin-Ovchinnikov (FFLO) like state [4,5] in the ferromagnetic layer.

The work was partially supported by INTAS (grant YSF 03-55-1856), BMBF (project MDA02/002), RFBR (project No 07-02-00963) and RFBR-Moldova (project No 18-R).

- [1] A.I. Buzdin, Rev. Mod. Phys. **77**, 935 (2005).
- [2] V.I. Zdravkov, A.S. Sidorenko, G. Obermeier, S. Gsell, M. Schreck, C. Muller, S. Horn, R. Tidecks, L.R. Tagirov, Phys. Rev. Lett. **97** (2006) 057004.
- [3] A.S. Sidorenko, V.I. Zdravkov, J. Kehrle, G. Obermeier, S. Gsell, M. Schreck, C. Muller, V.V. Ryazanov, S. Horn, R. Tidecks, L.R. Tagirov, Nature Physics (submitted).
- [4] P. Fulde & R. Ferrell, Phys. Rev. **135** (1964) A550.
- [5] A.I. Larkin & Yu.N. Ovchinnikov, Zh. Eksp. Teor. Fiz. **47**, (1964) 1136 [Sov. Phys. JETP **20** (1965) 762].

22RP-F-10

SUPERCONDUCTIVITY IN MULTI-PARTICLE SYSTEMS

Continentino M.A., Padilha I.T.

Instituto de Física, Universidade Federal Fluminense,
Campus da Praia Vermelha, Niteroi, RJ, 24.210-346, Brazil

We study superconductivity in a system of two types of quasi-particles using a BCS approximation. We allow for transmutation between these particles, such that, only their total number is conserved [1]. This study is relevant for cold atom systems, quark matter in the nucleus of neutron stars and inter-metallic systems. We focus here in the latter problem, specifically in a two-band metal, where hybridization due to overlap of the quasi-particle wave-functions transfers particles between these bands. In the presence of an inter-band attractive interaction, superconductivity becomes unstable as hybridization increases to a critical value V_c . This is due to the appearance of a soft mode at a characteristic wave-vector q^* . The zero temperature transition at V_c is first order and is associated with the appearance of a gapless metastable phase. In the case of intra-band interactions the transition between the normal and superconducting states is second order being associated at zero temperature with a quantum critical point (QCP). Since hybridization is due to the overlap of wave-functions associated with different orbitals, this QCP can be tuned by applying pressure in the system. We study the stability of an inhomogeneous FFLO phase characterized by the wave-vector q^* . We find this phase is unstable if the masses of the quasi-particles are different.

Partial support by CNPq, and FAPERJ is acknowledged.

- [1] M. A. Continentino and Igor T. Padilha, *J. Phys.:Condens. Matter*, **20** (2008) 095216.

22RP-F-11

PROPERTIES OF VORTEX STATES INDUCED BY PROXIMITY EFFECT IN HYBRID FERROMAGNET-SUPERCONDUCTOR SYSTEMS

Ader J-P.¹, Buzdin A.I.^{1,2}, and Mel'nikov A.S.³

¹CPMOH, University of Bordeaux I, 351 Cours de la Libération 33405 Talence cedex, France

²Institut Universitaire de France

³Institute for Physics of Microstructures, RAS, 603950 Nizhny Novgorod, GSP-105, Russia

We investigate theoretically the properties of a thin superconducting material (S) placed in electrical contact with a ferromagnet (F). This F metal can be a cylinder [1] or a sphere embedded in the superconductor. We study also the case of hybrid structures where the thin-walled superconducting shell is surrounded by the ferromagnet. The two geometries, cylinder and sphere are considered as well. The superconducting critical temperature, the order parameter structure and the effect of an applied external field, resulting in an analogous behaviour to the Little-Parks effect, are described in the dirty limit and in the presence of an exchange field through the Usadel equations. The superconducting material is sufficiently thin in such a way that variations of the Usadel function can be neglected in the superconducting shell. The boundary conditions at the different interfaces, which are of the usual Kuprianov-Lukichev type, are fully taken into account; in particular, the proximity effect caused by a finite F/S interface resistance is considered. In this model, associated with the orbital effect, spontaneous vortex states may appear, characterized by different winding numbers. A special attention is paid to the switching between states of different vorticities caused by the exchange field. The behaviour of the superconductivity in a magnetic field is also considered. Neglecting the variation of the flux inside the S metal we focus on the behaviour of critical temperatures for superconducting states with different vorticities, thus generalizing the Little-Parks effect [2].

[1] A.V. Samokhvalov, A.S. Mel'nikov, and A.I. Buzdin, *Phys. Rev. B* **76**, 184519 (2007)

[2] J-P. Ader, A.I. Buzdin, and A.S. Mel'nikov, to be published.

22RP-F-12

PROXIMITY EFFECT IN THE FINITE AND INCOMMENSURATE FERROMAGNET/SUPERCONDUCTOR SYSTEMS

Proshin Yu.N.¹, Luchkin R.G.¹, Khusainov M.G.^{1,2}

¹Kazan State University, Kazan 420008, Russia

²"Vostok" Branch, Kazan State Technical University, Chistopol' 422950, Russia

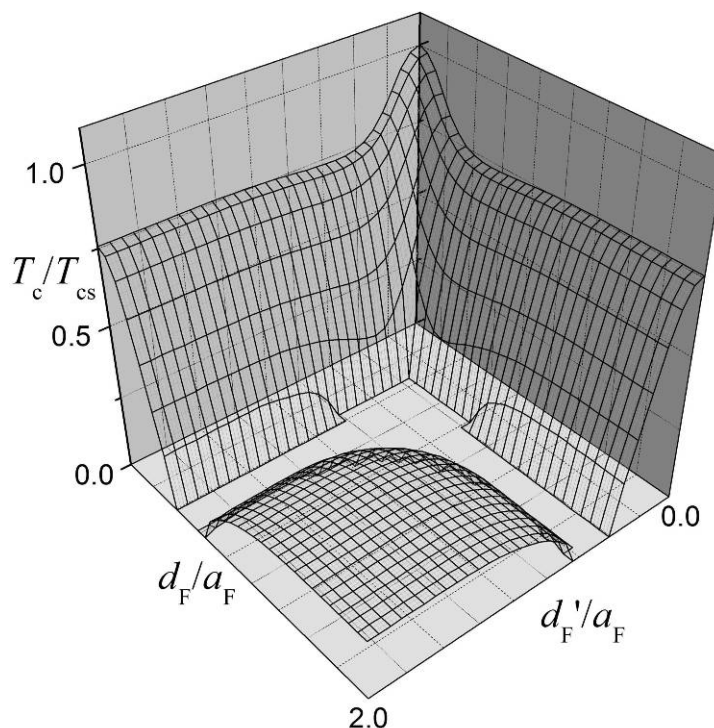
Last two decades the considerable success in the experimental and theoretical examination of proximity effect in the layered ferromagnetic metal/superconductor (F/S) systems [1,2] is reached. As a rule, the multilayered systems with a high degree of symmetry were explored.

In this report the original theory of a proximity effect is proposed for the F/S systems with finite number of layers. The bilayer (F/S), trilayers (F/S/F' and S/F/S') and four-layered systems (F/S/F'/S') are consistently reviewed in so called dirty limit. The distinctions in materials (S and S'; F and F'), in thicknesses (d_F and $d_{F'}$), in parameters interfaces (F/S and S/F), and in local environments of layers, leading to dissimilar boundary conditions for different layers made

of the same material, are considered among the causes of incommensurability of layers. We also take into account the complication of phase diagrams related to occurrence of the π -phase magnetism (in the F/S/F' and F/S/F'/S' systems) and π -phase superconductivity (in the S/F/S' and F/S/F'/S' systems). Along with a hierarchy of critical temperatures T_c for the finite layered systems [3] the peculiar $T_c(d_F, d_{F'})$ interference pattern is predicted for the systems with two F layers which thicknesses d_F and $d_{F'}$ may be disproportionated.

In the Figure the phase diagram with the $T_c(d_F, d_{F'})$ interference is presented for the F/S/F' system. The section $d_{F'} = 0$ corresponds to the $T_c(d_F)$ curve for the F/S bilayer. We see that addition of thin F' layer drastically can change the phase picture. The diagonal section $d_F = d_{F'}$ corresponds to the known picture from work [3] with reentrant superconductivity. All parameters of system also correspond to the ones from work [3]. Here T_{cs} is the critical temperature of bulk superconductor S, and thickness of the ferromagnetic layers made of an identical material are measured in units of length of spin stiffness a_F .

The possible applications to an observability of the spin-valve regime are discussed for three- and four-layered systems [3,4].



- [1] Yu.A. Izyumov, Yu.N. Proshin, M.G. Khusainov, *Physics - Uspekhi* **45** (2002) 109.
 [2] A.I. Buzdin, *Rev. Mod. Phys.* **77** (2005) 935.
 [3] Yu.N. Proshin, A. Zimin, N.G. Fazleev, M.G. Khusainov, *Phys. Rev. B* **73** (2006) 184514.
 [4] M. Fauré, A.I. Buzdin, D. Guskova *Physica C*, **454** (2007) 61.

22RP-F-13

π PHASE SUPERCONDUCTIVITY AND MAGNETISM IN FERROMAGNET/SUPERCONDUCTOR/FERROMAGNET TRILAYERS

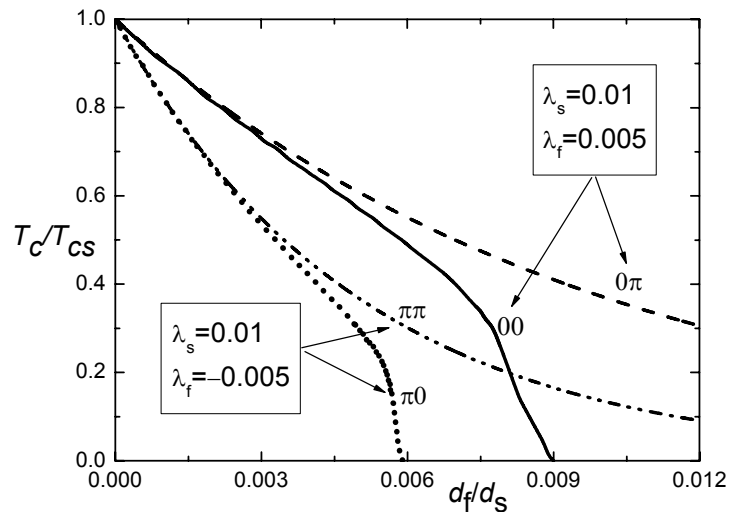
Khusainov M.G.^{1,2}, Proshin Yu.N.¹

¹Department of Theoretical Physics, Kazan State University, Kazan 420008, Russia

²Department "Vostok", Kazan State Tupolev Technical University, Chistopol' 422981, Russia

We investigate the proximity effect in the clean ferromagnet/superconductor/ferromagnet (F/S/F) trilayers. Having regard to the processes of mutual transformation between the Fulde-Ferrell-Larkin-Ovchinnikov (FFLO) and BCS pairs at the F/S boundary, the significantly new boundary conditions for the Eilenberger equations have been derived [1]. We also have taken into account possible electron-electron interaction in the F layers. The last assumption gives rise to the possibility of novel π phase superconducting states, which were deemed before impossible for this system [1,2]! We have shown that the F/S/F trilayer can have 4 different states ($\phi\chi$),

distinguished by the phases of superconducting (Δ) and magnetic (I) order parameters in neighbor F layers, where both phases take couple of values $\phi = (0, \pi)$; $\chi = (0, \pi)$. In the 0π and $\pi\pi$ states the F layers magnetizations are antiparallel to one another and their paramagnetic effect is mutual compensated due to ideal transparency and the Cooper limit. The critical temperature T_c of such 0π and $\pi\pi$ trilayers depends only upon the sign and magnitude of the interelectron coupling λ_f in the F



layers. Two alternative states 00 and $\pi0$ are realized at parallel orientation of both F layers magnetizations. These 00 and $\pi0$ states possess by intensified paramagnetic effect of the exchange field I and by lower T_c in relative to the 0π and $\pi\pi$ ones.

In the Figure the $T_c(d_f/d_s)$ dependencies are presented for all possible states $\phi\chi$ (T_{cs} is the critical temperature of the S film, $d_{s(f)}$ are the S(F) layer thickness). We see that at $\lambda_f > 0$ the two states are realized, and the 0π state wins. At $\lambda_f < 0$ the $\pi\pi$ state will possess greater T_c than the $\pi0$ state. The 00 and $\pi0$ FFLO states could be observed in the presence of the external magnetic field H greater than the coercive field of the F film if, of course, the averaged exchange field is not too strong.

To the point, our results can explain the unexpected weak depression of superconductivity which has been found in short period Gd/La superlattices at zero field cooling [3]. This means that in the Gd/La *superlattice* the 0π state is realized rather than $\pi\pi$ one and $\lambda_f \sim \lambda_s$, i.e. the electron-electron interaction in Gd *metal* corresponds to *attraction* but its own superconductivity depressed by exchange field $I \gg T_c$. On the other hand, also in accordance with our theory at the field cooling of the Gd/La superlattice the superconducting transition has been suppressed.

- [1] M.G. Khusainov, M.M. Khusainov, Yu.N. Proshin, *Chapter 3 in: Progress in Superconductivity Research*, Nova Science Publ., Inc., NY, (2008) 79.
- [2] Yu.A. Izyumov, Yu.N. Proshin, M.G. Khusainov, *Physics - Uspekhi* **45** (2002) 109.
- [3] J.P. Goff, et al., *J. Magn. Magn. Mater.*, **240** (2002) 592.

22TL-F-14

NOVEL TYPE OF PI - JUNCTION ON THE BASE OF JOSEPHSON S-(FNF)-S STRUCTURES

Karminskaya T.Yu.¹, Kupriyanov M.Yu.¹, Golubov A.A.²

¹Institute of Nuclear Physics Moscow State University, Leninskie Gory, Moscow 119992, Russia

²Faculty of Science and Technology, University of Twente, Enschede 7500 AE, The Netherlands

Supercurrent in an S-(FNF)-S Josephson junction is calculated within the framework of the quasiclassical Usadel formalism. The barrier of an analyzed structure consists of a

ferromagnetic (F) - normal metal (N) - ferromagnetic trilayer connecting two superconducting (S) electrodes, providing a supercurrent flow in the direction parallel to FN interfaces.

We assume that the dirty limit conditions are satisfied in all metals, effective electron - phonon coupling constants are zero in N and F layers and F films have single domain structure with magnetization vectors $\mathbf{M}_{1,2}$ parallel to the film planes. We suppose also that the transparency of SF and SN interfaces are small enough providing the opportunity to use linearized Usadel equations and that the effective exchange energy H is zero in N film.

We show that both the magnitude and the sign of the S-FNF-S junction critical current I_C depend essentially on the angle α between the directions of \mathbf{M}_1 and \mathbf{M}_2 . We argue that in the vicinity of $\alpha = \pi$ the interplay between singlet and triplet superconducting components in FNF weak link may produce a novel type of a π Josephson junction. The origin of such a π junction differs from known mechanisms based either on oscillatory behavior of a superconducting order parameter in F metal or on d-wave pairing in S electrodes. It is shown that effective control on both magnitude and sign of I_C can be achieved under small deviation of vectors \mathbf{M}_1 and \mathbf{M}_2 from antiferromagnetic orientation (\mathbf{M}_1 is anti parallel to \mathbf{M}_2).

In this case it is possible to find the angle α at which the difference between the magnitudes of I_C in "0" state ($I_C > 0$) and in " π " state ($I_C < 0$) can be even larger than under switching from ferromagnet (\mathbf{M}_1 is parallel to \mathbf{M}_2) to antiferromagnetic (\mathbf{M}_1 is anti parallel to \mathbf{M}_2) states [1].

This work was supported by the RFBR (grants 08-02-90105-mol-a, 07-02-00918-a).

[1] T.Yu. Karminskaya, M.Yu.Kupriyanov, *Pis'ma v ZhETF* **86** (2007) 61.

22 June Sunday

17:00-19:00

poster session

22PO-8

**“Nanomagnetism
and Nanostructures”**

22PO-8-1

ANODIC ALUMINA FILMS AS A HOST MATERIAL FOR PREPARATION OF MAGNETIC NANOWIRE ARRAYS

Napolskii K.S., Roslyakov I.V., Eliseev A.A., Lukashin A.V., Tretyakov Yu.D.
Department of Materials Science, Moscow State University, Moscow, Russia

Anodic aluminum oxide (AAO) membranes formed by two-step anodization technique, hard anodization process or nanoimprint technology are well-known to possess uniform pore structure with hexagonal arrangement of cylindrical channels and narrow pore size distribution. The use of different electrolytes, voltages and anodic oxidation times allows one to adjust pore diameter D_p , interpore distance D_{int} and film thicknesses L_f in a wide range ($D_p = 15\text{--}200$ nm; $D_{int} = 50\text{--}500$ nm; L_f up to several hundreds of micrometers). Combination of unique porous structure (straight pores of controllable diameter) with high thermal, mechanical and chemical stability makes anodic alumina films extremely attractive as a material for various applications in the fields of filtration, separation, storage, sensing, and the synthesis of one-dimensional nanostructures.

An important advantage of anodic alumina is the possibility to incorporate any compound by electrochemical methods, which enables precise control of deposit morphology and simple handling over loading values and, therefore, makes it possible to control the anisotropy parameters of nanostructures.

In the frames of present study we investigate the formation of magnetic Co, Ni and layered Ni/Cu nanoparticles in one-dimensional solid state nanoreactors formed by anodic alumina membranes with different pore diameters and film thicknesses. Nanocomposites were characterized by chemical analysis, SEM, TEM, XRD and magnetic measurements. It was showed that particles' shape and size are in good agreement with the shape and size of the pores, while the average length of nanowires could be controllably varied (see Fig. 1). Control of composition and morphology of nanoparticles enables to predetermine magnetic properties of nanocomposites. Thus, such nanocomposite materials may serve as a test system for information storage.

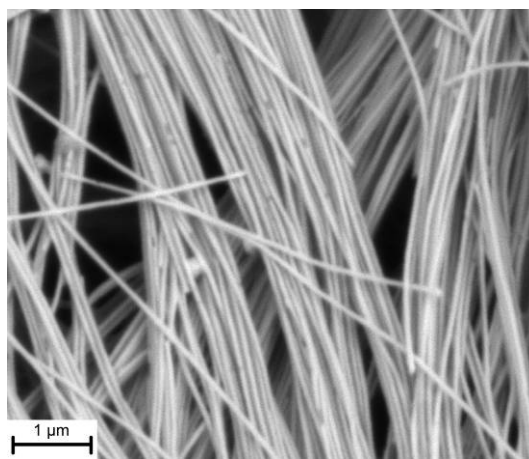


Fig. 1. SEM image of Co nanowires after dissolution of alumina matrix.

This work is supported by RFBR (06-03-89506, 06-03-33052) and FASI (02.513.11.3194).

22PO-8-2

MAGNETIC NANOCOMPOSITES BASED ON MICRO AND MESOPOROUS ALUMINOSILICATES

Vyacheslavov A.S., Lukatskaya M.R., Eliseev A.A., Lukashin A.V., Tretyakov Yu.D.

Department of Materials Science, Moscow State University,
Leninskiye Gory 1-3, 119992, Moscow

Today the improvement of the data storage density requires the development of principally new magnetic materials and storage techniques to solve the problems which appears with decreasing of magnetic bit size to atomic scale. The materials used as a recording media should possess large enough magnetic moment, remanence and coercive force, necessary both for steady reading the information, and it's time stability. However, small magnetic nanoparticles usually show superparamagnetic properties with low blocking temperatures and no coercivity at normal conditions. From the theoretical point of view, the solution to the problem is the use of anisotropic nanoparticles. Ordered system of anisotropic nanoparticles may be created by growing of clusters in one-dimensional pores such as cavities of zeolites and mesoporous matrices.

In the present work Co- and Fe-containing nanocomposites based on zeolites (ZSM-5) and mesoporous aluminosilicates were investigated. We used two different methods of metal-containing precursor intercalation: cation exchange and adsorption of neutral complexes into the pores of matrices. Then precursors were modified by thermal treatment at different temperature. Initial matrices and nanocomposites were investigated by XRD-analysis, TGA, TEM, BET, chemical analysis, magnetic measurement and Mossbauer spectroscopy.

XRD data for nanocomposites show that the decomposition of carbonyls and growth of particles don't result in the destruction of aluminosilicates lattice. The magnetic measurements indicate ferromagnetic behavior of samples even at room temperature that could be explained by the formation of anisotropic metal clusters in 1D-pores of matrices, that is in accordance with TEM data. Iron-containing nanocomposites have maximum coercivity of 670 Oe for Fe(CO)₅-ZSM sample annealed at 450 °C. Maximum of coercivity for cobalt-containing samples (790 Oe) corresponds to the thermal treatment of cobalt-containing ZSM-5 sample at 300 °C.

This work is supported by RFBR (№ 06-03-33052-a, 06-03-89506-NNS_a), FASI (№ 02.513.11.3120, 02.513.11.3352).

22PO-8-3

MAGNETIC GAMMA - IRON OXIDE NANOPARTICLES FOR BIOMEDICAL APPLICATIONS

Chekanova A.E.¹, Dubov A.L.¹, Petrova O.S.¹, Goodilin E.A.^{1,2}, Eremina E.A.², Maksimov Yu.V.³, Nikiforov V.N.⁴, Tretyakov Yu.D.¹

¹Department of Materials Science, Lomonosov Moscow State University, Moscow, 19991 Russia

²Department of chemistry, Lomonosov Moscow State University, Moscow, 19991, Russia

³N.N. Semenov Institute of Chemical Physics, Russian Academy of Science, Moscow, 19991 Russia

⁴Department of Low Temperature Physics and Superconductivity, Lomonosov Moscow State University, Moscow, 19991 Russia

Magnetic nanoparticles has attracted attention because of their current and potential applications as contrast agents for magnetic resonance imaging (MRI) or colloidal mediators for cancer magnetic hyperthermia. These applications are required non-toxic and biocompatible materials [1]. There are many known techniques for the synthesis of nanoparticles with required properties (particles size, magnetic properties, etc). Aerosol spray pyrolysis method permits to obtain highly disperse particles and also to control their micromorphology [2]. There is an evident idea to prevent the aggregation of nanoparticles and it demands new solutions because of a very high practical importance of such an approach. One of the solutions is the development of techniques yielding composites liberating nanoparticles after long-term storage upon a contact with water or medical liquids. Unfortunately, the behavior of magnetic nanoparticles entrapped in water soluble inorganic matrix has not yet investigated in details. Water/oil (W/O) microemulsions are media for the preparation of ultrafine particles due to the small water microdroplets contained inside which, under appropriate conditions, will contain the growth of the particles [3].

In the present work, an ultrasonic aerosol spray pyrolysis (ASP) and microemulsions methods were developed to prepare nontoxic and biocompatible nanostructured γ -Fe₂O₃ magnetic nanoparticles and γ -Fe₂O₃ nanoparticles entrapped in water soluble NaCl microgranules. Magnetic nanoparticles obtained by microemulsion method consisted of aggregates 0,5-1 μ m which are composed of 5-10 nm nanoparticles whereas nanoparticles obtained by ASP method consisted of hollow microspheres 0.1 - 2 μ m in diameter containing 5-20 nm nanoparticles of γ -Fe₂O₃.

The so-obtained biocompatible nanomaterials were characterized with Fourier transform infrared spectroscopy, transmission electron microscopy, magnetic measurements and Moessbauer spectroscopy. Moessbauer spectra confirm the superparamagnetic behavior of γ -Fe₂O₃ nanoparticles prepared by ASP and microemulsion methods. Obtained nanoparticles exhibit specific magnetic behaviour strongly affected by interparticle interactions and extremely low particle size.

[1] Ajay Kumar Gupta, Mona Gupta, *Biomaterials*, **26** (2005), 3995.

[2] Seiichi Suda, Seiji Takahashi, Mitsunobu Kawano, *Solid State Ionics*, **177** (2006), 1219.

[3] Deng Y, Wang L, Yang W, Fu S, Elaieassari A., *J. Magn Magn Mater*, **257(1)** (2003), 69.

22PO-8-4

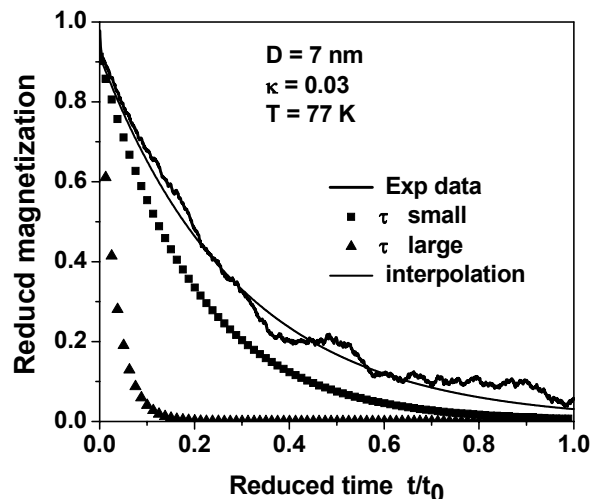
SUPERPARAMAGNETIC RELAXATION TIME OF A SINGLE-DOMAIN PARTICLE WITH A NON-AXIALLY SYMMETRIC DOUBLE-WELL POTENTIAL

Grebenshchikov Yu.B.¹, Usov N.A.^{1,2}

¹Institute of Terrestrial Magnetism, Ionosphere and Radio Wave Propagation, Russian Academy of Sciences, (IZMIRAN), 142190, Troitsk, Moscow region, Russia

²Ltd. "Magnetic and Cryogenic Systems", 142190, Troitsk, Moscow region, Russia

Magnetic nanoparticles are very promising for various technological applications such as high density magnetic recording, targeted drug delivery, etc. The measurement of relaxation times of superparamagnetic nanoparticles can provide important information about the particle volume V , saturation magnetization M_s , and anisotropy constant K . Theoretically, relaxation time can be determined by means of solution of Brown's equation [1] for distribution of magnetic moment orientations. However, the solutions of the Brown's equation are known for a few cases only. In this report a new approximate analytical solution is found for an important case of a nanoparticle with non-axially symmetric double-well potential. In particular, this solution describes the relaxation time of elongated nanoparticle whose easy anisotropy axis is inclined at arbitrary angle with respect to the shape anisotropy axis. The explicit analytical expressions are obtained for the relaxation times τ_s and τ_l of the nanoparticle in the limits of small, $\kappa \ll 1$, and large, $\kappa > 1$, values of the dimensionless damping parameter κ , respectively. To validate these results the numerical simulation of the relaxation process for a nanoparticle with non-axially symmetric double-well potential has been carried out using the stochastic Landau-Lifshitz equation. The relaxation process in the nanoparticles with diameter $D = 5-8$ nm has been studied numerically for a wide range of the damping parameter, $0.001 \leq \kappa \leq 2$, at a temperature $T = 77$ K. Importantly, the numerical simulation enables one to determine the actual bounds for the low and high dissipation regimes of relaxation. It is found, that for moderate reduced energy barriers, $\Delta E/T = 6 - 8$, the high damping limit occurs at $\kappa > \kappa_{large} = 1.0$, whereas low damping limit corresponds only very small value of the damping parameter, $\kappa < \kappa_{small} = 0.001$. For the intermediate κ values an interpolation formula for the relaxation time, $1/\tau_{in} = [1 - \exp(-\sqrt{\tau_l/\tau_s})]^2 / \tau_l$, is stated. It describes the results of numerical simulation with accuracy better than 10% for all values of the particle parameters investigated. Figure shows the relaxation process in a nanoparticle with diameter $D = 7$ nm and reduced energy barrier $\Delta E/T = 5.9$ for intermediate value of $\kappa = 0.03$. The characteristic time $t_0 = 4.4 \times 10^{-7}$ s. Irregular curve shows the numerical simulation data in comparison with analytical approximations for small (squares) and large (triangles) damping regimes, respectively. Smooth curve is drawn in accordance with the interpolation formula.



[1] W.F. Brown, Jr., *Phys. Rev.*, **130** (1963) 1677.

22PO-8-5

INVESTIGATIONS OF MFM TIP INDUCED REMAGNETIZATION EFFECTS IN COPT FERROMAGNETIC NANOPARTICLES

*Alekseev A.M.*², *Gribkov B.A.*¹, *Nikitushkin D.S.*¹, *Mironov V.L.*¹,
*Vdovichev S.N.*¹, and *Fraerman A.A.*¹

¹Institute for Physics of Microstructures RAS, Nizhny Novgorod, Russia

²NT-MDT Co, Moscow. Russia

Arrays of ferromagnetic nanoparticles with perpendicular anisotropy attract considerable attention at present time because of its possible applications as ultra high density magnetic storage media [1,2]. Also such arrays of ferromagnetic nanoparticles could be used as a controllable source of inhomogeneous magnetic field. In this work we present our results in the investigations of magnetic force microscopy (MFM) tip induced remagnetization reversal processes of ferromagnetic CoPt particles with dimensions from submicron size down to 35nm.

CoPt particles were fabricated by means of SEM lithography technique. Coercitivity of fabricated particles was about 200Oe. For performing controllable MFM tip induced remagnetization processes the non-contact single pass scanning procedure (also called 'flying mode') was used. This mode allows obtaining magnetic images of sample surface without scanning topography. High flying heights of MFM tip were used for getting non-perturbed MFM images of CoPt particles. Low heights were used for its remagnetization. Several types of samples were investigated: diameter of particles from 200nm down to 35nm; separation between neighbor particles in array was varied from 500nm down to 80nm. All samples initially were magnetized in perpendicular to plane direction in strong magnetic field 1kOe. As MFM investigations showed after that all particles in the array were oriented in similar direction according to magnetic field direction. The particle by particle remagnetization process contains several operations: (1) obtaining of MFM image at high flying height; (2) remagnetization of chosen particle using MFM tip at low scanning height; (3) observation of the remagnetization result. It's necessary to note, that performing of such tip induced remagnetization processes of vertical magnetized structures is possible only if ferromagnetic structures on the sample surface and MFM tip are magnetized towards to each other.

Finally we observed, that MFM technique allows controlling magnetic state of individual CoPt vertical magnetized particles with diameter down to 35nm and 80nm separation (density is approximately 50Gbit/inch²). At next step we will try to investigate the MFM tip induced remagnetization processes of CoPt particles with less diameter and separation.

Authors are thankful to N.I.Polushkin and his colleagues for CoPt films fabrication, to A.Yu.Klimov, S.A.Gusev and V.V.Rogov for samples fabrication. This work was partly supported by the RFBR, ISTC, and by EC through the NANOSPIN project (contract NMP4-CT-2004-013545).

[1] O.Hellwig, A.Berger, T.Thomson et. al. // Appl. Phys. Lett. 90, 162516, (2007)

[2] T.Thomson, G.Hu and D.Terris // Phys. Rev. Lett. 96, 257204, (2006)

22PO-8-6

OBSERVATION OF THE MAGNETIC DOMAIN STRUCTURES IN Cu_{0,47}Ni_{0,53} THIN FILMS AT LOW TEMPERATURES

Veshchunov I.S., Oboznov V.A., Rossolenko A.N., Prokofiev A.S., Vinnikov L.Ya.
Institute of Solid State Physics RAS, 142432 Chernogolovka, Moscow distr, Russia

The interest of investigating domain structure of weakly ferromagnetic Cu_{1-x}Ni_x (x~0.5) alloys is governed by their active use in thin film ferromagnet/superconductor heterostructures. The interaction between superconductivity and ferromagnetism leads to a number of interesting phenomena [1,2], which can be utilized in practical applications. The features of the intrinsic ferromagnet structure drastically affect the behavior of such systems. Besides, there is an inverse influence as experiments show.

Thin films of Cu_{0,47} Ni_{0,53} alloys with thickness of 10,20 and 50nm were grown by RF-sputtering on Si substrates at room temperature. The samples were investigated by high-resolution Bitter technique [3] at 4.2K well below the Curie point T_{Curie} of the films. In contrast to the magnetic force microscopy, this technique allows the visualization of the domain structure without its disturbance while the larger areas of the samples are probed.

Domain patterns reminiscent of maze domains typical for perpendicular magnetic anisotropy were found. The domain structure of 20nm thick film at magnetic field of 100 Oe is presented in Fig 1. Similar domain structures were observed for films of 10 and 50nm. The average domain size is found to be around 100 nm.

This work is supported by RFBR (07-02-00174) and Joint Russian-Israeli project MOST-RFBR (06-02-72025).

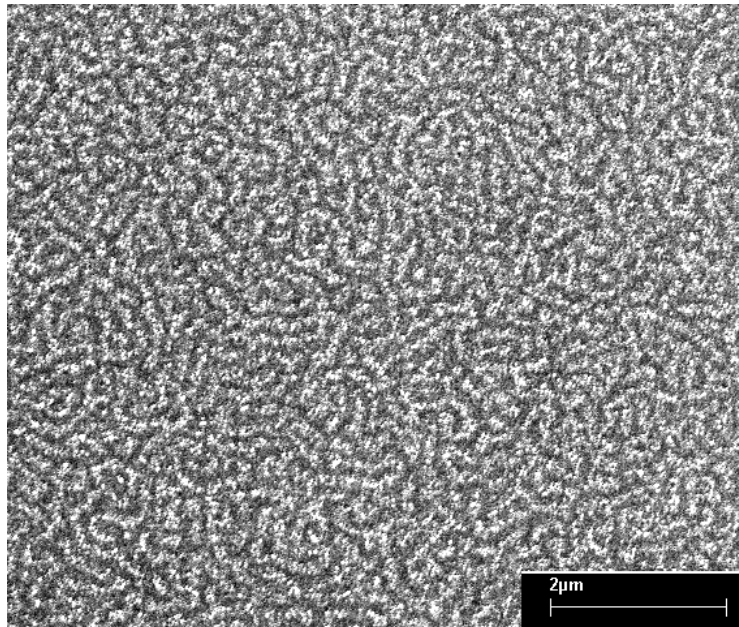


Figure 1

- [1] A.I. Buzdin, Rev. Mod. Phys. **77**, 935 (2005).
- [2] V.V. Ryazanov et al., Phys. Rev. Lett. **86**, 2427 (2001).
- [3] L.Y. Vinnikov et al., in The Real Structure of High-Tc Superconductors, edited by V. S. Shekhtman (Springer – Verlag, Berlin, Heidelberg, 1993), vol. **23** of Springer Series in Materials Science, p. 89.

22PO-8-7

MAGNETIC, THERMAL, AND TRANSPORT PROPERTIES OF HIGH-PRESSURE SYNTHESIZED NANOCRYSTALLINE EuC_6

*Tsvyashchenko A.V.¹, Sidorov V.A.², Fomicheva L.N.¹,
Thompson J.D.², Ronning F.², Ponomarev A.N.³*

¹Vereshchagin Institute for High Pressure Physics, RAS., 142190 Troitsk, Russia

²Los Alamos National Laboratory, Los Alamos, New Mexico 87545, USA

³Scientific Technical Center of Applied Nanotechnology, 198020 Saint-Petersburg, Russia

The graphite intercalated compound EuC_6 , where europium is in a Eu^{+2} state, orders magnetically below $T_N \sim 40$ K and exhibits a rich magnetic phase diagram [1]. Up to now only a thin layer of this compound could be obtained on the surface of the host graphite, even intercalation for weeks. We prepared bulk nanocrystalline EuC_6 by the route of high pressure and high temperature synthesis.

Europium powder and disordered carbon, prepared by STC of Applied Nanotechnology, were mixed, pressed to 8 GPa and heated by passing current through the mixture during a few minutes. The method of synthesis is similar to that used for preparation of other rare-earth compounds [2]. The structure and chemical composition of the samples were analysed with a transmission electron microscope JEM-2010. Magnetization, heat capacity and electrical resistivity measurements were performed between 2 and 350 K in magnetic fields up to 9 T in Quantum Design MPMS and PPMS devices.

X-ray and electron diffraction show amorphous-like patterns, with four main broad peaks having calculated d-spacings close to 0.34, 0.21, 0.17 and 0.12 nm. The transmission electron microscopy shows that pressure-synthesized samples consist of nanocrystals of the size 2-5 nm and chemical composition close to EuC_6 . The nanocrystals are formed by alternating carbon graphene-like layers and europium layers, with the europium atoms being disordered in these layers. AC-susceptibility exhibits a pronounced peak around ~ 25 K and a smaller peak at ~ 5 K that signals the appearance of ferromagnetic-like order. The position and amplitudes of these peaks do not change for months and indicate the relative stability of samples.

The electrical resistivity increases slightly from 9.2 $\text{m}\Omega\text{-cm}$ at 300 K to 9.7 $\text{m}\Omega\text{-cm}$ at 4 K, exhibiting the behavior of a strongly disordered material that contrasts with monocrystalline EuC_6 which is a good metal. The magnetic susceptibility obeys a Curie-Weiss law above ~ 60 K and the value of paramagnetic moment and Curie-Weiss temperature were found to be $\mu_{\text{eff}} = 2.48 \mu_B$ and $\theta_p = +12.5$ K, respectively. Magnetization measurements show that the material exhibits ferromagnetic behavior at low temperature. Its magnetic moment saturates at 2 K and 6 T to a value ~ 16 emu/gm which corresponds to $\mu_s \sim 0.64 \mu_B/\text{f.u.}$ Magnetic measurements show that europium atoms in the pressure synthesized EuC_6 are not in a purely Eu^{+2} state but rather in a mixed-valence state. Heat capacity at low temperature is high: C/T equals 20 mJ/mole-K^2 at 2 K and zero field and is suppressed to 9.3 mJ/mole-K^2 in a field of 9 T. $C(T)$ curves measured in different fields start to diverge below 25 K, the magnetic ordering temperature, implying that the main contribution to the low temperature heat capacity is due to magnetism.

This work was supported by the Russian Foundation for Basic Research (Grant 07-02-00280). Work at Los Alamos National Laboratory was performed under the auspices of the US DOE/Office of Science.

[1] H. Suematsu, K. Ohamatsu, T. Sakakibara et al., *Synth. Met.*, **8** (1983) 23.

[2] A.V. Tsvyashchenko, *J. Less-Common Met.*, **99** (1984) L9.

22PO-8-8

FERROMAGNETIC RESONANCE INVESTIGATIONS THIN MULTILAYER $[(\text{Fe}_{45}\text{Co}_{45}\text{Zr}_{10})_x(\text{Al}_2\text{O}_3)_{1-x}]_m/\{\alpha\text{-Si}\}_n$ FILMS

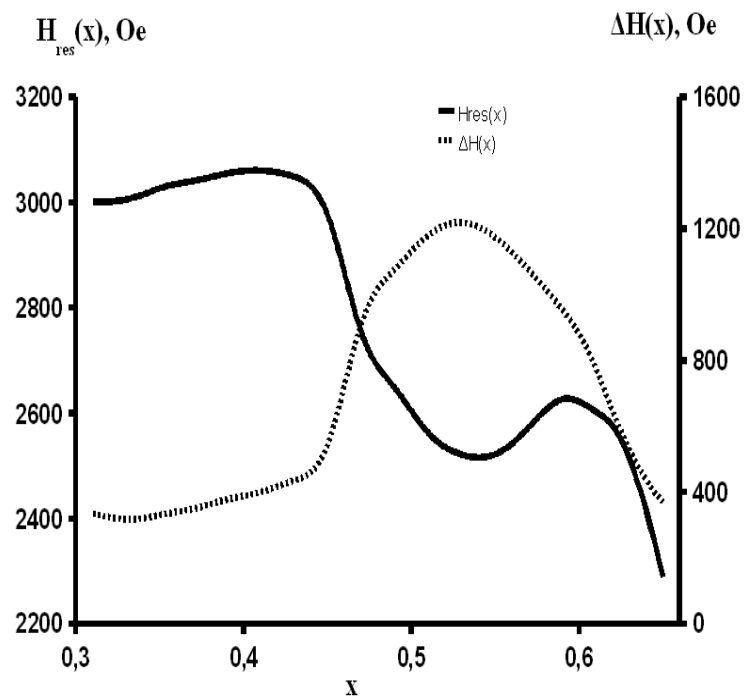
Efimets Yu.Yu.¹, Kotov L.N.¹, Kalinin Yu.E.², Sitnikov A.V.²

¹Syktyvkar State Univ., Radiophysics dept., Oktyabrsky Pr. 55, Syktyvkar 167001, Russia

²State Technical Univ., Physics of Solids, Moskovsky Pr. 14, Voronezh 394026, Russia

This work is devoted to the research on magnetic and relaxation properties of the films with the composition of $[(\text{Fe}_{45}\text{Co}_{45}\text{Zr}_{10})_x(\text{Al}_2\text{O}_3)_{1-x}]_m/\{\alpha\text{-Si}\}_n$ ($0,2 < x < 0,63$) and revealing their relationship with the nanostructure characteristics. The films with of a layer of a composite $1 \div 4$ nanometers were deposited on substrates of polycrystalline glass by the ion-beam sputtering method using compound targets of ferromagnetic and dielectric substances as previously described [1]. The films were received in an atmosphere of argon with pressure $P_{\text{Ar}} \approx 4 \cdot 10^{-2} \text{ Pa}$. The magnetic and relaxation properties of films have been characterized by means of ferromagnetic resonance (FMR). The FMR spectra were obtained by an electron paramagnetic spectrometer at 9.45 GHz using a standard modulation index meter [2, 3].

The FMR spectra were used to investigate the dependences of the resonant fields, FMR line widths and magnetization relaxation on concentration x in films. The FMR line width and the resonant fields are nonlinear depended to the metal phase percentage x (Figure) and thickness of layers. Features FMR line widths and magnetization relaxations are connected with dipole and exchange interaction between granules and layers. Significant changes in the shape of the FMR spectra lines are connected to nanostructural transformations in the ferromagnetic granules topology and sizes of metal alloy crystallites [2].



Support by RFBR (grant 06-02-17302).

[1] Y.E. Kalinin et al., *Phys. and Chem. of Processing of Materials*, (2001) 14.

[2] L.N. Kotov et al., *JMMM*, **316** (2007) 20.

[3] L.N. Kotov et al., *Mat. Sc. and Eng.*, **442** (2006) 352.

22PO-8-9

SYNTHESIS OF MAGNETIC NANOPOWDERS AND STUDY OF HEAT DISSIPATION UNDER AN ALTERNATING MAGNETIC FIELD

Sharapova V.A., Mysik A.A., Uimin M.A., Yermakov A.Ye.

Institute of Metal Physics, Ural Branch of RAS, 18, S.Kovalevskaya st., Ekaterinburg, Russia

Hyperthermia using magnetic nanoparticles is a promising field for cancer therapy, however at present its application is limited due to the choice of suitable magnetic nanoparticles which is capable to scatter the needed heat.

In our work we have been studied heat dissipation and magnetic properties of iron oxide Fe_3O_4 nanoparticles in axial and rotating alternating magnetic fields. Oxide nanopowders were prepared by gas-phase evaporation method of pure iron in the Ar atmosphere containing oxygen. To investigate the heat dissipation in nanoparticles due to reversal process the special device has been made, in where the container volume 480 mm^3 placed in magnetic field of constant frequency 70 kHz and controllable amplitude.

Characterization of powder has been made by different methods such as transmission electron microscopy (TEM), X-ray (phase composition, average size determination). We have been investigated the some samples with different average particles size within the range of 16 - 41 nm.

A sample of powder (average size 34 nm) was placed in solution of proxanol. It was shown that under the action of axial alternating magnetic field 170 Oe at 70 kHz, the specific heat energy dissipation was 11 W/g measured by using the initial part of the temperature dependence versus of time, but in a rotating magnetic field under the same conditions the heat dissipation was 32 W/g. In the given case the coercive force H_c was 30 Oe, and the magnetization was 11 emu/g. Measuring the square of hysteresis loops on the minor cycle in a field up to 170 Oe, we have indicated the specific hysteresis losses in the range of 0.44 W/g, which clearly mark the existence of additional rotational losses.

We should mention that a relatively coarse powder (average size 34 nm) was providing the high heat dissipation in the rotation field and was giving the poor heat effects in axial alternating magnetic field. On the contrary for the fine particle size (average size is about 16 nm) the heat effect in axial alternating field was much larger approximately 20 W/g. However, the hysteresis losses were 0.89 W/g, but when we fixed particles in paraffin, we have registered heat dissipation at the level of 9.9 W/g. It was demonstrated that in this case we have dealt with superposition of two fractions of powder (fine and coarse) which are providing the various contributions in the mechanism of heat losses at different field configurations.

At measurement of heat losses in an axial alternating field at frequency of 70 kHz using powder with average size of nanoparticles (16 nm) was found out that the growth of heat dissipation at increasing of amplitude of magnetic field can reach up 85 W/g.

In the paper we also discussed the nature of non-linear behavior of heat losses as a function of frequency, amplitude of field and powder concentration.

22PO-8-10

SILICA - METAL COMPOSITES AS FILLERS FOR BIOCOMPATIBLE POLYMERS

Bolbukh Iu.¹, Katok K.K.¹, Tertykh V.A.¹, Yurkov G.Y.², Volkov A.N.², Popkov O.V.²

¹Chemical Adsorption Department, Institute of Surface Chemistry by O.O. Chuiko, National Academy of Sciences of Ukraine, General Naumov, 17, 03164 Kyiv, Ukraine

(bolbukh@yahoo.com, <http://www.isc.gov.ua/>)

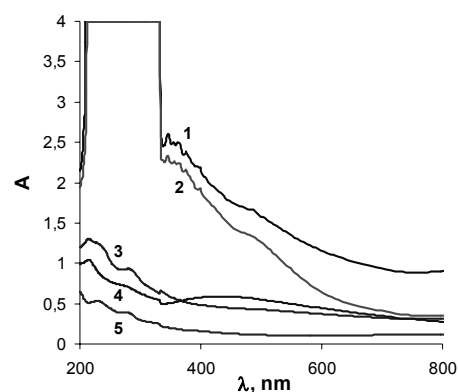
²Institute of General and Inorganic Chemistry, Russian Academy of Sciences, Leninsky prospect. 31, 119991 Moscow B-71, Russia (gy-yurkov@yandex.ru, <http://www.igic.ru/>)

Recent progress in nanofabrication have raised up challenging possibilities for designing novel composites based on filled polymers with new properties. Biocompatible nanocomposites filled with metal or oxides particles attract scientific attention due to their application as sensors, carriers of drug or biologically active substrates. Investigation of nanostructures self-organization via chemical or physical interaction in polymer matrixes, in particular at synthesis of magnetic sensitive materials, is one of fundamental task of nanotechnology.

The thermal treatment of salt or organometallic compounds at the present of strong reducer is one of the ways to obtain the uniform metal or oxide nanoparticles. Another way is synthesis of metal nanoparticles in surface layer of silica modified with groups that possess reducing properties. Such technique allows reducing the procedure temperature with controlling of metal particles size.

Structure of biocompatible nanocomposites is one of main factors of their functionality. That's why studying of such materials, in particular mechanisms of magnetic particles formation inside polymer (monomer) media and component interaction in system (polymer, magnetic particles, silica particles) is important for further development of this scientific direction.

In this work the nanocomposites based on biocompatible polymers and silica with silver or ferruginous particles as filler were investigated. At the first stage of the investigation the nanoparticles of ferric oxides were synthesized from salt aqueous solution in presence of modified silica with additional bubbling of ammonia. Synthesis of silver nanoparticles was carried out in result of interaction between silver nitrate solution and silica modified with functional groups that possess reducing properties. After reduction procedure silica with attached to surface silver particles or in mixture were dried at 20 or 120 °C. Obtained composites were studied by UV-Vis spectra. On Figure the UV-spectra of different ferric oxides (1-3) and silver particles (4) synthesized in the presence of modified silica are represent. Curve 5 corresponds to modified silica without metal. Presence of surface plasmon band in visible region at 400 nm provided evidence for silver nanoparticles formation.



Then the composites based on chitozan or 2-hydroxyethylmethacrylate were synthesized. The silica modified with nanoparticles of silver or ferruginous oxides were used as fillers. The polymer composites were obtained by drop-by-drop technique with and without fillers. Chitozan spheres were obtained at pH 3 or pH 10. It provided different state of amino groups of chitozan and macromolecules with correspondingly pseudospherical or linear shape.

Composites based on 2-hydroxyethylmethacrylate were synthesized by technique that excludes using of organic solvents. Structure of obtained samples was investigated with spectral methods. Developed techniques can be apply for synthesis of composites with immobilized medication.

22PO-8-11

MAGNETIC PROPERTIES OF EPITAXIAL COBALT FILMS GROWN ON A CORRUGATED $\text{CaF}_2(110)/\text{Si}(001)$ SUBSTRATE

Krichevtsov B.B., Kaveev A.K., Gastev S.V., Sokolov N.S.

Ioffe Physico-Technical Institute of RAS, 194021 St.-Petersburg, Russia

Ordered magnetic nanostructures, such as arrays of dots or wires, are now of particular interest, since they are considered to be promising materials for high-density memory systems and spintronic elements [1].

The magnetic properties of $\text{CaF}_2/\text{Co}/\text{CaF}_2(110)/\text{Si}(001)$ heterostructures fabricated by molecular beam epitaxy and having corrugated $\text{CaF}_2(110)$ buffer surface were studied by means of magneto-optical Kerr effects. The morphology of $\text{CaF}_2(110)/\text{Si}(001)$ heteroepitaxial substrates and cobalt films were analyzed by atomic force microscopy with lateral resolution about $\sim 7\text{nm}$. The growth of cobalt on CaF_2 has island character. In the initial stage of growth the individual islands form mainly in cubic fcc-modification as shows RHEED patterns. During the following growth, cobalt islands cover the entire surface however surface morphology still reflects the corrugation of the buffer layer. The studies of hysteresis loops using the longitudinal and transverse Kerr effects under oblique incidence and of magneto-optical phenomena under near-normal light incidence demonstrate that the corrugated structure of the surface leads to optical, magnetic and magneto-optical anisotropies. The magnetization reversal of such structures by in-plane magnetic field occurs via coherent magnetization rotation over a wide range of magnitude and orientation of magnetic field. The magnetic anisotropy of these structures is described by Gaussian distribution of easy axes of magnetization in cobalt granules or conglomerates of the granules around the direction parallel to the groove direction. The asymmetry of polarization plane rotation hysteresis loops observed at both oblique and normal light incidence is shown to be related to quadratic in magnetization \mathbf{M} components contributions ($\sim M_x M_y$) to the dielectric tensor ϵ_{ij} at optical frequencies.

The dependence of magnetic hysteresis loops on density of cobalt islands was studied. At low density of cobalt islands when the effective thickness d_{eff} of cobalt film is lower than the critical one $d_{\text{eff}} < d_{\text{eff}}^c$, the magnetic structure of the films may be described by array of superparamagnetic interacting particles characterized at $T=294\text{K}$ by small values of remanence M_r and coercive field $H_c \sim 10\text{ Oe}$. In this case the hysteresis loops do not exhibit noticeable anisotropy relative to the orientation of in-plane magnetic field. Decreasing the temperature one can observe in these films a considerable growth of M_r and H_c (up to $\sim 1\text{kOe}$) related to the transition of cobalt islands into blocked state. The blocking temperature is about $T_b \sim 280\text{K}$. Magnetic anisotropy parameter K and saturation magnetization M_s of the islands depend on the cobalt film growth temperature that influenced the dimensions of cobalt islands. The increase of effective thickness $d_{\text{eff}} > d_{\text{eff}}^c$ results at $T=294\text{K}$ in the jump-like growth of M_r and $H_c \sim 0.7\text{kOe}$ and appearance of hysteresis loops anisotropy induced by corrugated structure of CaF_2 buffer layer.

[1] J.M. Martin, J. Nogues, Kai Liy, J.L. Vicent, I.K. Schuller. JMMM, **256**,449 (2003)

22PO-8-12

FMR AND MAGNETIZATION CHARACTERIZATION OF ORDERED Ni NANOWIRES

Güner S.^{1,2}, Kazan S.³, Cemil Başaran A.³, Makarova T.L.⁴, and Dalchiele E.A.⁵

¹Department of Physics, Fatih University, 34500 Büyükçekmece / İstanbul, Turkey

²Center for Irradiation of Materials (CIM), Department of Physics, Alabama A&M University, Normal, AL 35762, USA

³Gebze Institute of Technology, 41400 Gebze- Kocaeli, Turkey

⁴Department of Physics, Umeå University, 90187 Umeå, Sweden

⁵Instituto de Física, Facultad de Ingeniería, Herrera y Reissig 565, C.C. 30, 11000 Montevideo, Uruguay

Magnetic and structural properties of nickel nanowire arrays electrodeposited into anodic alumina oxide (AAO) porous membranes with diameter of 180-200 nm were studied by Vibrating Sample Magnetometer (VSM) and Ferromagnetic Resonance (FMR) technique. The broad and multi FMR resonance lines of different Ni nanowire films which have been prepared at different electro-deposition potentials were observed and this unusual multi resonance lines for out of plane geometries (the oscillating magnetic field was in plane of nanowire film) were attributed to the spin waves along to wires. The magnetization was measured by VSM in both parallel and perpendicular positions of films with respect to the magnetic field.

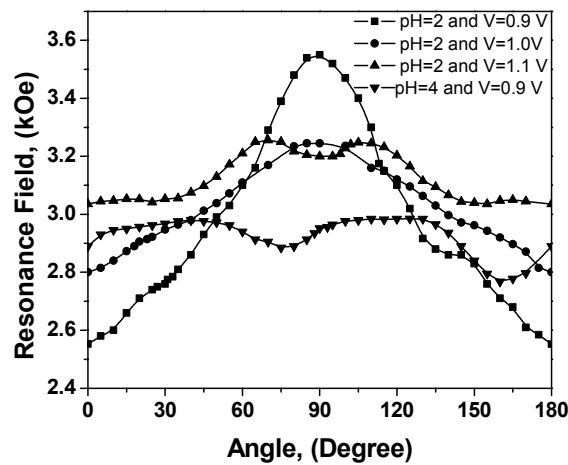


Fig. Angular dependence of ferromagnetic resonance fields at room temperature for the out of plane geometry case.

Support by Fatih University under Project No. P50010702 is acknowledged.

22PO-8-13

OPTICAL SPECTROSCOPY STUDY OF THE Dy^{3+} CRYSTAL-FIELD LEVELS AND MAGNETIC ORDERING IN THE CHAIN NICKELATE Dy_2BaNiO_5

Narozhnyy M.V.¹, Klimin S.A.¹, Mill B.V.², Popova M.N.¹

¹Institute of Spectroscopy RAS, Fizicheskaya 5, Troitsk 142190, Moscow region, Russia

²Moscow State University, Physics Department, 119899 Moscow, Russia

Dysprosium nickelate Dy_2BaNiO_5 is one of the members of the family of chain nickelates R_2BaNiO_5 . These compounds with R = rare earth or Y have attracted a considerable attention recently, after an observation of the Haldane gap in Y_2BaNiO_5 . Nickelates with R^{3+} carrying non-zero magnetic moment are known to exhibit a 3D magnetic ordering. Nevertheless the Haldane gap, being an intrinsic property of one-dimensional system composed of magnetic ions with integer-value spins, survives in nickelates even in a three-dimensional magnetically ordered state [1]. To get a deeper insight into this interesting model system, we have undertaken a detailed optical study of the crystal field levels and magnetic ordering in Dy_2BaNiO_5 .

In this work we have measured transmittance spectra of the polycrystalline sample Dy_2BaNiO_5 in a broad range of frequencies (2000-20000 cm^{-1}) and temperatures (4.2÷300K) using a Fourier-transform spectrometer BRUKER IFS 125HR and a closed-cycled helium cryostat Cryomech PT403. Positions of Dy^{3+} crystal-field levels in the ${}^6H_{15/2}$, ${}^6H_{13/2}$, ${}^6H_{11/2}$, ${}^6H_{9/2}+{}^6F_{11/2}$, ${}^6H_{7/2}+{}^6F_{9/2}$, ${}^6H_{5/2}$, ${}^6F_{7/2}$, ${}^6F_{5/2}$, ${}^6F_{3/2}$, and ${}^6F_{1/2}$ manifolds and exchange splittings in a magnetically ordered state of Dy_2BaNiO_5 have been determined. The establishment of a magnetic order is analyzed on the basis of temperature dependences of Kramers-doublet splittings. Our spectroscopic data allow to interpret some results of magnetic and heat capacity measurements on Dy_2BaNiO_5 .

This work was supported by the Russian Foundation for Basic Research under grant No. 08-02-00690, and by the Russian Academy of Sciences (program “Strongly correlated electrons and quantum critical phenomena”)

[1] A. Zheludev, J.M. Tranquada, T. Vogt, and D.J. Buttrey, *Phys. Rev. B* **54** (1996) 7210.

22PO-8-14

SYNTHESIS AND EFFECT OF SOME PARAMETERS THROUGH REVERSE MICELLES ROUTE OF IRON OXIDE NANOPARTICLES

Arabi H.^{1,}, Nateghi S.¹, Sadeghi S.²*

¹Physics department, faculty of science, University of Birjand, Iran

²Chemistry department, faculty of science, University of Birjand, Iran

*E-mail: arabi_h@yahoo.com

Superparamagnetic iron oxide nanoparticles have been widely used especially for numerous biomedical application such as vivo, tissue repair, hyperthermia, drug delivery and ultrahigh density magnetic storage, etc [1,2]. Various chemistry-based processing route have been developed to synthesise uniform and highly crystalline magnetic nanoparticles. Among these methods reverse micelles (using the restricted environments offered by surfactant water-in-

oil systems such as microemulsions) provides an excellent control over particle size, inter particle spacing and particles shape [3] Iron oxide nanoparticles with controlled size were synthesized by reverse micelles technique. In this process, all the steps of preparation were carried out under the argone atmosphere. Effect of some parameters, such as temperature of mixing two microemulsions, atmosphere, molar ratio of water to surfactant and concentration (ω paramete) of salt solution on size and properties of nanoparticles have been investigated.

There is no significant difference between samples prepared at 5°C, room temperature and 75 °C except a better crystalline at room temperature. X-ray powder diffraction (XRD), Transmission electron microscopy (TEM), and vibration sample magnetometer (VSM) were used to characterize the resultant samples. Both phase and estimated size of nanoparticles are measured by X-ray diffraction patterns. Increasing ω leads to producing particles with larger size (ie. for $\omega=16.83$, 11.22, and 5.6, particles size are 15.22, 11.66 and 10.5 nanometer, respectively The morphology of surface and precise size of particle was also determined with TEM Size of nanoparticles is in about of 9 to 20 nano meters.

The magnetic characterizations of nanoparticles were investigated by VSM. Magnetization loops of samples and approximate size of particles have obtained from magnetic measurements. As shown In Figure 1 the obtained nanoparticles have superparamagnetic behavior with smaller parameters of water to surfactant resulting to smaller particle size and lower saturation magnetization.

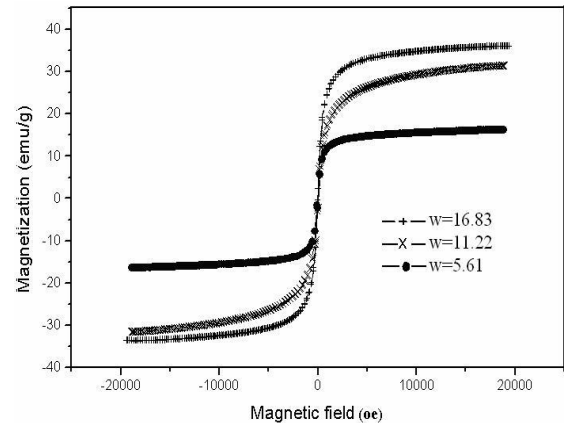


Fig. 1 Magnetization loops of Iron oxide Nanoparticles with different ω parameters

[1] A.K. Gupta, M.Gupta, Biomaterials., 26 (2005) 3995-4021

[2] H.Zeng, J.Li, J.P.Liu, Z.L.Wang, S.H.Sun, Nature 420 (2002) 395

[3] S. Morrison, C.L.Cahill, E.E. Carpenter, S.Calvin, and V.G. Harris, J. Nanoscience and nanotechnology, 5 (2005) 1323-1344.

22PO-8-15

FERROMAGNETISM AND SUPERPARAMAGNETIZM IN Fe/Co/Mo SUPERLATTICES

Antipov S.D., Goryunov G.E., Egov A.A., Smirnitskaya G.V., Senina V.A., Stetsenko P.N.
Faculty of Physic, Moscow State University

It is well known that multilayers and magnetic superlattices (MSL) containing Fe and Co ions have peculiar magnetic properties. The goal of present study was to obtain the Fe/Co/Mo MSL by means of cathode sputtering in discharge with Kr ions and oscillating electrons, and to investigate the influence of Fe, Co, Mo ions layers thicknesses on the basic magnetic parameters. To achieve this goal three series of MSL with constant thicknesses of Fe, Co; Fe, Mo; Co, Mo component and varied thicknesses of Mo, Co, Fe layers respectively were obtained and studied. The Fe/Co/Mo MSL were obtained on mica (muscovite) substrate at 70°C temperature. Magnetic measurements were carried out using an automated VSM with $2 \cdot 10^{-7}$ emu sensitivity in fields up to ± 8 kOe. The surfaces of MSL were imaged using scanning probe microscope (SPM) in

non-contact atomic force microscope mode at room temperatures of samples. The image shows the formation of island structure with a size distributions. The average size of islands was $\geq 2 \cdot 10^3 \text{ \AA}$ along the direction of magnetic field (Hd) at deposition and $\geq 1 \cdot 10^3 \text{ \AA}$ across Hd; the average height was $\approx 800 \text{ \AA}$ ($h=200-1400 \text{ \AA}$).

According XRD data the samples Fe/Co/Mo are in amorphous or nanocrystalline phases at room temperature.

The magnetic measurements showed that the most MSL in-plane have ferromagnetic behavior, but several samples Fe/Co/Mo MSL with variation of Co layers thicknesses revealed the existence of superparamagnetic states ($I_r=0$, $H_c=0$) at the $T > T_b$, where T_b is blocking temperature. For $[\text{Fe}(10 \text{ \AA})\text{Co}(10 \text{ \AA})\text{Mo}(12 \text{ \AA})] \cdot 100 T_b$ was about 230K. It is well known that by fitting the $I(H)$ data to Langeven function

$$I(T) = n\mu(\coth a - a^{-1})$$

where $a = \frac{\mu H}{k_B T}$, n is a number of microensembles per unit volume, μ is the magnetic moment of particular microensemble, k_B is Boltzmann's constant. Using μ as a fitting parameter it is possible to determine magnetic moment of superparamagnetic per microensemble: $\mu = 1.4 \cdot 10^3 \div 1.18 \cdot 10^4 \mu_B$.

It permitted to suppose the existence of long-range dipole and short-range exchange interaction among clusters in MSL Fe/Co/Mo.

The work is supported by RFBR grant 08-02-00970-a.

22PO-8-16

INDUCED MAGNETISM IN FeRh NANOPARTICLES STUDIED BY X-RAY MAGNETIC CIRCULAR DICHROISM

Smekhova A.¹, Ciuculescu D.², Lecante P.³, Wilhelm F.¹, Amiens C.², Rogalev A.¹, Chaudret B.²

¹European Synchrotron Radiation Facility, BP220, Grenoble Cedex, 38043, France

²Laboratoire de Chimie de Coordination, UPR 8241-CNRS, Toulouse Cedex 04, 31077, France

³Centre d'Elaboration de Materiaux et d'Etudes Structurales, UPR 8011-CNRS,
Toulouse Cedex 04, 31055, France

The nanoparticles (NP_S) are the subject of intense research activities in the last decade [1]. Progress in chemistry made it possible to synthesize nanoparticles in the wide range of sizes down to several nanometers [2,3], but at the same time NP_S exhibit large varieties of structural and, therefore, of electronic and magnetic properties. So, the further experimental investigations aimed at establishment of a correlation between structure and properties of NP_S are highly desirable.

Here, we concentrate our attention on bimetallic Fe_xRh_{100-x} nanoparticles ($x = 80, 50$) that could be considered as a good target to explore the relation between the chemical distribution and order inside NP_S and their magnetic properties [4]. Fe_xRh_{100-x} nanoparticles were synthesized according to a recently designed one-pot preparation method [5] by simultaneous decomposition of stoichiometric quantities of $Fe[N(\text{Si}(\text{CH}_3)_3)_2]_2$ and $Rh(\text{C}_3\text{H}_5)_3$ in mild conditions of temperature and hydrogen pressure but with addition of different reactants.

Magnetic properties of the Fe_xRh_{100-x} nanoparticles have been studied with X-ray absorption spectroscopy and X-Ray Magnetic Circular Dichroism (XMCD) near the K edge of Fe and the $L_{2,3}$ edges of Rh. Whereas the former technique is sensitive to the local electronic

structure and charge at the absorbing atom, the latter provides unique information about magnetic moments carried by the absorbing atom.

The XMCD measurements reveal different values of the spin and orbital magnetic moments at Rh atoms depending on iron concentrations and NPs preparation route. On the other hand, the orbital magnetic moment at Fe atoms monitored via magnetization of the 4p states is found to be nearly the same for all samples and reduced approximately twice in comparison with bulk value. The influence of NP_s structure on orbital and spin contributions of magnetic moment at Rh atoms are discussed.

- [1] S.Sun, C.B.Murray, D.Weller, L.Folks, A.Moser, *Science*, **287** (2000) 1989.
- [2] S.Stappert, B.Rellinghaus, M.Acet, E.F.Wassermann, *J.Cryst.Growth*, **252** (2003) 440.
- [3] D.Li, N.Poudyal, V.Nandwana, Z.Jin, K.Elkins, J.P.Liu, *J.Appl.Phys.*, **99** (2006) 08E911.
- [4] D. Ciuculescu, C.Amiens, M.Respaud, P.Lecante, A.Falqui, B.Chaudret, *Modern Phys. Lett. B*, **21** (2007) 1153.
- [5] D. Ciuculescu, C. Amiens, M. Respaud, A. Falqui, P. Lecante, R. E. Benfield, L. Jiang, K. Fauth, B. Chaudret, *Chem. Mater.*, **19** (2007) 4624.

22PO-8-17

MAGNETIC STATES OF FE IONS IN Fe/Co/Mo SUPERLATTICES

Antipov S.D., Goryunov G.E., Egov A.A., Smirnitskaya G.V., Senina V.A., Stetsenko P.N.

Faculty of Physics, Moscow State University

In this report the results on the investigation of magnetic states of Fe and Co ions in superlattice [Mo(12 Å)Co(21 Å)Fe(14 Å)]*100 are presented. The magnetic superlattice was obtained by means of cathode sputtering in high vacuum discharge with Kr gas at a pressure in the range 10^{-5} Torr in magnetic field 320 Oe in plane of sample with oscillating electrons. It is proved that this method forms small clusters deposited on the substrate (mica) at 70°C.

X-ray diffraction studies of [Mo(12 Å)Co(21 Å)Fe(14 Å)]*100 sample revealed broad halos in 2θ regions [$2\theta \approx 46^\circ \pm 5^\circ$, $\lambda(CoK_\alpha) \cong 1.791 \text{ \AA}$] indicating the formation of an amorphous phase. Magnetization loops of the cluster-assembled superlattices have been recorded by the vibrating sample magnetometer at the room temperature. The magnetic states of Fe and Co ions have been investigated using Mossbauer spectroscopy and electron spin resonance (ESR) experiments. The Mossbauer spectra of ^{57}Fe nucleus (MS) of sample and ESR measurements were performed at the room temperature. The ESR spectra were recorded on a Bruker (ELEXYS-506) spectrometer. The investigations of absorption spectra of MS and ESR were made for the as-deposited and after annealing at 450°C. (t=1h) at the pressure 10^{-5} Torr.

It was found that the spontaneous magnetization for the as-deposited sample is high 2000Gs. The increase of the coercivity for the annealed sample also found: $H_c(\text{as-deposited})=10$ Oe, $H_c(\text{after annealing})=105$ Oe.

We found that local magnetic states of the Fe ions for the as-deposited and after annealing are different. At room temperature in the ESR spectrum for the as-deposited we observed 6 lines with the effective gyromagnetic factors $g_{\text{eff}} = 16.3; 11.4; 8.2; 7.64; 7.16; 6.34$ and after annealing $g_{\text{eff}} = 41.8; 13.6; 7.4$ in plane of sample.

The results of our studies of states Fe and Co ions indicate that they correspond higher-spin states in clusters $Fe_n, Co_n, Co_n Fe_m, Fe_n Mo_m$ with small number of atoms n, m in clusters

and with large contribution of orbital moments in formation of total magnetization of superlattice [Mo(12 Å)Co(21 Å)Fe(14 Å)]*100.

The work is supported by RFBR grant 08-02-00970-a.

22PO-8-18

OSCILLATING DEPENDENCES OF SPONTANEOUS MAGNETIZATION IN Fe/Co/Mo SUPERLATTICES VERSUS Mo, Co, Fe LAYERS THICKNESSES

Antipov S.D., Goryunov G.E., Egov A.A., Smirnitskaya G.V., Senina V.A., Stetsenko P.N.
Faculty of Physics, Moscow State University.

In this work we report the result of experimental investigation of magnetic properties of three series Fe/Co/Mo magnetic superlattices (MSL) obtained by means of cathode sputtering in high-vacuum discharge with Kr gas at a pressure in the range 10-5 torr in magnetic fields up to 8000 Oe with oscillating electrons, a technique that is proved to form small clusters deposited on different substrates. The first set has constant Fe and Co layers and Mo layer thickness was varied. The second set of sample has Fe and Mo layers constant and Co layer thickness was varied. The samples incorporate up to 100 Fe/Co/Mo layer thirds.

The X-ray diffraction studies of Fe/Co/Mo magnetic superlattices revealed nanocrystalline or amorphous states of the samples. The crystallites sized about 300Å (Fe), 200-500 Å (Co) and 200Å (Mo).

The surfaces of MSL Fe/Co/Mo were imaged using scanning probe microscope (Solver PRO NT-MDT).

The hysteresis loops, magnetization measurements were performed in-plane and out-plane using a vibration sample magnetometer at room temperature. An in-plane magnetic anisotropy was demonstrated for majority Fe/Co/Mo samples.

The samples from the first set Fe/Co/Mo superlattices have shown non-monotonous oscillating dependence of spontaneous magnetization versus Mo layer thickness with a period of about 5Å. Similar oscillations of magnetization versus Co and Fe layers thicknesses were observed in second and third series, where the period equaled 6 Å. Such oscillations in the first case may be interpreted in terms of distance variations of magnetic exchange interactions and in terms of electron wave interference effects in Mo spacer due to partial reflections in interfaces in the second and third cases.

Several samples of Fe/Co/Mo magnetic superlattices possessed the spontaneous magnetization values exceeding that of bulk Fe. This may be described by:

- a) a change in Fermi-level density of states for Fe and Co ions at cluster surfaces
- b) unquenching of orbital moments of Fe and Co ions in clusters and in interfaces.

Similar oscillating dependences versus Mo, Co and Fe layers thicknesses were observed also for the remanent magnetizations and coercive field.

The work is supported by RFBR grant 08-02-00970-a.

22PO-8-19

PARAMAGNETIC CENTERS IN CuTe_2O_5

Gavrilova T.P., Eremina R.M.

Zavoisky Physical -Technical Institute (ZPhTI), Sibirsky tract, 10/7,
420029 Kazan, Russia

Observation of the spin-Peierls transition in CuGeO_3 [1] has stimulated searches of similar lowdimensional materials. Lemmens et al. [2] found that, as the temperature decreases, the magnetic susceptibility of CuTe_2O_5 , as well as that of CuGeO_3 , decreases along the three crystallographic directions. An analysis of the structural data allows the assumption that the dimerization of copper spins occurs in CuTe_2O_5 ; i.e., as in the case of CuGeO_3 , dimers with a singlet ground state are formed. It was established that at temperatures of 25 to 300 K, the EPR spectrum of copper ions consists of one Lorentzian-shaped line with $g \sim 2$. Near 25 K, the line splits into several components [3,4].

Figure 1 shows the angular dependences of position of the ESR lines in CuTe_2O_5 at a frequency of 34 GHz in the crystallographic plane bc measured at the temperature of 5 K. We connect the occurrence of these signals in ESR spectra with formation of the paramagnetic centers with $S=1$ in single crystal CuTe_2O_5 . Based on the assumption that pairs of Cu ions form dimers with $S=1$ we use the spin Hamiltonian:

$$H = DS_z^2 + E(S_x^2 - S_y^2) + \sum_{\alpha=a^*,b,c} g\mu_B H_\alpha S_\alpha,$$

where first two terms are presented in local axes of a pair, and the last term describes the interaction with the magnetic field.

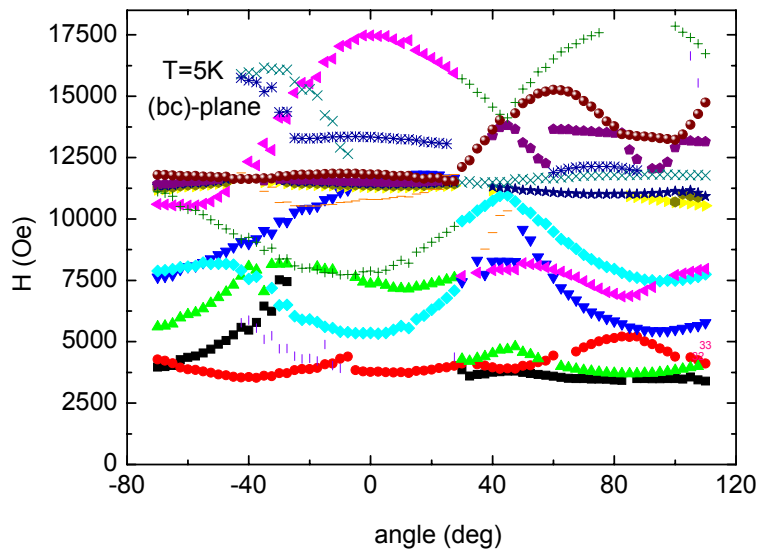


Fig.1. Angular dependences of position of the ESR lines in CuTe_2O_5 in the Q band in the crystallographic plane bc at $T=5$ K

This work was supported by the Russian Foundation for Basic Research (project no. 06-02-17401).

[1] M. Hase, I. Terasaki, and K. Uchinokura, Phys. Rev. Lett. 70, 3651 (1993).

[2] P. Lemmens, G. Guntherodt, and C. Gros, Phys. Rep. 375, 1 (2003).

[3] J. Deisenhofer, R.M. Eremina, A. Pimenov, T. Gavrilova *et al.*, Phys. Rev. B. 74, 174421 (2006)

[4] R. M. Eremina, T. P. Gavrilova, N.-A. Krug von Nidda *et al.*, Fizika Tverdogo Tela 50 №2, 273 (2008)

22PO-8-20

SPIN POLARIZATION IN LOW DIMENSIONAL INCOMMENSURATE SYSTEMS WITH HELICAL MAGNETIC STRUCTURE AS SEEN BY NMR

Gippius A.A.^{1,2}, Morozova E.N.^{1,2}, Okhotnikov K.S.¹, Moskvin A.S.³

¹Faculty of Physics, Moscow State University, Moscow, Russia

²Shubnikov Institute of Crystallography, Moscow, Russia

³Ural State University, Ekaterinburg, Russia

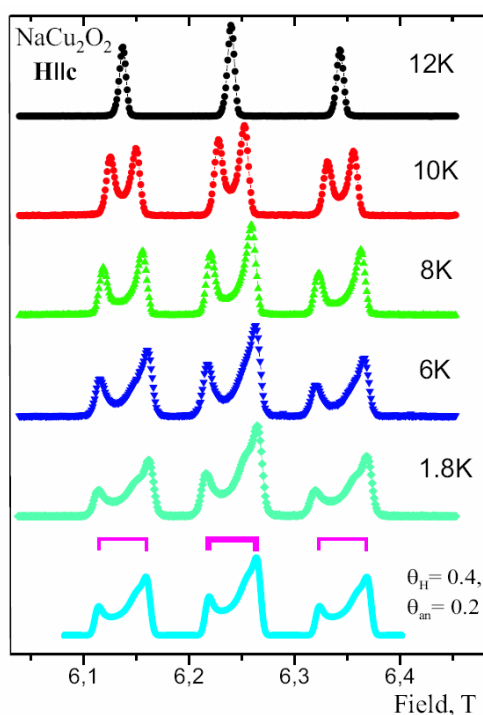
The magnetic phase transitions observed at low temperature in several edge-shared chain cuprates (e.g., LiCu₂O₂, LiVCuO₄, NaCu₂O₂, Li₂ZrCuO₄) are considered as an evidence for incommensurate (IC) helicoidal order with the propagation along the chain direction [1-3]. This picture based on strong in-chain frustration is supported by NMR, neutron diffraction and specific heat measurements. We have performed ²³Na NMR measurements on NaCu₂O₂ single crystal in the paramagnetic and in the ordered phase for the external field oriented along the main crystal axes H||**a**,**b**,**c** by sweeping H at fixed frequency of 70.0 MHz.

The NMR line shape for an incommensurate system can be calculated as follows:

$$F(\vec{H}) \propto \int \exp\left(-\frac{(|\vec{H} + \vec{H}_{loc}(\varphi)| - H_L)^2}{2\delta^2}\right) d\varphi$$

where \vec{H} is an external magnetic field, H_L – Larmor field, $\vec{H}_{loc}(\varphi)$ is a local field on Na site, δ is a homogeneous line width. The ²³Na NMR lineshape is strongly asymmetric pointing to the NMR response of an *bc*-plane polarized spin spiral. The ²³Na NMR lineshape at T=1.8 K can be successfully simulated with anisotropy parameter $\theta_{an}=0.2$ and Zeeman parameter $\theta_H=0.4$ (see figure).

The ²³Na NMR lineshape in NaCu₂O₂ shows clear signature of an IC static spin structure consistent with a spiral modulation of the Cu magnetic moments polarized in the *bc*-plane in contrast with the *ab*-plane polarization reported earlier [3]. It is the first experimental indication for spin polarization in a plane perpendicular to the plane of the basic CuO₄ plaquette in the edge-shared cuprates.



This work was supported by Russian Science Support Foundation.

[1] Drechsler S.-L., Richter J., Malek J. et al., JMMM. **345** (2005) 290.

[2] Gippius A.A., Morozova E.N., Moskvin A.S. et al., Phys. Rev. B **70** (2004) 020406.

[3] Capogna L., Mayr M., Horsch P. et al., Phys. Rev. B **71** (2005) 140402.

22PO-8-21

AB INITIO MOLECULAR DYNAMICS STUDY OF CARBON DISSOLUTION AND CLUSTERIZATION ON IRON SURFACES

Mutigullin I.V., Bazhanov D.I.

Physics Department, Moscow State University, Moscow, 119992, Russia

The recent intensive theoretical and experimental research activities were focused on the study of the influence of different metal catalysts based on transitional metals (Fe, Ni, Pd etc) on carbon graphitization process. These studies revealed the strong impact of catalyst surfaces on the growth morphology of carbon nanostructures (carbon nanotubes, nanofibers etc.) [1, 2]. However the formation processes of carbon nanostructures on an atomic scale are not well understood yet. On the other hand there was recently shown that carbon impurities can strongly affect the structural and electronic properties of catalyst [3]. That's why it is very important to study theoretically the dissolution and clusterisation properties of individual carbon adatoms on metal surfaces as an initial stage of carbon nanostructures growth.

In this work we present the first-principles molecular dynamics study of interaction and dissolution of carbon adatoms on (001) and (111) surfaces of ferromagnetic alpha-iron. This study was performed in the frame of density functional calculations with employment of plane-wave basis set and PAW potentials.

The theoretical investigations of carbon adatom interactions on low-index (001) and (111) surfaces have been carried out to study the formation process of carbon clusters on surfaces of metal catalysts. There was found, that interaction of carbon adatoms leads to their large distance mutual distribution on (001) and (111) surfaces and less packed carbon structures, which is in an agreement with previous studies of carbon on Fe (001) surface in works [4, 5]. We found that small carbon clusters have a larger binding energies on (111) surface than on (001) one, and form the growth centers for carbon nanostructures. The results of our calculations have shown also that deposition of carbon clusters up to one monolayer coverage on iron (001) surface leads to intermixing of carbon adatoms with upper metal layers. The dissolved carbon atoms produce the strong lattice distortion which impact the bonding and electronic properties of surrounding atoms.

[1] M. Yudasaka, Y. Kasuya, F. Kokai, K. Takahashi, M. Takizawa, S. Bandow, S. Iijima, *Appl. Phys. A* **74** (2002) 377

[2] Z.P. Huang, D.Z. Wang, J.G. Wen, M. Sennett, H. Gibson, Z.F. Ren, *Appl. Phys. A* **74** (2002) 387

[3] D.W. Boukhalov, Yu.N. Gornostyrev, M.I. Katsnelson, A.I. Lichtenstein, *Phys. Rev. Lett.* **99** (2007) 247205

[4] G. Panaccione, J. Fujii, I. Vobornik, G. Trimarchi, N. Binggeli, A. Goldoni, R. Larciprete, G. Rossi, *Phys. Rev. B* **73** (2006) 035431.

[5] C. Uebing, *Phys. Rev. B* **50** (1994) 12138.

22PO-8-22

MAGNETIC PROPERTIES AND SURFACE EFFECTS OF MAGNETITE NANOPARTICLES

Alkaev E.A.¹, Lyubutin I.S.¹, Lin C.R.², Chiang R.K.³,

¹Institute of Crystallography, Russian Academy of Sciences, Moscow 119333, Russia

²Department of Mechanical Engineering, Southern Taiwan University, Tainan 710, Taiwan

³Nanomaterials Laboratory, Far East University, Hsing-Shih, Tainan County 74448, Taiwan

In this study the compositions and magnetic properties of magnetic iron oxide nanoparticles were determined by Mossbauer spectroscopy. First we studied the phase composition of magnetic nanoparticles synthesized by thermal decomposition of hematite (α -Fe₂O₃) powder in the presence of high boiling point organic solvents. The mean crystallite size of the particles was about 40 nm. XRD patterns show that the phases of intermediate were composed of the spinel phase (Fe₃O₄ or/and γ -Fe₂O₃) and the corundum phase (α -Fe₂O₃). The ⁵⁷Fe Mossbauer spectra reveal that the spinel phase is originated from the magnetite Fe₃O₄ nanoparticles. Relative content of magnetite and hematite is dependent on the reaction time. The saturation magnetization and concentration of magnetite in the samples increases with the reaction time. The Moessbauer spectra show that 95% is magnetite and 5% is hematite after treatment for 28 hrs. The synthesized phase of hematite/magnetite composite has nonstoichiometric magnetite inside [1]. It was found from the Mossbauer spectra that not all B-site iron ions (Fe³⁺ and Fe²⁺) in magnetite nanoparticles experience the electronic exchange at temperatures above the Verwey point T_V which can be related to surface effects.

The monodisperse magnetic iron oxide nanoparticles were obtained as a result of slow dissolution of hematite powder in a mixture of unsaturated fatty acids and organic solvents. The transmission electron microscopy showed that the particles were monodisperse and spherically shaped with diameter of 19.2, 12.1, 10.6 and 8.8 nm depending on the preparation conditions. The Mossbauer spectra reveal that γ -Fe₂O₃ is preferentially precipitate out at lower ligand concentrations, while the Fe₃O₄ appears along with γ -Fe₂O₃ at higher ligand concentrations. Only the 19.2 nm particles exhibit a well-developed magnetic hyperfine splitting at 300 K. The content of Fe₃O₄ and γ -Fe₂O₃ in this compound is in the ratio 0.65 : 0.35. The Mossbauer spectra of the particles with sizes 12.1, 10.6 and 8.8 nm reveal superparamagnetic behavior with slow spin relaxation in the temperature range 80 – 300 K. In these particles, two Mossbauer components were found which exhibit different values of the blocking temperatures $T_{b1} = 150$ K and $T_{b2} = 220$ K. It seems that T_{b2} corresponds to core part of the particles whereas T_{b1} is related to the shell [2]. Here "core" is the central part of the ball-shaped nanoparticle, while "shell" is the surface layer of the particle. From the Messbauer data we have evaluated the relative volume of the core V_{core} and shell V_{shell} parts of the spherical-shaped particles. Than using the ratio

$$R_{particle} = r_{core} \sqrt[3]{\frac{V_{shell}}{V_{core}} + 1}$$

where $R_{particle}$ is the particle radius and r_{core} is the radius of the core part of the particle, we can estimate the thickness of the particles surface layer. For the 10.6 nm particles the thickness is $(R_{particle} - r_{core}) = 1.3 \pm 0.1$ nm.

We thank the Russian Academy of Sciences and National Science Council of Taiwan for financial support of the project.

[1] F.C. Voogt, T. Fujii, P.J.M. Smulders et al. , *Phys. Rev. B*, **60** (1999) 11193.

[2] F. Badker, M. F. Hansen, C. B. Koch, K. Lefmann, S. Morup, *Phys.Rev. B*, **61** (2000) 6826.

22PO-8-23

MAGNETIZATION CURVE IN TWO-PHASE NANOMAGNETS: THE MODEL OF MAGNETIC NANOCHAIN WITH RANDOM MAGNETIC ANISOTROPY

Smirnov S.I.¹, Komogortsev S.V.², and Iskhakov R.S.²

¹Krasnoyarsk State Pedagogical University, Krasnoyarsk, 660049 Russia;

²Institute of Physics, SB Russian Academy of Sciences, Krasnoyarsk, 660036 Russia;
e-mail: komogor@iph.krasn.ru

Two important characteristics of nanocrystalline ferromagnetic alloys are the orientation fluctuation of the local magnetization easy axes and the significant contribution of exchange interaction to the total magnetic energy. The radius of exchange interactions has the order of 1 nm. Therefore the exchange interaction between nanoparticles is absent in two-phase alloys where the uncoupled magnetic grains are distributed in a nonmagnetic matrix. Such materials show in a magnetic field either superparamagnetic behavior (Co-Cu, Co-Ag, Fe-Cu) or behave as a system of single-domain noninteracting ferromagnetic particles (for example, alloys FeCuNbSiB at temperature above Curie temperature of amorphous matrix phase) [1]. If the matrix phase is ferromagnetic, exchange interaction of a matrix with grains leads to the collective phenomena which cause outstanding applied characteristics both soft magnetic (FeCuNbSiB) and hard-magnetic (NdFeB) nanocrystalline alloys [2]. For understanding of macroscopic magnetic properties of such two-phase materials the convenient linear algebraic procedures of averaging are incorrect.

We have made numerical experiment to simulate the magnetization curve in a two-phase chain of ferromagnetic grains with random magnetic anisotropy. The method of calculation is based on the search of equilibrium distribution of magnetization in a chain with the exchange-coupled grains with random magnetic anisotropy. The equilibrium distribution of magnetization is found numerically from the differential equation:

$$\frac{d^2\theta(x)}{dx^2} = \frac{1}{\delta(x)^2} \sin(2(\theta_a(x) - \theta(x))) - h \sin(\theta(x)),$$

where $\theta(x)$ is a corner between magnetization vector and external field direction, $\theta_a(x)$ is random function of the deviation angle between the local magnetic anisotropy axis and the external field direction, $h = M_s H / 2K$ is external magnetic field, $\delta(x) = (A(x)/K(x))^{1/2}$, A is the exchange interaction constant, K is the local anisotropy energy, M_s is the saturation magnetization. Parameter $\delta(x)$ specifies the type of two-phase system. We have select the function $\delta(x)$ as a chain of rectangular impulses with the alternating amplitudes of two different values. For distributions $\theta(x)$ we calculate the correlation function of magnetization $K_m(R)$ and the average value of magnetization $M(h)$ at various values of h . It is occurred that the linear procedures of averaging for the magnetic two-phase nanocomposites are correct in the case when the size of the phase homogeneity more than a critical value – a size of stochastic magnetic domain. Otherwise the linear rules of averaging for magnetization in two-phase nanocomposite are invalid.

Support by the grant RFBR 07-02-01172-a; National Science Fund (2008, PhD RAS) are acknowledged.

[1] G. Herzer *IEEE Trans. On Magn.*, **25** (1989) 3327.

[2] A. Hernando *J. Phys.: Condens. Matter.*, **11** (1999) 9455.

22PO-8-24

MAGNETIC AND STRUCTURAL PROPERTIES OF NANOCOMPOSITE MELT-SPUN $Gd_2Fe_{14}B$ BASED ALLOYS

Bartashevich M.I.¹, Andreev S.V.¹, Bogatkin A.N.¹, Kozlov A.I.¹, Kudrevatikh N.V.¹, Markin P.E.^{1,2}, Milyev O.A.¹, Nizola A.A.¹, Gaviko V.S.², Pushin V.G.², Shreder L.A.²

¹Ural State University, 620083, Ekaterinburg, Lenin av. 51, Russia

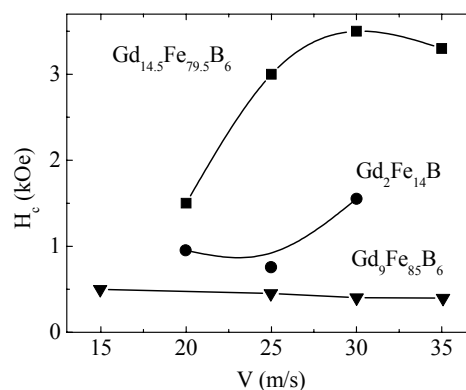
²Institute of Metal Physics, Ural Division of RAS, S. Kovalevskaya 18, 620041 Ekaterinburg, Russia

R–Fe–B alloys (R – rare earth metal) have been subject to extensive studies because of their excellent permanent magnet properties. Much of the published work has been dedicated to nanoscale rapid melt spun (RMS) hard magnetic materials (HMM) based on the R-Fe-B alloys system and used as the powder filler for permanent magnets. Usually, magnetic and highly anisotropic R element has been used to achieve the improved magnetic properties of the RMS HMM.

In order to reveal the role of the 3d transition metal with uniaxial anisotropy in formation of magnetic properties of RMS alloy, the structure and magnetic properties of RMS HMM based on the Gd-Fe-B alloys system in the region of phase structure 2-14-1 have been studied. In these systems Gd ion has zero orbital momentum (magnetically isotropic, $L = 0$), however it still persists rather high exchange interaction between rare earth and iron sublattices. RMS ribbons were prepared by centrifugal quenching method. Depending on composition, three main groups of alloys have been used: 1). "understoichiometric" - $Gd_9Fe_{85}B_6$, 2). "stoichiometric" - $Gd_2Fe_{14}B$, 3). "overstoichiometric" - $Gd_{14}Fe_{80}B_6$. Quenching wheel tangential surface speeds (V_s) were in the interval 10 - 40 m/s. Atomic and phase structure analyses have been performed by X-ray and electron microscopy methods. The coercivity dependence (H_c), the saturation magnetization (σ_s), the magnetization remanence (σ_r), the quantity of exchange increase ($\Delta\sigma_r = \sigma_r/\sigma_s - 0.5$) by the annealing temperature, melting temperature (T_L) and the moving tangential surface speeds have been studied.

The observed low value of H_c for the 1st group of alloys (see. Fig.) is explained by the large amount of metastable $Gd_2Fe_{17}B_x$ phase (up to 70 %) with planar anisotropy. This behavior is in contrast with isocompositional RMS alloys with Nd, where the metastable $Gd_2Fe_{17}B_x$ phase does not exist and H_c vs. V_s exhibits maximum. Maximum of H_c for the 3rd group of alloys and expected one for the 2nd group is explained by attaining the optimal grain size (about 45 nm) of the main HM $Gd_2Fe_{14}B$ phase. For all studied alloys H_c has extremum in the annealing temperature interval 600 - 900

⁰C. The maximum effect of exchange increase is achieved in the alloys of the 1st and the 2nd groups. The obtained results revealed the correlations between the magnetic properties, the final microstructure and phase composition and show that Fe sublattice can significantly contribute to the coercivity in R–Fe–B RMS HMM.



This work was supported by RF Program of High School Science Potential Development, project RNP.2.1.1.6945.

22PO-8-25

TRANSPORT AND MAGNETOTRANSPORT PROPERTIES OF AMORPHOUS METAL-DIELECTRIC NANOCOMPOSITES

Kalinin Yu.E., Sitnikov A.V., Stognei O.V.

Voronezh Technical State University, Voronezh, 394026, Russia

The results of investigation of electroresistivity as well as magnetoresistivity (MR) of granular metal-dielectric nanocomposites with amorphous structures are presented. The granular nanoclusters of pure metal or metal alloy (Co, Fe₄₅Co₄₅Zr₁₀, Co₄₁Fe₃₉B₂₀ or Co₈₄Nb₁₄Ta₂) randomly distributed in dielectric amorphous matrix (SiO₂, Al₂O₃, CaF₂ or MgO₂) were obtained by ion-beam sputtering of composite targets and deposition of the material to glassceramic substrates. The granular media from metal amorphous granules placed in dielectric matrix with wide and continuous spectrum of concentration were formed during simultaneous deposition of metal and dielectric phases owing to use of complicated non-symmetrical targets.

The density of electronic states on Fermi level ($g(E_F)$) were determined for the composites from temperature dependence of electrical resistivity. It has been determined that while concentration of the metal phase rises and approaches the percolation threshold the $g(E_F)$ values approach the values which are typical for the volume metal alloys which the granules are formed from. However the exact density of electronic states on Fermi level depends both on the material of the granules as well as on composition of dielectric matrix.

It has been established that concentration dependence of MR at room temperature is similar for all studied systems: nonmonoton MR dependence on metal concentration with maximum MR values near the percolation threshold and sharp decrease of MR behind the threshold with metal rise. The concentration position of the MR maximum is determined by geometrical (morphological) peculiarities of the composites: near the percolation threshold granule magnetic moments are not still correlated but the thickness of dielectric barriers between the granules is minimum therefore the probability of polarized electron tunneling is maximum.

The correlation between maximum values of MR and $g(E_F)$ for the composites was established. Magnetoresistivity is higher in composites which have larger values of density of electronic states on the Fermi level. The same correlation takes place for maximum values of MR and saturated magnetostriction of metal phase from which the nanogranules are formed. Magnetostriction of metal phase rise in the consequence CoNbTa → CoFeB → CoFeZr → Co, in the same consequence maximum values of MR rise if one compares composites with different metal phase. The observed correlation between saturated magnetostriction of metal phase and maximum values of magnetoresistivity can be explained by increase of d-electron contribution into spin-dependent tunneling. The contribution rises according to change of the metal phase in the composite in the same consequence: CoNbTa → CoFeB → CoFeZr → Co.

Support by the Russian Foundation for Basic Research (Grant N 08-02-00840) is acknowledged.

22PO-8-26

MAGNETIC AND ELECTRIC PROPERTIES NANOMULTILAYER STRUCTURES $[(\text{Co}_{45}\text{Fe}_{45}\text{Zr}_{10})_x(\text{Al}_2\text{O}_3)_{100-x}]/\{\alpha\text{-Si:H}\}_n$

Darinskii B.¹, Ivanov A.², Kalinin Yu.², and Sitnikov A.²

¹Voronezh State University, Voronezh, 394000, Russia

²Voronezh Technical State University, Voronezh, 394026, Russia

Multilayered structures have been received by ion - beam sputtering of two targets and deposition on a rotating substrate. Specific electric resistance (ρ) of $(\text{Co}_{45}\text{Fe}_{45}\text{Zr}_{10})_x(\text{Al}_2\text{O}_3)_{100-x}$ composite shows reduction of resistance of an alloy more than four order at increase of concentration of the metal phase from 32 up to 65 at. % that is typical for heterophase metal - dielectric systems. Similar dependences of ρ on the contents of a metal phase in a composite layer are characteristic for nanomultilayer structures $[(\text{Co}_{45}\text{Fe}_{45}\text{Zr}_{10})_x(\text{Al}_2\text{O}_3)_{100-x}]/\{\alpha\text{-Si:H}\}_n$. On the other hand, some features, which essentially distinguish the multilayers from the composite, were observed. The degree of change of specific electric resistance at increase of metal phase in the composites from 32 up to 65 at.% is much lower and reaches only one order of sizes. At $x=32$ at. % resistivity of multilayered structure is equal to $\sim 10^{-4}$ Ohm·m whereas in com-posite $(\text{Co}_{45}\text{Fe}_{45}\text{Zr}_{10})_x(\text{Al}_2\text{O}_3)_{100-x}$ the value of resistivity exceeds 0,5 Ohm·m.

Dependence of the real (μ') and imaginary part (μ'') of complex magnetic permeability on the contents of a metal phase in a composite layer for $[(\text{Co}_{45}\text{Fe}_{45}\text{Zr}_{10})_x(\text{Al}_2\text{O}_3)_{100-x}]/\{\alpha\text{-Si:H}\}_n$ nanomultilayer structures show, that in the region of concentration of a metal phase in the composite layer from 32 up to 42 at. % μ' and μ'' have high values and decrease with x growth. Such dependence lets us to assume that magnitoordered structure of ferromagnetic granules takes place. In the concentration region of $42 < x < 55$ at. % of the change of the real and imaginary parts of complex magnetic permeability is not significant. In this concentration region it is observed the high enough values of μ' , however these values are a little bit lower, than in a pure composite.

The mechanism of correlation between electrons in two metal inclusions separated by a thin layer from silicon atoms, resulting in an identical orientation of magnetization vectors of these two inclusions is offered. On a basis of the mechanism assumption of hybridization of electronic orbitals of silicon atoms and contacting metal particles has been made. The structure of silicon interlayer is not crystalline therefore the sp^3 -hybridization of silicon atomic orbital is not typical for it but the noncompensated p-states presents in large amount in the silicon. The p-states form hybrids with single-particle wave functions of electrons of contacting metals that leads to collinear spin directions in neighbor granules.

Work is executed at financial support of the Russian Foundation for Basic Research (grants № 08-02-00840) and grant MO and CRDF (project PG 05-010-1).

22PO-8-27

LATERAL BIAS AND ASYMMETRIC MAGNETIZATION REVERSAL IN A PATTERNED FERRO/ANTIFERROMAGNET STRUCTURE

Kabanov Yu.P.¹, Nikitenko V.I.¹, Tikhomirov O.A.¹, Egelhoff W.F.², McMichael R.D.², Shapiro A.J.², Shull R.D.²

¹Institute of Solid State Physics, Chernogolovka, 142432 Russia

²National Institute of Standards, Gaithersburg, MD 20899, USA

Artificial nanostructures consisting of two or more materials with drastically different magnetic characteristics are the subject of extensive studies in last few decades [1]. Proximity of ferromagnetic and antiferromagnetic layers of certain thickness gives rise to shifted hysteresis loops. Nanoscopic patterning of magnetic films, on the contrary, breaks the continuous exchange-induced correlation between spins in adjacent entities to replace it with magnetostatic interaction. Combination of such expedients, supported with modern achievements in sample engineering, provides a variety of possible magnetic configurations as well as different non-trivial scenarios of magnetization reversal.

We report magneto-optical indicator film investigation of kinetics of the magnetization reversal in a patterned ferro/antiferromagnetic bilayer - new class of magnetic materials with artificial periodic boundary conditions imposed along the surface. Successive images of a Ni₇₇Fe₁₄Mo₅Cu₄(300Å) film coupled to a rectangular network of antiferromagnetic FeMn(100Å) on top of it have been studied under the action of external in-plane magnetic field parallel or perpendicular to the unidirectional exchange anisotropy formed during the sample preparation.

Due to appreciable difference in anisotropy and coercivity of covered and bare parts of the sample, the magnetization reversal proceeds separately in two distinct stages. However, we have found undoubted influence of artificially created boundary conditions on the domain structure kinetics in a ferromagnetic film. First, the remnant state of a ferromagnetic layer becomes different for direct and backward branches if the ferromagnet is surrounded along the perimeter by the exchange-biased material. Further, the antiferromagnetic mesh is a preferable site for domains nucleation. The patterned structure facilitates nucleation of the opposite domains for one direction of the field, and retards their appearance for another one. As a result, the unidirectional shift of the whole magnetization cycle in bold ferromagnet is observed, similar to the well known exchange bias phenomenon caused by exchange interaction normal to layers. The likely reason of the observed asymmetry is magnetostatic interaction between covered and bold phases in case of canted orientation of their anisotropy axis.

Remarkable asymmetry of the magnetization reversal for direct and backward branches has been also observed. In the former case, new domains nucleate in the middle of bold squares and then spread laterally to the sides. In the latter one, the domain walls develop from the artificial boundaries between covered and not covered material and coagulate in the middle.

All described phenomena were observed in a magnetic field parallel to the exchange anisotropy axis. No lateral bias has been found for a perpendicular field orientation.

The work is supported by the Russian Fund of Basic Research.

[1] F. Radu and H. Zabel, Exchange Bias Effect of Ferro-/Antiferromagnetic Heterostructures. In: *Magnetic Heterostructures Advances and Perspectives in Spinstructures and Spintransport*, Eds. H. Zabel and S.D. Bader, Springer, 2008, pp.97-183.

[2] V.I. Nikitenko, V. S. Gornakov, A.J. Shapiro *et al.*, *Phys. Rev. Lett.* **84** (2000) 765.

[3] V.S. Gornakov, Yu.P. Kabanov, O.A. Tikhomirov *et al.*, *Phys. Rev. B* **73** (2006) 184428.

22PO-8-28

PHASE TRANSITION OF THE FIRST ORDER IN 3-LAYER Fe/Cr/Fe IN MAGNETIC FIELD

Bakulina N.B., Kurkin M.I., Gudin S.A., Gapontsev A.V., Ustinov V.V.
Institute of Metal Physics UrD RAS, Yekaterinburg, 620041, Russia

Multilayer Fe/Cr films with giant magnetoresistance effect are the primary materials for devices converting magnetic signals into electric ones. For effective work of such devices both the value of magnetization magnitude variation and its changing rate are important. The highest possible changing rate is achieved at the first order phase transition when magnetization amplitude changes stepwise.

The possibility of existence of the first order transitions induced by magnetic field in Fe/Cr films is determined by phase diagram of magnetic structures. We start from phase diagram obtained in [1] assuming the following: 1) exchange interactions inside Fe-Fe and Cr-Cr layers are much stronger than interlayer Fe-Cr interactions; 2) Fe atomic spins are ferromagnetically ordered; 3) Cr monolayer atomic spins are antiferromagnetically ordered forming a transversal linear polarized spin density wave with wave vector perpendicular to Fe/Cr interface. In this model magnetic moments of Fe layers can be ordered ferromagnetically, antiferromagnetically and uncollinearly depending on the exchange interaction parameters ratio of Fe-Fe, Cr-Cr and Fe-Cr. Boundary surfaces between these phases correspond to phase transitions of both the first and the second order.

We are interested in phases boundary surfaces that, firstly, correspond to phase transition of the first order, and secondly, can be shifted by the magnetic field. The observed steps of magnetization curves of the films under discussion can be related only to such boundaries. The example of boundaries satisfying this requirements are the phase interfaces corresponding to the first order phase transitions between magnetic states of films changing the phase of the spin density wave by $\pi/4$.

The calculation is performed for Fe/Cr/Fe films where there is no short period of ferromagnetic and antiferromagnetic phase change while varying the thickness of chromium. The variation of film energy density Δ is obtained

$$\Delta = \frac{H^2 M_{Fe}}{H_s}, \quad (1)$$

H — external magnetic field, M_{Fe} — Fe film magnetization

$$H_s = H_{in} - H_{ind}$$

- magnetic saturation field of the film, consisting of the induced anisotropy field H_{in} and induced indirect interaction field H_{ind} .

$$M = -\frac{\partial \Delta}{\partial H} = 2M_{Fe} \frac{H}{H_{Fe}} \quad (2)$$

describes the variation of film magnetization on the phase transition.

This work is performed under financial support of RFBR (project 08-02-00904), RAS Presidium («Quantum Macrophysics» program), «Dynasty» foundation.

[1] S.A. Gudin, A.V. Gapontsev, M.I. Kurkin, V.V. Leskovets, V.V. Ustinov, *JMMM.*, **300** (2006) e553.

[2] F. Fawcett, *Rev.Mod.Phys.* **60**, 209 (1988) 35.

22PO-8-29

FERROMAGNETIC RESONANCE IN MONOCRYSTALLINE FILMS Co/Cu

Iskhakov R.S.¹, Kim P.D.¹, Turpanov I.A.¹, Karpenko S.A.³, Stolyar S.V.^{1,2}

¹Kirenski Institute of Physics, Siberian Division, Russian Academy of Sciences,
Krasnoyarsk, 660036 Russia

²Siberian Federal University, Krasnoyarsk, 660041 Russia

³Krasnoyarsk Branch of Irkutsk State University of Railway Communications, st. Lado
Ketshoveli, 89, Krasnoyarsk, Russia

Analysis of ferromagnetic resonance spectra of monocrystalline epitaxial films Co/Cu grown on monocrystal MgO(001) allow to establishing pattern of they growth, determine effective value of crystallographic anisotropy field. It is established that in monocrystalline epitaxial films with the layer thickness $d_0 < 8$ nm and $d_0 > 8$ nm, $d_0 = d(\text{Co}) + d(\text{Cu})$, $d(\text{Co}) \approx d(\text{Cu})$, the easy axis direction coincides with (110) MgO direction. The value of crystallography anisotropy field is about 1 kOe. In monocrystalline epitaxial films with the layer thickness $d_0 \approx 8$ nm (crystalline lattices is coherently matched) it is established that there are two easy axis direction that coincides with : (110)-5° and (110)+5° directions. The value of crystallography anisotropy field here is about 0.2 kOe.

Support by RFBR, project no. 07-02-01172-a is acknowledged.

22PO-8-30

MAGNETIC STRUCTURE MODELLING OF Fe/V SUPERLATTICES WITH VARIABLE THICKNESS OF IRON LAYERS

Kudasov Yu.^{1,2}, Maslov D.¹

¹Sarov State Physics and Technology Institute, Dukhov str. 6, Sarov, 607188, Russia

²Russian Federal Nuclear Center – VNIIEF, Mira str. 37, Sarov, 607188, Russia

A magnetic ordering model of monocrystalline Fe/V superlattices with variable thickness of iron layers is discussed. Fabrication of such superlattices and their basic properties are well known. It is presumed that the superlattice consists of thin iron layers with thickness of 2-3 monolayers (Fe₂ and Fe₃) separated by vanadium spacers with thickness of 12 monolayers. From now on, antiferromagnetic interaction between iron layers is assumed.

According to Ref. [2] strong magnetic shape anisotropy of iron layers in combination with weak intraplane anisotropy allows analyzing a single iron layer within the framework of the XY-model. We used the spin-wave approximation of the XY-model [3] for low temperatures ($T \ll T_{BKT}$, where T_{BKT} is the Berezinsky-Kosterlitz-Thouless temperature). For high temperatures ($T \gg T_{BKT}$) system is in paramagnetic state but magnetic susceptibility of a single layer χ grows exponentially [4] with lowering the temperature. As a result we have dependence of magnetic moment

$$m(h, T) = m_0(h/T) \exp\left(a[T - T_{BKT}]^{-1/2}\right)$$

where a is the constant, $m_0(h/T)$ is the preexponential factor investigated in detail in Ref. [5]. In case of middle temperatures ($T \approx T_{BKT}$) we applied the results of the renormalization group theory [6].

The interlayer coupling is taken in the following form $J'(\mathbf{m}_i, \mathbf{m}_j)$, where J' is the parameter of interlayer coupling, \mathbf{m}_i is the magnetization of i -th iron layer. Thus the iron layer in the superlattice is described by the XY-model with an effective magnetic field, which is the sum of external and exchange fields.

By using self-consistent computations we got magnetic structures and full magnetizations of infinite and finite superlattices (Fe_2/V , Fe_3/V , $\text{Fe}_2/\text{V}_{12}/\text{Fe}_3/\text{V}_{12}$ and others). A distribution of magnetization at boundaries of the finite superlattices is determined. For superlattices $\text{Fe}_2/\text{V}/\text{Fe}_3/\text{V}$ we have obtained a good agreement with experimental data [2].

Support by ISTC, RFBR and «Dynasty» foundation is acknowledged.

- [1] B. Hjorvarsson, J.A. Dura, P. Isberg, T. Watanabe, T.J. Udovic, G. Andersson, and C.F. Majkrzak, *Phys. Rev. Lett.*, **79** (1997) 901.
- [2] B. Hjorvarsson, Yu. Kudasov, M. Wolff, T. Hase, C. Chacon, van Kampen M., P. Nordblad, A. Liebig, H. Zabel, *EPL*, **81** (2008) 17008.
- [3] V.L. Berezinsky, *Zhur. Eksp. Teor. Fiz. (Sov. Phys. -JETP)*, **59** (1970) 907.
- [4] J.M. Kosterlitz, *J Phys. C: Solid State Phys.*, **7** (1974) 1046.
- [5] I. Nakayama, T. Tsuneto, *Progr. Theor. Phys.*, **65** (1981) 1246.
- [6] M. Ito, *Progr. Theor. Phys.*, **66** (1981) 1129.

22PO-8-31

MAGNETIC PROPERTIES OF NANOCRYSTALLINE FeNi(P) COLUMNS IN POLYCARBONE MEMBRANES

*Iskhakov R.S.¹, Chekanova L.A.¹, Denisova E.A.¹, Komogortsev S.V.¹, Bukaemskiy A.A.²,
Polochanina S.V.³, Momot N.A.³*

¹Institute of Physics, SB Russian Academy of Sciences, Krasnoyarsk 660036, Russia

²Institut für Sicherheitsforschung und Reaktortechnik, Forschungszentrum Juelich GmbH, D-52425 Juelich, Germany

³Polytechnical Institute Siberian Federal University, Krasnoyarsk 660074, Russia

The synthesis and magnetic properties of the FeNi(P) alloy columns in polycarbone membranes are reported. The polycarbone membranes with diameters of holes from 0,1 up to 4 μ were used as the matrix material. The FeNi(P) alloy with the Ni content from 0 up to 100 % was chemically precipitated in to cylindrical holes oriented perpendicular to membrane's surface.

Samples are characterized by SEM – JEOL JSM – 840 coupled with the Energy Dispersive X-Ray analyzer (EDX). The well-structured cylindrical columns of the FeNi(P) alloy were found on the cross section of metal-filled membrane (Fig.1). Magnetic properties were measured by convenient ferromagnetic resonance UHF spectrometer (9.2GHz) and vibrating sample magnetometer.

The magnetization curves were measured perpendicular and parallel to membrane surface. The perpendicular magnetic anisotropy was detected (Fig.2). The magnetization curves and the FMR spectra obtained for various experimental geometries revealed a magnetic anisotropy in the direction of linear holes (oriented perpendicular to the membrane surface). The FMR data allowed the identifying the nature of this anisotropy as the shape anisotropy.

From magnetization curves the demagnetizing factor of a ferromagnetic material was estimated. The value of this factor was found to be close to 2π , what corresponds to the case of the ideal ferromagnetic cylinder with the length that is considerably exceeded its diameter. On the base of the analysis of the magnetic saturation curves it was shown, what the FeNi(P) alloy in investigated columns is in nanocrystalline state [1]. In the present report, the dependence of magnetic properties of the samples on the Ni content in the FeNi(P) alloys and on the column diameter are discussed.

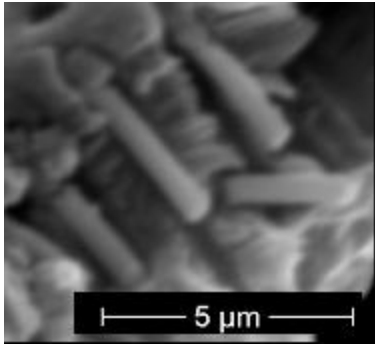


Fig.1 SEM image of FeNi(P) column on cross section of membrane.

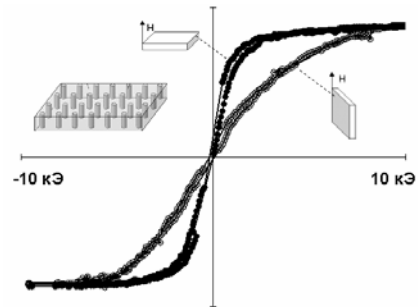


Fig.2 Magnetization curves received for various geometry of measurements.

Support by Russian program “Development of Science in High School” (2006-2008)–RNP.2.1.1.7376; the grant RFBR 07-02-01172-a; National Science Fund (2008, PhD RAS) are acknowledged.

[1] R.S. Iskhakov, S.V. Komogortsev, *Bull. Russ. Ac. Sc.: Phys.*, **71** (2007) 1620.

22PO-8-32

SHF-PROPERTIES AND SPIN-WAVE RESONANCE SPECTRA IN THE NANOGRANULAR FERROMAGNETIC FILMS AND PLANAR NANOCOMPOSITES

Iskhakov R.S.¹, Stolyar S.V.^{1,2}

¹Kirenski Institute of Physics, Siberian Division, Russian Academy of Sciences,
Krasnoyarsk, 660036 Russia

²Siberian Federal University, Krasnoyarsk, 660041 Russia

The SHF properties of multilayers “ferromagnetic/ferromagnetic”, trilayers “permalloy/Cu/permalloy”, bilayers DyCo/NiFe and nanocomposite films $(\text{CoFeB})_x(\text{SiO}_2)_{1-x}$ synthesized by different techniques were investigated. It is shown that FMR parameters of nanocomposite $(\text{CoFeB})_x(\text{SiO}_2)_{1-x}$ are depend from configuration of spatial packing of ferromagnetic grains in nanocomposites. The effect of exchange narrowing of magnetic resonance linewidth and fractal dimensionality of magnetic structure in nanocomposite closed to the percolation threshold. Twofold difference between exchange constants measured by FMR and from hysteresis curves is established in bilayers DyCo/NiFe.

It is shown that this is result from peculiar magnetic microstructure of DyCo layer. It is established by SWR technique that interlayer coupling in trilayers “NiFe/Cu/NiFe” initially are exchange and then it is substituted for magnetostatic with increasing of diamagnetic spacer thickness. The following increasing of diamagnetic spacer thickness is result in restoring

exchange coupling and then for the Cu thickness is more than $70E$ magnetostatic coupling is established finally.

For the first time distinctive modifications of spin wave resonance spectrum were discovered in multilayers “ferromagnetic/ferromagnetic” with the thickness $d = N(d_1+d_2)$. These results from the first stop-zone at $k_b = \pi/(d_1+d_2)$ in magnon crystal: the sudden change of exchange stiffness $\eta(k)$ is according by sudden change of resonance linewidth $\Delta H(k)$ for spin wave modes at $k = k_b$.

Support by RFBR, project no. 07-02-01172-a is acknowledged.

22PO-8-33

MAGNETIC AND ELECTRIC PROPERTIES OF TRILAYER Co/Ge/Co FILMS

Patrin G.S.^{1,2}, Turpanov I.A.¹, Velikanov D.A.¹, Yushkov V.I.^{1,2}, Patrin K.G.¹, Kobyakov A.V.²

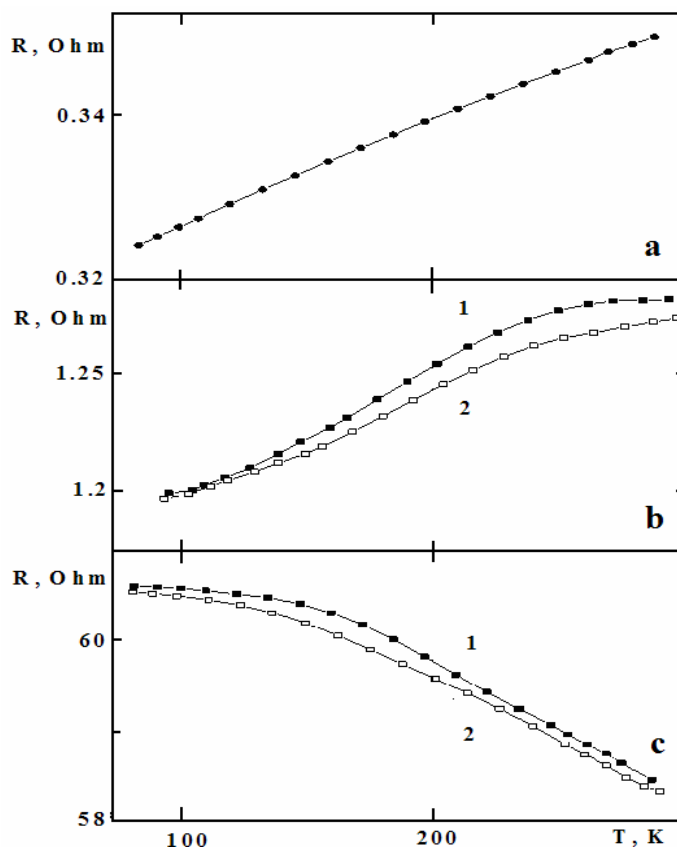
¹L.V. Kirensky Institute of Physics, Siberian Branch of Russian Academy of Sciences,
Krasnoyarsk, 660036, Russia

²Siberian Federal University, prospect Svobodny, 79, Krasnoyarsk, 660041, Russia

Films in *ferromagnetic metal/semiconductor* system are of noticeable interest for the latest years. First of all it is caused by presence of semiconducting component. In multilayer magnetic films with semiconducting spacer the interaction between ferromagnetic layers is realized through electron subsystem of semiconducting layer. In this case the possibility appears to control both of current carrier concentration and interlayer coupling by external influence. One of interest effect is the giant magnetoresistance and in this field magneto-heterogeneous materials, for instance, like granular magnetic films or manganites in range of electron phase separation are very perspective.

Therefore, the research of multilayer structure with semiconducting spacers in granular state is interestingly for us.

We have synthesized Co/Ge/Co films with different area-averaged thicknesses of nonmagnetic layer. Electron-microscopic investigations showed that the magnetic layers consist of mixture of cubic (fcc), hexagonal (hcp) and amorphous (am) phases. NMR experiments confirmed the conclusions of electron-microscopic investigations about presence of some magnetic phases in films. From the point of view of these data the behavior of magnetization in different conditions are due to that the



germanium particles induce the cobalt “coat” in the near environment with structure similar to germanium core one.

Also the temperature measurements of magnetoresistivity were made for films with different germanium thickness.

In figure the temperature dependences of electric resistivity are represented for trilayer construction of “cross” type

($t_{Co} = 15$ nm and $\mathbf{a} - t_{Ge} = 0$, $\mathbf{b} - t_{Ge} = 4$ nm, $\mathbf{c} - t_{Ge} = 38$ nm, $1 - H = 0$, $2 - H = 10$ kOe). It was received that the character of conductivity (metal or semimetal) depends on thickening regime of germanium layer (parts **b** and **c**). Apparently, at high velocity of Ge concretion the “jumpers lead” take a place and the conductivity is metallic. As it is seen from figure the absolute values of magneto-dependent additions of resistivity are more when the semiconducting character of conductivity takes place.

The current investigations are being undertaken at financial support of the Russian Foundation for Basic Research (Grant No. 08-02-00937-a).

22PO-8-34

MAGNETIC Co NANOPARTICLES IN THE MATRIX OF HIGH-POROUS AMORPHOUS CARBON

Iskhakov R.S.¹, Barnakov Ch.N.², Komogortsev S.V.¹, Mal'tsev V.K.¹, Momot N.A.³, Chekanova L.A.¹

¹Institute of Physics, SB Russian Academy of Sciences, Krasnoyarsk, Russia

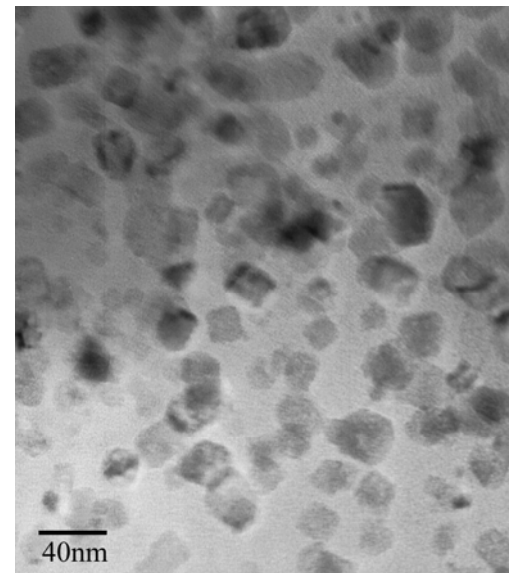
²Institute of Coal and Coal Chemistry SB RAS, Pr.Sovetskiy 18, Kemerovo, Russia

³Siberian Federal University, Kirenskiy street 26, Krasnoyarsk, Russia

The unique physical properties of nanoparticles, originating from surfaces effects or quantum-dimensional effects at the present are the object of intensive investigations.

Metallic nanoparticles are obtained as the ferrolíquids and inside the pores of various templates (polymers, zeolites, alumina, etc.). There are interesting phenomena in these materials: GMR, anomalous magnetocaloric effect, etc. Magnetic nanoparticles are of potential applications in the magnetic storage and recording systems, in magnetic-refrigerating systems, for the permanent magnets fabrication, as the magnetic sensors and for the medicine.

In this paper we report about synthesis and investigation of Co-nanoparticles in the matrix of amorphous high-porous carbon material [1]. Chemical reductions of Co from the solution in high-porous carbon material (pore diameter from 2 to 50 nm) were used for the Co nanoparticles synthesis. The TEM image (fig.1) of investigated material demonstrates that Co nanoparticles sizes in carbon matrix are vary in the range from 7 to 35 nm. There is fcc Co reflexes mostly revealed on the X-ray diffraction patterns, but on the several patterns there are weak hcp Co and CoO reflexes. The short range order of nanoparticles was investigated by nuclear magnetic resonance. The NMR spectra characterized by the peak with the frequency of 213.5 MHz – that is typical for the short range order of fcc Co. There are weak satellite of hcp Co (near by 220



MHz). The ferromagnetic resonance, magnetization curves and the temperature dependence of magnetization were investigated in our Co nanoparticles. The FMR spectrum parameters are sensitive to the quantity of cobalt oxide in the nanoparticle powders. The value of magnetic anisotropy field H_a was estimated from approach magnetization to saturation curves and its value was occurred close to $2\pi M_{Co}$, that points out the considerable dipole-dipole interactions in the system of investigated nanoparticles.

Support by Russian program “Development of Science in High School” (2006-2008)–RNP.2.1.1.7376; the grant RFBR 07-02-01172-a; National Science Fund (2008, PhD RAS) are acknowledged.

[1] Z.R. Ismagilov, M.A. Kerzhentsev, N.V. Shikina, A.S. Lisitsyn, L.B. Okhlopkova, Ch.N. Barnakov, Sakashita Masao, Iijima Takashi, Tadokoro Kenichiro. *Catalysis Today*, **102–103** (2005) 58.

22PO-8-35

EXCHANGE INTERACTION AND MAGNETIC STRUCTURES OF THE NANOCUSTER V_{15} IN STRONG MAGNETIC FIELDS

Kostyuchenko V.V.¹, Popov A.I.²

¹Institute of Microelectronics and Informatics RAS, 150007 Yaroslavl, Russia

²Moscow State Institute of Electronic Technology.124498 Moscow, Russia

At the present time, magnetic mesoscopic systems attract considerable interest. These systems exhibit both specific quantum features characteristic of individual atoms and classical features typical of bulk single crystals. Among these systems are clusters containing d – ions. In the present paper the process of rearrangement of the magnetic structure of the low – spin magnetic nanocluster V_{15} in magnetic field is theoretically investigated. The V_{15} cluster comprises fifteen vanadium ions, each of which has a spin of $S=1/2$. Vanadium ions are situated at the apexes of two planar hexagons and one triangle between them. The exchange interactions between ions are antiferromagnetic in nature and the V_{15} cluster has a low spin $S=1/2$ in the ground state. The magnetic field induces a transformation of the spin structure of the cluster from low-spin structure ($S=1/2$) to high-spin structure ($S=15/2$). In [1] it was shown that at $B=2.8$ T the magnetic structure of the cluster is changed with the result that the spin becomes equal to $3/2$. Further transformation of the magnetic structure occurs in the range of ultrastrong magnetic fields. This transformation occurs by discrete quantum jumps at low temperatures. The behavior of the magnetic susceptibility of the V_{15} cluster in ultrastrong magnetic fields of up to 550 T was experimentally studied in [2]. Anomalies in the susceptibility were found to exist in fields $B_1=200$ T and $B_2=350$ T. The fundamental parameters of the V_{15} cluster are exchange integrals which determine the magnetic structure of the cluster and its transformation under an external magnetic field. The spin – Hamiltonian of the cluster includes five basic exchange interactions. In the present paper by means of analytical and numerical (the modified Lanczos method) the energy spectra of the V_{15} cluster has been calculated as a function of the exchange constants. It allows to find the set of exchange constants giving rise to a good quantitative agreement between theoretical calculations and experimental data (behavior of the magnetization and the magnetic susceptibility of the V_{15} cluster) [1,2] both in low and high field region. After that we investigated the spin structure of the cluster and its transformation in ultrastrong magnetic fields. The existence of thin structure of the transitions from low – spin station to high – spin station is established. The transformation spin structure V_{15} in ultrastrong magnetic

fields manifests itself as a cascade of three discrete steps each of which is two quantum jumps, separated by short distance. It is shown that the last anomaly in the magnetic susceptibility of the cluster occurs at $B_3=600$ T and can be measured experimentally.

[1] B. Barbara, A. Muller, H. Bogge, W. Wernsdorfer, I. Chiorescu, *J. Magn. Magn. Mater.*, 221 (2000) 103.

[2] V.V. Platonov, O.M. Tatsenko, V.I. Plis, A.I. Popov, A.K. Zvezdin, and B. Barbara, *Phys. Solid State*, 44 (2002) 2104.

22PO-8-36

ANGULAR ORIENTATIONS OF THE IN-PLANE ANISOTROPY AND OF THE BIAS FIELDS IN NiO/Ni₈₁Fe₁₉ BILAYERS

Zighem F.¹, Roussigné Y.¹, Bouziane K.², Chérif S.M.¹, Moch P.¹

¹LPMTM CNRS, Institut Galilée, Université Paris 13, Av. J.-B. Clément (Villetaneuse), France

²Department of Physics, Sultan Qaboos University, P.O. Box 36, Al-Khodh 123, Oman

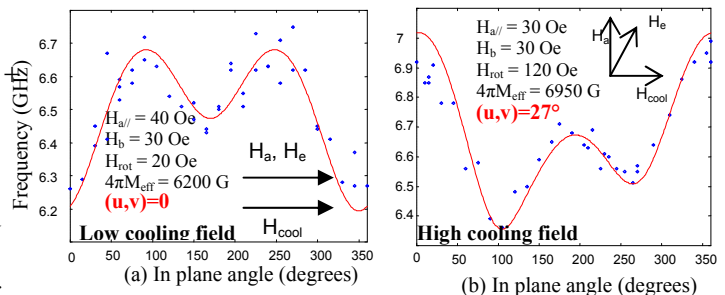
In this paper we show that, in thin films consisting of NiO/NiFe bilayers, the directions of the bias and of the in-plane uniaxial anisotropy fields depend upon the value of the magnetic field previously applied to induce the bias properties. The samples were prepared using RF sputtering [1], their structure is: Al₂O₃(10 nm)/Ag(8 nm)/NiO(t)/Py(d=10.4nm)/Al₂O₃(10 nm). The samples were first annealed just above the Néel temperature and subsequently cooled under an in-plane low (0.5 kOe) or high (5 kOe) magnetic field \mathbf{H}_{cool} . in order to favor the exchange bias. We studied their static and dynamic magnetic properties using vibrating sample magnetometry (VSM) and Brillouin light scattering (BLS) techniques. The experiments can be interpreted in the frame of an energy density writing as:

$$E = -\mathbf{H}\cdot\mathbf{M} + \frac{K_{\perp}}{M^2}(\mathbf{M}\cdot\mathbf{n})^2 + E_{exch.}$$

$$E_{dem.} + \frac{k}{M^2}(\mathbf{M}\cdot\mathbf{u})^2 + \frac{j}{M}(\mathbf{M}\cdot\mathbf{v})$$

\mathbf{H} and \mathbf{M} stand for the applied field and the magnetization. The three following terms are the perpendicular anisotropy, the exchange and the demagnetizing contributions.

The two last terms are the in-plane uniaxial and unidirectional anisotropies. The unit vectors \mathbf{u} and \mathbf{v} specify the directions of the in-plane anisotropy field $\mathbf{H}_{a//} = (2k/M)\mathbf{u}$ and of the bias field $\mathbf{H}_b = (j/M)\mathbf{v}$: in most of the cases, they are assumed to be parallel to \mathbf{H}_{cool} , in contrast of a part of the results of the present study. Finally, to account for the dynamical properties, it is necessary to introduce an additional rotatable field \mathbf{H}_{rot} . parallel to the static equilibrium magnetization. The BLS measurements under a rather large (above 500 Oe, approximately) in-plane applied magnetic field allows the determination of the magnetization M_{eff} ($M_{eff} = M + K_{\perp}/2\pi$) and of the exchange stiffness: for such large fields $H_{a//}$ and H_b do not appreciably affect the spin-wave frequencies. In contrast, for smaller applied fields, these terms significantly modulate the spin-wave frequencies: they are evaluated from the angular



Angular variations of the frequencies for a sample with $t = 28$ nm. Used parameters are given in each panel as well $d = 10.4$ nm; $A = 10^{-6}$ erg.cm⁻¹ and $q = 15.7 \times 10^4$ cm⁻¹.

dependence of the spectra generated by the rotation of the films around the direction \mathbf{n} normal to their plane. In the samples cooled under a low field, \mathbf{u} and \mathbf{v} are parallel to \mathbf{H}_{cool} . (Fig a). Whereas in the samples cooled under a high field \mathbf{u} is approximately normal to \mathbf{H}_{cool} . and the angle (\mathbf{u}, \mathbf{v}) significantly differs from 0. A typical behavior, compared to our best fit for j , k and (\mathbf{u}, \mathbf{v}) is shown on Fig b: a satisfactory agreement could not be obtained assuming $(\mathbf{u}, \mathbf{v}) = 0$. At evidence, the observed rotations of \mathbf{u} and \mathbf{v} under a high cooling field are due to a reorganization of the magnetic moments in the antiferromagnetic: $H_{a//}$ lies along the direction of the sublattice magnetization which shifts from parallel to perpendicular to the cooling field; the interpretation of the nonzero (\mathbf{u}, \mathbf{v}) value would necessitate an appropriate detailed model for the bias exchange which is still lacking.

[1] H. Hurdequint, extended abstract p 85-86, IWEBMN 2004, Anglet, 16-18 Sept (2004)

22PO-8-37

FIRST ORDER STRUCTURAL PHASE TRANSITION IN $\text{Na}_5\text{RbCu}_4(\text{AsO}_4)_4\text{Cl}_2$ SINGLE CRYSTAL

*Pashchenko M.¹, Bedarev V.¹, Gnezdilov V.¹, Pashkevich Yu.², Lemmens P.³, Zvyagin S.⁴,
Gnatchenko S.¹, Mo X.⁵, Queen W.⁵, and Hwu S.-J.⁵*

¹B.Verkin Institute for Low Temperature Physics and Engineering of the National Academy of Sciences of Ukraine, 47 Lenin Ave., Kharkov 61103, Ukraine

²A.Galkin Donetsk Physico-Technical Institute of the National Academy of Sciences of Ukraine, 72 R. Luxemburg Str., Donetsk 83114, Ukraine

³Institute for Physics of Condensed Matter, TU Braunschweig, Braunschweig D-38106, Germany

⁴Hochfeld-Magnetlabor, Forschungszentrum Rossendorf, 01328 Dresden, Germany

⁵Department of Chemistry, Clemson University, Clemson, SC 29634, USA

The discovery of high temperature superconductivity in the cuprates stimulates to search and study new families of materials with small spin and low dimensionality. Recently a new salt-inclusion copper arsenate $\text{Na}_5\text{RbCu}_4(\text{AsO}_4)_4\text{Cl}_2$ with a remarkable crystal structure was synthesized using a conventional solid-state reaction [1]. The low temperature crystal structure, which may have crucial implications for the distinct magnetic order, has not been determined until now. In the Ref. 2 two structural phase transitions around 74 K and 110 K seen by ^{87}Rb nuclear magnetic resonance were reported but their nature was not clarified.

To get more insight into the structural phase transitions in $\text{Na}_5\text{RbCu}_4(\text{AsO}_4)_4\text{Cl}_2$ we performed Raman scattering (RS) and optical birefringence experiments. RS measurements were performed in quasi-backscattering geometry with the excitation line $\lambda = 514.5$ nm of an Ar^+ laser. Experiments on the visual observations of the domain structure formed in the vicinity of the structural phase transition were carried in parallel.

The most characteristic Raman features related to the structural phase transition with decreasing temperature are the sudden splitting of some phonon modes and the appearance of new modes. Intuitively the character of changes allows us to suggest a first order nature of the phase transition. Visual studies and investigation of temperature dependence of birefringence allows us to define more precisely the order of the structural phase transition in $\text{Na}_5\text{RbCu}_4(\text{AsO}_4)_4\text{Cl}_2$. At the temperature dependence of birefringence at $T = 73$ K there is a sharp increase of optical birefringence which corresponds to a first order structural phase transition. The temperature hysteresis of birefringence by value of about 10 K is observed at the first order phase transition in the crystal of $\text{Na}_5\text{RbCu}_4(\text{AsO}_4)_4\text{Cl}_2$. In the low-temperature phase

the axes of optical indicatrix of the crystal are turned by an angle of 45° relative to axes of optical indicatrix before the phase transition.

Experimental results and group-theoretical analysis allow to assume that structural phase transition ($Fmmm \rightarrow C2/m$) in the single crystals $\text{Na}_5\text{RbCu}_4(\text{AsO}_4)_4\text{Cl}_2$ is related to the order-disorder transition of the Rb ion positions along the z axis within the ionic framework of mixed alkali metal chloride lattices.

[1] Shiou-Jyh Hwu, Mutlu Ulutagay-Kartin, Jeffrey A. Clayhold, Richard Mackay, Tina A. Wardojo, Charles J. O'Connor, and Mariusz Krawiec, *J. Am. Chem. Soc.* **124** (2002) 12404.

[2] R. Stern, I. Heinmaa, A. Kriisa, E. Joon, S. Vija, J. Clayhold, M. Kartin-Ulutagay, X. Mo, W. Queen, and S.-J Hwu arXiv:cond-mat/051272.

22PO-8-38

EFFECTS OF INTERACTION IN THE MAGNETIZATION REVERSAL KINETICS OF SUPERPARAMAGNETIC GRANULAR $\text{CoFeB} - \text{SiO}_2$ FILMS

Timopheev A.A.¹, Ryabchenko S.M.¹, Kalita V.M.¹, Lozenko A.F.¹, Trotsenko P.A.¹, Grishin A.M.², Munakata M.³

¹Institute of Physics NAS of Ukraine, Nauky prospect, 46, 03028, Kyiv, Ukraine

²Div. of Cond. Matter Phys., Royal Institute of Technology, Electrum 229, S-164 40 Kista, Stockholm, Sweden

³Energy Electronics Laboratory, Sojo University, Kumamoto 860-0082, Japan

e-mail: timopheev@iop.kiev.ua

In order to study the influence of magnetic interactions on the relaxation processes in superparamagnetic media magnetization, magnetostatic measurements were carried out on the granular $(\text{CoFeB})_x - (\text{SiO}_2)_{1-x}$ films with x values near percolation threshold. In-plane uniaxial anisotropy of the ferromagnetic nanoparticles in studied films has been originated by special

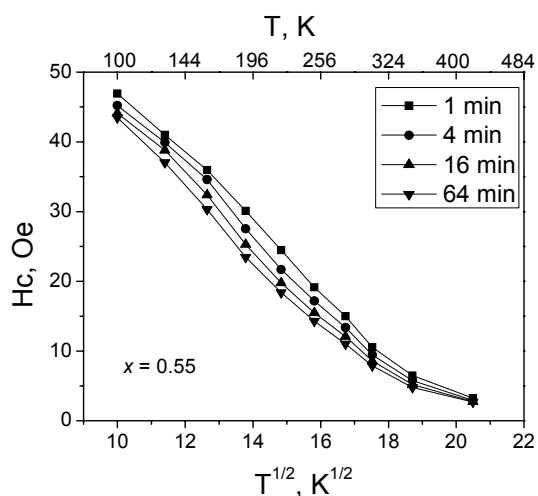


Fig1. Series of temperature dependences of coercivity for the sample with $x = 0.55$, which were registered with various values of measuring time.

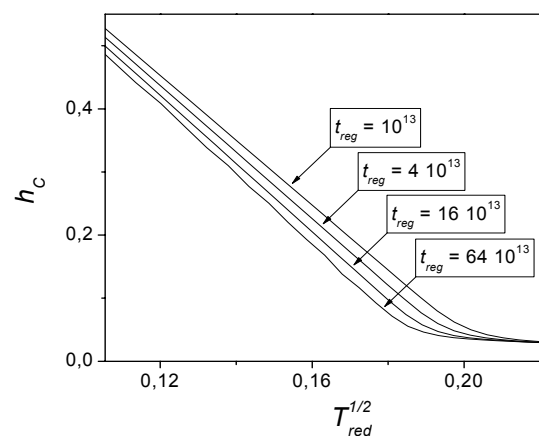


Fig2. Series of temperature dependences of coercivity, which were obtained by simulation with various values of measuring time t_{reg} . All units are dimensionless.

technological methods in the deposition process. The observed temperature dependence of the coercivity for the magnetization along easy axis of the samples shows two linear on \sqrt{T} parts with different inclination angles, which are crossed each other at the value of blocking temperature (T_b). The linear part of the curve, which corresponds to the temperature range below T_b , is dependent from the measuring time and is related to the thermoactivated nature of magnetization reversal process in the blocked superparamagnetic state. The linear part of the curve, which corresponds to the temperature range above T_b , is practically independent from the measuring time and may be related to existence of correlated state of superparamagnetic grains moments, i.e. superferromagnetic state. The method for simulation of the magnetization reversal curves based on the numerical solving of kinetic equation has been applied to explain observed experimental results. The interaction in ensemble has been taken into account in the mean-field approximation. The modeling results demonstrate two practically additive contributions in the temperature dependence of coercivity. The first contribution follows the well-known Neel-Brown formula and thus is strongly dependent from the measuring time, and the second one, which has weak measuring time dependence, characterize properties of superferromagnetic state. The modeling results demonstrate a good agreement with obtained results of experimental studies.

22PO-8-39

FMR ANALYSIS OF NUCLEATION CONDITIONS OF Co FILMS WITH VOLUME LIKE PROPERTIES OBTAINED BY ION-BEAM SPUTTERING

Pashkevich M.¹, Meshcheryakov V.^{2,3}, Fettar F.⁴, Stognij A.¹, Novitskii N.¹, and Pankov V.⁵

¹Scientific-Practical Materials Research Centre of NAS of Belarus, 19 P. Brovki Street, Minsk, 220072, Belarus, stognij@iftp.bas-net.by

²Moscow Institute of Radioelectronics and Automation, 78, Vernadskogo Avenue, Moscow, 119454, Russia

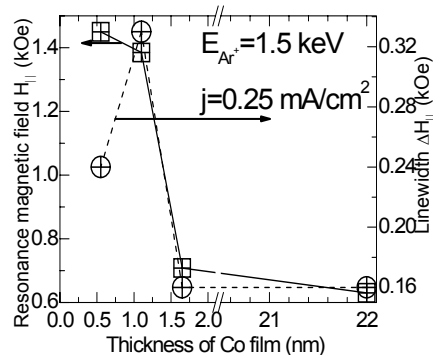
³Shubnikov Institute of Crystallography, 59, Leninskiy Avenue, Moscow, 119333, Russia

⁴Institut Neel, CNRS/UJF, B.P. 166, 38042 Grenoble Cedex 9, France

⁵Belarusian State University, 4, Nezavisimosti Avenue, Minsk, 220030, Belarus

At present work the features of transition of ferromagnetic Co films to volume like properties on the stage of their formation were investigated by the FMR. The FMR measurements were conducted at the frequency 9.55 GHz at room temperature. The direction of magnetic field was parallel (H_{\parallel}) and perpendicular (H_{\perp}) to the film plane. Such configuration let to determine Lande factor as well as saturation magnetization M_{SF} . Co films were grown by ion-beam sputtering (IBS) at working pressure of $2 \cdot 10^{-4}$ Torr by sputtering of Co target with Ar ion beam of energy changed from 0.5 to 2 keV at constant current density 0.25 mA/cm^2 . The flux of sputtered Co atoms deposited onto Si (100) substrate. The film thickness controlled by the deposition time. The film surfaces were covered by Au layer with thickness about 2 nm as protector.

The Co films of thickness from 10 nm obtained by sputtering by means of Ar ions with energy of 0.5 keV were found to possess $M_{SF} \geq 0.7M_S$ where M_S is the saturation magnetization of the bulk material ($M_S = 1420$ Gs). The Co films obtained by sputtering with Ar ions of



more than 1.5 keV at thicknesses from $\sim 2\text{-}3$ nm and more were already characterized by $M_{\text{SF}} \geq 0.8M_{\text{S}}$. The same values of critical thickness of transition to volume like properties were obtained in [1] where was found that the hcp crystal lattice start to form as Co thicknesses overcome 3 nm. One can explain the given features on the base of "auto-radiation" effect [2]. According to the calculations the high energy tail of Co atoms has energy higher than that of Si atom displacement threshold in substrate when the target was sputtered by Ar ion with the energy of more than 1.4 keV. This tail can penetrate in Co film up to thickness of 0.8 nm. Therefore the gradual increasing of M_{SF} , FMR linewidth (ΔH), and decreasing resonance magnetic field (H_{res}) are observed for Co films of thickness to 1 nm. On the other hand, both the sharp decay of H_{res} and ΔH together with M_{SF} surge are observed for Co films of thickness more than 1 nm. It is worthwhile that the increase of Ar ion energy more than 1.5 keV doesn't lead to sputtering rate growth and to improvement of film structure due to implantation processes on target surfaces and to form the developed relief.

According to the results presented the IBS method in optimal conditions lets to obtain the Co films with volume like properties beginning from the thickness more than 3 nm. Homogeneity and continuity of Co films reaches because of the specificity of IBS process. That implies the presence in flux the sputtered Co atoms of high energy component with mean energy more than 25 eV up to 30% of general flux of sputtered Co atoms.

- [1] A.I.Stognij, N.N.Novitskii, K.I.Yanushkevich et al., *XX International school-seminar "New magnetic materials of microelectronics (NMMM-XX)"*, Moscow (2006) 324
 [2] A.I.Stognij, N.N.Novitskii, O.M. Stukalov et al., *Tech. Phys. Lett.* **30** (2004) 256

22PO-8-40

ASYMMETRY OF MAGNETIZATION REVERSAL IN ULTRATHIN Co/Pt MULTILAYERS WITH PERPENDICULAR ANISOTROPY

Iunin Yu.L.¹, Nikitenko V.I.¹⁻³, Shapiro A.J.², Shull R.D.², Zhu L.Y.³, Chien C.L.³

¹Institute of Solid State Physics RAS, Chernogolovka, Russia

²National Institute of Standards and Technology, Gaithersburg, MD USA

³The Johns Hopkins University, Baltimore, MD USA

Investigations of the magnetization reversal of quasi-two-dimensional $[\text{Co/Pt}]_n$ multilayers with perpendicular anisotropy are important both for an understanding of the fundamental mechanisms of the domain dynamics within the ultrathin films and for potential use in the high-density data storage. In the earlier work [1] we reported the unusual asymmetry in the activity of nucleation centers in these materials, which is in sharp contrast to the observed symmetry of magnetic reversal in homogeneous bulk materials. In this work we investigated how this unusual feature depends on the number of Co layer repeats as well as on the magnitudes of magnetic fields.

We studied in detail the domain wall nucleation and motion in $\text{Pt}/[\text{Co/Pt}]_n/\text{Pt}$ multilayers ($n = 1, 2, 4, 16$) grown by magnetron sputtering on Si or glass substrates at room temperature. To study the magnetization reversal, the magnetic field was gradually reduced from the holding field exceeding the sample coercivity, to a point where magnetic domains began to nucleate and grow. We measured the number of asymmetrical nucleation centers in ultrathin Co films as a function of the holding field value. It was revealed that the number becomes zero after application of high holding fields (complete suppression of nucleation asymmetry) but grows rapidly when approaching to values close to the sample coercivity. We revealed that cycling magnetization reversal of single Co films with decreasing applied field results in the qualitative

change in the shape of domains. The dendrite-like domain structure forms instead of bubble domains.

In spite of the presence of nonmagnetic Pt interlayer, [Co/Pt]₂ multilayers demonstrate similar to single films behavior. The correlated formation and spreading of bubble domains are observed. The magnetization reversal of [Co/Pt]₄ multilayers also occurs by the formation of bubble domains with correlated spreading of domain walls. But, after magnetic field reverse, the domain walls do not move back as they do in [Co/Pt]_n samples with $n = 1, 2$. Instead, the magnetic reversal under magnetic field inversion occurs by the appearance of 'channels' with opposite magnetization and their subsequent thickening with increased negative field. Like in single Co films, the number of asymmetrical nucleation centers in multilayers with $n = 2, 4$ increases drastically with the decrease in holding field. The subsequent increase in the number of repeats up to 16 results in a qualitative change in the magnetization reversal. The dendritic domain structure is observed. Its formation occurs in stochastic manner, i.e. domains nucleate at different positions when cycling magnetic field.

Support by the Program of Presidium of the Russian Academy of Sciences "Quantum Macrophysics" and by the Russian Foundation for Basic Research (project no. 08-02-01268-a) is acknowledged.

[1] Yu. L. Iudin, Yu. P. Kabanov, V. I. Nikitenko, X. M. Cheng, D. Clarke, O. A. Tretyakov, O. Tchernyshyov, A. J. Shapiro, R. D. Shull, and C. L. Chien, *Phys. Rev. Lett.*, **98** (2007) 117204.

22PO-8-41

DOMAIN STRUCTURE OF INDIVIDUAL Fe LAYERS IN UNIAXIAL (210)[Fe/Cr]_n SUPERLATTICES

Ustinov V.¹, Milyaev M.¹, Gornakov V.², Kabanov Yu.², Romashev L.¹, Krinitsina T.¹

¹Institute of Metal Physics UD RAS, S. Kavalevskaya St.18, Ekaterinburg 620041, Russia

²Institute of Solid State Physics RAS, Chernogolovka 142432, Russia

The (210)[Fe/Cr]_n superlattices grown by MBE on (211)MgO substrates demonstrate the uniaxial in-plane anisotropy and unusual magnetic and transport properties namely the multi-step field dependence of both magnetization and magnetoresistance. The evolution of a magnetic state as a function of external magnetic field was investigated by polarized neutron reflectometry in the multilayer (210)[Fe(76E)/Cr(12.4E)]₁₂ [1]. The coexistence of antiferromagnetic and ferromagnetic ordering of magnetic moments of Fe layers in the multilayer stack was revealed in various magnetic fields. It was shown also that there is a possibility of magnetization reversal of individual Fe layer in the multilayer. The analysis of magnetic and magneto-resistive data for similar multilayer with Fe(85E) and Cr(13.6E) layers thicknesses have shown that magnetization reversal of the Fe layer cannot be due to rotation of magnetization in the film plane because of the high energy barrier for hard axis direction [2]. One may suppose that in a magnetic field, the magnetization reversal of the Fe layers occurs in such a way that domain walls appear and move inside of only one Fe layer whereas other Fe layers remain in the single domain state.

In this work, we study the domain structure of individual Fe layers in (112)MgO/Cr(80E)/ [Fe(85E)/Cr(13.4E)]₁₂ multilayer by magneto-optical indicator film technique [3], which visualizes the form of magnetic domains, as it is presented in Fig.1, and their evolution. The analysis of the data obtained allows us to reveal in what sequence of the Fe layers whose magnetizations are switched when magnetic field is changed. The possible mechanisms for this unusual behavior are discussed.

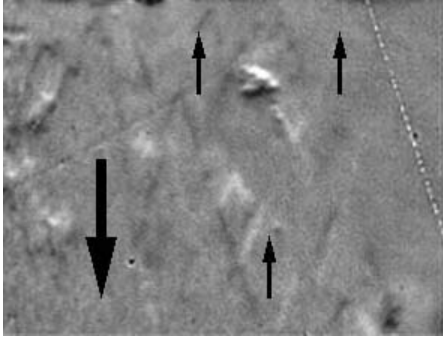


Fig. 1. Magneto-optical image of a region of the sample containing domains with different orientation of net magnetization of the multilayer (thick arrow) and magnetization in single Fe layer (thin arrows). Remagnetization field $H = 516$ Oe is applied along the easy direction in the film plane.

The work is supported by RFBR 07-2-01289-a, SS 3257.2008.2, program Presidium RAS “Quantum macrophysics”.

- [1] H.J. Lauter, V. Lauter-Pasyuk et al. *Physica B*, **335** 59-62 (2003).
- [2] V.V. Ustinov, M.A. Milyaev, et al. *Phys. Stat. Sol. (c)*, **3**, Iss. 5, 1249-1256 (2006).
- [3] V.S. Gornakov, V.I. Nikitenko, A.J. Shapiro et al. *JMMM* **246**, 80-85 (2002).

22PO-8-42

MECHANISM OF FORMATION OF MAGNETIC NANOPHASE IN POLYMER-BASED COMPOSITES

Volkov A.¹, Moskvina M.¹, Volynsky A.¹, Volkov I.²

¹Chemical Department, Lomonosov Moscow State University, Moscow, 119991 Russia

²Physics Department, Lomonosov Moscow State University, Moscow, 119991 Russia

We have studied the mechanism of formation and the structure of polymer nanocomposites prepared by the reaction of hydrolysis of bi- and trivalent iron chlorides carried out in the bulk of cross-linked polyvinyl alcohol matrix. The formation of magnetic nanophase is governed by the critical nucleation mechanism. Under certain conditions, primary ultrafine particles of magnetic nanophase (3–5 nm) reveal a tendency to agglomeration, which mediates the formation of large particles (20–60 nm) through the isothermal distillation process. We assume the following properties of the reaction medium to facilitate this process: i) high content of deprotonated hydroxyl groups and ii) relatively low microviscosity. Most likely, the migration of iron ions in the reaction medium proceeds from smaller particles to larger ones by means of macromolecular chains containing the deprotonated hydroxyl groups. From the analysis of TEM and XRD data obtained we have arrived at a conclusion that smaller particles (20–30 nm) are single-crystal objects, whereas larger ones (30–60 nm) are polycrystalline. The vibrating sample magnetometer and the SQUID-magnetometer have been applied for examination of magnetic properties of the prepared samples. The size dependences of the coercivity and the relaxation time observed for samples showing different particle coarsening effects suggest the single-domain behavior of magnetic nanophase.

22PO-8-43

SQUID-BASED RELAXOMETRIC DIAGNOSTICS OF MAGNETIC NANOPARTICLES

Volkov I.¹, Snigirev O.¹, Polyakov S.¹, Baranov D.², Volkov A.³, Tanaka S.⁴

¹Physics Department of Lomonosov Moscow State University, Moscow, Russia

²Institute of General and Inorganic Chemistry of RAS, Moscow, Russia

³Chemical Department of Lomonosov Moscow State University, Moscow, Russia

⁴Toyohashi University of Technology, Toyohashi, Japan

The method of SQUID-based relaxometric diagnostics has been applied to the ensembles of non-interacting near-spherical Fe₃O₄ and Co nanoparticles in order to reveal the behaviour of the anisotropy constant upon varying the mean size of nanoparticles in the ensemble (from 5 to 15 nm) and the type of ligand shell (dextran, chitosan, polyacrylic acid, etc.). The crystal structure of nanoparticles and the chemical structure of ligand shells have been analyzed by using XRD and IR-spectroscopy, respectively. The relaxation curves measured in the time range from 50 μs to several tens of seconds after application of a pulse (10 s) of dc magnetizing field (~ 10 G) have been approximated by theoretical dependences calculated within the framework of activation Néel–Arrhenius law with account for the size distribution function retrieved from the transmission electron microscopy data. The noticeable effects of the mean size of nanoparticles and the ligand shell on the anisotropy constant have been found. The observed behaviour of the anisotropy constant is discussed in terms of the surface anisotropy and variations in the electronic structure of near-surface ferromagnetic atoms caused by their interactions with the surrounding organic molecules.

22PO-8-44

SPIN GLASS BEHAVIOR OF Fe/Cr MULTILAYER STRUCTURES WITH ULTRATHIN IRON LAYERS

Drovosekov A.¹, Kreines N.¹, Kholin D.¹, Korolev A.², Milyaev M.², Romashev L.², Ustinov V.²

¹P.L.Kapitza Institute for Physical Problems RAS, 2 Kosygina St., 119334 Moscow, Russia

²Institute of Metal Physics UD RAS, 18 Sofia Kovalevskaya St., 620219 Ekaterinburg, Russia

Exchange coupled Fe/Cr magnetic multilayers (ML) have been an object of extensive investigations for several decades [1]. The most intriguing property of the system is the possibility of ferromagnetic (FM), antiferromagnetic (AFM) and non-collinear magnetic ordering of iron layers. Such ordered structures have been observed in the case of relatively thick iron layers ($t_{\text{Fe}} > 10E$). Recently, however, it was found that structures with very thin iron layers ($t_{\text{Fe}} \approx 2E$) demonstrate superparamagnetic (SP) behavior [2]. In this work, the evolution from SP to magnetically ordered structures was studied on a set of Fe/Cr samples with iron layer thickness in the 2–6E region.

Two series of samples were prepared by MBE technique: FM-type with $t_{Cr}=20E$ and AFM-type with $t_{Cr}=10E$ [2]. Each series consisted of three samples with $t_{Fe} \approx 2, 3, 5E$. The number of Fe/Cr layer pairs varied from 30 to 60 for different samples. Low angle X-ray reflectivity studies showed the presence of periodic layered structure for all the samples. Magnetic properties were investigated by SQUID-magnetometry and FMR technique in 2–400K temperature range.

Depending on temperature and nominal iron layer thickness, the samples showed three different regimes. At high temperatures, the SP and magnetically ordered ML structures were observed, depending on iron and chromium layer thicknesses [2]. At low temperatures, the presence of irreversible magnetic states was discovered in all the samples. The observed new magnetic phase demonstrates a set of typical spin glass (SG) properties:

1. The splitting of magnetization curves $M(T)$ obtained after zero field cooling (ZFC) and field cooling (FC) procedures.

2. Anomalous hysteresis loops with virgin curve lying below the remagnetizing one.

3. Frequency dependent maximum of the real part $\chi'(T)$ of AC susceptibility and non-zero value of the imaginary part $\chi''(T)$ below SG transition. The position of $\chi'(T)$ maximum shows a SG-like dependence on the frequency of the applied magnetic field.

4. “Slow” relaxation of irreversible magnetization with logarithmic time dependence.

As an example, some of the described properties are demonstrated in Fig.1 for one of the samples.

Qualitative $T - t_{Fe}$ phase diagrams for FM- and AFM-type structures are obtained.

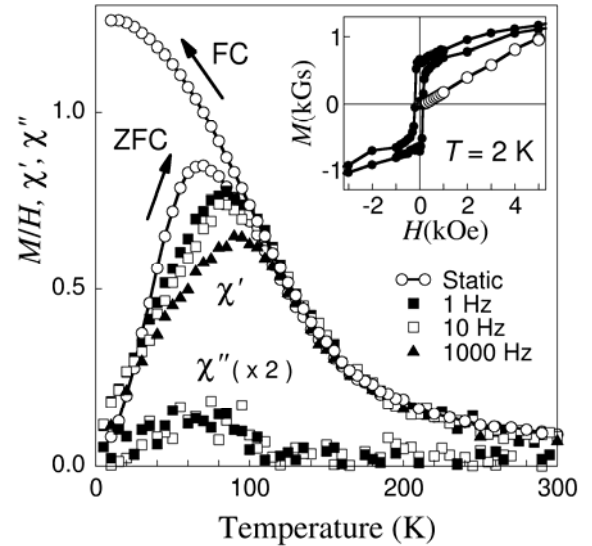


Fig.1: Temperature dependence of AC susceptibility in Fe(2.5E)/Cr(20E) multilayer sample measured at different frequencies (shown in the figure). The static $M(T)$ curves are obtained at $H=100$ Oe under FC and ZFC conditions. The inset shows anomalous hysteresis loop observed at low temperature. The virgin curve (open circles) lies outside the loop (solid circles).

[1] D.T.Pierce, J. Unguris, R.J. Celotta, M.D. Stiles, *J. Magn. Magn. Mater.* **200** (1999) 290.

[2] A.Drovosekov, N.Kreines, M.Milyaev *et al.*, *J. Magn. Magn. Mater.* **290-291** (2005) 157.

22PO-8-45

FERROMAGNETIC SPECTRA OF SILICON DIOXIDE FILMS WITH COBALT NANOPARTICLES

Lutsev L.¹, Khodzitskiy M.², Bagmut T.², Shipkova I.³, Tarapov S.², Stognij A.⁴, Novitskii N.⁴

¹Research Institute 'Ferrite-Domen', Chernigovskaya st. 8, St Petersburg, 196084, Russia

²Institute of Radiophysics and Electronics NASU, Ac. Proskura st. 12, Kharkov, 61085, Ukraine

³National Technical University "Kharkov Polytechnical Institute", Frunze st. 21, Kharkov, 61002, Ukraine

⁴Institute of Solid State and Semiconductor Physics, National Academy of Sciences of Belarus, P. Brovki st. 17, Minsk 220072, Belarus

We have studied the magnetic properties of heterostructures of amorphous silicon dioxide films with cobalt nanoparticles, $\text{Co}_x(\text{SiO}_2)_{100-x}/\text{GaAs}$, with the Co contents $x = 20 - 85$ at% by the electron spin resonance (ESR) method and by the vibrating sample magnetometer technique (VSM) [1]. The ESR investigation has been carried out to obtain ferromagnetic resonance (FMR) spectra in the frequency range of 25-28 GHz at room temperature. From FMR spectra we have found that an anomalous local fall in the dependence of the magnetization on the Co concentration of granular nanostructures has been detected in the vicinity of the percolation threshold (Fig. 1). According to the proposed theoretical model, the observed peculiarity of the magnetization dependence can be explained by the influence of semiconductor substrates on the spin polarization of Co particles in granular films.

FMR spectra of heterostructures $\text{Co}_{73}(\text{SiO}_2)_{27}/\text{Si}$ with different thicknesses at the frequency of 77.62 GHz at $T = 4.2$ K have been studied. It is found that in the magnetic field of 27 – 29 kOe additional peaks have appeared (Fig. 2). The magnetization of $\text{Co}_{73}(\text{SiO}_2)_{27}$ films decreases with decreasing thickness. For explanation of the observed peaks a model of spin wave excitations in disordered magnetic systems have been developed. In the framework of this model, which takes into account magnetic dipole and exchange interactions between spins, it is found that an additional longitudinal spin wave mode appears [2]. This mode is characterized by variations of the value of the magnetic moment density and corresponds to additional peaks on FMR spectra.

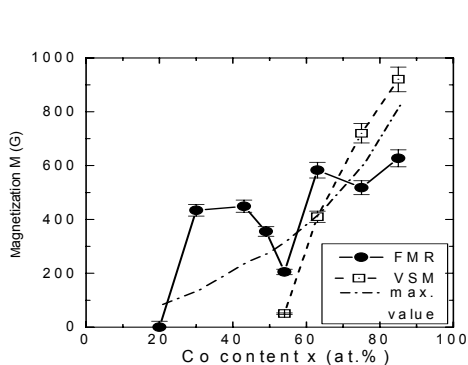


Fig. 1. Magnetization of $\text{Co}_x(\text{SiO}_2)_{100-x}/\text{GaAs}$ samples versus the Co concentration.

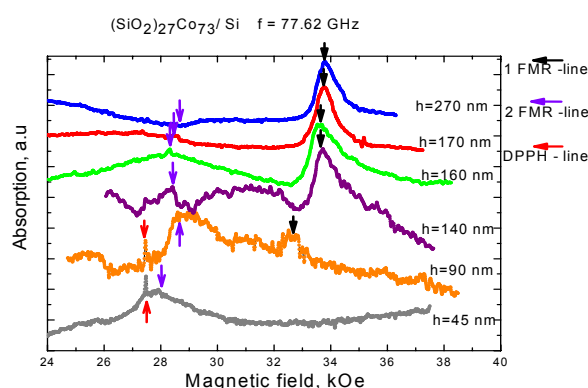


Fig. 2. FMR spectra of heterostructures $\text{Co}_{73}(\text{SiO}_2)_{27}/\text{Si}$.

This work was supported by the RFBR (grant N 06 - 02 - 17030).

[1] M. Khodzitskiy, L. Lutsev, S. Tarapov et al., *JMMM*, **320** (2008) L7.

[2] L.V. Lutsev, <http://arxiv.org/abs/0801.4633>

22PO-8-46

MAGNETIC MICROSTRUCTURE IN THE $\text{Co}_{41}\text{Fe}_{39}\text{B}_{20}\text{-SiO}_2$, Co-SiO_2 , Co-CaF NANOCOMPOSITE FILMS

*Iskhakov R.S.¹, Komogortsev S.V.¹, Denisova E.A.¹, Chekanova L.A.¹,
Kalinin Yu.E.², Sitnikov A.V.²*

¹Kirensky Institute of Physics SB RAS, 660036 Krasnoyarsk, Russia

²Voronezh State Technical University, Voronezh, Russia

The aim of this paper is to investigate (ferromagnetic metal–dielectric) granulated nanocomposite alloys Co-SiO_2 , Co-CaF , $\text{Co}_{41}\text{Fe}_{39}\text{B}_{20}\text{-SiO}_2$ using the magnetostructural technique. Giant magnetoresistance, giant anomalous Hall effect, intensification of magneto-optical effects, and other interesting physical effects were revealed recently in these materials. These effects are mainly result from the features of micromagnetic structure of these materials. The aim of our activity is to reveal these magnetic microstructure features.

Nanocomposites Co-SiO_2 , Co-CaF , $\text{Co}_{41}\text{Fe}_{39}\text{B}_{20}\text{-SiO}_2$ films were synthesized by the ion-beam sputtering. Films of the nanocomposites are composed of amorphous ferromagnetic alloy $\text{Co}_{41}\text{Fe}_{39}\text{B}_{20}$ or nanocrystalline Co nanograins dispersed in dielectric (nonmagnetic) matrix (disorder SiO_2 , crystalline CaF). Magnetostructural techniques are used to determine the exchange bond percolation limit in $(\text{Co}_{41}\text{Fe}_{39}\text{B}_{20})_x(\text{SiO}_2)_{1-x}$ ($x_c \approx 0.3$), Co-SiO_2 , Co-CaF nanocomposites, which separates the superparamagnetic and a ferromagnetic state of these materials. Investigations of ferromagnetic resonance spectra revealed that the transition from isotropic granular media to continuous magnetic film starts at $x \sim 36$ vol.%. It is found that the FMR linewidth of Co-CaF nanocomposites is much less than for nanocomposite with disorder SiO_2 matrix. Spin wave resonance spectra are measured in nanocomposites with $x > 52$ vol.%. Approach to magnetic saturation curves in the all nanocomposites follow Akulov's law $M(H) \sim (H)^{-2}$ in the applied fields up to 3 - 6 kOe. This allows us to determine the value of mean square fluctuations of local magnetic anisotropy field aH_a . The value of aH_a is occurred to decrease with the increasing the fracture of magnetic phase. In the field range from 1 to 3 - 6 kOe magnetization approaches to saturation as $M \sim H^\alpha$. The value of α changes from 0.5 to 1.4. It makes it possible to relate the revealed subdivision of the nanocomposite ferromagnetic region with respect to concentration into three subregions with the characteristic propagation of the magnetization ripples. As example in $(\text{Co}_{41}\text{Fe}_{39}\text{B}_{20})_x(\text{SiO}_2)_{1-x}$ case the threedimensional propagation of ripples is observed leading to the dependence $\Delta M \sim H^{1/2}$ for $x > 0.6$; for $0.39 < x < 0.6$, the two-dimensional propagation of short-wavelength ripples ($\Delta M \sim H^1$); for $0.33 < x < 0.38$, the fractal propagation of the magnetization ripples ($\Delta M \sim H^\alpha$) proceeds. It was calculated that the fractal dimension d varies from 1.2 to 1.9, depending on the metal concentration.

It is shown that, with respect to the singularities of the magnetization saturation curves, the ferromagnetic region is further subdivided into three regions differing in the character of the spatial propagation of the magnetization ripples or in the magnetic correlation function characteristics for all type of nanocomposite. The fractal dimension of the nanocomposite magnetic microstructure near the percolation threshold is detected.

Support by the grant RFBR 07-02-01172-a; National Science Fund (2008, PhD RAS) are acknowledged.

22PO-8-47

MAGNETIC PROPERTIES OF Fe-BASED NANOSTRUCTURAL POWDERS

Chekanova L.A., Denisova E.A., Iskhakov R.S., Bayukov O.A.
Institute of Physics SB RAS, 660036 Krasnoyarsk, Russia

Magnetic and structural properties of nanostructured $\text{Fe}_{100-x}\text{P}_x/\text{NiP}$ and $\text{Fe}_{82-x}\text{Zr}_x\text{P}_{18}/\text{NiP}$ powders prepared by chemical reduction were studied. The particles consist of core from Fe-P or Fe-Zr-P alloy with different phosphorous content surrounded by spherical shell from amorphous NiP alloy. Structural characterization of the powders was performed using X-ray diffraction, electron diffraction measurements and Mossbauer spectroscopy. It is shown that the $\text{Fe}_{100-x}\text{P}_x$ and $\text{Fe}_{82-x}\text{Zr}_x\text{P}_{18}$ core was nanocrystalline on-based α -Fe. There were two contributions in Mossbauer spectra of $\text{Fe}_{82-x}\text{Zr}_x\text{P}_{18}/\text{NiP}$ composite particles. The first - ferromagnetic α -Fe with $Z=8$, the second contribution was paramagnetic with electron structure closed to Fe^{3+} ($Z=6$). The Mossbauer spectroscopy data shown that the $\text{Fe}_{100-x}\text{P}_x/\text{NiP}$ powders were inhomogeneous. There were two ferromagnetic phases and one paramagnetic phase in Fe-Zr-P particles core.

Magnetic parameters such as the saturation magnetization, the exchange stiffness constant, the local magnetic anisotropy field, the FMR linewidth (ΔH), the coercivity of the powders were studied as a function of P and Zr content. The data show a strong dependence of the magnetic parameters on the phosphorous content. The saturation magnetization dependences of the $\text{Fe}_{100-x}\text{P}_x/\text{NiP}$ and $\text{Fe}_{82-x}\text{Zr}_x\text{P}_{18}/\text{NiP}$ powders were non monotonic. The saturation magnetization magnitude is determined by α -Fe content. It is found that the FMR linewidth is proportional to the saturation magnetization in FeP/NiP powders. Consequently the ΔH FMR is mainly determined by chain formation from composite particles.

Support by RFBR and KRSF, project no.07-03-96808 is acknowledged.

22PO-8-48

THE STUDY BY FERROMAGNETIC RESONANCE METHOD OF Fe/Ni MULTILAYER FILMS OBTAINED BY CHEMICAL PRECIPITATION METHOD

Iskhakov R.S.¹, Chekanova L.A.¹, Vazhenina I.G.²

¹Kirensky Institute of Physics, Academgorodok, Krasnoyarsk, 660036 Russia,

²Krasnoyarsk Institute of rail transport, Krasnoyarsk, 660028 Russia

e-mail: rauf@iph.krasn.ru

Planar metal multilayer systems are a new form of nanostructured materials which intensively are studied in modern material science and the magnetic effect physics. The entire series of the physical effects in multilayer metal film has experimentally been discovered caused by particular optical electric and magnetic property this properties, these properties find a technical application. The research has shown what physical properties of the multilayer are influenced by the thickness of individual layers, the number of layers which determine the partial correlation of the multilayer material to general volume interface state, individual layer graininess and other.

The research results with ferromagnetic resonance method (FMR) of multilayer films $[\text{Fe}(5\text{nm})/\text{Ni}(X\text{nm})]_N$ are presented in this paper, with the layer thickness Ni and layer number being changed. Specimens were obtained by chemical precipitation method from the solution onto thin copper foil and cover glass. The thickness of the individual iron layer was $d_{\text{Fe}}=5\text{ nm}$, the layer thickness Ni was changed from 1 to 9 nm. The general number of layers was changed so that the integral thickness of films was 200 nm.

The resonance curve were measured by standard spectrometer (pumping frequency is 9,2 GHz). The films were magnetized parallel to the surface in the field up to 20 kOe. The line width of FMR - ΔH and the value of the resonance field were measured. Effective magnetization of composition films was calculated with the help this data.

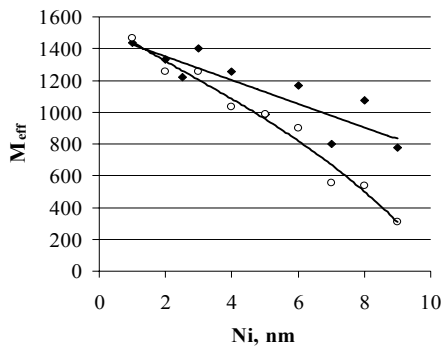


Fig. 1.

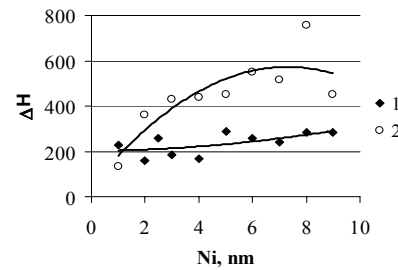


Fig. 2.

Dependences of effective magnetization M_{eff} and line width ΔH in Ni layer thickness are shown in fig. 1 and fig. 2 correspondingly (curve 1 presents the films precipitated on copper thin foil, curve 2 demonstrates the films precipitated on cover glass).

The magnetization of composition film precipitated on copper thin foil is monotonously, and almost linearly decreased by the increase of individual layer thickness of Ni. The films precipitated on cover glass shown other nature. The dependence ΔH is also characterized by a different character of behaviour. The line width of the resonance curve is caused first of all by the heterogeneous widening of the curve. It originates from the local variation of statistic and high-frequency magnetic field inside the ferromagnetic film. Every real film has a quantity of heterogeneity. One of possible explanations of in the difference of the dependence course M_{eff} and ΔH on Ni thickness is the increase of interaction between Fe and Ni on the interface of two adjacent layers.

Films precipitating on cover glass show more striking change in temper of adjacent layer interaction of Fe and Ni. It happens due to less abrupt difference in substrate surface heterogeneity.

22PO-8-49

MAGNETIC PROPERTIES OF NANOPARTICLES SYNTHESIZED ON THE BASE OF MCM-41

Komogortsev S.V.¹, Iskhakov R.S.¹, Chekanova L.A.¹, Denisova E.A.¹,
Balaev D.A.¹, Patrusheva T.N.², Kirik S.D.³, Khomchenko A.S.¹

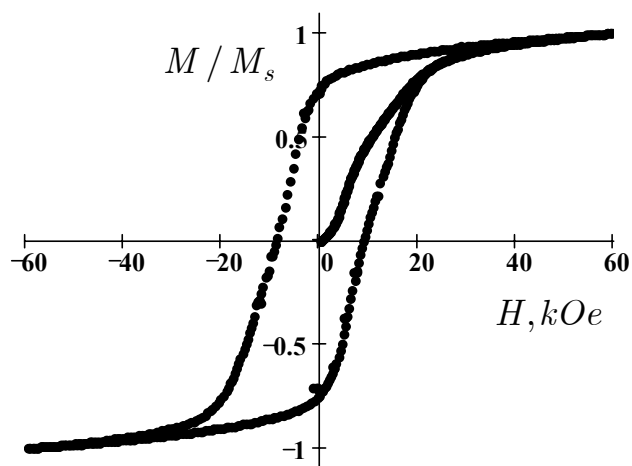
¹Institute of Physics, SB RAS, Krasnoyarsk, 660036 Russia

²Polytechnic Institute of Siberian Federal University, Krasnoyarsk, 660074 Russia

³Institute of Chemistry and Chemical Technology, SB RAS, Krasnoyarsk, 660036 Russia

e-mail: komogor@iph.krasn.ru

Single-domain nanoparticles Co and Co-ferrite are prospective materials for permanent magnets, magnetic recording and magnetic fluids. There are large magnetocrystalline anisotropy and magnetization in cobalt (hcp) and Co-ferrite particles. Theoretical predictions for coercivity H_c and reduced remanence M_r/M_s for the random system of spherical, non-interacting single-domain particles are: $H_c(5\text{ K}) = 25.2\text{ kOe}$, $H_c(300\text{ K}) = 5.3\text{ kOe}$, $M_r/M_s = 0.83$ [1] for the Co-ferrite nanoparticles and $H_c(5\text{ K}) = 5\text{ kOe}$, $H_c(300\text{ K}) = 3\text{ kOe}$, $M_r/M_s = 0.5$ for the hcp-Co nanoparticles. There are maximum experimental values in the literature for Co-ferrite nanoparticles: $H_c(5\text{ K}) = 14\text{ kOe}$, $H_c(300\text{ K}) = 1.8\text{ kOe}$ and $M_r/M_s(5\text{ K}) = 0.7$, $M_r/M_s(300\text{ K}) = 0.35$ [2]. In this work we report on magnetic properties of cobalt (hcp) and Co-ferrite particles synthesized by chemical deposition (hcp-Co) and selected pyrolytic decomposition on the template of mesoporous silicon oxide MCM-41. Investigation of X-ray



diffraction reveals that hcp-Co and CoFe_2O_4 nanoparticles formed without destruction of MCM-41 mesostructure. Synthesized powders are the hard magnetic material with following values of magnetic parameters: for the Co-ferrite particles coercivity $H_c(4.2\text{ K}) = 9.0\text{ kOe}$, $H_c(300\text{ K}) = 1.8\text{ kOe}$ and reduced remanence $M_r/M_s(4.2\text{ K}) = 0.78$, $M_r/M_s(300\text{ K}) = 0.4$; for the hcp-Co particles coercivity $H_c(100\text{ K}) = 1.5\text{ kOe}$, $H_c(300\text{ K}) = 1.3\text{ kOe}$ and reduced remanence $M_r/M_s(100\text{ K}) = 0.31$, $M_r/M_s(300\text{ K}) = 0.3$. Hysteresis loop for Co-ferrite nanoparticles in 4.2K is shown on the figure. The

interesting for the applications feature of investigated Co-ferrite nanoparticles is large value of reduced remanence in combination with isotropic nature of the powder sample. We assume that it is result of both the fact that magneto-crystalline anisotropy field is much than demagnetizing field (NM_s) and monodispersity of nanoparticles synthesized on the high ordered template (MCM-41).

The magnetization curves are successfully described on the base of Stoner-Wolfarth model for the randomly oriented single domain nanoparticles.

Support by Russian program "Development of Science in High School" (2006-2008)–RNP.2.1.1.7376; the grant RFBR 07-02-01172-a; National Science Fund (2008, PhD RAS) are acknowledged.

[1] J. Geshev, O. Popov, V. Masheva, M. Mikhov, *J. Magn. Magn. Mater.*, **92** (1990) 185.

[2] M. Grigorova, H.J. Blythe, V. Blaskov et. al., *J. Magn. Magn. Mater.*, **183** (1998) 163.

22PO-8-50

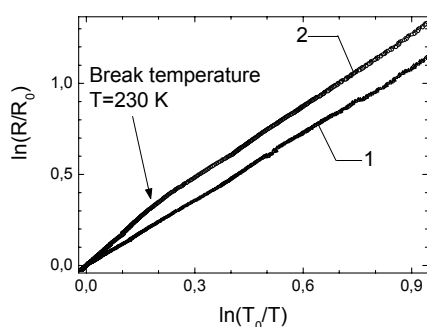
HYDROGEN INFLUENCE ON THE CONDUCTIVITY OF CoFeZr-AlO NANOCOMPOSITES

Grebennikov A.A., Stognei O.V., Sitnikov A.V.

Voronezh State Technical University, Voronezh, 394026, Russia

The hydrogen influence on conductivity in CoFeZr composites has been investigated. The studied composites have a nanogranular structures that is they are formed from the metal nanogranules randomly distributed in dielectric aluminum oxide matrix. All samples were obtained by Ar ion-beam sputtering of compound targets. The studied samples were a pre-percolated composites with nonmetallic type of conductivity. The electron transport, resistance value and temperature dependence of the composites resistance are determined in these pre-percolated materials by the conductivity through dielectric matrix. Actually there are two types of conductivity mechanism in pre-percolated composites: direct electron tunneling between metallic granules and electron tunneling via localized states in a dielectric matrix. The model of resonance electron tunneling via localized states [1] was used for analysis of temperature dependence of composites resistivity. This model allows calculating average number of local states between neighbor granules $\langle n \rangle$ which take part in the electron tunneling between these neighbor granules. The $\langle n \rangle$ values can be changed by external influence like heat treatment or high electric field [2,3] therefore one can expect that $\langle n \rangle$ would be changed by hydrogen absorption.

The studied CoFeZr-AlO samples exhibit high sensitivity to the hydrogen. The composite resistance sharply decreases when small amount of hydrogen is added to air atmosphere and degree of the resistivity change is proportional to the hydrogen amount. The $\langle n \rangle$ calculation was



Temperature dependence of electrical resistivity of the CoFeZr-AlO nanocomposite in as-deposited (1) and hydrogenated (2) state. The model [1] coordinates were chosen for plotting. T_0 and R_0 values were taken at 300 K

practically does not influence on $\langle n \rangle$ values in temperature interval 77 – 230 K. On the other hand the $\langle n \rangle$ values increases in higher temperature range (230 – 273 K) and the break on the $R(T)$ behavior is observed (see fig.). The $\langle n \rangle$ rise after hydrogenated was observed in wide pre-percolating range. This effect was observed just after hydrogenation, since some time (~ 70 hours) it disappears and the break on the curves vanishes.

The results are interpreted as a creation of new local states in composites dielectric matrix by hydrogen. These states are deep and are activated for conductivity only close to room

carried out based on temperature dependences of composites resistance that were measured in temperature range of 77- 293 K before and after hydrogenation. The hydrogenation of CoFeZr-AlO nanocomposites was realized at 590 K in pure hydrogen atmosphere under 250 Torr during 2 hours. Before the temperature measurements and hydrogenation all samples were annealed in vacuum at 640 K to provide the relaxation of their nonequilibrium structure. Therefore the relaxed samples were used for all following measurements.

In as-deposited state the experimental $R(T)$ curves of the composites were fitted by tunnel model quite well and this got a good opportunity of $\langle n \rangle$ calculation. The hydrogenization does not change the $R(T)$ behavior of the composites and

temperature. The states are not stable and destroyed as a result of usual relaxation process which leads to hydrogen desorption.

[1] L.V.Lutcev // *FTT* **44**, № 11 (2002) 1802-1810 (in Russian)

[2] O.V. Stognei et al. // *Microelectronic Engineering* **69**, № 2-4 (2003) 476-479

[3] M.N. Kopitin et al. // *J.of Nanostruct. Polymers and Nanocomposites* **2**, № 02 (2006) 67-72

22PO-8-51

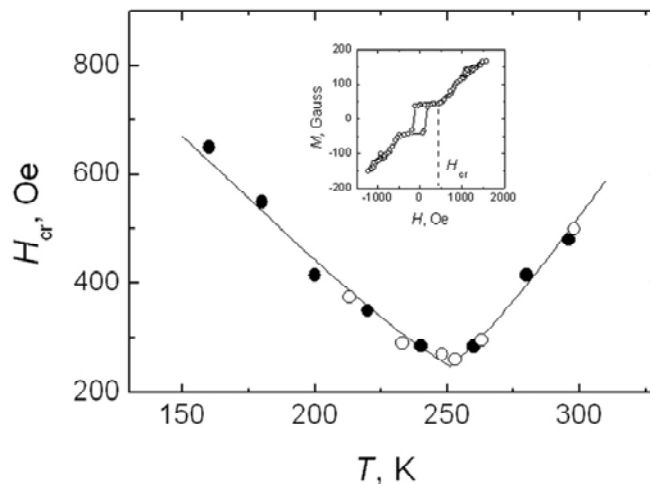
FEATURES OF MAGNETISATION PROCESS OF GdCo/Co FERRIMAGNETIC MULTILAYERS

Vas'kovskiy V.O., Balymov K.G., Svalov A.V., Sorokin A.N.

Ural State University named after A.M.Gorky, 620083, Ekaterinburg, Russia

Magnetization process of $[\text{Co}/\text{Gd}_{36}\text{Co}_{64}]_4/\text{Co}$ multilayers with complex magnetic structure had been studied in this work. The multilayered structures were obtained by rf-sputtering using corresponding targets for consecutive deposition of the required layers in argon atmosphere onto glass substrates. The composition of amorphous ferrimagnetic Gd-Co layers of the thickness of 24 nm was specially selected in order to guarantee the preponderating role of rare earth component in the formation of layer spontaneous magnetization up to the Neel temperature (~ 400 K). Thickness of polycrystalline Co layers was selected to be of 7 nm. Magnetic moments of the Co layers and magnetic moments of amorphous Gd-Co layers were ordered in a ferrimagnetic structure due to the interlayer exchange (which was positive for Co-Co system and negative for Co-Gd system) [1]. For such ferrimagnetic structure a compensation temperature of 255 K was obtained.

The analysis of the data of magnetic measurements (see inset of the figure), magneto-optical and magnetoresistive hysteresis loops showed that under application of the external magnetic field the initial collinear magnetic structure transforms into non-collinear as a consequence of the cut-off transition. The surface Co layers having reduced interlayer coupling with internal layers influence the critical field of the transition H_{cr} and features of the deformation of the magnetic structure at the beginning of the transition.



Interesting peculiarities of the torque curves were observed, namely the local extrema with the parameters which depend on the temperature and the value of the magnetic field. Satisfactory correlation was found between the experimental data and a model description of the deformation of the magnetic structure in a rotational magnetic field.

It was ascertained that the dependence of the critical field H_{cr} on the temperature T is a non-monotonous function (see figure) with the minimum near the magnetic compensation state. It was reasonably well described in frame of the model of bulk ferrimagnet with weak anisotropy when the role of the surface Co layers was taken into account by quantitative correction of the phenomenological constant of the interlayer coupling.

This work was supported by the RF project RNP.2.1.1.6945.

[1] V.O. Vas'kovskiy, A.V. Svalov, A.A. Yuvchenko, E.A. Kataeva. *Phys. Met. Metall.* **101** (2006) S84.

22PO-8-52

INVESTIGATION OF MAGNETIC PROPERTIES OF POLYMER NANOCOMPOSITES WITH MAGNETITE NANOPARTICLES

*Varfolomeev A.E.¹, Cherepanov V.M.¹, Zharkovsky A.E.¹,
Volkov A.V.², Volkov I.A.², Moskvina M.A.²*

¹RRC "Kurchatov Institute", 123182 Moscow, Russia, E-mail: varfol@imp.kiae.ru

²Lomonosov's Moscow State University, 119899 Moscow, Russia

Magnetic nanocomposites based on nanoparticles of Fe₃O₄ in polymer matrices of polyvinyl alcohol have been prepared and investigated in wide range of concentrations of magnetite from 1 up to 35 % vol. by use of XRD, magnetization measurements, Moessbauer spectroscopy. The influence of different conditions of synthesis of nanocomposites (temperature, magnetic field, concentration of nanoparticles) on their magnetic properties has been investigated.

The magnetization curves have been analyzed in wide range of concentration of magnetite by use of a Langeven function with a log-normal distribution of the size of nanoparticles. The magnetic coercitivities, saturation magnetization, magnetic diameter and density of nanoparticles have been found depending on the concentration of iron oxide by use of a magnetization curve fitting. It has been shown it is possible to obtain as single domain ferromagnetic as superparamagnetic nanoparticles in these nanocomposites. The transition between superparamagnetic-ferromagnetic nanoparticles has been investigated by use of Moessbauer spectroscopy in magnetic field. Due to wide range of concentrations the influence of cooperative effects on magnetic data has been investigated.

22PO-8-53

TEMPERATURE DEPENDENCE OF POSITIVE MAGNETORESISTANCE IN Co_x(AlO)_{100-x} GRANULAR NANOCOMPOSITES

Avdeev S.F., Stognei O.V., Sitnikov A.V., Doroshev N.N.

Voronezh State Technical University, Voronezh, 394026, Russia

Earlier it has been shown that granular nanocomposites Co_x(AlO)_{100-x} exhibit not only usual negative magnetoresistance (so-called tunnel magnetoresistance) but also unusual positive magnetoresistance (fig.1) [1]. It has been supposed that presence of the positive magnetoresistance (PMR) is related to the complicated structure of the nanocomposites: the nanocomposites with positive magnetoresistance contain both granules separated from each other as well as quite large metal clusters. There is a dipole interaction between clusters and neighbor granules therefore some sort of local magneto-correlated regions (correlation between

granules and clusters magnetic moment is taken into account) takes place in the composites at zero magnetic field. In such a case resistivity of the composites is not maximum. The conditions for maximum resistivity are fulfilled at some magnetic field (200 – 600 Oe) which destroys the magnetically correlated regions and makes the granules and clusters magnetic moments to be disordered. Presence of the PMR at certain temperature is determined by the certain ratio between the thermal energy (kT), the anisotropy energy of granules and clusters (E_a), the energy of dipole interaction between granules and clusters (E_{dip}).

The aim of the present investigation was to study the influence of temperature (influence of value of the thermal energy) on positive magnetoresistance in granular nanocomposites $\text{Co}_x(\text{AlO})_{100-x}$. The PMR at room temperature is observed in wide concentration region ($55 \leq x$, at. % ≤ 67) which coincide with percolation threshold. Increase of the measurement temperature to 373 K leads to shift of the PMR concentration region to larger metal concentration (fig.2). One should note that this temperature (373 K) does not lead to any structure relaxation and the observed temperature shift of the PMR values is reversible.

On the other hand the PMR is not observed at 77 K. Magnetic hysteresis and related with it hysteresis of magnetoresistance take place at 77 K but positive effect does not appear. According to the thermomagnetic measurements the values of bifurcation temperature in pre-percolated $\text{Co}_x(\text{AlO})_{100-x}$ nanocomposites are higher than 77 K and it explain presence of the hysteresis.

The experimental results confirm the point that not only morphological feature determined the PMR presence but also quantitative ratio between kT , E_a and E_{dip} (for example $kT \ll E_a$ at 77 K and this leads to the absence of PMR).

Strong dependence of the PMR on orientation between magnetic field and plate of thin film sample was established. When field is perpendicular to the plate the peak of PMR degenerates to a plateau. This is due to plane anisotropy of the composite morphology.

Support by the Russian Foundation for Basic Research (Grant N 08-02-90482) is acknowledged.

[1] O.V.Stognei et al. *Physics of the Solid State* **49** (2007) 164.

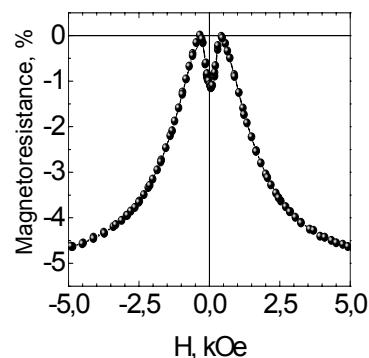


Fig. 1 Positive magnetoresistance of $\text{Co}_{57}(\text{Al}_2\text{O}_n)_{43}$ nanocomposite

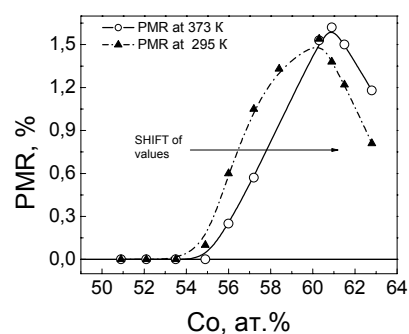


Fig. 2 PMR of $\text{Co}_x(\text{Al}_2\text{O}_n)_{100-x}$ measured at different temperatures

22PO-8-54

DETECTION OF CORRELATIONS OF INTERPARTICLE MAGNETIC INTERACTION PARAMETERS WITH SIZE AND SURFACE EFFECTS IN REAL SYSTEMS OF SMALL PARTICLES

Kamzin A.S.², Ol'khovik L.P.¹, Sizova Z.I.¹, Shurinova E.V.¹

¹Karazin Kharkov National University, Svobody Sqr. 4, Kharkov 61077

²Ioffe Physico-Technical Institute of Russian Academy of Sciences,
194021 St Petersburg, Russian Federation

Solution of the problem under consideration was guaranteed by purposive choice of the object of investigation in form of system of nanocrystals of highly anisotropic ferrimagnetic $\text{BaFe}_{12}\text{O}_{19}$. Particles of the given system (10-100 nm) in the range 300-750K have whole set of magnetic states, that are inherent in small particles: magnetostable, superparamagnetic and paramagnetic ones [1]. Along with that, the determining role in formation of magnetic properties of the particles belongs to open surface and adjacent to it structural-defective near-surface layers with skewed magnetic structure, which give partial contribution about (100-50)% to total particles volume [2].

For the considered close-packed system of highly anisotropic ferromagnetic nanocrystals it was established for the first time that the parameter Δm , which characterizes the intensity of interaction, has significant magnitude and changes sign with temperature growth. The idea to build the generalized (Δm -H-T) diagram of the magnetic state allowed us to establish whole row of critical temperatures and to find explanation to corresponding cardinal changes in the interaction parameters.

Two critical temperatures correspond to set up of the size effect: $T_{cr}^{(1)} \cong 420\text{K}$ – for transition of over 10% of particles from magnetostable state to superparamagnetic one; $T_{cr}^{(2)} \cong 450\text{K}$ – for modification of temperature dependence of low-field border of the particles distribution on the magnetic anisotropy field H_a^{\min} , which is also formed by the smallest particles of the system.

Manifestations of surface effects was unambiguously detected at $T_{cr}^{(3)} \cong 570\text{K}$ (change of sign of the “surface anisotropy” constant K_s) and at $T_{cr}^{(4)} \cong 670\text{K}$ (transition to paramagnetic state of the open surface in both superparamagnetic and magnetostable particles).

In order to confirm the determining role of magnetic moments of the surface ions Fe^{3+} in realization of interparticle magnetic interaction we carried out an additional experiment on a microcrystal (0,1-1,0 μm) system of barium hexaferrite. The essence of the latter was in alteration of physical and chemical state of the open surface and near-surface layer in the particles by means of hostile environments treatment (solutions HCl and NaOH). As the result we discovered changes not only in magnitude but also in sign of the parameter Δm , which is an experimental confirmation of the theoretical prediction [3].

[1] Z.V.Golubenko, A.S.Kamzin, L.P.Ol'khovik, Z.I.Sizova, *Fizika Tverdogo Tela*, **40** (1998) 1294.

[2] A.Kamzin, B.Shtall, R.Gellert, G.Klingelhofer, E.Kankelait, L.Ol'khovik, D.Vcherashniy, *Fizika Tverdogo Tela*, **42** (2000) 873.

[3] J.L.Dormann, D.Fiorani, E.Tronc, *Adv.Chem.Phys.*, **XCVIII** (1997) 283.

22PO-8-55

REFLECTION ELECTRON ENERGY LOSS SPECTRA AND INELASTIC ELECTRON SCATTERING CROSS SECTIONS FOR Fe/Si MAGNETIC LAYRED NANOSTRUTURES

Parshin A.S.¹, Alexandrova G.A.¹, Ovchinnikov S.G.², Varnakov S.N.²

¹Siberian State Aerospace University, 660014, Krasnoyarsk, Russia

²Kirenski Institute of Physics, SB RAS, 660036, Krasnoyarsk, Russia

Layered magnetic nanostructures with semiconductor interlayers, combining the semiconductor and magnetic properties, play an important role in electronics and optical devices (for example, in multiple quantum well lasers and optical mirrors) and are promising materials for spintronics.

The reflection electron energy loss spectra (REELS) for layered nanostructures Fe/Si(d) and Si/Fe(d) have been investigated experimentally. Layered structures are formed of an approximately 50-nm-thick substrate of Fe or Si and of a thin top layer, correspondingly, of Si or Fe, having different thickness in a range from 0.5 to 7 nm. Samples are obtained by vacuum evaporation on single-crystalline silicon substrates at room temperature in an ultrahigh-vacuum technological complex equipped with electron spectrometer. The base vacuum in the processing chamber was 10^{-7} Pa. The reflected electron energy-loss spectra were registered in the differential mode dN/dE (N is the number of electrons with energy E) with the primary electron energies of 600, 1100 and 1900 eV. After numerical integration of the experimental REELS spectra the products of the inelastic electron mean free path by differential inelastic electron scattering cross section from these spectra have been calculated with the package QUASESTM_XS_REELS [1].

We have applied to these layered structures the technique of definition of elements concentration of the composite samples Fe_xSi_{1-x} system advanced by us earlier [2]. Thus, for system Fe_xSi_{1-x} the product of the inelastic electron mean free path on differential inelastic electron scattering cross section determined from experimental REELS spectra can serve as quantitative measure of elements concentrations in the composite medium. The concentration of elements for layered structures determined by this method at different primary electrons energies appeared approximately equal. This result suggests to comparatively homogeneous composition of the top surface layers of the investigated structures.

This work was supported by the SB RAS integration project 3.5 and by the “Spintronics” program of the Division of Physical Sciences of the RAS.

[1] [http:// www.quases.com](http://www.quases.com).

[2] A.S. Parshin, G.A. Alexandrova, A.E. Dolbak, O.P. Pchelyakov, B.Z. Olshanetsky, S.G. Ovchinnikov, S.A. Kushenkov // International Conference “Functional Materials” (ICFM’ 2007): Abstracts. Ukraine, Crimea, Partenit, October 1-6, 2007. P 76.

22PO-8-56

DETECTION OF CORRELATIONS OF INTERPARTICLE MAGNETIC INTERACTION PARAMETERS WITH SIZE AND SURFACE EFFECTS IN REAL SYSTEMS OF SMALL PARTICLES

Kamzin A.S.², Ol'khovik L.P.¹, Sizova Z.I.¹, Shurinova E.V.¹

¹Karazin Kharkov National University, Svobody Sqr. 4, Kharkov 61077

²Ioffe Physico-Technical Institute of Russian Academy of Sciences, 194021 St Petersburg, Russian Federation

Solution of the problem under consideration was guaranteed by purposive choice of the object of investigation in form of system of nanocrystals of highly anisotropic ferrimagnetic $BaFe_{12}O_{19}$. Particles of the given system (10-100 nm) in the range 300-750K have whole set of magnetic states, that are inherent in small particles: magnetostable, superparamagnetic and

paramagnetic ones [1]. Along with that, the determining role in formation of magnetic properties of the particles belongs to open surface and adjacent to it structural-defective near-surface layers with skewed magnetic structure, which give partial contribution about (100-50)% to total particles volume [2].

For the considered close-packed system of highly anisotropic ferromagnetic nanocrystals it was established for the first time that the parameter Δm , which characterizes the intensity of interaction, has significant magnitude and changes sign with temperature growth. The idea to build the generalized (Δm -H-T) diagram of the magnetic state allowed us to establish whole row of critical temperatures and to find explanation to corresponding cardinal changes in the interaction parameters.

Two critical temperatures correspond to set up of the size effect: $T_{cr}^{(1)} \cong 420\text{K}$ – for transition of over 10% of particles from magnetostable state to superparamagnetic one; $T_{cr}^{(2)} \cong 450\text{K}$ – for modification of temperature dependence of low-field border of the particles distribution on the magnetic anisotropy field H_a^{\min} , which is also formed by the smallest particles of the system.

Manifestations of surface effects was unambiguously detected at $T_{cr}^{(3)} \cong 570\text{K}$ (change of sign of the “surface anisotropy” constant K_s) and at $T_{cr}^{(4)} \cong 670\text{K}$ (transition to paramagnetic state of the open surface in both superparamagnetic and magnetostable particles).

In order to confirm the determining role of magnetic moments of the surface ions Fe^{3+} in realization of interparticle magnetic interaction we carried out an additional experiment on a microcrystal (0,1-1,0 μm) system of barium hexaferrite. The essence of the latter was in alteration of physical and chemical state of the open surface and near-surface layer in the particles by means of hostile environments treatment (solutions HCl and NaOH). As the result we discovered changes not only in magnitude but also in sign of the parameter Δm , which is an experimental confirmation of the theoretical prediction [3].

[1] Z.V.Golubenko, A.S.Kamzin, L.P.Ol'khovik, Z.I.Sizova, *Fizika Tverdogo Tela*, **40** (1998) 1294.

[2] A.Kamzin, B.Shtall, R.Gellert, G.Klingelhofer, E.Kankelait, L.Ol'khovik, D.Vcherashniy, *Fizika Tverdogo Tela*, **42** (2000) 873.

[3] J.L.Dormann, D.Fiorani, E.Tronc, *Adv.Chem.Phys.*, **XCVIII** (1997) 283.

22PO-8-57

Co NANOPARTICLES IN Si OXIDES: MAGNETOOPTICAL SPECTRA

Edelman I.¹, Ivantsov R.¹, Vorotynova O.², Petrov D.², Seredkin V.¹,
Valeev V.³, Khaibullin R.³, Stepanov A.³

¹L.V. Kirensky Institute of Physics, Krasnoyarsk, 660036, Russia

²Siberian Federal University, Krasnoyarsk, 660041, Russia

³Kazan Physics-Technical Institute, Kazan, 420029 Russia

Magnetic and magneto-optical properties of the ion-synthesized cobalt nanoparticles in silica dioxide matrix are investigated. The ion Co^+ (40 keV) low energy implantation method at the ion dosage (D) $0.25 \cdot 10^{17}$, $0.5 \cdot 10^{17}$, $0.75 \cdot 10^{17}$ and $1.0 \cdot 10^{17}$ ion/cm² was used to fabricate Co nanoparticles. Spherical Co nanoparticles were detected with the electron microscope in transverse cross-section of samples. For the patterns with ion implantation dosage $1.0 \cdot 10^{17}$ ion/cm² the particle sizes are $\sim 3-8$ nm. Simulation of the distribution profile of Co ions implanted in glass demonstrate that Co implanted layer thickness is of the order of 30 nm and the Co-admixture concentration peak with implantation dosage growth increases and moves to the pattern surface.

Magnetization (top figure), Faraday and Kerr effects magnetic field dependencies demonstrate transition at room temperature from superparamagnetic behavior of the ensemble of Co nanoparticles to ferromagnetic response typical for thin magnetic films with in-plane anisotropy. The magnetization curve simulations both for superparamagnetic and for ferromagnetic cases allow estimating the Co nanoparticles mean size and the volume fraction in dependence on D.

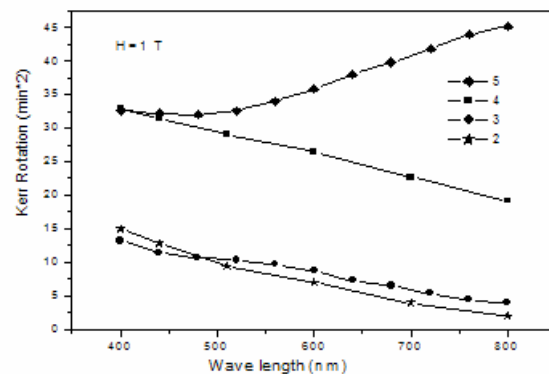
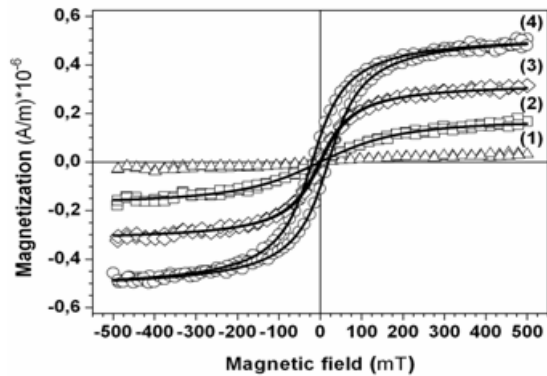
D 10^{17} ion/cm ²	Particles concentration 10^{18} cm ⁻³	Mean volume nm ³
0.50	3.4	37.8
0.75	5.1	44.6
1.00	5.9	61.6

An essential difference between Faraday and Kerr effect spectra (bottom) in Co ion-synthesized samples investigated and in homogeneous Co films is revealed. This difference is supposed to be due to the local excitation of free electrons in Co nanoparticles.

The Faraday and Kerr spectra simulation was made in frames of the effective medium approach [1] taking in to account the particles size and fraction factor derived from magnetic analysis. Spectra of the dielectric permeability tensor components of nanoparticles were obtained.

Support of RFBR (07-02-93174, 07-03-00320) is acknowledged.

[1] T.K. Xia, P.M. Hui, D. Stroud, *J. Appl. Phys.*, **67** (1990) 2736.



22PO-8-58

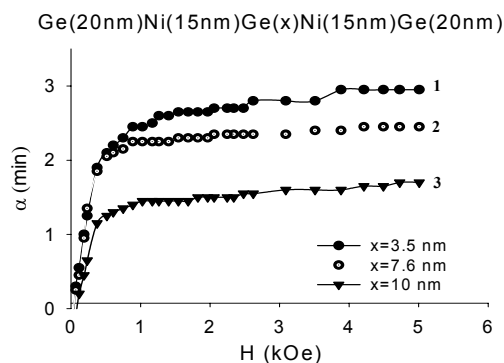
MULTILAYERED Ni-Ge FILMS: MAGNETIC AND MAGNETO-OPTIC PROPERTIES

*Edelman I.¹, Patrin G.^{1,2}, Velikanov D.^{1,2}, Chernichenko A.¹,
Turpanov I.¹, Bondarenko G.¹, Grebenkova Yu.²*

¹L.V. Kirensky Institute of Physics, SB RA Sciences, Krasnoyarsk, 660036 Russia ²Siberian Federal University, Krasnoyarsk, 660041 Russia

Magnetic and magneto-optical properties of the Ni-Ge multilayer films were studied. Films were prepared by the ion-plasma sputtering technique. Ni and Ge layers thickness varied from ~3 to ~20 nm. Magnetization was measured on a SQUID magnetometer at 4.2-300 K in the magnetic field H up to 1 kOe directed in the film plane. The magnetic field and spectral dependences of the Faraday and Kerr magneto-optical effects were measured in different geometries. Magnetization and Faraday Effect (FE) dependences on magnetic field are typical of the films with in-plane anisotropy. The saturation field H_s value and FE in H_s depend on the Ni layer thickness: both values decrease with the decrease of the Ni layer thickness. The most unusual thing is the strong decrease of the Faraday Effect value with an increase of Ge layers

situated between Ni layers (Fig). In-plane magnetization curves for all samples are the near-rectangular hysteresis loops, the coercive force H_c increases with a decrease in temperature approximately up to 70 K. As the temperature is further decreased, the hysteresis loop becomes asymmetric, less rectangular, and H_c reaches a magnitude of about 300 Oe at 4.2 K, i.e., it becomes an order of magnitude higher than H_c at room temperature. Moreover, the hysteresis loop at low temperatures is shifted along the field axis that is typical of the systems with exchange unidirectional anisotropy. Both effects - the increase in the coercive force and the appearance of the asymmetry in the



hysteresis loop - are observed in the film structures comprised of the ferromagnetic (FM) and antiferromagnetic (AFM) layers or of the soft and hard FM layers and are explained by the exchange interaction of these layers or the so-called exchange anisotropy. However, as a rule, the former effect occurs under weak exchange anisotropy in the FM-AFM or FM-FM layers and the latter effect occurs under strong anisotropy in the FM-AFM layers. A feature of the films under consideration is the appearance of both effects in one sample. The supposition is made that an interface of variable chemical composition conditioned by mutual diffusion of Ni into Ge is formed between Ni and Ge layers. On the Ni layer side, the Ni enrichment takes place and a compound that is similar to Ni_3Ge and has the ferromagnetic order is formed. Therefore, a pair of the Ni and Ni_3Ge layers in the interface can be considered as a structure comprised of the soft (Ni) and hard (Ni_3Ge) magnetic layers. As the distance from the Ni layer increases, the compound in the interface is enriched with Ge and the antiferromagnetic compounds are formed with a rather low Neel temperature. Since the magnetization curves at 77 K have no exchange shift, we can conclude that $T_N < 77$ K. Both FM layers at $T = 4.2$ K behave as an entity in the exchange field of the AFM layer. When Ge is the intermediate layer between Ni layers the picture became even more complex that forces strong decrease of FE value comparing to single-layer Ni film.

Support of RFBR (08-02-00397) is acknowledged.

22PO-8-59

NANOSTRUCTURES BASED ON GLASSES DOPED WITH 3d AND 4f ELEMENTS

Ivanova O.¹, Edelman I.¹, Ivantsov R.¹, Zablude V.¹, Zaikovskiy V.², Stepanov S.³

¹Kirensky Institute of Physics, Siberian Branch of RAS, 660036 Krasnoyarsk, Russia

²Boreskov Institute of Catalysis, Siberian Branch of RAS, 630090 Novosibirsk, Russia

³S.I. Vavilov State Optical Institute, St.-Petersburg 199034, Russia

Structure and magneto optical properties of potassium-aluminum-germanium glasses ($\text{Al}_2\text{O}_3\text{-K}_2\text{O-GeO}_2$) doped with Fe_2O_3 and R_2O_3 where R is Gd, Tb, Dy, Ho, or Yb, were investigated for the first time. Samples were fabricated with usual glass technology and subjected to additional thermal treatment at different temperatures and duration. Morphology and space distribution of components in the glasses were determined with transmission electron microscopy, Fourier filtered diffractometry, and energy dispersive spectroscopy (TEM - FFT - EDS). Spectral and magnetic field dependences of magneto optical Faraday Effect (FE) were obtained at room temperature.

Magnetic particles of different shape and size were observed in all samples, subjected to additional thermal treatment. Particles size changes, mainly, from 10 to 50 nm, however they consist of micro blocks of about 5 nm. Particles of isometric morphology prevail, some amount needle particles is observed too. Main part of Fe is included in to particles, rare earth elements are detected in the particles only. An example of TEM image is shown in figure for the sample with Dy. In most cases particles has crystal structure close to Fe_3O_4 (according to FFT).

For all samples FE spectra are close with each other independently of rare earth elements and differ from FE spectrum for Fe_3O_4 . Possibly such a discrepancy between FE and FFT data can be explain by an influence of rare earth components on the Fe ions electron spectrum. The second unusual phenomenon is FE hysteresis loops close to rectangular shape. Earlier, for particles of analogues sizes magnetization curves close to Langeven type were observed. Again, this effect can be ascribed to rare earth influence on the particles anisotropy.

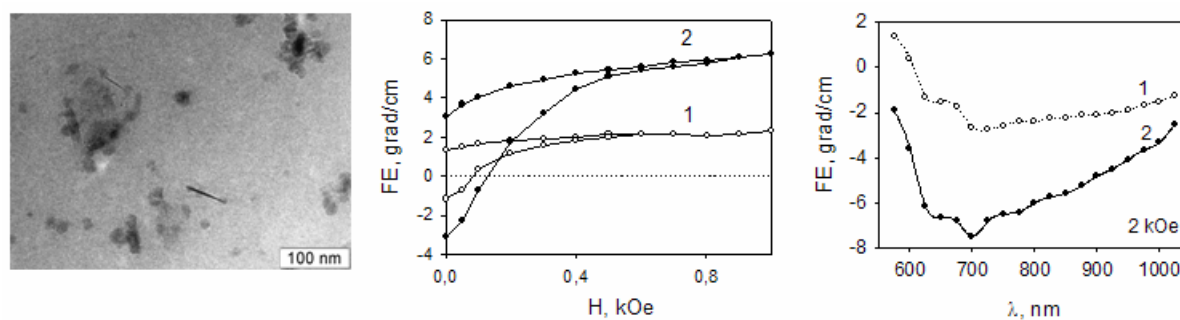


Fig. TEM image, FE field (750 nm) and spectral dependences for glass with Dy treated at 600 °C during 2 and 16 hours (curves 1 and 2).

Mechanisms are considered responsible for the FE behavior in the glasses under investigation in dependence on the particles morphology.

Support by RFBR (Grant 07-02-92174-CNRS) is acknowledged.

22PO-8-60

MAGNETIC AND MAGNETOOPTICAL PROPERTIES OF NANOGRANULAR Co-Ti-O FILMS

Polyakova K.P., Polyakov V.V., Seregin V.A., Zharkov S.M., Bondarenko G.V.
L.V.Kirensky Institute of Physics, SB RAS, 660036, Krasnoyarsk, Russia

Magnetic properties of granular films consisting of magnetic particles in dielectric matrix have been extensively described in last years. It is known that magneto-optical properties of composite system depend on properties of a dielectric matrix. The majority of researches are devoted metal particles in dielectric matrixes SiO_2 and Al_2O_3 . In this connection magneto-optical properties in TiO_2 matrix with the dielectric constant exceeding corresponding value of SiO_2 and Al_2O_3 are of interest.

Most widespread of granular film prepared method is the co-deposition of metal and insulator. In this case the nanoparticles distributed in matrix randomly. On successive deposition of metal and insulator it can be realized self-organization in metal particale formation.

In this report we present the magnetic and magneto-optical properties of Co-Ti-O granular films received in conditions of solid-state reaction in layered film structure [1]. Solid state reaction $\text{CoO} + \text{Ti} = 2\text{Co} + \text{TiO}_2$ was carried out in a mode of isothermal annealing at temperature 620-670 K in vacuum 10^{-6} Torr. Film structures with volume fractions of magnetic phase $X = 0.3, 0.46, 0.5, 0.66$ and 0.7 ($X = V(\text{Co})/V(\text{Co}+\text{Ti})$) have been received. Granular films of (50-100) nm thickness were prepared. The Co grain size was (10-100) nm. Investigations of magnetic properties of granular Co-Ti-O films have shown the following. The film magnetization curve of for $X=(0.46-0.70)$ specify ferromagnetic character of interaction between magnetic granules. Magneto-optical spectra have been investigated in the wavelength range of visible light in a magnetic field up to 14 Oe. It is established, that spectral dependence of polar Kerr rotation of $X=0.4-0.7$ are nonmonotonous unlike corresponding dependence of continuous Co films. It is shown also, that character of spectral dependence of Kerr rotation depends on magnetic fraction volume concentration of granular films. The curve of concentration dependence of polar Kerr rotation for contains tow maximum: of $X=0.46$ and of $X=0.65$. For $X=0.65$ the enhancement of rotation in 2-2,5 times in the wave length range of 400-650 nm with a maximum on length of a wave of 600 nm is observed. It was established the correlation of concentration dependences of Faraday rotation and polar Kerr rotation on wave length of 630 nm.

It is necessary to note that anomalies of magneto-optical spectra of the composite materials containing dielectric in the form of a layer or matrix, were observed [2] and have been predicted by theoretical calculation [3].

The mechanism of a magneto-optical rotation enhancement in granular films Co-Ti-O will be discussed.

[1] V.G. Miagkov, K.P. Polyakova, G.N. and V.V. Polyakov, *J.MMM*, **258-259** (2003) 358

[2] Yu.A. Dynnik, I.S. Edelman, T.P. Mopozova and A.Ya. Betenkova, *JETP Lett.*, **65** (1997) 531

[3] M. Abe and M. Gomi, *Jpn. J. Appl. Phys.*, **23** (1984) 1580.

22PO-8-61

MAGNETOOPTICAL PROPERTIES OF AMORPHOUS COMPOSITE FILMS

Buravtsova V.E.¹, Gan`shina E.A.¹, Ivanova O.S.¹, Kalinin Yu.E.², Kirov S.A.¹, Sitnikov A.V.²

¹Lomonosov Moscow State University, Physics Faculty, 119899, Moscow, Russia

²Voronezh State Technical University, 394006, Voronezh, Russia

In this study we have investigated multilayer structures $[(\text{Co}_{45}\text{Fe}_{45}\text{Zr}_{10})_Z(\text{Al}_2\text{O}_3)_{100-Z}]_X/(\alpha\text{-Si})_Y]_{40}$ prepared by ion-beam sputtering of two targets with deposition on rotating substrates [1]. Here Z is of the amorphous alloy content in the nanocomposites, X is the nanocomposites thickness, Y – thickness of the semiconductor interlayer.

Dispersion of the MO transversal Kerr effect (TKE) in the multilayer structures was studied in a wide energy range (0,5 – 4,2 eV). It was found that the frequency dependence and magnitude of the TKE strongly depend on thickness both of the semiconductor and granular ferromagnetic layers as well as the content of $\text{Co}_{45}\text{Fe}_{45}\text{Zr}_{10}$ in the nanocomposites.

The study of the TKE vs. layer thickness dependence $\delta(Y)$ revealed that in each series of the samples ($Z = 35$ at.%, 46 at.% and 100 at.%) the greatest TKE magnitudes were observed in the samples with different silicon layer thickness. Position of the maximum on the TKE thickness dependence $\delta(Y_{\text{cr}})$ strongly depends both on the silicon interlayer thickness and the ferromagnetic component concentration Z inside the $(\text{Co}_{45}\text{Fe}_{45}\text{Zr}_{10})_Z(\text{Al}_2\text{O}_3)_{100-Z}$ layers.

These particularities can be explained applying the minimization principle to the surface energy of the structure. During growth of a semiconductor film on the surface of the composite its nucleation centers tend to concentrate on the metallic granules since the surface energy density for the alloy $\text{Co}_{45}\text{Fe}_{45}\text{Zr}_{10}$ is 2,8 J/m² and the ones for Al_2O_3 and Si are 1,4 and 1,2 J/m² correspondingly [2]. For the samples from the $Z = 100$ at.% series the silicon particles can settle with equal probability in any position on the ferromagnetic film surface, and a continuous silicon layer is formed at $Y_{\text{cr}} \approx 1,2$ nm. Hence the changes of MO properties of the multilayer structures in the thickness range 1,2-2,1 nm can be attributed to the progressive growth of the Si interlayer on the ferromagnetic granules $\text{Co}_{45}\text{Fe}_{45}\text{Zr}_{10}$ – the island structure of the Si layer transforms into a continuous one. Since exchange interaction of ferromagnetic granules can proceed across thin silicon interlayers the number of granules which are exchange-coupled through an "island" grows and this results in the growth of the TKE magnitude.

Is the exchange interaction carried out by conductivity electrons of silicon or by the exchange interaction of the silicides formed on the ferromagnetic/Si interface is not yet clear and the problem requires further investigation.

This work was supported by Russian Foundation for Fundamental Research (Grant 05-02-17064)

[1] Yu.E.Kalinin, K.G.Korolev, A.V.Sitnikov. JETP Letters 32, 6 (2006) 61-67

[2] Yu.E.Kalinin, K.G.Korolev, A.V.Sitnikov. Vestnik VSTU (proceeds)

22PO-8-62

INVESTIGATION OF DISTRIBUTION OF MAGNETIC DOMAINS IN Co/Au MULTILAYER FILM BY MAGNETIC FORCE MICROSCOPY

Nurgazizov N.^{1,2}, Zhdan P.¹, Kisielewski M.³, Stobiecki F.⁴

¹University of Surrey, Guildford, UK

²Zavoisky Physical-Technical Institute, Sibirsky trakt 10/7, Kazan, Russia

³University of Bialystok, Bialystok, Poland

⁴Institute of Molecular Physics, Polish Academy of Sciences, Poznan, Poland

One of the main targets of the investigation of multilayer magnetic films (where a magnetic layer interchanges with nonmagnetic layer) represents the visualization of the magnetization distribution. The domains changes depend on a thickness of a magnetic layer, on a distance between these layers and quantity of layers [1]. The distribution of magnetic domains may be visualized by magnetic force microscope (MFM). However the MFM probe can bring distortions in the obtained image.

The multilayer Co/Au film was investigated. The film consisted from 15 Co layers (1 nm) interchangeable with 15 Au layers (1.5 nm). The measurements were carrying out by scanning probe microscopy Solver HV (NT MDT, Russia). For scanning the NSG 03 tips were used. The two types of magnetic probes have been prepared based on these tips. The first type of tips was covered by 25 nm of Co layer. The magnetic characteristics of this probe were identical to commercial magnetic probes. The second type of a probe had whisker on the end and was covered by 8 nm Co.

When we carried out the measurements by a standard two pass technique with the first type of probes the obtained magnetic images were unstable. It was connected with the sample remagnetization by a probe during the scan. The second type of probes had much less magnetic moment and it allowed to obtain stable magnetic images of the sample. It allows to investigate a distribution of magnetic domains and to estimate their width. For our sample the period of magnetic domains (the width of one black and one white stripe) was about 170-200 nm.

The MFM measurements carried out with different type of probes showed that for low coercivity sample the obtained images strongly depended on used probe. For obtaining the stable images of magnetic domains is necessary to use the probe with low magnetic moment or to use one pass MFM technique.

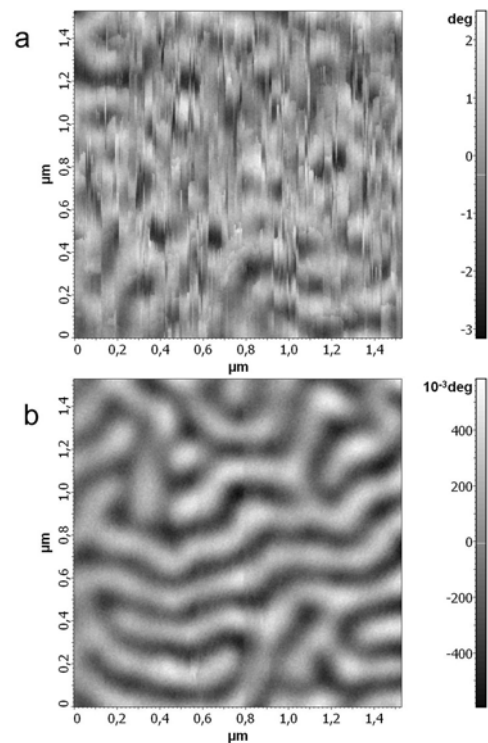


Fig. 1 MFM images of multilayer Co/Au film obtained by probes coated with 25 nm Co (a) and 8 nm Co (b).

Work was supported by project NANOMAG-LAB, No. 2004-003177 (European MC ToK).

[1] S. Hamada, N. Hosoi, T. Ono, T. Shinjo, *J. Mag. and Mag. Mat.*, **198-199** (1999) 496.

22PO-8-63

MAGNETIC MOMENT OF HELICAL NANOTUBES IN MAGNETIC FIELDS

Dunaevsky S., Grigor'kin A.

Petersburg Nuclear Physics Institute, Russian Academy of Sciences, Gatchina, Leningrad District, 188300, Russia

In recent years, the considerable interest in the investigation of the magnetic and transport properties of nanotubes has been motivated by their wide use in various devices of quantum electronics.

In this paper, we analyze the magnetic properties of a nanotube with helical symmetry, which is caused by the presence of a helical defect simulated by an extended δ potential. The violation of the symmetry of the structure with respect to the inversion of the coordinates leads to the appearance of specific features in the behavior of the physical properties of the electron gas in magnetic fields.

We consider the model [1] represented by a cylinder with infinitely thin walls and an extended helical δ potential wound on its surface. The potential has an amplitude V_0 and a period $T_z=2\pi/\alpha$ along the cylinder axis. In the limit $V_0 \rightarrow \infty$, the given model corresponds to the experimentally fabricated quasi-two-dimensional ribbon rolled into a helix [2]. For a finite amplitude of the potential, electrons can tunnel between neighboring turns in the system.

The single-electron spectrum $E_m(k)$ for this system has the form [1]:

$$E_m(k) = \varepsilon^* \left\{ \gamma \left(\frac{k}{\alpha} + \frac{\Phi}{\Phi_0} \right)^2 + \frac{\alpha^2 R^2 \Delta_m^2}{\gamma} \right\}$$

The magnetic moment of the nanotube will be sought under the assumption that the chemical potential μ of the electron gas is constant. In this case, the magnetic moment M is defined as the derivative of the thermodynamic potential with respect to the magnetic field B :

$$M = \frac{l}{\pi} \sum_m \int dk \frac{dE_m(k)}{dB} \rho_F(E_m(k))$$

$$\frac{dE_m(k)}{dB} = \frac{m_0}{m^*} \mu_B \left\{ \left(\frac{k}{\alpha} + \frac{\Phi}{\Phi_0} \right) - \frac{1}{2\alpha R^2 \varepsilon^*} \frac{dE_m(k)}{dk} \right\},$$

where ρ_F is the Fermi–Dirac function and l is the nanotube length.

The magnetic moment $M = M_0 + M_1$ of the system is studied as a function of the magnetic flux. It is demonstrated that the equilibrium magnetic moment M_0 at large amplitude of the δ potential is a smooth function of the magnetic flux or can exhibit kinks depending on the position of the Fermi level. The functional dependence of the equilibrium magnetic moment M_0 on the magnetic flux is determined in the limit $V_0 \gg E_F$.

An expression is derived for the magnetic moment M_1 induced in the given system for the case in which the electron current in a ballistic regime passes through the system.

[1] A. A. Grigor'kin and S. M. Dunaevskii, *Fiz. Tverd. Tela* (St. Petersburg) 49 (3), 557 (2007) [*Phys. Solid State* 49(3), 585 (2007)].

[2] V. M. Osadchii and V. Ya. Prinz, *Pis'ma Zh. Eksp. Theor. Fiz.* 72 (6), 451 (1998) [*JETP Lett.* 72 (6), 312 (1998)].

22PO-8-64

NON-EQUILIBRIUM MAGNETISM OF SINGLE-DOMAIN PARTICLES APPLIED FOR CHARACTERIZATION OF MAGNETIC NANOMATERIALS

Chuev M.A.

Institute of Physics and Technology, Russian Academy of Sciences, Nakhimovskii pr. 36-1,
117218 Moscow, Russia

A great interest of researchers in modern materials containing small magnetic particles or clusters (several nanometers, so that they are single-domain) is primarily due to the wide area of their application in the nanotechnology of magnetic and magneto-optic information-recording devices, ferrofluids, NMR tomography, chemical catalysis, color imaging devices, biotechnology, etc. For this reason, it is necessary to perform systematic investigations of the structural and magnetic properties of these materials by various methods in order to optimize the technology of their growth and to determine the fundamental characteristics of magnetism in an ensemble of magnetic nanoparticles. The most informative techniques to study the non-equilibrium magnetism of nanoparticles seem to be the conventional magnetization measurements and Moessbauer spectroscopy. The principal difference between them is that they can probe magnetic properties of the same material in different frequency ranges: the magnetization measurements are carried out at lower frequencies (of about 1-1000 Hz) while Moessbauer spectroscopy can reveal the magnetic dynamics of nanoparticles at higher frequencies due to the Mossbauer time window (10^{-11} – 10^{-6} s for ^{57}Fe nuclei). The only way to extract the reach information from the experimental data is to define a model of the magnetic dynamics in order to describe the whole set of the experimental data for the sample studied.

In the present contribution magnetic relaxation effects revealed in Moessbauer spectra and magnetization measurements of nanoparticles are discussed in the framework of a general model for magnetic dynamics of ensemble of single-domain particles which is based on a generalization of the well-known Stoner-Wohlfarth model within more accurate description of relaxation processes within the Neel's ideas and corresponding time-dependent hyperfine interactions in the magnetic system [1,2]. The generalized model allows one to treat numerically both Moessbauer spectra, including those in static and radiofrequency magnetic field, and magnetization curves in alternative low-frequency magnetic field as well as temperature demagnetization FC (field cooling) and ZFC (zero-field cooling) curves in a self-consistent way within the same set of physical parameters inherent to the system studied. A number of qualitative effects can be explained or predicted within the approach, which include interaction effects, relaxation-stimulated resonances in Moessbauer spectra under radiofrequency field excitation, specific shapes of Moessbauer spectra within precession of particle's uniform magnetization, and asymptotic high-temperature magnetization and susceptibility behavior different from the classical Langevin's high-temperature limit for ideal superparamagnetic particles. Corrections within more general models of magnetic dynamics based on the Landau-Lifshitz-Gilbert or Braun kinetic equations will be also discussed. Applications of the generalized model for analyzing the temperature- and magnetic field-dependent magnetization curves and Moessbauer spectra taken on nickel and iron nanoparticles in non-magnetic and weakly magnetic matrices will be presented.

This work is supported by the Russian Foundation for Basic Research (project No. 08-02-00388).

[1] A.M. Afanas'ev, M.A. Chuev and J. Hesse, *JETP*, **89** (1999) 533.

[2] M.A.Chuev and J.Hesse. *J. Phys.: Condens. Matter*, **19** (2007) 506201.

22PO-8-65

MAGNETORESISTIVE PROPERTIES OF Tb/Ti AND Tb/Si MULTILAYERS

Svalov A.V.^{1,2}, Vas'kovskiy V.O.¹, Barandiaran J.M.²,
Orue I.³, Sorokin A.N.¹, Kurlyandskaya G.V.²

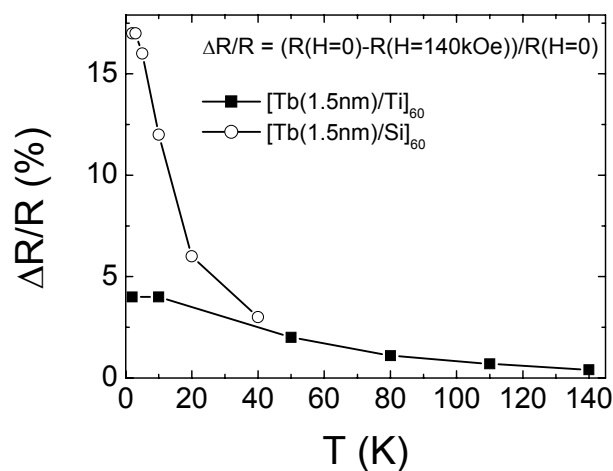
¹Ural State University named after A.M.Gorky, 620083, Ekaterinburg, Russia

²Universidad del País Vasco (UPV-EHU), Dpto. Electricidad y Electrónica, 48080 Bilbao, Spain

³SGiker, Universidad del País Vasco (UPV/EHU), 48080 Bilbao, Spain

Magnetoresistive properties of FM/NM multilayers and FM-NM granular structures (FM – is a ferromagnetic layer or clusters and NM – is non-magnetic spacer or matrix) are of special scientific interest from the point of view of both fundamental research and technological applications. Transition metals or their alloys have been usually employed as FM materials while rare earth have been much less studied as FM components [1-2]. However, one can expect peculiar magnetoresistance behaviour in such materials because the magnetism of rare earth metals is connected with localized $4f$ electrons, but conductivity is provided by $5d$ and $6s$ collective electrons [3].

In this work rf-sputtered multilayered structures of Tb/Ti and Tb/Si were studied. The thickness of the Tb layer was varied from 1.5 to 6 nm. The thickness of non-magnetic spacers of Ti or Si was kept constant (2 nm). Magnetoresistance (MR) was measured by a standard four points technique in a magnetic field up to 14 T in the temperature range of 2 to 200 K. Magnetic field and current were in plane of the sample. At low temperature both types of multilayer show large negative magnetoresistance, i.e. the resistance decreases with an increase of the magnetic field H . For temperatures $T < 40$ K $\Delta R/R$ is significantly higher for the samples with Si spacers (see figure). Below certain temperature T_0 for all multilayers (both with Ti and Si spacers) a hysteresis of the $MR(H)$ magnetoresistive curves was observed. T_0 depends on the thickness of terbium layer and on the type of the material of non-magnetic spacer. In this work the magnetoresistance and magnetic data are comparatively analyzed taking into account the results on the structure of Tb/Ti and Tb/Si multilayers.



This work was supported by the RF project RNP.2.1.1.6945, and Spanish MEC (project MAT_2005-06806-C04-03).

[1] F. Tsui, C. Uher, C.P. Flynn, *Phys. Rev. B*, **72** (1994) 3084.

[2] A.V. Svalov, V.O. Vas'kovskiy, G.V. Kurlyandskaya, J.M. Barandiaran, N.N. Schegoleva, A.N. Sorokin, *Chin. Phys. Lett.*, **24** (2007) 1717.

[3] S.A. Nikitin, *Magnetic Properties of Rare-Earth Metals and Alloys* (MSU, Moscow, 1989) [in Russian].

22PO-8-66

MAGNETIC FORCE MICROSCOPY ON Co/Pt MULTILAYERS*Karoutsos V.¹, Pouloupoulos P.¹, Angelakeris M.², Papaioannou E.Th.³, Fumagalli P.³ and Flevaris N.K.²*¹Materials Science Department, University of Patras, 26504 Patras, Greece²Department of Physics, Aristotle University of Thessaloniki, 54124 Thessaloniki, Greece³Institut für Experimentalphysik, Freie Universität Berlin, Arnimallee 14, D-14195 Berlin-Dahlem, Germany

Co/Pt multilayers is one of the best candidates for perpendicular magneto-optic recording. In this work, Co/Pt multilayers were prepared by electron-beam evaporation under ultrahigh vacuum conditions on silicon, glass and polyimide substrates. X-ray diffraction measurements revealed the high quality of multilayer stacking. Magneto-optic polar Kerr effect experiments were used in order to obtain magnetization hysteresis loops of the films. We have studied the magnetic-domain morphology on the surface of the films via Magnetic Force Microscopy. The field applied during these measurements was 2.3 kOe oriented perpendicular to the film plane; this field seems to stabilize and enhance out-of-plane stripe domains against in-plane domains that may be expected from magnetization curves. Finally, we observed that when the applied field approaches the magnetic saturation field, then the domain morphology turns to be dominated by bubble domains.

Work was supported by the Greek Secretariat for Research and Technology (GSRT), project PENED2003 03ΕΔ_667 'Self-assembled networks of magnetic nanoparticles for applications of permanent magnets, sensors and magnetic recording media'.

22PO-8-67

FINITE SIZE EFFECTS IN FIELD-INDUCED TRANSITIONS IN MAGNETIC MULTILAYERS*Kostyuchenko V.V.*

Institute of Physics and Technology RAS, Yaroslavl Branch, Yaroslavl 150007, Russia

The field-induced transitions in magnetic multilayers are the subject of intensive investigations since the discovery of the antiferromagnetic exchange interaction between magnetic layers via nonmagnetic spacer and the effect of giant magnetoresistance. Several peculiarities increase the complexity of theoretical investigations in this field of research. Finite size effect is one of the most important among them. In spite of a long time history of these investigations the regular method of analytical calculation of finite size effect is absent. Only in [1, 2] an attempt was made to study the finite size effects by using the methods of matrix analysis.

In the present work the new technique of finite difference equations is used for an analytical investigation of field-induced transitions in magnetic multilayers. As far as author knows this method was not used before. Heisenberg and biquadratic exchange interactions and uniaxial anisotropy are taken into account. At first, the values of critical fields determining the stability of phases are calculated for the case of infinite layers number. These calculations are

needed for comparison with the results obtained for the finite layers number. Next the values of critical fields were calculated for the arbitrary layers number N .

It is shown that the critical field value H_{C2} determining the stability of ferromagnetic phase is monotonically increased with increasing layers number and as N tends to infinity it coincides with the value of critical field for the infinite superlattice. It can be explained by the contribution by the boundary layers as far as they coupled by exchange interactions with one layers only. It gives rise to the decreasing of critical field value. With increasing layers number the relative contribution of boundary layers decreases and the critical field tends to the value obtained for the infinite layers number.

The value of critical field H_{C1} determining the stability of antiferromagnetic phase has cumbersome dependence on the layers number. In the case of even layers number the critical field H_{C1} does not depend on the layers number. For the odd layers number the critical field H_{C1} depends on the mutual orientation of the external field and the magnetization in the boundary layers. In the case of parallel orientation the critical field H_{C1} monotonically decreases with increasing layers number and as N tends to infinity the H_{C1} tends to H_{C1} value for infinite superlattice. In the case of antiparallel orientation the critical field H_{C1} monotonically increases with increasing layers number and as N tends to infinity the H_{C1} tends to H_{C1} value for even layers number. The smaller value of the critical field H_{C1} for the antiparallel orientation of the external field and the magnetization in the boundary layers is concerned with the nucleation of the surface spin-flop phase near the boundary layer.

In the interesting case of odd layers number and the perpendicular orientation of external magnetic field with respect to the easy axes the antiferromagnetic phase with perpendicular orientation of magnetization with respect to the easy axes can be stable. The stability condition for this phase strongly depends on the anisotropy value and the layers number.

[1] A. K. Zvezdin and V.V. Kostyuchenko, *Phys. Sol. St.*, **39** (1997) 155.

[2] A.L. Dantas and A. S. Carrigo, *Phys. Rev. B*, **59** (1999) 1223.

22PO-8-68

SUPERRADIANCE FROM MOLECULAR NANOMAGNETS

Henner V.K.¹, Kharebov P.V.¹, Yukalov V.I.²

¹Department of Theoretical Physics, Perm State University, Perm, 614990, Russia

²JINR, Laboratory of Theoretical Physics, Dubna, 141980, Russia

The goal of this work is to justify a possibility to obtain and observe coherent spin relaxation—the superradiance (SR) effect—in molecular nanomagnetic structures. We note that giant-spin molecules have the magnetic moments of the order of $10 \mu_B$ and possess substantial magnetic anisotropy. Moreover, to invoke SR, such a system should be polarized to a high extent. When put together, these factors rule out the conventional treatment used e.g. for optical SR, and invoke development of novel approaches.

The major manifestation of SR phenomena is that the radiation intensity is proportional to the squared number of the spins in the system. This implies collective magnetodynamics, which could be established when a large number of spins is tightly coupled by a long-range effective interaction. A simple way to create the latter is to place a sample in a passive resonance circuit which, in response to the magnetization motion, generates a feedback magnetic field common for all the spins of the system.

In our work we begin with a quantum microscopic Hamiltonian, which reflects all the features of the magnetic molecular spin system in question, and use it to obtain the Heisenberg

equations of motion for individual spins. Along with the Kirchhoff equation for the current induced in the resonator, it allows to reduce the initial description to a set of effective mean-field equations for “classical” spin vectors. The obtained set is essentially nonlinear and could be analyzed only by means of computer simulation.

The particular problem is formulated in the following way: a strongly polarized sample (a nanomagnetic molecular crystal) is subjected to a constant magnetic field \mathbf{B}_0 antiparallel to the initial polarization direction, so that the spin system is deliberately put in a non-equilibrium state. The axis of the inductance coil (the resonator), which encases the sample, is oriented perpendicular to \mathbf{B}_0 . In our simulations we consider several sample configurations viz. a cube cut out of a cubic spin lattice which side equals L lattice periods as well as 1D and 2D structures, i.e., spin chains and spin layers with various orientations of their axes with respect to \mathbf{B}_0 and to the resonator. The anisotropy parameter, the strength of the dipole interactions, the coupling to the resonator, the degree of initial polarization—all these factors prove to be crucial for obtaining the ultrafast SR relaxation. Of the variety of possible dynamic regimes we sort out those where SR in a system of molecular nanomagnets indeed takes place and analyze the conditions ensuring that.

22PO-8-69

COMPARATIVE ANALYSIS OF Fe_3O_4 NANOPARTICLES MAGNETIC INTERACTIONS IN DIFFERENT POLYMERIC NANOCOMPOSITES

Gendler T.S.¹, Novakova A.A.², Perov N.S.², Prudnikov V.N.², Aleksandrova G.P.³, Grishchenko L.A.³

¹Institute of Physics of the Earth RAS, B.Gruzinskaya 10, Moscow, Russia

²Moscow M.V. Lomonosov State University, Moscow, Russia

³Irkutsk Institute of Chemistry, Siberian Division RAS, Irkutsk, Russia

The investigations of an active role of support matrix, within which Fe-containing nanostructures are synthesized, are rather important in nanotechnology for creating of magnetic materials with desired physical properties.

The influence of different polymer matrix in addition to providing a means of particle dispersion on magnetic behaviour of nanosized Fe_3O_4 particles incorporated into polymer “in situ” was studied on two types polymer nanocomposites using low temperature (7-300K) VSM magnetometry and high temperature (300-973K) measurements of magnetization and remanent magnetization temperature dependences, natural remanent magnetization, hysteresis loops, Mossbauer spectra in 80-300K interval. The nanocomposites were prepared by alkalizing mixtures of Fe^{3+} - Fe^{2+} salts with varying iron content in the presence of amorphous polysaccharid arabinogalactan (AG) or polyvinyl alcohol (PVA). In the first case previously unknown iron derivatives of arabinogalactan, ferroarabinogalactan (FAG) was obtained [1], as the second synthesis results the PVA films of 200 μm thickness with different Fe_3O_4 concentrations [2]. For present comparative study the content of iron was ranged 3.5-5.1% for FAG and 0.6-5.7% for PVA films. The structure and dispersity of nanoparticles in FAG and PVA nanocomposites determined by X-ray, SEM and TEM identified a magnetite/ maghemite particles with average $d \sim 5.4$ nm as a core in shell of amorphous AG (microspheroids of 12 μm in size) and nonhomogeneous distribution of nanoparticles of about 10nm inside the films (isolated particles and chains along the film plain [3]). Mössbauer spectrum of FAG at 300K demonstrates unresolved doublet with significant relaxation broadening which indicates the magnetic ordering at this temperature resulted from interparticle interactions in contrast to SP behavior of

noninteracting particles. The spectrum gradually changes into well-resolved broadened sextet with reduced H_{hf} at 113K. The proposed magnetic interactions are confirmed by magnetization behavior versus temperature, showing insignificant decrease in low temperature region ($M_{300}/M_5=0.85$). The hysteretic loops revealed H_c decrease from 32 at 5K to 4.6 mT at 300K. The $M(T)$ curve of FAG has a convex shape with 3 characteristic points at 493K (destruction of AG shells), 573K (γ - α Fe_2O_3 irreversible transition) and 848K (T_c of stoichiometric magnetite). The spectra of the films with low iron particles concentration (from 0.6 to 5.7 volume %) reveal the combination of SP doublet (Ssp) and well resolved magnetic splitting from maghemite particles (Sm) with reduced as compared to bulk samples H_{hf} values. The central doublet width also as Ssp/Sm areas ratio increase with iron concentration indicating the growths of clusters number or layers inside the films involved in interparticle interactions. $M(T)$ dependences demonstrate the increase of M_{300}/M_5 ratio (from 0.54 up to 0.81) with iron concentration rise. So the matrixes play an active role in magnetic interaction of usually SP Fe- oxide nanoparticles.

[1] L.P. Feoktistova, A.N. Sapozhnikov, G.P. Aleksandrova, S.A. Medvedeva, and L.A. Grishchenko, *Inorg. Synth. Russian Journ.Appl. Chem.*, **75**, (2002), N 12, 1911-1915

[2] A.A. Novakova, V.Yu.Lanchinskaya, A.V.Volkov, T.S.Gendler, *JMM*, **258-259**, (2003), 354-357.

[3] Novakova A.A., Smirnov E.V., Gendler T.S., *JMM* **300**,N1, (2006), e354-e358

22PO-8-70

PATTERNING AND STUDY OF NANO-SCALE MAGNETIC ARRAYS

Gusev S.A.

Institute for Physics of Microstructures Russian Academy of Science,
GSP-105, 603950 Nizhny Novgorod, Russia
e-mail: gusev@ipm.sci-nnov.ru

Ordered arrays of metallic nanoparticles with sizes sub 100 nm have lately attracted great attention due to their unique optical, electrical and magnetic properties. Particularly, regular arrays of ferromagnetic nanoparticles are actively studied currently, because of their potential applications as media for ultrahigh density magnetic storage devices, and these systems are very interesting object for different basic studies of magnetism. In this report, we present short review of some experimental results relating to the fabrication and study properties of systems with fine ferromagnetic nanoparticles, which obtained in the IPM RAS.

The paper consists of two main parts. In the first part of the report, we concerned on the technological problems for the fabrication arrays of identical magnetic nanodiscs. In our experiments arrays of nanomagnets (circular or elliptical disks) were formed by electron-beam lithography (EBL) from permalloy (Ni_3Fe) and cobalt films, or multilayers based on Co thin films. We have used both usual EBL method (with positive PMMA resist and lift-off technique), and nanolithographic process developed by us with fullerene (C_{60}) films as negative electron resist [1]. The sensitivity of fullerenes as EBL resist is about 10^2 times less in comparison with PMMA. This parameter and small size of C_{60} molecules ensure us the similarity and reproducibility of dimensions of nanostructures with high accuracy. For example, that procedure we have used to fabricate fine particles with perpendicular magnetic anisotropy (from the Co-Pt multilayers) for magnetic force microscopy (MFM) experiments devoted to controllable remagnetization of nanomagnets. With "fullerene" technology we have formed periodical arrays of magnetic pillars with diameters of about 20 nm, and smallest distance between the particles equaled 15 nm. This procedure of nanomagnets fabrication is long and complex, as the method is

multi-stage, and it consist a few steps (up to 5-7) of reactive ion etching and ion milling. The EBL process with positive PMMA resist and lift-off technique is faster, but this way provide acceptable reproducibility of shapes and sizes of particles with dimensions about 100 nm and over.

In the second part of the paper, we report the demonstration of possibility of our technology to fabrication different systems with ferromagnetic arrays and some experimental results of investigation properties of these systems. Especially, we have used nanomagnets to control properties of superconducting systems (Nb microbridges and the Josephson junctions) and diluted ferromagnetic semiconductor GaMnAs structures. Some experiments have been made to study the magnetic chirality effects using elliptical Co nanoparticles with single vortex magnetic states. The magnetic properties of the structures were measured by MOKE technique (magneto-optical Kerr effect), Hall magnetometry and low-temperature electrical measurements. Local distribution of remanent magnetization and process of magnetization reversal of individual particles were studied by MFM (SPM "Solver", NT-MDT, Zelenograd, Russia). Lately we have set up the secondary electron detector with polarization analysis (SEMPA) on the scanning electron microscope to study the surface magnetism of ferromagnetic nanostructures.

This work was supported by the RFBR (Grant 08-02-00969).

[1] A.A. Fraerman, S.A. Gusev, L.A.Mazo et al., *Phys.Rev.B*, **65** (2002) 064424.

22PO-8-71

MAGNETIC PROPERTIES AND NONMAGNETIC PHASES FORMATION IN NANOSTRUCTURED FILMS (Fe/Si)_n

Varnakov S.N.^{1,2}, Komogortsev S.V.¹, Ovchinnikov S.G.¹, Bartolome J.³, Sese J.⁴

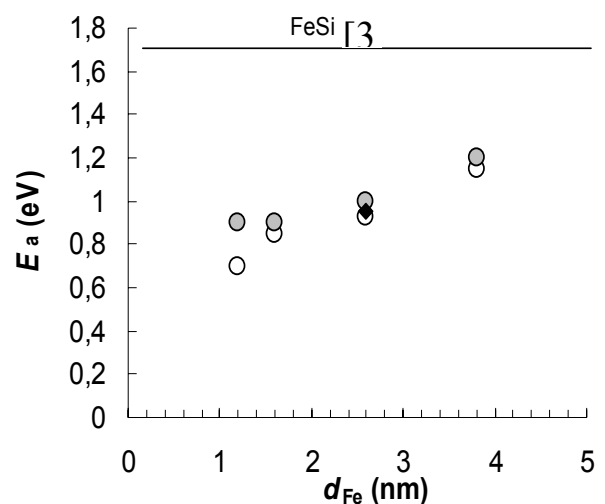
¹Kirensky Institute of Physics, Siberian Division, Russian Academy of Sciences, Akademgorodok, Krasnoyarsk, 660036 Russia

²Siberian Aerospace University, pr. im. gazety "Krasnoyarskii rabochii" 31, Krasnoyarsk, 660014 Russia

³Instituto de Ciencia de Materiales de Aragon, CSIC-Universidad de Zaragoza, Zaragoza, 50009 Spain

⁴Instituto de Nanociencia de Aragon, Universidad de Zaragoza, Zaragoza, 50009 Spain

The subject of this work is to find the relative amount of nonmagnetic phases which are formed both, during the synthesis process of (Fe/Si)_n films, and due to processes of silicides formation in high temperatures by magnetic measurements. The Si/Fe multilayers were grown on silicon substrates by evaporation of Si and Fe in ultrahigh vacuum (UHV) system including a hardware-software control complex of the UHV and the evaporation process [1]. The base pressure in the growth chamber was $2.1 \cdot 10^{-7}$ Pa. The thickness of Si layer was 1.5 nm, and Fe layer was in the range 1.2 - 5 nm. The magnetization M vs temperature T measurements for (Fe/Si)_n



multilayer was carried out on MPMS SQUID magnetometers [2] in external field $H = 700$ Oe and 4.2 - 800 K temperatures range.

There are two regions on $M(T)$ curves: reversible (4.2 - 350 K) and irreversible (350 - 800 K). Magnetization values obtained from low-temperature part of $M(T)$ (4.2 - 350 K) are reduced in comparison with pure bcc Fe films. It results from nonmagnetic phase formation at the interfaces in synthesis process. The volume fraction of such phases was estimated no more than 20%. Reduction of magnetization in high-temperatures (350 - 800 K) is irreversible (i.e. depends on both the time of measurement and the temperature value). It is caused by synthesis of nonmagnetic phases (iron silicides). This analysis allows us to obtain new information on the kinetic of iron silicide formation in Fe/Si multilayers. The values of activation energy E_a (fig.) and diffusion constant D_0 for the investigated films with different d_{Fe} , were determined.

This work was supported by the Russian Academy of Science program "Spintronics", the complex integration project of the Siberian Branch of the Russian Academy of Science №3.5, the Russian Foundation for Basic Research (grant 07-03-00320), the "Ramon y Cajal" program and project No. MAT 2005/01272 of Spanish Ministry of Education and Science.

[1] S.N. Varnakov, A.A. Lipeshev, S.G. Ovchinnikov, et al., *IET* **47** (2004) 839.

[2] J. Sese, J. Bartolome and C. Rillo, *Rev. Sci. Instrum.* **78** (2007) 046101.

[3] S.S.Lau, J.S.-Y. Feng, J.O. Olowolafe and M.-A. Nicolet. *Thin Solid Films*, **25** (1975) 415.

22PO-8-72

GIANT MAGNETORESISTANCE OF Ni NANOCONTACTS

Gatiyatov R.G., Bukharaev A.A., Ziganshina S.A.

Zavoisky Physical-Technical Institute of RAS, Kazan, 420029 Russia

Several years ago the giant magnetoresistance (GMR) effect was found in point ferromagnetic contacts fabricated between two Ni microwires using electrodeposition technique. It was proved that the observed effect was due to the contact break when the magnetic field was applied (essentially due to magnetostriction). This observation stimulated both theoretical and experimental investigations of the magnetoresistive properties of the point contacts. And the theory of ballistic magnetoresistance (BMR) was developed [1-2]. According to this theory the MR value of point ferromagnetic contact can reach hundred of percent at room temperature due to the strong reflection of carriers from the sharp domain wall located in the constriction (the ballistic transport of electrons is an important condition). It is well known that in the atomic contacts the conductance quantizes with the increase of the contact size due to the quantum size effect and this acts as an experimental criterion for the proof of ballistic transport.

Our group studied the GMR effect in Ni nanocontacts fabricated in the solution using electrodeposition technique at room temperature. Recently we found the GMR effect with magnitude of up to 210% in Ni contacts revealing the conductance quantization [3]. We discussed the origin of the observed effect in the framework of the BMR theory. However recent theoretical quantum-mechanical calculations [4] and our own further experimental investigations show that there could be a direct connection between the observed magnetoresistance of the nanocontacts and the influence of the solution or atomic rearrangement on the GMR effect. We reproduced the experimental results obtained by [5] and found that the MR effect was due to the experimental conditions of registering the conductance but not to the electronic origin. Thus when one deals with nanocontacts fabricated in the solution between two bonding pads with suppressed magnetostriction and even if there exists a conductance quantization it is not

guaranteed that the MR of nanocontacts will not be affected by other artifacts corresponding to the influence of the solution.

There are also several alternative methods of forming nanocontacts, e.g., ion etching or electromigration which are suitable for the formation of stable atomic scale contacts. We started with these methods for obtaining point contacts but no GMR effect was observed yet.

This work was supported by the Russian Foundation of Basic Research (Grant 05-02-16550) and by the Programs of RAS.

- [1] H.Imamura, N.Kobayashi, S.Takahashi, et al, *Phys. Rev. Lett.*, **84** (2000), 1003.
- [2] L.R. Tagirov, , B.P. Vodopyanov, K. B. Efetov, *Phys. Rev. B*, **63** (2001), 104468.
- [3] R.G. Gatiyatov, S.A. Ziganshina, A.A. Bukharaev, *JETP Letters*, **86** (2007), 412.
- [4] A. Bagrets, N. Papanikolaou, I. Mertig, et al, *Phys.Rev.B*, **75** (2007), 235448.
- [5] C.-S. Yang, C. Zhang, J. Redepenning, et al, *J. M. M. M.*, **286** (2005), 186.

22PO-8-73

EXCHANGE BIAS CRITICAL PARAMETERS IN F/AF SYSTEMS

Chechenin N.G.

Skobeltsyn Inst. of Nuclear Physics, Moscow St. University, 119991 Moscow, Russia

Exchange bias (EB) field H_{EB} at a ferromagnet (F)/antiferromagnet (AF) interface is a critical value for keeping the magnetic moment of the F-layer fixed. This is a prerequisite for a successful application of such a system in spin valves, MRAMs and other advanced spintronics devices. Though the exchange bias phenomena is known for more than 50 years [1], still there is a number of open issues in theoretical understanding as well as a large scatter and controversy in some of the experimental data available.

The unidirectional anisotropy constant is a characteristic parameter of the F/AF interface along with the blocking temperature T_B where the EB field and the unidirectional anisotropy of the F-layer disappear. Soft Fe-, Ni- or Co-based magnetic materials or their alloys are mostly used for F-layers. A large amount of oxides, metallic alloys and other types of AFs have been thoroughly investigated. While very few oxides have J_K and T_B large enough to be of a practical interest, a number of metallic Mn-based films are successfully used as AF-layers in spintronics devices. Though not ignoring the other Mn-based AFs, main focus of the report will be on the magnetic properties of IrMn AF-layers. Variation of the critical EB parameters H_{EB} , J_K and T_B with the alloy stoichiometry, type of F-material, type of substrate and seed layer, deposition condition, AF-microstructure and texture will be discussed basing on the published experimental results and theoretical analysis. Influence of the post-deposition thermal treatment in magnetic field on the critical EB parameters is analysed in connection with magnetic and microstructure re-ordering and interdiffusion of the layers.

The analysis of H_{EB} supports the linear dependence on the inverse thickness of the F-layer $1/t_F$ which corresponds to a constant J_K and in accordance with theoretical expectations (see, discussion in [2]). However, nonlinearities occur when the thickness of the F-layer becomes comparable or larger than the thickness of AF-layer where H_{EB} diminishes and where J_K is no more constant.

Support by Russian Agency of Science and Innovation (g/k # 02.513.11.3155) is acknowledged.

- [1] W. H. Meiklejohn and C. P. Bean, *Phys. Rev.* **105** (1957) 904
- [2] M. Kiwi, *JMMM*, **234** (2001) 584.

22PO-8-74

QUANTUM OSCILLATIONS OF MAGNETORESISTANCE IN ATOMIC-SIZE MAGNETIC NANOCONTACTS

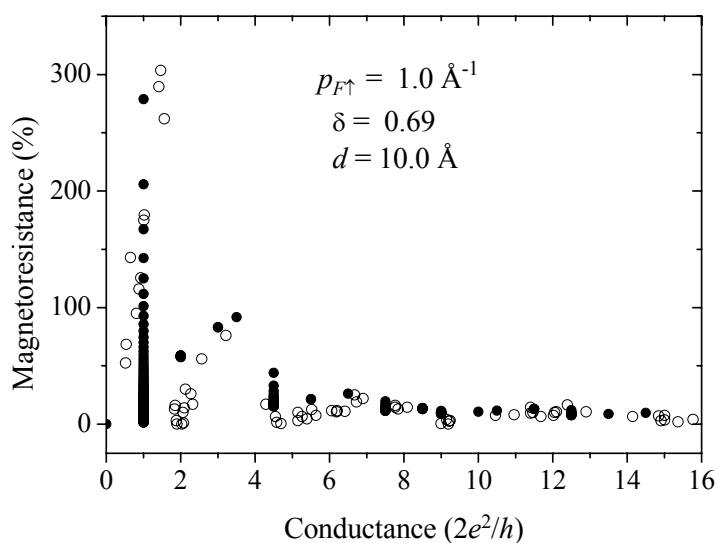
Useinov N., Tagirov L.

Solid State Physics Department, Kazan State University, Kazan, 420008, Russia

Magnetic nanocontacts reduced to an atomic size show unusual magnetoconducting properties which are connected with interaction between localized spins and conduction electrons. The influence of magnetism is twofold: (1) it introduces spin-splitting of the conduction electron band; (2) it creates a domain wall which can be a source of conduction electron scattering.

If size of a nanocontact is a few angstroms the conductance is quantized. The domain wall, which is most probably located in the nanocontact, serves as a quantum valve for the conduction electrons [1, 2]. The magnetic field governs domain state of the nanocontact, thus governing the quantized conduction through the nanocontact. The resulting magnetoresistance keeps footprint of the quantized nature of the conduction acquiring giant fluctuations as a function of number of open conduction channels [1]. Figure shows results of the magnetoresistance measurements in atomic-size cobalt nanocontacts [3]. The experimental data (open circles) show giant regular fluctuations of magnetoresistance superimposed on the gradual decay of the magnitude.

To describe the experimental data we assume a contact of the cylindrical shape with radius a and length d . It was shown in Ref. [4] that thickness w of the domain wall can be approximated by formula $w \approx 2a + d$. Within this model we calculated the quantized conductance and magnetoresistance of the magnetic nanocontact. The results of calculation are shown by solid circles. The values of parameters are displayed in the figure, $\delta = p_{F\downarrow} / p_{F\uparrow}$, where $p_{F\uparrow(\downarrow)}$ is



the Fermi momentum for the spin-up (down) conductance channel. Our calculations confirm quantum-fluctuation nature of magnetoresistance oscillations observed in the experiment [3], and allow to estimate the spin-polarization parameter of the material, $\delta \approx 0.69$.

The work was supported in part by RFFR, Grant 07-02-00963-a, and ministry of education and science of the Russian Federation.

[1] L.R. Tagirov, B.P. Vodopyanov, K.B. Efetov, *Phys. Rev. B* **65** (2002) 214419.

[2] M.E. Zhuravlev, E.Y. Tsymlal, J.J. Jaswal *et al*, *Appl. Phys. Lett.*, **83** (2003) 3534.

[3] H.D. Chopra, M.R. Sullivan, J.N. Armstrong, S.Z. Hua, *Nature Mater.*, **4** (2005) 832.

[4] V.A. Molyneux, V.V. Osipov, E.V. Ponizovskaya, *Phys. Rev. B* **65** (2002) 184425.

22PO-8-75

MAGNETIC PROPERTIES OF HEXAGONALLY ORDERED ARRAYS OF FE ANTIDOTS BY VACUUM THERMAL EVAPORATION ON NANOPOROUS ALUMINA TEMPLATES

Vega V.¹, Prida V.M.¹, Fernández A.¹, López-Antón R.^{2,3}, Pirota K.R.⁴, Vázquez M.⁴

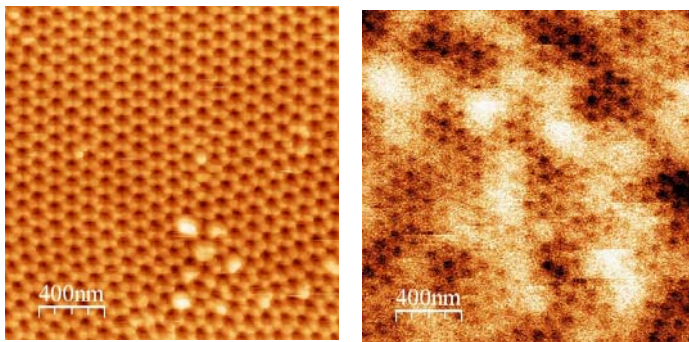
¹Dept. Física, Universidad de Oviedo, Calvo Sotelo s/n, 33007-Oviedo, Asturias, Spain

²Instituto de Ciencia de Materiales de Aragón, CSIC-Universidad de Zaragoza, Zaragoza, Spain

³ISIS Facility, STFC-RAL, Harwell Science and Innovation Campus, Didcot, United Kingdom

⁴Instituto Ciencia Materiales Madrid (ICMM-CSIC), Cantoblanco, 28049-Madrid, Spain

Periodic spacing antidot arrays formed by non-magnetic nanoholes in continuous magnetic films have recently attracted huge attention because of their potential applications in sensor devices [1]. Highly ordered arrays of Fe antidot films, with 40 ± 5 nm in diameter, 105 nm of periodic interspacing distance and 20 nm thickness, were fabricated by vacuum thermal evaporation on the top of nanoporous anodic alumina membranes used as templates [2]. The high quality of the hexagonally ordered and amorphous structure of the deposited Fe antidots film was checked by Electron Microscopy techniques. It is clearly seen, from Atomic Force Microscopy measurements (left), that the Fe antidots film retains the well-ordered structure of the alumina template. Meanwhile, in the Magnetic Force Measurements (right), magnetic contrast produced by magnetic stripe domains forming a maze pattern is found. Noteworthy, the magnetic domains are not pinned by the nanoholes (partially seen in the magnetic image in the form of regular darker circular spots forming) but, on the contrary, several antidots are included in each domain, in agreement with observed by Jaafar et al in similar nanostructures [3]. From in plane and out of plane hysteresis loops measurements, it is deduced that the easy magnetization axis of the Fe antidot array remains in the film plane, while the hard one lies perpendicular to the plane, which can be explained on the basis of the magnetostatic, stress and shape induced contributions of the nanoholes to the total magnetic anisotropy of the antidots film.



- [1] P. Candeloro et al, *Jpn. J. Apl. Phys.* 41, (2002) 5149
- [2] M. Tejedor et al, *J. Magn. Magn. Mater.* 59, (1986) 28
- [3] M. Jaafar et al., *J. Appl. Phys.* 101, (2007) 09F513

22PO-8-76

MAGNETIZATION REVERSAL IN FeNi/NiO/FeNi POLYCRYSTALLINE FILMS WITH THIN NiO LAYERS

Merenkov D.N.¹, Bludov A.N.¹, Gnatchenko S.L.¹, Savina Yu.A.¹, Novosad V.A.²

¹Institute for Low Temperature Physics & Engineering, Lenin Ave., 47,
Kharkov, 61103, Ukraine

²Materials Science Division, Argonne National Laboratory, Argonne, Illinois, USA

The polycrystalline films [Fe₂₀Ni₈₀(30E)/NiO(xE)/Fe₂₀Ni₈₀(30E)] with $x = 4, 8, 12$ E were investigated by magneto-optical longitudinal Kerr effect. The films were grown at a temperature 300 K by RF magnetron sputtering on a Si (100) oriented wafer in a in-plane magnetic field to induce uniaxial anisotropy in permalloy. The films had protective and buffer gold layers. The reversal process was investigated at magnetic field applied in the film plane. The incidence angle of light with wavelength $\lambda = 633$ nm was about 75° to normal.

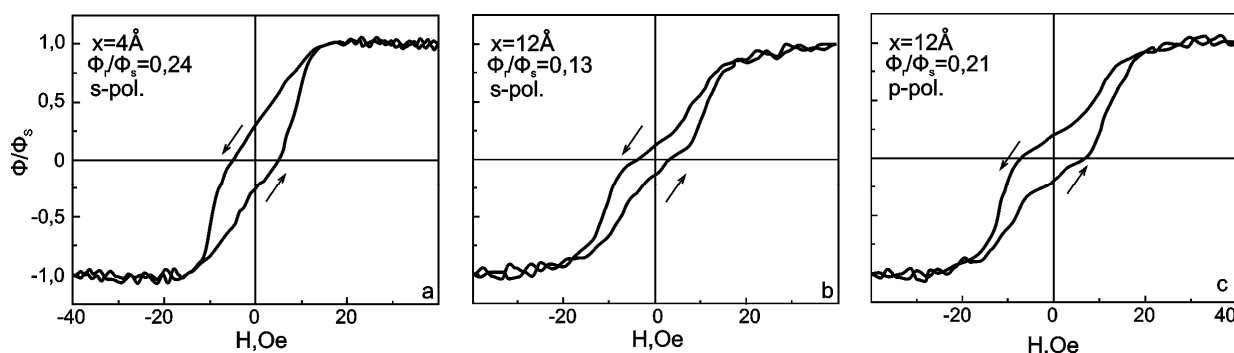


Fig.1. Field dependences of Kerr rotation of the FeNi/NiO(x)/FeNi trilayers in the external magnetic field applied along the hard axis of permalloy at 300 K.

The field dependences of Kerr rotation of the films shows evident hysteresis in the external magnetic field applied along the FeNi hard axis (Fig.1). The ratio of remanent rotation Φ_r to saturation rotation Φ_s changes depending on the antiferromagnetic NiO layer thickness (Fig.1a,b). This ratio increases for all films at the temperature decreasing. The value Φ_r/Φ_s for s- and p- polarizations of light was different for samples with $x = 8, 12$ E (for example, see Fig.1b,c). When the magnetic field is applied along FeNi easy axis all films shows the square, non-biased and symmetric hysteresis loop at 300 K.

The interpretation of experimental results was performed with consideration of Zeeman energy, magnetic anisotropy in the FeNi layers and exchange anisotropy. In external magnetic field applied along hard axis of permalloy the magnetization reversal occurred both rotation magnetic moments and first-order phase transitions. The existence of these transitions is caused by interlayer exchange coupling between NiO and FeNi. The Φ_r/Φ_s dependence from light polarization demonstrates the different influence of exchange anisotropy on top and bottom permalloy layers. This is concerned to different properties of interfaces FeNi/NiO and NiO/FeNi in as-deposited films. When external field was applied along the direction of sputtering field the magnetic moments are collinear with FeNi easy axes at magnetization reversal due to influence of Zeeman energy and uniaxial anisotropy in permalloy.

22PO-8-77

IMPURITY INDUCED MAGNETIC ORDER IN DOPED HALDANE SYSTEM $\text{SrNi}_{2-x}\text{Mg}_x\text{V}_2\text{O}_8$

Pahari B. and Ghoshray K.

ECMP Division, Saha Institute of Nuclear Physics, Kolkata-700064, India

Impurity effect in quantum spin chain with a singlet ground state is of great interest, since even a non magnetic defect may disturb the disordered ground state in a subtle manner and locally restore the magnetic behavior. A good example is the extra spin degrees of freedom localised near an open end of an integer spin Heisenberg chain, which has an excitation gap (Haldane gap) in the bulk. ^{51}V NMR results in $\text{SrNi}_2\text{V}_2\text{O}_8$ [1] reveals a spin liquid ground state with a spin gap of 25 K and intra chain exchange interaction $J/k_B = 106$ K. Interestingly this system lies very close to the phase boundary between the quantum disordered ground state and the Ising like ordered ground state in the Sakai Takahashi phase diagram [2]. Recently it has been observed from magnetic susceptibility and specific heat measurements that this compound undergoes a transition to an antiferromagnetically (AF) ordered state, for replacement of Ni^{2+} by Mg^{2+} , at a concentration of $x > 0.01$. Moreover, this impurity induced AF phase disappears in presence of an external magnetic field $H > 4\text{ T}$ [3]. Here, we report ^{51}V NMR studies in $\text{SrNi}_{2-x}\text{Mg}_x\text{V}_2\text{O}_8$ in presence of magnetic fields of 1.2 and 7 T respectively.

The ^{51}V NMR line shape in doped system show a continuous asymmetric broadening below 20 K. Whereas, the same in the pure compound shows a continuous narrowing in the range 4 – 60 K. The increase in line width in Mg-doped compound is attributed to the presence of $S = 1/2$ spins near the chain ends. The temperature dependence of spin-lattice relaxation rate $1/T_1$ and $1/T_1T$ i.e. $\chi''(\mathbf{q}, \omega)$ [Fig. 1] clearly reveal the suppression of the magnetic correlations in the presence of high magnetic field.

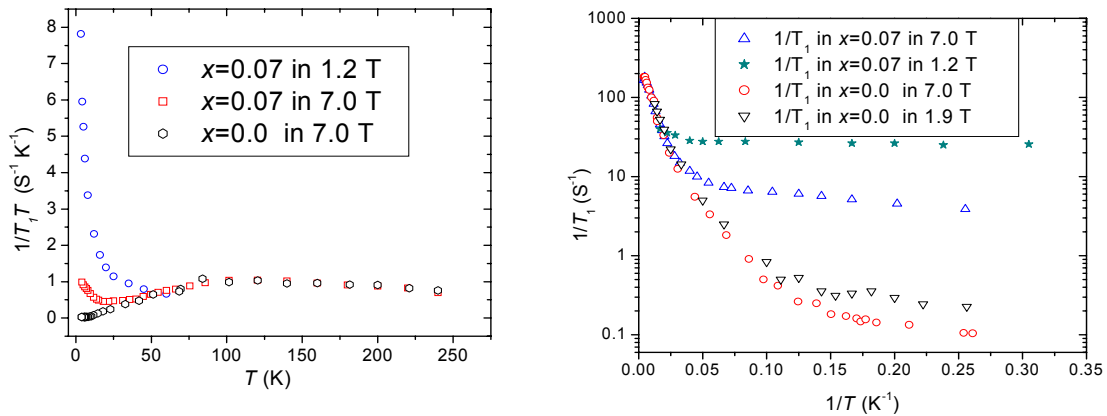


Fig. 1: $1/T_1T$ and $1/T_1$ for $\text{SrNi}_{2-x}\text{Mg}_x\text{V}_2\text{O}_8$ ($x = 0.07$) and pure compound at different magnetic field

- [1] B.Pahari et al., *Phys. Rev.* **B73** (2006) 012407
 [2] T. Sakai et al., *Phys. Rev.* **B42** (1990) 4537
 [3] B.Pahari et al., *Physica* **B395** (2007) 138

22PO-8-78

MAGNETOELASTIC AND CRYSTAL CONTRIBUTIONS IN TEMPERATURE DEPENDENCE OF MAGNETIC ANISOTROPY IN Co/Cu (111) SUPERLATTICES

Kutko K.V.¹, Kaplienko A.N.¹, Nikolova E.P.¹, Anders A.G.¹, Zorchenko V.V.², Stetsenko A.N.²

¹B.I.Verkin Institute for Low Temperature Physics and Engineering, NAS of Ukraine
47, Lenin Ave., Kharkov, 61103, Ukraine

²National Engineering university Kharkov Polytechnical institute
21 ul.Frunze, Kharkov, 61002, Ukraine

The temperature dependence of FMR spectra of superlattices Co/Cu was studied for determination of magnetic anisotropy mechanism.

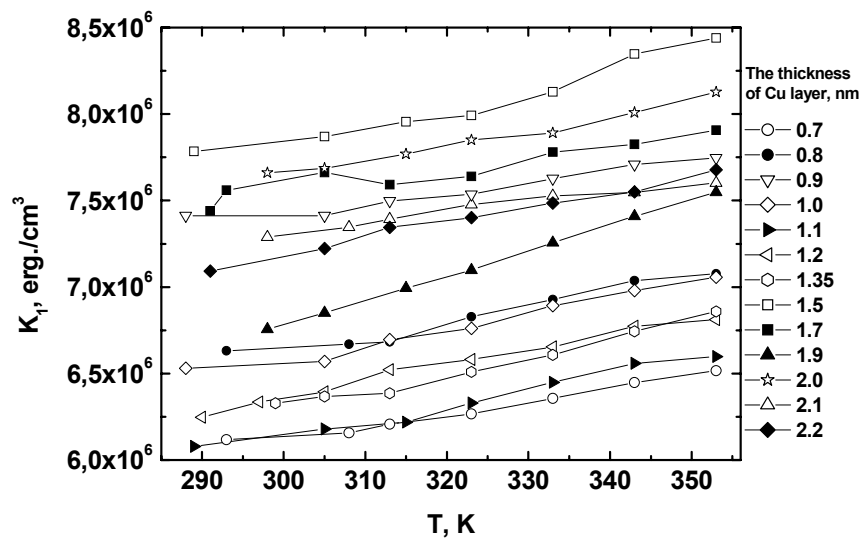
We have investigated the series of samples [Co/Cu(111)]₂₀ with fixed thickness of ferromagnetic cobalt layers $d_{Co} = 8$ E, while the thickness of nonmagnetic copper interlayers valid from 7 to 22 E with step 1-2 E. The samples were obtained on mica by magnetron sputtering method. The main measurements of ferromagnetic resonance (FMR) spectra were made with a JEOL-XK spectrometer in 3-cm wavelength range in temperature interval from 300 to 360 K.

The temperature dependence of anisotropy constant K_1 is close to linear behavior for all samples of series (see Fig.).

Such temperature dependence K_1 can be considered with magnetoelastic mechanism and the contribution of crystal anisotropy. In this work the calculation estimations of both contributions are made.

For given temperature interval the variations of magnetoelastic contribution to the anisotropy constant are about $4 \cdot 10^3$ erg/cm³, while in experiment the value $\Delta K_1 \approx (0,6 \div 0,9) \cdot 10^6$ erg/cm³ is observed. In this time the axial part of the crystal anisotropy makes about 10^6 erg/cm³.

So, the magnetoelastic contribution is not an appreciable source of temperature dependence of anisotropy in multilayered system under consideration. The main contribution to this dependence is given by the axial component of crystal anisotropy.



22PO-8-79

STRESS-INDUCED RESIDUAL DEFORMATIONS OF NANOCRYSTALS IN Fe-BASED FINEMETS AS A CAUSE OF TRANSVERSAL MAGNETIC ANISOTROPY

Ershov N.V.¹, Chernenkov Yu.P.², Fedorov V.I.², Lukshina V.A.¹, Potapov A.P.¹

¹Institute of Metal Physics, Ural Division of RAS, Yekaterinburg, Russia

²St.-Petersburg Institute of Nuclear Physics, RAS, Gatchina, Russia

Structural investigations with the aim to find a reason for the appearance of the magnetic anisotropy of “easy plane” type [1] oriented in the direction transversal to that of an application of a tensile load during annealing were performed in the transmission geometry with the use of a monochromatized radiation K_{α} Mo. Specimens of $\text{Fe}_{73.5}\text{Si}_{13.5}\text{B}_9\text{Nb}_3\text{Cu}_1$ alloy at first were prepared in the form of thin tapes via high-rate quenching from the melt on the rotating copper disk. Then they were annealed and subsequently cooled under tensile loading (520°C, 120 min; a load of 440 MPa). The Bragg and superstructure reflections were registered in conditions when the scattering vector lied in the plane of specimens. From the position of these reflections measured along and transverse to the tape axis, i.e., parallel and perpendicular to the tensile stress direction (TSD), the corresponding spacings between the planes in the FeSi phases were estimated. For the first time such an investigation of the samples of finemet with a silicon content of 15.5 % subjected to annealing under a load of different magnitude were performed by Ohnuma *et al* [2]. However, in [2] the position of only one reflection (310) was under study, which did not completely clarify the character of lattice residual deformations.

As in [2], in our case of annealing under tensile loading the interplanar spacings in TS direction show an increase. However, the lattice of nanocrystals is deformed nonisotropic, a change in the spacing d_{hkl} between the planes (hkl) is dependent of the angle between the direction of the wave vector $[hkl]$ when it is parallel to TSD and the closest axis $\langle 111 \rangle$. The greater the angle, the larger the deformation: the change Δd_{111} is minimum and Δd_{100} in the direction $[100]$ being an easy magnetization axis, of maximum magnitude. Thus, the lattice deformation of nanocrystals has a tetragonal character, with a greatest increase in an interplanar spacing of nanocrystals along the axis $\langle 100 \rangle$ the closest to TSD.

After cooling the deformed structure of nanocrystals is capable to fix due to the stiffness of the amorphous matrix. Since the nanocrystals with the silicon content approaching an Fe_3Si stoichiometry have a negative magnetostriction, magnetization in them upon tensile loading along the axis $[100]$ at a tetragonal deformation is induced in the plane with a normal parallel to TSD, namely, along one of the easy magnetization axes – either $[010]$ or $[001]$. Since we deal with a giant quantity of nanocrystals and their orientation distribution is not textured, the great number of the crystals deformed along the tape axis provides contribution to the transverse distribution of magnetization and cause the appearance of the magnetic anisotropy of easy plane type transversal to TSD – the direction of tensile stress application.

The authors are grateful for support from Russian Foundation for Basic Research, project no.06-02-17082.

[1] A.A. Glazer, et al. *Fiz. Met. Met.* **12** (1991) 56. (in Russian).

[2] M. Ohnuma, et al. *Appl. Phys. Lett.* **86** (2005) 152513-(1).

22PO-8-80

MAGNETIC PROPERTIES OF Co/Au MULTILAYER STUDIED WITH CIRCULAR POLARIZED X-RAYS

Smekhova A.¹, Wilhelm F.¹, Jergel M.², Majkova E.², Andreeva M.³, Szymanski B.⁴, Rogalev A.¹

¹European Synchrotron Radiation Facility, 6 rue Jules Horowitz, BP220, Grenoble, France

²Institute of Physics SAS, Dubravská cesta 9, SK 842 28, Bratislava, Slovak Republic

³M.V. Lomonosov Moscow State University, Leninskie Gory 1, Moscow, Russia

⁴Institute of Molecular Physics PAN, M. Smoluchowskiego 17, 60-179, Poznan, Poland

The artificial nanoscale periodical multilayers comprising a magnetic metal alternating with a nonmagnetic element attract a lot of attention since their complex internal electronic configuration and nontrivial magnetic redistributions inside the structure [1,2]. The induced moments in this case could manifest an presence of unusual intrinsic exchange processes and could play a crucial role in magnetic behaviour of the whole system.

Here, we concentrate our attention on circular polarized X-Ray reflectivity studies of [Co (4.2 nm) / Au (1.2 nm)]₁₀ / Ti / SiO₂ / Si multilayer prepared by evaporation method. Immiscibility of chosen Co and Au atoms and preparation route should allow us to obtain a multilayer of high quality with low roughness at the interfaces. The structural parameters of the multilayer were checked by X-ray diffraction with Cu K_α radiation and X-ray reflectivity at the Au L₃ absorption edge. Period of the multilayer, relative thicknesses and element concentrations in each atomic layer determined by the fitting procedure were found to be in a good agreement with data expected from growing process.

X-ray resonant magnetic reflectivity of circularly polarized radiation is an element selective technique with exceptional sensitivity to the magnetic properties of atoms over bilayer depth [3,4]. Analysis of asymmetry ratio behaviour over several Bragg peaks allows one to reveal the changes in magnetic moments in the repetition period of the system. In our case energy spectra of magnetic reflectivity for two opposite circular polarizations of the incident beam and for opposite directions of an applied magnetic field in L-MOKE geometry have been measured at the first four Bragg peaks of the system. The depth distribution of an induced Au 5*d* magnetic polarization has been determined by refinement the asymmetry ratio energy spectra for all measured Bragg peaks simultaneously using the dipolar approach of dynamical diffraction theory. Unexpectedly, we have found an antiferromagnetic-like ordering of induced magnetic moment at Au atoms which is discussed.

[1] P. F. Carcia, A. D. Meinhardt, A. Suna, *Appl. Phys. Lett.*, **47** (1985) 178.

[2] F. Wilhelm, P. Pouloupoulos, A. Scherz, H. Wende, K. Baberschke, M. Angelakeris, N. K. Flevaris, J. Goulon, A. Rogalev, *Phys. Status Solidi (a)*, **196** (2003) 33.

[3] N. Jaouen, G. van der Laan, T. K. Johal, F. Wilhelm, A. Rogalev, S. Mylonas, L. Ortega, *Phys. Rev. B*, **70** (2004) 094417.

[4] M.A. Andreeva, A.G. Smekhova, *Appl. Surface Science*, **252** (2006) 5619.

22PO-8-81

MAGNETO-OPTICAL INVESTIGATION OF THIN-FILM MAGNETIC SYSTEMS

Shalygina E.E.¹, Maximova G.V.¹, Komarova M.A.¹, Shalygin A.N.¹, Kozlovskii L.V.²

¹Faculty of Physics, Moscow State University, 119992, Moscow, Russia

²Department of Physics, Daugavpils University, Latvia

Results on the investigation of magnetic and magneto-optical properties nanocrystalline Fe (20 nm)/Zr ($t = 0.5$ - 10 nm) and Fe (2.5 nm)/Zr, Mo ($t = 0.3$ - 3.0 nm)/Fe (2.5 nm) thin-film systems are presented. The above samples are promising candidates for practical applications in modern microelectronics as ideal recording head pole materials. The examined systems were prepared by DC magnetron sputtering technique under a base pressure of less than 10^{-8} Torr and an argon gas pressure of 1×10^{-3} Torr. The existence of the periodic layer structures (well-defined interfaces) in the examined systems was confirmed by the low-angle XRD analysis. The studies of the magnetic and magneto-optical properties of the examined samples were carried out employing the magneto-optical magnetometer and the magneto-optical spectrometer by means of the transverse Kerr effect (TKE). Hysteresis loops were measured at two magnetic field directions (marked as D1 and D2). The D1 and D2 orientations of H were respectively parallel and perpendicular to the magnetic field direction, applied parallel to the substrate surface during the film depositions. The spectral measurements of TKE were performed in the $1.4 < \hbar\omega < 4.0$ eV photon energy range, at the 65° -angle of the light incidence from the sample normal and $H > H_S$ (H_S is the saturation field of the sample under study).

The hysteresis loops, measured at the D1 and D2 magnetic field orientations, were found to differ very strongly that show an in-plane magnetic anisotropy in the examined samples. The magnetization easy axis is parallel to the D1 direction that is caused by the magnetic field $H \sim 70$ Oe, applied during the film depositions. The hysteresis loops, observed for the bilayers at the D1 and D2 magnetic field orientations, have nearly square and anhysteretic shapes, respectively. With increasing t_{Zr} up to 4 nm, the magnitudes of the saturation field, H_S , and the coercivity, H_C , increase but at $t_{Zr} > 4$ nm, H_S and H_C decrease. The found dependences of $H_S(t_{Zr})$ and $H_C(t_{Zr})$ were explained by microstructural peculiarities of the Fe/Zr bilayers. It was found that the magnitudes of H_S of the trilayers along the magnetization easy axis oscillates as a function of t_{Zr} , t_{Mo} , a period of these oscillations, Λ , is about of 1.0 nm and the amplitude of H_S oscillations decreases with increasing t_{Zr} , t_{Mo} . This result was explained by the presence of the exchange coupling between ferromagnetic layers through the Zr (Mo) spacer and its oscillatory behavior with changing t_{Zr} , t_{Mo} . According to mechanism of the exchange coupling via an RKKY-like interaction, for most metals, Λ must be the order of $\pi/k_F \approx 0.3 - 0.4$ nm (k_F is a wave Fermi vector). The found value of $\Lambda \approx 1$ nm correlates with computations performed taking into account of quantum size effects, displaying in a change of ultra-thin film electronic structure as compared with a bulk sample (an appearance of so-named Quantum Well States).

The TKE spectra, observed for all samples, were revealed to be identical but the TKE values depend on the thickness of both the magnetic and nonmagnetic layers. The magneto-optical Kerr effect is known to be sensitive to the magnetization up to a certain depth range below the surface of ferromagnetic, called "a penetration depth of the light in media", t_{pen} . According to our experimental data, for metallic magnetic materials, the magnitude of t_{pen} does not exceed 22 – 30 nm in the photon energy range $1.5 < \hbar\omega < 5$ eV. The full thicknesses of the examined thin-film systems are smaller than the magnitude of t_{pen} . So, the observed variations of the TKE magnitudes can be explained by changing the thickness of both t_{Fe} and $t_{Zr, Mo}$.

22PO-8-82

THE NEEL TEMPERATURE AND SUBLATTICE MAGNETIZATION FOR THE STACKED TRIANGULAR-LATTICE ANTIFERROMAGNET

Ignatenko A.N.¹, Katanin A.A.^{1,2}, and Irkhin V.Yu.¹

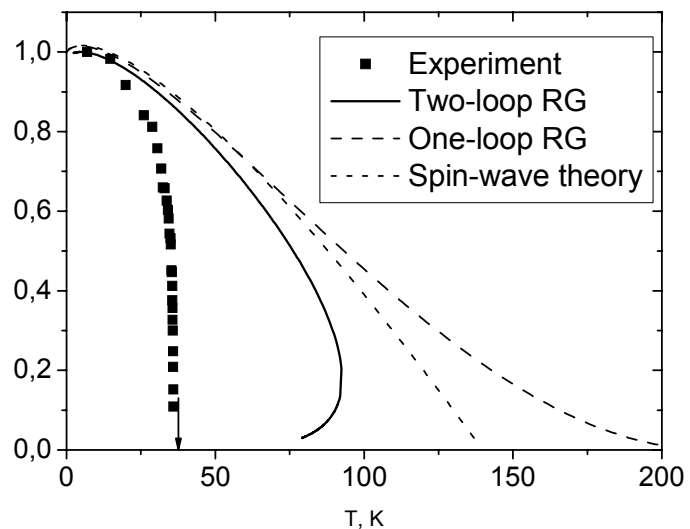
¹Institute of Metal Physics, Ekaterinburg, Russia

²Max Planck Institute for Solid State Research, Stuttgart, Germany

The quantum Heisenberg antiferromagnet on the stacked triangular lattice with the intralayer nearest-neighbor exchange interaction J , and the interlayer exchange J' , is considered within the non-linear σ -model with the use of the renormalization group (RG). For $J' \ll J$ the Neel temperature T_N is small in comparison with J , and the temperature behavior of the magnetic properties at $T < T_N$ is determined by spin waves and their interactions. The temperature is assumed to satisfy the inequalities $\sqrt{JJ'} \ll T \ll J$. The first inequality means that the main contribution to the thermodynamic comes from the two-dimensional (2D) magnetic fluctuations, while the second one constrains the temperature to the renormalized classical regime [1]. This allows one to describe the system by effective 2D classical RG equations (where the RG cut-off is temperature) and to take into account the interlayer interaction J' by means of the matching conditions.

A similar approach was used earlier [2] for the collinear antiferromagnets, quantitative agreement being obtained between the theory and experiment. However, in the present non-collinear case a large disagreement for the Neel temperature and sublattice magnetization curve was obtained (see the figure). The reason for this disagreement is the presence of topological \mathbb{Z}_2 -vortices that are similar to the vortices of the XY-model, but interact non-trivially with spin waves. Therefore T_N is estimated using the Monte-Carlo result for the 2D correlation length which has a Kosterlitz-type behavior near the temperature $T_{KT} = 0.28 JS^2$ where the vortices are activated [3]. We obtain $T_N = T_{KT} + 0.15 JS^2 / \ln^2(2J'/J)$. For VCl_2 ($J'/J = 0.006$) this formula gives $T_N = 37K$ (indicated by arrow in the figure) which is close to the experimental value $T_N = 36K$. This is in agreement with the assumption that the Neel temperature for the non-collinear antiferromagnets is determined by the vortices interacting with spin waves, but not by the spin waves alone.

Relative sublattice magnetization for VCl_2



[1] P. Azaria, B. Delamotte, D. Mouhanna, *Phys. Rev. Lett.*, **68**, (1992) 1762.

[2] V.Yu. Irkhin and A.A. Katanin, *Phys. Rev. B*, **57** (1998) 379.

[3] M. Wintel and H.U. Everts, *Phys. Rev. B*, **52** (1995) 13480.

22PO-8-83

NONUNIFORM RKKY MAGNETISATION IN THIN FILMS AND WIRES

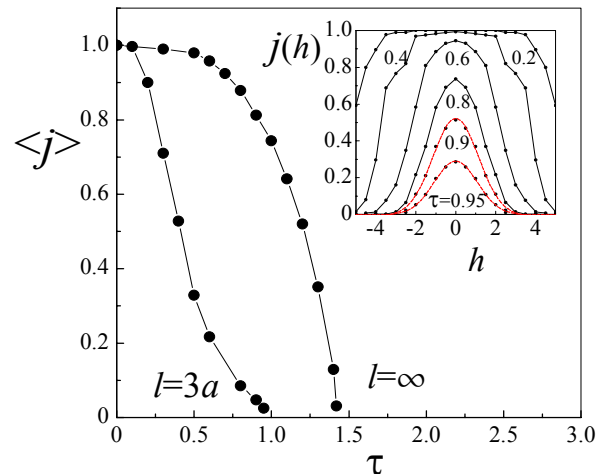
Meilikhov E., Farzetdinova R.

Kurchatov Institute, 123182 Moscow, Russia

Indirect Ruderman-Kittel-Kasuya-Yosida (RKKY) interaction of magnetic impurities is considered as one of the basic mechanisms of the magnetic ordering in systems with free carriers of high concentration (e.g., degenerate semiconductors with magnetic impurities). It is actual to consider how magnetic features of the relevant systems depend on their finite size. There are three parameters of the length dimension: the system size L by itself, the carrier wavelength $\lambda=2\pi/k_F$ defined by their concentration, and the characteristic interaction length l , coinciding, in the simplest case, with the carrier free path. Depending on the relation between those parameters, the following effects are possible and essential: (i) increasing the surface contribution - becomes apparent at $L<l$, (ii) the Fermi energy rise - appreciable at $L<\lambda$, (iii) energy levels quantization - comes to be essential at $L^2<l\lambda$. We have in mind systems like diluted magnetic semiconductors where carrier mobility b is small. With $b\sim 10\text{ cm}^2/\text{V}\cdot\text{s}$ (which is typical for the diluted GaAs(Mn) thin films) the last inequality is not fulfilled if $L>10\text{\AA}$. This means that the system grows *effectively three-dimensional*, and, therefore, we consider only two of the listed effects.

To obtain concrete results we use the mean-field theory extended over the case of the non-uniform effective magnetic field. The local effective field is defined by the relation $\mu H_{\text{RKKY}}(r)=n_{\mu}\int J(r-r')j(r')d^3r'$, where the integration is spread over the volume occupied by impurities, n_{μ} is their concentration, $J(r)$ is the energy of RKKY interaction between magnetic moments μ spaced at the distance r , and $0<j(r')<1$ is the reduced magnetization in the point r' . Contrary to the infinite system, the value of that integral depends on the position of a given point. The corresponding mean-field equation reads $j(h)=\tanh[(1/\tau)\int K(z,h)j(z) dz]$, where τ is the reduced temperature, and the kernel $K(z,h)$ should be specified for films or wires. This nonlinear integral equation determines the spatial distribution of the magnetization in the system.

Calculations show that the magnetization of films and wires is highly non-uniform. Results of calculating the spatial distribution $j(h)$ of the longitudinal magnetization in the wire of the diameter $2R=10a$ (a is the lattice constant) with the impurity concentration for which $4\pi n_{\mu}a^3=1$, and at the finite interaction length ($l=3a$) are represented in the Figure (insert): only the paraxial section of the wire has a significant magnetization, while its periphery is practically non-magnetic. Temperature dependencies of the average wire magnetization $\langle j \rangle$ at $l=3a$ and $l=\infty$ are also shown in the Figure. The distinguishing feature of the dependence corresponding to the finite interaction length is its negative curvature. The magnetization profile is strongly nonuniform if the interaction length is comparable with the wire radius, and at temperatures close to the Curie temperature that distribution is near Gaussian. The dependence of the Curie temperature on the film thickness has been found, along with the temperature dependencies of the average film and wire magnetization. Results could be used for describing properties of nanosized system based on the diluted magnetic semiconductors.



22PO-8-84

MAGNETIC FORCE MICROSCOPY OF MULTILAYER FERROMAGNETIC NANOPARTICLES

Mironov V.L.¹, Fraerman A.A.¹, Gribkov B.A.¹, Gusev S.A.¹, Hjorvarsson B.², Klimov A.Yu.¹, Nikitushkin D.S.¹, Rogov V.V.¹, Vdovichev S.N.¹, Zabel H.³

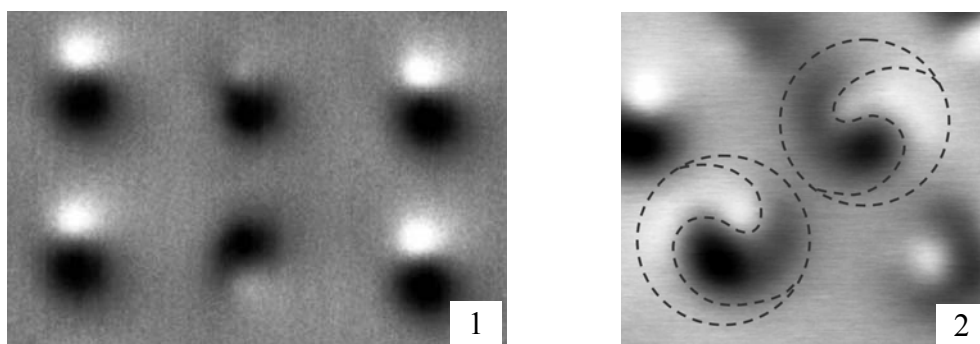
¹Institute for physics of microstructures RAS, Nizhniy Novgorod, Russia

²Uppsala University, Uppsala, Sweden

³Ruhr University, Bochum, Germany

We have used magnetic force microscopy (MFM) to investigate magnetic states in multilayer nanomagnets, consisting of a stack of single domain ferromagnetic disks separated by insulating nonmagnetic spacers. The nanomagnets were fabricated from a Co/Si multilayer thin film structure by electron beam lithography and ion beam etching. The electron microscopy and e-beam lithography were performed using a "JEOL – JEM 2000EX II" scanning electron microscope. The investigations of the stacks' magnetic states were carried out using a vacuum scanning probe microscope "Solver HV" ("NT-MDT" Company).

We investigated MFM tip induced transitions between states with ferromagnetic and antiferromagnetic ordering in the nanostacks consisting of two single-domain Co disks separated by nonmagnetic Si spacers. The stacks have elliptical shape with lateral sizes 300 - 150 nm. The thickness of upper Co layer was 15 nm and bottom layer 20 nm, thickness of Si spacer was 3 nm. The MFM tip induced states with different direction of magnetization in neighbor Co layers were observed (see central region in fig. 1).



The noncollinear helical states in multilayer nanomagnets consisting of three single-domain Co disks separated by nonmagnetic Si spacers were also investigated. The helical state originates from the competition of magnetostatic interactions between nearest and next nearest neighbouring ferromagnetic disks. A helical state occurs if the energy of magnetostatic interaction between next nearest neighbouring disks is sufficiently large compared to the interaction energy of neighbouring disks. The structural parameters (Co layer and spacer thicknesses) were optimised to obtain a clear spiral signature in the MFM contrast, taking into account the magnetostatic interaction between the layers. For optimized tri-layer nanomagnets (300 nm in diameter) with Co layer thicknesses of 16, 11, 8 nm and separated by 3 nm Si spacers, the spiral MFM contrast corresponding to the helical states with different chirality was experimentally observed [1] (see fig. 2).

This work was partly supported by the RFBR (07-02-01321, 08-02-01202), INTAS (# 03-51-4778) and by EC through the NANOSPIN project (contract NMP4-CT-2004-013545).

[1] A.A.Fraerman, B.A.Gribkov, S.A.Gusev et al. accepted in *J. Appl. Phys.*, (2008).

22PO-8-85

ELECTRON SPIN RESONANCE IN VO_x NANOTUBES

Chernobrovkin A.L.¹, Semeno A.V.¹, Glushkov V.V.¹, Sluchanko N.E.¹, Samarina N.A.¹,
Demishev S.V.¹, Grigorieva A.V.², Goodilin E.A.²

¹A.M.Prokhorov General Physics Institute of RAS, 38, Vavilov str., Moscow 119991, Russia

²Lomonosov Moscow State University, Lenin Hills, Moscow, 119992, Russia

Recently new nanoscale magnets, vanadium oxide multiwall nanotubes (VO_x-NT), have attracted attention due to a set of unusual magnetic properties [1]. This material demonstrates strong departures from Curie-Weiss law at temperatures $T > 100$ K, which has been explained by the presence of the antiferromagnetic (AF) dimers formed by the V⁴⁺ magnetic ions [1]. Some features of magnetization and NMR spectra have been assigned to the presence of trimers or another fragments of the V⁴⁺ S=1/2 spin chains in VO_x-NT.

In the present work we report results of the first study of electron spin resonance (ESR) in VO_x-NT aimed on checking of the aforementioned supposition. The sample preparation technique was similar to that used in Ref. [1]. ESR measurements at frequency 60 GHz have been carried out in the temperature range 4.2-200 K with an original cavity magneto-optical spectrometer [2]. The obtained results may be summarised as follows.

(1) Experimental ESR spectrum consists of two lines A and B, corresponding to the g-factors ~ 1.8 and ~ 2.5 respectively (see inset in fig. 1). The intensity of the line B decreases at low temperatures (main panel in fig. 1) and this resonant feature is not observed below $T \sim 100$ K allowing to assign this ESR signal to the AF dimers in qualitative agreement with [1]. However the integrated intensity data $I(T)$ suggest that for $T \sim 200$ K the ratio of the magnetic susceptibilities for the lines A and B is $\chi_A/\chi_B \sim 1$, in contrast to the analysis in Ref. [1], which gives $\chi_A/\chi_B \sim 9-10$.

(2) The temperature dependence of the ESR integrated intensity for the free spins (line A) demonstrate low temperature anomalies. The best fit of the data can be obtained with the help of the function $I \sim \chi = a/T^\alpha + \chi_0$ with $\alpha = 0.55$ and small negative χ_0 (solid line 1 in fig. 1) whereas Curie-Weiss and power laws provides poorer approximation (dash-dotted line 2 and dashed line 3 respectively in fig. 1). Thus the separation of the magnetic contributions carried out in [1], which is based on the postulating of the validity of the Curie-Weiss law for free spins in the whole temperature range, is not correct.

Summarizing, we report first direct experimental evidence of the presence of the AF dimers in VO_x nanotubes. Substantial discrepancies of the ESR data with the results obtained in [1] may be attributed to the higher dimer concentration in our samples as well as to incorrect ad hoc assumptions used in previous investigations.

Support from the Program of Russian Academy of Sciences ‘‘Strongly Correlated Electrons’’ is acknowledged.

[1] E. Vavilova, I. Hellmann, et al., *Phys. Rev. B*, **73** (2006) 144417.

[2] S.V. Demishev, A.V. Semeno et al., *Phys. Sol. State*, **49** (2007) 1295

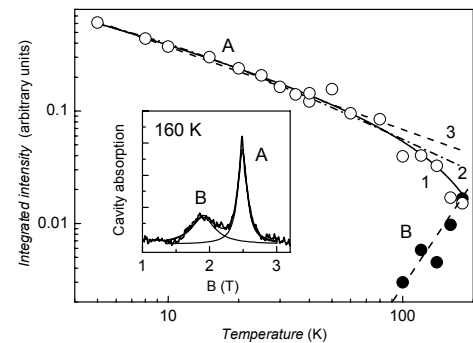


Fig. 1. High frequency ESR in VO_x-NT.

22PO-8-86

FORMATION OF γ -Fe BY THE SOLID-STATE SYNTHESIS IN EPITAXIAL Cu/Fe(001) THIN FILMS: STRUCTURAL AND MAGNETIC FEATURES

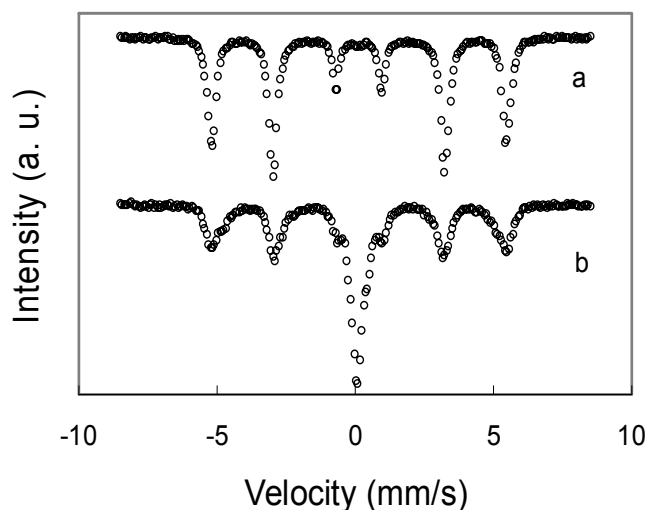
Myagkov V.G.¹, Bayukov O.A.¹, Bykova L.E.¹, Bondarenko G.N.²

¹L.V. Kirensky Institute of Physics, SB RAS, 660036 Krasnoyarsk, Russia

²Institute of Chemistry and Chemical Technology, SB RAS, 660049 Krasnoyarsk, Russia

Electric and magnetic properties of γ -Fe are the object of intensive study in the field of magnetism. Experimental investigations of magnetic properties of γ -Fe have been stimulated by first-principle calculations predicting the formation of a variety of spin states in γ -Fe depending on a lattice parameter. Lattice parameters of Cu and γ -Fe are close, therefore Cu is frequently chosen in experiments for γ -Fe stabilization at room temperature [1]. On one hand, repeated attempts to stabilize several γ -Fe single layers by epitaxial growth on the Cu(001) surface are undertaken. On the other hand, paramagnetic γ -Fe precipitates in the Cu matrix may exist at room temperature. Such samples are obtained by ageing a metastable solid solution of iron in copper at temperatures 300°C - 600°C [1].

In the present work, a new solid-state method of obtaining γ -Fe in a Cu matrix is proposed and justified. Our previous results showed that the mass transport and formation of compounds in bilayers and multilayers start at minimum temperature of a solid-state transformation in a given binary system. In the Fe-Cu system, the only eutectoid transformation with a temperature of 1123 K takes place. According to the above-mentioned assumption, structural transformations at the interface between iron and copper start only at temperature above 1123 K. Epitaxial Cu(001)/ α -Fe(001) bilayers were deposited onto a freshly-split MgO(001) surface. The structural and chemical characterization of the Cu/Fe interface was made by Moessbauer spectroscopy, X-ray diffraction, and magnetic analysis. Moessbauer spectra of the initial Cu(001)/ α -Fe(001) sample had only a sextet from the α -Fe phase (Fig. a). The samples were heated to a temperature of 1150 K, which exceeds the eutectoid transformation temperature 1123 K. Moessbauer spectra of these samples contain the γ -Fe phase singlet (Fig. b).



Magnetic measurement data and X-ray diffraction patterns also confirm the formation of the γ -Fe phase. This suggests that with temperature increasing above 1150 K the eutectoid reaction with the formation of the γ (Fe,Cu) solid solution layer at the interface between iron and copper is initiated. After cooling below 1123 K the eutectoid decay of the γ (Fe,Cu) solid solution leads to precipitation of γ -Fe coherent with a Cu matrix. Subsequent cycles (heating to 1200 K and cooling to liquid nitrogen) show the partial reversible $\gamma \leftrightarrow \alpha$ transition.

This study was supported by the Russian Foundation for Basic Research, project no. 07-03-00190.

[1] V.L. Sedov, Antiferromagnetism gamma-iron. Invar problem, M.: Nauka 1987.

22PO-8-87

GROWTH OF Co NANOSTRUCTURES ON Cu(110): ATOMIC SCALE SIMULATIONS

Stepanyuk O.V.¹, Negulyaev N.N.², Hergert W.², Saletsky A.M.¹

¹Faculty of Physics, Moscow State University, 119899 Moscow, Russia

²Physics Department, Martin-Luther-University Halle-Wittenberg,
Friedemann-Bach-Platz 6, D-06099 Halle, Germany

Magnetic properties of nanostructures on metal surfaces strongly depend on their atomic structure. Interplay between structure and magnetism is one of the most important issue in nanoscience. Self-organized growth of Co nanomagnets on Cu(110) has been reported [1]. Co initially grows via the formation of elongated along the (1-10) three-dimensional islands. However, in the submonolayer regime there was no detectable magnetic signal. It has been suggested that the interface intermixing suppresses ferromagnetism in Co nanoislands [2].

We perform molecular dynamics and kinetic Monte Carlo simulations to reveal the growth of Co nanoislands on Cu(110) at the atomic scale. Ab initio based many body interatomic potentials are used in our studies. We demonstrate that the interface intermixing is the driving force in early stages of the growth process. We find that Co atoms incorporate into the Cu substrate by an atomic exchange process. Such embedded Co atoms serve as the pinning centers for Cu adatoms. As the result the growth of Cu nanoislands occurs on the top of embedded Co adatoms (clusters). Orientation of nanoislands on Cu(110) is explained by anisotropic surface diffusion.

[1] S. Hope et al., *J. Appl. Phys.*, **85** (1999) 6094.

[2] S.M. York and F.M. Leibsle, *Phys. Rev. B*, **64** (2001) 033411.

22PO-8-88

FORMATION OF THE PLANAR DOMAIN WALL IN BI-LAYERS STUDIED BY MAGNETOSTRICTION

Li Jian-jun^{1}, Bobyl A.V.^{2*}, Jay J.-Ph.¹, Ben Youssef J.¹, Indenbom M.V.^{1#}*

¹Laboratory of magnetism of Brittany, CNRS/UBO, 6 av. Le Gorgeu, Brest 29200, France

²Ioffe Physico-Technical Institute, 26 Polytekhnicheskaya, St. Petersburg 194021, Russia

[#]e-mail : indenbom@univ-brest.fr

Bi-layer and multi-layer thin film magnetic structures are intensively studied last decades and a lot of practical applications of their fundamental properties have already greatly changed our life. One can mention, for example, the discovery of the giant magnetoresistance marked by the last Nobel Prize in physics [1]. In spite of the high progress in the understanding of the mechanisms involved it is still not always clear spin behaves at the interface between different thin films. Recently we have shown that all details of magnetisation of multilayers deposited onto thin substrates can be clearly revealed by simultaneous measurements of the substrate flexion and torsion [2]. This technique is complimentary to the ordinary vector magnetometer being capable to resolve the signal from a ferromagnetic (F) layer with the magnetisation negligible compared to the magnetisation of the other layers or even from an antiferromagnetic

(AF) layer and to study, for example, the formation of planar domain walls in a spring-magnet F/F bilayer or in an exchange-bias F/AF bilayer.

We will present our measurements and model calculations of the magnetisation of TbFe/F (F is FeNi, Fe or FeCo) nanometric bilayers with variable thickness of the TbFe film with giant magnetostriction. Unlike our previous studies of $(\text{TbFe}/\text{F})_n$ multilayers developed for magnetostrictive sensors and actuators (see, e.g., [2] and references there in), we are concentrated onto elementary effects of the interaction of two single layers. Already the modelisation of the strongly coupled films taking into account formation of the planar interface domain wall predicts a non-trivial non-monotonic TbFe-thickness dependence of the sample saturation flexion under the field perpendicular to the film easy axis. The experimental results demonstrate a much stronger decrease of the magnetostriction response at large thicknesses which we can explain in the framework of our model by a poor interlayer coupling.

In conclusion, we demonstrate the ability of the vector magnetostrictive magnetometer to reveal more details of the magnetisation at the interface of the magnetically coupled films. This technique can be extended to study the spin dynamics in antiferromagnetic films coupled to a ferromagnetic film and, thus, to understand better the exchange bias phenomenon, for example.

*Jian-jun Li is grateful to K.C. Wong Education Foundation for the financial support of his PhD thesis work in Brest and A.V. Bobyl acknowledges the University of Brest (UBO) for the financial support of his stay in the Laboratory of magnetism of Brittany.

[1] Charles Day – *Physics Today*, **60**, No.12, 12 (2007).

[2] J.-Ph. Jay, F. Petit, J. Ben Youssef, M.V. Indenbom, A. Thiaville, J. Miltat – *J. Appl. Phys.* **99**, 093910 (2006).

22PO-8-89

MAGNETIC PROPERTIES OF THE NANOSTRUCTURES BASED ON DISORDERED MULTILAYER SYSTEMS OF MAGNETIC NANOISLANDS

Boltaev A.P., Pudonin F.A.

P.N.Lebedev Physical Institute of the Russian Academy of Science, 119991, Moscow, Russia

New magnetic structures based on the multilayer system of magnetic nanoislands with ultrahigh sensitivity of weak variation of magnetic field and specific magnetic and magneto-optical properties are presented in this report. Electron transport and magnetoresistance were studied in those nanostructures.

The multilayer nanostructures from Co, FeNi, SmCo and CoNi nanoislands were grown on dielectric (siall) substrates by RF-sputtering method. AFM experiments show that the size of nanoislands in the each layer was 10-20 nm with distance 1.5-5.0 nm between them. Some sets of structures $(\text{FeNi-Co})_{10}$, $(\text{FeNi-CoNi})_{10}$, $(\text{FeNi-SmCo})_{10}$ and other with different nanoisland size were prepared with different islands sizes.

Weak temperature dependence of lateral conductivity (77-300K) indicates about mainly ohmic (metallic) mechanism of conductivity. Resistance of those structures lies in 100-1000 Ohm range. Magnetoresistance R_H (1-3% at H less than 30 Oe) has negative sign when magnetic field was applied perpendicular to current direction that indicates about GMR-effects in the structures. Very complicated $R(H)$ dependence was detected in other magnetic field directions. $R_H(\varphi)$ dependence (φ – angle between directions of magnetic field and electron current) has periodical saw tooth character like in anisotropic effect structures ($R(H) \sim \cos^2\varphi$). That means

that the two effects exist in nanoislands magnetic structures simultaneously. The mechanism of detected magnetoresistance at different orientation of magnetic and electrical fields is discussed in this report.

It is important that these systems of magnetic nanoislands have a monodomain magnetic structure. That means that the magnetization processes connect with magnetic momentum rotation and therefore it is possible to use modulation methods for investigation of field dependence of magnetoresistance.

The extra high sensitivity to super weak variation of magnetic field $\sim 10^{-5}$ - 10^{-6} Oe was discovered in islands structures. The multilayer systems of magnetic nanoisland detect super weak variation and direction of applying magnetic field in 77-300K temperature range.

This work was supported by the grants of RFBR.

22PO-8-90

MODELING HYSTERESIS OF NANOSTRUCTURED FePd ELEMENTS WITH TILTED ANISOTROPY

Niedoba H.¹, Labrune M.²

¹Groupe d'etude de la matiere condensee (GEMaC), CNRS / Universite de Versailles-St-Quentin
45, avenue des Etats-Unis, 78035 Versailles Cedex, France

²Laboratoire PMTM-CNRS, Universite Paris-13, 93430 Villetaneuse, France

Magnetic structures with dimensions on the nanometer scale have drawn increasing attention due to the opportunity of their applications and interest in understanding the related physical phenomena [1]. A large amount of work has been devoted to soft cylindrical dots exhibiting a vortex like ground state configuration. Another class of magnetic nanostructures far less studied corresponds to dots with a strong uniaxial perpendicular anisotropy in which size-dependent magnetic single domain versus vortex state stability has been explored [2]. Increasing the lateral dot's size leads first to a bi-domain state, either a stripe pattern with one straight wall separating up and down domains or a bubble state corresponding to two coaxial up and down domains limited by a circular wall especially observed in circular shaped dots.

Therefore, for particles with size just above a critical dimension the formation of domains inside each nanoelement is a crucial issue for technological applications. In view of recent developments of materials with large perpendicular anisotropies we study in this communication the magnetic behavior of isolated dots whose size allows for a remanent bi-domain pattern or two stripe domain structure. Opposite to highly symmetrical situation like cylindrical-shaped samples with perpendicular anisotropy where a bubble state is encountered, micromagnetic simulations are performed on rectangular-shaped ferromagnetic thin platelets. The main research problem we treat in this paper is the modification of the equilibrium domain pattern induced by a tilting of the uniaxial anisotropy with respect to the normal to the platelet. To model this effect, we have chosen FePd epitaxial layers which are known to grow in a single crystal phase on MgO substrates [3]. Effectively, one can expect to be able to control the tilting of the easy axis by growing epitaxial films on misoriented single crystal substrates. The substrate misorientation up to 20° was explored. The lateral size of the nanostructured elements was about 100 nm, and their thickness 42 nm.

Contrary to rectangular-shaped ferromagnetic thin platelets with perpendicular anisotropy in which only stripe domains are observed [4], tilting of the easy axis gives rise to the nucleation of a bubble like state when decreasing the magnetic field from saturation, followed by transitions to stripe domains in lower field values.

There are two additional significant effects: i) the presence of a double flux closure scheme for the magnetization distribution. In other words not only top and bottom surfaces are to be taken into account for flux closure as for normal anisotropy problem, but also two other faces of the dots on which magnetic charges do appear due to the canted easy axis need to be considered. ii) the magnetization reversal occurs with, at least, the occurrence of two pairs of Bloch-points injected successively during the magnetization process.

A precise description of various magnetization distributions encountered especially in relation with their winding or unwinding character will be fully presented. Special attention is paid to the intrinsic hysteresis phenomena occurring and the need of magnetic singularities to assist the magnetization reversal under an applied field.

[1] S.D. Bader, Rev. Mod. Phys **78**, 1-15 (2006).

[2] H.F. Ding, A.K. Schmid, Dogqui Li, K. Yu. Guslienko and S.D. Bader; Phys. Rev. Lett. **94**, 157202 (2005).

[3] P.R. Aitchison, J.N. Chapman, V. Gehanno, I.S. Weir, M.R. Scheinfein, S. McVitie and A. Marty ; J.Magn..Magn..Mater. **223**, 138-146 (2001).

[4] H. Niedoba and M. Labrune; Eur. Phys. J. B. **47**, 467-478 (2005).

22PO-8-91

COERCIVITY OF GRANULAR FERROMAGNETIC FILMS AND MULTILAYER STRUCTURES

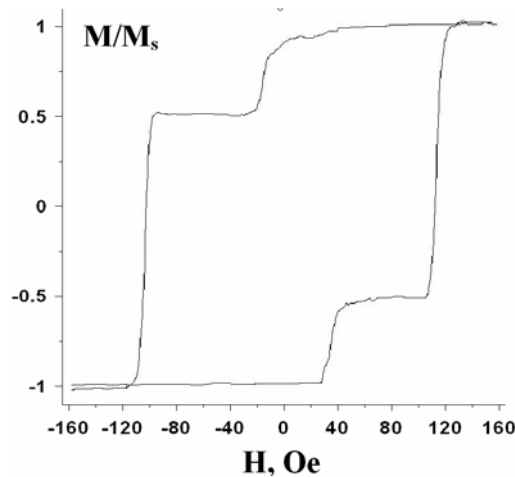
Vdovichev S.N., Gribkov B.A., Klimov A.Yu., Rogov V.V.
IPM RAS, 603950, GSP-105, N. Novgorod, Russia

In this work we suggest to pin coercivity of thin ferromagnetic (F) film by granular ferromagnet (GF) sub-layer. For formation structures GF-F we use well-known metastable Cobalt-Copper alloy and Cobalt as granular ferromagnet and ferromagnet, respectively.

The metastable alloy was fabricated by magnetron sputtering with annealing. We fabricated series of GF-F structures. One type of fabricated GF-F structures was $\text{Co}_{0.5}\text{Cu}_{0.5}\backslash\text{Co}$ with thickness of both $\text{Co}_{0.5}\text{Cu}_{0.5}$ and Co layer about 15 nm. A coercivity of individual $\text{Co}_{0.5}\text{Cu}_{0.5}$ and Co films on a Si substrate was 15 Oe and 200 Oe, respectively. The form of hysteresis loop of $\text{Co}_{0.5}\text{Cu}_{0.5}\backslash\text{Co}$ structure is close to rectangle and coercivity was about 120 Oe. Such effect is similar well-known "magnetic spring" effect [2].

Next we fabricated series of multilayer structures $[\text{Co}_{0.5}\text{Cu}_{0.5}\backslash\text{Co}](30\text{nm})\backslash\text{Si}(5\text{nm})\backslash\text{Co}(15\text{nm})$. The architecture of this multilayer magnetic structure is typical for magnetically engineered spintronic devices: element comprises a soft magnetic layer (Co) separated from a hard magnetic layer ($[\text{Co}_{0.5}\text{Cu}_{0.5}\backslash\text{Co}]$) using a thin insulating barrier (Si). The hysteresis loop is shown on the picture. It is essential to ferromagnetic and anti-ferromagnetic orders of the layers are stable.

Such multilayers can be used for fabrication of high resolution MFM tips [3]; for fabrication nanostructured controllable source of local magnetic field; for observation magnetic tunnel resistance (after optimization of thickness of insulator layer).



The hysteresis loop multilayer structure $[Co_{0.5}Cu_{0.5}\backslash Co](30nm)\backslash Si(5nm)\backslash Co(15nm)$

The work was supported by the RFBR, by BRHE #Y4-P-01-09 (V.S.N.) .

- [1] [7] J. R. Childress, C.L.Chien, J. Appl. Phys. 70, 5885(1991); Phys. Rev. B, 43, 8089 (1991).
 [2] E. Girgis, S. P. Pogossian, and M. Gbordzoe, J. Appl. Phys. 99, 014307 (2006)
 [3] Yihong W, Yatao Shen, Zhiyong Liu, Kebin Li, and Jinjun Qiu Nano, Appl. Phys. Lett., V.82, P. 1748 (2003).

22PO-8-92

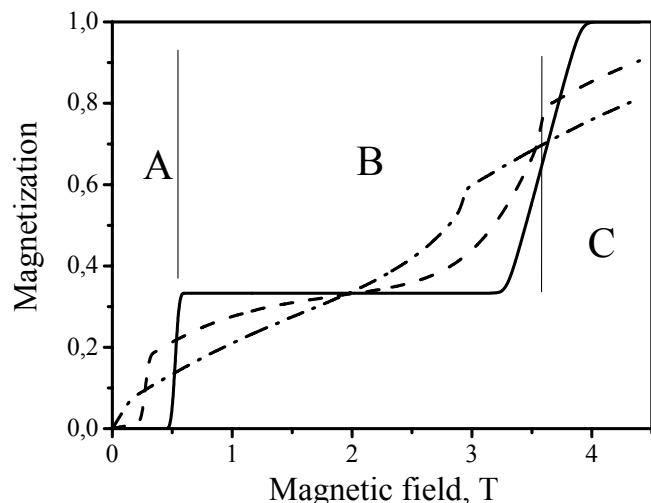
MAGNETIC PHASE DIAGRAM OF FRUSTRATED LATTICE OF ISING SPIN-CHAINS

Kudasov Yu.B.

Russian Federal Nuclear Center - VNIIEF, 37, Mira str., Sarov, 607188, Russia

There are few well-known groups of compounds in which Ising spin-chains are arranged in the triangular lattice. The chains are antiferromagnetic (AFM), e.g. in $CsCoCl_3$, $CsCoBr_3$ and related substances, or ferromagnetic (FM), e.g. in $Ca_3Co_2O_6$. A new compound ($Sr_5Rh_4O_{12}$) that do not contains magnetic 3d ions was recently discovered [1]. All the systems demonstrate complex magnetic behaviour due to the magnetic frustration.

Using the rigid chain model [2] at low temperatures it is shown that the differences in low-temperature phases in all the compounds stem from interactions between the next to the nearest neighbours. This interaction lifts the degeneracy of the 2D Ising model. An unusual step in the magnetization curve at low magnetic field in $Sr_5Rh_4O_{12}$ is explained by the stripe magnetic structure with two sublattices. To obtained the magnetization curves in the



whole temperature range we employ the model of Ref. [3].

The results of calculation of the magnetization curves in $\text{Sr}_5\text{Rh}_4\text{O}_{12}$ at different temperatures are shown in the figure. The solid, dash and dotted dash lines are obtained for $T=5$ K, $T=14$ K and $T=18$ K, correspondingly. They are in a good agreement with the experimental data from Ref.[1]. Three magnetic phases are distinguished in the figure: the stripe (A), ferromagnetic (B), and ferromagnetic (C) phases. It should be mentioned that the transition from the 1/3 plateau to the full magnetization remains smooth at any temperature. The stripe phase can be determined by means neutron scattering experiments.

The high-temperature behaviour is the same for all the substances (the honeycomb or partial AFM magnetic structure).

Support by ISTC and RFBR is acknowledged.

[1] G. Cao, V. Durairaj, S. Chikara, S. Parkin, P. Schlottmann, *Phys. Rev. B* 75 (2007) 134402

[2] Yu. B. Kudasov, *Phys. Rev. Lett.* 96 (2006) 27212

[3] Yu. B. Kudasov, *Eur. Phys. Lett.* 78 (2007) 57005

22PO-8-93

MAGNETIC AND MOSSBAUER STUDIES OF FeCo AND MULTILAYER FePt NANOSTRUCTURED THIN FILMS

Kamzin A.S.¹, Wei F.²

¹Ioffe Physicotechnical Institute, Russian Academy of Sciences, St. Petersburg, 194021 Russia

²Research Institute of Magnetic Materials, Lanzhou University, Lanzhou, 730000 China

To increase the recording density on magnetic media, one has, on the one hand, to develop magnetic materials with a high coercivity. On the other hand, in order to write information on the high coercivity media, recording head materials with high saturation magnetization, high permeability and low coercivity are required. In addition, the creation of the ultrahigh-density magnetic storage (UHDMS) systems of next generation requires magnetic materials as writing media with the minimum possible magnetic grain size, as well as miniaturization of the write/read magnetic heads. However, a decrease in the grain size is accompanied by a superparamagnetic effect, which is a serious problem at the creation of UHDMS media.

This report presents the results of investigations of the FeCo films for write/read magnetic heads an UHDMS recording, prepared by cosputtering on CoFe, NiFe, Cu or Fe underlayers.

In this report also are presented the results of studies of methods ensuring the formation for UHDMS applicable of multilayer L_{10} -[Fe/Pt] n films with controlled orientation of the easy axis and a high coercive field by means of the RF magnetron cosputtering onto heated glass substrates without post-growth annealing at high temperatures.

Our studies of FeCo and L_{10} FePt films have been focused on technological issues of high-density recording heads and media, respectively, as well as on the fundamental magnetic properties, such as the temperature dependence of the magnetic anisotropy constants and the exchange stiffness constant.

The film composition was determined using inductively coupled plasma spectroscopy. The magnetic properties were studied using a SQUID and vibrating-sample magnetometers. The microstructure of the films was determined by X-ray diffraction (XRD). The magnetic structure of the films was studied using conversion-electron Moessbauer (CEM) spectroscopy. The angle

Θ between the light axis orientation and the normal to the film plane determined using the relation of the 2nd(5th)/1st(6th) lines in the Zeeman sextet: $A_{25}/A_{16}=3(1-\cos\Theta)/(4\sin\Theta)$.

In result the FeCo nanostructured thin films with high M_s and low coercivity H_c were obtained by utilizing suitable underlayer and optimizing the deposition conditions. It was found that the improvement of soft magnetic properties for FeCo films with an underlayer is closely related to the film texture.

In the case of FePt L_{10} -phase multilayer $[\text{Fe}/\text{Pt}]_{xn}$ thin films have been obtained. The total thickness of multilayer $[\text{Fe}/\text{Pt}]_n$ was varied from 25 to 200 nm by changing the number n of deposited bilayers. We have studied the dependence of the microstructure, the magnetic structure, and the easy axis orientation in the $[\text{Fe}/\text{Pt}]_n$ films on the substrate temperature as well as the pressure of Ar during, the order and thicknesses of Fe and Pt layers; and the total film thickness.

This mmultilayers possess magnetocrystalline anisotropy (K_u) greater compared to the existing magnetic recording media, large coercivity and saturation magnetization, high chemical stability and corrosion resistance.

The results of our studies demonstrated that prepared L_{10} $[\text{Fe}/\text{Pt}]_{xn}$ multilayer and FeCo thin films can be use for future UHDMs systems.

22PO-8-94

DYNAMICS OF MAGNETIZATION IN FRUSTRATED SPIN-CHAIN SYSTEMS

Korshunov A.¹, Kudasov Yu.^{1,2}, Maslov D.², Pavlov V.¹

¹Russian Federal Nuclear Center – VNIIEF, Mira str. 37, Sarov, 607188, Russia

²Sarov State Physics and Technology Institute, Dukhov str. 6, Sarov, 607188, Russia

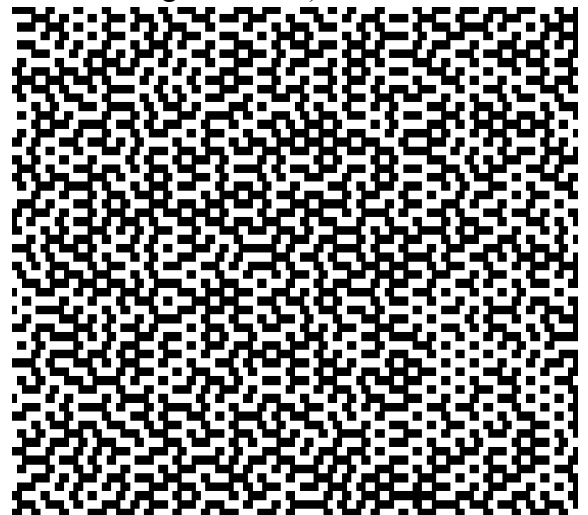
A complex magnetic behaviour of spin-chain compounds arises from a combination of low dimensionality and geometrical frustration. In $\text{Ca}_3\text{Co}_2\text{O}_6$ ferromagnetic Ising chains are packed into the triangular lattice. This substance demonstrate very unusual magnetization step-like curves at low temperatures and low sweep rate of the external magnetic field.

A two-dimensional Ising-like model for the triangular spin-chain lattice, where each spin-chain is treated as a rigid superspin, is proposed to investigate the dynamics of magnetization in frustrated triangular spin-chain systems. The superspins are assumed to interact with the nearest neighbours and external agency (heat reservoir and external magnetic field) that causes them to change their states randomly with time. The probability of spin flip per time unit is given by rules similar to the Glauber dynamics [1]

$$W(\sigma) = \frac{1}{2} \alpha \left[1 - \sigma \cdot \text{th} \left\{ \frac{J}{kT} \sum_i \sigma_i + \frac{\mu B}{kT} \right\} \right]$$

where α is the constant describing the interaction with the heat reservoir, σ is the superspin of the chain (up or down), J is the constant of the interchain coupling, kT is the temperature and μB is the external magnetic field.

The strong dependence of magnetization curve shape on the magnetic field sweep rate and temperature shows that the state of the system of



the spin-chains in the magnetic field is far from equilibrium [2]. We perform the investigation of the evolution of the system using the single-flip technique that was applied earlier to nonequilibrium dynamics of the AFM Ising model on the triangular lattice [3]. The initial structure for the dynamics simulation was prepared by means of a relaxation of the honeycomb structure. A fragment of the relaxed magnetic structure is presented in figure.

Starting with this initial state we investigated nonequilibrium evolution of the spin-chain systems. This technique allows to describe the steps in the magnetization curves observed in $\text{Ca}_3\text{Co}_2\text{O}_6$ and their dependence on the magnetic field sweep rate and temperature.

Support by ISTC (#3501) and RFBR (08-02-97018-r-povolzhje_a, 08-02-00508-a) is acknowledged.

[1] R. J. Glauber, *Jour. Mat. Phys.* **2** (1963) 294

[2] Yu. B. Kudasov, *Phys. Rev. Lett.* **96** (2006) 27212

[3] E. Kim, B. Kim, and S. J. Lee, *Phys. Rev. E* **68** (2003) 66127

22PO-8-95

SPECTROSCOPIC STUDY OF R-MIXED CHAIN NICKELATES $(\text{R}'_x\text{R}''_{1-x})_2\text{BaNiO}_5$. EVIDENCE FOR QUANTUM CRITICAL POINT IN $(\text{Nd}_x\text{Y}_{1-x})_2\text{BaNiO}_5$

Klimin S.A.¹, Popova E.A.²

¹Institute of Spectroscopy RAS, Fizicheskaya 5, Troitsk 142190, Moscow region, Russia

²Moscow State University, Physics Department, 119899 Moscow, Russia

There are two structural peculiarities of the family of chain nickelates with general formula R_2BaNiO_5 (R = rare earth {RE} or Y) important for experimental study of one-dimensional (1D) magnetism. First, there are straight, well separated from each other, 1D-chains of spins $S=1$ carried by Ni^{2+} ions in these compounds. Second, magnetic chains can interact with each other via magnetic R^{3+} ions that are situated between chains. Thus, Y_2BaNiO_5 (Y^{3+} is non-magnetic ion) from this family is a well known 1D Haldane system which does not order magnetically at least down to 100 mK. R_2BaNiO_5 with magnetic rare-earth RE ion R^{3+} is a 3D-magnetic system that orders at low temperatures (with Néel temperatures $T_N \sim 12\text{-}60$ K depending on R). The unique property of R-mixed nickelates $(\text{R}'_x\text{R}''_{1-x})_2\text{BaNiO}_5$ compounds is a possibility to change the interchain interaction by varying x . This promises a good opportunity for experimentalists to investigate the crossover from 1D quantum to 3D classical behavior for $(\text{R}_x\text{Y}_{1-x})_2\text{BaNiO}_5$ compounds. Recent quantum Monte Carlo simulations predict the existence of a quantum critical point that should manifest itself as a step in the T_N vs x dependence [1]. Quantum fluctuations in 1D-chains are strong enough and destroy a magnetic order. The interchain interaction should have a finite value to establish a magnetic order.

We have undertaken the study of the several R-mixed nickelates: $(\text{Y}_{1-x}\text{Er}_x)_2\text{BaNiO}_5$, $(\text{Y}_{1-x}\text{Nd}_x)_2\text{BaNiO}_5$, and $(\text{Er}_x\text{Gd}_{1-x})_2\text{BaNiO}_5$. The Néel temperatures were determined using spectroscopic technique of Kramers doublet splitting [2,3]. The analysis of the experimental data on the $(\text{Er}_x\text{Y}_{1-x})_2\text{BaNiO}_5$ [2] and $(\text{Er}_x\text{Gd}_{1-x})_2\text{BaNiO}_5$ [4] systems shows that the dependence of the ordering temperature on the magnetic rare earth concentration x (at least for $x \geq 0.1$) is well described by the mean-field theory. We did not observe any stepped behavior of the $T_N(x)$ dependence in the region $x \geq 0.1$. Quite recently, we have carried out a new spectroscopic investigation of nickelates $(\text{Nd}_x\text{Y}_{1-x})_2\text{BaNiO}_5$ with low concentration of Nd ($x = 0.075, 0.05,$

0.04, 0.02). In the $T_N(x)$ dependence we found a step-like feature that we attribute to a quantum critical point.

This work was supported by the Russian Foundation for Basic Research under grant No. 08-02-00690, and by the Russian Academy of Sciences (program “Strongly correlated electrons and quantum critical phenomena”)

- [1] J.V. Alvarez, H. Rieger, A. Zheludev, Phys. Rev. Lett. 93, 156401 (2004).
 [2] M.N. Popova, S.A. Klimin, E.P. Chukalina, B.Z. Malkin, R.Z. Levitin, B.V. Mill, and E. Antic-Fidancev., Phys. Rev B 68, 115103 (2003).
 [3] M.N. Popova, S.A. Klimin, E.P. Chukalina, E.A. Romanov, B.Z. Malkin, E. Antic-Fidancev, B.V. Mill, G. Dhalenne, Phys. Rev. B, 71, 024414 (2005)
 [4] M.N. Popova, S.A. Klimin, P. Higel, and G. Dhalenne, Physics Lett. A, **354**, 487 (2006).

22PO-8-96

THE INFLUENCE OF THE HYDROGEN IMPURITIES ON THE MAGNETIC PROPERTIES AND ATOMIC STRUCTURE OF PALLADIUM NANOCONTACTS

Smelova K.M.¹, Bazhanov D.I.¹, Stepanyuk V.S.², Hergert W.³, Saletsky A.M.¹, Bruno P.²

¹Faculty of Physics, Moscow State University, 119899 Moscow, Russia

²Max-Planck-Institut für Mikrostrukturphysik, Weinberg 2, 06120 Halle, Germany

³Fachbereich Physik, Martin-Luther-Universität, Halle-Wittenberg, Friedemann-Bach-Platz 6, D-06099 Halle, Germany

Recent progress in experimental techniques, such as the scanning tunneling microscope [1], transmission electron microscope [2], mechanically controllable break junctions [3] allow to fabricate metallic atomic-size nanocontacts (NC's) (the single metallic chain of few atoms or even one atom suspended between two electrodes). The fabrication of these structures allows to investigate a variety of phenomena at the ultimate limit of atomic scale. The quantum behavior of the electrons within NC's leads to the ballistic electronic transport [2,3]. The presence of

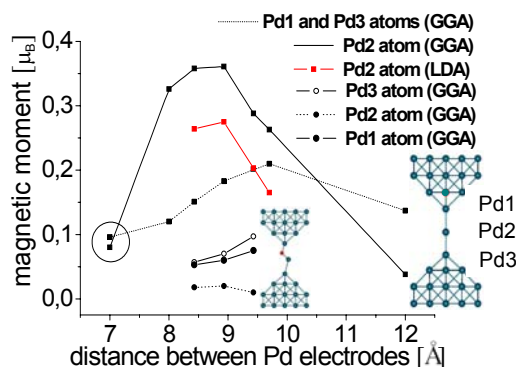


Fig. 1. Local magnetic moments of the Pd atoms in chains suspended between pyramidlike electrodes as a function of interelectrodes distance.

magnetism and its influence on quantum transport in different 3d-, 4d- and 5d-transition metal NC's have been extensively explored experimentally [1-3] and theoretically [5,6]. We present *ab initio* study based on density functional theory of the interplay between atomic structure and magnetic properties in palladium atomic-size contacts suspended between palladium electrodes using both GGA- and LDA-approximations for exchange correlation energy. This study was motivated by recent controversy about possible onset of magnetism in palladium NC's [5]. We have studied the effect of atomic arrangement and structure relaxations in contracted and elongated Pd contacts on their magnetic properties. We found that palladium contacts exhibit magnetic properties for a wide range of distances between separated electrodes (Fig.1) with large magnetic moment about $0,36 \mu_B$ [6]. We revealed an inhomogeneous distribution of the local magnetic moments within a

chain driven by strain relaxations. The onset of magnetism in Pd chain is caused by the reduced dimension of the contact. The contraction of Pd contacts leads to their structural transition from linear to zigzag atomic arrangement, which suppresses strongly their magnetic behavior. We have studied also the influence of gas impurity (hydrogen) on the magnetic properties and stability of Pd NC's, which could be present during experimental measurements. We found that presence of hydrogen impurities can strongly suppressed the magnetic properties of Pd NC's and can lead to their structural transition from linear to zigzag configuration (Fig.1).

- [1] H. Ohnishi *et al.*, *Nature*, **395** (1998) 780.
 [2] V. Rodrigues *et al.*, *Phys. Rev. Lett.* **91** (2003) 096801.
 [3] C. Untiedt, *et al.* *Phys. Rev. B* **66** (2002) 085418.
 [4] T. Matsuda and T. Kizuka, *Jpn. J. Appl. Phys.*, **45** (2006) L1337.
 [5] A. Delin *et al.* *Phys. Rev. Lett.* **96** (2006) 079702; S. Alexandre *et al.* *Phys. Rev. Lett.* **96** (2006) 079701.
 [6] K.M. Smelova, D.I. Bazhanov, V.S. Stepanyuk, W. Hergert, A.M. Saletsky, P. Bruno, *Phys. Rev. B* **77** (2008) 033408.

22PO-8-97

SPATIALLY ORDERED ARRAYS OF MAGNETIC NANOWIRES: SYNTHESIS AND PROPERTIES

*Eliseev A.A.¹, Napolskiy K.S.¹, Kolesnik I.V.¹, Lukashin A.V.¹, Tretyakov Yu.D.¹,
Grigorieva N.A.², Grigoriev S.³*

¹Department of Materials Science, Moscow State University, Moscow, Russian Federation.

²St-Petersburg State University, St-Petersburg, Russian Federation.

³St-Petersburg Nuclear Physics Institute, Gatchina, St.Petersburg, Russian Federation.

One of the important challenges in materials science today is the preparation of nanostructures with accurately controlled properties and dimensions which used as magnetic information carriers in storage devices. However, the use of the nanostructures is strongly restricted because of their low stability and one of the promising methods could be increased stability nanoparticles - the encapsulating of nanoparticles in a chemically inert matrix.

Thus, in the present study the influence of the anisotropy parameters of the magnetic metal (Fe, Ni, Pt, Fe-Co, Fe-Pt alloys, etc) and metal oxide (α -Fe₂O₃, γ -Fe₂O₃, Fe₃O₄, etc) nanowires formed in the structural cavities of solid state nanoreactors (zeolites, mesoporous silica and anodic alumina membranes) to the magnetic properties was carried out. Thus these types of nanoreactors made it possible to investigate the influence of anisotropy of nanowires on their magnetic properties in wide range of the aspect ratio of the nanoparticles.

Incorporation of metals were characterized by TEM, ED, SAXS, SANS, BET and magnetic measurements. It was showed that particles shape and size are in good agreement with that of the pores. Particles are uniform and well ordered in the matrices. Thus, our approach leads to functional materials with nanosized active elements in the matrices, which could find an application in various fields of engineering and technology.

This work is supported by RFBR (№ 06-03-33052-a, 06-03-08157, 06-03-89506-NNS_a), FASI (№ 02.518.11.7036, 02.513.11.3120, 02.513.11.3352).

22PO-8-98

ANGULAR DEPENDENCE OF MAGNETOSTRICTION IN OBLIQUELY MAGNETIZED FERROMAGNETIC FILMS

Fetisov Y.K.¹, Fetisov L.Y.², and Srinivasan G.³

¹MIREA, pr. Vernadskogo 78, 119454 Moscow, Russia

²Faculty of Physics, Moscow State University, 119992 Moscow, Russia

³Physics Department, Oakland University, 48309 Michigan, USA

The magnetostriction λ of samples with high shape anisotropy is determined by the material characteristics and the direction of applied magnetic field \mathbf{H} [1]. In particular, magnetostrictions of a ferromagnetic film magnetized parallel or perpendicular to its plane can differ in several times. However, no detail measurements or calculations of angular dependences of magnetostriction of ferromagnetic films magnetized in arbitrary direction have been done up to now.

In this paper the $\lambda(H)$ dependences for Ni film for three basic field orientations were measured and a method to calculate the film magnetostriction for any \mathbf{H} direction is described.

The Ni films with dimensions of $10 \times 10 \times 0.1 \text{ mm}^3$ and annealed at 800°C were used. The geometry of experiment is shown in Fig.1a. The λ was measured along y direction using a strain gauge. External magnetic field \mathbf{H} was directed at angles φ and β with respect to the x and z axes.

Figure1b shows measured dependences of longitudinal $\lambda_{11}(H)$ ($\mathbf{H} // y$), transverse $\lambda_{12}(H)$ ($\mathbf{H} // x$), and perpendicular $\lambda_{13}(H)$ ($\mathbf{H} // z$) magnetostrictions for the film. The VSM measurements of $M(H)$ curves showed that λ_{11} and λ_{12} increase linearly, and λ_{13} increases nonlinearly when magnetization M of the film is increased. Measured field dependences of λ_{11} , λ_{12} , and λ_{13} allow calculation of the film magnetostriction for arbitrary \mathbf{H} direction defined by the angles φ and β . The dependences were first approximated by analytical functions (shown by solid lines in Fig.1b) and then used to calculate the film magnetostriction using the formula

$$\lambda(H, \varphi, \beta) = \lambda_{11}(H \cdot \sin \beta \cdot \cos \varphi) + \lambda_{12}(H \cdot \sin \beta \cdot \sin \varphi) + \lambda_{13}(H \cdot \cos \beta).$$

As an example, Fig. 2 shows measured (dots) and calculated (solid lines) angular dependences of λ for the Ni film when the field \mathbf{H} rotates in longitudinal (λ_{1113}) or transverse (λ_{1112}) directions, respectively. It is seen that theoretical curves fit well the experimental data.

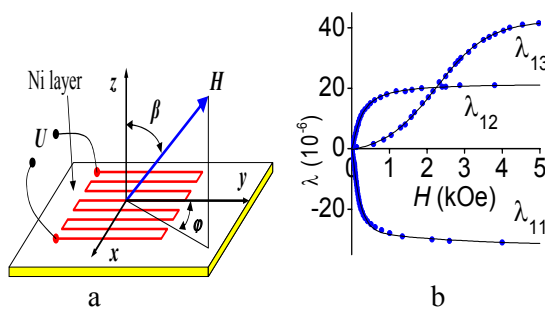


Fig.1. a – geometry of measurements;
b - magnetic field dependences of Ni film magnetostriction for basic H orientations

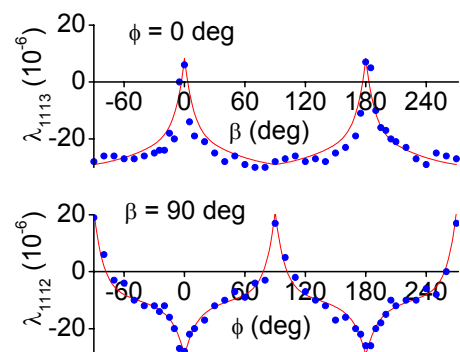


Fig. 2. Angular dependences of Ni film magnetostriction for $H = 1.18 \text{ kOe}$.

The research was supported by the Ministry of Education and Science of Russia and the Russian Fund for Basic Research.

[1] E. Tremolet de Lacheisserie, *Magnetostriction*, CRC Press, Inc., London, 1993.

22PO-8-99

MAGNETIC AND MICROWAVE PROPERTIES OF THIN FILMS CONSISTING OF Fe-Co-Ni NANO-PARTICLES OF VARIOUS SHAPES

Meshcheryakov V.F.¹, Fetisov Y.K.¹, Stashkevitch A.², and Viau G.³

¹MIREA, pr. Vernadskogo 78, 119454 Moscow, Russia

²LPMTM CNRS, University Paris-13, 93430 Villetaneuse, France

³ITODYS CNRS, University Paris-7, 75251 Paris, France

Composite magnetic materials consisting of magnetic nano-particles inserted in an insulating matrix have attracted considerable attention due to possibility of modifying their properties by choosing the particles content, shape, separation, and the shape anisotropy of the sample [1, 2].

In this paper we studied static (magnetization curves) and dynamic (ferromagnetic resonance absorption) properties of thin films (2-5 μm thick) fabricated from Fe-Co-Ni nano-particles of various shapes: $\text{Fe}_{0.12}[\text{Co}_{0.65}\text{Ni}_{0.5}]_{0.88}$ spheres with a diameter of 125-400 nm, $\text{Co}_{0.5}\text{Ni}_{0.5}$ disks with a diameter of 40 nm and 10 nm thick, $\text{Co}_{0.5}\text{Ni}_{0.5}$ rods with a diameter of 8 nm and 50-100 nm long. The nano-powders used were synthesized by the polyol method [3]. The shape and sizes of the particles were estimated by means of TEM and SEM imaging.

Typical magnetization curves for a film fabricated from magnetic nano-disks measured with a vibrating sample magnetometer at room temperature are shown in Fig.1. Dependences of the derivative of absorbed power as a function of the applied magnetic field measured at a constant frequency using a standard resonator technique are shown in Fig.2. Different curves correspond to external bias magnetic fields applied parallel (H_{\parallel}) or perpendicular (H_{\perp}) to the film plane.

The measurements showed that dipole-dipole interactions between the particles results in an effective magnetization M of the film which produces strong demagnetizing effects. Magnetic anisotropy of the static and dynamic characteristics of the film is mainly due to the shape anisotropy of the constituting magnetic particles and their chaotic orientation. The coercivity H_c , remanence M_r , and width of the hysteretic loop are increased for films fabricated from particles with pronounced shape anisotropy, i.e. disks and rods.

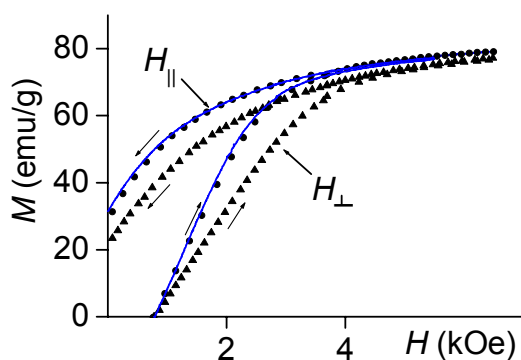


Fig. 1. Magnetization curves

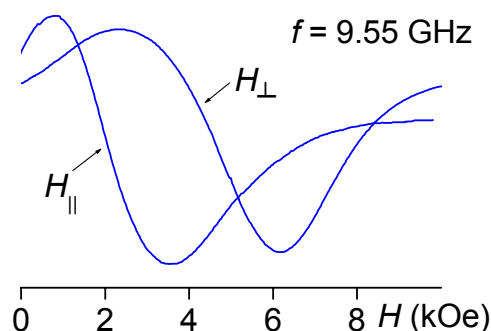


Fig. 2. Ferromagnetic resonance spectrum

The research was supported by grants from the Ministry of High Education and Science of Russia, Russian Fund for Basic Research and the French Ministry of National Education and Research (ACI NR0095 "NANODYNE").

[1] R.H. Kodama, JMMM, 200 (1999) 359.

[2] M. Vazquez, C. Luna, M.P. Morales et al., Physica B, 354 (2004) 71.

[3] G. Viau, F. Ravel, O. Acher, F. Fievet-Vincent, F. Fievet, JMMM, 140-144 (1995) 377.

23 June Monday

10:00-11:30

plenary lectures

23PL-A

23PL-A-1

SPIN-TRANSFER EFFECTS IN SPINTRONIC DEVICES

Dieny B.¹, Ebels U.¹, Houssamedine D.¹, Baraduc C.¹, Thirion C.¹, de Mestier N.¹, Petit S.¹, Manchon A.¹, Buda-Prejbeanu L.¹, Cyrille M.C.², Delaet B.², Vedyayev A.³

¹SPINTEC, URA CEA/CNRS, INAC, 17 rue des Martyrs, 38054 Grenoble cedex 9, France

²LETI/DIHS, CEA/Grenoble, 17 rue des Martyrs, 38054 Grenoble cedex 9, France

³Department of magnetism, Lomonosov University, Moscow, Russian Federation

Giant (GMR) and tunnel magnetoresistance (TMR) effects have already been widely studied and implemented in spin-electronic devices, in particular magnetoresistive heads used in magnetic recording technology and non-volatile magnetic memories (MRAM). In GMR and TMR, the magnetic configuration controls the flow of spin-polarized current throughout the magnetic stack. Spin-transfer effects were predicted and experimentally observed more recently. Spin-transfer describes the effect of a spin-polarized current on the magnetization dynamics. It can be viewed as the reciprocal effect of magnetoresistance. They play an important role in several classes of spin-electronic devices:

-In current-perpendicular-to-plane magnetoresistive heads, the current densities which are commonly used are in the range 10^7A/cm^2 - 10^8A/cm^2 . For these currents, spin-transfer has an observable influence on the magnetization dynamics of the sensing layer¹. Since in heads the magnetization of the sensing layer is biased at 90° from the magnetization of the reference layer, spin transfer most often induces additional noise in the sensor. However, we showed that in specifically designed embodiments, it is possible to benefit from the spin transfer to reduce the noise below the thermal noise.

-In non-volatile magnetic memories based on magnetic tunnel junctions (MRAM), magnetization switching induced by spin transfer torque (STT) can be used as a new write scheme which offers much better scalability (evolution of properties at decreasing lateral dimension) than the conventional approach based on field induced switching. We have conducted a thorough study of magnetization switching induced by field and current in MgO based MTJ. By fitting the critical switching lines in the (I,H) plane, we showed that the spin transfer in MTJ has two components of about equal importance: the Slonczewski spin-torque term of the form $a_j M^{\wedge}(M^{\wedge}P)$ and a field like term of the form $b_j M^{\wedge}P$ in which P represents the magnetization of the polarizing layer and M the magnetization of the switching layer. This contrasts with magnetic metallic stacks in which the Slonczewski term plays a very dominant role. These two terms are important to take into account in the design of STT MRAM.

-Spin transfer can also be used in certain geometries to generate steady magnetization excitations in a magnetic layer. This phenomenon is attractive in the design of frequency tunable radiofrequency oscillators for wireless communications. A geometry of particular interest consists in injecting in a layer with in-plane magnetization a current which is spin-polarized in the out-of-plane direction². This allows to generate a large angle precession of the free layer and therefore to maximize the output signal from the oscillator. Several regimes of oscillations were observed as a function of the current density flowing through the device.

The presentation will review the major results obtained concerning the spin transfer influence in these various classes of devices.

[1] Petit-S; Baraduc-C; Thirion-C; Ebels-U; Liu-Y; Li-M; Wang-P; Dieny-B, Physical-Review-Letters. (2007), 98(7): 077203/1-4

[2] D. Houssameddine, U. Ebels, B. Delaët, B. Rodmacq, I. Firastrau, F. Ponthenier, M. Brunet, C. Thirion, J. P. Michel, L. D. Buda-Prejbeanu, M. C. Cyrille, O. Redon, and B. Dieny, Nature Materials 6, 447 (2007).

23PL-A-2

COMPUTATIONAL QUANTUM MAGNETISM

Freeman A.J.

Morrison Professor of Physics, Northwestern University, Evanston, Illinois, USA

We are witnessing today a golden age of innovation with novel magnetic materials and with discoveries important for both basic science and device applications. Computation and simulation has played a key role in the dramatic advances of the past and those we are witnessing today. A goal driving computational science – simulations of every-increasing complexity on more and more realistic models has been brought into greater focus with greater computing power to run sophisticated and powerful software codes like our highly precise full-potential linearized augmented plane wave (FLAPW) method.

Indeed, significant progress has been achieved from advanced first principles FLAPW calculations for the predictions of surface / interface magnetism such as enhanced magnetic moments and magnetic phenomena induced by the spin-orbit coupling (SOC) – namely, MCA, MCD, and MOKE. One recently resolved challenging issue is the role of non-collinear magnetism (NCM) that arises not only through the SOC, but also from the breaking of symmetry at surfaces and interfaces. For this, we will further describe some specific advances we are witnessing today, including: complex magnetic phenomena from non-collinear magnetism with no shape approximation for the magnetization (perpendicular MCA in transition metal overlayers and superlattices; unidirectional anisotropy and exchange bias in FM and AFM bilayers; constricted domain walls important in quantum spin interfaces; and curling magnetic nano-scale dots as new candidates for non-volatile memory applications) and most recently providing new predictions and understanding of magnetism in novel materials such as magnetic semiconductors and multi-ferroic systems, and the effect of magnetism on phonon frequencies.

Supported by the NSF, AFOSR, and ONR.

23 June Monday

12:00-13:30

oral session

23TL-A

23RP-A

“Magnetophotonics”

23TL-A-1

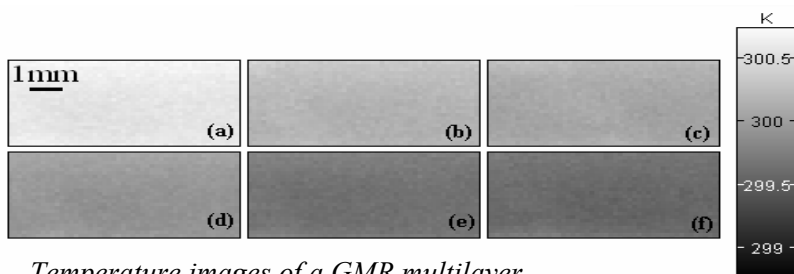
REMOTE SENSING OF MAGNETORESISTANCE USE THE MAGNETOREFRACTIVE EFFECT IN EMISSION

Thompson S.M., Stirk S., Mennicke R.T., Armstrong R., Stanton T., and Matthew J.A.D.
Department of Physics, University of York, York, YO10 5DD, UK

In the mid-far infra red (IR), the complex dielectric function depends on the electrical conductivity of a material. The transmissive, reflective, skin depth and emissive properties of the material can thus be employed to remotely sense Giant Magnetoresistance (GMR). This was first reported as the Magnetorefractive Effect (MRE) by Jacquet and Valet[1]. We have exploited this connection in reflection using Fourier Transform Infrared Spectroscopy, a fixed wavelength laser and used infrared fibre optics to create a portable instrument.

Measuring in emission presents advantages in sensitivity and lends itself to spatial resolution. A change in emissivity due to an applied magnetic field results in a change in IR power radiated from the material's surface, which is observed as a change in the observed temperature ΔT_{obs} . IR imaging techniques thus allow 2D images of GMR to be constructed, demonstrated for GMR and spin-valve multilayers down to a resolution of $30\mu\text{m}$ [2,3]. Assuming perfect thermal coupling between a thick sample and a detector at normal emission, in the long wavelength Hagen Rubens region the GMR is proportional to the fractional change in emissivity, ϵ , i.e. $(\Delta\epsilon/\epsilon)=\gamma$ GMR with a correlation factor $\gamma=0.5$. γ in magnetic thin films is investigated using a thin-film model of emissivity and is shown to depend upon film thickness, with γ weakening for films thinner than the skin depth. The spectral variation of γ is explored using a modified Drude-type expression for the refractive index combined with the thin film model. This is applied to a GMR multilayer and γ shown to have a similar spectral dependence

to that of the MRE in reflection.



Temperature images of a GMR multilayer

$\text{NiFeCr}[\text{CoFe}_{1.5\text{nm}}/\text{Cu}_{1.2\text{nm}}]_{25}\text{TaN}_{7\text{nm}}$ measured in an increasing magnetic field (a) 0.0T (301.03K) to (d) 0.85T (300.41K). IR camera: Infratec/Jenoptik Varioscans 3021ST ($8\text{-}12\mu\text{m}$)

the difference between the observed temperature $T_{obs}(0)$ and the temperature of the environment T_o is also small, then a simple relationship between the GMR and ΔT_{obs} is predicted:

$$\frac{\Delta\rho}{\rho} \approx \frac{1}{\gamma} \frac{\Delta T_{obs}}{T_{obs}(0) - T_o}$$
 as demonstrated in the temperature images of a CoFe/Cu multilayer in the figure.

We thank Seagate (Ireland) for the provision of the CoFe/Cu multilayer sample. This work was supported by the EPSRC [EP/F04027X] and the University of York Research Innovation Fund.

[1] J. C. Jacquet and T. Valet, in *Magnetic Ultrathin Films, Multilayers and Surfaces*, edited by E. Marinero (Materials Research Society, Pittsburgh, 1995).

[2] S. M. Stirk, S. M. Thompson, J. A. D. Matthew and A. F. Lee, *J. Magn. Magn. Mat.* **316**, (2007) e953.

[3] S. M. Stirk, A. J. Vick, S. M. Thompson, J. A. D. Matthew and A. F. Lee, *J. Appl. Phys.* **99**, (2006) 08T101

23RP-A-2

MAGNETOOPTICAL AND MAGNETOTRANSPORT PROPERTIES OF THE Fe/Cr NANOSTRUCTURE

Telegin A.¹, Sukhorukov Yu.¹, Milyaev M.¹, Romashev L.¹, Ustinov V.¹, Gan'shina E.²

¹Institute of Metal Physics, Ural Division of RAS, 620041 Ekaterinburg, Russia

²Moscow State University, 119992 Moscow, Russia

The nature of the effect of giant magnetotransmission (MT) in single crystals and manganite lanthanum films with colossal magnetoresistance (MR), as compared with Cr/Fe multilayers one is different essentially [1,2]. In work [2] devoted to the MT and magnetorefractive effect (MRE) of Cr/Fe multilayers investigation the data of MT(H) and MRE(H) dependences in different experiment geometries are absent. The spectral range MT(λ) and MRE(λ) were limited within energies 1000-5000 cm^{-1} , there is no comparison of the magneto-optical, magnetotransport and magnetic properties of Cr/Fe multilayers.

The investigation of magnetotransmission, magnetoreflection, Kerr and magnetoresistance effects in the nanostructure Cr(28 Å)/Fe(36 Å)/Cr(12.7 Å)/Fe(18 Å)/Cr(12.7 Å)/Fe(36 Å)/ Cr(28 Å) under different temperatures, magnetic fields and geometry of experiment (the magnetic field directed in-plane and out-plane of the film) was carried out in our work. The film was prepared on Al₂O₃ substrate by the molecular-beam epitaxial method. The spectrum of transmission and reflection of the light was measured in 600-12500 cm^{-1} range, magnetic field up to 10 kOe and in temperature interval of 80-370 K. Transversal Kerr effect was measured in an energy range 1-3.5 eV, magnetization and magnetoresistance were studied in a temperature interval 4-370 K.

It was obtained in our work: 1) the kind of a spectrum of magnetotransmission with a minimum at 5000 cm^{-1} is caused, possibly, both by the low-energy response on magnetoresistance and by the high-energy response on manifestation of the effective medium properties; 2) the sign of MRE is identical to a sign of magnetoresistance while the MT sign is opposite of MRE one, that is possibly caused by the influence of thickness of the nanostructure layers on optical properties of the sample; 3) the MT effect is practically temperature independent because of the optical response on magnetoresistance in the nanostructure Fe layers and demonstrate a weak influence of the optical response on tunnel magnetoresistance; 4) the form of the MR(H), MT(H) and MRE(H) dependences of Cr/Fe multilayers is related to the magnetic state of the multilayer characterized by orientation of magnetic moment of neighboring Fe layers.

Supported by the RAS program 'New materials and structures' and RFBR (grant No 07-02-00068 and 06-03-33070).

[1] E. Gan'shina, N. Loshkareva et. al. *J. Magn. Magn. Mater.* **300** (2006) 62.

[2] S. Uran, M. Grimsditch, E.E. Fullerton, S.D. Bader. *Phys. Rev. B.* **57** (1998) 5.

23RP-A-3

MAGNETO - OPTICAL EFFECTS ENHANCED BY SURFACE PLASMON RESONANCE IN NANO STRUCTURES

*Uchida H.¹, Tsunoda Y.¹, Koga M.¹, Fedyanin A.², Masuda Y.¹, Fujikawa R.¹,
Baryshev A.¹, Kim J.¹, Inoue M.¹*

¹Toyohashi University of Technology, Tempaku, Toyohashi, Aichi 441-8580, Japan

²Moscow State University, Moscow, 119992, Russia

Surface plasmon resonance is induced by coupling between light and electron wave in nanoscale structures, which can be excited by the total internal reflection, the nano-particle and the diffraction grating. So far, the magneto-optical effects affected by the plasma resonance was reported in metallic magnetic layer [1] and Au/Bi:YIG granular film [2].

In this study, to obtain the enhancement of magneto-optical effects assisted by surface plasmon resonance, we applied the methods utilizing noble metal nanoparticles and diffraction grating consisted of magnetic material.

For the first method, the Au nanoparticles embedded in bismuth substituted yttrium iron garnet (Bi:YIG) films were prepared, where the Au nano-particles were formed by heating an Au thin film at 750 °C. The Au nanoparticles were covered with Bi:YIG film. At the wavelength of the SPR absorption that appeared around 740 nm, the enhancement of Faraday rotation was obtained.

In the second method utilizing diffraction grating, we studied optical and magneto-optical effects for two-dimensional Ni dot structure. Fig.1 shows a SEM image of the Ni dot structure with a periodicity of 430 nm, a diameter of 200 nm and a height of 80 nm. Fig. 2 shows reflection and longitudinal Kerr rotation spectra for incident light angle of 6.5 °. The absorption of light around 540 nm corresponds to the SPR, which is known as Wood's anomaly [3]. At the same wavelength, Kerr rotation angle changed. Incident angle and polarization dependencies will be discussed.

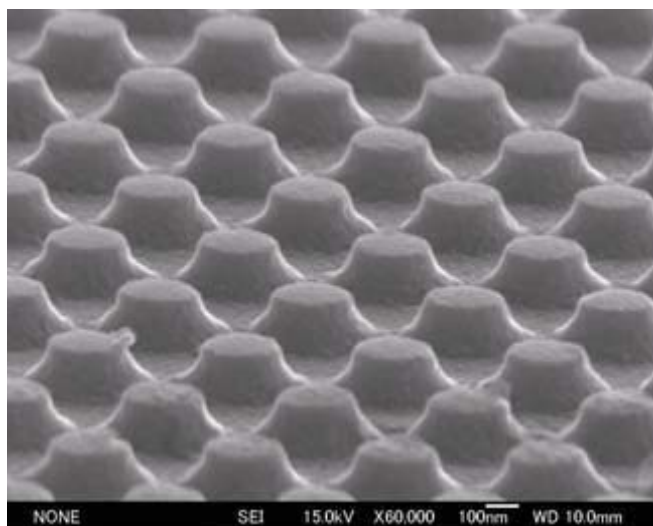


Fig. 1 SEM image of 2D Ni dot structure

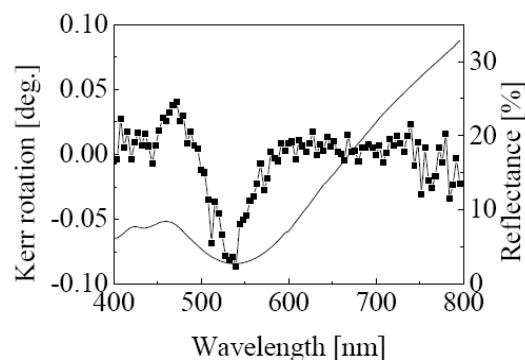


Fig. 2 Reflectance and longitudinal Kerr rotation spectra of the Ni dot structure.

P-polarized light , incident angle of 6.5 °.

[1] H. Feil, C. Haas, Phys. Rev. Lett. 58, (1987) 65.

[2] S. Tomita, T. Kato, S. Tsunashima, S. Iwata, M. Fujii, and S. Hayashi, Phys. Rev. Lett., 96 (2006) 167402.

[3] R. W. Wood, Philos. Mag. 4, (1902) 396.

23TL-A-4

ABSORPTION SUPPRESSION IN MAGNETIC PHOTONIC CRYSTALS

Figotin A., Vitebskiy I.

University of California at Irvine, Irvine, CA 92697-3875, USA

Magnetic materials play a crucial role in MW and optics. They are absolutely essential in numerous nonreciprocal devices. They can also provide tunability, miniaturization, better impedance matching, and other important features. A major obstacle for broader applications of magnetic materials is tied up with the issue of absorption. Many magnetic materials with otherwise perfect physical characteristics have been rejected because of strong losses. In this paper we explore the idea of composite structures having desired physical properties associated with magnetism but, at the same time, significantly suppressing the effects of absorption. In other words, we want to take advantage of the useful characteristics of a particular magnetic material, while drastically reducing its contribution to the energy dissipation.

Magnetic photonic crystals are spatially periodic composites with one of the components being a magnetic material, such as a ferromagnet or a ferrite. In comparison to uniform magnetic materials, magnetic photonic crystals can display much stronger nonreciprocal properties, such as magnetic Faraday rotation. In addition, the use of composite structures instead of uniform magnetic materials can dramatically reduce the size of non-reciprocal and other microwave and optical devices. The subject of our investigation is another important aspect of electrodynamics of composite materials. Namely, we show that properly design periodic array can dramatically reduce the losses associated with magnetic component [1]. Moreover, the broadband suppression of losses can be achieved in a combination with enhancement of nonreciprocal properties such as Faraday rotation. The possibility of absorption reduction is related to the fact that in most cases the absorption and the useful functionality of the particular magnetic material are related to different components of its permittivity and/or permeability tensors. Such a difference allows us to adjust the physical and geometric characteristics of the periodic structure so that the electromagnetic field distribution inside the photonic crystal suppresses the energy dissipation by the lossy magnetic component, while preserving or even enhancing its useful functionality. The way to address this problem essentially depends on the following three factors.

1. The useful functionality of the lossy material. In our example, it will be the nonreciprocal circular birefringence producing the Faraday rotation.

2. The dominant physical mechanism of absorption. For instance, energy dissipation caused by electric conductivity requires a different approach, compared to the situation where the losses are associated with the dynamics of magnetic domains, or some other physical mechanisms.

3. The frequency range of interest. The same periodic array can significantly reduce losses at some frequencies, while enhancing losses at different frequencies. In other words, the same periodic structure can be either effective or counterproductive, depending on the frequency range and the dominant physical mechanism of energy dissipation.

Another practical advantage of composite structure is that in some cases its size can be much smaller compared to that of the uniform magnetic sample with similar characteristics. Note, though, that a significant size reduction usually comes at the expense of the bandwidth.

Support by the Air Force Office of Scientific Research is acknowledged.

[1] A. Figotin and I. Vitebskiy. *Phys. Rev.*, B77 (2008) 104421.

23 June Monday

15:00-17:00

oral session

23TL-A

23RP-A

**“Biomagnetism
and Miscellaneous”**

23RP-A-5

MAGNETISM AT THE NANOSCALE*Wittborn J.¹, Rao K.V.¹, Proksch R.², Revenko I.², Dahlberg E.D.³, and Bazylinski D.A.⁴*¹Dept. of Condensed Matter Physics, KTH, Teknikringen 14, SE-10044 Stockholm, Sweden.²Asylum Research, Inc., Santa Barbara, CA, USA³School of Physics and Astronomy, University of Minnesota, Minneapolis, MN 55455, USA⁴Department of Microbiology, Iowa State University, Ames, Iowa, USA

There has been a renaissance in magnetism in the last several decades. In the area of micromagnetics (although in the modern context it should be nanomagnetics), major breakthroughs have resulted from the development of new magnetic imaging techniques [1]. A powerful magnetic microscope is the magnetic force microscope (MFM), a variant of the atomic force microscope. One of the frontiers in magnetism being pushed back is to understand the domain structure and the magnetization reversal in nanometer sized particles. We have utilized the high resolution MFM (30 nm) we developed [2] to increase our fundamental understanding of magnetism on this length scale.

We will discuss the magnetic reversal of chains of 50nm magnetite crystals (a magnetosome) extracted from magnetotactic bacteria (this includes a video of the bacteria trying to find food at the end of the magnetic rainbow) [3]. The original very long chains, up to 80 magnetosomes, were segmented with the MFM tip to create chains of various lengths. The MFM images of the chains were taken with variable *in situ* magnetic fields; the switching field distributions were determined from the images. Hysteresis loops with the applied magnetic field at various angles to the chain lengths were made. In general the coercivity was found to initially increase with increasing chain length and then remain constant with increasing chain length.

Supported by ONR and the University of Minnesota MRSEC.

[1] E. Dan Dahlberg and Jian-Gian Zhu, *Physics Today*, **48** (1995) 34.

[2] George D. Skidmore, Sheryl Foss, and E. Dan Dahlberg, *Appl. Phys.Lett.*, **71** (1997) 3293-3295.

[3] J. Wittborn, R. Proksch, S. Austvold, D. A. Bazylinski, I. Revenko, E. D. Dahlberg, K.V. Rao, *Nanostructured Materials*, **12** (1999)1149-52.

23RP-A-6

MAGNETOCARDIOGRAM(MCG) MEASURED BY HIGHLY SENSITIVE THIN FILM SENSOR

Yabukami S.¹, Kato K.¹, Ohtomo Y.¹, Ozawa T.², and Arai K.I.^{3,4}

¹Tohoku-Gakuin University, 1-13-1 Tagajyo, Japan

²Miyagi National College of Technology, 48 Nodayama, Medeshima-Shiote, Natori, Japan

³Res. Inst. for Elec. Magn. Materials, 2-1-1 Yagiyama minami, Taihaku-ku, Sendai, Japan

⁴National Inst. of Info. and Comm. Tech., 6-6-3 Minami-Yoshinari, Aoba-ku, Sendai, Japan

We developed a very sensitive high-frequency carrier-type thin film sensor with a pT resolution using a transmission line. The sensor element consists of Cu with a meander pattern (20 mm in length, 0.8 mm in width, 18 micro m in thickness, 1 turn), a ground plane, and amorphous-CoNbZr film (6 micro m in thickness) as shown in Fig. 1. The amorphous-CoNbZr film was deposited by RF sputtering, and a low anisotropy field of around 1.5 Oe was applied by annealing. Carrier current of around 800 MHz flows in the Cu meander pattern. A small AC magnetic field was applied to the sensor element and a very small phase change was detected using a Dual Mixer Time Difference method [1]. The phase of carrier drastically changed at 800 MHz which was ferromagnetic resonance frequency of the amorphous-CoNbZr film. A high phase change of 90 degree/Oe was observed. We obtained a magnetic field resolution of $3.0 \times 10^{-12} \text{ T/Hz}^{1/2}$ when very small AC field at 1 Hz was applied. The detectable magnetic field was limited by the $1/f$ noise of the sensing system. Fig. 2 shows a magnetocardiogram (MCG) signal which was measured using the sensor. The sensor was placed closely to a chest of a human body in the magnetically shielded room. Sampling rate was 15 kHz, we averaged these signals per 20 msec to reduce hum noise. Rapid changes were observed and these intervals between rapid changes were about 1 sec. Therefore we think the signal as R wave of MCG.

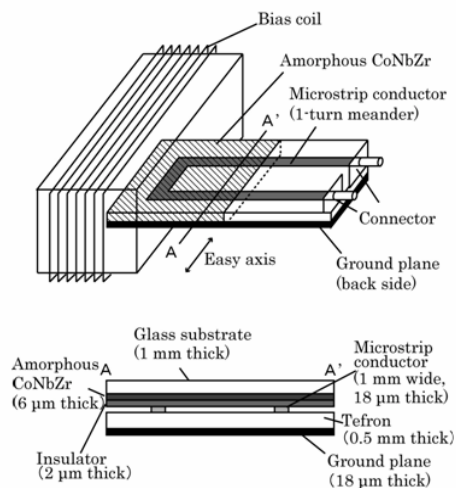


Fig. 1 A structure of sensor.

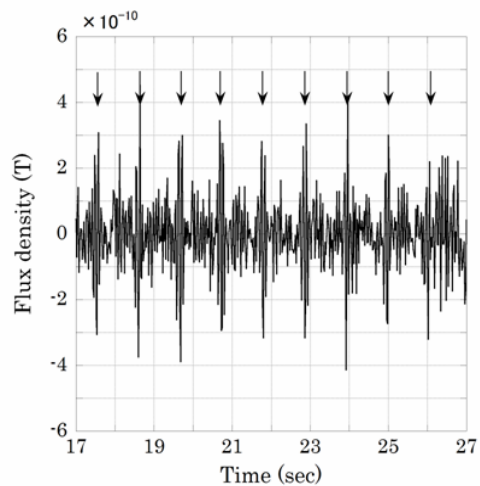


Fig. 2 MCG signal.

This study was partly supported by Development of System and Technology for Advanced Measurement and Analysis (Japan Science and Technology Agency). This study was partly supported by Grants-in-Aid for Scientific Research (Japan Society for the Promotion of Science).

[1] T. Ozawa, H. Mawatari, S. Yabukami, K. Ishiyama, and K.I. Arai., *J. Magn. Soc. Jpn*, 29, 831 (2005).

23TL-A-7

PHARMACOKINETICS OF RADIO ISOTOPE LABELED MAGNETIC NANOBEADS

Fu Chao-Ming^{1*}, Wang Yuh-Feng², Chuang May-Haw², Guo Yu-Feng¹, and Wu Yen-Wen³

¹Physics department, National Taiwan University, Taiwan

²Department of Nuclear Medicine, Buddhish Dalin TzuChi General Hospital, Taiwan

³Department of Nuclear Medicine, National Taiwan University Hospital, Taiwan

*e-mail: chaomingfu@phys.ntu.edu.tw

Biocompatible superparamagnetic nanoparticles such as magnetite have been widely utilized as targeting agents for directing the chemotherapeutic drug to a localized disease site. As well, there is utilization of magnetic nanoparticles to guide transport of radionuclides, which have an advantage of high concentrations of radioactivity to the target area.

We have developed an approach to directly label the radioactive Tc-99m with magnetite (Fe₃O₄) nanoparticles for diagnostic applications. Our approach of directly labelling of Tc-99m with ferrite nanoparticles no needs pre-process of chemical modification, yet achieving highly labeling efficiency and keeping bead's size small. As prepared radiolabeled ferrite nanoparticles can be utilized for diagnosis application or further conjugated with chemicals for therapeutic purposes, under magnetic assistance to the target area. For practical therapeutic or diagnostic applications, the knowledge of organ distribution of injected particles is necessary.

This presentation reports the study of the kinetics of *in vivo* bio-distribution of the radiomicrospheres upon injection, and the capability as prepared radiobeads conjugated with pharmaceutical chemicals. In this study, the *in vivo* bio-distribution of these beads, the Tc-99m labeled ferrite nanoparticles were intravenously injected into tail vein of rats. Then, the scintigraphic image were monitored by planar imaging, using a gamma camera. From the scintigraphic images, we have performed analysis on the time evolution of the radio-intensity of heart, lung and liver, respectively. It is observed that the uptake of particles by the organ is very fast and completed within first few minutes after intravenously injection. Modeling with dynamical equation for the fate of radiomicrospheres has been performed. Details will be reported.

Support by NSC Taiwan is acknowledged.

23TL-A-8

GIANT MAGNETOIMPEDANCE FOR BIOSENSING: ADVANTAGES AND SHORTCOMINGS

Kurlyandskaya G.V.^{1,2}

¹Universidad del País Vasco, UPV/EHU, Dpto. de Electricidad y Electrónica, P.O. Box 644, Bilbao 48080, Spain

²Ural State University named under A.M.Gorky, Dept. Magnetism and Magnetic Nanomaterials, Lenin Ave. 51, 620083, Ekaterinburg, Russian Federation

One of the important areas of modern sensor applications is biosensors. A biosensor is a compact analytical device incorporating a biological or biologically-derived sensitive element integrated in or associated with a physicochemical transducer [1]. There are different types of magnetic effects capable of creating magnetic biosensors: magnetoresistance, giant magnetoresistance, spin-valves, Hall effect, magnetoimpedance (MI) [1-3]. Magnetoimpedance phenomenon consists in the change of the total impedance, Z , of a ferromagnetic conductor in an external static magnetic field, H , when a high frequency alternating current flows through the conductor [4]. MI was proposed for biosensing in 2003 [1]. This work is a summary of the latest development of the GMI-biosensors. Both MI prototypes based on magnetic labels detection and label free detectors were designed and tested. In view of these results the advantages and shortcomings for potential applications of MI for biosensor will be discussed.

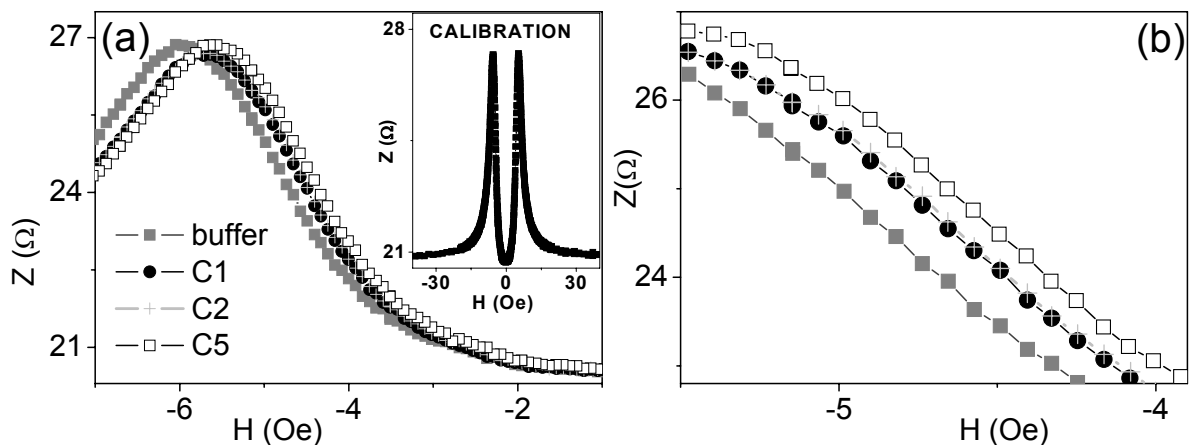


Figure. MI responses of FeNi/Cu/FeNi multilayered sensitive element without buffer (calibration) in ethanol buffer without and in presence of Dynabeads M – 480 for different bead concentrations: C1= 8.8×10^6 beads/ml; C2= 1.7×10^7 bead/ml C5= 4.4×10^6 beads/ml (measuring frequency $f = 50$ MHz).

Supports by MEC (“Ramon y Cajal” fellowship) an ACTIMAT grant and RF Program of High School Science Potential Development (project RNP.2.1.1.6945) are acknowledged.

- [1] G.V. Kurlyandskaya, M.L. Sánchez, B. Hernando, V.M. Prida, P. Gorria, M. Tejedor, Appl. Phys. Lett. 82 (2003) 3053.
- [2] D.R. Baselt, G. U. Lee, M. Natesan, S.W. Metzger, P.E. Sheehan, R. Colton, Biosens. Bioelectron. 13 (1998) 731.
- [3] G.V. Kurlyandskaya, V.I. Levit, Biosensors and Bioelectronics 20 (2005) 1611.
- [4] A. Antonov, S. Gadetsky, A. Granovsky, A. Diachkov, M. Sedova, N. Perov, T. Furmanova, A. Lagarkov, Physica A 241 (1997) 414.

23TL-A-9

MAGNETIC BASED TRANSLOCATION AND SENSING OF BIOMOLECULE TAGS FOR BIOMEDICAL DIAGNOSIS

Sun S., Kumal A., Bharat B., Kim K.W., Yoon S.S., Jung J.R., and Kim Cheol Gi

Division of Nanoengineering, Chungnam National University, Korea

e-mail : cgkim@cnu.ac.kr

Webpage: www.nanospin.net

Nanomagnetics are opening a new era not only in industrial application, especially related with information science and technology, but also in bioassays related to biomolecule translocation, biochip/sensors and multiplex bio-recognition channel. Ever since giant magnetoresistance (GMR) has been applied to a biochip sensor for biomolecule tags of magnetic particle in 1996, lots of researches has been carried out to enhance the resolution of the magnetic particle tags, corresponding to that of hybridized biomolecule pairs. At present, the several groups worldwide have succeeded to enhance the sensor resolution down to a few pairs of probe-target biomolecules.

In this talk, firstly, I will overview the current status on magnetic bioassay researches in worldwide. Secondly, I will introduce the translocation of biomolecules using the magnetic pathway and rotating magnetic field. Thirdly, the array using planar Hall Resistance (PHR) effect in magnetic multilayers and its performance of fabricated sensors are presented for high sensitive biomedical diagnosis. Finally, I will show some results on biomolecule manipulation, i.e., DNA immobilization, removal of non-specific hybridization using magnetic method.

23 June Monday

12:00-13:30

oral session

23TL-B

23RP-B

**“Nanomagnetism
and Nanostructures”**

23TL-B-1

THERMALLY INDUCED MAGNETOELASTIC ANISOTROPY IN ARRAYS OF Ni AND Co MAGNETIC NANOWIRES EMBEDDED IN ALUMINA MEMBRANES

Vázquez M., Pirota K.R., and Navas D.

Institute of Materials Science, CSIC. 28049 Madrid. Spain

The magnetic behaviour of arrays of magnetic nanowires are of relevance for their use in novel magnetic recording media, or functionalised magnetic sensors. The magnetic properties of such arrays are determined by the magnetic anisotropy of the nanowires as well as by the magnetostatic interactions among them. In previous works, such interactions were studied as a function of the geometrical characteristics of the hexagonal arrays, particularly the lattice constant that determines the distance between neighbouring wires.

In the present work, we focus on the study of the temperature dependence of their magnetic properties, namely the hysteresis loop of the whole array and its characteristic parameters as coercivity or remanence. In previous works [1] we have introduced the magnetic induced anisotropy as a consequence of the different nature of the metallic nanowires and the surrounding alumina matrix. In the present work we collect previous results and give a general view and characteristics of the magnetoelastic anisotropy induced by changes in the temperature.

Arrays of Ni and Co nanowires have been prepared by electroplating filling of the pores in alumina membranes. Their diameter was tailored between 35 and 65 nm, and the lattice constant of the array 105 nm. The magnetic behaviour has been determined by vibrating sample magnetometry in the temperature range between 5 and 300K.

It is observed that as temperature decreases magnetic anisotropy is induced resulting even in a change of magnetization easy axis. That is deduced from the evolution of the shape of the hysteresis loop with temperature and particularly its remanence magnetization. The trend of that evolution differs for Ni and Co interpreted to be due to the different magnetostriction sign. The crossing temperature at which the in-plane evolves into out-of-plane anisotropy and viceversa depends also on the length of the nanowires denoting the role of the magnetic shape anisotropy. Further analysis of the experimental results allows us to evaluate the nanoscale surface effect and surface tension in Ni and Co nanowires.

Support by MEC is acknowledged.

[1] K.R. Pirota *et al.*, Phys. Rev. B 76 (2007) 233410 ; D. Navas *et al.*, J. Appl. Phys. 103 (2008) 07D523

23RP-B-2

STRUCTURE AND MAGNETISM OF FePt₃ NANOCUBES

Spasova M., Margeat O., Tran M., and Farle M.

Universität Duisburg-Essen, Experimentalphysik – AG Farle, Fachbereich Physik and Centre of Nanointegration Duisburg-Essen (CeNiDE), Lotharstr. 1, 47048 Duisburg, Germany.

FePt₃ nanocubes with an edge length of 8 nm and narrow size distribution have been synthesized by methods of colloidal chemistry [1]. As-prepared cubes are in fcc chemically disordered phase with {100} crystal facets. Self-assembly of the nanocubes results in square superlattices with the <100> directions oriented perpendicular to the substrate plane. The average magnetic moment of 2.53 μ_B per FePt₃ formula unit and the Curie temperature ($T_c = 255$ K) of the particles are found to be reduced by 20% and approximately 30% with respect to those of the bulk alloy. The effective magnetic anisotropy energy density $K_{eff} = (6.7 \pm 1) \times 10^4$ J/m³ at 5 K is found to be larger by at least a factor of 2 with respect to this value for the bulk alloy. The temperature dependence of K_{eff} follows the magnetization M according to $K_{eff} \sim M(T)^{2.1}$. Thermal annealing of the FePt₃ nanocube superlattice results in formation of the chemically ordered L1₂ phase without particle aggregation. Annealed nanoparticles have lost their cubic shape keeping preferential crystallographic <100> orientation perpendicular to the substrate plane.

The work is supported by the European Union under contract MRTN – CT-2004-005567 (SyntOrbmag).

[1] O. Margeat et al. Phys. Rev. B 75 (2007) 134410

23RP-B-3

MAGNETIC EXCITATIONS IN (SiO₂)Co NANO-COMPOSITE FILMS: BRILLOUIN LIGHT SCATTERING STUDY

Stashkevich A.A.¹, Roussigné Y.¹, Stognij A.I.², Novitskii N.N.², Wurtz G.³, Zayats A.³, Viau G.⁴, Chaboussant G.⁵, Ott F.⁵, Lutsev L.V.⁶, Djemia P.¹, Kostylev M.P.⁷, and Belotelov V.⁸

¹LPMTM CNRS (UPR 9001), Université Paris 13, 93430 Villetaneuse, France

²Institute of Solid State and Semiconductor Physics, 220072 Minsk, Belarus

³Centre for Nanostructured Media, IRCEP, The Queen's University Belfast, BT7 1NN, UK

⁴ITODYS CNRS (UMR 7086), Université Paris 7, 75251 Paris, France

⁵Laboratoire Léon Brillouin (LLB-CNRS-CEA) CEA Saclay, 91191 France

⁶Research Institute 'Ferrite-Domen', 196084 Saint-Petersburg, Russia

⁷School of Physics – M013, University of Western Australia, Crawley, WA 6009, Australia

⁸Moscow State University, 119992 Moscow, Russia

In the present paper, the extensively discussed problem of SPM-to-SFM transition in nano-composite films has been re-addressed. This time it has been approached from a different side. We have investigated, by means of the Brillouin Light Scattering technique, the behavior of the magnetic excitations in a nano-composite Co_xSiO₂_{1-x} film during a transition from SPM to SFM state in the frequency range from 10 to 50 GHz with SW wavenumber varying from 3·10³ cm⁻¹ to 2·10⁵ cm⁻¹. The Cobalt concentration x varied from 50% to 80 % at.

Less concentrated samples ($x < 60\%$ at.) demonstrated SPM behavior, identical to that of a slightly under-saturated ferromagnetic film in the absence of exchange. It is characterized by a weakly pronounced SW dispersion and a reduced Stokes/anti-Stokes asymmetry. With the growth of the sample concentration, the features typical of the presence of non-vanishing exchange interactions begin to manifest themselves. The BVMSW degeneracy is removed and the contributions the DE and backward volume modes can be identified in the Stokes/anti-Stokes BLS spectral lines. Numerical analysis of the fine structure of these lines, based on the Dissipation-Fluctuation Theorem allowed estimation of the value of the effective exchange constant A_{eff} . It turned out to be three times less than of its bulk value for the Cobalt: $A = 1.8 \cdot 10^{-6}$ erg·cm⁻¹. Moreover, this analysis has indicated the presence of a relatively weak magnetic anisotropy of the order of several hundreds Oe. These two figures are corroborated by the experimental observation, by MFM/AFM, of weak stripe domains. The domain size was crosschecked by Grazing Incidence Small Angle Neutron Scattering.

A qualitative theoretical model has been proposed to explain the reduction of the value A_{eff} with respect to A . It has been shown that the “super-spin” approximation, identifying each nano-particle with a “magnetic point” with no internal structure, is insufficient to account for the description of the SW behavior of a concentrated nano-composite medium. The inter-particle exchange interaction invariably leads to a pronounced re-distribution of the dynamic magnetic field within each particle.

[1] S. Bedanta, T. Eimüller, W. Kleemann, J. Rhensius, F. Stromberg, E. Amaladass, S. Cardoso, and P. P. Freitas, *Phys. Rev. Lett.* 98 (2007) 176601.

[2] A. Butera, J.N. Zhou, and J.A. Barnard, *Phys. Rev. B* 60 (1999) 12270.

23RP-B-4

GAS FLOW SPUTTERING: A VERSATILE PROCESS FOR THE GROWTH OF NANOPARTICLES, NANOPILLARS, AND EPITAXIAL THIN FILMS

Sakuma H., Ishii K.

Department of Electrical and Electronic Engineering, Utsunomiya University,
7-1-2 Yoto, Utsunomiya 321-8585, JAPAN

Gas flow sputtering (GFS) [1] is a sputtering method, which can be used for the growth of some attractive structures of magnetic materials. The basic principle of GFS is illustrated in Fig. 1. GFS operates at a pressure around 1 Torr. This high pressure causes the mean free path of Ar atoms and sputtered atoms to be as short as 0.1 mm. Therefore, energetic particles lose their energies by collision with Ar atoms. The energy of the particles arriving at substrate is very low and various structures including nanoparticles and nanopillars are formed. However, sputtering at such a high pressure causes very low deposition rate. Ar gas flow of a few hundreds standard-cc-per-minute introduced from the back of sputtering target greatly improves the deposition rate. Another feature of GFS is the hollow cathode discharge with a tube or faced-plates target. Secondary electrons produced by the bombardment of ion to the target are confined in the hollow space, resulting in high plasma density. Therefore, high-density atomic vapor is generated.

The density of the atomic vapor increases with decreasing the inner diameter of the tube target. When the inner diameter is as small as 5 mm, the condensation of the sputtered atoms occurs in the gas flow [2]. Figure 2(a) shows the transmission electron microscope (TEM) image of Fe nanoparticles obtained by using GFS. For larger inner diameter, a thin film with columnar

structure is formed. The Co-Pt “nanopillars” shown in Fig. 2 (b) are the extreme cases of the columnar structure [3]. The magnetically separated nanopillar-structure is favorable for the magnetic recording application. By substrate heating, epitaxial thin films can be fabricated: Fe₃O₄/GaAs epitaxial thin films, which are difficult to deposit by any other methods, are fabricated by using GFS.

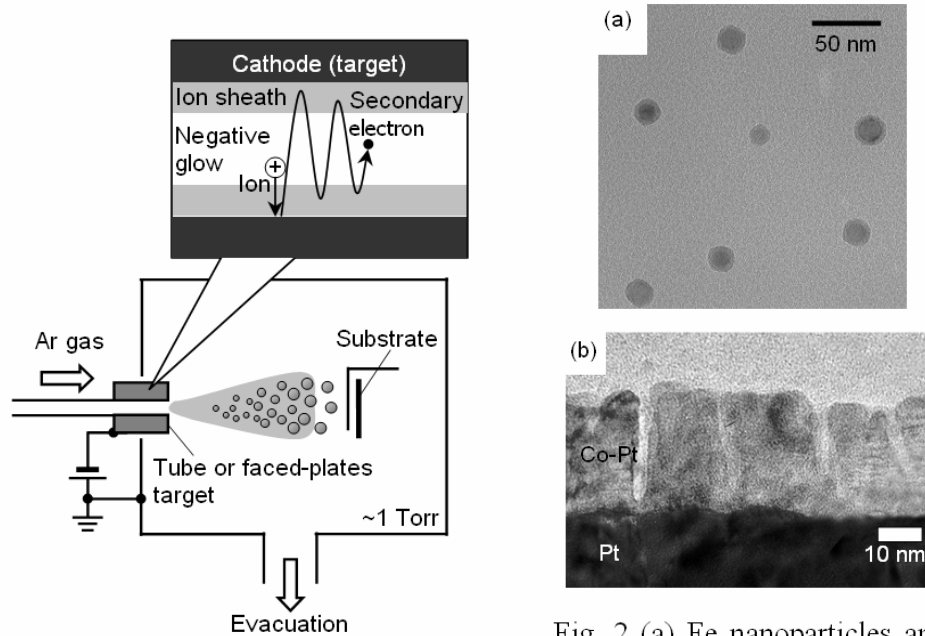


Fig. 1 Schematic illustration of GFS system

Fig. 2 (a) Fe nanoparticles and (b) Co-Pt nanopillars fabricated by using GFS

[1] K. Ishii, *J. Vac. Sci. Technol. A*, **7** (1989) 256, [2] H. Sakuma, H. Aoshima, K. Ishii, *J. Magn. (Korea)*, **11** (2006) 103, [3] S. Mifuji, H. Sakuma, K. Ishii, *J. Appl. Phys.*, **97** (2005) 10N102.

23RP-B-5

MAGNETIC PHASE DIAGRAM OF THE FRUSTRATED TWO - LAYER SYSTEM FERROMAGNET - ANTIFERROMAGNET

Morosov A.I.

Moscow State Institute of Radioengineering, Electronics and Automation
(Technical University), 78, Vernadski Avenue, 119454 Moscow, Russia

The magnetic phase diagram of a thin ferromagnetic film on an antiferromagnetic substrate is considered with account of the energy of single-ion anisotropy. The roughness of the interface between the layers of ferromagnet and uncompensated antiferromagnet, i.e. the presence of atomic steps at the interface, leads to frustration of the exchange interaction between the layers. Indeed, the spins of the ferromagnet located on different sides of a step are in contact with antiferromagnet spins belonging to different sublattices. For any sign of the exchange integral for neighboring spins belonging to different layers, the collinear orientation of ferromagnetic and antiferromagnetic order parameters on one side of the step corresponds to a minimum of the exchange energy of the interface, while on the other side of the step this energy is maximal. So, a frustration occurs that is caused by the atomic step. Thus the atomic steps

divide the interface into the regions of two types: in the regions of the first type the energy is lower at parallel orientation of ferromagnetic and antiferromagnetic order parameters, while in the regions of the second type the antiparallel orientation of the order parameters is preferable.

Within the exchange approximation, such a frustrated system was considered in papers [1,2]: we found the phase diagram of the system and predicted that for a large enough distance between step edges, the frustrations were responsible for 180° domains arising in the film and separated by domain walls of a radically new structure. The domain wall of such a new type is perpendicular to the film plane and coincides with the atomic step edge on the interface, the wall width being defined by the relation of the energies of exchange interaction within the layers and between them. Therefore at film thickness about 1-10 nm, the domain wall width should be of the same order of magnitude. Not far ago, the domain walls of just such a type have been observed experimentally [3,4]. For lower distances between the step edges, the frustration leads to perpendicular orientation of ferromagnetism and antiferromagnetism vectors and the static spin vortices arise at the interface.

It is possible to ignore the anisotropy energy if the characteristic spacing between the steps and the ferromagnetic film thickness are much smaller than the widths of conventional domain walls in the layers. If this condition is violated, one has to specify the orientations of easy axes in both layers and to take into account the anisotropy energy contribution to the system total energy.

The account of the single-ion anisotropy energy leads to a more complicated phase diagram with respect to that one obtained in the exchange approximation. If there is only one easy axis in each layer and the easy axes of film and substrate are parallel to one another, then for lower distances between the step edges a near- 90° Bloch exchange spring along with vortices arise near the interface.

[1] V.D. Levchenko, A.I. Morosov, A.S. Sigov, Yu.S. Sigov. *JETP*, **87** (1998) 985.

[2] V.D. Levchenko, A.I. Morosov, A.S. Sigov. *JETP Lett.*, **71** (2000) 373.

[3] U. Schlickum, N. Janke-Gilman, W. Wulfhekel, J. Kirschner. *Phys. Rev. Lett.*, **92** (2004) 107203.

[4] W. Wulfhekel, U. Schlickum, J. Kirschner. *Microscopy Research Technique*, **66** (2005) 105.

23 June Monday

15:00-17:00

oral session

23TL-B

23RP-B

“Spintronics”

23TL-B-6

ROLE OF INTERFACE RESONANCE STATES ON SPIN DEPENDANT TRANSPORT IN SINGLE CRYSTAL MAGNETIC TUNNEL JUNCTIONS

Schuhl A.

SPINTEC, Grenoble 38000, France

We present fundamental aspects on the physics of spin and symmetry filtering in single-crystal magnetic tunnel junctions. In such systems, the large TMR effect are determined by the different tunnelling mechanisms and symmetry-related decay rates of the Bloch waves for the majority and the minority spin channels, in the bulk but also at the interfaces. It has been shown that the magneto-transport properties of the junctions may be skilfully engineered by adjusting the interfacial chemical and electronic structure.

We then focus on the model system Fe/MgO/Fe, which have been strongly studied in the last decade. Beside the high magneto resistive effect observed in this system, it show several peculiar effects. For extremely small MgO thickness, the equilibrium tunnel transport in Fe/MgO/Fe systems leads to antiferromagnetic interactions. Moreover, the presence of interface states in the energy gap of minority Δ_1 -states has been theoretically predicted. Those states are coupled with the bulk Fe states and become available for conduction for small biased above the Fermi energy.

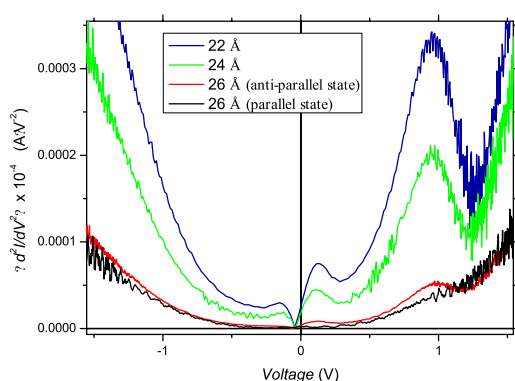


Fig. 1 : The second derivative of $I(V)$ characteristic, performed by using conducting AFM tip, show two peaks (at 0.2 and 1.12 V), but only for the anti-parallel state and by applying a positive biased voltage.

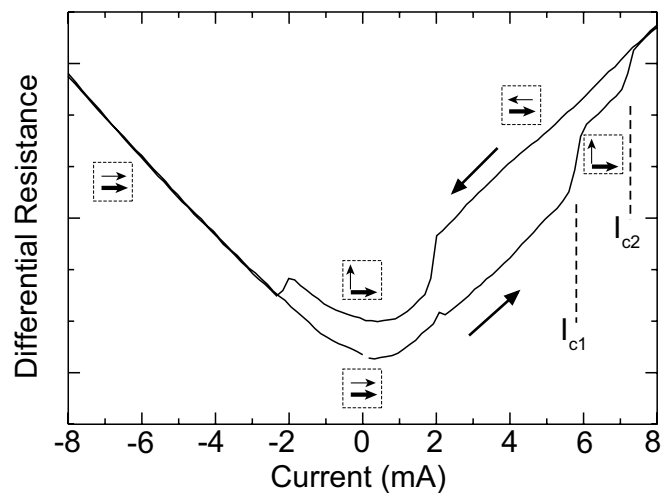
Finally, we discuss the experimental evidences of the role of the interface states on the spin dependant transport, and also on the magnetic interactions, at very low MgO thickness. Recently, we have observed intense sharp features in tunnelling spectra on asymmetric epitaxial Fe/MgO/Fe tunnel junction. Theses peaks are attributed to the density of states to two interface resonant states, both fundamental and first excited state.

23TL-B-7

SPIN-TRANSFER INDUCED DYNAMIC MODES IN SINGLE-CRYSTALLINE Fe/Ag/Fe NANOPILLARS

Bürgler D.E., Lehdorff R., Kakáy A., Hertel R., and Schneider C.M.
 Institut für Festkörperforschung – Elektronische Eigenschaften (IFF-9) and
 JARA-FIT, Research Center Jülich GmbH, D-52425 Jülich, Germany

A spin-polarized current entering into a ferromagnetic material exerts a torque on the magnetization by transferring spin angular momentum from the current to the ferromagnet. This so-called spin-transfer torque (STT) gives rise to current-driven magnetization dynamics with unprecedented properties like the switching of the magnetization without applying an external field or the excitation of persistent large-angle precessions of the magnetization with frequencies in the GHz range. We present measurements and simulations of STT effects in nanopillars containing a thin, circular, single-crystalline Fe nanomagnet with four-fold in-plane magnetocrystalline anisotropy as a free layer. The samples are fabricated from epitaxial, MBE-grown Fe/Ag/Fe(001) layered structures by a combination of optical and e-beam lithography [1]. The Fe(001) nanomagnets have diameters down to 70 nm and a thickness of 2 nm. The magnetocrystalline anisotropy inherent to *bcc*-Fe shows up in measurements of the giant magnetoresistance effect in the CPP geometry (CPP-GMR) and gives rise to a novel two-step switching behaviour. The nanomagnet magnetization consecutively switches at two different critical currents I_{c1} and I_{c2} (see Figure) by 90° from parallel to perpendicular and from perpendicular to antiparallel alignment to the fixed layer magnetization [2]. This feature enables us to investigate the angular dependences of CPP-GMR and STT and to compare them to theoretical predictions [3]. Additionally, the anisotropy gives rise to steady-state precession of the free magnetization at low or even zero applied magnetic field when the magnetizations are perpendicularly aligned. This low-field mode is governed by the interplay between the STT and the anisotropy, while the current-driven dynamics in large fields exceeding the coercive field results from the STT acting against the externally applied magnetic field. The two-step switching behaviour as well as the low-field excitations arise from significant asymmetries of the angular dependences of both CPP-GMR and STT, which have been predicted by Slonczewski [3], but have not been observed simultaneously so far. The asymmetries originate from strong spin accumulation at the Fe/Ag(001) interfaces in agreement with Ref. [4].



This low-field mode is governed by the interplay between the STT and the anisotropy, while the current-driven dynamics in large fields exceeding the coercive field results from the STT acting against the externally applied magnetic field. The two-step switching behaviour as well as the low-field excitations arise from significant asymmetries of the angular dependences of both CPP-GMR and STT, which have been predicted by Slonczewski [3], but have not been observed simultaneously so far. The asymmetries originate from strong spin accumulation at the Fe/Ag(001) interfaces in agreement with Ref. [4].

- [1] H. Dassow, R. Lehdorff, D.E. Bürgler, M. Buchmeier, P.A. Grünberg, C.M. Schneider, and A. van der Hart, *Appl. Phys. Lett.* **89**, 222511 (2006).
- [2] R. Lehdorff, M. Buchmeier, D.E. Bürgler, A. Kakáy, R. Hertel, and C.M. Schneider, *Phys. Rev. B* **76**, 214420 (2007).
- [3] J.C. Slonczewski, *J. Magn. Magn. Mater.* **247**, 324 (2002).
- [4] M.D. Stiles and D.R. Penn, *Phys. Rev. B* **61**, 3200 (2000).

23TL-B-8

CURRENT-INDUCED MAGNETIZATION DYNAMICS IN NANOMAGNET*Ono T.*

Institute for Chemical Research, Kyoto University, Uji 611-0011, Japan

The manipulation of magnetization by spin currents is a key technology for future spintronics. The underlying physics is that spin currents can apply a torque on the magnetic moment when the spin direction of the conduction electrons has a relative angle to the local magnetic moment. This leads us to a general concept that any type of spin structure with spatial variation can be excited by a spin-polarized current in a ferromagnet. We confirmed this concept for two typical noncollinear spin structures: magnetic domain wall (DW) [1]-[5] and magnetic vortex [6], [7].

Support by MEXT, JSPS, and NEDO is acknowledged.

- [1] A. Yamaguchi *et al.*, Phys. Rev. Lett. **92**, 077205 (2004).
- [2] A. Yamaguchi *et al.*, Appl. Phys. Lett. **86**, 012511 (2005).
- [3] A. Yamaguchi *et al.*, Jpn. J. Appl. Phys., **45**, 3850 (2006).
- [4] A. Himeno *et al.*, Appl. Phys. Lett. **87**, 243108 (2005).
- [5] H. Tanigawa *et al.*, Appl. Phys. Express **1**, 011301 (2008).
- [6] S. Kasai *et al.*, Phys. Rev. Lett. **97**, 107204 (2006).
- [7] K. Yamada *et al.*, Nature Materials **6**, 269 (2007).

23RP-B-9

A NEW METHOD FOR THE CALCULATION OF THE THERMAL STABILITY PARAMETER OF EXCHANGE-COUPLED TRILAYERS*Han J.K., Lee D.H., Kim K.S., and Lim S.H.*

Department of Materials Science and Engineering, Korea University, Anam-dong,
Seongbuk-gu, Seoul 136-713, Korea

There has been an increase in the use of an exchange-coupled trilayer with antiparallel magnetization alignment (often called synthetic antiferromagnet, composed of two magnetic layers separated by a nonmagnetic spacer) as a free layer structure in advanced device applications. Recently, exchange-coupled trilayers were used as a free layer structure in the current-induced magnetization switching (CIMS) of MgO-based magnetic tunnel junctions (MTJs) [1]. This indicates that exchange-coupled trilayers show significant potential for use as a high-density spin-transfer torque (STT) magnetic random access memory (MRAM) [2]. Although the thermal stability of high density MRAM is of critical concern, it is somewhat difficult to estimate the thermal stability parameter of exchange-coupled trilayers. This is mainly due to the poor definition of their anisotropy and magnetic volume. The main aim of this talk is to develop a new method for the calculation of the thermal stability parameter of exchange coupled trilayers. The key to this approach is the use of the total energy, including the magnetostatic energy expressed in an *analytical* form. When the total energy is in an analytical form, it is a relatively straightforward task to obtain the magnetic energy (and hence the thermal stability parameter). The magnetic energy is simply the energy barrier along the *lowest* energy

path linking the two energy minima (or two stable or metastable states). Since magnetostatic fields such as the self-demagnetizing field and interlayer magnetostatic field are very non-uniform, it will be difficult to express the total energy in a simple analytical form. This difficulty was overcome with the use of the *effective* magnetostatic fields by averaging over the entire magnetic volume. In this sense, the present approach is a hybrid one, combining an analytical method with a numerical method. The present was applied to a nanostructured exchange-coupled trilayer, Co-Fe-B (2 nm)/Ru (0.6 nm)/Co-Fe-B (2 nm) with lateral dimensions of 160 nm × 80 nm, as a free layer structure in MgO-based MTJs, where the experimental result for the thermal stability parameter is available [1]. Micromagnetic simulation is performed in order to obtain the equilibrium magnetic configuration, from which the effective magnetostatic fields are obtained. These are acquired by averaging over the entire magnetic layers and they are then used as inputs in an analytical equation for the total energy. Systematic calculations are performed, even considering the effects of edge rounding during nanofabrication and the thermal stability parameter is calculated to be within the range of 62 ~ 69, which concurs with the value of 68, as reported in the literature from the current induced magnetization switching experiments obtained by using the Slonczewski equation.

The Korea Science and Engineering Foundation (KOSEF) supported this work through the National Research Laboratory program, which is funded by the Korean Ministry of Science and Technology (Project No. M10600000198-06J0000-19810).

[1] J. Hayakawa et al., *Jpn J. Appl. Phys.*, **45** (2006) L1057.

[2] T. Kawahara et al., *Jpn J. Appl. Phys.*, in Proc. IEEE Int. Solid-State Circuits Conf. Dig. Tech. Papers, Feb. 2007, pp. 480-481.

23RP-B-10

MAGNETIC HETEROJUNCTION QUANTUM AMPLIFIER PUMPED BY SPIN-POLARIZED CONDUCTION ELECTRONS CURRENT

Ustinov V.V., Viglin N.A.

Institute of Metal Physics, Ural Division of Russian Academy of Sciences, Ekaterinburg, Russia

A promising idea to use the spin-polarized conduction electrons transport in a magnetic hetero-structure (MHS) for the inversion of charge carrier spin level occupancies in one of its layers to create an active environment for the electromagnetic radiation enhancement has been realized in a number of FMC/SC structures, where FMC is a ferromagnetic conductor and SC is a semiconductor. The *n*-InSb single crystals, possessing high mobility of charge carriers, a narrow ESR line and an anomalously high absolute value negative g-factor ($g = -52$), were used as SC. The following materials were used as FMC playing a role of electron polarizer: (i) Geisler alloys Co_2MnSn ($T_C = 826\text{K}$), Ni_2MnSn ($T_C = 340\text{K}$) and Co_2MnSb ($T_C = 478\text{K}$), (ii) ferromagnetic semiconductors $\text{EuO}_{0.98}\text{Gd}_{0.02}\text{O}$ ($T_C = 130\text{K}$) and HgCr_2Se_4 ($T_C = 120-130\text{K}$), (iii) manganites $\text{La}_{0.8}\text{Ba}_{0.2}\text{MnO}_3$ ($T_C = 250\text{K}$) and $\text{La}_{0.8}\text{Sr}_{0.2}\text{MnO}_3$ ($T_C = 308\text{K}$). We have demonstrated that the spin-polarized electrons injection into the *n*-InSb semiconductor from the above-mentioned ferromagnetic materials results in generation of the laser-type electromagnetic radiation.

The power P of the registered radiation is up to several tens microwatts. The radiation power $P(B, I)$ as a function of the magnetic field induction B and current I for all the MHS used is of a threshold character. The emission has been observed in the temperature range from 4.2 to T_C for the *n*- $\text{EuO}_{0.98}\text{Gd}_{0.02}\text{O}$ - and *p*- HgCr_2Se_4 -based MHS and in the range of 160 - 180 K for the

rest ones. In the most of MHS the radiation power slightly decreased down to the temperatures mentioned, and after that drastically fell down to zero. The radiation is observed only in case when electrons flow into a semiconductor from a spin polarizer. The results repeatability obtained using different materials as a spin polarizer allows to state that the phenomenon observed is determined mainly by the properties of ferromagnetics FMC and that of semiconductor SC, and to the less extent depends on the ohmic contact characteristics.

We demonstrate that the experimental results concerning the radiation power dependence on current and magnetic field are satisfactorily described in a model of light amplification by virtue of induced transitions in a medium with the inverse occupancy.

The conclusion that the radiation emission results from radiative transitions between the Zeeman levels is confirmed by the radiation frequency spectral analysis and by the measurement of the output power dependence on an angle between the magnetic field direction and the n -InSb crystal axes. It has been demonstrated that the radiation frequency corresponds to the transitions of conduction electrons ($|g|=52$) at Zeeman levels. A good agreement has been established between angle dependences of radiation power and probability of electro-dipole spin resonance on Zeeman levels of conduction electrons, testifying that the radiation occurs at electro-dipole transitions. This fact can be of great significance at the realization of laser generation, as the probability of induced electro-dipole transitions is by several orders of magnitude higher than that of magneto-dipole ones.

Thus, a new type of a solid state maser has been realized, namely, the spin injection maser controlled in frequency by a magnetic field and operating in a millimeter and submillimeter wave length range.

The research was partly supported by grants of RFBR and RAS.

23 June Monday

12:00-13:30

oral session

23TL-C

“Metamaterials”

23TL-C-1

ELECTRODYNAMIC MODELS OF THIN - LAYER METAMATERIALS AND RELATED DEVICES

Lagarkov A., Kisel V.

Institute for Theoretical and Applied Electromagnetics, Russian Academy of Sciences
Izhorskaya 13, Moscow, 125412, Russia

Some results of theoretical and practical investigations of thin-layer metamaterials, modeling and introduction of super-resolution devices are discussed in this review. Rigorous electrodynamic models not based on composite homogenization are proved preferable for modeling devices with metamaterials. It is shown that the application of averaged effective parameters is incorrect for investigating fields with point sources located in the vicinity of composite thin layers with resonance inclusion sizes comparable with the sample thickness. In this case the super-resolution is achieved due to a selective response of the “conductor-ring” pair to different (propagating and evanescent) field components. In comparing real composites and hypothetical homogeneous “metamaterial” parallels and differences are presented. As the result of electrodynamic modeling and numerical calculations it is proved possible to compensate losses in metamaterials with the help of active type inclusions; it is shown that those possibilities for “metamaterials” and real composites differ considerably. It is demonstrated that thin layer metamaterials permit to produce efficient devices in microwave field and to solve tasks of electromagnetic compatibility and data processing

23TL-C-2

HIGHLY LUMINESCENT MAGNETO - OPTICAL GARNETS: TOWARDS INTELLIGENT MAGNETO-OPTICS

Grishin A.M., Khartsev S.I.

Department of Condensed Matter Physics, Royal Institute of Technology,
SE-164 40 Stockholm-Kista, SWEDEN

Recently significant progress has been achieved in the synthesis of high performance all-garnet magneto-optical photonic crystals [1] and broad-color luminescent Er_2O_3 films [2]. These findings raise a challenging task to engineer garnet crystals that combine lasing/amplifying and non-reciprocal optical properties with a remanence. Luminescent magneto-optical garnets promise built-in *intelligence*: ability simultaneously recognize, process and store optical data, make color filtering and amplify optical signals. Novel epitaxial Er-doped $\text{Bi}_3\text{Fe}_5\text{O}_{12}$ and rare earth gallium garnet films were grown by rf-magnetron sputtering and pulsed laser deposition techniques. Under 514 nm and 980 nm pumping both magneto-optical iron based and non-magnetic gallium based garnet films show strong room temperature luminescence in the C-band at 1550 nm whereas the $^4I_{11/2} \rightarrow ^4I_{15/2}$ transitions appear to be very different. Luminescence at 980 nm was observed only in rare earth gallium garnets. Very fast multi-phonon decay of $^4I_{11/2}$ manifold due to relatively higher phonon energies completely extinguishes 980 nm luminescence in $\text{Er}:\text{Bi}_3\text{Fe}_5\text{O}_{12}$ films. A number of different pumping and lasing schemes can be realized through the proper design of Er-doped $[\text{Bi}_3\text{Fe}_5\text{O}_{12}/\text{Re}_3\text{Ga}_5\text{O}_{12}]^m$ photonic crystals: localizing light either in optically dense $\text{Bi}_3\text{Fe}_5\text{O}_{12}$ cavity or in $\text{Bi}_3\text{Fe}_5\text{O}_{12}$ mirrors in crystals with transparent $\text{Re}_3\text{Ga}_5\text{O}_{12}$ cavity.

- [1] S.I. Khartsev, A.M. Grishin, *J. Appl. Phys.* 101, 053906 (2007) and references therein.
[2] A.M. Grishin, E.V. Vanin, O.V. Tarasenko, S.I. Khartsev, P. Johansson, *Appl. Phys. Lett.* 89, 021114 (2006).

23TL-C-3

NEAR FIELD SENSORS AND MEMORY

Lozovik Yu.E., Merkulova S.P., Klyuchnik A.V., Kolesnikov A.A., Merkulov A.L.
Institute of Spectroscopy, 140190 Moscow region, Troitsk, Russia
e-mail: lozovik@isan.troitsk.ru

We studied optical near field based ultrahigh density memory both experimentally, theoretically and by computer simulations. Sensors based on near fields are also considered.

We consider three physical realizations: 1. apertureless near field originated by irradiation of STM tip by external laser pulses, 2. fiber based aperture near field, 3. near field created by fiber laser, 4. subwavelength hole array in metal film.

Large enhancement of local field (“hot spot”) of femtosecond laser pulses near tip of scanning probe microscope (SPM) was demonstrated. Spatial resolution better than $\lambda/40$ (λ is incident wavelength) was achieved in apertureless near field based nanolithography.

Enhancement of the electromagnetic field under the tip of a scanning probe microscope disposed over a substrate is analyzed in detail, arising due to the tip geometry (“lightning rod effect”) and to resonance excitation of local plasmon eigenmodes in the tip - substrate system.

Detailed FDTD calculations of local field enhancement of laser pulses for different systems to achieve optimal regime and configuration were performed. The spectrum of local plasmons is analyzed in detail for SPM tip – substrate system. The spatial structure of apertureless near field under the tip and far field are investigated for various external field sources in optical range - incident plane wave, decaying total internal reflection field, and dipole field of a nanoparticle placed near the tip.

Different physical processes under STM tip, excited by laser pulses are discussed.

We discuss possible uses of field enhancement in the subwavelength range for nanooptics, nanolithography and other nanotechnology applications. Other methods for excitation of plasmons to achieve ultrahigh spatial resolution will be considered.

We discuss possible methods of enhancement of near field optics sensitivity for sensor creation.

- [1] Lozovik Yu.E., Merkulova S.P, *Uspekhi Fiz.Nauk* 169, 348 (1999). (transl.:Physics-Uspekhi 42, N3 (1999))
[2] Yu.E. Lozovik and A.V. Klyuchnik, The dielectric function and collective oscillations inhomogeneous systems, in: “The Dielectric Function of Condensed Systems”, edited by L.V. Keldysh, et.al, Elsevier Science Publisher B.V.

23 June Monday

15:00-17:00

oral session

23TL-C

23RP-C

**“High Frequency
Properties”**

23TL-C-4

MICROWAVE AND MAGNETOSTATIC PROPERTIES OF MULTI-LAYER IRON-BASED FILMS

Iakubov I.T., Lagarkov A.N., Maklakov S.A., Osipov A.V., Rozanov K.N., Ryzhikov I.A., Samsonova V.V., Sboychakov A.O.

Institute for Theoretical and Applied Electromagnetics RAS, Izhorskaya 13,
Moscow 125412 Russian Federation

Thin ferromagnetic films with in-plane magnetic anisotropy are promising materials in view of obtaining high microwave permeability [1]. Magnetic properties of single-layer Fe-N films have been presented in [2]. Multi-layer films are advantageous over single-layer films in diminishing the effects of eddy currents and out-of-plane magnetization with the same or higher content of iron in the film [3]. The presentation reports on an experimental study of microwave and magnetostatic properties of multi-layer iron-based films.

The multi-layer films under study are deposited onto a 10 μm thick mylar substrate by a magnetron sputtering process performed in Ar atmosphere with controlled N_2 admixture. To produce laminated films, sputtered iron layers of 0.03–0.3 μm in thickness are alternated with SiO_2 layers of the same thickness. The microwave permeability is measured in the frequency range of 0.1 to 10 GHz by coaxial technique [4] that involves winding a film into a roll to produce a washer-shaped sample.

In multi-layer films, the damping factor of the ferromagnetic resonance is observed to increase as compared to that in single-layer films. The magnetoelastic effect is found to have a significant effect on the microwave properties of the wound samples used in the coaxial measurement.

To produce a bulk sample, the multi-layered films are stacked together and glued. Microwave permeability is measured in a rectangular waveguide. Magnetization curves of multi-layer films and the stacked sample are measured by a vibration sample magnetometer.

The measured static and microwave magnetic properties of the stack are found to be not equal to a sum of the properties of constituent films. This is an evidence for interactions between magnetic layers and is obtained even in case when interlayers between magnetic films are very thick, up to 10 μm . A theoretic model is developed to account for dipolar interactions between iron films in a multi-layer system. The model explains the anomalously high demagnetization field of the stack observed in the measurements.

Support by RFBR under grant 05-08-01212 is acknowledged.

[1] I.T. Iakubov, A.N. Lagarkov, S.A. Maklakov, A.V. Osipov, K.N. Rozanov, I.A. Ryzhikov, and S.N. Starostenko, *J. Magn. Magn. Mater.*, 300 (2006) e74.

[2] A.N. Lagarkov, I.T. Iakubov, I.A. Ryzhikov, K.N. Rozanov, N.S. Perov, E.P. Elsukov, S.A. Maklakov, A.V. Osipov, M.V. Sedova, A.M. Getman, A.L. Ulyanov, *Physica B: Condens. Matter.*, 394 (2007) 159.

[3] I.T. Iakubov, A.N. Lagarkov, S.A. Maklakov, A.V. Osipov, K.N. Rozanov, I.A. Ryzhikov, D.A. Petrov, and S.N. Starostenko, *J. Magn. Magn. Mater.*, 316 (2007) e813.

[4] K.N. Rozanov, N.A. Simonov, and A.V. Osipov, *J. Commun. Techn. Electron.*, 47 (229) 2002.

23TL-C-5

ON THE DETERMINATION OF THE PERMEABILITY TENSOR OF MAGNETIZED MATERIALS. APPLICATION TO THE DESIGN OF NONRECIPROCAL AND TUNABLE MICROWAVE DEVICES

Quéffélec P.¹, Guennou A.¹, De Blasi S.¹, Gelin P.²

¹Lab-STICC, University of Brest, 6 av. Le Gorgeu, CS 93837, 29238 Brest cedex 3 - France

²Lab-STICC, Telecom Bretagne, Technopôle Brest Iroise, BP 832, 29285 Brest cedex - France

Magnetized materials are widely used for the realization of microwave signal processing functions. They are at the very basis of the nonreciprocal effect in gyromagnetic devices (circulators, isolators). They are very good candidates for introducing new functionalities in RF circuits: tunability and miniaturization of filters, antennas, *etc.*

In practice, the nonreciprocity or the tunability of the device is obtained by applying an external dc magnetic field (fixed or variable in strength) on the magnetic sample integrated in the circuit. Magnetized polycrystalline ferrites or magneto-dielectric composites are anisotropic media due to the alignment of the magnetic moments in the dc field direction. Thus, their permeability is a tensor quantity and the design of a magnetic microwave device requires very accurate knowledge of this tensor. The off-diagonal components of the permeability tensor have often been ignored in the literature. This is partly due to the analytic complexity of handling such expressions and the difficulty in measuring them. Although they are negligible in some materials (thin layers with in-plane anisotropy), they can be large for others, with a magnitude of the same order than the diagonal terms. Moreover, for nonreciprocal devices where the magnetic material is assumed to be saturated by permanent magnets, studies have demonstrated the unsaturated character of regions in the ferrite puck due to the non-uniformity of the demagnetized fields and of the dc bias field [1], [2]. In that case, the analytical expressions commonly used to compute the frequency and dc-field dependences of the permeability tensor components of saturated media (Polder formulations) are not valid anymore.

In such a context, the design of microwave devices using magnetized materials needs the achievement of theoretical and experimental tools enabling the prediction and measurement of their dynamic behavior whatever their magnetization state. Up to now, no commercial electromagnetic simulator, no theoretical approach proposed in the literature, has been able to reach such a level of accuracy in the description of magnetized materials. Yet this condition is essential to the optimization of magnetic microwave device performances in terms of electromagnetic characteristics (band-width, insertion losses, operating frequency, tunability,...), size and cost.

In this review paper, we shall briefly recall the main microwave applications of magnetized materials. We shall present the theories developed to predict their dynamic behavior [3]. Then the measurement methods that enable us to compare the theoretical results with experimental data will be described. Prospects about the needs in new microwave magnetic materials for future applications will be finally discussed. We shall focus these prospects on self-biased ferrites for circulators and new magneto-dielectric composites for tunable functions, exhibiting permeability shifts under the action of a dc voltage through the piezoelectric/magnetostrictive inverse effects [4].

[1] A. Guennou *et al.*, *IEEE Transactions on Magnetics*, **43**, Sept. 2007.

[2] H. How *et al.*, *IEEE Trans. Microw. Theory Tech.*, **47**, Oct. 1999.

[3] P. Gelin, and P. Quéffélec, *IEEE Transactions on Magnetics*, **44**, Jan. 2008.

[4] S. De Blasi *et al.*, *IEEE Transactions on Magnetics*, **43**, June 2007.

23RP-C-6

HIGH-FREQUENCY BEHAVIOR OF MAGNETIC COMPOSITES

*Rozanov K.N.^{*1}, Lagarkov A.N.¹, Osipov A.V.¹, Petrov D.A.¹, Starostenko S.N.¹,
and Yelsukov E.P.²*

¹Institute for theoretical and applied electromagnetics RAS, Izhorskaya ul. 13, Moscow, Russia

²Physical-Technical Institute, Ural Branch of Russian Academy of Sciences, Izhevsk, Russia

*corresponding author, e-mail: k_rozanov@mail.ru

Developing composites with a good microwave magnetic performance is an important problem in view of many applications. In most magnetic composites, the frequency and concentration dependences of the microwave permeability are in agreement with the Maxwell Garnet mixing rule. This is attributed to the fact that the permeability contrast in the composite, i.e., the ratio of permeability of inclusions to that of the host matrix, is low at microwaves.

In many applications of microwave materials, the performance depends on both permittivity and permeability of the material. When the intrinsic permittivity of conductive inclusions is very high, the Maxwell Garnet mixing rule fails to provide an agreement with the permittivity data on a composite filled with such inclusions. For this case, more elaborated mixing rules, such as the Doyle–Jacobs model and Musal’s model have been introduced to predict the microwave properties of composites.

An example is presented of comparison of mixing laws with measured data on microwave frequency dispersion of permeability in magnetic composites. The composites under study are filled with iron powder, which is prepared by mechanical milling. The permittivity and permeability are measured by a coaxial technique in the frequency range of 0.01 to 3 GHz. The effective material parameters of the composites are shown to be affected greatly by the shape distribution of the powder particles. The measured data are compared to various mixing rules, such as Maxwell Garnet mixing rule, Doyle–Jacobs mixing rule, and the Ghosh–Fuchs theory, which is based on the Bergman–Milton spectral theory of composites. The Maxwell Garnet mixing law fails to approximate both the permittivity and permeability data. The Doyle–Jacobs mixing rule is shown to produce fake regions of magnetic frequency dispersion in many occasions. In contrast, the Ghosh–Fuchs theory provides an excellent agreement with the measured permittivity and permeability of the composites. The proposed analysis of the measured data on the frequency dependence of permittivity and permeability allows the frequency dependence of intrinsic permeability of the powder to be reconstructed.

Authors acknowledge partial support of the work from RFBR, grants nos. 06-08-00788 and 07-08-92111.

23RP-C-7

ENGINEERING OF FERRITE - BASED COMPOSITE MATERIALS FOR SHIELDING ENCLOSURES

Koledintseva M., Drewnia J., Zhang Y.

Missouri University of Science and Technology (former University of Missouri-Rolla), Rolla, Missouri, 65401, USA

A design of non-conductive absorbing shielding enclosures and gaskets for improving immunity of electronic equipment is important from the point of view of eliminating possible surface currents as culprits of undesirable emission. Combining dielectric or conducting inclusions with ferrite particles in a composite absorbing material may substantially increase the absorption level in the frequency range of interest. This paper presents an analytically modeled magneto-dielectric material with both frequency-dispersive permittivity and permeability (properties of this material will be specified), and a full-wave numerical model of a complex-shaped shielding structure that contains this magneto-dielectric material. The analytical model is based on the Maxwell Garnett rule for dielectric mixture, and on the Bruggeman's effective medium theory for permeability of a ferrite powder embedded in a dielectric host. Frequency dependencies of real and imaginary parts of effective permittivity and permeability of a composite, as well as shielding effectiveness (S.E.) for an infinitely wide sheet of this material with a given thickness and a normally incident plane wave have been modeled. After a composite with acceptable frequency characteristics is modeled, its permittivity and permeability are approximated by sums of Debye-like terms using a Genetic Algorithm optimization procedure [1], and then they are used in the full-wave numerical electromagnetic simulations of the geometry of interest.

The numerical model employs the EZ-FDTD code, developed by the UMR and IBM, and based on the finite-difference time-domain technique [1]. To treat simultaneously frequency dispersive permittivity and permeability, a new algorithm based on auxiliary differential material equations, discretized both in space and in time, has been implemented.

The geometry that contains a composite magneto-dielectric strip 50 mm wide and 3 mm thick in a gap (stitch) of the same size between two wide overlapping metal plates [2] has been modeled. The results of computations (Fig.1) show a

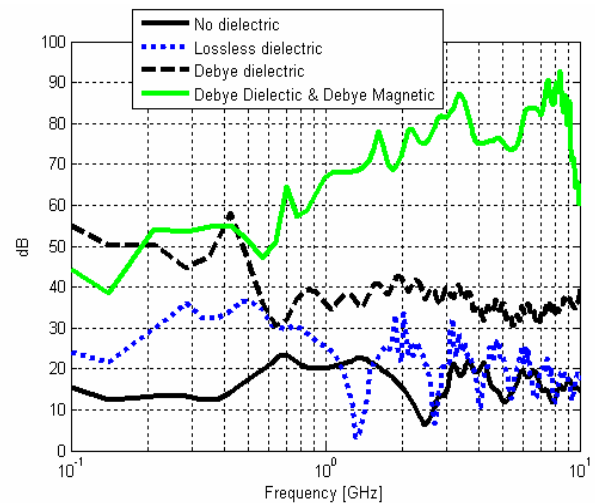


Figure 1. Shielding effectiveness in terms of E-field

substantial increase in the structure's S.E., compared to the cases of overlapping plates without any absorbing material, or with a dielectric material exhibiting the same permittivity as the effective permittivity of the modeled magneto-dielectric material. The results for a rectangular parallelepiped shielding enclosure will be provided in the full paper.

[1] M.Koledintseva, P.Ravva, et. al., *Proc. IEEE Int. Symp. Electromag. Compat.* Aug. 2005, Chicago, USA, vol. 1, 169-174.

[2] M. Koledintseva, S. Chandra, J.Drewniak, J.Lenn, *Int. IEEE Symp. Electromag. Compat.*, July, 2007, Honolulu, USA.

23TL-C-8

ON THE HIGH-FREQUENCY MEASUREMENT OF THE DYNAMIC PROPERTIES OF NANO-PARTICLE COLLOIDS

Fannin P.C.

Department of Electronic and Electrical Engineering, Trinity College, Dublin 2, Ireland

Ferrofluids are composed of colloidal suspensions of nano-sized particles in a carrier liquid and as such are ideally suited as a medium for the study of the magnetic properties of the constituent particles. In particular measurements in the MHz to GHz range of the ac complex susceptibility, $\chi(\omega) = \chi'(\omega) - i\chi''(\omega)$, by means of the transmission line technique [1, 2], enables one to study the resonant (f_{res}) properties of the samples under investigation. Also, by studying the behaviour of f_{res} in response to the application of an increasing external polarising field, from 0- H A/m in regular steps, one can obtain accurate data on the mean value of anisotropy constant, K , anisotropy field, H_A , gyromagnetic constant γ , and the damping parameter, α . Furthermore by then reducing the polarizing field from H to 0 A/m one can investigate the presence of any hysteresis effect which may arise due to the effect of the cyclic polarizing field.

From data on the imaginary component, $\chi''(\omega)$, one can determine the loss tangent, $\tan \delta$, of the samples and also a value of the precessional decay time τ_0 .

The transmission line technique is also suitable for the investigation of the magnetic properties of composite samples, thereby enabling an absorption peak in a chosen frequency range to be obtained.

In this paper a review of the above mentioned topics are presented with examples of results obtained for a number of samples, including colloidal suspensions of magnetite, manganese ferrite, nickel zinc ferrite and cobalt nano-particles, being presented.

[1] S.Roberts and A.R.von Hippel, *J. App.Phys.*, **17**, (1946) 610.

[2] P.C. Fannin, T. Relihan and S.W. Charles, *J. Phys. D:Appl. Phys.* **28**, (1995) 2003.

23 June Monday

12:00-13:30

15:00-17:00

oral session

23TL-D

23RP-D

**“Magneto-caloric Effect
and Shape Memory”**

23TL-D-1

MAGNETIC SHAPE-MEMORY AND MAGNETOCALORIC EFFECTS CLOSE TO FIRST ORDER TRANSITIONS IN HEUSLER-BASED MATERIALS

Acet M.¹, Aksoy S.¹, Wassermann E.F.¹, Moya X.², Mañosa L.², Planes A.²
¹Experimentalphysik, Universität Duisburg-Essen, 47048 Duisburg, Germany
²Universitat de Barcelona, 08028 Barcelona, Catalonia

Applying a magnetic field to ferromagnetic systems in the temperature vicinity of a first order structural transition can lead to magnetic field induced structural modifications and large magnetocaloric effects. Ni-Mn-Ga Heusler-type alloys are prototypes for systems showing large magnetic field induced strains related to twin boundary motion in the martensitic state, otherwise known as the magnetic shape memory effect. However, large magnetic field induced strain is not limited to Ni-Mn-Ga, and there is a rich variety of Heusler alloys that exhibit similar properties. In fact, practically any Heusler-based ferromagnetic alloy having the appropriate off-stoichiometric composition will undergo a first order martensitic transformation. When a field is applied close to the transition, not only are large strains induced, but also large magnetocaloric effects are observed. In many of these systems, the field-induced strain is due to a field induced reverse martensitic transformation to the austenitic state, rather than to twin boundary motion within the martensitic state. Also the magnetocaloric effect rather than being conventional, in which case a sample would heat on applying a magnetic field adiabatically, is an ‘inverse’ magnetocaloric effect, where the sample cools on applying a field. We discuss the mechanism of the inverse magnetocaloric effect and its relationship to the martensitic transformation.

23TL-D-2

PHASE TRANSITION AND MEMORY BEHAVIOR IN FERROMAGNETIC SHAPE MEMORY ALLOYS CHARACTERIZED BY HIGH-ENERGY X- RAY AND NEUTRON DIFFRACTION TECHNIQUES

Wang Y.D.¹, Ren Y.², Brown D.W.

¹Key Laboratory for Anisotropy and Texture of Materials (Ministry of Education),
Northeastern University, Shenyang 110004, China

²X-ray Science Division, Argonne National Laboratory, Argonne, IL 60439, USA

³Los Alamos Neutron Scattering Center, Los Alamos National Laboratory, NM 87545, USA

Materials that can reversibly change their dimension upon the application of external fields, such as magnetic or electric fields, have been used as actuators or sensors in many applications. Among them are magnetic-driven shape-memory alloys, which can be deformed by a magnetic field. The possibility of a magnetic-field control of the shape-memory effect has been demonstrated in the ferromagnetic Ni-Mn-Ga and Ni-Co-Mn-In alloys with a composition close to the Heusler structure. The synchrotron high-energy X-ray diffraction method and neutron diffraction technique based on the pulsed neutron source provide the ability to trace *in-situ* changes in the crystallographic structures and microstructures under the various environments (temperature, stress, and magnetic fields). In this presentation, some new progresses on the *in-situ* investigations of the phase transformation in the ferromagnetic shape memory alloys (FMSAs) and the FMSAs composites will be presented in all aspects, covering from the change

in structures, the phase-transformation kinetics, to the microstructural characteristics and selections of martensitic variants under the interactions of multiple external fields.

We greatly appreciate the financial supports by the National Natural Science Foundation of China (NSFC) (Grant Nos. 50725102 and 50531020) and the Ministry of Education of China.

23TL-D-3

THERMOELASTIC AND MAGNETIC PROPERTIES OF NiMnSn HEUSLER ALLOY

*Khovailo V.¹, Koledov V.¹, Kuchin D.¹, Shavrov V.¹, Zolotarev V.¹,
Kalashnikov V.¹, Afonina V.¹, Long Y.², Bao B.²*

¹Institute of Radioengineering and Electronics of RAS, 125009, Moscow, Russia

²School of Materials Science and Engineering, University of Science and Technology of Beijing 100083, People's Republic of China

The phenomena of magnetic field controlled shape memory effect (SME) and giant magnetocaloric effect (GMCE) are intrinsic properties of several ferromagnetic compounds with structural transitions. The new SME and GMCE alloys family Ni-Mn-Sn has attracted much interest in the recent years due to unclear nature of magnetic and structural transitions and high sensitivity of martensitic transition to magnetic field [1,2]. The subject of the report is the detailed study of SME, GMCE and other martensitic transition related phenomena in polycrystalline Ni₅₃Mn₃₄Sn₁₃ alloy.



a



b

Fig.1. Reversible change of surface relief of Ni₅₃Mn₃₄Sn₁₃ sample at transition from martensite (a) to austenite (b).

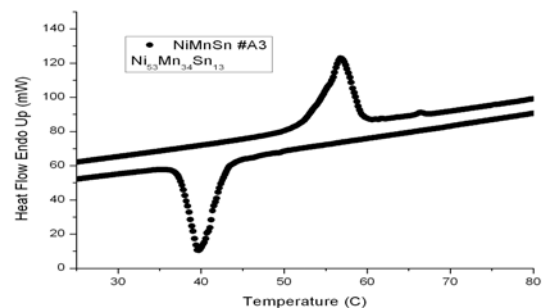
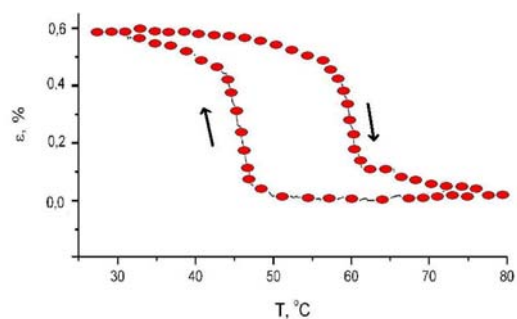


Fig.2. Thermoelastic martensitic transition and SME in Ni₅₃Mn₃₄Sn₁₃ alloy studied by strain-temperature measurements (a) and DSC (b).

The samples of Mn₅₃Ni₃₄In₁₃ alloy were produced by arc melting as described in [3]. The metallographic microscopic study (Fig. 1), DSC (Fig. 2 b) and low field magnetic susceptibility

measurements reveal the martensitic transition well above room temperature. The thermoelastic properties under bending stress were studied by the three point technique [4]. The typical strain vs. temperature dependence shows pure SME (Fig. 2a). The effects of magnetic fields on the martensitic twin structure and SME in $\text{Mn}_{53}\text{Ni}_{34}\text{In}_{13}$ are outlined in the report.

Support by RFBR grants Nos. 06-02-16266, 06-02-39030, 06-02-16984, is acknowledged.

- [1] Y. Sutou, et al. *Appl. Phys. Lett.* **85**, 4358 (2004).
 [2] T. Krenke, M. Acet, et al. *Phys. Rev.* **B72**, 014412 (2005).
 [3] V. Khovailo et al. *Mater. Sc. Eng. A.* **481-482** 322 (2008).
 [4] F. Albertini, et al. *J. Communications Technology and Electronics* **50**, 638 (2005).

23TL-D-4

MAGNETIC POWER CONVERSION WITH MACHINES CONTAINING FULL OR POROUS WHEEL HEAT EXCHANGERS

Egolf P.W., Kitanovski A., Diebold M., Gonin C., Vuarnoz D.

University of Applied Sciences of Western Switzerland, Thermal Sciences Institute IGT-SIT,
Route de Cheseaux 1, CH 1401 Yverdon les Bains, Switzerland

This article consists of two parts, a first part explaining the technology by the Curie wheel principle. If the wheel is stabilized by levitation, it corresponds to Palmy's wheel. These wheels show a full structure and, therefore, their uptake of heat by a flame (Curie wheel) or by solar light absorption (Palmy wheel) only on the periphery of their surface is very limited. Because of this, a variation of the principle as today applied in magnetic refrigerators by introducing a convective heat transfer into porous structures is proposed. By this the power conversion from the heat flux to mechanical power (and further to electric power) is much increased.

For the presented study the Curie and Palmy wheels yield the theoretical basis. A new thermodynamic theory is presented, which leads to a nonlinear ordinary differential equation which has periodic analytical solutions. These solutions describe the temperature field, which further on defines the magnetization distribution. With the magnetic field and the magnetization the force field is given. From this the total moment and torque are derived. The moment is the forcing term of a nonlinear pendulum equation describing the self-excited oscillatory and rotational mode of the wheel. Theoretical results are compared with experimental data obtained by Palmy.

The second main objective of the presentation and article is to present different applications of heat utilization, where magnetic power conversion presents a good alternative to conventional power conversion technologies. A selection of magnetic power conversion systems, which are most feasible and economic, is listed. Magnetic power generator machines based on permanent and superconducting magnets are analyzed for numerous heat source temperatures, magnetic field strength and rotational frequencies. The special analysis takes advantage of a new derived model, which permits to determine the thermodynamic efficiency, the exergy efficiency, the total mass and volume of a magnetic power conversion system. Preliminary results show that systems based on permanent magnets are limited to approximately 140-160°C heat source temperature, whereas systems with superconducting magnets could permit a much wider range of applications with an upper limit at approximately 600°C heat source temperature, if a magnetic field of 10 Tesla magnetic flux density is applied. This study shows that magnetic power conversion could beat conventional technologies in many aspects. This is especially the

case for low exergy heat sources, where most of the conventional energy conversion technologies cannot even operate. In contrast the magnetic power conversion technology for these sources leads to a high exergy efficiency of energy conversion. Despite of the low thermodynamic efficiency of machines operating with such sources, the available energy potential is nearly unlimited large. Another advantage of magnetic power conversion machines is that they work favourable with a temperature difference actually independent of the height of the temperature levels of the source and sink.

The Swiss Federal Office of Energy is acknowledged for their funding and support.

[1] M. Diebold, A. Kitanovski, D. Vuarnoz, P.W. Egolf, 2007. Second Workshop on Magnetostrictive Materials and Magnetic Refrigeration, 13-15 August, Vienna, Austria, 15-16.

23RP-D-5

A LANDAU-TYPE PARAMETRIZATION OF THE EQUATION OF STATE OF A FERROMAGNET

Kuzmin M.

Leibniz-Institut für Festkörper- und Werkstoffforschung, Dresden D-01171, Germany

An approximate equation of state is proposed for ferromagnets, with particular reference to magnetic refrigerants such as gadolinium. The equation is valid at an arbitrary magnetic field and a temperature not substantially higher than the Curie point, and is based on Landau's theory of second-order phase transitions, with Bloch's $3/2$ power law built in one of Landau's coefficients. The displacement of the maximum in the specific heat under applied magnetic field is demonstrated to be non-monotonic: the maximum shifts towards lower temperatures in a weak field but towards higher temperatures in a strong field.

23RP-D-6

APPLICATION OF MAGNETIC REFRIGERATION AND ITS ASSESSMENT

Kitanovski A., Egolf P.W.

University of Applied Sciences of Western Switzerland, Thermal Sciences Institute IGT-SIT,
Route de Cheseaux 1, CH 1401 Yverdon les Bains, Switzerland

Magnetic refrigeration has the potential to replace conventional refrigeration - with often problematic refrigerants - in several niche markets or even some main markets of the refrigeration domain. Based on this insight, for the Swiss Federal Office of Energy, a list of almost all possible refrigeration technologies was performed. Furthermore, the potential of magnetic refrigeration was evaluated for all these specific applications. A calculation tool to determine the coefficient of performance (*COP*) value and the exergy efficiency as a function of the magnetic field strength and the rotation frequency of a rotary-type magnetic refrigerator was developed. The evaluation shows that some application domains are more ideal for a replacement of conventional refrigerators by its magnetic counterparts than others. Four good examples - the household appliance without a freezing compartment, the room air conditioner, the supermarket display

cabinet (including the multideck) or glass door refrigerator and the central refrigeration or cooling unit were chosen for a more detailed study and presentation. While the first three applications are foreseen to be equipped with permanent magnet assemblies, the last would be more ideal for an application of superconducting magnet coils, especially for large scale units of a few MW cooling power. For different examples a comparison of the efficiency, mass and volume of conventional vapour compression applications and the equivalent magnetic refrigeration application is outlined.

[1] A. Kitanovski, M. Diebold, D. Vuarnoz, C. Gonin, P.W. Egolf, Application of magnetic refrigeration and its assessment, *Final report of project No. 101'776, Swiss Federal Office of Energy*, 2008.

23TL-D-7

GRAIN ORIENTED NiMnSn AND MnNiIn HEUSLER ALLOYS RIBBONS PRODUCED BY MELT SPINNING: MARTENSITIC TRANSFORMATION AND MAGNETIC PROPERTIES

Hernando B.¹, Sanchez Llamazares J.L.¹, Santos J.D.¹, Sanchez M.L.¹, Escoda Ll.², Sucol J.J.², Varga R.³, Garcia C.⁴, Gonzalez J.⁴

¹Departamento de Fisica, Universidad de Oviedo, Calvo Sotelo s/n, 33007 Oviedo, Spain

²Universidad de Girona, Campus Montilivi, edifici PII, Lluís Santalo s/n, 17003 Girona, Spain

³Institute of Physics, Faculty of Science, UPJS, Park Angelinum 9, 04154 Kosice, Slovakia

⁴Dpto Fisica de Materiales, Facultad de Quimica, UPV, 1072, 20080 San Sebastian, Spain

Since it was discovered that in some composition range Ni-Mn-Sn and Ni-Mn-In alloys show martensitic transformation with both phases ferromagnetically ordered [1], important attention is being paid to study their magnetic shape memory response, as well as magnetocaloric and magneto-transport properties, due to their potential technological applications. The alloys investigated have been bulk polycrystals obtained by arc or induction melting followed of high temperature homogenization annealing, or exceptionally single crystals grown by Czochralski method. Recently, we reported on the synthesis of alloys in both systems by rapid solidification using melt spinning technique [2, 3]. This may be of significant technological interest since melt spinning is a large-mass and continuous production technique that may become a single-step process to obtain single-phase alloys with homogeneous chemical composition avoiding, or reducing, the thermal annealing step to optimize their functional properties. In this contribution we outline the structural, microstructural and magnetic properties of melt spun ribbons of selected compositions in the $\text{Ni}_{50}\text{Mn}_{50-x}\text{Sn}_x$, $\text{Ni}_{50}\text{Mn}_{50-x}\text{In}_x$ and $\text{Mn}_{50}\text{Ni}_{50-x}\text{In}_x$, systems. Samples were produced by melt spinning in argon atmosphere at a high wheel linear speed of 48 ms^{-1} . Starting master alloys were prepared from highly pure elements (>99.9%) by argon arc melting. Samples were characterized by means of scanning electron microscopy, energy dispersive X-ray microanalysis (EDS), X-ray diffraction at different temperatures, and dc magnetization measurements. Ribbons produced were fully crystalline because of the fast crystallization and growth kinetics showed by these alloys. Ribbon flakes were typically of 1.5-2.0 mm in width, 6-7 mm in length and thickness of around 7-10 μm . EDS analyses showed that chemical elements homogeneously distribute in the alloys; the resulting average elemental chemical composition is slightly shifted with respect to the starting one. Alloys were found to be single-phase with ferromagnetic bcc austenite as room temperature phase. Ribbons tend to show an ordered columnar-like microstructure perpendicular to ribbon plane practically running through the entire

ribbon thickness. At low temperatures austenite transforms into a modulated martensite whose lattice symmetry depends on the alloy system. Field-induced reverse martensitic transition was observed in several alloys. Easy magnetization axis of both, austenite and martensite, lies along the rolling direction being perpendicular to the major axis of columnar grains.

Work supported by FICYT and MEC (COF07-013, MAT2006-13925 and NAN-2004-09203).

- [1] Y. Sutou, Y. Imano, N. Koeda, T. Omori, R. Kainuma, K. Ishida, K. Oikawa, *Appl. Phys. Lett.* **85** (2004) 4358.
 [2] J.L. Sanchez Llamazares, T. Sanchez, J.D. Santos, M.J. Perez, M.L. Sanchez, B. Hernando, Ll. Escoda, J.J. Socol, R. Varga, *Appl. Phys. Lett.* **92** (2008) 012513.
 [3] J.D. Santos, T. Sanchez, P. Alvarez, M.L. Sanchez, J.L. Sanchez Llamazares, B. Hernando, Ll. Escoda, J. J. Socol, R. Varga, *J. Appl. Phys.* **103** (2008) 07B326.

23RP-D-8

SOFT MAGNETIC MATERIALS FOR MAGNETIC REFRIGERATION: FIELD DEPENDENCE AND A UNIVERSAL CURVE

Franco V., Conde A.

Departamento de Física de la Materia Condensada. ICMSE-CSIC. Universidad de Sevilla.
P.O. Box 1065. 41080 Sevilla, Spain

Currently, the field dependence of the magnetocaloric effect is being studied intensively for two main reasons. From a fundamental point of view, the analysis of this field dependence for different types of materials can give further clues of how to improve the performance of refrigerant materials for the magnetic field range employed in actual refrigerators (generally 10 to 20 kOe). From a practical point of view, the knowledge of the laws governing the field dependence of the magnetic entropy change can provide tools for making plausible extrapolations to magnetic field values outside the available experimental range in some laboratories.

The theoretical description of this field dependence has usually been made on the basis of a mean field approach, which corresponds to a power law of the field with an exponent $2/3$. However, the authors have recently demonstrated that experimental data do not necessarily follow this $H^{2/3}$ law [1]. Instead, a relationship between the value of the exponent and the critical exponents of the material has been demonstrated.

The study of materials with a second order phase transition allowed finding a universal curve for the magnetic entropy change: not only the different magnetic entropy change curves of a material measured up to different maximum applied fields collapse onto a single curve, but also series of alloys with the same values of the critical exponent collapse onto the same curve [1,2]. This universal curve was initially derived in a purely phenomenological way using results of soft magnetic amorphous alloys. More recently, it has been applied to several crystalline rare earth alloys [3] and its existence can be demonstrated theoretically.

In this talk, the different procedures for constructing the universal curve will be described, outlining the demonstration of its existence and considering the particularities of different universality classes. This will be illustrated with experimental results from different types of materials, ranging from transition metal based amorphous alloys to rare-earth crystals and from bulk materials to nanoparticles. The practical applications of the universal curve (a tool for making extrapolations in temperature or field, and for enhancing the resolution of the experimental data close to the peak entropy change) will also be discussed.

Support by the Spanish Government and EU FEDER (Project MAT 2007-65227) and by the PAI of the Regional Government of Andalucía (Project P06-FQM-01823) is acknowledged.

- [1] V. Franco, J.S. Blázquez, and A. Conde, *Appl. Phys. Lett.* **89** (2006) 222512.
- [2] V. Franco, C.F. Conde, A. Conde, and L.F. Kiss, *Appl. Phys. Lett.* **90** (2007) 052509.
- [3] V. Franco, A. Conde, V.K. Pecharsky, and K.A. Gschneidner, Jr., *Europhys. Lett.* **79** (2007) 47009.

23 June Monday

12:00-13:30

15:00-17:00

oral session

23TL-F

23RP-F

**“Soft Magnetic
Matter”**

23TL-F-1

HEAT GENERATION IN A SUSPENSION OF MAGNETIC DIPOLES IN AN ALTERNATING FIELD

Raikher Yu.L.¹, Stepanov V.I.¹, Kashevsky B.E.²

¹Institute of Continuous Media Mechanics, Ural Branch of RAS, Perm, Russia

²A.V. Luikov Heat and Mass Transfer Institute, BAS, Byelarus

Medical hyperthermia that involves as a heat source the suspensions of magnetic single-domain particles driven by external AC field, is a well known method for anti-cancer treatment nowadays passing from laboratory to clinical practice. In its development, it had divided in a wide number of techniques depending on the size, type and functionalization of the particles as well as the frequency and amplitude of the field. However, there are a few simple problems which are basic and which comprehensive solution must precede all the further theoretical work.

One of such problems is the energy loss (heat generation) in an ensemble of non-interacting single-domain particles suspended in a Newtonian liquid and driven by a uniform AC magnetic field. We assume that the particles are magnetically hard enough to be considered as rigid dipoles and small enough to be sensitive to rotary Brownian motion. This model is one of a few that was addressed theoretically [1] and the results obtained there, due to the lack of any other, were widely employed for experiment interpretation. However, a closer analysis shows that the phenomenology [1] has a limited range of validity which is easy to be trespassed.

We build our consideration on the kinetic approach that is valid for arbitrary values of the field frequency and amplitude. From a numerically-exact solution of the Fokker-Planck describing the orientational motion of the particle magnetic moment, the dynamic magnetization is obtained, and the specific loss power (SLP) taking into account high-harmonic generation occurring under the fields of finite amplitude is evaluated. Comparison of our results with those derived in the phenomenological framework reveals the following:

- the frequency dependence of SLP holds its form practically independently of the approximation;
- in the weak field limit that is equivalent to a linear response theory approach, the phenomenological and kinetic model render SLP expressions that virtually coincide;
- it is the finite field amplitude case where the models notably deviate.

This latter difference is due mainly to the fact that the phenomenological model neglects the dependence of the magnetic relaxation time on the driving field strength. The effect is negligible in the weak-field limit but becomes important at higher fields. The field-frequency range where the phenomenology fails is determined by the condition

$$\xi_0 \omega \tau_B \geq 1, \quad (1)$$

with $\xi_0 = \mu H_0 / kT$ being the Langevin argument taken with respect to the driving field amplitude H_0 and $\tau_B = 3\eta V_h / kT$ being the Brownian rotary diffusion time; here μ and V_h are the particle magnetic moment and hydrodynamic volume, respectively, and η is the viscosity of the carrier liquid. For example, for a ferrite particle with the magnetic diameter 15 nm and hydrodynamic diameter 60 nm driven in water by the field with the amplitude 150 Oe, condition (1) becomes valid for $f = \omega / 2\pi \gtrsim 2$ kHz that is quite a low frequency for the hyperthermia treatment.

Support by RFBR under Project 06-02-81047 and by BRFFR under Project T06P-162 is gratefully acknowledged.

[1] R. E. Rosensweig, *J. Magn. Magn. Mater.* **252** (2002) 370.

23RP-F-2

MAGNETODYNAMICS AND SELF-ORGANIZATION IN STRONGLY NON-EQUILIBRIUM FERROSUSPENSIONS

Kashevsky B.E.¹, Kashevsky S.B.¹, Prokhorov I.V.¹, Raikher Yu.L.²

¹A.V. Luikov Heat and Mass Transfer Institute, BAS, Minsk, Belarus

²Institute of Continuous Media Mechanics, Ural Branch of RAS, Perm, Russia

We develop mesoscopic models appropriate for studies of the AC field-driven behavior of the ensembles of fine magnetic particles embedded in liquid matrices. In view of the diversity of the particles, liquid matrixes and the variants of the field application, this line of problems is actual for many areas of micro- and nanotechnologies. Our work presents some computational and experimental results concerning the ferrosuspensions where the particles are in strongly non-equilibrium conditions created by high-frequency (in comparison with the inverse time of the particle mechanical motion) magnetic fields. Two situations are considered, in particular.

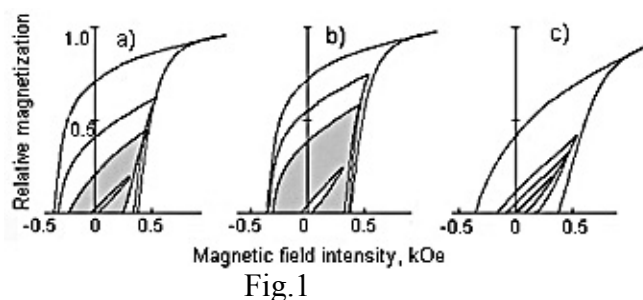


Fig.1

First is the dynamic magnetic hysteresis in a dilute suspension of highly-coercive particles subjected to a linearly polarized field $H(t) = H_0 \cos \omega t$. This problem is directly related to medical hyperthermia techniques. In each pane of Fig.1 four partial hysteresis loops measured under respectively equal fields on a liquid (*a* the increase, *b* the decrease of the amplitude) and a solid (*c*) dispersion of acicular $\gamma\text{-Fe}_2\text{O}_3$ grains are presented. Comparison reveals two consequences of the orientation freedom of the particles: (i) the enhanced squareness of the loops and (ii) the *memory effect* that is the dependence of the $M(H)$ loop on the direction of the field amplitude evolution. To clarify the origin of the memory effect, numeric simulations for anisotropic particles under coherent and incoherent (the chain-of-spheres model) conditions were performed. We find that at $\omega = \text{const}$ there exists an interval of H_0 within which two regimes—reversible and hysteretic—of the particle magnetic motion are possible. The actual number of the particles responding via a given mode depends on the orientational state of the ferrosuspension at which it “enters” this interval. At the increase of H_0 it is rather *easy-plane* while at its decrease it is virtually *easy-axis*; note that in the latter case the particle magnetic response is much higher. This theoretical analysis agrees well with the experimental evidence: inside the gray-filled area (borders included) of Fig.1 any loop induced by the field which amplitude grows (Fig.1a) is considerably smaller than the loop corresponding to the same amplitude of the field but obtained at H_0 diminution (Fig.1b).

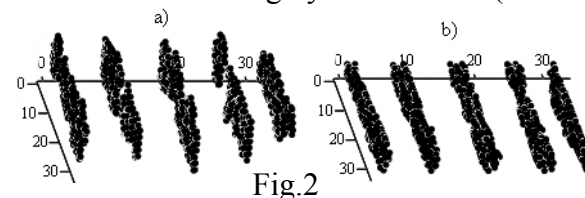


Fig.2

The second problem that we address is the dissipative self-organization of magnetically soft microparticles embedded in a thin layer of a polymer solution that is set under a rotating magnetic field. This problem is actual for polymer composite technologies. The process is studied in the high-frequency limit on the basis of a molecular dynamics model with allowance for the hydrodynamic interactions between the particles. In addition, we assume that the solvent is drying so that the thickness of the layer progressively reduces while the viscosity of the remaining particle-polymer film increases. Fig. 2

shows typical structure patterns corresponding to an as-prepared layer (*a*) and the same layer dried to one third of its initial thickness (*b*).

Support by BRFFR Project T06P-162 is acknowledged by the first three authors; support by RFBR Project 06-02-81047 is acknowledged by Y.L.R.

23RP-F-3

LANGEVIN DYNAMICS SIMULATIONS OF FAST REMAGNETIZATION PROCESSES IN FERROFLUIDS WITH INTERNAL MAGNETIC DEGREES OF FREEDOM

Berkov D.V.¹, Gorn N.L.¹, Schmitz R.²

¹Innovent Technology Development, Pruessingstr. 27B, D-07745, Jena, Germany

²Institute of Theoretical Physics C, RWTH Aachen, 52056 Aachen, Germany

In this talk we consider a model for numerical studies of a ferrofluid dynamics taking into account internal magnetic degrees of freedom of ferrofluid particles. In standard ferrofluid models magnetic moment of a particle is supposed to be fixed with respect to the particle itself. This assumption corresponds to the limit of a very high single-particle magnetic anisotropy, which is very rarely the case in real ferrofluids.

In contrast to this simple model, we take into account that in real systems magnetic moments of ferrofluid particles can rotate with respect to the particle themselves. Our model results in equations of motion describing both magnetic and mechanical degrees of freedom, where ‘magnetic’ equations are coupled to ‘mechanical’ ones via (*i*) the magnetodipolar interaction field which depend on the interparticle distances and magnetic moment orientations and (*ii*) mechanical torques acting on the particle which are determined by the particle anisotropy axes orientations with respect to the magnetic moments.

Using our model we have studied ferrofluid magnetization dynamics for various particle concentrations, i.e., for various magnetodipolar interaction strengths. In particular, we present numerical results for (a) magnetization relaxation of a ferrofluid after the external field is switched off and (b) frequency dependence of the ferrofluid *ac*-susceptibility. Comparing these results with the corresponding dependencies obtained for the rigid dipoles model, we demonstrate that for the magnetic anisotropy values typical for common ferrofluid materials (like magnetite) inclusion of ‘magnetic’ degrees of freedom is qualitatively essential to obtain a correct description of the ferrofluid dynamics.

Further we report the extension of our model towards aggregated ferrofluids, where internal magnetic degrees of freedom plays a crucial role by forming the magnetic structure of aggregates, which, in turn, determines the interaction between aggregates.

We conclude the talk with the discussion concerning the optimal calculation and physical effects arising from the hydrodynamic interparticle interaction.

23RP-F-4

MUON AND MUONIUM FRACTIONS BEHAVIOR IN FERROFLUIDS

*Balasoiu M.^{1,2}, Aksenov V.L.^{1,3}, Bica D.⁴, Vekas L.⁴, Barsov S.G.⁵, Vorobyev S.I.⁵,
Gritsaj K.I.¹, Duginov V.N.¹, Komarov E.N.⁵, Koptev V.P.⁵, Kotov S.A.⁵,
Mamedov T.N.¹, Mikirtychyants C.M.⁵, Shcherbakov G.V.⁵, Tripadus V.²*

¹The Joint Institute for Nuclear Research, 141980 Dubna, Moscow region, Russia

²Horia Hulubei National Institute for Physics and Nuclear Engineering Bucharest, Romania

³Russian Research Centre Kurchatov Institute, Moscow, Russia

⁴Center for Fundamental and Advanced Technical Research, Timisoara, Romania

⁵B.P. Konstantinov Petersburg Nuclear Physics Institute, Gatchina, Leningrad region, Russia

Ferrofluid on the basis of the Fe₃O₄ nanoparticles dispersed in heavy water (D₂O) have been investigated by means of the μ SR-method. It was revealed that the distinct muonium precession signal is observed simultaneously with muon (diamagnetic) precession signal. Behaviour of the muon and muonium fractions in ferrofluid is compared with those in the pure heavy water. Experiment was carried out at temperatures 25÷300 K in transverse magnetic fields of 8 and 278 Oe. It was observed that muon (diamagnetic) fraction is created in the ferrofluid approximately in the same proportion as in D₂O, however muon spin relaxation rate to a considerable extent higher in ferrofluid than in D₂O at temperatures T>150 K. Part of muonium fraction at these temperatures essentially less in ferrofluid than in D₂O. Precession frequencies of the muon and muonium spins in ferrofluid noticeable lower than in D₂O.

The investigation has been performed at the B.P. Konstantinov Petersburg Nuclear Physics Institute, and V.P. Dzhelepov Laboratory of Nuclear Problems, JINR.

Supports by JINR, Grants of Romanian Plenipotentiary are acknowledged.

[1] M. Balasoiu, S.G. Barsov, D. Bica, L. Vekas, S.I. Vorobyev, K.I. Gritsaj, V.N. Duginov, V.A. Zhukov, E.N. Komarov, V.P. Koptev, S.A. Kotov, T.N. Mamedov, C.M. Mikirtychyants, C. Petrescu, G.V. Shcherbakov, *Preprint PNPI 2745*, 2007 (in Russian).

23RP-F-5

SPIN GLASS BEHAVIOR IN STRONGLY INTERACTING NANOPARTICLE SYSTEMS

Dupuis V.¹, Parker D.², Ladieu F.², Dubois E.¹, Bouchaud J.P.², Perzynski R.¹, Vincent E.²

¹Universite Pierre et Marie Curie Paris-VI, LI2C UMR 7612 CNRS-UPMC-ESPCI, 4 place Jussieu, F-75252 Paris Cedex 05 France

²Service de Physique de l'Etat Condense, DSM/DRECAM/SCPEC CEA Saclay, 91191 Gif sur Yvette France

Ferrofluids are complex fluids composed of magnetic nanoparticles dispersed in a liquid, which are well known for their use in numerous technological applications. They are also

interesting from the viewpoint of basic research and constitute fascinating testing grounds to study the emergence of exotic behaviors resulting from complex particle-particle interactions.

In this talk I will report on a recent experimental investigation of the low temperature magnetic properties of concentrated ferrofluids using SQUID magnetometry [1]. Such frozen ferrofluids are found to share many similarities with spin glasses as they can be regarded as assemblies of randomly located nanoparticles bearing giant magnetic moments or superspins interacting via strong random long range dipolar interactions. I will discuss in particular the similarities and differences we observed between such superspin glasses and canonical spin glasses.

[1] D. Parker, V. Dupuis, F. Ladieu, J.-P. Bouchaud, E. Dubois, R. Perzynski, E. Vincent, *Phys. Rev. B* **77**, 104428 (2008).

23TL-F-6

MAGNETIC- AND ELECTRIC FIELD RESPONSIVE SOFT AND SMART MATERIALS

Zrínyi M.

Department of Physical Chemistry and Materials Sciences
Budapest University of Technology and Economics, Budapest, HUNGARY
Phone: 36-1-463322, Fax: 36.1 4633767
E-mail: zrinyi@mail.bme.hu

Many useful engineering materials, as well as living organisms have a heterogeneous composition. The components of composite materials often have contradictory, but complementary properties. Fillers are usually solid additives that are incorporated into the polymer to modify the physical properties. Fillers can be divided into three categories: those that reinforce the polymer system and improve its mechanical performance, those that are used to take-up space, and thus reduce material cost. The third, less common category is when filler particles are incorporated into the material to improve its responsive properties.

Composite materials consisting of rather rigid polymeric matrices filled with magnetic particles are long time known and called magnetic elastomers or magnetoelasts. These materials are successfully used as permanent magnets, magnetic cores, connecting and fixing elements in many areas. These traditional magnetic elastomers have low flexibility and practically do not change their size, shape and elastic properties in the presence of external magnetic field.

The new generation of magnetic gels and elastomers represent a new type of composites,



Fig. 1 Snapshot of shape change of a magnetite-loaded PDMS elastomer due to modulated magnetic field. The frequency of the field is 40 Hz.

consisting of small (mainly nano-sized) magnetic particles dispersed in a high elastic polymeric matrix. The particles couple the shape of the elastomer to the external magnetic fields. Since the particles cannot leave the polymer matrix, so that all of the forces acting on the particles are

transmitted directly to the polymer chains resulting in either locomotion or deformation. Shape distortion occurs instantaneously and disappears abruptly when external fields are applied or removed, respectively. Combination of magnetic and elastic properties leads to a number of striking phenomena that are exhibited in response to impressed magnetic fields. Giant deformational effect, tunable elastic modulus, non-homogeneous deformation and quick response to magnetic field (Fig. 1) open new opportunities for using such materials for various applications.

Synthesis of elastomers in uniform magnetic field can be used to prepare anisotropic samples. In uniform field there are no attractive or repulsive field-particle interactions therefore particle-particle interactions become dominant. In monomer solutions, containing dispersed magnetic particles, the imposed field orients the magnetic dipoles. If the particles are spaced closely enough, so that their field can reach their neighbours, mutual particle interactions present. These interactions can be very strong leading to significant change in the structure of the particle ensemble. The particles attract each other when aligned end to end, and repel each other when placed side by side. Due to the attractive forces pearl chain structure develops. The ordered structure can be fixed by cross-linking polymerisation.

The anisotropy manifest itself in both direction dependent elastic modulus as well as direction dependent swelling (Fig. 2). The magnetic field responsive elastomers have shown a change in compressive modulus under uniform magnetic field. Depending on the orientation of particle chains in the network and that of the magnetic field, the induced temporary reinforcement may exceed one order of magnitude.

These results suggest that magnetic field responsive gels and elastomers have several potential applications as tuned vibration absorbers, stiffness tuneable mounts and suspensions. Since the magnetic fields are convenient stimuli from the point of signal control, therefore it is of great importance to develop and study such soft and flexible magnetic systems.

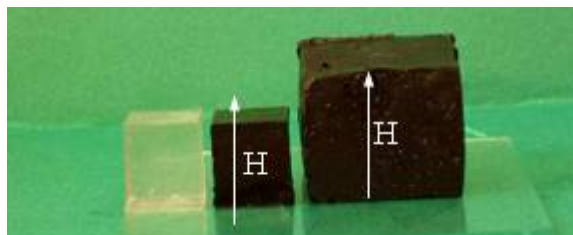


Fig. 2 Anisotropic swelling behaviour as seen by the naked eye. The arrow indicates the direction of the magnetic field during the preparation.

Quincke rotation is the rotation of non-conducting objects immersed in liquid dielectrics and subjected to a strong homogeneous DC electric field. The rotation is spontaneous when the field exceeds a threshold value. Wide range of applications (e.g. microscopic motor) motivates researchers to find materials with micro-fabrication possibilities. Polymer composites that fulfil these requirements have been developed for the first time. Electro-rotation of disk shaped polymer composites is studied as a function of electric field intensity.

Magnetic and electric field induced deformation, locomotion and rotation, as well as on/off switching control of magnetic polymeric membranes will be the subject of the oral presentation

[1] M.Zrínyi, L.Barsi, D.Szabó, H.-G.Kilian, *J.Chem Phys*, 108 (13), 5685-5692 (1997)

[2] D.Szabó, G.Szeghy and M.Zrínyi: *Macromolecules* **31**, 6541-6548 (1998)

[3] M.Zrínyi, D.Szabó and L.Barsi: *Polymer Sensors and Actuators* Springer, Verlag Berlin, Heidelberg (1999) p. 385-408

[4] M. Zrínyi, D. Szabó, G. Filipcsei and J. Fehér: *Polymer Gels and Networks*, Marcel Dekker, Inc., New York (2001) Chapter 11, p. 309-355

[5] G. Filipcsei, I. Csetneki, A. Szilágyi and M. Zrínyi: Magnetic Field-Responsive Smart

Polymer Composites (review article) *Advances in Polymer Science*, Springer, Verlag Berlin, Heidelberg 137-189, (2007)

23RP-F-7

MECHANICAL AND MAGNETIC PROPERTIES OF POLYDISPERSE MAGNETOELASTICS

Nikitin L.V.¹, Talipov R.A.¹, Kazakov A.P.¹, Stepanov G.V.²

¹Faculty of Physics, Moscow State University, Leninskie gory, Moscow, 119992 Russia

E-mail: nikitin@magn.ru

²State Research Institute of Chemistry and Technology of Organoelement Compounds, sh. Entusiastov 38, Moscow, 111123 Russia

This work is dedicated to researching new magnetic materials, magnetoelastics [1, 2]. It is an ensembles of disperse magnetic particles, which are set in polymeric flexible matrix. Magnetoelastics combine two properties: high magnetization and elasticity. Structure, elastic, magnetodeformational, viscosity and magnetic properties of these materials are considered.

In current work we studied polydisperse magnetoelastics, which are prepared on the base of two powders of particles with different sizes. We have used particles of three average sizes: 300A, 2 μ m and 50 μ m. The total mass concentration of magnetic phase was constant. We varied the relative concentration of magnetic particles of different size. Magnetic particles with average size of 2 μ m and 50 μ m were used in producing specimens for investigation of mechanical characteristics.

It was shown that magnetic field influences on the elastic and viscous properties of magnetoelastics. It was found that the application of a magnetic field leads to a considerable rise in the Young's modulus and in the viscosity of these materials.

We had considered the dependences of an elastic stress on relative elongation of magnetoelastic for different concentration of big magnetic particles under loading and unloading. Also the shear module for magnetoelastics with different concentration of big magnetic particles was measured.

Experiment for research of magnetoelastic properties by a method of twisting pendulum was advanced and process of registration and processing of experimental data is automated. Dependences character of the magnetoelastic twisting oscillation period from concentration of big magnetic particles was obtained.

It is established that results of magnetoelastics research by three various methods are well coordinated with each other and with existing magnetoelastic model.

Two series of specimens were prepared for investigation of magnetic properties of magnetoelastics. In first series were used particles of iron and their size was \sim 300A and \sim 2 μ m (series 1). In second series were also used particles of iron, and their size was \sim 2 μ m and \sim 50 μ m (series 2). The total mass concentration in all investigated specimens was constant.

Loops of magnetic hysteresis for magnetoelastics were obtained. The form of hysteresis loop for magnetoelastic depends from size of magnetic particles which are part of magnetoelastic. On hysteresis loops of specimens of series 1 was observed coercivity, which grows with growth of concentration of small particles. On hysteresis loops of specimens of series 2 was observed similarity to hysteresis. In other words, there is hysteresis on hysteresis loop, but it has zero coercive force and residual magnetization. We think that this phenomenon could be explained by contact interactions in structure of magnetic particles, which is formed by magnetic field.

[1] E.F.Levina, L.S.Mironova, L.V.Nikitin, G.V.Stepanov. Magnetocontrolled elastic composite materials. Russian patent N 2157013/2000.

[2] L.V.Nikitin, L.S.Mironova, K.G.Kornev, G.V.Stepanov. *Polymer Science, Ser. A*, Vol.46, No.3, 2004, p.498.

23RP-F-8

THE ROSENSWEIG INSTABILITY WITH A FERROGEL

Gollwitzer C.¹, Krekhova M.², Rehberg I.¹, Lattermann G.², Richter R.¹

¹Experimentalphysik V, University of Bayreuth, 95440 Bayreuth, Germany

²Makromolekulare Chemie I, University of Bayreuth, 95440 Bayreuth, Germany

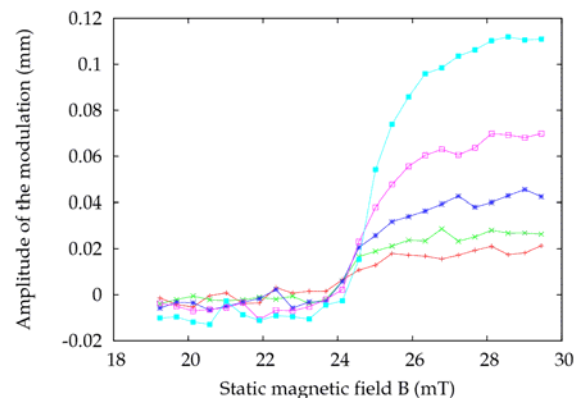
Ferrogels are an interesting new class of materials that enhance the properties of magnetic fluids by elastic components [1]. Due to the coupling of magnetic and elastic energies, they are able to change their shape and exert forces in response to external magnetic fields [2]. Large deformations could be achieved by gradient magnetic fields, utilizing the Kelvin force[3]. The deformation in homogeneous magnetic fields has not been studied to the same extent [4,5].

When applying a homogeneous magnetic field to a layer of ferrofluid, the surface becomes instable to liquid crests (the famous Rosensweig instability). This instability should also be possible in ferrogels. From a linear stability analysis [6], the critical magnetization is given by

$$M_c^2 = \frac{2}{\mu_0} \frac{1 + \mu}{\mu} \left(\sqrt{\rho g \sigma} + G \right)$$

where G is the shear modulus. For $G=0$ this coincides with the critical magnetization for a ferrofluid, i.e. the critical field is shifted to higher values due to the elastic forces. The critical wavenumber is predicted to remain the same.

We use a thermoreversible ferrogel [7] and expose it to a homogeneous magnetic field. By controlling the temperature we can easily change the elastic modulus over several orders of magnitude. The surface topography of the ferrogel is then recorded using an X-ray technique [8]. Because our ferrogel has no elasticity in the static limit, the instability is driven by a static field plus a sinusoidal modulation. We measure both amplitude and phase of the modulated surface deflection and compare it with the theory.



We'd like to thank S. Bohlius and H. R. Brand for fruitful discussion. Funding is provided by Deutsche Forschungsgemeinschaft via the project FOR 608.

[1] M. Zrinyi, L. Barsi, and A. Buki, *Polymer Gels and Networks* **5**, 415 (1997).

[2] M. Zrinyi, L. Barsi, and A. Buki, *J. Chem. Phys.* **104**, 8750 (1996).

[3] M. Zrinyi, L. Barsi, D. Szabo, and H.-G. Kilian, *J. Chem. Phys.* **106**, 5685 (1997).

[4] Y. L. Raikher and O. V. Stolbov, *J. Appl. Mech. Tech. Phys.* **46**, 434 (2005).

[5] C. Gollwitzer, A. Turanov, M. Krekhova, G. Lattermann, I. Rehberg, and R. Richter, Measuring the deformation of a ferrogel sphere in a homogeneous magnetic field, *accepted by J. Chem. Phys.* <http://arxiv.org/abs/0801.1244>.

[6] S. Bohlius, H. Brand, and H. Pleiner, *Z. Phys. Chem* **220**, 97 (2006).

[7] G. Lattermann and M. Krekhova, *Macromol. Rapid Commun.* **27**, 1373 (2006).

[8] R. Richter and J. Blasing, *Rev. Sci. Instrum.* **72**, 1729 (2001).

23RP-F-9

MAGNETIC PROPERTIES OF MAGNETOACTIVE ELASTOMERS IN FROZEN STATE

Stepanov G.V.¹, Borin D.Yu.², Odenbach S.², Gorbunov A.I.¹, Raikher Yu.L.³

¹State Scientific Research Institute of Chemistry and Technology of Organoelement Compounds, Moscow 111123, Russia

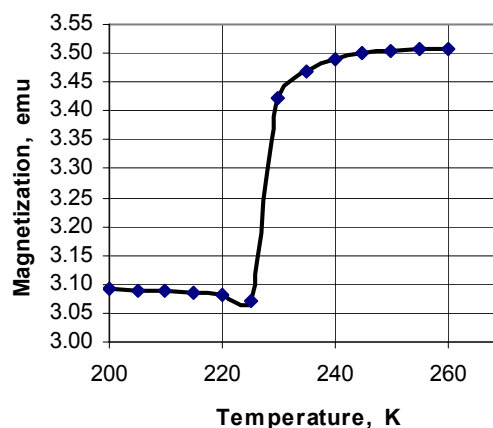
²Chair of MagnetoFluidDynamics, Technische Universitat Dresden, Dresden 01062, Germany

³Institute of Continuous Media Mechanics, Ural Branch of RAS, Perm, 614013, Russia

Magnetoactive elastomers (MAE) are composite smart materials with a strong response to an applied magnetic field. The major mechanism causing the change of their properties (elasticity, conductivity, etc.) is the dipole-dipole interaction between the nano- or microparticles of the magnetic filler. These changes become most vivid when under a magnetic field the material structurizes and inside it chains and/or clusters of particles form. For example, in [1] an anomalous increase of elasticity of a magnetized MAE under weak (0.5-5%) strain was found. In the present paper we report temperature measurements done on a MAE consisting of a siloxane rubber filled with carbonyl iron particles. To the best of our knowledge, this approach, successfully used for studies of magnetic fluids, has never ever been applied to MAE.

One should expect that the main temperature effect stems from vitrification of the polymer composite. A sharp increase of the mechanic modulus should as well impose arrest on the re-grouping of the particles thus fixing the structure of the ensemble in the sample. As the magnetic properties of MAE reflect its structural state, then when a cooled material will be heated under a constant field, its magnetization $M_H(T)$ should display a sharp growth at the glass transition point. From the thus obtained thermomagnetic curve $M_H(T)$ one would be able to establish the position of the vitrification point and to characterize the structure transformations which take place in the magnetodipole system of the sample. Therefore such experiments, being close analogues to the conventional Field Cooled-Zero Field Cooled magnetic tests, make an important source of material data on MAE.

The curve presented in the figure illustrates a typical thermomagnetic measurement. A MAE sample with the particles of 2-4 μm and the filler volume fraction 25% was at room temperature subjected to a uniform constant field 10 kOe and frozen to 200 K. Then the sample magnetization was measured in the field 3 kOe directed across the "freezing field" under slow (3 grad/min) heating. As seen, the magnetization indeed undergoes a sharp jump around 228 K, the width of the vitrification interval being about 5 K. The value of the jump gives a quantitative estimation for the contribution of the particle re-grouping to the magnetic properties of MAE. The experiments carried out with more large filler particles show that with the increase of the particle size, the structure contribution to the magnetization grows.



Financial support of RFBR Project 06-01-00723 is gratefully acknowledged by G.V.S., A.A.G. and Y.L.R.

- [1] G.Stepanov, L.Nikitin, E.Kramarenko, C.Abramchuk, D.Grishin, E. Suvorova, A.Gorbunov, MISM 2005, Moscow, 25-30 June 2005, 183-184.

23RP-F-10

NEMATIC LIQUID CRYSTALS DOPED BY FINE MAGNETIC PARTICLES OF DIFFERENT SHAPE

Kopčanský P.¹, Koneracká M.¹, Timko M.¹, Tomašovičová N.¹, Závašová V.¹, Tomčo L.³, Džarová A.¹, Šprincová A.^{1,2}, Éber N.⁴, Fodor-Csorba K.⁴, Tóth-Katona T.⁴, Vajda A.⁴, and Jadzyn J.⁵

¹Institute of Experimental Physics, SAS, Watsonova 47, 040 01 Košice, Slovakia

²JINR, Laboratory of Radiation Biology, Dubna, Russia

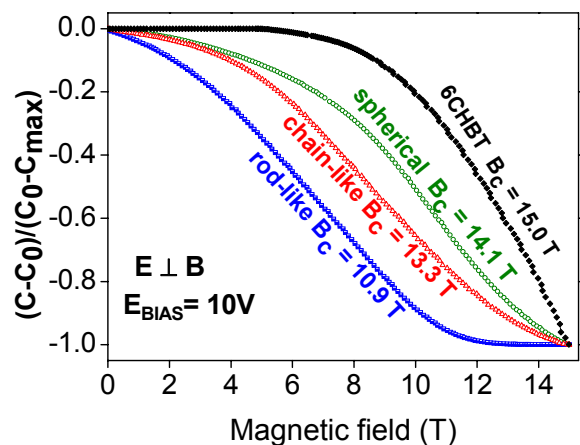
³Faculty of Aeronautics, Technical University, Rampová 7, 041 21 Košice, Slovakia

⁴Research Institute for Solid State Physics and Optics, HAS, H-1525 Budapest, Hungary

⁵Institute of Molecular Physics, PAS, Smoluchovskiego 17, 60179 Poznan, Poland

Liquid crystals can be oriented under magnetic or electric fields due to their anisotropic properties, but the response of liquid crystals to an external magnetic field is weak due to the small value of the anisotropy of diamagnetic susceptibility. Brochard and de Gennes [1] proposed doping liquid crystals with fine magnetic particles, i.e. to create ferronematics. Ferronematics are stable colloidal suspensions of fine magnetic particles in nematic liquid crystals. They attract considerable interest because their response to the external magnetic field exceeds substantially that of pure nematics. The most essential feature of these systems is an orientational coupling between the magnetic particles and the liquid crystal matrix. The influence of the magnetic field depends on the type of anchoring which is characterized by the density of anchoring energy and the initial orientation between liquid crystal molecules and the magnetic moment of magnetic particles.

The aim of this study was to investigate, how the shape of magnetic particles dispersed in the liquid crystal influences the threshold fields of structural transitions. The studied ferronematic samples were based on the thermotropic nematic 4-(trans-4'-n-hexylcyclohexyl)-isothiocyanatobenzene (6CHBT) doped with fine magnetite nanoparticles of different shape (nearly spherical, chain-like obtained from magnetotactic bacteria and rod-like). The structural changes were observed by capacitance measurements and showed significant influence of the shape and size of the magnetic particles on the magnetic field induced structural transitions (see figure). The experiments have indicated parallel initial orientation of the liquid crystal molecules and the magnetic moments of magnetic particles. Theoretical estimations based on the Burylov-Raikher theory [2] have confirmed that the anchoring between liquid crystal molecules and magnetic particles is soft in the case of spherical magnetic particles, while a rigid anchoring exists in the case of rod-like and chain-like magnetic particles.



Support by SAS VEGA 6166, Science and Technology Assistance Agency, contracts No. SK-MAD-02606 and APVV-0509-07, the Grenoble High Magnetic Field Laboratory, the Hungarian Research Funds OTKA K61075 and NKTH/KPf SK-19/2006 is acknowledged

[1] F. Brochard, P.G. de Gennes, *J. Physique (Paris)* **31** (1970) 691.

[2] S.V. Burylov, Y.L. Raikher, *J.Magn.Magn.Mater.* **122** (1993) 62.

23RP-F-11

ORIENTATION FLUCTUATIONS AND CORRELATIONS IN FERRONEMATICS

Burylov S.V.^{1,2}

¹Physics Faculty, National Taras Shevchenko University of Kyiv,
Prosp.Glushkova 2, bldg 1, Kyiv, 03680, Ukraine

²Institute of Transport Systems and Technologies, Pisargevskogo str. 5,
Dnepropetrovsk, 49005, Ukraine

Ferronematics (FN's), i.e. suspensions of fine ferromagnetic particles in nematic liquid crystals, present a specific class of soft magnetic materials. These materials, possessing optical properties of pure nematics, have the high magnetic susceptibility that is 2-3 orders of magnitude greater in comparison with usual liquid crystals [1, 2]. Owing to it, the ferronematics show specific optical effects in relatively weak ($\sim 10\div 100$ Oe) magnetic fields. It is very promising for applications of these magnetic materials in modern systems for processing and presenting information.

In this paper the effect of an external magnetic field on orientation fluctuations and correlations in ferronematics is studied. The continuum theory of ferronematics proposed in [3] is used for calculation of the free energy variations producing by three sources: (1) small local changes in the concentration of the disperse ferromagnetic phase, (2) spontaneous fluctuations in the director orientation of the nematic matrix and (3) fluctuations in the direction of the average magnetic moments of the ferroparticles. It is assumed that the homeotropic boundary conditions for the director of the nematic liquid crystal are specified on the surfaces of the ferroparticles and the long axis of such particles and their magnetic moments are oriented [4] perpendicularly to the director \mathbf{n} . We consider a case in which an external magnetic field \mathbf{H} is also perpendicular to the director.

It is shown that the small changes in the concentration of the ferromagnetic phase are statistically independent and do not effect on the fluctuations in the director orientation. At the same time, the external magnetic field $\mathbf{H} \perp \mathbf{n}$ lowers the fluctuation intensities in the direction of the average magnetic moments of the ferroparticles and, due to a strong orientation coupling between the fine ferroparticles and the nematic matrix, effects on the director fluctuations. We determinate the fluctuation intensities of the director \mathbf{n} depending on the external magnetic field, estimate the range of correlations of the orientation fluctuations and discuss the effect of the magnetic field on the birefringence of the ferronematic.

[1] P.Kopčanská, M.Koneracka, M.Timko, I.Potočová, L.Tomčo, N.Tomašovičová, V.Závišová and J.Jadzyn, *J. Magn. Magn. Mater.*, **300** (2006) 75.

[2] O.Buluy, E.Ouskova, Yu.Reznikov and P.Litvin, *Ukr. J. Phys.*, **49** (2004) A48.

[3] S.V.Burylov and Yu.L.Raikher, *Mol. Cryst. Liq. Cryst.*, **258** (1995) 107.

[4] S.V.Burylov and Yu.L.Raikher, *Phys. Rev. E*, **50** (1994) 358.

23RP-F-12

MAGNETO-HYDRODYNAMIC INTERACTION IN AN INCLINED FERROFLUID LAYER

Bozhko A.A.¹, Putin G.F.¹, Tynjälä T.²

¹Department of Physics, Perm State University, Perm 614990, Russia.

²Department of Energy and Environmental Technology, Lappeenranta University of Technology, P.O. Box 20, 53851 Lappeenranta, Finland

The instability of convection patterns representing a combination of vertical Rayleigh rolls and horizontal rolls resulting from longitudinal horizontal magnetic field is investigated in an inclined layer of magnetic colloid by experiments and numerical simulations. Visualization of convection patterns is provided by a temperature-sensitive liquid crystal film. Geometry of the studied case and examples of numerical and experimental results are shown in figure 1.

The rich spectrum of convection structures is observed against different values of inclination angles and uniform magnetic fields. If the horizontal longitudinal magnetic field is strong enough it extinguishes the convection perturbations along the field direction and stabilizes Rayleigh flows. However at small inclination angles the demagnetizing effect results in a horizontal orientation of the convection rolls. On the other hand when the magnetic field is small enough, the hydrodynamic orientation mechanism in the inclined layer predominates over the demagnetizing one, and the axis of convection rolls are lined up along the shear flow, i.e. perpendicular to the imposed magnetic field. The comparable contribution of both mechanisms leads to the formation of different types of oblique rolls and superposition structures. The appearance among listed above convection regimes the localized traveling vortices is the most interesting effect of nonlinear interaction convective modes in the inclined ferrofluid layer in the presence of magnetic field.

Besides, the wave and oscillatory character of convection requires taking into account and studying in detail along with the magneto-hydrodynamic interaction the influence of concentration gradient mainly generated in magnetic colloid due to the gravitational settling of magnetic particles and their aggregates.

The work was supported by the Russian Foundation for Basic Research and Government of Perm Region, Russia, under grant № 07-08-96039, and Finnish Academy grant 110852.

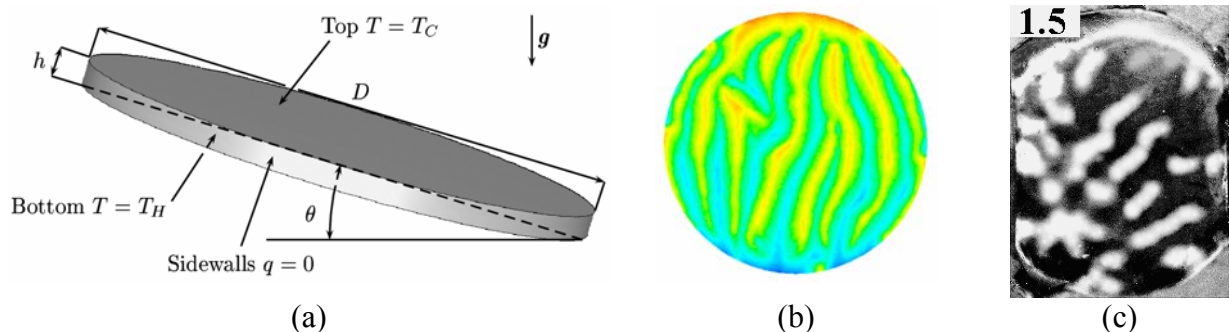


Figure 1 (a) Geometry of the studied case. (b) Simulated temperature contours for $\theta=25^\circ$, $H=1.5$ kA/m, $\Delta T/\Delta T_c=2$. (c) Liquid crystal visualization of temperature contours for $\theta=15^\circ$, $H=1.5$ kA/m, $\Delta T/\Delta T_c=2$.

23 June Monday

17:00-19:00

poster session

23PO-1

**“Magnetism and
Superconductivity”**

23PO-1-1

PROXIMITY EFFECT AS A PROBE OF ELECTRONIC CORRELATIONS AND EXCHANGE FIELD IN DIRTY FERROMAGNET/SUPERCONDUCTOR NANOSTRUCTURES

Ivanov N.M.¹, Terentieva L.A.¹, Parfenova E.L.¹, Proshin Yu.N.², Khusainov M.G.^{1,2}

¹Department "Vostok", Kazan State Tupolev Technical University, Chistopol' 422981, Russia

²Department of Theoretical Physics, Kazan State University, Kazan 420008, Russia

We originally investigate the interplay between the BCS and 2D Larkin-Ovchinnikov-Fulde-Ferrell (LOFF) states in the dirty thin ferromagnetic metal/superconductor (FM/S) bilayers. Moreover, in the corresponding FM/S/FM trilayers two novel π phase superconducting states with electron-electron repulsion in the FM layers have been predicted. The 2D modulated LOFF states are possible in such trilayers only in presence of the external magnetic field and at suitable parameters of the FM and S layers. In the FM/S superlattices there are the 0π and $\pi\pi$ states with compensation of the exchange field paramagnetic effect. This fact allows us to explain a surprisingly high $T_c \sim 5\text{K}$ in the short period Gd/La superlattice [1] and to predict the sign and magnitude of the electron-electron interaction in the Gd metal. On this base we originally propose the method of proximity effect probe of the order parameter symmetry and the magnitude and sign of the electronic correlations and exchange fields in various FM layers, if we use the well known S layer (i.e. the BCS superconductor) as a probe.

[4] J.P. Goff, et al., *J. Magn. Magn. Mater.*, **240** (2002) 592.

23PO-1-2

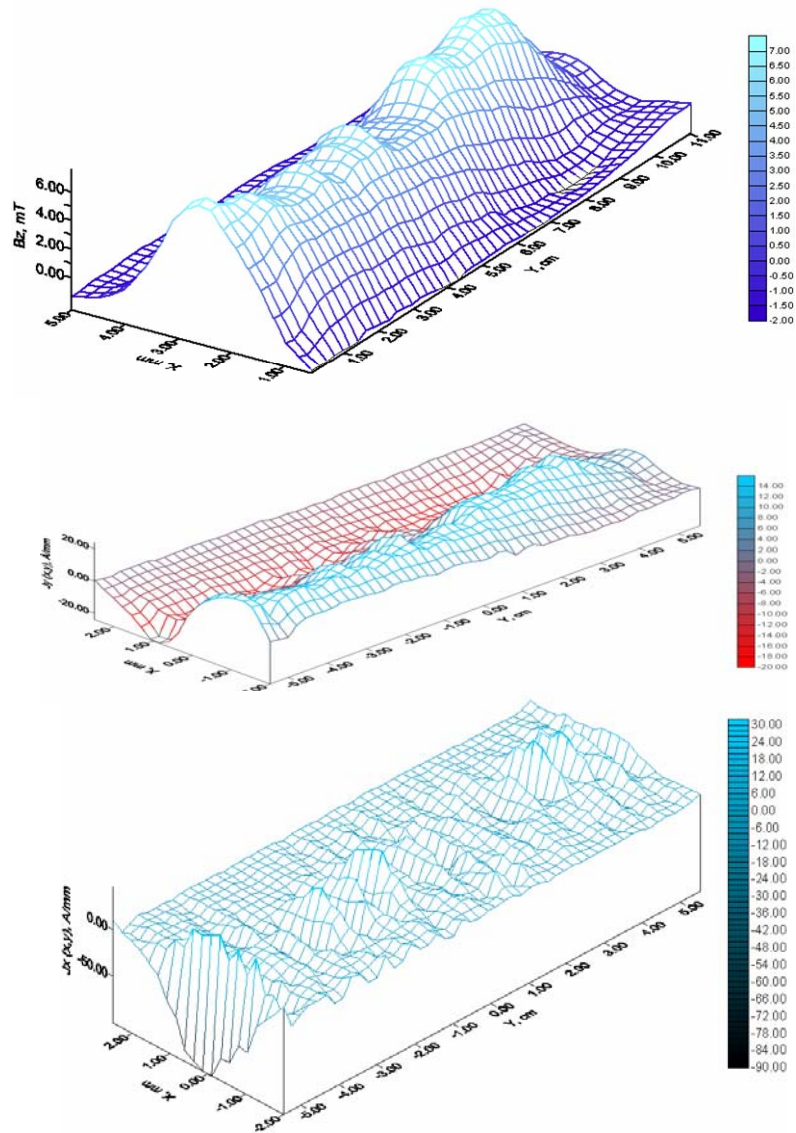
AN APPLICATION OF THE MAGNETIC MEASUREMENTS FOR A TWO-DIMENSIONAL CURRENT MAPPING IN THE SECOND GENERATION SUPERCONDUCTING TAPES

Rudnev I., Pokrovskii S., Podlivaev A.

Department of Superconductivity and Physics of Nanostructures,
Moscow Engineering Physics Institute, Russia

It is well known that the Hall probe magnetic imaging represents a powerful technique for the investigation of the magnetic field distribution in superconducting materials of many different types and geometries. In this report we present a new method of the evaluation of current distributions in thin superconducting tapes and films from the data of two-dimensional magnetic field profiles measured over the sample surface. We have analyzed standard algorithms of critical current calculation from the magnetic map and shown that the correct realization requires magnetic field mapping on the region in many times larger than the area of superconducting sample. To avoid this disadvantage we have developed a new modified calculation algorithm of two-dimensional 2D distribution of supercurrents. Realization of this modified algorithm needs sufficiently smaller area of measured magnetic field. An application of modified algorithm for 2D current mapping in superconductive tapes has shown a high efficiency of our approach. So, in the figure we present (from top to down) *i*) trapped magnetic field distribution that was measured by a scanning Hall-probe technique; *ii*) calculated 2D

distribution of y-component of supercurrent $J_y(x,y)$; *iii*) calculated 2D distribution of x-component of supercurrent $J_x(x,y)$. Obtained results may be used in real practical set-up for quality control of commercial superconductors.



Support by RFBR (grant 06-08-00551-a) is acknowledged.

23PO-1-3

PROXIMITY EFFECT IN Nb/Pd_(1-x)Fe_(x) AND Nb/Pd_(1-x)Fe_(x)/Ni_{0.80}Fe_{0.20} ($x=0.01$) HYBRID MULTILAYERS

Rusanov A.Yu., Egorov S.V., Golikova T.E., Prokofiev A.S., Stolyarov V.S.
Institute of Solid State Physics RAS, 142432 Chernogolovka, Moscow distr, Russia

Investigations of hybrid superconductor/ferromagnet (S/F) thin film structures are of a great interest [1-3] because of their potential use for different low temperature applications: RSFQ logic, cryoelectronics. Specifically, their functioning as a components of spintronic devices attracts huge attention.

We study the proximity effect in Nb/Pd_(1-x)Fe_(x) and Nb/Pd_(1-x)Fe_(x)/Ni_{0.80}Fe_{0.20} hybrid structures with $x = 0.01$. At this concentration of iron PdFe tends to show a strong dependence of Curie temperature versus film thickness, so the transition from the paramagnetic to the ferromagnet can be varied by just changing the F-film thickness. The situation changes dramatically if the additional strongly ferromagnetic Ni_{0.80}Fe_{0.20} layer is brought in the vicinity to PdFe layer. The critical temperature as a function of different film thickness both for superconductor and ferromagnet is measured together with the magnetotransport properties of the structures close to the transition from the normal into the superconducting state.

This work is supported by the Russian Foundation for Basic Research (project nos. 07-02-01026) and the Division of Physical Science, Russian Academy of Sciences (project no.5 “New Materials and Structures”)

[1] V.V. Ryazanov, V.A. Oboznov, A.Yu. Rusanov, et al., Phys. Rev. Lett. **86**, 2427 (2001).

[2] V.A. Oboznov, V.V. Bol'ginov, A.K. Feofanov, V.V. Ryazanov and A.I. Buzdin, Phys. Rev. Lett. **96**, 197003 (2006)

[3] A.Yu. Rusanov, S. Habraken, and J. Aarts, Phys. Rev. B **73**, 060505R (2006).

23PO-1-4

MAGNETISM AND SUPERCONDUCTIVITY OF RRh₄B₄ SYNTHESIZED UNDER HIGH PRESSURE

Tsvyashchenko A.V.¹, Sidorov V.A.¹, Fomicheva L.N.¹, Bauer E.D.², Thompson J.D.²

¹Vereshchagin Institute for High Pressure Physics, RAS, 142190 Troitsk, Russia

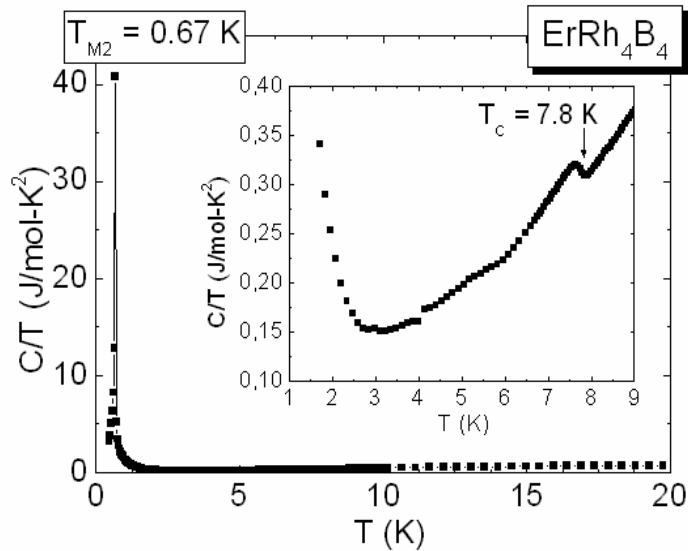
²Los Alamos National Laboratory, Los Alamos, New Mexico 87545, USA

A new group of RRh₄B₄ ternary borides has been synthesized at pressure of 8 GPa. These materials were also found to crystallize, like R(Rh_{0.85}Ru_{0.15})₄B₄, in a body-centered-tetragonal structure (type LuRu₄B₄) with space group I4₁/acd and 8 formula units per unit cell[1].

Magnetic measurements were made in a Quantum Design MPMS magnetometer. Electrical resistivity and specific heat measurements were performed in a Quantum Design PPMS with ³He insert down to 0.45K.

All compounds of the series (except Tb and Yb) become superconducting at low temperature. The superconducting transition at T_c in all compounds (except Lu and Y) develops from a weakly ferromagnetic state which appears at T_M. Inside the superconducting state, an antiferromagnetic transition at T_N is observed which is due to localized moments of the rare earth ions. Transition temperatures and lattice constants for new RRh₄B₄ compounds are shown in Table. Specific heat C(T)/T for ErRh₄B₄ is shown in Fig.

R	a (Å)	c (Å)	T _c (K)	T _N (K)	T _M (K)
Eu	7.438	15.093	5.5	-	-
Tb	7.459	14.865		4.2	58
Dy	7.453	14.950	4.6	3.3	38
Ho	7.452	14.862	6.2	1.5	23
Er	7.432	14.822	7.8	0.67	21
Tm	7.412	14.870	8.2	0.5	11
Yb	7.449	14.851	-	-	-
Lu	7.449	14.815	9.0	-	-
Y	7.434	14.934	10.7	-	-



This work was supported by the Russian Foundation for Basic Research (Grant 07-02-00280).

[1] D.C. Johnston, Solid State Communs, **24**, 699 (1977).

23PO-1-5

THE CRITICAL TEMPERATURE IN THE CLEAN FERROMAGNET/SUPERCONDUCTOR SUPERLATTICE

Khusainov M.G.^{1,2}, Khusainov M.M.¹, Popov I.I.¹, Proshin Yu.N.¹

¹Department of Theoretical Physics, Kazan State University, Kazan 420008, Russia

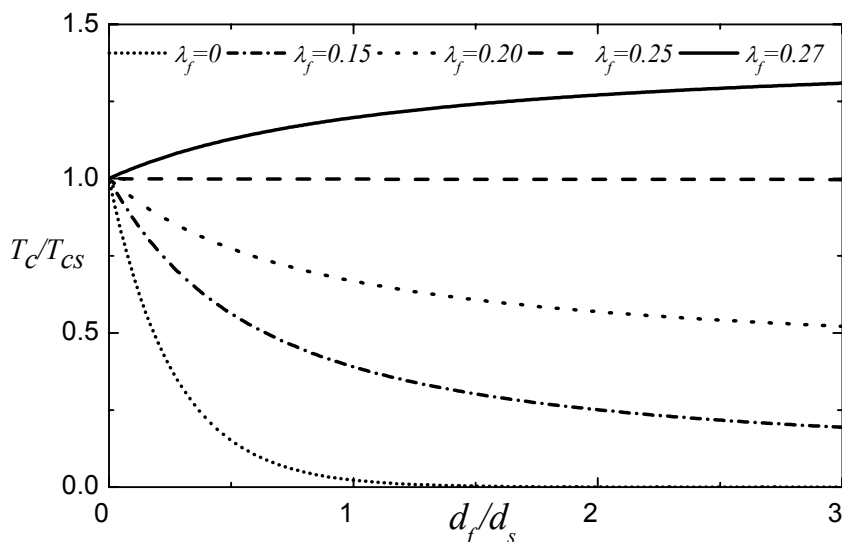
²Department "Vostok", Kazan State Tupolev Technical University, Chistopol' 422981, Russia

In present work we theoretically investigate the interplay between the possible superconducting and magnetic states in the layered FM/S nanostructures where FM is the clean ferromagnetic metal, and S is the clean superconductor. In the framework of the three-dimensional theory of the proximity effect [1] we take into account the electron-electron interaction in the FM layers. To find the dependence T_c versus thicknesses of layer FM (d_f) and S (d_s) for the FM/S superlattice in the Cooper limit we solve the Eilenberger equations in the case of ideal transparency of the FM/S interface. Two cases for mutual orientation of magnetizations in neighboring FM layers are considered: parallel one ("0" magnetic phase) and antiparallel one (" π " magnetic phase). It is shown that the 0 phase state can win only in case of external magnetic field presence only. In this case the unconventional Fulde-Ferrell-Larkin-Ovchinnikov pairing with nonzero 3D coherent momentum \mathbf{k} is realized in all layers. In the zero field condition the π phase is realized with the practically full compensation of paramagnetic effect of exchange field, and electrons are paired on the traditional BCS mechanism. The critical temperature T_c in the π phase state is determined by expression (T_{cs} is the critical temperature of the "bulk" S)

$$\ln \frac{T_c}{T_{cs}} = -\frac{c_f(\lambda_s - \lambda_f)}{\lambda_s(c_s\lambda_s + c_f\lambda_f)} + \frac{c_f\lambda_f}{(c_s\lambda_s + c_f\lambda_f)} \ln \left(\frac{\omega_D^f}{\omega_D^s} \right)$$

where $\lambda_{f(s)}$ is interelectron interaction constant in the FM (S) layers, ω_D is the Debye frequency, $c_{s(f)} = d_{s(f)}/(d_s + d_f)$ is relative weighting factor of the S (FM) layers.

It allows us to explain specific experimental results on the proximity effect in the Gd/La superlattices with unusual relation between the FM and S thicknesses ($d_{Gd} \approx 3d_{La}$) [2]. At zero field cooling the magnetic π phase state was realized with surprisingly high $T_c \sim 5K$, which practically coincides with T_{cs} for La. In the Figure the $T_c(d_f/d_s)$ dependencies for the various values of λ_f are shown for the pure Gd/La superlattice in the π magnetic phase. Thus the developed theory let us predict the magnitude and sign of constant $\lambda_f \approx 0.25 > 0$, that is slightly less than estimated value for the lanthanum $\lambda_s \approx 0.27$.



[5] M.G. Khusainov, M.M. Khusainov, Yu.N. Proshin, *JMMM.*, **300** (2006) 243.

[6] J.P. Goff, et al., *J. Magn. Magn. Mater.*, **240** (2002) 592.

23PO-1-6

INHOMOGENEOUS CURRENT DISTRIBUTION IN A BIMETAL FERROMAGNET/SUPERCONDUCTOR FILM IN A LONGITUDINAL MAGNETIC FIELD

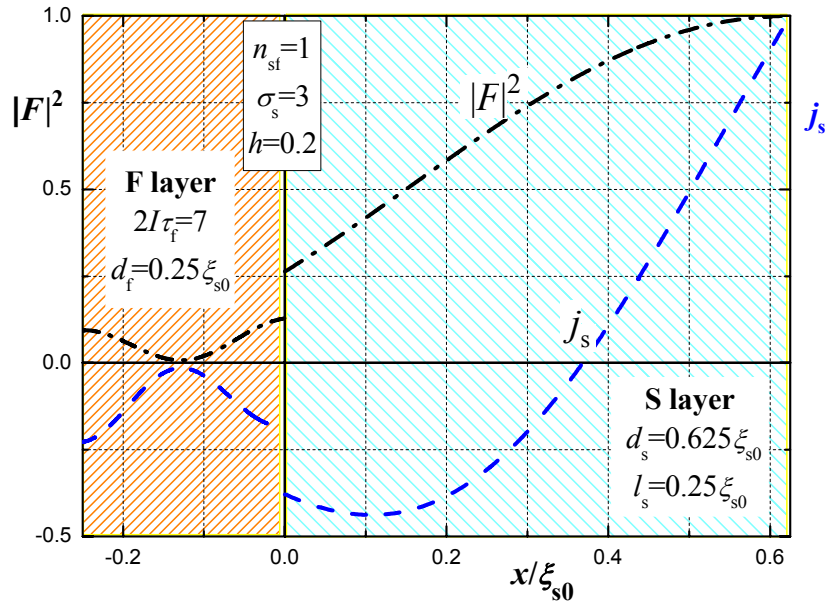
Avdeev M.¹, Khusainov M.², Proshin Yu.¹, Tsarevskii S.¹

¹Kazan State University, Kazan 420008, Russia

²“Vostok” Branch, Kazan State Technical University, Chistopol' 422950, Russia

It is well known that the proximity effect of thin ferromagnet metal/superconductor (F/S) bilayers depends heavily on the transparency of the S/F interface σ_s , the thicknesses of the F and S layers (d_f and d_s), the coherence length ξ_{s0} , and the relation between the parameters of the electron structure and electron interaction of the contacting metals. It should be noted also that the quasiparticle motion in the ferromagnet has the mixed diffusion – spin-wave character. The most striking feature of the F/S systems is the highly non monotonic behavior of the critical temperature T_c with the thickness of the ferromagnetic layer d_f [1,2].

In this report we consider a planar contact between a ferromagnetic metal film occupying the region $-d_f < x < 0$ and a superconductor film occupying the region $0 < x < d_s$ in the external magnetic field \mathbf{H} applied parallel to the film situated in the y - z plane ($d_f, d_s \ll \lambda$, where λ is the magnetic-penetration depth). In the applied magnetic field a superconducting current is induced both in the S and F films. We have assumed that S and F metals are dirty. For definition of a superconducting current density j_s we solve equations for the Usadel function F in the superconducting and ferromagnetic regions of space with relevant boundary conditions on $x = -d_f$, $x = 0$, $x = d_s$ [3]. The results of numerical calculations of $|F|^2$ and j_s as functions of x are presented in the Figure. Here I and τ_f are the effective exchange field, acting on the electron spin from localized spins, and the free path time in the F layer, correspondingly; n_{sf} is the electron structure parameter [1], l_s is the mean free path in the S layer; $h = H/H_c$ (H_c is the critical magnetic field of the superconductor).



As can be seen from the Figure, superconducting current is strictly inhomogeneous and it penetrates to the F layer. Calculations also show that the current inhomogeneity depends heavily on the transparency S/F-interface.

- [1] Yu.A. Izyumov, Yu.N. Proshin, M.G. Khusainov, *Physics - Uspekhi* **45** (2002) 109.
 [2] A.I. Buzdin, *Rev. Mod. Phys.* **77** (2005) 935.
 [3] Yu.N. Proshin, M.G. Khusainov, *JETP Lett.* **66** (1997) 562.

23PO-1-7

MAGNETIC SUPERCONDUCTORS IN SYSTEM OF SOLID SOLUTIONS Dy(1-x)YxRh4B4

Khlybov E.

Institute of high pressure physics, Troitsk 142190, Russia

In this work for the first time we give the evidence that compound $\text{Dy}_{1-x}\text{Y}_x\text{Rh}_4\text{B}_4$ with the tetragonal body-centered crystal structure LuRu_4B_4 is the ferrimagnetic at temperatures $T_{\text{Cur}} < 40\text{K}$, ferrimagnetic superconductor at $T_C < 10\text{K}$ and antiferromagnetic superconductor at $T_N < 3\text{K}$. No reentrant behavior was found down to $T = 0.32\text{K}$. The temperature of ferrimagnetic ordering T_{Cur} depends on x and with its increase falls down from $\approx 37\text{K}$ at $x=0$ up to $\approx 7\text{K}$ at $x=0.8$. YRh_4B_4 is a paramagnetic. At various x the basic features of ferrimagnetic behaviour of samples are found out and investigated: temperature dependence of reciprocal magnetic susceptibility $\chi^{-1}(T)$ at temperatures above T_{Cur} is hyperbolic; temperature dependences of spontaneous magnetization $M(T)$ are of P and N types on classification of Neel: absence of

saturation of $M(T)$ and presence of points of magnetic compensation. It is shown, that substitution of Dy by Y not simply reduces T_{Cur} , but essentially influences the ferrimagnetic structure. So, dependence of maximal spontaneous magnetization $M_{max}(x)$ on x is strongly nonmonotonic and it reaches the highest value at $x \approx 0.6$, exceeding $M_{max}(x)$ value for $DyRh_4B_4$ approximately 1.4 times. $DyRh_4B_4$, on preliminary data, is noncollinear ferrimagnetic with two Curie points. All results suggest the presence of the one-directional exchange anisotropy. The critical temperature appears linearly increasing from $\approx 5K$ for $x = 0$ up to $\approx 10K$ for $x = 1$. The change of the T_C seems to be correlated with the spin value of the system. For superconducting samples $DyRh_4B_4$ and $Dy_{0.8}Y_{0.2}Rh_4B_4$ the measurements of a heat capacity suggest that systems at temperature near 3K undergo ferrimagnetic- antiferromagnetic phase transition. This transition essentially influences temperature dependence of upper critical magnetic field H_{C2} . For the first time by means of a method of microcontact spectroscopy of Andreev reflection in point contact $Ag - Dy_{0.8}Y_{0.2}Rh_4B_4$ the value and temperature and field dependences of superconducting gap parameter $\Delta(T,H)$ in $Dy_{0.8}Y_{0.2}Rh_4B_4$ were measured. The value of $\Delta(0)$ is close to 1.0 meV, that gives the value of the $2\Delta(0)/kT_C \approx 4$. Some unusual features of $\Delta(T,H)$ dependences are observed, which give the evidence that unconventional triplet type of superconducting pairing of charges with the parallel spins is realized in the system $Dy_{1-x}Y_xRh_4B_4$.

23PO-1-8

SUPERCONDUCTOR – MAGNETICALLY ACTIVE LAYER– SUPERCONDUCTOR THIN FILM STRUCTURES

*Kislinskii Y.V.¹, Borisenko I.V.¹, Constantinian K.Y.¹, Komissinskiy P.V.^{1,2},
Ovysuannikov G.A.^{1,3}, Shadrin A.V.¹*

¹Institute of Radio Engineering and Electronics, RAS, Mokhovaya 11-7, Moscow, Russia

²University of Darmstadt, Darmstadt, Germany

³Chalmers University of Technology, S 41296 Geteborg, Sweden

Multilayer hybrid superconducting (S) structures with an interlayer consisting of a ferromagnetic or an antiferromagnetic (AF) material have aroused considerable interest [1, 2]. Recently S-AF-S thin film Josephson heterostructures Nb/Au/AF/YBa₂Cu₃O_{7- δ} with Ca_{0.5}Sr_{0.5}CuO₂ (CSCO) AF interlayer have been fabricated and experimentally studied at microwave frequencies [3]. The superconducting current–phase relation (CPR) has shown noticeable deviation from sinusoidal shape due contribution of the second harmonic, which was evaluated, using integer and non-integer Shapiro step measurements approach, described in [4].

However, a search for other magnetically active materials for interlayer may give intriguing opportunities for utilization of novel Josephson structures with enhanced weight of the second harmonic amplitude in CPR. Promising candidates are La_{0.68}Ca_{0.32}MnO₃ (LCMO) or LaMnO₃ (LMO). In this connection along with CSCO interlayer junctions we have fabricated and tested thin film sandwich-type structures with 20 ÷ 50 nm thick epitaxial grown LCMO and LMO over the YBa₂Cu₃O_{7- δ} film.

Preliminary measurements of structures with 20 nm LCMO interlayer have shown a drop in resistance versus temperature due superconducting transitions of YBa₂Cu₃O_{7- δ} and Nb films. Insulator – metal transition of structure with LCMO interlayer was observed at temperatures 90 ÷ 50 K. The transitions of a reference LCMO film was at 250 ÷ 200 K. Nonlinear I-V characteristics of Nb/Au/LCMO/YBCO (having R_{NS} of order of $10^{-3} \Omega \cdot cm^2$) have been registered with well defined conductance singularities which could be speculatively treated as a superconducting current with a density $10^{-1} A/cm^2$. The I-V characteristics of structures with

LMO interlayer were also nonlinear $V < 1$ mV. In order to verify existence of superconducting current and the Josephson effect a set of measurements are planned under applied microwaves.

- [1] L.B. Ioffe, et al. Nature, vol. 398, (1999) p. 679.
 [2] F.S. Bergeret, et al. Rev. Mod. Phys. 77, 1321 (2005).
 [3] P.Komissinskiy et al., Physical Rev. Letters, vol. 99, (2007) p. 017004.
 [4] Yu.V. Kisilinskii et al., JETP, vol. 101, (2005) p.494.

23PO-1-9

COEXISTENCE OF FERROMAGNETISM AND SUPERCONDUCTIVITY IN COMPLEX IRON-VANADIUM LAYERED NANOSTRUCTURES

*Aksenov V.L.^{1,2}, Khaidukov Yu.N.¹, Nikitenko Yu.V.¹,
Perov N.S.³, Jernenkov K.N.^{1,4}, Westerholt K.⁴, Zabel H.⁴*

¹Joint Institute for Nuclear Research, 141980 Dubna, Russia

²RRC Kurchatov Institute, 123182, Moscow, Russia

³Lomonosov Moscow State University, 119992 Moscow, Russia

⁴Ruhr-Universitat Bochum, D 44780, Bochum, Germany

Study of influence of superconductivity (S) on ferromagnetism (FM) in layered nanostructures is an actual problem both for fundamental science and for practical applications. Theoretically predicted, that due to proximity effects between S and FM layers various scenarios of influence of superconductivity on ferromagnetism are possible: formation of domain structure (so-called cryptoferromagnetic state [1]), effect of magnetization "leakage" from FM to S layer [2, 3], change of direct and indirect exchange coupling of FM layers [4], etc. In FM/S/FM structures with non-collinear magnetization the existence of triplet superconductor pairs is predicted. Such pairs are not subject to destroying influence of an exchange field [5] and therefore more "alive" in FM layer. Practical importance of studying of such systems for needs of spintronics is connected with non trivial magnetic response of such systems on occurrence of superconductivity.

In the present work results of research of influence of superconductivity on magnetism in complex systems of type "S/FM interface + GSW" are presented (GSW -is the generator of standing waves of neutrons contains Fe/V periodic layered system with period D_{GSW} and N times repeated). Measurements have been conducted at two samples (see table).

Table. Parameters of the samples

sample	S layer	FM layer	D_{GSW} , E	N	Tc, K
№ 1	V, 385 E	Fe, 32 E	64	20	3.8
№ 2	V, 365 E	Fe _{0.5} V _{0.5} , 47 E	94	10	3.3

Part of experimental data of polarized neutron reflectometry (PNR) with initial interpretation has been presented earlier in articles [6, 7]. In this work more detailed quantitative analysis of PNR data have been done, and data of VSM, X-ray and conductometry experiments has been added. Researches have shown, that in the given systems at transition into superconducting state there is a change of magnetic state both of S/FM interface and in GSW. Magnetic response of two samples has both the common moments, and differences.

- [1] P.W.Anderson, H. Suhl, Phys. Rev.,V.116 p. 898 (1959)
 [2] V.N. Krivoruchko and E.A. Koshina, Phys. Rev. B 66, 014521 (2002)
 [3] F. S. Bergeret, A. F. Volkov and K. B. Efetov, Phys. Rev. B 69, 174504 (2004)
 [4] Sa de Melo C.A.R. Phys.Rev. B 62 12303 (2000)
 [5] Volkov A. F., Bergeret F. S., and Efetov K. B. PRL. V 90. P 117006 (2003)
 [6] V.L. Aksenov, K.N. Jernenkov, Yu.N. Khaidukov et al, Physica B V. 356, 9-13 (2004)
 [7] V. L. Aksenov, Yu. V. Nikitenko, A. V. Petrenko et al, Crys. Rep. V.52(3),p. 381, 2007

23PO-1-10

MAGNETIC QUANTUM OSCILLATIONS IN DOPED ANTIFERROMAGNETIC INSULATORS

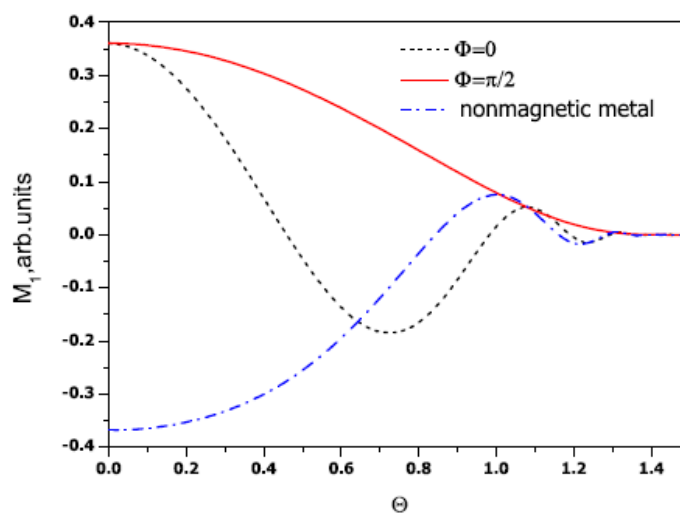
Kabanov V.V.¹, Alexandrov A.S.²

¹Jozef Stefan Institute 1001, Ljubljana, Slovenia

²Dept. of Physics, Loughborough University, Loughborough, UK

Energy spectrum of electrons (holes) doped into a two-dimensional antiferromagnetic insulator is quantized in an external magnetic field of arbitrary direction. A peculiar dependence of de Haas-van Alphen (dHvA) or Shubnikov-de Haas (SdH) magneto-oscillation amplitudes on the azimuthal in-plane angle from the magnetization direction and on the polar angle from the out-of-plane direction is found, which can be used as a sensitive probe of the antiferromagnetic order in doped Mott-Hubbard, spin-density wave (SDW), and conventional band-structure insulators.

In Fig. 1 we plot the dependence of the amplitude of the oscillations as a function of the angle Θ between the normal vector to the 2D plane and the direction of the magnetic field. $\Phi = 0$ corresponds to the rotation of the direction of the magnetic field in the plane determined by the direction of the magnetization of antiferromagnet and normal vector to the 2D plane. Here we assume that magnetization is parallel to the plane as in the case of high temperature superconductors. $\Phi = \pi/2$ corresponds to the rotation of the magnetic field in the plane perpendicular to the magnetization. The drastically different behaviour of the amplitude of quantum oscillations as a function of the angle is related to the strong anisotropy of the g-factors in doped antiferromagnets. It is interesting to note that angular dependence of the oscillations in doped antiferromagnetic insulators is very different from that in normal metals or semiconductors (see Fig.1).



These results are important in connection with the recent measurements of the dHvA and SdH oscillations in the underdoped phase of high-temperature superconductors. Analysis of the angular dependence of the oscillations may clarify if the oscillations are indeed connected to the opening of the small pockets of the Fermi surface in the doped antiferromagnetic phase.

[1] V.V. Kabanov, A.S. Alexandrov, *Physical Review B* (2008) (in press).

23PO-1-11

PRINCIPAL ROLE OF MAGNETISM FOR HIGH T_c IN CUPRATES: MAGNETIC PHASE TRANSITION PRECEDING SC ONE ($T_c < T_m$)

Mazov L.S.

Institute for Physics of Microstructures RAS, 603600 Nizhny Novgorod, Russia

In the beginning of 90th it was presented evidence for formation of modulated magnetic (AF SDW-like) structure before SC transition in high- T_c cuprates (see, e.g. [1] and references therein). In other words, cuprate system enters the SC state only when in the system there occurs a magnetic (AF SDW) phase transition from spin-disordered state to magnetically ordered one. In this sense, the additional (magnetic) order in the system can be considered as “stabilizer” which provides the conditions for Cooper pairing in cuprates at such high temperatures. This magnetic (SDW-like) state arises at $T = T_{SDW}^{onset} = T^*$ when in CuO_2 -plane it is formed a stripe-structure with alternating spin and charge stripes (10 \AA and 15 \AA in width, respectively), and at symmetrical parts of the Fermi surface the SDW(CDW)-gap (treated usually as pseudogap [1]) begins develop. This magnetically ordered state is completed at $T = T_{SDW}^{order} = T_c^{onset}$ below which temperature the cuprate system enters the (SC+SDW) state. The specificity of magnetically ordered state in HTSC is in its dynamical nature so that this magnetic ordering can be detected only by fast and local probes. Such a picture was mainly obtained on the basis of detailed analysis of in-plane resistivity measurements in magnetic field (see, [1]). The resistivity measurements can be included in list of fast and local experimental techniques since due to short conduction electron relaxation time, a magnetic structure is sampled on much shorter time scales as compared with many other techniques such as neutron scattering, Mossbauer effect etc. In this paper, it is demonstrated that above picture agrees well (not only qualitatively but quantitatively) with results of neutron, magnetic, optic, STM and other experiments in cuprates which appear since then. The reviewed results are further analyzed on the basis of the model with partial dielectrization of conduction electron energy spectra [3] (cf. with [4]). The practical recommendations on the possible using of above magnetic mechanism to further increase T_c are presented. The recent data with successful realization of twofold increase of T_c in artificial LSCO system, using, in fact, additional SDW-order, are also included.

- [1] L.S.Mazov, in: Symmetry and Heterogeneity in HTSC (ed. by A.Bianconi), NATO Sci., Ser.II, v.214, pp.217-228, Springer, Berlin, (2006).
 [2] R.A.Klemm, *Int.J.Mod.Phys. B* **12**, 2920 (1998).
 [3] L.S.Mazov, *J.Supercond.Nov.Magn.* **20**, 579 (2007).
 [4] A.N.Kozlov, L.A.Maksimov, *ZhETF* **48**, 1184 (1965).

23PO-1-12

ANOMALOUS MAGNETIC PROPERTIES OF Pr-BASED CUPRATES AND BOROCARBIDES

Narozhnyi V.N.

Institute for High Pressure Physics, Russian Acad. Sci., Troitsk, Moscow Reg., 142190, Russia

Magnetic properties of some Pr-based perovskite-like cuprates and quaternary borocarbides are discussed in interrelations to each other.

Magnetic behaviour of the high-quality Al-free $\text{PrBa}_2\text{Cu}_3\text{O}_{7-y}$ as well as mixed $\text{Y}_{1-x}\text{Pr}_x\text{Ba}_2\text{Cu}_3\text{O}_{7-y}$ and $\text{Gd}_{1-x}\text{Pr}_x\text{Ba}_2\text{Cu}_3\text{O}_{7-y}$ single crystals was experimentally investigated. An evolution of the magnetic anisotropy with temperature and magnetic field was determined for pure Pr-based and mixed (Y-Pr and Gd-Pr) systems. Magnetic phase diagrams have been obtained for $H \parallel c$ as well as for $H \perp c$. An indication on the pronounced interaction between the Pr and Cu(2) magnetic sublattices was found. Different signs of magnetic anisotropy were established for the Pr and Gd sublattices at low temperatures.

Quaternary borocarbides of the type $\text{PrNi}_2\text{B}_2\text{C}$ as well as mixed $\text{Y}_{1-x}\text{Pr}_x\text{Ni}_2\text{B}_2\text{C}$ system were studied. Magnetic properties of $\text{PrNi}_2\text{B}_2\text{C}$ single crystals as well as $\text{Y}_{1-x}\text{Pr}_x\text{Ni}_2\text{B}_2\text{C}$ polycrystalline samples were determined. No indication on superconductivity was observed for $\text{PrNi}_2\text{B}_2\text{C}$ down to $T = 0.35\text{K}$. Possible reasons for the absence of superconductivity and for the anomalously high Neel temperature (approximately 4K) in $\text{PrNi}_2\text{B}_2\text{C}$ are discussed.

Interaction of magnetism and superconductivity for both investigated systems (cuprates and borocarbides) is also discussed.

23PO-1-13

STRUCTURE STUDY OF THE 2H-NbSe₂ IN THE LOW-TEMPERATURE MAGNETIC ANOMALIES VICINITY

Sirenko V.A.¹, Eremenko V.V.¹, Ibulayev V.V.¹, Shvedun M.¹, Andre G.²

¹B.I. Verkin Institute for Low Temperature Physics NASU, Kharkov, Ukraine

²Laboratoire L. Brillouin (UMR12 CEA-CNRS) CEA-Saclay, 1 Gif-sur-Yvette Cedex, France

Albeit a comparatively simple crystal structure of the 2H-NbSe₂ the latter's behaviour in the low-temperature regime is unclear so far due to series of phase transitions and complex variance in topology of Fermi surface. In particular, the low-temperature magnetic anomalies were observed in crystals and powders of due to transformations in hybridized electronic states as was shown by experiments on irradiated samples [1].

The X-ray and neutron diffraction study of 2H-NbSe₂ around the temperature range of the observed magnetic peculiarities were performed. A drastic change of X-ray diffraction patterns were observed below which probably allows to consider these peculiarities as a precursor of the following transitions. A first direct evidence of X-ray scattering by electron modulation in charge-density wave irrelevant to a periodic lattice distortion (PLD) is presented for hexagonal modification of the layered niobium diselenide (2H-NbSe₂). The powder X-ray and neutron diffraction patterns measured concurrently on identical samples with magnetic and thermal properties close to best-quality single crystals revealed an amazing difference in scattering of X-rays and neutrons in the CDW state with their absolute identity above the transition temperature ($T_{\text{CDW}} \approx 35\text{K}$). Namely, few novel pronounced features appear in the X-ray diffraction patterns

below T_{CDW} independently of wavelength indexed in space group D_{3h}^1 with a doubled in-plane lattice parameter a and inversion symmetry axis instead of a screw one. Above a CDW transition, all measurements correspond to the space group D_{6h}^4 with lattice parameters $a=3.44\text{\AA}$, $c=12.8\text{\AA}$ in perfect agreement with published data. The observed difference is obviously explained by different mechanisms of neutron and X-ray scattering, either by spatial distribution of nuclei for the former case, or of electron density for the latter. A CDW formation in $2H\text{-NbSe}_2$ is then accompanied by spatial modulation of electron density with the periodicity $2a$ manifested by X-ray scattering, and a nuclei shift insufficient for appreciable neutron scattering. Indeed, numerous studies show enigmatic absence of Fermi-surface nesting in $2H\text{-NbSe}_2$. Within McMillans consideration, in such a case of long coherence length, electron modulation should dominate a distortion of periodic crystal potential rather than commonly observed periodic lattice distortion, e.g. in $2H\text{-TaSe}_2$.

Support by STCU №4119 , MECD MAT05/1272 and NANOARACAT

[1] J. Bartolome et al. *MISM-2008*

23PO-1-14

MAGNETO-ELASTIC PROPERTIES OF THE LAYERED $2H\text{-NbSe}_2$ SUPERCONDUCTOR

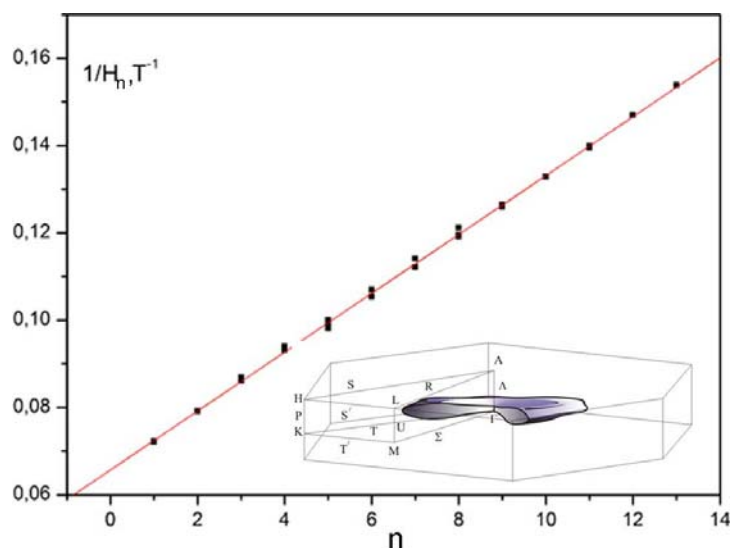
Eremenko V.V.¹, Sirenko V.A.¹, Bruk V.V.², Visser A.², Gasparini A.²

¹B.I. Verkin Institute for Low Temperature Physics NASU, Kharkov, Ukraine

²Zeeman and Van der Waalse University, Amsterdam, the Netherlands

The layered CDW superconductor $2H\text{-NbSe}_2$ was the first of *any* superconductors where magnetization [1] and magnetostriction (MS) [2] quantum oscillations were observed for the first time in the mixed state of superconductivity ($T_{SN}=7,2$ K). The earlier dHvA measurements of $2H\text{-NbSe}_2$ revealed the pan-cake sheet of the Fermi surface in agreement with the preceding band-structure calculations. Enhancement of the MS amplitude compared to those of magnetization was revealed and attributed to a pressure sensitivity of the relevant cross-section of Fermi surface [2], making MS measurements an effective tool for studying its complicated topology. Another important point is possibility to perform the MS measurements in a magnetic field oriented along crystallographic axis in contrast to the routine torque measurements of dHvA effect.

The MS capacitance measurements on a high-quality single-crystalline sample are analyzed for the temperature range 0.254-8K. Two MS oscillation frequencies are observed at the lowest temperatures with in-plane orientation of applied magnetic field H . Therefore, the Fermi-surface sheet in the first Brillouin zone has two cross-sections differing for three times (insert of Fig.1) rather than a conventional pan-cake. It means the presence of small electronic groups never reported before. Their nature can be considered



in a view of successive topological transition under CDW conditions and following competition of CDW and superconductivity in this compound. This finding compliments the reported in-plane anisotropy due to modulation along the pancake perimeter [1].

The MS oscillation–phase analysis was performed using the trivial plot $1/H_n(n)$ with n referred to the oscillation number (Fig. 1). The derived parameter proves a two-dimensional character of the Fermi-surface sheet responsible for the observed oscillations. Scaling in the peak-effect regime of longitudinal MS measurements along the c -axis direction with a succeeding unconventional normal-state behavior is discussed compared to the in-plane measurements.

Support by National Academy and Science & Technology Center of Ukraine under grant 4119.

[1] J.E. Graebner and M. Robbins *Phys. Rev. Lett.* 36 (1975) 422

[2] V.V. Eremenko, V.A. Sirenko, R. Shleser and P. Gammel *Low Temp. Phys. (AIP&ILTPE)* 27 (2001) 469

23PO-1-15

THERMODYNAMIC PROPERTIES OF Gd_2BaNiO_5

Popova E.A.¹, Vasiliev A.N.¹, Dhalenne G.², Berthet P.², Tristan N.³, Klingeler R.³, Buchner B.³

¹Low Temperature Physics Department, Moscow State University, 119991 Moscow, Russia

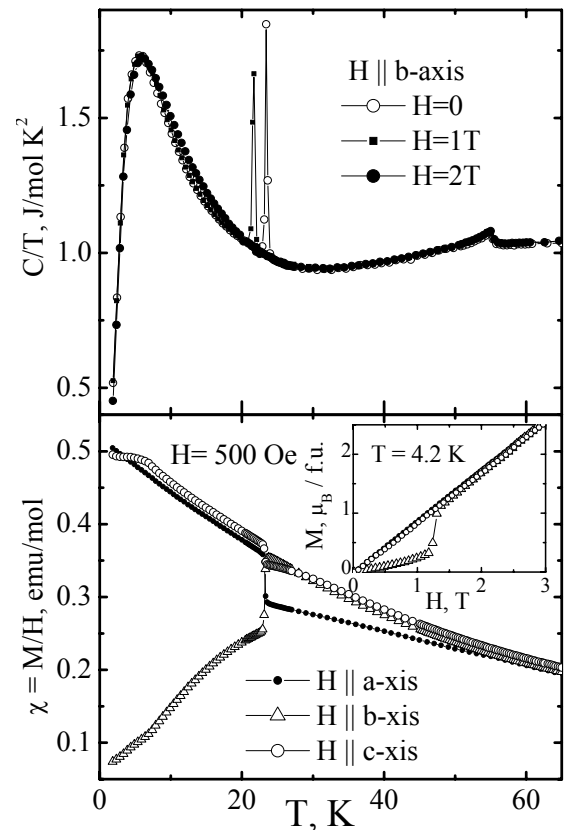
²Laboratoire de Physico-Chimie de l'Etat Solide, Universite Paris-Sud, F-91405 Orsay, France

³Leibniz Institute for Solid State and Materials Research, 01171 Dresden, Germany

The reference compound Y_2BaNiO_5 of the quasi-one-dimensional materials R_2BaNiO_5 (R-rare-earth ion or yttrium) is well known as a typical Haldane gap system. All other members of the family R_2BaNiO_5 have magnetic R^{3+} ions in addition to the spin $s=1$ Ni^{2+} ions and the system orders antiferromagnetically at T_N . Gd^{3+} is the rare-earth ion with no orbital moment in the ground state. The crystal structure of Gd_2BaNiO_5 contains flattened NiO_6 octahedra sharing their corners which form chains along the a -axis and are interconnected through Gd^{3+} and Ba^{2+} ions.

Specific heat and magnetization measurements are performed along a , b and c -axis of the Gd_2BaNiO_5 single crystal in the temperature range 1.8 - 300 K. As shown in figure, the specific heat data at zero magnetic field exhibit several pronounced features, i.e. a second order transition indicated by a λ -type anomaly at 53 K, a peak at first order phase transition at 24 K, and a Schottky anomaly at low temperatures. Strong anisotropy of magnetic properties is observed by magnetization measurement. Below 53K, magnetic susceptibility χ_a measured along a -axis is smaller than those measured along b - and c -axes. While the $\chi_b(T)$ fall down the $\chi_a(T)$ and the $\chi_c(T)$ rises upon cooling below 24K. Moreover, the spin-flop transitions in magnetization curves $M(H)$ are observed at $T < 24K$ in magnetic field $H \parallel b$ -axis, and above this temperature when $H \parallel a$ -axis.

The experimental data show that at $T_N=53\text{K}$, the antiferromagnetic ordering occurs, and spontaneous spin-reorientational phase transition takes place at 24K , which is in a good correspondence with Ref. [1]. The magnetic moments of both Ni and Gd subsystem are oriented mainly along the a-axis at $T_{sr} > 24\text{K}$, and are oriented mainly along the b-axis at $T_{sr} < 24\text{K}$. The application of external magnetic field $H\parallel b$ -axis facilitates the reorientation which occurs at lower temperature, as is seen in $C(T, H=1\text{T})$ dependence. The absence of sharp anomaly in $C(T, H=2\text{T})$ dependence at $H\parallel b$ -axis is due to the fact that the magnetic moments have been oriented along the a-axis, i.e. $\text{Gd}_2\text{BaNiO}_5$ is in the flop phase already. The Schottky anomaly in the specific heat is caused by a temperature-driven population of the upper components of the 8-times degenerated ground state of Gd^{3+} ions split by the internal magnetic field in ordered state. The shift of this anomaly to higher temperature in magnetic field $H\parallel b$ -axis of 2 T can be explained by difference of the value of external magnetic field acting on Gd ion in cases when magnetic moments are parallel to a- or b- axes.



[1] A.Butera , M.T.Causa, M. Tovar, S.B.Oseroff , S.-W.Cheong, JMMM **140-144** (1995) 1681

23PO-1-16

LOW TEMPERATURE HEAT CAPACITY STUDY OF $\text{Nd}_3\text{Ni}_{13-x}\text{Co}_x\text{B}_2$ SERIES

Arauzo A.¹, Bartolome J.², Rillo C.²

¹SIC-Area de Medidas Físicas, Universidad de Zaragoza, 50009 Zaragoza, Spain

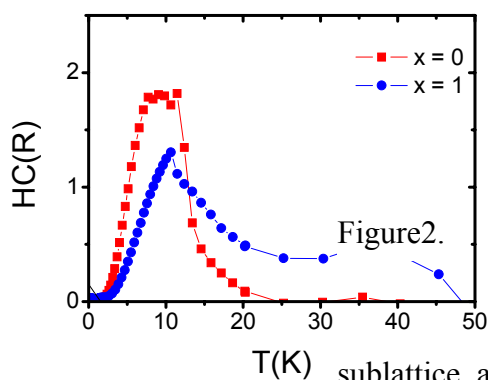
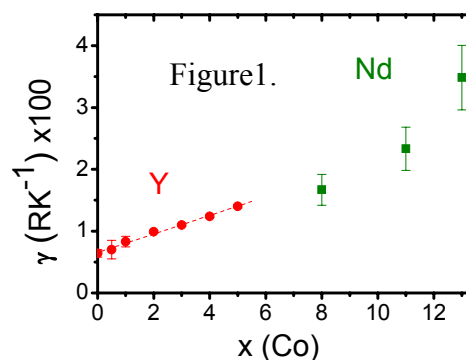
²Instituto de Ciencia de Materiales de Aragon, CSIC-Universidad de Zaragoza, 50009 Zaragoza, Spain

The low temperature Heat Capacity of the layered structure $\text{Nd}_3\text{Ni}_{13-x}\text{Co}_x\text{B}_2$ ($x = 0, 1, 3, 6, 8, 11$ and 13) solid solutions has been measured from 350 mK to RT. Magnetic phase diagrams of this series [1] show that these compounds order ferromagnetically for $x > 0$ and T_c increases linearly with increasing Co content. T_c is below 300 K for $x < 6$. The pure $\text{Nd}_3\text{Ni}_{13}\text{B}_2$ compound undergoes an AF ordering phase transition at 12 K . The electronic contribution to the low temperature heat capacity gives information about the density of states at the Fermi surface. Results of $\text{Y}_3\text{Ni}_{13-x}\text{Co}_x\text{B}_2$ ($x \leq 5$) series have been used to determine the origin of magnetism in these compounds [2]. Within this frame, low temperature heat capacity measurements have been performed, comparing the results with that of the $\text{Y}_3\text{Ni}_{13-x}\text{Co}_x\text{B}_2$.

For high Co content, $x \geq 10$, the Heat Capacity results below 20 K can be analysed in terms of three contributions, the hyperfine, the electronic and the phonon contribution:

$$C = C_{hf} + C_e + C_{ph} = \frac{\alpha}{T^2} + \gamma T + AT^3.$$

The magnetic term may be neglected in this case. The phonon term, C_{ph} , is almost independent of the Co substitution. The hyperfine contribution is explained as due to the interaction acting on the Co and the Nd nuclei. For increasing x the contribution depends linearly with the Co content. The hyperfine interaction with the Co nuclei is found to be larger than for the Y series [2]. The electronic constant also increases with Co content with similar trend that the one observed in the Y compounds (Figure1). The experimental value obtained for the pure $\text{Nd}_3\text{Co}_{13}\text{B}_2$ is $\gamma = 289.5 \text{ mJ/molK}^2$, to be compared with the theoretical value $\gamma_{th} = 215 \text{ mJ/molK}^2$



obtained with the calculated density of states at the Fermi surface.

For very low Co content, $x \leq 1$, an extra contribution to the HC at $T < 20\text{K}$ is observed, which can be attributed to a low dimensionality magnetic order transition (see Figure 2). In the case of the $\text{Nd}_3\text{Ni}_{13}\text{B}_2$ compound, an AF ordering has been reported at 12 K [1]. This order is attributed to the Nd-Nd interaction in the layered structure of this series. The introduction of Co, for $x=1$, induces disorder in the Nd sublattice, as is put in evidence by the broadening of the HC peak (Fig. 2). Moreover, the introduction of Co inhibits the Nd magnetic ordering for $x \geq 3$.

Support by MAT05-1272 is acknowledged.

[1] J. Bartolome et al., Journal of Alloys and Compounds 442 (2007) 11-16.

[2] C. Rillo et al., Journal of Magnetism and Magnetic Materials 316 (2007) 166-169.

23PO-1-17

MAGNETIC ANISOTROPY IN THE 2H-NbSe₂ ELECTRON IRRADIATED SINGLE CRYSTAL

Bartolome J.¹, Bartolome E.², Eremenko V.V.³, Ibulaev V.V.³, Sirenko V.A.³, Petrusenko Yu.T.⁴

¹Instituto de Ciencia de Materiales de Aragon. CSIC-University of Zaragoza, 50009 Zaragoza, Spain

²Escola Universitaria Salesiana de Sarria. Passeig Sant Joan Bosco, 74, 08017 Barcelona, Spain

³B.I. Verkin Institute for Low Temperature Physics NASU, Kharkov, Ukraine

⁴National Scientific Center "Kharkov Institute of Physics and Technology" NASU, Kharkov, Ukraine

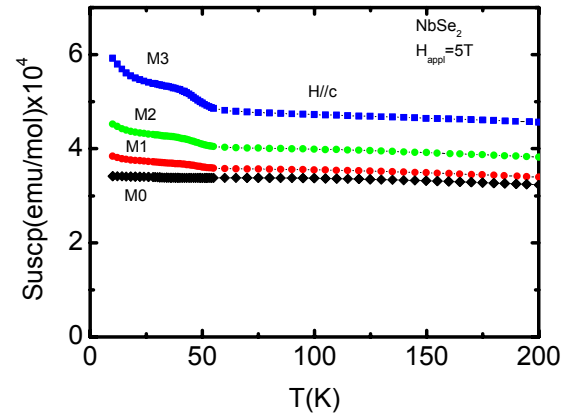
The hexagonal modification of the layered metallic compound 2H-NbSe₂ is of paramount interest due to the appearance of charge density wave, CDW state, when cooling below the temperature $T_{CDW}=32,5 \text{ K}$, and superconducting state when further cooling below $T_{SN}=7,2 \text{ K}$.

The effect of irradiation on the CDW region of NbSe₂ is far from understood, therefore, and considering the above antecedents on the same or similar systems, it was deemed of interest to investigate the anisotropic magnetic susceptibility as a function of temperature of 2H-NbSe₂, using therewith doping of the samples by electrons. The electron doses were M1=22 Mrad (1015 electron/cm²), M2=220 Mrad (1016 electron/cm²), M3=2200 Mrad (1017 electron/cm²). M0 corresponds to the pristine, non-irradiated, sample.

In the temperature range 50-150 K the magnetic perpendicular susceptibility χ_c of a pristine single crystal is almost independent of temperature (Fig.1) with a very small upturn in both χ_c or χ_{ab} , below 33 K. It is evident that this small increase upon cooling is related to the onset of the CDW transition.

In contrast to the pristine sample, for the irradiated samples the upturn sets-on at $T_S=54$ K, therefore, the mechanism for this feature is different to the former. All curves show Pauli paramagnetism, which increases with the irradiation dose. They all show a common tendency to decrease as temperature increases above 60 K, in fact, the temperature dependence is practically identical, independently of the irradiation dose. Besides, the anisotropy ratio $\chi_c/\chi_{ab} \approx 2.6$ is found for the pristine and lowest dose, very near to the theoretical prediction [1], and increases very strongly with irradiation dose, up to $\chi_c/\chi_{ab} \approx 3.8$.

The observed additive contribution superimposed to the Pauli paramagnetism in the low-temperature region is attributed to the presence of local paramagnetic centers, like vacants by displaced Nb ions, or dangling interatomic bonds created by electron irradiation. The observed anisotropy is related to spin-orbit effects on the hybridized electronic states. Irradiation affects the density of states at the Fermi surface, increasing both χ_P and the anisotropy.



Support by STCU №4119 , MECD MAT05/1272 and NANOARACAT

[1] A.H. MacDonald and D.J.W. Geldart. *Phys. Rev. B* 24 (1981) 469

23PO-1-18

EFFECT OF THE MAGNETIC TRAPPED FLUX ON THE HEAT CAPACITY OF THE SUPERCONDUCTING LEAD

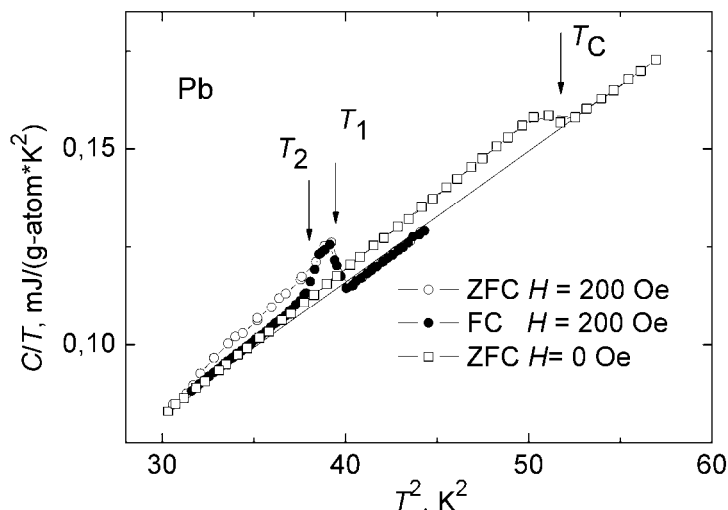
Podgornykh S.M., Dyakina V.P., Prekul A.F.

Institute of Metal Physics, Ural Division of the Russian Academy of Sciences,
S.Kovalevskya st., 18, 620041, Ekaterinburg, Russia

Effect of the magnetic prehistory on the temperature dependence of the heat capacity of Lead has been studied. It has long been known that there exists an intermediate state of a superconducting sample in a magnetic field $H_e < H_C$ (H_C is the critical magnetic field). The intermediate state is characterized by a subdivision of the specimen into superconducting and normal regions that the relative total volumes of these two types of region are determined by the

mean induction. At present the complicated data of the heat capacity in magnetic field are in consequence of that the Meissner effect is not enough perfect [1]. Firstly, the heat capacity in magnetic fields with trapped flux was observed for Ta [2]. The heat capacity of the metal in intermediate state is given by $C = C_n[1 - \frac{1}{D}(1 - \frac{H_e}{H_c})] + C_s[\frac{1}{D}(1 - \frac{H_e}{H_c})] + \frac{VT}{2\pi D} \frac{H_e}{H_c} (\frac{dH_c}{dT})^2$,

where C_n and C_s heat capacity in normal and superconducting phases, respectively, D is the demagnetizing factor [3]. Figure shows the heat capacity of the specimen of Lead in magnetic field $H=200$ Oe after zero field cooling (ZFC) and field cooling (FC).



In magnetic field two temperatures are observed: T_1 and T_2 are determined by the conditions $H_e = H_c(T_1)$ and $H_e = (1-D)H_c(T_2)$, respectively. The heat capacity for ZFC state surpasses one for FC state near T_c (Fig.1). We observed a difference of the heat capacity between the ZFC and the FC states in zero magnetic fields for the ring specimen with non zero trapped flux. The trapped flux was produced after the field was turned off. The difference between the ZFC and FC

heat capacity can not be interpreted in terms of the thermodynamics of the intermediate state. It is found that some temperature below the FC heat capacity C is smaller than the heat capacity both in the normal and in superconducting states: $C < C_n$ and $C < C_s$. We believe that the surface energy between the normal and superconducting phases changes and gives rise to the change of the heat capacity of the specimen. Up to now the contribution to the heat capacity from of the surface energy between normal and superconducting phases has never been considered. We think that this result is the first experimental evidence of the surface energy contribution to the heat capacity of the superconductors.

[1] D. Shoenberg, Superconductivity Cambridge (1952), Ch.III.

[2] W.H. Keesom, J.A. Kok, *Physica*, **1** (1934) 595.

[3] Peierls R., *Proc.Roy.Soc.*, **155A** (1936) 613.

23PO-1-19

YBa₂Cu₃O_{7-δ} THIN FILMS EMBEDDED WITH EPITAXIALLY GROWN Y₂O₃ INCLUSIONS

Boytsova O.V.¹, Samoilenkov S.V.², Gorbenko O.Yu.³, Kaul A.R.³

¹Department of Materials Science, Moscow State University, 119992 Moscow, Russia

²Institute of High Temperature RAS, Izhorskaja 13/19, 125412 Moscow, Russia

³Chemistry Department, Moscow State University, 119992 Moscow, Russia

Recently remarkable progress has been made worldwide in the fabrication process of YBa₂Cu₃O_{7-δ} (YBCO) superconducting films on flexible metal tapes for power applications. YBCO is an attractive material due to its high critical current density in high magnetic fields.

Best characteristics are achieved in films containing nanometer-sized defects or inclusions serving as efficient pinning centers for magnetic flux. One particular variant involves the deposition of alternating layers of YBCO and a non-reacting oxide that would grow epitaxially with it. One of these is yttria, Y_2O_3 , which has been used successfully to grow nanostructures in other growth procedures [1].

We have studied the relationship between the chemical nonstoichiometry of the film composition and the critical current density J_c in Y-rich (YBCO) films prepared by the metal-organic chemical vapor deposition (MOCVD). The growth conditions were found for obtaining c-axis orientation and homogeneity of the film. Microstructures of films with embedded particles of Y_2O_3 were analyzed by means of electron backscatter diffraction (EBSD). With this recently developed technique we could directly measure the crystallographic orientation of embedded particles with respect to YBCO matrix. Yttrium oxide particles typically grew with (001)-orientation.

Critical temperature of YBCO ($T_c \sim 90K$, $\Delta T_c = 1-2K$) was almost independent on yttria content in Y-rich films. We obtained high J_c values of $2.2MA/cm^2$ at 77K and self field. Superconducting properties, morphologies and structures of deposited films are reported.

The research was partly supported by RFBR grants 06-03-08050 and 06-08-00592.

[1] K. Matsumoto, T. Horide, A. Ichinose, S. Horii, Y. Yoshida and M. Mukaida *Jpn. J. Appl. Phys.* 2 44 (2005) L246

23PO-1-20

RESISTIVE TRANSITIONS IN S/F/S TRILAYERS

Prischepa S.L.¹, Kushnir V.N.¹, Cirillo C.², Attanasio C.², Vecchione A.², Bell C.³, Aarts J.³, Kupriyanov M.Yu.⁴

¹State University of Informatics and Radioelectronics, P. Browka str. 6, Minsk 220013 Belarus

²Laboratorio Regionale SuperMat, CNR-INFN Salerno and Dipartimento di Fisica "E.R. Caianiello", Università degli Studi di Salerno, Baronissi (Sa) I-84081 Italy

³Kamerling Onnes Laboratory, Leiden University, P.O. Box 9504, 2300 RA Leiden, The Netherlands

⁴Nuclear Physics Institute, Moscow State University, Moscow 119992 Russia

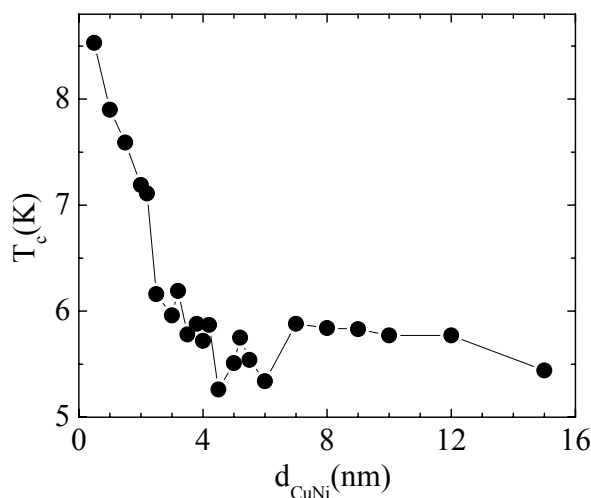
The phase transition of Nb(14 nm)/ $Cu_{0.41}Ni_{0.59}(x)$ /Nb(14 nm) trilayers from the normal to the superconducting state has been studied experimentally by measuring the temperature dependence of the electrical resistance, $R(T)$.

Samples were deposited on Si(100) substrates in a UHV dc diode magnetron sputtering system with a base pressure less than 10^{-9} mbar and sputtering Argon pressure of 4×10^{-3} mbar. The Nb and $Cu_{0.41}Ni_{0.59}$ layers were deposited at typical rates of 0.1 nm/s and 0.04 nm/s, respectively. The high quality layering of the samples was confirmed by X-Ray Reflectivity measurements. The roughness of $Cu_{0.41}Ni_{0.59}$ films did not exceed 0.8 nm.

In order to study the dependence of the superconducting critical temperature as a function of the ferromagnetic layer thickness, $T_c(d_F)$, samples with constant Nb thickness, $d_{Nb} = 14$ nm, and variable $Cu_{0.41}Ni_{0.59}$ thickness ($d_{CuNi} = 1-15$ nm) were grown. To prevent Nb oxidation a thin Al capping layer, 1 nm thick, was deposited on the top of the structures.

We observed, that with increasing d_{CuNi} , T_c exhibits first a rapid drop with a minimum for $d_{\text{CuNi}} \approx 5$ nm. After this point T_c slightly increases with d_{CuNi} saturating at larger $\text{Cu}_{0.41}\text{Ni}_{0.59}$ thickness, see Fig. This overall $T_c(d_F)$ behaviour is a signature of $0-\pi$ phase shift in S/F hybrids [1].

We obtained that, for $d_{\text{CuNi}} < 2$ nm and $d_{\text{CuNi}} > 8$ nm, and therefore in the 0 -phase and π -phase, respectively, the $R(T)$ curves show sharp phase transition from normal to superconducting state. The width of the transition is $\Delta T_c = 0.1$ K. On the contrary, in the thickness interval $2\text{ nm} < d_{\text{CuNi}} < 8\text{ nm}$ the $R(T)$ dependences are broadened and the ΔT_c value reaches 0.6 K. To explain this effect we supposed that for $2\text{ nm} < d_{\text{CuNi}} < 8\text{ nm}$ interval both 0 - and π - phases are realized in our samples due to roughness of S/F interfaces and the local fluctuations of Cu and Ni concentration in the $\text{Cu}_{0.41}\text{Ni}_{0.59}$ alloy. This leads to the existence of a network of both SNS and SFS Josephson junctions. The interaction between local 0 and π junctions in the network causes the fluctuations of the sample parameters and the observed spread of the $R(T)$ curves.



[1] A.I. Buzdin, *Rev. Mod. Phys.*, **77** (2005) 935.

23PO-1-21

FERROMAGNETISM, ANTIFERROMAGNETISM AND SUPERCONDUCTIVITY IN PERIODIC TABLE OF D.I. MENDELEEV

Koroleva L.I., Khapaeva T.M.

M.V. Lomonosov Moscow State University, Vorobyevy Gory, Moscow 119992, Russia

Basic tendencies in the distribution of ferromagnetic (FM), antiferromagnetic (AFM) and superconductive (SC) elements in the periodic table D.I. Mendeleev are observed. In every period, beginning from the fourth and in the group of lanthanides, at first SC elements start then AFM and FM elements (or elements, which possess neither of 3 types of ordering) follow and further SC elements appear again. One can see that ferromagnetism is observed at the elements in which $3d$ -shell is more than half-filled (the number of $3d$ -electrons $6 \leq n \leq 8$), and at the elements with $4f$ -shell, contained k electrons in $4f$ -shell, at which the sum $k + n \geq 8$. Estimation of the radii of the d -, f - and p - orbitals on Slater method [1] shown that $3d$ - and $4f$ -shells of ferromagnetics are more pressing, than the ones with smaller n and $k + n$, and are well separated in crystal. Antiferromagnetism is observed at the elements, at which $3d$ - or $4f$ -shells are precisely half-filled. Superconductivity is observed in the $3d$ -, $4d$ - and $5d$ -elements at $1 \leq n \leq x$, x grows from 3 in $3d$ -elements to 7 in $4d$ - and $5d$ -elements, and in 7-th period only at $n = 2$ and $k + n = 3$. Further, SC is observed at the elements, at which $3p$ -, $4p$ -, $5p$ - and $6p$ -shells are not completely filled and contain no more than 4 electrons. Let's remind that wave functions of p - and d -electrons are petal-shaped. In real crystalline materials the wave functions of neighbor atoms

recover each other. It is shown, that d -orbitals of SC approach closer to the nucleus of neighbor atom, than at FM and AFM. For example, in Fe group a difference $b-r_{3d}$ (r_{3d} is radius of $3d$ electronic shell and b is interatomic distance in the crystalline lattice) for SC is within limits 1.52 – 1.62 E whereas this difference for AFM equals 1.63 E at Cr and 1.65 E at Mn. For FM it is substantially greater: from 1.72 E at Fe to 1.86 E at Ni. It is well known that atoms have to be enough separated for the FM interaction. Only in this case exchange integral becomes positive. At smaller distances between atoms negative exchange interactions prevail and in crystal AFM order takes place [2].

In SC crystals the wave functions of external d - and p -electrons of each atom penetrate inside neighbor atoms and overlap with corresponding wave functions with smaller main quantum number than of central atom. So, in Lu crystal the $5d^1$ wave function of each atom overlaps with the $3d^7$ wave functions of neighbor atoms. This overlap of other elements take place between next wave functions: Hf – $5d^2$ with $3d^5$, Ta - $5d^3$ with $4d^2$, W - $5d^4$ with $3d^4$, Tl – $6p^1$ with $5p^2$, Zr - $4d^2$ with $3d^2$, Nb – $4d^2$ with $3d^5$, Mo - $4d^5$ with $3d^3$, In – $5p^1$ with $4d^4$, Sn – $5p^2$ with $4p^2$. Thus mentioned orbital is found in neighbor atoms in stronger electrical field than in own atom. It is known that in non superconductive crystals consisted of the one sort of atoms the zones are formed from the overlap of the identical wave functions of neighbor atoms. In superconductors the picture become complicated from listed above overlap: the wave functions of neighbor atoms with different main quantum numbers overlap, which energy levels differ on several ten eV. In this case the separation of spin and charge in electron is quite possible and the charges without spin become bosons. Spins obtained magnetic moments are ordered antiparallel by two. At transfer that pair in the parallel state by magnetic field its magnetic flux from component along of magnetic field is equal to 1 fluxon (quant of magnetic flux). In all probability that situation take place in superconductors of the second type at magnetic field $H_{C1} \leq H \leq H_{C2}$ in which magnetic field penetrates in sample through flux tubes contained at one fluxon each. In superconductors of the first type the situation is almost the same, but on account of more perfect lattice one tube, as it were, exists in which all the spins without charges are concentrated.

[1] J.C. Slater, Phys. Rev. 36 (1930) 57.

[2] R.J. Weiss, Phil. Mag. 9 (1964) 361.

23PO-1-22

MAGNETIC STRUCTURE OF SUPERCONDUCTING HIGH-PRESSURE PHASE DyRh_4B_4

*Makarova O.L.*¹, *Goncharenko I.N.*², *Tsvyashchenko A.V.*³, *Fomicheva L.N.*³

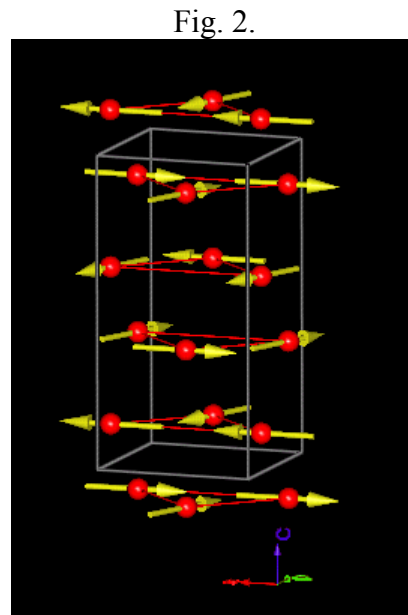
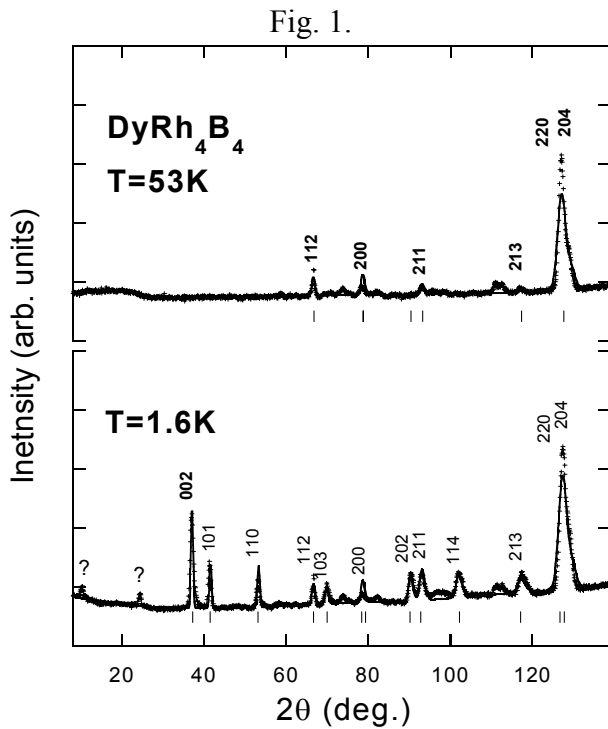
¹Russia Research Center “Kurchatov Institute”, 123182 Moscow, Russia

²Laboratoire Leon Brillouin, CEA-CNRS, CEA Saclay, 91191 Gif-Sur-Yvette, France

³Vereshchagin Institute for High Pressure Physics, RAS, 142190 Troitsk, Russia

The body -centered- tetragonal phase $\text{DyRh}_4^{11}\text{B}_4$ was prepared by melting and quenching the material under a high pressure of 8 GPa. The magnetic structure of the $\text{DyRh}_4^{11}\text{B}_4$ superconducting compound ($T_c = 4.6$ K) was studied by powder neutron diffraction at temperatures from 1.6 K to 53 K, using a G 6.1 diffractometer. The neutron diffraction wavelength was 4.74 Å. The diffraction patterns were measured in the angle range of $5^\circ < 2\theta < 141^\circ$. A 53 K neutron diffraction pattern revealed the absence of a magnetic contribution. The lines were identified in a tetragonal cell (space group $I4_1/a\ c\ d$) with the lattice parameters $a=7.47(3)$ Å

$c=14.96(8)$ E $c/a \sim 2$ (see Fig.1). At $T < 3.4$ K there emerge the lines forbidden in the space group $I4_1/a c d$. The analysis of the intensities of the superstructure peaks suggests the presence of the long-range magnetic order, characterized by a modulation vector 110 . A non-collinear magnetic structure which best describes the experimental spectrum is shown in Fig.2.



The work was supported by the Russian Foundation of Basic Research grant No. 07-02-00280.

23PO-1-23

DOMAIN WALL EFFECTS IN FERROMAGNET-SUPERCONDUCTOR STRUCTURES

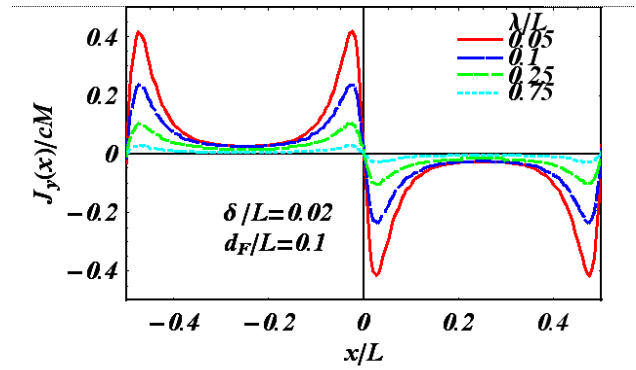
Burmistrov I.S., Chtchelkatchev N.M.

L.D. Landau Institute For Theoretical Physics RAS, 142432 Moscow Region,
Noginsky District, Chernogolovka, Russia

Superconductivity (S) and ferromagnetism (F) are two competing phenomena. It was argued that due to ferromagnetic domains vortices may appear in the superconducting film of a FS bilayer [1]. Recently, the generation of vortices by a magnetic texture of the ferromagnetic film in a FS bilayer has been demonstrated experimentally [2]. Our results presented below answer to the question, how a domain structure of the ferromagnetic film affects the properties of the superconducting film in FS bilayers. We consider the case of weakly coupled F and S films such that one can neglect the proximity effect. The coherence length ξ of the S film is assumed to be the smallest lengthscale in the problem. The magnetization in the F film is given as

$$M_a(x, z) = M\theta(z)\theta(d_F - z) \sum_{j=-\infty}^{\infty} (-1)^j m_a(x - jL), \quad m_x = 0, \quad m_y = \tanh \frac{x}{\delta}, \quad m_z = -\frac{1}{\cosh(x/\delta)}$$

where M is the absolute value of the magnetization, δ denotes the width of the Bloch domain wall, L the width of a domain, and $d_{F,S}$ widths of the F and S films, respectively. By solving the Maxwell-Londons equation for the FS bilayer, we find the distribution of current in the S film induced by the magnetic field of the domain walls. For the case $d_{F,S} \ll \lambda_L$, where λ_L is the London



penetration length, a typical current distribution in the S film averaged over its width is shown in Figure. If domain size $L \rightarrow \infty$, the maximal current was found to be [3]

$$|J_y^{\max}| = cM \begin{cases} \delta / \max\{\delta, \lambda_L\}, & d_F, d_S \gg \lambda_L \\ d_F / \max\{\delta, \lambda\}, & d_F, d_S \ll \lambda_L \end{cases} \quad \text{where } \lambda = \lambda_L^2 / d_S \text{ denotes Pearl's penetration length.}$$

For the case $d_{F,S} \ll \lambda_L$, we derive the "lower critical" magnetization of the F film for which vortices become to proliferate into the S film [3]:

$$M^c = \frac{H_{c1} \lambda}{4\pi d_F} \begin{cases} 2\lambda / \delta, & \pi\delta / 4\lambda \ll 1 \\ 1 - 32G\lambda / \pi^2\delta, & \pi\delta / 4\lambda \gg 1 \end{cases} \quad \text{where } G \approx 0.916 \text{ is the Catalan constant. We mention}$$

that our estimate for the magnetization is in reasonable agreement with the experimental data on FS bilayers [4].

Support by CRDF, RFBR, the Russian Ministry of Education and Science, Council for Grants of the President of Russian Federation, Dynasty Foundation, and Programs of RAS is acknowledged.

[1] V.L. Pokrovsky and H. Wei, *Phys. Rev. B* 69, 104530 (2004) and references therein.

[2] V.V. Ryazanov, V.A. Oboznov, A.S. Prokofiev, and S.V. Dubonos, *JETP Lett.* 77, 39 (2003).

[3] I.S. Burmistrov, N.M. Chtchelkatchev, *Phys. Rev. B* 72 (2005) 144520.

[4] C. Bell, S. Tursucu, J. Aarts, *Phys. Rev. B* 74 (2006) 214520.

23PO-1-24

SUPERCONDUCTING GAP OF Fe-INTERCALATED TiSe₂ USING ULTRAHIGH-RESOLUTION PHOTOEMISSION SPECTROSCOPY

Kuznetsova T.V.

Institute of Metal Physics RAS, 620041 Ekaterinburg, Russia

Intercalation of titanium dichalcogenides by 3d elements have a wide spectrum of physical properties compared with 1T-TiSe₂ and demonstrate ferromagnetic and antiferromagnetic behavior. These materials resemble artificial multilayer systems, in which thin layers of magnetic metal are separated by non-magnetic blocks. This can be employed to modify the physical properties of the material in a controllable way. The Fe_{0.5}TiSe₂ have antiferromagnetic type of interaction between intercalated atoms and the superconducting transition temperature about 5 K. The magnetic moment of an "impurity" is determined by its

valence state and hence by the chemical bonding between the intercalating element and the host lattice. Such bonding is well studied for intercalate compounds with alkali metals, where the host lattice acquires extra electron density and fixes the ionized guest species electrostatically. In the case of inserted *3d* elements this simple picture does not work, as magnetic moments of impurity atoms deviate considerably from free-ion values. The intercalation compression of interlayer distances in the compound TiSe_2 correlates with the ionization potential of the inserted ion. Such a behavior cannot be explained using the rigid band model, usually applied for intercalation compounds. One could describe this relation quantitatively, assuming the formation of a narrow band (of localized impurity states) just below the Fermi energy. Indeed, angle-resolved photoelectron spectroscopy (ARPES) indicated the formation of such bands for some TiS_2 , TiSe_2 , TiTe_2 -based intercalate compounds. Such bands are situated 0.5 to 1 eV below the Fermi level and exhibit no dispersion, thus indicating a considerable localization of corresponding states. As it was predicted from band calculations, the hybrid state band $\text{Ti}3d_{z^2}/\text{M}3d$ for $\text{M} = \text{Cr}, \text{Fe}$ should have spin splitting [1]. Evidently, when the splitting becomes significant it is possible to observe the gap between spin sub-bands. However the mechanism of so strong localization of the states with the energies so close to the Fermi level remained obscure. Another group of materials where one observed similar dispersionless bands close to the Fermi level are cuprate high-temperature superconductors. It is well known that low dimensionality is generally considered as a necessary ingredient for superconducting transition temperatures. Introducing metal atoms between the repeated layers of a host dichalcogenide layers can tune the interlayer spacing and charging of the dichalcogenide host through a variety of electronic ground states. One such ground state is superconductivity, which is not present in pure TiSe_2 . We study the Fermi surface and superconducting gap of $\text{Fe}_{0.5}\text{TiSe}_2$ using low-temperature ultrahigh-resolution angle-resolved photoemission spectroscopy. Angle-resolved photoemission spectroscopy (ARPES) is a powerful technique to investigate the occupied electronic states below the Fermi level in solids. The improvement of the energy and momentum resolutions enables visualization of detailed features of low energy excitation near the Fermi level: they are the topology of the Fermi surface, the superconducting gap and its anisotropic behavior, the pseudogap phenomenon in the normal state, the nature of quasiparticles in superconducting states and the effect of impurities and disorder. The opening of the superconducting gap as function of temperature, together with a narrow superconducting coherent peak with a shoulder structure located slightly below Fermi level is observed. The numerical fittings to the photoemission spectra for investigate the size and symmetry of the superconducting gap was performed. Also we focused on explaining the mechanism and origin of superconductivity in this system.

[1] T.V. Kuznetsova *et al*, *Phys. Rev. B* **72** (2005) 85418.

23PO-1-25

SUPPRESSION OF THERMO-MAGNETIC INSTABILITY IN SUPERCONDUCTORS

Yurchenko V.V.¹, Galperin Yu.M.¹, Lee S.I.², Johansen T.H.¹

¹Department of Physics, University of Oslo, P.Box 1048, Blindern, 0316, Oslo, Norway

²Department of Physics, Sogang University, Seoul 121-742, Republic of Korea

In most type-II superconductors (SC) magnetic field penetrates in the form of Abrikosov vortices forming a smooth flux front. Usually a slow increase of external magnetic field is accompanied by a gradual propagation of the front. However, in a fairly large family of the SC, for example MgB_2 , NbN , Nb , even a slow field increase may result in abrupt flux jumps, which

bring a great amount (from a few thousands to millions) of the vortices into the sample. The flux jumps, also called magnetic flux avalanches, are associated with a thermo-magnetic instability (TMI) of SC. The phenomenon that leaves fascinating traces of fractal dimension in a distribution of the flux inside the sample (see figure below), produces indeed a very destructing effect upon the performance of SC applications, such as: noise in superconducting electronics, jumps on magnetization curves etc. For a successful introduction of superconducting devices in practice, the avalanches should be suppressed or at least avoided. It is well documented in publications that the instability, that triggers the avalanches, exists only in a certain range of fields and temperatures. Furthermore, it has been shown that by depositing a thin metallic layer on top of a SC, one can suppress the avalanches. However, for a number of applications it may be desirable to have a superconducting part exposed.

In this work we suggest a new way of suppressing TMI by depositing a thin layer of gold only along the sample edges, i.e. exactly where the avalanches nucleate. We studied a series of MgB_2 samples with different width of gold rims by the mean of magneto-optical imaging, which allowed us to determine the range of fields and temperatures where the TMI exists. The obtained diagrams clearly show that by placing rims along the samples perimeter one can substantially reduce the region of the instability. The so called discontinuity lines, observed in the images of flux distribution, revealed a strong enhancement of the critical current in the protected parts of the SC. These effects are explained in the framework of a recently developed theoretical model for dendritic flux avalanches [2].

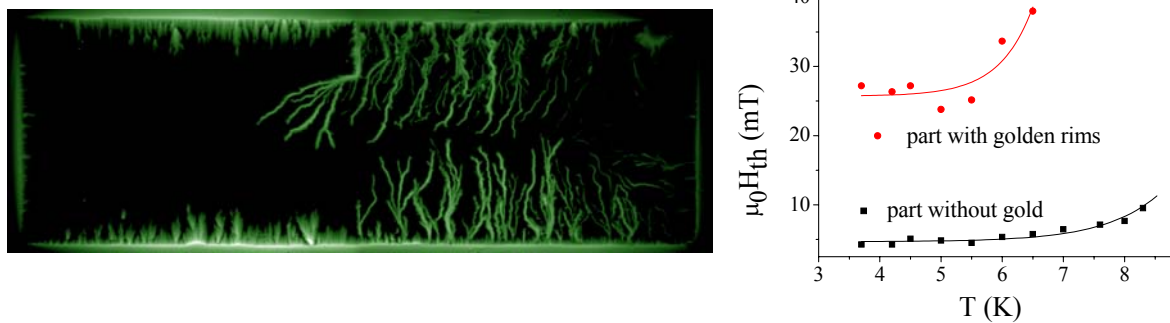


Figure 1. (left) Magneto-optical image of a flux distribution in MgB_2 superconductor film, left part of which is surrounded by a gold rim. (Right) Resulting phase diagram showing improved thermo-magnetic stability of the sample.

[1] D. V. Denisov, A. L. Rakhmanov, D. V. Shantsev, Y. M. Galperin, and T. H. Johansen, *Phys. Rev. B* **73** (2006) 014512

23PO-1-26

SPECIFIC HEAT OF KAGOME-LIKE COMPOUNDS REBaCo₄O₇ (RE = Dy, Ho, Er, Tm, Yb, Lu)

Markina M.¹, Vasilchikova T.¹, Vasiliev A.¹, Nakayama N.², Mizota T.², Ueda Y.³

¹Low Temperature Physics Department, Moscow State University, Moscow 119991, Russia

²Department of Advanced Materials Science and Engineering, Faculty of Engineering,
Yamaguchi University, Ube 755-8611, Japan

³Materials Design and Characterization Laboratory, Institute for Solid State Physics,
University of Tokyo, Kashiwa 277-8581, Japan

Specific heat measurements were performed on a new mixed valence cobalt oxides REBaCo₄O₇ (RE = Dy, Ho, Er, Tm, Yb, Lu) in a wide temperature range.

At room temperature, these compounds have a hexagonal crystal structure $P6_3mc$. At lowering temperature, the first order structural phase transitions from hexagonal to orthorhombic Cmc_21 phase were revealed by X-ray diffraction in REBaCo₄O₇ [1]. This transition was indicated by a peak-like anomaly in a specific heat dependencies at $T_S \sim 160$ K, 178 K, 224 K, and 280 K for RE = Lu, Yb, Tm, and Er correspondingly.

The compounds REBaCo₄O₇ are characterized by two magnetic subsystems: $4f$ rare earth ions system and $3d$ cobalt system (Co²⁺/Co³⁺). In a crystal structure two types of Co-O layers alternate along the c -direction. One of these layers contain a corner-sharing tetrahedra Co²⁺O₄ and Co²⁺ ions with spin only value $S = 3/2$ form a kagome-like network in the layer. The kagome-type magnetic structure is known for strong frustration of magnetic exchange that prevents a formation of a long range magnetic order. Second type of Co-O layers contain Co³⁺O₄ tetrahedra which have no connection in the layer and organize the links by corner-sharing tetrahedra between the Co²⁺-O and Co³⁺-O layers along the c -direction. The ratio Co²⁺:Co³⁺ in the REBaCo₄O₇ is equal 3:1, and Co³⁺O layers are rarefied as compare with Co²⁺O layers.

In spite of difficulties in magnetic order formation, the magnetic phase transitions were found in REBaCo₄O₇ by the magnetic susceptibility measurements [1]. We found the changes of slope on the $C(T)$ curves at corresponding temperatures. These anomalies were identified like Neel temperatures for Co-subsystem: $T_N \sim 50$ K, 74, K, 98 K and 98 K for RE = Lu, Yb, Tm, and Er, correspondingly. The rare-earth magnetic subsystem demonstrates no magnetic order to the lowest temperatures.

Note, that $C(T)$ curve for a Lu-compound LuBaCo₄O₇ demonstrates an additional anomaly at $T^* \sim 101$ K. This compound can be considered as a non-magnetic analogue regarding a rare-earth magnetic subsystem. At $T < 50$ K, the $C(T)$ curve for LuBaCo₄O₇ is lower then those in other compounds and at $T < 15$ K this curve can be described by βT^3 law. In other compounds the specific heat at low temperature contains an additional part from non-ordered RE - ions. Earlier for some compounds of REBaCo₄O₇ family the Mott-type conductivity at $T < T_S$ was found [1,2]. Since the specific heat at low temperatures contains the contributions from electronic and magnetic subsystems we can estimate the low limit of the Debye temperature θ_D only. From the estimations of θ_D values in a range 5 – 15 K the following Debye temperatures were found: $\theta_D \sim 200$ K, 219 K, 237 K, 248 K, 258 K, and 286 K for RE = Tm, Lu, Dy, Yb, Er and Ho, correspondingly.

This work is partially supported by RFBR Grants 06-02-16088a and 08-02-00406a.

[1] N. Nakayama, T. Mizota, A. Sokolov, A. Vasiliev, and Y. Ueda, JMMM, **300**, p. 98 (2006).

[2] H. Hao, C. Chen, L. Pan, J. Gao and X. Hu, Physica B, **387**, p. 98 (2007).

23PO-1-27

VALENCE STATES OF Ce ATOMS IN $[Y/Ce]_2 Sr_{2-x}Ba_xCu_{2-y}A_yO_9$ (A=B, P, S) STUDIED BY X-RAY ABSORPTION SPECTROSCOPY

Efremova N.N.¹, Shkvarin A.S.², Finkelstein L.D.², Kurmaev E.Z.²

¹Russian Scientific Center "Kurchatov Institute", 123182 Moscow Kurchatov square 1, Russia

²Institute of Metal Physics Russian Academy of Sciences – Ural Division,
620219 Yekaterinburg GSP-170, Russia

Formerly, several reports have described the partial substitution of a variety of oxy-anion (borate, phosphate and sulphate) at the copper site in the superconducting system $[Y/Ce]_2Sr_{2-x}Ba_xCu_3O_{9-y}$ [1]. The structure of this family (which is termed "223") is regarded as combination of the triperovskite ($YBa_2Cu_3O_{7.8}$)-type block and fluorite (CeO_2)-type block.

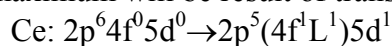
During a critical oxygen in O(1)-site the partial substitution of B, P or S at the Cu(1)-site has shaped the oxy-anion group in this component of structure, XPS [2] and x-ray emission spectroscopy [3] provide support for this view.

In the present report we introduce the investigations of Ce valence in this system by means of X-ray absorption spectroscopy.

Ce L_3 X-ray absorption spectra were measured using Johan-type X-ray spectrometer with position-sensitive detector. The white radiation was taken from the sealed tungsten X-ray tube. The curved ($R = 1.940m$) quartz crystal (10 $\bar{1}$ 1 plane) was used in the second order of reflection as crystal-analyzer. The energy resolution $E/\Delta E$ was about 8500. Measurements of solid samples were performed in transmission mode using a simple absorption cell.

Our research shows that when $x = 0$, Ce valence is close to that one in CeO_2 (≈ 3.82). But the intensity and position of relaxation maximum in Ce L_3 XAS are evidences of chemical bond change.

The origin of relaxation maximum was discussed by us in [4]. Its appearance was attributed to relaxation transition of electron from O 2p valence band on the vacant 4f-level involved by field of Ce 2p hole into Ce atom. In accordance with these ideas the formation of C maximum will be result of transition:



The investigation of Ce valence in $(Y_{1.5}Ce_{0.5})Sr_{2-x}Ba_xCu_{2.5}B_{0.5}O_{9-y}$ shows that substitution of bigger in size and more electronegative Ba for Sr results in decrease of valence from 3.84 ($x = 0$) to 3.67 ($x = 1.5$)

[1] P.R.Slater, C.Creves *Physica* **C215** (1993) 191

[2] E.Z.Kurmaev, V.V.Fedorenko, V.R.Galakhov, St.Bartkovski, St.Uhlenbrock, M.Neumann, P.R.Slater, C.Greaves *J. of Superconductivity*, **v.9 N1** (1996) 97-100

[3] E.Z. Kurmaev, S.N.Shamin, P.R.Slater, C.Greaves *Physica* **C225** (1994) 309-312

[4] L.D.Finkelstein, A.Postnikov, N.N.Efremova, E.Z.Kurmaev *Mater. Lett.* **14** (1992) 115

23PO-1-28

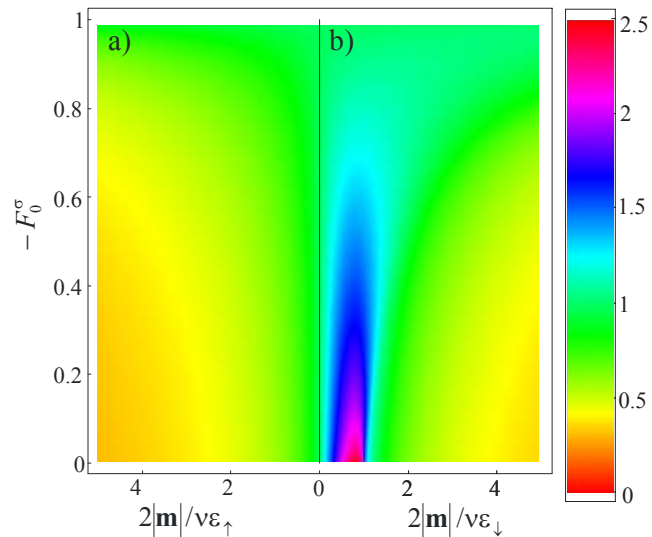
ENERGY RELAXATION IN THE SPIN-POLARISED ELECTRON LIQUID

Chtchelkatchev N., Burmistrov I.

L.D. Landau Institute for Theoretical Physics, 117940 Moscow, Russia

The study of the quantum electron kinetics in metallic conductors and, in particular, problems related to inelastic electron scattering represent the basic directions of mesoscopics [1-3]. Most part of theoretical and experimental research of the quantum transport in mesoscopic systems involves an estimate of the electron inelastic scattering time [or corresponding length scale]. Its comparison with the physical parameters of the system in hand allows us to understand when the concept of electrons with the well defined phase and energy is relevant for the electron transport description, when the non-equilibrium distribution function can be approximated by the Fermi-Dirac distribution with an effective electron temperature. The possibility to manipulate the inelastic scattering rates with the external fields, e.g., by a magnetic field, is one of the fundamental questions of electron kinetics.

We derive the QKE for the spin-polarized disordered electron liquid and find that the kernel of the collision integral, P , for the scattering with the electron spin flip depends strongly on the magnetic field [4]. For the small energy transfer, $|\omega| \leq |\bar{m}|/\nu$, this kernel saturates: $P_m \propto |\bar{m}|^{d/2-2}$, while for $|\omega| \geq |\bar{m}|/\nu$, $P_m \propto |\omega|^{d/2-2}$. At $\omega = 2|\bar{m}|\sigma/\nu$, where $\sigma = \pm 1$, this kernel has a pole related to electron paramagnetic resonance. Here, \bar{m} denotes the average spin density, ν is the thermodynamic density of states per one spin projection, and d is the space dimension. As a consequence, the inelastic scattering rate has non-monotonic dependence on the spin polarization of the electron system. For a wire, our results imply that the energy relaxation should be sensitive to the magnetization $|\bar{m}| \propto (1 + \gamma)H$ if $|\bar{m}|$ is larger than the Thouless energy. This prediction agrees qualitatively with the experiments [5] in which the Thouless energy of the wires corresponds to the magnetic field smaller than 0.1T and triplet dimensionless interaction amplitude $\gamma \approx 0.3$.



The density plot of the triplet channel energy relaxation rate dependence from the quasiparticle energy, magnetization and triplet Fermi-liquid interaction amplitude F_0^σ . The inelastic scattering rate has a highly non-monotonic dependence on the spin polarization of the system. The origin of this maximum has much in common with the electron paramagnetic resonance.

- [1] B.L. Altshuler and A.G. Aronov, in *Electron-Electron Interactions in Disordered Conductors*, ed. A.J. Efros and M. Pollack, Elsevier Science Publishers, North-Holland, 1985.
- [2] Y. Imry, *Introduction to Mesoscopic Physics*, (Oxford University Press, 1997).
- [3] F. Giazotto, T.T. Heikkila, A. Luukanen, A.M. Savin and J.O. Pekola, *Rev. Mod. Phys.* **78**, 217 (2006).
- [4] N.Chtchelkatchev and I.S. Burmistrov, *Phys. Rev. Lett.* (in press).
- [5] A. Anthore, F. Pierre, H. Pothier, D. Esteve, M.-H. Devoret, in *Proceedings of the XXXVIth Rencontres de Moriond, Electronic Correlations: From Meso- to Nano-physics*, Les Arcs, France (2001); A. Anthore, F. Pierre, H. Pothier, D. Esteve, *Phys. Rev. Lett.* **90**, 076806 (2003).

23PO-1-29

KINETICS OF MAGNETIZATION REVERSAL OF PERMALLOY IN Py/Nb HETEROSTRUCTURES

Uspenskaya L.

Institute of Solid State Physics RAS, Chernogolovka, 142432, Russia

Soft magnetic materials with ultra fast switching of magnetic polarization seem to be the ideal control item in spintronic devices based on superconductor/ferromagnetic multilayer heterostructures (SC/FM). Permalloy looks a possible candidate for this role when one takes into account magnetic properties of single layer Py-film. However it is known that the adjacent layers could significantly vary properties of the layer, e.g. the velocity of remagnetization of Py in Py/AFM heterostructures is reduced comparing with those in single Py-layer. More over, the mechanism of remagnetization could be changed because of the influence of the adjacent layer [1]. How the ferromagnetic layer will behave in heterostructures with superconductors is still open question, although many interesting applications for FM/SC heterostructures are predicted [2].

In this contribution, the effect of superconductor proximity on magnetic properties of Py film is reported. The magnetization reversal kinetics is studied by magneto-optic visualization technique in a wide temperature range. The alteration of ferromagnetic film anisotropy, the modification of a type of magnetic domain and domain walls structure (fig. 1), the reduction of domain wall mobility and the increase of coercivity are found. The comparison of magnetization reversal kinetics of Py/Nb at $T > T_c^{sc}$ and $T < T_c^{sc}$ with those of Py/FeMn and single Py-layer at low and room temperatures, figs.1-2, let the understanding of contribution of different interactions, which determine the found features.

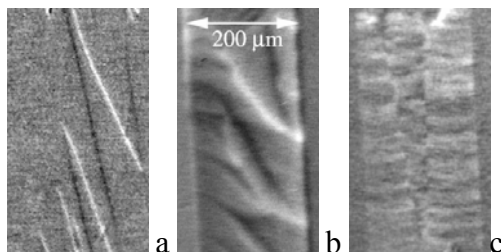


Fig.1. Magnetic domain structure of single Py-layer at $T=10$ K (a) and in Py/Nb heterostructure at $T=10$ K (b) and at $T=7$ K (c), i.e. Nb is in normal and superconducting state

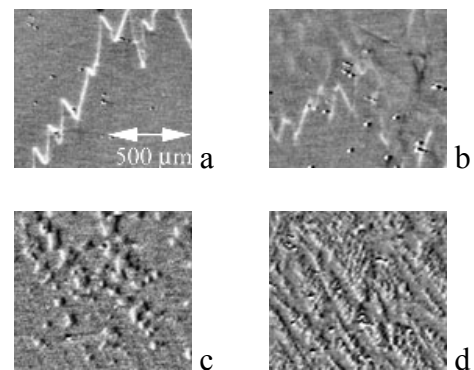


Fig.2. Variation of magnetic domain structure of Py-film in FM/AFM heterostructure with temperatures decrease: (a) - 295 K, (b) - 235 K, (c) - 110 K, (d) - 35 K

Support by the program “New materials and structures” of RAS is acknowledged. I’d like to thank S.Egorov (ISSS RAS, Russia) for samples preparation.

[1] L.S.Uspenskaya, V.I.Nikitenko, thesis and materials of EASTMAG2007, Kazan, Russia

[2] A.I. Buzdin, Rev. Mod. Phys. 77 (2005) 935

23PO-1-30

INHOMOGENEOUS PHASES IN HIGH-TEMPERATURE SUPERCONDUCTORS AND HEAVY-FERMION SYSTEMS

Martin I.

Los Alamos National Laboratory

Interplay between strong correlations and electronic kinetic energy naturally leads to intrinsically inhomogeneous phases. In the cuprates, many experimental probes, including elastic and inelastic neutron scattering, STM, and NMR, provide strong evidence for existence of stripe phases, in which the weakly doped antiferromagnetic regions alternate with highly-doped metallic or superconducting regions. Theoretically, such phases appear naturally in the Hubbard model treated at the unrestricted mean field level [1]. In the present work we demonstrate that similar phases can also generically occur in heavy fermion (HF) materials. The physics of HF materials is defined by the interplay between the localized band of f-electrons and conduction band of d-electrons. In the Kondo screened phase, the two bands effectively merge to form a single band of heavy electrons. Based on the Kondo-Heisenberg and Anderson-Heisenberg lattice models, we demonstrate that the remnants of the antiferromagnetic correlations in the Kondo screened phase can lead to formation of the inhomogeneous phase with alternating regions of well-screened and poorly screened f-electron moments. Our findings suggest universality of the frustrated phase separation physics in strongly correlated systems and may help to understand some of the surprising results indicating electronic inhomogeneity of some stoichiometric HF systems.

[1] Int J of Mod Phys, v. 14, pp. 3567-3577 (2000), Europhys. Lett., v. 56, 849 (2001)

23PO-1-31

PHASE TRANSITIONS IN SUPERCONDUCTIVE AND MAGNETIC SYSTEMS. TWO-LIQUID MODEL

*Boyarsky L.A.^{1,2}, Blinov A.G.^{1,2}*¹Novosibirsk State University, 630090, Novosibirsk, Russia²Institute of Inorganic Chemistry RAS, 630090, Novosibirsk, Russia

In the given report the speech will go about some features of phase transitions in strongly correlated electronic systems, such as high-temperature superconductors and antiferromagnetic metals. In one and other case at phase transitions there are features in an electronic spectrum - gaps, anisotropic gaps (nesting), pseudogaps. On our point of view similar type of realignment leads to separation of functions of various groups electrons in conducting zones. The part of electrons keeps the basic functions, and another is located at virtual levels. So there is probability for forming the clusters of spin density waves (SDW).

The published recently results of experiments (neutron diffraction, ARPES, NMR, quantum oscillations) confirm conclusions about magnetic character of a pseudogap's state in underdoped cuprates. It was shown, in particular, that the pseudogap phase coexists with superconductive one. The boundary curve $T^*(x)$ crosses a curve of the $T_c(x)$ in a tricritical point. At low temperatures first of the specified curves comes to a point of quantum phase

transition. So, to the left of a curve $T^*(x)$ in the superconductive area are exist the antiferromagnetic clusters.

As for the normal state of underdoped cuprate these kind of clusters were found out in 80th years by a neutron experiments. Per the same years at participation of the authors of the given report was shown, that in the cited normal phase the magnetoresistance contains the linear on a magnetic field component, likewise for antiferromagnetic metal, which magnetic ordering is connected to formation of spin density waves. The analysis given, and also some other experimental data, and theoretical accounts, has allowed us to state some assumptions. First of all, it is represented probable, that the destruction long-range antiferromagnetic order, characteristic for insulator phase of cuprate is accompanied the delocalization of the magnetic moments and occurrence the clusters of SDW. The similar phenomenon, by the way, takes place in the diluted alloys Chromium-Vanadium, in which pseudogap phase also was observed. Further, at a high level of doping at destruction of superconducting state in the phase transition is involves all the carriers of a charge near to a Fermi surface, but in underdoped samples in this process participates the part of carriers only. It is obvious, that the features of phase transitions as related to left and right with respect to thrucritical point should be various. Unfortunately, the basic heterogeneity of a condition of samples makes an opportunity of experimental check of this hypothesis almost improbable. Generalizing all stated facts, on our point of view, it is logical to state the assumption of applicability of the modified two-liquid model for the description of behavior of electronic systems in such, on the first sight, various systems as superconducting cuprates and antiferromagnetic metals.

Support by Project Siberian Branch RAS # 81 is acknowledged.

23PO-1-32

STRUCTURE AND MAGNETIC BEHAVIOR OF $\text{Nd}_6\text{Fe}_{13-x}\text{Co}_x\text{Cu}$ ALLOYS

Iranmanesh P.¹, Tajabor N.¹, Alinejad M.R.¹, Fruchart D.², Gignoux D.²

¹Department of Physics, Ferdowsi University of Mashhad, Mashhad, 91775-1436, Iran

²Neel Institute, CNRS, BP 166, 38042 Grenoble Cedex 9, France

The influence of Co substitution for Fe on the structure and magnetic properties of $\text{Nd}_6\text{Fe}_{13-x}\text{Co}_x\text{Cu}$ ($x = 0, 1, 2, 3$) compounds are investigated. The required alloys were prepared by arc melting of the pure (99.9%) constituent elements under Ar atmosphere processed by remelting in a high-frequency induction furnace and annealing at 550 °C within evacuated quartz ampoules for 40 days. X-ray diffraction and magnetometric methods were applied to determine the lattice parameter, ordering temperature and magnetization. The single phase samples with I4/mcm space group are formed only for $x = 0, 1$ while other compounds are multiphase. By substitution of one cobalt, the a and c lattice parameters decrease from 8.0865 to 8.0834 Å and from 22.2956 to 22.2861 Å, respectively. Results of the thermomagnetic measurements show that the curie temperatures of the compounds with $x = 0$ and 1 are 323K and 400 K, respectively. Magnetization curves indicate to the decrease of magnetic anisotropy with increasing Co content. In addition, the spin reorientation transition which was observed in $\text{Nd}_6\text{Fe}_{13}\text{Cu}$ compound at $T \approx 60$ K is disappeared by substitution of Co for Fe. These results were explained based on the improved T-T and R-T exchange interactions from one hand, and the influence of Co^{+3} ions on the crystal field anisotropy of 8f Nd sublattice, on the other hand.

23PO-1-33

LONG-RANGE ODD TRIPLET SUPERCONDUCTIVITY IN SUPERCONDUCTOR-FERROMAGNET STRUCTURES WITH NEEL WALLS

Fominov Ya.V.¹, Volkov A.F.^{2,3}, Efetov K.B.^{2,1}

¹L.D. Landau Institute for Theoretical Physics RAS, 142432 Chernogolovka, Russia

²Theoretische Physik III, Ruhr-Universität Bochum, D-44780 Bochum, Germany

³Institute of Radioengineering and Electronics RAS, 103907 Moscow, Russia

We consider a singlet superconductor – ferromagnet (SF) junction with the Neel domain structure in the F part. We demonstrate that an odd-frequency long-range triplet superconducting component is generated near domain walls; this component penetrates inside the domains on a length scale $\xi_T = (D/2\pi T)^{1/2}$ (we consider the diffusive limit, D is the diffusion constant). The length scale ξ_T is much larger than the usual short-range scale $\xi_h = (D/h)^{1/2}$ (where h is the exchange energy) which characterizes the penetration of superconductivity into a single-domain ferromagnet. We calculate the correction to the density of states due to the long-range triplet component and the Josephson current in the SFS junction due to this component. The presentation is based on the publications [1] and [2].

[1] Ya.V. Fominov, A.F. Volkov, and K.B. Efetov, Phys. Rev. B **75**, 104509 (2007).

[2] A.F. Volkov, Ya.V. Fominov, and K.B. Efetov, Phys. Rev. B **72**, 184504 (2005).

23PO-1-34

FMR AND CESR IN A METALLIC MAGNETIC THIN FILM

Hurdequint H.¹, Sergeeva N.¹, Le Graet C.², Ben Youssef J.²

¹Laboratoire de Physique des Solides, UMR 8502, Université Paris-Sud, 91405 Orsay, France

²Laboratoire de Magnétisme de Bretagne-CNRS-FRE 2697, UBO, 29285 Brest, France

Systematic investigations [1,2] of the spin resonance in magnetic films corresponding to **purely metallic** systems that we performed previously had revealed remarkable phenomena that we associated to the specific nature of the *interfacial coupling*[2] between a ferromagnetic and a normal metal, which implies the *diffusion* of the microwave magnetization of the *conduction electrons* from one metal to the other. We have recently reported results of FMR studies of single permalloy (Py) layers sandwiched, respectively, by **Ag** and by **Au**[3]. The FMR results have been systematically compared to the ones obtained on ‘control’ Py layers sandwiched by Al₂O₃ (a detailed report of FMR results is given in [4]) We report here and discuss the main results we have obtained in a detailed FMR investigation of (Py/Al) films (very different Py thicknesses) deposited by sputtering on Si substrates.

We study (at X-band) the angular variation of the resonance spectrum (angle θ_H of the dc field with the film normal). The detected signal [3] is characterized by an A/B ratio which is a unique function of the signal ‘phase’[1]. We highlight below the most remarkable phenomena observed for two samples corresponding to the two limits (*ultrathin* and *thick*) of the Py thickness range.

Sample F : ultrathin Py(3.5nm), sub/Al6/Py3.5/Al8). Continuously with the orientation θ_H the resonance spectrum is here composed of **two** lines. The main intense line corresponds to the

FMR line of the Py layer. A second partially resolved peak is observed: in higher field in parallel geometry and in lower field in the perpendicular one. We identify this second peak to the **CESR** line of the *conduction electron* spin accumulation of the metallic film[3]. A large variation of A/B is observed around the ‘*crossing*’ orientation (27 deg), corresponding to a large (132 deg) variation of the signal phase when going from the parallel to the perpendicular geometry. This observation corresponds to the **first evidence** of the spin accumulation **CESR signal** in a single magnetic layer metallic film.

Sample A : thick Py(40nm), sub/Al40/Py40/Al10). The linewidth ΔH presents (around $\theta_H = 10$ deg) a very *pronounced* peak ($\Delta H_{\max} = 1.15$ kOe), much larger in amplitude than the one observed (and well understood [4]) of a Py(43nm) control film . Beyond this orientation the **CESR** line of the metallic film is resolved in *lower* field and its characteristics (H^{res} , linewidth) can be followed nearly up to perpendicular geometry , increasing strongly the gain at detection .

The ensemble of observed phenomena may be well understood and analyzed in terms of the theory of the signal (sketched briefly in ref[3]) we have developed to describe analytically the resonance spectrum observable in a **bimetallic** film (ferro/normal metal). Taking appropriate boundary conditions at the metallic interface, the essential result obtained is that the resonance spectrum corresponds to the superposition of **two sources** of signal, associated respectively to the **two** eigenmodes (the ‘current’ and ‘spin-diffusion’ modes[5]) of propagation of the microwave magnetization in a metal. The crucial point is that these two sources of signal resonate at two *distinct* frequencies , respectively, the FMR eigenfrequency of the magnetic layer and the CESR frequency of the conduction electrons of the bimetallic film. Quite generally in a bimetallic film the two distinct H^{res} curves [H_{FMR} and H_{CESR}] will cross, the effect of the demagnetizing field being much weaker on the normal metal spin accumulation.

- [1] H. Hurdequint , J.Magn.Magn.Mater. **93** (1991) 336.
- [2] H. Hurdequint and G.Dunifer ,J.de Phys. **49** (1988) C8-1717.
- [3] H. Hurdequint , J. Magn.Magn. Mater. **310** (2007) 2061.
- [4] H. Hurdequint , J. Magn. Magn. Mater. **242-245** (2002) 521.
- [5] J.I.Kaplan , Phys.Rev. **115** (1959) 575.

23 June Monday

17:00-19:00

poster session

23PO-3

**“Soft Magnetic
Matter”**

23PO-3-1

MAGNETOPHORETIC BEHAVIOR OF A PANCREATIC CELL SUSPENSION

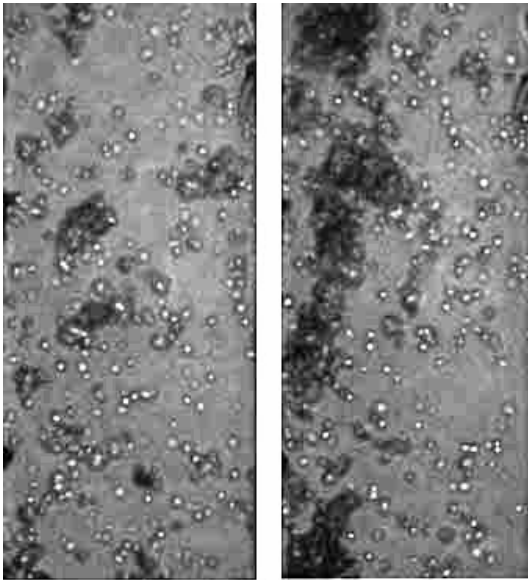
Kashevsky B.E.¹, Goranov V.A.², Prokhorov A.V.², Zholud A.M.¹

¹A.V. Luikov Heat and Mass Transfer Institute, BAS, Minsk, Belarus

²Belarus State Medical University, Minsk, Belarus

Medical technologies of cell transplantation depend on the progress of cell separation. The existing procedures are based on the difference of cells in bulk density and in receptor markers. The latter has found application in immunomagnetic separation of cells which is based on binding the cells to be separated to magnetic nanoparticle. This method is potentially damaging, costly, and it involves essential loss of specialized cells and a drop in viability of a sowing material. An example is the process of an enzymatic disintegration of specialized tissues for deriving functional cells, in particular, pancreatic cells. Due to impossibility to separate the completely disintegrated fraction from the reactor it is necessary, to preserve its functionality, to terminate the process of fermentation at early stages, thus losing considerable portion of functional cells in clusters with tissues and fibroblasts.

The ultimate goal of our studies is to increase the efficiency and purity of differentiation of beta cells from cell suspensions intended for cultivation and transplantation, making use of the difference of cell magnetic properties. The method of direct magnetic separation has principal advantages because it does not affect cells in any dangerous way. The present state-of-the-art concerning the direct magnetic separation of cells is rather superficial. The red blood cell represents a single instance which has aroused a noticeable interest (see [1]).



We present the results of a computer-aided video recording of magnetophoretic motion (following technique [2]) of a suspension of partially separated fetal rabbit pancreas (collagenase II, 0.5mg/ml - 5 min), settling in a liquid (cultural medium RPMI1640 with 10% fetal bovine serum) near a thin (0.5mm) vertical magnetic rod under the influence of the uniform magnetic field with induction of 0.8 T. The suspension included pieces of debris, single cells and islets composed of more than 6-8 cells. All these objects demonstrate contrasting magnetophoretic behavior. While single cells are practically insensitive to magnetic field, the pieces of debris (8-20 μ ID) are essentially paramagnetic (with respect to the liquid carrier) and move towards the magnetic rod with velocity of $\sim 30 \mu/c$ at a distance of 300 μ from the rod, and of

$\sim 100 \mu/c$ at 100 μ . At the same time, the islets are repelled from the rod (diamagnetic), their magnetophoretic velocity being only one tenth of the debris velocity. The pictures in the figure show the initial state of the suspension (left) and that attained after 2 minutes magnetic field action. The magnetic rod is situated on the right. The obtained results are analyzed on the basis of macroscopic theory which allows restoring magnetic properties of investigated cellular objects. We believe that our observations support the idea that direct magnetophoresis can be a promising trend in cell science and technology.

- [1] Zborowski M., Oстера G. R., Moor L. R., Milliron S. Chalmers J. J. and Schechter A. N. *Biophysical Journal*, **84** (2003) 2638.
- [2] Kashevskii B.E., Kashevskii S.B., Prokhorov I.V. Aleksandrova E.N., Istomin Yu.P. // *Biophysics*, **51**(6) (2006) 52.

23PO-3-2

NON-EQUILIBRIUM MAGNETIZATION OF A DILUTE SUSPENSION OF MAGNETIC PARTICLES

Tyatyushkin A.N.

Institute of Mechanics, Moscow State University, Michurinskiy Pr., 1, Moscow 119192, Russia

The possibility of using the magnetic hyperthermia as a method of cancer treatment attracted attention of investigators working in the field of magnetic soft matter [1]–[2]. In treating with this method, magnetic particles dispersed in a liquid are introduced into a treated carcinoma, and the latter is affected by an alternating magnetic field. The carcinoma saturated with magnetic particles is magnetized and, since the magnetization is non-equilibrium, heated. As the result, the temperature of the carcinoma increases up to the value at which the cancer cells perish.

In particular, the invention of the method of magnetic hyperthermia caused interest to investigation of the physical phenomena that play key role in its realization. One of those phenomena is the magnetic relaxation in a dispersion of magnetic particles in a liquid (i.e., in a magnetic fluid). Indeed, heating of a magnetic fluid in an alternating magnetic field takes place because the magnetization process is non-equilibrium, and the reason of the latter is just the magnetic relaxation.

It is important for effective control of magnetic hyperthermia to know how heating of a magnetic fluid depends on the parameters of the magnetization process and how those parameters depend on the properties of the magnetic liquid. Heating of a magnetic fluid in an alternating magnetic field is determined by the specific heat capacity at constant pressure, the heat conductivity, and the heat generation power density. The heat generation power density is determined by the magnetization process; meanwhile the influence of the latter on the specific heat capacity and the heat conductivity can be neglected. The heat generation power density depends on only the magnetic susceptibility and time of magnetic relaxation [3].

The magnetic susceptibility and time of magnetic relaxation are determined both by the interaction of a magnetic particle with the applied magnetic field and the surrounding viscous liquid and by the interaction with the other particles and their magnetic field. However, the importance of the second factor vanishes when the concentration of the magnetic particles is sufficiently low. Since the concentration of the magnetic particles in a carcinoma treated with the magnetic hypothermia cannot be high due to various reasons, the investigation of the first factor seems to be more important from the viewpoint of the application to the magnetic hyperthermia.

The goal of this work is to investigate theoretically non-equilibrium magnetization of a dilute suspension of magnetic particles determined by the magnetic relaxation due to interaction of particles of the suspension with the surrounding liquid and applied magnetic field.

A suspension of magnetic particles in a viscous liquid magnetized in an alternating uniform magnetic field is considered. The suspension is regarded as so dilute that interaction of a single particle with the applied magnetic field can be considered without taking into account the influence of other particles. The magnetic susceptibility and time of magnetic relaxation of the suspension are found as functions of the frequency of the applied magnetic field.

The present work is supported by the RFBR grants 08-01-00026 and 07-01-00026.

- [1] R.E. Rosensweig, *J. Magn. Magn. Mat.*, **252** (2002) 370.
- [2] W. Andra et al., *J. Magn. Magn. Mat.*, **194** (1999), 197.
- [3] V.A.Polyanskiy and A.N.Tyatyushkin, in: 11th International Ples Conference on Magnetic Fluids, Ples, Russia, 2004, pp.208–213 (in Russian).

23PO-3-3

MAGNETIC PROPERTIES OF BACTERIAL NANOPARTICLES SYNTHESIZED BY BIOMINERALIZATION PROCESS

*Timko M.¹, Džarová A.¹, Kováč J.¹, Závišová V.¹, Koneracká M.¹,
Kopčanský P.¹, Šprincová A.¹, Tomašovičová N.¹, Vávra I.²*

¹Institute of Experimental Physics, SAS, Watsonova 47, 040 01 Košice, Slovakia

²Institute of Electrical Engineering, SAS, Dubravská cesta 9, 841 04 Bratislava, Slovakia

Magnetic nanoparticles in diluted aqueous suspensions are an important tool in medical diagnostics as contrast agent for magnetic resonance imaging and in therapy for magnetic drug targeting and hyperthermia. For these applications, special nanoparticles so called magnetosomes were isolated, which consisted of a magnetic core covered by a protein-containing lipid membrane. Using of magnetosome was exerted for the immobilization of relatively large quantities of bioactive substances, for the introduction of DNA into cells, for the detection of mRNA, as a contrast agent for magnetic resonance imaging and tumor-specific drug carriers based on intratumoral enrichment, for biomedical applications. One of the special potential application areas of magnetic bacterial particles is hyperthermia. As it was pointed out recently an enhancement of specific heating power is of importance for reducing the useful dosage applied to the tumour. By this way a gain in reliability of magnetosomes as tumour therapy is expected.

In our experiments we compare the structural and magnetic properties of magnetite nanoparticles (magnetosomes) prepared by biomineralization of magnetotactic bacteria *Magnetospirillum sp.* – ABM. The morphology was studied by Transmission Electron Microscopy (TEM) and magnetic properties by SQUID magnetometer. The XRD powder diffraction peaks fit very well with standard Fe₃O₄ reflections. The average particle size (36 nm) was calculated by the Debye-Scherrer formula from XRD line width of the (311) peak what corresponds very well with TEM measurements (35 nm). In order to compare different samples we report temperature dependence of magnetization measurements in zero field (ZFC) and field cooling (FC) measurement mode. The sharp magnetic transition (Verwey transition) at 105K is clearly present in magnetosomes. One of the reasons for this behaviour can be attributed to the chain arrangement of magnetosomes. The chains act as long dipoles with enhanced magnetic anisotropy along the chains and thermal fluctuation are insufficient to overcome anisotropy barrier. In opposite this transition is missing in Fe₃O₄ powder, where the magnetic nanoparticles are separated, the magnetic fluctuations are strong to overcome magnetic anisotropy and randomize magnetic moment. The observed coercivity (71 Oe) at 293 K for magnetosomes can be connected with the fact that the mean diameter (36 nm) is larger than critical size for superparamagnetic behaviour of magnetosomes [1].

This work was supported by the Slovak Academy of Sciences (grant No. 6166) and by the Slovak Research and Development Agency under the contracts No. APVV-26-026505 and APVV-0173-06.

[1] N.H. Hai, R. Lemoine, S. Remoboldt, J..Mag. Mag. Mat. 293, 75, (2005).

23PO-3-4

MAGNETIC PROPERTIES BIOGENIC $\text{Fe}_2\text{O}_3 \cdot n\text{H}_2\text{O}$ NANOPARTICLES

*Stolyar S.V.^{1,2}, Gurevich Yu.L.³, Ladygina V.P.³, Iskhakov R.S.¹, Bayukov O.A.¹,
Petrakovskaya E.A.¹*

¹Kirensky Institute of Physics, Academgorodok, Krasnoyarsk, 660036, Russia

²Siberian Federal University, Krasnoyarsk, 660041 Russia

³Institute of Biophysics of SB of RAS, Russia

e-mail: rauf@iph.krasn.ru

Ferrihydrite $\text{Fe}_2\text{O}_3 \cdot n\text{H}_2\text{O}$ is an antiferromagnetic, with the magnetic ordering temperature above the room one ($T_N=340\text{K}$). As the particles are small (2--7 nm), magnetic moments of Fe^{3+} ions, which are situated on the particle surface, are uncompensated, and they form a "parasitic" integral magnetic moment of a separate particle. In human and animal tissues, in plants and bacteria, ferrihydrite is present in ferritin core. Ferritins of all types have identical molecular architecture. Ferritin is a spherical molecule 12 nm in outer diameter, containing a $5\text{Fe}_2\text{O}_3 \cdot 9\text{H}_2\text{O}$ core surrounded by 24 protein subunits. The aim of this paper is production and investigation magnetic properties of ferrihydrite synthesized by bacteria *Klebsiella oxytoca*. These bacteria were isolated from sapropel of the Borovoe Lake (Krasnoyarsk territory). The Moessbauer parameters show that all of Fe^{3+} ions have octahedral coordination. The sites can be divided into two groups: Fe(1) and Fe(2) sites (nanoparticles), with relatively small distortions of local site symmetry, $\text{QS}(\text{Fe}(1)) \sim 0.55 \text{ mm/s}$ and $\text{QS}(\text{Fe}(2)) \sim 1 \text{ mm/s}$; and Fe(3) and Fe(4) sites (cluster), with severe distortion of symmetry, $\text{QS}(\text{Fe}(3)) \sim 1.5 \text{ mm/s}$ and $\text{QS}(\text{Fe}(4)) \sim 1.8 \text{ mm/s}$. Redistribution of population in site groups depends on the age of bacterial culture. These clusters characterized by Fe(3) and Fe(4) sites are defective and have minimal sizes.

Ferromagnetic resonance (x-band) were used to study dynamic magnetic properties of nanoparticles (Fe(1) and Fe(2)) and clusters (Fe(3) and Fe(4)) in the range of temperatures $77 < T < 500\text{K}$.

Support by Russian program "Development of Science in High School" (2006-2008)–RNP.2.1.1.7376

23PO-3-5

KINEMATICS OF MOTION OF A GAS BUBBLE WITH DROP OF A MAGNETIC FLUID IN A NONMAGNETIC FLUID

Simonovsky A.Ya.¹, Travkina T.V.²

¹Institute of mechanics of Moscow State University, Moscow, Russia

²Stavropol State University, Stavropol, Russia

Laws of motion of a gas bubble are explored at emersion through a demarcation of a magnetic and nonmagnetic fluid in a magnetic field.

Experiment description: the cylindrical glass container was filled in bottom with a kerosene based magnetic fluid, and from above the transparent nonmagnetic fluid (water). Since a bottom of a vessel in volume of a magnetic fluid through a tube the gas bubble was blown out. At transiting by demarcation air traps magnetic and nonmagnetic fluids the bubble captured some volume of a magnetic fluid. Then the bubble with a magnetic fluid inside floated in water at action of an external homogeneous magnetic field produced by a Helmholtz coils. Bubble emersion was recorded by a digital camera (fig. 1).

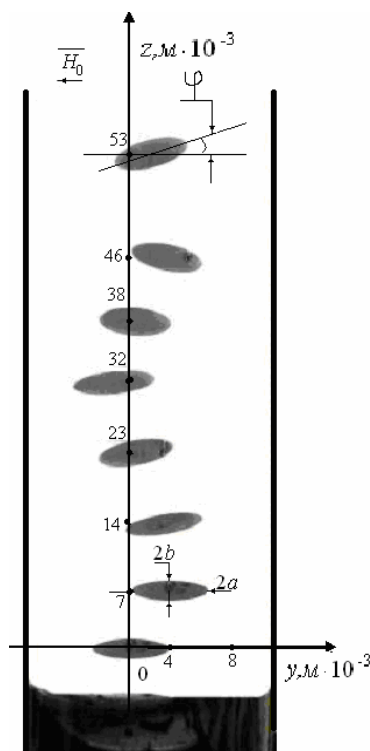


Fig. 1. Motion of a bubble of gas with a magnetic fluid.

We have counted a mechanical trajectory of a bubble which has appeared a spiral line. Cyclic oscillation frequencies of volume of a bubble and its precession concerning a magnetic field direction are computed.

The theoretical analysis has shown, that the bubble is drawn down in a magnetic field and makes small oscillations concerning a field direction. At motion in the transparent fluid the bubble volume varies also as well as an angle of deflection from a field direction. The bubble shape is an ellipsoid of revolution. Presence of a gas interlayer in a bubble oscillations of volume of a bubble and a precession of a semimajor axis concerning a field direction spot character of driving on a spiral line. The drop of a fluid after a gas discharge impinges downwards on absolute to other law, than the law of motion of a floating bubble. The law of falling drop without an air space is uniform linear motion.

Authors thanks RFBR (grant No.08-01-000-26) for work support.

23PO-3-6

MRI-MONITORING MAGNETIC DRUGS TARGETING, IMMOBILIZING AND HEATING IMPROVED CANCER TREATMENT

Brusentsov N.A.¹, Pirogov Y.A.^{2}, Lychnicer M.R.¹, Uchevatkin A.A.², Dubina A.I.²,
Ivanov A.V.¹, Polyanskiy V.A.³, Kupriyanov D.A.², Tischenko D.A.², Nikitin P.I.⁵,
Brusentsova T.N.⁵, Nikitin M.P.⁵*

¹N.N. Blokhin SE Russian Cancer Research Center RAMS, Moscow, 115478, Russia
(brusentsov2005@yandex.ru)

²Center for Magnetic Tomography and spectroscopy M.V. Lomonosov Moscow State University, Moscow 119992, Russia

³Institute of Mechanics, Moscow State University, Moscow 119192, Russia

⁴Institute of Bio-Chemical Physics N.M. Emanuel, RAN 119991, Kosygin st. 4 Russia

⁵Natural Science Center of General Physics Institute, Russian Academy of Sciences, 38 Vavilov St., Moscow 119991, Russia

In spite of nanotechnological advancements in the development of anticancer drugs, no known agent exhibits specific toxicity for cancer cells compared to normal tissues. A method for improving the efficacy of anticancer drugs is to incorporate them within a magnetically responsive sol (MS), which can be targeted and immobilized using non uniform magnetic field

(MF) and heated by AC MF [1], MRI-monitoring of this processes will be possible. For this purpose, permanent SmCo₅ or NdFeB magnets, magnetic bandages (MB) [2] (to 0.5 T induction) electromagnets (0.7 T) and superconducting electromagnets (to 7.0 T) are usually used to induce a non uniform MF. But, due to the sharp decrease of the MF with the increasing distance from the magnet surface, the MS can be immobilized only within a narrow zone near the magnet surface. It would appear more effective to generate an external MF using MB or superconducting coil (SC) and to induce a high field gradient for high magneto-immobilizing force with MB or ferrous flux concentrators (FC). By using FC of different sizes and geometry, it will be possible to alter the magnitude and spatial distribution of the magnetic force. Mobile MB and FC also could be used for navigating magnetic catheters and other devices in blood vessels. SC field strength would be sufficient to magnetically saturate both the MS and FC. In this paper, we present data concerning the immobilization of MS with MB, FC and SC. In experiments immobilizing MS, a high MF gradient in a selective region was induced by using FC made of magnetically soft iron. The MF near FC can be estimated analytically by considering the material magnetically saturated in the axial direction.

In our method, the external MF was generated by a SC with a horizontal axis. The coils generated 4 T and 7 T at the centre of the "warm" 8.0 cm and 30.0 cm aperture of the cryostat. The procedure of definition magnetically sensitive nano-materials in magnetically controlled antitumor drugs in vitro and in mice bodies on a limit of sensitivity of BioMag 2 [3] were designed.

Experiments in vitro and in vivo have shown that it is possible to target and immobilize magnetic drug carriers using magnetic bandages, magnetic flux concentrators and superconducting coils in regions to as adjacent to the pole.

This work was supported by the Russian Foundation for Basic Research, project No 08-01-00026.

[1] N.A. Brusentsov, T.N. Brusentsova, et al., *J. Magn. Magn. Mat.* 311, 176 (2007).

[2] U.O. Häfeli, K. Gilmour, A. Zhou, S. Lee, M.E. Hayden, *J. Magn. Magn. Mat.* 311, 323 (2007).

[3] P.I. Nikitin, P.M. Vetoshko, T.I. Ksenevich, *J. Magn. Magn. Mat.* 311, 445 (2007).

23PO-3-7

PECULIARITIES OF RELAXATION OF MAGNETISATION IN SILICON ORGANIC BASED MAGNETIC FLUIDS

Dikansky Yu.I.¹, Kunikin S.A.¹, Gladkikh D.V.¹, Radionov A.V.²

¹Stavropol State University, Stavropol, Russian Federation

²Scientific-Industrial Enterprise "Ferrohydrodynamika", Mykolayiv, Ukraine

Investigation of magnetic properties of magnetic fluids call the significant interest [1]. However the overwhelming majority of papers are devoted study of "classical" kerosene based magnetic fluids stabilized with oleic acid. In engineering devices as a rule ferrofluids based on more viscous liquids are used. In present work we investigate magnetic fluid based on silicon-organic liquid PES-3.

Magnetisation of magnetic fluids was measured by vibrational magnetometer and also a ballistic method. Complex magnetic susceptibility was measured by a bridge method on device LCR-817 (frequency range 0.02-10 kHz). By means of the same method the susceptibility of a rotating magnetic fluid in a stationary magnetic field was explored also.

According to experiment the explored fluid has anomalously great value of a susceptibility ($\chi = 6.36$) in low magnetic fields at saturation of magnetization $M_{\infty} = 26.9 \text{ A/m}$

Magnetogranulometrics, made on the experimental data, essential difference in particle sizes has shown: 6.9 nm in high fields and 20.6 nm in low fields. On the frequency dependence of an imaginary part of susceptibility of the sample under the action of external stationary magnetic field, which was directed parallel to a measuring field, there is a maximum at some value of external field. The maximum position depends on magnetic field intensity and at field increasing is biased in higher frequency area (fig. 1).

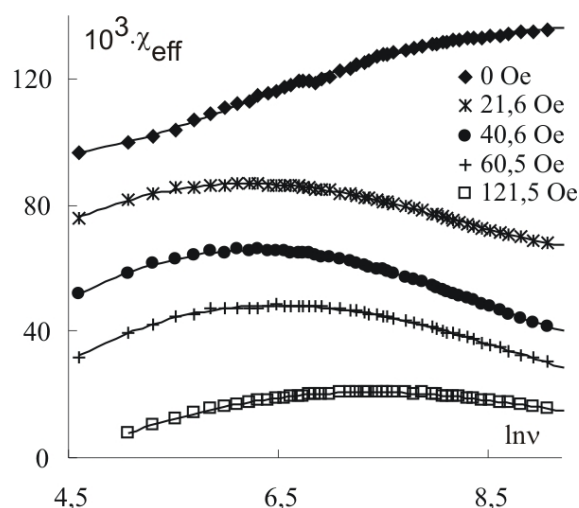


Fig. 1. Dependence of imaginary part of magnetic susceptibility on frequency at various magnetic fields

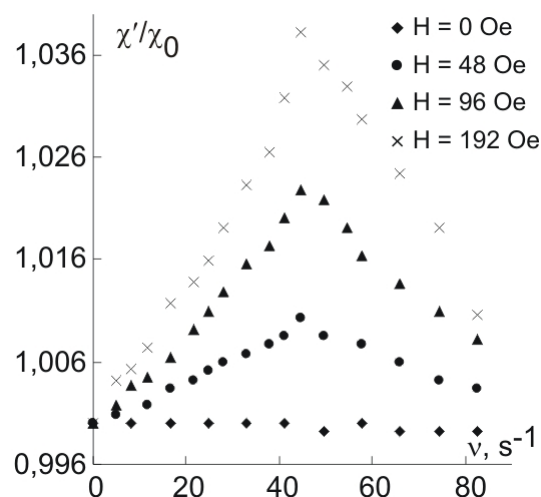


Fig 2. Dependence of real part of magnetic susceptibility on rotation speed at various magnetic fields

The real part of the susceptibility of magnetic fluid rotating in the homogeneous magnetic field, directed perpendicularly to measuring field has a maximum also at a rotational speed, close to frequency of a measuring sinusoidal field (fig. 2). For an explanation of results we extend the guess about possibility formation of magnetized structures of nanoparticles in such systems.

For confirmation of this fact we carried out the comparison of results of investigation of initial area of magnetisation curves and peculiarities of the anisotropic light scattering in a magnetic field for the explored sample and structurally resistant to kerosene based magnetic fluids.

Acknowledgements: this work was supported by Russian Educational Agency in Scientific Program "Development of Scientific Potential of High School".

[1] Blum E., Mayorov M., Cebers A. *Magnetic fluid*. Riga, 1986.

23PO-3-8

THERMOREVERSIBLE ORGANOFERROGELS: MORPHOLOGICAL, RHEOLOGICAL AND MAGNETIC PROPERTIES

Krekhova M., Lattermann G.

Makromolekulare Chemie I, Universität Bayreuth, D-95440 Bayreuth, Germany

Thermoreversible ferrogels (FG) obtained by physical gelation of ferrofluids (FF) have been described [1]. In principle, these systems offer some considerable advantages with respect to covalently crosslinked polymeric ferrogels. The gelation process can easily be repeated many times. For example, this allows a casting of a ferrogel ball in a mould and the measurement of the deformation of such a ball in a magnetic field in order to compare the results with theoretical predictions about such a magneto-deformation [2].

Two kinds of gelators of the type SEBS poly(styrene-*b*-(ethylene-co-butylene)-*b*-styrene) triblock copolymer (Kraton G 1650 and Kraton G 1652) with different molar masses were used. The original ferrofluid consists of magnetite colloidal nanoparticles in two types of paraffin oil with a different viscosity as selective solvent for triblock copolymer middle block (Finavestan A 80B and Finavestan A 50B). For both gelators, the concentration range, where stable, homogeneous organoferrogels are formed, is $c_{\text{gel}} = 4 - 10$ wt.% per paraffin oil. The magnetite concentration can be varied from 20 - 26 wt.% per paraffin oil.

Magnetic measurements of two ferrogel samples with either 5 wt.% G 1650 or G 1652 per paraffin oil A 50B and a magnetite concentration of $c_{\text{FF}} = 21$ wt.% per paraffin oil were performed. For both samples, a typical superparamagnetic behaviour at room temperature without any hysteresis loop is observed. Averaged over three measurements for each of the two FGs, we calculated the initial susceptibility, the saturation magnetisation and the particle size. For the G 1650 FGs we obtained $\chi_i = 0,32 \pm 0,01$, $M_s = 14,2 \pm 0,5$ kA/m, for the G 1652 FG the value of $\chi_i = 0,30 \pm 0,01$, $M_s = 13,4 \pm 0,5$ kA/m result. The numerical differences between two FGs lie within the experimental error range. The calculated particle diameters are $d_0 = (9.5 \pm 0.1)$ and $d_\infty = (6.2 \pm 0.1)$ nm. The results obtained from the magnetisation measurements are in a good agreement with the particle diameters determined by the transition electron microscopy (TEM) [3]. This indicates that the magnetite particles are not associated in the ferrogels.

TEM, cryo-TEM, CRF-TEM (cryo fracture replica TEM) analysis, falling ball method measurements and rheological studies have been performed. The magnetite particles are preferably located in the 'free' paraffin phase between micellar domains of the gelator. The ferrogels exhibit mostly higher softening temperatures than the neat gels. In general, the softening temperatures increase with the molar mass of the gelator and the viscosity of the paraffin oil.

Support by DFG (Research Group FOR 608, project 5) is acknowledged.

[1] G. Lattermann, M. Krekhova, *Macromol. Rapid Commun.* Vol. 27, 2006, pp. 1373-1379; Vol. 27, 2006, p. 1968.

[2] C. Gollwitzer, A. Turanov, M. Krekhova, G. Lattermann, I. Rehberg, R. Richter, arXiv:0801.1244v1. 2008

[3] M. Krekhova, G. Lattermann, *J. Mater. Chem.*, 2008, DOI:10.1039/b800692j.

23PO-3-9

PHYSICAL MODIFICATIONS INDUCED IN ELASTOMERS BY Fe PARTICLES DOPING

Balasoiu M.^{1,2}, Craus M.L.^{1,3}, Anitas E.M.³, Erhan R.³, Kuklin A.I.³, Islamov A.Kh.³, Kovalev Yu.S.³, Ivankov A.I.³, Lozovan M.², Muresan C.⁶, Tripadus V.¹, Savu D.⁴, Savu S.⁴, Bica I.⁴

¹Joint Institute of Nuclear Research, 141980 Dubna, Russia

²National Institute of Physics and Nuclear Engineering, Bucharest, Romania

³National Institute of Research&Development for Technical Physics, 700050 Iasi, Romania

⁴The West University of Timisoara, Department of Electricity and Magnetism, Timisoara, Timis County, Romania.

The doping of elastomers with a filler, considered as an indeformable material, leads to appearance of a local deformation of the matrix (local overstrain of chains) and also to a change of its mechanical properties. In the present work is studied the Fe particles doping effect on the physical properties of the polymer matrix (Fig.1). The samples were prepared at the West University of Timisoara, Department of Electricity and Magnetism.

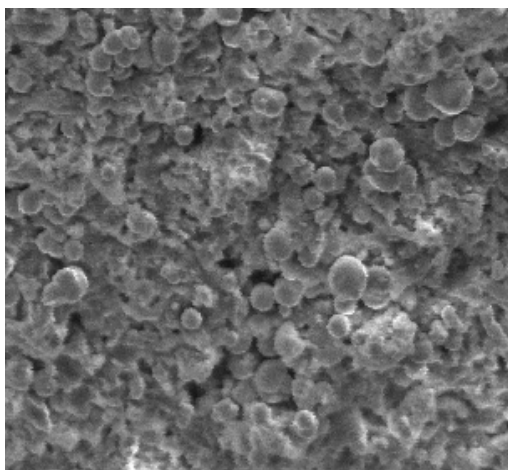


Fig1 TEM image of elastomer sample with magnetic particles.

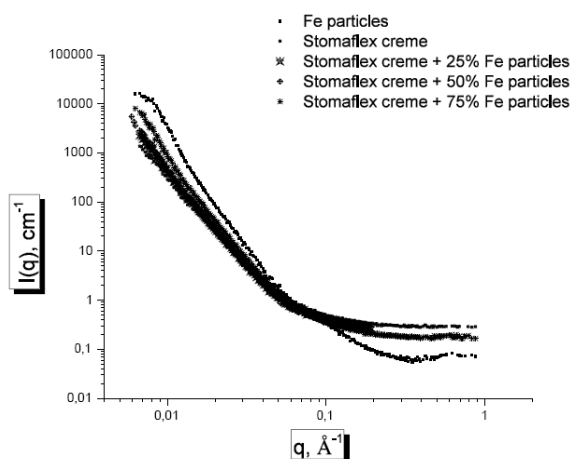


Fig.2 SANS experimental curves obtained at YUMO time of flight diffractometer.

We have investigated separately the filler and the elastomer by XRD and SANS. Magnetic properties of doped with magnetic particles were obtained by using a vibrating sample magnetometer between 200 and 340 K. Magnetic data indicated a change of the coercitive force with the particles concentration in the samples. In Fig.2 are presented SANS curves from experiments of nonpolarized neutrons carried out on YUMO small-angle time of flight diffractometer at the IBR-2 high pulsed reactor in JINR, Dubna. In agreement with the literature, the reinforcement factor, implicitly mechanical properties of the samples, depends on the filler concentration [1]. Our aim is to investigate the change of the matrix structure and the magnetic properties of the doped elastomers with the particles concentration.

Support by Joint Institute of Nuclear Research, Dubna, Russia is acknowledged.

[1] A. Botti, W. Pyckhout-Hintzen, V.Urban, J. Kohlbrecher, D. Richter, E. Straube, Appl. Phys. A 74 [Suppl.], S513–S515 (2002)

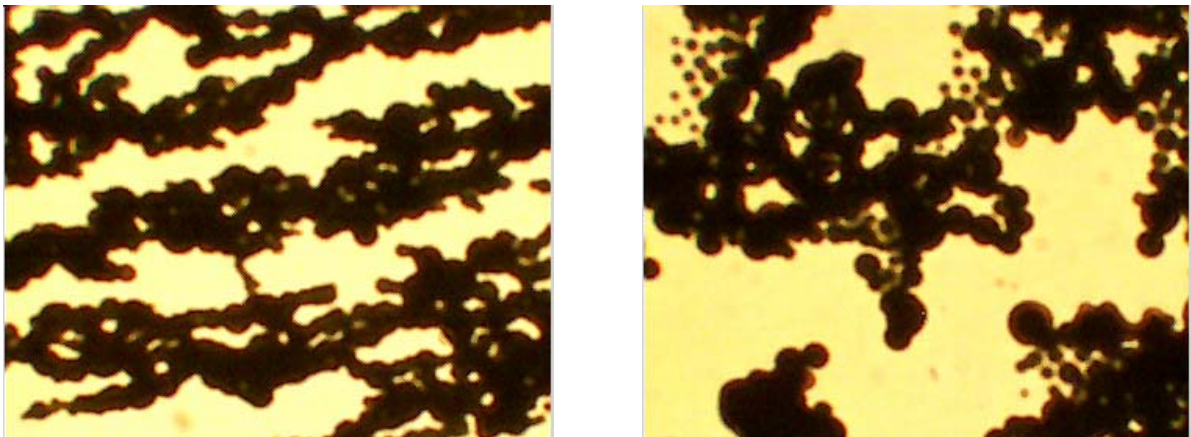
23PO-3-10

INVESTIGATION OF MAGNETORHEOLOGICAL SUSPENSIONS BY OPTICAL AND MAGNETO-OPTICAL METHODS

Nikitin L.V., Kudryavcev D.N., Shashkov I.V., Kazakov A.P.
Moscow State University, Vorob'evy gory, 119992 Russia

This work is dedicated to an investigation of processes of structuring of magnetorheological suspensions, which are used in producing magneto-dirigible materials – magnitoelastics [1, 2]. We studied these processes in thin layers (30-50 μm) of suspension in external magnetic field and without it. Spherical particles ($\sim 2 \mu\text{m}$) of iron were used as magnetic stuff. Solution of oligomer of the siloxane caoutchouc was used as liquid phase. We assembled plant for investigation of thin layers of magnetorheological suspensions using transmission microscope Olympus. Main feature of this plant was possibility to study our specimen in uniform and not uniform magnetic fields. Measurements were made in case of high concentration and low concentration (volume concentration varied from 0% to 20%).

We found out that processes of structuring occur both in magnetic field and without it. There is no chosen direction in structure of magnetic particles without magnetic field (see fig.). Considering processes of structuring we had determined velocities of single particles and character of growth of magnetic clusters. In polymerized suspension magnetic particles have less freedom to move. Also we had discovered an interaction between magnetic particles and polymer matrix.



Structures of magnetic particles with magnetic field (left) and without it (right), in case of high concentration of magnetic phase

In case of low concentration we observed that cluster that form of chains of magnetic particles [3] move for period of time and then stop, as if they run against invisible obstacle. Such a behavior can be explained by interaction of chains with centers of forming polymer matrix. Further growth of number of particles in cluster leads to new moving of magnetic chain in direction of gradient of magnetic field. Only chains with 10-15 particles can overpass these obstacles and reach poles of electromagnet or steel needle. We can calculate the local viscosity of forming polymer matrix if we rough estimate the force of interaction between magnetic needle and chain. So we think that polymer matrix bound magnetic clusters in one object.

We also had investigated magnitoelastics by magnito-optical methods.

[1] E.F. Levina, L.S. Mironova, L.V. Nikitin, G.V. Stepanov. Magnetocontrolled elastic composite materials. Russian patent N 2157013/2000.

- [2] L.V. Nikitin, L.S. Mironova, K.G. Kornev, G.V. Stepanov. *polymer Science, Ser. A*, Vol.46, No.3, 2004, p.498.
- [3] L.V. Nikitin, E.S. Nikitenko, *Proceedings of MISM, Moscow(2005)* 81

23PO-3-11

MAGNETIC FREDERICKSZ TRANSITION IN FERRONEMATIC LIQUID CRYSTALS UNDER SHEAR FLOW

Makarov D.V., Zakhlevnykh A.N.

Perm State University, 15 Bukirev St., Russia

The object of our investigations is a low concentrated suspension of monodomain anisometric magnetic particles in nematic liquid crystal (NLC). Such materials usually called ferronematic liquid crystals or ferronematics (FN). In this work we have analyzed the influence of shear flow on the magnetic-field-induced Fredericksz transition in a planar layer of a FN. Continuum approach has been used to describe the dynamics of a FN.

We have considered the magnetic field orientation which is perpendicular to the plane of the FN layer. Conditions of the planar rigid director coupling on the boundaries of the FN layer and linear distribution of a velocity inside the FN layer have been assumed. On the surfaces of the magnetic particles we have used soft homeotropic director coupling conditions. We have taken into consideration magnetic segregation effect in FNs and two mechanisms of the magnetic field influence on the FN orientational structure: diamagnetic (the influence on the NLC-matrix) and ferromagnetic (the influence on the magnetic particles). In the framework of generalized Leslie-Ericksen theory we have derived the set of integral equations describing the combined effect of shear flow and external magnetic field on the FN.

We have numerically obtained stationary solutions for the magnetic particle concentration, planar director and magnetization fields in the middle of the FN layer as functions of the magnetic field strength and different values of Frank elastic constants, the coupling energy, the segregation parameter, the reactive parameter, and the Ericksen number. The both cases for the so-called flow aligning and nonflow aligning NLC-matrices have been examined. We have derived analytical expressions for the critical magnetic field strength, the director and magnetization angles for the small Ericksen numbers and near critical points.

In the absence of shear flow we have found out that the magnetic-field-induced Fredericksz transition in a FN could be both the second and the first order phase transition. At weak magnetic segregation the orientational FN transition is the second order phase transition like conventional Fredericksz transition in pure liquid crystals. At strong magnetic segregation the transition in FN becomes the first order. In the framework of Landau expansion of FN free energy potential we have analytically obtained the critical value of the segregation parameter corresponding to the tricritical point.

In the presence of shear flow for the considered orientation of an external magnetic field the angular phase is observed. The threshold existing in the static case is "smoothed" with the increase of the velocity gradient (the Ericksen number) at any allowable values of the reactive parameter. The shear flow aligns the director at some nonzero angle to the direction of flow. The homeotropic phase is observed in special case when the reactive parameter is equal to unity, but the presence of shear flow leads to the symmetry breaking of perturbed FN orientation.

This work was partially supported by Grants 07-02-96007 and 08-02-00389 from Russian Foundation for Basic Research.

23PO-3-12

STRUCTURE FACTOR OF A MODEL BIDISPERSE FERROFLUID WITH CHAIN AGGREGATES

Pyanzina E.S.¹, Kantorovich S.S.^{1,2}, Ivanov A.O.¹

¹Urals State University, Ekaterinburg, Russia

²Max Planck Institute for Polymer Research, Mainz, Germany

Magnetic fluids are nanosystems with complex internal structure. Various types of clusters were observed in ferrofluids: chains of nanoparticles, fractal loose aggregates, drops with high density of magnetic phase, etc. One of the efficient ways of investigating the ferrofluid microstructure is to use the small angle neutron scattering and to analyze the structure factor. Theoretically the structure factor is nothing but the Fourier transform of the pair correlation function. Being the Fourier image, the structure factor might be easily calculated also in computer simulations.

It is well known that the microstructure of the ferrofluid is highly influenced by the particle polydispersity. That is why it is essential to take the particle size distribution into account when developing any theoretical model. Unfortunately, the chain formation might be described explicitly only for the bidisperse system which is a quite complicated subject to be properly prepared in the experiment. So, the main idea of the present work is to develop the theoretical model of the bidisperse ferrofluid structure factor, and to check it by means of computer simulations in which a bidisperse model might be exploited without any restrictions. To approximate a real ferrofluid by the bidisperse model system we will use the approach developed in [1] and compare the results to the data from [2].

The theoretical model described in [1] is based on the free energy functional minimization under the mass balance conditions which provides the equilibrium chain distribution. Having such a distribution at hand it is possible to construct the pair correlation function (for details see [3], for instance). The main idea of the method is to take a random particle and collect the information about the distances from it to its neighbors, and then to collect the number of neighbors situated at the same distance. In other words the ferrofluid is treated as a set of coordinating spheres the occupation of which is determined by the chain length distribution.

Any chain model is limited by relatively high values of the coupling parameter and moderately low concentrations of the magnetic material. So, the results of the present model are applicable only to these model systems. The developed model agrees well with computer simulation results. On the one hand it shows that these are chains that influence the anisotropy of the structure factor in the given range of parameters; on the other hand we show that the anisotropy decreases with the growth of small particle concentration. The latter fact allows to conclude that the structure factor is really sensitive not only to the presence of aggregates, but also to their sizes. It is very important to be able to trace this connection, as it might give a key to the interpretation of real experiments.

The research was carried out with the financial support of DFG-RFBR Grant No. HO 1108/12-1, CRDF Grant No. PG07-005-02, and a stipend to SK coming from the MPG. One of the authors (SK) was supported by CRDF Grant Y3-P-05-11, L'Oreal-Unesco Stipend, President RF Grant 412.2008.2, one of the authors (EP) is grateful to the Dynasty foundation.

[1] C. Holm et al, *J. Phys. Condensed Matter*, **18** (2006), S2737.

[2] J. P. Huang, Z. Wang and C. Holm. *Phys. Rev. E.*, **71**, (2005) 061203.

[3] M.P. Allen and D.J. Tildesley. *Computer Simulation of Liquids* (Clarendon, Oxford, 1987).

23PO-3-13

INSTABILITY OF MAGNETIC FLUID MICRODROP IN THE FLAT LAYER IN THE PERPENDICULAR MAGNETIC FIELD

Dikansky Yu.I.¹, Zakinyan A.R.¹, Nechaeva O.A.¹
 Stavropol State University, Stavropol, Russian Federation

Effects of instability of the kerosene based magnetic fluid microdrops shape, weighed in aviation hydraulic oil, which not immixed with a magnetic fluid under the action of a magnetic field was investigated.

Aviation hydraulic oil (AMG-10) provided rather small interphasic tension on boundary a drop – medium (about 10^{-5} N/m). The thin film of sample (100 μm) with drops of the magnetic fluid (diameter varied over the range from 15 to 70 μm) was located in an external homogeneous stationary magnetic field which was perpendicular to a film plane.

Under the action of a magnetic field drops of a magnetic fluid were extended along the field direction and reached walls of cell. At increasing of the field in a place of contact of drop to a cell wall formation and development fractal patterns was observed. In figure 1 typical star-like patterns are shown. With the field increasing the length of peaks of a “star” increases, and also formation of secondary peaks is observed. The similar pattern is formed both at bottom and at upper cell walls in a place of contact to them extended drop. At increasing of magnetic field to some critical quantity, the drop state becomes labile and there is its decay on some drops of the

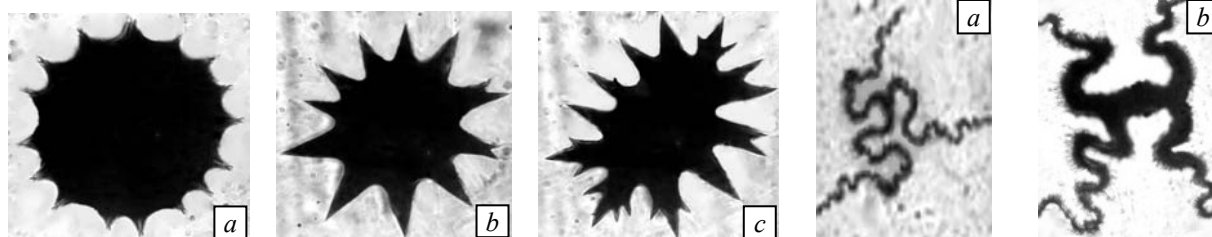


Fig. 1. The pattern observed in a place of contact of a drop with cell walls. The magnetic field creases from left to right.

Fig. 2. Decay of microdrops in high magnetic field

smaller size also elongated to a field direction and having star-like formations on the ends.

At the fast field increasing over critical value microdrops of a magnetic fluid break up at once to a considerable quantity of smaller drops. Thus decay occurs on several (depending on the size of drops) twisting fractal paths (fig. 2). Result of this decay is formation of a considerable quantity of small drops self-organised in hexagonal structure or the labyrinthine structure under certain conditions. The theoretical analysis of the observable phenomena has been made by us at use of the energy approach on the basis of minimisation of a total energy of system.

This work was supported by Russian Educational Agency in Scientific Program “Development of Scientific Potential of High School”.

23PO-3-14

DETERMINATION OF MAGNETIC MOMENTS OF MAGNETITE NANOPARTICLES AGGREGATES BY OPTICAL METHODS

Yerin C.V.

Stavropol State University, Stavropol, Russian Federation

Presence of aggregates of magnetite nanoparticles in magnetic fluids is confirmed by various methods, such as dynamic light scattering [1], pulsed birefringence in electric and magnetic fields [2], dichroism [3], magnetic measurements [4] at al. Experiments give values of the sizes of aggregates about 50-200 nanometers depending on the sample, i.e. each aggregate contains from several tens to several hundreds magnetite nanoparticles (diameter about 10-12 nm). Special interest is caused with character of magnetisation of aggregates and a problem of presence in them spontaneous magnetisation. Optical methods, such as a magnetic birefringence and a dichroism are one of the most effective for researches of colloids. Research of peculiarities of birefringence in pulsed and AC field allows to estimate the contribution of the constant and induced magnetic moments to orientation of a particle under the action of a magnetic field.

The sample was colloid of magnetite nanoparticles in kerosene with volume concentration 0.1 %. For measurement of effect of birefringence standard optical apparatus [2,4] was used. The magnetic field was created by Helmholtz coil which were connected to the pulse generator. Time of increase of a magnetic field to the peak value was 0.081 s.

The birefringence signal at action of an pulsed magnetic field by duration 0.01 s and amplitude 25 Oe is shown on fig. 1. By continuous line the magnetic field impulse is shown.

At action of a rectangular pulse of an external field birefringence of a colloid increases under the law [5].

$$\Delta n(t) = \Delta n_{\max} \left(1 - \frac{3R}{2(R+1)} \exp(-2Dt) + \frac{R-2}{2(R+1)} \exp(-6Dt) \right),$$

where D – rotational Brownian diffusion coefficient, parameter $R = \mu^2 / (\Delta\chi kT)$ – Spots a relation of the constant μ and induced moments $\Delta\chi H$ in a particle. In case $R=0$ orientation is carried out

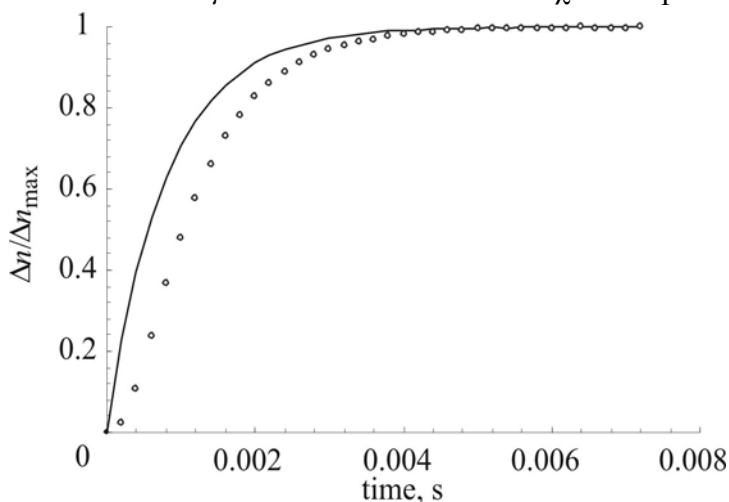


Fig.1.

under the action of the induced moment and at $R \gg 1$ under the action of the constant. In experiment it is impossible to achieve that the magnetic field switch on instantaneous and consequently it is necessary to consider influence on increasing of a birefringence of increasing of magnetic field in due course. It is made by us by means of the integral used in the electrical engineering for calculation of distortions of signals in electric circuits [2]. Calculations have shown, that parameter $R \ll 1$, that testifies to a prevailing role of an induced magnetic moment in orientation of aggregates under the action of a field.

This work was supported by Russian Educational Agency in Scientific Program “Development of Scientific Potential of High School”.

- [2] Padalka V.V., Yerin C.V. *Colloid Journ.* Vol. 62, No. 2 2001
[3] Reed W., Fendler J.H. *Journ. Appl. Phys.* Vol. 59. No. 8.,1986. P. 2914.
[4] Chikazumi S., Taketomi S. et al. *JMMM.* Vol. 65. 1987. P. 245.
[5] Stoylov S. *Adv. Coll. Int. Sci.* Vol. 3 (1), 1971, pp. 45.

23PO-3-15

EQUILIBRIUM DROP FORMS AND CONDITIONS OF A SEPARATION OF A HANGING DROP OF A MAGNETIC FLUID IN A MAGNETIC FIELD

Simonovsky A.Ya.¹, Yartseva E.P.²

¹Institute of mechanics Moscow State University, Moscow, Russia

²Stavropol State University, Stavropol, Russia

In the present work we represent results of research of process quasi-stationary growth and a separation of drops of a magnetic fluid at the expiration from a capillary aperture of a flat unlimited nonmagnetic substrate in an external magnetic and gravitational fields.

Kerosene based magnetic fluid stabilized with oleic acid we used in experiments. The scheme of experimental setup and methods of experiments is described recently [1]. Process of drop formation was registered by a digital videocamera. We measured volume of a separated drop in a magnetic field and without a field.

As have shown experiments behavior of a separated drop of a magnetic fluid depends on a magnetic field. In a magnetic field the volume of a coming off part of a drop of a magnetic fluid which we connect with increase in the capillary forces keeping a drop on a surface, at the expense of extension of a leg of a drop in a direction of the field.

The balance equation is the integro-differential equation which it is possible to lead to the nonlinear ordinary differential equation of the second order.

The equation has been solved by us numerically under the boundary conditions set from experiment (a regional corner and drop volume). As a result of numerical experiments borders of stability of the decision of the equation are mount and mechanisms of formation and a separation of separate parts of a drop are explained. The analysis of numerical decisions has shown, that the form of a drop of a magnetic fluid and volume of a separated part of a drop with increase in the size are defined by a surface tension of a fluid, magnetic properties and size of an external magnetic field and do not depend on viscosity and other mechanical characteristics of a fluid.

We thank RFBR (grant No. 08-01-000-26) for work support.

- [1] Simonovsky A.Ya., Chuenkova I.Yu., Yartseva E.P. *Magnetohydrodynamics*, 2007, No. 43(1), pp. 27-34.

23PO-3-16

CONTRAST VARIATION IN SMALL-ANGLE NEUTRON SCATTERING FROM MAGNETIC FLUIDS AS POLYDISPERSE AND SUPERPARAMAGNETIC SYSTEMS

*Feoktystov A.V.^{1,2}, Avdeev M.V.^{1,3}, Aksenov V.L.^{1,3}, Bulavin L.A.², Bica D.⁴, Vekas L.⁴,
Garamus V.M.⁵, Willumeit R.⁵*

¹Frank Laboratory of Neutron Physics, Joint Institute for Nuclear Research, Joliot-Curie 6,
141980 Dubna, Moscow region, Russia

²Taras Shevchenko Kyiv National University, Physics Department, Glushkova prosp. 6, k.I,
03022 Kyiv, Ukraine

³Russian Research Center "Kurchatov Institute", Akademika Kurchatova pl. 1,
123182 Moscow, Russia

⁴Laboratory of Magnetic Fluids, CFATR, Romanian Academy, Timisoara Division, Mihai
Viteazul blvd. 24, 300223 Timisoara, Romania

⁵GKSS Research Centre, Max-Planck-Str.1, 21502 Geesthacht, Germany

The contrast variation method in experiments on small-angle neutron scattering (SANS) is a powerful technique, which is now widely applied for studying colloidal systems. It is based on the detection of changes in the scattering from the system when varying the contrast $\Delta\rho$ (difference between the mean scattering length densities of the studied particles, $\bar{\rho}$, and the solvent, ρ_s , where these particles are located). The latter is achieved by partial substitution of hydrogen with deuterium in the solvent. The classical approach [1] deals with systems of monodisperse multicomponent and non-magnetic nanoparticles. For magnetic fluids, which are polydisperse and superparamagnetic systems, the method of the contrast variation requires some modifications [2].

In the present work SANS curves obtained at different contrasts for two kinds of magnetic fluids (magnetite/myristic acid/benzene and magnetite/oleic acid/benzene) are treated in terms of modified basic functions approach [2]. Analysis of the obtained basic functions makes it possible to conclude about the inner structure of nanoparticles in magnetic fluids together with the size polydispersity function. Also, the cluster formation effect is considered. Dependence of the apparent radius of gyration as a function of the inversed contrast gives information about the characteristic radius $(\langle R^8 \rangle / \langle R^6 \rangle)^{1/2}$ of the whole (magnetite plus surfactant) particle in the fluid. For magnetic fluid with oleic acid this radius (10.3 nm) is twice larger compared to that for the fluid with myristic acid (5.1 nm), which is in agreement with the data of polarized neutrons scattering [3]. It is shown that the used approach can be efficiently used as a method complementary to the direct modeling of the SANS curves.

[1] H.B. Stuhrmann, In: Small-angle X-ray scattering, Eds. O. Glatter, O. Kratky, London: Acad. Press, 1982.

[2] M.V. Avdeev, *J. Appl. Cryst.*, **40** (2007) 56.

[3] M.V. Avdeev, D. Bica, L. Vekas, et al., *J. Mag. Mag. Mater.*, **311** (2007) 6.

23PO-3-17

SANS OF INTERACTING MAGNETIC MICROSIZED PARTICLES IN A POLYMER MATRIX

Anitas E.^{1,2}, Islamov A.Kh.¹, Erhan R.¹, Balasoiu M.^{1,3}, Bica I.², Osipov V.A.¹, Kuklin A.I.¹

¹Joint Institute for Nuclear Research, 141980 Dubna, Moscow region, Russian Federation

²The West University of Timisoara, Blvd. V. Parvan, No. 4, 300223 Timisoara, Romania

³Horia Hulubei National Institute of Physics and Nuclear Engineering, Bucharest, Romania

The reinforcement of polymeric matrix with fine-particle metallic fillers is of considerable scientific interest [1-2] when one needs to understand and control their microstructure for improving physical properties. Small angle neutron scattering and electron microscopy were used for structural investigations of these magnetic elastomers in a broad length scale. The polymer matrix consist of: a) Paste Alpha Omega PDMS, calcium carbonate, pigments, taste ingredients and b) Catalysts: dibutildilaureate, benzyl silicate and pigments. The magnetic particles used have a mean diameter of $d = 2.24 \mu\text{m}$ [3]. Experimentally the high fraction of reinforcement of magnetic particles, respectively 25%, 50% and 75% mass concentration induce a strong increasing of scattering intensity with concentration, at very small angles. We present an analysis of scattering-intensities from these magnetic elastomers. The results gives new insights on the structural properties of magnetic elastomers at micrometric scale.

[1] A.V. Shenoy – *Rheology of Filled Polymer Systems*, Springer, 1999.

[2] J.- F. Gerard – *Fillers and Filled Polymers*, Wiley-VCH, 2001.

[3] Mat. Sci. and Eng. **B98** (2003) pp. 89-93.

23PO-3-18

MODELLING OF AIR CAVITIES IN A MAGNETIC FLUID NEAR TO THE FERROMAGNETIC CONE

Avdeeva O.A.¹, Simonovsky A.Ya.²

¹Stavropol State University, Stavropol, Russia

²Institute of mechanics of Moscow State University, Moscow, Russia

Equilibrium shapes of a free surface of a magnetic fluid near to a ferromagnetic cone are experimentally and theoretically investigated. The ferromagnetic cone was installed in nonmagnetic cuvet between electromagnet poles. The axis of symmetry of a cone placed vertically and the magnetic field direction - is horizontal. In a magnetic field to a cone surface consistently incremented portions of a magnetic fluid moved. Distribution of the free surface of a magnetic fluid near to a cone surface was registered by a digital camera.

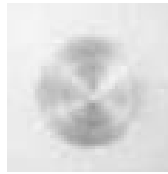


Fig. 1. Photo of distribution of the free surface of a magnetic fluid near to a cone without a magnetic fluid (a view from an edge).

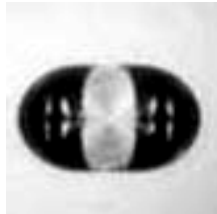


Fig. 2. Photo of distribution of the free surface of a magnetic fluid near to a cone at bulk volume of a magnetic fluid in a cuvet of 0.4 cm^3 .

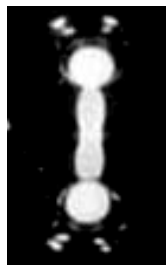


Fig. 3. Photo of distribution of the free surface of a magnetic fluid near to a cone at volume of a magnetic fluid in a cuvet of $110,0 \text{ cm}^3$.

As observations have shown the magnetic fluid sticks to those parts of a surface of a cone which are located under a corner 0 and 180° to a external magnetic field direction. At a surface of a cone located under corner $\pm 90^\circ$ to magnetic field direction aerial cavities are formed. Photos shows the cone coated with a magnetic fluid. At centre of fig. 1 the cone surface free from a magnetic fluid at the sight of from an edge is shown.

In fig. 2 the photo of a cone coated in small volume of a magnetic fluid are shown. At centre of fig. 2 the light surface of a cone is visible. Dark stains at the left and to the right of cone vertex it is drops of a magnetic fluid the surfaces located near to surface located under a corner 0 and 180° to a direction of an exterior magnetic field. The vector of an exterior magnetic field is directed from left to right and lays in a plane of drawing. In fig. 3 the photo of a cone coated in great volume of a magnetic fluid is shown. Light strips at photo centre it is sections of a surface of a cone free from a magnetic fluid. Round white spots from above and from below a vertex of a cone it is air cavities in close surface of a cone. We are counted by a numerical methods the p distribution of free surface of a magnetic fluid

near to a magnetised cone. Results of modeling are well agrees to a experimental results.

Authors thanks the Russian Found of Basic Researches (project No.08-01-000-26) for the work support.

23PO-3-19

EVALUATION OF THE INFLUENCE OF THE VARIOUS FACTORS ON THE MAGNETO-OPTICAL PROPERTIES OF THE ULTRAFINE MEDIUM BY STATISTICAL METHOD

Kalandadze L.

Department of Physics, Batumi State University, 35 Ninoshvili street, Batumi 6010, Georgia

In general, the magneto-optical properties of magnetic fluids are very different from the properties of the bulk ferromagnetic. This fact causes the changes of the magneto-optical effects of the spectral and angular dependences. Therefore, it is important to define the conditions of the magneto-optical experiment. In this case it occurs much easier to interpret the magneto-optical spectrums, which provides information on magnetized magnetic fluids surface layer, electronic energy structure of fine magnetic particles and the properties of carrier fluids. In specific experimental conditions the amount of equatorial Kerr effect is proportional to q , which is the

occupancy of the volume of the magnetic fluid with magnetic particles [1]. On the example of magnetite magnetic fluids in references [2] was decided to evaluate the percent of the influence of q on the variation of the frequency dependences equatorial Kerr effect comparing to other factors. Calculations showed that the influence of only q factor on the amount of the frequency dependences equatorial Kerr effect is 53 %. Another significant factor which influences the magneto-optical properties of magnetic fluids is ϵ_0 , dielectric permittivity of the medium. According to the calculations part of influence of ϵ_0 is 37% comparing to others [3]. For these calculations have been used correlation analyses methods - the rule of dispersion summarizing.

We did analogous researches for Faraday rotation. According to this result, as for equatorial Kerr effect, in specific experimental conditions the values of the Faraday rotation prorate to q and spectral dependences of effect in ultrafine medium and in the proper bulk magnetic are similar. This result is in good relation with the experiments [4], where Faraday rotation has been studied in magnetite magnetic liquids. This research also shows obviously the linear dependence of Faraday rotation to q .

The researches done for Faraday rotation have only confirmed the results produced for equatorial Kerr effect. Particularly, it has been concluded that basically q and ϵ_0 factors exert influence on the value of the effect but the part of all of the rest factors consists of 10%.

We would like to underline that these results will be also suitable to all magnetic ultrafine medium, the optical constants of the material of which, n and k , holds following relation $k^2 \propto n^2$. Moreover, these results give us a really good opportunity to forecast the magneto-optical properties of ultrafine medium and therefore, to receive the proper parameters of ultrafine medium.

[1] L.G. Kalandadze, L.V. Nikitin and O.M. Nakashidze, *Proc. of BSU (Batumi)*, **3** (2001)78.

[2] L. Kalandadze, *J. Sensor Letters*, V.5, **1** (2007) 13.

[3] L. Kalandadze, *Book of Abstracts, Thirteenth International Conference on Liquid and Amorphous Metals*, Ekaterinburg, (2007)61

[4] A. Akram, Rousan, M. Hassan, El-Ghanem and A. Yusuf, *J. IEEE Transactions on Magnetism*, V.25, **4** (1989) 3121

23PO-3-20

EFFECT OF MAGNETIC FIELD ON TURBULENCE AND TRANSITION IN HYDRODYNAMIC FLOWS

Zikanov O.

University of Michigan – Dearborn, Dearborn, MI 48128, USA

We consider the effect of imposed steady magnetic fields on transition to turbulence and turbulence itself in flows of electrically conducting, but non-magnetic fluids. The focus of the work is on understanding fundamental properties of flow transformation, although the results have direct implications for the geodynamo theory and for control and optimization of technological processes in such areas as steel casting, aluminium primary production, and semiconductor crystal growth.

In the limit of low magnetic Reynolds number (large magnetic diffusivity) the effect of the flow on magnetic field can be neglected. The opposite effect is, however, strong at a sufficiently strong magnetic field and can lead to spectacular modification of the flows. In particular, Joule dissipation of induced electric currents results in suppression of turbulence and instabilities. Furthermore, the anisotropy is introduced into the flow by the preferred direction of

the magnetic field. As an example, figure 1 shows transformation of a turbulent pressure under impact of vertical magnetic field.

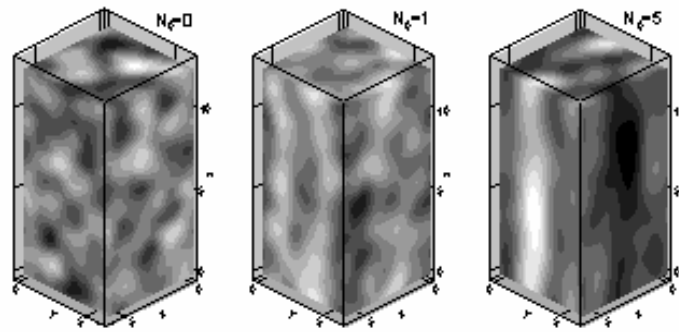


Figure 1. Results of numerical simulations [1]. Instantaneous pressure distributions for zero ($N=0$), moderate ($N=1$) and strong ($N=5$) vertical magnetic field.

We report numerical investigations of flow transformation in idealized well-defined settings. The results are extended to development of turbulence models valid for low Rm magnetohydrodynamics.

Support by the US Department of Energy (Grant DE FG02 03 ER46062) is acknowledged.

- [1] A. Vorobey, O. Zikanov, P. Davidson, B. Knaepen, *Phys. Fluids*, **17**, N12, 125105, 2005.
- [2] A. Thess, O. Zikanov, *J. Fluid Mech.* **579**, 383-412, 2007.
- [3] A. Vorobey, O. Zikanov, *J. Fluid Mech.* **574**, 131-154, 2007.
- [4] O. Zikanov, A. Thess, *J. Fluid Mech.*, **358**, 299-333, 1998.

23PO-3-21

STRUCTURAL SELF-ORGANISATION AT MAGNETIC FLUID DROP EVAPORATION IN A MAGNETIC FIELD

Zubenko E.V.¹, Simonovsky A.Ya.²

¹Stavropol State University, Stavropol, Russia

²Institute of mechanics of Moscow State University, Moscow, Russia

Magnetic fluid drops evaporation on a flat horizontal nonmagnetic surface at surface temperatures above 100°C is investigated.

Measurements have shown, that the magnetic field essentially influences evaporation rate of drops of a magnetic fluid. Effect of a magnetic field depends on concentration of magnetic corpuscles dmagnetic fluids and surface temperatures of the heater.

Magnetic field effect on evaporation rate of drops of a magnetic fluid determines by a character of structuring in volume of a drop of a fluid at evaporation. At surface temperature of the heater 110°C in the first shares of second there is an unmixing of a drop to formation quasi-solid kern consisting of magnetite particles and molecules of surfactant.

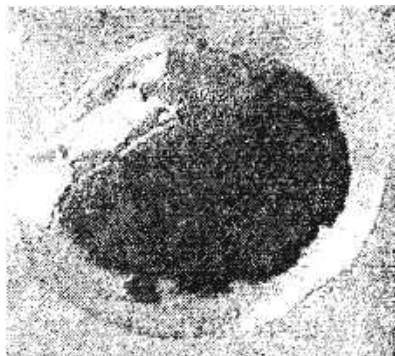


Fig. 1. Quasi-solid kern and liquid shell of drop.

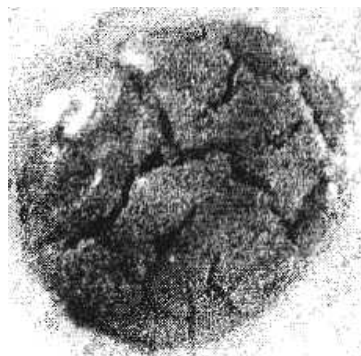


Fig. 2. Decrepitates of quasi-solid kern.

The kern is enclosed by a drop of water (fig. 1). At first there is an intensive evaporation of a liquid envelope of a drop. Then quasi-solid kern decrepitates at the expense of thermal and magnetic stresses (fig. 2). The organised fractures increment an evaporating surface. At the further evaporation in a precipitate layer the self-organising start to be formed. Depending on type and quantity of a magnetic field these structures can take the form of labyrinths, rings or other (fig. 3, 4). Structuring of a precipitate and increasing of evaporating surface it is possible to interpret effect of a magnetic field on evaporation rate of magnetic fluid drops.

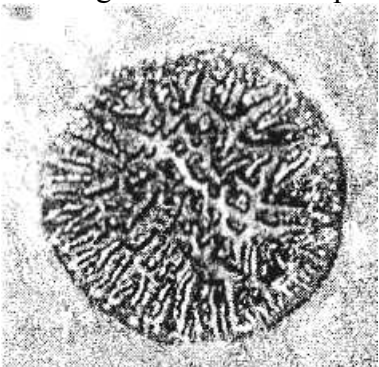


Fig. 3. Evaporation of a high concentrated magnetic fluid drop in AC magnetic field.

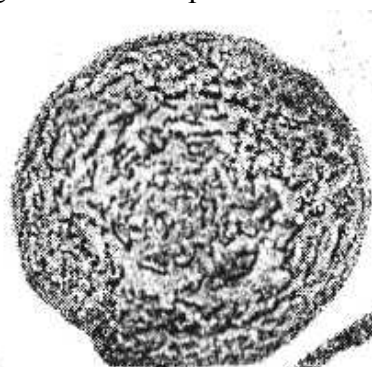


Fig. 4. Evaporation of a low concentrated magnetic fluid drop in AC magnetic field.

Authors thanks RFBR (grant No.08-01-000-26) for work support.

23PO-3-22

ORIENTATIONAL STRUCTURE OF BISTABLE FERRONEMATICS IN MAGNETIC FIELD

Semenova O.R., Zakhlevnykh A.N.

Perm State University, Bukirev St. 15, Perm 614990, Russia

Within the framework of continuum theory the orientational transitions in a bistable cell of ferronematic (i.e. dilute suspension of needle-like magnetic particles on the base nematic liquid crystal) in external magnetic field were investigated. Soft homeotropic coupling between the ferroparticles and the director was assumed. An external magnetic field was applied normal to the cell.

The bistability of the cell consists in the fact that the lower boundary of a layer supposes two stable anchoring conditions. The top boundary of a layer exhibits rigid homeotropic anchoring. The bottom bistable surface allows both homeotropic and planar anchoring, with both

of these surface states are of equal energy and locally stable. So in such a cell there is one of two possible ferronematic states. These states correspond to homogeneous homeotropic alignment or to hybrid homeotropic-planar alignment.

First the set of equations of the orientational and concentrational equilibration of ferronematic with weak bistable surface anchoring was obtained and the basic state of ferronematic was investigated. The influence of external magnetic field on switching of orientation between homeotropic and homeotropic - planar states in a cell was studied. The cases both positive and negative diamagnetic anisotropy of a ferronematic were considered. It is found that at the increase of a magnetic field the threshold values of anchoring energy increase for ferronematic with positive diamagnetic anisotropy, and they decrease for a ferronematic with negative diamagnetic anisotropy. In both cases the conditions have been determined at which the bistability of the cell can be observed.

The effect of segregation on the orientational structure of a ferronematic in both states of the cell was also investigated. It is found, that in a hybrid homeotropic-planar phase the particles migrate to bistable surface at the increase of a magnetic field. In homeotropic phase at the inclusion of a magnetic field the particles accumulate in the middle of a layer, but if the strength of a magnetic field is higher than some critical value, the distribution of particles concentration becomes homogeneous, as well as in a case when the field is switched off.

This work was partially supported by grant No. 07-02-96007 of Russian Foundation for Basic Research.

23PO-3-23

BASIC MAGNETIC STATE OF AN ASSEMBLY OF SINGLE-DOMAIN PARTICLES CONFINED IN A SPHERICAL LAYER

Melenev P.V.¹, Rusakov V.V.¹, Raikher Yu.L.¹, Perzynski R.²

¹Laboratory of Complex Fluids, Institute of Continuous Media Mechanics
Ural Branch of the Russian Academy of Sciences, Perm, 614013, Russia

²Laboratoire des Liquides Ioniques et Interfaces Chargees UMR CNRS 7612

Universite Pierre et Marie Curie, case 51, 4, place Jussieu, 75252 Paris Cedex 05, France

A prospective multi-purpose object in magnetic nanotechnologies and their biomedical applications is a cluster of a finite number (10-1000) of single-domain nanoparticles [1]. In this variety, a separate class make magnetic systems of reduced dimensionality emerging in result of adsorbing or assembling of nanoparticles at platelets, spheres, tubes or other surfaces with intrinsic 2D geometry, see [2], for example. For ideal magnetic manipulations, these objects should possess zero spontaneous magnetic moment and become magnetized only when the field is applied, i.e., be perfectly superparamagnetic. Accordingly, they are modeled as such [3]. It often happens, however, that a cluster is assembled of the particles which have a substantial extent of ferromagnetism, and the question of the residual magnetic moment \mathcal{M} of such an entity turns up. In view of the afore-mentioned, we study the properties of the systems of $N = 100$ and 200 identical magnetically isotropic nanoparticles (each with a permanent magnetic moments μ) confined at the surface of a sphere. The surface density of the particles is about 20%; at such concentrations the particles strongly interact but yet have plenty of room for re-grouping.

Two model situations are investigated. In the first one the nanoparticles are uniformly distributed over the surface of a sphere (the particle locations are determined by solving a pertinent Thomson problem) and pinned in their positions. Thus, the basic state of the cluster is

attained only with respect to the orientational degrees of freedom. In the second case, the particles are initially distributed at random and then allowed to move freely over the sphere surface as well as to rotate their magnetic moments. In both cases the basic state of an assembly is found via a Monte-Carlo procedure multiply repeated: 100 plus realizations. In the second case, to accelerate the calculations, temporal grouping of the particles in sub-clusters is allowed. With the statistics obtained two main integral characteristics of a “magnetic spherical shell” are evaluated: the overall magnetic moment \mathcal{M} and the toroid moment \mathcal{Q} , i.e., the net magnetic vorticity that determines the orientation of the cluster in a vortex magnetic field.

Comparison of the results shows the following. In a layer with $N = 200$ fixed particles \mathcal{M} is about 8% and in a same layer with movable particles it is about 10% of the saturation value μN . The toroid moment is also more suppressed in a layer with fixed particles. However, as it is for smaller systems [4], \mathcal{Q} “dies harder”: for $N = 200$ its values are yet 0.13 and 0.15 of the maximal one. Along with that, our simulations reveal a new and interesting fact: in any cluster the directions of \mathcal{M} and \mathcal{Q} in the basic state are with high accuracy perpendicular to one another.

Support of RFBR Project 06-01-00723 and ECONET Programme 16274QL is acknowledged.

- [1] J.F. Berret, N. Schonbeck, F. Gazeau, D. El Kharrat, O. Sandre, A. Vacher, M. Airiau, *J. Amer. Chem. Soc.* **128** (2006) 1755.
- [2] S. Lecommandoux, O. Sandre, F. Checot, J. Rodriguez-Hernandez, R. Perzynski, *Advanced Materials*, **17** (2005) 712.
- [3] L. Clime, T. Veres, *J. Magn. Magn. Mater.*, **314** (2007) 11.
- [4] P.V. Melenev, V.V. Rusakov, Yu.L. Raikher, *Techn. Phys. Lett.*, **34** (2008) 50.

23PO-3-24

STRUCTURING IN FERROCOLLOIDS AS POSSIBLE BASIS OF MAGNETORECEPTION

Nikolaev I.¹, Nikulina V.², Netsvetov M.², Khizenkov P.³, Makmak I.³

¹Debit consulting, 21/122, Mosfilmovskaya Str., Moscow, 119285, Russia

²Donetsk National University, 46, Shorsa Str., Donetsk, 83050, Ukraine

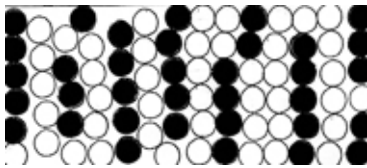
³Donetsk Institute for Physics and Engineering NAS of Ukraine, 72, R. Luxemburg str.,
Donetsk, 83114, Ukraine

Geomagnetic field is used by large number of species for orientation. There are a few hypotheses that explain a mechanism of magnetoreception. One of them is based on the interaction of biogenic magnetic crystals with ambient field. In its context several models can be carried out: transmission of energy of interaction and Earth magnetic field to magnetic structures, for example, to nerve; changing of the optical properties of the layer of biological magnetic liquid; structuring of non-magnetic environment of magnetic nanoparticles. The latter is described below. So far it is a well-known fact that nanoparticles of magnetite in colloids form a structure by itself in the external magnetic field and efficiently structure components of its non-magnetic environment, as it is shown in [1, 2] for mono- and polydisperse styrene microspheres in the layers of ferrocolloids.

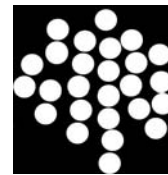
It is impossible to see the picture of structuring biological non-magnetic particles that are commensurated with particles of magnetite. For example it is impossible for big organic ions or biopolymers because of their small size. But here the same as in: it is possible to simulate using

magnetized balls. Proposed model differs from the known with compound magnetic components with non-magnetic (balls, ellipsoids, cylinders etc).

When putting a layer of such compound into magnetic field H_{\parallel} rearrangement of composed elements doesn't occur. Only magnetic axis of the balls orientate along the vector H . A layer is in a "frozen" state. The factor, that promote the movement of the particles (balls) in the layer can be light mechanical or magnetic vibration (V), that imitate actions of thermic energy and fuse of the system. With effects of H_{\parallel} and V at the same time magnetic balls move in the layer as a result of magnetodipole interaction and assemble into chain aggregates. Chaotic allocation of elements in the layer turns into arranged with alternation of magnetic and non-magnetic chains which are drawn along the field. It is impossible to define it visually if one doesn't know which elements of the compound are magnetic or non-magnetic. For biological object such structurization means that total structurization of the magnet containing areas in the cells or other formations may provide functioning not only optical, but electrical, acoustic and obviously other channels of perception of natural and artificial magnetic fields. For ML changing of electrical and acoustic properties under effect of magnetic field is known and described.



Structurization of the monolayer of the compound of magnetic (●) and non-magnetic (○) spheres (diameter 2 mm)



Diameter of the magnetic particles of nickel (●) 20-50 mkm and non-magnetic (○) spheres (diameter 2 mm)

[1] A.T Skjeltorp, *J. Appl. Phys.*, **55** (1984) 2587-2588.

[2] P.K. Khizenkov, M.V. Netsvetov, I.M. Makmak *Structuring magnetic fluids* (Donetsk Institute for Physics and Engineering NAS of Ukraine, Donetsk, 2007).

23PO-3-25

MAGNETIC NANO- AND MICROTECHNOLOGIES IN THE SOIL SCIENCE

Nikolaev I.¹, Romensky M.², Nikulina V.², Netsvetov M.², Khizenkov P.³

¹Debit consulting, 21/122, Mosfilmovskaya Str., Moscow, 119285, Russia

²Donetsk National University, 46, Shorsa Str., Donetsk, 83050, Ukraine

³Donetsk Institute for Physics and Engineering NAS of Ukraine, 72, R. Luxemburg str., Donetsk, 83114, Ukraine

In the work the modified method of magnetic liquation was applied [1] for the modeling of the movement process of colloidal particles and particles of micrometer size in the soil as a component of hydro flux or under the action of vibration. Magnetic particles of carbonyl iron (diameter 5 nm) and nickel (5 nm-200 mkm) were used.

In the run of experiments on the soil we measured time, which took magnetic particles to sank inside the samples, which were taken from the different horizons in the profile (fig. 1.).

Particles of all fractions need minimal time for deepening into volume of samples, which were taken from the depths of 45-55 sm and maximal time from the depths of 70-80 sm. There are explicit differences in the time of movement of the different fractions' particles. Especially there is a big difference between particles of 20 mkm and bigger than 100 mkm. If convert the time into arbitrary units of the speed it may be clearly seen the character of its changing subjects to depths of horizon. Most probably the expressed nonlinearity of the speed of movement of the particles in the profile shows the character of the direction of the process of the soil formation and conforms to textural differentiation of the soil. It is interesting an interesting fact to mention that in the depths of 45-55 sm the speeds of movement of the particles 5 nm – 20 mkm and 20-100 mkm equalize. In extrapolation under natural conditions that may mean facilitated migration not only colloids but even bigger particles and aggregates in conformable genetic horizon.

The introduced model allows to estimate comparative transmission capacity of the different horizons in the limit of the profile. The process of mechanical movement of the nanoparticles (carbonyl iron) registers clearly in the dry samples of the soil. The speed of the vertical movement of the particles depends on their size and micro- and macro organization of horizons of the soil profile.

[1] P.K. Khizenkov, M.V. Netsvetov, I.M. Makmak *Structuring magnetic fluids* (Donetsk Institute for Physics and Engineering NAS of Ukraine, Donetsk, 2007).

23PO-3-26

DC SQUID MODULATION ELECTRONICS FOR OPERATION WITH HTS DC SQUID MAGNETOMETERS IN THE UNSHIELDED ENVIRONMENT

Burmistrov E.¹, Slobodchikov V.Yu.², Khanin V.V.¹, Maslennikov Yu.V.², Snigirev O.V.¹

¹MSU, Physics faculty, Moscow, Russia

²IREE RAS, Moscow, Russia

The new variant of DC SQUID modulation electronics for functioning with HTS DC SQUID magnetometers in the unshielded environment, was designed, manufactured and tested. The electronics, was optimized for operation with new ultrasensitive HTS DC SQUID magnetometer with magnetic field resolution of about 15 fT/Hz^{1/2} at frequencies above 10 Hz and 30 fT/Hz^{1/2} at 1 Hz.

The functional scheme of electronics is presented on Fig. 1. On Fig. 2 one can see the spectrum of background magnetic field, measured in the center of Moscow, using our electronics with ultrasensitive HTS DC SQUID magnetometer.

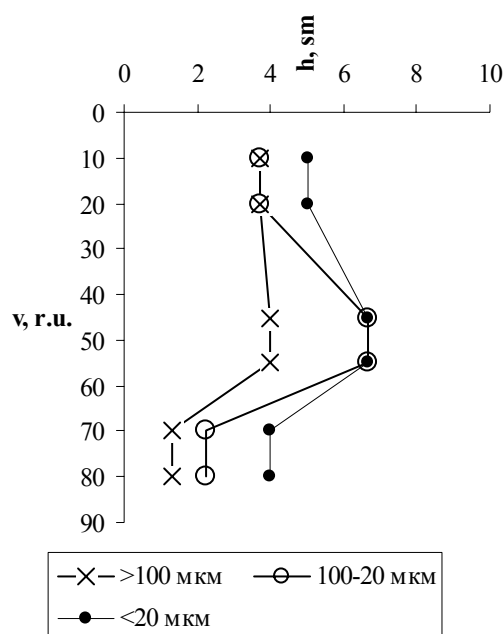


Fig. 1. Comparative speed of vertical movement of the particles in the soil subjects to depths of horizon (b).

The central commutation core of electronics was based on EPLD (Electronic Programmable Logic Device) and allowed to include into the channel the system of a bias reversal and the system of compensation of modulation signal in the feedback, in the bias supply, and in the main signal nets circuits. Such variant provides the stable work independently of configuration of supplying wires in the dipstick or cryostat and configuration of HTS DC SQUID. The electronics was manufactured in one compact box with size 110 mm x 60 mm x 15 mm. The channel has standard bandwidth of about 100 kHz with greatly increased dynamic range due to high coupling ($8 \text{ mV}/\Phi_0$) of feedback signal with main SQUID's loop.

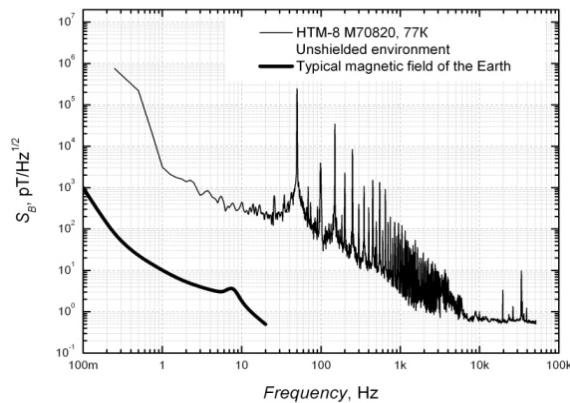
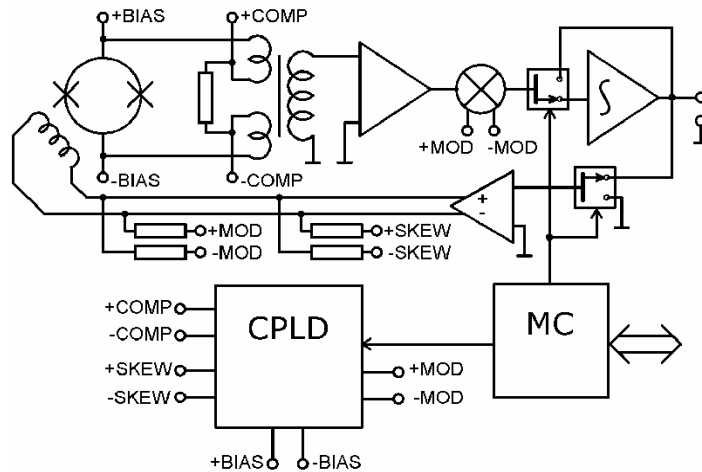


Fig. 2

[1] Faley M.I., Poppe U., Urban K., Paulson K. and Fagaly K. // A New Generation of the HTS Multilayer DC-SQUID Magnetometers and Gradiometers, Journal of Physics: Conference Series **43** (2006) 1199–1202

23PO-3-27

THIN FERROFLUID FILM BREAKUP IN A CAPILLARY TUBE SUBJECTED TO AN AXIAL MAGNETIC FIELD

Kazhan V.A.¹, Korovin V.M.²

¹Moscow State University of Environmental Engineering, 127550 Moscow, Russia

²Institute of Mechanics, M.V. Lomonosov Moscow State University, 119192 Moscow, Russia

The considerable number of publications have been devoted to the investigating the influence of applied magnetic fields on the cylindrical configurations of magnetic fluids, such as an annular layer covering a straight current-carrying cylindrical conductor, a round jet as well as a ferrofluid thread, see, e.g., the bibliography in [1]. Unlike existing papers, we examine the effect of an applied longitudinal magnetic field H_0 on the instability and breakup of an annular ferrofluid film of slowly varying thickness which covers the inner side of a straight unmagnetized capillary tube.

It is well known, that a wetting unmagnetized liquid film of uniform thickness initially at rest inside a cylindrical capillary tube is unstable due to the surface tension acting on a distorted liquid-gas interface. As a result, a cylindrical liquid film of a small relative thickness $\gamma = \delta/a < 0.09$ disintegrates into regularly arranged stable collars [2]; here δ is the thickness and a is the inner radius of the cylindrical film. Characteristic volume of a liquid collar is determined by the wave length $\lambda_m^0 = 2\sqrt{2}\pi a$ of the most rapidly growing normal mode.

We focus our attention on the case where the dynamics of magnetic fluid film is controlled by capillary, viscous and bulk magnetic forces whereas the inertial forces are negligible. Using the simplified ferrohydrodynamic equations [3] which describe the surface tension-driven motion of a ferrofluid in the case $\gamma \ll 1$, $\beta = M_s/H_0 \ll 1$ and considering the normal modes proportional $\exp[i(kz - \omega t)]$, we have derived the following dispersion equation

$$\omega = \frac{i\alpha\delta^3}{3\eta a^2} k^2 \left\{ 1 - (ka)^2 [1 + Mc I_0(ka) K_0(ka)] \right\}, \quad Mc = \frac{a\mu_0}{\alpha} M_s^2,$$

where $I_0(ka)$, $K_0(ka)$ are the modified Bessel functions of the first and second kind, Mc is the magnetocapillary interaction number, α and η are, respectively, the ferrofluid surface tension and viscosity, $\mu_0 = 4\pi \cdot 10^{-7} \text{ H/m}$ is the magnetic constant and M_s is the saturation magnetization of the ferrofluid.

In the absence of a magnetic field ($Mc = 0$) we have the well-known expression for the cutoff wave number $k_c^0 = a^{-1}$ when developing the capillary instability of a long cylinder of viscous unmagnetized fluid. It is easy to see that magnetic forces stabilize a certain range of modes with wave lengths $\lambda > 2\pi a$ that are unstable when there is no magnetic field. With the help of the dispersion equation we have found the following approximate expression for the wave length λ_m of the most rapidly growing mode

$$\lambda_m = \lambda_m^0 (1 + 0.29Mc + 0.04Mc^2).$$

The relative error of this formula does not exceed 3% at $0 \leq Mc \leq 4$. Thus in the case of a strong magnetic field, the magnetic forces essentially increase the volume of collars formed at final stage of the capillary instability of the ferrofluid film.

This work was supported by the Russian Foundation for Basic Research (grant No. 08-01-00026).

[2] P.A.Gauglitz, C.J.Radke, Chem. Eng. Sci., **43** (1988) 1457.

[3] V.M.Korovin, Tech. Phys., **53**, No. 5 (2008) in press.

23PO-3-28

CRYSTAL STRUCTURES AND SUPERFERROMAGNETISM IN 2D MAGNETIC COLLOIDAL MONOLAYERS WITH STRONG DIPOLAR INTERACTIONS

Zhukov A.V.

Institute of Mechanics, Moscow State University, Michurinskiy Prospekt 1, Moscow, Russia

The magnetic ordering, structure and stability of crystal lattices formed by identical spherical ferromagnetic single-domain nanoparticles in two-dimensional (2d) colloidal monolayers on a planar surface exposed to an external magnetic field are studied numerically by lattice sum minimizations. We consider the idealized case where the interaction energy between the particles is much larger than the thermal energy $k_B T$. It is shown that the ferromagnetic single-domain nature of particles may lead to spontaneous orientational order even in the absence of an external magnetic field, as in dipolar soft sphere model of thin films [1].

In the case of the uniform magnetization inside each of the particles the magnetic part of the pair potential reduces to the point dipole-dipole interaction with constant moments but varying orientations of dipoles, as in dipolar hard sphere model. In addition, for the repulsive part of the particle interactions we consider two different models - Yukawa (for electrolyte-based suspensions) and Lennard-Jones potentials. Then, using the periodic approach, we study lattice systems with one particle per unit cell but different dipole orientations of the particles. We assume that these orientations are themselves periodic with respect to a multiple $L_1 \times L_2$ cell, so the problem reduces to the global minimization of the energy per particle $E_1(L, \mathbf{s}_1, \dots, \mathbf{s}_N; \mathbf{H}, \alpha_b)$, where the orientations $\mathbf{s}_i \in S^2$, $N = L_1 L_2$ and the lattice L are variable, but the magnetic field \mathbf{H} and various interaction parameters α_b are fixed. For the minimization the simulated annealing and random particle search methods were used up to $L_1 \times L_2 = 32 \times 32$. In many cases, however, the result may be obtained by solving the spherical model and the optimal dipolar configuration exhibits the 2×2 (Luttinger-Tisza) periodicity.

For $\mathbf{H} = \mathbf{0}$ the found dipolar ground states are ferromagnetic. For $\mathbf{H} \neq \mathbf{0}$ there exist also anti-ferromagnetic ground states with 2×2 (as a rule, with 1×2) periodicity, as well as stripe states with the dipoles oriented mainly in the same direction, and some dipolar chains oriented in the different direction. The found 2d crystal structures, as in the case of fixed dipolar moments [2], represent various rectangular, oblique, chain-like oblique and rhombic lattices, with both first- as well as second-order transitions between them. The mean volume magnetization as a function of \mathbf{H} has the break point at the first-order transitions.

Some generalizations (several particles per unit cell, two-layered structures) are also discussed.

Supported by the Russian Foundation for Basic Research, Grant No. 07-01-00026.

[1] S. H. L. Klapp, M. Schoen, *J. Chem. Phys.*, **117** (2002) 8050.

[2] V.A. Froltsov, R. Blaak, C.N. Likos, H. Lawen, *Phys. Rev. E*, **68** (2003) 061406.

23PO-3-29

EFFECT OF SURFACTANT EXCESS IN NON-POLAR FERROFLUIDS BY SMALL-ANGLE NEUTRON SCATTERING

Petrenko V.I.^{1,2}, Avdeev M.V.¹, Aksenov V.L.^{3,1}, Bulavin L.A.², Rosta L.⁴

¹Joint Institute for Nuclear Research, Frank Laboratory of Neutron Physics, Joliot-Curie 6, 141980 Dubna, Moscow reg., Russia

²Kyiv Taras Shevchenko National University, Physics Department, Glushkova 6/1, 03022 Kyiv, Ukraine

³Russian Research Center "Kurchatov Institute", Acad. Kurchatova 1, 123182 Moscow, Russia

⁴Research Institute for Solid State Physics and Optics, Konkoly-Tege 29-33, Budapest, Hungary

The understanding of mechanisms of ferrofluids stability is an important factor in the synthesis of highly stable magnetic colloids with defined properties. In the present work the microstructure of ferrofluid magnetite/oleic acid/benzene with excess of surfactant (oleic acid) is investigated by small-angle neutron scattering (SANS). The studied type of ferrofluids is characterized by extremely high stability; it allows record volume fractions of dispersed magnetite (above 20 %). In the initial ferrofluid there is an optimal content of surfactant corresponding to full coating of magnetite particles, no free surfactant takes place in bulk solvent. The ratio between the magnetite and surfactant contents is about 1:1. During experiments surfactant is added to this type ferrofluid (volume fraction of magnetite 1 %) up to volume fraction of 25%. For higher values a sharp break in the ferrofluid stability occurs following coagulation and precipitation. Below, influence of the surfactant excess to the ferrofluid stability is insignificant within the time of experiment (order of days); no particle aggregation, as well as surfactant agglomeration (micelles) is observed by SANS. Slight changes are detected after one year from the first experiment. The interaction of free acid molecules in the ferrofluid is compared with that for their solutions in pure benzene. A significant increase in attraction is observed for acid molecules in the ferrofluid, which is probably the main reason of the loss of stability at high excess.

The work is done in the frame of the project RFBR-Helmholtz (HRJRG-016).

23PO-3-30

NUMERIC CALCULATION OF A MAGNETIZABLE ELASTIC BODY DYNAMIC IN A MAGNETIC FIELD

Zimmermann K.¹, Naletova V.A.^{2,3}, Zeidis I.¹, Turkov V.A.³, Kalmykov S.A.^{2,3}, Lukashevich M.V.³

¹Faculty of Mechanical Engineering, Technische Universitat Ilmenau, 98684, Germany

²Department of Mechanics and Mathematics, Moscow State University, Moscow, 119992, Russia

³Institute of Mechanics, Moscow State University, Michurinsky Pr. 1, Moscow, 119192, Russia

A creation of a motion using deformation of magnetizable materials in the magnetic field is a very actual problem. Such devices have some characteristics, which allow to use them in

medicine and biology. For example, it does not contain solid details contacting with a surrounding medium.

The cylindrical body made with a magnetizable polymer is considered. The body is located in a cylindrical channel. An alternate magnetic field is applied so the body moves along a channel. It was found experimentally that a motion of the elastic body in a traveling magnetic field of special structure depends on different parameters and the direction of the motion is opposite to a direction of a traveling magnetic field [1]. The static body deformation was studied and calculation of the body velocity for small magnetic field frequency was made in [2].

In the present paper the dynamic of the magnetizable elastic body in an alternate magnetic field is studied numerically. Within the frame of pin-type rod model following dynamic equations are obtained:

$$\frac{1}{\alpha} \cdot \frac{\partial \mathbf{P}}{\partial l_0} + \mathbf{K} = \rho S_w \frac{\partial^2 \mathbf{r}}{\partial t^2}, \quad (1)$$

$$\frac{1}{\alpha^4} EI \left[\frac{\partial \mathbf{r}}{\partial l_0} \times \frac{\partial^3 \mathbf{r}}{\partial l_0^3} \right] + \mathbf{K} = \frac{1}{\alpha} \left[\mathbf{P} \times \frac{\partial \mathbf{r}}{\partial l_0} \right], \quad (2)$$

$$\mathbf{P}_\tau = \frac{S_w E}{2} [\alpha^2 - 1], \quad \alpha = \frac{\partial l}{\partial l_0}, \quad S_w = \frac{S_{w0}}{\alpha}. \quad (3)$$

Here l_0 and l are lengths of a centerline of the non-deformed and deformed body (Lagrange coordinates of non-deformed and deformed body), S_{w0} is the cross-section area of the non-deformed body, $S_w(l)$ is the cross-section area of the deformed body, $\mathbf{r}(l)$ is a radius-vector (x - and y - coordinates) of a centerline, \mathbf{P} is a force of internal tension, $\mathbf{P}_\tau = (\mathbf{P} \mathbf{t})\mathbf{t}$, $\mathbf{t} = \partial \mathbf{r} / \partial l$, \mathbf{K} is a external force per unit length of body, E is the polymer Young's modulus, I is the moment of inertia of the body cross-section, ρ is the polymer density. The polymer is incompressible, $S_w dl = S_{w0} dl_0$. The external force \mathbf{K} includes the magnetic force, the gravity force, the dissipation forces and the reaction forces on the channel walls.

Calculations of a movement and deformation of a body using these equations are done for a series of bodies with different physical parameters. The numerical results are compared with the experimental data.

This work was in part supported by the Russian Foundation for Basic Research (projects 08-01-91955, 08-01-00401), DFG Zi 540-11/1 and Grant Sci.Sc.-610.2008.1.

[1] K. Zimmermann, V.A. Naletova, I. Zeidis, V.A. Turkov, M.V. Lukashevich, E. Kolev, G.V. Stepanov, *J. Magn. Magn. Mater.*, **311** (1) (2007) 450.

[2] K. Zimmermann, V.A. Naletova, I. Zeidis, V.A. Turkov, E. Kolev, S.A. Kalmykov, Calculation of a magnetizable worm deformation in a magnetic field, *Magnetohydrodynamics*, (2008) (in print).

23 June Monday

17:00-19:00

poster session

23PO-4

**“Spintronics and
Magnetotransport”**

23PO-4-1

DYNAMICAL MAGNETIC EQUATIONS AND SPIN RELAXATION PROCESSES IN COMPLEX MAGNETIC SYSTEMS

Kuzemsky A.L.

Joint Institute for Nuclear Research, 141980 Dubna, Moscow Reg., Russia

The fundamental properties of magnetization dynamics, magnetization magnitude conservation, energy balance, etc., are of great importance for characterization of a magnetic material. Magnetic dynamics is usually described both the Landau-Lifshitz (LL) and Landau-Lifshitz-Gilbert (LLG) equations. It should be noted that these equations are merely phenomenological equations, which were used to explain the time decay of the average magnetization. Spintronic devices have peculiar properties of great technological promise, but exhibit many complicated problems of fundamental and applied character. One of the main fundamental problems in the theoretical description of various spintronic phenomena is their inherent nonequilibrium nature. The main examples are the current-induced magnetization reversal and domain wall motion. Moreover, there are some evidences that the conventional micromagnetic approach may not be valid for higher temperatures. Thus a successive theory of spin transport and spin relaxation processes in magnetic systems, constructed in a general statistical-mechanical way is highly desirable. To elucidate the nature of transport and relaxation processes in spin systems, in papers [1,2] the generalized kinetic equations for magnons and general transport and evolution equations for spins in solids were derived within the method of the nonequilibrium statistical operator (NSO) [3]. This theory permits one to analyse relaxation dynamics and spin diffusion in various spin subsystems. In the present work, these results were extended to describe the relaxation dynamics and spin transport in relevant complex magnetic systems, having in mind the spintronic devices. The aim was to formulate a successive and coherent microscopic description of the magnetic relaxation dynamics. The approach is general, and is based on a previously developed statistical-mechanical theory [3]. The emphasis was on suitable definition of the local magnetization density $M(\mathbf{r})$, i.e. the expectation value of the magnetic moment per unit volume due to the spins (and orbital) motion of unpaired electrons averaged over a few lattice cells. The number of cells must be selected in such a way that it will permits one to smooth out microscopic fluctuations in the magnitude and orientation of the magnetization field at an atomic level. From the other hand, the number of cells must be small enough to avoid smearing out the complicated domain structure. On the basis of the dynamical equations derived in the framework of this approach, the problem of dissipative magnetization dynamics was discussed approximately. It is known that for the semiclassical dynamical description of damped gyromagnetic precession the LL and LLG equations can be used. The aim was to clarify the complicated question of whether Landau-Lifshitz (LL) damping or Gilbert (G) damping provides the more suitable physical picture. The discussion of certain physically relevant cases, where this theory can be applied, was given. The possibility of the generalisation of the present approach for studying of the spin transport in fluid suspensions of magnetic particles was discussed briefly.

[1] A.L. Kuzemsky, *Int.J. Mod. Phys.*, B19 (2005) 1029.

[2] A.L. Kuzemsky, *J. Low Temp. Phys.*, 143 (2006) 213.

[3] A.L. Kuzemsky, *Int.J. Mod. Phys.*, B21 (2007) 2821.

23PO-4-2

SPINTRONICS IN ANTIFERROMAGNETS: PHENOMENA INDUCED BY SPIN-POLARISED CURRENT

Gomonay H., Loktev V.

National Technical University of Ukraine "KPI", 37, ave Peremogy, Kyiv, 03056, Ukraine

The phenomenon of spin torque transfer from a hard to free ferromagnetic layer predicted by Slonczewski and Berger [1] is widely used in the present-day data storage devices. The transferred spin-torque can induce magnetization switching, stable precession of magnetization or even generation of spin-waves. Recent experiments [2,3] show that the analogous effects may also take place in antiferromagnetic (AFM) materials. In the present paper we study theoretically the influence of spin-polarised current on the dynamics and equilibrium states of thin AFM layer.

Our model is based on the following assumptions: *i*) magnetic structure of AFM can be adequately described in terms of macroscopic vectors of sublattice magnetizations \mathbf{S}_j ($j=1, 2, \dots, n$) mutual orientation of which is kept fixed due to the strong exchange coupling; *ii*) spin-torque is transferred to each of sublattice magnetizations independently.

The dynamics of AFM in the presence of spin-polarised current is thus described on the basis of the Landau-Lifshitz-Gilbert equations for each of sublattice magnetizations \mathbf{S}_j supplemented with the Slonczewski term for spin torque $\mathbf{T}_j = \sigma I \mathbf{S}_j \times (\mathbf{S}_j \times \mathbf{p}_{\text{curr}}) / S_0$, where \mathbf{p}_{curr} is the unit vector parallel to spin-polarization, I is electric current flowing through the AFM layer, constant σ is proportional to the spin-transfer efficiency, $S_0 = |\mathbf{S}_j|$, ($j=1, 2, \dots, n$).

Analysis of the dynamic equations shows that the spin-polarised current may induce *i*) reorientation (spin-flop) of AFM vectors; *ii*) stable precession of AFM vectors (in steady current); *iii*) parametric downconversion in the presence of ac current; *iv*) shift of the eigenfrequencies of spin waves. In contrast to ferromagnets, characteristic value of critical current at which the switching between the different dynamic regimes takes place depends upon anisotropy of magnetic interactions and is comparable or smaller than that in typical ferromagnets. In the collinear AFMs dissipation of current transferred energy is possible only through the circular polarised spin waves. In the linearly polarised excitations pumping and dumping of oscillations in different sublattices is compensated exactly.

We discuss application of the developed model to the metallic AFMs like FeMn and Mn_3NiN .

[1] J. C. Slonczewski, *JMMM*, **159** (1996) L1; L. Berger, *Phys. Rev. B* **54**, (1996) 9353.

[2] Z. Wei, A. Sharma, A. S. Nunez, *et al*, *Phys. Rev. Lett.*, **98** (2007) 116603

[3] S. Urazhdin, N. Anthony, *Phys. Rev. Lett.*, **99** (2007) 046602.

[4] Yu. V. Gulyaev, P. E. Zil'berman, E. M. Epshtein, *JETP Lett.*, **84** (2006) 34.4.

23PO-4-3

SPIN CONTROLLED CHARGE TRANSPORT IN DISORDERED MEDIA

Bozhko A.D.¹, Demishev S.V.¹, Glushkov V.V.¹, Kataeva E.A.¹, Sluchanko N.E.¹, Lyapin A.G.²

¹A.M.Prokhorov General Physics Institute of RAS, 38, Vavilov str., 119991 Moscow, Russia

²Institute for High Pressure Physics of RAS, 142190 Troitsk, Moscow Region, Russia

The transport in disordered solids occurring via hopping between localized states is not generally recognized as a spin controlled process. In the present work we provide both theoretical and experimental arguments that even in non-magnetic materials the spin degree of freedom defines the process of the charge transfer for the hopping conductivity (HC) in magnetic field. This circumstance opens new opportunities for creating materials prospective for the spintronic applications.

First of all, it is possible to show [1] that the accounting of the spin effects in HC in the frame of the known Zeeman mechanism [2] fails and provides incorrect description of the experimental data. We argue that the correct approach can be obtained in a recently developed spin polarization (SP) theory [1,3], which is based on the separate treatment of the spin and orbital degrees of freedom in HC process. According to [1,3], just the polarization of the spin part of the wave function controls the probabilities of the hops between the single and double occupied localized states and, moreover, the spin polarization process can be treated as in the S=1/2 paramagnet.

The fingerprint of the SP mechanism is the universal scaling of the magnetoresistance: $\ln[\rho(H)/\rho(0)] = \xi_c \cdot F(x)$ (here

$\xi_c = (T_0/T)^\alpha$ defines resistivity in zero field, $\ln \rho \sim \xi_c$, and scaling parameter is $x = \mu^* H / k_B T$).

However, in general case the SP effects coexist with the ordinary shrinkage of the wave function in magnetic field, which may mask the spin dependent HC transport [1]. Nevertheless, it is found that in disordered media prepared of a mixture of fullerenes C_{2N} under high pressure [4] the SP mechanism of magnetoresistance dominates whereas the shrinkage effects are negligible. This is proven by validity of the scaling relation expected in the SP theory (fig. 1). Interesting, that taking into account the analytical expression for $F(x)$ [1] it is possible to describe well the experimental data (solid line in fig. 1) and show that an effective magnetic moment of electron in non-magnetic carbon-based disordered media surprisingly becomes renormalized: $\mu^* \sim (0.7 - 0.8)\mu_B$. In conclusion, we discuss a possible way of creation of the HC systems with the SP colossal magnetoresistance.

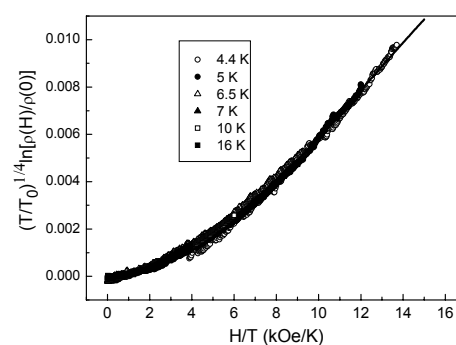


Fig. 1 The SP scaling for the HC with $\alpha=1/4$ in a C_{2N} sample

Support from the program of RAS “Quantum macrophysics” is acknowledged.

[1] S.V. Demishev, A.A. Pronin, *Phys. Solid State*, **48** (2006) 1363

[2] K. A. Matveev, L. I. Glazman, et al., *Phys. Rev. B* **52** (1995) 5289.

[3] S.V. Demishev, A.D. Bozhko, *Fiz. Tv. Tela*, (2008), *in press*

[4] A.A. Pronin, V.V. Glushkov, et al., *Phys. Solid State*, **49** (2007) 1403

23PO-4-4

A FUNDAMENTAL RELATIONSHIP BETWEEN HYSTERETIC RESPONSES OF MAGNETIZATION AND RESISTIVITY IN HALF-METALLIC FERROMAGNETS

Krivoruchko V.N.¹, Revenko Yu.F.¹, Melikhov Y.², Jiles D.C.²

¹Donetsk Physics & Technology Institute, NASU, 72 R. Luxemburg Str.,
Donetsk 83114, Ukraine

²Wolfson Centre for Magnetism, Cardiff University, Newport Rd.,
Cardiff, CF24 3AA, Wales, U.K.

Half-metallic ferromagnets (HMFs) are magnetic metals with an unusual band structure due to which electrons (or holes) with spin, for example, parallel to magnetization are conducting while charge carriers with the opposed spin direction are localized. Thanks to this fact, the charge carrier probes the magnetisation on a very short length scale (that is typically the distance of about a lattice parameter). In the report, we argue for some *fundamental relationships* between *magnetization hysteresis* and *magnetoconductivity hysteresis* for HMFs. The magnetoresistance – that is the dependence of resistance on magnetic field – is described in terms of the system evolution through a sequence of Barkhausen-like jumps to localized free energy minima. Within this model, both the magnetization hysteresis and resistivity hysteresis of HMFs can be described with a few simple assumptions common to description of hysteresis phenomena [1]. Some of the analytical relations between magnetization $M(H)$ and magnetoresistance which are observed experimentally have been found. Specifically, in the case of low magnetic disorder (high-field limit with $M \rightarrow M_S$, M_S is a saturation magnetization), the following expression for an “irreversible” conductivity has been obtained: $\sigma_{irr}(H) \sim \exp[M(H)/M_S]$. In the limit of strong magnetic disorder (low-field limit with $M_S \gg M \rightarrow 0$), calculations lead to the following relation between magnetization hysteresis $M(H)$ and conductivity hysteresis $\sigma(H)$: $\sigma_{irr}(H) \sim (M(H)/M_S)^2$. Indeed, the data obtained on a series of manganites oxides demonstrate that the electric resistivity and the magnetization can be described by these relationships [2].

For the external work performed on the system due to an infinitesimal transformation dM , we have $\delta W = \mu_0 H dM + d\sigma(|M|)/dM E^2 dM$, where M varies at constant temperature T and electrical field E , μ_0 is the Bohr magneton and the second term describes the work by electric current due to variation of conductivity. For the internal entropy production we obtain:

$$T \delta S_i = 2\mu_0 M_s \int_0^\infty dh_c h_c P(h_c, b(h_c)) |\delta b(h_c)| + E^2 \int_0^\infty dh_c [2M_s \frac{d}{dM} \sigma(|M|)] P(h_c, b(h_c)) |\delta b(h_c)|, \quad (1)$$

and for the system free energy we can write: $F = F_{MF} + 2\mu_0 M_s \int_0^\infty dh_c \int_0^{b(h_c)} h_i P(h_c, h_i) dh_i$. Here $P(h_c, h_i)$

is a probability distribution function, which describes the density of the elementary hysterons which have switching fields h_c and h_i ; F_{MF} describes reversible mean-field effects; $b(h_c)$ represents a given field history [1]. Eq. (1) generalises Eq. (4) of Ref. [3] for the entropy production on the case when work variables are not conjugate ones. The results obtained support the fundamental postulate for a description of hysteretic phenomena of the existence of the distribution which determines in what proportion the work performed by external sources will be subdivided into heat in a Barkhausen event, and will be stored reversibly in such an event.

[1] G. Bertotti, *Hysteresis in Magnetism* (NY: Academic, 1998).

[2] M. B. Salamon, M. Jaime, *Rev. Mod. Phys.*, **73**, 583 (2001).

[3] G. Bertotti, Phys. Rev. Lett. **76**, 1739 (1996).

23PO-4-5

**ANOMALIES OF TEMPERATURE–CONCENTRATION DEPENDENCE
OF ELECTRICAL RESISTANCE
OF AN ORDERING $\text{Fe}_{1-c}\text{Co}_c$ ALLOY BASED ON A B.C.C. LATTICE**

Repetsky S.P.¹, Melnyk I.M.¹, Tatarenko V.A.^{1,2}, Len E.G.², Vyshivanaya I.G.¹

¹Taras Shevchenko Kyiv National University, Physics Department, Functional-Materials Physics
Chair, 2 Academician Glushkov Prosp., 03680 Kyiv, Ukraine

²G. V. Kurdyumov Institute for Metal Physics, N.A.S.U. Department of Solid State Theory,
36 Academician Vernadsky Blvd., 03680 Kyiv-142, Ukraine

A theory of energy spectrum and electrical conductivity of ordered magnetic alloys is developed as applied to the b.c.c.-Fe–Co alloy with different concentrations of Co, c . The theory is based on the cluster expansion for one- and two-particle Green's functions of an ordered magnetic alloy without a long-range atomic order (after the quenching from high temperatures) that allows to take into account the electron scattering on the potentials of ions and fluctuations of both the spin and charge densities of electrons of an alloy at issue. The causes of predicted nonmonotonic temperature dependence of electrical resistance of the quenched alloy are governed by the presence of a quasi-gap in the electron-energy spectrum. Such a quasi-gap appears because of strong correlations between electrons in conditions of their Coulomb repulsion depending on the mutual orientation of their spins (*viz* magnetic moments localized on atoms at sites of a b.c.c. lattice) and due to the developed short-range order of substitutional atoms. As known, the temperature dependence of electrical resistance is conditioned not only by the change of the electron relaxation time but also by the change of the energy spectrum because of the electron scattering by thermal vibrations of a lattice. In consequence of decreasing of the electron-subsystem relaxation time over the electron scattering by lattice vibrations, the electrical conductivity decreases at temperature rise on condition that the energy spectrum is unchanged. On the other hand, as revealed, the electron scattering by lattice vibrations leads to the effect of the energy quasi-gap 'tailing'. The mentioned effect leads to the increase of electron density of states at the Fermi level if the Fermi level is within the quasi-gap interval. The contrary dependence of increasing electrical conductivity with temperature rise takes place at the dominating contribution of the indicated factor. (In the general case, predominance of one or another factor of influence on electrical conductivity is determined by the electronic and atomic structures of an alloy.) As shown, the well-known relatively-weak dependence of electrical resistance of quenched $\text{Fe}_{1-c}\text{Co}_c$ alloys (for different c) on the temperature within the range from 0 K to 300 K may be explained on the basis of calculations by the compensation of an action of indicated factors of the temperature influence on both the relaxation time and the energy spectrum of electrons.

23PO-4-6

HALL EFFECT IN HOB₁₂

Sluchanko N.E.¹, Sluchanko D.N.¹, Glushkov V.V.¹, Demishev S.V.¹, Shitsevalova N.Yu.²

¹A.M. Prokhorov General Physics Institute of RAS, 38, Vavilov str., Moscow, 119991, Russia

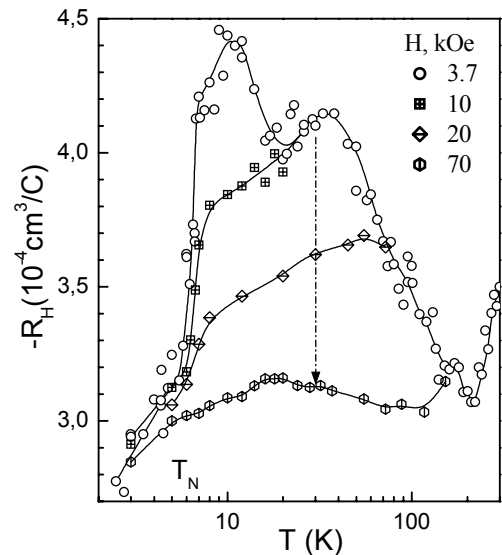
²Institute for Problems of Materials Science of NASU, 3, Krzhizhanovsky str.,
Kiev, 03680, Ukraine

The rare earth (RE) and transition metal dodecaborides RB₁₂ demonstrate a variety of physical properties and ground states, among them are the antiferromagnetic (AF) metals with incommensurate magnetic structure (TbB₁₂-TmB₁₂), paramagnetic insulator YbB₁₂ with homogeneous intermediate valence of Yb ion and superconductors (YB₁₂, ZrB₁₂ and LuB₁₂). For RE dodecaborides in vicinity of mixed valence compound YbB₁₂ an anomalous behaviour of charge carriers' mobility $\mu_H(n_{4f})$ (n_{4f} is the filling factor of $4f$ shell) has been deduced from the Hall effect measurements [1] with very unusual drastic decrease of $\mu_H(n_{4f})$ in the filling number range $10 \leq n_{4f} \leq 13$ between HoB₁₂ and YbB₁₂. The enhancement of magnetic scattering with n_{4f} contradicts obviously to the monotonous diminishing of the de-Gennes' factor

$G(n_{4f}) = (g-1)^2 J(J+1)$ to the end of the RE series and has been interpreted in [1] in terms of gradual intensification of spin and charge fluctuations from HoB₁₂ to YbB₁₂.

To verify the role of spin fluctuations in the Hall effect of the RB₁₂ a high precision measurements of angular, temperature and magnetic field dependences of the Hall resistivity $\rho_H(\varphi, T, H)$ have been undertaken in present study for HoB₁₂ compound with Neel temperature $T_N \approx 7.4$ K and complicated H - T magnetic phase diagram [2].

The study was carried out within a wide temperature range of 1.8-300K in high magnetic fields up to 80 kOe. The temperature dependences of the Hall coefficient $R_H(T)$ (Figure) were deduced from the $\rho_H(\varphi, T, H)$ data obtained by rotating the sample in the magnetic fields $H_0 = 3.7, 10, 20$ and 80 kOe. The results presented on Figure demonstrate negative values of $R_H(T)$ with noticeable anomalies at 30 K, 12 K and T_N which depressed evidently by applied magnetic field. Analysis of the data obtained allowed us to separate normal and anomalous contributions to the Hall effect and to conclude in favor of $5d$ -state magnetic polarization (the spin-polaron effect) in paramagnetic and AF-phases of HoB₁₂.



Support by the RAS Program "Strongly Correlated Electrons in Semiconductors, Metals, Superconductors and Magnetic materials" and RFBR is acknowledged.

[1] N.E. Sluchanko et al., phys. stat. sol. (b), **243** (2006) R63.

[2] K. Siemensmeyer et al., J. Low Temp. Phys., **146** (2007) 581.

23PO-4-7

CROSSOVER IN MAGNETORESISTANCE OF RB₁₂

Sluchanko N.E.¹, Sluchanko D.N.¹, Bogach A.V.¹, Glushkov V.V.¹, Demishev S.V.¹,
Shitsevalova N.Yu.², Flachbart K.³

¹A.M. Prokhorov General Physics Institute of RAS, 38, Vavilov str., Moscow, 119991, Russia

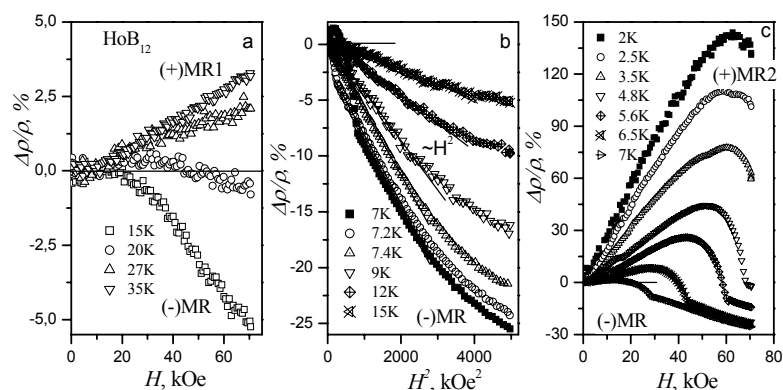
²Institute for Problems of Materials Science of NASU, 3, Krzhizhanovskiy str.,
Kiev, 03680, Ukraine

³Center of Low Temperature Physics, IEP SAS, 04001 Košice, Slovakia

B₁₂ - cluster compounds have attracted considerable interest in recent years due to the unique combination of their physical properties, such as high melting point, hardness, thermal and chemical stability, and rich magnetic properties. Among them, the rare earth dodecaborides RB₁₂ (R-Tb, Dy, Ho, Er, Tm) are metals which order antiferromagnetically (AF) and monotonous decrease of the Neel temperature (T_N) is observed along the RB₁₂ series with a filling of the 4*f* shell of rare earth ions.

To shed more light on the charge scattering mechanisms in paramagnetic and AF phases of these compounds the transverse magnetoresistance (MR) measurements have been carried out in this study on single crystalline samples of RB₁₂ (Ho and Er) at helium and intermediate temperatures (1.8-80K) in magnetic fields up to 70 kOe. As a nonmagnetic reference compound lutetium dodecaboride LuB₁₂ was also investigated. The example of the data obtained for HoB₁₂ is shown in Figure.

It was established evidently that the only regime of positive magnetoresistance (+MR) is observed for nonmagnetic LuB₁₂ that may be described by semi-empirical Koler relation $\Delta\rho/\rho=f(\rho(0,300K)H/\rho(0,T))$. For the magnetic RB₁₂ (R-Ho, Er) three different regimes of MR behavior have been found: (i) at



$T > 20K$ magnetoresistance is small, positive (+MR1) (Fig.a) and similar to that one observed for LuB₁₂, (ii) in the range of temperatures $T_N \leq T \leq 15K$ above the magnetic phase transition the magnetoresistance becomes negative (-MR) and it demonstrates quadratic dependence $\Delta\rho/\rho \sim H^2$ with the tendency to saturation in strong magnetic fields (Fig.b) and, then, (iii) in AF phase at $T < T_N$ a crossover to large positive MR (+MR2 on Fig.c) is observed. It was shown that the above mentioned negative contribution (-)MR can be interpreted quantitatively in the framework of Yosida model [1]. Moreover, the results of the magnetoresistance measurements have allowed us to find new details and reconstruct the magnetic H - T phase diagrams of HoB₁₂ and ErB₁₂.

Support by the RAS Program “Strongly Correlated Electrons in Semiconductors, Metals, Superconductors and Magnetic materials” and RFBR is acknowledged.

[1] K. Yosida, Phys. Rev. , **107** (1957) 396.

23PO-4-8

REALIZATION OF TWO INPUT LOGIC GATES WITH MAGNETIC RESONANT TUNNELING DIODES

Sarkar D.

Department of Electronics Engineering, ISM University, Dhanbad, India

Aggressive downscaling of device dimensions has led to dramatic increase in the computing power of modern computers [1]. However, this method is approaching its physical limitations [2]. Thus novel alternate technologies need to be explored for future computers. Spintronics devices have the features of faster computing, higher integration density with low heat dissipation. In this paper a novel technique has been proposed for the implementation of the spintronics 2-input logic gates using the concept of magnetic resonant tunneling diode [3]. By changing the width (W) of the quantum well (QW), the position of the quantized energy levels can be controlled. Both the QW and the injector are made of dilute magnetic semiconductor (DMS) which exhibit giant Zeeman splitting on application of magnetic field. Two separately controllable fields are used for the two regions. The field in the injector region is to be kept ON always at a fixed value to give a constant desired splitting of the energy levels (E_{dn}, E_{up}) between the down and up spin electrons, while the field in the QW is switched on and off and it acts as one of the input bits. A gate is provided around the QW region so that shifting of the quantized energy levels in the well is possible by application of proper gate bias which acts as the second input bit. The spin of the electron is taken to be the output bit. Here the principle of operation of an AND and an OR gate has been elaborated.

For realization of AND gate the device structure parameters (W and manganese concentration (x) in DMS) are chosen in such way that E_{dn} is aligned with E_0 , thus we get spin down electrons (S=0) at zero magnetic field ($C_0 = 0$) and zero gate bias ($C_1 = 0$). Now application of magnetic field ($C_0 = 1$) splits the energy sub-bands and aligns E_{2dn} with E_{dn} and application of proper gate bias ($C_1 = 1$) lowers E_1 and brings it to the same level as E_{dn} . In both the cases we get spin down electrons (S=0) at output. When $C_0 = 1$ and $C_1 = 1$, none of the levels in the QW are aligned with E_{dn} , but E_{2up} aligns with E_{up} (The well is designed such that after lowering of E_2 due to gate bias and its upward movement due to Zeeman splitting, E_{2up} aligns with E_{up}). Therefore, spin up electrons (S=1) are obtained at the output. Thus we find that an AND gate is implemented. In my design, I have chosen $W=30\text{nm}$, $x= 15.8\%$ and constant magnetic field (B') of 5T at the injector and the gap between gate and QW (t_{gap}) being 190nm. $B=0$ ($C_0 = 0$), $B= 8\text{T}$ ($C_0 = 1$) and $V_g = 0$ ($C_1 = 0$), $V_g = 1.4\text{V}$ ($C_1 = 1$).

For realization of OR gate, E_{dn} is made to align with E_0 just as was the case for AND gate, thus S=0 when $C_0 = 0$ and $C_1 = 0$. Application of magnetic field ($C_0 = 1$) aligns E_{1up} with E_{up} and application of proper gate bias ($C_1 = 1$) lowers E_3 to E_{up} , thus we get spin up electrons (S=1) at output. On application of both magnetic field

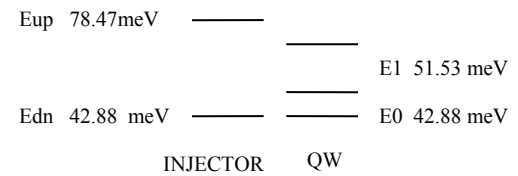


Fig . 1 Energy band diagram for implementation of AND

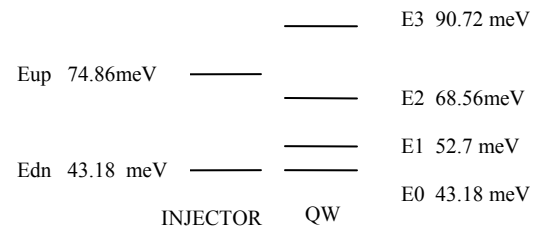


Fig . 2 Energy band diagram for implementation of AND

and gate voltage ($C_0=1$, $C_1=1$), E_{2up} aligns with E_{up} and thus again $S=1$. For the above purposes to be served, I have chosen $W=28.5\text{nm}$, $x=16\%$, $B'=4\text{T}$ and $t_{gap}=40\text{nm}$.

In conclusion it can be said that, by properly choosing the width of the QW, the Mn concentration in the DMS, the fixed magnetic field and the gap between gate and QW, the positions of spin up and down levels in the injector and the quantized levels in the well can be accurately controlled. Thus any logic function with two bit input can be realized with the help of magnetic RTD by proper control of these parameters.

[1] R.R. Schaller, "Moore's law :past, present and future", IEEE Spectr., vol. 34, no.6, pp. 52–59, Jun.1997.

[2] M. Schulz, "The end of the road for silicon?", Nature, vol. 399, pp. 729–730, Jun.1999]

[3] A. Slobodskyy, C. Gould, T. Slobodskyy, C.R. Becker, G. Schmidt, and L.W. Molenkamp, Phys. Rev. Lett., 90, 246601 (2003)

23PO-4-9

HIGH FIELD MAGNETORESISTANCE BEHAVIOR IN PrB_6 AND NdB_6

Anisimov M.¹, Glushkov V.², Demishev S.², Samarin N.², Shitsevalova N.³, Sluchanko N.²

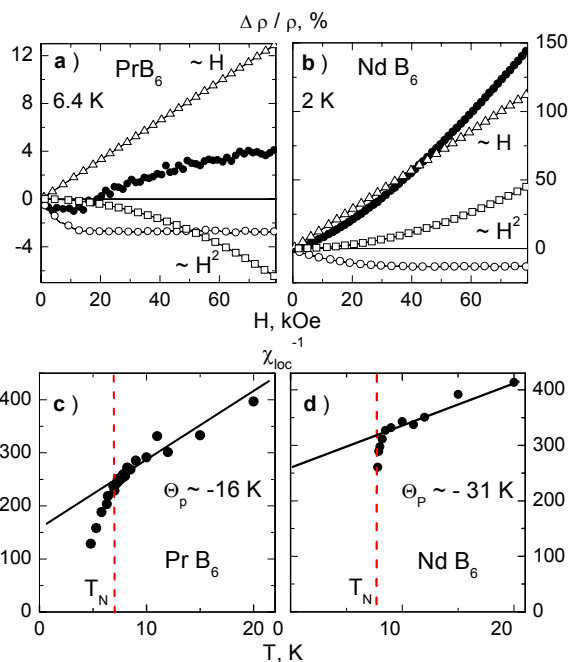
¹Moscow Institute of Physics and Technology, Institutskii street, 9, Dolgoprudnii, Moscow Region, 141700, Russia

²Low Temperatures and Cryogenic Engineering Department, A.M. Prokhorov General Physics Institute of Russian Academy of Science, Vavilov street, 38, 119991, GSP-1, Moscow, Russia

³Department of Refractory Materials, Institute for Problems of Material Science of Ukrainian National Academy of Science, Krzhizhanovskii street, 3, 03680, Kiev, Ukraine

Due to their simple cubic structure the rare-earth hexaborides (RB_6) are the convenient model objects for studying the nature of magnetic interactions which strongly influenced by electron correlations in these compounds. For instance, the variation of 4f shell occupation of the light hexaborides ($R = \text{Pr}, \text{Nd}$) results to the increase of antiferromagnetic (AF) ordering temperature: from $T_N \sim 7.0\text{K}$ (PrB_6) to $T_N \sim 7.8\text{K}$ (NdB_6) [1]. The increase of T_N is accompanied by the depression of the incommensurate (IC) magnetic state detected in PrB_6 in the interval $4.2\text{K} < T < T_N$. Note that the genesis of the intermediate phase in PrB_6 is still the subject of discussion [2].

To obtain more information about the paramagnetic and AF- phases in PrB_6 and NdB_6 the comprehensive study of low temperature magnetoresistance (MR) has been carried out on PrB_6 and NdB_6 single crystals in the wide range of temperatures (2-20K) and magnetic fields (up to 8T). The negative $\Delta\rho/\rho$ was found in the paramagnetic state at $T > T_N$ for both compounds. The analysis of the experimental data allows us to establish three contributions to MR (see Fig. a, b). In addition to the main Brillouin type



component $\Delta\rho/\rho \sim M^2 \sim H^2$ that can be interpreted in the framework of Yosida theory [3] both the linear (2) ($\sim H$) and nonlinear (3) magnetic contributions were also deduced. According to the conclusions of [4] where these contributions were naturally interpreted for CeAl_2 in terms of spin-polaron model, the last one component should be ascribed to the ferromagnetic (FM) nanodomains embedded in the metallic matrix. The estimation of local magnetic susceptibility $\chi_{\text{loc}} = (1/H(d(\Delta\rho/\rho)/dH))^{1/2}$ which was determined directly from quadratic part of negative MR reveals Curie-Weiss type behavior in paramagnetic phase with Weiss temperature $\Theta_p \sim -16\text{K}$ and -32K for PrB_6 and NdB_6 , correspondingly (Fig. c, d). The results of undertaken analysis allows to conclude in favour the concurrence between AF and FM interactions as the main reason of IC magnetic structures formation in RB_6 .

[1] Y. Onuki, A. Umezawa et al., *Phys. Rev. B*, **40** (1989) 11195.

[2] M. Sera et al., *J. Phys. Soc. Jpn.*, **73** (2004) 3422.

[3] K. Yosida, *Phys. Rev.*, **107** (1957) 396.

[4] N.E. Sluchanko et al., *JETF*, **98** (2004) 793.

23PO-4-10

ELECTRONIC STRUCTURE OF HEUSLER ALLOYS- SEMICONDUCTORS INTERFACES

Eremeev S.^{1,2}, Kulkova S.^{1,2}, Bazhanov D.³

¹Institute of Strength Physics and Materials Science SB RAS, pr. Akademicheskoy 2/1,
Tomsk 634021, Russia

²Tomsk State University, pr. Lenina 36, Tomsk, 634050, Russia

³Moscow State University, GSP-2, Leninskie Gory, Moscow, 119992, Russia

Half Heusler alloys with composition XYZ and X_2YZ were recently examined in the light of their possible spintronic applications because they behave as half-metals and, therefore, exhibit 100% spin polarization at the Fermi level (E_F). In last decade structural, electrical and magnetic properties of Heusler alloys were a focus of numerous experimental and theoretical studies. For spintronic applications, minimizing interfacial reactions and controlling the growth of Heusler alloys thin films on semiconductor substrate are very important task. In this connection the investigation of structural and magnetic properties of systems incorporating Heusler alloys are desirable. In present work we present ab-initio calculations of electronic structure and magnetic properties in the series Heusler alloys with varying of one or two components of alloy. Since the loss of half-metallicity is observed at surfaces of Heusler alloys and their interfaces with semiconductors we study also the electronic structure of low-index surfaces and (001) interfaces between NiMnZ or Co_2MnZ with $\text{InP}(001)$ and $\text{GaAs}(001)$. We also study the influence of structural defects on half-metallic behavior in the bulk, at surface and interfaces. The (001) interface between Heusler alloy and semiconductor was simulated by two models consisting of two different contacts (Fig. 1, left) and two equivalent interfaces (Fig. 1, right). The influence of tetragonal distortion of the alloy film by the semiconductor substrate was taken into account. The calculations of surface and interface ES were performed within the density functional theory in the generalized gradient approximation for the exchange-correlation functional.

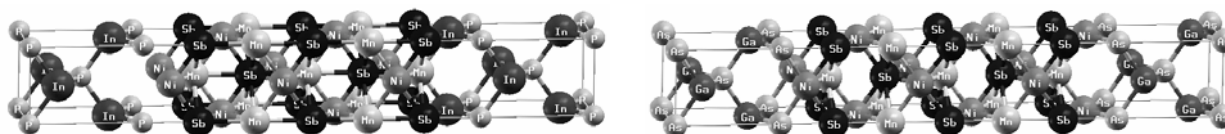


Fig. 1. Atomic structures for Ni/P and MnSb/In contacts (left) and Ni/As contact (right) in the case of NiMnSb interface with InP(001) and GaAs(001).

It was shown that in the series Co_2MnZ half-metallicity is preserved in all cases of considered defects excepting Co antisite one. In the case of MnMn termination of $\text{Co}_2\text{MnSi}(\text{Ge})(001)$ surface the well defined gap at E_F was obtained. However this surface termination with Mn antisite defect as ideal MnSi(Ge) ones does not preserved half-metallicity at the interface (001) with semiconductors. The origin of the interface states is discussed. The estimation of the spin polarization at E_F were performed for all considered contacts. It was found that in the case of NiMnSb on InP(GaAs) Ni/P(As) contacts show high degree of spin polarization of $\sim 77\%$ while the pinning of the Fermi level is observed in the cases of Ni/In and Ni/Ga. In the case of $\text{Co}_2\text{MnSi}/\text{GaAs}$ interface highest value of spin polarization was obtained for Co/As contact ($\sim 42\%$), i.e. about 70 % of electrons at E_F are of majority spin character. We demonstrate that the partial replacement of the interface Co atoms by Cu leads to sharp increase of the spin polarization up to $\sim 81\%$ for the Co/As contact. Thus, the obtained results allow us to identify the electronic origin of the interface states and to predict the interfaces with a high spin polarization at the Fermi level.

Support by RFBR (05-02-16074) is acknowledged.

23PO-4-11

X-RAY DIAGNOSTICS OF MATERIALS FOR SPINTRONICS

Likhachev I.A.¹, Pashaev E.M.¹, Chuev M.A.^{1,2}, Subbotin I.A.^{1,3}, Kvardakov V.V.¹,
Aronzon B.A.¹, Rylkov V.V.¹, Golovanov A.Ye.¹

¹Kurchatov Center for Synchrotron Radiation and Nanotechnology, Russian Research Center
“Kurchatov Institute”, Moscow, Russia

²Institute of Physics and Technology, Russian Academy of Sciences, Moscow, Russia

³Institute of Crystallography, Russian Academy of Sciences, Moscow, Russia

Studies of magnetic effects in diluted magnetic semiconductors (DMSC) containing up to 10% magnetic impurity are among the most intensively developing field in solid state physics. The major efforts in investigations of such two-dimensional DMSC structures have been naturally focused on a detection of magnetic ordering into their transport characteristics, while an essentially lower attention has been paid to studies of structural characteristics of the samples really grown, first of all, to a disorder inherent to DMSC. These materials demonstrate a number of non-trivial electronic and magnetic properties which are perspective in creating devices for magnetic writing and storage of information so that structural investigations of the materials are of special interest.

In the present contribution the results of the high-resolution X-ray diffraction and X-ray glancing-incidence mirror reflection studies of structural characteristics of the quantum-well GaAs/Ga_{1-x}In_xAs/GaAs DMSC grown by MOS CVD-hydride epitaxy are presented. A Mn δ -layer of 0.5-1.8 ML thickness has been also grown and separated the Ga_{1-x}In_xAs ($x = 0.1-0.2$) quantum well by the GaAs spacer of 3 nm optimal thickness [1]. Structural characterization of

magnetic digital alloys consisting of a periodic structure of sub-monolayers of magnetic atoms separated by semiconducting nano-thickness layers as a superlattice of Mn and GaSb layers has been also performed by the high-resolution X-ray glancing-incidence mirror reflection [2].

A detailed treatment of the experimental X-ray data has allowed us to understand non-conventional behavior of transport and magnetic characteristics of the heterostructures studied. As a result, we have found a strong correlation between structural, magnetic, electro-physical and optical properties of the DMSC systems [1] as well as shown that the electron density of the Mn-layers in digital-alloy superlattices corresponds to a mixture of Mn and GaSb into the layers, which has allowed us to estimate the diffusion depth of Mn atoms into adjacent GaSb thicker layers.

This work was financially supported by the Russian Foundation for Basic Research (grants 08-02-01462, 08-02-00719).

[1] M.A. Chuev, B.A. Aronzon, E.M. Pashaev, M.V. Kovalchuk et al. *Russian Microelectronics* **37** (2008) No. 3 (to be published)

[2]. M.A. Chuev, I.A. Subbotin, E.M. Pashaev, V.V. Kvardakov, and B.A. Aronzon. *JETP Lett.* **85** (2007) 21.

23PO-4-12

FMR STUDIES OF THIN PERMALLOY LAYERS SANDWICHED BY Cu

Hurdequint H.¹, Sergeeva N.¹, Grollier J.², Cros V.², Deranlot C.²

¹Laboratoire de Physique des Solides, UMR 8502, Université Paris-Sud, 91405 Orsay, France

²Unité Mixte de Physique CNRS/Thales and Université Paris-Sud, 91767 Palaiseau, France

Systematic investigations [1,2] of the spin resonance in magnetic films corresponding to **purely metallic** systems performed previously had revealed remarkable phenomena associated to the specific nature of the *interfacial coupling* [2] between a ferromagnetic and a normal metal. This coupling implies the **diffusion** of the microwave magnetization of the conduction electrons from one metal to the other. Recently the results of FMR studies of single permalloy (**Py**) layers sandwiched by **Ag** and by **Au** have been reported [3]. The FMR results have been systematically compared to the ones obtained on “control” **Py** layers sandwiched by **Al₂O₃** [4]. We report here and discuss the main results obtained in a systematic FMR investigation of (**Py/Cu**) films corresponding to single **Py** layers (4 different **Py** thicknesses were studied $d=3.5, 4, 7, 12$ nm) sandwiched by **Cu** and deposited by sputtering on thermally oxidized Si substrates.

We study (at X-band) the angular variation of the resonance spectrum (angle θ_H of the DC field with the film normal). We investigated, in parallel, the modifications induced on the characteristics of the FMR spectrum (lineshape, H^{res} , linewidth ΔH) by the three following effects: a short time *annealing* (at $T_{an}=150\div 180^\circ C$); the variation of the **Cu base layer thickness**; the presence of a **Ta** (10nm) *seed layer* before the growth of the **Cu** base layer.

Short time annealing. The analysis [4] of the angular variation of H^{res} of the film (sub/**Cu**(6nm)/**Py**(3.5nm)/**Cu**(6nm)) gives $H_i = 8.087 kOe$ for the total perpendicular anisotropy field which is completely dominated here by the demagnetizing field $4\pi M$. It was observed that after annealing during 5 minutes at $T_{an}=180^\circ C$ the H_i value is lower, $H_i = 6.88 kOe$. This reduction of H_i is well consistent with the observed reduction (of the same relative amplitude) of the saturation magnetization obtained by SQUID measurements.

Effect of the Cu base layer thickness. For the film (*sub/Cu(6nm)/Py(7nm)/Cu(6nm)*) the angular variation of the linewidth can be accounted for essentially in terms of the intrinsic contribution characterized by the damping parameter α . We get $\alpha = 8.5 \cdot 10^{-3}$, a value slightly larger than the one found [4] for the (*Py/Al₂O₃*) system. The results of the angular variation of the linewidth obtained for the film (*sub/Cu(50nm)/Py(7nm)/Cu(6nm)*) indicate that the quality of the *Py* layer is basically preserved for this thick *Cu* base, the inhomogeneous contribution [4] to the linewidth remaining weak.

Presence of a Ta seed layer. The following films have been studied: (*sub/Ta(10nm)/Cu(60nm)/Py(4nm)/Cu(6nm)*), (*sub/Ta(10nm)/Cu(60nm)/Py(12nm)/Cu(6nm)*). By contrast to the preceding case of films without *Ta* layer, the observed linewidth, characterized by a much larger value at maximum, is dominated by a strong inhomogeneous contribution. The principal source of inhomogeneity of the polycrystalline *Py* layer is to be associated to the dispersion of heights of the crystallites at the *Cu* base surface.

Support from the contract RTRA 2007-35 CODES is acknowledged.

- [1] H.Hurdequint, J.Magn.Magn.Mater., **93** (1991) 336.
- [2] H.Hurdequint, G.Dunifer, J.de Phys., **49** (1988) C8-1717.
- [3] H.Hurdequint, J.Magn.Magn.Mater., **310** (2007) 2061.
- [4] H.Hurdequint, J.Magn.Magn.Mater., **242-245** (2002) 521.

23PO-4-13

LOCAL FMR SPECTROSCOPY

Leksikov A., Naletov V.V., Klein O.

Service de Physique de l'Etat Condense, CEA Saclay, 91191 Gif-sur-Yvette, France

Development of innovative tools, which are capable of measuring the high frequency magnetization dynamics on nano-meter length scale, is an object of fundamental interest. In this work, we shall present how magnetic resonance force microscope (MRFM) [1-5] can be applied to perform local ferromagnetic resonance (FMR) spectroscopy of extended thin films. The MRFM technique is directly inspired from magnetic force microscopy (MFM). A soft cantilever with a magnetic tip is placed above the sample to be studied. The dipolar coupling between the tip and the sample creates a small flexion of the cantilever beam, which is detected optically by deflection of a laser beam. The pitch angle is produced by the vertical component of the force applied on the cantilever. The sample magnetization is excited by a microstrip antenna placed in its vicinity. Exciting the sample at a fixed frequency, spectroscopy is achieved by recording the cantilever motion as a function of the perpendicular dc applied field, H_{ext} , produced by an electromagnet. When an FMR resonance is excited by the antenna, the induced change ΔM_z in the longitudinal component of the magnetization (component along the precession axis) diminishes the force on the cantilever. We shall present here measurements obtained on a

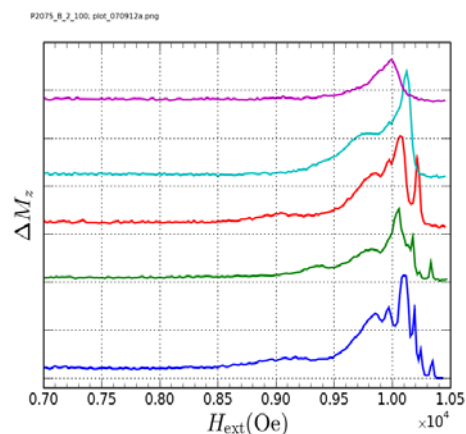


Figure.1: FMR spectrum of the extended film measured at 1.43 GHz as a function of the separation between the tip and the sample. The separation diminishes from top to bottom. The grid shows steps of about 400nm and the bottom spectrum is almost at contact.

metallic GMR multilayer stack Cu(60)/Py(30)/Cu(10)/Py(4)/Au(25), deposited on a Si substrate and whose composition consists mainly of a Permalloy bi-layer separated by a thin normal metal layer of Cu. The film is perpendicularly magnetized in the saturated state. The magnetic tip is a 1 μm FeSi_{3%} sphere glued on to the cantilever and uniformly magnetized parallel to the sample. Figure.1 shows the recorded FMR spectrum as a function of the separation between the tip and the surface. Far away from the surface, a single mode is detected at high field. The resonance position of this mode corresponds to the FMR excitation of the thick layer. The polarity of the force suggests that the induced force on the tip is repulsive during resonance (i.e. the cantilever moves up when the magnetization in the film diminishes). As the tip gets closer to the surface, new FMR modes appear and they multiply in number as the separation vanishes. These new modes are clearly induced in the vicinity of the probe and open up the possibility of a local FMR spectroscopy, which is sensitive to the local differences. We will attempt to analyze, the position, amplitude and the linewidth of these new modes.

- [1] G. de Loubens, V. Naletov, O. Klein *et al.*, *Phys. Rev. Lett.*, **98** (2007) 127601.
 [2] V. Naletov, G. de Loubens, V. Charbois, O. Klein, V. Tiberkevich, and A. Slavin, *Phys Rev. B*, **75** (2007) 140405
 [3] G. de Loubens, V. Naletov, O. Klein, *Phys. Rev. B*, **71**(2005) R180411
 [4] O. Klein, V. Charbois, V.V. Naletov *et al.*, *Phys. Rev. B*, **67** (2003) R220407
 [5] V.V. Naletov, V. Charbois, O. Klein *et al.*, *Appl. Phys. Lett.*, **83**(2003) 3132

23PO-4-14

MACROSPIN AND MICROMAGNETIC APPROACHES FOR SIMULATION OF MAGNETIC DYNAMICS EXCITED BY THE SPIN TORQUE EFFECTS IN LAYERED MAGNETIC NANOSTRUCTURES

Chinenkov M.Yu.^{1,3}, Khvalkovskiy A.V.², Popkov A.F.^{1,3}, Zvezdin K.A.², Zvezdin A.K.²

¹F.V. Lukin State Scientific-Research Institute of Physical Problems, 103460, Moscow, Russia

²A.M. Prokhorov General Physics Institute of RAS, 119991, Moscow, Russia;

³Moscow Institute of Electronic Technology, 124498, Moscow, Russia

Numerical investigation of excitation of magnetic nanostructures by spin transfer effect is very important in view of recent experimental results [1]. In such numerical studies a macrospin approach which is a one-domain single spin approximation is widely used. This approach is rigorously true for very small lateral sizes of the structure. In this view it is of vital importance to make a comparison of the results of numerical simulations for macrospin approach and full scale micromagnetic simulations. We analyze spin dynamics by solving within the macrospin and micromagnetic approaches the Landau-Lifshitz equations that includes the additional term due to the spin current [2] for a spin-valve nanopillar structure with one unpinning magnetic layer:

$$\frac{d\mathbf{M}}{dt} = -\gamma[\mathbf{M} \times \mathbf{H}_{eff}] - \gamma JG[\mathbf{M} \times [\mathbf{s} \times \mathbf{M}]] + \frac{\alpha}{M}[\mathbf{M} \times \frac{d\mathbf{M}}{dt}]$$

For the macrospin model we have made a bifurcation analysis of spin dynamics equations in the phase space of the dynamical system using qualitative and numerical calculations. Micromagnetic simulations were performed using the solver SpinPM. An example of current-field diagram of steady spin states got within two models is presented on Fig1. The main conclusions are as follows. Calculations show the first excited mode (for not very values of the external magnetic field and spin polarized current) is a uniform mode that may be present in the macrospin simulations.

However at larger field and currents non-uniform modes are excited. At even larger currents many modes may be excited simultaneously that leads to quasi-chaotic oscillations. Such excitations present for even very small samples may not be got by macrospin approach. Particular very-non-uniform modes such as vortex motion and auto-oscillations of domain walls are also observed. Spin precession modes and their frequency change with the current variation are calculated. We hope that carried out analysis may be helpful in the comparison of theoretical investigations with experimental results and their understanding. They are important also for design nano-scale voltage generators, working in Ghz frequency scale [3].

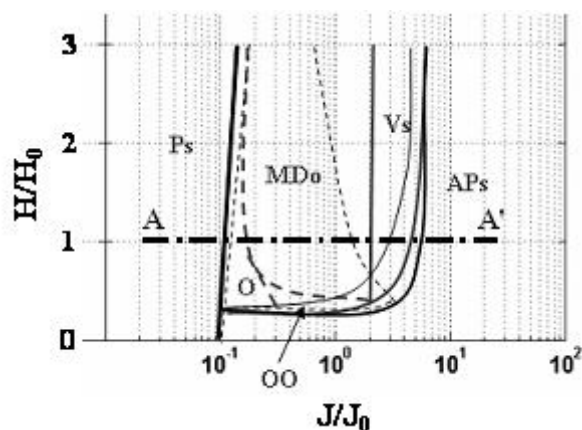


Fig.1 Phase diagramm

Steady states: Ps - parallel, APs - antiparallel, Vs - vertical, O – light-amplitude precession, OO – strong-amplitude precession, MDo – multi-domain precession.

The work is supported by RFBR (grants № № 07-02-91589, 06-02-08028)

- [1] S. I. Kiselev, J. C. Sankey, I.N. Krivorotov, N.C. Emley, R.J. Schoelkopf, R. A. Buhrman, D.C. Ralph, Nature 425, 380 (2003).
- [2] J.Slonczewski, JMM159, L1-L7 (1996).
- [3] A.D.Kent, B. Ozyilmaz, and E. del. Barco, Appl. Phys. Lett. **84**, 3897 (2004).

23PO-4-15

THERMAL RELAXATION OF THE THERMO-ELECTROMOTIVE FORCE IN COMPOSITES WITH METAL NANOPARTICLES COFeB IN THE DIELECTRIC MATRIX MgO_n

Kalinin Yu., Kudrin A., Sitnikov A.

Voronezh Technical State University, Voronezh, 394026, Russia

The heat treatment effect of the concentration dependence of electrical resistivity and thermal electromotive force (e.m.f.) of the amorphous composites with metal nanoparticles CoFeB in the dielectric matrix MgO_n has been investigated. Samples of composites with a wide range of concentrations of the metal phase were obtained by ion-beam sputtering in an atmosphere of argon under pressure of 2×10^{-4} Torr. An electrical resistance was measured by amperemeter-voltmeter method. In the process of the thermal e.m.f. measurement the temperatures of the hot and cold ends of the samples were maintained in the range of $T_1 = 105 \pm 5$ °C and $T_2 = 22 \pm 2$ °C respectively. As a measuring material probes were used a silver wire with 0.6 mm diameter.

An electrical resistance dependency of the composites of the metal concentrations has the characteristic S-shaped appearance for percolation systems with the inflection point in the corresponding percolation threshold. The heat treatment of those composites, not leading to crystallization, increases the electrical resistance of alloys that are up to a percolation threshold, and reduces – over the percolation threshold. At the point of intersection of concentration

dependencies of the electrical resistance of composites in the initial and annealed state has been defined threshold leakage.

The dependence of the thermal e.m.f. of concentration of the metal phase is kind of monotone changing curve from $-5 \mu\text{V/K}$ to $-8.5 \mu\text{V/K}$. At the same time, the thermal e.m.f. absolute values for composites with concentrations up to a percolation threshold are higher than that of composites below the threshold leakage. All measured values of the thermal e.m.f. are negative, which indicates that the electric charge carriers are electrons.

An analysis of the dependency shows that the thermal annealing of amorphous composites, at temperatures not leading to the crystallization of amorphous structure, contributes to a negligible increase in the whole range of concentrations of the metal phase as the temperature processing.

Granulated nanocomposites also showed a nonlinear dependence of the thermal e.m.f. of the magnetic field.

Work is executed at financial support of the Russian Foundation for Basic Research (grants № 08-02-00840) and grant MO and CRDF (project PG 05-010-1).

23PO-4-16

AB-INITIO STUDY OF ELECTRONIC AND MAGNETIC PROPERTIES OF GASB/MN AND GAAS/MN DIGITAL HETEROSTRUCTURES

Titov A.^{1,4}, Kulatov E.¹, Uspenskii Yu.A.², Tugushev V.V.³, Michelini F.⁴, Mariette H.⁵

¹A.M. Prokhorov General Physics Institute of RAS, 38 Vavilov str. Moscow 119991, Russia

²P.N. Lebedev Physical Institute of RAS, 53 Leninskii prosp. Moscow 117924, Russia

³RRC Kurchatov Institute, Kurchatov Sqr. 1 Moscow 123182, Russia

⁴IM2NP-UMR CNRS 6242, Faculte des Sciences St.-Jerome - case 142 Marseille 13397, France

⁵Institut Neel, 25 av. des Martyrs BP 166, 38042 Grenoble cedex 9, France

Diluted magnetic semiconductors (DMS) are considered today as promising materials for spintronics. However the Curie temperature (T_C) of the semiconductors is below room temperature and this fact limits their practical application. To increase T_C one should increase concentration of magnetic impurity in host semiconductor. In DMS the concentration is limited by low solubility of magnetic impurities in these materials. This limitation can be overcome in digital heterostructures where thin layers with a high concentration of magnetic impurities are produced.

In this work digital GaSb/Mn and GaAs/Mn heterostructures are studied using *ab-initio* calculations. Electronic structure and magnetic properties of the heterostructures were calculated by the APW method implemented in the WIEN2k code [1]. Calculated electronic structures of GaSb/Mn and GaAs/Mn heterostructures are rather similar: $3d$ states of Mn (spin up) are situated deep in the valence band, below the Fermi level, and they are almost fully occupied by electrons; at the same time $3d$ states of Mn (spin down) are above the Fermi level and they are essentially empty. Such a distribution of Mn $3d$ states implies the same $2+$ state of Mn in the both materials and similar x-ray absorption properties related to empty $3d$ states of Mn.

Magnetic interaction between two Mn layers in GaSb/Mn and GaAs/Mn heterostructures as a function of interlayer distance was studied. The interlayer exchange interaction falls rapidly as the interlayer distance increases and the exchange energy become close to zero for interlayer distances larger than $2a_0$ (a_0 – lattice parameter). For smaller interlayer distances the exchange interaction is ferromagnetic and it is significantly stronger in GaSb than in GaAs for the least possible interlayer distance ($a_0/2$). Therefore GaSb semiconductor is more suitable for

heterostructures where interlayer distance is very small. This corroborate well with experimental findings of room temperature ferromagnetism in GaSb/Mn heterostructures which contain quasi-2D Mn islands [2]. In practice it is difficult to create heterostructures with a very small distance between neighbour Mn layers, so GaSb semiconductor with 3D Mn clusters can be also considered as a prospective material for room temperature applications.

Support by Russian Foundation for Basic Research (projects 07-02-01177-a, 07-02-00114-a), Department of Physical Sciences of the Russian Academy of Sciences (Program “Strongly correlated electrons in semiconductors, metals, superconductors and magnetic materials”) and French Embassy in Moscow is acknowledged.

[1] P.Blaho, K.Schwarz, G.K.H.Madsen, D.Kvasnicka, and J.Luitz, Wien2k, An Augmented Plane Wave+Local Orbitals Program for Calculating Crystal Properties (Karlheinz Schwarz, Techn. Universitat Wien, Austria, 2001), ISBN 3-9501031-1-2.

[2] B.D.McCombe, M.Na, X.Chen et al. *Physica E*, **16** (2003) 90.

23PO-4-17

MAGNETOTHERMOPOWER IN MAGNETIC NANOCOMPOSITES “AMORPHOUS FERROMAGNET $\text{Co}_{45}\text{Fe}_{45}\text{Zr}_{10}$ -AMORPHOUS DIELECTRIC Al_2O_n ”

Belousov V.¹, Granovsky A.², Kalinin Yu.¹, Sitnikov A.¹

¹Voronezh Technical State University, Voronezh, 394026, Russia

²Moscow State University, Faculty of Physics, Moscow, 119991, Russia

The concentration and temperature dependences of the resistivity, thermopower and magnetothermopower of composites containing of amorphous nanoparticles $\text{Co}_{45}\text{Fe}_{45}\text{Zr}_{10}$ embedded in the Al_2O_n dielectric matrix are investigated. Below the percolation threshold, i.e., in the tunnelling conduction region, the absolute values of the thermopower of the composites under investigation are less than those above the percolation threshold. It is revealed that, in the tunnelling conduction region, the slope of the temperature dependences of the thermopower changes at a temperature of ~ 205 K. This can indicate that the thermopower is sensitive to a change in the mechanism of conduction from the Mott law to a power relation that corresponds to the model of inelastic resonant tunnelling through a chain of localized states in the dielectric matrix.

Magnetothermopower is negative for nanocomposites fabricated with introduction of oxygen in the course of sputtering, but it is positive if nanocomposites are obtained in the atmosphere of both oxygen and argon. Our measurements lead to the following conclusions:

1. The magnetothermopower is even in $\text{Co}_x(\text{Al}_2\text{O}_n)_{100-x}$ composites, and while $\text{CoFeZr}_x(\text{Al}_2\text{O}_n)_{100-x}$ composites exhibit strong asymmetry relative to the field direction.

2. The $\text{CoFeZr}_x(\text{Al}_2\text{O}_n)_{100-x}$ composites obtained in the argon and nitrogen atmosphere also exhibit magnetothermopower; however, asymmetry to the field direction is even higher than in the composites obtained in the argon atmosphere.

3. It is shown that the developed theory of the tunnelling magnetothermopower is consistent with the obtained data. The observed asymmetric behavior of magnetothermopower in $\text{CoFeZr}_x(\text{Al}_2\text{O}_n)_{100-x}$ nanocomposites prepared in the argon or argon and nitrogen atmosphere points to the existence of anisotropy in these systems [1].

This study was partly supported by the Russian Foundation for Basic research (project . 08-02-00840).

[1] V.A. Belousov, A.B. Granovsky, Yu.E. Kalinin, and A.V. Sitnikov, *Zh. Eksp. Teor. Fiz.* **132** (6), 1393 (2007).

23PO-4-18

MAGNETIZATION DYNAMICS IN POINT CONTACTS TO SINGLE CO FILMS UNDER THE HIGH-FREQUENCY IRRADIATION

*Balkashin O.P.¹, Yanson I.K.¹, Fisun V.V.¹, Triputen L.Yu.¹
Konovalenko A.², Korenivski V.²*

¹B. Verkin Institute for Low Temperature Physics and Engineering, National Academy of Sciences of Ukraine, 61103, Kharkiv, Lenin av. 47, Ukraine

²Nanostructure Physics, Royal Institute of Technology, 10691, Stockholm, Sweden

The electric conduction of point contacts between ferromagnetic (F) Co films 5, 10 and 100 nm thick and a nonmagnetic metal (Cu, Ag) needle has been measured. The measurements were made on contacts exposed to electromagnetic microwave irradiation in the external magnetic field of different strengths and directions and on non-irradiated contacts. For the first time two basically different mechanisms of a response to high-frequency (HF) irradiation have been detected experimentally for this type of contacts. One mechanism is caused by the rectification HF alternating current and operates typically in any contact having a nonlinear I-V characteristic. The other is related to resonant excitation of various spatial modes of precession dynamics in the magnetization of the ferromagnet under the influence of the external HF field. The results obtained suggest that point contacts between a single ferromagnetic film and a nonmagnetic metal needle exhibit all the static and dynamic effects caused by the transfer of the spin moment in high-density current flows (surface spin-valve [1]) similar to the effects in spin-valve F-N-F structures.

[1] I. K. Yanson, Yu. G. Naidyuk, V. V. Fisun, A. Konovalenko , O. P. Balkashin, L. Yu. Triputen, and V. Korenivski, *Nano Letters*, **7** (2007) 927

23PO-4-19

MAGNETIC FORCE MICROSCOPY AND DECOMPOSITION OF DOMAIN-WALL MOLECULES IN NIFE NANO RINGS

Sasage K.¹, Okamoto N.¹, Tsujikawa H.², Yamaoka T.², Saitoh E.¹

¹Department of Applied Physics and Physico-Informatics, Keio University, 3-14-1 Hiyoshi, Kohoku, Yokohama, Kanagawa 223-8522, Japan

²SII NanoTechnology Inc., 2-15-5 Shintomi, Chuo, Tokyo 104-0041, Japan

Magnetic properties of nano scale magnets are actively being studied for the purpose of practical applications, such as ultra high density magnetic storage media and magnetic logic gate. In these researches, observations of nano-scale magnetization distribution are essential. Magnetic

force microscopy (MFM) is an excellent technique to measure the nano-scale magnetic structures with high spatial resolution. However, stray fields from a MFM probe often disturb the small magnetic domain structures of a sample [1], a situation which has limited the application range of MFM.

We have investigated the influence of a stray field from a MFM probe using magnetic domain walls (DWs) in a magnetic nano-ring array. The sample used in the present study is an array of a $\text{Ni}_{81}\text{Fe}_{19}$ ring with various values of the interspace distance d . The diameter, the linewidth, and the thickness of the ring are 2 μm , 160 nm, and 15 nm, respectively. The sample were fabricated by means of electron beam lithography and lift-off technique. $\text{Ni}_{81}\text{Fe}_{19}$ was deposited by electron beam evaporation in a high vacuum on a thermally oxidized Si substrate.

When a strong external magnetic field $H_{\text{ext}} = 10$ kOe is applied to a sample, the magnetization in the ring is saturated along the field. After removing the external field, the magnetization is directed along the ring due to strong magnetic-shape anisotropy, and head-to-head and tail-to-tail magnetic DWs are produced at the opposite side of each ring.

Figure 1 shows the MFM images of the sample. The bright and the dark signals represent head-to-head and tail-to-tail DWs, respectively. When $d = 320$ nm (see Fig.1 (a)), signals corresponding to the DW drag appear. This indicates that the DWs are pushed due to a stray magnetic field from the MFM probe. On the other hand, when $d = 200$ nm (see Fig. 1 (b)), no DW-drag signals were observed. This is attributed to the interaction between the head-to-head and the tail-to-tail DWs in the rings next to each other. The pinning potential due to the DW-DW magnetostatic interaction can be estimated as a function of d in terms of the micro magnetic simulation. Since the pair of the DWs are decomposed when the magnetic potential due to the stray filed from the MFM probe is greater than the pinning potential, the drag potential is estimated from the measurement.

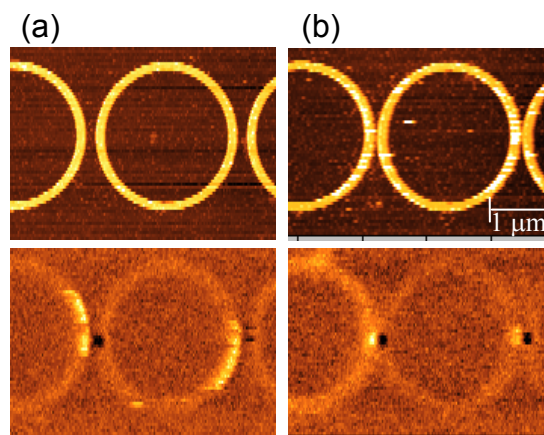


Fig. 1. MFM images of the sample.

[1] T. Yamaoka, K. Watanabe, Y. Shirakawabe, K. Chinose, E. Saitoh, H. Miyajima, *Jpn. J. Appl. Phys.*, **45** (2006) 2230.

23PO-4-20

SIMULATION OF SWITCHING AND DYNAMICS OF TOROIDAL MOMENTUM IN FERROMAGNETIC NANO-RING

Gonkov K.V., Khvalkovskiy A.V., Zvezdin K.A.

A.M. Prokhorov General Physics Institute, Vavilova str. 38, 119991 Moscow, Russia

We study the process of switching between right and left flux-closure vortex states in nano-ring (outer diameter $D=1000$ nm, inner diameter $d=800$ nm and thickness $t=2$ nm). The current-induced dynamics of magnetization was calculated by micromagnetic simulations in the framework of the Landau-Lifshitz-Gilbert (LLG) equation with a spin-transfer term and subject to magnetostatic field, exchange energy and energy of anisotropy. In our simulation the current flows through the structure of nano-ring perpendicular to its plane. It is shown, that there are notable differences in dynamics induced by nonpolarized current and dynamics induced by spin-polarized current. We also investigate the influence of different directions of current polarization on the process of switching.

Today, much attention is paid to magnetic properties and switching of ring-shaped nanomagnets [1]. This is not only due to the fact that these structures allow for the investigation of fundamental physical properties [2], but they also have important applications such as in magnetic random access memory (MRAM) cells [3]. In this letter, we study the switching of ferromagnetic nano-ring under two mechanisms permanently: under magnetic field induced by current and under spin-transfer mechanism [4]. The stable states of the studied object are flux-closure vortex states in which the total magnetic moment is zero. The aim of our research is to simulate the switching between two stable states (clockwise and counterclockwise orientation of the magnetization). Simulations were computed by solving the micromagnetic equilibrium equation for each applied field induced by current on a square mesh, with a 5 nm cell size. We use toroidal momentum calculated relative to the centre of nano-ring as a suitable quantity for description of the switching. It is shown, that toroidal momentum take on a maximum absolute value, when the studied object is in the flux-closure vortex state. Also, the switching of the nano-ring goes with the change of sign of the toroidal momentum.

In summary, we take current-induced magnetization switching loops for the nano-ring. It is shown, that the use of spin-polarized current can constitutive decrease the critical current of switching.

Support by RFBR project 07-02-91589-ASP is acknowledged.

- [1] M. Klaui et al. *J. Magn. Magn. Mater.* **272–276** (2004) 1631–1636.
 [2] L. D. Landau and E. M. Lifshitz, *Physik Z. Sowjetunion* **8**, 153 (1935).
 [3] J. G. Zhu, Y. Zheng, and G. A. Prinz, *J. Appl. Phys.* **87**, 6668 (2000).
 [4] J.C. Slonczewski. *J. Magn. Magn. Mater.* **159**, L1 (1996).

23PO-4-21

PULSED LASER DEPOSITION OF EPITAXIAL MAGNETIC THIN FILMS

Goikhman A.¹, Lebedinski Yu.¹, Zenkevich A.¹, Mantovan R.², Fanciulli M.², Chernykh P.³

¹Moscow Engineering Physics Institute (state university), 115409 Moscow, Russia

²Laboratorio Nazionale MDM CNR-INFN, Agrate Brianza (MI), Italy

³Lomonosov Moscow State University Skobeltsyn Institute of Nuclear Physics,
119991 Moscow, Russia

Magnetic tunnel junctions (MTJs) consisting of two ferromagnetic electrodes separated by an ultrathin insulating layer are promising functional structures for non-volatile storage cells in magnetic random access memories (MRAM). Up to date, the highest room-temperature tunneling magnetoresistance (TMR), i.e. the dependence of the tunnelling current on the relative orientation of the FM electrodes magnetization, have been achieved in fully epitaxial MTJs based on FM(001)/MgO(001)/FM(001) (FM=Fe, Co, CoFe) [1-3]. To get even better characteristics, the search for and the development of novel, technologically relevant thin film ferromagnetic (FM) materials as well as FM/oxide systems is of great interest.

Ferromagnetic half-metals attract special attention since they are predicted to exhibit high spin polarization values which determines the TMR of MTJ. Among those, the ferromagnetic iron silicide phase Fe₃Si with a Curie temperature of ~800 K, and in the thin film form it has a 45% spin polarization [4]. Another promising candidate with a similar Curie temperature is Fe₃O₄ (magnetite) [5], which in addition exhibits much higher coercivity (H_c~350 Oe) compared to Fe, Co, Fe₃Si (H_c~10-50 Oe), and thus can be expected to provide independent switching of FM electrodes in MTJ.

In this contribution, we report on the research efforts towards fabrication of fully epitaxial MTJs based on ferromagnetic half-metals [Fe₃Si(001)/MgO(001)/Fe₃O₄(001)] by Pulsed Laser Deposition (PLD) technique. Different approaches including the ablation of the stoichiometric Fe₃Si and Fe₃O₄ targets, the co-deposition of Fe and Si, and the deposition of Fe in the O atmosphere are used to grow epitaxial layers on MgO(001) substrate at elevated temperature. Ultrathin (~2 nm) epitaxial MgO layers as insulating barriers are successfully grown by deposition of Mg in O at low pressure ($P \sim 10^{-7}$ Torr) at room temperature. The chemical composition of the grown layers and of the forming interfaces was revealed *in situ* with x-ray photoelectron spectroscopy (XPS). Low energy ion spectroscopy (LEIS) was used also *in situ* to check the thickness uniformity and the continuity of the ultrathin MgO barrier layer. Rutherford backscattering spectrometry (RBS)/channeling technique is employed *ex situ* for structural characterization as well as to reveal the elemental composition and the thickness of the grown layers. By using enriched ⁵⁷Fe-enriched tracer layers, we perform conversion electron Mossbauer spectroscopy (CEMS) to reveal phase composition and magnetic properties of FM layers as well as at FM/MgO interface. The magnetic properties of the successfully grown epitaxial films are measured with superconducting quantum interference device (SQUID).

The preliminary results demonstrate that PLD provides a promising approach to fabricate fully epitaxial MTJ based on ferromagnetic half-metals.

- [1] S.S.P. Parkin, C. Kaiser, A. Panchula, P.M. Rice, B. Hughes, M. Samat, S. Yang, *Nature Mat.*, **3** (2004) 862.
 [2] S. Yuasa, T. Nagahama, A. Fukushima, Y. Suzuki, K. Ando, *Nature Mat.*, **3** (2004) 868.
 [3] S. Yuasa, A. Fukushima, H. Kubota, Y. Suzuki, K. Ando, *Appl.Phys.Lett.*, **89** (2006) 042505.
 [4] A. Ionescu *et al.*, *Phys. Rev. B* **71** (2005) 94401.
 [5] P. Seneor, A. Fert, J.L. Maurice, F. Montaigne, F. Petroff, A. Vaures, *Appl. Phys.Lett.* **74** (1999) 4017.

23PO-4-22

HALL EFFECT IN LaB₆ AND NdB₆

Samarin N.¹, Anisimov M.², Bogach A.¹, Glushkov V.¹,
 Demishev S.¹, Shitsevalova N.³, Sluchanko N.¹

¹Low Temperatures and Cryogenic Engineering Department,

A.M. Prokhorov General Physics Institute of RAS, 38 Vavilov str. 119991 Moscow, Russia

²Moscow Institute of Physics and Technology, 9 Institutskii str.,

Dolgoprudnii 141700 Moscow Region, Russia

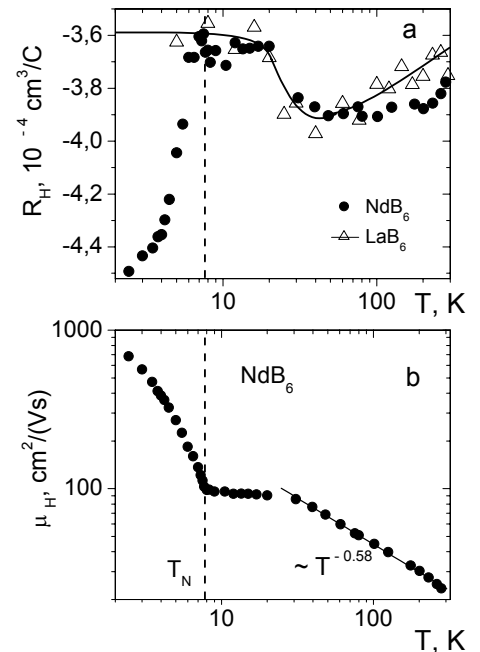
³Department of Refractory Materials, Institute for Problems of Material Science of NASU,

3 Krzhizhanovskii str. 03680 Kiev, Ukraine

It is well known that the ground state of the rare earth hexaborides (RB₆) is strongly influenced by the interaction between localized 4*f*-states and itinerant 6*s*/5*d* electrons [1-3]. For instance, CeB₆ is generally considered as a typical dense Kondo system with heavy fermions [1], the mixed valence compound SmB₆ is a narrow band semiconductor with the gap value $E_g \sim 19$ meV [2], while PrB₆ and NdB₆ are the metals with localized magnetic moments demonstrating antiferromagnetic (AFM) ordering [3]. However, the microscopic mechanisms of the strong electron correlations occurred in RB₆ are intensively discussed up to now [1-4].

To shed more light on the peculiarities of ground state formation in RB_6 the Hall effect in AFM NdB_6 and nonmagnetic LaB_6 has been investigated on the single crystals at temperatures $2\text{ K} < T < 300\text{ K}$ in magnetic fields $H < 8\text{ T}$. The Hall coefficient R_H and resistivity ρ have been measured by the sample rotation technique in fixed magnetic field to be perpendicular to the axis of rotation ($\langle 110 \rangle$ for LaB_6 and $\langle 100 \rangle$ for NdB_6). A very similar temperature behavior of $R_H(T)$ with a step-like feature at $T \sim 25\text{ K}$ (Fig. a) has been established for both AFM NdB_6 and nonmagnetic LaB_6 at intermediate temperatures $T > 10\text{ K}$. The temperature independent behavior of Hall coefficient ($R_H(LaB_6) \sim 3.58 \cdot 10^{-4}\text{ cm}^3/\text{C}$, $R_H(NdB_6) \sim 3.72 \cdot 10^{-4}\text{ cm}^3/\text{C}$) observed in the interval $10\text{ K} < T < 20\text{ K}$ (Fig. a) allowed to estimate the reduced charge carriers concentration $n \approx 1.25 - 1.3$, which differs considerably from $n \approx 1$ provided by a nominal valence of Nd ions ($v=3$) [4]. The significant decrease of Hall coefficient ($\sim 30\%$) induced by the AFM ordering [2,4] was detected for NdB_6 below $T_N = 7.7\text{ K}$ (Fig. a).

The Hall mobility $\mu_H(T) = R_H(T)/\rho(T)$ estimated for LaB_6 and NdB_6 was shown to be well fitted by the power law $\mu_H \sim T^{-\alpha}$ ($\alpha(LaB_6) \approx -1.53$, $\alpha(NdB_6) \approx -0.58$) in the range $30\text{ K} < T < 300\text{ K}$ (Fig. b). The drastic decrease of the Hall mobility μ_H and the exponent α is discussed in terms of magnetic scattering enhancement of itinerant electrons on the localized $4f$ -states of Nd ions.



The financial support from the RAS Program “Strongly Correlated Electrons” is acknowledged.

- [1] A. Takase et al., Sol. St. Commun. **36** (1980) 461.
- [2] N.E. Sluchanko et al., Phys. Rev. B **61** (2000) 9906.
- [3] Y. Onuki et al., Phys. Rev. B **40** (1989) 11195.
- [4] J. Stankiewicz et al., Phys. Rev. B **71** (2005) 134426.

23PO-4-23

HALL EFFECT AND MAGNETIC ORDERING IN RB_{12}

Baranovskiy A.E.¹, Grechnev G.E.¹, Shitsevalova N.Yu.², Sluchanko N.E.³, Sluchanko D.N.³,
Glushkov V.V.³, Demishev S.V.³, Ischenko T.V.³

¹B.Verkin Institute for Low Temperature Physics of NASU, Kharkov, 61103, Ukraine

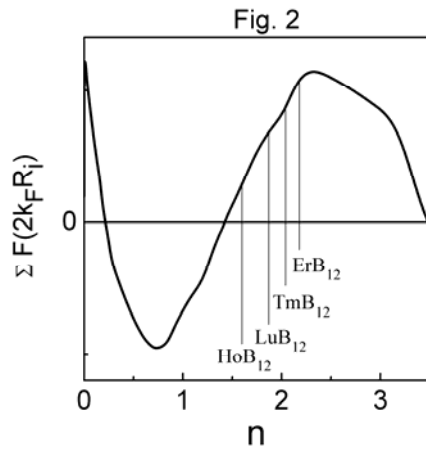
²Institute for Problems of Materials Science of NASU, Kiev, 03680, Ukraine

³A.M. Prokhorov General Physics Institute of RAS, 38, Vavilov str., Moscow, 119991, Russia

Rare earth (RE) dodecaborides RB_{12} demonstrate antiferromagnetic (AFM) ordering with complicated incommensurate magnetic structures (TbB_{12} - TmB_{12}). For the heavy RE dodecaborides, close to the Kondo insulator YbB_{12} , an anomalous behaviour of charge carriers' mobility $\mu_H(n_{4f})$ (n_{4f} is the occupation number of $4f$ shell) has been deduced from the Hall effect measurements. An unusually sharp decrease of $\mu_H(n_{4f})$ within the $4f$ -shell occupation range $10 \leq n_{4f} \leq 13$ was found in series from HoB_{12} till YbB_{12} . The expected enhancement of magnetic scattering does not fit to the monotonous diminishing of the de-Gennes' factor $G(n_{4f}) = (g-$

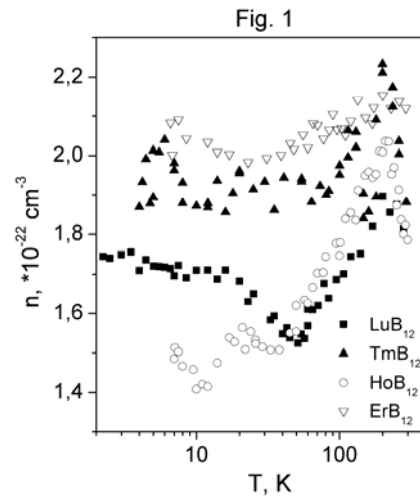
$1)^2J(J+1)$ towards the end of the RE series and can be interpreted in terms of substantial increasing of spin and charge fluctuations.

To elucidate a nature of magnetic ordering in RB_{12} the high precision measurements of the Hall resistivity $\rho_H(\varphi, T, H)$ are carried out for RB_{12} compounds HoB_{12} , ErB_{12} , TmB_{12} and LuB_{12} within a temperature range of 1.8-300 K in magnetic fields up to 80 kOe. The evaluated temperature dependences of the concentration of carriers are presented in Fig. 1



and considered as primary mediators of magnetic ordering in RB_{12} . The complementary *ab initio* electronic structure calculations have been performed for paramagnetic (PM), ferromagnetic (FM) and antiferromagnetic (AFM) phases of the RB_{12} compounds by

using FP-LMTO method. The magnetic stability of the AFM ordering in RB_{12} has been examined and confirmed within comprehensive total energy calculations for PM, FM and AFM phases. Also it is appeared in accordance with the analysis based on the RKKY model, as can be seen in Fig. 2. It is also proved, that *5d*-states of RE ions play an important role in AFM ordering via polarization with conduction *s,p*-states of RB_{12} .



Support by the RAS Program “Strongly Correlated Electrons in Semiconductors, Metals, Superconductors and Magnetic materials” and RFBR is acknowledged.

23PO-4-24

FMR STUDY OF FM/AFM STRUCTURES FOR SPINTRONICS DEVICES

Khomenko E.V.¹, Chechenin N.G.¹, Cherhykh P.N.¹, Goikhman A.Yu.², Zenkevich A.V.²

¹Skobeltsyn Inst. of Nuclear Physics, Moscow St. University, 119991 Moscow, Russia

²Moscow Engineering Physics Institute (state university), 115409 Moscow, Russia

Exchange biasing at ferromagnet (F)/antiferromagnet (AF) interface is an important physical effect which is known for more than 50 years, though not yet completely understood in spite of an evident applications in spintronics devices such as spin valves, reading heads and MRAMs. Ferromagnetic resonance (FMR) is a powerful tool for study the intrinsic magnetic properties of the materials. Here we report on FMR study of Co/IrMn and Fe/IrMn structures where IrMn AF-layer is a reasonably thermally stable due to a fairly high Neel and blocking temperatures.

The films were deposited prepared by the Pulsed Laser Deposition technique at room temperature in ultra-high vacuum (base pressure $P \sim 10^{-8}$ Torr). The thickness of ferromagnetic (F), t_F , and antiferromagnetic (AF), t_{AF} , layers varied in the range of 5 to 100 nm. Ta layers were deposited in between the substrate (Si/SiO₂) and the film, as a seed layer, and on the top of the structure as an oxidation protection layer. After the deposition the samples were annealed at the temperature $T_{ann} = 100 \div 500$ °C in Ar-atmosphere and slowly cooled in the presence of magnetic field of 1200 Oe. The FMR resonance field, H_r , absorption linewidth, ΔH_r , were analysed as a

function of t_{ATF} and t_{F} thicknesses. For the external magnetic field applied parallel to the film plane under the angle α with respect to the easy direction for FMR resonance condition in the AF/F structure with unidirectional exchange bias field at the interface, H_{EB} , and bidirectional uniaxial anisotropy field, H_{K} , we have [1]:

$$H_r = \frac{\omega^2}{4\pi M_s \gamma^2} - H_{\text{EB}} \cos \alpha - H_{\text{K}} \cos 2\alpha, \quad (1)$$

where ω is the FMR frequency, γ is the gyromagnetic constant, M_s is the saturation magnetization of the F-film. Setting $\alpha = 0^\circ$, 90° and 180° the H_{K} - and H_{EB} - fields were obtained. In the report we discuss the variation of the exchange bias field as a function of the annealing temperature, thicknesses of F- and AF- layers in comparison with published data.

Support by Russian Agency of Science and Innovation (g/k # 02.513.11.3155) is acknowledged.

[1] A. Layadi, W.C. Cain, J.-W. Lee and J.O. Artman, *IEEE Trans. Magn.* **MAG-23** (1987) 2993.

23PO-4-25

FMR STUDY OF SANDWICHED MAGNETIC STRUCTURES

Kupriyanova G.¹, Goikhman A.²

¹I. Kant Russian State University, 236000, Kaliningrad, Russia

²Moscow Engineering Physics Institute (state university), 115409 Moscow, Russia

Sandwiched magnetic structures, such as ferromagnetic(FM)-insulator(I)-ferromagnetic, also known as magnetic tunnel junctions (MTJs) are basic elements of novel nonvolatile magnetic random access memory (MRAM), which works on tunnel magnetoristance (TMR) effect. [1]

The main goal in MTJ fabrication is to reach high value of TMR, but prior to observe any magnetoristance in FM-I-FM structure, the problem of independent switching of FM layers often arises. The main reason of such problem is in interlayer exchange coupling between upper and lower magnetic layers. [2]

Ferromagnetic resonance (FMR) is acknowledged as a fingerprint method of identification of magnetic phase and magnetic statement for magnetic materials.

In this work we report on FMR research either single thin magnetic layers such as Fe₃Si, Co, Fe and Fe₃O₄, or sandwiched magnetic structures Fe₃Si/SiO₂/Co, Fe₃Si/MgO/Co and Fe₃O₄/MgO/Fe₃Si, both epitaxial and polycrystalline, all grown by pulsed laser deposition. By single magnetic thin film study, we found magnetic anisotropy as a function of thickness and chemical statement of layer (some of this data is interesting in comparison with [3]). As for FM-I-FM structures, there were found two different FMR signals from upper and lower FM layers respectively. Moreover, for some of three-layer samples we observed shift of FMR signal from one or two FM layers in comparison with signal from same single-layer samples. The observed shift of FMR signal corresponds to interlayer coupling between upper and lower FM layers. For this reason, coupling study of MTJs depending on insulating layer thickness was done.

[1] S.S.P. Parkin, C. Kaiser, A. Panchula, P.M. Rice, B. Hughes, M. Samat, S. Yang, *Nature Mat.*, **3** (2004) 862.

[2] S. Demokritov¹, J. A. Wolf and P. Grunberg, *Europhys. Lett.* **15** (1991) 881-886.

[3] Kh.Zakeri, I.Barsukov, N.K.Utochkina, F.M.Romer, J.Lindner, R.Meckenstock, U. von Horsten, H.Wende, W.Keune, and M.Farle, *Phys. Rev. B*, **76** (2007), 214421

23PO-4-26

EFFECT OF THE TOPOLOGICAL CHANGE OF THE FERMI SURFACE ON THE MAGNETOTRANSPORT IN A 2D RASHBA SYSTEM

Buchinsky D.I.¹, Novokshonov S.G.²

¹Ural State Technical University, Ekaterinburg, 620002, Mir str., 19, Russia

²Institute of Metal Physics, Ural Division of RAS, Ekaterinburg, 620041, S. Kovalevskaya str., 18, Russia

The energy spectrum of two-dimensional (2D) electron gas with Rashba spin-orbit interaction contains two degenerate at $p=0$ subbands, $E_{\pm}(p) = \varepsilon(p) \pm \alpha p$, where $\varepsilon(p) = p^2/2m$, and α is the spin-orbit coupling. An orthogonal magnetic field lifts this degeneracy and modifies quasi-classical dispersion laws $E_{\pm}(p) = \varepsilon(p) \pm \sqrt{\hbar^2 \omega_c^2 \delta^2 + m\alpha^2 \hbar \omega_c + 2m\alpha^2 \varepsilon(p) + \hbar \omega_c} / 2$. Here $\omega_c = eB/mc$ and $\delta = (g-2)/4$ is the relative deviation of the Zeeman coupling from its ideal value. This evolution of $E_{\pm}(p)$ exerts effect on kinetic properties of 2D electron Rashba system. This influence is most pronounced in the vicinity of topological change of the Fermi surface that takes place when Fermi level, E_F , passes through bottom of the upper energy subband. Such situation can be achieved in the structures with strong enough spin-orbit coupling [1,2].

We study the effect of the magnetic field induced topological change of the Fermi surface on the density of states and conductivity tensor of degenerate 2D Rashba system calculated in the self-consistent Born approximation and ladder approximation respectively [3].

If E_F lies above bottom of the upper subband, then the Fermi surface consist of two contours belong to different subbands. The Fermi level remains constant as function on the magnetic field, $n = m(E_F + m\alpha^2)/\pi$, where n is the total electron concentration. In this case, the smooth parts of the magnetoresistance and Hall coefficient are independent on the magnetic field and equal to corresponding classical values. The period of the Shubnikov – de Haas oscillation (SdHO) is defined by usual formula $\Delta(1/B) = |e|/\pi\hbar n$ which holds true for arbitrary spin-orbit coupling magnitude. Finally, the period of the SdHO beatings is defined by magnetic field depending frequency of the spin precession $\hbar\Omega_B = \sqrt{8m\alpha^2 E_F + 4m^2\alpha^4 + 4\hbar^2\omega_c^2\delta^2}$ [3,4].

As the magnetic field increases, the bottom of upper subband is enhanced and eventually intersects the Fermi level. It leads to the drastic topological change of the Fermi surface due to collapse of one from two its contours. First of all, it is accompanied by disappearance of the SdHO beatings. Secondly, the Fermi level turns to monotone decreasing function on the magnetic field and, consequently, the simple relation between period of SdHO and electron concentration is violated. Furthermore, it leads to appearance of the smooth magnetic field depending part (parallel with the oscillating part) in the Streda like term of the Hall conductivity.

The work was done within RAS Program (project № 01.2.006 13395) with partial support of RFBR (grant № 06-02-16292).

- [1] W. Yang, Kai Chang, X.G. Wu, *et al.*, *Appl. Phys. Lett.*, **89** (2006) 132112.
 [2] E. Cappelluti, C. Grimaldi, R. Marsiglio, *Phys. Rev. Lett.*, **98** (2007) 167002.
 [3] S.G. Novokshonov, A.G. Groshev, *Phys. Rev. B*, **74** (2006) 245333.
 [4] S.I. Dorozhkin, *Phys. Rev. B*, **41** (1990) 3235.

23PO-4-27

GIANT MAGNETORESISTANCE IN PLANAR FERROMAGNETIC CONTACTS

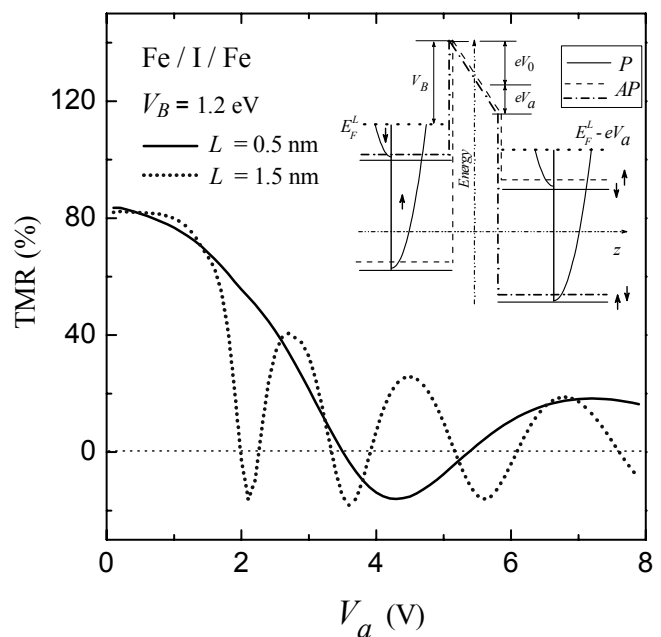
Useinov A., Dudnik M., Tagirov L.

Kazan State University, Kremlevskaya str.18, Kazan, Russia

In this paper we develop a quasiclassical theory of tunneling magnetoresistance (TMR) FM/I/FM planar ferromagnetic contacts.

Our objective is to analyze bias voltage dependence of TMR and material parameters issues within the quasiclassical approach to TMR. As a particular case we choose parameters which are close to iron as a ferromagnetic metal electrodes and magnesium oxide as a tunneling barrier material.

In the main stream of calculations we follow the work [1], on boundary resistance in planar contacts, however, we use a ferromagnetic metal for both electrodes and an insulating barrier in between. The model of spin-conserving coherent tunneling is employed in our model. Figure shows the bias dependence of TMR calculated for the biased trapezoidal-shape barrier with thickness L and height V_B , where $V_B = 1.2$ eV is the barrier's height over Fermi level (see inset of the figure), $E_F^{L(R)} = p_{FL(R)}^2 / 2m$. Bias $eV = eV_0 + eV_a$, where eV_0 is difference between potentials on the two metal's contact without applied bias potential eV_a .



Our quasiclassical theory produces the low bias voltage TMR magnitude as high as 80%, which fits well the experimental data in such systems. The high-voltage behavior of TMR strongly depends on the barrier height and thickness (see figure).

- [1] B.P. Vodopyanov, L.R. Tagirov, *J. Phys. Cond. Matter* **18**, (2006) 1545.

23 June Monday

17:00-19:00

poster session

23PO-12

“Theory”

23PO-12-1

RELATION OF PARAMETERS OF THE ELECTROMAGNETIC INTERACTION WITH PROPERTIES OF A PHYSICAL VACUUM

Astafurov V.I.¹, Georgieva M.I.², Marennyy A.M.¹, Webb N.V.²

¹JSC "Radiation and Ecology Investigations", Schukinskaya st., 40, Moscow, Russia

²Offshore Technology Development, Pte Ltd, Gul Road, 55, Singapore

The work [1] offers a new model of the material continuum, allowing to consider all fundamental interactions within a frame of one physical presentation. The physical vacuum is presented in this model as wave vector continuum, where space vector \mathbf{R} , having three constituencies (three degrees of freedom), characterizes the space and electromagnetic vector \mathbf{Q} , having two constituencies (two degrees of freedom), characterizes electromagnetic quality of the matter. The physical vacuum is considered as a sum of interconnected oscillators, forming hierarchy structures. The oscillators, defining qualitative different levels of material interactions, are called fundamental oscillators. The smallest natural oscillator, or «absolute oscillator», appears to be the basic elementary cell of the physical vacuum and forms its structural basis.

The equation, connecting space parameters of fundamental interactions [1], appears as follows (logarithmic form):

$$\log R_i = \log R_{abs.} + f_R^i \log K_0, \quad (1)$$

where R_i – radius of the i -th fundamental oscillator; $R_{abs.}$ – radius of the absolute oscillator; f_R – density of the gravitational environment; K_0 – non-dimensional coefficient, characterizing the material continuum; $i = 0, 1, \dots, 5$. The value of $i = 3$ corresponds a fundamental oscillator, defining the electromagnetic interaction. The upper limit of this oscillator is connected to Compton's wave length of an electron by a relation: $R_3 = \lambda_{comp}/2$. Strong, electromagnetic, weak and gravitational interaction comprise in such obtained consequence a continuous row with meanings of i as follows 2, 3, 4, 5.

The equation [1] can be considered as a correlation dependency, connecting parameters of fundamental interactions with qualities of a physical vacuum. The last can be understood as a space-electromagnetic nature of the vacuum and dimensionality of its structural components. The calculated values, obtained by this equation are in well agreement with the experimental data.

The equation, connecting force parameters of the fundamental interactions [1, 2], appears as follows (logarithmic form):

$$\log F_i = \log F_{abs.} + f_R^i \log k_0, \quad (2)$$

where $F_{abs.}$ and F_i – physical parameters, having dimension of a force; $k_0 = K_0^{-1}$. The calculations show that among the structural components of the absolute oscillator act connecting forces such great in dimension, that a conclusion is drawn from this about impossibility to divide these components, at least in the frame of modern theoretical presentations.

The equation (2) allows calculation of the relative values of the intensity of the fundamental interactions.

[1] V.I. Astafurov, V.A. Borisov, M.I. Georgieva, A.M. Marennyy, *Preprint VNIINM*, **2007-1** (2007).

[2] V.I. Astafurov, *Preprint VNIINM*, **5-52** (1989).

23PO-12-2

DISPERSION CHARACTERISTICS OF THE DIPOLE-EXCHANGE SPIN WAVES IN PLANAR MAGNETIC PERIODIC STRUCTURES

Grigorieva N.Yu., Kalinikos B.A.

St. Petersburg Electrotechnical University, St. Petersburg, 197376 Russian Federation

In recent years the magnetic periodic structures attract attention in connection with the investigation of the properties of nonlinear waves in dispersive medium in general as well as nonlinear spin wave effects in the artificial magnetic materials (metamaterials) in particular [1-3]. As it is well known, an efficient formation of the spin wave envelope solitons takes place in the spectral regions of high dispersion near the dipole “gaps” in the spin wave spectrum. Planar periodic structures provide a unique opportunity to have a region with high dispersion in any desired place in ω - k space. Modern technology allows one to fabricate a magnetic periodic structure with previously specified parameters. Thus, one of the main problems is to describe theoretically the dispersion parameters of the considered structures.

In this work we extend the existing analytical theory of the dipole-exchange spin-wave spectrum for a single magnetic film [4] to the tangentially magnetized planar periodic magnetic structure. In doing so, we apply a common transfer matrix approach [5]. As an example, the structure consisting of a thin ferromagnetic film with periodic metallic grating is considered. It is assumed that the grating is placed at a distance b from one of the film surfaces (Fig.1). This model takes into account the dipole-dipole and exchange interaction inside the ferromagnetic film and includes the influence of the surface anisotropy through the surface spin-pinning conditions on both sides of the film. An analytical solution in zero-order of perturbation theory for the spin-wave spectrum is obtained.

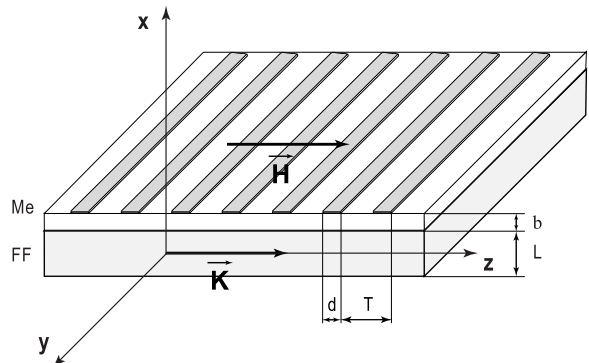


Fig.1

The spin-wave spectrum contains stop bands and allowed bands. Wave propagation within the stop bands is prohibited. It is shown that the position and the width of the stop bands depend not only on the geometric parameters of the structure but also are strongly influenced by the surface anisotropy of the ferromagnetic film.

This work was supported in part by Russian Foundation for Basic Research, Grant No. 08-02-00959, Russian Federal Agency for Education, Projects RNP/2.1.1.1382 and NSh-2124.2008.2.

[1] Niu-Nui Chen, A. N. Slavin, and M.G. Cottam, *Phys. Rev. B.*, **47** (1993) 8667.

[2] S. A. Nikitov and Ph. Tailhades, C.S. Tsai, *JMMM*, **236** (2001) 320.

[3] P.A.Kolodin and B. Hillebrands, *JMMM*, **161** (1996) 199.

[4] B. A. Kalinikos, Dipole-exchange spin-wave spectrum of magnetic films. *Linear and nonlinear spin waves in magnetic films and superlattices. ed. M.G. Cottam*, Singapore: World Scientific Publishing Co. 1994.

[5] A. Yariv and P. Yeh, *Optical waves in crystals*. A Wiley-Interscience Publication, NY 1984.

23PO-12-3

THE ANALYSIS OF THE MECHANISM OF MAGNETIC INTERACTIONS WITH ENGAGING OF AN ACOUSTIC MODEL OF QUASIELASTIC PHYSICAL VACUUM

Stukalov V.I.¹, Shalyapin A.L.²

¹Urals State Technical University, High Mathematics Chair,
Mira Str. 19, Ekaterinburg, 620002, Russia

²Institute of Engineering Science, Urals Branch, Russian Academy of Sciences, Komsomolskaya
Str. 34, Ekaterinburg, 620219, Russia

In a magnetostatics, and also in an electrodynamics the basic properties of a magnetic field are postulated on the base of experience. The additional clearing about a nature of this field cannot be received, proceeding from transformations of the Lorentz at passage to mobile frames or from positions of the quantum theory. The edge between a mathematical formalism and modeling of mechanisms of formation of field of forces is not always carried out. This contributes certain uncertainty in the understanding of magnetic interactions between particles.

In the work the attempt is made to reveal the mechanism of magnetic interactions through reviewing of scattering of acoustic waves of physical vacuum as a quasielastic medium. The reality of existence of physical vacuum as material medium is proved in works [1, 2]. Thus in the beginning, in an outcome of scattering of casual acoustic waves of physical vacuum by electrons, is formed a spherical symmetrical Coulomb field representing a stream of spherical longitudinal Coulomb waves. Then, at driving of electrons in physical vacuum, at the expense of delay of spherical scattered waves and deforming a spherical symmetrical field, the magnetic field as a secondary effect from a Coulomb field is formed.

At acceleration of electrons occurs the transversal modulation of longitudinal Coulomb waves with forming the transversal electromagnetic waves. The magnetic field in the given model is calculated with the help of lagging force potentials of Lienar-Vihert under the laws of a classical wave mechanics and acoustics.

As shown in works [3, 4, 5], the considered model reduces in numerous interesting outcomes, which completely will be agreed experimental dates.

Support by USTU, IES is acknowledged.

[1] St. Marinov. Rotating coupled mirrors experiments. *Ind. J. Theor. Phys.*, **31**, N 2 (1983) 93-96.

[2] J.P. Wesley, C. Monstein. Solar System Velocity from Muon Flux Anisotropy. *Apeiron*, **3**, N 2 (April 1996) 33-37.

[3] A.L. Shalyapin, V.I. Stukalov. Introduction to the classical electrodynamics and atomic physics. – Ekaterinburg, USTU-UPI, 1999.

[4] A.L. Shalyapin, V.I. Stukalov. Introduction to the classical electrodynamics and atomic physics. – Ekaterinburg, USTU-UMC, 2006.

[5] A.L. Shalyapin, V.I. Stukalov. Analysis of mechanism of magnetic interactions with attraction acoustic quasielastic physical vacuum models. – Proceeding of reports XIX international school-seminar "NMMM", MSU, 28 June - 2 July 2004, Moscow.

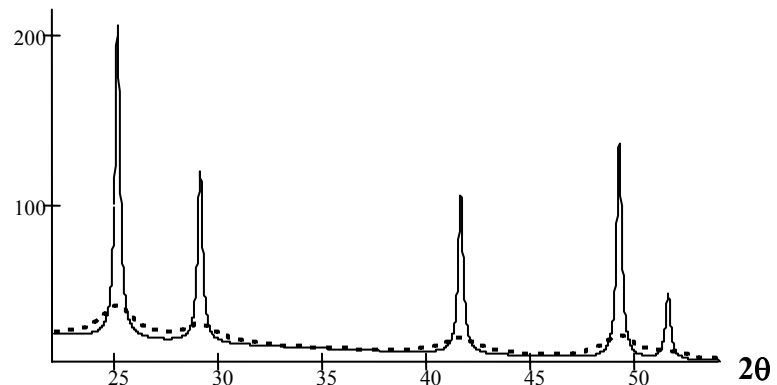
23PO-12-4

FERROMAGNETISM OF URANIUM MONOCHALCOGENIDES

Kassan-Ogly F.A., Filippov B.N.

Institute of Metal Physics, Ural Division of Russian Academy of Sciences, Russia

We consider US, USe, and UTe, the compounds crystallizing in a cubic NaCl structure at high temperatures and undergoing phase transitions from paramagnetic to ferromagnetic phase with simultaneous rhombohedral distortion at the Curie point. A very peculiar feature of all of them is that they possess so strong magnetic anisotropy that now available magnetic fields are not enough to change the magnetization orientation in them. Thus, as the initial point, we use not the conventional Heisenberg model, but rather the model of utmost strong anisotropy, magnetic modified 8-state Potts model [1]. The experimental studies of magnetic form-factor for uranium ions show that depending on the concrete surrounding they can be slightly distorted from ideal spherical shape: either prolate or oblate ellipsoids of revolution. Using this fact and the available from literature radii of S, Se, Te, and U ions, we carried out the quantitative crystallographic analysis (as it is done in cubic crystals [2]) of phase transformations in US, USe, and UTe. We analytically derived a system of transcendental equations for the four-component order parameter and an algorithm for its numerical solution at any temperature. On the basis of the crystallographic analysis we specified the relations between four components of the order parameter and lattice parameters that allowed calculating the unit cell volume and rhombohedron angle as temperature functions. We also derived the analytic expressions for spin-spin correlation functions and calculated the temperature dependence of elastic magnetic scattering of neutrons (The figure shows scattering calculated above and below the Curie point).



The theory [3] developed on the base of synthesis of magnetic modified 8-state Potts

model [1] and concepts of structural phase transitions in cubic crystals [2] makes it possible to describe simultaneous magnetic and structural phase transitions in magnetic compounds with a NaCl structure and a strong cubic magnetic anisotropy, to calculate thermodynamic, magnetic, and structural characteristics and to predict the magnetic moment directions in such structures. The theory explains the origin of diffuse magnetic neutron scattering, its temperature evolution and its transformation into magnetic Bragg reflections below the Curie point, i.e. the unified nature of magnetic scattering and Bragg reflections. The theory also predicts an impossibility of magnetic ordering and structural transformation in crystals with a certain ratio ($R_c/R_a < 0.414$) of cation and anion ion radii.

Support by RFFI, grant №06-02-17082 is acknowledged.

[1] F.A. Kassan-Ogly, *Phase Transitions*, **72** (2000) 223.

[2] F.A. Kassan-Ogly, V.E. Naish, I.V. Sagaradze, *Phase Transitions*, **49** (1994) 89.

[3] F.A. Kassan-Ogly, B.N. Filippov, *Physics of Metals and Metallogr.*, **105** (2008) 227.

23PO-12-5

THE INFLUENCE OF THE QUANTUM FLUCTUATIONS ON THE GROUND STATE AND SPECTRAL PROPERTIES OF 2D MAGNETS WITH CUBIC SYMMETRY FOUR-SPIN EXCHANGE INTERACTION

Valkov V.V.^{1,2}, Valkova T.A.², Jolobova N.N.^{1,3}

¹L.V. Kirensky Institute of Physics SB RAS, Krasnoyarsk, 660036, Russia

²Siberian Federal University, Krasnoyarsk, 660041, Russia

³Krasnoyarsk State Pedagogical University, Krasnoyarsk, 660049, Russia

The discovery of the high-temperature superconductivity has stimulated the investigations of the two-dimensional antiferromagnets (2D-AFM). One of the important questions of these systems theory is the question about quantum fluctuations in the problem of Neel phase stability. In the simple case of the isotropic Heisenberg 2D-AFM with nearest neighborhood approximation the influence of the quantum fluctuations is not essential even with minimum spin $S=1/2$.

In the case of non-Heisenberg 2D-AFM, when not only quadratic invariants are taken into account, the stability problem of the Neel phase has remained unproved. Four-spin exchange interactions on square lattice give rise to anisotropic terms. Accordingly, the excitation spectrum has energy activation. From this point of view the anisotropic four-spin interactions must stabilize the Neel phase. On the other hand four-spin interactions are responsible for additional quantum fluctuations. By this means the mechanism of the stabilization is in competition with the mechanism of the destruction of the Neel phase for anisotropic non-Heisenberg AFM.

In this work the influence of the anisotropic four-spin interactions on the ground state and spectrum properties of 2D-AFM has been analyzed. Three invariants of the four-spin interactions have been taken into account. Self consistent form of the Bogolubov transformation has been used for development of the nonlinear theory of the anisotropic non-Heisenberg 2D-AFM. In the framework of such theory the influence of the cube anisotropy and frustrations on the stability regions of the Neel phase has been investigated. It is shown that quantum fluctuations in anisotropic non-Heisenberg 2D-AFM may destroy the Neel phase.

This work was supported by the program of Presidium of RAS Quantum macrophysics, Russian Foundation for Basic Research (project no. 07-02-00226), and Integration project 3.4 SB RAS.

23PO-12-6

REJUVENATION EFFECTS IN THE SPHERICAL P-SPIN MODEL OF SPIN GLASSES

Busiello G.¹, Gazeeva E.², Saburova R.², Khaibutdinova I.²

¹Dipartimento di Fisica "E.R.Caianiello" and unita CNISM, Universita di Salerno,
Salerno, Italy

²Kazan State Power University, Kazan, 420066, 51 Krasnosel'skaya st, Russia

Chaos, rejuvenation, memory and aging are the fascinating properties of spin glasses which have been intensively studied during the last years [1-4]. In particular, to clarify the nature of spin glass phase below the transition temperature, the aging behaviour has been actively investigated.

In randomly frustrated systems such as spin glasses, directed polymer in random media and vortex glasses, the equilibrium ordered state could be completely reorganized by an infinitesimally small change perturbation, such as changes in temperature, field and in (disorder) bond interaction (chaos properties). The characteristic behaviours as rejuvenation and memory were interpreted in terms of chaos concept, leaving the door open to different mechanisms.

In this paper we have analytically and numerically calculated the bond and temperature shifts in the p-spin spherical quantum model of glass related to the quantum environment and subjected to the action of external fields. The effects of aging and recovery (rejuvenation) is revealed using solutions of coupled integro-differential equations for the correlation and response functions [5].

The results may be interpreted in terms of bond and temperature chaos or in terms of the existence of a time dependent coherence length as a consequence of which the rejuvenation effect is due to the freezing of small length scale modes which were fast at higher temperature. This freezing changes the correlations on small scales.

[1] R. Arai, K. Komatsu, T. Sato, cond-mat/0601248 (2007).

[2] J. Kurchan, Nature **433** (2005) 222.

[3] L. Berthier, J-P. Bouchaud. Phys. Rev. **B66** (2002) 0544041.

[4] M. Sasaki, K. Hukushima, M. Yoshino, H. Takayama, Phys. Rev. Lett. **95** (2005) 267203.

[5] L.V. Keldysh, Zh. Eksp. Teor. Fiz. **47** (1964) 1515.

23PO-12-7

ON THE MAGNETIC SUSCEPTIBILITY OF DIPOLAR SPIN GLASSES

Busiello G.¹, Gazeeva E.², Saburova R.², Khaibutdinova I.²

¹Dipartimento di Fisica “E.R.Caianiello” and unita CNISM, Universita di Salerno,
Salerno, Italy

²Kazan State Power University, Kazan, 420066, 51 Krasnosel'skaya st, Russia

Very interesting magnetic phenomena are observed in systems which have negligible exchange interactions, so the dominant magnetic interactions are of dipolar type [1,2]. These kind of interactions are, in many respect, similar to RKKY interaction and its long-range character give rises to many non trivial properties. At low temperature the dilute magnet LiHo_xY_{1-x}F₄ has dipolar spin glass order which is very sensitive to weak perturbations. The nature of quantum or classical phase transition in this Ising magnet in transverse field is a recent questionable topic [3,4].

In this paper we investigate the dissipative part of the linear magnetic dynamical susceptibility of the system of randomly diluted, dipolar coupled, magnetic impurities in crystal, interacting each other and with the lattice oscillations. It is shown that the linear response of the system to an external ac magnetic field consists of a resonant part and a relaxation one. It is found an anomalous temperature dependence of the dissipative part of the magnetic susceptibility at the transition (at enough high concentrations of the magnetic dipoles) from paramagnetic to ordered phase. In particular has been considered the dependence of the linear susceptibility from concentration, transverse field and on the magnetic dipole-phonon interaction. Some experimental measurements on the afore mentioned dipolar magnet qualitatively agrees with our results.

[1] J. Brooke, T.F. Rosenbaum, G. Aeppli *et al*, Nature **413** (2001) 610; **425** (2005) 48; **448** (2007) 567.

- [2] H.M. Rannow *et al*, Science **308** (2005) 389.
 [3] C. Ancona-Torres *et al*, cond-mat/08012181 (2008).
 [4] P. E. Jonsson *et al*, cond-mat/08031357 (2008).

23PO-12-8

SPIN-AND-ORBITAL EFFECTS IN MOTT-HUBBARD OPTICAL BANDS IN TWO LIMITS OF JAHN-TELLER INSTABILITY: LaMnO_3 vs. YTiO_3

Kovaleva N.N.^{1,2}, Boris A.V.^{1,2}, Maljuk A.^{1,3}, Stoneham A.M.⁴, Keimer B.¹

¹Max-Planck-Institut für Festkörperforschung, Heisenbergstr. 1, D70569, Germany

²Department of Physics, Loughborough University, Leicestershire, LE11 3TU, UK

³Hahn-Meitner-Institut Berlin, Glienickerstr. 100, 14109 Berlin, Germany

⁴London Centre for Nanotechnology, University College London, Gower Str., WC1E 6BT, UK

Spectral ellipsometry is used to study temperature dependences of the optical conductivity of the Mott-Hubbard bands, associated with intersite $d-d$ transitions, in LaMnO_3 and YTiO_3 . In LaMnO_3 , the optical spectral weight of the $d-d$ transitions exhibits a strong anomaly at the Neel temperature $T_N = 139$ K, due to enhanced antiferromagnetic spin-spin correlations. In YTiO_3 , the spectral weight evolves smoothly through the onset of a ferromagnetic long-range order at $T_C = 30$ K, with no discernible anomaly at the Curie temperature. However, a distinct anomaly is observed at about 100 K, far above T_C , but coincident with a deviation of the uniform magnetization from the mean-field Curie-Weiss behaviour. These observations imply an important qualitative difference between LaMnO_3 and YTiO_3 . Almost undistorted octahedra in YTiO_3 indicate a small Jahn-Teller instability, resulting from the weak coupling between two nearly degenerate electronic ground states. The Jahn-Teller instability may disappear if there is sufficiently large splitting of two nearly degenerate levels by small perturbation, in particular, by the spin-orbit interactions [1]. The orbital degrees of freedom may be essentially quenched in the magnetically ordered state, when the ground multiplet experiences splitting into two doublets, with concomitantly a partial uncoupling of the spin and orbital moments. Then, the temperature dependence in such a system is largely determined by the interplay between the spin-orbit coupling and the Jahn-Teller effect. In such a case, the establishment of the spin-spin correlations in approaching the ferromagnetic transition will give rise to complex *spin-orbit-lattice* effects, peculiar to the system with orbital degrees of freedom. By contrast, the orbital degrees of freedom are quenched in LaMnO_3 by a large static Jahn-Teller distortion, and the redistribution of the optical spectral weight is in a good agreement with a superexchange model, which attributes these shifts to the temperature dependent *spin-spin* correlations.

Discussions at Landau Seminar of Physics Department at Loughborough University are acknowledged.

- [1] U. Öpik and M. H. Pryce, Proc. R. Soc. London, Ser. A 238 (1957) 425.

23PO-12-9

MODELING OF THE DYNAMIC DOMAIN PATTERNS

Maltsev V.N.

Urals State University, 620083, Lenin av.51, Yekaterinburg, Russia

In ferrite-garnet film, with uniaxial anisotropy, in the presence of alternated harmonic magnetic field along the easy direction, the dynamic domain structures of various forms exist, for instance spiral domains, systems of concentric circular domains and others [1]. Each type of the domain structure appears and exists under some amplitudes and frequencies of the external field. The typical frequencies, under which patterns exist belong to region 0,01 Hz – 30 kHz. The typical amplitudes from half of the saturation field. The dynamic domain structures influence on the hysteresis properties of film.

Modeling such domain structures is difficult enough, because it demand to take account of the magnetic dipole interaction and the vector character of the magnetization distribution. In the earlier models, to avoid these problems the discrete magnetization [2] or only z-component of magnetization [3] were considered. The structure of the domain wall was not taken into account, consequently in these model the chiral effects were absent, which are responsible to origin of spiral domains. Besides, modeling was conducted for quasi-static the field. In this work the results of modeling of two-dimensional dynamic patterns are present on base of two approaches: phenomenology and micromagnetics, which complement each other. In micromagnetics approach the was suggested that on thickness of sample the magnetization distribution is not changed. In simulations are got two-dimensional magnetic patterns in the sample placed in alternated magnetic field for different moments of time. That allows to research the processes of formation, existence and the destruction of these patterns. The getting types of patterns, were observed in experiments. However, for understanding of these processes it is necessary to use a phenomenology model, in which it is possible to define the condition of existence of these structures. For this the patterns with given forms are considered in suggesting about the freedom degrees. For instance, for spiral domain his form and sizes are assigned, as well as is taken into account that change of his form and size can occur when increase of his length, change of his width and distorting the form of his walls? whereupon it is researched the stability of the given form of patterns for small change of the amplitude, frequencies of the field and geometric parameters of patterns. The numeric results are in a good conformity with experiments. It is possible that given approach will allow simulate all types of observed patterns and define the condition of their formation.

[1] G.S.Kandaurova, *Uspekhi Fizicheskikh Nauk*, **45** (2002) 1051.

[2] A. Magni, G. Vertesy, *Phys.Rev. B*, **61** (2000) 3203.

[3] E.A. Jagla, *Phys. Rev. E*, **70** (2004) 046204

23PO-12-10

NEW MATHEMATICAL MODEL OF A PHYSICAL VACUUM AND ITS APPLICATION TO THE PROBLEM OF MAGNETIC CHARGES

Astafurov V.I.¹, Georgieva M.I.², Marennyy M.A.¹

¹JSC “Radiation and Ecology Investigations”, Schukinskaya st., 40, Moscow, Russia

²Offshore Technology Development, Pte Ltd, Gul Road, 55, Singapore

The physical vacuum is represented as a vector continuum, where space vector \mathbf{R} , having three constituencies (three degrees of freedom), characterizes the space and electromagnetic vector \mathbf{Q} , having two constituencies (two degrees of freedom), characterizes electromagnetic quality of the matter. Having accounted the thesis about universality of a wave motion, the model appears to have discrete-continuous character. The physical vacuum is considered as an aggregate of interconnected oscillators, forming hierarchy structures [1]. Oscillators, determining qualitative different levels of material interactions, have been called fundamental oscillators. Smallest natural oscillator or “absolute oscillator” appears to be an elementary cell of the physical vacuum and compiles its structural basis.

Developed model allows consideration of all fundamental interactions within one physical presentation. The equation, connecting space parameters of the fundamental interactions [2], appears as follows (logarithmic form):

$$\log R_i = \log R_{abs.} + f_R^i \log K_0,$$

where R_i – radius of the i -th fundamental oscillator; $R_{abs.}$ – radius of the absolute oscillator; f_R – density of gravitational environment; K_0 – non-dimensional coefficient; $i = 0, 1, \dots, 5$. Calculated values obtained by this equation agreed well with the experimental data.

According to the developed model, the magnetic charges appear to be part of the vacuum structure. The absolute oscillator contains in its structure two opposite by sign elementary magnetic charges. They have been represented as compounds of the vector \mathbf{Q} in the mathematical model of the vacuum. The process of creation of a pair electron-positron is considered as a transformation of the magnetic charges into electrical and process of annihilation of an electron and positron – as a transformation of the electrical charges into magnetic. A conclusion is drawn from the model about the equality of magnetic and electrical elementary charges, as well as the mass and spin of their bearers.

So the magnetic monopole exists only in the structure of the physical vacuum in the composition of interconnected pairs of opposite magnetic charges. Bipolarity of any constant magnet is stipulated from the bipolarity of the structure of the physical vacuum and is interconnected with it. Single-polar magnet is not possible to obtain. The Dirac’s monopole and any other magnetic monopole don’t exist as an individual magnetic particle in the nature.

A magnetic field around a constant magnet appears to be a field of quasi-elastic deformation of a vacuum structure. The character of deformation is directed towards minimizing of the potential energy of the interconnected system “magnet – vacuum”. As a consequence of superposition of different oscillating processes, the magnetic field has a specific structure, close to interferential. Electromagnetic waves can be considered as strain oscillations of the vacuum.

[1] V.I. Astafurov, *Preprint VNIINM*, **4-51** (1989).

[2] V.I. Astafurov, V.A. Borisov, M.I. Georgieva, A.M. Marennyy, *Preprint VNIINM*, **2007-1** (2007).

23PO-12-11

NONPERTURBATIVE SCALING THEORY OF FREE MAGNETIC MOMENT PHASES IN DISORDERED METALS

Zhuravlev A.K.¹, Zharekeshev I.², Gorelov E.², Lichtenstein A.I.², Mucciolo E.R.³, Kettemann S.²

¹Institute of Metal Physics, 620041 Ekaterinburg, Russia

²Institut für Theoretische Physik, Universität Hamburg, 20355 Hamburg, Germany

³Department of Physics, University of Central Florida, Orlando, Florida 32816-2385, USA

The crossover between a free magnetic moment phase and a Kondo phase in low-dimensional disordered metals with dilute magnetic impurities is studied. We perform a finite-size scaling analysis of the distribution of the Kondo temperature obtained from a numerical renormalization group calculation of the local magnetic susceptibility for a fixed disorder realization and from the solution of the selfconsistent Nagaoka-Suhl equation. We find a sizable fraction of free (unscreened) magnetic moments when the exchange coupling falls below a critical value J_c . Between the free moment phase due to Anderson localization and the Kondo-screened phase we find a phase where free moments occur due to the appearance of random local pseudogaps at the Fermi energy whose width and power scale with the elastic scattering rate $1/\tau$.

The Kondo problem is of central importance for understanding low-temperature anomalies in low-dimensional disordered metals such as the saturation of the dephasing rate and the non-Fermi-liquid behavior of certain magnetic alloys. For a clean metal, the screening of a spin-1/2 magnetic impurity is governed by a single energy scale, the Kondo temperature T_K . Thermodynamic observables and transport properties obey universal functions which scale with T_K . Thus, in a metal where nonmagnetic disorder is also present, two fundamental questions naturally arise: (i) Is the T_K modified by nonmagnetic disorder? (ii) Is the one-parameter scaling behavior still valid? It is well known that magnetic moments can remain unscreened when conduction electrons are localized. However, in weakly disordered two-dimensional systems, the localization length is macroscopically large and is not expected to influence the screening of magnetic moments for experimentally relevant values of exchange coupling J . Another way of quenching of the Kondo effect is the existence of a *global pseudogap* at the Fermi energy E_F , namely, $\rho(E) \sim (E-E_F)^\alpha$, where $\alpha > 0$. In clean metals, the pseudogap quenches the Kondo screening when J falls below a critical value $J_c(\alpha)$.

In this Letter [1] we examine the quantum phase diagram of magnetic moments diluted in two-dimensional disordered metals using a modified version of the numerical renormalization group (NRG) method. We find a free moment phase which we attribute to the random occurrence of *local pseudogaps*. The existence of free moments is confirmed directly with the NRG by the Curie-like behavior of the local magnetic susceptibility at low temperatures at particular sites for a given disorder realization. Finite-size scaling is performed to demonstrate the robustness of our finding. Furthermore, the distribution of T_K s obtained from the NRG is found to agree well with earlier results based on the solution of the Nagaoka-Suhl equation.

[1] A. Zhuravlev, I. Zharekeshev, E. Gorelov, A.I. Lichtenstein, E.R. Mucciolo, S. Kettemann «Nonperturbative scaling theory of free magnetic moment phases in disordered metals», *Physical Review Letters*, **99**, 247202 (2007)

23PO-12-12

EFFECTS OF CROSS CORRELATION BETWEEN INHOMOGENETIES OF THE EXCHANGE AND ANISOTROPY ON THE SPIN-WAVE SPECTRUM

Ignatchenko V.A.¹, Polukhin D.S.²

¹Kirensky Institute of Physics, Siberian Branch of RAS, 660036 Krasnoyarsk, Russia

²Siberian Federal University, 660041 Krasnoyarsk, Russia

Joint effects of inhomogeneities of the exchange and anisotropy on the spectrum and damping of spin waves in a ferromagnet are considered. Stochastic properties of the inhomogeneities are described by correlation functions with the arbitrary correlation radius r_c . Side by side with the autocorrelations of inhomogeneities of each physical parameter, the cross correlations between inhomogeneities of different parameters are taken into account. Effects of cross correlations and autocorrelations on the spin-wave spectrum and damping are much more developed themselves for the wave numbers k of spin waves which correspond to the correlation wave number $k_c = r_c^{-1}$. The most considerable distinction of the dispersion law from the quadratic law and the damping law from its usual form occurs in this region of k .

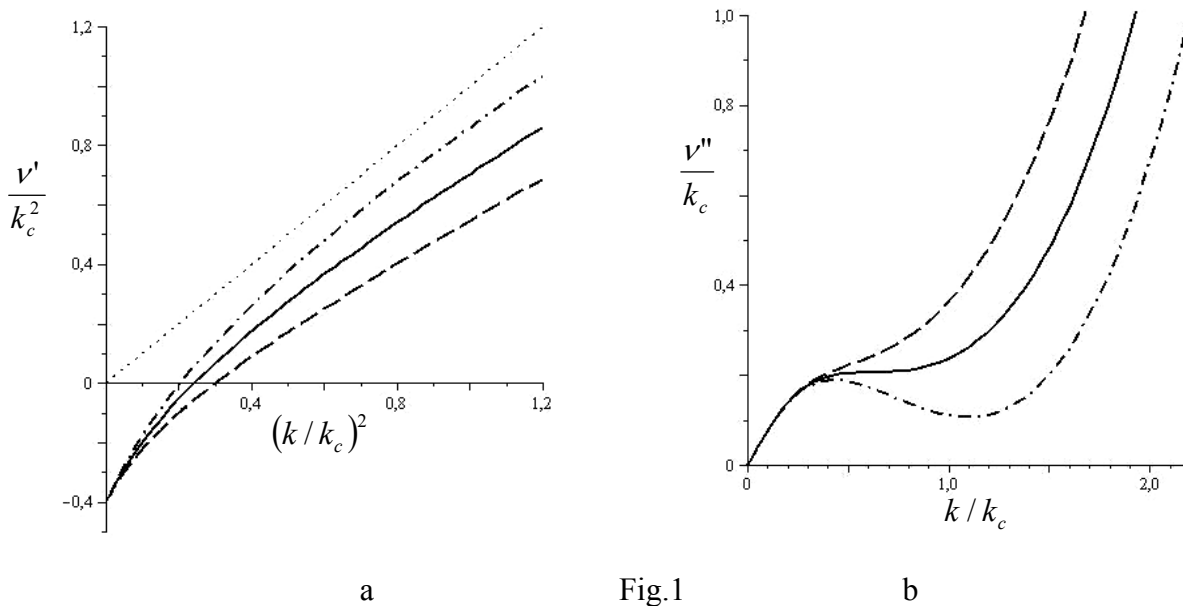


Fig.1

In Fig.1a,b the dependencies of the real and imaginary parts of the complex spin-wave frequency $\nu = \nu' - i\nu''$ on k are shown. Here $\nu = (\omega - \omega_0) / \alpha g M$, where α is the exchange constant, g is the gyromagnetic ratio, M is the magnetization and ω_0 is the frequency of the ferromagnetic resonance. Solid curves in both these figures correspond to joint effects of inhomogeneities of the exchange and anisotropy on the spin-wave spectrum (Fig.1a) and damping (Fig.1b) in the absence of the cross correlations. Dashed curves describe effects of these inhomogeneities in the presence of the positive cross correlations and dotted-dashed curves describes effects of the negative cross correlations. The dotted curve in Fig.1a corresponds to the unperturbed dispersion law $\nu = k^2$. It is seen that the positive cross correlations lead to the larger difference of the dispersion law $\nu'(k)$ from the unperturbed dispersion law as compared with the joint action of inhomogeneities without cross correlations. The positive cross correlations lead also to the increase of the damping of waves. The negative cross correlations lead to the opposite effects: both the modification of the dispersion law and damping decrease. The change of the damping

law forme is also occurred and the distinctive “window of transparency” appears for k in the vicinity of k_c .

This work was supported by the Grant of the RF President, SS-3818.2008.3.

23PO-12-13

INVESTIGATION OF MAGNETIC AND THERMAL PROPERTIES OF MODEL Fe/V SUPERLATTICES

Khizriev K.Sh.¹, Murtazaev A.K.¹, Uzdin V.M.²

¹Institute of Physics Dagestan SC RAS, Yaragskogo Street, 94, Makhachkala, 367003, Russia

²ICAPE, St.Petersburg State University, 14 linia V.O., 29, 199178, St. Petersburg, Russia

The manipulation by interlayer exchange coupling, magnetoresistance and other magnetic properties of the multilayers via hydrogen adsorption in the non-magnetic layers allows creation of the structures, where the continuous transition from 3-dimensional toward 2-dimension magnetism can be realized experimentally. For simulation of magnetic phase transition in multilayers we suggested a model of superlattice Fe/V. Superlattice Fe/V represents structure where there is an alternation of magnetic (Fe) and nonmagnetic (V) layers. In superlattice Fe/V inside monolayers of iron exchange interaction $J_{||}$ ferromagnetic interaction (an intralayer interaction). Also there is an interaction J_{\perp} between “iron” layers through layers of vanadium (an interlayer interaction). The size and a sign of this interaction can change from thickness of an layer of vanadium. The Curie temperature for magnetic layers has minimum at zero interlayer coupling when the system was found to be quasi-two-dimensional. One can wait that critical behavior, as a whole, will depend strongly on the interlayer exchange parameter. For today there are various experimental and theoretical investigations of such superlattices. These works, mainly, are devoted to reception of superlattices and investigation of their structure and some magnetic properties. All these works score, that superlattices are ideal for investigation of transition from three-dimensional to two-dimensional magnetism.

One of techniques for modeling and investigations of such superlattices is the Monte-Carlo method. The Monte Carlo method is exactly effective at examination of nanoscale systems what are superlattices. In the given work the iron-vanadium model of a superlattice is offered and results of investigation of magnetic phase transition of this model are resulted by a method of Monte-Carlo. The Hamiltonian of a superlattice model could be presented as

$$H = -\frac{1}{2} \sum_{i,j} J_{||} (S_i^x S_j^x + S_i^y S_j^y) - \frac{1}{2} \sum_{i,k} J_{\perp} (S_i^x S_k^x + S_i^y S_k^y) - m_0 H_0 \sum_i S_i$$

where the first sum took into account an exchange interaction of every iron atoms with all nearest neighbours inside a layer with the exchange interaction $J_{||}$, and the second sum was the contribution to a Hamiltonian of interaction of iron atoms through vanadium layers with an interaction parameter J_{\perp} , S were magnetic moments (spins) of atoms Fe. Hamiltonian views planar orientation of magnetic moments Fe (XY-model).

Investigations were performed using by a single-cluster algorithm of a Monte-Carlo method for systems with periodic boundary conditions. The relation between interlayer and intralayer exchange coupling was varied in a wide limit. We have calculated spontaneous magnetization, susceptibility and specific heat as functions of the temperature and exchange parameters. The accurate method of Binder cumulants have been used for definition of the critical temperature. Temperature dependences of magnetization, susceptibility and a heat capacity for several models of a superlattice are received. In model with two and three layers of

iron ($\text{Fe}_2/\text{V}_n/\text{Fe}_3$) are found two maximums of a heat capacity at small values of a relation of interlayer and intralayer exchanges. Temperature dependences of thermodynamic values testify to presence in model of a superlattice $\text{Fe}_2/\text{V}_n/\text{Fe}_3$ of two phase transitions.

The investigation is supported by the program of “Russian Science Support Foundation”, by the Russian Foundation for Basic Research (project № 06-02-96602, 07-), by grant of a scientific school (SS-4526.2008.2).

23PO-12-14

ANISOTROPICALLY RIGID MAGNETIC MATERIALS. CLASSIFICATION AND PROPERTIES

Golubiatnikov A.N.

Mech. and Math. Dept., MSU, Vorobyovy Gory, 119992 Moscow, Russia

Within the framework of general theory of anisotropic continua interacting with electromagnetic field [1] and the theory of thermodynamics stability of such media [2], an approach to the description of magneto-rigid media with geometrical constraints is developed.

The theory is based on the classification of continuum models according to the continuous groups of affine symmetries including rotations, shears and dilations of Lagrangian variables. There exist 99 types of such groups, of which only two groups are the ones of pure rotation. The invariants of all this groups as the functions of Lagrangian components of metric tensor and magnetization vector are calculated. In theory of anisotropically rigid media for every group of affine symmetry, all these invariants (or their part) are fixed. The absolutely rigid body with the frozen-in magnetization and the incompressible magnetic fluid with the magnetization saturation are examples of such media.

The equations of motion, energy and magnetic field are derived taking into account the dissipative processes. In non-dissipative case the possible shock conditions are investigated. In certain cases the constraint equations almost completely determine the motion law and the magnetization, but the equations of motion and field serve for determination of Lagrange multipliers (of pressure type).

In general case, the class of solutions with homogeneous deformations is indicated. Plane problem is discussed. The method of resolution of the nonlinear constrain equations for media with one-parametric groups of two-dimensional transformations is proposed. As the example, the solution to stationary problem of flow of the incompressible medium, consisting of non-extensible magnetized filaments, around an rigid obstacle is given.

The work is supported by the RFBR (projects 08-01-00026 and 08-01-00401) and the grant of the President of the RF (project NSh-610.2008.1).

[1] A.N. Golubiatnikov, *Uspehi mehaniki*, **2**, No. 1 (2003) 126.

[2] A.N. Golubiatnikov, *Uspehi mehaniki*, **4**, No. 3 (2006) 3.

23PO-12-15

APPLILCATION OF THE MEAN-FIELD APPROXIMATION TO THE MAGNETIC AND SUPERCONDUCTING PHASES OF QUASI-ONE-DIMENSIONAL METAL

Rozhkov A.V.

Institute for Theoretical and Applied Electrodynamics,
ul. Izhorskaya 13/19, 124512, Moscow, Russian Federation

Quasi-one-dimensional (Q1D) metals show a variety of magnetic and superconducting ordered phases. However, straightforward application of the mean-field approximation to such systems might lead astray. The main goal of this work is to investigate under which conditions it is permissible to use the mean-field approach to study ordered phases of Q1D metals.

Here we map the phase diagram of a model system: an array of one-dimensional (1D) conductors coupled together by short-range single-electron hopping. It is assumed that the transverse hopping amplitude t is much smaller than $v_F A$, where v_F is the Fermi velocity and A is the cutoff.

If such a system is studied within the mean-field approximation, then the spin-density wave (SDW) is the only stable ordered phase. This magnetic order vanishes through a continuous phase transition at high temperatures or upon destruction of the Fermi surface nesting.

Despite general appeal, this approach is incorrect. The source of our trouble is strong 1D-like fluctuations unaccounted at the mean-field level. They are important since the electronic kinetic energy is extremely anisotropic.

The proposed solution to this difficulty is to apply the mean-field approximation not to the bare Hamiltonian H , but rather to the effective Hamiltonian H_{eff} . The high-energy 1D-like fluctuations are hidden in the renormalized parameters of H_{eff} .

It is possible to derive H_{eff} at such scale where the effective transverse hopping is comparable to the cut-off. At this energy scale the mean-field approximation for H_{eff} should be sufficient: indeed, the anisotropy ratio $t_{\text{eff}}/(v_{F,\text{eff}}A_{\text{eff}})$ is of the order of unity, thus, 1D fluctuations are suppressed.

To map the phase diagram, therefore, we must know the effective Hamiltonian. Provided that the anisotropy is strong, term $g_{2k_F,ij}^\perp \rho_{2k_F,i} \rho_{-2k_F,j}$ experiences the strongest renormalization [i and j are chain indices, $g_{2k_F}^\perp$ is the coupling constant, ρ_{2k_F} is the oscillating component of the density operator]. This structure of the effective interaction is a consequence of high-energy 1D physics, as such, it is insensitive to the exact nesting properties of the Fermi surface which is a low energy feature.

Within the mean-field approximation for H_{eff} we obtain two phases. At good nesting the most stable order is SDW. When nesting becomes poor SDW transition temperature quickly reaches zero. At that point superconductivity appears. The order parameter is stabilized due to the term $g_{2k_F,ij}^{\perp,\text{eff}} \rho_{2k_F,i} \rho_{-2k_F,j}$ [it can be cast as $-2g_{2k_F,ij}^{\perp,\text{eff}} (\Delta_{ij}^+ \Delta_{ij} + \vec{d}_{ij}^+ \vec{d}_{ij})$ where Δ_{ij} (\vec{d}_{ij}) is d_{xy} -wave (f -wave) order parameter, and chains i and j are nearest neighbours]. The superconductivity is insensitive to the nesting and remains stable even when the latter is poor.

The emergent superconducting order has four important properties. First, Cooper pair corresponding to our order parameter consists of a fermion with spin σ on chain i and a fermion with spin $-\sigma$ on chain j . That way the fermions avoid paying large penalty due to strong in-chain repulsion. Second, superconducting gap has nodes on the Fermi surface. The presence of the nodes may be checked experimentally. Third, the superconductivity becomes possible due to 1D-

like fluctuations which must be taken into account properly. Fourth, the orbital symmetry and the spin state of the order parameter is a non-universal property of the system.

Support by RFBR through grants 08-02-00212, 06-02-16691, 06-02-91200 is acknowledged.

23PO-12-16

INFLUENCE OF ELECTRON CORRELATIONS ON MAGNETIC PROPERTIES OF TRANSITION METALS IN VIEW OF DEGENERATION

Shilov V.E., Shilova E.V.

Mari State University, 424001 Yoshkar Ola, a sq. Lenin 1. Russia.

In compound of transition metals with narrow bands the behaviour of strong electron-electron correlations it is caused by degeneration. Degeneration on orbital quantum number is removed by a crystal field only in part. In work [1] it is marked, that electron correlation d^5 ions, of iron in hematite Fe_2O_3 may to be realized as in low-spin and high-spin state. Weak distortion of octahedron field results in fact, that cubic representation t_{2g} is split on $a_{1g} + e_g^\pi$ and e_g^σ . In used Hamiltonian we take into account such features of a spectrum for a case, when e_g^σ there are two equivalent Hubbard orbitals, a_{1g} - a narrow band. In work [2] it is shown, that in pure metals Fe, Co, Mn the system resounds between low-spin state and high spin state and it appears ferromagnetic. We consider a case when the system resounds between two and three-hole high spin states, and the spectrum of spin waves is determined in case of transitions between these states on Hubbard orbitals, proceeding from equation Daison [3]:

$$-\omega + \vec{\lambda} \cdot \vec{\alpha}(+++ , L^\sigma) - \text{Re} \sum_{L^\sigma}^{+++}(\vec{k}, \omega) = 0,$$

Where $\vec{\lambda}$ - a vector made of own values, $\vec{\alpha}(+++ , L^\sigma)$ - root vectors of twice degenerated Hubbard model, $\sum_{L^\sigma}^{+++}(\vec{k}, \omega)$ - an own - power part in a case double - triplet transitions. Twice differential section of dispersion of a neutron on a spin wave:

$$\frac{d^2\sigma}{d\Omega d\omega} \propto \delta\left(\omega - \omega_{L^\sigma}^{+++}\right) = \delta(E_{p'} - E_p \pm \hbar\omega_S(q)),$$

Where

$$\hbar\omega_S(q) = \vec{\lambda} \cdot \vec{\alpha}(+++ , L^\sigma) - \frac{q^2}{2m^*} \cdot \frac{(1-c^*)}{\sqrt{2}} \left/ \sqrt{1 + \frac{V_0}{2(d-c)^2}} \right.,$$

m^* - the effective weight determined by energy of tunneling, c^* - concentration of electron in a of three-particle states band, $(d-c)$ depends on Coulomb interaction, Hund exchange interaction, atomic energy and hybridization of Anderson V_0 .

Dependence of an optical gap from initial is established (one-site) power structure of a spectrum. The represented results show dependence of an optical branch on parameter of hybridization of Anderson, concentration in a narrow hole band, Hund exchange energy in case of transitions on Hubbard orbitals. The received result shows clear distinction in a spectrum of magnetic excitations for degenerated and not degenerated cases for the accepted model and is interesting from the point of view of application of a method of dispersion of slow neutrons at studying magnetic dynamics.

[2] Zaitsev R. O., JETP, **123**, №2, (2003), 325.

[3] Vedjaev A.V., Ivanov V.A., Shilov V.E., TMF, **64**, (1985),163,.

[4] Shilov V.E., Shilova E. V., Digest of Mari State University, **1**(2), (2007), 130.

23PO-12-17

FIELD-INDUCED HELICAL MAGNETIC STRUCTURE IN THE TWO-SUBSYSTEM FRUSTRATED ANTIFERROMAGNET

Martynov S.N.

Kirensky Institute of Physics, SB RAS, Krasnoyarsk, 660036, Russia

The equilibrium orientation of spins and self-consistent magnetizations of subsystems in the two-subsystem geometrically frustrated antiferromagnet with hamiltonian

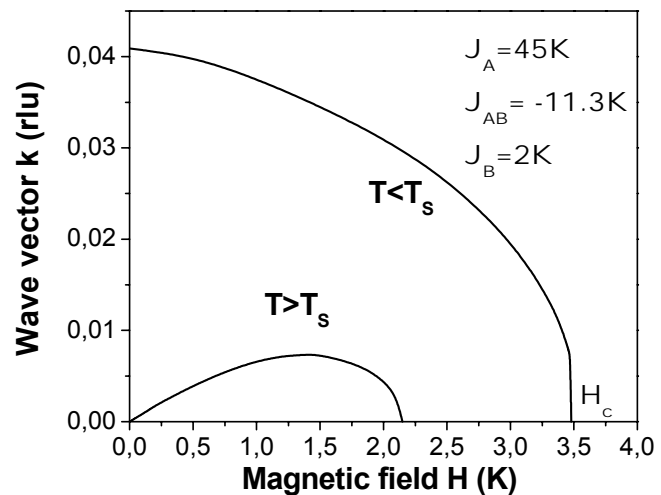
$$H = J_A \sum_i \mathbf{S}_i^A \cdot \mathbf{S}_{i+1}^A + J_B \sum_i \mathbf{S}_i^B \cdot \mathbf{S}_{i+1}^B + J_{AB} \sum_{ij} \mathbf{S}_i^A \cdot \mathbf{S}_j^B + H \sum_{ij} (\mathbf{S}_i^A + \mathbf{S}_j^B) \quad (1)$$

are investigated. According to classical theory of ground-state spin configurations for such two-subsystem magnets with competing exchange as a spinels [1] the collinear or triangular (Yafet-Kittel-type) configurations of spins are unstable if the threshold conditions on the values and geometry of the exchange interactions are satisfied. Antiferromagnetic intersubsystem exchange interactions $J_A, J_B > 0$ and geometrically frustrated exchange J_{AB} between subsystems leads to a formation of incommensurate magnetic structure of helicoid type [2] For a system with a

sufficiently different ordering temperatures of each subsystem ($J_A \gg J_B$, or a low dimension of the magnetic interactions within B-subsystem) the magnetizations of each system have a different temperature dependence. For $J_A \gg J_B$ the spontaneous helicoid magnetic structure with an absence of magnetic field is appeared with an appearance of magnetization in the “weak” B-subsystem at $T_s = T_C^B \ll T_C^A$. An external magnetic field at $T < T_s$ lead to decrease of spiral wave vector and disappearance of spiral at $H = H_c$ [2].

The numerical and analytical

minimization of the free energy of system (1) in the framework of mean field approximation shown, that on presence of the magnetic field the helicoid magnetic structure is appeared at higher temperatures $T_s < T < T_1 < T_C^A$. The wave vector of the induced long-period helicoid magnetic structure have a nonmonotonic field dependence (Fig.)



[1] D.H.Lyons, T.A.Kaplan, Phys.Rev. **120**,(1960) 1580.

[2] S.N.Martynov, A.D.Balaev, Pis'ma v Zh.Eksp.Teor.Fiz. **85**,(2007) 785 [JETP Letters **85**,(2007) 649].

23PO-12-18

CONDITIONS FOR THE SPIN-SPIRAL STATE IN ITINERANT MAGNETS

Timirgazin M.A., Arzhnikov A.K.

Physical-Technical Institute,
Ural Branch of Russian Academy of Sciences,
Kirov str. 132, Izhevsk 426001, Russia

In the last years noncollinear magnetic states have aroused a growing interest. The studies available in the literature have not clarified entirely the conditions for these states in transition metals and their alloys.

We investigate the conditions of stabilization of the spin-spiral (SS) type of magnetization in itinerant magnets. The main role in stabilization of the SS states belongs to the hybridization between the spin up and spin down electrons, the mixing of the spin states and the appearance of a hybridization gap in the dispersion law. This feature can be realized in the Hubbard model that is known to well reproduce main peculiarities of itinerant magnets to which the transition metals are subsumed.

Consideration of noncollinearity of magnetic moments results in a phase diagram which consists of regions of the SS and paramagnetic states depending on the number of electrons n_{el} and the parameter U/t (U is the Hubbard repulsion, and t is an overlap integral). The phase diagram has been found for the cubic and square lattices. For the square lattice we have obtained more correct diagram in comparison with [1, 2]. The SS state is found to be the ground one in transition metals in a wide range of the parameters of the model. The ferromagnetic and antiferromagnetic orders are realized as special cases of the SS state, and their regions are much narrowed in comparison with the collinear magnetic phase diagram.

Temperature behavior of the conditions for the SS ordering in plane square lattice is studied in the functional integration formalism.

The data obtained can be used in the first-principles calculations of magnetic structure of the transition metals and their alloys.

A perspective to control the SS wave length with the help of pressure or by change of the composition of alloy looks promising for technology.

[1] M. Dzierzawa, *Z. Phys. B*, **86** (1992) 49.

[2] B.-G. Liu, *J. Phys.: Cond. Mat.*, **6** (1994) L415.

23PO-12-19

ELECTRONIC, MAGNETIC AND LATTICE DYNAMICS PROPERTIES OF Co_3Al PHASES

*Nikitin N.Yu.¹, Bondarenko N.G.¹, Isaev E.I.^{1,2,3}, Vekilov Yu.Kh.¹, Johansson B.^{3,4},
Abrikosov I.A.²*

¹Theoretical Physics Department, Moscow State Institute of Steel and Alloys (Technological University), 4 Leninskii prospect, Moscow 117049, Russia

²Department of Physics, Chemistry and Biology (IFM), Linköping University, SE-581 8

³Condensed Matter Theory Group, Physics Department, Uppsala University, S-751 21 Uppsala, Sweden

⁴Applied Materials Physics, Materials Science Department, The Royal Technological University, SE-100 44 Stockholm, Sweden

Co-based alloys recently attracted of great interest due to elaboration of $\text{Co}_3(\text{W},\text{Al})$ alloy with possible high operating temperature combined with high strength [1]. In fact, L1_2 Co_3Al intermetallic compound has to be considered as a metastable phase, because it is absent in the available experimental equilibrium phase diagram for the Co-Al system and it can exist either in highly defective lattice [2] or in the perovskite type Co_3AlC phase [3] when the cubic lattice is stabilized by C which occupies the octahedral positions in fcc structure. In order to investigate the structural, electronic, magnetic and dynamical properties of L1_2 Co_3Al and related compounds we have performed first-principles calculations based on density functional perturbation theory [4], ultrasoft pseudopotentials [5,6], and generalized gradient approximation (GGA) to the exchange-correlation functional [7]. We have calculated the band structure and electron density of states (DOS) for nonmagnetic Co_3Al and Co_3AlC , and ferromagnetic Co_3Al . For the latter we found that magnetic moment Co_3Al is around $4.50 \mu_B$ per cell. As concerns correlation between the structural stability and DOS at the Fermi level, ferromagnetic Co_3Al is preferred compared to nonmagnetic one. Calculated phonon spectra indicate the dynamical stability for both ferromagnetic Co_3Al phase and nonmagnetic Co_3AlC , as well as dynamical instability for nonmagnetic Co_3Al at the equilibrium lattice parameter.

Financial support from RFBR (06-02-17542 and 07-02-01266) is acknowledged.

- [1] J. Sato, T. Omori, K. Oikawa, I. Ohnuma, R. Kainuma, K. Ishida, *Science*, **312** (2006), 90.
- [2] V. K. Portnoi, K. V. Tret'yakov, and V. I. Fadeeva, *Inorganic Materials*, **40**(9), (2004) 1073.
- [3] W. Fu-Gao, H. Keum-Yeon, M. Yoshinao, *Intermetallics*, **9** (2001) 671
- [4] S. Baroni, S. De Gironcoli, A. Dal Corso, and P. Giannozzi, *Rev. Mod. Phys.*, **73** (2001) 515.
- [5] D. Vanderbilt. *Phys. Rev. B.*, **41**(11) (1990) 7892.
- [6] A. M. Rappe, K. M. Rabe, E. Kaxiras, and J. D. Joannopoulos, *Phys. Rev. B*, **41** (1990) 1227.
- [7] J. P. Perdew, K. Burke, and M. Ernzerhof, *Phys. Rev. Lett.*, **77** (1996) 3685.

23PO-12-20

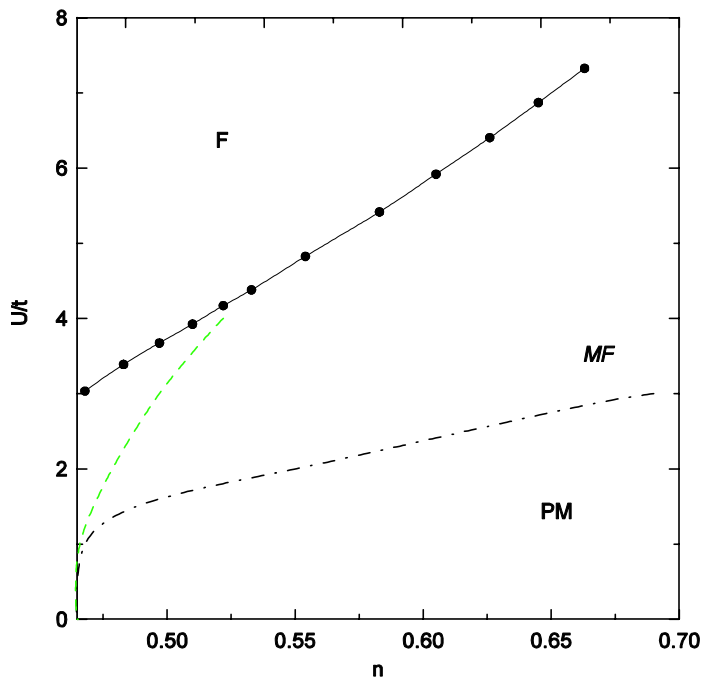
MAGNETIC FLUCTUATIONS AND ITINERANT FERROMAGNETISM IN TWO-DIMENSIONAL SYSTEMS WITH VAN HOVE SINGULARITIES

Igoshev P.A.¹, Katanin A.A.^{1,2}, Irkhin V.Yu.¹

¹Institute of Metal Physics, Ekaterinburg, Russia

²Max Planck Institute for Solid State Research, Stuttgart, Germany

The criterion of ferromagnetism for a two-dimensional (2D) itinerant electron system on the square lattice is analyzed. We assume that the Fermi level is near the Van Hove singularity (VHS), so that the electronic spectrum has the form $\varepsilon_k = -2t[\cos(ak_x) + \cos(ak_y)] + 4t'[\cos(ak_x)\cos(ak_y) + 1]$, $t'=0.45t$, a being a lattice parameter, t and t' the transfer integrals for nearest and next-nearest neighbors.



We obtain the spin-fermion model as a result of separation of the particle-hole channel from the single-band Hubbard electron-electron interaction U . This is correct for the paramagnetic state at low temperature provided that the ground state is ferromagnetically ordered. The spin-fermion model describes the interaction of electrons with collective paramagnon excitations which give the main contribution to thermodynamics. It was argued that relevant magnetic fluctuations in this case are purely static and constrained to fluctuate together on different sites. The criterion of ground-state ferromagnetic ordering originates from the requirement of the stability of the paramagnon spectrum. We use it to

determine the critical values of U at different values of electronic concentration n . The quasistatic approach is applied. The phase diagram in the $n-U/t$ plane is shown in the figure (calculated phase separation line is solid, dashed line is the functional renormalization group result, and dot-dashed line is the mean-field result, n being referred to the Van Hove filling $n_{\text{VH}} = 0.466$). The critical interaction U_c remains finite at the Van Hove filling and exceeds considerably the value obtained from the Stoner criterion because of the incommensurate spin fluctuations which are expected to be important near the ferromagnetic quantum phase transition.

The results obtained may give a basis for further investigations of itinerant systems in the vicinity of the ferromagnetic instability in the presence of VHS. More detailed investigations of the vicinity of the quantum phase transition and of the role of non-analytic corrections in the system with VHS are required. It is also of interest to investigate a possibility of triplet pairing in such systems.

[1] P. A. Igoshev, A. A. Katanin, V. Yu. Irkhin, *Sov. Phys. JETP* **105** (2007) 1043.

[2] P. A. Igoshev, A. A. Katanin, V. Yu. Irkhin, ArXiv:cond-mat/0709.3219v1.

23PO-12-21

MAGNETISM OF FeN FROM FIRST PRINCIPLES

Kartsev A.I.², Isaev E.I.^{1,2,3}, Vekilov Yu.Kh.¹, Abrikosov I.A.³, Johansson B.^{2,4}

¹Theoretical Physics Department, Moscow State Institute of

Steel and Alloys (Technological University), 4 Leninskii prospect, Moscow 117049, Russia

²Condensed Matter Theory Group, Physics Department, Uppsala University, S-751 21 Uppsala, Sweden

³Department of Physics, Chemistry and Biology (IFM), Linköping University, SE-581 83 Linköping, Sweden

⁴Applied Materials Physics, Materials Science Department, The Royal Technological University, SE-100 44 Stockholm, Sweden

Using first principles density functional perturbation theory [1] and ab initio ultrasoft pseudopotentials [2,3] and generalized gradient corrections to the exchange-correlation functional [4], we have investigated structural, electronic, magnetic and dynamical properties of stoichiometric iron mononitrides within NaCl, CsCl, ZnS (zinc blend and wurtzite), NiAs, and NbO phases. According to results of our total energy calculations nonmagnetic zinc blend FeN is the most stable phase and under high hydrostatic pressure it should transform to nonmagnetic NiAs-type phase in contrast to previous calculations. According to phonon dispersions calculated zinc blend FeN is dynamically unstable, but it can be stabilized by a small lattice expansion. The existence range for zinc blend FeN is rather small, $a_0=4.331\text{--}4.359\text{\AA}$, and further small lattice expansion yields dynamically stable zinc blend type FeN with antiferromagnetically ordered Fe atoms in the [110] plane. Our results suggest that different phases obtained experimentally for FeN films can be explained as a substrate effect. Obviously, the stresses between the substrate and sample are appeared during the growth process, and depending on substrate and temperature, FeN film is expanded that allows FeN to crystallize in dynamically stable zinc blend type structures.

Financial support from RFBR (06-02-17542 and 07-02-01266) is acknowledged.

[1] N. E. Zein, *Fiz. Tverd. Tela*, Leningrad, **26** (1984) 3024 [*Sov. Phys. Tech. Phys.*, **26** (1984) 1825]; S. Baroni, S. De Gironcoli, A. Dal Corso, and P. Giannozzi, *Rev. Mod. Phys.*, **73** (2001) 515.

[2] The pseudopotential was originally generated by A. Dal Corso, for details see <http://www.pwscf.org/pseudo.htm/>.

[3] A. M. Rappe, K. M. Rabe, E. Kaxiras, and J. D. Joannopoulos, *Phys. Rev. B*, **41**, (1990) 1227.

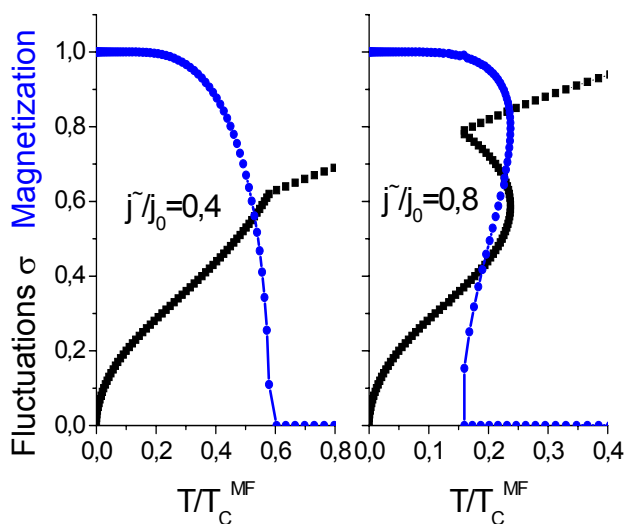
[4] J. P. Perdew, K. Burke, and M. Ernzerhof, *Phys. Rev. Lett.*, **77** (1996) 3685.

23PO-12-22

A FLUCTUATING FIELD THEORY FOR SYSTEMS OF LOCALIZED MAGNETIC MOMENTS

Grebennikov V.I.

Institute of Metal Physics RAS, Ekaterinburg, 620041, Russia, e-mail: greben@imp.uran.ru



Recent progress in the theory of itinerant-electron magnetism is based on representation electron-electron interactions through the fluctuating exchange field [1-3]. Here we develop a self-consistent fluctuating field (FF) theory for the localized-magnetic-moment systems. It generalizes the well-known mean field (MF) theory and describes ferromagnets at all temperatures including phase transitions. As distinct from the MF theory with one unknown value \bar{V} , the FF theory deals with two unknowns: an average value

\bar{V} of field V , and its dispersion σ^2 . As a result the equations obtain new classes of solutions. In particular, besides the usual second-order transitions, they describe the first-order transitions, too. The FF approach is very useful for simulation of low-dimensional and anisotropic systems by setting preferred direction of fluctuating field.

Let's consider a system of located spin moments S and introduce fluctuating exchange field using the Stratonovich-Hubbard transformation. Calculating free energy in the second-order over ΔV , we obtain equations FF theory in the following simplified form. An average value \bar{V} of exchange field V is determined by standard Brillouin function $B_S : \bar{V} = j_0 S \langle B_S(V/T) \rangle$. Here j_0 is the exchange integral at zero wave vector; the angle brackets denote integration with the normal law function: $f(V) = \exp\{-(V - \bar{V})^2 / 2\sigma^2\} / \sigma\sqrt{2\pi}$ with a dispersion value $\sigma^2 = \tilde{j}T / [1 - (\tilde{j}S/T) \langle B_S(V/T) \rangle]$, where T is temperature and \tilde{j} stands for effective exchange integral in single-site susceptibility. At $\sigma \rightarrow 0$ our equations go into ordinary MF theory. Results for spin $S = 1/2$ are shown at the figure for two cases: weak (left) and strong fluctuations (right). Average value \bar{V} (magnetization) and root-mean-square fluctuations σ are given in the units of $V_0 = Sj_0$; temperature T is specified in units of the Curie temperature in the MF theory T_C^{MF} .

The basic results: (1) Fluctuations reduce considerably critical temperature T_C of phase transition. (2) A slope of magnetization curve near T_C increases in systems with strong fluctuations. (3) The first-order transition accompanied by temperature hysteresis arises in systems with large single-site susceptibilities. The unstable branch with an inverse inclination on temperature is shown in the right figure.

Work is supported by the Russian Foundation for Basic Researches (the project No 08-02-00904).

[1] J. Hubbard, *Phys. Rev. B* **20** (1979) 4584.

[2] V.I. Grebennikov, Yu.I. Prokop'ev, O.B. Sokolov, E. Turov, *Fiz. Met. Metalloved.* **52** (1981) 679.

[3] V.I. Grebennikov, *JMMM* **84** (1990) 59.

23PO-12-23

IMPURITY ASSISTED INTERLAYER EXCHANGE COUPLING IN IRON/SILICON MULTILAYERS

Menshov V.N.¹, Tugushev V.V.¹, Kulatov E.T.²

¹Russian Research Center Kurchatov Institute, Kurchatov sq.1, 123182, Moscow, Russia

²A.M.Prokhorov General Physics Institute, Vavilov st.38, 119991, Moscow, Russia

During the last years the iron/silicon multilayers became a particular topic of experimental and theoretical researches, due to their unusual yet not fully explained magnetic properties. Though a number of works have been done to understand the mechanism of interlayer exchange coupling (IEC), i.e. the coupling between Fe layers across the Si spacer, the results are still controversial. The most intriguing are the unusual dependences of the IEC integral $J(T,L)$ on the temperature (T) and the spacer thickness (L); the main features of the $J(T,L)$ dependence are still unexplained. The antiferromagnetic character of $J(T,L)$ is well established for all temperatures at large $L > L_{\max}(T)$, where the characteristic thickness $L_{\max}(T)$ lies in the wide

range of L , from $\sim (8-10) \text{ \AA}$ up to $\sim (18-20) \text{ \AA}$. Experiments have shown the pronounced maximum of $J(T,L)$ at $L_{\max}(T)$ and the change of type of IEC from antiferro- to ferromagnetic at small $L < L_{\max}(T)$. Interpretation of the IEC data in terms of a simple tunneling between metallic layers across the semiconductor spacer is hampered by the lack of knowledge about the spontaneously formed iron-silicide interlayer, due to Fe diffusing into Si spacer through the Fe/Si interface. There were various suggestions on the composition of this interlayer, from the nonmagnetic semimetal with the bcc structure (c-FeSi) to the more complex compounds.

Here we develop a new approach to IEC in Fe/Si multilayers, based on the idea that contact induced ferromagnetic phase of body-centered-cubic iron silicide and spin-polarized interfacial states are formed at the Fe/Si boundaries. We show that strong exchange coupling between Fe layers can be effectuated by means of the superexchange between the spin-polarized interfacial states through the deep impurity states in strongly compensated non-degenerated semiconductor spacer. We calculated the IEC integral using the averaged T-matrix approximation for the electron-impurity scattering. The complex and unusual dependence of IEC on the spacer thickness and composition can be successfully explained in terms of competition between antiferromagnetic and ferromagnetic components of the impurity assisted superexchange. Our model qualitatively explains all existing experimental results.

The work is supported by the grant of RFBR 07-02-01252-a.

23PO-12-24

INVESTIGATION OF THE CRITICAL PROPERTIES IN THE 3D SITE-DILUTED POTTS MODEL

Murtazaev A.K., Babaev A.B., Aznaurova G.Ya.

Institute of Physics, Daghestan Scientific Center, Russian Academy of Sciences,
ul. Yaragskogo 94, 367003 Makhachkala, Russia

The investigation of phase transitions and critical phenomena of magnetics containing the impurities and other structure defects is of great theoretical and experimental interest [1]. A majority of real solids contain impurities and other structure defects which influence on their thermodynamic characteristics, particularly, a behavior of the systems of the phase transitions. Therefore lately the attempts of researchers are directed at understanding how the structure defects influence on a behavior of different systems at the phase transitions. When study the critical properties of disordered spin systems are distinguished the systems with quenched and annealed impurities. In solids the impurities are usual quenched. A presence of quenched impurities is revealed as random disturbance of the local critical temperature. In a case of the spin systems, experiencing the first order phase transitions in a homogeneous state, the impurities lead to smoothing of this transition close to induction the second order phase transition in them.

In this work, the influence of quenched nonmagnetic impurities on the phase transitions in the three-dimensional Potts model with the number of spin states $q=3$ was studied by the Monte-Carlo method. The Hamiltonian of studied system can be written as:

$$H = -\frac{1}{2} J \sum_{i,j} \rho_i \rho_j \delta(S_i, S_j), \quad S_i = 1, 2, 3, \quad (1)$$

where $\delta(S_i, S_j) = \begin{cases} 1, & \text{если } S_i = S_j \\ 0, & \text{если } S_i \neq S_j \end{cases}$, $S_i, S_j = \pm 1$, $\rho_i = 1$, if a site i is occupied by the magnetic atom, and $\rho_i = 0$, if in a site i locates the nonmagnetic impurity, J is the exchange interaction. The

investigation is carried out on the basis of Wolff single-cluster algorithm [2] for systems with linear sizes $L=20\div 46$ at the spin concentrations $p=1.0; 0.9; 0.8; 0.7; 0.65$.

By means of the fourth order Binder cumulants method the second order phase transition is shown to be observed in this model at spin concentration $p=0.9; 0.8; 0.7; 0.65$, and for pure model ($p=1.0$) to be occurred the first order phase transition. On the basis of the finite-size scaling theory are calculated the static critical exponents of heat capacity α , susceptibility γ , magnetization β and exponent of correlation radius ν .

This work was supported by the Russian Foundation for Basic Research (Project No. 07-02-00194), the State Program of Support for Leading Scientific Schools of the Russian Federation (Project No. NSh-5547.2006.2). A.K.M. acknowledges the support of the Russian Science Foundation.

[1] S.-k. Ma. *Modern Theory of Critical Phenomena* (Benjamin/ Cummings, London, (1976).

[2] K. Binder, *Z. Phys. B* **43**, 119 (1981).

23PO-12-25

THE INVESTIGATION OF 3D ANNNI MODEL BY THE MONTE-CARLO METHODS

Murtazaev A.K., Ibaev J.G.

Institute of Physics DSC RAS, 367003 RD s. Makhachala st. M. Yaragsckogo 94, Russia

The investigation of phase transitions in complex magnetics is still remains a basic problem of the condensed matter physics. As theoretical investigation of such models are connected with significant difficulties of principle character in the foreground stand different numerical methods. The most popular is Monte-Carlo methods.

Till recently these methods have been applied to investigate the simple models of the first approximation. Lately they are used for investigation of exotic systems such as crystal superstructures, impure and frustrated systems, long-periodic modulated structures.

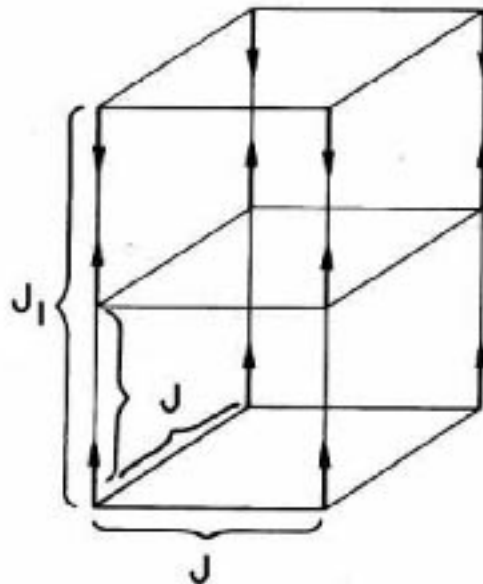
In the work we study the long-periodic modulated structures of 3D ANNNI model by means of Monte-Carlo methods on the basis of Metropolis standard algorithm. This model has been offered in 60-s of the last century [1] and till now remains as most simple and universal model of the static physics applied for qualitative description of modulated magnetic structures.

The Hamiltonian of the studied model can be shown as

$$H = -\frac{1}{2}J\sum_{i,j}(S_i \cdot S_j) - \frac{1}{2}J_1\sum_i(S_i \cdot S_{i+1})$$

where $J>0$ is a parameter of ferromagnetic interaction of first nearest neighbors $J_1<0$ is a parameter of antiferromagnetic interaction of the second nearest neighbors on Z axis direction.

The investigations are carried out in cubic shape systems with periodic boundary conditions and sizes $L=8, 12, 16, 20, 24, 28, 32, 50, 64$. The number of spins N_{eff} in simulated systems is 512, 1728, 4096,



8000, 13824, 21952, 32768, 6400, 12500 и 262144. The Markovian chain up to 10^5 MC steps per spin are generated in a computer. To bring the system in to the equilibrium state there are cut off the nonequilibrium sections of up to 10^4 MC steps per spin.

We consider a character of the temperature dependence of thermodynamic parameters and the wave vector of modulated structures. Also we carried out the Furie analysis of appeared structures and determined the stability boundaries of different phases appeared in the system.

This work was supported by the Russian Foundation for Basic Research (Project No. 07-02-00194), the State Program of Support for Leading Scientific Schools of the Russian Federation (Project No. NSh-5547.2006.2). A.K.M. acknowledges the support of the Russian Science Foundation

[1] R.J. Elliot *Phys. Rev.* **124** (1961) 346

23PO-12-26

TEMPERATURE HYSTERESIS IN THE DYNAMIC SPIN-FLUCTUATION THEORY FOR STRONG FERROMAGNETS

Reser B.I.¹, Grebennikov V.I.¹, Melnikov N.B.²

¹Institute of Metal Physics, Ural Branch of the Russian Academy of Sciences,
18, Kovalevskaya St., 620219 Ekaterinburg, Russia

²Department of Computational Mathematics and Cybernetics,
Moscow State University, 119992 Moscow, Russia

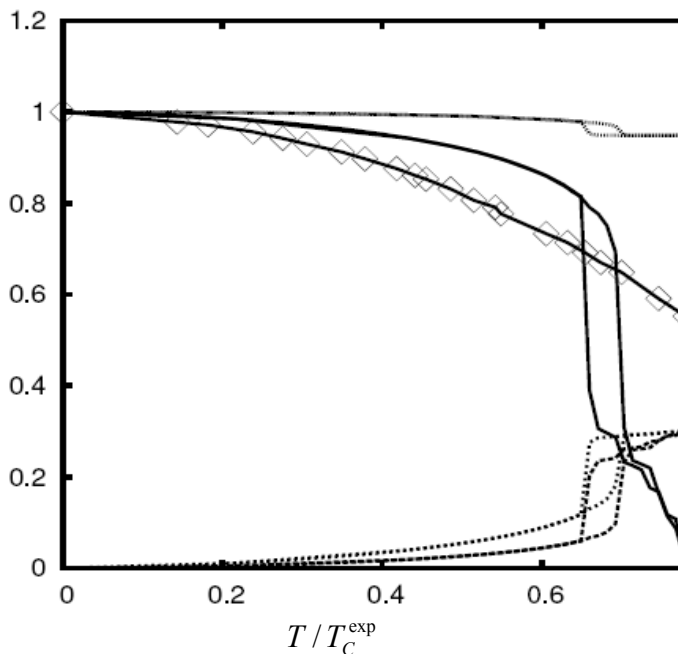


Fig. 1. The magnetization $m(T)/m(0)$ (— calculation, $\diamond\diamond$ experiment [3]), the mean square of fluctuations $\langle \Delta V_x^2 \rangle(T)$ (.....) and $\langle \Delta V_z^2 \rangle(T)$ (---) in units of $\langle V_z \rangle^2(0)$, the reciprocal paramagnetic susceptibility

Calculations showed that the solution to the system of equations of the spin-fluctuation theory can become unstable below the Curie temperature, T_C . It is especially pronounced in Fe [1] and Fe-Ni alloys [2], where spin fluctuations increase sharply in this region (Fig. 1).

In [4, 5], by the example of the $\text{Fe}_{0.65}\text{Ni}_{0.35}$ invar, we investigated the temperature dependence of magnetic properties in the dynamic nonlocal approximation of the spin-fluctuation theory (DSFT) using several numerical methods. The methods give satisfactory results over a wide range of temperatures and produce a discontinuous jump near the phase transition temperature. The calculation with the cyclic change of temperature shows that the jump of the magnetic characteristics in the DSFT is of hysteresis type. This yields that the instability is not related to the

calculation method, but to the system of equations itself. Hence we conclude about the effectiveness and applicability of the numerical methods. Furthermore, applying the methods of the catastrophe theory, we show that the hysteresis can be eliminated by small changes in the initial data. Finally, we discuss the improvements of the DSFT directed towards better description of the experiment at high temperatures.

Support by RFBR (grant no. 06-01-00148) is acknowledged.

- [1] B.I. Reser, V.I. Grebennikov, *Phys. Met. Metallogr.*, **85** (1998) 20
- [2] B.I. Reser, *J. Phys.: Condens. Matter*, **16** (2004) 361
- [3] J. Crangle, G.C. Hallam, *Proc. Roy. Soc., A* **272** (1963) 119
- [4] N.B. Melnikov, B.I. Reser, in *Proc. Dynamic Systems and Appl.*, vol. 5, Atlanta, 2008
- [5] B.I. Reser, N.B. Melnikov, *J. Phys.: Condens. Matter*, **20** (2008), submitted

23PO-12-27

FIRST-PRINCIPLES CALCULATIONS IN THE MOSSBAUER SPECTRA PROCESSING

Arzhnikov A.K., Dobysheva L.V.

Phys.-Techn.Inst., Ur.Br., Rus.Ac.Sci., 426001 Izhevsk, Kirova str, 132, Russia

Analysis of the Mossbauer spectra (MS) of alloys, disordered materials, or nano-sized structures is a complicated task. First, from the mathematical point of view, this is a noncorrect task, the spectrum can be described by different sets of subspectra with equal accuracy. Second, from the point of view of physics, often one cannot surely bind up the set of subspectra obtained with certain peculiarities of crystalline or chemical structure of the sample. Modern first-principles calculations can give a reliable information on hyperfine magnetic fields (HFF), isomer shifts (IS), quadrupole splittings (Q), local magnetic moments (M) and so forth, which allows one to limit possible solutions of the inverse problem in the processing of spectra and correctly understand the physical picture in the sample.

With the help of concrete examples, the paper demonstrates different aspects of the use of the first-principles calculations for the analysis of the MS of the Fe-Si, Fe-Sn, $\text{Fe}_3(\text{Si}_{1-x}\text{Ge}_x)$, Fe_5SiC , Fe_3C systems. In the Fe-Si alloys with Si concentration 13-33 at. %, ordered by the DO3 type, shown is a possibility to analyse the chemical environment up to the third coordination sphere of atomic environment using the experimental data, and the calculations show reliability and admissible interpretations of the experimental information obtained. Similar analysis of the $\text{Fe}_{75}(\text{Si}_{1-x}\text{Ge}_x)_{25}$ alloys allows one to colligate the MS peculiarities with a deviation of the Fe concentration from 75 at. %. The preliminary processing of MS of the Fe_5SiC compound, recently obtained with mechanical alloying, raised doubts as the intensities of the components did not correspond with the structure. Using the calculated HFF, IS and Q results in a more correct MS processing. The first-principles calculations of the Fe_3C cementite show that absence of the quadrupole splitting in the MS under the Curie temperature is not due to a special angle between the HFF and electric field gradient (55 grad) as it was believed earlier, but is a consequence of a superposition of two subspectra from non-equivalent iron positions.

23PO-12-28

SPIN FLUCTUATIONS AND STRUCTURAL PHASE TRANSITIONS IN ITINERANT PARAMAGNETS

Solontsov A.^{1,2}

¹State Center for Condensed Matter Physics, 123060, Rogova str.5a, Moscow, Russia

²A.A.Bochvar Institute for Inorganic Materials, 123060, Moscow, Russia

It is well known that spin fluctuations (SF) in itinerant electron magnets may strongly influence the stability of magnetic phases and cause magnetic transitions due to spin anharmonicity resulting in their coupling with the magnetic order parameter. Besides that SF may be strongly coupled to the crystal lattice affecting thermal expansion and giving rise to the Invar anomaly observed in transition metals. Recently it became clear that in itinerant magnets besides thermal SF an essential role is paid by quantum zero-point SF, which give rise to strong spin anharmonicity and essentially affect magneto-volume phenomena [1].

However, up to now SF were not related to structural phase stability and structural transitions in itinerant paramagnets though experiments in some rare earths and actinides presented direct evidence for coupling of structural transformations to their magnetic properties. First we shall point to the isostructural $\gamma \rightarrow \alpha$ transition in fcc paramagnetic *Ce* accompanied by a $\sim 12-17\%$ volume contraction in the low-temperature α - phase, with a more than 3 times drop in the magnetic susceptibility and essential softening of the elastic moduli. The structural transformation was shown to be suppressed in magnetic fields $\sim 56\text{T}$. Together with the observed by inelastic neutron scattering SF this directly points to the magnetic origin of the $\gamma \rightarrow \alpha$ transition in *Ce*, driven by SF.

Another candidate for the magnetic mechanism of phase transitions is paramagnetic plutonium which possesses a cascade of phase transformations with a 25% volume change between monoclinic α - and fcc δ - phases, and discontinuities of the magnetic susceptibility $\sim 5\%$ at structural transitions also suggesting strong magneto-volume coupling and a magnetic mechanism of $\delta \rightarrow \alpha'$ structural transition caused by SF.

Here we suggest a novel mechanism of structural phase transitions in itinerant paramagnets based on the essential role of SF acting according to the following scenario we have briefly outlined recently [2]. In the low-temperature α -(or α') phase the bulk modulus is negative due to electronic correlations resulting in the attractive effective interactions of Fermi quasiparticles. The stabilisation of the low-temperature phase then results from its contactation described by the order parameter related to the volume strain. We show that the SF contribution to the bulk modulus is positive and raises with the temperature proportionally to the total squared amplitude of SF, accounting for the both thermal and zero-point contributions. As a result, the bulk modulus changes its sign near the temperature of the phase transition making the high-temperature γ -(or δ) phase stable. We believe that the suggested SF mechanism may explain the $\gamma \rightarrow \alpha$ and $\delta \rightarrow \alpha'$ transitions in *Ce* and *Pu* compounds where the transitions are affected by both SF and softening of bulk moduli.

Financial support by the Russian Federal Agency for Atomic energy is gratefully acknowledged. The work was also supported by the Russian Foundation for Basic Research under the grant No 06-02-17291a and the programme "Strongly Correlated Electrons in Semiconductors, Metals, Superconductors, and Magnetic Materials" of the Russian Academy of Sciences. The Federal support of the leading scientific schools of Russia (grant No SH- 4122.2006.2) is also appreciated.

[1] A. Solontsov, *Int. J. Mod. Phys. B*, **19** (2005) 3631.

[2] A. Solontsov, A. Mirmelshtein, *Phys. Lett. A*, **372** (2008) 2086.

23PO-12-29

QUANTUM MONTE CARLO STUDY OF PSEUDOGAPS IN HUBBARD MODEL

Kenjaev Z.M.¹, Mukimov Z.M.², Kenjaev A.M.³

¹Bukhara State University, 705018 Bukhara, Uzbekistan

²Applied Physics Institute of NUUZ, 700174 Tashkent, Uzbekistan

³Tashkent University of Informational Technology, 700011 Tashkent, Uzbekistan

We study the pseudogaps in the spectra of the half-filled 2D Hubbard model using dynamical cluster approximation (DCA) quantum Monte Carlo calculations. A charge pseudogap, accompanied by non-Fermi liquid behaviour in the self energy, is shown to persist in the thermodynamic limit. The DCA method systematically underestimates (overestimates) the width of the pseudogap. A spin pseudogap is not seen at half-filling.

This research was supported by the Fundamental Research Foundation under Grant OT – Φ 2 – 086.

23PO-12-30

STUDY OF THE MAGNETIC STRUCTURE OF THE LOW-DIMENSIONAL MAGNETS UPON ORBITAL ORDERING BY QUANTUM MONTE CARLO METOD

Piskunova N.I.¹, Aplesnin S.S.^{1,2}, Moskvin A.I.¹

¹M.F. Reshetnev Siberian Aerospace State University, Krasnoyarsk, 660014, Russia

²L.V. Kirensky Institute of Physics, SB RAS, Krasnoyarsk, 660036, Russia

e-mail: apl@iph.krasn.ru , piskunova@sibsau.ru

Magnetic materials with double orbital quasi-degeneration are characterized not only by spin-dependent interaction, but also by the dependence of the exchange integral on the mutual position of the orbitals. The interplay of spins with the charge-orbital ordering changes not only magnetic properties, but also transport characteristics, for example, gives rise to giant magnetoresistance in manganites. The orbital ordering forms a quasi-low-dimensional structure in $KCuF_3$ [1] and possibly results in the formation of quantum states without the long-range magnetic order in $KCuF_3$.

This study is aimed to determination of the effect of the exchange interaction between e_g electrons on the ordering $d_{2x^2-z^2-y^2}$ and $d_{x^2-y^2}$ orbitals in a Mott insulator and estimation of a region of the parameters, at which the magnetic order dimensionality changes from quasi-two-dimensional antiferromagnetic. We propose a new mechanism of the formation of a gapless spin liquid state and the occurrence of a plateau in the field dependence of magnetization.

Let us consider a model with antiferromagnetic anisotropic exchange alternation in a chain and a square lattice for a spin $S=1/2$ with the exchange interaction $J(1 + \delta)$, $J(1 - \delta)$ ($J < 0$)

between electrons located at the nearest $d_{2x^2} - d_{2x^2}$, $d_{x^2-y^2} - d_{x^2-y^2}$, $d_{x^2-y^2} - d_{2x^2}$ orbitals in the external magnetic field.

As a calculation method, the quantum Monte Carlo method is used that combines two algorithms [2, 3], namely the world-line algorithm and the continuous time one for the spin $S=1/2$. Monte Carlo calculations are carried out with the nonuniform exchange distribution and periodic boundary conditions in the Trotter direction and on the chain $L=400$ [4].

We have found the exchange parameters associated with the relation of the exchange interaction of electrons on the $d_{2x^2} - d_{2x^2}$ and $d_{x^2-y^2} - d_{x^2-y^2}$ orbitals and exchange anisotropy, at which the ordering of pair of the $d_{2x^2} - d_{2x^2}$ and $d_{x^2-y^2} - d_{x^2-y^2}$ orbitals forms a gapless quantum spin liquid with a finite correlation radius and the quasi-low-dimensional antiferromagnetic state [4]. The phase boundary of the transition from a spin liquid to the antiferromagnetic state induced by suppression of the quantum fluctuations in magnetic field has been determined in a plane magnetic field-exchange alternation. The regions of existence of an antiferromagnet with a stripe structure in dependence on the relation of exchange anisotropy parameters and exchange interaction alternation have been calculated.

This work was supported by the Russian Foundation for Basic Research project no.05-02-97710.

- [1] K.I. Kugel', D.I. Khomsky, *Sov. Phys. Usp.*, **25** (1982) 231.
- [2] N.V. Prokof'ev, B.V. Svistunov, *Phys. Rev. Lett.*, **81** (1998) 2514.
- [3] S.S. Aplesnin, *JETP* **97** (2003) 969.
- [4] S.S. Aplesnin, N.I. Piskunova, *JETP Letters*, **85** (2007) 644.

24 June Tuesday

10:00-11:30

plenary lectures

24PL-A

24PL-A-1

ELECTRIC FIELD ACTIVATION OF MAGNETISM IN METALS

Givord D.¹, Weisheit M.^{1,2}, Fähler S.^{1,2}, Marty A.³, and Souche Y.¹

¹Institut Néel, CNRS/UJF, Grenoble, France

²IFW Dresden, Institute for Metallic Materials, Dresden, Germany

³INAC-CEA Grenoble, France

Electric field activation of the magnetic properties may emerge as an alternative to magnetic field or electric current activation to control the properties of various types of micro-actuators developed today to fulfil functions required by modern technology. With respect to usual activation procedures, substantial gain in terms of device architecture and power consumption is expected since no permanent electric current is required. Recent results in this field, obtained in insulating magnetic systems, will be summarised. In metals, electric field activation was essentially neglected, based on the argument that an electric field does not penetrate into bulk metals, thus reducing dramatically the size of the expected effects. This does not apply in the case of nanomaterials where the surface to volume ratio is high. We demonstrated that the magnetocrystalline anisotropy of ordered iron-platinum (FePt) and iron-palladium (FePd) intermetallic compounds can be reversibly modified by an applied electric field when immersed in an electrolyte [1]. A voltage change of -0.6 volts on 2-nanometer-thick films altered the coercivity by -4.5% and by $+1\%$ in FePt and FePd, respectively. Attributing the modification of the magnetic parameters to a change in the number of unpaired d electrons in response to the applied electric field, semi-quantitative agreement with electronic structure calculations is obtained. Potential applications of electric field activation in metals will be discussed finally.

[1] .Weisheit, S.Fähler, A.Marty, Y.Souche, C.Poinsignon, D.Givord, Science, 315 (2007) 349

24PL-A-2

COEXISTENCE OF SUPERCONDUCTIVITY AND MAGNETISM IN MULTILAYERED SUPERCONDUCTOR-FERROMAGNET STRUCTURES

Ryazanov V.V.

Institute of Solid State Physics, Institutskaya 2, Chernogolovka, Moscow district, 142432 Russia

The talk reviews recent achievements in the field of fabrication and investigation of artificial multilayered superconductor-ferromagnet (SF-) structures with mutual interplay of superconductivity and magnetism. For many years the coexistence of these two classes of phenomena have not been considered as an exciting and challenging thing because of their incompatible electron spin ordering: the exchange field, in a magnetically ordered state, tends to align spins of Cooper pairs in the same direction, therefore preventing pairing effect [1]. However, recent measurements have confirmed a number of theoretical predictions for SF-structures like so-called π -state in SFS junction [2] and the FSF-spin valve effects [3]. Observation of superconductivity with a triplet pairing [4] and inverse magnetization in a superconductor close to the SF-interface [5] are the next in turn.

The review is mostly based on the works related to the proximity and magneto-resistance effects in SF-systems that were carried out with the author's participation. Among the effects are

nonmonotonic behavior of the SFS junction critical currents vs. F-layer thickness with two nodes and reentrant temperature dependence of the critical current [6]; half-integer Shapiro steps and half-flux-quantum period of the Fraunhofer patterns resulting from anomalies of Josephson current-phase relation at the point of $0-\pi$ -transition. The transition to the π -state also manifested itself in the half-period shift of the magnetic field dependence of the critical current in the triangular SFS arrays and in the appearance of spontaneous supercurrents in the arrays even in case of zero magnetic field [7]. Experiments show that π -junctions and 'self-frustrated' superconducting networks with π -junctions may be used for the realization of the superconducting quantum bit and new superconducting 'complementary' electronics based on the analogy with complementary metal-oxide-semiconductor (CMOS) logic family, as well as for implementation a new modification of Rapid Single Flux Quantum superconducting logics.

A number of magneto-resistive experiments on SF-bilayers and FSF-trilayers will be also presented. The effects observed caused by electron and spin processes at SF-interfaces and influence of magnetic domain structure [8].

Support by Russian Foundation of Basic Researches and INTAS is acknowledged.

- [1] P.G. De Gennes, G.J. Sarma, *J. Appl. Phys.*, **34** (1963) 1380; J.J. Hauser, H.C. Theuerer, N.R. Werthamer, *Phys. Rev.*, **142** (1966) 118; N.V. Zavaritskii, V.N. Grigor'ev, *JETP Lett.*, **14** (1971) 73.
- [2] A.I. Buzdin, *Rev. Mod. Phys.*, **77** (2005) 935.
- [3] L.R. Tagirov, *Phys. Rev. Lett.*, **83** (1999) 2058.
- [4] F.S. Bergeret, A.F. Volkov, and K.B. Efetov, *Rev. Mod. Phys.*, **77** (2005) 1321.
- [5] F.S. Bergeret, A.F. Volkov, and K.B. Efetov, *Phys. Rev. B*, **69** (2004) 174504.
- [6] V.A. Oboznov, V.V. Bol'ginov, A.K. Feofanov, V.V. Ryazanov and A.I. Buzdin, *Phys. Rev. Lett.* **96** (2006) 197003.
- [7] S.M.Frolov, M.J.A.Stoutimore, T.A.Crane, D.J. Van Harlingen, V.A.Oboznov, V.V.Ryazanov, A.Ruosi, C.Granata, and M. Russo. *Nature Physics* **4** (2008) 32.
- [8] V.V. Ryazanov, V.A. Oboznov, A.S. Prokofiev, and S.V. Dubonos, *JETP Lett.* **77** (2003) 39.

24 June Tuesday

12:00-13:30

oral session

24TL-A

24RP-A

**“Diluted Magnetic
Semiconductors”**

24TL-A-1

ANISOTROPIC MAGNETORESISTANCE PHENOMENA IN FERROMAGNETIC SEMICONDUCTORS AND METALS

Jungwirth T.

Institute of Physics ASCR in Prague and University of Nottingham,
Prague 162 53, Czech Republic

Anisotropic magnetoresistance (AMR) sensors replaced in the early 1990s classical magneto-inductive coils in hard-drive readheads launching the era of spintronics. Their utility has, however, remained limited partly because the response of these ferromagnetic resistors to changes in magnetization orientation originates from generically subtle spin-orbit interaction effects. In this talk we demonstrate that despite the quantum-relativistic nature of the AMR the microscopic physical origin of the effect can be readily explained in ferromagnetic semiconductor ohmic devices and that the phenomenology of the AMR, containing non-crystalline and crystalline components, can be very rich. We then focus on AMR effects in tunnelling (TAMR) and Coulomb blockade (CBAMR) devices whose size can be orders of magnitude larger than the AMR in ohmic devices and, in the case of the CBAMR, can be electrically tunable in magnitude and sign. Both ferromagnetic semiconductor and metal TAMR and CBAMR structures will be discussed.

24TL-A-2

MAGNETIC AND MAGNETOTRANSPORT PROPERTIES OF 2D GaAs/InGaAs/GaAs STRUCTURES WITH Mn DELTA LAYER

Aronzon B.A.^{1,2}, Lagutin A.S.¹, Rylkov V.V.^{1,2}, Lashkul A.³, Laiho R.³

Zvonkov B.N.⁴, Danilov Yu.A.⁴

¹Russian Research Center “Kurchatov Institute”, Moscow, 123182 Russia

²Institute of Applied and Theoretical Electrodynamics, Russian Academy of Sciences,
Moscow, 127412 Russia

³Wihuri Physical Laboratory, Department of Physics, University of Turku, FIN-20014, Finland

⁴Physico-Technical Research Institute of N. Novgorod State University, 603950 N. Novgorod,
Gagarine Av., 32/3, Russia

e-mail: aronzon@imp.kiae.ru

A search for materials with the controllable spin polarization of charge carriers is among of the most topical issues of spintronics. In this connection, Dilute Magnetic Semiconductors (DMS) and especially Si and A³B⁵-type semiconductors attract currently a widespread attention. In such materials we have achieved the above room temperature ferromagnetic behavior. However for spintronics the 2D materials are very promising being compatible with modern technology. Having this in mind, we manufactured GaAs/InGaAs/GaAs quantum wells with a Mn δ -layer introduced into one of the GaAs layers and observed a magnetic ordering and different manifestations of the spin polarization of charge carriers. Here, we present the experimental data on the magnetization, anomalous Hall effect, magnetoresistance, and spectral density of the voltage noise, as well as the results of X-ray structural studies. The X-ray diffraction data demonstrated the absence of Mn in the quantum well. This favors the relatively

high mobility of carriers ($2000 \text{ cm}^2/\text{Vs}$) as compared to the DMS-based 2D structures studied earlier and implies that the exchange interaction between the magnetic moments of Mn is nonlocal and is mediated by the charge carriers located outside the Mn layer. Due to the high mobility value the spectrum of holes is really 2D resulting in observation of the Shubnikov-de Haas oscillations and the quantum Hall effect accompany with ferromagnetic behavior, in particular, the anomalous Hall effect at relatively high temperatures (60 K). As far as we know this is the highest Curie temperature value observed in really 2D systems based on dilute magnetic semiconductor which demonstrate quantum Hall effect and other 2D properties. The magnetic ordering in the structure under study is also detected by magnetization measurements and its unusual behavior will be also discussed. The magnetic ordering is responsible for the peculiarities in the structure transport properties, giving rise to the anomalous Hall effect and the hump in the temperature dependence of the electrical resistance $R(T)$, which is typical for systems with the ferromagnetic ordering. The temperature corresponding to the maximum in the $R(T)$ curve agrees well with the Curie temperature calculated assuming that ferromagnetic ordering is mediated by carriers inside the quantum well. The magnitude of the anomalous Hall effect is in a good agreement with its theoretical estimations for the 2D structures based on the assumption that the dominant mechanism underlying this effect has an intrinsic origin.

24RP-A-3

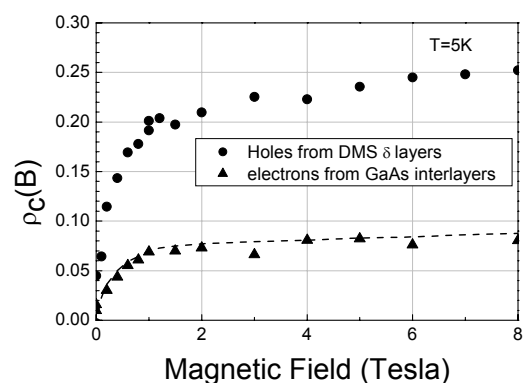
CARRIER SPIN POLARIZATION IN FERROMAGNET-SEMICONDUCTOR GaMn/GaAs STRUCTURES

Sapega V.F.^{1,2}, Kolovos-Vellianitis D.¹, Trampert A.¹, Ploog K.H.¹

¹Paul-Drude-Institut für Festkörperelektronik,
Hausvogteiplatz 5-7, D-10117 Berlin, Germany

²Ioffe Physico-Technical Institute, Russian Academy
of Sciences, 194021 St Petersburg, Russia

The effect of ferromagnetic layers on the spin polarization of holes and electrons in ferromagnet-semiconductor MnAs/GaAs structures is studied by means of hot electron photoluminescence (HPL). A set of superlattices with a fixed Mn δ layer thickness of 0.11 nm and different GaAs interlayer thicknesses varying in the range from 2.5 to 14.4 nm and a fixed number of periods (40) were grown by low temperature beam epitaxy to study the effect of interlayer distance on ferromagnetic properties of the structure. The HPL and its circular polarization in a magnetic field provide information on the acceptor binding energy and the spin polarization of holes [1] and free or bound electrons. Here, our study of the HPL demonstrates that the holes in δ layers of (Ga,Mn)As DMS occupy predominantly the Mn acceptor impurity band. The width of the impurity band decreases with the increase of the interlayer distance. The decrease of the impurity band width detected in the HPL spectra is explained by compensation of impurity bound holes by electrons supplied from the GaAs interlayers. These electrons originate from As antisites (double donors), which were also observed in the X-STM studies and from interstitial Mn (double donors). We found also that an



increase of the GaAs interlayer thickness softens the magnetic properties of the ferromagnetic layers as well as reduces the carrier polarization. The decrease of the hole polarization is explained by the in-plane stress induced by thick GaAs interlayers in-between the Mn δ sheets. Careful analysis of our data demonstrates that the increase of the distance between the DMS δ layers reduces the ferromagnetism in the studied structures in two ways. First of all, electrons coming from the interlayer regions effectively compensate the impurity band holes mediating ferromagnetism of ferromagnetic DMS δ layers. On the other hand, thicker interlayer regions induce stress in the DMS δ sheets. Due to this stress, the ground state of the impurity band becomes unpolarized. The spin polarization of free or donor bound electrons in the interlayer regions is studied. We show that electrons in the GaAs interlayers experience strong exchange interaction with the ferromagnetic interfaces. Comparison of the magnetization curves (Fig.1) of holes located in the ferromagnetic δ layers with that of electrons located in the interlayer regions demonstrates that holes in the DMS δ layers and electrons in the interlayer regions experience the same internal magnetic field originating from the ferromagnetic δ sheets. This internal field decreases rapidly with increasing distance between the ferromagnetic δ layers.

Support by RFBR (Grant No. 06-02-16245) is acknowledged.

[1] V. F. Sapega, M. Ramsteiner, O. Brandt, L. Deweritz, and K. Ploog, Phys. Rev. B **73**, 235208 (2006).

24RP-A-4

SPIN-DEPENDENT ELECTRON TRANSPORT IN A TYPE II GAINASSB/P-INAS HETEROJUNCTION DOPED WITH MN IN QUANTISED MAGNETIC FIELDS

*Moiseev K.D.¹, Parfeniev R.V.¹, Averkiev N.S.¹, Berezovets V.A.^{1,2}, Mikhailova M.P.¹,
Nizhankovskii V.², Kaczorowski D.³*

¹A.F. Ioffe Physico-Technical Institute, RAS, Saint Petersburg, 194021, Russia

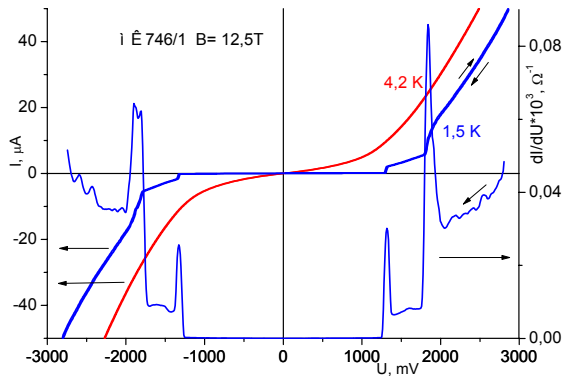
²International Laboratory of High Magnetic Fields and Low Temperatures,
Wroclaw, 50-204, Poland

³Institute of Low Temperature and Structure Research PAN, Wroclaw, 50-950, Poland

This report is devoted to a study of spin-transport properties in unique layered heterostructures containing δ -layer of atomic Mn and grown on InAs substrate doped with Mn. Planar and vertical quantum magnetotransport in a 2D electron-hole system at a single type II broken-gap InAs/GaInAsSb heterointerface has been studied in high magnetic fields under the quantum Hall regime up to 15 T at low temperatures $T=1.5$ K.

Lattice-matched GaIn_{0.09}As_{0.16}Sb/p-InAs single heterostructures with planar and abrupt heteroboundary were grown by LPE [1]. The quaternary p-GaInAsSb solid solution was both unintentionally doped and had a hole concentration of $p=2 \times 10^{16}$ cm⁻³ and doped with Te up to electron concentration of $n=2 \times 10^{17}$ cm⁻³ at 77 K. The p-type InAs(100) substrate was heavily compensated with Mn to a hole concentration of $p \sim 10^{17}$ cm⁻³ at $T=300$ K. 2 ML of atomic Mn was deposited on the 0.5 μ m-thick GaInAsSb epilayer and followed by p-GaSb cap layer by MOCVD using laser deposition. Since the top of the valence band of the solid solution enriched GaSb is lying higher in energy than the bottom of the InAs conduction band, self-consistent quasi-triangular quantum wells for 2D-electrons and holes have been forming at both sides of the type II broken-gap p-GaInAsSb/p-InAs heteroboundary. Filling of these wells is determined by

electron transfer across the interface owing to the doping level of contacting materials. An asymmetric potential profile of the quantum wells at the heteroboundary leads to Rashba spin-splitting of 2D-electron states near Fermi level in an absence of a magnetic field [2]. Presence of Mn ions in the InAs substrate and taking into account of their s-d exchange with 2D-electrons results in an enhancing of Landau levels spin-splitting which was found from Shubnikov-de Haas oscillations.



Spin-related structures for the lowest Landau level of 2D-electrons at the interface and magnetic moments of Mn δ -layer were observed as steps in I-V characteristics and spikes in the tunneling conductance measured at quantum Hall regime ($B > 12$ T) at 1.5 K. For filling number of $\nu = 2$ the value of dI/dU in co-linear case was higher in an order than for one in non-co-linear case and their ratio increases with magnetic field increasing.

Support by RBRF grant #06-02-16470, by programs of the Presidium of RAS and Leading Scientific Schools is acknowledged.

- [1] M.P. Mikhailova, K.D. Moiseev, Yu.P. Yakovlev, *Semicond. Sci. Technol.*, **19**, (2004) R109
 [2] E.I. Rashba, *Sov. Phys. Solid States*, **2**, (1960) 1109

24 June Tuesday

15:00-17:00

oral session

24TL-A

24RP-A

“Magnetic Oxides”

24TL-A-5

OUT OF EQUILIBRIUM PHASES IN PEROVSKITES AND CONTROL OF MESOSCOPIC PHASE SEPARATION

Bianconi A., Fratini M., Poccia N., Vittorini-Orgeas A.

Department of Physics, University of Rome "La Sapienza", P.le A. Moro 2, 00185 Rome, Italy

The search for the quantum critical point relevant for understanding the physics of doped perovskites (cuprates and manganites), in spite of the large amount of work, remains object of debate. In manganites it is getting clear that mesoscopic phase separation (MePhS) occurs in the proximity a critical point at a critical chemical pressure (tolerance factor) and critical doping where the long range polaronic charge ordering phase occurs. In this report we show that the relevant critical point for cuprates (where the static long range charge and spin ordered phase competes with the long range superconducting order) appears at a critical doping $N_c=1/8$ and a critical anisotropic chemical pressure P in the new 3D phase diagram of doped perovskites (T, N, P) [1]. The anisotropic chemical pressure is controlled by the lattice mismatch between the CuO_2 monolayers and the intercalated rocksalt layers. The phase diagram for all cuprates (T_c, N, P) is obtained by measuring P via the Cu-O microstrain by EXAFS and X-ray diffraction in all cuprate families and it is shown to be similar to that of manganites. Here we report the investigation of multiscale mesoscopic phase separation by high-resolution X-ray microdiffraction using synchrotron radiation in a cuprate $\text{La}_2\text{CuO}_{4+y}$ with y such that it is very close to the hole doping $N_c=1/8$. We have obtained the x-ray mapping of the charge ordered domains at different oxygen doping in single crystals of $\text{La}_2\text{CuO}_{4+y}$. We report evidence for the power law distribution of ordered domains of the crystalline electronic phase of ordered polarons with commensurate periodicity in competition with high- T_c superconducting striped bubbles with incommensurate periodicity [2-5]. We determine the power-law exponent and the exponential cut-off that changes with the distance from the quantum critical point at (N_c, P_c) showing that the chemical pressure in cuprates is as important as in manganites to tune these system in the critical region where complex electronic phases appear. In these phases, we report evidence for metastability and we show that we can manipulate the mesoscopic phase separation by photo-induced phase transition.

[1] A. Bianconi, G. Bianconi, S. Caprara, D. Di Castro, H. Oyanagi, N.L. Saini, *J. Phys. C: Condens. Matter*, **12** (2000) 10655.

[2] D. Di Castro, M. Colapietro, G. Bianconi, *Int. J. Mod. Phys. B*, **14** (2000) 3438.

[3] A. Bianconi, D. Di Castro, G. Bianconi, A. Pifferi, N.L. Saini, F.C. Chou, D.C. Johnston, M. Colapietro, *Physica C*, **341-348** (2000) 1719.

[4] D. Di Castro, G. Bianconi, M. Colapietro, A. Pifferi, N. L. Saini, S. Agrestini, Bianconi, *Eur. Phys. J. B*, **18**, (200) 617.

[5] F.V. Kusmartsev, D. Di Castro, G. Bianconi, A. Bianconi, *Phys. Lett. A*, **275** (2000) 118.

24TL-A-6

PHASE SEPARATION IN STRONGLY CORRELATED ELECTRON SYSTEMS WITH DIFFERENT KINDS OF CHARGE CARRIERS

Kugel K.I., Rakhmanov A.L., Sboychakov A.O.

Institute for Theoretical and Applied Electrodynamics, Russian Academy of Sciences,
Izhorskaya str. 13, Moscow, 125412 Russia

Extending our earlier study of the phase separation in the materials with localized and itinerant charge carriers (doped manganites and related magnetic oxides) [1, 2], we considered the two-band Hubbard model to analyze a possibility of a non-uniform charge distribution in a strongly correlated electron system with two types of charge carriers. It was demonstrated that in the limit of strong on-site Coulomb repulsion, such a system has a tendency to phase separation into the regions with different charge densities even in the absence of magnetic or any other ordering [3]. This tendency turned out to be specially pronounced, if the ratio of the bandwidths is large enough. The characteristic size of inhomogeneities was estimated accounting for the surface energy and the electrostatic energy related to the charge imbalance.

A similar approach was also used to describe the characteristic features of band structure and phase separation in multiband superconductors, especially in cuprates [4]. We predicted a large peak in the density of states at the Fermi level in the case of optimum doping corresponding to the minimum energy difference between the centers of two hole bands. For strong interband hybridization, a metal-insulator transition occurs near this optimum doping level. The suggested mechanism of phase separation is related to the redistribution of holes between two Hubbard bands rather than to the usual antiferromagnetic correlations. As a result, the superconducting critical temperature T_c ceases to be directly determined by the doping level and remains near its maximum value within a broad doping range.

We also analyzed the situation typical of orbital ordering when the charge carriers can be characterized by different values of orbital quantum number. The effect of orbital ordering on the phase separation was studied employing a minimal model including itinerant charge carriers at the orbitally ordered background. It was shown that at low doping, the phase separation may appear in systems with orbital degeneracy even without taking into account the magnetic structure. We consider this effect using two versions of the model. In the first one, we assume that in the absence of doping, the orbital structure results from the interaction of core electrons with the lattice. The electrons appearing due to doping move on this background. In an alternative model, the same electrons take part both in formation of the band structure and of the orbital ordering.

The work was supported by the European project CoMePhS (contract NNP4-CT-2005-517039), International Science and Technology Center (grant no. G1335), and Russian Foundation for Basic Research (project no. 08-02-00212)

- [1] K.I. Kugel, A.L. Rakhmanov, and A.O. Sboychakov, *Phys. Rev. Lett.*, **95** (2005) 267210.
- [2] A.O. Sboychakov, A.L. Rakhmanov, and K.I. Kugel, *Phys. Rev. B*, **74** (2006) 014401.
- [3] A.O. Sboychakov, K.I. Kugel, and A.L. Rakhmanov, *Phys. Rev. B*, **76** (2007) 195113.
- [4] A.O. Sboychakov, Sergey Savel'ev, A.L. Rakhmanov, K.I. Kugel, and Franco Nori, *arXiv:0706.0082*; submitted to *Phys. Rev. B*.

24TL-A-7

MAGNETIC STRUCTURE DETERMINATION USING POLARISED RESONANT X-RAY SCATTERING

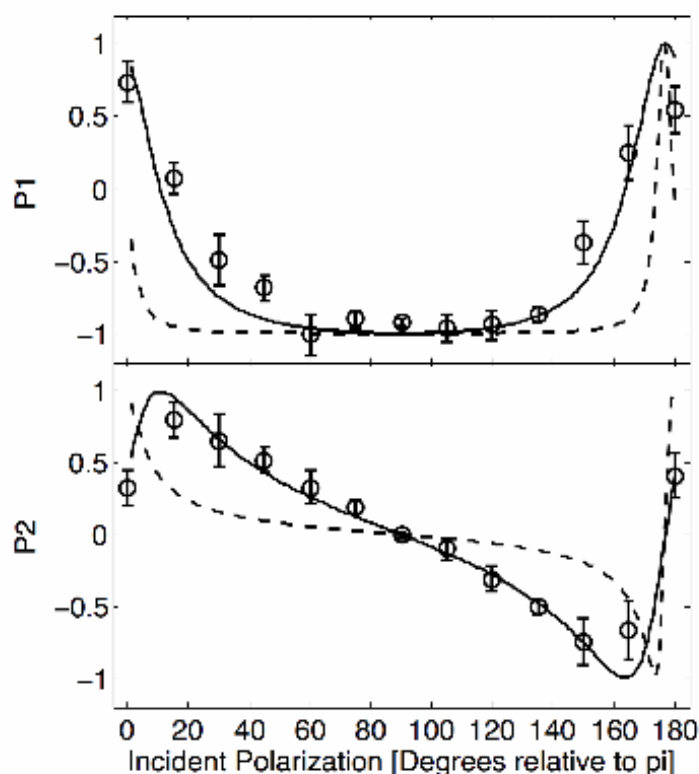
Hatton P.D.¹, Johnson R.D.¹, Bland S.R.¹, Beale T.A.W.¹, Mazzoli C.², Wilkins S.B.³

¹Department of Physics, Durham University, South Road, Durham DH1 3LE, UK

²European Synchrotron Radiation Facility, Biote Postal 220, F-38043, Grenoble Cedex, France

³Brookhaven National Laboratory, Long Island, N.Y., U.S.A

The determination of magnetic structures relies principally on neutron diffraction, but resonant X-ray scattering techniques are continuing to develop. In this talk I will review the latest advances in polarised resonant magnetic X-ray scattering using synchrotron radiation. New experimental techniques including the use of diamond phase plates to rotate the polarisation of the incoming X-ray beam [1] can be combined with energy and azimuthal scans to give atomic and band-specific information on the magnetic ordering and structure. As an example, recent results of the multiferroic material TbMn_2O_5 will be presented [2]. By tuning the incident beam to the terbium L3 edge, the specific magnetic behaviour of the rare earth ions can be probed, and the unusual magneto-electric coupling studied [3]. The extension of these techniques into the soft X-ray scattering regime including the terbium M, manganese L and oxygen K edges will also be addressed.



Scattered intensity of the (4.5, 4, 0.25) magnetic reflection at the Tb L3 edge defined in terms of Poincare-Stokes parameters, P1 & P2, as a function of incident polarization.[2] The solid (dashed) line shows simulation when scattering from Mn4+ (Mn3+) sites. This result confirms that the continuum states of terbium are polarised by the Mn4+ spin density, as predicted by G. R. Blake *et al.*[3]

Support by EPSRC and STFC is acknowledged.

[1] C. Mazzoli *et al.* Phys. Rev. B **76**, 195118 (2007)

[2] R. D. Johnson *et al.* to be published...

[3] G. R. Blake *et al.* Phys. Rev. B **71**, 214402 (2005)

24RP-A-8

ELASTIC PROPERTIES OF LANTHANUM MANGANITES*Bebenin N.G., Zainullina R.I., Ustinov V.V.*

Institute of Metal Physics, UD RAS, Kovalevskaya St. 18, Ekaterinburg 620041, Russia

The interest in lanthanum manganites $\text{La}_{1-x}\text{D}_x\text{MnO}_3$, $D = \text{Ca}, \text{Sr}, \text{Ba}$, is stimulated by the colossal magnetoresistance (CMR) effect that is observed near the Curie temperature T_C . Although the role of the lattice in forming the properties of the CMR compounds is universally recognized, the lattice properties as such remain weakly investigated. It is sufficient to note that in the CMR reviews, the elastic properties have not been discussed.

The purpose of this paper is to give a short overview of the data on the elastic properties of the CMR manganites published during last decade. The results of measurements on single crystal samples are preferably considered. The focus is on how magnetic and structural phase transitions manifest themselves in the temperature dependence of sound velocity and sound damping. The effect of charge ordering is also discussed.

We first consider the low frequency data for $\text{La}_{1-x}\text{Sr}_x\text{MnO}_3$ and $\text{La}_{1-x}\text{Ba}_x\text{MnO}_3$ in which the magnetic transition is second order. In these crystals, the $Pnma-R\bar{3}c$ structural transformation results in the longitudinal sound velocity jump, which can be as high as 20%, while the anomaly near the Curie temperature is weak. The yttrium doping suppresses the structural $Pnma-R\bar{3}c$ transition.

The $Pnma-R\bar{3}c$ transition is accompanied by the giant thermal hysteresis (GTH). The phenomenological theory for describing the GTH effect is presented. The dependence of the GTH effect on polarization of the ultrasound waves is considered. The specific effects observed in high frequency region are discussed.

Unlike the La-Sr and La-Ba manganites, in the $T-x$ phase diagram for La-Ca system, there is the tricritical point. If the Ca content is greater than 0.25; the magnetic transition at T_C is first order. The first order ferromagnetic-to-paramagnetic transition results in significant fall in the longitudinal sound velocity. The internal friction in the paramagnetic state is much greater than in the ferromagnetic state, indicative of strong interaction ultrasonic waves with spin fluctuations.

Support by grants RFBR 06-02-16085 is acknowledged.

24RP-A-9

INFRARED STUDY OF SmMnO_3 CRYSTAL FIELD EXCITATIONS*Jandl S.¹, Nekvasil V.², Mukhin A.A.³, Ivanov V.Yu.³, and Balbashov A.M.⁴*¹Université de Sherbrooke, Département de Physique, 2500 Boulevard Université,
Sherbrooke, Canada J1K 2R1²Institute of Physics, Czech Academy of Sciences, Cukrovarnická 10,
CZ-162 53 Prague 6, Czech Republic³General Physics Institute of the Russian Academy of Sciences, 38 Vavilov St.,
119991 Moscow, Russian Federation⁴Moscow Power Engineering Institute, 14 Krasnokazarmennaya St.,
105835 Moscow, Russia

Intensive efforts have been devoted to the understanding of the rare earth manganites magneto-transport properties. Substitution in $\text{R}_{1-x}\text{A}_x\text{MnO}_3$ of the rare earth ion R^{3+} by a divalent cation A^{2+} generates, due to charge compensation, Mn^{4+} that leads to double exchange interactions and simultaneous observation of metallic and ferromagnetic character [1]. The study of a manganite parent compound, such as SmMnO_3 phonons and crystal field (CF) excitations, is an important starting point to the understanding of the more complex interactions in the doped systems.

Effect of antiferromagnetic phase transition on phonons and CF excitations in SmMnO_3 ($T_N \sim 60$ K) is studied by micro-Raman scattering and infrared transmission as a function of temperature. Similarly to the orthorhombic RMnO_3 family, SmMnO_3 structure is distorted by static Jahn-Teller effects consistent with the D_{2h}^{16} space group. The antiferromagnetic phase transition influences the most intense Raman active B_{2g} stretching mode (~ 607 cm^{-1}) which softens below T_N reflecting a modulation of the exchange integral by lattice vibrations. Such softening can be described by the following relation: $\Delta\omega = (2/m\omega) (\delta^2 J/\delta u^2) (M(T)/4\mu_B)^2$. where ω represents the B_{2g} mode frequency, m the oxygen mass, J the superexchange integral, u the oxygen displacement, and $M(T)$ the ferromagnetic sublattice magnetization per Mn^{3+} ion.

The same antiferromagnetic phase transition influences the Sm^{3+} ion CF excitations through the lifting of their Kramers doublet degeneracies due to the Mn^{3+} - Sm^{3+} temperature dependent magnetic interaction [2]. We have observed, in the 1800-6000 cm^{-1} range, several infrared active Sm^{3+} CF transitions between the lowest ${}^6\text{H}_{5/2}$ ground state level and the ${}^6\text{H}_{7/2}$, ${}^6\text{H}_{9/2}$, ${}^6\text{H}_{11/2}$, and ${}^6\text{H}_{13/2}$ excited levels. We have calculated the energies of the Sm^{3+} CF levels by using CF parameters obtained for NdMnO_3 [4] and found that they are in good agreement with the observed transitions. The ground state Kramers doublet energy splittings below T_N vary from 3.8 cm^{-1} at 40 K up to 5.8 cm^{-1} at 2 K reflecting the Mn^{3+} - Sm^{3+} magnetic interaction strengthening, in good agreement with submillimeter data for direct transitions inside the ground state doublet [3].

[1] D. I. Khomskii and G. A. Sawatzky, *Solid State Commun.* **102** (1997) 87.

[2] V. Yu. Ivanov, A. A. Mukhin, A. S. Prokhorov, and A. M. Balbashov, *Phys. Stat. Sol. (b)* **236** (2003) 445.

[3] A.A. Mukhin, V. Yu. Ivanov, V. D. Travkin, et al., *JMMM* **272-276**, (2004) 96.

[4] S. Jandl, V. Nekvasil, M. Divis, A. A. Mukhin, J. Hölsä, M. L. Sadowski, *Phys. Rev.* **71**, (2005) 024417.

24 June Tuesday

12:00-13:30

15:00-17:00

oral session

24TL-B

24RP-B

**“Spintronics and
Magnetotransport”**

24TL-B-1

MAGNETO-STRUCTURAL COUPLING IN ITINERANT SYSTEMS.*Abrikosov I.A.¹, Alling B.¹, Ponomareva A.V.², Liot F.¹, Asker C.¹, Ekholm M.¹, and Ruban A.V.³*¹Department of Physics, Chemistry and Biology (IFM),
Linköping University, SE-581 83 Linköping, Sweden²Theoretical Physics Department, Moscow Institute of Steel and Alloys, Moscow, Russia³Applied Materials Physics, Department of Materials Science and Engineering, Royal Institute of
Technology, SE-10044, Stockholm, Sweden

It is often assumed that the electronic, magnetic, and vibrational degrees of freedom can be separated in theoretical treatment of itinerant magnets due to the fact that their excitations usually have different time scales. Moreover, while it is well known that the crystal structure is of primary importance for an understanding of magnetism in these systems, the fact that a magnetic state of the system has very strong impact on its structural properties is appreciated much more seldom. We show that magnetic and chemical interaction in itinerant magnets are deeply interconnected, and strongly affect each other. We start with relatively simple examples, and show that there exists very strong dependence of thermodynamic properties, like elastic constants, structural distortions, and mixing enthalpies, on the underlying magnetic state in Fe alloys with Cr, Mn and Ni. This will be traced to the strong influence of the magnetism on the interatomic interactions in itinerant systems. We then illustrate the effect of the underlying magnetic state on the interactions and phase stability in Fe-Si alloys, and show that the crystal structure of samples quenched from the high-temperature magnetic state differs from the ground state DO₃ structure. In its own turn, the crystal structure has, of course, a pronounced effect on the magnetic properties, and therefore its modification allows one to tune the magnetic properties of the alloys. We illustrate this idea by results of a theoretical study of the effect of doping the half-Heusler alloy NiMnSb with the magnetic 3d-metals Cr, Mn, Fe, Co and Ni, both with respect to energetics and magnetic properties. Starting from the formation energies we discuss the possibility of placing the dopant on different crystallographic positions in the alloy. We calculate total and local magnetic moments, effective exchange interactions as well as the density of states and outline strategies to tune the magnetic properties of the alloy. Doping of NiMnSb with Cr as well as substituting some Ni with extra Mn has the largest impact on magnetic interactions in the system while preserving the half metallic property. Therefore, we suggest the possibility that these dopants increase the thermal stability of half-metallicity in NiMnSb with implications for its possible usage in spintronics applications.

24TL-B-2

SPINTRONICS WITH MULTIFERROICS

Bea H.^{1,2}, *Gajek M.*¹, *Bibes M.*¹, *Bouzehouane K.*¹, *Fusil S.*¹, *Catalan G.*³, *Paruch P.*², *Warot-Fonrose B.*⁴, *Petit S.*⁵, *Cherifi S.*⁶, *Herranz G.*¹, *Jacquet E.*¹, *Deranlot C.*¹, *Fontcuberta J.*⁷, *Bartholome A.*¹, and *Fert A.*¹

¹UMP CNRS/Thales, route departementale 128, 91767 Palaiseau, France

²DPMC, Universite de Genève, 24 quai E. Ansermet, 1211 Genève 4, Switzerland

³Center for Ferroics, Departments of Earth Sciences, University of Cambridge, Cambridge CB2 3EQ, United Kingdom

⁴CEMES-CNRS, 29, rue Jeanne Marvig, 31055 Toulouse Cedex, France

⁵Laboratoire Leon Brillouin, CEA Saclay, 91191 Gif-sur-Yvette, France

⁶Institut Neel, NANOscience department, 38042 Grenoble, France

⁷Institut de Ciència de Materials de Barcelona, CSIC, 08193 Bellaterra, Catalunya, Spain

Multiferroics belong to a class of compounds which show several ferroic orders as ferroelectricity and ferro-(or antiferro-)magnetism for instance. They are very interesting for applications due to both their multifunctionality and the magnetoelectric coupling between these two orders - that allows the change of the magnetic order by an electric field or vice versa the electric polarization by a magnetic field. We will present experiments performed on multiferroic based heterostructures in order to check the potential of such multifunctional materials in the field of spintronics. Two materials have been studied: the ferromagnetic-ferroelectric $\text{La}_x\text{Bi}_{1-x}\text{MnO}_3$ (LBMO) ($x \leq 0.1$) and the antiferromagnetic-ferroelectric BiFeO_3 (BFO).

First, the ferromagnetism and ferroelectricity of LBMO offers the unique opportunity to encode information independently in electric polarization and magnetization to obtain four different logic states. Magnetic tunnel junctions with a $\text{Au/LBMO}/(\text{La,Sr})\text{MnO}_3$ structure have been measured, LBMO being used as a magnetic barrier, and $(\text{La,Sr})\text{MnO}_3$ as a magnetic counterelectrode. A 100% change of the tunnel resistance is obtained at 3K depending on whether the magnetizations of LBMO and $(\text{La,Sr})\text{MnO}_3$ are parallel or opposite, thus showing a spin filtering effect in the LBMO barrier [1]. In addition, the ferroelectric character of the compound is exploited to give rise to two different resistance states related to the direction of the polarization. The resulting electroresistance phenomenon goes up to 20% at low temperature [2]. A four resistance state device has thus been obtained.

On the other hand, we have studied the antiferromagnetic-ferroelectric BFO in thin films. The ferroelectric character has been shown to remain down to very low thicknesses of 2nm [3]. Thanks to its insulating and epitaxial properties, BFO ultrathin films has been used as tunnel barriers to obtain a large tunnel magnetoresistance up to +100% in magnetic tunnel junctions with Co and $(\text{La,Sr})\text{MnO}_3$ ferromagnetic electrodes [4]. The antiferromagnetic order of BFO thin films has been demonstrated by neutron diffraction measurements and used to induce a sizeable (~60 Oe) exchange bias on ferromagnetic films of NiFe and CoFeB, at room temperature. The observed mechanisms of this exchange bias [5] open a way of an electrical control of the magnetization via the magnetoelectric coupling which is very promising for spintronics.

[1] M. Gajek et al., *Phys. Rev. B* **72**, 020406(R) (2005)

[2] M. Gajek et al., *Nat. Mat.*, **6**, 296 (2006)

[3] H. Bea et al., *Jpn. J. of Appl. Phys.*, **45**, L187 (2006)

[4] H. Bea et al., *Appl. Phys. Lett.*, **89**, 242114 (2006)

[5] H. Bea et al., *Phys. Rev. Lett.* **100**, 017204 (2008)

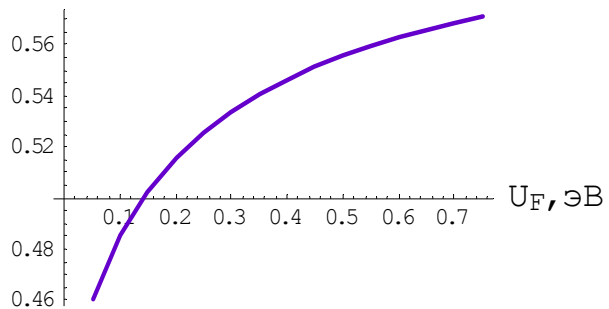
24RP-B-3

RESISTANCE AND TMR SWITCH IN ASYMMETRIC FERROELECTRIC TUNNEL JUNCTIONS

Zhuravlev M.Ye.

N.S. Kurnakov Institute of General and Inorganic Chemistry of RAS,
119991 Moscow, Leninskii prosp., 31, Russia
e-mail: myezhur@gmail.com

We present a model investigation of electron transport in asymmetric ferroelectric tunnel junctions. The asymmetric ferroelectric tunnel junctions can be obtained either by two different electrodes separated by a thin ferroelectric barrier, or by placing additional layer (conducting or insulating) between one of the electrodes and the ferroelectric layer. In the last case, which is considered in this work, the electrodes are identical. A significant change of conductance of the system takes place when the



polarization of the ferroelectric layer switches. The Figure represents the calculated ratio of the electroresistance for two opposite directions of the polarization as the function of the ferroelectric barrier height. The height of the additional insulating barrier was chosen as $U_I = 0.1$ eV, its thickness, $b_I = 15E$ and the thickness of the ferroelectric layer, $a = 10E$. Our calculation shows that in the case when the electrodes are the narrow-band ferromagnetic conductors (e.g. ferromagnetic semiconductors), the reversal of the polarization of the ferroelectric causes the sizable change of spin polarization of the current. The tunneling magnetoresistance demonstrates considerable change as well. These effects are caused by a different potential profile for the two opposite polarization orientations seen by transport electrons. The effects are similar to giant electroresistance switch and tunneling magnetoresistance switch in ferroelectric tunnel junction with different electrodes. [1,2].

[1] M. Ye. Zhuravlev, R. F. Sabirianov, S. S. Jaswal, and E. Y. Tsymbal, Phys. Rev. Lett. **94**, 246802 (2005)

[2] M. Ye. Zhuravlev, R. F. Sabirianov, S. S. Jaswal, and E. Y. Tsymbal, Appl. Phys. Lett. **87**, 222114 (2005)

24RP-B-4

CONCEPT OF THE FIELD DRIVEN DOMAIN WALL MOTION MEMORY

You Chun-Yeol

Dept. of Physics, Inha University, Korea

Recently, a new kind of memory concept of current induced domain wall motion (CIDWM) using spin transfer torque is actively investigated [1]. The race-track memory has superior advantages of the hard disk drive by replacing the mechanical part with a domains motion, while it keeps the density and the non-volatility. Since the domain wall motion is

occurred with spin transfer torque, an angular momentum deposition from conduction spins to the localized spins, it must involve huge number of electrons. Such huge current density yields serious Joule heating problems, and it causes a loss of the magnetic information, or thermally active random domain wall motion. Furthermore, the physics of spin dynamics in the spin transfer torque is not yet clear. The role or physical origin of the non-adiabatic term is still controversy.

Recently, we proposed a new concept of the memory device based on field driven domain wall motion (FDDWM) instead of CIDWM. The physics of the FDDWM is clearly established and simple, but the conventional longitudinal FDDWM will destroy the information which is stored in a domain. In our study, we employ the non-uniform transverse magnetic field. With non-uniform transverse magnetic field, a transverse domain wall moves to the maximum field position as illustrated in Fig. 1. Under the non-uniform transverse field, the magnetization of the longitudinal domains rotate just small angles to the moderate strength transverse field, the magnetization of the domain wall acts as a single dipole to the non-uniform transverse field. Therefore the domain wall moves to the energy minimum position where the field has a maximum strength in order to minimize the Zeeman energy. Therefore the domain can be shifted with carefully designed non-uniform magnetic field, so that FDDWM memory concept is possible.

We perform micromagnetic simulations and solve the equation of the motion for the domain wall motion under the non-uniform magnetic field. We find that the rigid domain motion is possible with micromagnetic simulation. The details of the equation of the motion for the domain wall and micromagnetics results will be discussed.

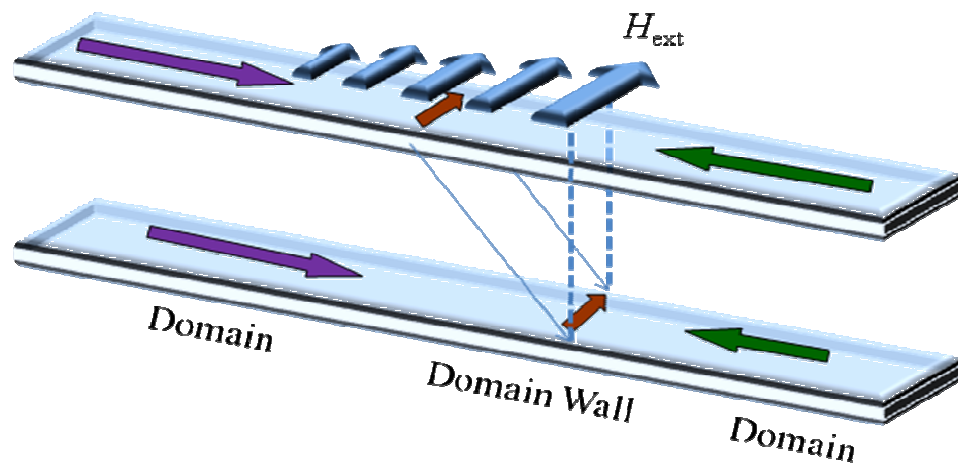


Fig. 1 Schematic Diagram of the concept of non-uniform transverse magnetic field driven domain wall motion. The transverse domain wall moves to the position of maximum field strength.

[1] L. Thomas, M. Hayashi, X. Jiang, R. Moriya, C. Rettner, and S. S. P. Parkin, *Nature* **443**, 197 (2006), and references therein.

[2] C.-Y. You, submitted to *Appl. Phys. Lett.* (2008).

24TL-B-5

SPIN INJECTION DRIVEN SWITCHING IN A MAGNETIC JUNCTION

Epshtein E.M., Gulyaev Y.V., Chigarev S.G., Krikunov A.I., Panas A.I., Zilberman P.E.

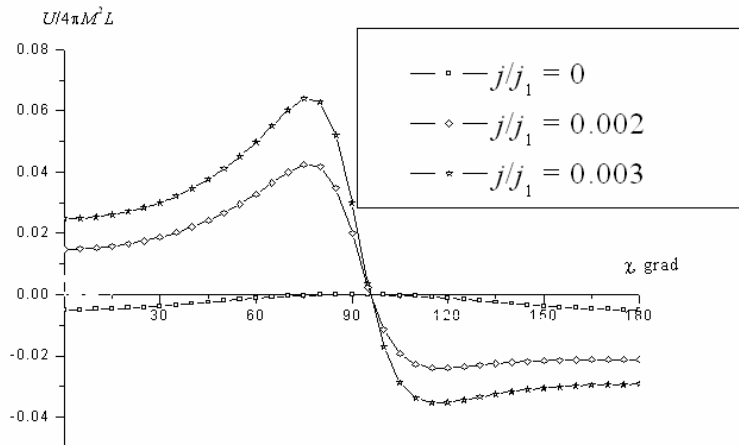
Institute of Radioengineering and Electronics RAS, Fryazino Moscow Region, 141190, Russia

Matching conditions for spin resistances are found at the interfaces of a magnetic junction. These conditions provide high current driven spin injection level. Essence of the conditions consists of creating an effective injection at input interface and suppressing the injection at the output one. These conditions combined with parallel magnetization orientation leads to orders of magnitude lowering of instability threshold. Contrary to this, stability preserves completely for antiparallel magnetization orientation and for any direct current magnitude. However, new effect of population inversion of spin subbands is predicted in the situation.

Perpendicular electric current creates a non-equilibrium spin injection in the structure of contacting thin ferromagnetic layers (ferromagnetic junction). We calculate net spin polarization of the junction for very high level of the injection when non-equilibrium spin density is comparable with the equilibrium one. Spin resistances are introduced for each layer of the three layered junction, namely, Z_1, Z_2, Z_3 , where $Z_i = \rho_i l_i / (1 - Q_i)$, ρ_i - specific resistance, l_i - average spin relaxation length and Q_i - spin polarization degree of current for the layer of number "i" = 1, 2, 3. As it is shown, the conditions $Z_1 \gg Z_2$ and $Z_3 \gg Z_1$ provide the most high injection level at a given current density j in the forward direction $1 \rightarrow 2$, the first condition providing strong spin injection into the layer 2 and the second condition providing lock of spins in the layer 2.

If the conditions are fulfilled, the junction demonstrates some interesting new properties. First of all the injection suppresses completely the so called spin-transfer torque. Then the situation becomes different depending on parallel or antiparallel is the mutual magnetization orientation of neighboring ferromagnetic layers. The proper junction magnetization waves become unstable at current density exceeding some threshold value for parallel orientation. It is significant to note that this threshold appears many orders of magnitude lower than it is in the commonly used low injection regime. For example, the threshold may reach $j_{th} \sim 10^5 \text{ A/sm}^2$ instead of an ordinary value $j_{th} \sim 10^7 \text{ A/sm}^2$.

In contrast to this, lattice becomes stable at any current for parallel orientation of the neighbor ferromagnetic layers. This is seen from figure where magnetic energy U versus angle χ of magnetization is shown. Current removes minimum at $\chi = 180^\circ$, but creates an additional minimum at $\chi \approx 70^\circ$.



Supported by grant RFBR # 06-02-16197.

24TL-B-6

SPIN POLARIZED VACUUM TUNNELING THROUGH COBALT(0001)*Ding H.F.*

National Laboratory of Solid State Microstructures and Department of Physics,
Nanjing University, Hankou Rd. 22, Nanjing, 210093 (China)

We present the study of the bias-voltage and gap-width dependence of tunneling magnetoresistance (TMR) through a vacuum barrier. The TMR observed by spin-polarized scanning tunneling microscopy between an amorphous magnetic tip and a Co(0001) sample is almost independent of the bias voltage at large tip-sample separations. At small tip-sample separations, a pronounced minimum in the experimental TMR was found at +200 mV bias. The experimental findings are compared with bias-voltage dependent first-principles calculations for ballistic tunneling and qualitative agreement is obtained. By varying the tip-sample separation in a controlled way, the TMR was measured as a function of the gap width. At large gap widths the TMR is constant. At gap widths below ≈ 0.45 nm, a drop of the TMR was found in contrast to predictions of the Jullière model. The drop of the TMR is found to correlate with drop of the imaginary electron momentum inside the barrier and we compare our experimental results with the predictions of the Slonczewski model.

*In collaboration with W. Wulfhekel and J. Kirschner (MPI-Halle)

24TL-B-7

WHAT CAN WE LEARN FROM NOISE STUDIES IN MAGNETIC TUNNEL JUNCTIONS*Aliev F.G.*

Departamento de Física de la Materia Condensado C-III, Universidad Autónoma de Madrid,
28049 Madrid, Spain

Magnetic tunnel junctions (MTJs) are nowadays one of the most active areas of material science and spintronics. Here we review our recent studies of conductance and noise as a function of applied bias and magnetic state in different types of MTJs. Such combined measurements have recently demonstrated to be a powerful tool to understand and optimise electron tunnelling processes in polycrystalline (with Al_2O_3 barrier) and in fully epitaxial (with MgO barrier) magnetic tunnel junctions devices with room temperature Tunnelling Magneto-Resistance (RT-TMR) exceeding 100% [1-3]. We shall compare the data on the control Fe/MgO(001)/Fe MTJs and one obtained for the MTJs with carbon-doped bottom Fe/MgO interface. Such doping was previously shown to lead to strongly asymmetric TMR vs. bias, providing a root for creation of high-output voltage device applications [4].

The experimental on the shot noise clearly indicate the absence of electron correlations and/or sequential tunnelling phenomena for negative bias when the electrons are injected from the top Fe/MgO towards the bottom Fe-Fe-C/MgO interface in carbon doped MTJs. When electrons are injected from bottom to upper electrodes, the shot noise also shows the Fano factors close to 1, except the narrow region close to 0.5V when some resonant tunnelling (presumably through asymmetrically situated oxygen vacancies) suppresses weakly (Fano decreases to about 0.9) the shot noise. In general, the data on the shot noise proves that both parallel (P) and anti-

parallel (AP) spin-dependent conductance are due to pure (direct) tunnelling between electron bands. The high MTJs quality and coherent tunnelling is further confirmed by the large breakdown voltage of the MTJs (up to 3 V) [2].

Low frequency noise analysis performed on our fully epitaxial MTJs show extremely low 1/f noise levels [3]. We have found that the normalized noise (Hooge factor) asymmetry between parallel and antiparallel states may strongly depend on the applied bias and its polarity. Fully epitaxial Fe/C/MgO/Fe(001) MTJs exhibit record low Hooge factors being at least one order of magnitude smaller than previously reported.

(*) In collaboration with D.Herranz, R.Guerrero, R.Villar, F.Greullet, C.Tiusan, M.Hehn, F.Montaigne

Support by Spanish-French Integrated Action project, Spanish MEC and European Science Foundation (FONE-SPINTRA) is gratefully acknowledged.

[1] R.Guerrero, et al., Phys. Rev. Lett., 97, 0266602 (2006).

[2] R. Guerrero et al, Appl. Phys. Lett. 91, 132504 (2007).

[3] F.G.Aliev, et al., Appl. Phys. Lett. 91, 232504 (2007)

[4] C. Tiusan et al, Appl. Phys. Lett. 88, 062512 (2006).

24RP-B-8

DOMAIN WALL MOTION IN MAGNETIC MULTILAYERS DUE TO THE SPIN CURRENT FLOWING PERPENDICULARLY TO THE LAYERS

Khvalkovskiy A.V.^{1,2}, Zvezdin K.A.¹, Gorbunov Ya.V.³, Grollier J.², Cros V.², Zvezdin A.K.¹

¹A.M. Prokhorov General Physics Institute, Vavilova str. 38, 119991 Moscow, Russia

²Unite Mixte de Physique CNRS/Thales and Universite Paris Sud 11, route departementale 128, 91767 Palaiseau, France

³Institute of Microtechnology - Spin MT, Lomonosovskiy prosp.15, Moscow 119311, Russia

Most of the studies devoted to a motion of a domain wall (DW) by spin polarized current consider the current flowing along the system axis, a current-in-plane (CIP) configuration. Few previous works, in which the polarized current flowing perpendicularly to the plane of a magnetic layer with DW is considered. In such systems the effect of the current on the DW motion is strongly affected by interaction with the edges or other DWs. Here we present some results of a micromagnetic study of a motion of a single DW due to the spin current, that flows perpendicularly to the layers of a spin valve-like structure. Four types of spin valves are considered having in each case a magnetic layer containing a DW and a second magnetic layer with a fixed magnetization being magnetized either in the film plane or perpendicularly to it. From the simulations, we predict that for sufficiently small current densities, the spin transfer effect brings the DW into a steady motion with unchanged DW shape and velocity. For current densities larger than a given threshold value, the DW is transformed by the current and the character of its motion is strongly affected. The predicted velocities of the steady DW motion may be more than two orders of magnitude larger than those previously given for the current with the same density flowing in the plane of the magnetic film. Implying that the distribution of the current is non-uniform in the vicinity of the DW in CIP spin valve structures, our results may possibly reveal the reason of a large difference in the observed thresholds for DW depinning in one- and three-layer CIP structures.

Support by RFBR project 07-02-91589-ASP and “RTRA- Triangle de la physique” is acknowledged.

24RP-B-9

SPIN WAVES EXCITED BY SPIN-POLARIZED CURRENT IN NANOPILLAR SPIN VALVES: A MICROMAGNETIC STUDY

Khvalkovskiy A.V.^{1,2}, Grollier J.¹, Georges B.¹, Gorbunov Ya.V.³, Zvezdin K.A.², Zvezdin A.K.², Cros V.¹, Jaffres H.¹, Fert A.¹

¹Unite Mixte de Physique CNRS/Thales and Universite Paris Sud 11, route departementale 128, 91767 Palaiseau, France

²A.M. Prokhorov General Physics Institute, Vavilova str. 38, 119991 Moscow, Russia

³Institute of Microtechnology - Spin MT, Lomonosovskiy prosp.15, Moscow 119311, Russia

In this report we present the results of a micromagnetic analysis of our experimental data on the spin-wave excitation in the free layer of nanopillar spin valves by spin-polarized current. The measurements are made on a Py(X = 15, 30)/Cu(10)/Py(Y=2.5, 4) structures (in nm). The thin Py free layer (FL) is defined by electron-beam lithography and ion-milling and is designed with elliptical shapes with different sizes. The magnetic field is applied perpendicular to the plane of the structures. In the experimental results, several large-amplitude spin-wave modes are sequentially excited in the free layer by the spin transfer torque (STT)[1]. Each mode may be characterized by its frequency, linewidth and emitted power, and by the dependence on these intrinsic features on the applied current and magnetic field.

The micromagnetic simulations are performed using our home-made solver SpinPM by numerical integration of the Landau-Lifshitz equation, that includes an additional spin-transfer torque term. In the simulations, we do take into account the Oersted field due generated by the current and the thermal fluctuations. A two-dimensional mesh is used and both the free and the reference layers are taken into account in the simulations.

We discuss the influence of several parameters, such as the shape of the sample, the material parameters, the direction of the applied field, the magnetization distribution in the reference layer of the spin valve or the current distribution. We emphasize that these parameters that are seldomly known with a sufficient precision affects drastically the characteristics of the actual excited spin waves modes. This could explain the remaining discrepancy, not only in our case but in a general way, between the experimental data and the micromagnetic simulations. To be pro-active, we suggest some experimental sample characterizations that should be performed in order to provide a base for adequate interpretations of the experimental data about the current-induced spin wave excitations.

Support by “RTRA-triangle de la physique”, RFBR project 07-02-91589-ASP is acknowledged.

[1] S. I. Kiselev, J. C. Sankey, I. N. Krivorotov, et al., *Nature (London)*, **425** (2003) 380.

24 June Tuesday

12:00-13:30

15:00-17:00

oral session

24TL-C

24RP-C

“Metamaterials”

24TL-C-1

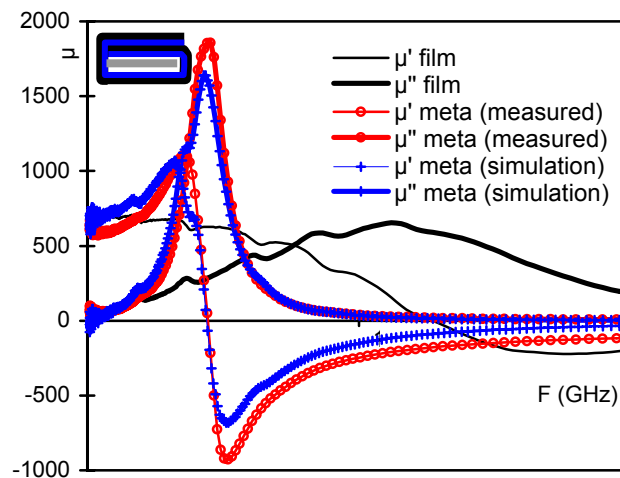
PERMEABILITY ENHANCEMENT OF MAGNETIC THIN FILMS THROUGH METAMATERIAL STRUCTURES

Acher O.

CEA Le Ripault, BP 16, F-37260 Monts

The considerable interest related to metamaterials during the present decade has led to numerous advances in the field of microwave materials. Among many other results, it has been shown that materials with large permeability levels could be produced, without any conventional magnetic constituent such as ferrite or ferromagnetic materials.

However, until recently [1], no metamaterial structure had been proposed, that could replace or supplement individual magnetic thin films. In this paper, a metamaterial structure is proposed, based on a conventional high permeability thin film, which boosts the film permeability to much higher levels. It can be manufactured using deposition and patterning techniques commonly used in the semiconductor industry. It can handle a planar magnetic field just as a single thin film usually does. A sketch of the metamaterial structure wrapped around a $1\mu\text{m}$ ferromagnetic layer is presented in the inset of the Figure. The permeabilities measured on the thin film and on the metastructure are also reported. It can be clearly seen that the permeability levels close to the resonance have been significantly increased. A simple model gives a fair account of the measured properties.



A theoretical approach is proposed, that outlines to what extent metafilms may challenge conventional magnetic films. In particular, sum rules on the imaginary permeability are extended to the case of metamaterials with a magnetic core. At very high frequencies, the figure of merit associated to metamaterials can exceed that associated to conventional magnetic films. However, for low frequency operation, it is shown on rigorous bases that the figure of merit associated to metamaterials are somewhat lower than the figure of merit associated to their magnetic constituents. This is associated with the intrinsically narrower resonance band of metamaterials.

[1] O. Acher, *J. Magn. Magn. Mater.*, in press.

24TL-C-2

ACTIVE PLASMONIC METAMATERIALS

Zayats A.V.

Centre for Nanostructured Media, The Queen's University of Belfast, Belfast BT7 1NN, UK

Plasmonic metamaterials have recently attracted significant attention due to their promise in numerous applications in nanophotonics and opto-electronics [1]. Coupling of light to plasmonic excitations, that are collective electronic excitations near a metal surface, allows one to confine the electromagnetic field on the sub-wavelength scale and manipulate it with high precision. Surface plasmon polaritons (SPPs) play a crucial role in determining optical properties of nanostructured metal surfaces and films, such as reflection, transmission, scattering, second-harmonic generation, surface enhanced Raman scattering, etc. Two-dimensional optics of surface polaritons has been developed that provides tools to manipulate and direct SPP waves on a metal surface. Various elements of SPP optics, including mirrors, lenses, resonators, plasmonic lasers, planar waveguides have been implemented.

Optical properties of plasmonic metamaterials can be controlled via modification of surface plasmon modes by varying geometry of the nanostructure and its dielectric environment. In order to achieve useful functionalities, active control of optical properties and spectral tuneability are required. In this talk we will overview how optical response of plasmonic metamaterials can be actively controlled with various control signals such as electric [2,3] and magnetic [4] field and all-optically with light [5,6]. Surface-plasmon optics provides a basis for implementation of novel photonic functionalities and development of a new class of active photonic devices for optical signal processing and all-optical integrated circuits. Numerous possible applications of surface plasmon polaritons can be envisaged in nanophotonics, optical data storage, classical and quantum optical information processing and optical communications.

- [1] A. V. Zayats, I. I. Smolyaninov, A. A. Maradudin, *Phys. Rep.* **408** (2005) 131.
- [2] W. Dickson, G. A. Wurtz, P. R. Evans, R. J. Pollard, A. V. Zayats, *Nano Lett.* **8** (2008) 281.
- [3] P. R. Evans, G. A. Wurtz, W. R. Hendren, R. Atkinson, W. Dickson, A. V. Zayats, *Appl. Phys. Lett.* **91** (2007), 043101.
- [4] G. A. Wurtz, L. Le Guyader, A. Kirilyuk, Th. Rasing, I. I. Smolyaninov, A. V. Zayats, to be published.
- [5] G. A. Wurtz, R. Pollard, A. V. Zayats, *Phys. Rev. Lett.* **97** (2006) 057402.
- [6] W. Dickson, G. A. Wurtz, P. Evans, D. O'Connor, R. Atkinson, R. Pollard, A. V. Zayats, *Phys. Rev. B* **76** (2007) 115411.

24TL-C-3

OPTICAL MAGNETIC MATERIALS AND PLASMONIC NANOLASER

Sarychev A.K.

Institute of Theoretical and Applied Electrodynamics RAS, Moscow, Russia

We consider plasmonic nanoantennas immersed in active host medium. Specifically shaped metal nanoantennas can exhibit strong magnetic properties in the optical spectral range

due to the excitation of magnetic plasmon resonance. A case when a metamaterial comprising such nanoantennas can demonstrate both left handedness and negative permeability in the optical range is considered. We show that high losses predicted for optical left-handed materials can be compensated in the gain medium. Gain allows achieving local generation in such magnetic active metamaterials. We propose plasmonic nanolaser, where the metal nanoantenna operates similar to a resonator. The size of the proposed plasmonic laser is much smaller than the wavelength. Therefore, it can serve as a very compact source of coherent electromagnetic radiation.

Extending the range of electromagnetic properties of naturally occurring materials motivates the development of artificial metamaterials. For example, it has been demonstrated recently that optical metamaterials may exhibit such exotic properties as, negative dielectric permittivity, negative magnetic permeability, and even both. Situations when a negative refractive index can be realized in practice are particularly interesting because of possibility of the perfect lens with subwavelength resolution, which is not restricted by the diffraction limit. Negative refraction and subwavelength imaging has been demonstrated in the microwave and optical range. However, the loss becomes progressively important with decreasing the wavelength towards the optical range. High loss inside the left-handed superlens dramatically reduces the resolution of such lens and made a dream of a full-scale superlens unattainable. To reduce the loss we suggest filling the metal plasmonic resonator with an active medium. We consider the interaction of such nanoantenna with a two-level amplifying system, which can be represented by quantum dot in the semiconductor host, quantum well, dye molecules, or another high gain medium.

24TL-C-4

ENGINEERING ELECTROMAGNETIC RESPONSE FROM COMPOSITES WITH FERROMAGNETIC WIRES

Panina L.V., and Makhnovskiy D.P.

University of Plymouth, Plymouth, United Kingdom

e-mail: lpanina@plymouth.ac.uk

Microwave signals have numerous scientific and industrial applications in modern technology. Many of the desirable properties such as selectivity, adjustability, multifunctionality, subwavelength imaging etc, are difficult or impossible to achieve with natural materials but could be realised with specially designed structures. In this work, we aim at the development of artificial dielectrics containing ferromagnetic microwires, which have a tuneable response for scattering or transmission of the incident electromagnetic waves in the GHz range. Such materials are foreseen to find applications in reconfigurable networks, tuneable 'microwave windows', antenna engineering, and structural health monitoring.

The response of a material to electromagnetic radiation at the microscopic scale is bundled into two macroscopic parameters, the electric permittivity and magnetic permeability. Similarly, with artificially structured materials, one can define effective parameters that characterise the average response of the materials at larger scales. Manipulating material design, previously inaccessible values of permittivity and permeability can be produced. Achievements of material engineering include negative refraction materials, band-gap materials, frequency selective and magnetically active surfaces. A recent trend is to achieve adjustability in these structures. In the context of our research, we propose to use ferromagnetic microwires to engineer a tuneable dielectric response. The effective permittivity of such a composite may have

a strong dispersion in the GHz range, producing a highly frequency selective (band-gap or bandpass) propagation regime.

In thin conducting wires the currents are constrained with the associated resonances determined by the geometrical parameters. The current resonances are damped due to the wire impedance which may result in a strong dependence of the permittivity on the wire magnetic properties owing to the magnetoimpedance (MI) effect. In soft ferromagnetic amorphous wires subjected to an external magnetic field or a stress MI is in the range of 100% even at frequencies of few GHz, as was reported by us and other groups. This makes it possible to sensitively tune the electromagnetic response from magnetic wire composites by external stimuli: a magnetic field, stress or temperature. The relationship between the electric effective permittivity and magnetic properties of constituent wires is a new phenomenon, which contrasts with most results on tuneable microwave materials where it is common to tune the permittivity through an electric field. We have recently provided first experimental verification of this effect, demonstrating enhanced transmission (by more than 10 dB) in a narrow frequency region near 2 GHz through a silicon layer containing Co-rich amorphous wires in the presence of a magnetic field or stress.

24TL-C-5

ON MICROSCOPIC PROPERTIES OF MAGNETIC METAMATERIALS

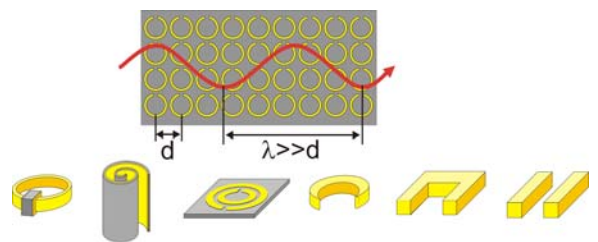
Shamonina E.¹, Sydoruk O.¹, Tatartschuk E.¹, Radkovskaya A.²

¹School in Advanced Optical Technologies, University of Erlangen-Nuremberg, Paul-Gordan-Str. 6, D-91052 Erlangen, Germany

²Magnetism Department, Faculty of Physics, Moscow State University, Leninskie Gory, Moscow 119991, Russia

Magnetic metamaterials (Fig.1) consisting of resonant elements with a strong magnetic response have developed into an important branch of the metamaterials research. The aim of this lecture is to provide an overview of microscopic properties of magnetic metamaterials in view to their applications as near field manipulating devices.

Fig. 1 Magnetic metamaterials (top) consist of small resonant “magnetic atoms“, e.g. capacitively loaded pipe, swiss roll (MHz-elements), split ring resonator (GHz-elements), nano-crescent, nano-U or a pair of nanorods (THz-elements) (bottom, from left). Metal (yellow), dielectric (grey).



To understand the way how magnetic metamaterials can be employed to manipulate the near field we need to understand their “microscopic” properties, i.e. the way how the electric and magnetic fields are created and transformed by resonant elements constituting the unit cells.

We will start with the analysis of properties of individual elements and discuss equivalent circuits capable of describing both low-frequency (MHz range) and high-frequency (GHz to THz) resonators [1]. In the second part of the lecture we will analyse mechanisms of the near-field coupling between elements, pointing out at different approaches in the description of low-frequency [2] and high-frequency metamaterials [3,4]. Properties of slow waves of coupling, known for low-frequency metamaterials as magnetoinductive (MI) waves, and the possibility of tailoring the dispersion characteristics of metamaterials will be discussed [5,6]. In the concluding part of the lecture we will review recent advances in the development of near field manipulating

devices such as miniaturised subwavelength waveguide components [7-10] and near-field lenses [11] in a wide range of frequencies, from radio frequencies, with a potential for medical applications in magnetic resonance imaging, to the IR and visible range aiming at fast signal processing.

- [1] A. Radkovskaya, M. Shamonin, C.J. Stevens et al., *MOTL* 46 (2005) 473.
- [2] E. Shamonina, V.A. Kalinin, K.H. Ringhofer and L. Solymar, *J. Appl. Phys.* 92 (2002) 6252.
- [3] A. Radkovskaya, M. Shamonin, C.J. Stevens et al., *J. Magn. Magn. Mat.* 300 (2006) 29.
- [4] F. Hesmer, E. Tatartschuk, O. Zhuromskyy et al., *phys. stat. sol. (b)* 244 (2007) 1170.
- [5] O. Sydoruk, A. Radkovskaya, O. Zhuromskyy et al., *Phys. Rev. B.* 73 (2006) 224406.
- [6] R.R.A. Syms, E. Shamonina, V. Kalinin and L. Solymar, *J. Appl. Phys.* 97 (2005) 064909.
- [7] E. Shamonina and L. Solymar, *J. Phys. D: Appl. Phys.* 37 (2004) 362.
- [8] R.R.A. Syms, E. Shamonina and L. Solymar, *IEE Proc. MAP* 153 (2006) 111.
- [9] A. Radkovskaya, O. Sydoruk, M. Shamonin et al., *IET Microw. Ant. Prop.* 1 (2007) 80.
- [10] A. Radkovskaya, O. Sydoruk, M. Shamonin et al., *MOTL* 49 (2007) 1054.
- [11] O. Sydoruk, M. Shamonin, A. Radkovskaya et al., *J. Appl. Phys.* 101 (2007) 073903.

24TL-C-6

EXACT AND ASSYMPTOTIC EXPRESSIONS FOR EFFECTIVE MAGNETO-RESISTANCE TENSOR COMPONENTS OF GENERIC THREE-DIMENSIONAL PERIODICAL COMPOSITE WITH CONDUCTING INCLUSIONS

Strelniker Y.M.¹, Bergman D.J.²

¹Department of Physics, Bar-Ilan University, IL-52900 Ramat-Gan, Israel

²Raymond and Beverly Sackler School of Physics and Astronomy, Tel Aviv University,
IL-69978 Tel Aviv, Israel

The strong-field magneto-transport in a generic three-dimensional composite with periodical microstructure where all the constituents are normal metals is considered. The macroscopic response in such systems turns out to be considerably simpler than it is in the absence of a magnetic field. Closed form asymptotic expressions are found for the microscopic current distributions and macroscopic effective magneto-resistance tensor components. Numerical calculations of the current distributions and effective magneto-resistance tensor components are also performed and compared with the closed form asymptotic expressions. A new critical point and the associated critical behavior are found. The ways and conditions for a possible experimental verification of the predicted phenomena, as well as their possible applications for magnetic field sensing are discussed.

24RP-C-7

EXTRAORDINARY TRANSMISSION THROUGH A METAL FILM WITH RANDOM ARRAY OF SUBWAVELENGTH HOLES

Bykov I.V., Dorofeenko A.B., Ilyin A.S., Ryzhikov I.A., Sedova M.V., Vinogradov A.P.
Institute for Theoretical and Applied Electromagnetics, Russian Academy of Sciences,
Moscow 125412, Russia

It has been experimentally shown that in near and medium IR-wave bands the transmittance of 17 nm silver layer deposited onto a lavsan film with an irregular system of small holes is 2 – 6 times higher than that of the same layer deposited onto a uniform lavsan film. The effect is of a broadband type covering the wave range of 1500 – 5000 nm. The study of system's microstructure with the help of AFM and electronic microscope shows that the silver film is corrugated with the same system of holes as the lavsan substrate is. The evaluation made within the frames of physical optics approximation has shown that due to smallness of holes' diameter (200nm) the additional transmittance through the holes is much less than the observed effect. A supposed mechanism of extraordinary light transmittance is discussed.

24RP-C-8

MAGNETIC METAMATERIALS AS NEAR FIELD LENSES

Radkovskaya A.¹, Sydoruk O.², Shamonina E.²

¹Magnetism Department, Faculty of Physics, Moscow State University, Leninskie Gory,
Moscow 119991, Russia

²School in Advanced Optical Technologies, University of Erlangen-Nuremberg, Paul-Gordan-
Str. 6, D-91052 Erlangen, Germany

The idea of near-field imaging based on the recovery of the evanescent part of the electromagnetic spectrum [1] has been a driving force in the rapid development of the field of metamaterials. The aim of this lecture is to overview our work on magnetic metamaterials employed as subwavelength lenses.

A magnetic metamaterial consists of artificial "magnetic atoms", resonant elements with a strong magnetic response, and can be seen as a lattice of LCR circuits coupled to each other magnetically. The coupling between individual resonators may lead to propagation of slow magnetoinductive (MI) waves with the wavelength much shorter than that of the electromagnetic radiation. This opens up a possibility of effective manipulation of magnetic fields on a subwavelength scale and creation of near field lenses.

Experimentally, the so-called Swiss Roll lens (a single layer of resonant Swiss Rolls, see Fig.1a) was shown to be able to transfer subwavelength information from the object to the image plane with a view to MRI applications [2]. The proposed device works well only far away from the resonant frequency, resulting in low signal-to-noise ratio. The imaging is not possible in the vicinity of the resonant frequency where a series of spatial resonant modes of MI were excited that prevented the pixel to pixel transmission and distorted the observed picture [3].

A bi-layered structure (see Fig.1b) offers a better alternative [4]. Both layers of the lens, each one capable of propagating a MI wave, form a “biatomic” metamaterial [5-7] exhibiting a complete stop band for MI waves around the resonant frequency providing conditions for near field imaging [8]. Experiments in the MHz frequency range agree with the theory [8]. However, in the design of a near field lens operating in the GHz frequency range both effects of retardation [9] have to be taken into account. Nanofabrication led to the increase in the magnetic resonance frequency of metamaterials up to the visible range [10] making near-field manipulating magnetic metamaterial devices feasible even in the visible region.

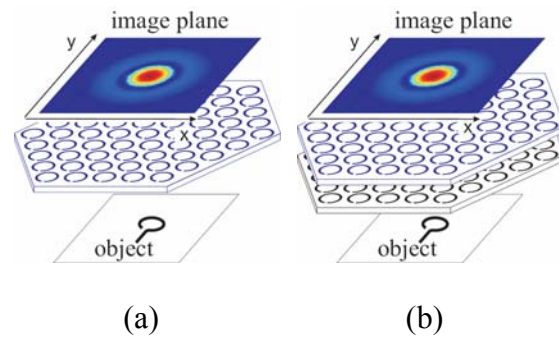


Fig. 1: Near-field imaging with magnetic metamaterials. (a) Single- and (b) double-layered lens.

- [1] J.B. Pendry, *Phys. Rev. Lett.* 85 (2000) 3966.
- [2] M.C.K. Wiltshire, J.B. Pendry, I.R. Young et al., *Science* 291 (2001) 849.
- [3] O. Zhuromskyy, E. Shamonina, and L. Solymar, *Opt. Expr.* 13 (2005) 9299.
- [4] M. J. Freire and R. Marques, *Appl. Phys. Lett.* 86 (2005) 182505.
- [5] O. Sydoruk, A. Radkovskaya, O. Zhuromskyy et al., *Phys. Rev. B.* 73 (2006) 224406.
- [6] A. Radkovskaya, O. Sydoruk, M. Shamonin et al., *IET Microw. Ant. Prop.* 1 (2007) 80.
- [7] A. Radkovskaya, O. Sydoruk, M. Shamonin et al., *Microw. Opt. Techn. Lett.* 49 (2007) 1054.
- [8] O. Sydoruk, M. Shamonin, A. Radkovskaya et al., *J. Appl. Phys.* 101 (2007) 073903.
- [9] A. Radkovskaya, M. Shamonin, C.J. Stevens et al., *J. Magn. Magn. Mat.* 300 (2006) 29.
- [10] G. Dolling, C. Enkrich, M. Wegener et al., *Appl. Phys. Lett.* 89, 231118 (2006).

24 June Tuesday

12:00-13:30

15:00-17:00

oral session

24TL-D

24RP-D

**“Magnetocaloric
Effect”**

24TL-D-1

MAGNETOCALORIC EFFECT: POWERFUL TOOL TO UNDERSTAND VARIOUS PHENOMENA IN MAGNETIC MATERIALS

Das I.

Saha Institute of Nuclear Physics, 1/AF, Bidhannagar, Kolkata-700 064, India.

E-mail: indranil.das@saha.ac.in

Magnetocaloric effect (MCE) is the adiabatic temperature change ΔT_{ad} [= T(H) - T(0)] or the isothermal entropy change ΔS [= S(H) - S(0)] of a magnetic materials with the application of magnetic field. MCE has a tremendous technological interest for its energy saving, environment friendly future application in the cooling technology. Recently we have discovered new material with highest magnetic cooling power [1] compared to any known materials in the literature. Besides the technological interest of MCE, our study indicates, MCE can be use as a powerful tool to understand various phenomena in magnetic materials. I will be discussing with the help of our own contributions how the nature of magnetic transitions even for very small amount of magnetic impurity phase in the host magnetic material can be detected [2], which is difficult by the other technique. I will also be discussing our remarkable finding, the similar dependence of MCE and magnetoresistance (MR) [3]. It has been shown by us that the comparative study of MR with MCE is a method to distinguish major contributions to the MR, namely the change in carrier number and the change in conduction electron relaxation time with the application of magnetic field. Finally I will be discussing our recent work how the magnetic field verses temperature phase diagram can be generated with the help of magnetocaloric effect [4]. MCE can also be utilized to analyze charge order state in manganites [5].

- [1] Tapas Samanta, I. Das and S. Banerjee, *Appl. Phys. Lett.*, **91** (2007) 082511.
 Tapas Samanta, I. Das and S. Banerjee, *Appl. Phys. Lett.*, **91** (2007) 152506.
- [2] R. Rawat and I. Das, *Phys. Rev. B*, **64** (2001) 052407.
- [3] R. Rawat and I. Das, *J. Phys.: Condens. Matter*, **13** (2001) L379.
 I. Das and R. Rawat, *Solid State Communications*, **115** (2000) 207.
 Tapas Samanta and I. Das, *Phys. Rev. B*, **74** (2006) 132405.
- [4] Tapas Samanta, I. Das and S. Banerjee, *Phys. Rev. B* (communicated)
- [5] Anis Biswas, Tapas Samanta, S. Banerjee and I. Das, *Appl. Phys. Lett.*, **92** (2008) 012502.
 Anis Biswas, Tapas Samanta, S. Banerjee and I. Das, *J. Appl. Phys.*, **103** (2008) 013912.

24TL-D-2

REARRANGEMENT OF CRYSTALLOGRAPHIC DOMAINS DRIVEN BY MAGNETIC FIELD IN Fe-BASED FERROMAGNETIC SHAPE MEMORY ALLOYS AND CoO SINGLE CRYSTAL

Kakeshita T.

Department of Materials Science and Engineering, Graduate School of Engineering,
 Osaka University, 2-1, Yamada-oka, Suita, Osaka 565-0871, Japan

Recently, it has been found that a large recoverable strain of several percent appears in some ferromagnetic shape memory alloys by applying magnetic field. This phenomenon is of interest because magnetic field influences not only its intensive variable but also another variable

of strain. This large magnetic field-induced strain in ferromagnetic shape memory alloy is not due to conventional magnetostriction, but due to the rearrangement of crystallographic domain of the martensite under a magnetic field. In addition, it is clarified that one crystallographic domain corresponds to one magnetic domain. In this presentation, we will show such behavior in three kinds of ferromagnetic shape memory alloys of Fe-31.2Pd, Fe₃Pt ($S = 0.8$) and Ni₂MnGa. In addition, rearrangement of crystallographic domain in antiferromagnetic CoO will be demonstrated. Also, the crystallographic domains of charge ordered phase formed by charge ordering transition in Pr_{0.55}Ca_{0.45}MnO₃ and Nd_{0.5}Sr_{0.5}MnO₃ single crystals will be presented.

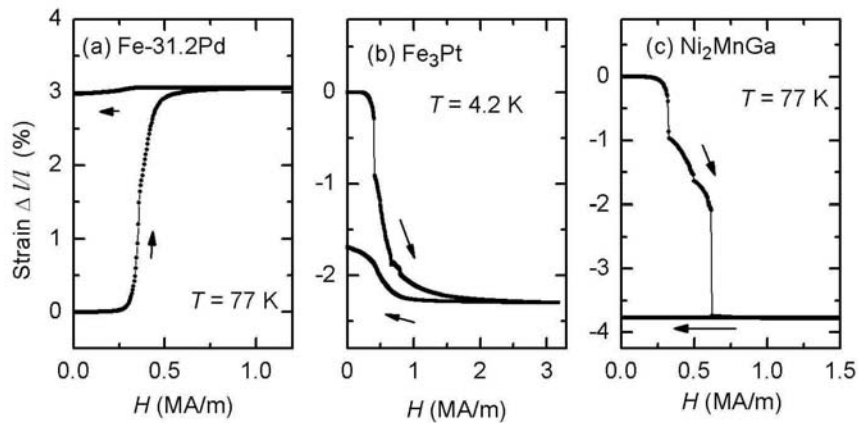


Figure 1 Magnetic field-induced strain in ferromagnetic shape memory alloys. The specimen was cooled down to the set temperature (indicated in each panel) without applying magnetic field. Then a magnetic field was applied in the [001] direction, which corresponds to either the magnetization easy axis or the hard axis depending on crystallographic domain, and then the field was removed. During the process, the strain was measured in the [001]_p direction.

24TL-D-3

MAGNETIC PROPERTIES ON SHAPE MEMORY ALLOYS Ni₂Mn_{1+x}In_{1-x}

*Kanomata T.¹, Yasuda T.¹, Sasaki S.¹, Nishihara H.², Kainuma R.³, Itoh W.⁴,
Oikawa K.⁴, Ishida K.⁴, Neumann K.-U.⁵, Ziebeck K.R.A.⁵*

¹Faculty of Engineering, Tohoku Gakuin University, Tagajo 985-8537, Japan

²Faculty of Science and Technology, Ryukoku University, Otsu 520-2194, Japan

³Institute for Multidisciplinary Research for Advanced Materials, Tohoku University, Sendai 980-8577, Japan

⁴Department of Materials Science, Graduate School of Engineering, Tohoku University, Sendai 980-8579, Japan

⁵Department of Physics, Loughborough University, LE11 3TU, UK

More recently, the present authors' group has found an magnetic-induced reverse martensitic transition from a nonmagnetic martensite phase to a ferromagnetic austenite one in the Ni-Co-Mn-In Heusler alloys[1]. These alloys open up to the possibility of utilizing the magnetic-induced shape memory effect. Since then, the magnetic shape memory alloys Ni-Mn-

Z(Z=In, Sn, Sb) have attracted much attention from the point of view of high performance materials being controlled by a magnetic field.

To understand the magnetic-induced shape memory effect in Ni-Mn-Z(Z=In, Sn, Sb) alloys, we have investigated the magnetic and crystallographic properties of $\text{Ni}_2\text{Mn}_{1+x}\text{In}_{1-x}$ ($0 \leq x \leq 0.60$) alloys.

X-ray powder diffraction and magnetization measurements were done on $\text{Ni}_2\text{Mn}_{1+x}\text{In}_{1-x}$ ($0 \leq x \leq 0.60$) alloys. Based on these experimental results, the phase diagram of the $\text{Ni}_2\text{Mn}_{1+x}\text{In}_{1-x}$ ($0 \leq x \leq 0.60$) alloys was determined. The alloys with $0 \leq x \leq 0.32$ crystallize in the cubic $L2_1$ structure and exhibit the ferromagnetic behavior. X-ray diffraction patterns indicate that the excess Mn atoms occupy the vacant Sn sites. Furthermore, magnetization measurements make clear that the Mn atoms, which substitute for Sn sites, are coupled ferromagnetically to the ferromagnetic manganese sublattices. The alloys with $0.32 \leq x \leq 0.60$ undergo the martensitic transition from the high temperature $L2_1$ structure to a monoclinic one. These alloys show a variety of magnetic transitions. A magnetic phase diagram of the $\text{Ni}_2\text{Mn}_{1+x}\text{In}_{1-x}$ ($0 \leq x \leq 0.60$) alloys is discussed qualitatively on the basis of the interatomic dependence of the exchange interactions.

[1] R. Kainuma et al., *Nature* **439** (2006) 957.

24TL-D-4

MARTENSITIC TRANSFORMATION TEMPERATURE HYSTERESIS NARROWING AND MAGNETOCALORIC EFFECT IN FERROMAGNETIC SHAPE MEMORY ALLOYS

Kokorin V.V.¹, Konoplyuk S.M.¹, Perekos A.E.², Kozlova L.E.¹, Semenova Yu.S.¹

¹Institute of Magnetism, 03680 Kiev, Vernadskogo 36b, Ukraine

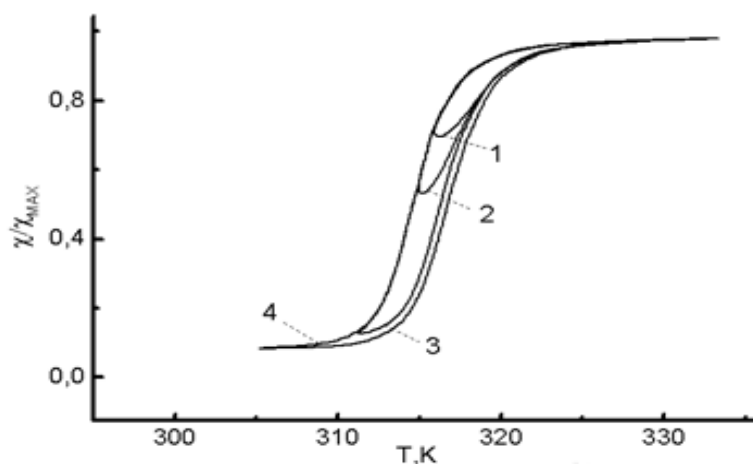
²Institute of Metal Physics, 03680 Kiev, Vernadskogo 36, Ukraine

The ferromagnetic shape memory alloys and particularly Ni-Mn-Ga ones are of significant interest due to the existence of substantial magnetic field induced strain in martensite phase [1] and large magnetocaloric effect (MCE). There is some potential for the practical applications of these alloys.

A temperature hysteresis of martensitic transformation is an important characteristic of the shape memory alloys, the values $\Delta T = 10 \div 100$ K are typical for the thermoelastic martensitic transformations.

The hysteresis width decrease is favorable to enhance MCE especially when the Curie temperature (T_C) coincides with martensitic start temperature (M_S).

The hysteresis narrowing was considered using the alloys Ni-Mn-Ga and Fe-Ni-Co-Ti. The $\text{Ni}_{54}\text{Mn}_{24}\text{Ga}_{22}$ (alloy 1), $\text{Ni}_{51.9}\text{Mn}_{27}\text{Ga}_{21.1}$ (alloy 2) and $\text{Fe}_{34.7}\text{Co}_{35.6}\text{Ni}_{14.8}\text{Ti}_8\text{Cu}_{6.9}$ (alloy 3) were melted in



argon atmosphere and used for the research. The alloy compositions were selected in order to study an influence of a number of factors on a hysteresis width. An effect of martensite crystal lattice softening due to the intermartensitic transition (IT) taking place immediately after austenite – martensite (AM) transformation on the hysteresis width was studied using the alloy 1.

The alloy 2 was selected to measure a temperature change at the expense of MCE in case of a coincidence T_C and M_S after long time annealing for a hysteresis narrowing. An iron – cobalt based alloy 3 having considerably higher magnetization in comparison with the alloys 1 and 2 was studied to find out an effect Cu addition on a temperature hysteresis width of martensitic transformation and to measure MCE in temperature interval of martensitic transformation.

As a result, it was demonstrated that in Ni-Mn-Ga alloys, the hysteresis width reaches a value $\Delta T \approx 2$ K (see figure) if IT is enough close to a main AM transition. The figure shows the temperature dependence of low field magnetic susceptibility (χ) for the partial cycles heating-cooling (χ_{MAX} – maximum value of χ in measured temperature interval), curves 1, 2, 3, 4 correspond to a cooling to 316, 315, 311, 305 K, respectively. A temperature change due to MCE has a maximum at $T \approx T_C \approx M_S$ and reaches 0.25 K at field $H = 7.5$ kOe. An Cu addition to Fe-Co-Ni based alloys has given rise to the hysteresis narrowing up to $\Delta T \approx 50$ K that is half as much as ΔT for these alloys without Cu. A magnetocaloric temperature change for alloy 3 is not essential at $T \approx M_S$.

[1] K.Ullakko, J.K.Huang, C.Kantner, V.V.Kokorin, R.C.O'Handley, J.Appl.Phys., **69** (1996) 1966.

24TL-D-5

MAGNETORESISTANCE OF $Ni_{2-x}Mn_{1+x}Ga$

Barman S.R.¹, Banik S.¹, Rawat R.¹, Mukhopadhyay P.K.², Ahuja B.L.³, Chakrabarti A.⁴

¹UGC-DAE Consortium for Scientific Research, Khandwa Road, Indore, 452001, India

²LCMP, S. N. Bose National Centre for Basic Sciences, Kolkata, 700098, India

³Department of Physics, M. L. Sukhadia University, Udaipur 313001, India

⁴Raja Ramanna Centre for Advanced Technology, Indore, 452013, India

Nowadays there is enormous interest in the Ni-Mn-Ga magnetic shape memory alloys because of large strain and fast actuation by magnetic field. Here, we report the magnetoresistance (MR) and magnetic properties for a series of $Ni_{2-x}Mn_{1+x}Ga$ ferromagnetic shape memory alloys with $-0.35 \leq x \leq 1$ spanning both the Ni and Mn excess compositions. Systematic increase is observed at room temperature in the magnitude of negative MR from 0.2% to 7.3% at 8 T, as x decreases from 1 (Mn_2NiGa) to -0.35 ($Ni_{2.35}Mn_{0.66}Ga_{0.98}$). Isothermal magnetization at RT does not track the MR behaviour. The saturation magnetization is found to be highest for Ni_2MnGa ($x=0$) and decreases for both Ni and Mn doping. The MR behavior can be explained by the s-d scattering model on the basis of the monotonic increase in Curie temperature over the studied composition range.

MR for Ni_2MnGa ($x=0$) varies almost linearly in the austenitic and pre-martensitic phases with magnetic field up to 8 T, while in the martensitic phase it shows a cusp-like shape.[1] An unusual negative-positive-negative switching of magnetoresistance has been observed in $Ni_{1.75}Mn_{1.25}Ga$ ($x=0.25$) as a function of temperature. The negative MR behaviour in the austenitic phase between 300 and 120K can be explained by the s-d scattering model. Curiously, below 120 K, MR of $Ni_{1.75}Mn_{1.25}Ga$ is positive, while at still lower temperatures in

the martensitic phase, MR is negative again. The positive MR cannot be explained by Lorentz contribution and is related to a magnetic transition. Evidence for this is obtained from a decrease in magnetization, resistivity upturn at 120 K and *ab initio* density functional theory. The density functional theory calculations using full potential augmented plane wave method show that a ferrimagnetic state with antiferromagnetic alignment between the excess Mn atoms and the remaining Mn atoms is the energetically favoured ground state. A similar ferrimagnetic state with antiferromagnetic coupling between Mn atoms has been reported recently for Mn₂NiGa.[2] In the martensitic phase, the MR is influenced by two competing factors: a dominant negative trend up to the saturation field due to decrease of electron scattering at twin and domain boundaries; and a weaker positive trend due to the ferrimagnetic nature of the magnetic state.

Funding from Ramanna Research Grant (Department of Science and Technology, India) and Partner Group project (Max Planck Institute, Germany) are acknowledged.

[1] C. Biswas, R. Rawat, and S. R. Barman, *Appl. Phys. Lett.*, 86, 202508 (2005).

[2] S. R. Barman, S. Banik, A. K. Shukla, C. Kamal, and A. Chakrabarti, *Europhys. Lett.* 80, 57002 (2007).

24RP-D-6

MAGNETIC ENTROPY CHANGES AND PHASE FORMATION IN COMPOUNDS $\text{La}_{1-x}\text{Pr}_x\text{Fe}_{10.725}\text{Co}_{0.91}\text{Si}_{1.365}$

*Shi Puji**, *Fu Bin*, *Bao Bo*, *Long Yi*, *Ye Rongchang*, *Chang Yongqin*, *Wan Farong*

School of Materials Science and Engineering, University of Science and Technology of Beijing,
100083, P R China

E-mail: shipuji@163.com

The structure and magnetic entropy changes ΔS of compounds $\text{La}_{1-x}\text{Pr}_x\text{Fe}_{10.725}\text{Co}_{0.91}\text{Si}_{1.365}$ ($x=0, 0.2, 0.4, 0.6$) have been experimentally investigated. The room-temperature powder XRD patterns show these compounds crystallized in a very clean single phase with a cubic NaZn₁₃-type structure. The increasing Pr content enhances the magnetic entropy changes ΔS sharply, but leads to a reduction of the Curie temperature T_C . The influence of Co doping on itinerant electron magnetic transition and magnetic entropy changes are discussed. Consequently, the economical compounds $\text{La}_{1-x}\text{Pr}_x\text{Fe}_{10.725}\text{Co}_{0.91}\text{Si}_{1.365}$ can be used as magnetic refrigerant materials working at near room temperature.

24RP-D-7

MAGNETOCALORIC EFFECTS IN Ni-Mn-X BASED HEUSLER ALLOYS WITH X=Ga, Sb AND In

Dubenko I., *Pathak A.K.*, *Gautam B.R.*, *Khan M.*, *Stadler S.*, and *Ali N.*

Southern Illinois University, Department of Physics, Carbondale, IL 62901 USA

The Mn-based Heusler alloys encompass a rich collection of useful materials from highly spin-polarized systems to shape memory alloys and, now, to magnetocaloric materials.

Substantial magnetocaloric effects (MCE's) are expected at phase transitions driven by temperature and/or magnetic fields. We have studied magnetostructural transitions from paramagnetic austenite to ferromagnetic martensite phase at T_{MC} in Ni_2MnGa based alloys, and martensitic transitions from ferromagnetic austenite to the martensite state at T_M in off-stoichiometric Ni-Mn-(In/Sb) Heusler alloys. The phase transition temperatures and respective magnetic entropy changes (ΔS) depend on composition in these systems and have been determined from magnetization measurements in the temperature interval 5-400K and in magnetic fields up to 5T. Magnetocrystalline transitions near room temperature have been observed in the following Heusler alloys: $Ni_2Mn_{0.75}Cu_{0.25-x}Co_xGa$, $Ni_2Mn_{0.7}Cu_{0.30}Ga_{0.95}Ge_{0.05}$, $Ni_2Mn_{1-x}Cu_xGa$, $Ni_{2+x}Mn_{1-x}Ga$, and $Ni_2Mn_{0.75-x}Cu_xGa$. It was found that the ΔS associated with T_{MC} persists in a range $-(40-60)$ J/(KgK) for a magnetic field change $\Delta H = 5T$ in each system. The transition temperatures vary from 270K to 370K with composition. The evolutions of the phase transition

temperatures and entropy changes with small variations in composition in $Ni_{50}Mn_{37-x}Sb_{13+x}$ and $Ni_{50}Mn_{50-x}In_x$ compounds have been evaluated. It was found that the martensitic transformation results in inverse MCE's in both systems. The maximum value of entropy changes was found to be $\Delta S = 38$ J/(KgK) for a magnetic field change $\Delta H = 5T$ for $Ni_{50}Mn_{35}In_{15}$.

We find that these systems present an opportunity to study the different types of magnetization behaviours in the vicinity of complex phase transitions, and that they may lead to advances in the field of MCE.

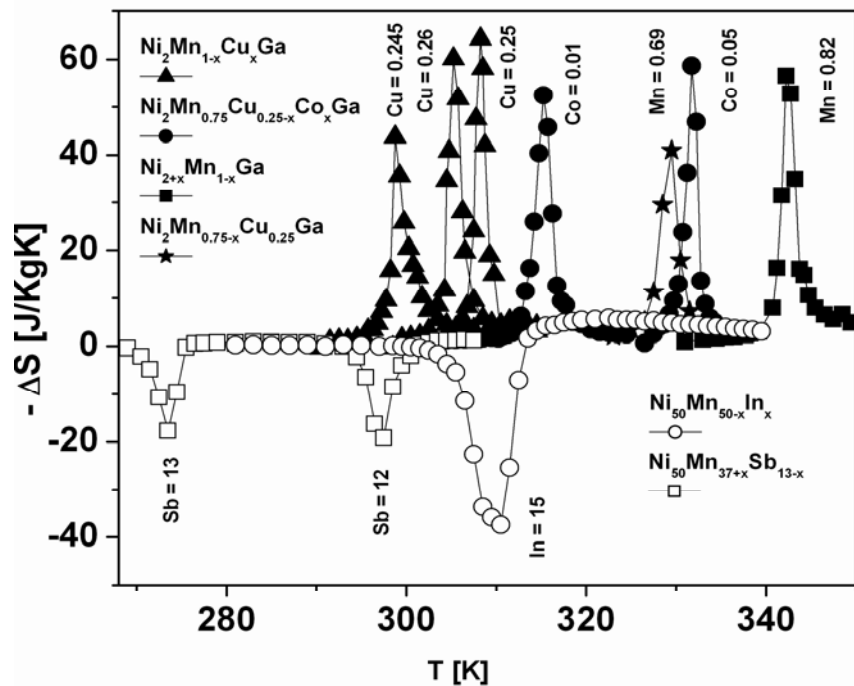


Fig.1 $\Delta S(T)$ for the some compounds of the Ni-Mn-X (with X=Ga, Sb and In) systems for $\Delta H = 5T$

Support from the US DOE and Research Corporation is acknowledged.

24RP-D-8

FePd MELT-SPUN RIBBONS AND NANOWIRES: FABRICATION AND MAGNETO-STRUCTURAL PROPERTIES

Vega V.¹, Prida V.M.¹, Franco V.², Sánchez Llamazares J.L.¹, Pérez M.J.¹, Santos J.D.¹, Escoda Ll.³, Suñol J.J.³, Hernando B.¹

¹Departamento de Física, Universidad de Oviedo, Calvo Sotelo s/n, 33007 Oviedo, Spain

²Dept. Física Materia Condensada, ICME-CSIC, Universidad de Sevilla, 41080 Sevilla, Spain

³Universidad de Girona, Campus Montilivi, Lluís Santaló s/n, 17003 Girona, Spain

FePd(30%Pd) bulk alloys are of considerable interest due to their exciting magnetic shape memory (SMA) behaviour that may lead to their applications in sensors and microactuators as intelligent/smart materials [1], as well as the possibility of also exhibiting other magnetic properties of applicative interest as giant magnetostrictive properties, magnetoresistance (MR) and magnetocaloric (MCE) effects, which can be controlled either by changing the temperature in a certain range or by applying an external magnetic field at constant temperature. These interesting phenomena, characteristics of the thermoelastic properties of these FePd SMA alloys, are related to its austenite-to-martensite reversible transformation from a face centered cubic (fcc) to face centered tetragonal (fct) martensitic transformation that is driven by either varying temperature or applied magnetic field [2]. However, bulk thermoelastic SMAs are not suitable for their use in rapid actuation of microsensors or actuators because of the response speed of actuators is significantly limited by the heat conduction of the material itself. One possibility for overcoming this disadvantage consist of fabricating nanostructured SMA alloys, well in form of thin films [3], or as arrays of self-ordered nanowires embedded into nanoporous anodic alumina membranes (NAAM) [4], where high uniaxial shape anisotropy enables FePd nanoparticles to overcome thermal fluctuations even in very small sizes.

In this work, we report on the microstructure, composition and magnetic properties of $\text{Fe}_{1-x}\text{Pd}_x$ ($x=0.3$) alloys, with ribbon and nanowire geometry. Ribbon samples were produced by melt spinning technique under argon atmosphere, starting from master alloys that were prepared from pure elements (>99.9%) by argon arc melting. On the other hand, FePd nanowires having about 35 nm in diameter, 105 nm inter-nanowires distance and around 4 microns in length, were synthesized by alternating pulsed electrodeposition of the plating bath solution into NAAMs used as templates (see Fig. 1). Samples were characterized by scanning electron microscopy (SEM), energy dispersive X-ray microanalysis (EDX) and dc magnetization measurements up to 1.5 T, in the temperature range between RT up to 1000 K. EDX analysis of ribbons shows that chemical elements were homogeneously distributed in the alloys that shown an average atomic composition of Fe(73.2%) and Pd(26.8%). $M(T)$ measurements exhibit a reversible behaviour in the temperature range between RT to 720 K, but around 770 K a clear irreversible transformation takes place.

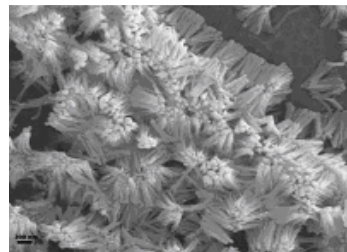


Fig. 1 SEM image of an array of FePd nanowires, after partial dissolution of the NAAM template in NaOH acid.

Financial support under Spanish MEC and FICYT research projects MAT2006-13925, NAN-2004-09203, COF07-013 and PCTI_FC06-PC041 is also acknowledged.

[1] D. Vokoun, C.T. Hu, *Scripta Mater.*, **47** (2002) 453.

[2] H. Uchida, Y. Matsumura, H. Uchida, H. Kaneko, *J. Magn. Magn. Mater.*, **239** (2002) 540.

[3] F. Wang, S. Doi, K. Hosoiri, H. Yoshida, T. Kuzushima, M. Sasadaira, T. Watanabe, *Electrochim. Acta*, **51** (2006) 4250.

[4] X.L. Fei, S.L. Tang, R.L. Wang, H.L. Su, Y.W. Du, *Solid State Commun.*, **141** (2007) 25.

24RP-D-9

NEUTRON DIFFRACTION AND BAND STRUCTURE CALCULATIONS IN MAGNETOCALORIC R_2Fe_{17} ($R = Pr, Nd$) ALLOYS

Gorria P.¹, Piñeiro A.², Pardo V.², Baldomir D.², Sánchez Llamazares J.L.¹,
Sánchez-Marcos J.^{3,4}, Blanco J.A.¹

¹Departamento de Física, Universidad de Oviedo, Calvo Sotelo, s/n, 33007 Oviedo (Spain)

²Departamento de Física Aplicada. Facultad de Física and Instituto de Investigaciones Tecnológicas. Universidad de Santiago de Compostela, E-15782. Santiago de Compostela, Spain

³ILL, BP 156, 6, rue Jules Horowitz, 38042 Grenoble Cedex 9, France

⁴Instituto de Ciencia de Materiales de Madrid, CSIC, Cantoblanco, 28049 Madrid, Spain

Intermetallic R_2Fe_{17} compounds crystallizes in the rhombohedral Th_2Zn_{17} -type crystal structure ($R\bar{3}m$) when R is a light rare earth metal [1]. Ferromagnetic order with T_C values around room temperature are observed for $R = Pr$ and Nd , with a high value for the spontaneous magnetisation [2]. In addition, both compounds exhibit strong magneto-volume effects below T_C , such as anomalous thermal expansion and a negative value for dT_C/dP [2], and a moderate magneto-caloric effect around room temperature [3, 4].

As expected from the Campbell's model describing the exchange interactions in 3d-4f systems, the magnetic moments of Fe and R in R_2Fe_{17} compounds are parallel, with magnetic moments around $2.5 \mu_B/at$ and $2 \mu_B/at$ for the rare earth and Fe respectively, and with both magnetic moments lying in the basal plane of the hexagonal unit cell [2]. However, it has been proposed recently an antiparallel configuration between the magnetic moments of the rare-earth and Fe atoms based in band structure calculations [5]. Hence, the explanation of the magnetic behaviour remains controversial, although these compounds have been largely studied during the last decades, which in turn, this fact is of primary importance in order to completely understand the magneto-caloric effect and the magneto-volume anomalies exhibited by these Fe-rich intermetallic alloys.

In this work we will report our recent results concerning magnetic structure determination from low temperature neutron powder diffraction in both Pr_2Fe_{17} and Nd_2Fe_{17} . The different proposed magnetic moment configurations are taken into account. Values of the magnetic moment for each of the four inequivalent sites (6c, 9d, 18f and 18h) occupied by the Fe atoms as well as that for the unique 6c site occupied by the R atom will be given. Besides that, results from band structure calculations will be shown and the discrepancies between calculated and refined magnetic structure will be discussed.

Financial support from Spanish MEC under projects NAN2004-09203-C04, MAT2005-06806-C04-01 and MAT2006/10027 is acknowledged.

[1] Q. Johnson et al., Acta Cryst., B25 (1969) 464.

[2] D. Givord, R. Lemaire, IEEE Trans. Mag., MAG-10 (1974) 109.

[3] S.Yu. Dan'kov et al., Adv. Cryog. Eng. 46 (2000) 397.

[4] P. Gorria et al., submitted.

[5] Yu.V. Knyazev et al., Phys. Rev. B, 73 (2006) 094410.

24 June Tuesday

12:00-13:30

15:00-17:00

oral session

24TL-F

24RP-F

“Theory”

24TL-F-1

TWO DIMENSIONAL ELECTRON GAS IN A PERIODIC MAGNETIC FIELD

Lacroix C.¹, Taillefumier M.^{1,2,3}, Dugaev V.K.^{4,5}, Canals B.¹, Bruno P.^{2,6}

¹Institut Neel, CNRS – UJF, BP 166, 38042 Grenoble Cedex 9, France

²Max-Planck Institut für Mikrostruktur Physik, Weinberg 2, 06120 Halle, Germany

³Department of Physics, Norwegian University of Science and Technology, N-7491, Trondheim, Norway

⁴Department of Mathematics and Applied Physics, Rzeszow University of Technology, Al. Powstancow Warszawy 6, 35-959 Rzeszow, Poland

⁵Department of Physics and CFIF, Instituto Superior Tecnico, Universidade Tecnica de Lisboa, Av. Roviso Pais, 1049-001 Lisbon, Portugal

⁶ESRF, BP 220, 38043 Grenoble Cedex, France

We study the energy spectrum and electronic properties of a spin-less two-dimensional electron gas in a periodic magnetic field of zero average, which has the symmetry of a triangular lattice, and perpendicular to the electron layer. In this case the magnetic field creates a 2D periodic potential and Bloch theorem can be applied.

We demonstrate how the structure of electron energy bands can be changed with the variation of the field strength, so that we can start from nearly free electron gas for small field, and transform it continuously to a system of essentially localized electron states for large magnetic field with a very small group velocity.

For small fields, the electrons are delocalized over the unit cell, avoiding the regions of large magnetic field, while for large fields, we find that the electrons localize near some minima of the effective potential which correspond to the regions where the periodic magnetic field is close to zero; these localized electrons are responsible for occurrence of dissipationless persistent currents creating a lattice of current contours along the lines of zero magnetic field. These persistent currents are a consequence of the chiral character of the electronic structure.

The topological properties of the electron energy bands are also varied with the intensity of the periodic field. We calculated the topological Chern numbers of several lower energy bands as a function of the field. The variation of these Chern numbers with magnetic field seems to be rather chaotic, tending to zero when the field is increasing. The corresponding Hall conductivity is nonzero and, when the Fermi level lies in a gap, it is quantized.

24TL-F-2

CHARGE AND SPIN PAIRING INSTABILITIES IN HUBBARD NANOCCLUSERS

Kocharian A.N.¹, Fernando G.W.², Palandage K.², and Davenport J.W.³

¹Physics Dept., California State University, Los Angeles, CA 90032

²U-46, Physics Dept., University of Connecticut, Storrs, CT 06269

³Brookhaven National Laboratory, Upton, NY 11973

Electron charge and spin pairing instabilities in various cluster geometries are studied exactly with emphasis on tetrahedron and square pyramid of octahedral structure under variation of interaction strength, electron doping and temperature [1-3]. The exact diagonalization, level

crossing degeneracies, spin-charge separation and separate condensation of paired doubled of electron charge and opposite spins yield intriguing insights into the origin of magnetism, ferroelectricity and superconductivity in nanoscale level [4-9]. Calculations of charge and spin collective excitations and pseudogaps demonstrate mapping between repulsive and attractive Hubbard clusters in charge and spin sectors respectively. Using this analogy for one hole off half-filling in repulsive and low spin region attractive models we show the equivalency between corresponding phase diagrams in the ground state and finite temperatures. The attractive Hubbard model exhibits Fulde-Ferrell-Larkin-Ovchinnikov phase separation into spin-rich and spin-poor regions analogous to hole-rich and hole-poor inhomogeneities in the positive Hubbard model at optimally doped regime [2]. The electron pairing at strong coupling regime provides a mechanism of electron instability with spontaneous saturated ferroelectric moment similar to Nagaoka ferromagnetism in frustrated and bipartite cluster geometries. The condition for existence of BCS like coherent charge and spin pairings gaps of equal amplitude is found at relatively low temperatures relevant to possible superconductivity. Criteria for spin-charge separation and reconciliation driven by interaction strength, next nearest coupling and temperature are also obtained [3]. Phase diagrams resemble a number of inhomogeneous, coherent and incoherent nanoscale phases seen recently in high T_c cuprates and manganites nanomaterials. Separate condensation of electron charge and spin degrees at various crossover temperatures offers a new route for superconductivity, different from the BCS scenario. The electronic instabilities found for various geometries, in a wide range of interaction strength and temperatures, will be useful for the prediction of electron pairing, ferroelectricity and possible superconductivity in nanoparticles, doped cuprates and multiferroic nanomaterials. The calculated phase diagrams resemble a number of inhomogeneous paired phases, superconductivity and ferroelectricity found in Nb nanoparticles [3]. The phase separation and electron pairing, monitored by electron doping and magnetic field in the family of doped high T_c cuprates surprisingly resemble incoherent electron pairing with spontaneous ferroelectricity in multiferroic materials [4-8].

- [1] A.N. Kocharian *et al.*, *Phys. Rev.* **B74** (2006) 024511; *Phys. Lett.* **A364** (2007) 57.
- [2] G.W. Fernando *et al.*, *Phys. Rev.* **B75** (2007) 085109.
- [3] A.N. Kocharian *et al.*, *to be published* (2008).
- [4] R. Moro *et al.*, *Phys. Rev. Lett.* **93** (2004) 086803, *ibid* **95** (2005) 237209.
- [5] Y. Kohsaka *et al.*, *Science* **315** (2007) 1380.
- [6] H.E. Mohottala *et al.*, *Nature Materials* **5** (2006) 377.
- [7] K.K. Gomes *et al.*, *Nature* **447** (2007) 569.
- [8] T. Valla *et al.*, *Science* **314** (2006) 1914.
- [9] H.E. Mohottala *et al.*, *Nature Materials* **5** (2006) 377.

24TL-F-3

EFFECTS OF INHOMOGENEITIES WITH EXTENDED CORRELATIONS ON THE SPIN-WAVE SPECTRUM IN NANOCRYSTALS AND SUPERLATTICES

Ignatchenko V.A., Mankov Yu.I.

L.V. Kirensky Institute of Physics SB RAS, 660036, Krasnoyarsk, Russia

The first part of this talk is dedicated to the theory of the spectrum and damping of spin waves in partially randomized superlattices (SLs). The SL with one-dimensional (1D), two-

dimensional (2D) and tree-dimensional (3D) inhomogeneities (IHs) is considered which models random displacements of interfaces from their initial periodic arrangement and random deformations of the interfaces, respectively. We derive the correlation function (CF) of the SL and show that effects of IHs on the wave spectrum strongly depend on the asymptotic behavior of this CF. The CF for 1D IHs tends to zero for $r_z \rightarrow \infty$, while for 3D IHs it tends to nonzero asymptote. This leads to a sharp decrease in the wave damping and an increase in the effective gap at the boundary of the SL Brillouin zone in the 3D case as compared to the 1D case. Effects of a mixture of IHs of both 1D and 3D dimensionalities are studied with taking account cross correlations between 1D and 3D IHs. It is shown that positive cross correlations partly suppress effects of 1D and 3D IHs on the wave spectrum: the gap at the boundary of the Brillouin zone increases and wave damping decreases. When the gap is closed under the action of the 1D IHs, the phenomenon of the partial opening of this gap, that is, of partial restoration of the wave spectrum of the SL is found when the 3D IHs cross correlated with the 1D IHs add to the SL. It is shown that all these effects are due to the slowly decay ($\propto r^{-1}$) of the CF of cross-correlated IHs. The unusual mechanism of the forbidden zone closing under the action of the 2D IHs is found.

In the second part of the talk the theory of effects of the 1D and 3D IHs of the magnetic anisotropy and exchange on the frequencies and widths of the FMR and SWR lines is developed. The calculation of the effects of the magnetic anisotropy IHs is carried out by the method of the averaged Green's function in the coherent potential approximation (CPA). The resonance frequencies and linewidths are obtained for the first time for the whole region of values of the correlation wave number of IHs k_c ($r_c = k_c^{-1}$ is the correlation radius, $2r_c = D$ is the value of grains in poly- or nanocrystals). For the FMR at $k_c = 0$ the linewidth is maximum and corresponds to the well-known limiting case of independent grains. When $k_c > 0$ the effect of exchange narrowing of the FMR line switches on as a consequence of the exchange coupling between the grains. In the limiting case of the strongly bounded grains (large k_c) the dependence of the linewidth on k_c corresponds to the law obtained from the scaling arguments. Large narrowing of the FMR and SWR linewidths with the decrease of the correlation radius of IHs is the substantiation of the main advantage of the nanocrystalline and amorphous materials over usual polycrystals when they are used at high frequency devices. We calculate also effects of IHs of the exchange and elastic force constants. The standard CPA can not be used in this case because these values are nonlocal parameters of the Hamiltonian. We develop the Green's function formalism and derive the analog of the Dyson and CPA equations for the long-wave IHs of the nonlocal parameters. We apply this obtained CPA equation to the study of effects of the 1D IHs of the exchange on the spectrum of spin waves in a ferromagnet.

These works were supported by the Grant of the RF President, SS-3818.2008.3.

24TL-F-4

FORMATION OF SPIN-SLIP SPIRALS IN Fe – Al ALLOYS

Arzhnikov A.K., Dobysheva L.V.

Phys.-Techn.Inst., Ur.Br., Rus.Ac.Sci., 426001 Izhevsk, Kirova str, 132, Russia

Experimental studies have revealed that a diversity of magnetic structures is realised in the Fe-Al alloys at different temperature, concentration and external magnetic field. In particular, at temperature lower than 120 K and at the Al concentration of 34-43 at % the spin-density waves are detected by neutron diffraction measurements [1]. The Hubbard model shows that

there is a wide region of the parameters at which a spin-spiral (SS) state is ground. So, the appearance of incommensurate SS waves is a natural phenomenon and they can be realized in an itinerant magnetic with changing the number of d-electrons through alloying or with pressure.

This work studies the spin-spiral state in Fe_9Al_7 and $\text{Fe}_{10}\text{Al}_6$ supercells with the help of the first-principles calculations. In the [001] direction these structures have atomic planes consisting of solely Al that hedge three planes: two adjoining planes containing iron atoms with small magnetic moment (the decrease of moment occurs due to many Al atoms in environment) and an inner plane between them containing both Al and high-spin Fe atoms. An incommensurate SS is characterized by a wave vector q which describes a long-distance angle of the moment rotation in the SS, and an angle φ between the Fe moments in the inner and outer planes. We have considered the SSs in dependence of q and φ and received that the state with minimum energy has angle φ different from that corresponding to q . So, the Al planes lock in the SS and there exist spin slips in the SS. A possibility to change the parameters of SS using pressure is discussed.

[1] D.R. Noakes, A.S. Arrott, M.G. Belk, S.C. Deevi, Q.Z. Huang, J.W. Lynn, R.D. Shull and D. Wu, Phys. Rev. Let. 91, 217201 (2003).

24TL-F-5

AB-INITIO CALCULATION AND COMPARISON OF THE PROPERTIES OF DIGITAL MAGNETIC HETEROSTRUCTURES AND DILUTED MAGNETIC SEMICONDUCTORS OF IV AND III-V GROUPS

Uspenskii Yu.A.¹ and Kulatov E.²

¹P.N. Lebedev Physical Institute of RAS, 53 Leninskii prosp. Moscow 119991, Russia

²A.M. Prokhorov General Physics Institute of RAS, 38 Vavilov str. Moscow 119991, Russia

Diluted magnetic semiconductors (DMS) and digital magnetic heterostructures (DMH) are both considered as materials promising for spintronics. In many cases these materials have identical chemical composition and differ only in the spatial distribution of magnetic atoms, which are inserted into a semiconductor as isolated impurities (DMS) or atomic layers (DMH). In this presentation we discuss our first-principles calculations of DMS and DMH on the base of the semiconductors of IV and III-V groups and magnetic transition 3d-atoms. The key element of the electronic structure of both the materials is a spin-polarized impurity 3d-band, which falls mostly in the semiconducting gap. In DMS this band is narrow, of 1 eV width, while in DMH it covers all the gap and is highly anisotropic. This difference in the electronic structure of DMS and DMH is the starting point of our analysis of their thermodynamic, magnetic, transport, and optical properties of these materials. Existing experimental facts agree with our predictions and indicate on the realistic character of our analysis,

This research was supported in part by the grant 07-02-01177a of the Russian Fund for Basic Research and by the program "Strongly correlated electrons in semiconductors, metals, superconductors and magnetic materials" of RAS.

24RP-F-6

AB INITIO STUDY OF MN-STABILIZED ZIRCONIA AND HAFNIA

Ostanin S.

Max-Planck Institute of Microstructure Physics, D-06120 Halle, Germany

Spintronics devices must possess the ability both to generate and to manipulate electronic spin at room temperature and above. Any good spintronics material must be stable and compatible with conventional semiconductors and metals. In dilute magnetic semiconductors and magnetic oxides, a variety of factors continue to keep Curie temperature far below room temperature. From the basis of ab initio calculations we propose that Mn-stabilized cubic zirconia (Mn-SZ) and hafnia (Mn-SH) can match all criteria of spintronics [1]. Pure zirconia is a high dielectric constant insulator which is thermally stable on Si and SiGe substrates. The cubic phase is stabilized at room temperature by the addition of 3 to 40 mol per cent MnO. Mn-SZ and Mn-SH may remain ferromagnetic up to 300 K, and it seems that they meet all requirements for incorporation into a field effect transistor.

We use the multiple scattering Korringa-Kohn-Rostoker theory, combined with the coherent-potential approximation to handle both the local moment disorder and randomly distributed impurities. The effect of short-range order of the magnetic impurities was studied using the supercell approach. In a ferromagnet, thermally induced spin fluctuations destroy the long-range magnetic order and the overall spin polarization. It can be modelled by the local moment degrees of freedom which vary very slowly on the timescale of the electronic motions. By taking appropriate ensemble averages over the orientational configurations, we do this in two complementary ways using the disordered local moment theory and the frozen-magnon method.

The density of states of Mn-SZ shows a pronounced half-metallicity. Its origin comes from the Hund rule that the majority spin 3d impurity states are fully occupied. The minority spin states lie partially in zirconia's band gap. Regarding the effect of oxygen vacancies, we show that Curie temperature remains high when there is up to one vacancy for every three Mn. When the number of vacancies approaches the number of Mn, the system is no longer ferromagnetic. For keeping T-C above 300 K, the Mn oxidation state should vary between 4+ and 3+ that corresponds to the system doped with MnO₂. We infer that the high levels of Mn in Mn-SZ will prevent its magnetic degradation at room temperature.

[1] S. Ostanin et al., Phys. Rev. Lett., 98 (2007) 016101.

24RP-F-7

UNIVERSAL SCALING OF FOREST FIRE PROPAGATION

Porterie B.¹, Zekri N.², Kaiss A.¹, Zekri L.², and Clerc J.-P.¹

¹Universite de Provence, IUSTI/UMR CNRS 6595, 5 Rue E. Fermi,
13453 Marseille Cedex 13, France

²Universite des Sciences et de la Technologie d'Oran, LEPM,
BP 1505 El Mnaouer, Oran, Algeria

As revealed by satellite maps the spread of forest fires is fractal¹, which suggests a new mathematical model². Until now this spread has been modelled using regular networks³⁻⁶. However there is some evidence that networks with only local contacts do not mimic real fires very well⁷⁻⁹ as they cannot take into account physical effects beyond the nearest neighbours of a

burning site (i.e. an item of vegetation), especially radiation from flames. Moreover, wind and topography may induce anisotropy, which in turn reduces the effective dimension of the propagation to less than two. This gives an idea of the second-order phase transition for a dimension ranging from one to two¹⁰. In the percolation theory¹¹, critical exponents are universal. To address the question of the universality of the wildfire propagation/non-propagation transition, we used a new two-dimensional timeweighted- site network model, which is a variant of the Watts-Strogatz small-world network¹². Here we show that forest fire patterns are fractal and transition scaling laws remain universal whatever the conditions of anisotropy and the network symmetry. Universality tells us that the characteristic critical behaviour of propagation in real (amorphous) forest landscapes can be extracted from the simplest network model. In addition to its capacity to mimic the phenomena of fire spread in nature, the present model produces super-real-time simulations of fire.

24RP-F-8

MICROSCOPIC MECHANISMS OF SPIN-DEPENDENT ELECTRIC POLARIZATION IN 3d OXIDES

Moskvin A.S.¹, Drechsler S.-L.²

¹Ural State University, 620083 Ekaterinburg, Russia

²Leibniz Institut für Festkörper- und Werkstofforschung Dresden, D-01171, Dresden, Germany

We present both a critical overview of different microscopic models of nonrelativistic and relativistic magnetoelectric coupling including so-called “*ab initio*” calculations and a systematic microscopic theory of spin-dependent electric polarization in 3d oxides starting with a generic three-site two-hole cluster [1]. A perturbation scheme realistic for 3d oxides is applied which implies the quenching of orbital moments by low-symmetry crystal field, strong intra-atomic correlations, the *dp*-transfer effects, and rather small spin-orbital coupling. An effective spin operator of the electric dipole moment is deduced incorporating both nonrelativistic $\propto (\mathbf{s}_1 \cdot \mathbf{s}_2)$ and relativistic $\propto [\mathbf{s}_1 \times \mathbf{s}_2]$ terms. The nonrelativistic electronic polarization mechanism related with the effects of the redistribution of the local on-site charge density due to *dp* covalency and exchange coupling is believed to govern the multiferroic behaviour in 3d oxides. The relativistic exchange-dipole moment is mainly stems from the nonrelativistic one due to the perturbation effect of Dzyaloshinsky-Moriya coupling and is estimated to be a weak contributor to the electric polarization observed in the most of 3d multiferroics.

As an actual application of the microscopic approach we discuss recent observations of multiferroic behaviour concomitant the incommensurate spin spiral ordering in $s=1/2$ chain cuprates LiCuVO_4 and LiCu_2O_2 which challenge multiferroic community [2]. At first sight, these cuprates seem to be prototypical examples of 1D spiral-magnetic ferroelectrics revealing the relativistic mechanism of “ferroelectricity caused by spin-currents” [3]. However, we argue that multiferroicity observed in these cuprates has nothing to do with “spin-currents” and can be consistently explained if one takes into account the nonrelativistic exchange-induced electric polarization on the Cu^{2+} centers substituting for the positions native for the Cu^+ -ions in LiCu_2O_2 or the positions native for the Li^+ -ions in LiCuVO_4 , respectively [4,5]. These substituent centers are proved to be an effective probe of the spin incommensurability and magnetic field effects.

Support by RFBR Grant № 08-02-00633 (ASM) is acknowledged.

[1] A.S. Moskvin, S.-L. Drechsler, arXiv:cond-mat/0710.0496.

- [2] Y. Yasui et al., *J. Phys. Soc. Jap.* **77**, (2008) 023712; S. Park et al., *Phys. Rev. Lett.* **98**, (2007) 057601.
 [3] H. Katsura, N. Nagaosa, and A.V. Balatsky, *Phys. Rev. Lett.* **95**, (2005) 057205.
 [4] A.S. Moskvina and S.-L. Drechsler, *Europhys. Lett.* **81**, (2008) 57004.
 [5] A.S. Moskvina, Yu.D. Panov, S.-L. Drechsler, arXiv:cond-mat/0801.1975.

24RP-F-9

MAGNETIC PROPERTIES OF THE ANISOTROPIC ANTIFERROMAGNETIC WITH DIMER ORDERING

Aplesnin S.S.^{1,2}, Petrakovskii G.A.², Miroshnichenko N.S.¹

¹M. F. Reshetneva Aircosmic Siberian State University, Krasnoyarsk, Russia

²L.V. Kirenskii Institute of Physics, Siberian Branch of the RAS, Krasnoyarsk, Russia

In recent years, much attention has been devoted to investigation into the properties of low-dimensional quantum spin system. These are given by the close proximity of competing phases with long range order or short range correlated states, for example Neel order and a spin liquid. The dynamic of such system is governed even at finite but low temperatures by quantum fluctuations instead of thermal fluctuations.

Unusual magnetic properties reveal the two-dimensional $\text{Cu}_3\text{B}_2\text{O}_6$ [1] crystal. The temperature dependence of the magnetic susceptibility passes through a broad maximum near 40 K, followed by a sharp decrease at temperatures below 10 K and a rise at 5 K. Incidentally, the magnetization is only $\sim 0.05 \mu_B$ in a magnetic field of 30 T at 1.5 K. Heat capacity has an anomaly at $T_N=9.8$ K, that depends on magnetic field approximately as H^2 . The elastic and inelastic neutron scattering experiments did not reveal the long-range magnetic order in this compound down to a temperature of 1.5 K. The analysis of the experimental data suggest that spin subsystem consists of single spins, clusters of pairs and fours of spins interacting with one another.

In this report, we study the Heisenberg model with alternating exchange $J(1\pm\delta)$ and spin $S=1/2$ in the square lattice in which interaction between spins is realized per strong dimer bonds. Quantum fluctuation enhanced by dimer ordering may give rise to instability AF order and lead to formation of spin liquid state. Our aim is to determine the magnetic state and thermodynamic characteristics anisotropic magnet having odd spin numbers in unit cell with special exchanges topology.

As a calculation method, we take the quantum Monte Carlo method unifying two algorithms, world-lines and continuous time. To eliminate the influence of finite lattice size using by MC simulation we restrict to investigation of AFM with the exchange anisotropy $\eta=(J^{zz}-J^{xx})/J^{zz} < 1$. There are two local exchange field $E_1=4(1-\delta)JS$ and $E_2=2JS$. In limit case $\delta \rightarrow 1$ magnetic structure consists from part of spins located in small exchange field and the pairs of spins in the singlet state. Energy related to one bond is $E/J=0.44$ for chain and $E/J=0.75$ for the dimer and $E/J=0.34$ for square lattice. The effective antiferromagnetic interaction derived from integrating out the singlets formed by the dimer bonds is $J_{\text{eff}} = 0.5J(1-\delta)^2 / (1+\delta)$ and energy is $E/J=0.68 J_{\text{eff}}$. Disordered ground state described by a resonating valence bond is $E_{\text{dimer}}=1.5(1+\delta)J$. More exact energy value can be calculated by Monte Carlo.

The exchange alternating enhances the quantum fluctuations that causes a reduction of spin value on site. Neel temperature (T_N) is determined from the $\langle S^z(0)S^z(r) \rangle$ correlation function, the sublattice magnetization, susceptibility at the various parameters of exchange anisotropy. Dependence T_N versus alternation is well fitted by $T_N(\delta)/T_N(0)=1,7(1-\delta)^2/(1+\delta)$ at $\delta > \delta_c \approx 0.3$. Magnetization field dependence reveals plateau in the field region of $H_1 < H < H_2$, that

arises from two local anisotropic exchange fields $E_{1,2}$ in the unit cell and lead to the noncollinear spin configuration.

This work was supported by the Russian Foundation for Basic Research project no. 08-02-00364-a.

[1] G.A. Petrakovskii, L. N. Bezmaternykh and et. al. , *Phys. Sol. St.*, **49** (2007) 1315.

24RP-F-10

STRONG SHORT-RANGE ORDER IN THE FRUSTRATED FCC LATTICE AND ITS POSSIBLE ROLE IN THE STRUCTURAL TRANSFORMATION OF IRON

Ignatenko A.N.¹, Katanin A.A.^{1,2}, and Irkhin V.Yu.¹

¹Institute of Metal Physics, Ekaterinburg, Russia

²Max Planck Institute for Solid State Research, Stuttgart, Germany

The quantum Heisenberg antiferromagnet on FCC lattice with the nearest- and next-nearest neighbour exchange interactions J_1 and J_2 is considered. We use the self consistent spin-wave theory (SSWT) [1]. The dependence of the Neel temperature T_N on the ratio J_2/J_1 is shown in Fig. 1. Near the point of frustration $J_2/J_1=0.5$, T_N is small. In the Tyablikov method T_N is smaller that in SSWT, except for the narrow region near the point $J_2/J_1=0.5$. Although for non-frustrated magnets the result $T_N^{\text{Tyabl}} < T_N^{\text{SSWT}}$ is reasonable, near the point of frustration the results of SSWT are more reliable since it treats adequately quantum fluctuations, contrary to the Tyablikov theory which does not consider short-range order (SRO). The calculated temperature dependence of the averaged (over the nearest and next nearest neighbours) SRO is shown in Fig. 2 for different values of the ratio J_2/J_1 . One can see that there exists a broad temperature region of SRO above T_N .

The strong SRO is possibly relevant for the γ - α structural transformation in the Fe. It is known that FCC γ -Fe is magnetically frustrated (see, e.g. [2]). Though the determination of J_1 and J_2 for γ -Fe can be difficult because of existence of the non-Heisenbergian exchange, the presence of strong SRO can provide a magnetic-fluctuation mechanism of the structural transformation.

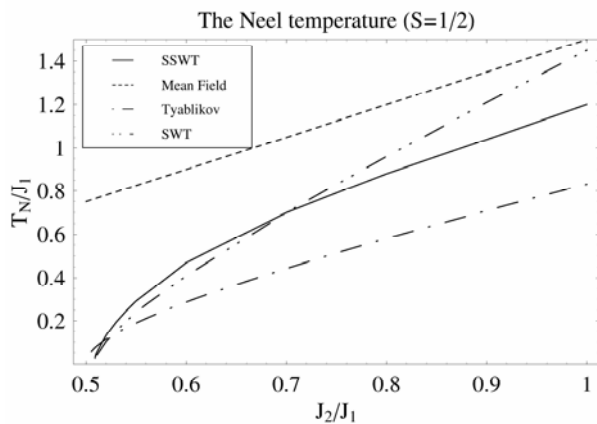


Fig. 1

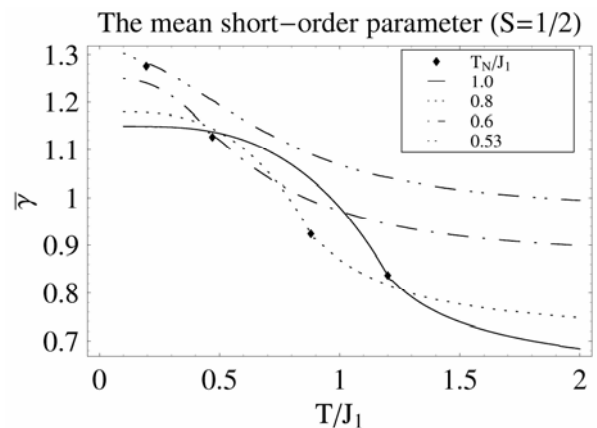


Fig.2

- [1] M. Takahashi, Phys. Rev. B, **40**, (1989) 2494; D. J. Yoshioka, Phys. Soc. Jpn., **58**, (1989) 3733; V.Yu. Irkhin, A.A. Katanin and M.I. Katsnelson, Phys. Rev. B, **60**, (1999) 1082.
- [2] O.N. Mryasov et al, J.Phys.: Cond.Matter, **3**, (1991) 7683; D.W. Boukhvalov, Yu.N. Gornostyrev, M.I. Katsnelson et al. Phys. Rev. Lett., **99**, (2007) 247205.

24 June Tuesday

17:00-19:00

poster session

24PO-6

**“Diluted Magnetic
Semiconductors”**

24PO-6-1

MOSSBAUER SPECTROSCOPY OF RUTILE IMPLANTED WITH IRON IONS AT HIGH FLUENCES

Dulov E.N.¹, Ivoilov N.G.¹, Khripunov D.M.¹, Khaibullin R.I.², Valeev V.F.², Nuzhdin V.I.², Tagirov L.R.^{1,2}

¹Kazan State University, Kremlevskaya str. 18, 420008 Kazan, Russian Federation

²Kazan Physical-Technical Institute, Sibirsky Trakt 10/7, 420029 Kazan, Russian Federation

The (1 0 0)- and (0 0 1)-monocrystalline plates of rutile (TiO₂) were implanted by 40 keV ⁵⁷Fe-isotope enriched (50%) Fe⁺ ions with fluences of 1.5·10¹⁷ ion/cm² and the ion current density of 8 μA/cm². The implantation was performed at two values of the substrate temperature – 300K (room temperature, cold implantation) and 900K (hot implantation). All of the four synthesized samples have ferromagnetic properties at room temperature.

The Mossbauer spectra of two kinds of cold-implanted samples show no significant differences. Visually they are identical. Fe-containing phases of these samples include ferromagnetic α-Fe (~60% area of the spectra) and some paramagnetic phase. The partial spectrum of the paramagnetic phase has two doublets ascribed to Fe²⁺ and Fe³⁺ ions. Using known result of the work [1], we identify this paramagnetic phase as Fe-substituted rutile Fe_xTi_{1-x}O₂. Because of native valence Ti⁴⁺ of Ti atoms in TiO₂, the Fe-substituted rutile should have oxygen vacancies. The observed quadrupole splitting for Fe²⁺ is larger than for Fe³⁺ that confirms existence of the vacancies. All implanted samples should have large number of the oxygen vacancies, because concentration of Fe²⁺ atoms is larger than concentration of Fe³⁺. Recently, the vacancy-enhanced ferromagnetism in iron-doped rutile was predicted in [2]. We report about the absence of the ferromagnetism at room temperature for strongly defected Fe_xTi_{1-x}O₂.

The Mossbauer spectra of two hot-implanted samples are significantly different both in comparison with the cold-implanted samples and between each other. The spectrum of the hot-implanted (0 0 1) sample has similar phase composition with the cold-implanted samples, but less area of the ferromagnetic sextet (~30%). A new ferromagnetic phase, Fe₃O₄, appears in the spectrum of the (1 0 0) sample. Total content of the ferromagnetic phases in this sample is ~90% (by the area of the spectrum). Ratio of the areas of the two sextets of Fe₃O₄ is 1:2, and their linewidths are close to the minimal instrumental linewidth corresponding to a good crystalline spinel.

The experimental technique (DCEMS with flowing-gas proportional detector, and sample holder with fixed working window) allows direct comparison between measured samples. At this condition, the ratio of the area of a spectrum and the area below the baseline is proportional to the total amounts of Fe atoms in the near-surface layer ~200 nm (maximal penetration depth for the conversion electrons). If this ratio is set up as 1 for the cold-implanted sample (1 0 0), then it would be 0.9 for the cold-implanted sample (0 0 1), 0.7 for the hot-implanted sample (1 0 0) and 0.3 for the hot-implanted sample (0 0 1). It is clear that such difference between the iron content in the samples can be explained by anisotropy of the interstitial thermo-diffusion [3] of Fe atoms during the implantation process. From these simple estimations we deduce that ratio of the diffusion coefficients in directions (1 0 0) and (0 0 1) is approximately 1:1000, respectively.

The work was supported by RFBR, grants 07-02-00559-a and 04-02-97505-r_ofi; CRDF BRHE Program Y3-P-07-01, the RF Ministry of Education and Science RNP.2.2.2.3.1184.

[1] T.R. Sandin, D. Schroerer, C.D. Spencer, *Phys. Rev. B* **13** (1976) 4784.

[2] J. Chen, P.Rulis, L.Ouyang, S. Satpathy, W.Y.Ching, *Phys. Rev. B* **74** (2006) 235207.

[3] K. Ruebenbauer, U.D. Wdowik, M. Kwater, *Phys. Rev. B* **54**, №6 (1996) 4006.

24PO-6-2

A MANGANESE IONS GROUND STATE IN Mn_xSi_{1-x} : NEGATIVE-U PROPERTIES CENTRE?

Yakubanya S.M.

RRC “Kurchatov Institute”, 123182, Moscow, Russia

e-mail: seryak56@mail.ru

The problem of a manganese ions ground state in Mn_xSi_{1-x} is discussed in the present work. Two limiting cases are considered (1): a concentration manganese ions is infinitesimal; (2) : concentration of Mn is close to one of Si. In the first case Mn ions can be treat as a doping impurity of Si crystal.

The concept of double defect model is used in the case (1) has been formulated earlier (see ref. [1,2]). The essence of model consists in that that the ion, acting as a doping impurity, can occupy different positions in a lattice of the basic crystal. The interstitial and substitution defects are considered as a two limiting cases in double defect model. A silicon vacancy acts as a partner for the Mn impurity ions in the suggested double defect.

At that when,

- distance between partners is infinity, interstitial defect type is realized;
- distance between partners is an infinitesimal value, we have substitution defect type;

The intermediate case, when distance between partners is of the order lattice period and only one valence bond saturated exist between partners. Such type defects has been named by the pairing defects. A plenty of pairing defects different types may exist (depending on overlapping integral of wave functions partner's and number of nonequivalent crystallographic positions in a lattice). Single type of pairing defects is realized in silicon only. The special attention is given to Jahn-Teller effect (including full-symmetrical vibration mode), which result on electronic structure of the manganese ions ground state in such system. In MnSi binary compound corresponding to case (2), there are the strong correlation effects between Mn ions, absent in strongly diluted systems (case (1)). Obviously, that correlation effects affect the electronic structure of manganese ions ground state. A possibility of such effects observation in lattice dynamics studied by neutron scattering, temperature dependence of the magnetic susceptibility, etc. are discussed in work.

[1] S.M.Yakubanya, *Fizika Tverdogo Tela (Soviet)* ,**33** (1991) 1462.

[2] S.M.Yakubanya, *Fizika Tverdogo Tela (Soviet)*, **33** (1991) 1470.

24PO-6-3

OBSERVATION OF FERROMAGNETISM IN Mn-SUBSTITUTED ZINC OXIDE NANOSTRUCTURES

Granovsky S.A.¹, Gaidukova I.Yu.¹, Markosyan A.S.², Lu Jia G.³, Chien C.J.³, Doerr M.⁴, Papageorgiou T.⁵, Wosnitza J.⁵

¹M.V.Lomonosov Moscow State University, 119991 Moscow GSP-1 Leninskie Gory, Russia

²SCCMP, 115569, mar. Zakharov str. 6, 3, Moscow, Russia

³Department of Chemical Engineering and Materials Science, University of Southern California, CA 92697, USA

⁴Institut für Festkörperphysik, TU Dresden, 01062 Dresden, Germany

⁵Hochfeld-Magnetlabor Dresden, Forschungszentrum Rossendorf, 01314 Dresden, Germany

Since the first observation of ferromagnetism in Mn-doped InAs, diluted magnetic semiconductors are intensively under the investigation. In this contribution we present our recent results on magnetic properties of undoped and Mn-doped quasi one-dimensional ZnO nano-wires formed as dendrite crystals of different width, for which the room-temperature ferromagnetism was reported [1].

Samples were synthesized by catalytic CVD method on silicon substrates and were doped by Mn by thermal diffusion. Depending on the synthesis conditions substrates with different nanowire width were obtained. Amount of Mn atoms implanted to wurtzite structure was controlled by EDX method. The magnetization versus magnetic field ($H < 50$ kOe) and temperature ($1.8 \text{ K} < T < 300 \text{ K}$) dependencies were measured by a SQUID magnetometer.

Mn-doped ZnO nanowires studied exhibit ferromagnetic properties with magnetic ordering temperature c.a. 40 K. No significant dependence of T_C on the width of the matrix nanowires was revealed. A small magnetic signal observed up to the room temperature is not intrinsic to the nanostructure and comes from a secondary phase formed during synthesis.

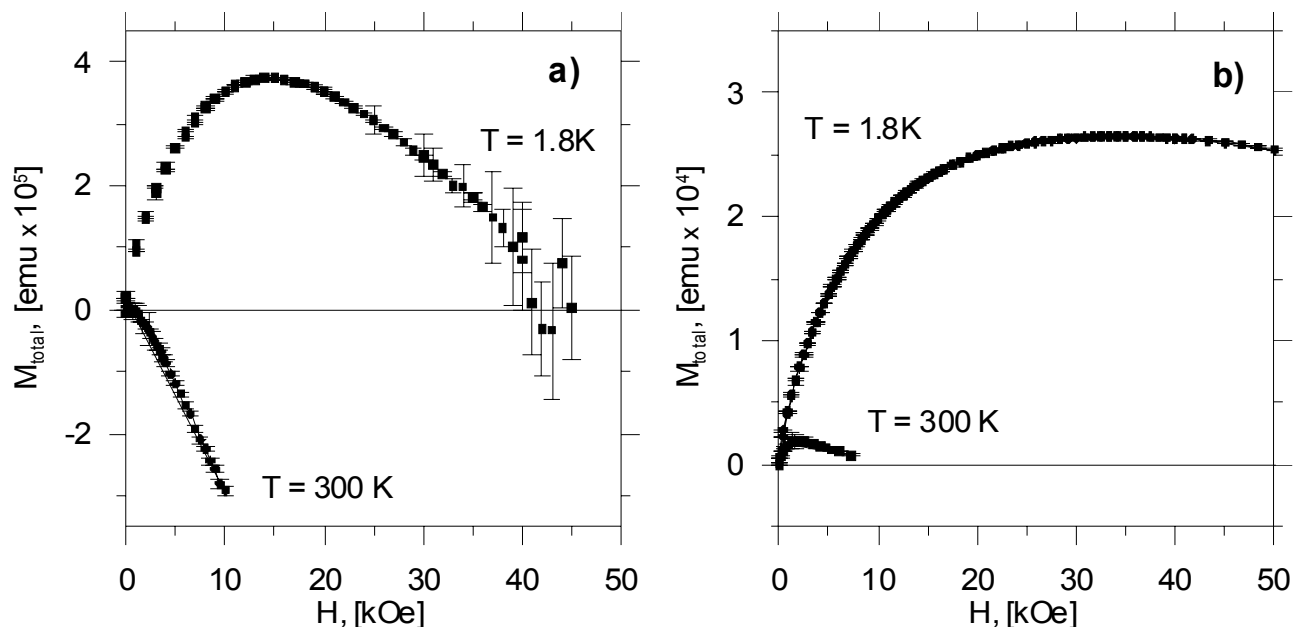


Fig. 1. Magnetization isotherms of Mn-doped ZnO nanowires with the average size $d \approx 200$ nm (a), and $d \approx 30$ nm (b).

This work was supported by RFBR (Grant # 06-02-17291)

[1] P.Sharma et.al., *Nature*, **2** (2003) 673.

24PO-6-4

ELECTROLUMINESCENCE OF InGaAs/GaAs QUANTUM SIZE HETEROSTRUCTURES WITH GaAs BARRIER MODIFIED BY DELTA-Mn DOPING

*Dorokhin M.V.¹, Danilov Yu.A.¹, Demina P.B.¹, Kulakovski V.D.², Prokof'eva M.M.¹,
Vikhrova O.V.¹, Zaitsev S.V.², Zvonkov B.N.¹*

¹Physico-Technical Research Institute of Nizhny Novgorod State University, 603950 Nizhny
Novgorod, Gagarine Av., 23/3, Russia

²Institute of Solid State Physics, RAS, 142432 Chernogolovka, Institutsky pr. 2, Russia

The important feature of currently developing newest light-emitting devices (LEDs) is the capability of emitting a circularly polarized light. The latter feature makes such LED's attractive as a key element of the spintronics [1]. Prospective devices of this kind are the light-emitting Au/*n*-GaAs Schottky diodes with a δ <Mn>-doped layer inserted near an InGaAs/GaAs quantum well (QW). Our previous investigations have shown the possibility of obtaining both high electroluminescence (EL) intensity and circular polarization [2]. In the present work we investigate the properties of InGaAs/GaAs heterostructures with δ <Mn>-doped GaAs barrier.

The structures were grown by two-stage epitaxial growth method. An In_xGa_{1-x}As/GaAs QW ($x = 0.1-0.2$) and the thin (3 nm) spacer GaAs layer were grown on *n*⁺-GaAs (or *i*-GaAs) substrates by MOCVD at 600°C. At the next stage the δ <Mn>-doping and a GaAs cap layer growth were carried out at 400°C in the same reactor by the laser sputtering of a Mn and GaAs targets, respectively. The details are described elsewhere [2]. The nominal thickness of δ <Mn> layer (Q_{Mn}) was varied from 0.1 to 1.8 monolayers (ML). The reference sample contained no δ -layer.

The type of conductivity and 2D concentration of carriers in the QW/ δ <Mn> structure were determined by the Hall effect measurements of the samples grown on *i*-GaAs substrates. All samples have a *p*-type conductivity with concentrations of holes up to $1 \times 10^{12} \text{ cm}^{-2}$ at 77 K and 1.5×10^{13} at 300 K. The hole mobility was up to $685 \text{ cm}^2/\text{V}\cdot\text{s}$ at 77 K and $70 \text{ cm}^2/\text{V}\cdot\text{s}$ at 300 K

It was found that a conduction channel in the QW remains even at low temperatures.

The forward bias EL at 77 K demonstrate d strong enhancement of the EL intensity in comparison with that of the similar samples without δ -doping. The EL intensity non-monotonously depends on the Mn content as well as on a spacer layer thickness. The maximum of the EL was obtained for the sample with $Q_{Mn} = 0.1$ ML. The best thickness of a spacer between δ <Mn> and a QW was found to be 10 nm. The enhancement of the EL is believed to be due to increased hole injection into the QW with a help of the inserted acceptor δ <Mn>-layer. This supposition is approved by *I-V* characteristics measurements that show the peculiarities on the *I-V* curves related with additional hole current flowing.

The EL at the magnetic field was measured at 1.5 K in a liquid He cryostat with the superconducting magnet. The magnetic field *B* was normal to the QW plane. In the magnetic field the EL radiation becomes circularly polarized. The degree of polarization varies for different samples from 12% to 48 % and strongly depends on the δ <Mn> parameters. However the polarization degree for samples with δ <Mn>-doping always exceeds that of reference samples evidencing about the affect of δ <Mn> on hole spin polarization in the QW.

This work was supported by RFBR (projects 08-02-00548 and 08-02-97038), Ministry of Education of Russian Federation (project 2.2.2.2.4737).

[1] A.M. Nazmul, S. Sugahara, M. Tanaka // Phys. Rev. B. **67**, 241308, (2003).

[2] Yu.A. Danilov, P.B. Demina, M.V. Dorokhin, et.al. // Euro-Asian Symp. "Magnetism on a nanoscale". Abstract Book. Kazan, 23-26 August 2007, P.121.

24PO-6-5

STUDY MAGNETIC EXITATIONS IN $\text{Ni}_c\text{Mg}_{1-c}\text{O}$ SOLID SOLUTIONS

*Mironova-Ulmane N.¹, Kuzmin A.¹, Ulmanis U.¹, Sildos I.², Pärs M.²
Cazzanelli E.³, Mariotto G.⁴*

¹Institute of Solid State Physics, University of Latvia, Kengaraga street 8

²Institute of Physics, Riia street 142, EE-2400 Tartu, Estonia

³INFN and Dipartimento di Fisica, Università della Calabria, I-87036 Arcavacata di Rende (Cosenza), Italy

⁴INFN and Dipartimento di Fisica, Università di Trento, I-38050 Povo (TN), Italy

In this paper we reviewed recent experimental data and their interpretation for $\text{Ni}_c\text{Mg}_{1-c}\text{O}$ solid solutions with an emphasis on the exchange interactions between Ni^{2+} ions. We show that different experimental methods provide with complementary information and allow deeper understanding of $\text{Ni}_c\text{Mg}_{1-c}\text{O}$ system. It was found that a dilution of nickel oxide with magnesium ions affects strongly atomic structure and optical, magnetic and vibrational properties.

A magnetic phase diagram of $\text{Ni}_c\text{Mg}_{1-c}\text{O}$ system has been established in the past by elastic magnetic neutron scattering and SQUID magnetometry. There are four domains (1) a homogeneous antiferromagnet ($0.63 \leq c \leq 1$); (2) a tricritical region or a frustrated antiferromagnet ($0.4 \leq c < 0.63$); (3) a spin-glass state ($0.25 \leq c < 0.4$) and (4) a diamagnet ($c \leq 0.2$). Complementary information on the magnetic ordering in $\text{Ni}_c\text{Mg}_{1-c}\text{O}$ single-crystals has been obtained from microscopic magneto-optic investigations of the composition and temperature dependence of the domain structure. It was found that the regular domain structure is more sensitive to the concentration of magnesium ions than T_N and appears upon cooling at temperatures well below T_N . The above mentioned techniques provide with while direct but macroscopic view on the magnetic ordering of solid solutions. Below we will discuss the experimental results, which shed light on magnetic interactions in $\text{Ni}_c\text{Mg}_{1-c}\text{O}$ system at the microscopic level. Opposite to conventional point of view, the local symmetry at Ni^{2+} ions sites lowers upon dilution due to magnetic interactions between neighbouring nickel ions. The magnetic interactions can be accessed through the study of optical and Raman spectroscopy, since both one-magnon and two-magnon excitations contribute strongly to optical and Raman spectra. We found that one-magnon energy dependence on composition shows unexpected trend which can be explained by strong decrease of the spin-spin correlation length upon dilution, however further studies are required to understand this behaviour.

A comparison of Raman scattering by phonons and magnons in $\text{Ni}_c\text{Mg}_{1-c}\text{O}$ with ones for pure NiO and MgO allowed us to withdraw several conclusions. First, the two-magnon band becomes invisible for $c < 0.7$, that agree perfectly with the magnetic phase diagram of $\text{Ni}_c\text{Mg}_{1-c}\text{O}$ system. Second, upon dilution by magnesium, a relative increase of one-phonon scattering is observed, whereas the two-phonon contribution disappears completely at $c < 0.5$. This phenomenon is explained by the local symmetry lowering at nickel sites, caused by chemical substitution and "off-centre" displacement of nickel ions.

The one-magnon Raman scattering was studied in $\text{Ni}_c\text{Mg}_{1-c}\text{O}$ solid solutions as a function of temperature and composition. The peak due to one-magnon scattering was well detected for $c \geq 0.5$ at $T \sim 25$ K and shows typical behaviour with increasing temperature [1].

[1] E. Cazzanelli, A. Kuzmin, G. Mariotto and N. Mironova-Ulmane, Phys. Rev. B 71 (2005) 134415:1-5.

24PO-6-6

MAGNETO-OPTICAL SPECTROSCOPY OF DILUTED MAGNETIC OXIDES $\text{TiO}_{2-\delta}:\text{Co}$

Gan'shina E.A.¹, Granovsky A.B.¹, Orlov A.F.², Perov N.S.¹, Vashuk M.V.¹

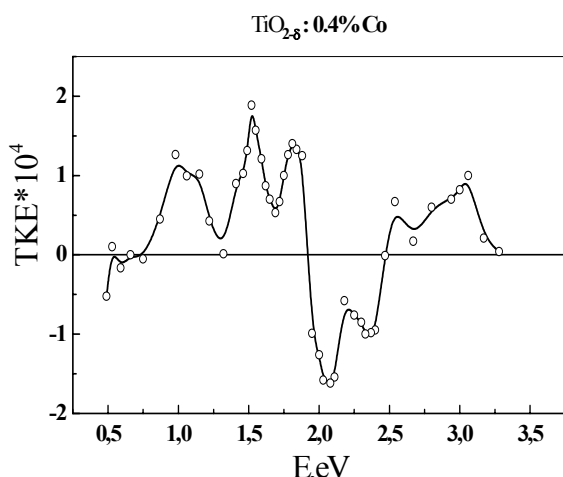
¹Faculty of Physics, Moscow State University, Moscow 119991, Russia

²State Research Institute for the Rare-Metal Industry, Moscow 119017, Russia

e-mail: eagan@magn.ru

We used magneto-optical spectroscopy to study magnetic properties of diluted magnetic oxides $\text{TiO}_{2-\delta}:\text{Co}$. The $\text{TiO}_{2-\delta}:\text{Co}$ thin films were deposited on $\text{LaMnO}_3(100)$ substrates by magnetron sputtering in an argon–oxygen atmosphere with different partial oxygen pressures. Magneto-optical spectra were measured in the transverse Kerr effect geometry (TKE) by the dynamic method in the 0.5–4.5 eV energy range from 77 to 300K in the applied magnetic field up to 3.0 kOe.

It was obtained that TKE spectra are extremely sensitive to the Co volume fraction, the crystalline structure, the film thickness and technological parameters such as the oxygen pressure, the growth rate, annealing conditions. Our investigations confirmed above room



temperature ferromagnetism in both anatase and rutile phases in the limited range of the charge-carrier concentration [1-3]. Moreover, we found intrinsic ferromagnetism at low Co volume fraction (<1%) and coexistence of extrinsic and intrinsic ferromagnetism at larger Co content. Magneto-optical spectrum in $\text{TiO}_{2-\delta}:\text{0.4\%Co}$ is shown in Fig. It consists of 6 peaks, which are not typical for metallic Co clusters and resemble optical transitions for Co^{2+} ions. With increasing Co volume fraction this structure disappears and the magneto-optical response becomes similar to that for metallic Co clusters in Co-based nanocomposites. The value of TKE was larger for an anatase phase. Despite of a small

doping level, for the anatase film in the range of transparency of the matrix, the effect has the greater value, even exceeding the value of TKE for bulk Co. It makes these diluted magnetic oxides promising for magnetophotonics.

This work was supported by the Russian Foundation for Basic Research.

- [1] Y. Matsumoto, M. Murakami, T. Shono, *et al.*, Science **291** (2001) 854.
- [2] L.A. Balagurov, S.O. Klimonsky, S.P. Kobeleva, *et al.* JETP Lett. **79** (2004) 98.
- [3] A.F. Orlov, N.S. Perov, L.A. Balagurov, *et al.* JETP Lett. **86** (2007) 405

24PO-6-7

CALCULATION OF CARRIER SCATTERING AND NEGATIVE MAGNETORESISTANCE IN Mn-DOPED GaAs/InGaAs/GaAs QUANTUM WELL WITH FERROMAGNETISM

Kulbachinskii V.¹, Shchurova L.², Kuznetsov N.¹

¹M.V. Lomonosov Moscow State University, Low Temperature Physics Department,
Physics Faculty, Moscow, Russia

²P.N. Lebedev Physical Institute of RAS, Moscow, Russia

The temperature dependences of resistance (in the temperature interval $4.2 < T < 300$ K), magnetoresistance (magnetic field up to 6 T was applied perpendicular to the sample plane), Hall effect and magnetic moment have been measured in doped with Mn and carbon structures with GaAs/In_xGa_{1-x}As/GaAs quantum well [1]. The ferromagnetism up to 400 K was detected with SQUID magnetometer. All samples had *p*-type conductivity and high hole mobility. In the temperature range between 50 and 100 K at zero magnetic field a kink in the temperature dependence of sheet resistance was observed due to hole mediated ferromagnetic transition in Ga_{1-x}Mn_xAs solid solution. At higher temperatures the resistance increases with temperature. Negative magnetoresistance was detected in the temperature interval $4.2 < T < 35$ K. The magnetoresistance changes from colossal negative to enhanced positive with increasing temperature above 35 K. Transport properties of ferromagnetic InGaAs quantum well doped with Mn have revealed interesting features resulting from the interplay between carrier transport and magnetism.

The calculations of temperature dependence of resistance and magnetoresistance for doped with Mn and carbon GaAs/In_xGa_{1-x}As/GaAs quantum well with low Mn concentration have been carried out. The resistance varies with temperature reflecting the change of free hole density in quantum well, and because of change of the scattering mechanisms determining resistance. The thermodynamic calculations of equilibrium free hole concentration (dependence of two-dimensional hole density and Mn ion concentration on temperature) are carried out. According to calculations at low temperatures ($T < 20$ K) the hole density in a quantum well is defined by the concentration of carbon acceptors. The density of free holes increases with temperature because the degree of Mn ionization raises, and the potential of Mn ionization differs in ferromagnetic and nonmagnetic phases.

We have calculated the effects of various scattering mechanisms to hole transport in quantum well. The calculation of the temperature dependence of resistance due to scattering by interface roughness, LA and LO phonons, alloy scattering, ionized impurities and localized magnetic moments have been carried out. Coulomb scattering and also spin-flip scattering give comparable contributions to the sheet resistance at temperatures less than 50 K. At high temperatures the influence of phonon scattering on resistance is the most essential.

Negative magnetoresistance is caused by influence of spin polarization of holes in ferromagnetic material. It was supposed, that in not quantized magnetic field, when cyclotron orbits are not formed, nevertheless there is the splitting of spin hole states. The value of spin splitting depends on magnetic field. The degree of population of spin hole states in examined area of temperatures and concentration is calculated for intermediate Fermi-Boltzman statistics. The negative magnetoresistance is explained quantitatively as the reduction of spin polarization and spin-flip scattering by aligning spins by magnetic field.

[1] B.A. Aronzon, V.A. Kul'bachinski, P.V. Gurin, A.B. Davydov, V.V. Ryl'kov, A.B. Granovski, et al, JETP Letters, **85** (2007) 27 (Pis'ma ZETF, **85** (2007) 32).

24PO-6-8

ROOM-TEMPERATURE FERROMAGNETISM IN InMnAs LAYERS, DEPOSITED BY PULSE LASER ABLATION

Danilov Yu.A.¹, Kudrin A.V.¹, Vikhrova O.V.¹, Zvonkov B.N.¹, Drozdov Yu.N.², Sapozhnikov M.V.², Perov N.S.³, Semisalova A.S.³, Nicolodi S.⁴, Zhiteytsev E.R.⁵, Carmo M.C.⁵, Sobolev N.A.⁵

¹Physico-Technical Research Institute of Nizhny Novgorod State University, 603950 Nizhny Novgorod, Gagarine Av., 32/3, Russia

²Institute for Physics of Microstructures, RAS, 603950 Nizhny Novgorod, Russia

³Faculty of Physics, Moscow State University, 119992 Moscow, Leninskie gory, Russia

⁴Instituto de Física, UFRGS, av. Bento Gonçalves, 91501-970 Porto Alegre, RS, Brazil

⁵Departamento de Física and I3N, Universidade de Aveiro, 3810-193 Aveiro, Portugal

Mn-doped III-V semiconductors, such as GaMnAs and InMnAs, exhibit ferromagnetic (FM) properties and are therefore promising materials for use as injectors of spin-polarized carriers in spintronic devices [1]. For many applications of FM semiconductors, the Curie temperature must be above room temperature (RT). In the present work, the InMnAs layers were grown in a quartz reactor by YAG:Nd pulse laser ablation of solid targets (InAs and Mn) in hydrogen and arsine flow. The quantity of Mn (controlled by sputtering time ratio of Mn and InAs, $Y_{Mn} = t_{Mn}/(t_{InAs}+t_{Mn})$) was varied. The temperature of GaAs (001) substrate was in range of 280 - 320°C, the layer thickness was 100 – 400 nm. The crystal quality and the phase composition were studied by x-ray diffraction. The electrical properties were derived from the Hall effect and magnetoresistance measurements at 77 and 300 K. The longitudinal magneto-optical Kerr effect (MOKE) and alternating gradient field magnetometry (AGFM) measurements were performed at RT and with magnetic field applied in sample plane. Magnetic properties also were measured with a vibrating sample magnetometer Lakeshore (resolution about 10^{-6} emu) in the temperature range 77 - 400 K. Ferromagnetic resonance measurements were performed with a Bruker ESP 300E spectrometer operating in the X-band (9.38 GHz) at temperatures varying from 4 to 300 K.

The $\Theta/2\Theta$ x-ray diffraction curves for samples comprising highly Mn doped InAs layers contain, besides the (002) peaks from the GaAs substrate and InAs in layer, additional maxima lying closely to peak positions of the MnAs hexagonal phase. Hence, the InMnAs layers with $Y_{Mn} = 0.25-0.33$, while having a good crystal quality, are not of a single phase. The InMnAs layers throughout the entire range of Mn quantity ($Y_{Mn} = 0.05 - 0.33$) exhibit FM properties as detected by magnetic and magneto-optical measurements at RT. Magnetization vs. magnetic field curves are similar for AGFM (after extraction of the diamagnetic contribution from the GaAs substrate) and MOKE measurements. The saturation magnetization monotonically increases with Y_{Mn} value, however, the coercive field is practically independent (≈ 300 Oe) on the Mn quantity. The InMnAs layers revealed the *p*-type conduction. The Hall resistance exhibited a nonlinear dependence on the magnetic field and shown hysteretic behavior both at 77 and 300 K. The carrier concentration at RT reached $\sim 1 \cdot 10^{19}$ cm⁻³, and the hole mobility was ≈ 30 cm²/(V·s). At 77 K the hole concentration decreases by a factor of 2 to 4, and the mobility increases up to ≈ 60 cm²/(V·s). The FMR measurements on Mn-containing samples revealed broad temperature-dependent anisotropic spectral bands that did not appear in reference InAs samples. Therefore, the InMnAs layers can be used as RT FM components, e.g., in spin light-emitting diodes.

This work was supported by RFBR (projects 08-02-00548 and 08-02-97038), Ministry of Education of Russian Federation (project 2.2.2.2.4737), and FTC of Portugal (projects POCI/FIS/61462/2004 and PTDS/FIS/72843/2006).

[1] I. Žutić, J. Fabian, S. Das Sarma, *Rev. Mod. Phys.*, **76** (2004) 323.

24PO-6-9

BAND STRUCTURE CALCULATIONS AND MAGNETIC RELAXATION IN CORRELATED SEMICONDUCTORS FeSb_2 AND RuSb_2

Okhotnikov K.S.¹, Gippius A.A.^{1,2}, Baenitz M.³, Shevelkov A.V.⁴

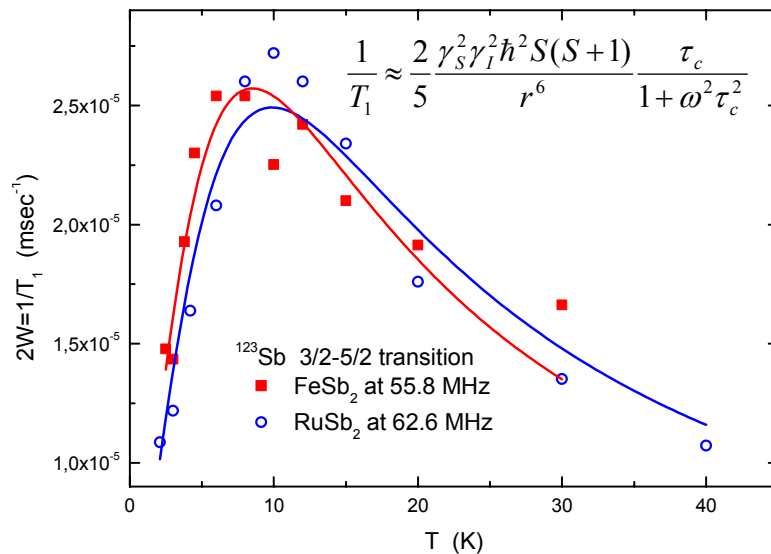
¹Faculty of Physics, Moscow State University, Moscow, Russia

²Shubnikov Institute of Crystallography, Moscow, Russia

³Max Planck Institute for Chemical Physics of Solids, Dresden, Germany

⁴Faculty of Chemistry, Moscow State University, Moscow, Russia

NQR spectra and nuclear spin-lattice relaxation of $^{121,123}\text{Sb}$ were measured in novel compounds FeSb_2 and RuSb_2 , exhibiting promising thermoelectric properties [1-3]. The Sb spectra consist of 3 lines of ^{123}Sb isotope and 2 lines of ^{121}Sb isotope in the range 45–105 MHz. The most important information about electronic structure and properties of FeSb_2 and RuSb_2 comes from Sb spin-lattice relaxation ($1/T_1$) study and *ab-initio* band structure calculations. The temperature dependence of $1/T_1$ consists of two distinct intervals. In FeSb_2 the high temperature range (above 40 K) the $1/T_1$ behavior determined by the activation law with the gap value $\Delta = 430$ K, in RuSb_2 this dependence is more close to T^2 behavior characteristic for phonon relaxation mechanism. In the low temperature regime $1/T_1$ follows dipolar electron-nuclear relaxation mechanism caused by the high spin d^5 impurity Fe^{3+} (Ru^{3+}) state for both compounds (see Figure). The existence of such impurity is caused by intrinsic non-stoichiometry of these compounds. The extra electron occupies the d_{xy} orbital of $\text{Fe}(\text{Ru})$ and form the narrow energy level of localized spins $S = 5/2$ near the bottom of the conduction band. The concentration of these paramagnetic centers extracted from the best fit of $1/T_1$ data to Bloembergen function (see figure) is about 0.3% per unit cell.



The dominant contribution to the calculated DOS comes from Fe $3d$ states and Sb $5sp$ states in FeSb_2 and from Ru $4d$ states and Sb $5sp$ states in RuSb_2 . The $g(E)$ function in FeSb_2 is in excellent agreement with results of [4]. Our calculations provide smaller gap value in FeSb_2 than in RuSb_2 : $E_g = 0.083$ eV (946 K) and $E_g = 0.19$ eV (2166 K), respectively.

This work was supported by RFBR grant 07-03-00435 and Russian Science Support Foundation.

[1] Slack G.A. In CRC Handbook of Thermoelectrics. (1995).

[2] Sales B.C., Mandrus D., Williams R.K., *Science* **272** (1996) 1325.

[3] Chepin J., Ross J., *J.Phys.:Cond.Mat.* **3** (1991) 8103.

[4] Bentien A., et al, *Phys. Rev. B* **74** (2006) 205105

24PO-6-10

MAGNETIC PROPERTIES OF DILUTED MAGNETIC SEMICONDUCTORS $Pb_{1-x}V_xTe$

Skipetrov E.P.¹, Zvereva E.A.¹, Golovanov A.N.¹, Pichugin N.A.¹, Primenko A.E.¹, Savelieva O.A.¹, Zlomanov V.P.², Vinokurov A.A.²

¹Faculty of Physics, Moscow State University, 119991 Moscow, Russia

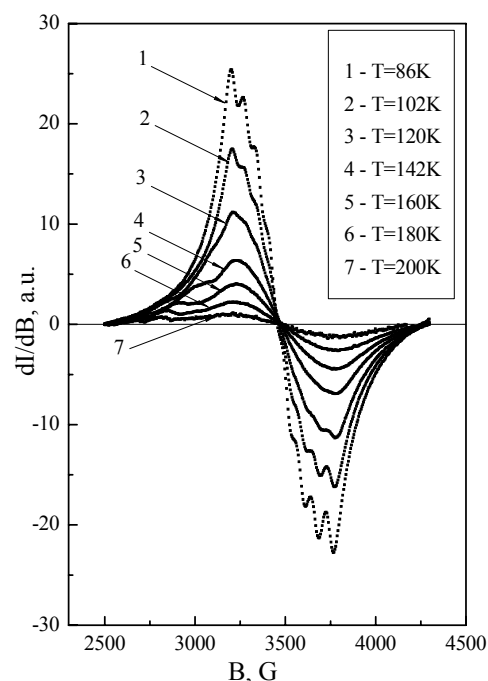
²Faculty of Chemistry, Moscow State University, 119991 Moscow, Russia

Doping of IV-VI semiconductors with rare-earth (Eu, Gd, Yb) and transition (Mn, Fe, Cr) metals turns them into the diluted magnetic semiconductors (DMS), which have attracted attention due to the effects arising from the exchange interaction between charge carriers and local magnetic moments. It is known that some of these materials demonstrate ferromagnetic behavior with the Curie temperature up to the room temperatures. In order to reveal new IV-VI DMS and investigate the correlation between electronic structure and magnetic properties of these materials in the present work the temperature and magnetic field dependences of magnetization ($T=5-300$ K, $B \leq 0.5$ T) as well as electronic paramagnetic resonance (EPR) ($f=9.4$ GHz, $T=80-250$ K, $B \leq 0.5$ T) in $Pb_{1-x}V_xTe$ ($x \leq 0.02$) alloys were studied.

Single crystals $Pb_{1-x}V_xTe$ were grown using the Bridgman method. Crystallographic analysis, performed by X-ray diffraction using a $Cu K_\alpha$ source, show the absence of the second phases in the investigated samples. It was shown that samples with low vanadium content demonstrates weak paramagnetism due to the competition between the temperature independent diamagnetic contribution of the host semiconductor lattice and Curie-Weiss paramagnetic contribution of the isolated magnetic vanadium ions in the alloys. With the increase of vanadium concentration the paramagnetic response gradually increases, indicating monotonous increase of the magnetic centers concentration, while the temperature dependences of magnetization remains paramagnetic in the whole investigated temperature range.

EPR spectra were measured in the paramagnetic phase of investigated alloys at $T > 80$ K. The values of Lande factor g were deduced from the center of the main line of the first-derivative absorption EPR spectra. It was found that g -factor is smaller well-known experimental values for V^{2+} ($g=1.97$) and V^{3+} ($g=1.98$) ions in paramagnetic vanadium salts and virtually independent on temperature ($g=1.904 \pm 0.010$). Unfortunately, extremely small difference between g -factors of V^{2+} and V^{3+} states did not allow us to determine the charge state of V ions in the samples.

Obtained experimental results were discussed assuming appearance of deep vanadium level near the bottom of conduction band [1], redistribution of electrons between localized and band states and transition of vanadium ions from V^{2+} state to V^{3+} state under the increase of the impurity concentration.



[1] A.A. Vinokurov, S.G. Dorofeev, O.I. Tananaeva et al., *Neorg. Mater.*, **42** (2006) 1445.

24PO-6-11

FERROMAGNETISM IN DILUTED MAGNETIC SEMICONDUCTORS

$\text{Pb}_{1-x-y}\text{Ge}_x\text{Cr}_y\text{Te}$

*Skipetrov E.P.¹, Mikheev M.G.¹, Pichugin N.A.¹, Kovalev B.B.¹, Skipetrova L.A.¹,
Slynko E.I.², Slynko V.E.²*

¹Faculty of Physics, Moscow State University, 119991 Moscow, Russia

²Institute of Material Science Problems, 274001 Chernovtsy, Ukraine

Doping with chromium induces an appearance of deep impurity states in the electronic structure of PbTe-based alloys. So the magnetic activity of impurity ions and magnetic properties of these materials should be dependent on their electronic structure (on the mutual arrangement of the deep impurity level, allowed band edges and Fermi level). In order to study the influence of electronic structure on the magnetic properties in the present work temperature dependences of magnetic susceptibility ($T=4.2-300$ K, $B \leq 0.5$ T) and magnetic field dependences of magnetization and Hall coefficient ($T=4.2$ K, $B \leq 8$ T) in the $\text{Pb}_{1-x-y}\text{Ge}_x\text{Cr}_y\text{Te}$ alloys were studied.

Single crystal $\text{Pb}_{1-x-y}\text{Ge}_x\text{Cr}_y\text{Te}$ ingot was grown by the Bridgman technique. The chemical composition was determined using the X-ray fluorescence analysis, which revealed that the concentration of Ge and Cr increase exponentially along the axis of the ingot ($x=0.02-0.20$, $y=0.01-0.08$). The crystal structure was investigated by X-ray diffraction. It was shown that there are no second phases in the samples at least up to the alloy composition $x=0.10$, $y=0.03$.

It was found that, according to the previously known experimental data, at low temperatures ($T < 40$ K) temperature dependences of magnetic susceptibility $\chi(T)$ contain paramagnetic Curie contribution, connected obviously with the existence of magnetically active Cr^{3+} ions in the samples. However, additional ferromagnetic contribution on the $\chi(T)$ dependences and the ferromagnetic hysteresis on the magnetization curves were revealed. The ferromagnetic share and Curie temperature ($T_C=160-280$ K) almost monotonously grow while the paramagnetic contribution decreases and disappears with the increase of Ge and Cr content in the alloys. In accordance with the Curie-Weiss law the concentration of paramagnetic ions in the samples were determined and dependence of this concentration on the matrix composition were obtained.

In the samples with $x \leq 0.07$ magnetic field dependences of the Hall voltage at $T=4.2$ K are linear indicating independence of the Hall coefficient R_H on the magnetic field. But in the alloys with $x \geq 0.10$ absolute value of the Hall coefficient decreases with the increase of magnetic field. The character of these dependences indicates that there are at least two types of conductivity mechanisms in the investigated samples – conduction band conductivity and conductivity via impurity band states. In terms of two-band conduction model the theoretical $R_H(B)$ dependences, which satisfactory agree with experimental data, were calculated and the main parameters for each type of charge carrier were determined.

Obtained experimental results are discussed in the frame of the model, assuming the metal-insulator transition due to the shift of the chromium impurity band from the conduction band to the gap under the increase of Ge content and variable electrical and magnetic activity of Cr ions. The origin of ferromagnetism in the alloys is unclear yet. However, our X-ray diffraction data allow us to suggest that it is not connected with formation of macroscopic ferromagnetic second phases in the samples. We suppose that it may be attributed to the new mechanism of exchange interaction, taking into account direct exchange interaction of the band states and localized spins and hybridization of the band states with the localized impurity states [1].

[1] V.K. Dugaev, V.I. Litvinov, J. Barnas et al, *J. Supercond.: Incorp. Nov. Magn.*, **16** (2003) 67.

24PO-6-12

MAGNETIC PROPERTIES OF COBALT OXIDE POLYMORPHS

Archer T., Hanafin R. and Sanvito S.

School of Physics and CRANN, Trinity College Dublin, Ireland

Diluted magnetic semiconductors (DMS) are a new class of materials in which magnetic dopants are introduced into a host semiconductor. The dopants provide localized spins and in some cases free charges, which would ideally arrange into a ferromagnetic ground state at low concentrations and high Curie temperatures. These materials are potentially the material foundation of future “spintronics” technologies.

(Ga,Mn)As is by far the most studied among the DMS, however the extreme difficulties in reaching Curie temperatures exceeding room temperature, has stimulated experimental activity towards other host materials and in particular towards oxide based DMS ZnO.

Room Temperature ferromagnetism in ZnO:Co was first demonstrated by Ueda et al.[1]. Subsequent experimental reports show a range of properties for this system including paramagnetism[2,3] and spin-glass[4]. As yet there is little understanding on the mechanism behind the observed ferromagnetic signal.

When ferromagnetism is detected in ZnO:Co the saturation magnetization is always small[2,5]. A possible explanation is that Co atoms congregate into clusters forming a secondary phase. Uncompensated spins on the surface of these clusters would produce the observed ferromagnetic signature. This has recently been proposed by Dietl et.al[6] as a mechanisms behind the plethora of experimental results observed for ZnO:Co.

In this work we report first principles calculations using the LSDA+U method for wurtzite and zinc-blende phases of cobalt oxide. By fitting our results to a Heisenberg Hamiltonian we are able to apply classical Monte-Carlo to show that both structures have a frustrated antiferromagnetic ground state with Neel temperatures well below room temperature.

[1] K. Ueda, H. Tabate and T. Kawai. Appl. Phys. Lett. **79** 988-990 (2001).

[2] A.C. Tuan et.al, Phys. Rev. B **70**, 054424 (2004).

[3] S.C. Wi et.al. Appl. Phys. Lett. **84** 4233-4235 (2004).

[4] Y.Z. Peng et.al, J. Appl. Phys. **98**, 114909 (2005).

[5] H.J. Lee et.al. Appl. Phys. Lett. **81** 4020-4022 (2002).

[6] T. Dietl et.al. PRB **76** 155312 (2007)

24PO-6-13

ANTIFERROMAGNETIC ORDERING OF THE 3D IONS IN THE NEW COMPOUNDS WITH $\text{Ca}_3\text{Ga}_2\text{Ge}_4\text{O}_{14}$ STRUCTURE

Ivanov V.Yu.¹, Mukhin A.A.¹, Prokhorov A.S.¹, Mill B.V.²

¹Prokhorov General Physics Institute RAS, Vavilov str.38, Moscow, Russia

²Lomonosov Moscow State University, Leninskie gory, Moscow, 119992 Russia

We have investigated magnetic properties of new magnetically frustrated compounds with the crystal structure of the $\text{Ca}_3\text{Ga}_2\text{Ge}_4\text{O}_{14}$ -type topologically equivalent to a Kagome lattice. The well known non-magnetic langasite series, the prototype of which is the $\text{La}_3\text{Ga}_5\text{SiO}_{14}$ have the same crystal structure and exhibit excellent piezoelectric properties. Recently, an attempt to

obtain a magnetic ordering in these materials has been attacked by replacing La for magnetic ions Nd and Pr, however nothing of ordered states were observed up to lowest temperatures due to magnetic frustrations [1]. In this work we have tried to achieve the magnetic ordering by implantation of the magnetic 3d ions Co^{2+} and Mn^{2+} to other crystallographic site of the $\text{Ca}_3\text{Ga}_2\text{Ge}_4\text{O}_{14}$ structure. Recently, such new compounds $\text{Pb}_3\text{Te}^{6+}\text{M}^{2+}_3\text{M}^{5+}_2\text{O}_{14}$ ($\text{M}^{2+} = \text{Zn, Co, Mg, Mn}$; $\text{M}^{5+} = \text{P, V, As}$) have been prepared [2]. These compounds have the space group $P321$. The Pb^{2+} ions occupy $3e$ site (symmetry 2), eight coordinated by oxygen anions. The Te^{6+} site ($1a$, symmetry 32) is octahedrally coordinated. Both Pb and Te form layers at $z = 0$. The M^{5+} ions ($2d$ site, symmetry 3) and the M^{2+} ions ($3f$ site, symmetry 2) are both in tetrahedral coordination and form another layer at $z = 1/2$. Triangles composed of M^{2+} ions form the trigonal net in the tetrahedral layer with distances $\text{M}-\text{M} \sim 3.5$ and 4.5 Å in the layer and ~ 5 Å between layers. For magnetic Co^{2+} and Mn^{2+} ions, one can expect a magnetic ordering at low temperatures. Polycrystalline samples were prepared at $700\text{-}900^\circ\text{C}$ by solid-state reactions in compacted mixtures of corresponding salts and oxides. Phase composition was controlled by XRD.

Magnetic properties of Co and Mn compounds were investigated by vibrating sample magnetometer in magnetic fields up to 14 kOe at the temperature range from 4.2 to 340 K. The field dependencies of magnetization show a linear character at all temperatures without any evidence of residual magnetization and hysteresis. Above 20 K, the temperature dependencies of magnetic susceptibility obey well the Curie-Weiss law with negative paramagnetic Curie temperatures varying between -10 and -40 K. This indicates an existence of antiferromagnetic interactions between 3d ions. For $\text{Pb}_3\text{TeMn}_3\text{P}_2\text{O}_{14}$, an effective moment per one Mn^{2+} ion $\mu_{\text{eff}} = (5.9 \pm 0.1) \mu_B$ that corresponds the value calculated for Mn^{2+} ion with spin $S = 5/2$. For $\text{Pb}_3\text{TeCo}_3\text{P}_2\text{O}_{14}$ and $\text{Pb}_3\text{TeCo}_3\text{V}_2\text{O}_{14}$, the experimental $\mu_{\text{eff}} = (4.6 \pm 0.1) \mu_B$ exceeds the calculated value for Co^{2+} ion with $S = 3/2$ at $g = 2$, that may be resulted from a contribution of orbital magnetic moment similar to other Co-compounds. Temperature dependencies of magnetization measured at fixed magnetic fields reveal rather sharp maxima at low temperatures, testifying for antiferromagnetic ordering. The found Neel temperatures T_N are ~ 14 K for $\text{Pb}_3\text{TeCo}_3\text{P}_2\text{O}_{14}$, ~ 11 K for $\text{Pb}_3\text{TeCo}_3\text{V}_2\text{O}_{14}$, and ~ 7 K for $\text{Pb}_3\text{TeMn}_3\text{P}_2\text{O}_{14}$.

Thus, clear evidence of long range antiferromagnetic ordering in new compounds with a Kagome lattice has been obtained.

This study was supported by the Russian Foundation for Basic Research (project no. 06-02-16601).

[1]. P. Bordet, I. Gelard, K. Marty et al., *J. Phys: Cond. Mat.* **18** (2006) 5147.

[2]. B.V. Mill, *Rus. J. Inorg. Chem.* (submitted).

24PO-6-14

FERROMAGNETISM FROM INDUCED COBALT NANO-NECKLACES IN ANNEALED COBALT DOPED ZINC OXYDE SUB-MICROMETRIC POWDERS

Barroy P.R.J.¹, Jouini N.¹, Cherif S.M.¹, Idri B.¹, Molinie Ph.², Leone Ph.², Richard V.¹

¹LPMTM-CNRS-UPR 9001, Université Paris-13, 99 av. J. B. Clément,
93400 Villetaneuse, France

²Institut des Matériaux Jean Rouxel, 2 Chemin de la Houssinière, F-44072 Nantes, France

The aim of this work is to discuss the relative influence of the synthesis method and the heat treatment on the magnetic properties of ZnO (Co) semi-conductor material. In a first step $Zn_{1-x}Co_xO$ ($0 < x < 0.33$) has been elaborated by chimie douce method namely forced hydrolysis in polyol medium [1] in order to avoid the formation of secondary phases. The as-produced powders were found to be constituted of homogenous submicrometric particles made of ZnO with Co(II) ions substituted in the würtzite lattice. Observations by means of Energy Filtered Transmission Electron Microscopy show metallic cobalt to be uniformly distributed in the whole particle (Fig. 1). The collective behavior of these particles is paramagnetic. In a second step, annealing of the as-obtained powder under hydrogen and nitrogen has been conducted. This brought ferromagnetism for temperatures above 400°C (Fig. 2). In both cases, by calculating the reduced magnetic moment per Co element, a dual magnetic contribution of Co(II) ions and metallic Co seem to occur in both annealed powders. Energy Filtered Transmission Electron Microscopy shows here that metallic Co is segregated on the borders of the submicrometric particles, producing nano-necklaces in both H₂ and N₂ annealed powders (Fig. 3). The presence of cobalt particles is confirmed in this case by X-ray diffraction analysis.

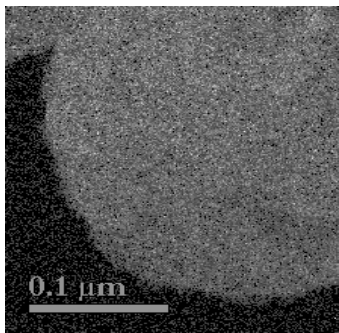


Fig. 1: As-prepared powder

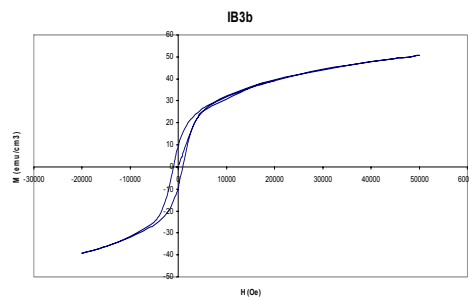


Fig. 2 : Typical hysteresis cycle of an annealed ferromagnetic sample

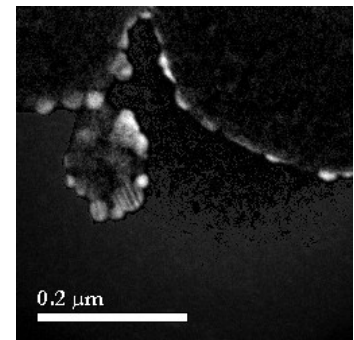


Fig. 3 : Powder annealed at 400°C under H₂

This leads us to conclude that the ferromagnetism in these powders appears to be an extrinsic property due to secondary phases induced by the heat treatment rather than an intrinsic property as predicted by Dietl et al. [2].

[1] L. Poul, S. Ammar, N. Jouini, F. Fiévet and F. Villain ; Solid State Sciences **3** (2001) 31 – 42.

[2] T. Dietl, H. Ohno, F. Matsukura, J. Cibert, and D. Ferrand, Science **287** (2001) 1019.

24PO-6-15

MAGNETORESISTANCE IN LOW-DENSITY P-TYPE Si/SiGe HETEROSTRUCTURES IN AN IN-PLANE MAGNETIC FIELD

Drichko I.L.¹, Smirnov I.Yu.¹, Suslov A.V.², Mironov O.A.³

¹A.F. Ioffe Physico-Technical Institute, St.Peterburg, 194021, Russia

²National High Magnetic Field Laboratory, Tallahassee, 32310, USA

³Warwick SEMINANO R&D Centre, UK

We have done measurements of DC magnetoresistance ρ_{xx} in the in-plane field up to 18 T in the heterostructures *p*-Si/SiGe (with the holes density $p=8.2$ and $16 \times 10^{10} \text{ cm}^{-2}$, mobility $10^4 \text{ cm}^2/\text{Vs}$) in the temperature range 0.3-2 K with two orientations against the direction of current *I*: $B \perp I$ and $B \parallel I$. At the fields $B=0-7$ T magnetoresistance in both samples demonstrates a metallic

behavior. In the sample with $p=8.2 \times 10^{10} \text{ cm}^{-2}$ the metallic state is suppressed at $B=7.3 \text{ T}$ and the magnetic field induced MIT occurs. It turned out that in the fields $B > 8 \text{ T}$ magnetoresistance shows drastic increase; furthermore it demonstrates an anisotropy with respect to the current direction: at $T=0.3 \text{ K}$ and $B=18 \text{ T}$ $\rho_{xx}/\rho_0 \approx 200$ for $B \parallel I$, and $\rho_{xx}/\rho_0 \approx 700$ for $B \perp I$. In the lowest density sample MIT wasn't observed at all, moreover, $\rho_{xx}/\rho_0 = 2$ is relatively small even at $B=18 \text{ T}$.

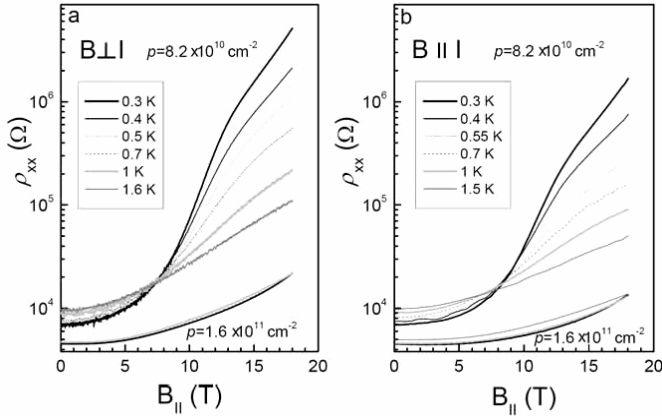


Fig.1 The dependences of ρ_{xx} on magnetic field at different temperatures: for $B \perp I$ (a) and $B \parallel I$ (b).

Large in-plane magnetoresistance is generally attributed to the modification of spin system of the electrons/holes. Indeed orbital motion of charge carriers is suppressed, and the Zeeman splitting arising in a parallel field lifts spin degeneracy.

However, in such systems like p -Si/SiGe heterostructures spin effects couldn't be considered as responsible for observed in-plane magnetoresistance. Really, in this system the heavy holes – light holes degeneracy is splitted due to a strain in SiGe. So the heavy holes are responsible for conductivity. Wave functions of the heavy holes have $(j=l+s) j=3/2$, and $m=\pm 3/2$. In this case the Zeeman splitting is completely determined by normal component of applied magnetic field.

To explain a giant in-plane magnetoresistance observed in our experiments we used the theory suggested in [1]. Authors explain the GMR as arising from the coupling of the parallel field to the carrier orbital motion due to the finite thickness in the low density of the 2D-layer.

Support by RFFI 08-02-00852, Presidium of RAS, the Program of Branch of Physical Sciences "Spintronika", NHMFL IHRP is acknowledged.

[1] S. Das Sarma and E.H. Hwang, Phys. Rev. Lett. **84**, 5596 (2000).

24PO-6-16

X-RAY DICHROISMS STUDIES OF COMPLEX MAGNETISM IN DILUTED MAGNETIC SEMICONDUCTORS

Wilhelm F., Rogalev A., Smekhova A., Goulon J.

European Synchrotron Radiation Facility, 6 rue Jules Horowitz, BP220, 38043 Grenoble, France

Recently, diluted magnetic semiconductors (DMS), where transition-metal atoms are incorporated into the semiconductor hosts, have become promising materials for future spintronics device applications. However, because those materials are synthesized using molecular beam epitaxy under thermal non-equilibrium conditions, the microscopic

characterization of their atomic and electronic structures has not been straightforward. Polarization dependent X-ray absorption spectroscopy, X-ray Linear Dichroism (XLD) and X-ray Magnetic Circular Dichroism (XMCD) in particular, is a very powerful technique for the studies of DMS since it is an element-specific probe and therefore can be used to study local electronic and magnetic properties. In particular, XLD and XMCD at the absorption edges of transition metals can be used to identify the valence state, magnetic moments, and local symmetry of the transition-metal ions in DMS. By measuring the temperature and magnetic-field dependences of XMCD signals, one can disentangle the ferromagnetic component from the paramagnetic and diamagnetic components, and study the local electronic structure of ions responsible for each component. In this talk, results are presented for various DMS which were speculated to be ferromagnetic at room-temperature, (GaMn)N [1], (GaGd)N [2], (ZnCo)O [3], (TiCo)O₂, as well as for a prototypical DMS (GaMn)As [4].

[1] E. Sarigiannidou, F. Wilhelm, E. Monroy *et al.*, *Phys. Rev. B*, **74** (2006) 041306.

[2] A. Ney, T. Kammermeier, E. Manuel *et al.*, *Appl. Phys. Lett.*, **90** (2007) 252515.

[3] A. Barla, G. Schmerber, E. Beaurepaire, *et al.*, *Phys. Rev. B*, **76** (2007) 125201.

[4] A. A. Freeman, K. W. Edmonds, G. van der Laan *et al.*, *Phys. Rev. B*, **77** (2008) 073304.

24PO-6-17

ELECTRICAL AND MAGNETIC PROPERTIES OF CdGeAs₂ LOW-DOPED BY Mn

Kochura A.V.^{1,2}, Laiho R.³, Lashkul A.³, Lahderanta E.², Shakhov M.S.⁴, Vlasenko L.S.⁴, Ivanenko S.G.¹, Marenkin S.F.⁵, Mikhailov S.G.⁵, Molchanov A.V.⁵

¹Kursk State Technical University, 305040, ul. 50 let Oktyabrya 94, Kursk, Russia

²Department of Physics, Lappeenranta University of Technology, Lappeenranta, PO Box 20, FIN-53851, Finland

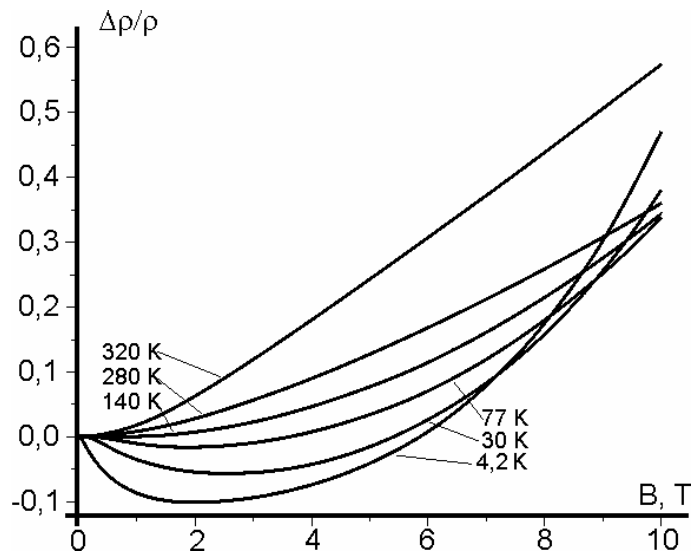
³Wihuri Physical Laboratory, University of Turku, Turku, FIN-20014 Finland

⁴A F Ioffe Physico-Technical Institute, 194021 St Petersburg, Russia

⁵Kurnakov Institute of General and Inorganic Chemistry, Russian Academy of Sciences, Leninskii pr. 31, Moscow, 119991 Russia

Cadmium germanium arsenide (CdGeAs₂) belongs to the ternary chalcopyrite family of II-IV-V₂ semiconductors. These compounds are structurally and chemically closely related to the III-V group. The discovery of hole-mediated ferromagnetic order in (III,Mn)-V with Curie temperature (T_c) up to 173 K (for (Ga,Mn)As) and observation of room-temperature ferromagnetism in II-IV-V₂ Mn doped semiconductors (e.g. CdGeAs₂, CdGeP₂, ZnGeP₂, ZnGeAs₂) encourages detailed investigations of Mn centers in II-IV-V₂ semiconductor compounds.

Single crystals of CdGeAs₂ doped with 0,006 mass % Mn have been synthesized by the vertical



Bridgman technique. Hall effect measurements indicated p-type conductivity. The room temperature carrier concentration was $4,5 \cdot 10^{15} \text{ cm}^{-3}$. The hole mobility behavior looks like that in the case of III-V semiconductors with maximum $\mu_p \sim 320 \text{ cm}^2/(\text{V} \cdot \text{sec})$ occurring at $T \sim 80 \text{ K}$. Activation energy $E_a = 170 \text{ meV}$ exceed the limit (160 meV) for native defects in undoped CdGeAs₂ crystals.

The weak paramagnetic signal was detected with help of superconducting quantum interference device (SQUID) magnetometer in magnetic field 5 T.

The electron paramagnetic resonance spectra was taken at temperature 12 K. Six-line structure of uncoupled Mn²⁺ ions was observed as well as broad signal of cation vacancy. There were no signs of Mn⁴⁺ centers.

The dependences of the magnetoresistance $\Delta\rho/\rho = (\rho - \rho_0)/\rho_0$ on magnetic field are shown in Fig. At low temperatures magnetoresistance consisted of two components: positive quadratic term (ordinary magnetoresistance) and a negative term, which depend of $B_{5/2}$ Brillouin function. Such a behaviour can be explained assuming the p-d exchange interaction between spin-polarized charge carriers and Mn²⁺ ions ($S = 5/2$) localized outside the magnetically-ordering regions.

This work was supported by RFBR under grant No 07-03-00810 and INTAS under grant No 06-100014-5792.

24PO-6-18

MAGNETOTRANSPORT AND MAGNETIC PROPERTIES OF SiMn LAEYRS WITH THE HIGH Mn CONTENT

*Rylkov V.V.^{1,2}, Aronzon B.A.^{1,2}, Lagutin A.S.¹, Nikolaev S.N.¹, Podolskii V.V.³, Lesnikov V.P.³,
Perov N.S.⁴*

¹Russian Research Center “Kurchatov Institute”, Moscow, 123182 Russia

²Institute of Applied and Theoretical Electrodynamics, Russian Academy of Sciences,
127412 Moscow, Russia

³Physics-Technical Institute of the Nizhnii Novgorod State University,
603950 Nizhnii Novgorod, Russia

⁴Moscow State University, Vorob'evy gory, Moscow, 119992 Russia

The SiMn layers with the thickness of about 50-60 nm having the Mn contents around 35% are prepared by means of method of the laser epitaxy on Al₂O₃ substrates. The temperature of the epitaxy growth of layers was 300 °C. Magnetotransport and magnetic properties of these samples are studied in the temperature range from 5K to 300K in magnetic fields up to 2 T. It is shown that SiMn layers possess the metal type of conductivity alongside with the existence of magnetization till the room temperature. For the first time the anomalous Hall effect is observed in systems based on Si and 3d-metal, and its sign is opposite to the type of conductivity (the hope type) of SiMn (Fig.1). The anomalous Hall effect has essentially the hysteresis-like character at low temperatures, and the coercitive force reaches 0.34 T at $T = 5\text{K}$ (see Fig.1). It is found that the anomalous component of the Hall effect defines its behavior completely till the room temperature keeping the hysteresis-like character up to 230 K (Fig.2).

It is impossible to explain strong ferromagnetism of the studied films as the result of the formation of Mn silicides, because the Curie temperatures of those materials (for Mn₄Si₇, etc.) don't exceed 50 K [1]. We believe that the free carriers play the essential role in the exchange

interaction, the concentration estimate of which in these layers appreciably exceeds 10^{21} cm^{-3} in our case.

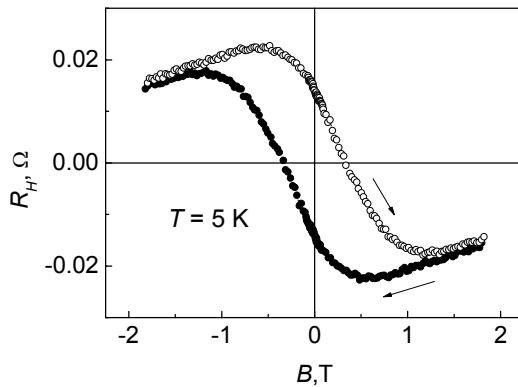


Fig. 1. Dependent of the Hall effect on magnetic field in SiMn at $T = 5 \text{ K}$

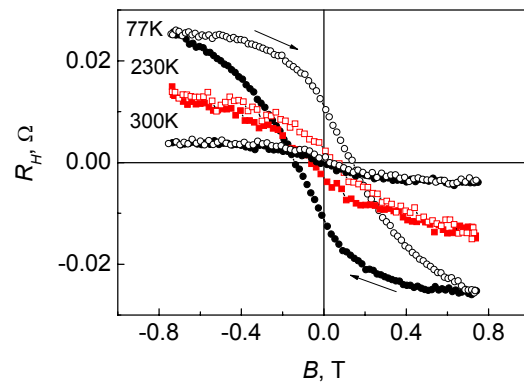


Fig. 2. Dependencies of the Hall effect on magnetic field in SiMn at high temperatures

[1] U. Gottlieb, A. Sulpice, B. Lambert-Andron, O. Laborde. *J. Alloys Comp.* **361**, 13 (2003).

24PO-6-19

MAGNETIC PROPERTIES OF Mn-DOPED ZnO NANOWIRES

Granovsky S.A.¹, Gaidukova I.Yu.¹, Markosyan A.S.², Lu Jia G.³, Chien C.J.³, Chang P.C.³, Bannikova E.M.¹, Rodimin V.E.¹

¹M.V.Lomonossov Moscow State University, 119991 Moscow GSP-1 Leninskie Gory, Russia

²SCCMP, 115569, mar. Zakharov str. 6, 3, Moscow, Russia

³Department of Chemical Engineering and Materials Science, University of Southern California, CA 92697, USA

Small amounts of $3d$ - and $4f$ - elements embedded in a host matrix of some non-magnetic semiconductors are found to be inducing ferromagnetic order. This phenomenon can be caused by hybridization of the $3d$ - ($4f$ -) electronic states with the hole states of a semiconductor or due to indirect magnetic couplings. For a Mn-doped zinc oxide (wurtzite B4 structure, $P6_3mc$) room-temperature ferromagnetism was reported in [1]. Characteristics of nano-sized ZnO materials are not systematically studied as yet. We studied structural, transport and magnetic properties of Mn-doped quasi one-dimensional ZnO nano-wires formed by dendrite crystals of different width (sample N with diameter $d \sim 200 \text{ nm}$, and sample UF with $d \sim 30 \text{ nm}$).

ZnO nanowires were synthesized by modified CVD method [2]. They were subsequently Mn-doped by thermal diffusion using Mn powder. The total Mn content was analyzed by SEM and XRD methods. Magnetic properties were measured in the temperature range $1.8 \text{ K} < T < 300 \text{ K}$ using SQUID magnetometer.

While undoped ZnO samples are diamagnets, all Mn-doped nanowires exhibit a ferromagnetic behavior, which is significantly temperature dependent (Fig.1). A small magnetic signal detected up to the room temperature could be caused by small amounts of magnetic impurities. Analysis of the temperature dependencies of magnetization shows that the observed magnetic properties can be caused by the host ferromagnetic matrix with Curie temperature $T_c \approx 35 \text{ K}$.

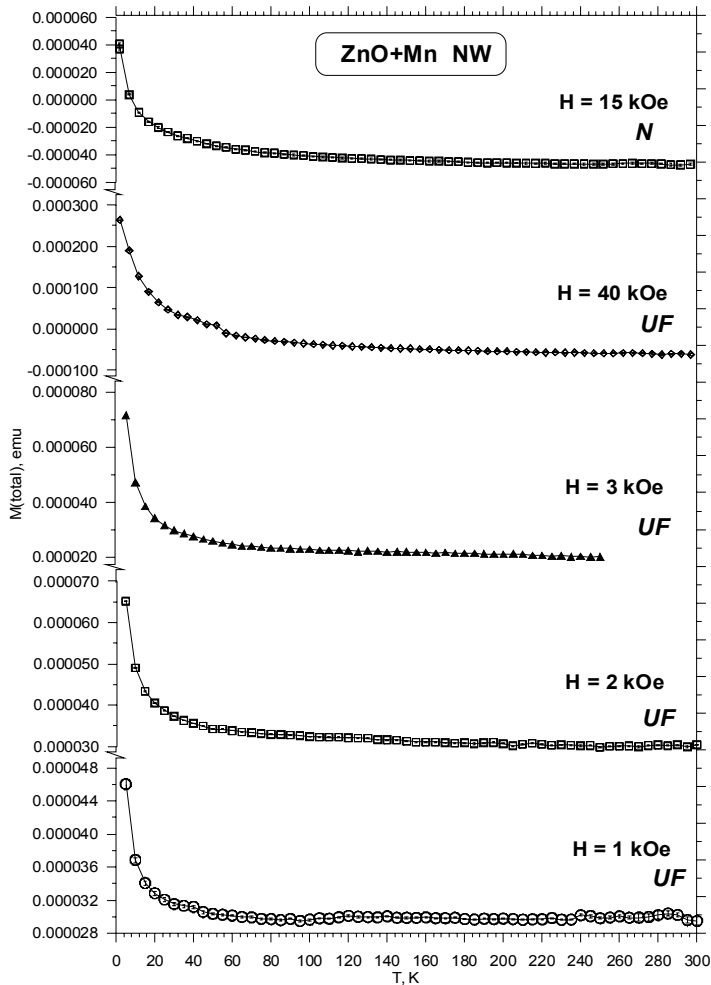


Fig.1. Magnetisation versus temperature curves, obtained for different Mn-doped ZnO samples in various fields.

This work was supported by RFBR (Grant # 06-02-17291)

[1] P.Sharma et.al., *Nature*, **2** (2003) 673.

[2] P.-C. Chang et.al., *Chem. Mater.*, **16** (2004) 5133.

24PO-6-20

PHYSICAL PROPERTIES OF THE $\text{CuM}_x\text{Cr}_{1-x}\text{S}_2$ ($\text{M}=\text{V}, \text{Fe}$) DISULFIDES

Abramova G.^{1,2}, Petrakovskiy G.^{1,2}, Szymczak R.³, Rasch J.⁴, Mazalov L.⁵, Vorotynev A.¹, Velikanov D.¹, Gerasimova J.¹, Sokolov V.⁵, Bovina A.¹, Kiselev N.¹

¹L.V. Kirensky Institute of Physics, Akademgorodok, Krasnoyarsk 660036, Russia

²Siberia Federal University, Svobodnyi ave 49, Krasnoyarsk 660041, Russia

³Institute of Physics PAS, Al. Lotnikow 32/46, Waszawa PL-02-668, Poland

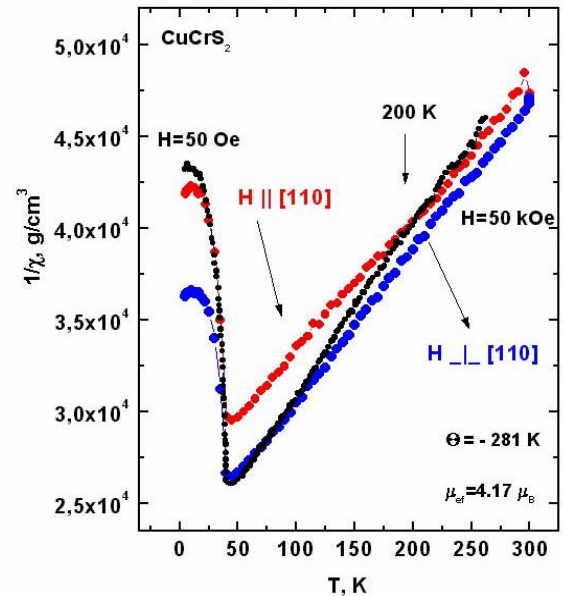
⁴Institute Laue-Langevin, 6 rue Jules Horowitz, BP 156, 38042 Grenoble, Cedex 9, France

⁵Nikolaev Institute of Inorganic Chemistry, Laventyev ave. 3, Novosibirsk 630090, Russia

There has been considerable interest over the last decade in the study of transition-metal dichalcogenides and their intercalated complexes because they show a wide range of very different physical properties and have found numerous technical applications, for example, for spintronics [1]. In the present paper, we report the studies results of the structural, electrical, magnetic properties, EPR, XAS, XES and Raman spectra of the layered intercalated $\text{CuM}_x\text{Cr}_{1-x}$.

xS_2 ($M=V$) with the different synthesis technology: the polycrystalline, ceramic and single-crystal samples. From XRD analysis we found that the samples have the lattice parameters of the rhombohedral $R\bar{3}m$ structure, which is typical for $CuCrS_2$.

Figure shows the temperature dependencies of the magnetic susceptibility of $CuCrS_2$ at different magnetic field. The anisotropy of the magnetic (figure) and electric properties with its strong dependency on the synthesis technology was found for the $CuCrS_2$ single-crystal. The ESR spectra of the samples at near room temperatures may be explained by the presence of the two paramagnet Cu and Cr ions. These data are in agreement with the XAS and XES experimental data. The splitting of the Cr EPR line and CMR was found for the $CuV_{0.1}Cr_{0.9}S_2$ at temperature range about 100 K. The powder $CuCrS_2$ has the similar splitting of the Cr line below 14 K. The experimental Raman spectra $CuM_xCr_{1-x}S_2$ ($M=V$) agree with the data of the theoretical analysis of the IR and Raman spectra for the $CuCrS_2$ with the Cu ions in the lattice tetra-position. An important founded property of the $CuCrS_2$ sulfide is the frequencies of the IR active phonon modes are equal to the frequencies of the Raman active phonon modes. These data indicate that $CuCrS_2$ crystal has no centre of inversion. The low-dimensional modulated magnetic structures (helicoids) with the large period and certain direction of the magnetization vector rotation (chirality) may occur in the magnets without the centre of inversion. The helicoidal incommensurate magnetic structure was observed by the DMC powder neutron diffraction for the $CuCrS_2$.



This study was supported by the INTAS (Project № 06-100013-9002) and the “Spin-dependent Effects in Solids and Spintronics” program of the Division of the Physical Sciences of RAS (Project № 2.4.2 SB RAS).

[1] G. M. Abramova, G. A. Petrakovskiy, et al, *JETP Letters*, **83**, (2006) 118.

24PO-6-21

INTERACTION OF A TWO SPIN SUBSYSTEMS WITH THE DIFFERENT WAVE VECTORS

Bolsunovskaya O.¹, Petrakovskii G.¹, Popov M.²

¹L.V. Kirensky Institute of Physics, Siberian Branch of the Russian Academy of Sciences, 660036, Krasnoyarsk, Russia

²Siberian Federal University, 660041, Krasnoyarsk, Russia

The attention to the problem pointed in the title has been attracted by a number of works on study of the properties of a CuB_2O_4 copper metaborate in strong magnetic fields at temperatures below 10K. In the absence of a field in this temperature region the magnetic structure of the crystal represents a helicoid along the tetragonal axis [1]. Further neutron

diffraction study [2-3] and magnetic resonance measurements [4] showed that with an increase in magnetic field intensity a transition from a phase incommensurate with the crystal lattice to the phase whose magnetic structure reveals the step occurrence of both a commensurate wave and an incommensurate wave with a shorter period. The transition to the completely commensurate structure occurs upon further increasing of the external field. The experiments on inelastic neutron scattering [3] showed that the commensurate wave in the discovered intermediate phase is formed by spins of the copper ions occupying the 2b-position in an elementary cell of the crystal, whereas the incommensurate wave is formed by spins of the copper ions occupying the 4d-position. Therefore, the latter phase may be named “semi- incommensurate”.

The analysis reported in [5] demonstrated the possibility of phenomenological description of the novel phase in the magnetic system of the copper metaborate. In the present work, the possibility of the coexistence of two magnetic subsystems with different wave vectors is studied in the mean field approximation

- [1] B. Roessli, J. Schefer, G. Petrakovskii et al., *Phys. Rev. Lett.*, **86** (2001) 1885.
 [2] J. Schefer, M. Boehm, B. Roessli et al., *Appl. Phys. A*, **74** (2002) S1740.
 [3] M. Boehm, B. Roessli, J. Schefer et al., *Physica B*, **378-380** (2006) 1128.
 [4] Y. Yasuda, H. Nakamura, Y. Fujii et al., *J. Phys.: Condens. Matter*, **19** (2007) 145277.
 [5] M.A. Popov, G.A. Petrakovskii, O.A. Bolsunovskaya, *Fiz. Tverd. Tela*, **50** (2008) 871.

24PO-6-22

TRANSPORT AND MAGNETIC PROPERTIES OF MnSe AND MnTe

*Ryabinkina L.I.¹, Romanova O.B.¹, Aplesnin S.S.^{1,2}, Balaev D.A.¹,
 Demidenko O.F.³, Yanushkevich K.I.³ and Bandurina O.N.²*

¹L.V. Kirensky Institute of Physics, Siberian Branch of the Russian Academy of Sciences,
 660036, Krasnoyarsk, Russia

²Reshetnev Siberian State Aerospace University, 660014, Krasnoyarsk, Russia

³Incorporated Institute of Solid State and Semiconductor Physics, National Academy of
 Sciences of Belarus, 220072, Minsk, Belarus

In this work we present the results of measurements of the conductivity in manganese chalcogenides MnSe and MnTe under thermal cycling in the temperature range $80 < T < 300$ K in magnetic fields up to 5 kOe. MnTe crystallizes in a NiAs-type hexagonal structure and MnSe undergoes a structural phase transition from the cubic of NaCl-type to the hexagonal of NiAs-type structure in the temperature range $248 < T < 266$ K [1]. Manganese chalcogenides are antiferromagnets and have *p*-type semiconducting conductivity. The temperature dependence of the electrical resistivity of MnTe provides evidence for a transition from the metallic to semiconducting state. The $\rho(T)/\rho_{295K}=f(T)$ dependence reveals a maximum in the electrical resistivity near $T_N = 320$ K and a sharp change of the resistivity by order of magnitude. The MnSe samples exhibit the magnetoresistance in the magneto-ordered cubic phase. It increases as one approaches the Neel temperature. Indeed, the magnetoresistance $\delta_H = (\rho(H)-\rho(0))/\rho(H) = -4.8\%$ at $T = 100$ K and $H = 5$ kOe while $\delta_H = -14\%$ at $T = 113$ K in the same field. MnSe exhibits a strong maximum in magnetic susceptibility in the temperature range $T = 160-180$ K, i.e., above the Neel temperature ~ 135 K for the cubic modification. At $T \sim 200$ K the temperature dependence of the magnetic susceptibility for MnSe passes through a minimum, which cannot be assigned to superposition of susceptibilities for the antiferromagnetic MnSe having a cubic and a nickel-arsenide structures.

Neutron diffraction studies of the magnetic and crystal structures of MnSe performed in [2] furnish direct evidence for the existence of orbital ordering. The temperature corresponding to the break in the temperature dependence of the intensity at 181 K fits well the calculated temperature of orbital ordering. Orbital (charge) ordering entails a decrease in the magnetic moment on a site, and in the limiting cases of strong interaction between the spin and orbital subsystems it will lead to disappearance of long-range order and formation of the spin liquid state. This model accounts for the decrease in the magnetic moment in MnSe down to $\mu = 4.45\mu_B$, and in MnTe to $\mu = 4.7\mu_B$ [3]. Competition between the exchange and orbital interactions induces incommensurate orbital ordering in the temperature range $T_{orb} < T < T_N$ and can give rise to spin-glass effects, which reveal in specific features in the behaviour of the temperature dependences of the electrical resistivity. The specific features revealed in the temperature dependences of the magnetic susceptibility and the electrical resistivity in some temperature ranges are accounted for in terms of orbital ordering, which is explained by the interaction of the pseudoorbital moments with spins.

This work is supported by the Russian Basic Research Foundation (RFFI – BRFFI, project no. 08–02–90031 Bel_a) and the FFI RB project n. $\Phi 08P-037$.

[1] D. L. Decker and R. L. Wild, *Phys. Rev. B: Solid Stat*, **4**, (1971), 3425.

[2] G. I. Makovetskii and A. I. Galyas, *Sov. Phys. Solid State*, **24**, (1982), 1558.

[3] S. J. Youn, B. I. Min, and A. J. Freeman, *Phys. Status Solidi B*, **241**, (2004), 1411.

24PO-6-23

PECULIARITIES OF THE CONDUCTIVITY AND MAGNETIC PROPERTIES OF THE COBALT- MANGANESE SULPHIDES

*Romanova O.B.¹, Ryabinkina L.I.¹, Petrakovskii G.A.¹, Velikanov D.A.¹, Balaev A.D.¹,
Balaev D.A.¹, Yanushkevich K.I.²*

¹L.V. Kirensky Institute of Physics, Siberian Branch of the Russian Academy of Sciences,
660036, Krasnoyarsk, Russia

²Incorporated Institute of Solid State and Semiconductor Physics, Belarus National Academy of
Sciences, 220072, Minsk, Belarus

In the last time it is actively developed the new scientific direction - spintronic [1] dependence of the conductivity on the magnetic structure. Creation and research of the new compounds with strong interaction between magnetic, elastic, electric and optical properties are important in connection with possible technical applications in spintronic. The sulphides of 3d-metals $Me_xMn_{1-x}S$ (Me = Cr, Fe, Co) belong to the disordered systems, which exhibit various structural, magnetic and electronic transitions at the different temperatures. Interest to these compounds is caused by the discovery of the concentration metal–insulator transition and colossal negative magnetoresistance effect [2].

In present work the measurements of the transport and magnetic properties of $Co_xMn_{1-x}S$ ($0 \leq x \leq 0.4$) sulphides are carried out in the temperature range of 4.2-1000K and magnetic field up to 70 kOe. According to X-ray analysis data $Co_xMn_{1-x}S$ samples are the solid solutions with fcc lattice of NaCl-type. The solid solutions with $x \leq 0.3$ are the semiconductors with conductivity hole type (coefficient of thermoelectromotive force $\alpha > 0$). In these samples the transition from the impurity to the intrinsic conductivity at $T > 600$ K is observed. The value of the band-gap ΔE for α – MnS and solid solutions $Co_xMn_{1-x}S$ was determined at $T > 600$ K. Increasing of the cobalt concentration (X) decreases ΔE from 1.46 eV for MnS (X=0) up to

0.42 eV ($X=0.3$). For $\text{Co}_X\text{Mn}_{1-X}\text{S}$ sulphides with $X = 0.4$ the metallic type of conductivity ($\alpha < 0$) has been established. In $\text{Co}_X\text{Mn}_{1-X}\text{S}$ system the metal-insulator transitions both at the concentration ($X_c=0.4$) and the temperature ($T_c=950\text{K}$ for $X=0.4$) are realized that is typical for the disordered systems [3]. In antiferromagnetic compounds $\text{Co}_X\text{Mn}_{1-X}\text{S}$ the spontaneous magnetic moment is found out in magneto-ordering region below T_N that is confirmed by existence of the hysteresis loop in this temperature range. There are observed the hysteresis effects in temperature dependence of the magnetization and resistivity. For sample with $X=0.3$ in the temperature range 4.2-50K in magnetic field 10 kOe hysteresis of magnetization correlates with hysteresis of the resistivity measured at $H=0$ under heating and cooling of the sample.

This work is supported by the Russian Basic Research Foundation (RFFI – BRFFI, project no. 08–02–90031 Bel_a) and the FFI RB project n. $\Phi 08\text{P}-037$.

[1] A.V. Vedyayev, *Usp.Fiz.Nauk*, **172** (2002) 1458.

[2] L.I. Ryabinkina, O.B. Romanova, G.A. Petrakovskii and et al., *Phys. Met. and Metallog.*, **99** (2005) S77.

[3] N.F. Mott Metal - insulator transitions. *Taylor and Francis LTD, London* (1974) 344p.

24PO-6-24

COMPLEX EXCITONIC ORDER PARAMETER BY SPIN-ORBIT COUPLING AND BEC-BCS CROSSOVER

Ali Can M. and Hakioglu T.

Department of Physics and UNAM Institute of Material Science and Nanotechnology, Bilkent University, 06800 Ankara, Turkey

The condensation of electron-hole (e-h) pairs is studied at zero temperature and in the presence of a weak magnetic field, a controllable Rashba and an intrinsic Dresselhaus type spin-orbit couplings in coupled quantum wells. Under realistic conditions, a weak SOC can have observable effects in the order parameter of the condensate. Firstly, the fermion exchange symmetry is absent. In result, the condensate spin has no definite parity. Additionally, the excitonic SOC breaks the rotational symmetry yielding a complex order parameter in an unconventional way, i.e. the phase pattern of the order parameter is a function of the condensate density. This is manifested through finite off diagonal components of the static spin susceptibility, suggesting a new experimental method to confirm an excitonic condensate.

24PO-6-25

ANOMALOUS MAGNETISM IN $\text{Eu}(\text{Ca})\text{B}_6$

Glushkov V.¹, Anisimov M.¹, Bogach A.¹, Demishev S.¹, Samarin N.¹, Kuznetsov A.²,
Levchenko A.³, Shitsevalova N.³, Flachbart K.⁴, Sluchanko N.¹

¹A.M.Prokhorov General Physics Institute of RAS, 38, Vavilov str., Moscow 119991, Russia

²Moscow Engineering Physics Institute, 31, Kashirskoe Shosse, Moscow, 115409 Russia

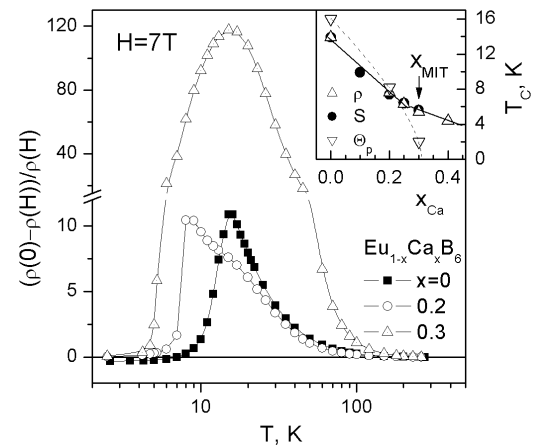
³Institute for Problems of Materials Science NAS, 3, Krzhizhanovsky str., 03680, Kiev, Ukraine

⁴Centre of Low Temperature Physics, IEP SAS and IPS FS UPJS, SK-04001Košice, Slovakia

The effect of colossal magnetoresistance (CMR) in europium hexaboride EuB_6 primarily determines the great interest of researchers to this low carrier density ferromagnetic metal with Curie temperature $T_C \approx 13.9\text{K}$. Although a lot of experimental data and theoretical investigations are available for the EuB_6 based CMR systems (see, e.g., [1-2]), the nature of the dramatic reduction of the resistivity accompanied by the onset of ferromagnetism is still under question.

To shed more light on the origin of CMR in these compounds, the comprehensive study of transport and magnetic properties was carried out on the single crystals of $\text{Eu}_{1-x}\text{Ca}_x\text{B}_6$ ($0 \leq x \leq 0.4$) in a wide range of temperatures (1.8-300 K) and magnetic fields (up to 8 T). The obtained data allowed to identify a metal-to-insulator transition (MIT) at the critical Ca concentration $x_{\text{MIT}} \approx 0.3$, which agrees well with the predictions of double exchange model [1]. It was shown that the charge transport in $\text{Eu}_{1-x}\text{Ca}_x\text{B}_6$ for $x < x_{\text{MIT}}$ is influenced by a strong renormalization of the charge carriers' effective mass $m_{\text{eff}} \approx 30m_0$ (m_0 – free electron mass) resulting from the spin polaronic states' formation in the paramagnetic phase of this compound [3]. The gradual decrease of m_{eff} to the low temperature values $m_{\text{eff}}(T \leq T_C) \approx 0.2-1m_0$ seems to reflect the evolution of the phase separated state with low resistive ferromagnetic nano-sized regions (ferrons) in the high resistive paramagnetic matrix of $\text{Eu}_{1-x}\text{Ca}_x\text{B}_6$.

When approaching to MIT in $\text{Eu}_{1-x}\text{Ca}_x\text{B}_6$, a huge enhancement of CMR is observed for $x=0.3$ below 100K (see Figure). The comparison between the $T_C(x)$ values obtained from resistivity $\rho(T)$ and thermopower $S(T)$ data and paramagnetic Curie temperature $\Theta_P(x)$ evaluated from the magnetic and magnetotransport measurements (see inset in the Figure) reveals a drastic decrease of Θ_P in the vicinity of x_{MIT} . This observation favors to the quantum MIT scenario proposed in [1] for this low carrier density system. Thus the anomalies of transport properties detected for $\text{Eu}_{1-x}\text{Ca}_x\text{B}_6$ in this work could be naturally ascribed to the features of phase separated state realized in the vicinity of the concentration driven quantum MIT. However, the crossover from the electron-like ($x < x_{\text{MIT}}$) to the hole-like ($x > x_{\text{MIT}}$) conductivity doesn't agree with the Anderson mechanism of quantum MIT scenario [1-2] and requires further investigations of spin polaronic effects in this CMR system.



Support by RFBR 05-08-33463 and 07-02-90903 projects and the RAS Program “Strongly Correlated Electrons” is acknowledged.

[1] V.M. Pereira et al., *Phys. Rev. Lett.*, **93** (2004) 147202.

[2] G. Caimi et al., *Phys. Rev. Lett.*, **96** (2006) 016403.

[3] V. Glushkov et al., *Phys. B* **403** (2008) 820.

24 June Tuesday

17:00-19:00

poster session

24PO-7

“Magnetic Oxides”

24PO-7-1

THE EFFECT OF OXYGEN ISOTOPE SUBSTITUTION ON Pr_{0.5}Ca_{0.5}MnO₃ MANGANITE DOPED WITH CHROMIUM AND RUTHENIUM

Babushkina N.A.¹, Taldenkov A.N.¹, Inyshkin A.V.¹, Maignan A.²

¹RRC "Kurchatov Institute", Kurchatov sq. 1, 123182 Moscow, Russia

²Laboratoire CRISMAT, ENSICAEN, 6 bd. du Marechal Juin, 14050 Caen Cedex 4, France

The formation of inhomogeneous states with the phase separation into nanoscale ferromagnetic (FM) metallic and antiferromagnetic (AF) insulating regions is typical of doped manganites. The situation is especially intriguing when the AF phase exhibits also a charge ordering (CO). This is just the case for the half-doped Pr_{0.5}Ca_{0.5}MnO₃ manganite. At low temperatures, it is an AF insulator with the checkerboard-type CO arising at $T_{CO} \sim 250$ K, whereas the Neel temperature T_N for the CE-type AF ordering is about 165 K. In high magnetic fields (10–30 T), the AF CO state is "melted", and the system transforms to the FM metallic state. At the same time, the FM state can be also induced by substitution Mn with Cr, Ru and other transition metals [1]. For example, the substitution of Mn by 2 at.% of Cr is sufficient to attain the FM state even at zero magnetic field.

Here, we use the oxygen isotope substitution as a unique tool for investigation the complex magnetic oxides and especially for revealing the specific features of the phase separation in them. We studied the effect of $^{16}\text{O} \rightarrow ^{18}\text{O}$ substitution in Pr_{0.5}Ca_{0.5}MnO₃ manganite doped with Cr and Ru. Such a doping suppresses the CO state and favors the formation of FM phase. However, Cr⁺³ and Ru⁺⁴ ions produce different effect on the zigzag FM chains, being characteristic feature of CE-type AF state with the charge ordering. This leads to a stronger FM interaction in the Ru-doped compound and hence to the higher temperature of FM transition T_{FM} . The measurements of magnetization, ac magnetic susceptibility, and magnetoresistance were performed for ceramic samples of Pr_{0.5}Ca_{0.5}(Mn_{1-x}Cr_x)¹⁶⁻¹⁸O₃ with $x = 0, 0.02, 0.05$, and Pr_{0.5}Ca_{0.5}(Mn_{1-x}Ru_x)¹⁶⁻¹⁸O₃ with $x = 0, 0.01, 0.02, 0.05$. The obtained experimental data show that the $^{16}\text{O} \rightarrow ^{18}\text{O}$ substitution leads to the increase of the charge ordering temperature T_{CO} by 4-8 K both for Cr- and Ru-doped samples ($T_{CO}=250$ K at $x = 0$). In contrast, the isotope effect for the FM phase induced by Cr and Ru dopants has the opposite sign. For the samples with Cr ($x = 0.02$ and 0.05), we found $T_{FM} \sim 130 - 150$ K, which decreased by about 30 K after the $^{16}\text{O} \rightarrow ^{18}\text{O}$ substitution. For the samples with Ru ($x=0.02$) we obtained $T_{FM} \sim 180 - 215$ K with the isotope shift $\Delta T_{FM} \sim 30$ K also. But for the samples with Ru ($x=0.05$) we got $T_{FM} \sim 250$ K and negligible isotope shift. The decrease of ΔT_{FM} with the increase of T_{FM} is a rather usual feature of the FM manganites. The isotope effect becomes more stronger with the narrowing of the conduction band leading to the shift of T_{FM} to lower temperatures. The most pronounced oxygen isotope substitution effect on this system is observed in compounds with $x = 0.02$, having minimum T_{FM} . This doping level corresponds to the region of coexistence of phases with different order parameters.

Support by the Russian Foundation for Basic Research (N 07-02-00681 and N 07-02-91567 NNIO_a) is acknowledged.

[1] C. Martin, A. Maignan, M. Hervieu, C. Autret, B. Raveau, and D.I. Khomskii, *Phys. Rev. B* **63** (2001) 174402.

24PO-7-2

INFLUENCE OF Mn-SITE DOPING ON CHARGE AND ORBITAL ORDERING IN MANGANITES (M=Ni, Ga, Fe, Ti, Mg)

Orlova T.S.¹, Laval J.Y.², Monod Ph.², Bassoul P.², Noudem J.³

¹Ioffe Physico-Technical Institute, 26 Polytekhnicheskaya, St. Petersburg 194021, Russia

²Laboratoire de Physique du Solide, CNRS ESPCI, 10 Vauquelin, 75231 Paris, France

³Laboratoire de Cristallographie et Sciences des Matériaux, ISMRA, 6 bl. du Marechal Juin, 14050 Caen, France

The origin of charge and orbital ordered phases in the manganese perovskites ($RE_{1-x}^{3+}AE_x^{2+}MnO_3$, where RE is rare earth and AE is alkaline earth) is still the subject of debate [1, 2]. Charge-orbital modulation has been traditionally seen as the ordering of Mn^{3+} and Mn^{4+} ions followed by arrangement of a Jahn-Teller distortion of the $Mn^{3+}O_6$ octahedra: $d(z^2)(Mn^{3+})$ orbitals are oriented perpendicular to the c -axis and form a series of ordered (zigzag) chains within the $(a-b)$ basal plane. The lattice distortion ordering can be perfectly detected in transmission electron microscopy (TEM). In $La_{1-x}Ca_xMnO_3$ system for special dopings ($x=1/2, 2/3, 3/4$) the superstructural modulation with the averaged wave vector $q=(1-x)a^*$ (a^* is the reciprocal lattice vector) was observed by TEM [3]. However, according to some recent experimental findings the charge difference between two Mn sites is only 0.16 electrons [1] that is too far from $3d^3$ and $3d^4$. Thus more studies are needed to shed light on charge and orbital ordering phenomena. Modifying of Mn^{3+} -O- Mn^{4+} bonds, which are responsible for interplay between ion, orbital and spin ordering, through Mn site doping could be an efficient key in understanding main factors affecting the charge-orbital ordering in the manganites.

Effects of initial doping of the Mn-sites in $La_{1/3}Ca_{2/3}MnO_3$ by various cations (without d orbital, with d^0, d^{10} or d^n) on striped charge-orbital ordering have been systematically studied by combining transmission electron microscopy with magnetic and transport measurements. It was shown that the temperature T_{CO} of charge ordering (CO) transition gradually decreases with dopant concentration regardless on doping element (Fe, Ni, Ga, Ti, Mg). Temperature dependences of magnetization $M(T)$ and resistivity $\rho(T)$ showed that the doping does not change their behaviour at $T < T_{CO}$ which remains typical for CO state. Weiss temperature estimated from $M(T)$ dependence also gradually decreases with the concentration of dopants.

TEM studies revealed that effect of doping on the formation of extended striped superstructure critically depends on filling d -shell of doping cation. Diamagnetic cations ($Ga^{3+}, Ti^{4+}, Mg^{2+}$) on Mn-site completely suppress long-range superstructure. In compounds doped by magnetic cations such as Fe^{3+} and Ni^{3+} the long-range striped superstructure is kept, but strongly modified compared with the parent $La_{1/3}Ca_{2/3}MnO_3$ manganite. Such doping leads to incommensurability of the superstructure which arises due to local variation in periodicity of $Mn^{3+}O_6$ and $Mn^{4+}O_6$ stripes arrangement and shifts along a direction. As a result in Fe- and Ni-doped compounds with dopant concentration $0.03 \leq y \leq 0.07$ q -parameter of superstructure is 17-20% lower than in undoped sample.

It was concluded that the tolerance factor (the cation size of dopant) is not decisive factor in suppression of long-range superstructure. The determining role of d -shell filling on stabilization of long-range striped superstructure is discussed.

[1] M. Coey, *Nature*, **430** (2004) 155.

[2] G.C. Milward, M.J. Calderon, P.B. Littlewood, *Nature*, **433** (2005) 607.

[3] S. Mori, C.H. Chen, S.-W. Cheong, *Nature*, **392** (1998) 473.

24PO-7-3

EFFECT OF Y-DOPING ON THE MAGNETIC AND CHARGE ORDERINGS IN $\text{Nd}_{2/3}\text{Ca}_{1/3}\text{MnO}_3$

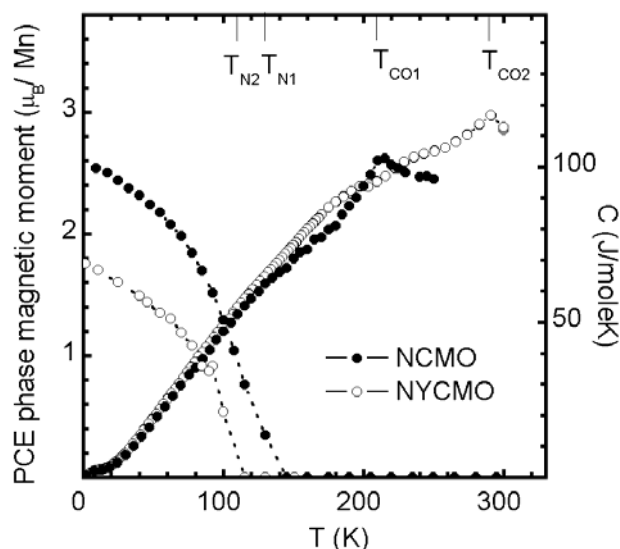
*Fertman E.*¹, *Beznosov A.*¹, *Desnenko V.*¹, *Kajnakova M.*², *Feher A.*²

¹Institute for Low Temperature Physics and Engineering NASU, Kharkov, Ukraine

e-mail: fertman@ilt.kharkov.ua

²Centre of Low Temp. Physics of the Faculty of Science UPJŠ and IEP SAS, Košice, Slovakia

Three different long-range magnetic orderings consistent with a phase separation scenario have been observed in the doped colossal-magnetoresistance compound $(\text{Nd}_{0.9}\text{Y}_{0.1})_{2/3}\text{Ca}_{1/3}\text{MnO}_3$ (NYCMO) at low temperatures: the antiferromagnetic (AF) orderings of PCE and DE types existing below ~ 110 K (T_{N2}) and ~ 60 K, respectively, and the ferromagnetic (FM) one of B type existing below ~ 40 K. The revealed temperatures of the magnetic transformations are shifted by ~ 20 - 30 K compared with the corresponding ones earlier reported for the parent compound $\text{Nd}_{2/3}\text{Ca}_{1/3}\text{MnO}_3$ (NCMO) as ~ 130 K (T_{N1}), ~ 80 K and ~ 70 K, respectively [1]. It is characteristic that Y-doping has been revealed to have the opposite effects on the magnetic and charge ordering temperatures (T_{CO}): the last one appeared to be shifted by ~ 80 K towards the high temperatures (Figure). T_{CO} in NCMO and NYCMO have been defined as ~ 212 K (T_{CO1}) and ~ 290 K (T_{CO2}) respectively, where typical anomalies of the temperature dependent heat capacity has been found (Figure). Corresponding anomalies of the temperature dependent magnetization and resistivity have been found as well. The higher T_{CO} of the doped compound is consistent with the higher level of the coherent Jahn-Teller (JT) distortions σ_{JT} of the MnO_6 octahedra. For NYCMO at 160 – 295 K $\langle\sigma_{JT}\rangle \approx 1.4 \times 10^{-2}$ is 28% higher than that for the parent NCMO compound. The more distorted NYCMO oxygen octahedra cause the increase of



T_{CO} since their ordering provides for the increased energy gain (following to [2] we consider the charge ordered structure as a wave of the distortions of the oxygen octahedra). On the other hand magnetic moments of Mn- and Nd- ions are coupled by exchange forces. The diluting of the system of the magnetic Nd ions by the nonmagnetic Y ions results in a loss of the exchange energy of the system and thus in a decreasing of the temperatures of the magnetic transitions.

Figure. Refined magnetic moments of the long-range AFM phase with the PCE-ordering type (left); heat capacity of NCMO and NYCMO compounds (right).

The work is partly based on the experimental results obtained at SINQ, PSI Villigen (Switzerland). Authors are grateful to D. Sheptyakov for collaboration.

[1] E. Fertman, D. Sheptyakov, A. Beznosov, V. Desnenko, D. Khalyavin, *J. Magn. Magn. Mater.* **293** (2005) 787.

[2] D. I. Khomskii, *J. Magn. Magn. Mater.* **306** (2006) 1.

24PO-7-4

RELAXATION OF STRUCTURAL DEFECTS IN ANTIFERROMAGNETIC CuO

Arbuzova T., Naumov S.

Institute of Metal Physics of Ural Division, RAS, 620041 Ekaterinburg, Russia

The comparison of the magnetization relaxation processes taking place after electron irradiation and the intensive deformation is performed for the copper monoxide within the magnetic ordered phase. CuO has a monoclinic crystal lattice and it is low-dimensional antiferromagnet with Neel temperature $T_N=230\text{K}$. Magnetic properties of CuO are conditioned by a strong antiferromagnetic superexchange of Cu^{2+} ($S=1/2$) ions via O^{2-} ions in the $[10\bar{1}]$ direction and a weaker ferromagnetic bond in all other directions. The magnetic structure can be represented in the form of zigzag Cu-O-Cu antiferromagnetic chains extended along the $[10\bar{1}]$ direction. Competition of the intrachain and interchain exchange interactions leads to a 3D-collinear antiferromagnetism below $T=212\text{K}$. In the temperature range $230\text{K}<T<560\text{K}$ the interaction between the chains is vanishingly small and the system transforms into low-dimensional antiferromagnetic state. The magnetic order depends on the angle and the distance between the nearest magnetic ions. The distortions of the crystal lattice caused by external actions can lead to the frustration of exchange couplings and to the modification of the magnetic order.

In this work we studied the influence of radiation defects on the magnetic properties of CuO. The electron bombardment by the fluence $F=5\cdot 10^{18}\text{e/cm}^2$ led to the sharp increase of the susceptibility in ordered region (fifty times as much at $T=77\text{K}$). After the electron irradiation the most probable point defects are the ions of oxygen and copper displaced from their positions. These defects lead to the modification of the distances and the angles between magnetic ions and to the change of the competing exchange interactions. The great values of the susceptibility may be explained by the formation of magnetic polarons with the large magnetic moment in the antiferromagnetic matrix. After storage for 3 years at room temperature the susceptibility of the irradiated samples decreased, but did not reach the initial value. Perhaps, not all displaced ions returned to point of departure, therefore the magnetic state remained inhomogeneous. The elastic strains after shock action led to the lesser increase of the susceptibility (five times as much at $T=77\text{K}$), that is conditioned by the lesser concentration of the structural defects. In CuO the relaxation of elastic strain created with shock waves led to the complete restoration of the antiferromagnetic order in 3 years [1]. The boundaries of grains are good channels for the relaxation of elastic strains. Thus, structural defects lead to the disturbance of long-range magnetic order. The relaxation of point radiation defects is more lasting in comparison with the relaxation of elastic strains.

Support by Program "New materials and structure" of the Department of Physics of Russian Academy of Sciences is acknowledged.

[1] T.I.Arbuzova, S.V.Naumov, E.A.Kozlov, *Phys. of Solid State* **47** (2005) 1358.

24PO-7-5

BOUND MAGNETIC POLARONS WITH EXTENDED SPIN DISTORTIONS ON REGULAR AND FRUSTRATED AFM LATTICES

Kagan M.Yu.¹, Ogarkov S.L.¹, Kugel K.I.², Rakhmanov A.L.², Sboychakov A.O.²

¹Kapitza Institute for Physical Problems, Russian Academy of Sciences, Kosygina str. 2,
Moscow 119334, Russia

²Institute for Theoretical and Applied Electrodynamics, Russian Academy of Sciences,
Izhorskaya str. 13, Moscow 125412, Russia

We analyze the structure of magnetic polarons (ferrons) in lightly doped antiferromagnets with 3D cubic, 2D square and 2D triangular lattices in the framework of Kondo-lattice model in the double exchange limit [1]. The nearest-neighbor (NN) and next nearest-neighbor (NNN) exchange interactions are taken into account. NNN exchange interaction leads to the frustration of lattice in the cases of cubic and square lattices. Triangular lattice has strong geometrical frustration without NNN exchange interaction. In addition, the crystal is assumed to have uniaxial magnetic anisotropy.

The conduction electron is assumed to be bound by a nonmagnetic donor impurity and to form a ferromagnetic core of the size about the electron localization length (bound magnetic polaron). We find that the magnetic polaron can produce rather extended spin distortions of the antiferromagnetic background around the core. In a wide range of distances, these distortions decay as $1/r^4$ for cubic lattice and as $1/r^2$ for square lattice. On triangular lattice, spin distortions decay slower (as $1/r$) because of strong geometrical frustration of the lattice. The characteristic size of this ‘coat’ decreases with increase of NNN interaction or with increase of magnetic anisotropy. In first case, the critical value of ratio J'/J (J' and J are the exchange integrals of NNN and NN exchange interactions, respectively), at which the ‘coat’ disappears, is close to that corresponding to the transformation of magnetic configuration in the background. This suggests that the ‘coated’ magnetic polaron is a stable object within a wide range of parameters. Nevertheless, the frustration of lattice results in the disappearance of the ‘coat’.

We calculate the energy of ‘coated’ magnetic polaron and compare it with the energy of ‘bare’ magnetic polaron (ferromagnetic core without extended distortions – this magnetic polaron is usually considered in literature). We show that, at not too high values of anisotropy constant K , the ‘coated’ magnetic polaron is favorable in energy in comparison to the ‘bare’ one. If we increase the magnetic anisotropy constant K , the ‘coated’ magnetic polaron becomes less favorable – this situation is similar to the 1D case, where the ‘coated’ magnetic polaron was found to be a metastable object [2].

We obtain our results in the limit of strong electron-impurity coupling V . In this case, the wave function of the conduction electron is nonzero only at the sites, nearest to the impurity. At finite V , the wave function extends over larger distances, and we should calculate the magnetic structure simultaneously with it. Despite of this, the tails of the wave function only stabilize polaronic state and do not change qualitatively our results.

The work was supported by the EU project CoMePhS, International Science and Technology Center (grant no. G1335), and Russian Foundation for Basic Research (project no. 08-02-00212).

[1] S.L. Ogarkov, M.Yu. Kagan, A.O. Sboychakov, A.L. Rakhmanov, K.I. Kugel, *Phys. Rev. B*, **74** (2006) 014436.

[2] I. Gonzalez, J. Castro, D. Baldomir, A.O. Sboychakov, A.L. Rakhmanov, K.I. Kugel *Phys. Rev. B*, **69** (2004) 224409.

24PO-7-6

MICROSCOPIC MODEL OF DOUBLE EXCHANGE WITH SYMMETRY LOWERING: FERROMAGNETISM VERSUS NONMAGNETIC GROUND STATE

Nikolaev A.V.¹, Michel K.H.²

¹Institute of Physical Chemistry of RAN, Leninskii pr. 31, Moscow 117915, Russia

²University of Antwerp, Groenenborgerlaan 171, Antwerp 2020, Belgium

From the theory of many electron states in atoms we know that there exists a strong Coulomb repulsion, which results in the electronic term structure of atoms and is responsible for Hund's rules. By expanding the Coulomb on-site repulsion in multipolar series we derive this interaction and show that it is also present in solids.

Of particular interest is the case when this interaction couples states of localized and delocalized electrons (double exchange). We show that the interaction is bilinear in terms of creation/annihilation operators for localized electrons and bilinear in terms of the operators for conduction electrons. This form is very different from the linear one, which is commonly used for the interaction in the Anderson Hamiltonian.

In order to study the effect of double exchange, a simple model with one localized f-electron and one itinerant s-electron per crystal site is considered. It is shown that depending on the low-lying excitation spectrum, the model can lead to ferromagnetism and/or to a nonmagnetic state. The model is relevant for solids with lanthanide and actinide atoms.

[1] A.V. Nikolaev, *Phys. Rev. B*, **71** (2005) 165102.

[2] A.V. Nikolaev, P.N. Dyachkov, *Int. J. Quantum Chem.*, **89** (2002), 57; **93** (2003), 375.

24PO-7-7

ELECTRON-DOPED $\text{Sm}_{1-x}\text{Sr}_x\text{MnO}_3$ PEROVSKITE MANGANITES: CRYSTAL AND MAGNETIC STRUCTURES AND PHYSICAL PROPERTIES

Kurbakov A.I.¹, Martin C.², Maignan A.²

¹Petersburg Nuclear Physics Institute of the Russian Academy of Sciences, 188300 Gatchina, Leningrad region, Russia

²Laboratoire CRISMAT, UMR 6508 ISMRA et Universite de Caen, Bd. du Marechal Juin, 14050 Caen, France

The crystal and magnetic structures of the $^{152}\text{Sm}_{0.45}\text{Sr}_{0.55}\text{MnO}_3$ and $^{152}\text{Sm}_{0.37}\text{Sr}_{0.63}\text{MnO}_3$ perovskite manganites have been established by high resolution neutron powder diffraction. These data are compared with the magnetic and transport properties of these compounds.

The temperature dependences of the resistivity of both samples demonstrate the absence of clear metal-insulator (MI) transition, which is characteristic of $\text{Sm}_{1-x}\text{Sr}_x\text{MnO}_3$ manganites exhibiting colossal magnetoresistance (CMR). However $\rho(T)$ curves of $^{152}\text{Sm}_{0.45}\text{Sr}_{0.55}\text{MnO}_3$ exhibit a maximum for $T \cong 160$ K indicating a more conducting regime below this temperature. This local resistivity maximum attributed to the metallic character of the ferromagnetic (FM) planes of the *A*-type antiferromagnetic (AFM-*A*) structure that takes place around this temperature. This is confirmed by the isothermal magnetic field dependent magnetization curve.

These $M(H)$ curves collected at 2.5 and 5 K reveal maximal magnetization values reaching only $\cong 0.16 \mu_B/\text{Mn}$ in 5 T, i.e. much lower than expected for a fully saturated ferromagnetic order ($\cong 3.45 \mu_B/\text{Mn}$). Furthermore, instead of a tendency towards saturation, these curves exhibit a faster increase of magnetization for $H > 4$ T characteristic of the beginning of a smooth metamagnetic transition.

A comparison of microscopic characteristics of the manganites has shown, that the changes in the MnO_6 octahedral tilt system at room temperature are directly related to changes in the low temperature magnetic structures.

Although $^{152}\text{Sm}_{0.45}\text{Sr}_{0.55}\text{MnO}_3$ and $^{152}\text{Sm}_{0.37}\text{Sr}_{0.63}\text{MnO}_3$ compounds, differ insignificantly in the strontium doping level, are homogeneous antiferromagnetic insulators ($T_N \sim 180$ and 250 K), and do not exhibit CMR, they have different crystal symmetries in the entire temperature range under study (1.5 - 300 K) (orthorhombic $Pnma$ and tetragonal $I4/mcm$), differ in the type of spin ordering at low temperatures (AFM-A and AFM-C), are characterized by different orbital polarizations ($d_{x^2-y^2}$ and $d_{3z^2-r^2}$), and possess two- and one-dimensional magnetic and transport properties, respectively.

The lack of magnetoresistance for these compositions is explained by the lack of coexisting magnetic phases involving double exchange ferromagnetism, in contrast to what is observed for the magnetoresistive $\text{Sm}_{1-x}\text{Sr}_x\text{MnO}_3$ compounds, that is with $x \leq 0.52$.

The critical concentration range governed by the average A-cation size $\langle r_A \rangle$ and the local A-cation size mismatch (σ^2) has been determined for the samarium–strontium manganites, in which the concentration driven structural transition from the orthorhombic to tetragonal crystal symmetry accompanied by a crossover in orbital and magnetic ordering takes place: $\langle r_A \rangle \approx 1.24 \text{ \AA}$ and $\sigma^2 \approx 0.0077 \text{ \AA}^2$.

24PO-7-8

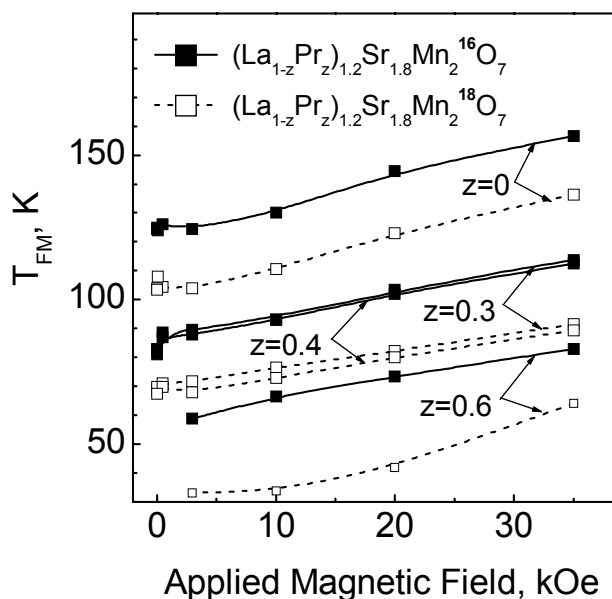
OXYGEN ISOTOPE EFFECT IN LAYERED MANGANITES

Taldenkov A.N.¹, Babushkina N.A.¹, Inyushkin A.V.¹, Suryanarayanan R.²

¹RRC Kurchatov Institute, Kurchatov sq.1, 123182 Moscow, Russia

²Laboratoire de Physico-Chimie de l'Etat Solide UMR8648, CNRS, Universite Paris XI, Bat-414, 91405 Orsay, France

The oxygen isotope effect in ceramic bi-layered manganite $(\text{La}_{1-z}\text{Pr}_z)_{1.2}\text{Sr}_{1.8}\text{Mn}_2^{16-18}\text{O}_7$ ($z = 0, 0.3, 0.4, 0.6$) has been investigated. Real and imaginary parts of magnetic susceptibility, magnetization and magnetoresistance were measured at temperatures from 4.2 K to 320 K in applied magnetic field up to 40 kOe. Substantial decrease of ferromagnetic (FM) transition temperature T_{FM} under oxygen isotope substitution $^{16}\text{O} \rightarrow ^{18}\text{O}$ was found. This positive isotope effect amounts to more than 20 K. In addition, a large decrease of concentration of FM phase was inferred in compounds with heavy oxygen isotope. Doping with Pr



suppresses the FM ordering, so as at highest Pr concentration ($z = 0.6$) we do not observe any sizable amount of FM fraction. Applied magnetic field induced FM ordering and caused transition temperature to increase (see the figure). Nevertheless, the isotopic shift remained large to consider bi-layered manganites as manganites with anomalous oxygen isotope effect. The temperature profile of the resistance and magnetoresistance demonstrated the clear evidence of metal-insulator transition. The peak of magnetoresistance was shifted down in temperature in the samples with oxygen-18, thus confirming the existence of the anomalously large isotope effect observed in magnetic measurements.

A number of additional transitions of ferromagnetic type were observed at $T > 170$ K. These transition temperatures were also shifted under oxygen isotope substitution, demonstrating the positive isotope effect. Based on the published data, we propose that samples under investigation contained impurity phases of the Ruddlesden-Popper structure [1] with the number of layers more than two. The obtained results are compared with those observed in other manganite systems where the large isotope effect was found. From this we conclude that the main features of oxygen isotope effect in low-dimensional Ruddlesden-Popper phases are in accordance with the earlier results observed in cubic manganites.

This work was supported by the Russian Foundation for Basic Research (RFBR Project N 07-02-00681 and RFBR-NNIO Project N 07-02-91567_a).

[1] S.N. Ruddlesden and P. Popper // *Acta Crystallogr.*, 1958, v. 11, p. 54.

24PO-7-9

ELECTROMAGNONS IN MULTIFERROIC MANGANITES WITH MODULATED SPIN STRUCTURE

Mukhin A.A.¹, Travkin V.D.¹, Ivanov V.Yu.¹, Pimenov A.V.², Shuvaev A.M.², Loidl A.³

¹A.M. Prokhorov General Physics Institute of the RAS, 119991 Moscow, Vavilov St., 38, Russia

²Experimentelle Physik 4, Universitat Wurzburg, 97074 Wurzburg, Germany

³Experimentalphysik V, Universitat Augsburg, 86135 Augsburg, Germany

Recently interesting multiferroic properties exhibiting a strong interplay between ferroelectricity and modulated (sinusoidal or cycloidal) spin structures were observed in some pure and substituted orthorhombic manganites RMnO_3 ($R = \text{Gd, Tb, Dy}$) [1,2] and $\text{Eu}_{1-x}\text{Y}_x\text{MnO}_3$ [3,4] with frustrated exchange interactions controlled by rare-earth ionic radius r_R . We have revealed in these multiferroics fundamentally new spin excitations: electromagnons, representing spin waves excited by ac electric fields. Using a submillimeter backward-wave-oscillator quasi-optical technique ($3\text{-}40\text{ cm}^{-1}$) we have observed in dielectric $\epsilon^*(\nu)$ spectra of GdMnO_3 , TbMnO_3 [5], DyMnO_3 and $\text{Eu}_{1-x}\text{Y}_x\text{MnO}_3$ ($0 \leq x \leq 0.5$) strong wide absorption lines at frequencies $15\text{-}25\text{ cm}^{-1}$ identified as the electromagnons. The electro-active origin of the observed modes was determined by independence of their excitation conditions on a polarization of ac magnetic field and a strong dependence on the polarization of ac-electric one: the modes were observed for $e \parallel a$ -axis. The electromagnon contribution to the dielectric function $\Delta\epsilon_a$ amounts to $\sim 1 - 5$. In all compositions the electromagnons appear as a broad Debye-like contribution in the sinusoidally-modulated antiferromagnetic phase and transform to well-defined excitations as the magnetic structure transforms into the spiral state at lower temperatures. At lowest temperatures fine structure of electromagnons is observed reflecting increasing complexity of the magnetic structure. Besides electromagnons, usual antiferromagnetic resonance modes excited by ac magnetic field, were also observed at the similar resonance frequencies which exhibited

significant broadening as compare to canted antiferromagnetic phase. In external magnetic fields $H \parallel c$ -axis the ferroelectric cycloidal structures can be suppressed due to transition to the usual canted state and the electromagnons are wiped out, thereby inducing considerable changes in the index of refraction from dc up to THz frequencies. These transitions are accompanied by a transfer of the corresponding spectral weight to the lowest lattice vibration (GdMnO_3), demonstrating the strong coupling of phonons with electromagnons [6].

Symmetry analysis shows a key role of the inhomogeneous magnetoelectric interaction in observed phenomena both in an appearance of spontaneous polarization in cycloidal structure and electroactive spin excitations. The observed electromagnons can be interpreted as spin oscillations with non-zero wave vectors \mathbf{k} corresponding to a wave vector of the modulated magnetic structure ($\mathbf{k}_0 \parallel b$ -axis), which interact with homogeneous ac electric field. The tuning of electromagnon contribution to the refraction index by moderate magnetic fields in a wide frequency range allows a design of new optoelectronic devices.

This work was supported in part by RFBR (06-02-17514).

- [1] T. Kimura, T. Goto, H. Shintani, K. Ishizaka, T. Arima, Y. Tokura, *Nature*, **426**, 55 (2003).
- [2] T. Kimura, G. Lawes, T. Goto, Y. Tokura, A.P. Ramirez, *Phys. Rev. B*, **71**, 224425 (2005).
- [3] V. Yu. Ivanov, A. A. Mukhin, V. D. Travkin, et al., *JMMM*, **300**, e130 (2006).
- [4] J. Hemberger, F. Schrettle, A. Pimenov, P. Lunkenheimer, V.Yu. Ivanov, A.A. Mukhin, A.M. Balbashov, A. Loidl, *Phys. Rev. B*, **75**, 035118 (2007).
- [5] A. Pimenov, A. A. Mukhin, V. Yu. Ivanov, et al., *Nature Physics* **2**, 97 (2006).
- [6] A. Pimenov, T. Rudolf, F. Mayr, A. Loidl, A. A. Mukhin, A. M. Balbashov, *Phys. Rev. B*, **74**, 100403(R) (2006).

24PO-7-10

MAGNETOELECTRIC PROPERTIES AND LOCAL INDUCED STATES IN LOW-DOPED MANGANITES

Mamin R.F.

Zavoisky Physical-Technical Institute, RAS, Sibirskii trakt 10/7, Kazan, Russia

The complicated interplay among charge, spin and lattice degrees of freedom in manganites is believed to induce the unexpected magnetic and transport phenomena, such as the colossal magnetoresistance (CMR). Manganites display also a variety of useful multiferroic properties such as colossal magnetocapacitance effect and high dielectric constant [1]. In multiferroics ferromagnetic order can be controlled by an electric field, or ferroelectric order can be controlled by a magnetic field. Among them, $\text{La}_{1-x}\text{Sr}_x\text{MnO}_3$ is the most attractive candidate for multiferroic applications because of a combination of desirable properties. In this work we report the observation of extremely high dielectric permittivity exceeding 10^9 and magnetocapacitance of the order of 10000% in the single crystals of complex manganites $\text{La}_{1-x}\text{Sr}_x\text{MnO}_3$ (LSMO), $x=0.1, 0.11, \text{ and } 0.125$, which all display a CMR effect accompanied with a sufficiently high conductivity. We also found the piezoelectric effect after the application of high local electric field to the surface of $\text{La}_{0.89}\text{Sr}_{0.11}\text{MnO}_3$ crystals. We carried out the studies of the low-frequency dielectric properties in LSMO and of the magnetic field effect on these properties. An experimental results of such studies was get for LSMO crystal with $x=0.125$. The permittivity possesses a strong peak as a function of temperature, while other parameters, dc-conductivity change rather smoothly. The external magnetic field strongly affects the charge separation in these materials and the strong magnetocapacitance effect is consequently observed.

Similar results have been observed for $x=0.1$ and 0.11 , but in these cases also at room temperature.

The distinct contrast of the electric field induced charged states are observed in LSMO-0.1 and LSMO-0.11 single crystals. The electric-field-induced contrast is observed in Kelvin mode (KFM) confirming local modification of the surface properties of manganites. Piezoelectric effect of the induced states is assessed using Piezoresponse Force Microscopy (PFM). The piezoelectric contrast is observed in these states pointing to the existence of a local polar state at some volume. These results are complemented by the measurements of piezoresponse hysteresis and surface potential hysteresis loops at some area in standard pulse *dc* mode. The injection of the additional conductivity currents promotes the occurrence of the polar charged states. The induced polar charged states relax with characteristic time constant of about 80 hours at room temperature, which exceeds Maxwell relaxation time by many orders of magnitude. The long relaxation time for the induced charged state might be explained by the existence of the intrinsic inhomogeneous states. These effects may be the consequence of a strong competition and interplay between the charge, orbital and spin degrees of freedom resulting in above mentioned phenomena. We believe that this effect occurs due to the dynamic charge separation in pre-percolation regime. Holes are not totally confined to a single polaron, and we may characterize this state as the nanocomposite with nanoscale charge segregation. Therefore, the low-frequency behavior of high dielectric permittivity can be explained by the charge dynamics of these nano-patches and can be called a “dynamic intrinsic Maxwell-Wagner effect”. At applying of an external electrical field these positively charged nano-patches shift with respect to the negative insulated matrix and then they are fixed on new positions. The surface charge and the charge on the interphase boundary stabilize this new structure. As a result, the area with polarization is induced in the sample.

[1] R. F. Mamin, T. Egami, Z. Marton, S.A. Migachev, *Phys. Rev. B* **75**, 115129 (2007).

24PO-7-11

EFFECT OF THE RARE-EARTH IONS ON MAGNETOELECTRIC, MAGNETOELASTIC AND MAGNETIC PROPERTIES OF $RFe_3(BO_3)_4$

Kadomtseva A.M.¹, Ivanov V.Yu.², Mukhin A.A.², Popov Yu.F.¹, Vorob'ev G.P.¹, Kuzmenko A.M.², Pyatakov A.P.¹, Zvezdin A.K.², Prokhorov A.S.², Bezmaternikh L.N.³

¹M.V. Lomonosov Moscow State University, 119992 Moscow, Russia

²A.M. Prokhorov General Physics Institute of the Russian Acad. Sci., 119991 Moscow, Russia

³Institute of Physics SB RAS, 660036 Krasnoyarsk, Russia

Recent observation of magnetic field induced electric polarization in rare-earth iron borates $RFe_3(BO_3)_4$ ($R=Gd, Nd$) [1] makes it possible to consider this interesting class of magnetic compounds as multiferroics in which magnetic, electric and elastic order parameters coexist. In this work we have performed a complex high-magnetic field study of magnetic, ferroelectric, ac dielectric and elastic properties of iron borates as a function of the rare-earth ions for $R= Y, Eu, Gd_{0.5}Nd_{0.5}, Pr, Tb$ and Dy . Magnetic measurements showed antiferromagnetic ordering at $T \leq T_N \sim 40$ K with a spin orientation either in the *ab*-plane ($R= Y, Eu, Gd_{0.5}Nd_{0.5}$) or along trigonal axis ($R=Pr, Tb, Dy$). The observed ground state is determined by magnetic anisotropy of the R-ions exchange coupled to the antiferromagnetic Fe-subsystem. In all the studied easy axis iron borates the field-induced spin reorientation to the *ab*-plane was observed for $H||c$ -axis which was accompanied by jumps of magnetization, magnetostriction and electric polarization. The values of the corresponding threshold fields are 45, 37 and 27 kOe at $T=4$ K for

R= Pr, Tb and Dy, respectively, and show a noticeable increase at higher temperatures. In the easy plane iron borates magnetization, magnetostriction and electric polarization revealed also anomalies in the field $H \sim 5-8$ kOe perpendicular to c -axis which correspond to the iron spins reorientation in the ab -plane perpendicular to the H . Pyroelectric measurements showed a considerable dependence of the value and the sign of electric polarization on reciprocal orientation of the polarization and magnetic field in the ab -plane that is in good agreement with a symmetry consideration of the magnetoelectric coupling [1]. The lowest electric polarization ($\sim 1.5 \mu\text{C}/\text{m}^2$) induced by the field at the spin-reorientation in ab -plane was observed in $\text{YFe}_3(\text{BO}_3)_4$. However, this value increased up to $10-20 \mu\text{C}/\text{m}^2$ in $\text{EuFe}_3(\text{BO}_3)_4$ and reached the largest value ($\sim 100 \mu\text{C}/\text{m}^2$) in $\text{Gd}_{0.5}\text{Nd}_{0.5}\text{Fe}_3(\text{BO}_3)_4$, thus revealing strong contribution of the rare-earth ions to the magnetoelectric coupling and its significant dependence on R-ion type. It is interesting that even in the case of the Eu^{3+} ion its Van-Vleck contribution to the polarization increases noticeably. The measurements in high pulsed magnetic fields up to 250 kOe revealed a change of the polarization sign $P_a(H_{a,b})$ due to the competition of R-Fe exchange and Zeeman rare-earth contributions which enabled to estimate the R-Fe effective fields. In the easy axis iron borates the observed jumps of the polarization at the spin-flop transition $P_{a,b}(H_c)$ were smaller as compared with $\text{Gd}_{0.5}\text{Nd}_{0.5}\text{Fe}_3(\text{BO}_3)_4$ due to a specific magnetic anisotropy of the Pr^{3+} , Tb^{3+} and Dy^{3+} ions having easy c -axis and thus do not show a significant magnetization in the ab -plane. In particular, the Tb^{3+} behaves like Ising ion, the Pr^{3+} has a singlet ground state with the easy c -axis thus resulting in a weak ab -plane susceptibility of the Van-Vleck origin which is responsible for a small contribution to the polarization. The magnetoelastic measurements did not show a significant dependence on the R-ions and revealed magnetostriction values (jumps at a spin reorientation) in the range $10^{-6}-10^{-5}$. The temperatures of structural phase transitions studied by ac dielectric measurements exhibited a monotonic dependence on the R-ion radius from ~ 50 K (Eu) up to ~ 370 K (Y).

This work was supported by RFBR (07-02-00580).

[1] A.K. Zvezdin, G. P. Vorob'ev, A. M. Kadomtseva, et al., JETP Letters, **83**, 509 (2006).

24PO-7-12

NONLINEAR CHARGE TRANSPORT IN THE EPITAXIAL $\text{La}_{0.7}\text{Sr}_{0.3}\text{MnO}_3$ FILM: EFFECTS OF MAGNETIC FIELD AND OPTICAL RADIATION

Volkov N.V.¹, Eremin E.V.¹, Tsikalov V.S.¹, Kim P.D.¹, Seong-Cho Yu², Dong-Hyun Kim²,
Nguyen Chau³

¹L.V. Kirensky Institute of Physics SB RAS, Krasnoyarsk, 660036 Russia

²Department of Physics, Chungbuk National University, Cheongju 361-763, Korea

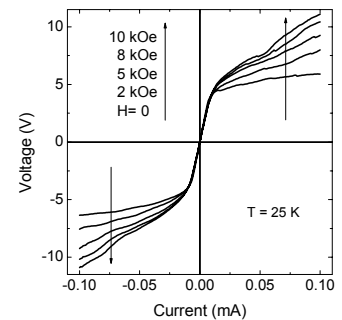
³Center for Materials Science, National University of Hanoi, 334 Nguyen Trai, Hanoi, Vietnam

The intriguing properties of manganites with the perovskite-type structure are determined, to a great extent, by strong sensitivity of these materials to external perturbations. Magnetic and electronic states of the manganites can be considerably modified by application of magnetic and electric fields, pressure, current bias, and light or x-ray illumination (see, for example, [1]).

Here we report the experiments on the effect of the electric current on resistivity and magnetoresistance (MR) of an epitaxial $\text{La}_{0.7}\text{Sr}_{0.3}\text{MnO}_3$ film. Also, we demonstrate the influence of optical radiation on the magneto-transport properties of the film. The thin film was deposited

onto a SiO₂/Si(001) substrate and characterized using x-ray diffraction, scanning and transmission electron microscopy, and magnetization measurements.

Characteristic current-voltage (I - V) curves for the film under study are shown in Figure. The I - V characteristics are linear at small currents up to about 8 μ A; at larger currents the curves show nonlinear behavior. Qualitatively similar dependences are observed in the temperature range from 4.2 to 300 K. The film exhibits the negative MR effect, at which in the low temperature region MR is determined mainly by the magnetic tunnel mechanism. Down to 30 K, the MR value is independent of current bias. Below this temperature, the film exhibits the positive MR effect in the region of bias currents where the I - V characteristics are nonlinear. The positive MR value depends on bias current and can considerably exceed the negative MR value observed at low currents (see Figure). Thus, we have apparently observed for the first time the effect of the colossal positive MR induced by the transport current in manganites.



In addition, we have detected the effect of optical radiation ($\lambda=1 \mu$ A) on the transport and magneto-transport properties of the film. This effect is not heat in origin. The strongest effect of optical radiation is observed below 30 K. The applied magnetic field suppresses photo-induced changes in the transport properties of the film.

The results obtained are discussed in terms of the spin-polarized tunnel conduction mechanism. The film possesses of the granular microstructure, which results in the formation of the cooperative network of magnetic tunnel junctions. The features near 30 K are related to the appearance of magnetic ordering at the grain boundaries which form potential barriers between the neighboring contacting grains.

This study was supported by the RFBR, Project No. 08-02-00259-a, the KRSF-RFBR “Enisey-2007”, Project No. 07-02-96801-a, and the Division of Physical Sciences of RAS, Program “Spin-dependent Effects in Solids and Spintronics” (Project No 2.4.2 of SB RAS).

[1] N. Volkov, G. Petrakovskii, K. Patrin et al., *Phys. Rev. B*, **73**, 104401-1-10 (2006).

24PO-7-13

MAGNETIC STRUCTURES AND EXITATIONS IN FERROMAGNETIC – NONMAGNETIC METALL MULTILAYERS

Ignatchenko V.A., Laletin O.N.

L.V. Kirensky Institute of Physics, Academgorodok, 660036 Krasnoayrsk, Russia.

The ferromagnetic layers in the multilayer structure ferromagnetic – nonmagnetic metal are coupled to each other by the indirect exchange coupling through conduction electrons of the metallic layers. Since the indirect exchange coupling is appreciable for the spins on the surfaces of the ferromagnetic layers and the magnetic field acts on all spins, the inhomogeneous distribution of the magnetization $\mathbf{M}(z)$ along the thickness of the ferromagnetic layers should arise. To find this distribution the boundary-value problem is solved in which the equations for the polar angles θ_i at the orientation of the magnetic field along the z axis have the forms

$$\alpha M \theta_i'' - H \sin \theta_i + 4\pi M_0 \sin \theta_i \cos \theta_i = 0, \tag{1}$$

where $i = 1, 2$ are the layer numbers, α is the exchange constant, H_i^m is the demagnetizing field. Coupling between the layers is described by the boundary conditions at the right boundary of the first layer $z = l/2$ and at the left boundary of the second layer $z = l/2 + r$, where l and r are the thicknesses of the ferromagnetic and nonmagnetic layers, respectively:

$$\alpha \theta_1' \Big|_{z=l/2} = -A \cos \theta_1 \Big|_{z=l/2} \sin \theta_2 \Big|_{z=l/2+r}. \tag{2}$$

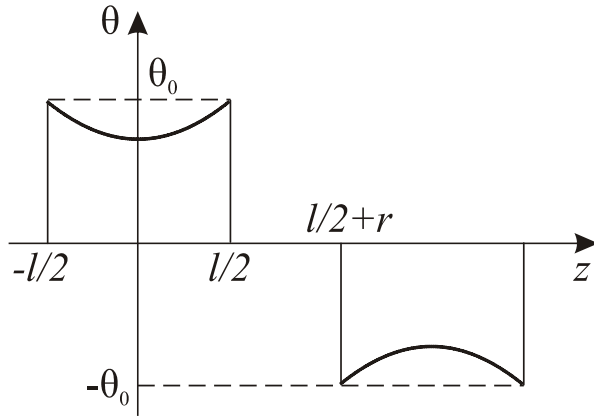


Fig. 1.

Here A is the indirect exchange coupling constant between the spins on the surfaces of the adjacent ferromagnetic layers, its sign depends periodically on the distance r between the layers. The case of antiferromagnetic coupling between the layers is investigated ($A < 0$). The two situations are considered: magnetization reversal in the plane of the layers along the x axis and magnetization reversal along the z axis. For the both cases the distribution of the orientation of the magnetization in the layers has the same character in workmanlike manner (Fig. 1). At $H \neq 0$ the maximum angle $2\theta_0$ between the orientations of the magnetization \mathbf{M}_1 and \mathbf{M}_2

corresponds to the edges of the adjacent ferromagnetic layers and the angle decreases to the middle of the layer. The averaged value of the projection $\langle M_z \rangle = M_0 \langle \cos \theta \rangle$ is calculated, the dependence of which on H describes the magnetization curve of the multilayer structure. For the both cases under consideration the magnetization curves are similar in the form in spite of

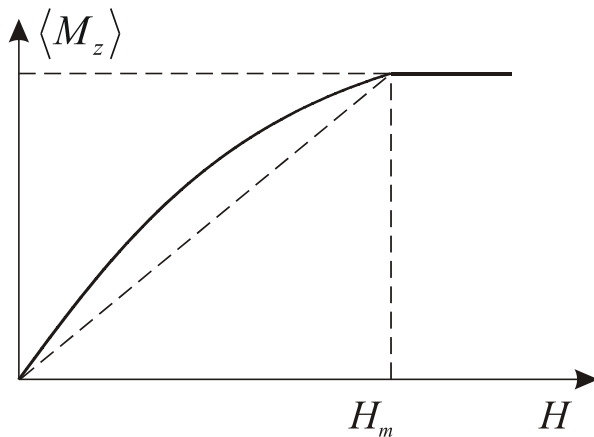


Fig. 2.

considerable quantitative difference (Fig. 2). One can see that instead of the linear dependence corresponding to the homogeneous orientation of the magnetization in the layers the nonlinear curves should be observed with the greater initial susceptibility. At magnetization in the xy plane the magnetic saturation field $H_m = 2AM/l$ and at magnetization along the z axis $H_m = (4\pi + 2A/l)M$. Magnetic excitations propagating in such multilayer structures is studied at $H > H_m$.

This work was supported by the Grant of the RF President, SS – 3818.2008.3.

24PO-7-14

PENETRATION OF RF ELECTROMAGNETIC FIELD THROUGH THIN FILMS OF $\text{La}_{0.67}\text{Sr}_{0.33}\text{MnO}_3$ MANGANITE

Nosov A.^{1}, Rinkevich A.¹, Gribov I.¹, Moskvina N.¹, Vassiliev V.², Vladimirova E.², Szymczak H.³, Lewandowski S.³, Gierlowski P.³, Abaloshev A.³, Ranno L.⁴*

¹Institute of Metal Physics, UD of RAS, Ekaterinburg, Russia

²Institute of Solid State Chemistry UD of RAS, Ekaterinburg, Russia

³Institute of Physics, Polish Academy of Sciences, Warszawa, Poland

⁴Institut Nreel, CNRS-UJF, BP 166, 38042 Grenoble Cedex 9, France

Doped lanthanum manganites are strongly correlated materials in which complex interaction of spin, structural, and charge degrees of freedom is observed. They attracted considerable interest after discovery of “colossal” magnetoresistance. Investigations of manganites by radio-frequency methods received much less attention. In this frequency range the observed effects have much greater values than the ones measured under *dc* conditions and important information about the dynamic properties of spin system can be obtained.

Penetration of electromagnetic waves through thin films of $\text{La}_{0.67}\text{Sr}_{0.33}\text{MnO}_3$ manganite grown by pulsed laser deposition on (100) SrTiO_3 and LaAlO_3 substrates was investigated and compared to the data obtained for the bulk specimens of the same composition. Experiments were carried out in the frequency range from 20 kHz to 30 MHz in the temperature range below and above the Curie temperature T_C . A manganite sample was placed between a pair of identical coils and was used as an element screening the receiving coil from the exciting one. The exciting coil created the high-frequency magnetic field which penetrated through a manganite sample and excited the signal in the receiving coil. Experimentally the modulus of the transmission coefficient, *i.e.* the ratio of signal in the receiving coil to the one in the exciting coil was measured as a function of the *dc* magnetic field applied in the plane of a sample.

Strong frequency-dependent variations of penetration coefficient in the *dc* magnetic field were observed both for ferromagnetic and paramagnetic temperatures. Changes of the transmission coefficient both for thin films and the bulk target were qualitatively similar. In the ferromagnetic state below T_C for all frequencies variations of the transmission coefficient in the *dc* magnetic field are positive and are mostly caused by the dynamic magnetic permeability. In the paramagnetic state above T_C at low frequencies the contribution from magnetic permeability prevails, while at high frequencies the contribution from magnetoresistance is more important. The experimental data obtained confirm preservation of a local dynamic magnetic ordering in the paramagnetic temperature range by 1,10÷1,22 times higher the Curie temperature, which weakly depends on the microstructure of the films. The value of upper frequency limit of the dynamic polaron correlations in the paramagnetic phase was estimated.

Support by the Program of Presidium of RAS “Quantum macrophysics”, the NSh-3257.2008.2 grant, programs of scientific cooperation between RAN and PAN, RAN and CNRS, IEEE, ARC, and ARCNN is acknowledged.

24PO-7-15

POLARON IN-GAP STATES IN CMR MANGANITES

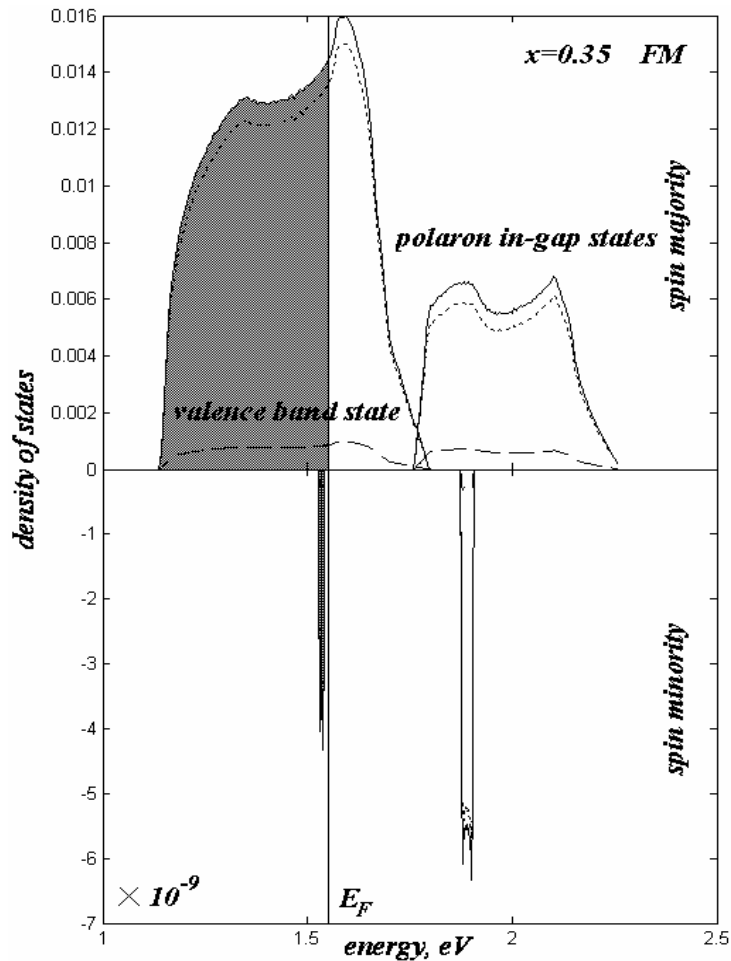
Gavrichkov V.^{1,2}, Ovchinnikov S.^{1,2}

¹Siberian Federal University, av. Svobodnyi 79, Krasnoyarsk 660041, Russia

²L.V. Kirensky Institute of Physics, Siberian Branch of RAS, Krasnoyarsk, 660036, Russia

The electronic structure undoped and doped manganites $La_{1-x}Sr_xMnO_3$ is investigated within the frameworks of the generalized tight binding method with the obvious account for the strong intratomic electronic correlations [1]. As follows at our calculations of, the ground state of the orbital nonordering undoped antiferromagnetic LaSrMnO₃ would be metal, despite of the Mott-Hubbard correlation gap in spectra of the quasiparticles.

Due to the orbital ordering the ground dielectric state, both in antiferromagnetic and paramagnetic phases is stabilized for the materials. Near to a top of valence band we observe the in-gap hole states of the polaron nature with a spectral weight proportional to the concentration doping in $La_{1-x}Sr_xMnO_3$ (see figure). With increasing doping in a ferromagnetic phase at zero temperature there is a ground state of metal with the metal character for one of the spin subbands of electronic structure and the dielectric type for other spin subband. The figure illustrates a specific metal character of ground states in FM phase (at T=0K), so-called the “half-metal” ground state.



The dotted line corresponds to d - and dashed line – p -contributions.

Support by Presidium of RAS program “Quantum macrophysics”, Integration Grant of Siberian and Ural Branches of RAS #74, RFFI-BNTS Grant 06-02-90537, and Grant WTZ project 1/2006.

[1] V.A. Gavrichkov, A.A.Borisov, S.G.Ovchinnikov, *Phys.Rev.***B64**, (2001) 235124.

24PO-7-16

MAGNETOELECTRIC EFFECT FOR COLOSSAL MAGNETORESISTIVE MANGANITES

Kadomtseva A.M.¹, Popov Yu.F.¹, Vorob'ev G.P.¹, Kamilov K.I.¹, Ivanov V.Yu.², Mukhin A.A.², Balbashov A.M.³

¹Moscow State University, 119992 Moscow, Leninskie Gory Russia

²A.M. Prokhorov General Physics Institute of RAS, Moscow, Vavilov st. 38, Russia

³Moscow Power Institute 105835 Moscow, Russia

Field-induced electric polarization was observed for the first time in $\text{Pr}_{1-x}\text{Ca}_x\text{MnO}_3$, $\text{Nd}_{1-x}\text{Ca}_x\text{MnO}_3$ and $\text{Gd}_{1-x}\text{Sr}_x\text{MnO}_3$ ($x \sim 0.5$) single crystals by complex study of their magnetoelectric, magnetic, magnetoelastic properties in high magnetic fields. It is commonly known that for these compounds Mn ions exhibit either CE-type charge and orbital ordering of $\text{Mn}^{3+}/\text{Mn}^{4+}$ ions or Zener polaron ordering with e_g -electrons placed in the middle of Mn-O-Mn bond. Both of these states has a center of symmetry that forbids an appearance of spontaneous electric polarization. However, it was predicted [1] that new type of ordering with non-zero electric dipole moment may appear in doped manganites with $x \sim 0.5$ in a case of asymmetry distribution of the e_g -electrons between neighboring Mn ions. Such compounds with coexistence of different types of ordering (magnetic, electric and sometimes elastic) are called multiferroics and their investigations are both of fundamental and practical interest.

Recently in our work [2] jumps of electric polarization were found in $\text{Gd}_{1/2}\text{Sr}_{1/2}\text{MnO}_3$ single crystal at magnetic-field suppression of charge ordered spin-glass state upon a phase transition to a ferromagnetic conductive phase. A sign of induced polarization revealed a strong correlation with a sign of poling electric field applied to the crystal during cooling, thus indicate an existence of spontaneous polarization in the charge ordered state.

Similar sharp changes of electric polarization were found in $\text{Pr}_{0.6}\text{Ca}_{0.4}\text{MnO}_3$ and $\text{Nd}_{0.6}\text{Ca}_{0.4}\text{MnO}_3$ single crystals in magnetic fields $H_{\text{cr}} \sim 65$ kOe and 80 kOe ($T=4.2$ K), respectively, at field suppression of the charge ordered antiferromagnetic state and phase transition to the ferromagnetic metallic state. The dependence of induced electric polarization sign on polarity of poling electric field reveals ferroelectric order coexisting with the antiferromagnetic states. The found spontaneous polarization associates with the predicted non-centrosymmetric structures for half-doped rare-earth manganites [1].

Thus our investigations of the half-doped manganites $\text{Pr}_{0.6}\text{Ca}_{0.4}\text{MnO}_3$, $\text{Nd}_{0.6}\text{Ca}_{0.4}\text{MnO}_3$ and $\text{Gd}_{1/2}\text{Sr}_{1/2}\text{MnO}_3$ have shown new (ferroelectric) type of ordering in addition to the known antiferromagnetic (spin-glass) charge-ordered states.

The work was partially supported by RFBR (06-02-17192-a).

[1] D.V. Efremov, J. van den Brink, D.I. Khomskii, *Nature Materials*, 10, 1038 (2004)

[2] A.M. Kadomtseva, Yu.F. Popov, G.P. Vorob'ev, V.Yu. Ivanov, A.A. Mukhin, A.M. Balbashov, *JETP Lett.*, 82, 590 (2005).

24PO-7-17

CRYSTAL FIELD DISTORTIONS OF YVO_3

Beale T.A.W.¹, Johnson R.D.¹, Hatton P.D.¹, Bouchenoir L.²,
Prabhakaran D.³, Boothroyd A.T.³

¹Department of Physics, Durham University, South Road, Durham, DH1 3LE, UK

²European Synchrotron Radiation Facility, Boite Postal 220, F-38043 Grenoble Cedex, France

³Department of Physics, University of Oxford, Clarendon Laboratory, Parks Road,
Oxford, OX1 3PU, UK

The vanadate series RVO_3 ($R = \text{rare earth}$) form a distorted cubic structure, displaying a range of magnetic and orbital order phases. We describe recent resonant X-ray scattering results at the vanadium K edge sensitive to the crystal field distortions and associated orbital order. The sample undergoes a variety of phase transitions, with a distorted room temperature crystal forming a G-type orbital ordered system below 200 K. Further cooling induces a C-type magnetic ordering at 118 K. These orbital and magnetic orders simultaneously undergo a further transition at 77 K [1], where the orbital order flips from G-type to C-type and the magnetic order from C-type to G-type (Fig. 1a). The resonant spectra of the (010) reflection illustrates the complex crystal field, showing a dramatic change at the low temperature, 77 K, orbital and magnetic transition (Fig 1b). By comparison, the higher orbital and magnetic phase transitions are much less apparent and appear to have little effect on the distortions.

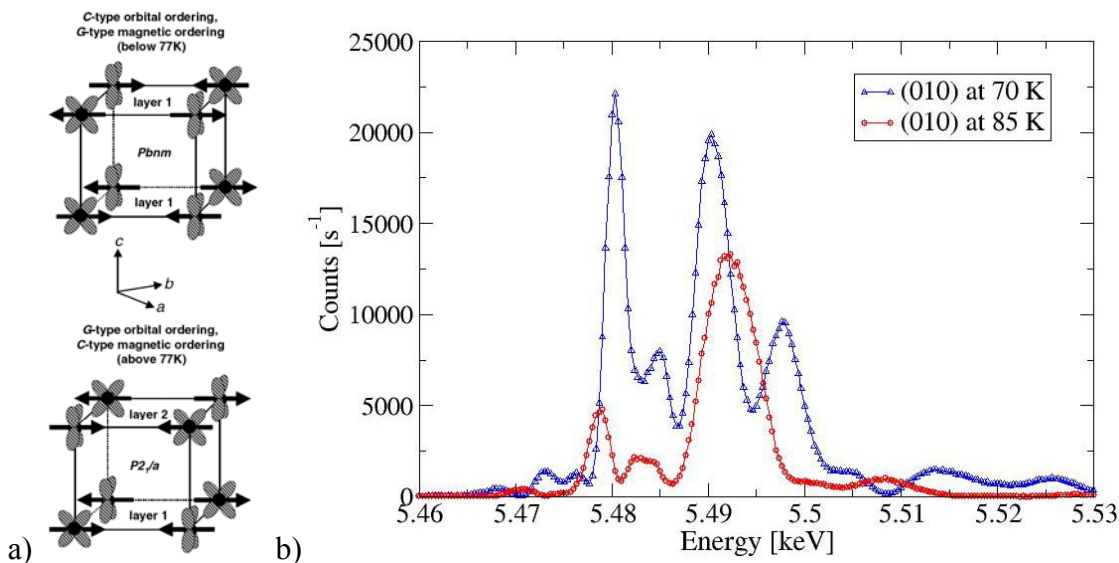


Fig. 1 a) The orbital and magnetic occupancies in each phase [1]. b) Resonance spectra of the (010) forbidden Bragg reflection above and below the magnetic and orbital transition.

[1] G.R. Blake, T.T.M. Palstra, Y. Ren, A.A. Nugroho and A.A. Menovsky PRL **87** 245501 (2001)

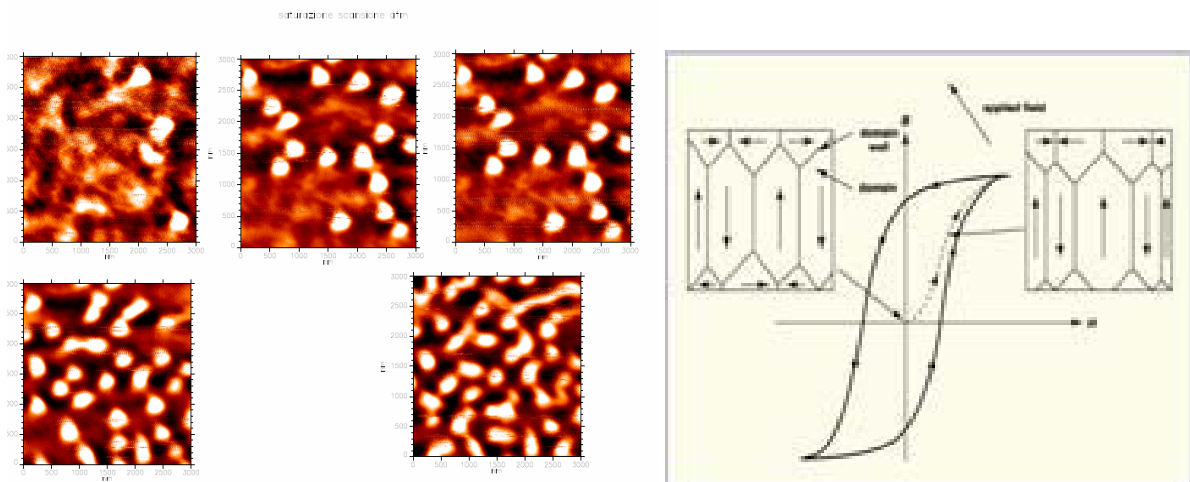
24PO-7-18

LOW TEMPERATURE MFM EXPERIMENTS ON $\text{La}_{0.7}\text{Ca}_{0.3}\text{MnO}_{3-\delta}$ -THIN-FILMS

Bobba F., Scarfato A., Longobardi M., Giubileo F., Piano S., Cucolo A.M.

Dipartimento di Fisica "E. R. Caianiello", Università degli Studi di Salerno, via S. Allende,
84081 Baronissi (SA)

By using Frequency Modulation AFM and MFM techniques we have performed an extensive study of the effect of the substrate induced strain in $\text{La}_{0.7}\text{Ca}_{0.3}\text{MnO}_{3-\delta}$ (LCMO) thin films. Highly epitaxial thin films were realized by DC sputtering system, in the same deposition run, both on STO substrates, inducing a tensile strain, and on compressive LAO substrates. The thickness of the films were varied from 10 to 100 nm. NC-AFM images were performed at room temperature while MFM images were acquired with a Co/Cr coated tip both above and below the metal-insulator transition temperature. Topographic analysis showed surfaces with low roughness formed by atomically flat. The low temperature MFM images have shown that for thinner films magnetization is mainly in the film plane while in thicker sample the magnetization start to be out of plane and for LCMO/STO the magnetization appears to be more "out of plane" oriented than LCMO/LAO films. In external applied magnetic field normal to the film surface, a complete contrast saturation has been found at $H=0.1$ T for the LCMO/LAO and at $H > 6$ T for the LCMO/STO samples. When the thickness of LCMO films is increased "out of plane" circular shaped magnetic domains starts to dominate in LCMO/STO samples while maze shape domains appear in LAO. By following the evolution of the magnetic domains structure in the external applied magnetic field and in temperature we discuss here the influence of the substrate induced strain on the micromagnetic configuration of the LCMO films.



Barkhausen effect and nucleation of the magnetic domains. The nucleation has been observed in correspondence of a magnetic field of about 850mT perpendicular to the film. The coloured dots indicate the position along the hysteresis cycle.

24PO-7-19

ELECTRON- AND MAGNETO- TRANSPORT IN EPITAXIAL MANGANITE FILM UNDER SUBSTRATE INDICED STRAIN

Ovsyannikov G.A.^{1,2}, Petrzhik A.M.¹, Borisenko I.V.¹, Klimov A.A.¹, Demidov V.V.¹, Nikitov S.A.¹

¹Institute of Radio Engineering and Electronics, Russian Academy of Sciences,
Mokhovaya 11, bld 7, 125009 Moscow Russia

²Chalmers University of Technology, SE-41296 Gothenburg, Sweden

Electrical transport and magnetic properties of epitaxial, optimally doped ($x=0.3$) $\text{La}_{1-x}\text{Sr}_x\text{MnO}_3$ epitaxial films were investigated by dc, magneto-optic, and microwave resonance techniques. Substrates with the lattice mismatch from 0.9% to -2% related to LSMO material were used: (110) NdGaO_3 , (001) SrTiO_3 , and (001) LaAlO_3 . Magnetic and electric properties depend strongly on uniform and biaxial distortions. The insulator-metal transition and Curie temperatures dependence both on bulk and Jahn-Teller strains as Millis theory predicted [1]. The temperature dependence of the resistance $R(T)$ for all investigated films is proportional to $T^{2.5}$ with asymptotic constant resistance R_0 at low temperatures as it was observed previously [2]. Temperature dependence term represents at low temperature the coupling between hopping disorder and low energy magnons in the system and produces a resistivity that increases as $T^{2.5}$ [3]. A small (0.2%) orthorhombic distortion due to the (110) NdGaO_3 substrate caused an anisotropy of the magnetic parameter in the plane of the substrate. Only in-plane and out-of-plane anisotropies were observed for LSMO films grown on (001) SrTiO_3 and (001) LaAlO_3 substrates. The deviation of the form of ferromagnetic resonance from a Lorenz one clearly indicates the presence of a second magnetic phase in the film.

Support in partially by programs of Physics Department of RAS, project NMP3-CT-2006-033191 of FP6 EU, programs AQDJJ and THIOX of ESF and project N3743 by ISTC.

[1] A.J. Millis, T. Darling, and A. Migliori, *J. Appl. Phys.*, 83, 1588 (1998)

[2] P. Schiffer, A.P. Ramirez, W. Bao and S.-W. Cheong, *Phys. Rev. Lett.*, 75, 3336 (1995)

[3] M.J. Calderon, L.Brey, *Phys. Rev. B*64, 140403® (2001).

24PO-7-20

SPIN WAVES SPECTRUM OF FERROMAGNETIC LANTHANUM MANGANITE

Karpenko B.V.¹, Falkovskaya L.D.¹, Kuznetsov A.V.²

¹Institute of Metal Physics, Ural Branch of Russian Academy of Sciences,
Ekaterinburg 620041, S. Kovalevskaya str.18, Russia

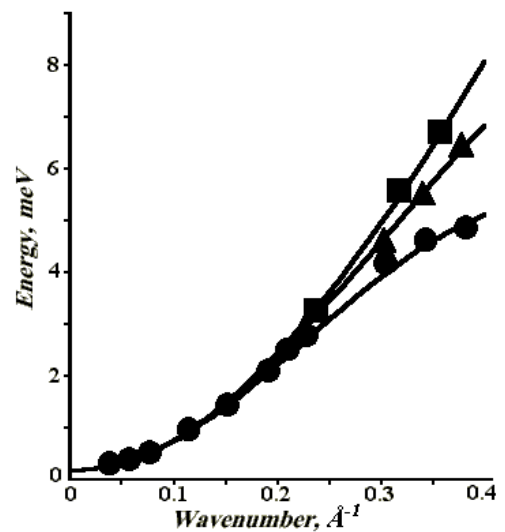
²Ural State University, Ekaterinburg 620083, Lenin str.51, Russia

The theoretical expressions for spin waves spectrum of cubic compound $\text{La}_{1-x}\text{Ca}_x\text{MnO}_3$ with ferromagnetic ordering containing mixed valence ions are obtained. The model of homogeneous spin alloy which supposes that the system is the mixture of ions Mn^{3+} and Mn^{4+} is used. Each site of magnetic sub-lattice with probability $1-x$ is occupied by ion Mn^{3+} and with probability x – by ion Mn^{4+} . The Heisenberg superexchange, double exchange and one-ion anisotropy are taken into account. Interactions with magnetic ions from four coordinate spheres

are taken into account resulting in eighteen interaction parameters. The formulas for spin waves energies are valid in the full Brillouin zone.

The theoretical curves for three major crystallographic axes [001], [110], and [111] are compared with experimental ones obtained in paper [1] by the method of inelastic neutron scattering in compound $\text{La}_{0.83}\text{Ca}_{0.17}\text{MnO}_3$. Experimental results are presented on the figure by circles for direction [001], by triangles for directions [110] and [101] and by squares for direction [111]. The solid lines are least square fits which give the following values of summary exchange parameters for four coordinate spheres: $J_1 = 2.405$, $J_2 = -1.088$, $J_3 = 0.606$, $J_4 = 0.384$ (in meV). These values of exchange parameters lead to the magnitude of energy gap 0.136 meV. It should be noted that gap in our model appears not only due to anisotropy energy but also as a result of the superexchange and double exchange interactions. The reason of this is presence of ions with different spins, namely 2 and 3/2.

In conclusion we need to explain why we have considered interactions up to the neighbors of the fourth order. The reason lies in the fact that for direction [001] the point of inflection is at $q < 0.4$ while the nearest neighbors approximation with dependence $\cos(aq)$ can give the inflection at $q > 0.4$ (if $a = 3.89 \text{ \AA}$). The needed inflection can be given by harmonic $\cos(2aq)$ which appears only with neighbors of the fourth order.



The work is supported by Program “New materials and structures” of the Department of Physics of RAS.

[1] M. Hennion, F. Moussa, *New J. Phys.*, 7 (2005) 1

24PO-7-21

TUNNELING OF SPIN-POLARIZED CHARGE CARRIERS IN $\text{La}_{0.8}\text{Ag}_{0.1}\text{MnO}_{3+\delta}$ FILMS WITH THE VARIANT STRUCTURE

*Sukhorukov Yu.*¹, *Telegin A.*¹, *Gan'shina E.*², *Vinogradov A.*², *Kaul A.*², *Gorbenko O.*², *Melnikov O.*²

¹Institute of Metal Physics, Ural Division of RAS, 620041 Ekaterinburg, Russia

²Moscow State University, 119992 Moscow, Russia

e-mail: suhorukov@imp.uran.ru

It has been shown in a lot series of our works that both of the single crystals and the films of lanthanum manganites with the colossal magnetoresistance ($\text{CMR} = \rho_{\text{H}} - \rho_0 / \rho_0 = \Delta\rho / \rho$) there are optical analogue CMR magnetotransmission effect ($\text{MT} = \Delta I / I$, I-transmission of IR radiation) and on metal-insulator transition (MI) near the Curie temperature (T_{C}). It has been demonstrated also, that a high epitaxial homogeneous manganite films has the similar dependence of $\rho(T)$ and $I(T)$, $\Delta I / I(T)$ and $\Delta\rho / \rho(T)$ and possess the coincidence temperatures of maxima CMR and MI-transition near the T_{C} , for example, $\text{La}_{1-x}\text{Ag}_x\text{MnO}_3$ films ($x_{\text{Ag}} = 0.05, 0.10, 0.15$ and 0.25) on SrTiO_3 substrate [1]. In the present work on an example of the $\text{La}_{0.8}\text{Ag}_{0.1}\text{MnO}_{3+\delta}$ films with the variant structure grown on $\text{ZrO}_2(\text{Y}_2\text{O}_3) - \text{ZYO}$ substrates it has been shown that there are the

significant difference in the $\rho(T)$ and $I(T)$, $\Delta I/I(T)$ and $\Delta\rho/\rho(T)$ dependences in it artificially created charge- and the magnetic nonuniformities within films [2].

Films with variant structure differ from polycrystalline materials by the presence of high conducting structural domains divided by the fixed low conducting high angle boundaries (19.5° , 70.5° and 90°). In contrast to films without variant structure in $\text{La}_{0.8}\text{Ag}_{0.1}\text{MnO}_{3+\delta}$ films on ZYO the metal-insulator transition occurs at the temperatures on ~ 80 K below the T_C while optical analogue CMR are close to $T_C=313$ K. The distinction in position of these critical temperatures is caused by a competition of the contributions to conductivity inside of structural domains and through boundaries one. The Curie temperature measured onto the film surface and onto the substrate back has revealed the different values that testified to magnetic inhomogeneity of the films.

It has been shown, that unlike usual manganites films in films with variant structure besides of CMR there is a contribution in magnetoresistance connected with tunneling spin-polarized of electrons through high angle boundaries of structural domains - so-called tunnel magnetoresistance which increases at downturn of temperature.

As the magnetotransmission achieves a maximum $\sim 6-9\%$ at temperature close of T_C , the comparison of $\rho(T)$ and $I(T)$, $\Delta I/I(T)$ and $\Delta\rho/\rho(T)$ dependences has allowed us to divide contributions of CMR and tunnel magnetoresistance in $\text{La}_{0.8}\text{Ag}_{0.1}\text{MnO}_{3+\delta}$ films with variant structure. It was shown, that tunnel magnetoresistance is described by the formula $\Delta\rho/\rho(T)=a+b/(T)^{1/2}$, where a and b are constants. Extrapolation of a curve $\Delta\rho/\rho(T)$ on an axis of ordinates made us possible to estimate the spin-polarizations (P) of electrons by the expression $\Delta\rho/\rho=2P^2/(1-P^2)$: $P\sim 0.5$ in these $\text{La}_{0.8}\text{Ag}_{0.1}\text{MnO}_{3+\delta}$ films on ZYO substrates.

Supported by the RAS program 'New materials and structures' and RFBR (grant No 07-02-00068 and 06-03-33070).

[1] E. Gan'shina, N. Loshkareva et. al., *J. Magn. Magn. Mater.*, **300** (2006) 62.

[2] O.V. Melnikov, Yu.P. Sukhorukov et. al., *J. Phys.: Cond. Matt.*, **18** (2006) 3753.

24PO-7-22

CHARGE STATE AND MAGNETIC MOMENT OF Mn IONS IN MIXED-VALENCE $\text{Ca}_{1-x}\text{La}_x\text{MnO}_{3-\delta}$ ($x\leq 0.1$) MANGANITES WITH ELECTRON TYPE DOPING

Gizhevskii B.A.¹, Galakhov V.R.¹, Loshkareva N.N.¹, Elokhina L.V.¹, Fedorenko V.V.¹, Neumann M.²

¹Institute of Metal Physics, Ural Division, Russian Academy of Science,
620041 Yekaterinburg, Russia

²University of Osnabrück, D-49069 Osnabrück, Germany

The manganese perovskite oxides of $\text{A}_{1-x}\text{La}_x\text{MnO}_{3-\delta}$ ($A=\text{Ca}, \text{Sr}, \text{Ba}$) have wide range of homogeneity. High level of defects both in cation and in anion sublattices results in change of charge state (valence) of cations. For understanding of electron and magnetic properties of manganites it is important to know stoichiometry of compound as well as charge state and magnetic moment of Mn ions. Manganites $\text{Ca}_{1-x}\text{La}_x\text{MnO}_{3-\delta}$ with $x<0.5$ have electron type of conductivity. In contrast of hole doped manganites ($x>0.5$) electron doped ones tend to oxygen deficiency. Manganites with electron type doping demonstrate interesting magnetic, transport and optical properties different from those of hole doped compounds [1].

In this work we studied cation and oxygen nonstoichiometry as well as charge state and effective magnetic moment of Mn ions in $\text{Ca}_{1-x}\text{La}_x\text{MnO}_{3-\delta}$ ($x=0, 0.05, 0.1$) single crystals. Manganites single crystals were grown by A. Balbashov. Cation composition of manganites was measured by x-ray microanalysis. For determination of Mn charge state and oxygen deficiency we used the Mn 3s x-ray photoelectron spectra [2]. The spectral splitting of the 3s core-level x-ray photoelectron spectra in compounds of transition metals originates from the exchange coupling between the 3s hole and the 3d electrons. The magnitude of the splitting is proportional to $(2S+1)$, where S is the local spin of the 3d electrons in the ground state. This method provides a possibility to determine charge state and spin of Mn ions.

We find that the composition of $\text{Ca}_y\text{MnO}_{3-\delta}$ single crystal is $\text{Ca}_{0.854}\text{MnO}_{2.75}$ and the composition of $\text{Ca}_y\text{La}_x\text{MnO}_{3-\delta}$ sample ($x=0.05$ for initial reaction powder) is $\text{Ca}_{0.845}\text{La}_{0.03}\text{MnO}_{2.73}$. Charge state and effective magnetic moment μ_{eff} of Mn ions for these samples are equal $3.8+$, $4.06 \mu_B$ and $3.6+$, $4.20 \mu_B$ accordingly. In the case of $\text{Ca}_y\text{La}_{0.1}\text{MnO}_{3-\delta}$ sample Mn ion has charge state $3.5+$ and $\mu_{\text{eff}}=4.43 \mu_B$. Average valence $3.5+$ means that one-half of manganese ions is Mn^{4+} and half of Mn ions is Mn^{3+} . These effective magnetic moments of $\text{Ca}_y\text{La}_x\text{MnO}_{3-\delta}$ single crystals are larger than ones defined from measurements of magnetic susceptibility $\chi(T)$ [1]. In nonstoichiometric and defect manganites magnetic heterogeneity may have a pronounced effect on magnetic measurements. Contrary to magnetic data the Mn 3s x-ray photoelectron spectra are free from action of magnetic ordering and magnetic heterogeneity. We believe that 3s x-ray photoelectron spectroscopy is the effective method for study of charge state (valence) and magnetic moments of 3d ions in defect and nonstoichiometric compounds.

This work is supported by the Russian Foundation for Basic Research, Grant No 07-02-00540 and by the Program "New Materials and Structures" of the Department of Physics, Russian Academy of Science.

[1] N.N. Loshkareva, et al., *Phys. Met. Metallog.*, **103** (2007) 251.

[2] V.R. Galakhov, et al., *Phys. Rev. B*, **65** (2002) 113102.

24PO-7-23

MAGNETIC PROPERTIES OF $\text{La}_{1-x}\text{Ag}_y\text{MnO}_{3+\delta}$ POWDERS AS MATERIALS FOR LOCAL HYPERTHERMIA

Markelova M.¹, Melnikov O.¹, Gorbenko O.¹, Kaul A.¹, Atsarkin V.², Demidov V.², Roy E.³, Odintsov B.^{2,3}

¹Moscow State University, 119991 Moscow, Russia

²Institute of Radio-engineering and Electronics of RAS, 125009, Russia

³University of Illinois at Urbana-Champaign, USA

e-mail:pomar-ka@yandex.ru

Local hyperthermia is the method of intensive cancer therapy. Malignant cells perish upon heating up to 43°C much more effectively than normal cells. Within the past decades a technique of local hyperthermia was put forward using the electromagnetic heating of ferromagnetic nanoparticles introduced into the tumor. In our work we propose a new material for local hyperthermia based on lanthanum-silver manganites. It possesses the Curie temperature (T_C) in the range of tumor hyperthermia interest ($40\text{-}50^\circ\text{C}$).

Using the spray pyrolysis method the spherical particles of lanthanum-silver manganite were prepared. Spray of La, Ag and Mn nitrates water solution was generated by ultrasonic

applicator. Spray was admitted through tubular oven heated up to 1000°C. Then powder was annealed in oxygen at 700°C or 800°C 5 h. For optimization of synthesis conditions some series of $\text{La}_{0.8}\text{Ag}_y\text{MnO}_{3+\delta}$ with different silver doping ($y = 0 \div 0.2$) were investigated including samples made by the paper synthesis [1]. According to X-rays diffraction the products were identified as single phase rhombohedral perovskites. The index of oxygen non-stoichiometry δ was determined by iodometric titration. $M(H)$ loops revealed typical soft ferromagnetic behavior of the samples. It was found that T_C depends on the temperature of synthesis and the silver content. T_C increases gradually with silver content. We studied the heating of powder water suspensions subjected to alternating magnetic field at ~ 800 kHz. Temperature kinetics shows clear thermostatic behavior for a long time, the stabilization temperature (T_{st}) being close to T_C . This is very useful for cancer hyperthermia because of avoiding the overheating problem. Stabilization temperature was found to be rather insensitive to the amplitude H_1 of the A.C. magnetic field within the range of 7.8-13 kA/m. It is found that the material with $y = 0.15$ made by paper synthesis is most effective and can be applicable for local hyperthermia due to the proper T_C value of 43 °C and sufficiently high specific absorption rate, $\text{SAR} \approx 80 \text{ W/g}_{\text{Mn}}$. High biocompatibility of the lanthanum-silver manganite powders has been supported by the *in vivo* tests.

Supported by the grants from RFBR (07-03-01019a, 08-02-00040-a) and HFSP (№ RGP 47/2007).

[1] O.Yu.Gorbenko, O.V. Melnikov, A.R. Kaul, A.M.Balagurov, S.N.Bushmeleva, L.I. Koroleva, R.V. Demin, *Materials Science and Engineering B*, **116** (2005) 64.

24PO-7-24

OPTICS AND MAGNETO-OPTICS OF CHROMITES: A THEORETICAL CONSIDERATION

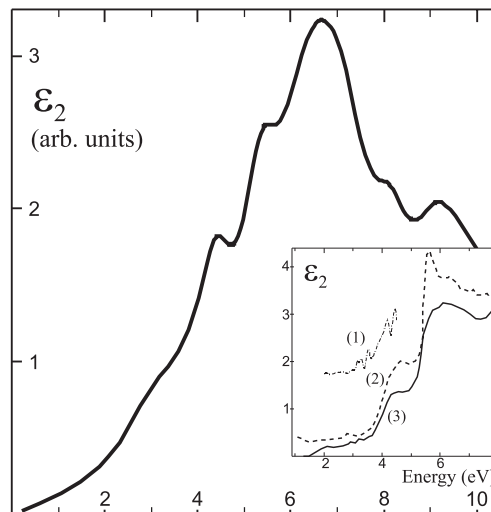
Zenkov A.V.¹, Zenkov E.V.¹, Sazanova L.A.²

¹Radio Engineering Institute, Ural State Technical University, 620002 Ekaterinburg, Russia

²Ural State Economical University, 620219 Ekaterinburg, Russia

e-mail: andreas@2-u.ru

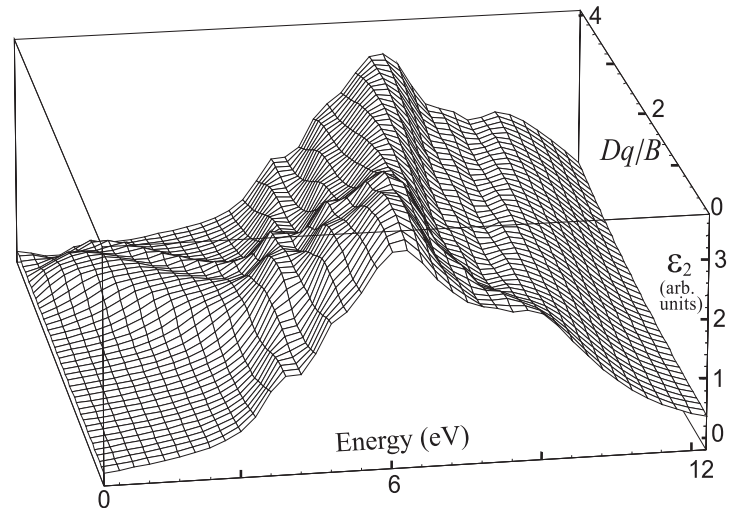
Specific features of the charge-transfer (CT) states and CT transitions of the $\text{O}_{2p} - \text{Cr}_{3d}$ type in octahedral complexes $(\text{CrO}_6)^{9-}$ are considered in the cluster approach. Using the Racah algebra for spins and quasimomenta, the reduced matrix elements of the electric dipole transition operator are calculated on the many-electron wave functions of the complexes corresponding to the initial and final state at CT transitions. The energies of the many-electron CT transitions and their intensities are calculated within the Tanabe-Sugano theory taking into account the mixing of different configurations of the same symmetry. The corrections to the energies of the levels due to the 2p hole – 3d shell interaction are made.



A self-consistent description of the CT band in perovskite-type oxide compounds like YCrO_3 is presented which allows to correct the current interpretation of the optic and magneto-optic spectra. We have performed the theoretical model simulation of the $\text{O}_{2p} - \text{Cr}_{3d}$ CT optic and magneto-optic band in these compounds generated by electric dipole allowed ${}^4\text{A}_{2g} - {}^4\text{T}_{2u}$ CT transitions in CrO_6 octahedra. The influence of crystal field magnitude and electron-electron d-d interaction on the spectrum structure are examined. The analysis shows an intricate multi-band structure of the CT optic and magneto-optic response. Predictions of the model are in a satisfactory agreement with experimental data available.

The upper figure shows the computed spectral dependence of ε_2 – the imaginary part of the diagonal permittivity tensor component. The inset shows the experimental data on ε_2 for $\text{Lu}_{0.85}\text{Y}_{0.15}\text{CrO}_3$ [1], YCrO_3 and LaCrO_3 [2] (curves 1, 2 and 3, respectively).

The lower figure shows the spectral dependence of ε_2 vs. the crystal field magnitude.



This work is supported by the Russian Foundation of Basic Research, Project No. 07-02-96036.

[1] E.A. Ganshina et al., *Fiz. Tverd. Tela*, **35** (1993) 343.

[2] T. Arima, Y. Tokura, *J. Phys. Soc. Jap.*, **64** (1995) 2488.

24PO-7-25

HEAT CAPACITY AND MAGNETOCALORIC EFFECT IN MANGANITES

$(\text{La}_{1-y}\text{Eu}_y)_{0.7}\text{Pb}_{0.3}\text{MnO}_3$ (y: 0.2; 0.6)

*Kartashev A.V.*¹, *Flerov I.N.*^{1,2}, *Volkov N.V.*^{1,2}, *Sablina K.A.*¹

¹L.V. Kirensky Institute of Physics SB RAS, Krasnoyarsk, 660036, Russia

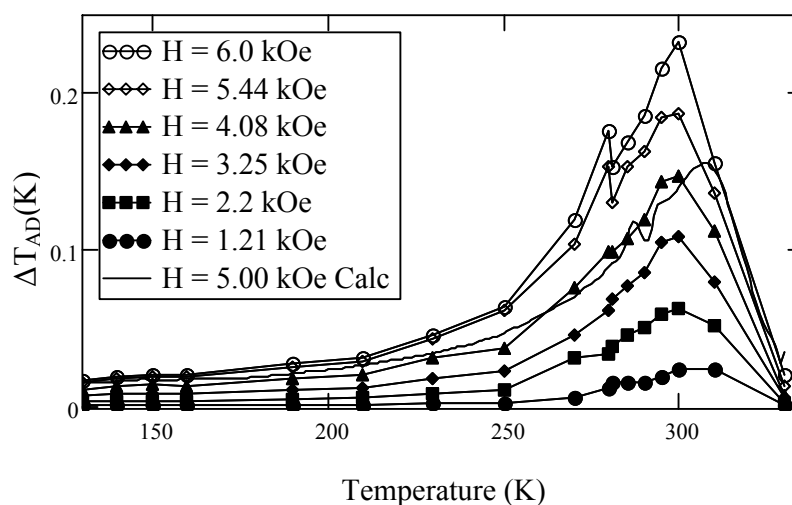
²Siberian Federal University, Krasnoyarsk, 660079, Russia

Recently intrinsic magnetic inhomogeneity was observed and studied in the system of $(\text{La}_{1-y}\text{Eu}_y)_{0.7}\text{Pb}_{0.3}\text{MnO}_3$ single crystals [1]. It was found that increase of the Eu ion concentration lead to the decrease of the Curie temperature as well as the change of the crystal symmetry at room temperature from rhombohedral (y=0; 0.2) to orthorhombic (y=0.4) and then to tetragonal (y=0.6) one. Solid solutions with y = 0 – 0.4 are characterized by the coexistence of para- and ferro-magnetic phases in a limited temperature range above as well as below T_C . Two ferromagnetic phases with different directions of the magnetic moments which are coupled by antiferromagnetic exchange interaction exist in the tetragonal crystal at $T < T_C$. In accordance with the results of comprehensive studies [1] it has been suggested that europium ions are in trivalent nonmagnetic state in manganites $(\text{La}_{1-y}\text{Eu}_y)_{0.7}\text{Pb}_{0.3}\text{MnO}_3$.

In this paper we present the results of magnetothermal properties studies in two solid solutions $(\text{La}_{1-y}\text{Eu}_y)_{0.7}\text{Pb}_{0.3}\text{MnO}_3$ (y = 0.2; 0.6) differed from each other by the coexisting phases below T_C . The aim of investigations is to reveal, firstly, the peculiarities of magnetothermal properties behaviour depending on the type of inhomogeneous magnetic state in crystal;

secondly, the influence of isovalent substitution of La^{3+} ions by nonmagnetic Eu^{3+} ones on magnetocaloric effect.

The heat capacity as well as the adiabatic temperature change was measured directly by means of adiabatic calorimeter. Increase of Eu ion concentration lead to remarkable decrease of the heat capacity anomalies at T_C as well as the value of intensive magnetocaloric effect ΔT_{AD} . Experimental data $\Delta T_{AD}(T)$ are compared with the results of calculations using the magnetic properties [1] (see Figure). Relative cooling power associated with both adiabatic temperature change and entropy is determined and considered in combination with other manganites



Support by the Council of Grants from the President of the Russian Federation for Support of Leading Scientific Schools (project no. NSh -1011.2008.2) is acknowledged.

[1] N. Volkov, G. Petrakovskii, P. Boeni, E. Clementyev, K. Patrin, K. Sablina, D. Velikanov, A. Vasiliev. *J. Magn. Magn. Mater.* 309, (2007), 1

24PO-7-26

ELECTRONIC STRUCTURE AND MAGNETIC PROPERTIES OF Sr_2FeMO_6 DOUBLE PEROVSKITES (M=Sc, Ti, ..., Ni, Cu) ACCORDING TO FLAPW-GGA CALCULATIONS

Bannikov V.V., Shein I.R., Kozhevnikov V.L., Ivanovskii A.L.

Institute of Solid State Chemistry, Ural Branch of the Russian Academy of Sciences, 620041 Ekaterinburg, Russia

The present communication is devoted to the investigations of electronic structure and magnetic properties of the SrFeO_3 -based double perovskites family Sr_2FeMO_6 (M=Sc, Ti, ..., Ni, Cu). The properties of these systems are in interest being the initial approach to investigate the properties of more complicated SrFeO_3 -based systems: with multi-cation doping, with vacancies in oxygen sublattice and some others. In the frameworks of full-potential linearized method of augmented plane waves (FLAPW) with generalized gradient approximation (GGA) of exchange-correlation potential [1] we have performed the calculations of electronic and magnetic properties, namely, band structures, total and partial densities of states (DOS), atomic magnetic moments and DOS on Fermi level for all these systems (see Table). The results reveal the picture of electronic states qualitatively different from that one which may be forecasted from simple "rigid band" model. The latter predicts the metallic state for all the compounds of the family

meanwhile the results of our calculations show that some of them may possess the half-metallic or semiconducting properties.

The most important results following from our band calculations may be summarized as follows:

- 1) Depending on the kind of M 3d-atom the Sr_2FeMO_6 compounds may exhibit the properties of magnetic semiconductor, magnetic half-metal or magnetic metal.
- 2) The magnetic properties of Sr_2FeMO_6 compounds with $M=\text{Sc}, \text{Ti}, \text{V}, \text{Cu}$ are mainly determined by magnetism of Fe-sublattice.
- 3) In Sr_2FeMO_6 compounds with $M=\text{Cr}, \text{Mn}, \text{Co}, \text{Ni}$ the contributions of Fe- and M-sublattices into magnetization of these compounds are comparable.
- 4) The features of band structure and magnetic characteristics of Sr_2FeMO_6 compounds depend on concentration of valence electrons and on energy of orbital states of M 3d-atoms. The first point determines the degree of filling of double perovskite valence band and the second one determines the degree of M- $3d_{\uparrow,\downarrow}$ states mixing to SrFeO_3 valence band.

<i>Compound</i>	$\mu(M) (\mu_B)$	$\mu(Fe) (\mu_B)$	<i>Conductivity state</i>
$\text{Sr}_2\text{FeScO}_6$	-0.011	2.360	Magnetic semiconductor
$\text{Sr}_2\text{FeTiO}_6$	-0.040	1.661	Magnetic half-metal
Sr_2FeVO_6	-0.157	2.929	Magnetic metal
$\text{Sr}_2\text{FeCrO}_6$	1.518	3.128	Magnetic metal
$\text{Sr}_2\text{FeMnO}_6$	3.108	2.656	Magnetic metal
$\text{Sr}_2\text{FeCoO}_6$	2.712	2.369	Magnetic metal
$\text{Sr}_2\text{FeNiO}_6$	1.527	2.400	Magnetic metal
$\text{Sr}_2\text{FeCuO}_6$	0.223	2.352	Magnetic metal

[1] J.P. Perdew, S. Burke, M. Ernzerhof, *Phys. Rev. Lett.*, **77** (1996) 3865

24PO-7-27

ELLIPSOMETRIC STUDY OF OPTICAL PROPERTIES OF $\text{La}_{1-x}\text{Ba}_x\text{MnO}_3$ SINGLE CRYSTALS ($x=0.15, 0.20, 0.25$)

Makhnev A.A., Nomerovannaya L.V., Bebenin N.G.

Institute of Metal Physics, UD RAS, Kovalevskaya St. 18, Ekaterinburg 620041, Russia

The ferromagnetic lanthanum manganites $\text{La}_{1-x}\text{Ba}_x\text{MnO}_3$ exhibit colossal magnetoresistance (CMR) near Curie temperature T_C . To find the origin of the CMR effect, one needs information on energy bands below and above T_C . Such information can be extracted from optical data but a systematic study of the optical properties of La-Ba manganites seems not to be published so far. The aim of this work is to fill the gap in part.

We report the ellipsometric study of real, $\varepsilon_1(\omega)$, and imaginary, $\varepsilon_2(\omega)$, parts of the complex permittivity and the optical conductivity spectrum, $\sigma(\omega)$, of $\text{La}_{1-x}\text{Ba}_x\text{MnO}_3$ single crystals ($x=0.15, 0.20, 0.25$; $T_C = 214, 252, 300$ K, respectively) in the spectral range of 0.22-4.8 eV taken at temperatures 95, 300, and 400 K.

At $T = 300$ and 400 K, the optical conductivity spectra of all samples are characterized by the intensive broad absorption band at 2.5-4.5 eV and the low energy maximum at ≈ 1.5 eV ($x=0.15$), 1.3 eV ($x=0.20$), and 1.3 eV ($x=0.25$).

In the ferromagnetic state ($T = 95$ K), the behavior of $\sigma(\omega)$ depends on barium concentration. If $x = 0.15$ or 0.20 , the low energy peak is situated at lower energy than at $T > T_C$, the peak intensity is higher, but the peak value ($1000-1200 \Omega^{-1}\text{cm}^{-1}$) is about the Mott minimum metallic conductivity, which in the CMR manganites is known to be about $10^3 \Omega^{-1}\text{cm}^{-1}$. In the infrared region, the real part of the complex permittivity is positive, which indicates that bound carriers dominate $\sigma(\omega)$. In the case of $x = 0.25$, lowering temperature results in broader low energy hump shifted to towards lower energies. It is important that $\epsilon_1(\omega)$ pass through zero at 0.6 eV and is negative below this energy, which points to essential contribution of free charge carriers. The optical response is however strongly incoherent in character (no Drude-like behavior in the range from 0.2 to 0.6 eV).

The increase of Ba content leads to the systematic shift of the optical conductivity spectrum as a whole and transfer of the spectral weight from the optical transitions at $2.5-4.5$ eV to lower energies. This type of behavior of $\sigma(\omega)$ was observed in many doped perovskite manganites. The shift of the absorption edge of peak at $1.3-1.5$ eV for insulating paramagnetic phase to lower energy with increasing Ba content suggests the decrease of the energy gap.

Support by grant RFBR 06-02-16085 is acknowledged.

24PO-7-28

MAGNETORESISTANCE OF $\text{La}_{0.54}\text{Ho}_{0.11}(\text{Sr/Ca})_{0.35-x}(\text{K/Na})_x\text{MnO}_3$ MANGANITES

Craus M.-L.^{1,2}, *Cornei N.*³, *Lozovan M.*², *Balasoiu M.*¹

¹Joint Institute of Nuclear Research, 141980 Dubna, Russia

²National Institute of Research&Development for Technical Physics, 700050 Iasi, Romania

³Chemistry Faculty of "Al.I.Cuza" University, 700506 Iasi, Romania

The $\text{La}_{1-x}\text{A}_x\text{MnO}_3$ manganites, where $\text{A}=\text{RE}$ or Alk ($\text{RE}=\text{rare earth as Nd, Sm, Tb, Ho, Dy etc}$ and $\text{Alk}=\text{Sr, Ba, Ca, Na, K}$) are known as magnetoresistive materials, a change of the resistivity appearing when is applied a magnetic field [1, 2]. The transport and magnetic properties of manganites can be explained by means of double exchange mechanism, proposed by Zener and later developed by Anderson and Hasegawa. Zener supposed that the e_g electrons jump, by means of p orbitals of oxygen, from a Mn^{3+} cation to a Mn^{4+} cation. The Hund's rule enhances the hopping of the e_g electrons between neighboring Mn^{3+} and Mn^{4+} cations by a factor $\cos(\theta_{ij}/2)$, where θ_{ij} is the angle between t_{2g} spins. The substitution of the rare earth with alkali (earth) cations should modify the $\text{Mn}^{3+}/\text{Mn}^{4+}$ concentrations, implicitly the magnetic moment and the transport properties. The $\text{La}_{0.54}\text{Ho}_{0.11}(\text{Sr/Ca})_{0.35-x}(\text{K/Na})_x\text{MnO}_{3+\delta}$ manganites were obtained by sol-gel and ceramic standard methods using oxides/acetates and treated in air between 1000 and 1200°C .

The samples were investigated by X-ray diffraction using a Huber diffractometer with a $\text{CuK}\alpha$ radiation. Transport and magnetic properties were determined between 77 and 500 K, by using a four probe method and, respectively, a vibrating sample magnetometer. Space group, lattice constants, positions of cations/anions in the unit cell, average size of the crystalline blocks were tested, respectively, determined, by using CeckCell, PowderCell and GSAS programs. The samples obtained by sol-gel method contain a perovskite phase, with orthorhombic structure (S. G. – Pmna); superstructure lines were also observed (s.Fig.1). We have discussed the influence of the K/Na substitution on structure, magnetic and transport properties of $\text{La}_{0.54}\text{Ho}_{0.11}(\text{Sr/Ca})_{0.35-x}(\text{K/Na})_x\text{MnO}_{3+\delta}$ manganites.

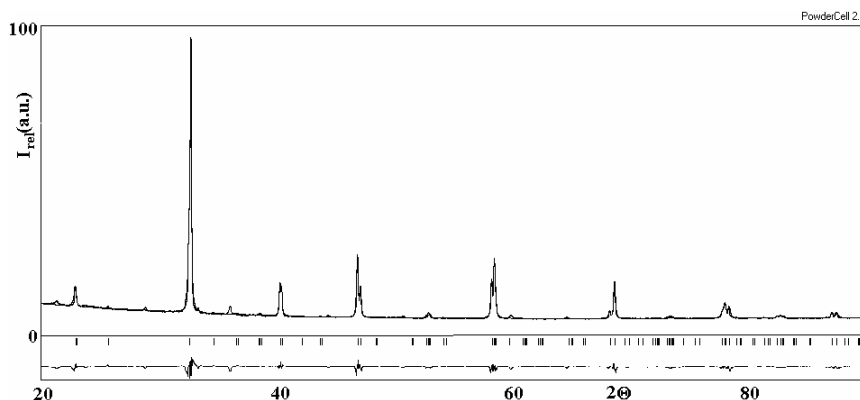


Figure 1 Diffractogram (observed, calculated and difference) of $\text{La}_{0.54}\text{Ho}_{0.11}\text{Sr}_{0.30}\text{K}_{0.05}\text{MnO}_3$ manganites

Support by Joint Institute of Nuclear Research, Dubna, Russia is acknowledged.

[1] H. Terashita and J. J. Neumeier, *Phys.Rev. B*, **71**, (2005) 134402

[2] G. Venkataiah, D.C. Krishna, M. Vithal, S.S. Rao, S.V. Bhat, V. Prasad, S.V. Subramanyam, P. Venugopal Reddy, *Physica B* **357** (2005) p.370–379

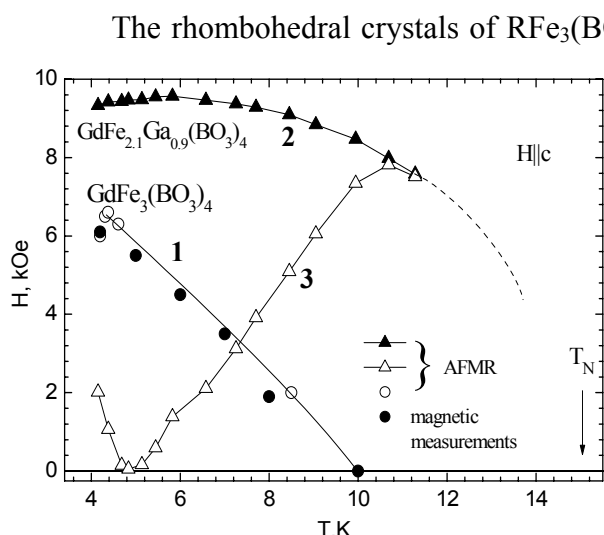
24PO-7-29

MAGNETIC AND RESONANCE PROPERTIES OF $\text{GdFe}_{2.1}\text{Ga}_{0.9}(\text{BO}_3)_4$ AND $(\text{Gd-Nd-Ho})\text{Fe}_3(\text{BO}_3)_4$ SINGLE CRYSTALS

Pankrats A.¹, Petrakovskii G.¹, Tugarinov V.¹, Khabarov I.¹, Bezmaternykh L.¹, Gudim I.¹, Szymczak R.²

¹L.V. Kirensky Institute of Physics SB RAS, Krasnoyarsk, 660036, Russia

²Institute of Physics, Polish Academy of Sciences, 02-668, Warsaw, Poland



Temperature dependencies of critical fields (1,2) of $\text{GdFe}_3(\text{BO}_3)_4$, $\text{GdFe}_{2.1}\text{Ga}_{0.9}(\text{BO}_3)_4$ and resonance fields (3) of $\text{GdFe}_{2.1}\text{Ga}_{0.9}(\text{BO}_3)_4$ for $H\parallel c$

The rhombohedral crystals of $\text{RFe}_3(\text{BO}_3)_4$ family with *huntite* structure is a new kind of rare earth magnets. They exhibit interesting magnetic properties due to competing subsystems of Fe^{3+} and R^{3+} magnetic ions. In the present work we study magnetic properties, antiferromagnetic resonance (AFMR) and magnetic phase diagrams of $\text{GdFe}_3(\text{BO}_3)_4$ with diamagnetic substitution of Fe^{3+} by Ga^{3+} ions and investigate the influence of R^{3+} ions on magnetic properties of rare earth huntites.

The AFMR investigations of pure $\text{GdFe}_3(\text{BO}_3)_4$ showed [1] that the competition of Fe^{3+} and Gd^{3+} contributions to total magnetic anisotropy of the crystal results in spontaneous reorientation at $T=10$ K between states with “easy plane” (EP) and “easy axis” (EA) anisotropy.

$\text{GdFe}_{2.1}\text{Ga}_{0.9}(\text{BO}_3)_4$. Diamagnetic substitution of Fe^{3+} ions increases the gap for EA state and decreases the gap for induced EP state in comparison with pure $\text{GdFe}_3(\text{BO}_3)_4$ due to

state and decreases the gap for induced EP state in comparison with pure $\text{GdFe}_3(\text{BO}_3)_4$ due to

reducing of the contribution of Fe^{3+} -subsystem to a magnetic anisotropy. This effect leads also to increasing of critical field of spontaneous transition to the EP state at $H||c$ (see figure) and decreasing of the Néel temperature to $T_N \approx 15$ K.

It is important that the temperature dependences of resonance field have no anomalies up to the Néel temperature. It means that spontaneous reorientation does not occur and the crystal remains in EA state in all ordering area. At the same time there is no phase transition to the induced EP state in the magnetic field lying in basal plane, at least, up to 60 kOe.

$\text{NdFe}_3(\text{BO}_3)_4$. The frequency-field dependencies of this crystal are characteristic for EP antiferromagnet with $T_N=30$ K that confirms the data of elastic neutron scattering [2]. The resonance data have no peculiarities at $T=19$ K at which a phase transition to slightly incommensurate magnetic structure with very long period along the rhombohedral axis is found [2]. In the system $\text{Nd}_x\text{Gd}_{1-x}\text{Fe}_3(\text{BO}_3)_4$ the energy gap for high frequency AFMR changes from 120 GHz for $x=1$ till 31 GHz for $x=0$.

$\text{Ho}_x\text{Gd}_{1-x}\text{Fe}_3(\text{BO}_3)_4$. The AFMR in this system is studied and the magnetic phase diagram for $x=0.06$ is obtained. The magnetic properties of $\text{HoFe}_3(\text{BO}_3)_4$ are studied in the temperature range 2-300 K in magnetic field up to 5 T. The EP state below the Néel temperature 38 K and the spontaneous reorientation to EA one at $T_{SR}=5$ K are found.

The work was supported by RFBR, grant 06-02-16255.

[1] A.I. Pankrats, G.A. Petrakovskii, L.N. Bezmaternykh, O.A. Bayukov. JETP **99**, 766 (2004).

[2] P. Fischer, V. Pomjakushin, et al., J. Phys.: Condens. Matter, **18**, 7975 (2006).

24PO-7-30

CRITICAL BEHAVIOR OF THE SPECIFIC HEAT OF $\text{La}_{1-x}\text{Ag}_x\text{MnO}_3$ ($x=0.1; 0.15; 0.2$) MANGANITES

*Gamzatov A.G.¹, Batdalov A.B.¹, Khizriev K.Sh.¹, Aliev A.M.¹, Abdulvagidov Sh.B.¹,
Melnikov O.V.² and Gorbenko O.Y.²*

¹Institute of Physics of Daghestan Scientific Center of RAS, 367003, Makhachkala, Russia

²Department of Chemistry, Moscow State University, 119899, Moscow, Russia

An interest expressed by researchers in the study of doped manganites, which have a perovskite structure and exhibit a giant magnetoresistance effect, is associated not only with the prospects of their practical applications, but also with their fundamental physical properties.

For the most part, works on manganites have been devoted to investigations into the giant magnetoresistance effect. Little attention has been focused on the study of anomalies of different thermal properties (for example, the heat capacity) in the vicinity of the magnetic phase transition and calculations of universal critical parameters [1].

Earlier [2,3] we have in detail researched a critical behavior of the manganite heat capacity $\text{La}_{0.9}\text{Ag}_{0.1}\text{MnO}_3$ (with fusion parameters $T=1100$ C, $t=5$ h) nearby a temperature of the magnetic phase transition in an interval $3 \times 10^{-3} \leq t \leq 1.8 \times 10^{-2}$ both at $T > T_C$ and at $T < T_C$, and obtained a numerical value of the critical exponent $\alpha = -0.127 \pm 0.009$, which is close to theoretically predicted estimation $\alpha = -0.12$ [4] for the isotropic Heisenberg magnetics.

In this work is studied a critical behavior of the manganite heat capacity $\text{La}_{1-x}\text{Ag}_x\text{MnO}_3$ ($x=0.1; 0.15; 0.2$) (with fusion parameters $T=1100$ C, $t=20$ h) nearby a temperature of the magnetic phase transition. The heat capacity is measured by means of original version of the modulation

calorimetry [5]. A critical behavior of an abnormal part of the heat capacity ΔC_p is described as follows [4]:

$$\Delta C_p = \frac{A}{\alpha} |t|^{-\alpha} (1 + D|t|^\theta), \quad (1)$$

where A is critical amplitude of the heat capacity, D is correction amplitude for scaling, θ is a correction index for scaling (in our case $\theta=55$, what is corresponding to Heisenberg model [4]), α is critical exponent for the heat capacity, $t=(T-T_C)/T_C$ is a reduced temperature.

The critical behavior approximation for the heat capacity is carried out by means of least-squares nonlinear method. An approximation interval is chosen in such a way that a value of root-mean-square error R would be minimal at the approximation of our data by the Formula (1). Thus we derive a numerical value of the critical exponent $\alpha=-0.114$, -0.105 and -0.105 for $\text{La}_{0.9}\text{Ag}_{0.1}\text{MnO}_3$, $\text{La}_{0.85}\text{Ag}_{0.15}\text{MnO}_3$ and $\text{La}_{0.8}\text{Ag}_{0.2}\text{MnO}_3$ correspondingly, which are close to theoretically predicted estimation $\alpha=-0.12$ for 3D isotropic Heisenberg magnetics. It should be noted that the critical exponent value α for the sample $x=0.1$ calculated in this work and a value α in work [2,3] are in good agreement with each other despite the fact that fusion conditions for these samples are different.

So, the magnetic phase transition in $\text{La}_{1-x}\text{Ag}_x\text{MnO}_3$ nearby Curie temperature is studied by means of the scaling theory of phase transitions.

- [1] M.B. Salamon, M. Jaime. *Rev. of Modern Phys.* **73** (2001) R5901.
- [2] A.G. Gamzatov, A.M. Aliev et al, *Physica B* **390** (2007) 155.
- [3] A.G. Gamzatov, S.B. Abdulvagidov et al, *Physics of the Solid State* **49** (2007) 1769.
- [4] I. K. Kamilov, A. K. Murtazaev, and Kh. K. Aliev, *Usp. Fiz. Nauk* **169** (1999) 773.
- [5] S.B. Abdulvagidov, G.M. Shakhshayev, I.K. Kamilov, *Prib. Tekh. Eksp.* **5** (1996) 134.

24PO-7-31

ELECTRIC FIELD DRIVEN MAGNETIC DOMAIN WALL MOTION IN FERRITE GARNET FILMS

Logginov A., Meshkov G., Nikolaev A., Nikolaeva E., Pyatakov A.

Physics Department, M.V. Lomonosov MSU, Leninskie gori, Moscow, 119992, Russia

Magnetoelectric effect attracts the attention of scientists and engineers in the context of increasing storage density in hard disc drivers (HDD) and MRAM. Currently most of experiments concerning magnetoelectric interaction imply either low temperatures or electric and magnetic subsystems to be spatially separated (composite materials). In this report the control of magnetization distribution is realized in single phase material at room temperature by usage electric field only, not implying electric current.

In our experiments we used the epitaxial ferrite garnet films grown on a $\text{Gd}_3\text{Ga}_5\text{O}_{12}$ substrate with various crystallographic orientations: (111), (110), (210). The electric field of high strength was produced by a tip electrode (curvature radius $\sim 10\mu\text{m}$), the magneto-optical technique in Faraday geometry was used to observe the micromagnetic structure (the experimental details are described elsewhere [1]). In the local area near the tip electrode we observed the domain wall displaced while the field was applied, and returned to equilibrium state after switching off the field (fig. 1). The effect took place in the films with low symmetry ((210) and (110) substrate orientation) and was not observed in high symmetry (111) films. The direction of domain wall displacement in electric field depends on the electric polarity and doesn't depend on the direction

of magnetization in the domains. These features evidence for magnetoelectric nature of the effect under study [1].

For dynamic measurements the high speed photography technique was used: the pulses of electric field (pulse width ~ 300 ns, the rise time ~ 20 ns) were followed by pulses of laser illumination (duration ~ 10 ns) to get an image of the structure. Varying the time delay between field and laser pulses enabled us to observe the consecutive positions of domain wall and thus investigate its dynamics.

In dynamic measurements with maximum field strength 400 kV/cm the domain wall velocity achieved 50 m/s that was equivalent to the effect of magnetic field ~ 50 Oe. The effect of electric field on micromagnetic structure was still discernible at voltages of 100 V and this value can be scaled down to several Volts by means of further miniaturization of the electrode to nanometric size. This effect opens new exciting possibilities in the field of micro- and nanomagnetism, providing the means for electric field control of magnetization distribution.

Support by RFBR #08-02-01068-a is acknowledged.

[1] A.S. Logginov, G.A. Meshkov, A.V. Nikolaev, A.P. Pyatakov, JETP Letters, **86** (2007) 115.

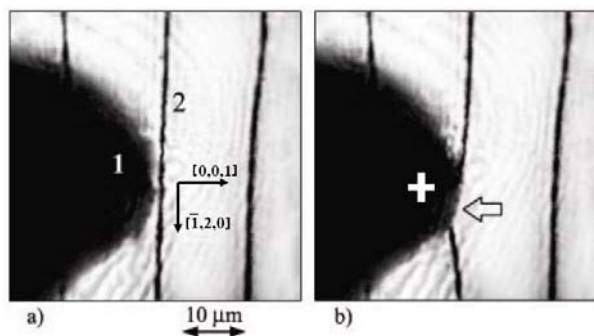


Fig.1 The effect of electric field in the vicinity of electrode (1) on magnetic domain wall (2) in the films of ferrite garnets: a) initial state b) at the voltage of $+1500$ V applied.

24PO-7-32

MAGNETIC PHASE TRANSITIONS INDUCED BY ELECTRIC FIELD IN MULTIFERROICS

Zvezdin A.K.¹, Zhdanov A.G.², Shust V.A.², Pyatakov A.P.^{1,2}

¹Institute of General Physics RAS, Vavilova St., 38, Moscow 119991, Russia

²Physics department, M.V. Lomonosov, Moscow State University, Moscow, 119992, Russia

Multiferroics, i.e. materials possessing simultaneously at least two types of ordering (magnetic, ferroelectric or ferroelastic), are considered to be promising materials for microelectronics due to the ability of controlling their *magnetic* state by the applied *electric* field. [1] Bismuth ferrite BiFeO₃ is the most widely studied and the most interesting multiferroic for practical applications due to its uniquely high temperatures of ferroelectric and antiferromagnetic (AFM) ordering ($T_C = 1083$ K; $T_N = 643$ K, respectively) (rev. [1] and reference therein).

In [2] the electric field control of AFM vector in BiFeO₃ is reported. Electric field causes the switching of electric polarization between main diagonals of the quasi-cubic cell. AFM vector switches only for the case of 109° polarization switching, i.e. the AFM vector tends to stay in plane of the film perpendicular to the direction of polarization. The switching electric field in experiment [2] is $\sim 2 \cdot 10^7$ V/m.

In [3] slabs of BiFeO₃ with (100) plane orientation are studied. These samples can be considered to be bulk and AFM vector forms cycloidal structure. Its period obtained both theoretically [1] and experimentally [3] is equal 64 nm. Experimental results reported in [3] show that in the case of application of electric field along (100) direction of quasi-cubic cell only

cycloid with wave-vector along the surface of the sample (0-11) survives. In the absence of electric field three cycloids with wave-vectors (0-11), (10-1), (-110) exist simultaneously.

The aim of the current work is to study theoretically electric field induced magnetic phase transitions both in thin films and bulk samples. Theoretical calculations are made using Landau-Ginzburg approach of minimization of free-energy functional.

Electric field induced spin-flop phase transition corresponding to direct coupling of electric and magnetic systems is shown to be expected at the values of electric field $\sim 2 \cdot 10^9$ V/m. Such values of electric field seem to be unrealistic due to finite conductance of the material.

Theoretical calculations based on free energy minimizing procedure show that critical fields for 109° and 71° are nearly the same and amount 52% from the value of critical field for 180° switching. This 109° and 71° switching is an example of electric field induced magnetic phase transition between various AFM domains in thin films.

(100)-oriented thick film of BiFeO₃, corresponding to experiment [3] is also considered in the current work. In the presence of electric field energetic profit for *in-plane* (0-11) cycloid is proportional to E^2 . Such results find themselves in a good agreement with experimental data and can be interpreted as phase transition between different states of cycloidal spin structure in bulk samples.

The work is supported by grant of RFBR #08-02-01068-a and "Dynasty" foundation.

[1] A. M. Kadomtseva, Yu.F. Popov, A.P. Pyatakov, G.P. Vorob'ev, A.K. Zvezdin, and D. Viehland, *Phase Transitions*, **79** (2006) 1019-1042.

[2] T. Zhao, A.Scholl, F. Zavaliche et al, *Nat. Mat.*, **5** (2006) 823.

[3] D. Lebeugle, D. Colson, A. Forget, M. Viret, A. M. Bataille, and A. Gukasov, *Cond. Mat.*, **0802** (2008) 2915.

24PO-7-33

MAGNETIC RESONANCE AND DIELECTRIC PROPERTIES OF IRON BORATES $R_3Fe_3(BO_3)_4$ AT SUBMILLIMETER WAVELENGTHS

*Kuzmenko A.M.¹, Mukhin A.A.¹, Ivanov V.Yu.¹, Prokhorov A.S.¹,
Kadomtseva A.M.², Bezmaternikh L.N.³*

¹A.M. Prokhorov General Physics Institute of the RAS, 119991 Moscow, Vavilov St., 38, Russia

²M.V. Lomonosov Moscow State University, 119992 Moscow, Russia

³Institute of Physics SB RAS, 660036 Krasnoyarsk, Russia

Rare-earth iron borates $R_3Fe_3(BO_3)_4$ attract a considerable interest in the last years due to their remarkable magnetic, magnetoelectric and other properties which are substantially determined by an exchange interaction of antiferromagnetic Fe and paramagnetic rare-earth (R) subsystems. In this work we have performed the first study of submillimeter magnetic resonance and dielectric properties of these materials in order to get additional data on their spin structure, magnetic interactions and structural phase transitions. Polarization measurements of transmission spectra of single crystalline $YFe_3(BO_3)_4$, $EuFe_3(BO_3)_4$, $TbFe_3(BO_3)_4$, $Gd_{0.5}Nd_{0.5}Fe_3(BO_3)_4$ plates (a-cut of a trigonal crystal) were carried out by a submillimeter quasioptical backward-wave-oscillator spectrometer at the frequency range $3-20$ cm^{-1} at the temperatures 3-300 K. The antiferromagnetic resonance modes of the Fe-subsystem were observed in easy plane $YFe_3(BO_3)_4$ and $EuFe_3(BO_3)_4$ as well as in easy axis $TbFe_3(BO_3)_4$ crystals. The corresponding resonance frequencies ν_{AF} increase with lowering temperature and amount to ~ 4.5 , 6 and 15 cm^{-1}

at 4 K, respectively, in Y, Eu and Tb borates. The increasing of the v_{AF} in $\text{EuFe}_3(\text{BO}_3)_4$ as compared with $\text{YFe}_3(\text{BO}_3)_4$ indicates on the additional anisotropic Eu^{3+} Van-Vleck contribution stabilizing the easy ab -plane $(\chi_{\perp c}^{VV} - \chi_c^{VV})H_{ex}^2$ which is in a good agreement with observed anisotropy of the Van-Vleck susceptibility $\chi_{\perp c}^{VV} > \chi_c^{VV}$ and allows to estimate the Eu-Fe exchange field $H_{ex} \approx 140$ kOe. A noticeable increase of the v_{AF} in the easy axis $\text{TbFe}_3(\text{BO}_3)_4$ revealed not only a change of the sign of the effective anisotropy constant but its significant negative value due to a strong contribution $-\chi_c^{\text{Tb}}H_{ex}^2$ of the Ising Tb^{3+} ions with easy c -axis. The extracted value of the Tb-Fe exchange field $H_{ex} \approx 35$ kOe corresponds nicely to static magnetic data for the spin-flop transition in $H \parallel c$ -axis. In easy plane $\text{Gd}_{0.5}\text{Nd}_{0.5}\text{Fe}_3(\text{BO}_3)_4$ two wide absorption lines were observed at $\sim 8 \text{ cm}^{-1}$ and $\sim 14\text{-}17 \text{ cm}^{-1}$ which were identified with rare-earth modes in Nd and Gd subsystems, respectively, determined by the R-Fe exchange splitting of the ground multiplets of the R ions. A strong anisotropy of the Nd-mode contribution to the permeability parallel and perpendicular trigonal c -axis was observed and explained by the anisotropy of the g -factor ($g_{\perp c} \gg g_c$) for the ground Nd^{3+} doublet. A noticeable increase of the Nd and Gd mode contribution (intensity) for ac field $\mathbf{h} \parallel ab$ -plan was revealed in the external magnetic field H in the ab -plane ($\mathbf{H} \perp \mathbf{h}$) and was explained by the field-induced spin reorientation in the ab -plane.

Temperature dependencies of the complex dielectric permittivity along and perpendicular to the c -axis were also obtained for the studied borates. Anomalies (jumps) in the permittivity behavior were revealed at $T_{str} \approx 55$ K, 200 K and 370 K, respectively, in the Eu Tb and Y iron borates which were associated with the structural phase transitions from high temperature R32 trigonal phase to the slightly less symmetry $P3_121$ one. A significant dielectric anisotropy ($\epsilon_c' > \epsilon_{\perp c}'$) were found in the R32 phase ($\epsilon_c' \approx 16\text{-}20$ and $\epsilon_{\perp c}' \approx 13$) which, however, was reduced in the low temperature phase due to the permittivity jumps along the c -axis $\Delta\epsilon_c \approx 1\text{-}3$. In $\text{Nd}_{0.5}\text{Gd}_{0.5}\text{Fe}_3(\text{BO}_3)_4$, where the transition is absent, the dependence of the $\epsilon_{c, \perp c}(T)$ remains weak, while its anisotropy becomes strong ($\epsilon_c/\epsilon_{\perp c} \sim 1.7$ at 4 K). The observed frequency dispersion of the permittivity is positive with increasing up to 5-10 % in the studied frequency range.

This work was supported by RFBR (07-02-00580).

24PO-7-34

OPTICAL SPECTROSCOPY OF MULTIFERROIC TbMn_2O_5

Chukalina E.P., Korotkov N.M.

Institute of Spectroscopy RAS, Fizicheskaya 5, Troitsk 142190, Moscow region, Russia

Multiferroic TbMn_2O_5 is one of the family of oxides with the general formula RMn_2O_5 (R =rare earth, Y or Bi). These compounds all ordered antiferromagnetically below 50 K and their properties dependence on the type of the R^{3+} ion. This is related to the complexity of the RMn_2O_5 crystal structure. RMn_2O_5 crystallize in the orthorhombic space group $Pbam (D_{2h}^9)$. The Mn^{4+}O_6 octahedra and Mn^{3+}O_5 square pyramids are connected by their corners and form the layers in the ab -plane. These layers are stacked along the c -axis and separated by planes of R^{3+} ion. The octahedra share their edges forming ribbons along the c -axis. The R^{3+} ion is surrounded by eight oxygen ions and occupies the site with C_s point group symmetry. RMn_2O_5 compounds with R =Eu, Gd, Tb Dy, Ho, and Y have attracted considerable attention during the last years as a materials with giant magnetoelectric effects. Despite the appearance and of a large number of studies, the microscopic nature of giant magnetoelectric effects is not understood until now. Nevertheless, spectroscopy of the R^{3+} ion in RMn_2O_5 and the crystal-field effects in RMn_2O_5 were not reported, as far as we know.

Recently, neutron diffraction measurements on TbMn_2O_5 have revealed a series of phase transitions (see, e.g., [1]): at $T_1=43$ K the appearance of incommensurate antiferromagnetic ordering, at $T_C=38$ K the onset of ferroelectricity, $T_2=33$ K the magnetic order transforms into a commensurate structure, at $T_3=24$ K the magnetic order transforms into an incommensurate structure again, and, finally, at $T_4=10$ K the phase transition coincides with a major increase of the terbium ordered moment.

To account for the crystal-field effects in TbMn_2O_5 , we have undertaken the optical spectroscopy study of the f-f transitions of the Tb^{3+} ion in TbMn_2O_5 . Optical absorption polarized spectra of single crystalline TbMn_2O_5 samples in the spectral region $1800\text{-}10000\text{ cm}^{-1}$ at a resolution 1 cm^{-1} were measured using a Fourier-transform spectrometer Bruker IFS 125HR and InSb liquid-nitrogen-cooled detector. The sample was in a closed-cycle optical cryostat with Cryomech ST403 pulse tube system at a variable (3.5-300 K) temperature stabilized within 0.01 K. From the analysis of the temperature-dependent polarized spectra the energies of the ${}^7\text{F}_{6,5,4,3,2,1,0}$ multiplets of the Tb^{3+} ion in TbMn_2O_5 were determined and some peculiarities connected with observed earlier phase transitions were found.

This work was supported by the Russian Academy of Sciences under the Programs for Basic Research. We are grateful to R.V. Pisarev and M.N. Popova for a helpful discussions. We thank K. Kohn for TbMn_2O_5 single crystals.

[1] C. Chapon, G.R. Blake, M.J. Gutmann, S. Park, N. Hur, P. G. Radaelli, and S-W. Cheong, *Phys. Rev. Lett.*, **93** (2004) 177402.

24PO-7-35

HYPERFINE INTERACTION ON ${}^{17}\text{O}$ ISOTOPE IN MANGANITES

Agzamova P., Nikiforov A.

Ural State University, Lenin av. 51, Yekaterinburg, Russia

The interest to manganites study is caused by interplay of spin, charge and orbital degrees of freedom in these strongly correlated electron materials.

At present the question of which picture of charge ordering is indeed true in $R_{1-x}A_x\text{MnO}_3$ systems at some concentrations x is a hotly discussed both theoretically and experimentally.

Two microscopic alternative models of the charge ordering mechanisms in manganites were considered in literature: site-centered model [1] and bond-centered model [2].

One of the local experimental methods for the investigation of the charge-ordering states in manganites is nuclear magnetic resonance (NMR) observed on isotope ${}^{17}\text{O}$ [3, 4]. This method is sensitive to the local magnetic environment of oxygen atom. Indeed, being placed between two Mn ions each ${}^{17}\text{O}$ nucleus probes the spin and orbital configuration of the corresponding Mn pair through the transferred spin density.

Theoretically, in order to investigate the charge-ordered states it is necessary to consider separately the contributions of trivalent and tetravalent manganese ions to the transferred spin density.

This report is devoted to the investigation of the magnetic hyperfine interactions formation mechanism on ${}^{17}\text{O}$ isotope in CaMnO_3 system (where Mn^{4+} ions are exist only), PrMnO_3 (where Mn^{3+} ions are exist only) and $\text{Pr}_{0.5}\text{Ca}_{0.5}\text{MnO}_3$ (where both Mn^{4+} and Mn^{3+} or $\text{Mn}^{3.5+}$ ions are exist).

Hyperfine interaction on ^{17}O isotope is determined by interplay of $2s$ - oxygen shells with $3d$ -manganese shell through transferred spin density (isotropic interaction) and through polarization of $2p$ - oxygen shells by $3d$ - manganese shell (anisotropic interaction). Moreover, we propose that the contributions from p_{σ} - and p_{π} - polarization are different.

It is well known that manganites have a perovskite structure. In the ideal perovskite structure there is only anisotropic contribution to magnetic hyperfine interaction associated with p_{π} - oxygen orbital polarization.

The real crystal structure of $\text{Pr}_{1-x}\text{Ca}_x\text{MnO}_3$ systems is distorted. In distorted crystal structure oxygen atoms are shifted so that the distortion angles (θ , φ) of Mn-O-Mn bonds appears, and the Mn-O distances (R) of various Mn-O pairs become different. In this case energy levels of Mn-O molecular orbital are shifted that leads to polarization s - and p_{σ} - oxygen shells. Consequently, additional contributions to hyperfine field on ^{17}O isotope appear.

In order to take into account the magnetic structure of manganites $\text{Pr}_{1-x}\text{Ca}_x\text{MnO}_3$ we write the magnetic hyperfine interaction Hamiltonian via the components of the magnetic structure vectors (F , A , C , G). Then, we can write down the expression for the magnetic hyperfine field:

$$^{17}\mathbf{H}_{MHF} = -\frac{1}{\gamma_n \hbar} \sum_k (A^F(R_k, \theta_k, \varphi_k) \mathbf{F} + A^C(R_k, \theta_k, \varphi_k) \mathbf{C} + A^A(R_k, \theta_k, \varphi_k) \mathbf{A} + A^G(R_k, \theta_k, \varphi_k) \mathbf{G}) \mathbf{I},$$

where $A(\theta_k, \varphi_k, R_k)$ are magnetic hyperfine interaction parameters. These parameters are tensors.

Thus, by means of this formula we calculate Mn^{3+} and Mn^{4+} contributions to hyperfine field in PrMnO_3 and CaMnO_3 correspondingly and both contributions in charge-ordered $\text{Pr}_{0.5}\text{Ca}_{0.5}\text{MnO}_3$. Obtained results agree with experiments.

This report is supported by “Dynasty” foundation.

[1] J. Goodenough, *Phys. Rev.* **100** (1955) 564.

[2] C. Zener, *Phys. Rev.* **82** (1951) 403.

[3] A. Yakubovskii, A. Trokiner, S. Verkhovskii, A. Gerashenko, and D. Khomskii, *Phys. Rev. B* **67** (2003) 064414.

[4] A. Trokiner, A. Yakubovskii, S. Verkhovskii, A. Gerashenko, and D. Khomskii, *Phys. Rev. B* **74** (2006) 092403.

24PO-7-36

ELECTRONIC AND MAGNETIC STATES OF IRON IONS IN $(\text{Bi}_{1-x}\text{Sr}_x)\text{FeO}_{3-y}$ MULTIFERROIC PEROVSKITES

Cherepanov V.M.¹, Pokatilov V.S.²

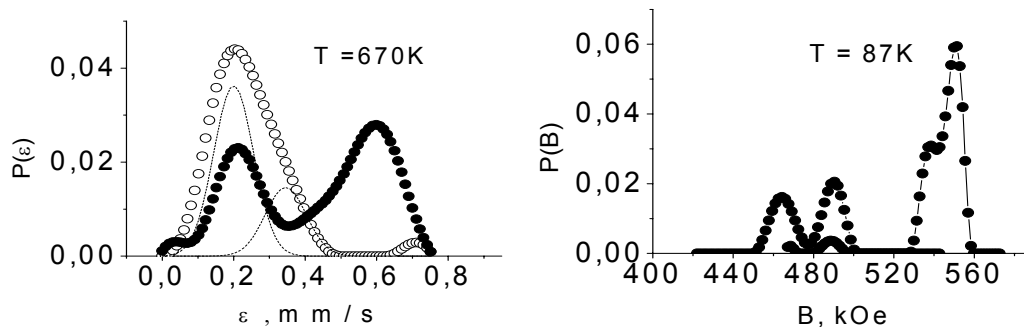
¹RRC “Kurchatov Institute”, 123182 Moscow, Kurchatov sq., 1, Russia

²Moscow State Institute of Radioengineering, Electronics and Automation (Technical University), 119454 Moscow, pr. Vernadskogo, 78, Russia

The magnetically ordered perovskites based on BiFeO_3 attract a great attention since these materials exhibit interesting multiferroic properties. BiFeO_3 is well known as a magnetoelectric compound with the magnetic and electric transition temperatures $T_N \approx 640\text{K}$ and $T_C \approx 1100\text{K}$, correspondingly. The compound has a rhombohedral distorted crystal structure and a spatially modulated cycloid antiferromagnetic Fe^{3+} spin structure. The modulation period $\lambda \approx 620\text{\AA}$ is incommensurate with the crystal lattice parameters. SrFeO_3 is a cubic perovskite with a screw antiferromagnetic structure ($T_N \approx 134\text{K}$) containing only Fe^{4+} .

In the present work the mixed perovskites $(\text{Bi}_{1-x}\text{Sr}_x)\text{FeO}_{3-y}$ ($x=0.07, 0.14, 0.25$ and 0.50) were studied by ^{57}Fe Moessbauer spectroscopy in the temperature range 80–700K. The samples were prepared by the well-known ceramic technology [1] with 10% ^{57}Fe isotope enrichment. X-ray diffraction measurements showed that the samples were single-phase and had a rhombohedral structure at $x=0.07$ and a cubic one at $x=0.14-0.50$. There was only one study of this mixed system at $x=0.20-0.67$ where only room temperature Moessbauer spectra were presented manifesting two different Fe^{3+} sites [1].

The Neel temperatures T_N of the $(\text{Bi}_{1-x}\text{Sr}_x)\text{FeO}_{3-y}$ studied were measured on the data of the Moessbauer effect temperature scans. As x increases $T_N(x)$ increases from 643K ($x=0$) to 669K ($x=0.25$) and then decreases to 640K ($x=0.5$). The same concentration behaviour was found for the hyperfine field values $B(x)$ at $T=87\text{K}$. A model interpretation of the spectra was performed using the SPECTR program and the distribution functions of a hyperfine field $P(B)$, an isomer shift $P(\delta)$ and a quadrupole shift $P(\varepsilon)$ were restored using the DISTRI program [2]. The experimental spectra are satisfactorily described by four Fe^{3+} states with the room temperature isomer shift values in the range 0.2-0.4mm/s, which correspond to the iron sites with 4, 5 and 6 oxygen ion neighbours. Therefore, the substitution of Sr^{2+} for Bi^{3+} leads to oxygen deficiency in the $(\text{Bi}_{1-x}\text{Sr}_x)\text{FeO}_{3-y}$. Fig.1 (left) shows the distribution of the quadrupole shifts $P(\varepsilon)$ at $T=670\text{K}$ and Fig.2 (right) – the distribution of the hyperfine magnetic field $P(B)$ at $T=87\text{K}$ for $x=0.50$ manifesting four Fe^{3+} sites.



This work was supported by the Russian Foundation for Basic Research, project No 06-2-16636a.

[1] J.Li, et al., *J. Alloys and Comp.*, **315** (2001) 259.

[2] V.S.Rusakov. Moessbauer spectroscopy of locally inhomogeneous systems. Almaty, 2000, p.430 (in Russian).

24PO-7-37

HYPERFINE PARAMETERS IN $\text{Bi}_{1-x}\text{La}_x\text{FeO}_3$ (0 - 1)

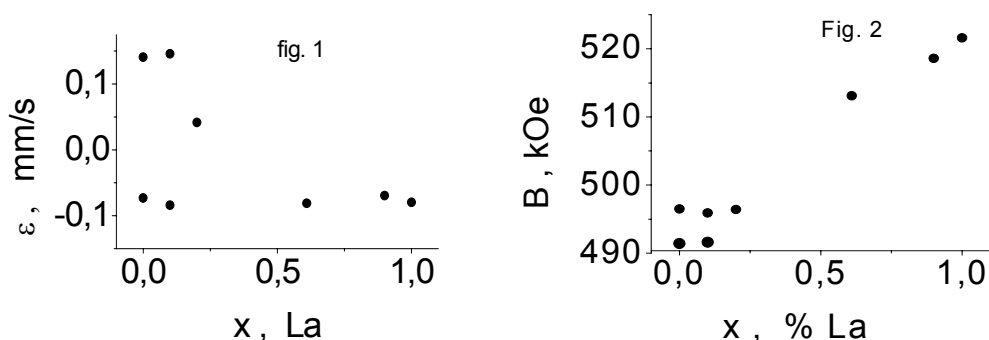
Pokatilov V.V., Pokatilov V.S.

Moscow State Institute of Radioengineering, Electronics and Automation (Technical University),
Vernadsky pr. 78, Moscow 117454, Russia.

The perovskites based on BiFeO_3 attract great research attention since these materials exhibit interesting ferroelectric-ferromagnetic properties. BiFeO_3 has space modulated magnetic structure (SMMS) of cycloidal type (the period of the modulation $\lambda = 620 \text{ \AA}$). SMMS is incommensurate with the crystal lattice parameters [1]. The ^{57}Fe -NMR data confirmed an

existence of the SMMS structure in BiFeO_3 [2]. The crystal and magnetic structures of $\text{Bi}_{1-x}\text{La}_x\text{FeO}_3$ ($x=0, 0.07$) were studied by neutron diffraction [3]. The ^{57}Fe -NMR study of $\text{Bi}_{1-x}\text{La}_x\text{FeO}_3$ ($x = 0, 0.1$ and 0.2) showed that the SMMS-type structure was present in $\text{Bi}_{0.9}\text{La}_{0.1}\text{FeO}_3$ as well [4]. In the case of SMMS-structure, the NMR spectrum has symmetric lineshape limited by two-edge singularities B_1 and B_2 . B_1 and B_2 are the hyperfine fields at ^{57}Fe nuclei for spin directions parallel $B_{//}$ and perpendicular B_{\perp} to the crystal c -axis [2]. There were no ^{57}Fe Mossbauer study of the perovskites based on BiFeO_3 , which considered an influence of the SMMS structure on the Mossbauer hyperfine interactions and the local valence and magnetic states of the iron ions in these compounds. In present work the hyperfine parameters (hyperfine field B , isomer δ and quadrupole shift ϵ) and the valence and magnetic states of the iron ions were studied by ^{57}Fe Mossbauer spectroscopy in $\text{Bi}_{1-x}\text{La}_x\text{FeO}_3$ ($x=0-1$) at room temperature.

On using the hyperfine fields B obtained in $\text{Bi}_{1-x}\text{La}_x\text{FeO}_3$ ($x=0, 0.1$) by NMR the isomer δ and quadrupole shift ϵ were measured from Mossbauer spectra. On fitting of these spectra by the program Univem, two six-lines components with fixed B_{\perp} and $B_{//}$ for $x=0$ and 0.1 the hyperfine parameters were obtained. These parameters are presented in fig.1 together with those for the whole concentration range $x=0-1$ at room temperature. The hyperfine field distribution $P(B)$ were determined by the program DISTRI for all the samples. Our data showed that there were the $P(B)$ (with two peaks at $B_{//}$ and B_{\perp}) and $P(\epsilon)$ distributions in $\text{Bi}_{1-x}\text{La}_x\text{FeO}_3$ ($x=0, 0.1$). It should note that $P(B)$, B_{\perp} , $B_{//}$ and the width of $P(B)$ are essentially in accord with the NMR data [4]. The iron ions are in single (octahedral) state with a valence of +3 in the concentration range of $x=0-1$. The local magnetic moments of the iron ions were determined as well.



This work is supported by the Russian Foundation for Basic Research, projects № 06-02-16636a

- [1] Sosnowska I et al., J. Phys. C, **15** (1982) 4835.
- [2] Zalesky A.V. et al., Europhys. Letter **50** (2000) 547.
- [3] Sosnowska I. et al., JMMM **160** (1996) 384.
- [4] Zalesky A.V. et al., FTT **45** (2003) 134.

24PO-7-38

THE TEMPERATURE DEPENDENCE OF EPR LINEWIDTH IN $\text{La}_{1-x}\text{Ba}_x\text{MnO}_3$

Yatsyk I.V.¹, Eremina R.M.¹, Mukovskii Ya.M.², Krug von Nidda H.-A.³, Loidl A.³

¹Kazan Physical Technical Institute, Kazan, Sibirskii trakt 10/7, Kazan, 420029, Russia

²Moscow State Institute of Steel and Alloys, Technological University, Leninskiĭ pr. 4, Moscow, 119049, Russia

³Experimentalphysik V, Universitat Augsburg, 86135 Augsburg, Germany

The colossal magnetoresistance is observed in $\text{La}_{1-x}\text{Me}_x\text{MnO}_3$ doped with the divalent ions $\text{Me}=\text{Sr}, \text{Ba}, \text{Ca}$, etc. The phase diagram of these compounds is very rich [1, 2] and can include regions with phase stratifications [3].

The $\text{La}_{1-x}\text{Ba}_x\text{MnO}_3$ single crystals were grown by the crucibleless zone melting method with radiative heating [4]. The measurements of the EPR spectra were performed using Bruker ER 086 CS and Varian E – 12 spectrometers equipped with temperature blows for measurements in the temperature range from 200 K to 600 K at frequency 9.4 GHz. The $\text{La}_{1-x}\text{Ba}_x\text{MnO}_3$ single crystals with $x=0.05, 0.1, 0.12, 0.15, 0.2$, and 0.3 are studied. The single crystals were preliminarily oriented using the x – ray diffraction. For EPR study, discs 3 mm in diameter and 0.5 mm in height are cut from the single crystals so that the disc plane is perpendicular to the [110] crystallographic axis for $x=0.1$ and 0.15 and to the [001] crystallographic axis for $x=0.12, 0.2$ and 0.3 . We measured the temperature dependencies of magnetic susceptibility in $\text{La}_{1-x}\text{Ba}_x\text{MnO}_3$ ($x=0.1; 0.12; 0.20$) on the SQUID Oxford design from 4.2K to 400K.

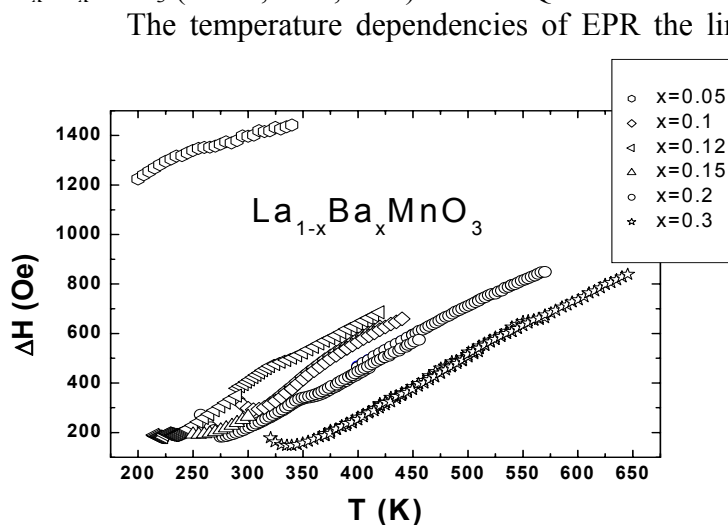


Fig. 1. The temperature dependence of the EPR linewidths of single crystals $\text{La}_{1-x}\text{Ba}_x\text{MnO}_3$

The temperature dependencies of EPR the linewidths in single crystals $\text{La}_{1-x}\text{Ba}_x\text{MnO}_3$ with $x=0.05, 0.1, 0.12, 0.15, 0.2$, and 0.3 in the temperature interval from 200 to 420 K (X-band) are shown in Fig. 1.

It has been found [5], that the temperature dependence of the EPR linewidths in the manganites was described by the simple formula: $\Delta H(T) = [\chi_0(T) / \chi(T)] \Delta H_{p.p.}(\infty)$, where $\Delta H(T)$ denotes the linewidth at temperature T , $\chi_0(T)$ is the free spin (Curie) susceptibility $\chi_0(T) \propto T^{-1}$, and $\chi(T)$ is the measured susceptibility. The symbol $\Delta H(\infty)$ is a temperature – independent constant. Since $\chi_0(T) \rightarrow \chi(T)$ as $T \rightarrow \infty$, $\Delta H(\infty)$ is identified with the high-temperature

limit of the linewidth. Using this expression does not give possibility to describe of the temperature dependencies of EPR linewidth in single crystal $\text{La}_{0.9}\text{Ba}_{0.1}\text{MnO}_3$.

This work was supported by the Russian Foundation for Basic Research, project no. 06 – 02 – 17401

- [1] J. Zhang, H. Tanaka, T. Kanki, J.-H. Choi, and T. Kawai, *Phys. Rev. B* **64** (2001), 184404
 [2] H.L. Ju, Y.S. Nam, J. E. Lee, and H.S. Shin, *J. Mag. Mater.* **219** (2000), 1
 [3] E. L. Nagaev, *Usp. Fiz. Nauk* **166** (1996), 833 [*Phys. Usp.* **39** (1996), 781]

[4] D. Shulyatev, N. Kozlovskaya, R. Privezentsev, et al., *J. Cryst. Growth* **291** (2006), 262

[5] D. L. Huber, G. Alejandro, A. Caneiro, et al., *Phys. Rev. B* **60** (1999), 12155

24PO-7-39

MAGNETIC AND TRANSPORT PROPERTIES OF $\text{La}_{0.7}\text{Ca}_{0.3}\text{MnO}_3$ SINGLE CRYSTAL IN THE FERROMAGNETIC STATE

Zainullina R.I.¹, Bannikova N.S.¹, Elokhina L.V.¹, Bebenin N.G.¹,
Mukovskii Ya.M.², Shulyatev D.A.²

¹Institute of Metal Physics, UD RAS, Kovalevskaya St. 18, Ekaterinburg 620041, Russia

²Moscow State Steel & Alloys Institute, Leninskii prospekt, 4, Moscow 119049, Russia

The analysis of the literature data indicates that the mechanism of the colossal magnetoresistance (CMR) in La-Ca crystals may differ from that in other lanthanum manganites but the available data on kinetic properties of $\text{La}_{1-x}\text{Ca}_x\text{MnO}_3$ crystals remain insufficient to make a certain conclusion. To fill the gap in part, we have performed the study of magnetic properties and electronic transport in $\text{La}_{0.7}\text{Ca}_{0.3}\text{MnO}_3$ single crystal. The results of measurements of the field and temperature dependence of the magnetization, resistivity, thermopower, and Hall effect are reported.

The single crystal was grown by the floating-zone method. Since the La-Ca rods produced by the floating-zone technique are always inhomogeneous, the element distribution along the rod was measured with an electron-probe microanalyzer and then the region was chosen where the Ca content is equal to 0.30 ± 0.01 . The magnetization measurements were performed using a vibrating sample magnetometer, the resistivity ρ was measured by a four-probe technique. The Hall effect measurements were carried out in two opposite directions of the magnetic field and the electric current.

Below 220 K, the manganite under study is in the ferromagnetic state, the magnetization depending on temperature weakly. The resistivity increases with increasing T and is as high as $1.87 \cdot 10^{-3} \Omega \text{ cm}$ at $T=220 \text{ K}$. The normal Hall coefficient R_o is positive, therefore holes dominate conductivity. The negative sign of the thermopower below 94 K indicates, however, that there are charge carriers of electron type that play a role of minority carriers. The value of the thermopower is small, which points to metallic type of electronic transport. The Hall mobility μ_H defined as $\mu_H = R_o / \rho(H=0)$ is small in value. Taking into consideration that the estimates made for a CMR manganite suggest minimum metallic conductivity σ_m to be of order $10^3 (\Omega \text{ cm})^{-1}$ we infer that in the low temperature region, the single crystal behaves as a "bad" metal, which is at the threshold of localization at $T = 220 \text{ K}$.

The spontaneous Hall coefficient R_s is proportional to ρ , which indicates that R_s is dominated by skew scattering.

Support by grants RFBR 06-02-16085 and NSh-3257.2008.2 is acknowledged.

24PO-7-40

KINETIC AND THERMODYNAMIC PROPERTIES OF CHARGE - DISPROPORTIONATED COMPOUND $\text{La}_{1/3}\text{Sr}_{2/3}\text{FeO}_3$

Vasilchikova T.M.¹, Troyanchuk I.O.², Lin J.-Y.³, Vasiliev A.N.¹

¹Low Temperature and Superconductivity Department, Moscow State University, Moscow 119991, Russia

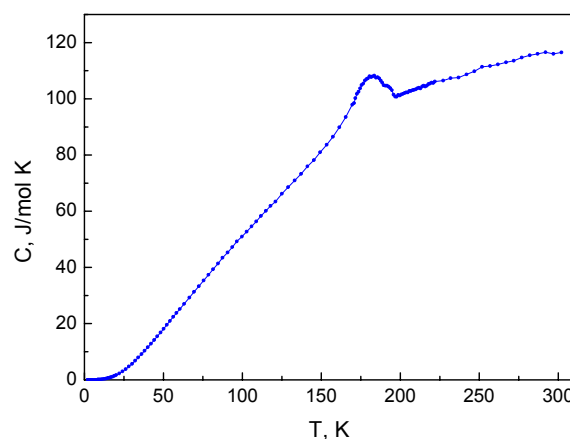
²Institute of Solid State Physics and Semiconductors, NAS, Minsk 220072, Belarus

³Institute of Physics, National Chiao Tung University, Hsinchu 30050, Taiwan

Below $T_C \sim 200$ K, the metaloxide compound $\text{La}_{1/3}\text{Sr}_{2/3}\text{FeO}_3$ exhibits a unique phenomenon of charge disproportionation [1], nominally denoted by $\text{Fe}^{4+} + \text{Fe}^{4+} \rightarrow \text{Fe}^{3+} + \text{Fe}^{5+}$ reaction. This effect is motivated by the system's intention to escape from Jahn – Teller instability in Fe^{4+}O_6 octahedra. At T_C , the compound experiences simultaneous metal – insulator transition and canted antiferromagnetic spin ordering with weak ferromagnetism [2].

In present work, basic kinetic and thermodynamic properties of $\text{La}_{1/3}\text{Sr}_{2/3}\text{FeO}_3$ were studied in a wide temperature range 2 – 350 K. At $T < T_C$, the temperature dependence of resistance shows an activation behavior. The temperature dependence of magnetic susceptibility measured in both zero – field – cooled and field – cooled regimes presents a peak – like anomaly at T_C and small divergence at low temperatures indicating probably a formation of a spin glass state. The field dependence of magnetization is of hysteretic type in agreement with canting of antiferromagnetic sublattices. The temperature dependence of specific heat, shown in the Figure, displays a broad peak below T_C and release of significant magnetic entropy at low temperatures.

Preliminary measurements of the x-ray absorption spectra on Fe ions indicate that the charge disproportionation is not complete resulting in reaction $\text{Fe}^{4+} + \text{Fe}^{4+} \rightarrow \text{Fe}^{+4-\delta} + \text{Fe}^{+4+\delta}$ with relatively small δ .



[1] Takano, M., and Y. Takeda, 1983, Bull. Inst. Chem. Res., Kyoto Univ. **61**, 406.

[2] Battle, P. D., T. C. Gibb, and P. Lightfoot, 1990, J. Solid State Chem. **84**, 271.

24PO-7-41

**INFLUENCE OF OXYGEN DEFICIENCY ON MAGNETIC,
MAGNETORESISTIVE AND MAGNETOELASTIC PROPERTIES
OF $\text{La}_{1-x}\text{Sr}_x\text{MnO}_{3-y}$ MANGANITES**

*Zashchirinskii D.M.¹, Koroleva L.I.¹, Khapaeva T.M.¹,
Gurskii L.I.², Kalanda N.A.², Trukhan B.M.²*

¹M.V. Lomonosov Moscow State University, Leninskie gory, 119992 Moscow, Russia

²Institute of Solids and Semiconductor Physics, P. Brovka str. 17, 220072 Minsk, Belarus

The influence of oxygen deficiency on magnetization, paramagnetic susceptibility, electrical resistivity, magnetoresistance and magnetostriction of $\text{La}_{1-x}\text{Sr}_x\text{MnO}_{3-y}$ ($x = 0, 0.2, 0.4$; $y = 0, 0.05, 0.13, 0.2$) is studied. All samples were single-phase on X-ray data. Magnetization on formula unit (f.u.) M of compounds with $x = 0.2$ and 0.4 , $y = 0.05$ and 0.13 is understated as compared with compounds with $y = 0$. The Curie temperature (T_C) reduction, anomalous disposition of T_C and the paramagnetic Curie point θ ($T_C > \theta$) and difference of FC and ZFC magnetizations are also observed. These peculiarities point out the presence in these samples of ferromagnetic (F) – antiferromagnetic (AF) magnetic two-phase state (MTPS). In compounds with $x = 0.2$ and 0.4 , $y = 0.2$ the $M(T)$ -dependence obeys to Langevin function with the magnetic moment of superparamagnetic clusters $m = 40 \mu_B$ for the former and $130 \mu_B$ for the latter. The $M(T)$ -dependence in $H = 16$ kOe of LaMnO_{3-y} with $y = 0.13$ and 0.2 obeys to Langevin function with the magnetic moment of $m = 77 \mu_B$ and $m = 86 \mu_B$ correspondingly except small T -region around 132 K in which maximum, typical for AF, is observed. By this means in these compounds MTPS take place that consists of the F clusters in AF host. The F clusters occupy ~ 0.1 of the sample volume only. There are single-charged acceptors (Sr^{2+}) and doubly-charged donors (oxygen vacancies) in $\text{La}_{1-x}\text{Sr}_x\text{MnO}_{3-y}$ system. At $T \sim 0$ K in compound with $x = 0.4$ and $y = 0.13$ the all electrons left the donor centers and acceptor centers in amounts of 0.14 on f.u. remain unchanged; in compound with $x = 0.4$ and $y = 0.2$ the all donors and acceptors are ionized. Therefore the magnetic and electrical properties of latter compound and LaMnO_3 are similar. So its $M(T)$ -dependence obeys to Langevin function with $m = 130 \mu_B$ and electrical resistivity is more than two orders of magnitude greater than for compound with $y = 0$. The electrical resistivity of compound with $y = 0.13$ is more than in compound with $y = 0$ by a factor of 30. Magnetoresistance (MC) and volume magnetostriction (VM) compounds with $x = 0.4$ and $y = 0.13, 0.2$ are negative and their modules in $y = 0.13$ reach of maxima in T_C -region. The values of MC and VM in $H = 8$ kOe do not exceed 1.4 % and 6×10^{-6} correspondingly. It is known that colossal MC and giant VM in manganites are explained by presence in them of F regions of ferron type. Therefore the absence of colossal MC and giant VM in $y = 0.13$ testifies to absence of ferrons near Sr^{2+} -ions which are remained non-compensative. There appears to be the presence of broken connections Mn-O-Mn in sites with oxygen absence suppresses of the ferron formation. Electron type of conductance is realized in compounds $\text{La}_{0.8}\text{Sr}_{0.2}\text{MnO}_{3-y}$ with $y = 0.13$ and 0.2 in a result of compensation. Compounds with $y = 0.13$ and 0.2 have 0.03 and 0.1 non-ionized vacancies on f.u. at $T \sim 0$ K correspondingly. The magnetic moment on f.u. of compound with $y = 0.2$ would can to be larger than of compound with $y = 0.13$ if the electrons of donors have strong $s-d$ exchange with Mn ions, surrounding donors, and form F droplets of ferron type. But a pattern, observed experimentally, is opposing to the speculating one: $M = 2.05 \mu_B/\text{f.u.}$ for $y = 0.13$ and $0.93 \mu_B/\text{f.u.}$ for $y = 0.2$. Apparently in $\text{La}_{1-x}\text{Sr}_x\text{MnO}_{3-y}$ the $s-d$ exchange of electrons is weaker than of holes and spins of two electrons of the oxygen vacancy are ordered in antiparallel $\{(1S)^2$ state in helium-like model but the non- $(1S)(2S)$ one in which 2S-electron forms the ferron. The broken connections Mn-O-Mn in sites of lattice with the ionized oxygen vacancies break F exchange interactions in these sites decreasing the mean magnetic moment on

f.u. Thus in compounds with $y = 0.05, 0.13$ the oxygen vacancies, as ionized as non-ionized, decrease the mean magnetic moment on f.u., exciting a break-up of long F order in compound with $y = 0.2$ on superparamagnetic clusters. F –AF MTPS, presented in sample, is not associated with $s-d$ exchange since in compounds with the oxygen deficit MR and VM are small.

24PO-7-42

INVESTIGATION OF LaMnO_3 IN ULTRA-HIGH MAGNETIC FIELDS

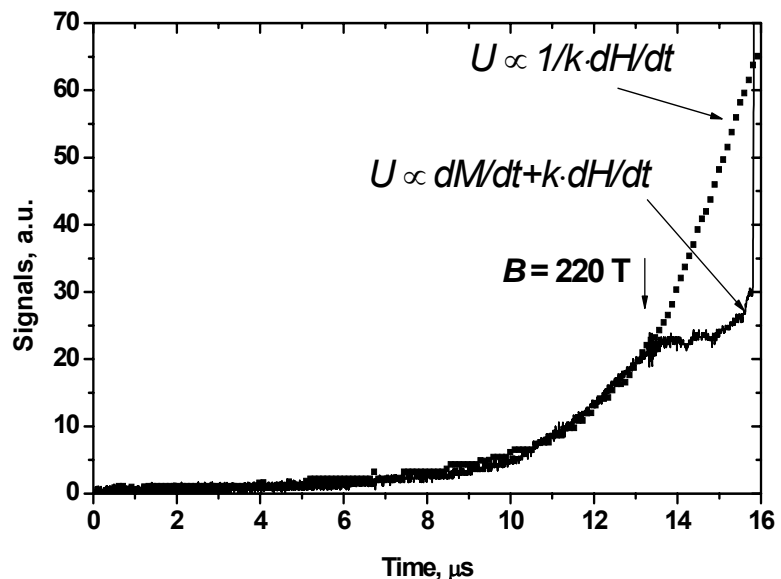
Korshunov A.S., Kudasov Yu.B., Platonov V.V., Selemir V.D.

RFNC-VNIIEF, 37, Mira str., Sarov, 607188, Russia

SarFTI, 6, Dukhova, Sarov, 607188, Russia

Magneto-induced phase transitions in a single crystal LaMnO_3 under ultrahigh magnetic fields at 5 K have been investigated. Magnetocumulative generator MC-1 was used for generation of high magnetic fields [1]. The differential magnetic susceptibility was measured by inductive compensation coils [2]. The signals from probes of magnetic field and compensation coils are presented in the figure. The solid line shows the signal from the compensation coils and the dotted line is the background signal due to the decompensation. The coefficient k is the value of coils decompensation of coils in the magnetization probe.

In our experiments the sensitivity of the field probe is very dependent on the field derivative. That is why, the spin-flop transition in fields 18 T [3] was hardly resolved. The sharp spin-flip transition was observed at about 70 T for the orientation of the magnetic field along the c -axis ($H \parallel b$). The transition became smooth for $H \parallel b$ [3]. In our experiments this transition manifests itself as a bending of the differential magnetic susceptibility. The saturation field increases with rise of temperature and reaches the full saturation in fields nothing less than 100 T. With further increasing of the magnetic fields an anomaly in differential magnetic susceptibility was well observed at about 220 T. This anomaly indicates the presence of magneto-induced transition to a metallic state of LaMnO_3 with conductivity about $10^5 \text{ Ohm}^{-1} \text{ m}^{-1}$.



The electronic structure of LaMnO_3 under ultrahigh magnetic fields was calculated by means of LDA+U technique. Our results support the possibility of the transition of the LaMnO_3 to the metallic state due to suppression of the AFM order and Jahn-Teller distortion.

Support by ICTC 3501, and RFFI is acknowledged.

- [1] A.I.Pavlovskii et.al. *Megagauss Physics and techniques*, edited by P.Turchi, Plenum Press, New York 1980.
- [2] I.S.Dubenko et.al. *JETP Lett*, **64**, 3, 1996, 202.
- [3] A. Kirste et.al., *Proceeding Megagauss X*, Berlin, 2005, 295.

24PO-7-43

INFLUENCE OF RARE-EARTH Nd AND La SUBSTITUENTS ON MAGNETIC PROPERTIES OF BiFeO_3 MULTIFERROIC

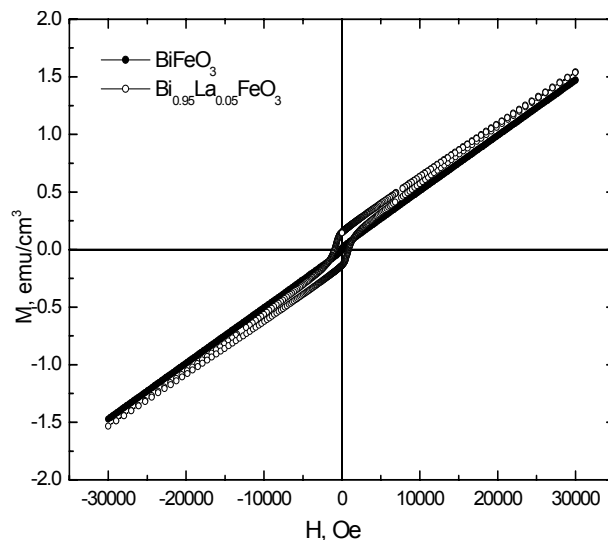
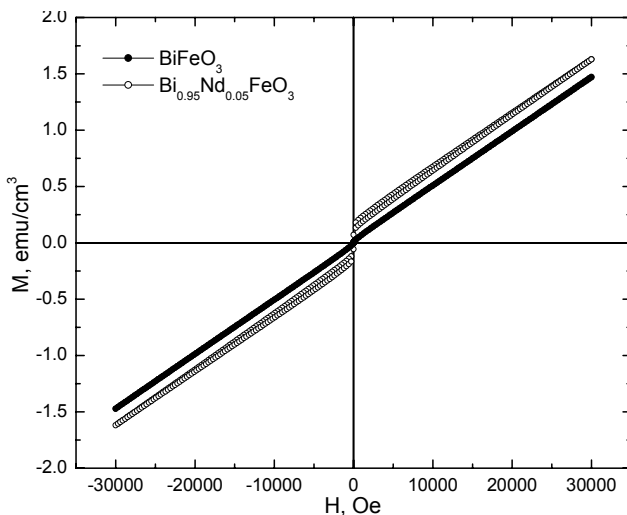
Amirov A.A.¹, Badtalov A.B.¹, Reznichenko L.A.², Razumovskaya O.N.², Verbenko I.A.²

¹Institute of Physics, Dagestan Scientific Center of RAS, 94 Yaragskogo Street, Makhachkala, 367003, Russia

²Institute of Physics, South Federal University, 194 Stachki Street, Rostov-na-Donu, 344090, Russia

Compounds on base of BiFeO_3 are very perspective multiferroic materials due to high temperatures of magnetic and ferroelectric phase transitions, bad conductivity and simple chemical structure [1-2]. Symmetry of BiFeO_3 allows existence of the magnetoelectric (ME) effect, but space-modulated spin structure (SMSS) suppress it. Substitution Bi by rare-earth ions, preparing BiFeO_3 thin films, synthesis solid solution with PbTiO_3 increases ME effect and magnetic properties.

In present paper we report the results of magnetic investigation of BiFeO_3 , $\text{Bi}_{0.95}\text{La}_{0.05}\text{FeO}_3$ and $\text{Bi}_{0.95}\text{Nd}_{0.05}\text{FeO}_3$ ceramics. The ac-susceptibility vs. temperature measurements is carried out on a modulating magnetometer with amplitude 0.5 Oe. The magnetization vs. temperature is studied using a vibrating sample magnetometer at room ($T=300\text{K}$) and liquid nitrogen ($T=77\text{K}$) temperatures. The ac-susceptibility vs. temperature curve of BiFeO_3 has sharp peak at 646 K which corresponds to the antiferromagnetic phase transition and it is confirmed by literature data [3-4]. A rare-earth substitution change temperature of antiferromagnetic order. Magnetization curves for all present samples at the room temperature are shown in figure. The magnetization of pure BiFeO_3 is small and grows linearly with magnetic field. Such type of magnetization curve is typical for antiferromagnetic materials. La and Nd substitution leads to increase of BiFeO_3 magnetic properties. They have a hysteresis typical for ferromagnetic materials and area of the loop larger than for pure BiFeO_3 . Similar behavior observes in the case of $T=77\text{K}$. The magnetic properties change occur not only on account of magnetic moment and



ionic radiuses (lanthanum atom has no its magnetic moment), but also because of La and Nd ions magnetic moments anisotropy. Rare-earth substituents can change the anisotropy constant, so that the presence of SMSS would be energy-wise disadvantageously [5].

- [1] J. Wang et al., Science, **299** (2003) 1719
 [2] A.K. Zvezdin and A.P. Pyatakov, Sov. Phys. Usp., **47** (2004). 8
 [3] I. Sosnowska and A. K. Zvezdin, J. Magn. Magn. Mater, **140–44** (1995) 167
 [4] P. Fischer and M. Polomska, J. Phys. C: Sol. Stat., **13** (1980) 1931
 [5] A. M. Kadomtseva, A. K. Zvezdin et. al., Sov. Phys. JETP, **79** (2004) 705

24PO-7-44

THE TEMPERATURE DEPENDENCE OF SUBLATTICE MAGNETIZATION IN MANGANITES AND RELATED COMPOUNDS

Gontchar L.E., Mozhegorov A.A., Nikiforov A.E., Leskova Y.V., Firsov I.A.
Urals State University, 51 Lenin Av., Ekaterinburg, Russia

The temperature dependence of sublattice magnetization is the important description stage of various experiments like nuclear magnetic resonance measurements (NMR), antiferromagnetic and ferromagnetic resonance measurements (ARMR and FMR, correspondingly), magnetic susceptibility study. In this connection, the manganites investigation is of great interest.

In the current work, two models of temperature dependence are presented. The comparison of these models is useful in order to choose one of the in the certain temperature range.

The spin-Hamiltonian, used in the current work, is as follows [1]:

$$\hat{H} = \sum_{i>j} J_{ij} (\mathbf{S}_i \cdot \mathbf{S}_j) + \sum_i \hat{H}_i^{an},$$

where \hat{H}_i^{an} is single-ion anisotropy of i-th magnetic ion.

The first calculation is made within the framework of mean field approximation:

$$\langle S_i \rangle = S \cdot B_S \left(\frac{S \cdot \langle H_{eff}^{(i)} \rangle}{k_B T} \right),$$

where $H_{eff}^{(i)}$ is the effective magnetic field, acting on each sublattice. This model gives an overestimation of critical temperatures [2]

The second calculation is carried out within the framework of spin-wave approximation:

$$\langle S_i^z \rangle = S - \frac{1}{NS} \sum_k \mathbf{n}_k = S - \frac{1}{NS} \int d\omega \frac{D(\omega)}{\exp\left(\frac{\hbar\omega}{k_B T}\right) - 1},$$

where $D(\omega)$ is the density of spin-wave states, and ω is the spin-wave frequency.

The densities of spin-wave states are obtained for different manganites compounds $\text{La}_{1-x}\text{Ca}_x\text{MnO}_3$ ($x=0, 0.5, 0.667$) and titanate LaTiO_3 . The strong effect of single-ion anisotropy (in manganites) and anisotropic exchange (in titanate) upon these dependences is shown.

The strong affection of anisotropic magnetic interactions appears as well in temperature dependences. The different models of insulating manganites description give the different temperature dependences.

Because of peculiarities of mentioned models, they are applied in different temperature range: the mean-field model is more useful near Neel temperature, and the spin-wave model is used at low temperatures.

The NMR spectra in the both models are calculated.

This investigation is partially supported by CRDF REC-005 (BRHE program).

[1] Gontchar L. E., Nikiforov A. E., Popov S. E., JMMM, 223, p.175 (2001)

[2] Gontchar L. E., Nikiforov A. E., Phys. Rev. B, 66, p.014437 (2002)

24PO-7-45

HYPERFINE INTERACTIONS IN IMPURITY CHARGE-ORDERING MANGANITES

Leskova J.V., Nikiforov A.E., Gonchar L.E., Popov S.E., Mozhegorov A.A.
Ural State University, Ekaterinburg, Russia

^{139}La NMR a sensitive tool in respect to particular spin and orbital configuration of the neighboring Mn. The local magnetic field at ^{139}La ion originates from the Fermi-contact interaction with the transferred s- spin density of electrons and dipole-dipole interaction with the transferred p-spin density. We consider La NMR in charge ordering compound $\text{La}_{0.5}\text{Ca}_{0.5}\text{MnO}_3$ and $\text{La}_{0.33}\text{Ca}_{0.67}\text{MnO}_3$.

The crystal and charge structures of mentioned compounds are taken from experimental works [1]. The crystal and charge structures are forming the orbital structures of the both compound. Using the model of the orbitally-dependent exchange and single-ion anisotropy interactions [2], we can predict the magnetic structure. The magnetic structure of a half-doped manganite is of a CE-type with the moments mainly directed along c-axis of the orthorhombic reference frame. The magnetic structure of the manganite with a doping rate 2/3 is frustrated. The magnetic moments could be joined together into trimers with strong ferromagnetic interaction, containing three manganese ions ($\text{Mn}^{4+}-\text{Mn}^{3+}-\text{Mn}^{4+}$) and coupled with the weak antiferromagnetic interaction. The trimers are mainly directed along x-and y-axes of pseudoperovskite reference frame.

The magnetic structure was used for calculation of NMR spectra. The gradient of the electrical field on the ions of the rare-earth metals was calculated in the assumptions of the point charges. The calculation of local magnetic field has shown that hyperfine field, induced by s-wave spin polarization, is rather small. We investigate a spectrum of a nuclear magnetic resonance for polycrystalline $\text{La}_{0.5}\text{Ca}_{0.5}\text{MnO}_3$ at various temperatures. It contains two peaks with close frequencies. However the shape of lines for different peak is various. The temperature dependence of La NMR spectra in polycrystalline $\text{La}_{0.33}\text{Ca}_{0.67}\text{MnO}_3$ has been studied. It consists of two lines with frequencies near 11 MHz and 23 MHz. In the experiment [3], the La resonance line at zero field is centered at 24.4 MHz.

The increase of temperature is accompanied by decrease of NMR frequencies in both compounds. This effect is connected with a reduction of a sublattice magnetization of manganese subsystems. Thus, we have shown that La NMR provides a direct probe of the Mn spin and orbital correlations in the charge-ordered phase of manganites.

The work is partially supported by CRDF REC-005, "Dynasty" foundation.

- [1] P.G. Radaelli, D.E. Cox, M. Marezio, S-W. Cheong, *Phys. Rev. B*, **55**, 3015(1997); P.G. Radaelli, D.E. Cox, L. Capogna, S.-W. Cheong, *Phys. Rev. B*, **59** (1999) 14440
 [2] L.E. Gontchar, A.E. Nikiforov, *JMMM*, **223** (2001) 175
 [3] Cz. Capusta, P.C. Riedi, M. Sikora, M.R. Ibarra, *Phys.Rev.B* **84** (2000) 4216

24PO-7-46

GIANT MAGNETOSTRICTION OF DILUTED NICKEL FERRITE $\text{NiGa}_{0.8}\text{Al}_{0.8}\text{Fe}_{0.4}\text{O}_4$ WITH FRUSTRATED MAGNETIC STRUCTURE

Antoshina L.G., Korshak A.B.

Faculty of Physics, M.V. Lomonosov Moscow State University,
 Lenin Hills, 1-2, GSP-1, Moscow, Russia, 119991

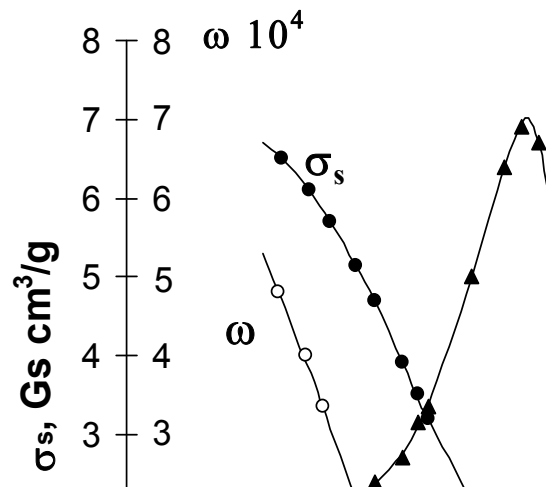
The anomalous behaviour of spontaneous magnetization $\sigma_s(T)$, coercive force $H_c(T)$ and magnetostrictions $\lambda_{\parallel}(T)$ and $\lambda_{\perp}(T)$ is revealed for sample $\text{NiGa}_{0.8}\text{Al}_{0.8}\text{Fe}_{0.4}\text{O}_4$ with frustrated magnetic structure. It is shown, that the sharp reduction of the σ_s value takes place at temperatures (T_t), lower than the temperature of the sharp decreasing of H_c (T_C). It is established, that at $T = 295$ K the sample has a tetragonal-distorted spinel structure with $c/a = 1.016$, with $a = 8.20$ Å.

By method of thermodynamic coefficients for the diluted ferrite $\text{NiGa}_{0.8}\text{Al}_{0.8}\text{Fe}_{0.4}\text{O}_4$ it is established, that a long-range magnetic order occurs at the temperatures lower than temperature $T_t = (172 \pm 15)$ K in the sample under consideration. The Curie temperature $T_C = (250 \pm 10)$ K of this sample was defined as the temperature at which coercive force H_c value vanished.

It is established, that two phase magnetic transitions take place for the diluted ferrite at temperatures T_C and T_t . Reduction of temperature to T_C results in a magnetic phase transition from paramagnetic state to a phase, which consists of spontaneously magnetized regions formed by short-range magnetic order (clusters). A second transition from spin glass phase to the state with frustrated magnetic structure takes place at lower temperature T_t .

Anomalous behaviour of coercive force $H_c(T)$ at the temperature $T > T_t$ is established. It is shown that in the spin glass state H_c value increases at $T > T_t$, reaches the maximum value and then decreases to zero when the temperature $T > T_C$.

It was found, that for the ferrite $\text{NiGa}_{0.8}\text{Al}_{0.8}\text{Fe}_{0.4}\text{O}_4$ the anomalous behaviour of magnetostriction takes place which is different from that for usual ferrimagnetic structures, where the long-range magnetic order penetrates all volume of a sample. For example, both parallel λ_{\parallel} , and perpendicular λ_{\perp} magnetostrictions in the whole investigated interval of temperatures from 78 K up to 275 K in all fields have only positive sign and are practically equal in size. Volume magnetostriction $\omega = \lambda_{\parallel} + 2\lambda_{\perp}$ increases with reduction of temperature and reaches very large (that is to say "giant") sizes. So at the temperature 78 K volume magnetostriction $\omega \sim 5 \cdot 10^{-4}$.



It is known, that the unit cell of a spinel lattice contains eight molecules. It is established, that for the investigated ferrite in a spin glass phase (at the $T_i < T < T_C$) clusters are formed by short-range magnetic order, that is exchange interaction within the scale of one or two coordination spheres. Therefore, it is possible to assume, that at the $T_i < T < T_C$ the size of clusters is about 3 nm.

24PO-7-47

TRANSPORT AND DIELECTRIC PROPERTIES AND HEAT CAPACITY OF THE $\text{Pb}_3\text{Mn}_7\text{O}_{15}$ MIXED-VALENT MANGANESE OXIDE

Eremin E.¹, Volkov N.^{1,2}, Sablina K.¹, Flerov I.^{1,2}, and Kartashev A.¹

¹Kirensky Institute of Physics SB RAS, Krasnoyarsk, 660036 Russia

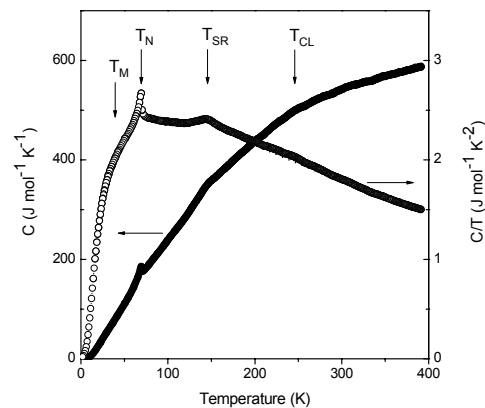
²Siberian Federal University, Krasnoyarsk, 660041 Russia

Perovskite-like manganites, layered manganites of a Ruddlesden-Popper series, and other manganese oxides in which Mn ions are in the 3+/4+ mixed-valence state have been a popular subject of research due to their fascinating properties, such as colossal magnetoresistance (CMR), competing magnetic order, magnetic phase separation, and charge and orbital ordering.

Previously, we reported some magnetic properties of the $\text{Pb}_3\text{Mn}_7\text{O}_{15}$ crystal with approximately equal concentrations of Mn^{3+} and Mn^{4+} ions [1]. The observed anomalies in magnetization behavior suggest that in the temperature region under study (2–900 K) several magnetic phases can be distinguished.

Here we present the results of specific heat measurements made on a $\text{Pb}_3\text{Mn}_7\text{O}_{15}$ single crystal. In Fig. 1 the results of the heat capacity measurements are shown. In the temperature dependence of the heat capacity near 70 K one can clearly see a lambda-shape anomaly associated with the onset of long-range antiferromagnetic ordering. The temperature at which this peak takes place is consistent with the critical temperature T_N determined from the magnetization data. Also, there is a broad hump in the temperature dependence of the heat capacity around 160 K, specifically in the same temperature region where the clear maximum in ac and dc magnetizations versus temperature curves is observed. This suggests that the observed feature in the heat capacity behavior is magnetic in origin and apparently related to the onset of the cooperative effect in the magnetic subsystem of the crystal. At the same time, thorough analysis of the measurement results shows that the specific feature in magnetization behavior does not correspond to the occurrence of the long-range magnetic order. Most likely, in the temperature region near 160 K only short-range antiferromagnetic ordering starts forming.

At higher temperatures, the experimental C versus T dependence is not a smooth function as it can be expected in the case of the only lattice contribution to the total heat capacity. One can clearly see the presence of the hump near $T_{CL} \approx 250$ K in the C/T versus T curve. In addition, at these temperatures we have found anomalies in behavior of both dc-conductivity and the dielectric properties. The complex dielectric constant has been investigated



in the temperature range 77 – 273 K at frequencies from 0.1 to 100 kHz. The temperature dependences of ϵ' and ϵ'' reveal anomalies at 130 – 190 K, which shift towards higher temperatures with an increase in frequency. Such a behavior is typical of the charge relaxation processes.

[1] N.V. Volkov, K.A. Sablina, O.A. Bayukov, E.V. Eremin, G.A. Petrakovskii, D.A. Velikanov, A.D. Balaev, A.F. Bovina, P. Boeni and E. Clementyev, J. Phys.: Condens. Matter **20** (2008), 055217.

24PO-7-48

MAGNETIC PROPERTIES OF THE $\text{La}_{0.50}\text{Ba}_{0.50}\text{MnO}_3$ NANOMANGANITES

Trukhanov A.V.^{1*}, *Stepin S.G.*¹, *Trukhanov S.V.*², *Botez C.E.*³, *Szymczak H.*⁴

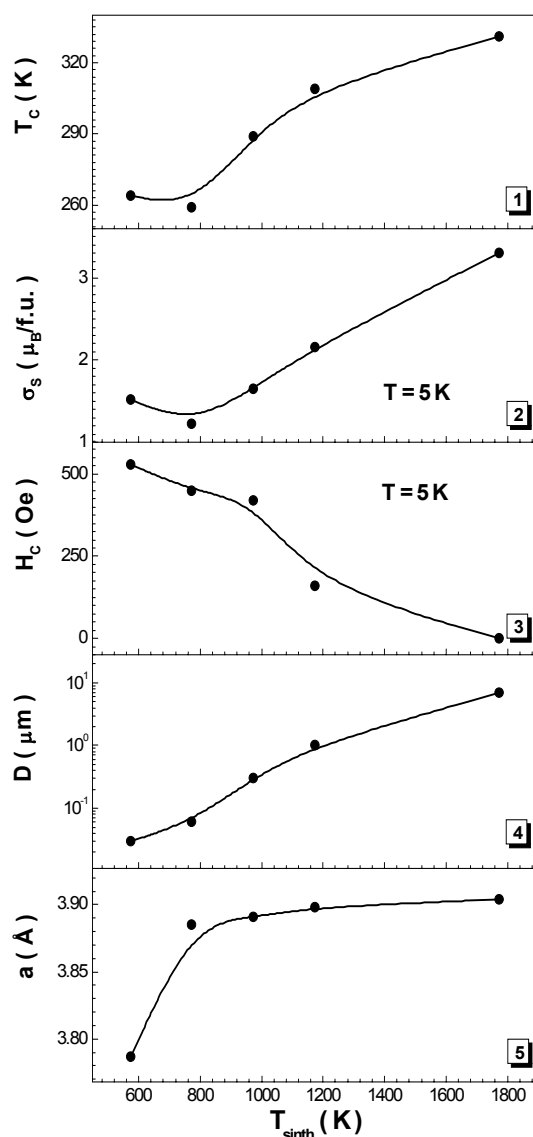
¹Chemistry Department, Vitebsk State University, 210036 Vitebsk, Belarus

²Scientific-Practical Materials Research Centre NAS of Belarus, 220072 Minsk, Belarus

³University of Texas at El Paso El Paso, TX 79968-0515, USA

⁴Institute of Physics of PAS, 02-668 Warsaw, Poland

*e-mail: truhanov86@mail.ru



From the other manganites Ba-doped ones are interesting, that they have Curie point close to room temperature. So, the $\text{La}_{0.50}\text{Ba}_{0.50}\text{MnO}_3$ has $T_C \sim 270$ K [1]. In vicinity this temperature the peak of magnetoresistance is observed. Recently, it has been revealed that the Curie point of manganites depends on the size of crystallite in nanoscale region [2]. $\text{La}_{0.50}\text{Ba}_{0.50}\text{MnO}_3$ nanosample has been synthesised using modified sol-gel method. The $\text{C}_3\text{H}_8\text{O}_3$ glycerin has been used as organic matrix. Parent nanosample has been annealed in air at $T_{\text{synth}} = 500$ °C, 700 °C, 900 °C and 1500 °C.

Fig. Curie temperature (1), spontaneous magnetic moment (2), coercivity (3), average crystallite size (4) and unit cell parameter (5) vs. annealed temperature for the obtained $\text{La}_{0.50}\text{Ba}_{0.50}\text{MnO}_3$ samples.

Average size of crystallite increases with annealed temperature from $D \sim 30$ nm to ~ 7 μm (Fig.1). The stoichiometry was correct. All the samples had cubic perovskite-like unit cell with increasing parameter from a ~ 3.787 Å to ~ 3.904 Å as average size of crystallite increases. Pressure effect is maximum for the sample with $D \sim 30$ nm. Temperature Curie and spontaneous magnetic moment have non-monotone behavior and increases from $T_C \sim 264$ K to ~ 331 K and from $\sigma_S \sim 1.52$ $\mu_B/\text{f.u.}$ to ~ 3.31 $\mu_B/\text{f.u.}$ (Fig.), respectively. Anomalous magnetic properties of the $\text{La}_{0.50}\text{Ba}_{0.50}\text{MnO}_3$ is explained by frustration of Mn^{3+} -O-

Mn⁴⁺ exchange interactions [3] and compression of the crystal lattice as a result of nanograin formation [4].

[1] F. Millange, V. Caignaert, B. Domenges, B. Raveau, E. Suard, Chem. Mater. V. 10, P. 1974-1983 (1998).

[2] K.S. Shankar, S. Kar, G.N. Subbanna, A.K. Raychaudhuri, Solid State Commun. V. 129, P. 479-483 (2004).

[3] S.V. Trukhanov, A.V. Trukhanov, C.E. Botez, A.H. Adair, H. Szymczak, R. Szymczak, J. Phys.: Condens. Matter. V. 19, P. 266214-18 (2007).

[4] N. Das, P. Mondal, D. Bhattacharya, Phys. Rev. B V. 74, P. 014410-6 (2006).

24PO-7-49

SUPPRESSION OF CHARGE-ORDERED STATE IN La_{0.50}Ca_{0.50}MnO₃ NANOMANGANITE

Trukhanov S.V.^{1,}, Trukhanov A.V.², Botez C.³, Szymczak H.⁴*

¹Scientific-Practical Materials Research Centre NAS of Belarus, 220072 Minsk, Belarus

²Chemistry Department, Vitebsk State University, 210036 Vitebsk, Belarus

³University of Texas at El Paso El Paso, TX 79968-0515, USA

⁴Institute of Physics of PAS, 02-668 Warsaw, Poland

*e-mail: truhanov@ifttp.bas-net.by

Two ceramic La_{0.50}Ca_{0.50}MnO₃ manganites have been synthesized using “two-step” reduction-reoxidation method [1]. One of samples La_{0.50}Ca_{0.50}MnO₃-I has micrograins with average size ~ 5.964 μm (fig.1). Other sample La_{0.50}Ca_{0.50}MnO₃-II has nanograins with average size ~ 138 nm (fig.1). The microsample demonstrates two magnetic phase transitions with decrease of temperature. At ~ 260 K the paramagnet-ferromagnet transition occurs (fig.2).

At ~ 170 K the charge-ordered antiferromagnetic state is formed (fig.2). At ~ 170 K the spontaneous magnetic moment is ~ 2.66 μ_B/f.u. which indicates ~ 76 % parallel ordering of all the spins of the Mn³⁺ (μ_{total} = 4 μ_B) and Mn⁴⁺ (μ_{total} = 3 μ_B) cations. At ~ 5 K the spontaneous magnetic moment is only ~ 0.05 μ_B/f.u. The nanosample demonstrates only one magnetic phase transition with decrease of temperature. At ~ 240 K the paramagnet-ferromagnet transition occurs. The charge-ordered antiferromagnetic state is not formed (fig.2). At ~ 5 K the spontaneous magnetic moment for nanosample is ~ 1.31 μ_B/f.u. which indicates ~ 37 % parallel ordering of all the spins of the Mn³⁺ (μ_{total} = 4 μ_B) and Mn⁴⁺ (μ_{total} = 3 μ_B) cations. The size of grains influences the properties of the crystal structure. A decrease in grain size to nanometer scale reduces the unit cell volume, which can be explained by an increase in the surface tension as compared to elastic forces in the bulk material [2]. The compression of the unit cell produces the increase of the ferromagnetic interactions intensity and suppresses the charge ordering [3].

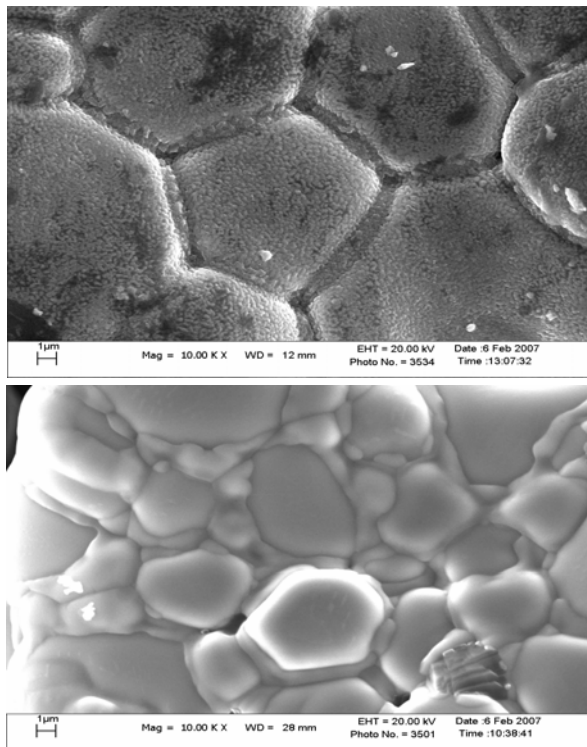


Fig.1. Grain topography for the micrograin (bottom) and nanograin (top) samples.

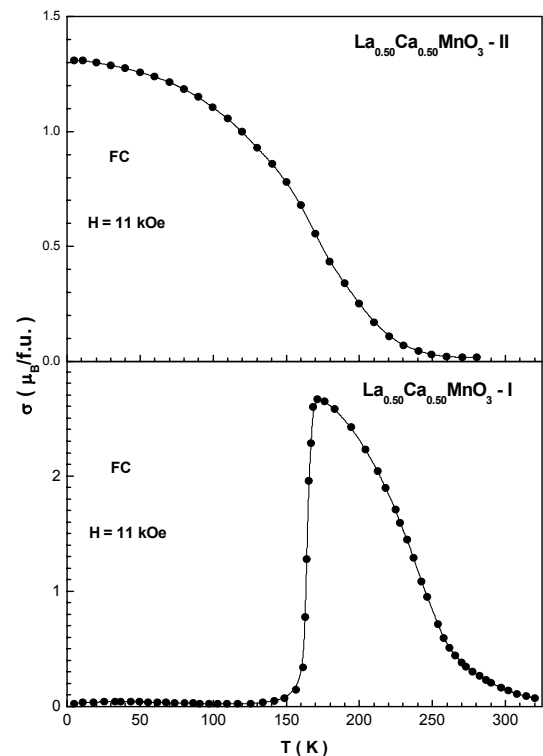


Fig.2. Temperature magnetization in field of 11 kOe for the micrograin (bottom) and nanograin (top) samples.

- [1] S.V. Trukhanov, JETP V. 101, № 3, P. 513-520 (2005).
 [2] K.S. Shankar, S. Kar et al., Solid State Commun. V. 129, P. 479-483 (2004).
 [3] S.S. Rao, S. Tripathi, D. Pandey et al., Phys. Rev. B V. 74, P. 144416-5 (2006).

24PO-7-50

INHOMOGENEOUS STATES IN SYSTEMS WITH ORBITAL ORDERING

Sboychakov A.O.¹, Khomskii D.I.², Kugel K.I.¹, Rakhmanov A.L.¹

¹Institute for Theoretical and Applied Electrodynamics, Russian Academy of Sciences, Izhorskaya Str. 13, 125412 Moscow, Russia

²II. Physikalisches Institut, Universitaet zu Koeln, Zuelpicher Str. 77, 50937 Koeln, Germany

The existence of inhomogeneous states is a characteristic feature of magnetic oxides, especially those containing Jahn-Teller (JT) ions. In the crystal lattice, the JT ions usually give rise to the orbital ordering (OO), which is typical of insulating compounds. The doping can destroy the OO since

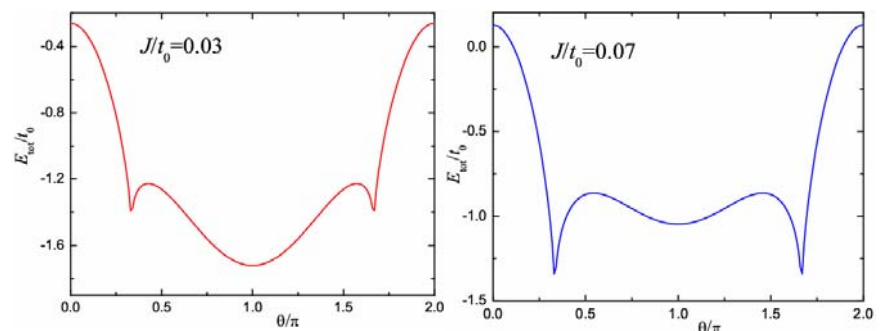


Fig. 1. The energy of ferro-OO droplet vs angle θ at $J < J_{cr}$ (left) and $J > J_{cr}$ (right)

the itinerant charge carriers favor the formation of a metallic state without OO. However, at low doping levels, we have a competition between the charge localization and metallicity, which can lead to the so-called electronic phase separation (PS). This phenomenon is often observed in, e.g., doped manganites and is usually related to some specific type of the magnetic ordering. In the usual treatment of PS, the OO is not taken into account.

We study the two-dimensional (2D) lattice with one e_g electron per site, forming a regular antiferro-OO array with alternating $|\theta_0\rangle$ and $|\theta_0\rangle$ orbitals. Here $|\theta_0\rangle$ is a linear combination of the basis orbitals $|x^2-y^2\rangle$ and $|2z^2-x^2-y^2\rangle$: $|\theta_0\rangle = \sin(\theta_0/2)|x^2-y^2\rangle + \cos(\theta_0/2)|2z^2-x^2-y^2\rangle$. Owing to the doping, some lattice sites become empty (we have a hole at each such site). Even without any magnetic ordering, the hole becomes self-trapped, forming a ferro-OO region with occupied $|\theta\rangle$ orbitals around it due to the gain in kinetic energy. The size of such an orbital polaron is about several lattice constants. The effective Hamiltonian for a hole is

$$H^\theta = -2t_0 [Q_x^2(\theta) + Q_y^2(\theta)] + t_0 \left[Q_x^2(\theta) \frac{\partial^2}{\partial x^2} + Q_y^2(\theta) \frac{\partial^2}{\partial y^2} \right], \quad Q_{x,y}(\theta) = \left| \sin\left(\frac{\theta}{2} \mp \frac{\pi}{6}\right) \right| \quad (1)$$

where t_0 is a hopping integral.

Using Hamiltonian (1), we solve the Schrodinger equation for a hole within a finite region, which we choose in the shape of an ellipse with semiaxes $Q_x \rho_0$ and $Q_y \rho_0$. The formation of ferro-OO region results in the energy cost of antiferro-orbital ordering, which can be written as $E_{OO} = \pi Q_x Q_y \rho_0^2 J(\theta)$, where the function $J(\theta)$ depends on the structure of antiferro-OO matrix. Minimization of the total energy with respect to ρ_0 gives us the energy of ferro-OO droplet:

$$E_{tot} = -t_0(2 + \cos\theta) + j_{0,1} \left| \frac{1}{2} - \cos\theta \right|^{1/2} \sqrt{\frac{2\pi J(\theta)}{t_0}}, \quad (j_{0,1} \cong 2.405 \text{ is } 1^{\text{st}} \text{ zero of Bessel function } J_0)$$

To analyze the shape of ferro-OO droplets, we assume that $J(\theta) = \text{const}$ and minimize E_{tot} with respect to θ . The result depends on the value of parameter J/t_0 . At small J/t_0 , we have $\theta = \pi$, that is, occupied $|x^2-y^2\rangle$ orbitals (see Fig. 1). In this case, droplets have the shape of a circle. With the growth of J/t_0 above some critical value ($J_{cr}/t_0 \cong 0.05$), the system exhibits a jump-like transition to the state with $\theta = \pi/3$ or $5\pi/3$. In this case, we have the chains of $|x^2-z^2\rangle$ or $|y^2-z^2\rangle$ orbitals and hence nearly one-dimensional droplets are stretched along x or y axes.

The work was supported by the EU project CoMePhS (NNP4-CT-2005-517039), International Science and Technology Center (grant no. G1335), and RFBR (project no. 05-02-17600).

24PO-7-51

SYNTHESIS AND MAGNETIC PROPERTIES OF MANGANITE $\text{Pr}_{1-x}\text{Ca}_x\text{MnO}_3$ FILMS

*Patrin G.S.^{1,2}, Polyakova K.P.², Patrusheva T.N.¹, Velikanov D.A.², Volkov N.V.², Balaev D.A.²,
Patrin K.G.², Klabukov A.A.²*

¹Siberian Federal University, Krasnoyarsk, 660041, Russia

²L.V.Kirensky Institute of Physics, SB RAS, 660036, Krasnoyarsk, Russia

The properties of manganites with perovskite structure considerably depend on conditions of reception and the subsequent heat treatment. To an even greater degree it is possible to expect influence of preparation conditions on physical properties of a thin-film dilute manganites [1,2].

In it work the results of research of magnetic properties of $\text{Pr}_{1-x}\text{Ca}_x\text{MnO}_3$ ($x=0,25; 0.3;$

0.35) polycrystalline films, prepared by an extraction-pyrolytic method, are presented.

The essence of the extraction-pyrolysis method consists in component extraction from water solutions, mixing them in a required proportion, deposition of the solution on a substrate and the subsequent pyrolysis. As a substrate the plates of a fused quartz were chosen. The films were applied on substrates by centrifuging at 300 rpm. The solution with concentration of 2 % has been used [3]. After pyrolysis at temperature 770 K within 5-10 minutes the film was spent annealing on air within 2 hours at temperatures 1000 K (film N1) and 1070 K (film N2).

The X-ray diffraction showed that the films obtained in the stage of pyrolysis (prior to the annealing) exhibited an X-ray amorphous structure. The subsequent annealing in air led to the formation of a polycrystalline single-phase perovskite. Diffraction patterns of films of different thickness and of annealing temperatures were made.

Research of magnetic properties was carried in a magnetic field up to 30 kOe in the temperature range 4.2-350 K. In particular investigations of manganite $\text{Pr}_{0.7}\text{Ca}_{0.3}\text{MnO}_3$ films noted the high fields of saturation for both films: 15 kOe (a film 1) and 12 kOe (a film 2). Essential difference is observed in temperature dependences of saturation magnetization of films, received at various annealing temperatures. Character of temperature dependence of film 1 is closer to ferromagnetic behaviour, unlike corresponding dependence of film 2. Value of saturation magnetization of film 1 is below that of a film 2. Curie temperature of a film 1 is equal ~ 60 K. The curve of temperature dependence of the saturation magnetization of film 2 most likely is superposition of corresponding curves with Curie temperatures 60 K and 120 K. Investigation of temperature dependence of the magnetic moment in fields up to 500 Oe accepted presence thermomagnetic effects and properties similar to those spin glasses.

[1] T.Li, B.Wang, H.Dai, et al., *J.Appl.Phys.*, **98** (2005) 123505.

[2] S.L. Cheng, J.L.Lin, *J.Appl.Phys.*, **98** (2005) 114318.

[3]. G.S. Patrin, K.P. Polyakova, T.N. Patrusheva, D.A. Velikano, *Pis'ma v ZTF*, **33** (2007) 30 (in Russia).

24PO-7-52

OBSERVATION OF DOMAIN WALL RESISTANCE IN $\text{La}_{0.7}\text{Ca}_{0.3}\text{MnO}_3$ FILMS

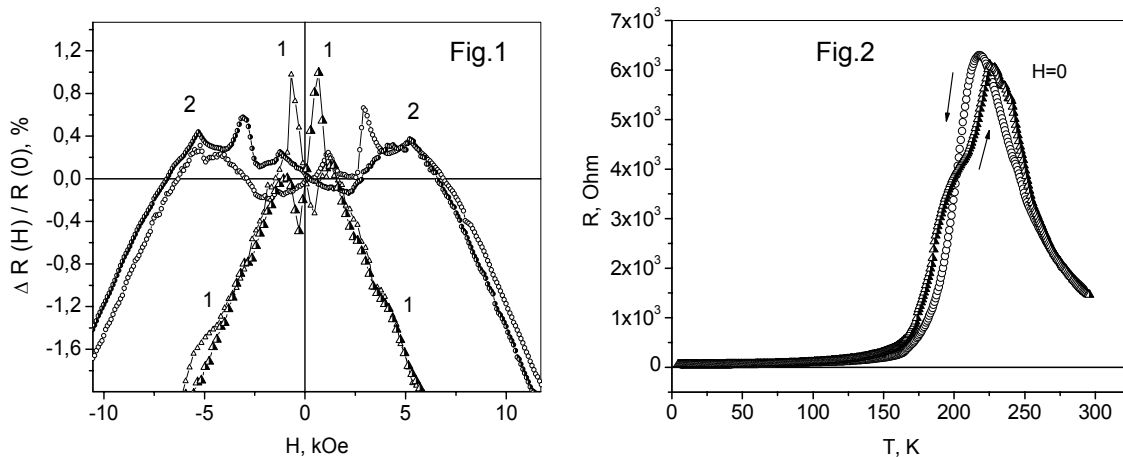
Dyakonov K.V., Popov V.V.¹, Dyakonov V.P., Gierlowski P., Lewandowski S.J., Szymczak H.²

¹Ioffe Physico-Technical Institute of the Russian Academy of Sciences 194021, Russia

²Institute of Physics, Al. Lotnikow 32/46, 02-668 Warszawa, Poland

Magnetic and transport properties of thin colossal magnetoresistance ferromagnetic manganite films depends of its thickness, interfaces strains and grain structure [1]. Domain wall scattering result in an additional contribution to the electrical resistance. The study of magnetoresistance in low-field region can provide information about domain wall dynamics and peculiarity of structural discontinuities in thin films as source of domain-wall pinning. We report the study of the resistivity and magnetoresistance in epitaxial films of the $\text{La}_{0.67}\text{Ca}_{0.33}\text{MnO}_3$ type deposited onto Y-cut of single-crystalline LiNbO_3 (LNO) substrates by pulsed-laser deposition in an on-axis geometry. The KrF excimer laser was used to ablate the stoichiometric ceramic target. The substrate temperature was 730°C. The deposition was carried out at oxygen pressure of 300 mTorr, and was followed by cooling down to the room temperature in an oxygen atmosphere with the rate of about 20°C min. The film thickness, as measured by optical interferometry, was between 100 and 200 nm. According to the x-ray diffraction analysis, the films are single phase, epitaxial, and (211) oriented with the pseudocubic lattice parameter $a = 0.3853$ nm.

Fig.1 shows results for magnetoresistance $\Delta R(H)/R(0)=(R(H)-R(0))/R(0)$ at 77K. Measurements were performed by means of for-point dc method. Curves 1 corresponds to transversal orientation of magnetic field and film plane, and curves 2 – to field in the plane of the film. All curves shows the hysteresis loops indicating interplay between coercive magnetization and electrical resistance. There are three jumps occurs in the resistance, presents by curve 2, after reversing the magnetic field. This jumps reflects the presence of a number of pinning centers for domain walls. The domain walls bend between individual pinning centers with increase magnetic field, and switching when the field reaches a critical value.



Apparently, a lattice deformation due to substrate mismatch, which leads to a biaxial distortion of the film, may be probable origin of such strong pinning centers. This confirms with hysteresis type of resistivity temperature dependence near Curie temperature $T_c \sim 203\text{K}$. (T_c obtained from maximum slope of cooling-off curve $R(T)$ (Fig.2)).

This work was supported by the grant “Leading scientific school”- HIII-5596.2006.2

[1] A-M.Haghir-Gonset, J-P.Renard. J.Phys. D: Appl.Phys.,36, (2003), R127-150.

24PO-7-53

MAGNETIC AND DIELECTRIC PROPERTIES, PHASE TRANSITIONS AND MAGNETOTRANSPORT IN SEMICONDUCTOR MANGANITE-MULTIFERROIC $\text{Eu}_{0.8}\text{Ce}_{0.2}\text{Mn}_2\text{O}_5$

Golovenchits E.I., Sanina V.A., Zaleskii V.G., Scheglov M.

A.F. Ioffe Physical Technical Institute, 26 Polytechnicheskaya, 194021, Russia

New doped single crystals of semiconductor manganite – multiferroic $\text{Eu}_{0.80}\text{Ce}_{0.20}\text{Mn}_2\text{O}_5$ have been grown and investigated. The initial dielectric multiferroic EuMn_2O_5 have close temperatures of magnetic and ferroelectric ordering (40 and 30 K, respectively). Investigations of the doped crystals have shown, that they have coupled magnetic and polar states in a wide temperature range, from 180 K to the temperatures above the room one. They have been found to possess a giant dielectric permeability ($\epsilon' \sim 10^3 - 10^4$) and ferromagnetic orientation of manganese ion spins.

The anisotropy of magnetic, dielectric, magnetotransport properties, and ac – conductivity in the crystal have been studied in the frequency range $10 - 10^6$ Hz, at temperature interval 5 – 350 K, in magnetic field up to 7 T. Analysis of dielectric properties and ac-conductivity has led to the conclusion that at $T \geq 180$ K phase separation with dynamic periodic distribution of quasi-2D layers of manganese ions of variable valency, i.e. charge ferroelectricity, occurs in this crystal. At low temperatures ($T < 100$ K) the crystal have a small phase volume occupied by as-grown quasi-2D layers with doping impurities and charge carriers, and the basic crystal volume occupied by a dielectric phase without charge carriers. A thermal activation of the hopping conductivity gives rise to a phase transition into the state of charge ferroelectricity at $T \approx 180$ K caused by self-organization of charge carriers in the crystal matrix with ferroelectric frustrations.

X – ray study at the room temperature shows the superstructure existence also. Magnetic properties, magnetoresistance, and phase transitions in a magnetic field of $\text{Eu}_{0.80}\text{Ce}_{0.20}\text{Mn}_2\text{O}_5$ have also been studied. These investigations have confirmed the ideas on the formation of the state with a giant dielectric permeability inferred from analysis of dielectric properties. A rather high magnetic field has been found to lead to the shift of the phase transition from 180 K to higher temperature (225 K).

The study is supported by RFBI and by Presidium of Academy Sciences of Russia.

24PO-7-54

MAGNETIC AND DIELECTRIC PROPERTIES, PHASE TRANSITIONS AND MAGNETOTRANSPORT IN SEMICONDUCTOR MANGANITE-MULTIFERROIC $\text{Eu}_{0.8}\text{Ce}_{0.2}\text{Mn}_2\text{O}_5$

Golovenchits E.I., Sanina V.A., Zalesskii V.G., Scheglov M.

A.F. Ioffe Physical Technical Institute, 26 Polytechnicheskaya, 194021, Russia

New doped single crystals of semiconductor manganite – multiferroic $\text{Eu}_{0.80}\text{Ce}_{0.20}\text{Mn}_2\text{O}_5$ have been grown and investigated. The initial dielectric multiferroic EuMn_2O_5 have close temperatures of magnetic and ferroelectric ordering (40 and 30 K, respectively). Investigations of the doped crystals have shown, that they have coupled magnetic and polar states in a wide temperature range, from 180 K to the temperatures above the room one. They have been found to possess a giant dielectric permeability ($\epsilon' \sim 10^3 - 10^4$) and ferromagnetic orientation of manganese ion spins.

The anisotropy of magnetic, dielectric, magnetotransport properties, and ac – conductivity in the crystal have been studied in the frequency range $10 - 10^6$ Hz, at temperature interval 5 – 350 K, in magnetic field up to 7 T. Analysis of dielectric properties and ac-conductivity has led to the conclusion that at $T \geq 180$ K phase separation with dynamic periodic distribution of quasi-2D layers of manganese ions of variable valency, i.e. charge ferroelectricity, occurs in this crystal. At low temperatures ($T < 100$ K) the crystal have a small phase volume occupied by as-grown quasi-2D layers with doping impurities and charge carriers, and the basic crystal volume occupied by a dielectric phase without charge carriers. A thermal activation of the hopping conductivity gives rise to a phase transition into the state of charge ferroelectricity at $T \approx 180$ K caused by self-organization of charge carriers in the crystal matrix with ferroelectric frustrations.

X – ray study at the room temperature shows the superstructure existence also. Magnetic properties, magnetoresistance, and phase transitions in a magnetic field of $\text{Eu}_{0.80}\text{Ce}_{0.20}\text{Mn}_2\text{O}_5$

have also been studied. These investigations have confirmed the ideas on the formation of the state with a giant dielectric permeability inferred from analysis of dielectric properties. A rather high magnetic field has been found to lead to the shift of the phase transition from 180 K to higher temperature (225 K).

The study is supported by RFBI and by Presidium of Academy Sciences of Russia.

24PO-7-55

MAGNETIC PHASE TRANSITION AND COLOSSAL MAGNETORESISTANCE IN $\text{La}_{0.7}\text{Ca}_{0.3}\text{MnO}_3$ SINGLE CRYSTAL

Bebenin N.G., Zainullina R.I., Bannikova N.S., Ustinov V.V.

Institute of Metal Physics, UD RAS, Kovalevskaya St. 18, Ekaterinburg 620041, Russia

The lanthanum manganites $\text{La}_{1-x}\text{D}_x\text{MnO}_3$, $D = \text{Ca}, \text{Sr}, \text{Ba}$, are ferromagnets in the range of $0.1 < x < 0.5$. Near Curie temperature T_C , they exhibit colossal magnetoresistance (CMR). In La-Sr and La-Ba crystals the ferromagnetic-to-paramagnetic phase transition is second order, in $\text{La}_{1-x}\text{Ca}_x\text{MnO}_3$ with calcium content around 0.33 the transition is most likely to be first order although some authors believe that it is second order at arbitrary x . It follows that the mechanism of the CMR effect in La-Ca crystals may differ from that in La-Sr and La-Ba manganites.

We have performed the study of magnetic properties and electronic transport in $\text{La}_{0.7}\text{Ca}_{0.3}\text{MnO}_3$ single crystal. Below 220 K, the crystal is shown to be in the ferromagnetic state in which magnetization M depends on temperature T weakly; above 250 K, the manganite is in the paramagnetic state and the transition region occupies the range of 220-250 K.

In the transition region, there are two peculiarities at the M - T curves: the first one is at ≈ 227 K and does not depend on magnetic field; the second is the inflection point, which we identify as the Curie temperature T_C . The thermal hysteresis is observed around 227 K on the $\rho(T)$ curve. We believe that at $T_S = 227$ K, the crystal undergoes the structural transition between two orthorhombic $Pnma$ phases.

The rapid decrease of the magnetization indicates that the magnetic transition is first order. This is confirmed by the negative sign of the slope of the isotherm H/M against M^2 for $T = 240$ K, which according to the Banerjee criterion, is an evidence for the first order transition.

In the CMR manganites, $|\Delta\rho/\rho|$ is typically decreased as Curie temperature grows up. The opposite holds in our case: the magnetoresistance of $\text{La}_{0.7}\text{Ca}_{0.3}\text{MnO}_3$ is much higher than that of $\text{La}_{0.82}\text{Ca}_{0.18}\text{MnO}_3$ where the magnetic transition is second order. This suggests that the origin of the CMR effect in the $x=0.18$ crystal differs from that in the $x = 0.3$ one. In $\text{La}_{0.82}\text{Ca}_{0.18}\text{MnO}_3$, as in the La-Sr and La-Ba crystals, near the Curie temperature, the reduction of the resistivity in a magnetic field results from the suppression of magnetic fluctuations. The situation in $\text{La}_{0.7}\text{Ca}_{0.3}\text{MnO}_3$ is opposite in the sense that near T_C , there is a mixture of metallic phase and semiconductor one. Application of a magnetic field increases the first order magnetic transition temperature increasing thereby the volume of the low resistivity. Since the resistivity of the paramagnetic phase is much higher than that of the metallic one, the magnetoresistance in $\text{La}_{0.7}\text{Ca}_{0.3}\text{MnO}_3$ is very great.

Support by grants RFBR 06-02-16085 and NSh-3257.2008.2 is acknowledged.

24PO-7-56

SEARCH FOR CRITERIA TO PREDICT INDUCED-MULTIFERROICS ON THE BASIS OF STRUCTURAL DATA

Volkova L.M.

Institute of Chemistry, Far East Branch RAS, Vladivostok, Russia

Search of new induced-multiferroics has been recently attracted a significant interest. The main condition of ferroelectric transition in these materials consists in the fact that polar atomic displacements should be induced by magnetic ordering occurring under external magnetic field [1-3]. The objective of the present work was to find criteria for searching new multiferroics on the basis of structural data. To implement this objective, we have studied three known multiferroics TbMnO_3 and RMn_2O_5 ($R = \text{Mn}$ and Bi) by a phenomenological method [4] that we had been earlier developed to estimate quantitatively the coupling parameters (strength of magnetic couplings and type of spin ordering) from the structural data.

We have shown that the reason of magnetic frustration of TbMnO_3 consists in a competition of the AF J_1 nearest and AF J_2 next-to-nearest neighbors couplings in linear chains along the sides of the square lattice in the ab plane. Magnetic ordering (MO) emerging at transition of J_2 couplings from AF to FM state under magnetic field and spontaneous polarization (P_s) along the c axis are mutually dependent. It is related to the fact that both of the above phenomena could be as reasons as consequences of the same effect – slight displacement of the O1 ions, which are in critical positions, along the c -axis.

The crystal structure of RMn_2O_5 is not typical for ferroelectrics, since in the paraelectric phase it contains atomic groups in the forms of Mn^{4+}O_6 octahedra and Mn^{2+}O_5 pyramids having constant dipole moments; however, coupling in these groups is of substantially ionic character. Since dipoles in these groups are oriented in different directions, they should be ordered for emerging P_s . Changing of orientation of dipole moments of octahedra and pyramids is possible due to displacement of specific ions, because couplings in these dipole groups are not “rigid”. According to the calculations, the paraelectric phase of RMn_2O_5 is a frustrated antiferromagnetic. In linear chains along the c -axis the nearest AF J_1 and J_2 couplings compete with next-to-nearest-neighbor (J_n) couplings. In addition, J_1 and J_2 couplings compete with all strong AF couplings between linear chains and dimers along the a - and b -axes. For emerging MO in RMn_2O_5 it is sufficient to eliminate or transform into FM the AF state of J_1 and J_2 couplings. It is possible through slight displacements of ions (O2 and O3 from the line -Mn1-Mn1- along the a -axis and ions O4 along the c -axis), which are in critical positions. However, these MO-accompanying displacements are not polar, they just induce changes of bond valence of Mn1 and Mn2, thus creating instability of the crystal structure. To approximate again the bond valence to an ideal value under MO conditions is possible only due to displacement of Mn2 (or O1) and O4 ions along the b axis that is the reason of ferroelectric transition. To obtain direct experimental evidence of structural changes accompanying P_s , it is necessary to perform diffraction studies of induced-multiferroics under high magnetic fields.

To conclude, the induced-multiferroics should be searched among the frustrated magnets, where intermediate ions are located in critical positions in the local space between magnetic ions, when displacement from them results in anomalous force change or reorientation of spins of magnetic interactions resulting in magnetic ordering. The displacements accompanying MO should be polar ones themselves or create conditions necessary for polar displacements emerging. All the above parameters can be determined on the basis of the structural studies data.

[1] T. Kimura et al., *Nature*, **426** (2003) 55.

[2] N. Hur et al., *Nature*, **429** (2004) 392.

[3] S-W. Cheong and M. Mostovoy, *Nature* (London) **6** (2007) 13.

[4] L.M. Volkova et al., *J. Supercond.*, **18** (2005) 583; *J. Phys.: Condens. Matter.*, **18** (2006) 11177; **19** (2007) 176208.

24PO-7-57

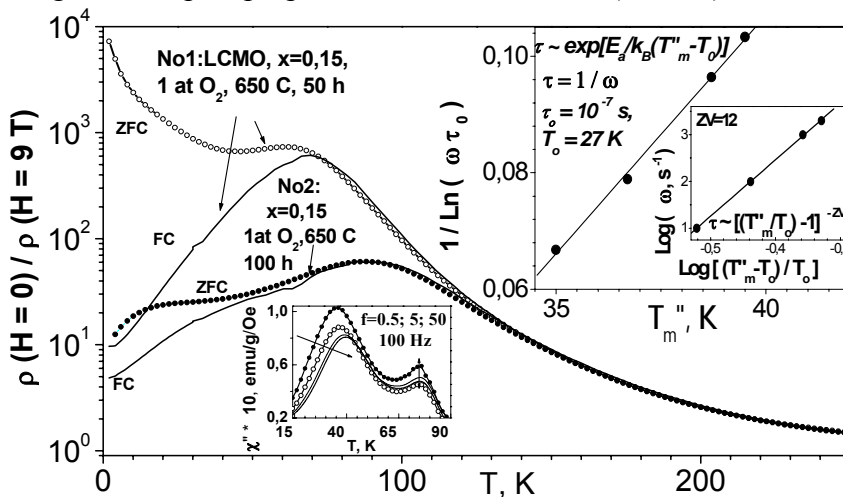
GIANT INTERCLUSTER MAGNETORESISTANCE IN DISORDERED WEAKLY DOPED LANTHANUM MANGANITES

Solin N.I.^{*}, Chebotaev N.M., Korolev A.V.

Institute of Metal Physics, 620041, Ekaterinburg, ul. S.Kovalevskoy, 18, Russia

e-mail: ^{*} solin@imp.uran.ru

A responsibility for the magnetoresistance in lanthanum manganites may rest with i) phase separation [1]; ii) strong electron – phonon coupling caused by Yahn-Teller effect [2]; iii) localization of electrons on spin polarons caused by magnetic disorder and by electron-electron interaction [3]. We have studied the influence of the magnetic disordering on the magnetic and magnetotransport properties of $\text{La}_{1-x}\text{Ca}_x\text{MnO}_3$ (LCMO), $x \leq 0.15$.



Ceramics $\text{La}_{1-x}\text{Ca}_x\text{MnO}_3$ was prepared by usual technology. Final annealing was performed in the air at 1300°C for 50 h. Some of specimens were homogenized by annealing in a vacuum at 650°C for 25 h. These specimens had the phase diagrams and low values of magnetoresistance that is typical for $\text{La}_{1-x}\text{Ca}_x\text{MnO}_3$ with $x \leq 0.15$. The other part of specimens (№1)

became inhomogenized after short annealing in the O_2 atmosphere. Their properties were changed dramatic: the Curie temperature T_C decreased from 140 K to 78 K, spin-glass-like temperature dependencies of magnetic susceptibility χ_{ac} with parameters typical for superparamagnetic particles (insets in Fig.) were found. The temperature dependence of electrical resistance ρ from 300 K to T_C is described by $\text{Log} \sim T^{-1/2}$ [3] that is typical for tunneling processes between metal nanoclusters [4]. The magnetoresistance $\text{MR} = \rho(H=0)/\rho(H)$ appears from 300 K, increases up to $10^6\%$ at the field $H=9\text{T}$ after zero magnetic field cooling (ZFC) and decreases up to $10^3\%$ after 9T magnetic field cooling (FC) (Fig.). Long annealing of the specimen (№2) decreases MR up to $10^3\%$ (Fig.).

Magnetotransport properties (№1) are explained by occurrence of cation vacancies during annealing in O_2 atmosphere, by frustration because of the competition of the superexchange $\text{Mn}^{+3} - \text{Mn}^{+3}$ and the double exchange $\text{Mn}^{+3} - \text{Mn}^{+4}$, by the inhomogeneity of crystallites through the low diffusion rate of cation vacancies and by decomposition of crystallites to superparamagnetic clusters. In the absence of magnetic field the electron tunneling between disordered small-sized magnetic clusters results in semiconductor kind of the conductivity. The magnetic field raises the magnetic order and the cluster sizes, reduces the energy of Coulomb blockade and determines high value of MR. Long annealing of the specimen (№2) or FC regime (№1) order the specimen, increase the cluster sizes and eliminate the reason of high MR.

This work was supported by Programs of RAS "New materials and structure" and "Quantum macrophysic", by Scientific Program of Far Eastern Division and Ural Division RAS.

- [1] E. L. Nagaev. Phys.Usp. **39**, 781 (1996)]; E. Dagotto, New J. Phys. **7**, 67 (2005).
 [2] A. J. Millis, P. B. Littlewood, and B. I. Shraiman. Phys.Rev. Lett. **74**, 5144 (1995).
 [3] C. M. Varma. Phys. Rev. B **54**, 7328 (1996).
 [4] P.Sheng et al. Phys. Rev. Lett. **28**, 34(1972); J.S.Helman, B.Abeles. Phys. Rev. Lett. **37**, 1429(1976).

24PO-7-58

ELECTRON-ELECTRON INTERACTION IN HYBRIDIZED IMPURITY STATES AS A CAUSE OF THE CONCENTRATION DEPENDENCE OF CONDUCTION ELECTRON G-FACTOR

Okulov V.I.¹, Pamyatnykh E.A.², Alshansky G.A.¹

¹Institute of Metal Physics UD RAS, 620219, Ekaterinburg, Russia

²Ural State University, 620083, Ekaterinburg, Russia

In low-temperature magnetic properties of semiconductors with the impurities of transition elements the hybridized electron states may manifest themselves. Such states arise when donor energy d-level of the impurity falls within the conduction band of a crystal. Electron density of hybridized states contains homogeneous contribution related to the electron free movement and contribution localized on the impurity, which conforms to the peak in energy dependence of the density of electron states. The degree of filling this peak defines relative fraction of localized electron density at the given concentration of donor impurities. The hybridization of states can be manifested in the anomalies of concentration and temperature dependencies of kinetic properties. The most marked anomalies of this kind were detected in gapless semiconductor – mercury selenide with impurities of iron and other transition elements[1,2]. Recent experiments on the observations of quantum Shubnikov - de Haas and de Haas - van Alphen oscillations in the same systems have revealed non-monotone concentration dependence of conduction electron g-factor, related to the hybridization. In the present work it has been shown that the above effect is caused by the Fermi-liquid electron interaction and its theory is developed. Our study is based on the quantum theory of electron liquid, generalized to electron hybridized states, with using the same model assumptions that were applied to studying the impurity part of magnetic susceptibility [3]. As a result the following expression for g-factor of conduction electrons is obtained:

$$g_e = g_0 \left(1 - \tilde{\psi}_{re} \frac{\eta_r}{1 + \tilde{\psi}_r \eta_r} \right),$$

where $g_0 = 2/(1 + \psi_{ee} \eta_e)$, $\tilde{\psi}_r = \psi_{rr} - \psi_{re}^2 \tilde{\eta}_e$, $\tilde{\psi}_{re} = \psi_{re} - \psi_{re}^2 \tilde{\eta}_e$, $\tilde{\eta}_e = \eta_e / (1 + \psi_{ee} \eta_e)$; η_e , η_r are the densities of states on the Fermi surface for distributed and localized contributions to electron states; ψ_{ee} , ψ_{rr} , ψ_{re} are the parameters of electron-electron interaction for distributed contributions, localized ones and mixed case, respectively. In case, when Fermi energy is large in comparison with the width of resonance interval, the quantity η_e (and, therefore, g_0 and $\tilde{\psi}_{re}$, $\tilde{\psi}_r$) almost do not depend on the impurity concentration n_d . In this case, the dependence

on n_d appears in the above formula mainly through the density of states of localized electrons η_r , which is proportional to

$$(n_d/\pi n_0) \sin^2(\pi n_0/n_d),$$

where n_0 is resonance electron concentration. According to this result the g-factor can have maximum or minimum in depending on the sign of the Fermi-liquid parameter ψ_{re} , describing the interaction of localized and delocalized contributions to electron states.

This study was supported by Russian Academy of Sciences project (subject № 01.2.006 13395), by the Russian Foundation for Basic Research, grant № 06-02-16919, and by grant EK-005-00(REC-005) of Russian-American Program BRHE.

[1] V.I. Okulov, *Low. Temp. Phys.*, **30** (2004) 1194; *Fizika Metall. i Metalloved.*, **100**, 2005) 23.

[2] V.I. Okulov, et al., *Low. Temp. Phys.*, **33**, (2007) 282.

[3] V.I. Okulov, E.A. Pamyatnykh, and A.V. Gergert, *Fizika Metall. i Metalloved.*, **101**, (2006) 7.

24PO-7-59

MAGNETO-OPTICAL PROPERTIES OF BULK NANOSTRUCTURED YTTRIUM IRON GARNET $Y_3Fe_5O_{12}$

Gizhevskii B.A.¹, Sukhorukov Yu.P.¹, Loshkareva N.N.¹, Ganshina E.A.², Telegin A.V.¹, Pilugin V.P.¹, Gaviko V.S.¹, Lobachevskaya N.I.³, Gilyatidinova N.M.²

¹Institute of Metal Physics, Ural Division, Russian Academy of Sciences,
Ekaterinburg, 620041 Russia

²M.V. Lomonosov Moscow State University, Moscow, 119992 Russia

³Institute of Chemistry of Solids, Ural Division, Russian Academy of Sciences,
Ekaterinburg, 620041 Russia

Production of bulk (massive) magnetic nanomaterials is the important problem of modern material science. We prepared high density bulk nanostructured Yttrium Iron Garnet $Y_3Fe_5O_{12}$ (nano-YIG) by high pressure torsion method and studied IR absorption spectra, Faraday rotation and transversal Kerr effect (TKE) of a number of nano-YIG samples. High pressure torsion was realized by means of a 100-t press and Bridgman anvils. The initial coarse-grain YIG powder was placed between anvils and pressed at pressure of as high as 9 GPa. Shear deformation was achieved by rotation one of the anvils. The degree of strain was specified by anvil rotation angle. Crystallite size quickly saturates with increase of the degree of strain. So we obtained a series of nano-YIG samples with close crystallite size 20-40 nm and various microdeformations and concentration of point defects.

IR absorption spectra of nano-YIG demonstrate 2 new bands near 2 and 3.1 μm and strong broadening well known band near 1 μm in comparison with IR spectra of single crystals. The band $\sim 1 \mu\text{m}$ is due to the transition ${}^6A_1 \rightarrow {}^4T_1$ of the octahedral ion Fe^{3+} and forms the high frequency absorption edge of YIG. Intensity of the band $\sim 2 \mu\text{m}$ is varied under deformations. This band may be connected with Fe^{2+} or Fe^{4+} ions because severe plastic deformations produce change degree of oxidation of oxides. The peak near 3.1 μm is likely impurity band. Broadening of absorption edge is due to action of random fields of defects on Fe^{3+} ions in octahedral positions. Faraday rotation $F(\lambda)$ of YIG arises from transitions in Fe^{3+} ions and frequency independent Faraday effect in the middle and far IR region of spectrum. The value of Faraday rotation of nano-YIG is less than of single crystal one but spectral dependence is similar to $F(\lambda)$

of single crystals. Faraday rotation value of nano-YIG rises near the absorption edge $\sim 1 \mu\text{m}$ with increase of deformations because of enhancement of optical transitions in this spectral region.

Spectral dependence of TKE for all nano-YIG samples displays extremum near 3 eV. This peak corresponds to charge transfer transition from the oxygen p-band to Fe^{3+} orbitals. Intensity of such kind interband transition decreases with increase in concentration of defects and the peak shifts to low energy. It is known that the gap of wide-band compounds is broadened in nano-state (blue shift of fundamental absorption edge). In the case of nano-YIG we observed opposite effect. Shift of the band $\sim 3 \text{ eV}$ is similar to red shift of the absorption edge of nano-CuO [1]. The high degree of deformation (1 revolution of anvils or more) causes partly amorphisation of YIG. Samples of this type demonstrate decrease of Faraday rotation and TKE.

In conclusion, optical and magneto-optical properties of nanostructured samples of YIG depend on not only crystallite size but concentration of defects and microdeformations.

The work is supported by the Russian Foundation for Basic Research, Grant 06-03-72003, and by Program "New Materials and Structures" of the Department of Physics, Russian Academy of Sciences and Ural Division of Russian Academy of Sciences.

[1] B.A. Gizhevskii, Yu.P. Sukhorukov, A.S. Moskvina, et al., *JETP*, **102** (2006) 297.

24PO-7-60

MAGNETIZATION AND ELECTRICAL CONDUCTIVITY STUDY OF $\text{Gd}_{0.9}\text{A}_{0.1}\text{CoO}_3$ (A=Ba, Sr)

Kazak N.V.¹, Ivanova N.B.², Michel C.R.³, Balaev A.D.¹, Ovchinnikov S.G.^{1,4}

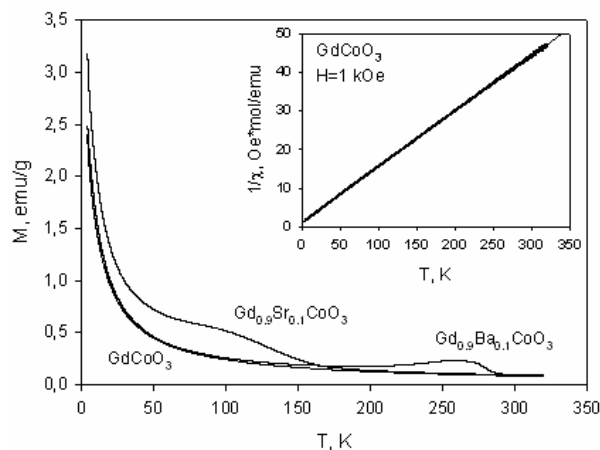
¹Kirensky Institute of Physics, Siberian Branch of Russian Academy of Sciences, 660036, Akademgorodok, Krasnoyarsk, Russia

²Polytechnical Institute, Siberian Federal University, 660074, Kirensky str. 26, Krasnoyarsk, Russia

³Departamento de Fisica, C.U.C.E.I., Universidade de Guadalajara, Blvd. Marcelino Garcia Barragan 1421, 44430 Guadalajara, Jalisco, Mexico

⁴Institute of Natural and Humanitary Researches, Siberian Federal University, 660041, pr. Svobodnii 79, Krasnoyarsk, Russia

The magnetic and electron transitions in polycrystalline $\text{Gd}_{0.9}\text{A}_{0.1}\text{CoO}_3$ (A=Ba, Sr) cobaltites have been investigated by magnetization and electrical conductivity measurements [1]. The parent GdCoO_3 was found to demonstrate paramagnetic behaviour within wide temperature interval (4.2-320 K). The Curie-Weiss law fitting has revealed weak antiferromagnetic coupling between Gd ions with effective magnetic moment close to the theoretical one. An average value of the exchange interaction was estimated to be $J/k = -0.124 \text{ K}$. The replacement of Gd^{3+} by Ba^{2+} and Sr^{2+} with larger ionic radii leads to dramatic change in magnetic and electrical properties. The ferromagnetic phase transitions were found at 280 K for Ba-doped sample and at 130 K for Sr-doped one. Below these temperatures the divergence between ZFC and FC curves is



observed. The field induced hysteresis appears below magnetic transition temperature and remains down to 4.2 K in $\text{Gd}_{0.9}\text{Sr}_{0.1}\text{CoO}_3$. In the case of Ba-sample magnetic hysteresis takes place in the range $180 < T < 300$ K. The doped cobaltites with variable valence and spin states of Co ions demonstrate intriguing antiferromagnetic – ferromagnetic competition which results in the cascade of magnetic phase transitions from paramagnetic to antiferromagnetic state in $\text{Gd}_{0.9}\text{Ba}_{0.1}\text{CoO}_3$ and to ferromagnetic state in $\text{Gd}_{0.9}\text{Sr}_{0.1}\text{CoO}_3$ through spin-glass state. The complicated magnetic behaviour can be interpreted on basis of electronic phase separation known in the cobaltites [2]. The analysis of the inverse magnetic susceptibility curves shows the change of the slope at 305 K in Ba-doped sample and 230 K in Sr-doped one and corresponding change of effective magnetic moment. These singularities point to the spin transition of Co^{3+} ions. The magnetic results have revealed that in GdCoO_3 and Ba-doped cobaltite the Co ions are most likely in low-spin state up to room temperature unlike Sr-doped one where the considerable cobalt contribution to magnetic moment is observed at low temperatures.

The Ba and Sr doping leads to the conductivity increase by several orders. The gradual metal-insulator transition takes place in the all studied materials within the temperature interval 600-800 K.

This study was supported by “Strongly correlated Electrons” program of the Department of Physical Sciences of RAS.

[1] N.B. Ivanova, N.V. Kazak, C.R. Michel, et al., *Phys. Solid State* **49** (2007) 1498.

[2] R. Caciuffo, D. Rinaldi, G. Barucca, et al., *Phys. Rev. B* **59** (1999) 1068.

24PO-7-61

OPTICAL ABSORPTION OF MULTIFERROIC HoMnO_3

Loshkareva N.¹, Sukhorukov Yu.¹, Moskvina A.², Balbashov A.³

¹Institute of Metal Physics of Ural Division, RAS, 620041 Ekaterinburg, Russia

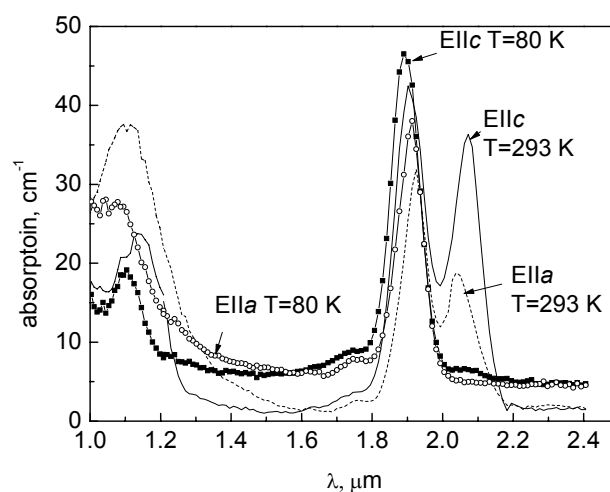
²Ural State University, 620083 Ekaterinburg, Russia

³Moscow Power Engineering Institute, 105835 Moscow, Russia

Hexagonal manganite HoMnO_3 reveals a ferroelectric order below $T_C = 875$ K and the antiferromagnetic order below $T_N = 76$ K. HoMnO_3 is a typical multiferroic with the magnetic phase of both the Mn^{3+} and Ho^{3+} sublattices controlled by the electric field [1].

We have performed optical study of HoMnO_3 single crystal in the infrared range (0.8 - 30 μm) using a high sensitive prism-type spectrometer. The hexagonal HoMnO_3 single crystal was grown by the floating-zone method. The parameters of lattice are: $a=6.140$ Å, $c=11.408$ Å. HoMnO_3 reflection spectrum measured in unpolarized light reveals the onset of the light interaction with lattice vibration (residual spectrum) at 12.5 μm (800 cm^{-1}). The residual spectrum of HoMnO_3 for polarization $E \perp c$ starts with 16.3 μm (620 cm^{-1}) [2]. Polarization measurements of optical absorption $\alpha(\lambda)$ were carried out using thin (0.6 mm) plate with (110) crystal plane for polarization $E \parallel c$ and $E \parallel a \perp c$. Several spectral features were found in the transparency window of HoMnO_3 . Weak lines and the absorption rise at the long wave length edge $\lambda > 5$ μm are associated with overtones or combinations of phonon modes. These manifest a strong anisotropy with a dichroism $(\alpha_a - \alpha_c)/(\alpha_a + \alpha_c)$ on the order of 50 % in the range 7-9 μm .

Spectral features nearby 2 μm and 1.1 μm may be assigned to transitions $^5I_8 \rightarrow ^5I_7$ and $^5I_8 \rightarrow ^5I_6$ within the $4f^{10}$ electron configuration of Ho^{3+} ion, respectively. Their energies are practically the same as in the case of holmium iron garnet $\text{Ho}_3\text{Fe}_5\text{O}_{12}$ [3]. The line at 1.1 μm seems to be more pronounced for $E||a$, than for $E||c$. The spectral feature nearby $\lambda=2 \mu\text{m}$ has a distinct two-peak structure with a strong temperature dependence. For both polarizations the low-energy (2.04, 2.07 μm , respectively) line weakens under cooling and disappears below 80 K that can be explained as a result of a depopulation of an initial Stark level. In other words, the two-peak structure of the $\lambda=2 \mu\text{m}$ feature is a result of the f-f transitions from the ground and first excited Stark levels of the 5I_8 multiplet to the Stark levels of the 5I_7 multiplet. Fluorescence transition at 2.09 μm for $\text{Ho}_3\text{Fe}_5\text{O}_{12}$ which occurs with sufficient intensity for laser action was studied in [4].



Supports by RFBR project 08-02-00633, Program "New materials and structure" of the Department of Physics of Russian Academy of Sciences are acknowledged.

- [1] T. Lottermoser, T.Lonkai, U.Amann et al., *Nature*, **430** (2004) 541.
 [2] A. P. Litvinchuk, M.N.Iliev, V.N.Popov et al., *J. Phys.: Condens. Matter*, **16**, (2004) 809.
 [3] D.L.Wood, J.P.Remeika, *J. Appl. Phys.*, **38** (1967) 1038
 [4] L.F.Johnson, J.P.Remeika, J.F.Dillon, *Phys. Letters*, **21** (1966)37

24PO-7-62

MULTIFERROIC $\text{LuMnO}_3 - \text{Pr}_{1-x}\text{Sr}_x\text{MnO}_3$ THIN FILM NANOCOMPOSITE

Akbashev A.R.¹, Gorbenko O.Yu.²

¹Department of Materials Science, Moscow State University, 119991 Moscow, Russia

²Department of Chemistry, Moscow State University, 119991 Moscow, Russia

A growing interest towards multiferroics is an outcome of the general tendency to creating smaller electronic devices, which has lead to the making use of the spin state of electrons as the carrier of the information bit. Multiferroics, the most promising materials important for spintronic devices, allow us to convert a magnetic field to an electric field and vice versa. Composite multiferroics made of the ferroelectric and ferromagnetic materials coupled together by magnetostriction or electrostriction provide an essential material flexibility and higher magnetoelectric effect.

In this work we propose new composite multiferroic thin film system $\text{Pr}_{0.7}\text{Sr}_{0.3}\text{MnO}_3$ - LuMnO_3 including CMR perovskite manganite $\text{Pr}_{0.7}\text{Sr}_{0.3}\text{MnO}_3$ with MIT near the room temperature and ferroelectric matrix of the hexagonal non-perovskite LuMnO_3 . The composite material was prepared in-situ on single-crystalline (111) $\text{ZrO}_2(\text{Y}_2\text{O}_3)$ substrate using metallorganic chemical vapor deposition (MOCVD) with flash evaporation precursor source. $\text{Pr}(\text{thd})_3$, $\text{Lu}(\text{thd})_3$, $\text{Mn}(\text{thd})_3$, $\text{Sr}(\text{thd})_2$ (where thd = 2,2,6,6-tetramethylheptane-3,5-dionate) were

used as volatile precursors. Deposition was carried out at 700-800°C and total gas pressure 8 mbar (partial pressure of oxygen 2 mbar).

The thin film samples prepared were characterized by XRD, SEM, EDX, optical and magneto-optical techniques. It was found that two-phase composite $\text{Pr}_{0.7}\text{Sr}_{0.3}\text{MnO}_3$ - LuMnO_3 was formed in-situ due to the miscibility gap between perovskite and layered hexagonal manganite phases. XRD revealed that LuMnO_3 forms c-oriented epitaxially strained matrix of the layered hexagonal phase which demonstrates ferroelectric properties (due to the non-centrosymmetrical space group $\text{P6}_3\text{mc}$), while $\text{Pr}_{0.7}\text{Sr}_{0.3}\text{MnO}_3$ crystallized in form of the random nanometric inclusions of the perovskite phase (metallic and ferromagnetic below the RT) inside the ferroelectric matrix without percolation of the metallic regions. According to SEM, no secondary phase inclusions were sticking out of the smooth surface of the composite films. Thus, a combination of ferromagnetic nanodomains with high magnetostriction and ferroelectric matrix in the composite thin films was realized by an in-situ deposition.

The work was supported by FRBF grant N 06-03-33070.

24PO-7-63

MAGNETOELASTIC PROPERTIES OF THE RARE-EARTH FERROBORATES $\text{RFe}_3(\text{BO}_3)_4$

Volkov D.V.¹, Demidov A.A.², Kolmakova N.P.², Vasiliev A.N.¹

¹M.V. Lomonosov Moscow State University, 119992 Moscow, Russia

²Bryansk State Technical University, 241035 Bryansk, Russia

The trigonal 4f-3d crystals $\text{RFe}_3(\text{BO}_3)_4$ demonstrate various magnetoelastic effects depending strongly on the rare-earth element R. The iron subsystem in these compounds orders antiferromagnetically with the Neel temperature in the interval 30-40 K. The magnetic anisotropy is governed by the rare-earth.

Theoretical investigations of magnetoelastic properties are performed for the rare-earth ferrobates $\text{RFe}_3(\text{BO}_3)_4$ with $\text{R} = \text{Tb}$ and Pr . In particular, we have considered the anomalies of magnetostriction caused by the spin-flop transition in the iron subsystem which is induced by magnetic field applied along the trigonal axis of the crystal. Comparative analysis is carried out for the curves of longitudinal magnetostriction of these compounds, which differ by the value of splitting of the lowest-lying energy levels of rare-earth ions in the ordered phase.

New experimental data [1, 2] for the magnetostriction curves of the compounds under consideration at the field along the trigonal axis show that the magnetostriction is small for $B < B_{\text{sf}}$ ($B_{\text{sf}} \approx 3.5$ T for $\text{R} = \text{Tb}$ and $B_{\text{sf}} \approx 4.5$ T for $\text{R} = \text{Pr}$ at $T = 4.2$ K), experiences a jump at B_{sf} , this jump is 2 times smaller in $\text{PrFe}_3(\text{BO}_3)_4$ than in $\text{TbFe}_3(\text{BO}_3)_4$, and at $B > B_{\text{sf}}$ grows linearly with field. Calculated multipole moments of the Tb^{3+} ions in terbium ferrobate allowed us to obtain following results. It is established that the quadrupole approximation is sufficient for accounting for the observed regularities of magnetostriction. This situation differs from the situation with magnetostriction in $\text{NdFe}_3(\text{BO}_3)_4$ [3], where quadrupole approximation is not sufficiently convincing [4]. Different signs and values of jumps of longitudinal and transversal magnetostrictions at B_{sf} and their mutual correlation are explained. When interpreting the magnetostriction curves, estimates of relevant coefficients are performed, these coefficients are combinations of elastic constants and magnetoelastic coefficients of the compound. For $\text{PrFe}_3(\text{BO}_3)_4$ with the aim to calculate field and temperature dependences of multipole moments of the Pr^{3+} ion, the crystal-field parameters were deduced from experimental data [2] for temperature dependences of initial magnetic susceptibility along the trigonal axis and in the basal

plane and for magnetization curves at the field along trigonal axis. Other necessary parameters were taken from literature. A singlet ground state of the Pr^{3+} ion in the paramagnetic phase of compound and weakly-magnetic wave functions of the low-lying singlet states are responsible for small contributions of rare-earth subsystem both to the magnetization in the collinear phase and to the magnetization jump at spin-flop transition. Calculated values of jumps of multipole moments of the Pr^{3+} ion at the spin-flop transition, main ones being the quadrupole moments just as in the case of Tb compound, give possibility to account for the linear field dependences of longitudinal magnetostriction both in the collinear and flop phases, which are observed in experiment, and for a smaller value of magnetostriction jump experimentally observed in $\text{PrFe}_3(\text{BO}_3)_4$, than in $\text{TbFe}_3(\text{BO}_3)_4$.

Support by ISTC (project 3501) is acknowledged.

- [1] A.M. Kadomtseva, Yu.F. Popov, G.P. Vorob'ev et al., in *Proc. Intern. Meeting Multiferroics'2007*, p. 188.
 [2] A.M. Kadomtseva, Yu. F. Popov, G.P. Vorob'ev et al., *JETP Lett.* **87** (2008) 45.
 [3] A.K. Zvezdin, G.P. Vorob'ev, A.M. Kadomtseva et al., *JETP Lett.* **83** (2006) 509.
 [4] A.A. Demidov, N.P. Kolmakova, L.V. Takunov, D.V. Volkov, *Physica B* **398** (2007) 78.

24PO-7-64

LOW TEMPERATURE MAGNETIC PROPERTIES OF MANGANITE

$\text{Nd}_x\text{Mn}_{1-x}\text{O}_{3+\delta}$

Rykova A.¹, Khatsko E.¹, Cherny A.¹, Bukhanko F.²

¹B.I.Verkin Institute for Low Temperature Phys. & Engineering of NASU, 47 Lenin Ave.,
 Kharkov, 61103, Ukraine

²A.A. Galkin Donetsk Physico-Technical Institute of NASU, 72 R. Luxemburg Str.,
 Donetsk, 83114, Ukraine

The manganese oxides RMnO_3 (where R=La, Pr, Nd, Sm...) are extensively studied due to the existence of complex magnetic phases and their transformation, as well as the possibility of using these compounds in microelectronics techniques. The NdMnO_3 with the orthorhombic structure has an A-type antiferromagnetic antiferromagnetic (A-AF) structure, where the ferromagnetic MnO_2 layers are coupled antiferromagnetically along the *c*-axis at low temperature [1]. It is an insulator. In the present time a great scientific and practical significance has been produced by the synthesis of manganites with a surplus of oxygen, because the changing of the composition of oxygen of the manganese it is possible to form a ratio of concentration $\text{Mn}^{4+}/\text{Mn}^{3+}$ and thus to influence on the magnetic status of manganese.

The complex magnetic investigation of a lightly self-doped insulating ceramic sample $\text{Nd}_x\text{MnO}_{3+\delta}$ ($x=1$, $\delta=0.1$) with nanoscale phase separation was carried out in detail.

The field and temperature dependence of magnetization of the sample in the temperature range 300-0.5 K and magnetic field up to 20 kOe was studied. The temperature dependence of the *dc* magnetization *M* in external magnetic fields 35, 50, 70, 525, 1050, 1750, 3500 Oe in the temperature range from 0.5 to 100 K are measured using the different regimes of cooling (ZFC and FC regimes). The presence in oxides of areas with different densities of electrons results in the coexistence of ferromagnetic metal and antiferromagnetic insulator nanoscale phases. It is necessary to note that such a cluster structure can persist above T_c (like superparamagnetic). This leads to a clear-cut distinction between $M_{\text{ZFC}}(T)$ and $M_{\text{FC}}(T)$ curves at all fields. The all *M* (*T*) dependences demonstrate two singularities close to 11 K and 60 K. Below 60 K the sample is ferromagnetic. At

temperatures above T_c the measured magnetic susceptibility temperature dependence is described by Curie-Weiss law quite well, but the value of Curie-Weiss constant Θ changes with change of external field. The dependence of $\Theta(T)$ at different external magnetic fields has the complicated character, but sing of Curie-Weiss constant always remain positive. This is explained by small shift of equilibrium between different types of magnetic exchange (anti-, ferromagnetic) under influences of magnetic field. Near 11 K the competition between the ferromagnetic double exchange and antiferromagnetic superexchange interaction lead to antiferromagnetic or ferrimagnetic ordered state.

The dependence of magnetization from external magnetic field of $\text{Nd}_x\text{Mn}_{1-x}\text{O}_{3+\delta}$ is studied in temperature range 0.5 -100 K and magnetic field up to 20 kOe. The $M(H)$ curves shows a sophisticated hysteresis loops. The value of coercitivity H_k decreases with increase of temperature and the dependence of $H_k(T)$ have the exponential character. It is characteristic for similar systems with phase separation.

[1] E.O. Wollan and W.C. Koehler, *Phys. Rev.*, **100** (1955) 545.

24PO-7-65

EFFECT OF Ga SUBSTITUTION ON STRUCTURE AND Tb MAGNETIC ORDER IN MULTIFERROIC $\text{TbMn}_{1-x}\text{Ga}_x\text{O}_3$ CRISTALS

Prokhnenko O., Aliouane N., Feyerherm R., Maljuk A., Argyriou D.N.
Hahn-Meitner-Institut, Glienicke Str.100, D-14109 Berlin, Germany.

We have prepared ceramic $\text{TbMn}_{1-x}\text{Ga}_x\text{O}_3$ ($0 \leq x \leq 0.2$) samples by a conventional solid state synthesis. Single crystals have been grown by the floating zone technique using the 4-mirror type image furnace. All single crystalline and ceramic samples are impurities free from X-ray and neutron powder diffraction measurements. Tb magnetic ordering was studied by using neutron powder diffraction, neutron and X-ray resonant synchrotron single crystal diffraction, magnetization measurements on substituted $\text{TbMn}_{1-x}\text{Ga}_x\text{O}_3$ ($x = 0.0, 0.04, 0.1, 0.2$) samples. We show that keeping the same crystal structure for all compositions, Ga for Mn substitution leads to the linear decrease of both $T_N(\text{Mn})$ and $\tau(\text{Mn})$ reflecting the decrease of $J(\text{Mn-Mn})$ and the increase of the Mn-O-Mn bond angles, respectively. At the same time the observed strong decrease (for $x = 0.04$) and disappearance (for $x = 0.1$) of the Tb-magnetic ordering above $T_N(\text{Tb})$ verifies that this magnetic ordering is of induced character and its presence in the ferroelectric phase (FE) of TbMnO_3 may reflect the symmetry breaking at T_{FE} . Even 4% of Ga for Mn substitution suppresses not only the induced Tb magnetic ordering but also its own long range magnetic ordering that becomes of short range below 7 K. It is in the agreement with our recent investigations showing that Mn-Tb interactions are involved in stabilizing the Tb-magnetic ordering even below $T_N(\text{Tb})$.

24PO-7-66

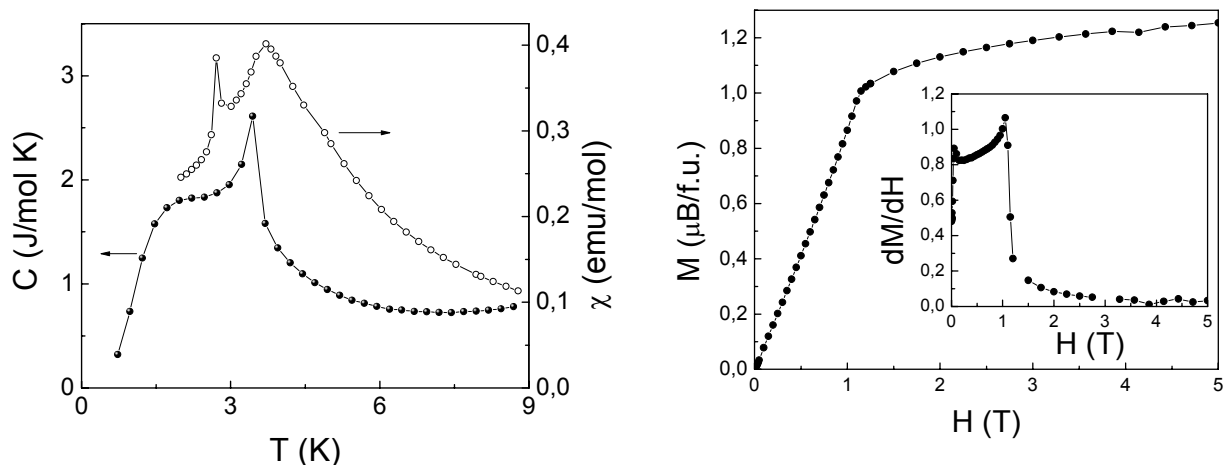
THERMODYNAMIC PROPERTIES OF NEW QUASI – ONE – DIMENSIONAL CUPRATE $\text{Cu}(\text{NO}_3)_2 \times \text{H}_2\text{O}$

Volkova O.¹, Morozov I.¹, Lapsheva E.¹, Shutov V.¹, Klingeler R.², Büchner B.², Vasiliev A.¹

¹Moscow State University, 119991 Moscow, Russia

²Institute for Solid State and Materials Research, 01069 Dresden, Germany

The trihydrate copper nitrate $\text{Cu}(\text{NO}_3)_2 \cdot 2.5\text{H}_2\text{O}$ was namely the substance which study opened the field of low – dimensional magnetism. It is a spin – gap compound due to the alternation of magnetic exchange interaction within the chain [1]. At water extraction the topology of the magnetic chain changes basically. In monohydrate copper nitrate $\text{Cu}(\text{NO}_3)_2 \cdot \text{H}_2\text{O}$ it is uniform. The measurements of specific heat and magnetization indicate that this compound reaches the long range magnetic order at low temperatures. As shown in the left panel of the Figure the specific heat C passes through sharp peak at $T_N \sim 3.5$ K and shows a broad shoulder at lower temperatures. This shoulder signals the release of some additional degree of freedom, most probably in the magnetic subsystem. At high temperatures, the magnetic susceptibility of $\text{Cu}(\text{NO}_3)_2 \cdot \text{H}_2\text{O}$ follows the Curie – Weiss law with positive Weiss temperature $\Theta \sim 10$ K. At low temperatures, the $\chi(T)$ dependence passes through broad maximum. The temperature of this maximum is slightly higher than the temperature of the sharp peak at $C(T)$ dependence. Strictly speaking, the Neel temperature roughly coincides with the peak in the derivative $\chi'(T)$. Unexpected feature in the temperature dependence of magnetic susceptibility is the sharp peak at about 2.7 K. The rise of χ at this temperature can be tentatively ascribed to the cancellation of various contributions to the magnetic anisotropy of $\text{Cu}(\text{NO}_3)_2 \cdot \text{H}_2\text{O}$. The right panel of the Figure represents the field dependence of magnetization M taken at 2 K. Two characteristic magnetic fields can be identified follow the field dependence of the derivative $M'(H)$. The lower field $H_1 \sim 0.06$ T can be associated with the spin – flop transition, while the upper field $H_2 \sim 1.05$ T signifies the spin – flip transition.



This work is supported by RFBR grants N 06-02-16088, 07-02-91580, 07-02-00350 and DFG grant KL1824.

[1] J.C. Bonner, S.A. Friedberg, H. Kobayashi, D.L. Meier, H.W.J. Blöte, Phys. Rev. B **27** (1983) 248.

24PO-7-67

UNCORRELATED SPIN POLARONS IN $\text{LaMnO}_{3+\delta}$ *Arbuzova T., Naumov S.*

Institute of Metal Physics of Ural Division, RAS, 620041 Ekaterinburg, Russia

The paper presents the results of magnetic investigation of the $\text{LaMnO}_{3+\delta}$ ($\delta = 0.06, 0.11, 0.16$) polycrystals in the wide paramagnetic region. The colossal magnetoresistance (CMR) effect in manganites is conditioned by intrinsic electronic inhomogeneities. Nanocluster phase-separated states are peculiarity of these compounds. Uncorrelated local structural distortions (Jahn-Teller polarons) and correlated distortions (charge-ordered nanoclusters) exist in the paramagnetic region. The orbital correlations play the key role in the effect of CMR [1]. Uncorrelated structural distortions are present in all crystallographic phases of manganites. Charge-ordered nanoclusters are revealed only in the insulating orthorhombic structure within the range of magnetic order and in paramagnetic range. It is interesting to study the influence of structural correlations on the magnetic properties of manganites. The magnetic measurements at high temperatures $T > T_c$ can provide the information about the existence of the new temperature scale above T_c , where polarons start forming [2].

The sample of $\text{LaMnO}_{3.06}$ (№1) contained 70% of orthorhombic phase (Pnma space group) and 30% of rhombohedral phase (R-3c space group) at room temperature. The sample $\text{LaMnO}_{3.11}$ (№2) had 35% and 65%, of O and R phases, respectively. $\text{LaMnO}_{3.16}$ (№3) had rhombohedral structure. A Curie temperature decreased from $T_c = 150\text{K}$ to $T_c = 127\text{K}$ with an increase the content of Mn^{4+} ions. Curie-Weiss law $\chi = C/T - \theta$ began to carry out above $T \sim 440\text{K}$. Below this temperature (T_{pol}) the uncorrelated paramagnetic polarons with the effective magnetic moment larger than that of the appropriate average moments of Mn^{3+} ($S=2$) and Mn^{4+} ($S=3/2$) ions are created. They are the spin-polarized clouds around localized charges. At further decrease of the temperature $T < T_{\text{pol}} = 300\text{K}$ the correlated magnetic polarons with $\mu_{\text{eff}} = 6.04\mu_B$ are formed. Their susceptibility depends from applied magnetic field. For the sample №3 Curie-Weiss law is carried out above $T = 480\text{K}$. In the region $300\text{K} < T < 480\text{K}$ the higher effective moment retains invariable. Bellow $T = 300\text{K}$ μ_{eff} increases continuously, that can be explained by increase of the number of the polarized spins. It is possible to conclude that the temperature range of the correlated magnetic polarons $T_c < T < T^*$ and the uncorrelated polarons $T^* < T < T_{\text{pol}}$ are present in the orthorhombic phase of $\text{LaMnO}_{3+\delta}$. The values of T^* and T_{pol} practically do not depend on ion concentration of Mn^{4+} . In the rhombohedral phase of $\text{LaMnO}_{3+\delta}$ only uncorrelated individual polarons are realized in the paramagnetic region.

Support by Program "New materials and structure" of the Department of Physics of Russian Academy of Sciences is acknowledged.

[1] V.Kiryukhin, *New J.Phys.*, **7** (2005) 67

[2] E.Dagotto, *New J.Phys.*, **6** (2004) 155

24PO-7-68

MAGNETOELECTRIC EFFECTS IN FERRITE-PIEZOELECTRIC NANOSTRUCTURES AT ELECTROMECHANICAL RESONANCE

Petrov V.¹, Bichurin M.¹, Srinivasan G.²

¹Novgorod State University, 41, B. St.-Petrburgskaya, Veliky Novgorod 173003, Russia

²Oakland University, Rochester MI, 48309, USA

Materials which reveal the ferromagnetic and ferroelectric ordering simultaneously in the same phase and allow coupling between the two are known as magnetoelectric (ME) multiferroics. Most of the known single-phase ME materials show weak ME coupling. Relatively large ME coefficients, however, have been obtained in layered composites consisting of piezoelectric and magnetostrictive materials. The ME effect in a composite is related to the interaction between the magnetostrictive and piezoelectric subsystems through the mechanical deformation. Investigations on the ME effect in nanostructures in the shape of wires, pillars and films are important for increased functionality in miniature devices.

Since the appearance of polarization in such composite materials under the action of a magnetic field is associated with the occurrence of mechanical stresses, it is reasonable to expect that the magnitude of this effect will be much greater in the region of the electromechanical resonance (EMR) [1]. This work is focused on modeling the ME effect in ferrite-piezoelectric nanostructures in EMR region.

Calculation of ME voltage coefficient α_E which is the ratio of induced electric field to applied magnetic field is carried out by solving the equation of medium motion using the appropriate boundary conditions, magnetostatic and electrostatic equations, Hooke's law and lattice mismatch effect. Changes in the piezoelectric and piezomagnetic coefficients, permeability and permittivity of components arising from lattice mismatch between the nanostructure and substrate are evaluated from the classical Landau-Ginsburg-Devonshire phenomenological thermodynamic theory. We consider here piezoelectric and ferrite films with thickness much larger than the ferroelectric and ferromagnetic correlation length for both phases so that the size effects may be neglected. The frequency dependent ME voltage coefficients have been estimated for field orientations corresponding to minimum demagnetizing fields and maximum α_E . The dependence of ME voltage coefficients on components volume fractions is obtained. The effect of substrate or template clamping has been described in terms of dependence of α_E on their dimensions.

We consider here the longitudinal mode for nanobilayers and thickness mode for nanowires and nanopillars. Numerical estimations are made for the nanobilayer, nanowire and nanopillar of nickel ferrite and lead zirconate titanate on MgO substrate. With increasing substrate thickness, the theory predicts a shift in the resonance frequency of bilayer along with a decrease in the ME interaction due to the clamping effect. A similar effect is obtained at increasing the template radius for nanowire of same composition. The strongest interactions are expected for ferrite nanopillars in a piezoelectric matrix when the pillar height is large compared to substrate thickness.

The model is useful for measurements of ME constants and for the design and analysis of ME material based electronic devices.

Support by RFBR (project 06-08-00896-a) and Russian Ministry for Education and Science (Program "Development of Higher School Scientific Potential") is acknowledged.

[1] M.I. Bichurin, D.A. Filippov, V.M. Petrov, V.M.Laletsin, N.Paddubnaya and G.Srinivasan, Phys. Rev.B **68**, 132408 (2003).

24PO-7-69

DYNAMICS OF DOMAIN WALLS IN MULTIFERROICS

Gerasimchuk V.S.¹ and Shitov A.A.²

¹National Technical University of Ukraine “Kyiv Polytechnic Institute”

37 Peremohy Ave., 03056 Kyiv, Ukraine

²Donbass National Academy of Civil Engineering and Architecture

2 Derzhavin Str., 86123 Makeevka, Ukraine

The nonlinear dynamics of 180-degree domain walls in multiferroics with the crystal symmetry C_{2v} is theoretically investigated. The two-sublattice model of a weak ferromagnet with domain walls of ab-type is described. This model can be used for the description of rhombic multiferroics of the type of Ni-Cl boracites or rare-earth manganites [1].

The density of Lagrange function written in terms of unit antiferromagnetism vector is used for the description of nonlinear dynamics. All basic types of interactions are taken into account: exchange interaction, Dzyaloshinskii interaction (a weak ferromagnetism takes place in a plane perpendicular to the pyroelectric axes [2]), magnetic anisotropy energy, energy of interaction with an external variable magnetic field, and linear magnetoelectric interaction.

Under the assumption of smallness of magnetic and electric fields amplitudes, one of the versions of perturbation theory for solitons is used for the analysis of the movement of a domain wall [3]. We obtain the equations for oscillatory and translational movements (drift) of domain wall, respectively, which are linear and quadratic on the amplitude of a variable field. We find the dependence of the domain wall drift velocity on the frequency and polarisation of external fields

$$V_{dr} = \nu_0 [A_1(\omega, \chi) + D_1(\omega, \chi)] H_{0x} H_{0y} + \tilde{\nu}_0 [A_2(\omega, \chi) + D_2(\omega, \chi)] H_{0z} E_{0y},$$

where ν_0 and $\tilde{\nu}_0$ are the mobilities of the domain wall depending on parameters of a material, H_{0i} is the amplitude of a magnetic field, E_{0y} is the amplitude of electric field, and $A_j(\omega, \chi)$ and $D_j(\omega, \chi)$ are the terms depending on the frequency ω and phases shift χ . The term $D_j(\omega, \chi)$ is connected with the presence of Dzyaloshinskii interaction in multiferroics, the term $A_j(\omega, \chi)$ does not depend on Dzyaloshinskii interaction and is nonzero in “pure” antiferromagnet.

The comparative analysis of the contributions $A_j(\omega, \chi)$ and $D_j(\omega, \chi)$ into the drift velocity depending on the frequency and phases shift is performed. In the region near the frequency of activation of the lower branch of volume spin waves the functions $A_j(\omega, \chi)$ and $D_j(\omega, \chi)$ have the resonances and peculiarities of the “resonance-antiresonance” type. In a vicinity of these frequencies in external fields $H_{0i} \sim 1 \div 10$ Oe, $E_{0y} \sim 0,1$ CGSE units, the drift velocity of domain walls can reach several cm/c, and even several m/c under certain conditions.

[1] T.K. Soboleva and E.P. Stefanovskii, *Low Temp. Phys.* **10**, 620 (1984).

[2] I.H. Brunskill and H. Schmid, *Ferroelectrics* **36**, 395 (1981).

[3] A.L. Sukstanskii and V.S. Gerasimchuk, *Ferroelectrics* **162**, 1-4, 293 (1994).

24PO-7-70

MAGNETIC INTERMEDIATE STATE IN THE TERBIUM IRON BORATE $\text{TbFe}_3(\text{BO}_3)_4$

*Bedarev V.A.*¹, *Bezmaternykh L.N.*², *Gnatchenko S.L.*¹, *Pashchenko M.I.*¹, *Temerov V.L.*²

¹B. Verkin Institute for Low Temperature Physics and Engineering of the National Academy of Sciences of Ukraine, 47 Lenin Ave., Kharkov 61103, Ukraine

²L.V. Kirenskii Institute of Physics, Siberian Branch of RAS, 660036 Krasnoyarsk, Russia
e-mail: bedarev@ilt.kharkov.ua

Spin-orientation first order phase transition is observed in an external magnetic field in the terbium iron borate $\text{TbFe}_3(\text{BO}_3)_4$ [1]. In the vicinity of first order phase transition a magnetic intermediate state (MIS) with periodical domain structure can arise in antiferromagnetic [2]. The main cause of MIS appearing is demagnetization magnetic field which arises in antiferromagnetic in a magnetic field. In this report the results of the magneto-optical and visual investigations of MIS in the crystal $\text{TbFe}_3(\text{BO}_3)_4$ are presented.

In this study the $\text{TbFe}_3(\text{BO}_3)_4$ single crystal plate was cut perpendicular to the c axis. Crystal dimensions were $2,5\text{mm} \times 2,5\text{mm} \times 110\mu\text{m}$. The investigations of MIS were carried out by means of visual observations of the magnetic domain structure formed in the vicinity of the first order phase transition and with studying of the field dependences of the Faraday rotation.

By using visual observations it was established that the antiferromagnetic state and high field magnetic phase coexist in the vicinity of spin-orientation phase transition. As a rule, a high field magnetic phase appears as cylindrical magnetic domains in the magnetic field H_1 . The cylindrical domains transform into labyrinth magnetic domain structure with the increasing of magnetic field. The further increasing of magnetic field to H_2 results to the homogeneously magnetic state. The fields H_1 and H_2 were measured by means of the visual observation and studying of the field dependences of Faraday rotation at different temperatures. It was made possible to define the area of existence of MPS in H - T plane in the interval of temperatures from 6 to 15 K.

The energy of domain wall between an antiferromagnetic and high field magnetic phase was calculated using the experimental dates. This energy is determined by the following expression [3]:

$$\sigma = \frac{D^2 \cdot \Delta M^2 \cdot F(\rho)}{t} \quad (1)$$

Here t is a thickness of the plate, D – is a period of labyrinth magnetic domain structure, ΔM is a jump of magnetization at the first order phase transition, ρ is a concentration of magnetic phase, $F(\rho)$ is a function depending on ρ . Substitution of experimental parameters $\Delta M \approx (H_2 - H_1)/4\pi \approx 310 \text{ G}$, $D = 16 \mu\text{m}$, $t = 110 \mu\text{m}$, and value $F(0,5) \approx 7,9 \times 10^{-2}$ [4] in (1) results in $\sigma \approx 1,8 \text{ erg/cm}^2$.

[1] Ritter C., Balaev A., Vorotynov A. et al., *J.Phys.: Condens. Matter* **19** (2007) 196227.

[2] Baryakhtar V.G., Bogdanov A.N. et al., *Usp. Fiz. Nauk.* **156** (1988) 47.

[3] Baryakhtar V.G., et al., *Zh. Eksp. Teor. Fiz.* **62** (1972) 2233.

[4] Popov V.A. *Fiz. Niz.Temp.* **1** (1975) 1020.

24PO-7-71

**CORRELATION BETWEEN IONIC RADIUS OF SUBSTITUTING
ELEMENT AND MAGNETIC PROPERTIES OF $\text{Bi}_{1-x}\text{A}_x\text{FeO}_{3-x/2}$
(A= Ca, Sr, Pb, Ba) MULTIFERROICS**

Khomchenko V.A.¹, Kopcewicz M.², Pogorelov Y.G.³, Araujo J.P.³, Vieira J.M.¹, Kholkin A.L.¹

¹Department of Ceramics and Glass Engineering & CICECO, University of Aveiro,
3810-193 Aveiro, Portugal

²Institute of Electronic Materials Technology, Wolczynska street 133,
01-919 Warsaw, Poland

³IFIMUP/ Department of Physics, University of Porto, Rua Campo Alegre 687,
4169-007 Porto, Portugal

Multiferroics have become an object of growing interest due to the coexistence of magnetic order and ferroelectric polarization combined in a single-phase material. This interest is motivated by their great potential due to the mutual control of magnetic and polar states and by the rich physics that is expected in this class of solids. However, most magnetic ferroelectrics tend to have low magnetic ordering temperature and are often antiferromagnets, in which the magnetoelectric effect is intrinsically small. BiFeO_3 perovskite, in which the stereochemical activity of the Bi lone electron pair gives rise to ferroelectric polarization, while the partially filled 3d orbitals of the Fe^{3+} ions cause G- type antiferromagnetic order, seems to be the most suitable object for multiferroic research in view of its high magnetic and ferroelectric ordering temperatures ($T_N \sim 640$ K, $T_C \sim 1100$ K). On the other hand, spiral spin modulation, superimposed on the G- type antiferromagnetic spin ordering, cancels out any possible net magnetization and inhibits the observation of linear magnetoelectric effect.

One of the ways to suppress the spiral spin modulation in BiFeO_3 is a chemical substitution in the A-sublattice of the ABO_3 perovskite. Spontaneous magnetization was revealed both for the $\text{Bi}_{1-x}\text{RE}_x\text{FeO}_3$ (RE= Nd, Sm, Tb) solid solutions doped by magnetically- active rare-earth ions and for the diamagnetically- substituted $\text{Bi}_{1-x}\text{A}_x\text{FeO}_3$ (A= La, Ba, Pb) compounds. It was found that value of net magnetization depends strongly on the kind of the diamagnetic substituting element. For instance, the spontaneous magnetization of the Ba- doped samples is at least an order of magnitude greater than that observed for the La- doped solid solutions at the same doping concentration. While the dependency between a kind of the substituting element and the magnetization value might be natural for the rare-earth substitution, which can induce additional magnetic contribution at sufficient concentrations (at low temperature), the nature of a correlation between the kind of a diamagnetic dopant and magnetic properties of samples is not quite clear.

In order to unveil the main regularities of changes of crystal structure, ferroelectric and magnetic properties of the BiFeO_3 -based multiferroics under diamagnetic A- site substitution, we have performed synthesis and investigation of the $\text{Bi}_{1-x}\text{A}_x\text{FeO}_3$ (A= Ca, Sr, Pb, Ba; $x = 0.2, 0.3$) polycrystalline samples. It has been shown that the heterovalent A^{2+} substitution result in the formation of oxygen vacancies in the host lattice. The solid solutions have been found to possess a rhombohedrally distorted perovskite structure described by the space group R3c. Piezoresponse force microscopy have revealed signs of existence of the ferroelectric polarization in the samples at room temperature. Magnetization measurements have shown that magnetic state of these compounds is determined by the ionic radius of the substituting elements. The highest values of the magnetization were observed for the samples doped by the biggest ionic radius ions (Pb^{2+} , Ba^{2+}), suggesting their ability to have an effective influence on the parameters controlling the magnetic anisotropy in the spin magnets and to induce the transition from a spatially- modulated antiferromagnetic spin structure to a homogeneous weak ferromagnetic state.

24PO-7-72

MAGNETIC PROPERTIES OF Co-DOPED CuB_2O_4 *Udod L.V.¹, Sablina K.A.¹, Pankrats A.I.¹, Szymczak R.²*¹L.V. Kirensky Institute of Physics SB RAS, Akademgorodok, 660036, Krasnoyarsk, Russia²Institute of Physics, Polish Academy of Sciences, 02-668, Warsaw, Polande-mail: luba@iph.krasn.ru

The magnetic properties of CuB_2O_4 have been presented in numerous works for last years. Neutron elastic scattering studies showed that, in the absent the magnetic field, incommensurate magnetic state with the structure wave vector oriented along the tetragonal axis is established below $T^* = 9,5$ K [1]. It was shown by magnetic and resonance investigations that for CuB_2O_4 in temperature range of 9.5 – 20 K there occurs a phase transition from the state without a spontaneous moment to the field-induced weak ferromagnetic state. It is assumed that a long-periodic modulate structure is formed in this temperature range [2]. The distinguishing feature of CuB_2O_4 is the presence of two magnetic subsystems of copper ions with distinct magnetic dimension and order. The subsystem (A) is strong one which is magnetically ordered below $T_N = 20$ K and the weak subsystem (B) ordered partially by the exchange interaction with Cu^{2+} of subsystem (A) [3]. Although the subsystem (B) is weak it plays an important role in the formation of the magnetic incommensurate modulate state forming with a subsystem (A) the spiral magnetic structure.

The effect of Cu^{2+} substitution by Ni^{2+} and Mn^{2+} ions occurring mainly in weak B-subsystem results in the change of magnetic state CuB_2O_4 at $T > 9.5$ K [4]. We report the magnetic properties of Co-doped CuB_2O_4 in this paper. The single crystals of $\text{Cu}_{0.98}\text{Co}_{0.02}\text{B}_2\text{O}_4$ were grown by spontaneous crystallization. The magnetic measurements of Co-doped CuB_2O_4 were carried out using SQUID magnetometer at various temperatures and magnetic field perpendicular to the tetragonal axis of the crystal. A drastic increase of magnetization is observed for Co-doped samples in comparison with pure CuB_2O_4 . The deviation of reciprocal susceptibility from Curie-Weiss law for CuB_2O_4 is begins approximately at $T = 140$ K whereas for Co-doped samples this deviation begins at $T = 40$ K. The value of the paramagnetic Curie temperature reduced from $\theta_{\perp} = -23$ K for pure CuB_2O_4 down to $\theta_{\perp} = -8$ K for $\text{Cu}_{0.98}\text{Co}_{0.02}\text{B}_2\text{O}_4$ crystals. The temperature dependence of magnetization for $\text{Cu}_{0.98}\text{Co}_{0.02}\text{B}_2\text{O}_4$ measured in magnetic field of 1.5 Oe shows that the temperatures T^* and T_N are decreased. It can be supposed that the Co ions replaced Cu ions not only in B-subsystem but also in A-subsystem. The field dependence of magnetization for $\text{Cu}_{0.98}\text{Co}_{0.02}\text{B}_2\text{O}_4$ shows that the phase transition from modulate state to the field-induced weak ferromagnetic state is absent in temperature range 9.5-20 K. The change of the critical fields of phase transition from incommensurate spiral magnetic structure to commensurate one was observed for Co-doped CuB_2O_4 . Substitution Cu^{2+} ions by Co^{2+} mainly in B-subsystem is resulted to destruction of spiral incommensurable structure at lower temperatures.

Thus, our experimental data confirm the important role of subsystem (B) in formation of complex magnetic state in CuB_2O_4 .

[1] B. Roessly, J. Schefer, G. Petrakovskii, et.al. Phys. Rev. Lett. 86, 1885 (2001).

[2] A.I. Pankrats, G.A. Petrakovskii, et.al. JETP Letters, v.78, p.569 (2003).

[3] M. Boehm, B. Roessli, J. Schefer, A.S. Wills et.al., Phys. Rev. B, 68, 024405 (2003).

[4] G.A. Petrakovskii, L.V. Udod, K.A. Sablina et.al. Phys. Met. and Metallog. v. 99, suppl. 1 pp. S53-S56 (2005)

24PO-7-73

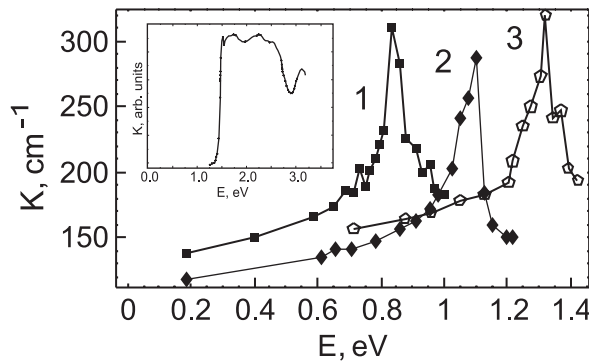
TITLE OF CONTRIBUTION BY CAPITALIZE LETTERS

Zenkov E.V.

Ural State Technical University, 620002, Ekaterinburg, Mira 19, Russia

We propose a semi-quantitative model to account for the unconventional behaviour of optical absorption spectra of copper oxide CuO with respect to the polarization, observed after the bombardment of the samples with alpha-particles. It was found [1], that the optical spectrum, measured in natural light, displays a novel peak (curve 3) within the range 1.2 - 1.4 eV, that is absent in any of two independent orthogonal polarizations (curves 1 and 2).

Clearly, such an effect cannot be understood within the linear response approach, assuming that the unpolarized light may be regarded as a random superposition of two normal modes with different polarizations, that propagate independently through the medium. We show, that these findings may be explained within the model of optical switching centers [2]. Each center is a structure, that is normally frozen in one of its two metastable states, but can switch between



them when absorbing the photons of an appropriate energy, required for the center to jump over the potential barrier. The key point of the model is the special selection rule, imposed on these photon-activated processes: while the transition of the center from state 1 to the state 2 is allowed in a certain photon polarization, the reverse transition from 2 to 1 is only possible in complementary (orthogonal) polarization. When exposed to the natural light, where the photons of both polarization are present, the center will switch continuously between the two states, thus giving rise to the novel channel of optical absorption. This makes it possible to explain the observed anomalous polarization dependence of the spectra. From a microscopic viewpoint, the center can have a variety of prototypes among the systems with spontaneously broken symmetry. Besides the Jahn-Teller molecular cluster, considered in [2], examples include also the magnetic systems and the so-called "purely electronic" analogue of the Jahn-Teller effect in strongly correlated systems [3], that consists in the correlational shift of the electron shells, similar to the conventional vibronic distortion of the lattice.

The work is supported by Grant 07-02-96036 RFBR URAL 2007.

[1] N.N. Loshkareva, Yu.P. Sukhorukov, B.A. Gizhevskii, A.S.Moskvin, T.A. Belykh, S.V. Naumov, A.A. Samokhvalov, *Phys.Solid State* **40** (1998) 383.

[2] E.V. Zenkov, *J. Phys. Chem. of Solids*. **68** (2007) 1973.

[3] A.S. Moskvin, V.A. Korotaev, Yu.D. Panov, M.A. Sidorov, *Physica C* **282** (1997) 1735.

24PO-7-74

SOLITON LATTICE AND ELECTRIC POLARIZATION IN MULTIFERROIC RMn_2O_5

Men'schenin V.V.

Institute of Metal Physics Ural Division of the RAS, S. Kovalevskaya, 18, GSP-170, Russia

At present, there has arisen a great interest in materials known as multiferroics, in which magnetic ordering and electric polarization coexist and are mutually coupled. These materials open up the opportunity to influence using magnetic field and electric field on the electric polarization and the magnetic degrees of freedom, respectively. The manganese oxides with a general formula RMn_2O_5 (R= rare earth) are in particular referred to the multiferroics. The characteristic peculiarities of these oxides are the presence of a large number of the magnetic phase transitions and the complicated magnetic structures. Usually, the transition from paramagnetic to incommensurate magnetic phase takes place upon cooling these materials immediately below the Neel temperature. On further cooling, the existence of a ferroelectric ordering has been established. In the case of $TbMn_2O_5$, for example, the appearance of the electric polarization is not accompanied by the crystal structure change [1], as it would occur upon the ferroelectric phase transition in which the space inversion should vanish as an element of symmetry because the electric polarization changes its sign under the action of the inversion. The further cooling through a "lock-in" temperature results in a new magnetic phase transition, though to a commensurate antiferromagnetic phase.

The purpose of the investigation was to analyze, based on the Landau phase transition theory, in the frame of symmetry description these magnetic phase transitions in $TbMn_2O_5$ and consider the reason of the absence of a structural phase transition when the ferroelectric ordering arises.

It is shown that the thermodynamical potential giving a description of the transition from the paramagnetic to incommensurate phase contains the Lifschit's invariant and admits the appearance of the accompanying ordering parameter, namely, electric polarization with the orientation along the Y axis of the crystal. Hence, the appearance of the magnetic spiral ordering results in the emergence of the irregular electric polarization without a change in the crystal symmetry. On further cooling below the Neel temperature, the magnetic soliton lattice is formed and the system is separated into magnetic and electric domains. The polarization inside the domain is constant. The vectors of polarizations of the nearest neighboring domains are antiparallel to each other. Consequently, in this case the measured values of the polarizations are small. At the temperatures below the "lock-in" temperature the soliton lattice vanishes and there appears one magnetic and one electric domain. It means that there takes place the magnetic transition to the commensurate antiferromagnetic structure.

[1]. G. R. Blake, L.C. Chappon, P.G. Radaelli, S. Park, N. Hur, S-W. Cheong and J.Rodriguez-Carvajal. Rhys.Rev. B **71**, 214402 (2005).

24PO-7-75

MAGNETIC AND MAGNETORESONANCE PROPERTIES OF INITIAL AND QUENCHED SPIRAL ANTIFERROMAGNET LiCu_2O_2

Pankrats A.^{1,2}, Petrakovskii G.^{1,2}, Sablina K.¹, Popov M.^{1,2}, Szymczak R.³

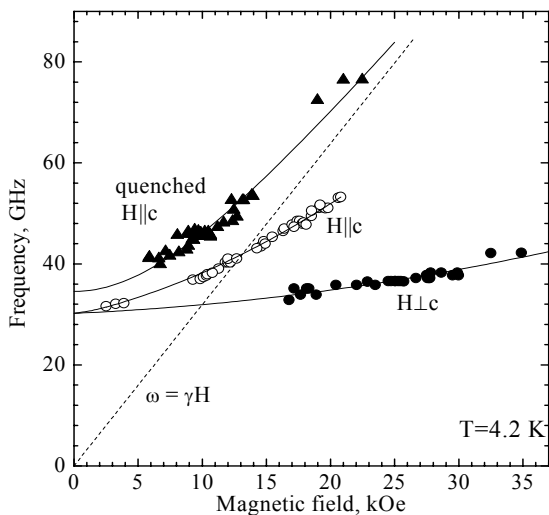
¹L.V. Kirensky Institute of Physics SB RAS, Akademgorodok, 660036, Krasnoyarsk, Russia

²Siberian Federal University, 660079, Krasnoyarsk, Russia

³Institute of Physics, Polish Academy of Sciences, 02-668, Warsaw, Poland

The crystal structure of orthorhombic quasi-one-dimensional compound LiCu_2O_2 is formed by double chains of Cu^{2+} ions that run along the crystallographic \mathbf{b} -axis. The chains are separated by similar chains with Li^+ ions in (\mathbf{ab}) plain and by nonmagnetic layers of Cu^+ ions along \mathbf{c} -axis. The crystal has a tendency to chemical disorder because Li^+ and Cu^{2+} ions have similar oxygen surroundings and some part of ions can change their places. We studied the magnetic and magnetic resonance properties of initial (i.e. as grown) and quenched single crystals of LiCu_2O_2 with various extent of chemical disorder.

The high temperature parts (above ~ 30 K) of magnetic susceptibility of initial LiCu_2O_2 for $\text{H}\parallel\mathbf{c}$ and $\text{H}\perp\mathbf{c}$ are well described by model of interacting antiferromagnetic chains with



effective exchange parameters $J_{\text{eff}} = 33.1$ K in a chain and $|J'| = 8.2$ K between chains. Magnetic resonance study of initial LiCu_2O_2 revealed the energy gap $\nu_c = 31.3$ GHz at $T = 4.2$ K for both $\text{H}\parallel\mathbf{c}$ and $\text{H}\perp\mathbf{c}$ directions (see Figure, open and close circles). The existing of the gap indicates the magnetic order which appears below $T_N = 22.5$ K probably due to: (a) exchange coupling through Cu^{2+} bridge ions arising due to the some chemical disorder and (b) exchange interaction through sequences Cu-O-Me-O-Cu where $\text{Me} = \text{Li}^+$ or Cu^+ for coupling in (\mathbf{ab}) layer and between layers, accordingly.

The unusual frequency-field dependencies crossing the $\omega = \gamma H$ dotted line are caused by spiral magnetic order of initial LiCu_2O_2 with spiral plane close to (\mathbf{ab}) one and propagation vector along \mathbf{b} -axis [2,3]. The spiral order is explained by the strong in-chain frustration of ferromagnetic nearest- and antiferromagnetic next-nearest-neighbor (nn and nnn) interactions.

Using the tendency of lithium and copper ions to change positions we can control the exchange interactions both in chains and between them. The temperature dependencies of magnetic susceptibility of LiCu_2O_2 quenched from $T = 920^\circ\text{C}$ consist of two contributions. One of them is similar to that for initial crystal but with diminished value of effective parameter of in-chain exchange interaction $J_{\text{eff}}^q = 26.1$ K and the second contribution obeys the Curie-Weiss law.

The last contribution is paramagnetic and most likely is concerned with arising of fragments of Cu^{2+} chains with uncompensated spins due to strong chemical disorder. The disorder is probably a reason of some diminishing of in-chain exchange parameter and of the change of the frustration parameter for nn and nnn interactions. As a result the frequency-field dependency of quenched LiCu_2O_2 (close triangulars) becomes usual for orthorhombic antiferromagnets tending asymptotically to $\omega = \gamma H$ line.

[1] A.Vorotynov, A.Pankrats, G.Petrakovskii, et al., *JETP*, **86** (1998) 1020.

[2] Masuda T., Zheludev A., Bush A., et al., *Phys. Rev. Lett.*, **92** (2004) 177201.

[3] A.A.Gippius, E.N.Morozova, A.S.Moskvin, et al., *Phys. Rev.B*, **70** (2004) 020406.

24PO-7-76

LOW-DIMENSIONAL SPIN-1/2 SYSTEMS IN VANADIUM OXIDES: MAGNETIC PROPERTIES OF $\text{Ag}_2\text{VOP}_2\text{O}_7$ and AgVOAsO_4

Tsirlin A.A.¹, Nath R.², Geibel C.², Rosner H.²

¹Department of Chemistry, Moscow State University, 119992 Moscow, Russia

²Max Planck Institute CPFS, Noethnitzer Str. 40, 01187 Dresden, Germany

Low-dimensional spin-1/2 systems attract attention due to a number of unusual quantum phenomena (spin liquid ground state, magnetoelectric effect, ballistic heat transport) that are of interest in both fundamental and applied aspects. The search for novel materials realizing low-dimensional spin systems remains a challenging task of solid state science. The scope of the respective studies is often restricted to the compounds of Cu^{+2} , although other transition metal cations can also provide unusual low-dimensional magnetism. In particular, V^{+4} is interesting due to its similarity to Cu^{+2} in the electronic configuration and the difference in the orbital state. Basically, vanadium oxides and cuprates can show similar physics with different energy scale of magnetic interactions. Exchange couplings in many vanadium oxides are usually weak enabling high-field studies as an additional possibility to influence the ground state of the system.

In this contribution, we present the magnetic properties of two silver vanadium oxides, $\text{Ag}_2\text{VOP}_2\text{O}_7$ and AgVOAsO_4 . To get a proper understanding of the respective spin systems, we use both experimental and computational techniques. Experimental methods include magnetic susceptibility measurements and the analysis of the data using model expressions, while computational methods deal with band structure calculations, estimates of individual exchange couplings, and a construction of reliable microscopic models for the systems under investigation.

Crystal structures of both the compounds are composed of V^{+4}O_6 octahedra and non-magnetic PO_4 (AsO_4) tetrahedra that form layers in $\text{Ag}_2\text{VOP}_2\text{O}_7$ and three-dimensional framework in AgVOAsO_4 . Silver cations are located between the layers in $\text{Ag}_2\text{VOP}_2\text{O}_7$ or in the voids of the V–As–O framework in AgVOAsO_4 . In the former compound, VO_6 octahedra are not directly connected to each other, while in the latter one the octahedra share corners and form chains. Despite the differences in the crystal structure, the magnetic properties of the two compounds are somewhat similar. Magnetic susceptibility data reveal a spin gap-type behavior.

Band structure calculations enable to interpret the observed magnetic properties on the microscopic level. In case of $\text{Ag}_2\text{VOP}_2\text{O}_7$, one of the nearest-neighbor interactions is strong (~ 30 K), and spin dimers are formed. Inter-dimer couplings (both nearest- and next-nearest-neighbor) are weak (below 5 K) and frustrated. The spin system can be described as an alternating zigzag chain close to the dimer limit. The respective spin model has been extensively studied theoretically, and its experimental realization in $\text{Ag}_2\text{VOP}_2\text{O}_7$ may be helpful for verifying the theoretical results. From the structural point of view, the formation of spin dimers in $\text{Ag}_2\text{VOP}_2\text{O}_7$ is highly unexpected. Two nearest-neighbor superexchange pathways have similar geometry, but only one of these pathways gives rise to strong magnetic interactions.

In case of AgVOAsO_4 , the crystal structure suggests one-dimensional magnetic behavior caused by the chains of corner-sharing VO_6 octahedra. However, these chains are uniform and incompatible with the spin gap-type magnetic behavior. Our computational analysis shows that the spin system of AgVOAsO_4 is really one-dimensional, but the magnetic chains do not coincide with the structural ones. Non-magnetic AsO_4 tetrahedra provide two nonequivalent pathways along the chains resulting in alternating spin chains ($J_1 = 41$ K, $J_2 = 26$ K) and spin gap-type behavior. The interchain couplings are frustrated.

Our work presents novel unusual low-dimensional spin systems in vanadium oxides and emphasizes the importance of electronic structure based microscopic modeling for the proper understanding of the respective systems.

Financial support of RFBR (07-03-00890), GIF (I-811-275.14/03), and the Emmy Noether Program of the DFG is acknowledged.

24PO-7-77

INVESTIGATION OF STRUCTURAL AND MAGNETIC PROPERTIES OF COMPLEX COMPOUNDS OF Mn, Co AND Ni WITH CARBAMIDE AND ATHETAMIDE

*Kuvandikov O.K.¹, Shakarov X.O.¹, Nasimov Kh.M.², Shodiyev Z.M.¹, Amonov B.U.¹,
Salakhitdinova M.K.¹, Eshmirzaeva M.¹, Qobilova N.¹, Dustmuhammedov Kh.¹*

¹Samarkand State University, Department of Physics. University blvd. 15, Samarkand, 703029, Uzbekistan, e-mail: kuvandikov@rambler.ru

²Samarkand State University, Department of Chemistry. University blvd. 15, Samarkand, 703029, Uzbekistan

The aim of this work is synthesis and study of structure and magnetical properties of pseudoligand complexes of chloride on the base of Mn, Co and Ni with carbamide and athetamide $[\text{Mn}\cdot\text{KA}\cdot\text{AA}]\text{SO}_4$, $[\text{Mn}\cdot\text{KA}\cdot\text{TKA}]\text{SO}_4$, $[\text{Co}\cdot\text{KA}\cdot\text{AA}]\text{SO}_4$, $[\text{Co}\cdot\text{KA}\cdot\text{TKA}]\text{SO}_4$, $[\text{Mn}\cdot\text{KA}\cdot\text{TKA}\cdot 4\text{H}_2\text{O}]\text{Cl}_2$, $[\text{Ni}\cdot\text{KA}\cdot\text{TKA}\cdot 6\text{H}_2\text{O}]\text{SO}_4$ where KA is carbamide $\text{CO}(\text{NH}_2)_2$, AA is athetamide CH_3CONH_2 and TKA is thiocarbamide $\text{CS}(\text{NH}_2)_2$. The absorption spectra of samples have been obtained by spectrophotometer SPEORD-75 ($400\text{-}4000\text{ cm}^{-1}$) POE and NICAM ($200\text{-}4000\text{ cm}^{-1}$) with application pressing of KBr method. Thermo-analysis was carried out on derivatograph of Paulic-Paulic-Erdoy system with rate 10 deg/min and mass 0.1 g .

Magnetic studies were carried out by Faraday-Seksmit method. Magnetic properties of studied samples represent more complicated picture in complex compound on base of nickel. The temperature dependence of magnetic susceptibility $\chi^{-1}(T)$ reveals straight line with breaks at temperature $60\text{ }^\circ\text{C}$. The reason of the break in dependence $\chi^{-1}(T)$ of studied samples one can explain, obviously, by polymorphic transformation that takes place in their crystalline lattices as depending on concentration of added ligands. In complex compound on the base of Co at temperature increase the magnetic susceptibility $\chi^{-1}(T)$ is linearly increased. It is explained that magnetic susceptibility of this complex compound follows Curie-Weiss law. Obtained results are discussed on the base of the field theory of ligands of crystalline lattice.

24PO-7-78

SYNTHESIS OF MnGeO_3 POLYCRYSTALLINE AND SINGLE CRYSTAL SAMPLES AND COMPARATIVE ANALYSIS OF THEIR MAGNETIC PROPERTIES

Sapronova N.¹, Volkov N.^{1,2}, Sablina K.¹, Petrakovskii G.^{1,2}, Bauykov O.¹, Velikanov D.¹, Vorotynova A.¹, Bovina A.¹

¹Kirensky Institute of Physics SB RAS, Krasnoyarsk 660036, Russia

²Siberian Federal University, 660079 Krasnoyarsk, Russia

Among manganese oxides there are compounds that exhibit magnetoelectricity. The formation of magnetoelectric domains in $\text{Mn}_{0.94}\text{Mg}_{0.06}\text{GeO}_3$ single crystals was reported [1]. Previously, the magnetoelectric effect in MnGeO_3 polycrystalline samples below $T_N=16$ K was observed [2]. This study is devoted to the investigation of the magnetic properties of MnGeO_3 single crystals grown by the flux method. These crystals are characterized by orthorhombic symmetry with space group P_{bca} . Magnetic measurements carried out on the MnGeO_3 single crystal have revealed higher values ($T_N=38$ K, $\theta=-100$ K) as compared to the data for polycrystalline samples reported in the literature ($T_N=10$ K, $\theta=-54$ K; $T_N=16$ K, $\theta=-46$ K). For polycrystalline samples synthesized by us these magnetic parameters are close to the literature data.

We show that the magnetic behavior of MnGeO_3 is sensitive even to minor impurity amount and to synthesis conditions.

The MnGeO_3 magnetic structure and one of possible reasons causing the effect of impurities on the MnGeO_3 magnetic properties are considered in the framework of a simple indirect coupling model. The study of magnetoelectric properties of MnGeO_3 are in progress.

[1] P.J. Brown, J. B. Forsyth, F. Tasset, *Solid State Science* **7** (2005) 682.

[2] G.Gorodetsky. *Phys.Letters* **39A** (2005) 155.

25 June Wednesday

10:00-11:30

12:00-13:30

oral session

25TL-A

25RP-A

**“Diluted Magnetic
Semiconductors”**

25TL-A-1

HOMOPOLAR BOND FORMATION IN FRUSTRATED SPINELS NEAR THE ITINERANT ELECTRON LIMIT

Baldomir D.^{1,2}, Pardo V.^{1,2}, Blanco-Canosa S.³, Rivadulla F.³, Khomskii D.I.⁴, Wu Hua⁴, Piñeiro A.^{1,2}, Arias J.E.², Rivas J.¹

¹Departamento de Física Aplicada, Universidade de Santiago de Compostela, E-15782, Spain

²Instituto de Investigacións Tecnolóxicas, Universidade de Santiago de Compostela, E-15782, Spain

³Departamento de Química-Física, Universidade de Santiago de Compostela, E-15782, Spain

⁴II Physikalisches Institut, Universität zu Köln, Zùlpicher Str. 77, D-50937 Köln, Germany

The transition between an antiferromagnetic insulator and a paramagnetic metal is associated to some of the most intriguing experimental observations in solid state physics. Unconventional forms of superconductivity, electronic phase separation, and a variety of non-Fermi liquid behaviour are well known examples.

Our work focuses on trigonally distorted V spinels, where the V atoms form a pyrochlore lattice, where the AF interactions are highly frustrated, leading to small T_N/\square_{CW} ratios.

Previous results [1] show that these V spinels approach, under pressure, a metal-insulator transition on reducing the V-V distance. We propose that electron delocalization leads to structural instabilities, not related to orbital ordering, that occur due to the proximity of the material to the itinerant-electron boundary. This mechanism naturally couples charge and lattice degrees of freedom in magnetic insulators close to the itinerant-electron crossover.

This could be the case of ZnV_2O_4 , which is very close to the itinerant-electron limit, according to previous experimental observations [1]. For analysing the properties of this material close to itinerancy, electronic structure calculations have been carried out in the compound. These were based on the density functional theory using a full-potential, all-electron method including strong-correlation effects by means of the LDA+U method. We have relaxed the structural positions in the material. For small values of the on-site Coulomb repulsion U (closer to itinerant behaviour), the most stable structure forms V-V dimers. The V-V distances along the [011] and [101] directions become alternately shorter-longer. Of these, the shorter distance is below the itinerant electron limit for V^{3+} compounds with direct V-V interactions.

Support by the Spanish Ministry of Science and Technology (MEC) through the projects MAT2006/10027 and HA2006-0119 and also by the Xunta de Galicia through the project PXIB20919PR is acknowledged. We also thank the CESGA (Centro de Supercomputación de Galicia) for computing facilities. F.R. also acknowledges MEC for support under program Ramón y Cajal.

[1] S. Blanco-Canosa, F. Rivadulla, V. Pardo, D. Baldomir, M. García-Hernández, J.S. Zhou, J. Rivas and J.B. Goodenough, *Phys. Rev. Lett.*, **99** (2007) 187201.

25RP-A-2

GIANT MODULATION OF RESONANT SPIN-FLIP RAMAN SCATTERING IN CdTe/CdMnTe QWs

Kusrayev Yu.G.¹, Koudinov A.V.¹, Wolverson D.², Davies J.J.², and Wojtowicz T.³

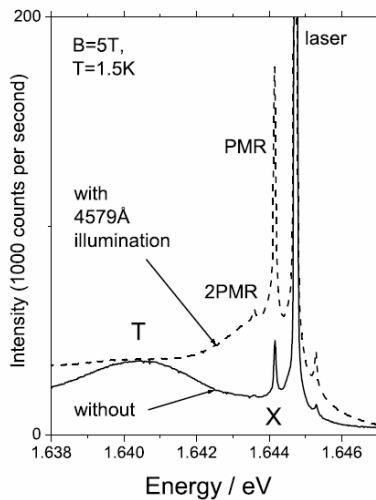
¹A.F.Ioffe Physico-Technical Institute, 194021 St. Petersburg, Russia

²University of Bath, Bath BA7 2AY, UK

³Institute of Physics, Polish Academy of Sciences, 02-668 Warsaw, Poland

Spectroscopy of the near-bandedge optical features in semiconductors and semiconductor nanostructures (QWs, QDs, etc.) can provide massive information about symmetry, band structure and electronic properties of these systems. Such studies generally imply possibility of an additional influence on the system under study.

In the present Letter, we report for the first time the dramatic effect of the additional above-barrier illumination on the resonant spin-flip Raman scattering (SFRS) by diluted magnetic quantum wells CdTe/CdMnTe. We observed up to order-of-magnitude changes of the



intensity of the Raman scattering signal associated with the $\text{Mn}^{2+} 3d^5$ electrons (PMR) or band electrons when the sample was illuminated by rather weak blue-green light. Moreover, in different (but nominally very similar) samples the effect showed opposite sign, and our observations ranged from 5-times increase (see Figure) to 10-15-times decrease of the SFRS intensity when the blue-green light was switched on.

Based on the summary of the observations, we suggest a consistent interpretation of the effect of blue-green light on SFRS intensity. Phenomenologically, this interpretation implies the change of the nonradiative homogeneous linewidth of the excitonic QW states. Microscopically, this change originates from the change of concentration of resident charge carriers in the QW, which may work through, e.g., the rate of trapping the

neutral excitons into trion states. We note that, according to our interpretation, the striking value of the effect on the SFRS intensity is not specific for the SFRS itself. But one factor indeed seems essential – that the SFRS mediated by the neutral exciton states represents truly (or quasi) *doubly-resonant* processes, unlike many other optical processes do.

The suggested interpretation of the main effect involves the idea of variable homogeneous broadening, i.e., variable lifetime of the intermediate exciton states. We believe that the additional illumination supplies the QW by a surplus charge carriers of certain type. Depending on the type of the “dark” 2D gas contained in the QW, this either enriches or depletes the QW layer by charge carriers. Consequently, trapping of neutral excitons into the trion states becomes faster or slower, and it is this process that controls the broadening Γ of the exciton states by means of Heisenberg uncertainty principle.

The large value of the effect in the spin-flip Raman scattering is caused by the strong dependence on Γ , namely Γ^{-3} . Such sensitivity may be used for fine control of the concentration of electron or hole gas in QWs and, in explored systems, for determination of the type of “dark” 2D conductivity of the very dilute gas. We note that the physical situation studied in this Letter looks by no means exceptional. Presence of excitons and trions is a typical feature of QWs in many systems, and these systems are frequently active in resonant SFRS.

Support by Russia Foundation for Basic Research and Academy of Sciences is acknowledged.

25RP-A-3

NOVEL FERROMAGNETIC Mn-DOPED ZnSiAs₂ CHALCOPYRITE WITH CURIE POINT EXCEEDED ROOM TEMPERATURE

Marenkin S.F.¹, Novotortsev V.M.¹, Fedorchenko I.V.¹, Varnavskii S.A.¹, Koroleva L.I.², Zashchirinskii D.M.², Khapaeva T.M.², Szymczak R.³, Krzymanska B.³, Dobrowolski V.³, Kilanski L.³

¹Institute of General and Inorganic Chemistry RAS, Leninskii str. 31, 119991 Moscow, Russia

²M.V. Lomonosov Moscow State University, Vorobyevy Gory, 119992 Moscow, Russia

³Institute of Physics PAS, Lotnicow al., Warsaw 02668, Poland

Diluted magnetic semiconductors have recently new interest because of possible applications in spintronics devices. In this work a new ZnSiAs₂:Mn chalcopyrite is described in which Curie point exceeds room temperature. The value of these compositions is in the fact that they are combined with “siliceous technology”, i.e. it is possibility to make on them of epitaxy and other technological processes allowed to create the devices of the solid state electronics. The samples of ZnSiAs₂ with 1 and 2 wt % Mn were obtained by melting of stoichiometric proportion of Si, ZnAs₂ and Mn high purity powders. To improve the manganese solubility cooling rates were chosen to be 5-10 K/s. Components content was controlled use of a fluorescence analysis. No traces of MnAs or related compounds were found in them by accurate X-ray measurements. The magnetization M was determined using SQUID magnetometer and the electrical resistivity ρ by a four-probe method. Hall effect was measured by standard d.c. method. The temperature dependence of magnetization $M(T)$ has a complicated character: at $T < 15$ K it obeys by Langevin function, that is evidence of superparamagnetic behavior. Difference between FC and ZFC magnetization and shift of the hysteresis loop of FC sample, observed at $T = 5$ K, confirms the superparamagnetic clusters presence. At $T > 15$ K appears a spontaneous magnetization. At $T > 15$ K the magnetization is sum of: spontaneous magnetization M_S and magnetization of superparamagnetic clusters. Spontaneous part of magnetization was separated. It is found that spontaneous magnetic moment on formula unit very understand comparison with the one at total ferromagnetic ordering of spins of Mn²⁺ ions or antiferromagnetic ordering of spins Mn²⁺ and ions Mn²⁺, that is these compounds are frustrated magnetics. Therefore their Curie points were determined by extrapolating the steepest part of $M_S(T)$ curve to intersection with T -axis. They are 325 and 337 K for samples with 1 and 2 wt % correspondingly. Contrary to the conventional superparamagnets in these compounds magnetic moments of clusters depend from the magnetic field value H : 12000 and 20000 μ_B at $H = 0.1$ kOe, 52 and 55 μ_B at $H = 11$ kOe, 8.6 and 11 μ_B at $H = 50$ kOe of compounds with 1 and 2 wt % correspondingly. The $\rho(T)$ -dependence is semiconductive character with an activation energy 0.12 – 0.38 eV at $124 \leq T \leq 263$ K (both compounds). Mobility and concentration of the charge carriers (holes) are 1.33, 2.13 cm²/Vs and 2.2×10^{16} , 8×10^{16} cm⁻³ at $T = 293$ K compounds with 1 and 2 wt % correspondingly. Magnetoresistance of both compounds does not exceed of 0.4 % in $H = 10$ kOe. The peculiarities of magnetic properties are explained by competition of the superexchange and the exchange through the charge carriers. In work [1] was shown that modified RKKI interaction of Mn atoms positioned in the neighbor sites of Ga-sublattice in Ga_{1-x}Mn_xAs leads to their attraction and promotes their clustering. One would expect a conclusion of [1] can be justly for chalcopyrite structure since it is crystallochemical analog of A^{III}B^V. In this case the cluster formation occurs in the same manner as in Ga_{1-x}Mn_xAs.

[1] E.Z. Meilikov, R.M. Farzetdinova, *Phys.Rev.*, **B 75** (2007) 052402.

25RP-A-4

ANISOTROPY OF MAGNETORESISTANCE IN Be CODOPED GaMnAs*Parchinskiy P.B.^{1,2}, Yu Fucheng¹, Chandra Sekar P.V.¹, Kim Dojin¹*¹Department of Materials Science and Engineering, Chungnam National University

220 Gung-dong, Yuseong-ku, Daejeon, 305-764 Korea

²National University of Uzbekistan, Tashkent, 700174, Uzbekistan

Since the discovery of ferromagnetic – paramagnetic transition in InMnAs and GaMnAs grown by low temperature molecular beam epitaxy (LT MBE) Diluted Magnetic Semiconductors (DMS) based on III – V compound alloy doped with 3d magnetic transitional metals attracted great attention as the promising materials for spintronics (area of nanoelectronics based on spin – related phenomena). Because of the processing compatibility with the established semiconductor technologies, this material could easily be integrated with III-V nonmagnetic semiconductor system to create devices that depend on electron charges as well as on their spins.

Among the other properties of DMS, magnetic anisotropy phenomena is one of the most important for successful realization of the spintronics' devices and structures. Although it has been established, that magnetic anisotropy in GaMnAs epitaxial films strongly depends on stress within the film, carriers concentration and temperature some questions about origin of anisotropy phenomena (in particular anisotropy of magnetic properties along equivalent crystalline directions) remain unclear. Hence, detail investigations of anisotropy phenomena in GaMnAs epitaxial films, is necessary from both – basic science and practical point of view. Codoping with Be – which is an effective acceptor nowadays is often used for improving the magnetic properties of GaMnAs. Beryllium atoms, also as the Manganese atoms occupy Ga position in GaAs crystalline lattice. Hence codoping with Be could effect on magnetic anisotropy in GaMnAs as through increasing of hole concentration as well as through alteration of the stress' parameters in the epitaxial layer. However, effect of Be codoping on magnetic anisotropy phenomena in GaMnAs has been hardly studied until now.

Recently it has been demonstrated that information about magnetic anisotropy could be successfully obtained by means magnetoresistance measurements. In this context we have studied the anisotropy of magnetoresistance in GaMnAs epilayers codoped with Be. It was shown that MR effects in both low field and high field region depend on the magnetic field and measuring current relative orientation as well as on crystalline direction of the GaMnAs epilayers. We observed anisotropic magnetoresistance (AMR) in GaMnAs:Be when magnetic field was applied parallel to epilayer surface. However parameters of the AMR in GaMnAs:Be is significantly different from parameter of the AMR in non codoped GaMnAs. The origin of anisotropy phenomena in GaMnAs codoped with Be has been discussed.

25RP-A-5

MAGNETIC PROPERTIES OF SINGLE CRYSTAL $\text{Pb}_2\text{Fe}_2\text{Ge}_2\text{O}_9$

Petrakovskii G.^{1,2}, Balaev A.¹, Sablina K.¹, Bayukov O.^{1,2}, Bovina A.¹, Boehm M.³

¹Kirensky Institute of Physics SB RAS, 660036 Krasnoyarsk, Russia

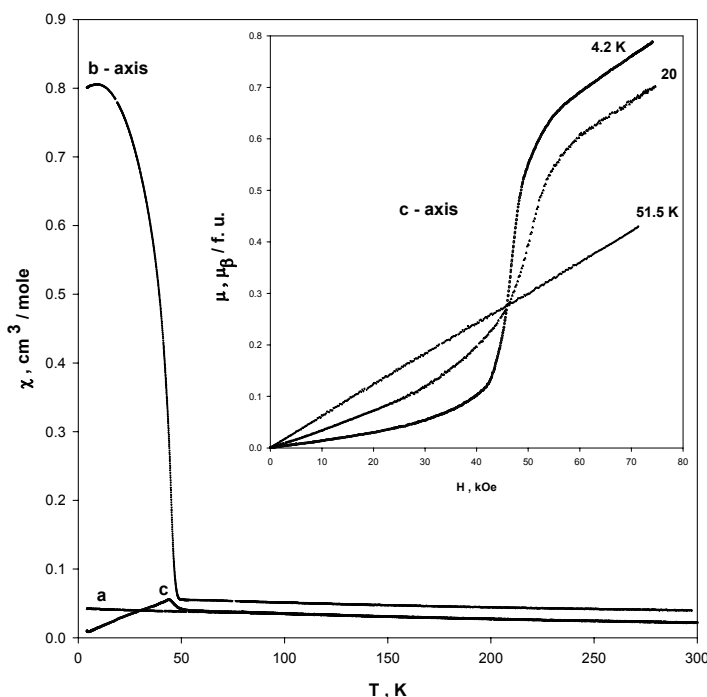
²Siberian Federal University, 660079 Krasnoyarsk, Russia

³Institut Laue-Langevin, Grenoble, France

The single crystal $\text{Pb}_2\text{Fe}_2\text{Ge}_2\text{O}_9$, the germanate analogue of the silicate mineral melanotekite, was grown by a method of spontaneous crystallization from melt with excess PbO and GeO_2 in eutectic ratio. The orthorhombic crystal structure of $\text{Pb}_2\text{Fe}_2\text{Ge}_2\text{O}_9$, the space group Pbcn, consists the zig-zag rows of edge-sharing Fe^{3+}O_6 octahedrons running along [001]direction. The structure contains channels parallel to the a-axis, filled by stereoactive lone pairs of the Pb^{2+} cations. Such compounds are interest as catalysts, electrode materials, adsorbents [1] and can reveal magnetoelectric multiferroic properties [2]. We have investigated the magnetic properties of the $\text{Pb}_2\text{Fe}_2\text{Ge}_2\text{O}_9$. The Neel temperature is about 46 K. The elastic neutron scattering measuring showed that the long range antiferromagnetic ordering takes place at the temperature below 46K.

Figure shows the magnetic susceptibilities χ versus temperature in three directions of magnetic field with respect to the crystallographic axis, $H=1$ kOe. Below T_N pronounced susceptibility anisotropy is observed. For magnetic field applied parallel to the *b*- axis weak ferromagnetic moment arises and one increases below T_N with a decrease in temperature. Along *c*-axis χ has sharp peak near T_N and $\chi_c(T) \rightarrow 0$ at $T \rightarrow 0$. Along *a*-axis χ weak depends on the temperature.

The inset of fig. shows the field dependences of the magnetisation along *c*-axis at the different temperatures. In magnetic ordering phase the spin-flop phase transition at the magnetic field about 45 kOe is observed. The $\text{Pb}_2\text{Fe}_2\text{Ge}_2\text{O}_9$ magnetic structure is considered in the framework of indirect coupling model and it will be discussed.



The inset of fig. shows the field dependences of the magnetisation along *c*-axis at the different temperatures. In magnetic ordering phase the spin-flop phase transition at the magnetic field about 45 kOe is observed. The $\text{Pb}_2\text{Fe}_2\text{Ge}_2\text{O}_9$ magnetic structure is considered in the framework of indirect coupling model and it will be discussed.

[1] S. Barbato *et al*, *ElectroChim. Acta*, **46** (2001) 2767.

[2] D. Khomskii, *JMMM*, **306** (2006) 1.

25RP-A-6

ELEMENT SPECIFIC MEASUREMENTS OF THE STRUCTURAL QUALITY AND MAGNETISM IN $\text{Co}_x\text{Zn}_{1-x}\text{O}$

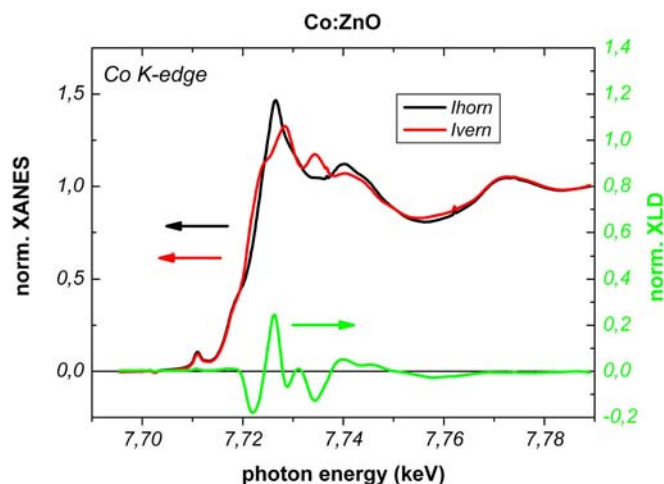
*Kammermeier T.¹, Ney V.¹, Ye S.¹, Ollefs K.¹, Ney A.¹,
Wilhelm F.², Rogalev A.², Kaspar T.³, and Chambers S.³*

¹Experimentalphysik, Universitat Duisburg-Essen, Lotharstr. 1, D-47057 Duisburg, Germany

²European Synchrotron Radiation Facility (ESRF), 6 Rue Jules Horowitz, BP 220, 38043 Grenoble, France

³Pacific Northwest National Laboratory, Richland, Washington 99352, USA

Sparked by theoretical predictions [1], $\text{Co}_x\text{Zn}_{1-x}\text{O}$ is one of the most favoured materials within the search for a doped semiconductor with ferromagnetic properties at room temperature – an essential prerequisite for spintronics. Despite early reports of high temperature ferromagnetism [2] - mainly based on SQUID measurements - the topic becomes more and more controversial since recent reports, claim a paramagnetic behaviour of the Co-sublattice [3] or suggest extrinsic origins of the observed ferromagnetism [4]. Here we present studies on Co:ZnO samples grown either by reactive magnetron sputtering or pulsed laser deposition (PLD). We used X-ray absorption near edge spectroscopy (XANES) at the Co K-edge and the Zn K-edge, respectively. By means of X-ray linear dichroism (XLD) we could examine the local structural environment of the dopant and the cation atoms – an information not accessible by other methods. XLD-simulations using the FDMNES code [5] were calculated to investigate deviations from the ideal wurtzite signature including small clusters of the dopant atom. For PLD-grown samples virtually all Co atoms are on Zn substitutional sites [6]. X-ray diffraction was additionally used for probing the global crystal structure quality. The element specific magnetic properties, as measured by X-ray magnetic circular dichroism (XMCD), are compared to the integral magnetic properties that were investigated by SQUID and electron magnetic resonance. We show that ferromagnetism in Co:ZnO is not likely to be an intrinsic feature. Possible extrinsic origins will be discussed by means of sputtered samples having varying oxygen content.



- [1] T. Dietl et. al. *Science* **287**, 1019 (2000)
- [2] K. Ueda et al. *Appl. Phys. Letters* **79**, 988 (2001)
- [3] A. Barla et. al. *Phys. Rev. B* **76**, 125201 (2007)
- [4] M. Venkatesan et. al. *Appl. Phys. Lett.* **90**, 242508 (2007)
- [5] Y. Joly, *Phys. Rev. B* **63**, 125120 (2001)
- [6] A. Ney et al. (*Phys. Rev. Lett.* (in press, 2008))

25RP-A-7

DEFECT - MEDIATED FERROMAGNETISM IN INSULATING Co-DOPED ANATASE TiO₂ THIN FILMS

Rashkeev S.^{1,2}, Griffin Roberts K.³, Varela M.⁴, Pantelides S.T.^{2,4}, Pennycook S.J.^{4,2}, Krishnan K.M.³

¹Center for Advanced Modeling, Idaho National Laboratory, Idaho Falls, ID 83415, USA

²Dept. Physics and Astronomy, Vanderbilt University, Nashville, TN 37235, USA

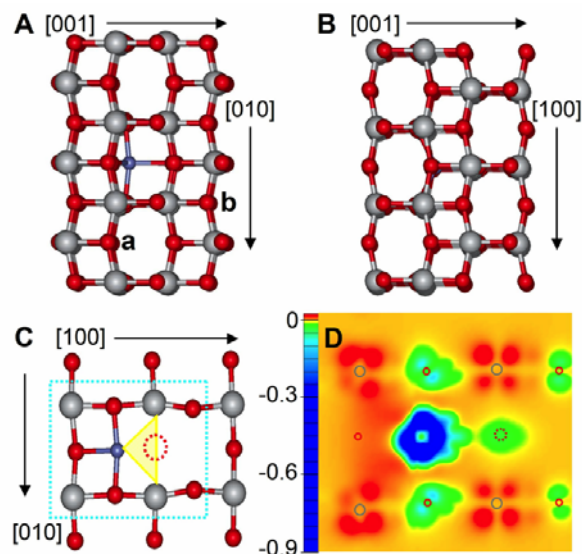
³Dept. Materials Science and Engineering, University of Washington, Seattle, WA 98195, USA

⁴Materials Science and Technology Division, Oak Ridge National Laboratory, Oak Ridge, TN 37831, USA

With the discovery of room-temperature ferromagnetism (RTFM) in Co-doped anatase TiO₂ [1], transition-metal (TM) doped oxides/nitrides have been a major focus in spintronics research. However, the origin of FM and its relationship to semiconducting properties and film microstructure in single-phase TM doped oxides is not well understood. Conventional FM theories cannot explain magnetism in insulators where the dopant concentration is well below the percolation threshold. Similarly, theories of carrier-induced FM are not applicable to these materials which are highly insulating.

Here we report atomic-resolution Z-contrast scanning transmission electron microscopy (STEM) images showing that Co atoms are dispersed and occupy preferred interstitial sites. Density-functional calculations find that these sites are the lowest-energy configuration of Co in anatase and that O vacancies (V_O), introduced by annealing, anchor the Co atoms into Co-Ti⁺³-V_O complexes. The calculated magnetic moment of these defects is in agreement with the measured value and their presence is confirmed by imaging and spectroscopy.

The activation of RTFM in highly insulating anatase Co_{0.03}:TiO₂ is defect-mediated and involves the formation of ordered Co-Ti⁺³-V_O defect complexes. A vacuum annealing process is required to form an ordered distribution of defect complexes by the creation and diffusion of V_O's to Co ions. Because undoped anatase TiO₂ becomes conducting when annealed, it is clear that O vacancies create carriers. However, the presence of a few at% Co creates a superstructure of specific defect complexes which then trap these carriers and mediate the ferromagnetism.



The work was supported through the INL LDRD program under DOE Idaho Operations Office Contract DE-AC07-051D14517. Research at VU was partially supported by the McMinn Endowment. The work at the UW was funded by NSF/ECS No. 0224138 and the Campbell Endowment with partial support (KG) received from UW-PNNL JIN fellowship. Research at ORNL was sponsored by the Office of Basic Energy Sciences, Division of Materials Sciences and Engineering.

[1] Y. Matsumoto *et al.*, *Science* **291**, (2001) 854.

25RP-A-8

ELECTROCHEMICAL PREPARATION OF TRANSPARENT FERROMAGNETIC Fe-Zn-O HETEROGRANULAR FILMS

Izaki M.

Toyohashi University of Technology, Production System Engineering, 1-1 Hibarigaoka, Tenpaku-cho, Toyohashi, 441-8580 JAPAN

Hetero-granular films composed of semiconductor matrix and ferromagnetic nano-sized particles have attracted increasing attentions for electronics applications due to the unique magnetic and electrical characteristics. The use of semiconductor matrix opens new door to fabricate an electronics device with correlation among the charge and spin of electrons. Electrochemical process has several advantages over gas-phase deposition techniques widely used for fabricating electronics devices. The author developed an electrochemical process for preparing a semiconductor high-quality ZnO film.[1,2] And a chemical process for introducing impurities into the ZnO was developed.[3] A transparent Fe-Zn-O hetero-granular film was prepared by combining the electrochemical deposition and chemical introduction and exhibited ferromagnetic and semiconducting features. Here, the characteristics of the Fe-Zn-O hetero-granular films and the structures related to the origin of the ferromagnetic feature are presented.

The ZnO films were deposited on a conductive glass substrate by cathodic electrodeposition in a simple zinc nitrate aqueous solution at 333K and then the ZnO-coated substrate was immersed into an aqueous solution containing iron nitrate at ambient temperature for introducing the Fe impurity into ZnO. The structure was characterized using a transmission electron microscopy(TEM) and X-ray Absorption Fine Structure (XAFS) measurements carried out in Japan Synchrotron Radiation Research Center, SPring8.

The Fe-Zn-O film showed optical transmission around 70% at wave length of 400-800nm, ferromagnetic feature of 6.9 emucm^{-3} in saturation magnetization and n-type semiconductivity of 10^{10} cm^{-3} in carrier concentration and $3.6 \text{ cm}^2 \text{ V}^{-1} \text{ s}^{-1}$ in mobility. Figure shows the TEM image and electron diffraction pattern of the Fe-Zn-O film. The Fe-Zn-O film was composed of wurtzite ZnO hexagonal grains and thin plates (represented by arrows) of about 3 nm in thickness and 70nm in length between the close-packed ZnO grains. And, XAFS measurement exhibited that the thin plate grains was identified as a zinc ferrite with Fe deficient nonstoichiometry. The process composed of the electrochemical oxide formation and chemical impurity introduction is a viable process for fabricating smart materials with controlled characteristics.

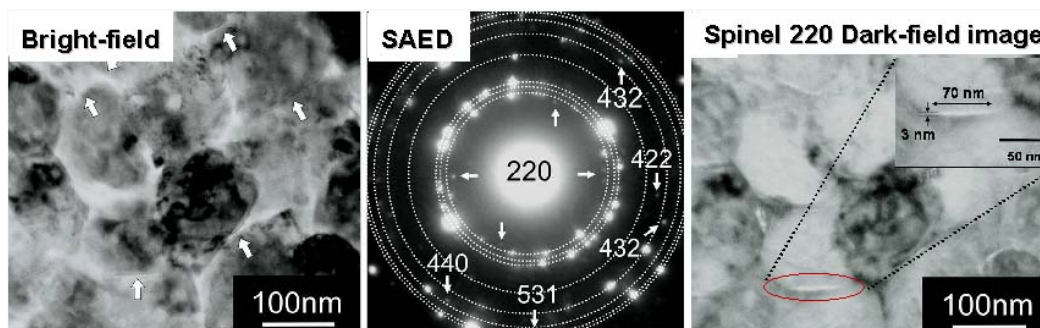


Figure TEM image and SAED patterns for Fe-Zn-O film

[1] M. Izaki, et al., *Appl. Phys. Lett.*, **68**(1996), 2439.

[2] M. Izaki, et al., *Advanced Materials*, **15**(2003),2000.

[3] T. Shinagawa, M. Izaki, et al., *J. Electrochem. Soc.*, **152**(2005), G736.

25RP-A-9

EVIDENCES OF NEARLY-CRITICAL SPIN AND CHARGE FLUCTUATIONS IN HIGH- T_c SUPERCONDUCTING CUPRATES

Caprara S., Di Castro C., Enss T., and Grilli M.

Dipartimento di Fisica – Università di Roma “Sapienza”, Piazzale Aldo Moro, 2 - ITALY

Many experiments and theoretical predictions indicate that the physics of high- T_c superconducting cuprates might be controlled by the proximity to a quantum critical point. One of the candidates for the corresponding ordered phase is a finite-wavelength charge and spin modulation, possibly in the form of stripe-like textures. The question then arises whether and how fingerprints of nearly-critical charge and spin collective modes are seen in various experiments.

We discuss here the evidences of these fluctuations in low-frequency optical [1] and Raman spectra [2], within an effective model of fermion quasiparticles coupled to nearly-critical charge and spin collective modes, which is apt to describe the physical properties of high- T_c superconducting cuprates near a stripe instability.

Recently, the lack of an evident scaling in the far-infrared optical spectra of the cuprates was interpreted as an evidence against quantum criticality. Instead, we argue that optical conductivity might be severely conditioned by momentum conservation, and should vanish in a clean Galilean-invariant system, unless the fermion charge carriers are coupled to dynamical degrees of freedom which dissipate the current. If these degrees of freedom are nearly critical collective modes, this coupling introduces non-universal frequency scales, leaving the way open to a variety of phenomena, ranging from partial scaling of the optical spectra, to the absence of any evident feature to be associated with quantum criticality, in agreement with the experimental findings [3].

On the contrary, Raman spectroscopy is not constrained by momentum conservation. Moreover, the Raman vertices of various symmetries have a characteristic momentum dependence, which might directly probe different regions of the quasiparticle Fermi surface, giving precise indications on the typical wavevectors of the collective modes. We are thus able to explain both the background of the Raman spectra and the critical dispersing peaks which are experimentally observed in the underdoped region of the phase diagram of the cuprates, as well as their specific temperature, doping, and symmetry dependence [4].

Part of this work was supported by the MIUR-PRIN 2005, prot. 2005022492. CDC and TE were also partly supported by the Alexander von Humboldt foundation.

[1] S. Caprara, C. Di Castro, S. Fratini, and M. Grilli, *Phys. Rev. Lett.*, **88** (2002) 147001.

[2] S. Caprara, C. Di Castro, M. Grilli, and D. Suppa, *Phys. Rev. Lett.*, **95** (2005) 117004.

[3] S. Caprara, M. Grilli, C. Di Castro, and T. Enss, *Phys. Rev. B*, **75** (2007) 140505(R).

[4] S. Caprara, C. Di Castro, T. Enss, and M. Grilli, to appear in *J. Phys. Chem. Solids* (2008).

25RP-A-10

GRAIN-BOUNDARY INDUCED FERROMAGNETISM IN DOPED AND UNDOPED NANOCRYSTALLINE ZnO

Straumal B.B.¹⁻³, Mazilkin A.A.², Protasova S.G.², Myatiev A.A.³, Straumal P.B.^{3,4}, Schütz G.¹, Goering E.¹, Baretzky B.¹

¹Max-Planck-Institut für Metallforschung, Heisenbergstrasse 3, 70569 Stuttgart, Germany

²Institute of Solid State Physics, Russian Academy of Sciences, Chernogolovka, Moscow district, 142432 Russia

³Moscow Institute of Steel and Alloys (Technological University), Leninsky prospect 4, 119991 Moscow, Russia

⁴Institut für Materialphysik, Universität Münster, Wilhelm-Klemm-Str. 10, D-48149 Münster, Germany

Ferromagnetic wide band-gap semiconductors like ZnO are very promising materials for the potential device applications in spin-based information processing technologies (spintronics). The ferromagnetism with high Curie temperature (T_c) above room temperature in ZnO was first theoretically predicted by Dietl et al. in 2000. This work stimulated further theoretic developments and huge amount of experimental studies. However, the ferromagnetism in diluted doped ZnO is far from understood. The presence or absence of ferromagnetism in doped ZnO critically depends on the synthesis method. The reasons for this controversy remain unclear. Here we present the results showing that zinc oxide has a definite threshold value, s_{th} , of specific area of intercrystalline boundaries (grain boundaries, GBs), s_{GB} . For Co-doped ZnO $s_{th} = 4 \times 10^6 \text{ m}^2/\text{m}^3$ nearly corresponding to the grain size of 10^{-6} m . If the $s_{GB} < s_{th}$, the Co-doped ZnO is paramagnetic. If $s_{GB} > s_{th}$, the Co-doped ZnO is ferromagnetic. For pure (undoped) ZnO the threshold value of specific GB area is more that two orders of magnitude higher than for the Co-doped one, namely $s_{th} = 1.1 \times 10^8 \text{ m}^2/\text{m}^3$. Using the novel "liquid ceramic" method we succeeded to obtain dense (poreless) nanocrystalline ZnO films with GB specific area above s_{th} . These films possess very reproducible ferromagnetic behavior and T_c above room temperature.

Support by RFBR, DAAD, DFG and BMBF is acknowledged.

25RP-A-11

MAGNETIC PROPERTIES OF GaAs/ δ <Mn>/GaAs/ $\text{In}_x\text{Ga}_{1-x}\text{As}$ /GaAs QUANTUM WELLS

Aronzon B.A.¹, Lagutin A.S.¹, Rylkov V.V.¹, Tugushev V.V.¹, Lashkul A.², Laiho R.², Danilov Yu.A.³, Zvonkov B.N.³

¹Russian Research Center „Kurchatov Institute“, 123182, Moscow, Russia

²Wihuri Physical laboratory, Department of Physics, University of Turku, FIN-20014, Turku, Finland

³Physics-Technological Institute of the Lobachevskii Nizhnii Novgorod State University, 603950 Nizhnii Novgorod, Russia

Magnetic properties of GaAs/ δ <Mn>/GaAs/ $\text{In}_x\text{Ga}_{1-x}\text{As}$ /GaAs quantum wells ($x = 0.16-0.21$) with high mobility of holes ($\mu \approx 1300 \text{ cm}^2/\text{V}\cdot\text{s}$ at 77 K) are studied in steady magnetic fields up to 6 T at temperatures from 3K to 300 K.

The width of these quantum wells was from 90 to 100 nm, and they were prepared on semi-insulating GaAs (100) substrates by means of the metal-organic vapor phase epitaxy using the laser evaporation of a Mn target. Thickness of a GaAs spacer between the 2D channel and Mn δ -layer was around 3 nm, and its thickness was varied from 0.5 up to 1.8 ML.

It was observed that the temperature dependence of magnetization $M(T)$ in structures with the lowest Mn content demonstrate the spin-glass behavior in moderate magnetic fields (0.5 ÷ 1.5 T, see Fig.1) in contrast with structures, where the content of Mn was maximal. The last have shown the appearance of a ferromagnetic ordering in these fields (see insert in Fig.1) at low temperatures, and $M(T)$ curves for “Zero field cooled” and “Field cooled” samples coincide.

It was found that in the quantum wells with the highest Mn content the first order transition takes place at $T < 40\text{K}$ induced by the external magnetic field (Fig.2), and the hysteresis loop reaches 1.5 T at 3 K. In order to explain these experiments a theoretical model was developed assuming the coexistence of interacting ferro- and antiferromagnetic areas inside a GaAs spacer.

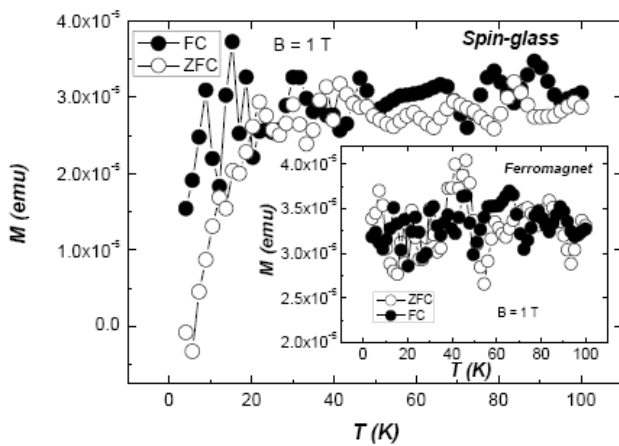


Fig.1

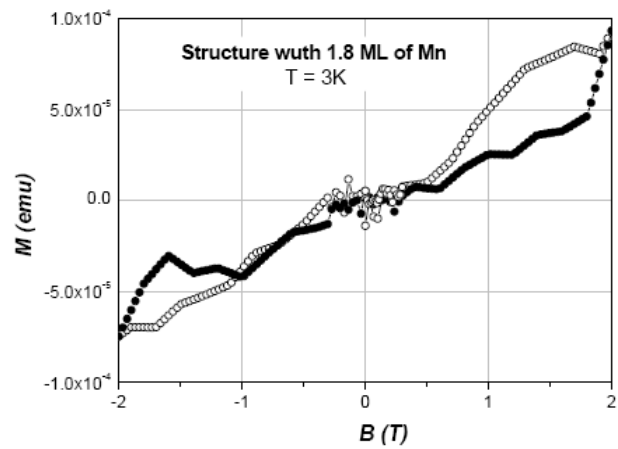


Fig.2

25 June Wednesday

10:00-11:30

12:00-13:30

oral session

25TL-B

25RP-B

**“Amorphous and
Nanocrystalline
Materials”**

25TL-B-1

RECENT PROGRESS IN EXCHANGE ENHANCED NANOCOMPOSITE RARE EARTH-IRON-BORON-BASED HARD MAGNETIC ALLOYS

Davies H.A.¹ and Betancourt I.^{1,2}

¹Dept. Engineering Materials, University of Sheffield, Mappin St., Sheffield S1 3JD, U.K.

²Permanent address: Depto. Materiales Metalicos y Ceramicos, Inst. de Investigaciones en Materiales, UNAM, Mexico, D.F. 04510, Mexico

Rare earth-iron-boron magnets processed via melt spinning to thin ribbon have the advantage over their sinter-route counterparts in being chemically more stable, largely because of their homogeneous microstructure of ultra fine RE₂Fe₁₄B crystallites (typically having a mean diameter d_g of ~ 100 nm). On the other hand, the maximum energy density $(BH)_{\max}$ is substantially limited by the fact that the grain orientations are random, in contrast to the coarser grained sinter-route magnets, which are amenable to field alignment prior to sintering. It has been demonstrated, however, that progressive refinement of d_g below 60 nm results in a progressively increasing degree of ferromagnetic exchange coupling between crystallites, such that the remanent polarisation J_r is progressively enhanced above the Stoner-Wohlfarth limit of $J_s/2$, where J_s is the saturation polarisation (i.e. $J_r > 0.8T$ for (Nd/Pr)₂Fe₁₄B) [1]. This, in turn, gives technologically useful increases in $(BH)_{\max}$ (up to 145kJ/m³ vs. 105kJ/m³ for the conventional commercial alloys).

Further increases in J_r and BH_{\max} can be achieved by employing Fe-rich, off-stoichiometric compositions which yield nanocomposite structures, such as RE₂Fe₁₄B/ α -Fe or RE₂Fe₁₄B/Fe₃B, resulting in additional exchange coupling between the hard and soft phase crystallites and hence in further enhancement of J_r and $(BH)_{\max}$. A prime requirement of such a structure for full exploitation of the effect is that the soft phase crystallites should have d_g smaller than the exchange length l_{ex} (~ 35 nm for the bcc α -Fe) [2]. This requirement is achieved relatively easily under laboratory conditions for alloy ribbon in the as-spun state. However, for production of bonded magnets on a commercial scale it is necessary to use melt spun ribbon that is processed by overquenching to the amorphous state, followed by a controlled devitrification anneal, in order to ensure that the nanostructure and magnetic properties are consistent within and between batches. But a major disadvantage for unmodified, Fe-rich compositions is that such anneals at temperatures below the glass transition temperature yield soft phase grains which are larger than l_{ex} , with a resulting degradation of the squareness of the second quadrant of the BH loop and reduction in $(BH)_{\max}$.

As a consequence of this limitation, recent research has concentrated on doping the Fe-rich alloys with early transition metals such as Nb, Zr, Ta and/or Ti and enhancing the B content in order to impede the interatomic diffusion during the devitrification and to retard the growth rate(s) of the soft phase grains. This strategy has proved to be remarkably successful in yielding good loop squareness and excellent combinations of $(BH)_{\max}$ and intrinsic coercivity iH_c by the overquench/anneal route (e.g. 140kJ/m³/910kA/m for a 2at.% doping with Nb in a (Nd/Pr)₁₀Fe_{80-x}Nb_xB₁₀ alloy [3]). The allowable concentrations of such dopants are, however, restricted by their adverse effects on J_s and on the Curie temperature T_c for the 2/14/1 phase. The reduction in T_c can, nevertheless, be compensated for by partial substitution of Fe by Co without significant degradation of the other magnetic properties.

The present paper will briefly review these recent developments aimed at improving the magnetic properties and the processability of nanocomposite REFeB magnets. The functions of the various alloying modifications will be analysed and the potential for designing compositions

which may be cast to the amorphous state in bulk (section thicknesses $>1\text{mm}$) in order to facilitate small net-shape magnets will also be considered.

- [1] A Manaf, R A Buckley, H A Davies and M. Leonowicz, *J Magn Magn Mater*, 101, 360-362 (1991).
 [2] A Manaf, R A Buckley and H A Davies, *J.Magn.Magn.Mater*, 128, 302-306 (1993).
 [3] I. Betancourt and H.A. Davies, *Appl Phys Lett* 87, 162516-1-3 (2005).

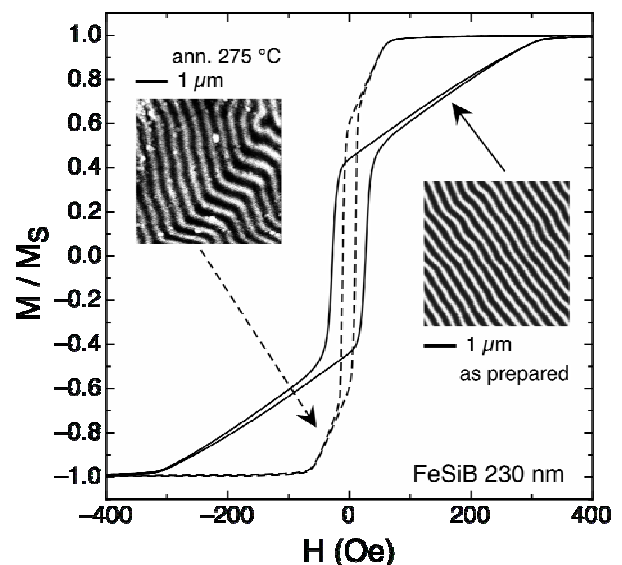
25TL-B-2

STRIPE DOMAINS AND SPIN REORIENTATION TRANSITION IN FeSiB THIN FILMS PRODUCED BY RF SPUTTERING

Coisson M., Vinai F., Tiberto P., Celegato F.

INRIM, Electromagnetism Division, strada delle Cacce 91, I-10135 Torino (TO), Italy

The development of a perpendicular anisotropy in ferromagnetic thin films is still widely studied because of applications in data storage. As a consequence, the discovery more than a decade ago of a spin-reorientation transition (SRT), consisting in a spontaneous switching of the magnetic anisotropy from in-plane to out-of-plane, has attracted much interest [1,2]. In this study, FeSiB thin films have been produced by rf sputtering from a target made by amorphous ribbons. As a function of film thickness t , samples display SRT, from in-plane ($t < 100\text{ nm}$) to out-of-plane ($t > 100\text{ nm}$) anisotropy; in the latter case, stripe domains develop, as observed by magnetic force microscopy (MFM). The stripe domain pattern evolves with t : stripes get larger and for samples thicker than 600 nm tend to become more irregular, and a dominant in-plane magnetization is spontaneously restored. The origin of the observed SRT has probably to be searched in the stresses quenched in the samples during their preparation; their effect is enhanced by the large magnetostriction constant of the studied alloy. Stress relaxation can then be induced by furnace annealing in vacuum, at temperatures up to 375 °C for 60 min for the thickest films; stripe domains on annealed samples become more irregular on increasing annealing temperature (as shown, together with the respective hysteresis loops, in the figure for the sample 230 nm thick in the as prepared state, compared with the one annealed at 275 °C for 60 min), and eventually disappear. Magnetization curves measured with a vector VSM by applying the magnetic field at different angles with respect to the sample allow for a precise determination of the anisotropy constants. A proper vector model for the anhysteretic magnetization process provides a full understanding of the role played by shape and uniaxial (out-of-plane) anisotropies. The effect of thickness and annealing temperature has also been followed on all samples by measuring hysteresis loops and comparing them with magnetic force microscopy images taken at magnetic remanence. SRT can also be induced in samples with in-plane anisotropy at room temperature by cooling down at low temperature, where a spontaneous out-of-plane anisotropy appears. A reversible switch back to in-plane anisotropy is observed on



heating up to room temperature. In spite of the presence of a uniaxial out-of-plane anisotropy responsible for the observed stripe domains on thicker samples, a large fraction of the magnetization of these FeSiB thin films lies in the sample plane, as pointed out by in-plane hysteresis loops. The in-plane component of the magnetization is probably responsible for the direction of the stripe domains, whose orientation is seen by magnetic force microscopy to abruptly change by applying in-plane magnetic fields in the interval where VSM measurements detect the largest in-plane magnetization jump.

[1] D.P. Pappas, K.-P. Kmpfer, H. Hopster, Phys. Rev. Lett. **64**, 3179 (1990).

[2] R. Allenspach, M. Stampanoni, A. Bischof, Phys. Rev. Lett. **73**, 3344 (1990).

25TL-B-3

RECENT ADVANCES IN STUDIES OF MAGNETICALLY SOFT AMORPHOUS MICROWIRES

Zhukov A.^{1,2}, Ipatov M.¹, Gonzalez J.¹, Blanco J.M.³, and Zhukova V.³

¹Dpto. Física de Materiales, Fac. Químicas, UPV/EHU, 20009 San Sebastian, Spain

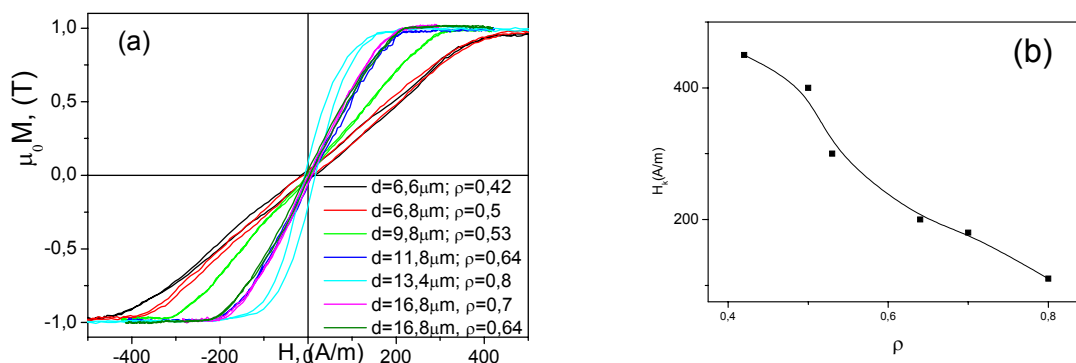
²TAMAG Ibérica S.L., Paseo Mikeletegi 56, 1ª Planta, 20009 San Sebastian, Spain

³Dpto. de Física Aplicada, EUPDS, UPV/EHU, 200018, San Sebastian, Spain

Thin ferromagnetic metallic glass coated microwires exhibit a number of outstanding magnetic properties such as magnetic bistability and GMI effect [1]. Recent studies allow tailoring magnetic properties by selection of appropriate chemical composition, applying appropriate heat treatment and modifying the microwire geometry (the ratio, ρ , of the metallic nucleus diameter to the total microwire diameter). In fact this is important to obtain quite thin microwires with enhanced soft properties and GMI effect for development of micro-sensors, since the demagnetizing factor affects the domain structure and magnetic properties when the geometric ratio of microwire diameter to its longitude becomes low enough [2].

In this paper we present the GMI effect (GMI ratio, $\Delta Z/Z$, and the off-diagonal impedance tensor $\zeta_{\phi z}(H_{ex})$) and hysteretic magnetic properties of amorphous glass-coated microwires with different compositions possessing nearly-zero, positive and negative magnetostriction constant and metallic nucleus diameter ranging within 6 and 16 μm . Special emphasis has been paid to development of stress and temperature sensitive magnetic properties.

Both $\Delta Z/Z$, and hysteresis loops of nearly-zero $\text{Co}_{67.1}\text{Fe}_{3.8}\text{Ni}_{1.4}\text{Si}_{14.5}\text{B}_{11.5}\text{Mo}_{1.7}$ microwires magnetostrictive exhibit strong sensitivity to the ratio, ρ . The hysteresis loops exhibit low coercivity (below 15 A/m) with well defined magnetic anisotropy field, H_k (see Fig. 1a). H_k increases when ρ decreases (see Fig. 1b).



Field dependence of the off-diagonal voltage response of nearly zero magnetostriction ($\lambda_s \approx -3 \times 10^{-7}$) $\text{Co}_{67.1}\text{Fe}_{3.8}\text{Ni}_{1.4}\text{Si}_{14.5}\text{B}_{11.5}\text{Mo}_{1.7}$ with metallic nucleus diameter of 6.0, 7.0 and 8.2 μm exhibits anti-symmetrical shape with almost linear growth within the field range, ΔH .

The obtained results allow us to tailor the microwire magnetic properties for magnetic sensors applications through selection of their composition and/or geometry and by thermal treatment.

[1] D.C. Jiles, *Acta Materialia* **51** (2003) 5907.

[2] A. P. Zhukov, M. Vázquez, J. Velázquez, H. Chiriac and V. Larin, *J. Magn. Magn. Mater.* **151** (1995) 132.

25RP-B-4

SUPERSONIC DOMAIN WALL IN THIN FERROMAGNETIC WIRES

Varga R.¹, Richter K.¹, Zhukov A.², Larin V.³

¹Inst. Phys., Fac. Sci., UPJS, Kosice, Slovakia

²Dept. Física de Materiales, Fac. Química, UPV/EHU, San Sebastian, Spain

³MFTI, Kishinev, Moldova

The domain wall propagation is used in different devices to store (race-track memory [1]) or transfer (domain wall logic [2]) information. The domain wall is driven either by magnetic field or by electric current. In both cases, the speed of such devices depends directly on the propagating domain wall velocity.

Amorphous glass coated microwires with positive magnetostriction are ideal material for study the single domain wall dynamics [3]. Due to their low anisotropy, the studied domain wall is very fast [4], even exceeded the sound velocity in magnetic microwire [5]. Such fast domain wall brings new unexpected effects that could occur its propagation.

Here, we present a single domain wall dynamics study on amorphous glass-coated microwires with different composition. The maximum velocities obtained in our measurement exceeded few times the sound velocity. The supersonic velocities of domain wall has already been observed in ferrites [6,7], however, such fast domain walls are not usual for ferromagnetic materials with high magnetization.

We try to explain the existence of such fast domain wall in terms of presence of two perpendicular (however low) anisotropies, as well as the presence of the outer radial domain structure that shields the domain wall from the pinning on the surface. Moreover, due to the presence of magnetoelastic anisotropy, the interaction of the domain wall with the phonons can be recognized similarly to that published in [6], when the domain wall overcomes the sound velocity.

Support by VEGA 1/3035/06 and APVT 20-007804 is acknowledged.

[1] S. S. Parkin, "Shiftable Magnetic Shift Register and Method of Using the Same," U.S. Patent 6834005, 2004;

[2] D. A. Allwood, G. Xiong, C. C. Faulkner, D. Atkinson, D. Petit, and R. P. Cowburn, "Magnetic Domain-Wall Logic," *Science* vol.309 (2005), pp.1688-1692.

[3] R. Varga, K.L. Garcia, M. Vázquez, P. Vojtanik, "Single-DomainWall Propagation and Damping Mechanism during Magnetic Switching of Bistable Amorphous Microwires," *Phys. Rev. Lett.* vol.94 (2005), 017201.

- [4] R. Varga, A. Zhukov, J.M. Blanco, M. Ipatov, V. Zhukova, J. Gonzalez, P. Vojtanik, "Fast magnetic domain wall in magnetic microwires," *Phys. Rev. B* vol.74 (2006), 212405.
- [5] R. Varga, A. Zhukov, V. Zhukova, J.M. Blanco, J. Gonzalez, "Supersonic domain wall in magnetic microwires," *Phys. Rev. B* vol.76 (2007), 132406. C.D. Ee, F.G. Hhh, *J. Appl. Phys.*, **33** (1999) 133.
- [6] S.O. Demokritov, A. Kirilyuk, N.M. Kreines, V. Kudinov, V.B. Smirnov, M.V. Chetkin, "Interaction of the moving domain wall with phonons," *J. Magn. Magn. Mater.* vol.102 (1991), pp. 339-353.
- [7] M. V. Chetkin, Yu. N. Kurbatova, T. B. Shapaeva, and O. A. Borshchegovskii, "Generation and Gyroscopic Quasi-relativistic Dynamics of Antiferromagnetic Vortices in Domain Walls of Yttrium Orthoferrite", *J. Exp. Theor. Phys*, vol. 103, (2006), pp. 159–164.

25RP-B-5

GYROSCOPIC DYNAMICS OF ANTIFERROMAGNETIC VORTICES IN ORTHOFERRITE DOMAIN WALL

Chetkin M.V., Kurbatova Yu.N., Shapaeva T.B.

Physical Department of M.V.Lomonosov Moscow State University, Moscow, Russia

Solitary deflection waves accompanying antiferromagnetic vortices on supersonic domain walls of yttrium orthoferrite have been observed experimentally and investigated in our laboratory for some time [1,2]. Two- and threefold high speed digital photography using Faraday rotation in the plates cut perpendicular to the optical axis were used in the real time scale. After local deceleration of supersound domain wall we observed solitary deflection waves moving along the domain wall under influence of gyroscopic force. In the center of antiferromagnetic vortices magnetic G_y phase takes place [3]. This phase has higher energy than $G_z F_x$ inside the domain wall. The energy for G_y phase was obtained from supersound part of the domain wall. The observed amplitudes of solitary deflection waves vary from one to several tens of microns. The head-on collision of two vortices with different topological charges can be used for generation of vortices with small topological charges. Strongly nonlinear dependencies of solitary deflection wave velocity along the domain wall $u(v)$ and its full velocity $w(v)$ as function of domain wall velocity v were investigated up to $v=20\text{km/s}$ equal to limiting spin wave velocity. After a fast increase the experimental dependence $u(v)$ follows the relation $u^2+v^2=c^2$. Position of the maximum on this dependence is the function of the topological charge of antiferromagnetic vortex. Threefold high speed photography of solitary deflection waves of small amplitudes makes possible registering small topological charges of antiferromagnetic vortices. The real force that moves the antiferromagnetic vortices in orthoferrites domain wall can be only the gyroscopic force as it was pointed out in our previous experimental works. Yet this force was considered to be zero [4]. Recently a new theory of nonzero gyroscopic force in the orthoferrites was proposed [5]. This force is proportional to Dzialoshinski field, to the exchange field in the orthoferrites. As a result we have the quasirelativistic gyroscopic dynamics of antiferromagnetic vortices in the orthoferrites on quasirelativistic domain wall.

Support by RFBR grant 07-02-00832-a.

- [1]. M.V. Chetkin, Yu.N. Kurbatova, *IEEE Trans. on Magn.* **34**, (1998) 1075.
- [2]. M.V. Chetkin, Yu.N. Kurbatova, T.B.Shapaeva, O.A. Borschegovsky, *Phys. Lett. A*, **337**, (2005) 235

- [3]. M.M. Farztdinov, M.A. Shamsutdinov, A.A. Khalfina, *Fiz.Tverd. Tela* 21, 1522 (1979) [*Sov. Phys. Solid State* 21 (1979)].
- [4]. V.G.Bar'yakhtar, M.V.Chetkin, B.A.Ivanov, S.N.Gadetskiy. *Dynamic of Topological Magnetic Solitons. Experiment and Theory. Springer tracts in modern Physics*, vol. 129, 1994.
- [5]. A.K.Zvezdin, V.I.Belotelov, A.K.Zvezdin, *JETP Letters* 87, (2008) 443.

25RP-B-6

DIRECT STUDY OF REMAGNETIZATION ELEMENTARY EVENTS IN FERROMAGNETIC FILM WITH UNIDIRECTIONAL ANISOTROPY

Uspenskaya L.S.¹, Nikitenko V.I.^{1,2,3}, Shapiro A.J.², Shull R.D.², Zhu F.Q.³, Chien C.L.³

¹Institute of Solid State Physics RAS, 142432, Chernogolovka, Russia

²21218National Institute of Standards and Technology, Gaithersburg, Maryland 20899

³The Johns Hopkins University, Baltimore, Maryland

It is well established that ferromagnetic film exchange coupled with antiferromagnetic one in ferromagnetic/antiferromagnetic heterostructures (FM/AFM) is determined by a nucleation and evolution of lateral domains in ferromagnetic layer and by penetration of heterophase partial domain wall (exchange spring) into antiferromagnetic layer. The results of direct experimental study of dynamics of magnetization reversal process of FM/AFM heterostructure are presented in this report. The dynamical properties of the domain walls in ferromagnetic FeNi thin film exchange coupled with antiferromagnetic FeMn layer were measured for the first time.

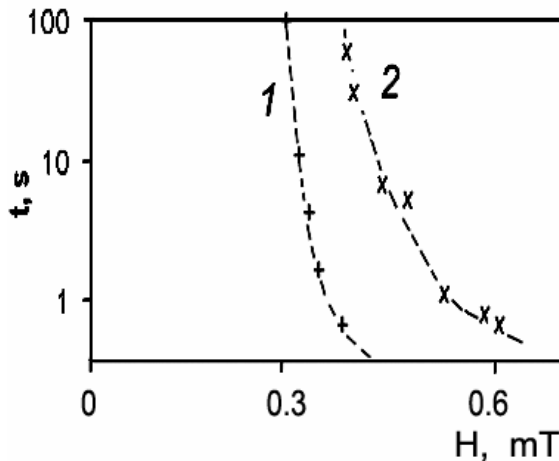


Fig.1. Dependence of the time of domain walls nucleation upon the field; 1 – the magnetic field is applied parallel to unidirectional anisotropy, 2 – the field is applied in opposite direction.

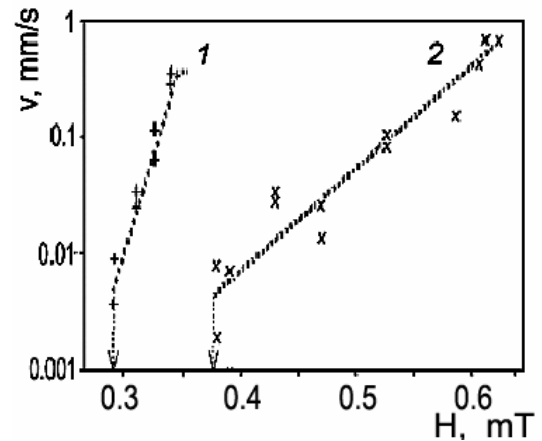


Fig.2 Variation of domain wall velocity with the field strength, 1 – the field direction coincides with the direction of unidirectional anisotropy, 2 – the field is applied in opposite direction

The use of magneto-optical indicator film technique let us to observe for the first time the stages of the processes of domain wall nucleation during the magnetization reversal, the time of nucleation of domain walls in ferromagnetic layer (Fig.1) and the velocity of the walls in depend upon the strength of applied magnetic field (Fig.2). The crucial dependence of the nucleation time upon the field direction is found.

It is shown that the formed domain walls started to move with constant velocity, which depends exponentially upon the field strength, Fig.2. A new phenomenon, an asymmetry in the domain wall (DW) mobility has been revealed. The Barkhausen activation volume values for the DW motion in opposite directions differ more than by a factor of four. Possible microscopic mechanism of magnetization process responsible for observed phenomena are discussed.

Support by RFBR grant # 08-02-01268 and by the program "New materials and structures" of RAS is acknowledged.

25RP-B-7

SOLITON COLLISIONS IN SOFT MAGNETIC NANOTUBES

Usov N.A.^{1,2}, Gudoshnikov S.A.^{1,2}, Palvanov P.S.¹

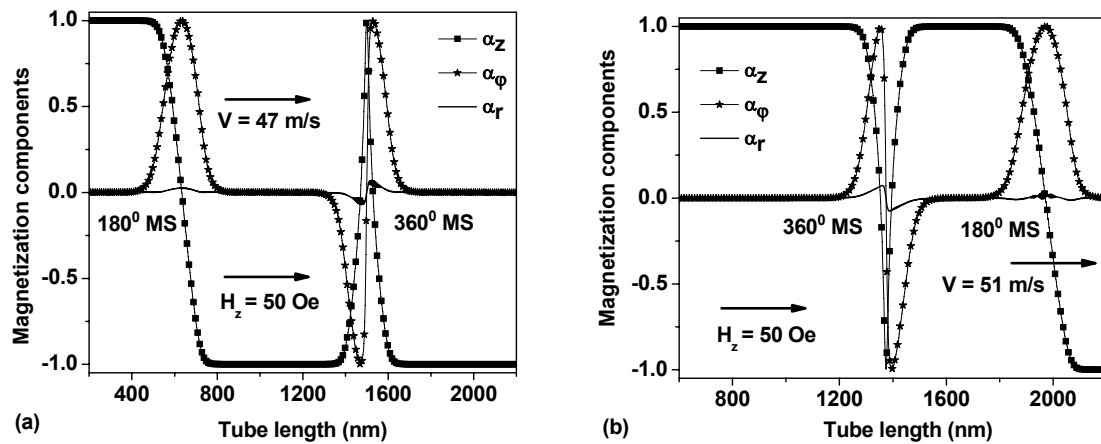
¹Pushkov Institute of Terrestrial Magnetism, Ionosphere and Radio Wave Propagation, Russian Academy of Sciences, (IZMIRAN), 142190, Troitsk, Moscow region, Russia

²Ltd. "Magnetic and Cryogenic Systems", 142190, IZMIRAN, Troitsk, Moscow region, Russia

Recently [1], the dynamical properties of a head to head domain wall (DW) in a soft magnetic nanotube with positive uniaxial anisotropy constant, $K > 0$, have been studied by means of 2D numerical simulation. The unit magnetization vector of the DW can be approximately described in the cylindrical coordinates (r, φ, z) as follows

$$\alpha_z = \cos \theta(z) = \tanh(z/\delta); \quad \alpha_\varphi = \pm \sqrt{1 - \alpha_z^2}; \quad \alpha_r \approx 0, \quad (1)$$

where δ is the DW width. This wall is a 180° isolated magnetic soliton (MS), because the angle $\theta(z)$ changes from 0 to 180° when passing through the DW center. The fact that both signs of the α_φ component in Eq. (1) are possible enables one to construct topologically stable MSs of higher order. The 360° MS is immobile in external magnetic field H_z parallel to the tube axis, because it separates the domains with the same sign of the α_z component (see Fig. 1a). However, if H_z is opposite to the domain magnetizations, a 180° MS starts at one of the tube ends at $|H_z| > H_n$, where H_n is the nucleation field of the 180° MS at the tube end. This process is shown in Fig. 1a for a nanotube with inner, $d = 32$ nm, and outer, $D = 40$ nm, diameters, respectively (tube saturation magnetization $M_s = 1000$ emu/cm³, $K = 10^5$ erg/cm³). If the sign of the α_φ component of 180° MS is positive, as shown in Fig 1a, a collision of 180° and 360° MSs leads to creation of 540° MS. The latter is mobile one, though its mobility is found to be considerably lower than that of 180° MS. Furthermore, there is a critical magnetic field, H_{zc} , for 540° MS propagation. At $H_z > H_{zc}$ 540° MS becomes unstable and transforms into immobile 360° MS and mobile 180° MS. The 180° MS propagates finally through the nanotube to complete the magnetization reversal process, as Fig. 1b shows. On the other hand, if $\alpha_\varphi < 0$, the result of collision of mobile 180° MS and immobile 360° MS is a single 180° MS that propagates along the nanotube and remagnetises it finally.



It is shown also that for a long nanotube stable periodic and aperiodic domain structures can be constructed. They consist of chains of solitons of various order.

[1] N.A. Usov, A. Zhukov, J. Gonzalez, *J. Magn. Magn. Mater.*, **316** (2007) 255.

25RP-B-8

EXPERIMENTAL DETERMINATION OF LIMIT ANGLE OF HELICAL ANISOTROPY IN AMORPHOUS MAGNETIC MICROWIRES

Chizhik A.¹, Zhukov A.¹, Blanco J.M.², Gonzalez J.¹, Gawronski P.³, Kulakowski K.³

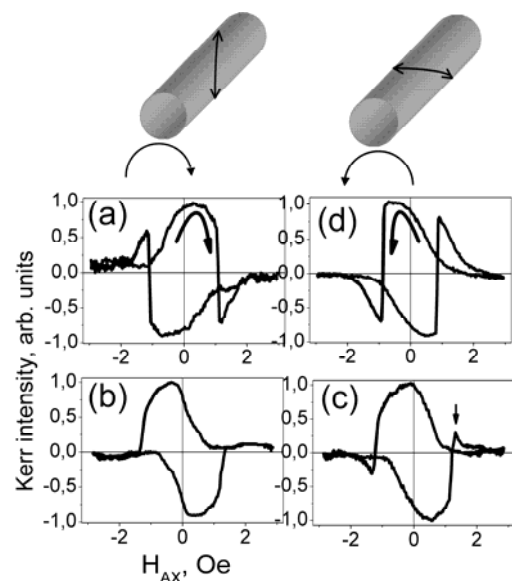
¹Dpto. Fisica de Materiales, Facultad de Quimica, UPV, 1072, 20080 San Sebastian, Spain

²Departamento Fisica Aplicada I, EUPDS, UPV/EHU, Plaza Europa, 1, 20018 San Sebastian, Spain

³Faculty of Physics & Applied Computer Science, AGH University of Science & Technology, 30-059 Cracow, Poland

Glass covered amorphous microwires exhibiting nearly zero negative magnetostriction, of nominal composition $\text{Co}_{69.5}\text{Fe}_{3.9}\text{Ni}_{11.8}\text{Si}_{10.8}\text{Mo}_2$ (metallic nucleus diameter $19\mu\text{m}$, glass coating thickness $2.6\mu\text{m}$) have been investigated using the transverse magneto-optical Kerr effect (TMOKE) in axial magnetic field. The intensity of the reflected light is proportional to the magnetization oriented perpendicularly to the plane of the light polarization, i.e. to the circular projection of the magnetization in the surface area of the microwire. The torsion stress have been applied to the microwire during the experiments.

The process of surface magnetization reversal in the presence of the torsion stress of different amplitude and directions has been studied. Figure presents examples of the TMOKE



dependencies on the axial magnetic field with the amplitude of the torsion stress as a parameter: (a) $\tau = -22 \pi \text{ rad m}^{-1}$, (b) $\tau = -2.2 \pi \text{ rad m}^{-1}$, (c) $\tau=0$, (d) $\tau=8.9 \pi \text{ rad m}^{-1}$. Insets: schematically pictures of the inclination of the axis of helical anisotropy induced by the torsion stress.

The applied torsion stress induces strong transformation of the surface hysteresis loops. The most essential feature of this transformation is the stress induced change of the value and direction (sign) of the jump of the Kerr intensity ΔI (the circular magnetization ΔM_{CIRC}).

The obtained results are related to the torsion induced change of the helical anisotropy. The analysis of the experimental results has been performed taking into account the existence of a helical magnetic anisotropy in the wire [1]. The comparative analysis of the experimental results and the results of the calculations permits us to determine and construct for the first time, the dependence of the angle of the helical anisotropy on the applied torsion stress. The obtained results are in agreement with the model [2] which consider the torsion stress as a interference of two tensile stresses of opposite signs (pressing and straining) directed at 45° and 135° relative to the longitudinal axis of the wire. Now we have the method which permits us to present the results of the experiments with torsion stress as a dependence on the angle of helical anisotropy.

This work was supported by MEyC under project PCI2005-A7-0230.

[1] A. Chizhik, et al., *IEEE Trans. Magn.*, **42** (2006) 3889.

[2] M.J. Sablik, and D.C. Jiles, *Phys. D: Appl. Phys.*, **32** (1999) 1971.

25RP-B-9

GLASS-COATED Cu-Mn-Ga MICROWIRES PRODUCED BY TAYLOR-ULITOVSKY TECHNIQUE

Prida V.M.¹, Vega V.¹, Sánchez Llamazares J.L.¹, Santos J.D.¹, Escoda Ll.², Suñol J.J.², García C.³, Hernando B.¹

¹Departamento de Física, Universidad de Oviedo, Calvo Sotelo s/n, 33007 Oviedo, Spain

²Universidad de Girona, Campus Montilivi, edifici PII, Lluís Santaló s/n, 17003 Girona, Spain

³Dpto Física de Materiales, Facultad de Química, UPV, 1072, 20080 San Sebastián, Spain

Glass-coated Cu-Mn-Ga microwires were successfully fabricated by Taylor-Ulitovsky technique. Starting alloys of nominal composition $\text{Cu}_{50}\text{Ga}_{25}\text{Mn}_{25}$ were prepared by argon arc melting from pure elements (>99.9%). A preliminary study of their physical dimension, elemental chemical composition and magnetic behaviour was performed by means of energy dispersive spectroscopy microanalysis (EDS), scanning electron microscopy (SEM), and magnetization measurements in the temperature range of 10 K-350 K. The samples produced were quite homogeneous from the geometric point of view exhibiting average inner and outer diameters of 24 μm and 33 μm , respectively (see Fig. 1). After a systematic study by EDS of the fracture cross-section and cylindrical surface of an appreciable number of microwire pieces we determined the average alloy composition $\text{Cu}_{55.1}\text{Ga}_{27.4}\text{Mn}_{17.5}$. None appreciable contamination with silicon impurity was observed. It is believed that Mn deficiency is due to evaporation during the melting process. The temperature dependence of magnetization measured at a low field of 200 Oe showed that two ferromagnetic phases co-exist (Fig. 2). The Curie temperature determined for the major magnetic phase was 125 K, while that of the second phase is above room temperature. Hysteresis loops measured at 50 K and 350 K, underlined that both phases are ferromagnetic with coercive field values, H_C , of 387 Oe and 45 Oe at 50 K and 350 K, respectively.

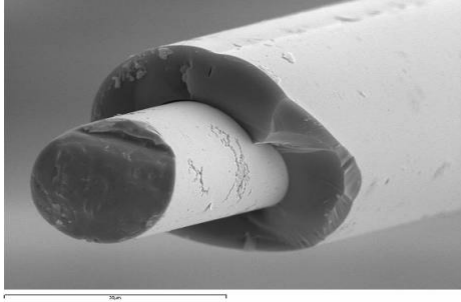


Fig. 1. SEM micrograph of as-cast Cu-Mn-Ga microwires fabricated showing their typical inner and outer diameter. Scale: 30 μm .

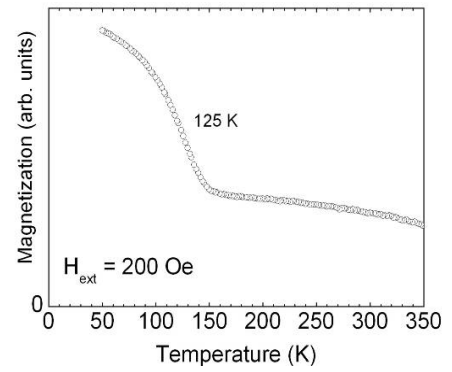


Fig. 2. Magnetization as a function of temperature under a field of 200 Oe for as-cast Cu-Mn-Ga microwires.

Financial support under Spanish MEC and FICYT research projects MAT2006-13925 and COF07-013 is acknowledged.

25 June Wednesday

10:00-11:30

oral session

25TL-C

25RP-C

**“Nanomagnetism
and Nanostructures”**

25TL-C-1

VORTEX-CORE REVERSAL DYNAMICS AND VORTEX RANDOM ACCESS MEMORY

Kim Sang-Koog, Lee Ki-Suk, Choi Youn-Seok,

Yu Young-Sang, Guslienko K. Yu., and Jeong Hyeon-Seong

Research Center for Spin Dynamics and Spin-Wave Devices (ReC-SDSW), Nanospinics Laboratory, Department of Materials Science and Engineering, College of Engineering, Seoul National University, Seoul 151-744, Republic of Korea

The magnetic vortex (MV) is now a well-known magnetic microstructure typically observed as ground and/or dynamic states in patterned [1] or continuous soft magnetic thin films [2]. The MV consists of two parts: One is the in-plane curling magnetizations as most part and the other is the out-of-plane magnetizations at the tiny core region, so called the vortex core (VC). The VC has either upward or downward magnetization orientation, so that it can be used as information carrier of binary digits “0” and “1” [3]. Over the past five years, our group has found the nontrivial novel dynamic properties of magnetic vortices in geometrically confined magnetic thin-film dots, such as ultrafast vortex-core reversals by oscillating magnetic fields and currents with extremely low power and by circularly rotating fields in the film plane, its detailed mechanism [4], physical origin [5], universal criterion [6], as well as linear and nonlinear gyrotropic motions [7]. On the basis of those novel static and dynamics properties of vortices, we propose a conceptual design of new classes of nonvolatile random access memory (RAM) using magnetic vortex arrays. In particular, the use of circular rotational fields of frequencies close to the eigenfrequency of a given vortex allows us to select a vortex for its core reversal and detecting its core orientation for information recording and writing, respectively, with low power consumption as small as 10 Oe, and with excluding transistors assigned to individual cells for reliable writing and reading operation [3].

The results provide a new as well as more detailed physical understanding of vortex-related dynamics in soft magnetic nanodots, and allow for an effective manipulation of vortex motions and VC switching, as well as its practical application to information storage devices such as vortex-RAM (VRAM) coined by us, for the first time.

Supported by Creative Research Initiatives (ReC-SDSW) of MOST/KOSEF

- [1] T. Shinjo, T. Okuno, R. Hassdorf, K. Shigeto, T. Ono, *Science*, **289** (2000) 930.
- [2] S.-K. Kim, K.-S. Lee, B.-W. Kang, K.-J. Lee, J. B. Kortright, *Appl. Phys. Lett.*, **86** (2005) 052504.
- [3] S.-K. Kim, K.-S. Lee, Y.-S. Yu, Y.-S. Choi, *Appl. Phys. Lett.*, **92** (2008) 022509.
- [4] K.-S. Lee, K. Y. Guslienko, J.-Y. Lee, S. -K. Kim, *Phys. Rev. B*, **76** (2007) 174410 .
- [5] K. Y. Guslienko, K.-S. Lee, S.-K. Kim, *Phys. Rev. Lett.*, **100** (2008) 027203.
- [6] S.-K. Kim, Y.-S. Choi, K.-S. Lee, K. Y. Guslienko, D.-E. Jeong, *Appl. Phys. Lett.*, **91** (2007) 082506.
- [7] K.-S. Lee, S.-K. Kim, *Appl. Phys. Lett.*, **91** (2007) 132511.

25RP-C-2

TRANSPORT PROPERTIES OF NON COPLANAR MAGNETIC NANOSTRUCTURES

Fraerman A.A., Udalov O.G.

Institute for Physics of Microstructures RAS, Nizhny Novgorod, Russia

Investigations of spin and spatial degrees of freedom for electrons and their interplays are of great interest from both theoretical and practical points of view. When Hamiltonian contains Zeeman term (for example, ferromagnetic metals in the frames of s-d approximation) the symmetry of an electron energy spectrum depends on a magnetic field (or magnetization) spatial distribution. In particular, a momentum-reversal symmetry is broken in a non-coplanar system. This can lead to the peculiarities of transport properties of crystals in a non-coplanar magnetic field (with non-coplanar magnetization distribution). In the report we are going to discuss some aspects of the problem. Namely

- phenomenological and microscopic theory of “topological” Hall effect [1] in ferromagnetic nanoparticles with vortical magnetic state.

- phenomenological and microscopic theory of rectification effects in the medium with helical magnetic structure. It was shown that rectification effect is connected with asymmetry of group velocity and scattering asymmetry of carriers in non coplanar magnetic systems and what is more, with asymmetry of probabilities for transitions of electrons between different spin branches under the action of electromagnetic wave (photo galvanic effect) [2,3]. Possibilities for experimental observation of predicted effects are discussed.

- helix magnetic state in laterally confined magnetic multilayers. The spiral state in the system originates from the magnetostatic interaction taking into account interplay between nearest and next nearest neighboring magnetic layers. The system was fabricated by electron beam lithography from a multilayer Co/SiO₂ thin film structure grown by magnetron sputtering. Magnetic force microscopy method was used for observation of helix state in such systems [4].

This work was supported by the RFBR (#07-02-01321-à).

[1] Y. Aharonov, A. Stern, Phys. Rev. Lett. **69**, 25, 3593 (1992)

[2] A.A. Fraerman, O.G. Udalov, Phys.Rev. B, **77**, 1 (2008)

[3] A. A. Fraerman, O.G. Udalov, JETP Lett., in press

[4] A.A.Fraerman, B.A.Gribkov, S.A.Gusev et al, J. Appl.Phys., in press

25RP-C-3

COUPLING EFFECTS ON THE PRECESSIONAL DYNAMICS IN LATERAL FERROMAGNETIC HETEROSTRUCTURES

Polushkin N.P.

Institute for Physics of Microstructures, Russian Academy of Sciences, GSP-105 603950,
Nizhniy Novgorod, Russian Federation (e-mail: nip@ipm.sci-nnov.ru)

Precessional dynamics in (ferro)magnetic nano-objects is well described by the Landau-Lifshits equation for the motion, which can be reduced to that for a simple linear (or even nonlinear) oscillator. What happens in their system if individual magnetic nano-oscillators are

closely packed and excited? A common answer here would be that the coupled oscillators should synchronously resonate either in phase (acoustic mode) or anti-phase (optic mode) with respect to each other.

We find a *diversity* of collective oscillation modes in periodic arrays of patterned magnetic stripes with no any separation between adjacent stripes but with different saturation magnetizations in them [1]. In the microwave absorption (MA) spectra of such heterostructures, we observe multiple resonances, whose intensity strongly depends on the ratio of stripe widths and the structure period. Such a behavior contrasts to that typically occurring in thin ferromagnetic films and laterally confined structures where the intensities of resonant modes are insensitive to the structure dimensions [2]. To explain the observed anomaly, a linear response theory has been formulated for stripe structures with arbitrary profile of the saturation magnetization over the period. The developed theory (i) supports an existence of dipolar standing-wave resonances in the arrays where stripes are separated from each other; (ii) establishes basic differences between the resonant modes occurring in individual stripes and, on the other hand, in our heterostructures; (iii) allows us to assign the measured MA resonances to specific oscillation regimes.

Finally, the obtained results indicate the existence of coupled oscillations of a new type. These oscillations are standing-wave-like modes of the dynamic magnetization, which are extended through a whole heterostructure period. In the lowest (acoustic-like) mode, such a standing wave has nonzero minima of the oscillation amplitude instead of the nodes. In the higher (optic-like and hybrid) modes the distances between the nodes are smaller than a half of wavelength of an usual standing wave.

Work was supported by the Russian Foundation for Basic Research (# 07-02-01305).

[1] N. I. Polushkin *et al.*, *Phys. Rev. Lett.*, **97** (2006) 256401.

[2] M. Sparks, *Phys. Rev. B*, **1** (1970) 3831.

25RP-C-4

STRUCTURE AND MAGNETIC PROPERTIES OF Fe IMPLANTED SrTiO₃

Mikhailov F.A.^{1,2}, Kazan S.¹, Onan A.G.¹, Gatiyatova Ju.I.³, Valeev V.F.³, Khaibullin R.I.³

¹Department of Physics, Gebze Institute of Technology, Gebze, 41400, Kocaeli, Turkey

²Institute of Physics, Azerbaijan Academy of Sciences, 370143, Baku, Azerbaijan

³Kazan Physical-Technical Institute, 10/7, Sibirsky Trakt, 420029 Kazan, Russia

The results of detailed XRD, SEM, magnetic resonance and magnetization measurements of Fe implanted strontium titanate (SrTiO₃) perovskite crystal are presented. The samples were prepared by Fe ion implantation into (111)-oriented single crystalline substrates of SrTiO₃ with 40 keV iron ions at doses in the range of 0.5-1.5×10¹⁷ ion/cm² and with an ion current density of 8 μA/cm². The temperature of substrate was 700°C during ion irradiation to minimize the radiation damage of SrTiO₃ crystalline structure.

It has been revealed that the microstructure of Fe implanted SrTiO₂ is characterized by the presence of linearly ordered iron clusters of average sizes of approximately 20 nm over the layer of thickness of some micrometers near the crystal surface. The implantation of Fe into single-crystal SrTiO₃ on different doses of metal concentrations produces a remarkable ferromagnetic behaviour, which is characterized by well-defined magnetic hysteresis loop at room temperature. Analysis of the hysteresis loops measured in in-plane and out-of-plane

geometries of the strontium titanate plate shows that the ferromagnetic Fe:SrTiO₃ system displays easy plane magnetic anisotropy. It has been shown that the magnetization and coercivity of ferromagnetic state depends on the dose of implantation. The FMR spectra measurements taken at different crystalline orientations of substrate with the respect to the applied magnetic field show an out-of-plane uniaxial magnetic anisotropy in Fe-implanted SrTiO₃. Additionally, EPR spectra from two magnetically equivalent Fe centers in SrTiO₃ crystal structure have been observed. The observed phenomena are discussed on the base of strong magnetic dipolar interaction between Fe nanoparticles due to diminishing of interparticle distance with increasing of implantation dose.

Support from The Scientific & Technological Research Council of Turkey (TÜBİTAK) is acknowledged (Project No.106M540) by FAM.

Authors from Kazan Physical-Technical Institute, Russia, acknowledge support of RFBR, grant 07-02-00559-a, and OFN RAN Programme "New material and structures".

25RP-C-5

MAGNETIC - FIELD BEHAVIOR OF HETEROGENEOUS MAGNETIC MATERIALS

Shalygina E.E.¹, Maximova G.V.¹, Komarova M.A.¹, Melnikov V.A.¹, Shalygin A.N.¹, Molokanov V.V.²

¹Faculty of Physics, Moscow State University, 119992, Moscow, Russia

²Institute of Metallurgy and Metallovedeniya named A.A. Baikova, RAS, Russia

Results on the investigation of the magnetic properties of nanocrystalline Co (2 nm)/Fe (1 nm)/Ni (0.5 nm), Fe (2.5 nm)/Zr ($t = 0.3- 3$ nm)/Fe (2.5 nm) thin-film systems and Fe_{80.5}Nb₇B_{12.5} ribbons are presented. The Co/Ni/Fe and Fe/Zr/Fe samples were prepared by magnetron sputtering technique under a base pressure of less than 10⁻⁸ Torr. The ribbons of the 30-microns thickness were obtained by a planar flow casting method from the melt. The ribbon samples were annealed in vacuum for 1h at temperature $T = 380-650$ °C. The near-surface regions of the annealed ribbons display the nanocrystalline and amorphous layer microstructure. The study of the magnetic properties of the above samples was carried out employing by a vibrating sample magnetometer (VSM) and magneto-optical micromagnetometer.

It is known that magneto-optical Kerr effect (MOKE) is sensitive to the magnetization up to a certain depth range below the surface of ferromagnetic, called "a penetration depth of the light in media", t_{pen} . According to our experimental data, for metallic magnetic materials, the magnitude of t_{pen} does not exceed 22 – 30 nm in the $1.5 < \hbar\omega < 5$ eV photon energy range. The full thicknesses of the thin-film systems are smaller than the magnitude of t_{pen} . As a result, their bulk and near-surface hysteresis loops were found to be identical. At the same time, it was revealed that the VSM hysteresis loops of the as-cast FeNbB ribbon are habitual but the MOKE ones of all thin-film samples and annealed ribbons display complicated forms. According to [1], only heterogeneous layer magnetic systems can exhibit the unusual hysteresis loops. That can be explained by the following. The Co/Fe/Ni samples consist of layers, characterizing by different magnitudes of anisotropy constant and the saturation magnetization. Stray fields, created by neighboring layers, have opposite direction as compared to the applied external magnetic field. So, the strong modifications of the MOKE hysteresis loops, observed for these systems, are caused by the magnetostatic interaction between the above layers.

The complicated MOKE hysteresis loops of the Fe/Zr/Fe samples can be ascribe to the presence of the exchange coupling between ferromagnetic layers through the Zr spacer and its

oscillatory behavior with changing t_{Zr} : the switch from the ferromagnetic (F) to the antiferromagnetic (AF) coupling. The saturation field of AF-coupled trilayers is more than H_S of the F-coupled ones that is caused by an additional energy expense for overcoming the AF exchange coupling between magnetic layers. The magnetic-field behavior of the AF-coupled trilayers is similar to that of classic antiferromagnetic. As a result, at the magnetic field, parallel to the AF magnetization orientation, these samples exhibit the complicated hysteresis loops.

In the annealed FeNbB ribbons, the forward and reverse hysteresis branches were found to be shifted in opposite directions, i. e., inverted near-surface hysteresis loops are observed. Actually, a negative remanent magnetization is observed upon removing the positive applied magnetic field to zero (and vice versa). The partially and completely inverted MOKE hysteresis loops of the FeNbB annealed ribbons can be explained by the presence of two phases near its surfaces and the interface antiferromagnetic exchange between them.

[1] A. Aharoni. J. Appl. Phys. **76** (1994) 6977.

25 June Wednesday

12:00-13:30

oral session

25TL-C

25RP-C

“Theory”

25TL-C-6

NUMERICAL MICROMAGNETICS FOR QUASISTATICS AND DYNAMICS: STATE OF THE ART AND ROADMAP FOR THE FUTURE

Berkov D.V.

Innovent Technology Development, Pruessingstr. 27B, D-07745, Jena, Germany

Numerical simulations of quasistatic and dynamic remagnetization processes are currently widely used to study the behaviour of a large variety of magnetic systems - from disordered assemblies of single-domain particles up to extended thin films and patterned nanoelement arrays.

In the introduction we briefly address the foundations of micromagnetics as a phenomenological theory developed to study magnetization configurations in ferromagnets on a mesoscopic (from ~ 10 nm to ~ 10 μ m) length scale. We list main contributions to a free energy of a ferromagnetic body and discuss their finite-different approximations suitable of numerical simulations.

The first part of the talk is devoted to the study of static magnetization configurations and slow (quasistatic) remagnetization processes in ferromagnets under different external conditions. We present examples of numerical simulations of ripple structures in thin films, hysteretic switching in nanodots and nanowires arrays, complicated 3D magnetization states in Fe nanoislands etc. Comparing simulations results with experimental data, we demonstrate that micromagnetics provides a reliable and efficient tool for studying quasistatic magnetization configuration of a large variety of mesoscopic magnetic systems.

Next, we consider numerical simulations of the magnetization dynamics, which require the solution of the (stochastic) Landau-Lifshitz-Gilbert equation of the magnetization motion. Here we first discuss three methodological questions crucial for such Langevin dynamics simulation: (i) influence of the finite-element discretization on the simulated dynamics, (ii) choice between the *Ito* and *Stratonovitch* stochastic calculus (for simulations by $T > 0$) and (iii) correlation properties of the random field used in such simulations. Afterwards we present several applications of the Langevin dynamics for studying fast remagnetization processes in magnetic nanodevices. These examples include remagnetization of a soft magnetic element in a pulsed field, studies of the magnon spectrum in confined magnetic nanostructures, and domain wall motion in nanowires. We conclude this parts with the analysis of the strongly non-linear remagnetization processes driven by the spin-polarized current injection.

Finally we list several open problems which solution is considered as being especially important for further progress of analytical and numerical micromagnetism: chaotic dynamics in continuous magnetic systems, vortex-antivortex creation-annihilation processes in case of strong excitations, stability of non-linear modes and calculation of (dynamic) energy barriers between them.

25RP-C-7

MULTIELECTRON APPROACH TO THE ELECTRONIC STRUCTURE AND MECHANISMS OF SUPERCONDUCTIVITY IN HIGH- T_c CUPRATES

Ovchinnikov S.G.^{1,2,}, Gavrichkov V.A.^{1,2}, Korshunov M.M.^{1,3}, Shneyder E.I.¹, Nekrasov I.A.⁴,
Kokorina E.E.⁴, Pchelkina Z.V.⁵, Ambrosch-Draxl C.⁶, Spitaler J.⁶*

¹L.V. Kirensky Institute of Physics, Siberian Branch of RAS, Krasnoyarsk, 660036, Russia

²Siberian Federal University, av. Svobodnyi 79, Krasnoyarsk 660041, Russia

³Max-Planck-Institut für Physik Komplexer Systeme, Dresden, Germany

⁴Institute for Electrophysics, Ural Division of RAS, Ekaterinburg, Russia

⁵Institute for Metal Physics, Ural Division of RAS, Ekaterinburg, Russia

⁶University of Leoben, Leoben, Austria

*e-mail: sgo@iph.krasn.ru

A review of the LDA+GTB results of the electronic structure calculations with exact treatment of strong local Coulomb correlations for undoped and doped LSCO and NCCO is given. For undoped cuprates, the antiferromagnetic ground state is a charge transfer insulator, where the dispersion of the valence band is in agreement with ARPES data. Upon doping in-gap states appear, and for small hole concentrations the chemical potential is pinned by them. In the paramagnetic underdoped region the spin liquid effects are important for the band dispersion via the spin correlation function. It is shown that the low energy effective model Hamiltonian has the form of the $t-t'-t''-J^*$ model, where all parameters for LSCO and NCCO are calculated from first principles. At low doping the Fermi surface consists of 4 small hole pockets around $(\pi/2, \pi/2)$. With increasing doping there are two quantum phase transitions with a change of the Fermi surface topology near optimal doping and in the overdoped region. The $t-J^*$ model with account for 3-site correlated hopping leads to a magnetic pairing mechanism due to exchange coupling and provides the $T_c(x)$ dependence with a maximum at $x_{opt}=0.16$. The latter is close to the experimental value, while in our mean-field approach T_c is larger than the experimental one.

The electron-phonon interaction is incorporated in the GTB scheme within the tight binding model. Phonon frequencies and eigenvectors have been calculated for all $q=0$ modes with the LAPW method. The electronic bands have been calculated for undistorted and distorted atomic structures and hence provide the electron phonon matrix elements for these modes.

A mean field BCS type theory of superconductivity with both, magnetic and phonon mechanisms of coupling has been developed. In the d-symmetry channel of pairing the concentration dependence of T_c and the isotope effect have been investigated. The phonon mechanism enhances the magnetic one thereby conserving the shape of the $T_c(x)$ dome. The non-monotonic doping dependence of the isotope effect in the underdoped regime of LSCO originates from the competition of bare electron-phonon interaction and electron-phonon coupling induced by spin correlation.

This work has been financially supported by the Presidium of RAS program "Quantum macrophysics", Integration Grant of Siberian and Ural Branches of RAS #74, RFFI-BNTS Grant 06-02-90537, RFFI Grant 06-02-16100, and Grant WTZ project 1/2006.

25RP-C-8

FIRST-PRINCIPLES STUDY OF ELECTRONIC AND OPTICAL PROPERTIES OF GROUPS IV AND III-V DIGITAL MAGNETIC HETEROSTRUCTURES

Kulatov E.¹, Tugushev V.², Uspenskii Yu.³

¹A.M. Prokhorov General Physics Institute of RAS, 38 Vavilov str. Moscow 119991, Russia

²RRC Kurchatov Institute, Kurchatov Sq. 1 Moscow 123182, Russia

³P.N. Lebedev Physical Institute of RAS, 53 Leninskii prosp. Moscow 117924, Russia

Ferromagnetic diluted semiconductors attract considerable attention for semiconductor-based spintronics, as in these devices the spin degree of freedom of carriers can be magnetically and electrically manipulated. Recently semiconductor superlattices were employed to create a new class of III-V, Mn doped, dilute magnetic semiconductors (DMS) that promise to advance our understanding of the interplay between electronic and magnetic coupling in this family of materials. These phenomena are, however, difficult to investigate in random alloys due to the multiple effects of Mn doping. In digital ferromagnetic heterostructures (DFH) these problems may be overcome by using the δ -doped Mn layers. On the other side technology for Si based devices is more mature, and they might be more readily manufactured, if corresponding half-metallic devices could be engineered. Prediction of the ferromagnetic order in Mn-doped bulk Si and Ge DFH [1-3], in GaAs/Mn and GaSb/Mn DFH [4-6] and in wurtzite GaN/Mn [7,8] have been reported. The experimental results are particularly encouraging because the measured Curie temperature is near room temperature.

Density-functional calculations presented here are performed within a supercell scheme and by the FLAPW method. Our supercells are constructed by piling the diamond, zinc-blende and wurtzite cells in z-direction. We simulate DFH by replacing the group IV and III atomic sites by 3d TM atoms (TM= Cr, Mn, Fe, Co) in Si, Ge, GaAs, GaSb and GaN semiconductor hosts. All atomic positions in cells were optimized by minimization of the total energy. The energy difference between ferromagnetic and antiferromagnetic collinear orderings was calculated for *intralayer* and *interlayer* geometries. Our calculated optical spectra of all DFH show marked features in the infrared region, due to the optical interband transitions between impurity-induced states. Calculated magneto-optical spectra are also presented and discussed. Comparison of the optical spectra, calculated with various doped TM atoms, with experimental optical data could help to understand the basic physics for digitally doped layers.

Support by Russian Foundation for Basic Research (projects 07-02-01177-a, 07-02-00114-a) and Program of Russian Academy of Sciences "Strongly correlated electrons in semiconductors, metals, superconductors and magnetic materials" is acknowledged.

- [1] H. Weng *et al*, *Phys. Rev. B*, **71**, (2005) 035201.
- [2] M.C. Qian *et al*, *Phys. Rev. Lett.*, **96**, (2006) 027211.
- [3] A. Continenza *et al*, *Phys. Rev. B*, **70**, 035310 (2004).
- [4] B.D. McCombe *et al.*, *Physica E.*, **16**, 90 (2003).
- [5] R.K. Kawakami *et al*, *Appl. Phys. Lett.*, **77**, (2000) 2379.
- [6] X. Chen *et al*, *Appl. Phys. Lett.*, **81**, (2002) 511.
- [7] J. Furthmüller *et al*, *Phys. Rev. B*, **73**, (2006) 224409.
- [8] J.I. Hwang *et al*, *Appl. Phys. Lett.*, **91**, (2007) 072507.

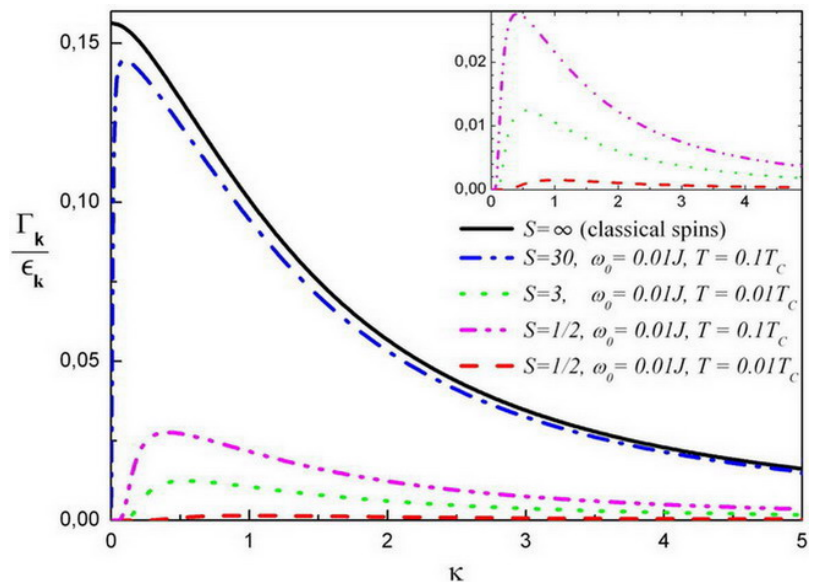
25RP-C-9

SPIN-WAVE INTERACTION IN TWO-DIMENSIONAL FERROMAGNETS WITH DIPOLAR FORCES

Syromyatnikov A.V.

Petersburg Nuclear Physics Institute, Gatchina, St. Petersburg 188300, Russia

I discuss the spin-wave interaction in 2D Heisenberg ferromagnet (FM) with dipolar forces at $T_c \gg T \geq 0$ using $1/S$ expansion. A comprehensive analysis is carried out of the first $1/S$ corrections to the spin-wave spectrum. Similar to 3D FM discussed in [1], I observe quite an unusual phenomenon: the spin-wave interaction leads to the *gap* Δ in the spectrum ϵ_k renormalizing greatly the bare gapless spectrum at small momenta k . Expressions for the spin-wave damping Γ_k are derived self-consistently and it is concluded that magnons are *well-defined quasi-particles* in both quantum and classical 2D FMs at small T . I observe thermal enhancement of both Γ_k and Γ_k/ϵ_k at small momenta. In particular, a peak appears in Γ_k/ϵ_k at small k and at any given \mathbf{k} direction. The peak in quantum 2D FM is lower than that of the classical 2D FM found at $k=0$ which height is small only *numerically*: $\Gamma_0/\epsilon_0 \approx 0.16$ for the simple square lattice (see the figure that is for \mathbf{k} parallel to magnetization, where ω_0 is the characteristic dipolar energy, J is the exchange coupling constant and $\kappa = k\sqrt{J\omega_0}/\Delta$). Frustrating next-nearest-neighbor exchange coupling increases Γ_0/ϵ_0 in classical 2D FM only slightly. I find expressions for spin Green's functions and the magnetization. The latter differs from the well-known result [2]. The effect of the exchange anisotropy and higher order corrections to the spectrum are also discussed.



I demonstrate that the spin-wave gap that has been steadily ignored in the literature is crucial for some very peculiar features of FMs with dipolar forces reported so far (infrared divergent corrections to the longitudinal spin susceptibility [3] and to the spin-wave stiffness [4] in 3D FM, and existence of the diffusion spin-wave mode at small k in 2D FM [5]). For more details, see [1,6].

[1] A.V. Syromyatnikov, *Phys. Rev. B*, **74** (2006) 014435.

[2] S.V. Maleev, *Sov. Phys. JETP*, **43** (1976) 1240.

[3] B.P. Toperverg, A.G. Yashenkin, *Phys. Rev. B*, **48** (1993) 16505.

[4] T.S. Rahman, D.L. Mills, *Phys. Rev. B*, **20** (1979) 1173.

[5] A. Kashuba, Ar. Abanov, V.L. Pokrovsky, *Phys. Rev. Lett.*, **77** (1996) 2554; *Phys. Rev. B*, **56** (1997) 3181.

[6] A.V. Syromyatnikov, arXiv:0802.0958.

25 June Wednesday

10:00-11:30

oral session

25TL-D

**“High Frequency
Properties”**

25TL-D-1

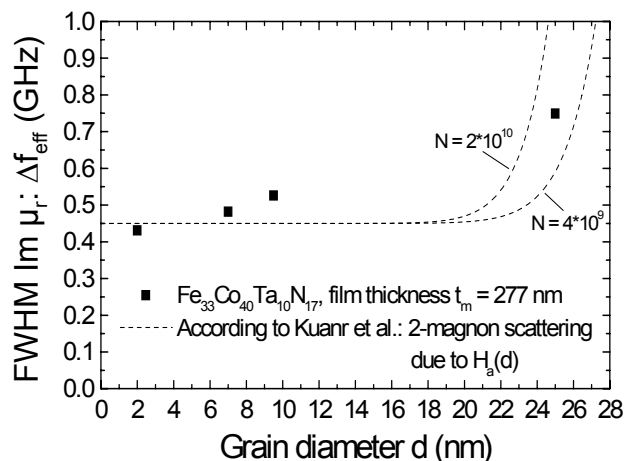
INFLUENCE OF GRAIN GROWTH ON THE HIGH FREQUENCY BEHAVIOUR OF FERROMAGNETIC Fe-Co-(M)-N (M = Ta, Hf) NANOCOMPOSITE FILMS

Seemann K., Leiste H.

Forschungszentrum Karlsruhe in der Helmholtz-Gemeinschaft, Institut für Materialforschung I,
Hermann-von-Helmholtz-Platz 1, D-76344 Eggenstein-Leopoldshafen, Germany

In the present paper, CMOS compatible ferromagnetic Fe-Co-(M)-N (M = Ta, Hf) films were investigated with regard to their grain size dependent frequency behaviour.

Predominantly $\text{Fe}_{33}\text{Co}_{40}\text{Ta}_{10}\text{N}_{17}$ films were deposited by reactive r.f. magnetron sputtering on oxidised $5 \times 5 \text{ mm}^2 \times 380 \text{ }\mu\text{m}$ (100) silicon substrates by means of a 6-inch $\text{Fe}_{37}\text{Co}_{46}\text{Ta}_{17}$ target. These films were compared to Fe-Co-Hf-N films. In order to induce an in-plane uniaxial anisotropy H_u as well as to investigate the grain growth behaviour, the films were annealed at temperatures between $300 \text{ }^\circ\text{C}$ and $600 \text{ }^\circ\text{C}$ in a static magnetic field of 50 mT. The grain size of the films was determined by TEM imaging and amounts from a few nanometers for films heat treated at $300 \text{ }^\circ\text{C}$ to more than 20 nm at $550 \text{ }^\circ\text{C}$. The in-plane uniaxial anisotropy of around 4 mT as well as a good soft magnetic behaviour -the coercitive field was quantified to be between 0.2 mT and 0.9 mT- with a saturation polarisation of approximately 1.2 to 1.4 T could be observed after heat treatment at the above mentioned temperatures which drove these films to a high frequency suitability. Ferromagnetic resonance frequencies (FMR) of approximately up to 2.4 GHz could be achieved according to the Kittel theory. Depending on the heat treatment, high-frequency losses through energy dissipation was made conspicuous by means of the full width at half maximum (FWHM) $\Delta f_{\text{eff}} = \Delta f_{\text{int}} + \Delta f_{\text{ext}}$ of the imaginary part of the frequency-dependent permeability. Δf_{int} and Δf_{ext} are attributed to effects causing intrinsic and extrinsic broadening, respectively. This FWHM was basically discussed in terms of two-magnon scattering theories (extrinsic broadening), in combination with the Herzer random anisotropy model. Scattering occurs due to magnetocrystalline anisotropy H_a and/or nonmagnetic scatterers both functioning as inhomogeneities causing magnetic fluctuations inside the magnetic films. In order to correlate the resonance line broadening with a phenomenological damping parameter resulting in $\alpha_{\text{eff}} = \alpha_{\text{int}} + \alpha_{\text{ext}}$ and which ranged from about 0.0125 to 0.028, the modified the Landau-Lifschitz-Gilbert equation [1] was used to fit and describe the permeability spectra of the ferromagnetic films. It can be seen in the FWHM plot that for continuous grain growth the line width increases. Due to the fairly high magneto-crystalline anisotropy coefficient K_1 of about 10000 J/m^3 for the, e.g., above introduced $\text{Fe}_{33}\text{Co}_{40}$ fraction of the Fe-Co-Ta-N film the measured data can be obviously described according to Kuanr et al. [2], where α_{int} (for $d \rightarrow 0$) and a number of "defects" (grains) N were taken as fit parameters.



[1] K. Seemann, H. Leiste, V. Bekker, J. Magn. Magn. Mater. 278 (2004) 200.

[2] B. K. Kuanr, R. E. Camley, Z. Celinski, J. Magn. Magn. Mater. 286 (2005) 276.

25TL-D-2

INTEGRATED ON-CHIP INDUCTORS USING MAGNETIC MATERIAL*Gardner D.S.¹, Schrom G.², Paille F.², Karnik T.², Borkar S.²*¹Circuits Research Lab, Intel Labs, 3065 Bowers Ave., Santa Clara, CA, 94040, USA²Circuits Research Lab, Intel Labs, 2111 N.E. 25th Ave., Hillsboro, OR, 97124 USA

On-chip inductors with magnetic material are integrated into both advanced 130 and 90 nm CMOS processes. The inductors use aluminum or thick copper metallization and amorphous CoZrTa magnetic material. Increases in inductance of up to 28 times corresponding to an inductance density of up to 1300 nH/mm² were obtained, significantly greater than prior values for on-chip inductors with magnetic material. In comparison, air-core spiral inductors can achieve inductance densities of up to about 50 nH/mm². With such improvements, the effects of eddy currents, skin effect, and proximity effect become clearly visible at higher frequencies. The CoZrTa was chosen for its good combination of high permeability, good high-temperature stability (>250 °C), high saturation magnetization, low magnetostriction, high resistivity, minimal hysteretic loss, and compatibility with silicon technology. The CoZrTa alloy can operate at frequencies up to 9.8 GHz, but trade-offs exist between frequency, inductance, and quality factor. The effects of increasing the magnetic thickness on the permeability were measured and modeled including skin depth effects, eddy current dampening, and the effects of the demagnetization field. The inductors use magnetic vias and elongated structures to take advantage of the uniaxial magnetic anisotropy. Techniques are presented to extract a sheet inductance and examine the effects of magnetic vias (vias that allow complete closure in the magnetic flux) on the inductors. Comparisons of measurements of different via width and of structures with versus without laminations demonstrate the effectiveness of this technique with thin cobalt oxide. Comparing inductors with maximum Q-factors at different frequencies was accomplished by plotting the inductance over ac resistance time constant (L/R_{ac}) versus frequency, then including contours representing constant quality-factor values. Simulations of magnetic flux density and eddy current densities and analytical models were used to gain a good understanding of the effects of laminations. The inductors with thick copper and thicker magnetic films were successfully demonstrated to have L/R_{ac} time constants about 20× higher than earlier aluminum-based inductors with resistances as low as 0.04 Ω and quality factors of up to 8 at frequencies as low as 40 MHz.

25TL-D-3

DESIGN, SYNTHESIS, AND MEASUREMENT OF CATION SITE SELECTION IN FERRITE MATERIALS

Harris V.G.^{1,2}, Geiler A.^{1,2}, Yang A.¹, Zuo Xu³, Yoon Soack Dae¹, Chen Yajie¹, Vittoria C.^{1,2}

¹Center for Microwave Magnetic Materials and Integrated Circuits, Northeastern University,
Boston, MA 02115 USA

²Department of Electrical and Computer Engineering, Northeastern University,
Boston, MA 02115 USA

³College of Information Technical Science, Nankai University, 94 Weijin Road,
Tianjin 300071, CHINA

Ferrites have long been studied and optimized for high frequency applications. There are few new compositions left for materials scientists to discover. Alternatively, new materials processing tools, techniques, and approaches are ubiquitous that provide scientists with new abilities to tailor chemistry, morphology, shape, crystal structure, and atomic and electronic structure. These new processing schemes often allow for new properties and applications for this important class of materials. In this presentation, we will review the latest advances in the use of alternating target laser ablation deposition (ATLAD) in which the user controls the type and distribution of cations in the spinel structure in order to derive new and useful properties for microwave applications. In one such example, epitaxial manganese substituted M-type barium ferrite thin films are deposited by ATLAD from BaFe₂O₄, Fe₂O₃, and MnFe₂O₄ targets to manipulate Mn cations in specific interstitial sites of the M-type barium ferrite unit cell. The distribution of Mn cations has been confirmed experimentally by extended x-ray absorption fine structure (EXAFS) and predicted from first principle theory. As a result of specific site selection, the saturation magnetization increased 12-22% and the Néel temperature increased by 40-60 K compared to bulk material. This represents one of the first successful demonstrations of the ATLAD technique and suggests an effective methodology to the design and processing a new generation of ferrite, oxide and alloy materials.

25 June Wednesday

12:00-13:30

oral session

25TL-D

25RP-D

“Magnetic Oxides”

25TL-D-4

OPTICAL SPECTROSCOPY OF LOW-DIMENSIONAL RARE-EARTH IRON BORATES

Popova M.N.

Institute of Spectroscopy RAS, Fizicheskaya 5, Troitsk 142190, Moscow region, Russia

Borates with general formula $RM_3(BO_3)_4$, where R stands for a rare earth (RE) or yttrium and $M = Al, Ga, Fe, Cr,$ or Sc , crystallize in the huntite type non centrosymmetric trigonal structure. MO_6 octahedra form spiral chains along the high symmetry axis, which leads to *quasi-one-dimensional magnetic properties* in the case of magnetic M ions. Aluminate from this family combine good luminescent and nonlinear optical properties with excellent physical characteristics and chemical stability. Nd and, to a less degree, Yb containing alumoborates were thoroughly investigated and used in self-frequency doubling and self-frequency summing lasers and minilasers. Recently, single crystals of the whole series of RE iron borates have been grown. Borates with magnetic M ions have interesting new properties and promising new application potential. In this talk, I'll briefly review a spectroscopic research of RE iron borates carried out in my group in cooperation with the Kazan' University (Russia) and the Laboratory of Chemistry of Condensed Matter (Paris, France). The crystals of good optical quality have been grown in the L.V. Kirensky Institute of Physics (Krasnoyarsk, Russia). The spectroscopic methods used were temperature-dependent high-resolution absorption and FIR reflection Fourier spectroscopy.

FIR spectra evidence the weak first-order structural phase transition in $RFe_3(BO_3)_4$, $R = Gd, Tb, Y,$ and Er , at $T_s = 156, 198, 345,$ and 340 K, respectively, from the R32 trigonal structure to the less symmetric $P3_121$ one. $NdFe_3(BO_3)_4$ and $PrFe_3(BO_3)_4$ do not change their structure down to the lowest temperature used (3 K).

We have undertaken a detailed crystal-field study of the compounds $RFe_3(BO_3)_4$, $R = Pr, Nd$ [1], $Eu, Tb, Ho,$ and Er . The analysis of the temperature-dependent polarized spectra has revealed the energies and, in some cases, symmetries and exchange splittings of R^{3+} Kramers doublets. The crystal-field calculations starting from the exchange-charge model were performed, the sets of crystal-field parameters were obtained, wave functions and magnetic g-factors were calculated. The values of the local effective magnetic field at the R^{3+} sites and the R – Fe exchange integrals have been determined from the experimentally measured R^{3+} ground-state splittings. To check reliability of our sets of crystal field parameters we modeled the magnetic susceptibility data from literature. A dimer containing two nearest-neighbor iron ions in the spiral chain was considered to partly account for quasi-one-dimensional properties of iron borates, and then the mean-field approximation was used. The results of calculations with the exchange parameters for Fe^{3+} ions obtained from fitting agree well with the experimental data.

This work was supported by the Russian Foundation for Basic Research (grant №07-02-01185) and by the Russian Academy of Sciences under the Programs for Basic Research.

[1] M.N. Popova, E.P. Chukalina, T.N. Stanislavchuk, B.Z. Malkin, A.R. Zakirov, E. Antic-Fidancev, E.A. Popova, L.N. Bezmaternykh, and V.L. Temerov, *Phys. Rev. B*, **75** (2007) 224435.

25RP-D-5

TIME RESOLVED MAGNETOOPTICAL KERR EFFECT IN (Pr,Ca)MnO₃ THIN FILMS

Mertelj T.^{1,2}, *Yusupov R.*¹, *Gradišek A.*¹, *Filippi M.*³, *Prellier W.*³, *Mihailovic D.*^{1,2}

¹Jozef Stefan Institute, Jamova 39, 1000 Ljubljana, Slovenia

²Faculty of Mathematics and Physics, Univ. of Ljubljana, 1000 Ljubljana, Slovenia

³Laboratoire CRISMAT, CNRS UMR 6508, Bd du Marechal Juin, F-14050 Caen Cedex, France

Time resolved Magneto-optical Kerr effect (TRMOKE) in insulating ferromagnetic phase in (Pr_{0.6}Ca_{0.4})MnO₃ thin films on LaAlO₃ and SrTiO₃ substrates was measured upon photoexcitation in magnetic fields up to 1.1T. The photoinduced Kerr rotation and ellipticity show remarkably different magnetic-field dependence (see Fig. 1). From comparison with the static Kerr rotation and ellipticity we conclude that two different magnetic phases are present in the samples at low temperatures. According to small angle neutron scattering results in bulk [1] one of the phases originates from nanoscopic ferromagnetic metallic clusters. Comparison of temporal dependence of the photoinduced Kerr signals with the photoinduced reflectivity indicates that upon photoexcitation changes of the volume fractions of these phases take place on a timescale of ten picoseconds.

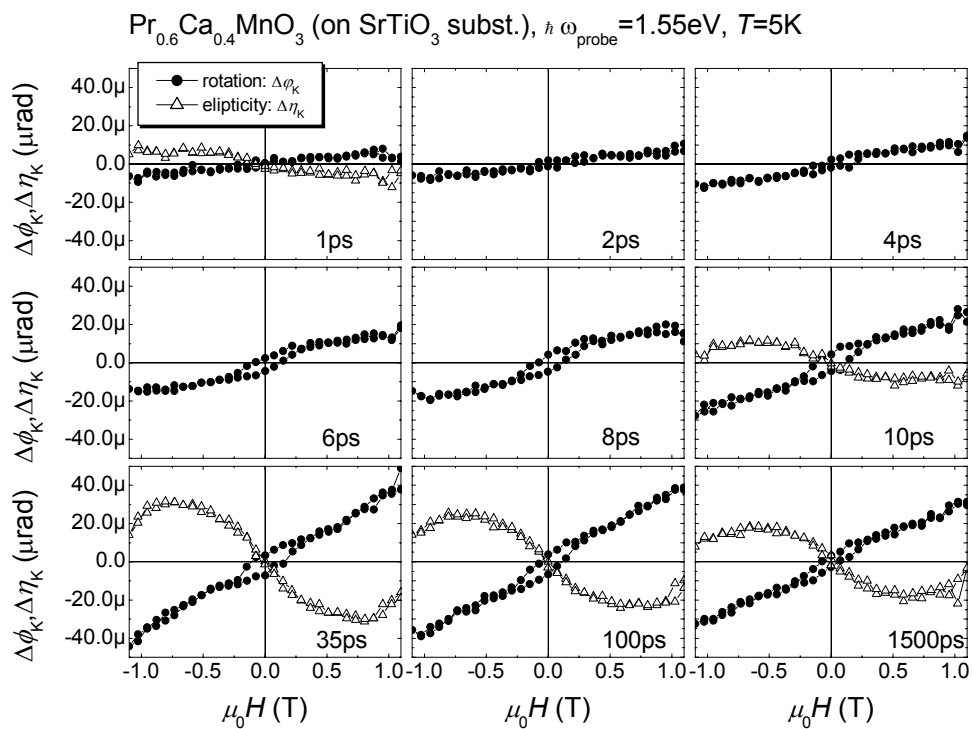


Fig. 1. Delay dependence of the photoinduced Kerr rotation and ellipticity in (Pr_{0.6}Ca_{0.4})MnO₃ thin film on SrTiO₃ substrate.

The work was supported within the FP6, project NMP4-CT-2005-517039.

[1] D. Saurel, A. Brûlet, A. Heinemann, C. Martin, S. Mercone, and C. Simon, *Phys. Rev.* **B 73**, 094438 (2006).

25RP-D-6

PHASE SEPARATION WITH DYNAMIC CHARGE SELF-ORGANIZATION IN SEVERAL SEMICONDUCTOR MANGANITES-MULTIFERROICS

Sanina V.A.¹, Golovenchits E.I.¹, Zalesskii V.G.¹, Lushnikov S.G.¹, Gvasaliya S.N.², Kawaji H.³, Atake T.³

¹A.F. Ioffe Physical Technical Institute, 26 Polytechnicheskaya, 194021, Russia

²Lab. for Neutron Scattering ETHZ, Paul Scherrer Institut, CH-5232 Villigen PSI, Switzerland

³Tokyo Institute of Technology, 4259 Nagatsuta-cho, Midori-ku, Yokogama, 226-8503 Japan

New doped semiconductor manganites – multiferroics $Tb_{0.95}Bi_{0.05}MnO_3$, $Gd_{0.75}Ce_{0.25}Mn_2O_5$, and $Eu_{0.80}Ce_{0.20}Mn_2O_5$ have been grown and investigated. The initial dielectric multiferroics $TbMnO_3$ and RMn_2O_5 ($R = Gd$ and Eu) have similar temperatures of magnetic and ferroelectric ordering, of the order of 30 – 40 K. In the crystals studied, the states with a giant dielectric permeability and ferromagnetism have been found to coexist at room temperature. Analysis of dielectric properties of these crystals has led to the conclusion that at $T \geq 180$ K phase separation with dynamic periodic distribution of quasi-2D layers of manganese ions of variable valency, i.e. charge ferroelectricity, occurs in these crystals. At low temperatures ($T < 100$ K) the crystals have been found to have a small phase volume occupied by as-grown quasi-2D layers with doping impurities and charge carriers and the basic crystal volume occupied by a dielectric phase without charge carriers. A thermal activation of the hopping conductivity gives rise to a phase transition into the state of charge ferroelectricity at $T \approx 180$ K caused by self-organization of charge carriers in the crystal matrix with ferroelectric frustrations.

Magnetic properties, heat capacity, magnetoresistance, and phase transitions in a magnetic field in $Tb_{0.95}Bi_{0.05}MnO_3$ and $Eu_{0.80}Ce_{0.20}Mn_2O_5$ have also been studied. The experimental investigations have confirmed the ideas on the formation of the state with a giant dielectric permeability inferred from analysis of dielectric properties. At low temperatures magnetization and heat capacity of $Tb_{0.95}Bi_{0.05}MnO_3$ exhibit singularities at the phase transition temperatures of a pure $TbMnO_3$ crystal. The ferromagnetic moment has also been observed at all temperatures. In a magnetic field, jumps in resistance due to metamagnetic transition in the quasi-2D layers with Mn^{3+} and Mn^{4+} ions have been observed at the layer boundaries. At $T \geq 180$ K a periodic variation of resistance in a magnetic field demonstrating the process of charge carrier self-organization has been observed. A rather high magnetic field has been found to lead to the shift of the phase transition from 180 K to higher temperatures and to induce additional phase transitions.

The study is supported by RFBI and by Presidium of Academy Sciences of Russia.

25RP-D-7

SPECTROSCOPIC STUDY OF ELECTROMAGNONS IN MULTIFERROICS

Sushkov A.B.¹, Valdés Aguilar R.¹, Drew H.D.¹, Cheong S.W.²

¹Department of Physics, University of Maryland, College Park, Maryland 20742, USA

²Department of Physics and Astronomy, Rutgers University, Piscataway, New Jersey 08854, USA

Electromagnons are coupled magnon-phonon excitations. Coupled phonon and magnon branches shift in frequency and exchange electric and magnetic dipole activity. Detection of the electric activity at magnon frequencies is a direct and the most reliable method of observation of electromagnons. Although theoretically electromagnons are studied for more than 40 years, only recently electromagnons were observed by the infrared spectroscopy in some orthorhombic $RMnO_3$ [1] and in some RMn_2O_5 [2] multiferroics. In agreement with the theoretical picture, strong phonon-electromagnon effects are observed in $RMnO_3$ compounds [1,3]. I will present our new data on electromagnons in magnetic field and discuss the possible role of Heisenberg type and Dzyaloshinsky-Moria type exchanges in formation of electromagnons.

Support by the NSF-MRSEC at the University of Maryland, DMR # 0520471 is acknowledged.

[1] A. Pimenov, A.A. Mukhin, V.Y. Ivanov, V.D. Travkin, A. Balbashov, and A. Loidl, *Nature Phys.* **2**, (2006) 97.

[2] A.B. Sushkov, R. Valdés Aguilar, S. Park, S.W. Cheong, and H.D. Drew, *Phys. Rev. Lett.*, **98** (2007) 027202.

[3] R. Valdés Aguilar, A.B. Sushkov, C.L. Zhang, Y.J. Choi,² S.W. Cheong, and H.D. Drew, *Phys. Rev. B*, **76** (2007) 060404.

25RP-D-8

SPIN STATE ORDER AND SPIN STATE PHASE SEPARATION IN LAYERED COBALTITES $RBaCo_2O_{5.5}$ (R=Y, Tb, Dy and Ho)

Pashkevich Yu.¹, Luetkens H.², Gnezdilov V.³, Lemmens P.⁴, Ambrosch-Draxl C.⁵, Lamonova K.¹, Gusev A.¹, Stingaciu M.², Pomjakushina E.², Conder K.², Klauss H.H.⁴, Barilo S.⁶

¹A.A. Galkin Donetsk Phystech NASU, 83114 Donetsk, Ukraine

²Lab. for Muon-Spin Spectroscopy PSI CH-5232 Villigen, Switzerland

³B.I.Verkin Inst. for Low Temp. Physics NASU, 61164 Kharkov, Ukraine

⁴IPCM, TU Braunschweig, D-38106, Braunschweig, Germany

⁵University Leoben, A-8700 Leoben, Austria

⁶Inst. of Phys. of Solids & Semiconductors, 220072 Minsk, Belarus

Layered cobaltites $RBaCo_2O_{5.5}$ (R= rare earth or Y) belong to the family of strong electron correlated systems. They exhibit a manifold of interesting properties like giant-magneto resistance, high thermoelectric power, orbital order, and metal-insulator (MI) transitions while Co ions remain in the nominally trivalent state and crystallographic lattice remains perfect. $RBaCo_2O_{5.5}$ shows a series of magnetic phase transitions, namely ferro(ferri)magnetic (FM) transition at $T_C \sim 300K$ well below a metal-insulator transition at $T_{MI} \sim 350K$, a FM to

antiferromagnetic (AFM1) at $T_{N1} \sim 220\text{K}$ and a AFM1 to antiferromagnetic (AFM2) phase transition at T_{N2} . Such properties are peculiar to manganites and cuprates both with intrinsic inhomogeneities caused by a doping and with variable valency of metallic ions. In comparison with former compounds, an additional degree of freedom adds to the complexity of the cobaltate system, the crystal electric field splitting of the Co 3d-states is of the same order of magnitude as the Hund's exchange coupling. Therefore it is possible for the $3d^6 \text{Co}^{3+}$ ion to adopt the high-spin (HS: $S=2$), intermediate-spin (IS: $S=1$), or low-spin (LS: $S=0$) state, depending on both crystallographic environment and temperature. The lattice's features promote easy switching of Co spin state while complex interplay of electron-spin-orbital-lattice degree of freedom can create a nonuniform spin state distribution - spin state order (SSO).

Using muon spin resonance (μSR) spectroscopy, Raman spectroscopy, *ab-initio* band structure and lattice dynamic calculations we uncovered that in layered cobaltites SSO plays a part of intrinsic inhomogeneities like doping in cuprates and manganites. From the observed spontaneous muon spin precession frequencies in the FM phase we conclude a ferrimagnetic SSO of IS and HS states in the octahedra with antiferromagnetically ordered IS in the pyramids. However, the HS-IS type of SSO contains intrinsic magnetic frustrations which lead to the instability of the FM phase and following series of magnetic phase transitions. We show that such kind of SSO, which appears below T_{MI} , serves as a new mechanism of metal-insulator phase transition. We succeeded in assignment of all μSR signals from both AFM phases and in restoring of their magnetic structures. We show that as a result of a first order phase transition the homogeneous FM phase develops in a phase separated AFM1 phase which consists of phases with different type antiferromagnetic and spin state order (AFM/SSO). Below T_{N2} a rearrangement of phase separated regions occurs again in which part of them survive and new AFM/SSO phases appear forming the AFM2 phase. The details of this scenario as well the volume fraction of a given AFM/SSO phase depend on R while all AFM structures are realized on a fixed set of SSO which include different combinations of HS/LS and IS/LS states on octahedra sites. The estimated size of phase separated regions is no less than hundred lattices constant. We demonstrate that both phase separation and magnetic structures of AFM/SSO phases are responsible for the observed features of magneto-resistance phenomenon, namely, a strong anisotropy which depends on current/field/lattice geometry.

25 June Wednesday

13:30-15:00

poster session

25PO-13

“Magnetic Materials”

25PO-13-1

SYNTHESIS OF SUBMICRON SrFe_{12-x}Al_xO₁₉ PARTICLES WITH VERY HIGH COERCIVITY

Trusov L.A.^{1*}, Zaitsev D.D.¹, Kazin P.E.², Jansen M.³

¹Department of Materials Science, Moscow State University, 119991, Moscow, Russia

²Chemistry Department, Moscow State University, 119991, Moscow, Russia

³Max-Planck-Institut für Festkörperforschung, D-70569, Stuttgart, Germany

Magnetically hard M-type hexaferrites (AFe₁₂O₁₉, A = Ba, Sr) are oxide solids which play the dominant role on the permanent-magnet market due to their high magnetocrystalline anisotropy, chemical stability and low cost [1].

Monodomain submicron hexaferrite particles have excellent hard magnetic properties. One of the most efficient methods of their synthesis is crystallization of oxide glass precursor [2], e.g. in the SrO-Fe₂O₃-B₂O₃ system. This technique allows wide variation in chemical composition and thermal treatment conditions, thus particle size and, consequently, magnetic properties of the material can be controlled. Also the improvement of hexaferrite properties can be achieved by substitution of iron ions by aluminum. The glass crystallization is very suitable way to obtain aluminum doped monodomain hexaferrite particles at relatively low temperatures.

This work is concerned with synthesis of fine strontium hexaferrite particles by crystallization of glasses in the SrO-Fe₂O₃-Al₂O₃-B₂O₃ system.

The glasses were prepared by rapid quenching of initial reagents melt (SrCO₃, Fe₂O₃, Al₂O₃, H₃BO₃) between two steel rollers. The glass-ceramic samples were formed during heat treatment of glasses at 650-950 °C and fine hexaferrite powders were derived by dissolving of glass ceramics. The materials obtained were characterized by XRD, DTA, SEM, TEM, EDX, ICP AES and magnetic measurements (Faraday balance and SQUID magnetometers). The dependence of structure and phase composition on thermal treatment conditions was determined. Also the influence of sodium oxide additives on glass crystallization was studied.

The SrFe_{12-x}Al_xO₁₉ particles obtained demonstrate hexagonal platelet shape. The particle size varies from 40 nm × 5 nm to 450 nm × 150 nm depending on annealing temperature and glass composition. The sodium oxide additives decrease glass synthesis temperature from 1400 to 1200 °C but slightly reduce the coercive force of corresponding glass-ceramics.

The coercivity of the samples rises while the annealing temperature increases. This occurs because of more profitable aspect ratio of hexaferrite particles formed at higher temperatures. Also the increase of coercivity is associated with aluminum substitution for iron.

The glass-ceramic materials exhibit very high coercivity values up to 10.18 Oe [3]. The substitution rate *x* in the record sample equals to 1.3. The hexaferrite powder obtained from this glass-ceramic sample has the saturation magnetization value of 49.6 emu/g and corresponding coercivity. Crystal structure of the powder was refined by Rietveld method and distribution of Al atoms on Fe sites was determined. Al atoms occupy 41% of 2a sites, 14% of 12k sites and 5% of 4e(1/2) sites, while 4f sites are not affected.

The work was supported by the Federal Target Program “Research and Development in Priority Areas of Science and Technology in Russia for 2007–2012” (Section 1.3, Project no. 02.513.11.3115) and RFBR Project no. 07-03-00569.

[1] J.M.D. Coey, *J. Magn. Magn. Mater.*, **226-230** (2001) 2107.

[2] B. Shirk, W. Buessem, *J. Am. Cer. Soc.*, **53** (1970) 192.

[3] Kazin P.E., *et al.*, *J. Magn. Magn. Mater.*, **320** (2008) 1068.

25PO-13-2

INFLUENCE OF OXYGEN CONTAMINATION ON MAGNETIC PROPERTIES OF AMORPHOUS AND NANOCRYSTALLIZED FeCuSiNbB THIN FILMS

Moulin J.¹, Kaviraj B.², Oubensaid E.-H.³, Alves F.², Gupta A.⁴, Dufour-Gergam E.¹

¹IEF UMR 8622 CNRS-Univ. Paris Sud XI, 91405 Orsay, France

²LGEP UMR8507 CNRS-Supelec-Univ. Paris Sud XI-UPMC, 91192 Gif sur Yvette, France

³Present address: GREMI Université d'Orléans Polytech Orleans, 445067 ORLEANS, France

⁴UGC-DAE Consortium for Scientific Research, Univ. Campus, 452017 Indore, India

Thin films of 400 nm thick Finemet® type alloy of composition $(\text{Fe}_{75}\text{Cu}_6\text{Si}_9\text{Nb}_3\text{B}_7)_{100-x}\text{O}_x$ were prepared on SiO_2/Si substrates by RF sputtering with the following conditions: residual vacuum $3 \cdot 10^{-7}$ mbar and argon working pressure 3 mtorr. Samples with different oxygen ratio (from 4 to 12 %) were prepared by varying the RF power, all other parameters remaining constant. In this situation, oxygen adsorption in the film is constant and deposition rate of the alloy is driven by the RF power. The O-content in the films was measured using EDS technique. Its linearity with deposition rate confirmed that water vapor in the sputtering chamber is responsible for the contamination of the films. It allowed although to estimate the adsorption coefficient of the oxygen on the film.

The hysteresis cycles of the samples have been drawn at room temperature using an AGFM. As for other Fe-based type alloys [1], the coercive field is highly dependent of the oxygen content in the as-deposited film, up to a factor 15. On the other hand, the magnetization is slightly influenced by this parameter.

The films have been annealed at temperature between 250 and 450 °C. Magnetic measurements show that the annealing temperature giving the softest materials is around 250-300 °C for all samples and does not depends on oxygen contamination. This optimal temperature corresponds to the relaxation of strains due to sputtering deposition. It is although related to the beginning of the nanocrystallisation that is unfavorable to magnetic softness for films thinner than the exchange length in such alloys [2].

However, the oxygen contamination influences highly the softness of the crystallized films, more than in the as-deposited state, up to a factor 35. The film microstructure has been studied using X-ray diffraction and Mossbauer spectroscopy. It is supposed that hardness of the crystallized films is due to the limitation of the magnetic exchange between FeSi grains by the formation of a paramagnetic phase in the amorphous matrix.

The electrical resistivity of the films was measured by 4 probes technique. It was found that its value depends directly on the oxygen content in the as-deposited films but poorly on the microstructure, except for the film containing 12% of oxygen, what is consistent with magnetic measurement.

Support by french Agence Nationale pour la Recherche.

[1] Y.J. Liu, I.T.H. Chang, M.R.Lees, *Scripta Mater.*, 22 (2001), 2729-2734

[2] A. Neuweiler, H. Kronmüller, *J. Magn. Magn. Mat.*, **177-181** (1998), 1269-1270.

25PO-13-3

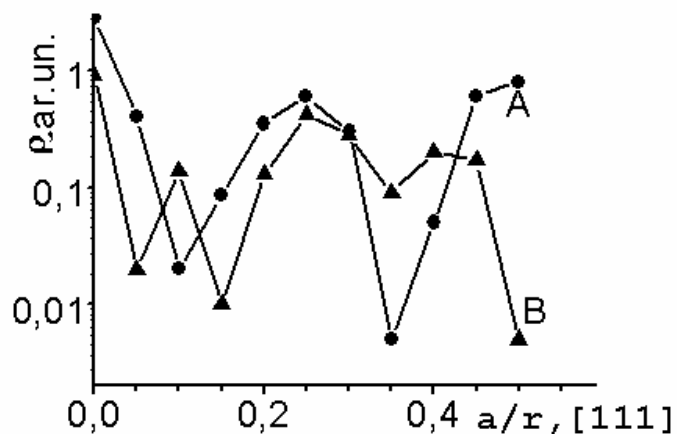
DISTRIBUTION ELECTRONIC DENSITY IN CELLS AND MAGNETIC PROPERTIES OF CRYSTALS OF Mn-Zn SPINEL

Kotov L.N., Petrakov A.P.

Syktyvkar State Univ., Physics dept., Oktyabrsky Pr. 55, Syktyvkar 167001, Russia

It was previously established that the manganese zinc spinel crystals $\text{Mn}_a\text{Zn}_b\text{Fe}_{2+c}\text{O}_4$ ($a+b+c=1$) grown by the Verneuil method (type A samples) are characterized by the existence of a temperature interval in which the first magnetic anisotropy constant K_1 changes the sign while the second constant K_2 remains negative which is manifested by a change in the easy magnetization direction from [100] to [111] with decreasing temperature [1]. While the crystals of a close composition grown by the Bridgman method (type B samples) showed a absence of changes the sign K_1 . In order to check for the proposed difference in the properties of type A and B crystals, we have studied these spinels by X-ray diffraction. The samples were studied on a four-axle X-ray diffractometer (Mo K α radiation, the ω - mode). The diffractometer was supplied with the carbon monochromator. The results showed that the crystal structures of the two samples were identical, the lattice parameters calculated by the X-ray data being $a=8.370(7)$ Å and $8.472(5)$ Å for type A and B crystals, respectively. However, the crystal of type B exhibited a very small deviation from cubic to tetragonal symmetry: $a/c = 1.009 \pm 0.001$. Also, we have studied by X-ray diffraction distribution electronic density ρ in cells on direction from [111] of manganese-zinc spinel crystals of types A and B (Figure: a- parameter of a lattice, r - distance in cells). As follows from figure various distribution of electronic density ρ in a cell of crystals of types A and B is observed. Hence will be various distinction of an indirect exchange along various axes which leads to ordering of the magnetic moments next Fe^{2+} and Fe^{3+} ions.

We may conclude that the observed difference in the magnetic properties of manganese-zinc spinels with close compositions grown by different methods is explained by various distribution of an electronic density in cells of types crystals A and B and by the different exchange electron interaction between Fe^{2+} and Fe^{3+} ions in the octahedral and tetrahedral voids of the spinel lattice. These distinctions are related to differences in the crystal growth methods.



Support by RFBR (grant 06-02-17302) and the program of development of scientific potential of the higher school (DSP.2.1.1.3425)

[1]. L.N. Kotov, S.N. Karpachev. *Technical Phys. Lett.*, **28** (2002) 49.

25PO-13-4

HYPERFINE INTERACTION ANISOTROPY OF ^{57}Fe NUCLEI IN $\text{Yb}_{(1-x)}\text{Y}_x\text{Fe}_2$ ALLOYS

*Rusakov V.S., Ilyushin A.S., Nikanorova I.A., Umhaeva Z.S.,
Tsvjatshenko A.V., and Shkurenko A.V.*
Faculty of Physics M.V. Lomonosov Moscow State University,
Leninskie gory, Moscow, 119992, Russia

The hyperfine interaction anisotropy of ^{57}Fe nuclei in high pressure phases $\text{Yb}_{1-x}\text{Y}_x\text{Fe}_2$ isostructural to MgCu_2 (C15) is studied by methods of Mössbauer spectroscopy. For each compound the orientation of easy magnetization axis and the parameters of the hyperfine interactions such as the Mossbauer line shift δ and the quadrupole interaction constant e^2qQ (fig. 1), isotopic A_{is} and anisotropic A_{an} hyperfine magnetic field (fig. 2) are found in the scope of the tensor description.

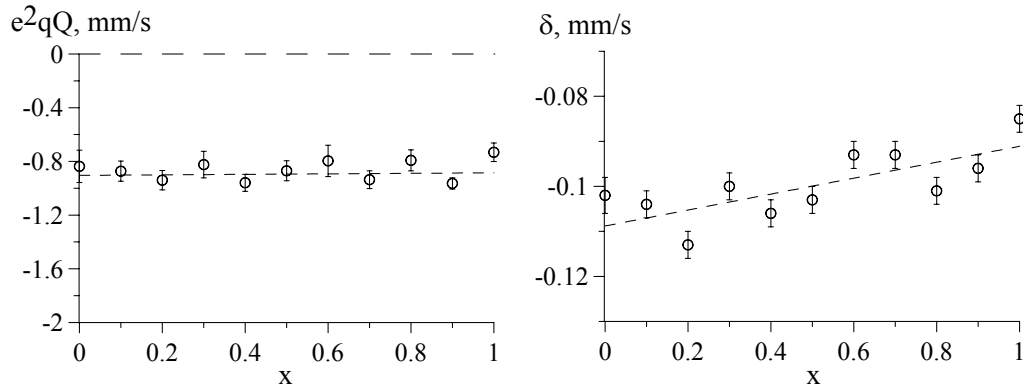


Fig. 1

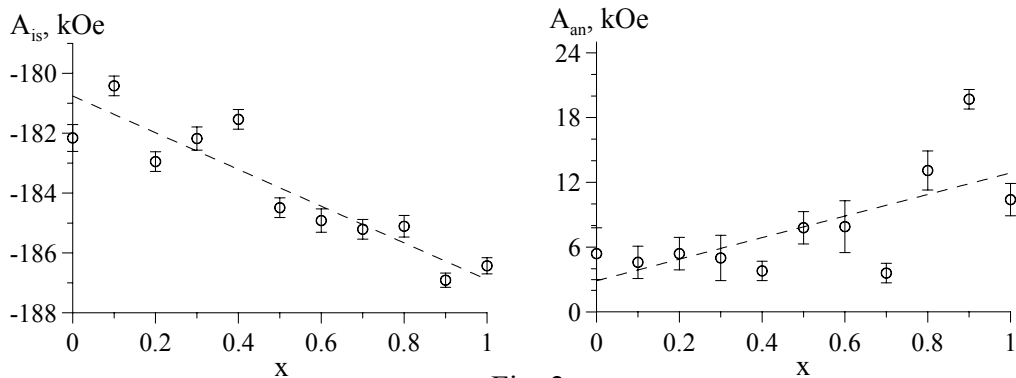


Fig. 2

We have found that the orientation of the easy magnetization axis and quadrupole interaction constant e^2qQ are insensitive to the composition. The Mössbauer line shift δ of ^{57}Fe nuclei, and the hyperfine magnetic fields A_{is} , A_{an} are correlated with the structural parameters of the alloys. We show that the nonmagnetic dilution of Yb atoms by Y atoms, that is accompanied by the nearly linear increase of the distance between Fe atoms, leads to the linear increase in δ and A_{an} in contrast with the decrease of A_{is} .

25PO-13-5

ALTERATIONS IN LOCAL ORDERING OF SI ATOMS IN Fe-Se ALLOYS UNDER MAGNETIC FIELD OR STRESS ANNEALING

Kleinerman N.M., Lukshina V.A., Ershov N.V., Serikov V.V.

Institute of Metal Physics, Ural Division of RAS, Yekaterinburg, Russia

Fe-Si-based soft magnetic alloys possess an important and helpful property: magnetic-field or stress annealing result in the formation in them of a state (named anisotropy of magnetic properties or, to say short, “magnetic anisotropy”) in which their magnetic properties depend on the direction of measurements. In [1,2], it was already experimentally shown that the origin of magnetic anisotropy in crystalline α -FeSi alloys is related to a directional ordering of pairs of Si atoms (local order of the B2 type), which are oriented parallel to the magnetic anisotropy axis induced upon magnetic-field or stress annealing.

To quantitatively characterize the local ordering in the $\text{Fe}_{1-x}\text{Si}_x$ ($x = 0.05, 0.06, \text{ and } 0.08$) alloys, the Mössbauer spectra were taken and their treatment, using the program package [3], allows one to pick out contributions from different atomic configurations in the nearest neighborhood of an Fe^{57} atom (within one-two coordination shells) and to determine volume fractions of the configurations and their changes upon magnetic-field or stress annealing that produce the anisotropy of magnetic properties to a different extent. The magnetic state of samples was monitored by the domain structure patterns.

It is shown that the results of the NGR spectroscopy do not contradict the X ray data gained before and reveal the fact that the configuration with two Si atoms in the first coordination shell of an Fe atom (6:2) is made of a pair of the nearest atoms Si-Si (second neighbors) with its axis aligned with the $\langle 100 \rangle$ direction. The heat treatments, which involve short annealing and cooling of the samples in a dc or ac magnetic field and under or without a tensile load, result in a decrease in the degree of structure separation but increase the volume fraction of the configuration in which an Fe atom has one Si atom in the first and in the second coordination shell, these two atoms being the fourth neighbors.

In the samples that underwent quenching from the temperature of disordering or annealing for the induction of a uniaxial magnetic anisotropy along one of the easy magnetization axes $\langle 100 \rangle$, there is gained the maximal volume fraction of coordination 6:2. Therefore, a conclusion can be made that the formation of a directional order proceeds via a redistribution of Si atoms under the dc field or stress annealing. After annealing in an ac magnetic field the degree of ordering lowers as well as the volume fraction of coordination 6:2.

The significance of the results of the study performed consists in that the processes of local ordering in iron rich Fe-Si alloy and their part in the formation of magnetic properties, as well as such an important phenomenon as magnetic anisotropy, have been quantitatively investigated for the first time.

The authors are grateful for support to RFBR, project no.06-02-17082.

[1] Yu.P. Chernenkov, V.I. Fedorov, V.A. Lukshina, B.K. Sokolov, N.V. Ershov. *The Physics of Metals and Metallography*, **92** (2001) 193.

[2] Yu.P. Chernenkov, N.V. Ershov, V.A. Lukshina, V.I. Fedorov, and B.K. Sokolov. *Physica B: Condensed Matter*, **396** (2007) 220.

[3] V.S. Rusakov. Mössbauer spectroscopy of locally heterogeneous systems. Alma-Ata (2000).

25PO-13-6

EFFECT OF ANNEALING ON FePd THIN FILMS DEPOSITED BY PULSED LASER DEPOSITION(PLD)

Karamat S., Mahmood S., Lee P., Tan T.L., and Rawat R.S.

Natural Science and Science Education, National Institute of Education, Nanyang Technological University 637616

It is very important to control the microstructure of the magnetic materials because the textured or anisotropic magnetic materials usually show better performance in technical applications [1]. Tetragonal intermetallic phases, such as FePt, CoPt, MnAl and FePd, are of interest as active ferromagnetic materials in thermally stable thin film data storage media with ultra-high information density [2]. Utilization of these intermetallic phases, promises up to about one order of magnitude increase in data storage densities with respect to current Co based media [3].

In the present work, FePd thin films were deposited from commercial targets of Fe₅₀Pd₅₀(Kurt J.lesker) by pulsed laser deposition technique using Nd:YAG laser (532 nm, 10 ns) at a repetition rate of 10 Hz . The laser was focused on a rotating FePd target surface in a stainless steel chamber at the base vacuum pressure of 5×10^{-5} mbar. The ablated material were deposited on a Si (100) substrate maintained at room temperature for 10000 shots .The thickness of the thin films measured by surface profilometer were found to be 40nm. Post annealing were done for different temperatures (400 °C - 600 °C) in vacuum. New phase exist in thin films which was investigated from spectra measured by XRD (SIEMENS D5000) equipped with Cu-K_α source. The formation of nanoparticles was investigated on thin films by using JEOL 6700F field emission Scanning electron microscope (SEM). The corresponding change in magnetization with respect to annealing temperature were measured by hysteresis curves obtained from Lakeshore 7400 vibrating samples magnetometer. Rest of things will be discuss in paper.

[1] D.S. Li, H. Garmestani, S.S Yan, M. Elkawni, M.B. Bacaltchuk, H. J. Schneider-Muntau, J. P. Liu, S. Saha, J.A. Barnard *J.Magn.Magn.Mat* **281** (2004) 272–275

[2] H. Xua, H. Heinrichb, J.M. K. Wiezoreka, *Intermetallics* **11** (2003) 963–969

[3] Weller D, Moser A. *IEEE Trans Magn* **35** (1999) 4423.

25PO-13-7

DEFECTS IN Fe-RICH AMORPHOUS MICROWIRES

Palvanov P.S.¹, Gudoshnikov S.A.^{1,2}, Borshagovskaya L.S.¹, Liubimov B.Ya.¹, Usov N.A.^{1,2}

¹Pushkov Institute of Terrestrial Magnetism, Ionosphere and Radio Wave Propagation, Russian Academy of Sciences, (IZMIRAN), 142190, Troitsk, Moscow region, Russia

²Ltd. "Magnetic and Cryogenic Systems", 142190, IZMIRAN, Troitsk, Moscow region, Russia

Amorphous glass coated Fe-rich microwires are very promising for application in microelectronic devices due to their unique physical properties such as nearly rectangular hysteresis loop with a small coercive field $H_c < 1$ Oe, as well as very high mobility of isolated magnetic solitons that can propagate along the wire length. For technical applications one has to control basic magnetic parameters of the microwires, i.e. saturation magnetization, M_s , saturation magnetostriction constant, λ_s , amplitude of the residual quenching stresses, etc. In this report we

show that the physical properties and technological quality of amorphous ferromagnetic microwires are also determined by the presence of various types of local defects both in a ferromagnetic core and in a glass shell of the wire. It is shown that the local defects distributed along the wire length can considerably reduce the value of external magnetic field, H_n , necessary for the domain wall nucleation at a given point of a long microwire. They influence also on the domain wall mobility, dV_{dw}/dH , where V_{dw} is the domain wall velocity, and the characteristic threshold field, H_{th} , for domain wall propagation. The effect of natural and artificial defects on the microwire local nucleation field and the propagation of the isolated magnetic solitons (i.e. head to head domain walls) along the wire length have been investigated by means of the original installation [1].

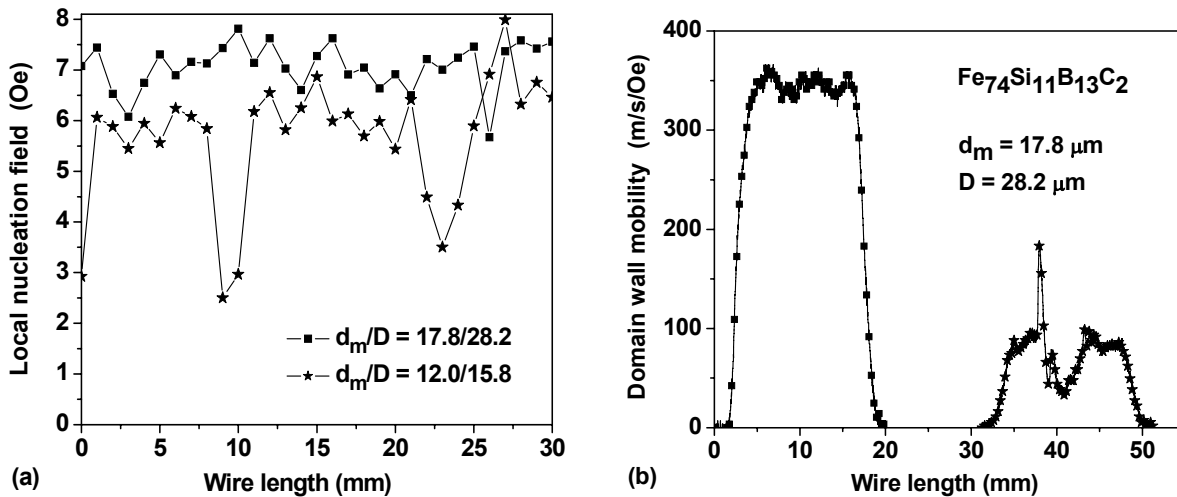


Fig. a) shows the local nucleation field as a function of the wire length for two $Fe_{74}Si_{11}B_{13}C_2$ wires with different metal core diameters d_m and total diameters D (the sizes are given in μm). The positions of the strong localized defects for the second wire correspond to the deep holes where H_n value is considerably reduced. Fig. b) shows the head to head domain wall mobility is presented for two different sections of $l = 17$ mm length of the same Fe-rich microwire. One can assume that the defect density is much higher for the second section where mobility is much lower and is an irregular function of the coordinate along the wire length.

[1] S.A. Gudoshnikov et. al., RF Patent No. 68713 (2007).

25PO-13-8

CERAMIC SUPERCONDUCTORS MAGNETOMETERS COMPARISON CHARACTERISTICS AS APPLIED TO THE BIOMEDICINE

Ichkitidze L.P.¹, Belodedov M.V.²

¹Moscow State Institute of Electronic Technology (Technical University), proezd 4806, 5, Zelenograd, Moscow, 124498, Russia. E-mail: leo852@inbox.ru

²Moscow University of Printing Arts, Prianishnikova str., 2a, Moscow, 125008, Russia. E-mail: m.belodedov@gmail.com

High-temperature superconducting ceramic materials (HTSC) as a rule are granular superconductors, represent "josephson medium" with a high nonlinear magnetic susceptibility in a weak magnetic fields $B \leq 1$ mT. This property is used in magnetomodulation magnetometers

(MMM), using as a magnetosensitive elements moderate cylindrical sample (with a diameter 1-10 mm and a length 5-20 mm) made of ceramic HTSC material. MMM principles of operation are analogous those of a flux-gate magnetometer. Using MMM based on the ceramic HTSC permits to measure magnetic field absolute value (both constant and slow changing), they are easy for manufacturing and servicing and have a cost much less than that of HTSC SQUID magnetometers.

Pilot MMM models based on ceramic HTSC material of Y-123 system are operating at liquid nitrogen temperature ($T \sim 77$ K) with sensibility $\delta B \sim 10^{-11}$ T and dynamic range $D \sim 110$ dB [1-2]. MMM characteristics greatly improve on using ceramic HTSC material Bi-2223 system as a magnetosensitive element [3]. Indeed HTSC materials with composition Bi-2223 have higher critical temperature T_c , than that of Y-123 materials. Difference between the critical temperature and the temperature at operations $\Delta T = T_c - T$ in liquid nitrogen is equal $\Delta T \sim 30$ K for Bi-2223 materials and $\Delta T \sim 14$ K for Y-123 materials, and this leads to the spectrum noise density decreasing in Bi-2223 in comparison with Y-123, and hence lower δB value in Bi-2223. Furthermore, Josephson current density between granules in Bi-2223 materials by $T \sim 77$ K much higher as in Y-123. Therefore, quadratic component response in it must be presented until far greater external magnetic field values ($B^* \sim 1$ mT) than those in Y-123 materials ($B^* \sim 0.3$ mT).

Thus, lower assessed value of sensitivity $\delta B < 10^{-12}$ T and higher limiting value of measuring field $B^* \sim 1$ mT in HTSC ceramic Bi-2223 in comparison with those in ceramic Y-123 permit to create on basis of them the MMM with the parameters values $\delta B \leq 10^{-12}$ T and $D \geq 140$ dB which are closely related to corresponding HTSC SQUID parameters. Proposed MMM parameters make them attractive for using them in biomedicine applications, in particular for liver, lungs, other internal organs and tissues and other biomedicine objects diagnostics.

Prof. Selischev S.V. is acknowledged for supporting this work.

- [1] Belodedov M. V., Chernykh S. V. // [Instr. and Exper. Techniques](#), 2001, No.4. P. 157-161.
 [2] Golovashkin A.I., Kuzmichev N.D., Slavkin V.V. // JTP, 2006. V.76, No.3. P. 81-85.
 [3] Grigorashvily Y. E., Ichkitidze L. P., Volik N.N. // Physica C. 2006. V.435. P. 140-143.

25PO-13-9

ROLE OF MAGNETO-ELASTIC ANISOTROPY IN A FORMATION OF COERCIVE FORCE VALUE OF NANOCRYSTALLINE FeZrN FILMS

Sheftel E.N.¹, Ivanov A.N.², Inoue M.³, Fujicawa R.³, Moiseev A.U.², Usmanova G.Sh.¹, Sidorenko P.K.¹, Blinova E.N.⁴

¹Baikov Institute of Metallurgy and Material Science, RAS, Leninsky pr. 49, Moscow, Russia

²Moscow Institute of Steel and Alloys, Leninsky pr. 4, Moscow, Russia

³Toyohashi University of Technology, Japan

⁴Bardin Central Research Institute for the Iron and Steel Industry, Vtoraya Baumanskaya ul. 9/23, Moscow, Russia

Films of Fe-Zr-N alloys are perspective materials for the high-sensitive magnetic sensors fabrication. It is shown that at proper composition after treatment at specific annealing conditions two-phase (α Fe+ZrN) nanodimension structure forms in the films. The structure provides unique combination of high value of saturation magnetization M_s and extremely low value of coercive force H_c [1]. The films investigated in this work are $\text{Fe}_{79-80}\text{Zr}_{10}\text{N}_{10-11}$ 0,7 μm and 2 μm thickness synthesized by RF reactive magnetron sputtering, annealed after that in

vacuum at 300 ... 700 °C for 1 hour. In this work we investigate influence of annealing temperature on the H_C magnitude (vibrating sample magnetometer), grain size (TEM) and magnitude of macrostresses (XRD) of films.

The common theoretical basis for the understanding magnetic properties, in particularly, magnitude of coercive force H_C of nanocrystalline ferromagnets is the random magnetic anisotropy model of averaging out magnetocrystalline anisotropy [2]. However, the model doesn't consider a role of magneto-elastic anisotropy ($\lambda_S\sigma$) on the H_C magnitude.

In this work the influence of magneto-elastic anisotropy ($\lambda_S\sigma$) on the H_C magnitude of films with ferromagnetic phase grain size more less than ferromagnetic exchange length L_{EX} is studied. The investigated films after sputtering are in compression ($\sigma < 0$). The annealing temperature increase the compressive macrostress decrease and exhibit a zero value at 400-500 °C. At higher temperature the films are in tension ($\sigma > 0$). It is shown, that the annealing temperature increase α Fe phase ($\lambda_S < 0$) grain size increases resulting in decrease of volume fraction of disordered grain boundaries ($\lambda_S > 0$). In this case minimum values of λ_S is reached by compensation of negative λ_S of grain bodies and positive λ_S of grain boundaries at proper parity of its volume fractions [3].

In the investigated films the minimal values of H_C , zero value of macrostress and minimum value of λ_S are reached after the annealing at 400–500 °C.

Support by RFFI grant 08–03–00104–a is acknowledged.

[1] E.N. Sheftel, O.A. Bannykh, *Russian Metallurgy* No 5(2006)394-399.

[2] Herzer G. Nanocrystalline soft magnetic materials // *Journal of magnetism and magnetic materials* /. – 1992. – v. 112. – p. 258–262.

[3] O. A. Bannykh, E.N. Sheftel et.al, *New magnetic material in microelectronic, XV All-Russian school-seminar, Moscow* (1996), pp.70-71

25PO-13-10

EFFECTS OF ANNEALING ON MAGNETIC PROPERTIES AND STRUCTURAL FEATURES OF NANOCRYSTALLINE $Fe_{79}Zr_{10}N_{11}$ FILMS

Sheftel E.N.¹, Iskhakov R.S.², Komogortsev S.V.², Sidorenko P.K.¹, Utitskikh S.I.¹, Perov N.S.³

¹Institute of Metallurgy and Materials Science RAS, Moscow 119991, Russia

²Institute of Physics SB RAS, Krasnoyarsk 660036 Russia

³Faculty of Physics, Moscow State University, Moscow 119992, Russia

Nanocrystalline Fe-Zr-N films are perspective materials for the high-sensitive magnetic sensors fabrication. There is unique combination of high value of saturation magnetization M_s and extremely low value of coercive force H_C in these films of the certain composition annealed under certain conditions. It is established that the effect of annealing is two-phase (α Fe+ZrN) nanodimension structure formation in the films [1]. The correlation between the phase composition and structural state of the films and their magnetic properties should be studied.

In this work we investigate soft magnetic films $Fe_{79}Zr_{10}N_{11}$ with the thickness 0.7 μm, synthesized by high-frequency reactive magnetron sputtering and then annealed at 475 °C and 600 °C during 30, 60, 120 and 180 min. Phase composition, structure and magnetic properties of the films in dependence on annealing condition were investigated. Their magnetic inhomogeneity is revealed on ferromagnetic resonance spectra of $Fe_{79}Zr_{10}N_{11}$ films – two Lorenz-type peaks are needed to fitting experimental resonance absorption curves. The annealing results in some homogenization – for the annealing at 475 °C the weight of one Lorenz-peak

occur considerably much than another; for the annealing at 600⁰C only one Lorenz-peak is needed to fitting experimental resonance absorption curves. The common theoretical basis for the understanding magnetic properties of nanocrystalline ferromagnets is the random magnetic anisotropy model. In this work we use a technique developed on the base of this model – correlation magnetometry – investigation of approach to ferromagnetic saturation curves [2]. The values of local magnetic anisotropy fields (H_a), and the values of correlation radius of magnetic anisotropy (R_c) reduced to the value of $\delta = (A/K)^{1/2}$. It is established that dependences of R_c/δ and H_a on the duration of annealing (τ_{an}) are qualitatively differ for the annealing at 475⁰C and 600⁰C. The annealing at 475⁰C results in decreasing R_c/δ for $\tau_{an} \leq 120$ min. With the annealing duration (at 475⁰C) to 180 min. the value of R_c/δ is increased. The minimal value of coercive force is reached for annealing at at 475⁰C and $\tau_{an} = 120$ min. The annealing at 600⁰C results in increasing the value of R_c/δ for all investigated durations of annealing. There is the correlation $H_c \sim (R_c/\delta)^3$ for the all annealed films of Fe₇₉Zr₁₀N₁₁ alloy. The mixed structure consisting of two basic nanocrystalline phases - the bcc solid solution of N in α -Fe with a grain size of 4-5 nm and Zr_xN_{1-x} with an fcc structure and a grain size of 1-2 nm, and the amorphous (in terms of X-ray analysis) -is formed upon deposition. The annealing results in crystallization of the amorphous phase. As the annealing temperature and duration increases the follow changes of the bcc phase occur: volume fraction increases; content of N decreases; the value of microdistortion decreases; the average grain size increases up to ~7-8 nm at 475⁰C, $\tau_{an} = 180$ min and at 600⁰C for all durations. Observed magnetic characteristics changes in the films were compared with their structural changes.

Support by the grant RFBR 07-02-01172-a; and RFBR08 -03-00104-a, National Science Fund (2008, PhD RAS) are acknowledged.

[1] E.N. Sheftel, O.A. Bannykh, *Russian Metallurgy No5(2006)394-399*

[2] R.S. Iskhakov, S.V. Komogortsev, *Bull. Russ. Ac. Sc.: Phys.*, 71 (2007) 1620.

25PO-13-11

DYNAMIC REARRANGEMENT OF DOMAIN STRUCTURE AND LOSSES IN THIN Fe-3%Si SHEETS IN ROTATING MAGNETIC FIELDS

Tiunov V.F., Filippov B.N.

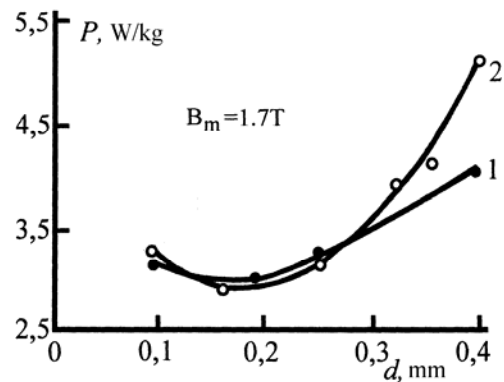
Institute of Metal Physics, Ural Division of Russian Academy of Sciences

At the heart of the magnetic losses physics the dynamic processes, occurring in both domain walls and domain structures, as a whole, in ac magnetic fields, are situated [1]. These processes are well investigated and the essential understanding of the nature of magnetic losses in the case of linearly polarized magnetic fields is achieved. Such understanding does not exist in the situation, when an external field is rotating. Many devices work just in the mode of rotating fields. In this connection the experimental study of domain structures dynamic rearrangement in rotating fields presents an important problem, to which this work is devoted. We processed new experimental equipment allowing observing instant magnetization structures in different phases of rotating field on the whole surface of a sample. As a result it is established:

1. At small amplitudes of induction B_m (up to 0.5 T) the dynamic magnetic reversal of a sample in general is connected with periodic oscillations of domain walls. However amplitudes of various walls oscillations can differ from one another in several times. In such situation the induction of a sample is not a harmonic function of the time.

2. At higher values of B_m the situation greatly varies. So at B_m equal to 0.8 T and higher the oscillations of strip domain walls is accompanied by their drift as a single whole.

3. At $B_m \sim 1.4$ T magnetic reversal of a sample in rotating the field is accompanied by strong dynamic refinement of a domain structure (effect of dynamic splitting of a structure), resulting in reduction of average width of domains in comparison with the initial sizes almost 2-2.5 times. This effect is shown in some induction interval close to $B_m \sim 1.4$ T. The effect is absent both at lower and higher inductions. It is especially strongly pronounced when there is an inclination of [001] easy magnetization axis at a small angle to the sample surface. In this case splitting is connected with favorable conditions for a growth of closing drop-like domains, which exist in plenty, as observations show, on a sample surface. The observed splitting on the samples with $\beta \neq 0$ results in decreasing the level of magnetic losses by rotary magnetic reversal in comparison with the values observed on samples with "ideal" magnetisation orientation (see the figure.).



Fe-3%Si. Here 1- $\beta = 0$, 2- $\beta = 1.5^\circ$
Magnetic losses power on rotary magnetization reversal upon specimen thickness

Support by RFFI, grant №06-02-17082 is acknowledged.

[1] Filippov B.N., Tankeev A.P. Dynamic effects in ferromagnetic with domain structure. Moscow, Nauka, 1987, 216 c.

25PO-13-12

EXPERIMENTAL AND THEORETICAL STUDIES OF THE PROCESSES OF ORDERING IN A SOFT- MAGNETIC IRON-SILICON ALLOY

Gornostyrev Yu.N.^{1,2}, Ershov N.V.¹, Kuznetsov A.R.^{1,2}, Gorbatov O.I.², Lukshina V.A.¹, Serikov V.V.¹, Kleinerman N.M.¹, Chernenkov Yu.P.³, Fedorov V.I.³

¹Institute of Metal Physics, Ural Division of RAS, Yekaterinburg, Russia

²Institute of Quantum Material Science, CJSC, Yekaterinburg, Russia

³St.-Petersburg Institute of Nuclear Physics, RAS, Gatchina, Russia

Using methods of X-ray diffraction and Mössbauer spectroscopy we performed structural investigations of the soft-magnetic alloys $Fe_{1-x}Si_x$ with silicon content within the α field of the phase diagram to show that in the bcc solid solution for $x = 0.05, 0.06$ takes place a concentration-related separation into regions depleted of silicon that exhibit inclusion of the clusters typical of $B2$ ordering. The domains of DO_3 phase were found to appear and co-exist with the $B2$ clusters in the alloy at $x = 0.08$. A local ordering of $B2$ type is revealed even after quenching at a rate of 400 K/s from the temperature 850°C and does not show a pronounced change upon subsequent low-temperature annealing at 450°C – a treatment when the relative fraction of the regions of overwhelming presence of the DO_3 phase gradually increases. After anneal, for all the specimens we have registered a growth in the volume fraction for a configuration that corresponds to one atom of silicon to be located in the first, and another one, in the second coordination shell of the iron atom, both of Si atoms being the fourth neighbors to each other.

To elucidate the mechanism of formation of a short-range order in dilute solid solutions of silicon in iron, on the base of electronic density functional theory by using PAW-VASP method [1] we calculated the enthalpy of Si dissolution, atomic displacements in the vicinity of Si, and the energies of an effective interaction between Si atoms in ferromagnetic iron. It is shown that dissolution of Si atoms in the bcc Fe is energetically beneficial, and the directional character of the Si–Fe chemical bond due to hybridization of p Si and d Fe states entails anisotropy of the atomic displacements in the close vicinity of silicon atoms. The results of calculation show the growth of energy with decreasing in the distance between two Si atoms that is in agreement with the existence of a wide concentration interval of dissolution for Si in Fe. With rising concentration, the Si atoms are prefer to occupy sites in one of sublattices, which results in the formation of the ordered phases in accordance with the phase diagram for the system Fe – Si.

Calculations of the energy of the pairwise and many-body Si–Si interactions as a function of the magnetic state of a bcc Fe were carried out in coherent potential approximation with the use of Green function method [2]. It is established that for a paramagnetic state the Si–Si interaction is considerably weaker in comparison with the case of ferromagnetic state and, thereby, the formation of short range order of Si atoms at $T > T_C$ is hardly feasible. Using the results of calculated Si-Si interactions we performed Monte-Carlo simulation for the formation of the regions of short-range order and determined their atomic and magnetic configurations. It is shown that a most energetically preferable is the configuration where two atoms of Si are in the position of the 3-rd or 4-th neighbors. The results of the calculations and Monte-Carlo simulation for the alloy $Fe_{0.92}Si_{0.08}$ in dependence on temperatures make it possible to explain specific features of the short-range ordering that have been experimentally observed in the Fe–Si alloy.

The authors are grateful for support to RFBR, project no.06-02-17082.

[1] VASP, <http://cms.mpi.univie.ac.at/vasp>.

[2] A.V. Ruban, S. Shallcross, S. I. Simak, H.L. Skriver, *Phys. Rev. B* **70** (2004) 125115.

25PO-13-13

AFMR AND MAGNETOELECTRIC INTERACTION IN HEMATITE PIEZOELECTRIC STRUCTURES

Fetisov Y.K.¹, Meshcheryakov V.F.^{1,2}

¹MIREA, pr. Vernadskogo 78, Moscow, 119454, Russia

²Shubnikov Institute of Crystallography, Leninskiy pr. 59, Moscow, 119333, Russia

Composite structures consisting of magnetic and piezoelectric layers attract great attention recently due to high efficiency of magnetoelectric interactions. These structures are considered as a basis for new generation of magnetic field sensors [1] and electrically controlled microwave signal processing devices [2]. Electrical field applied to the piezoelectric layer results in a deformation of mechanically coupled magnetic layer followed by a change in the ferromagnetic resonance frequency of the structure thus allows control of microwave signal characteristics. In this work the hematite (α -Fe₂O₃) single crystal and piezoelectric lead zirconium titanite (PZT) ceramic element was the system, in which the influence of the static and alternating deformations, created by PZT ceramic, on antiferromagnetic resonance (AFMR) in hematite was investigated. This constructions were placed in external permanent magnetic field H directed parallel to the surface of the hematite plate and perpendicularly to C₃ axis of the crystal. The voltage U up to 300 V was applied to the metalized surfaces of PZT elements. AFMR spectra of the structures were measured at the frequency 36.6

GHz and room temperatures for different values of U and different mechanical stress applied to the structure. The mutual orientation of the magnetic field, stress a HF magnetic field component could be changed. Three configurations were investigated: a) – hematite and PZT plates connected by their surfaces, b) - hematite sample placed inside the PZT ring, and c) – hematite and PZT samples connected in series. An epoxy glue was used to provide mechanical coupling between magnetic and piezoelectric elements. The following results have been obtained:

- The AFMR line width was equal to 70-100 Oe for all the configurations in the absence of static strain. For (a-c) configuration a shift of the AFMR linewidth up to ~ 5 oe was observed when voltage 300 V was applied to the PZT plate. The shift's sign depended on the U polarity.

- For (b) configuration the AFMR line shift up to 900 Oe [3] and increase of the line width was observed due to unsymmetrical strain created by the PZT ring in the absence of voltage U . Sign of the AFMR shift changed when H was rotated in the basis plate of hematite crystal.

- For (c) configuration an increase in the AFMR signal intensity up to $10\div 100$ times was observed when ac modulation of strain created by PZT element was used instead of traditional magnetic field modulation. The signal intensity didn't depend on the orientation of the field H with respect to the strain direction. The calculations have shown, that magnetoelastic interaction does not influence on excitation conditions of the both branches AFMR spectrum. If for static striction u_{xy} and u_{xz} ($x \parallel H$, $z \parallel C_3$) deformations are equal to zero, then only these components determine types of homogeneous acoustic oscillations branch, coupled with AFMR low-frequency branch.

[1] Y.K. Fetisov, K.E. Kamentsev, A.Y. Ostashchenko et al, IEEE Sensors, **6**, 935, (2006).

[2] G. Srinivasan, Y. Fetisov, Ferroelectrics, **342**, 65 (2006).

[3] A.S. Borovik-Romanov, E.G. Rudashevsky, JETP (Rus), **47**, 2095 (1964).

25PO-13-14

MAGNETIC PHASE TRANSITIONS IN AMORPHOUS ALLOYS BASED ON RARE-EARTH METALS

Bondarev A.V., Barmin Yu.V., Balalaev S.Yu., Ozherelyev V.V.

Voronezh State Technical University, 14 Moskovski prospekt, 394026 Voronezh, Russia

e-mail: bondarev@vmail.ru

Amorphous alloys based on rare-earth metals (REM) are of great interest due to their unique magnetic properties. Since heavy REM have large magnetic anisotropy and exchange interaction can vary in the magnitude and sign, in the amorphous alloys based on REM one can observe many types of magnetic ordering (spero-, aspero- or sperimagnetic). In this work we report on the experimental investigation of magnetic properties of binary amorphous alloys of REM with nonmagnetic 5d-transition metals which were almost not studied so far.

Amorphous alloys of the Re-T^{4f} ($T^{4f} = \text{Gd, Tb, Dy, Ho, Er}$) systems were produced by ion-plasma sputtering method. At the low temperatures in these alloys in a wide compositional region the sharp maximum (cusp) on temperature dependence of dynamic magnetic susceptibility $\chi(T)$ and irreversibility of magnetization $M(T)$ are observed. The observed magnetic phase transition is typical for spin glasses. The dependencies of the transition temperatures T_f on the concentration of magnetic ions are linear functions. The slope of these lines decreases with increasing of the number of 4f-electrons of REM. The $\text{Re}_{100-x}\text{-Gd}_x$ amorphous alloys represent the more complex case: at the intermediate concentrations ($x=33-65$

at. %) they turn into the reentrant spin-glass state. All these phase transitions take place if the concentration of the REM atoms exceeds some critical value $x_c=8-20$ at. %.

In order to study the influence of the sort of nonmagnetic atoms on magnetic properties, we additionally prepared the $Tb_x-T^{5d}_{100-x}$ ($T^{5d} = Hf, Ta, W, Re$) ($x=10-90$ at. %) amorphous alloys and measured their temperature dependence of low-field ac susceptibility $\chi(T)$ and dc magnetization $M(T)$. The susceptibility also exhibits a cusp at the temperature T_f , and these alloys undergo the spin-glass like transition. It was revealed that the nature of the T^{5d} element (the number of 5d-electrons) does not influence the T_f values. The only exception are Tb_xHf_{100-x} ($x>50$) alloys with the increased values of T_f . The possible mechanism of this anomalous behaviour is proposed.

25PO-13-15

MAGNETIC STRUCTURE OF $GdMn_2Ge_2$ STUDIED BY NEUTRON DIFFRACTION AND XRMS METHODS

Granovsky S.A.¹, Kreyssig A.², Doerr M.³, Ritter C.⁴, Feyerherm R.⁵, Goldmann A.I.², Loewenhaupt M.³

¹M.V.Lomonossov Moscow State University, 119991 GSP-1 Moscow, Russia

²Ames Laboratory USDOE, Iowa State University, Ames, IA 50011, USA

³TU Dresden, Institut für Festkörperphysik, D-01062, Dresden, Germany

⁴Institut Laue-Langevin, 38042 Grenoble Cedex 9, France

⁵Hann-Meitner-Institute, BESSY, D-12489, Berlin, Germany

Among the large variety of magnetic materials containing rare earth and 3d elements, the ternary RMe_2X_2 compounds ($R =$ rare earth and Y , $Me =$ transition metal, $X = Ge$ or Si) are of the special interest. These compounds exhibit a wide range of physical phenomena: superconductivity, mixed valence, Kondo and heavy-fermion behaviour. Whereas RMe_2X_2 compounds with $Me = Co, Fe$ and Ni have non-magnetic 3d sublattice, magnetic properties of the manganese-containing RMn_2X_2 are determined by two subsystems formed by rare earth and manganese ions. Various magnetic structures and a number of field-, temperature- or pressure-induced magnetic phase transitions were observed in these compounds due to the interplay between exchange interactions of the different types.

The RMe_2X_2 compounds crystallize in the $ThCr_2Si_2$ -type tetragonal structure (space group $I4/mmm$). The R, Mn and Si/Ge layers form a sequence $R-X-Mn-X-R$ perpendicular to the tetragonal axis. The Mn -atoms occupy a primitive tetragonal sublattice in this structure in which the distance between the Mn -atoms in the layer is approximately a half the distance between the adjacent layers. This feature leads to a significant spread of the manganese 3d electrons within the layers, and, as a result, the strength and the sign of magnetic interactions significantly depend on the both inlayer and interlayer $Mn-Mn$ separations.

According to results of magnetisation, resistivity and thermal expansion experiments, below $T_C \cong 96$ K the collinear ferrimagnetic structure, in which Gd -moments are coupled antiparallel to Mn moments is formed in $GdMn_2Ge_2$. With increasing the temperature the strength of the f-d exchange is decreasing and at T_c magnetic moments rearranged to the collinear antiferromagnetic structure. The transition ferrimagnetism-antiferromagnetism is a first-order type and is accompanied by a significant lattice expansion ($\Delta V/V \cong 3.2 \times 10^{-3}$) [1] and an anomaly of the temperature-dependent electrical resistivity [2]. Being compensated by molecular field of neighbour Mn atoms, Gd do not carry the magnetic moment in the antiferromagnetic phase. So the "separate" magnetic ordering of Mn -moments is established in this temperature

region. Moreover, observation of the high-temperature weak ferromagnetic phase above the Néel point is described in [3].

In this contribution the first direct probe on magnetic structure of GdMn_2Ge_2 is reported. Results of the hot neutron powder diffraction and X-ray resonant magnetic scattering experiments on a single-crystalline sample are presented.

This work was supported by RFBR (Grant # 06-02-17291).

[1] I.Yu.Gaidukova, Guo Guanghua, S.A.Granovsky, I.S.Dubenko, R.Z.Levitin, A.S.Markosyan, V.E.Rodimin, *Fiz.Tverd.Tela* **41**, (1999), 2053. (in Russian).

[2] T. Fujiwara, H.Fujii, *Physica B* **300** (2001) 198.

[3] T.Shigeoka, H.Fujii, H.Fujiwara, K.Yagasaki, T.Okamoto, *J.Magn.Magn.Mater* **31-34** (1983) 209.

25PO-13-16

MIXED MAGNETO-OPTICAL CONTRAST IN THE MAGNETIC FILMS WITH PLANE ANISOTROPY CAUSED BY A NON-UNIFORM MAGNETIC FIELD

Ivanov V.

Ural State University, 620083, Ekaterinburg, Russia

An action of a non-uniform magnetic field gives rise analog magneto-optic (MO) contrast in bismuth-substituted ferrite-garnet films with planar anisotropy [1]. The ferrite-garnet films have been used for the visualization of magnetic fields of various origins.

In our work the pictures of MO-contrast caused by a non-uniform magnetic field of permanent magnet (fig. 1) arising in the metallic and amorphous films with planar anisotropy are analyzed.

In geometry of polar Kerr effect contrast in the form of the light and dark strips above edges of a magnet (fig. 2a) is observed. In geometry of longitudinal Kerr effect there are fragments of longitudinal Kerr effect and polar Kerr effect contrast. This picture we interpret as mixed magneto-optic contrast that was caused by change of horizontal (J_x) and vertical (J_z) magnetizations components of a display film.

Decoding of observable pictures is lead at the account of coordinate distribution of magnetization $\mathbf{J}_s(x)$ (magnetic structure) in the display film and gradation of the brightness simulated in the assumption of additivity both MO-effects corresponding this distribution. Distribution $\mathbf{J}_s(x)$ was minimization of energy $E = -\mathbf{J}_s(x)\mathbf{H}(x) + K_p$, where K_p - an effective constant of anisotropy.

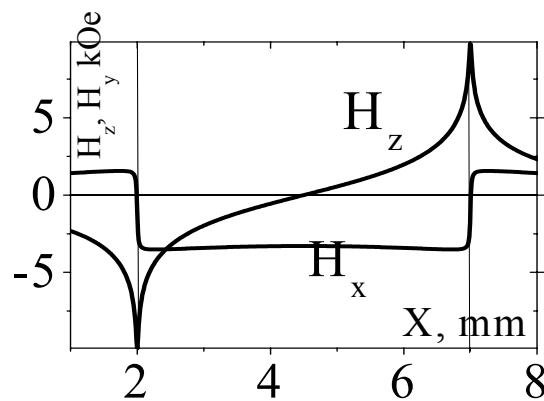


Fig.1

The intermediate result of simulation considering gradation of brightness, caused only tangential magnetizations components $J_s(x)$ shows presence of precise border directly above edge of a magnet (fig. 2c). Summation of these pictures veils these borders (fig. 2d) that qualitatively agrees with experiment.

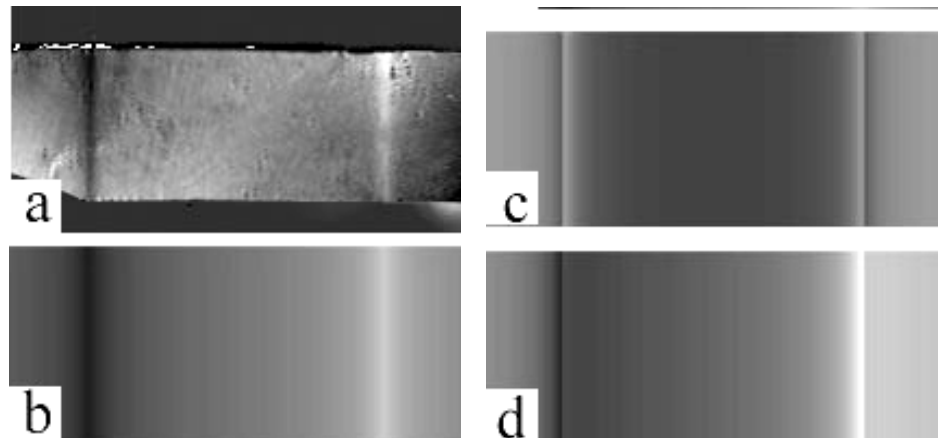


Fig.2

[1] Grechishkin R.M., Goosev V.Yu., Il'yashenko S.E., Neustroev .S./J. Magn. Magn. Mater. 1996. Vol. 157/158, P. 305-306.

25PO-13-17

MAGNETIC PROPERTIES OF NANOSTRUCTURAL Y-Fe-B ALLOY RIBBONS PREPARED BY CENTRIFUGAL MELT-SPUN METHOD

Kudrevatykh N.V.¹, Bogatkin A.N.¹, Kozlov A.I.¹, Andreev S.V.¹, Markin P.E.^{1,2}, Milyaev O.A.¹, Bartashevich M.I.¹, Emelina T.N.¹, Pirogov A.N.², Pushin V.G.²

¹Ural State University, 620083, Ekaterinburg, Lenin av. 51, Russia

²Institute of Metal Physics, Ural Division of RAS, S. Kovalevskaya 18, 620041 Ekaterinburg, Russia

Objects of research in work were rapidly quenched alloys (RQA) of Y-Fe-B system in the vicinity of $Y_2Fe_{14}B$ phase composition, prepared by the centrifugal quenching method [1].

As a magnetism of such objects is entirely originates from Fe- ions subsystem, this circumstance allowed to establish explicitly a role of Fe subsystem in magnetism of $R_2Fe_{14}B$ RQA in general (including RQA where R is magnetically active ion).

Another task of this work was the realization in Y-Fe-B RQA a nanocrystalline structure and finding out the conditions of occurrence and the value of remanence enhancement effect $\Delta\sigma_r=(\sigma_r/\sigma_s-0.5) >0$ and also an opportunity of a nanograins texture formation.

Depending on composition, they were divided into three groups: "overstoichiometric" – $Y_{14,5}Fe_{79,5}B_6$ (alloy A); stoichiometric- $Y_{12}Fe_{82}B_6$ (alloy B); "understoichiometric" – $Y_9Fe_{85}B_6$ (alloy C) and $Y_9Fe_{79}B_{12}$ (alloy D).

Phase and atomic structure analyses have been performed by X-ray, electron and neutron diffractions methods. Subatomic structure has been studied by a scanning electron and atomic force microscopy methods and by a small angle neutron scattering techniques. The magnetic properties have been measured with a vibrating sample magnetometer (in fields up to 20 kOe) and by induction method in pulse magnetic fields (H) up to 100 kOe.

It is revealed, that contrary to the isocompositional RQA with Nd, in understoichiometric RQA the multiphase heterogeneous structure with a presence of minimum four different phases is realized: $Y_2Fe_{14}B$, YFe_7 , α -Fe and amorphous (AP), close probably to 2-14-1 composition.

Their content depends on the chilling wheel surface speed $-V_s$, and the melt temperature $-T_L$ at the moment of spinning procedure. For all RQA coercivity (iH_c) value as function of V_s and T_L has a maximum on both arguments. By neutron diffraction and X-rays methods it is established, that with T_L lowering the content of an amorphous phase in RQA prepared at $V_s \geq 30$ m/s is increased. Short-time heat treatment of RQA in a temperatures range 400-900°C can significantly change a morphological structure, phase content and magnetic properties of annealed materials. The maximal iH_c and residual specific magnetization σ_r values are realized after annealing treatment in the narrow temperature interval 700-800 °C.

It is worth notice that the effect of remanence enhancement in the isotropic uniaxial magnetic material above the level of 0.5, as far as the $iH_c = 3.5$ kOe were observed in this alloys for the first time. It allows to consider them as a perspective filler materials for bonded magnets.

From comparison of $\sigma(H)$ dependences for nanocrystalline isostructural A, B and C alloys, the value of the effective field causing the remanence enhancement effect $\Delta\sigma_r > 0$ in B and C alloys has been inferred.

This work was supported by RF High School Science Potential Development Program -project RNP.2.1.1.6945.

[1] V.I. Pushkarsky, N.V. Kudrevatykh, L.A. Pamyatnykh, S.V. Andreev, Proc. Of 9-th Int. Conference On Rapidly Quenched & Metastable Mater.-Bratislava, 1996.-Abstr. Book, P.92.

25PO-13-18

ATOMIC ORDERING OF Fe-Co ALLOYS IN THIN MAGNETIC FILMS AT ROOM TEMPERATURE

Repina N.M.

Krasnoyarsk Institute of Railway Engineering, 89, L.Ketskhoveri St, Krasnoyarsk, 660028, Russia

It is known that the process of atomic ordering in Fe-Co alloys proceeds comparatively fast. Therefore it is very difficult to receive a disordering condition of alloy 50 at.% - 50 at.% Co in massive specimens.

The investigations of epitaxial magnetic films 50 at.% Fe-50 at.% Co show that this alloy may be received in the disordering condition comparatively easily.

Originally the processes of ordering in epitaxial films Fe-Co at the room temperature were studied.

Single (001) films of Fe-Co alloys were grown by the method of vacuum condensation on the surfaces of the splits of LiF and MgO crystals.

The electronographical investigations of the films were conducted with the amplication "the method of the small makeweights" theoretic proposed by Krivoglas and experimentally was confirmed by us. Au up to 1 at.% and Pd up to 2 at.% were used as makeweights. Just condensed films super structure phase of films is absent. The diffuse background on the electronograms of films appears after two days, which is intensified during the time.

On the eighth day the weak reflects type $\{100\}$ appears, and a diffuse background on the electronograms of films begins to weaken, however it does not disappear completely.

In the given work it was investigated the changes of magnetic anisotropy, electro resistance and coercive force at natural aging were investigated. The process of atomic ordering in this films may take place at the room temperature and even at much lower temperatures.

In the course of the investigation of magnetocrystalline anisotropy stoichiometric compositions specimens the epitaxial films it was discovered that the first constant of this anisotropy changes its value from -5×10^5 to $-0,5 \times 10^5$ erg/sm³. The changes of K_1 are insignificant during three days. The principal changes of K_1 films begin for three days and they finish for nine days. The energy of activation of the change K_1 process during the natural aging ($E = 0,25$ eV) was measured. The change K_1 films at natural aging are similar to the change K_1 at ordering annealing of massive specimens.

The electroresistance R was measured. It was researched that increasing of R corresponds to the appearing of the diffuse background in the electron diffraction pattern. The decreasing of R leads to the weakening of diffuse background and appearing of super-lattice reflexes.

The coercive force was measured under the magnetization reversal of films along one of the easy magnetic axis. During three days the changes of H_C were absent. After three days of aging the coercive force of film begins to decrease slowly. Between the seventh and tenth days of aging the sharp (approximately 1,5 time) decrease of H_C was observed.

The role of covalent and metallic bonds in the effect and mechanism of ordering will be discussed.

The results of the above described the researches allow to make the conclusion that in film specimens Fe-Co may be received in the disordering condition comparatively easily. This condition of alloy is metastable and at the room temperature it takes place gradually in the atomic ordering condition. These scientific data facilitate the study of atomic ordering influence on the physical properties of alloy.

25PO-13-19

THE EFFECT OF DISORDERING ON MAGNETIC PROPERTIES OF Fe-Al ALLOYS

Voronina E.¹, Yelsukov Eu.¹, Korolyov A.², Nagamatsu Sh.³, Fujikawa T.³, Miyanaga T.⁴

¹Physical-Technical Institute of UrB RAS, 132 Kirov Str., 426000 Izhevsk, Russia

²Institute of Metal Physics UrB RAS, S.Kovalevskoi Str., 620041 Ekaterinburg, Russia

³Chiba University, 1-33 Yayoi-cho, Inage, Chiba 263-8522, Japan

⁴Hirosaki University, 3-Bunkyo-cho, Hirosaki, Aomori 036-8561, Japan

Up to date bcc binary Fe-Al alloys attract great attention in magnetic interactions and magnetic structure aspect. B2 or DO₃-type ordered alloys with Al content from 25 to 35 at.% and the disordered by mechanical activation alloys with Al content from 35 to 60 at.% have abnormal magnetic properties, that can not be explained by well-known canonical microscopic models of magnetic moments arrangement. The magnetization curves for both groups of alloys are not saturated in external fields up to 5T. The hysteresis loop is not shifted and the alloys do not demonstrate a true temperature hysteresis if the strength of external magnetic field exceeds the value of confluence of ascending and descending branches of hysteresis loop. ZFC and FC curves in low magnetic fields exhibit a clearly distinguished maximum. Both ordered and disordered alloys show qualitatively similar temperature and in-field dependences of magnetization, magnetic susceptibility and ⁵⁷Fe hyperfine magnetic field.

The earliest [1] and recent [2] neutron scattering studies of the ordered alloys indicate existence of magnetic inhomogeneities on a nanometer scale. Temperature studies of magnetization show its superparamagnetic-like behaviour and give the estimation of Fe atoms number in fluctuating clusters $\sim 10^3$ - 10^4 at.

For the ordered and disordered alloys the model of magnetic structure in ground (energy) state was proposed. The model supposes that the Fe atom local magnetic moments are collinear with magnitude and direction depending on the number of Al atoms in the Fe nearest neighbourhood (Mattis' magnet model). The model fits empiric concentration dependence of saturation magnetization for the alloys in the concentration intervals referred to above. In the ordered alloys this model accounts for the formation of nanometer magnetic inhomogeneities (regions with magnetic moments directed opposite to the total magnetization).

The results of polarized Moessbauer spectroscopy studies [4] for the disordered Fe-Al alloys allow the existence of Fe atom magnetic moments directed antiparallel to the total magnetization. X-ray magnetic circular dichroism measurements (XMCD, Fe K-edge absorption spectra) of disordered Fe-Al alloys indicate the essential changes in XMCD –signal as Al content exceeds 40 at.%. Theoretical XMCD-calculations performed for the above model of collinear magnetic moments reproduce the changes observed in the experimental XMCD-signal. A great number of defects in atoms arrangement proper to the disordered alloys block the formation of extended magnetic inhomogeneities similar to those in the ordered alloys. Analysis of these data along with results of magnetometric and Moessbauer studies carry inference that magnetic state of the disordered Fe-Al alloys is adequate describable by Mattis' magnet model.

Support by RFBR (Grant N 06-02-16179-a) is acknowledged.

[1] J.W. Cable, L. David, R.Parra, *Phys.Rev.B*, **16**(1977)1132.

[2] D.R.Noakes, A.S.Arrott, M.G.Bells et al, *Phys.Rev.Lett.* **91**(2003)217201.

[3] K. Szymacsky, D. Satula, L.Dobrzycsky, E.Voronina et al, *Phys.Rev.B*, **72**(2005)104409.

25PO-13-20

MOSSBAUER SPECTRA ^{57}Fe OF AMORPHOUS Co-BASED MATERIALS

Prokoshin A.F.¹, Pokatilov V.S.², Dmitrieva T.G.², Balmashov S.A.²

¹Central Scientific Research Institute for Ferrous Metallurgy by I.P. Bardin, 105007, Moscow, 2nd Baumanskay str., Russia

²Moscow State Institute of Radio Engineering, Electronics and Automation, . 119454, Moscow, pr. Vernadskiy 78, Russia

The amorphous soft magnetic wire and ribbon-shaped materials of the CoFeSiB system are of great interest due to their technological application in the field of electronics. It is well known that investigation of the short-range order and spin texture is important for understanding of peculiarity of such magnetic materials. The present work devotes to investigation of the hyperfine interaction (HFI) (hyperfine field B, isomer δ and quadrupole ϵ shifts and spin texture) of the ribbon-shape $\text{Co}_{75.3}\text{Fe}_{4.6}\text{B}_{20.1}$ (1), $\text{Co}_{74.5}\text{Fe}_{0.5}\text{B}_{10}\text{Si}_{15}$ (2), $\text{Co}_{66}\text{Fe}_9\text{B}_{10}\text{Si}_{15}$ (3) and glass-coated microwires $\text{Co}_{66}\text{Fe}_9\text{B}_{10}\text{Si}_{15}$ (4) at 87K and room temperature (RT). Mossbauer spectra show broadened lines due to the occurrence of HF field distributions typical for amorphous alloys. The distribution functions of HFF $P(B)$, isomer shift $P(\delta)$ and quadrupole shift $P(\epsilon)$ were reconstructed using the DISTRI program [1]. The average HFF B_{av} , isomer δ_{av} and quadrupole ϵ_{av} shifts and also the widths of the distribution $P(B)$ are given in Table for some samples at RT.

№	Composition, at. %	B_{cp} , kOe	ΔB , kOe	Δ_{av} , mm/s	ε_{av} , mm/s
1	$Co_{75.3}Fe_{4.6}B_{20.1}$	268,5 (± 2)	61,53 (± 2)	0,12 ($\pm 0,01$)	-0,00 ($\pm 0,01$)
2	$Co_{74.5}Fe_{0.5}Si_{15}B_{10}$	233,73 (± 2)	55,26 (± 2)	0,18 ($\pm 0,01$)	-0,01 ($\pm 0,01$)
3	$Co_{66}Fe_9Si_{15}B_{10}$	254,31 (± 2)	55,18 (± 2)	0,17 ($\pm 0,01$)	-0,00 ($\pm 0,01$)
4	$Co_{66}Fe_9Si_{15}B_{10}$	244,35 (± 2)	59,96 (± 2)	0,17 ($\pm 0,01$)	-0,00 ($\pm 0,01$)

The substitution of Si for B decreases the average HFF and increases the average isomer shift. From these results it may be concluded that silicon adds more electrons to the iron 3d band than boron. Short-range order and spin texture are considered in these amorphous alloys as well.

[1] V.S.Rusakov. Mossbauer spectroscopy of locally inhomogeneous systems. Almaty, 2000, p.430 (in Russian).

25PO-13-21

ANNEALING TEMPERATURE DEPENDENCE OF DOMAIN STRUCTURES AND MAGNETIZATION REVERSAL IN CoNbZr THIN FILMS

Gornakov V.S.¹, Lee C.G.², and Hamid E.²

¹Institute of Solid State Physics RAS, Chernogolovka, Moscow distr., 142432, Russia

²Changwon National University, Changwon, Gyeongnam 641-773, South Korea

The amorphous CoNbZr layer exhibits good thermal stability, soft magnetic properties, and small magnetostriction. Thus it has been used for many applications: high-frequency carrier-type thin-film magnetic field sensors with a high sensitivity and quick response, recording and read heads and solid-state memory, ferromagnetic RF integrated thin film inductors and electromagnetic noise suppressors, which are currently used in modern information technology. The physical properties of such a thin films are strongly depending on their domain and real crystalline structures and domain wall displacement [1]. In this report, we observed statically and dynamically domain structures of the thin CoNbZr films and investigated an annealing temperature influence on the structure and magnetization reversal in the films with two different thicknesses.

Films were prepared by the reactive RF magnetron sputtering with a base pressure less than $2 \cdot 10^{-6}$ Torr and the Ar gas pressure of 8 mTorr during sputtering. The films of 20 nm and 135 nm thickness were deposited on Si substrates from a CoNbZr target. Domain structures and magnetization reversal process were studied by magneto-optical indicator film (MOIF) technique. Hysteresis loops were measured by a vibrating sample magnetometer. The electrical resistivity of the thin film was determined by the four-point probe method. The film structures were investigated by X-ray diffractometry and transmission electron microscopy.

Non-uniform magnetization distribution in ground state of thin amorphous ferromagnetic films is revealed. These films are shown to possess dispersions of a uniaxial magnetic anisotropy. We have studied magnetization reversal processes in CoNbZr films using the MOIF technique and magnetometry. As-deposited films have had square hysteresis loops of 2.2 Oe and 8.2 Oe coercive forces for 135 nm and 20 nm thicknesses, respectively. The MOIF images

clearly reveal, when the external magnetic field is oriented along the easy anisotropy axis, the remagnetization occurs by two steps. Initially, there is a weak local magnetization rotation, further increasing of the external magnetic field results in the nucleation and motion of domain walls. It was shown that reversal of the thinnest films is controlled by new domain nucleation inside them, whereas the thicker film reversal is done by same process at the edges. The magnetic reversal centers were observed when the field was oriented far away from the easy axis at some angle. X-ray diffractometry has shown that in these films can form Co and Nb clusters, which have different structure and magnetic properties and might play an essential role in the reversal of the samples. It was shown that an annealing temperature up to 500°C for 30 min doesn't practically influence on the real structure, whereas it is leading to the change of the magnetization reversal process.

This work was partially supported by Grant 08-02-01268 from the Russian Foundation for Basic Research.

[1] M. Takezawa and J. Yamasaki, *IEEE Trans. Magn.*, **37** (2001) 2034.

25PO-13-22

MAGNETIC PROPERTIES OF FeSi CRYSTALS WITH Co IMPURITIES

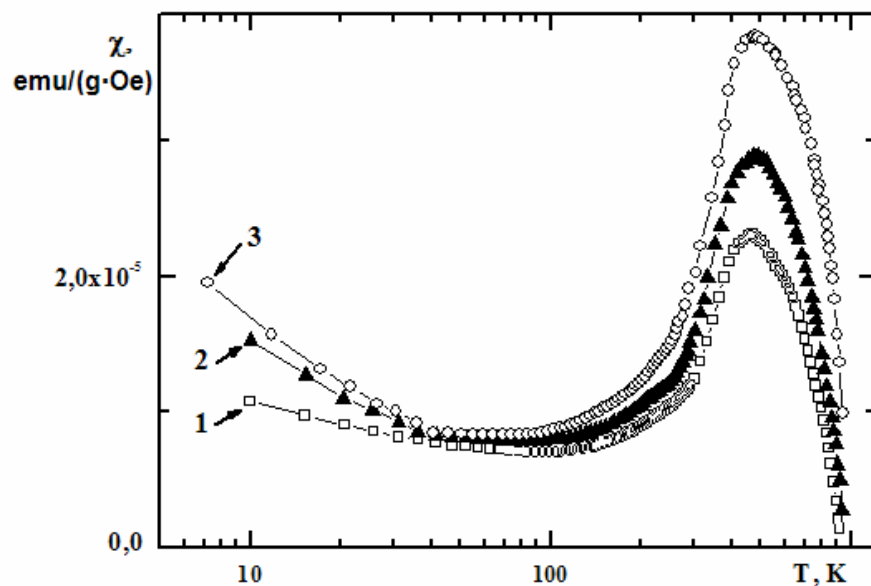
Patrin G.S.^{1,2}, Beletsky V.V.², Velikanov D.A.¹, Yurkin G.Yu.¹

¹L.V. Kirensky Institute of Physics, Siberian Branch of Russian Academy of Sciences, Krasnoyarsk, 660036, Russia

²Siberian Federal University, prospect Svobodny, 79, Krasnoyarsk, 660041, Russia

Owing to unique properties the FeSi crystal attracts attention of researches in the course of many years. In this crystal the behavior of magnetic susceptibility, thermal and electric parameters are unusual. According to some features FeSi crystal is related either to Kondo class of compounds [1] or material showing semiconductor-metal transition. By increasing temperature up to $T = 90$ K the magnetic susceptibility ($\chi \sim 10^{-4}$ to 10^{-6}) falls and then it is noticeably rises, running up to maximum at $T = 500$ K [2].

The CoSi crystal is isostructural to FeSi crystal. Present isolated experiments show that the addition of Co ions to FeSi host results in cardinal change of magnetic properties [3]. Primordial FeSi is paramagnetic and CoSi is diamagnetic, but $\text{Fe}_{1-x}\text{Co}_x\text{Si}$ solid solutions ($x \geq 0.1$) are ferromagnetic. We have made an attempt to investigate in what way the change of magnetic state occurs with doping Co ions in an impurity limit. Our researches were made with polycrystalline samples.



X-ray measurements were carried out with several samples chosen in different locations of crucible. For every samples synthesized the X-ray data agree with data presented in paper. Magnetic properties of $\text{Fe}_{1-x}\text{Co}_x\text{Si}$ crystals with $x \geq 0.1$ are quite similar to ferromagnetic ones.

In figure the temperature dependences of magnetic susceptibility are represented for $\text{Fe}_{1-x}\text{Co}_x\text{Si}$ crystals with: 1 – $x = 0.001$, 2 – $x = 0.005$, 3 – $x = 0.01$. It is seen that with increasing cobalt ion content the rise of magnetic susceptibility takes place both at low temperatures and at high temperatures. Field dependences of magnetization for crystals with $x = 0.001$ и $x = 0.005$ have practically linear form both at low temperatures and at high temperatures, and only for crystal with $x = 0.01$ deviation from linearity becomes apparent. At low temperatures the rise of χ one can explain by direct influence of doped cobalt ions and at high temperatures, apparently, by influence of cobalt ions on states of neighbor iron atoms, that results in additional magnetic contribution because of formation of Co-Fe complex. Thus, one can contend that the addition of cobalt ions results in reconstruction of electron spectrum.

[1] G. Aeppli, Z. Fisk. Comments Cond. Matter Phys., **16** (1992) 155.

[2] M. Imada, A. Fujimori, Y. Tokura. Rev. Mod. Phys., **70** (1998) 1039.

[3] S. Asanabe, D. Shinoda, Y. Sasaki. Phys. Rev., **134** (1964) 774.

25PO-13-23

MAGNETIC PROPERTIES OF $\text{Fe}_{1-x}\text{Co}_x\text{Si}$

Yurkin G.¹, Patrin G.^{1,2}, Velikanov D.^{1,2}

¹Kirensky Institute of Physics, 660036 Krasnoyarsk, Russia

²Siberian Federal University, 660049 Krasnoyarsk, Russia

We report temperature $\sigma(T)$ and magnetic field $\sigma(H)$ measurements of the magnetic susceptibility for polycrystalline samples of $\text{Fe}_{1-x}\text{Co}_x\text{Si}$ with $x=0$ and 0.01 . The samples were prepared by standard melting technique. FeSi compound is formed congruently at 1410°C . This compound exists at Si content from 49 to 50,8 % (at.), which corresponds to ϵ -phase. The low temperature measurements were carried out by SQUID at temperature range from 4.2 to 300 K and high temperature measurements were carried out by VSM at temperature range from 300 to 1000 K. We have found the unusual behavior of magnetic properties of FeSi, there is a broad maximum in temperature dependence of magnetic susceptibility [1]. We illustrate the temperature dependence of susceptibility of samples on Figure 1. Figure 1 shows that infusion of slight amount of Co resulted in significant increasing and changing FeSi susceptibility. The

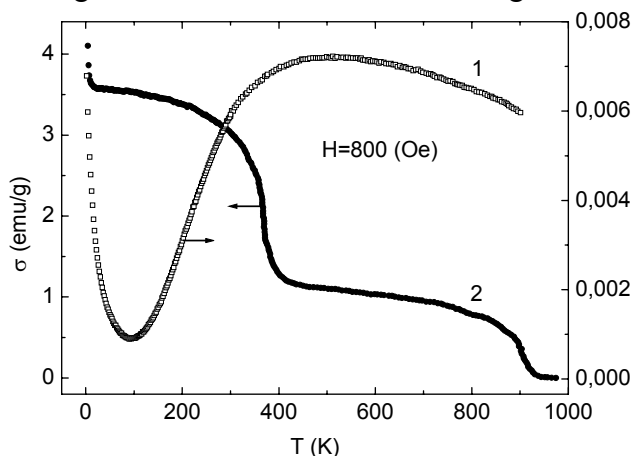


Fig.1. Temperature dependence $\sigma(T)$ of polycrystalline FeSi (1) and $\text{Fe}_{0.99}\text{Co}_{0.01}\text{Si}$ (2).

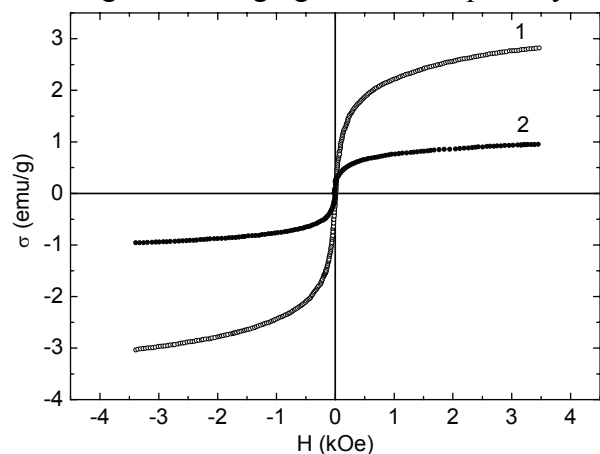


Fig.2. Magnetic field dependence $\sigma(H)$ polycrystalline $\text{Fe}_{0.99}\text{Co}_{0.01}\text{Si}$ at temperatures 300K (1) and 700K (2).

magnetic field dependence of susceptibility of FeSi samples is linear. Figure 2 shows magnetic field dependence of $\text{Fe}_{0.99}\text{Co}_{0.01}\text{Si}$ susceptibility at temperatures 300 and 700 K.

[1] Mihalik M. et al. Magnetic properties and gap formation in FeSi, *JMMM.*, **157** (1996), 637.

25PO-13-24

ELECTRONIC STRUCTURE AND MAGNETIC PROPERTIES OF EuB_6 AND YbB_6

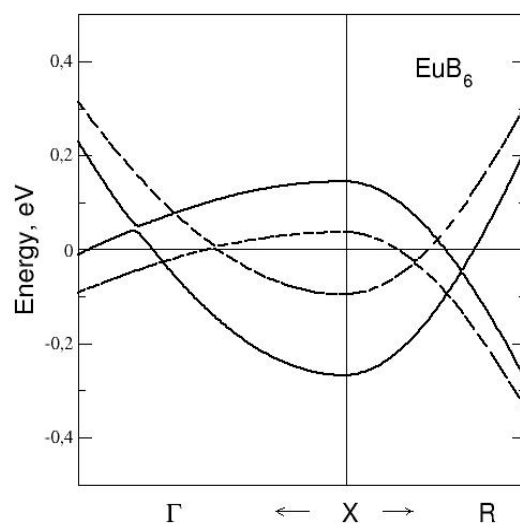
Grechnev G.E.¹, Logosha A.V.¹, Panfilov A.S.¹, Svechkarev I.V.¹, Shitsevalova N.Yu.²

¹B.Verkin Institute for Low Temperature Physics and Engineering, Kharkov, 61103, Ukraine

²Institute for Problems of Material Science, Kiev, 03680, Ukraine

Rare-earth hexaborides attract considerable interest due to their peculiar physical properties, such as Kondo and valence fluctuation effects (CeB_6 and SmB_6), anomalous magnetic and narrow gap semiconducting properties (EuB_6 and YbB_6). The main objective of this contribution was to determine the principal electronic states and interactions responsible for intriguing magnetic properties of EuB_6 and YbB_6 compounds. In particular, we are focused on theoretical and experimental studies of the atomic volume effect on electronic structure and magnetic properties of the hexaborides. Reliable *ab initio* electronic structure calculations have been carried out for paramagnetic (PM), ferromagnetic (FM) and antiferromagnetic (AFM) phases of the RB_6 compounds by using the full potential linear muffin-tin orbital method. The magnetic stability of FM and AFM phases of RB_6 has been examined. The temperature and pressure dependencies of magnetic susceptibility were experimentally studied for the PM phases of EuB_6 , GdB_6 and $\text{EuB}_{6-x}\text{C}_x$. For EuB_6 the paramagnetic Curie temperature is found to be increasing with pressure, $d\theta/dP=0.44\pm 0.03$ K/Kbar, whereas in related GdB_6 compound with the same f -shell configuration (f^7) the pressure effect is lower in magnitude but opposite in sign: $d\theta/dP=-0.17\pm 0.03$ K/Kbar. The calculations have confirmed that stability of FM phase in EuB_6 is enhanced by applying pressure, in accordance with increasing of T_C under pressure. The band overlap at the X point is found for all phases of EuB_6 (see the Figure), and the corresponding tiny electron pockets provide the RKKY-like interaction between Eu atoms.

The Figure shows a transformation of the band overlap at X under lattice parameter expansion (about 5%, dotted lines). On the other hand, the compression enhances the band overlap and conduction electron concentration and increases T_C . Our studies on $\text{EuB}_{6-x}\text{C}_x$ show that the carbon doping is favourable for transition to the AFM phase. The same trend takes place with increasing of the lattice constant in EuB_6 , where the total energy difference between the FM and AFM phases decreases, as well as the extent of the band overlap at X (see the Figure). According to our calculations, the opening of a band gap for the minority spin states is expected in the FM phase under the lattice expansion (e.g. by epitaxial growth on a substrate). This can induce a half-metallic semimetal, which has electron and hole pockets for majority spin states and the opening of a band gap for minority spin states. The



opening of a band gap for the minority spin states is expected in the FM phase under the lattice expansion (e.g. by epitaxial growth on a substrate). This can induce a half-metallic semimetal, which has electron and hole pockets for majority spin states and the opening of a band gap for minority spin states. The

calculations have confirmed a semiconducting ground state of YbB_6 at ambient conditions. A possibility of transition to the Yb^{+3} state with the lattice parameter variations is investigated.

25PO-13-25

MAGNETIC PROPERTIES OF THE DIPOLE FERROMAGNET DyF_3

*Savinkov A.V.¹, Korableva S.L.¹, Rodionov A.A.¹, Kurkin I.N.¹, Malkin B.Z.¹,
Tagirov M.S.¹, Suzuki H.², Matsumoto K.², Abe S.²*

¹Kazan State University, 420008 Kazan, Russian Federation

²Kanazawa University, Kakuma-machi, 920-1192 Kanazawa, Japan

The heavy-rare-earth fluorides, from SmF_3 to YbF_3 , having an orthorhombic $\beta\text{-YF}_3$ structure, show a variety of magnetic behavior and attract interest as model systems for theoretical studies of magnetic ordering in rare-earth insulators with competing dipole and exchange interactions. The magnetic ordering was found in TbF_3 , HoF_3 (canted ferromagnets with $T_C=3.95$ and 0.53 K, respectively) and ErF_3 (antiferromagnet with $T_N=1.05$ K) trifluorides. Low temperature magnetic properties of DyF_3 were not described in the literature, however the λ -type anomaly in the specific heat due to the ferromagnetic ordering of Dy^{3+} moments along the b -axis below $T_C = 2.53$ K was communicated in Ref.[1].

In the present study temperature dependences of the principal values of the magnetic susceptibility tensor in DyF_3 were obtained from direct measurements of magnetization in weak external magnetic fields. The ordered state was found at temperatures below $T_C = 2.55(2)$ K. For the magnetic field directed along the b -axis, the susceptibility in the ordered state does not depend on temperature (Fig.1) and is determined by the demagnetizing factor of a sample that gives evidence for the ferromagnetic state induced by magnetic dipole-dipole interactions

between the Dy^{3+} ions. Magnetic moments of Dy^{3+} ions in the ordered state were determined from magnetization measurements in strong magnetic fields up to 5.5 T in paramagnetic phase (see insert in Fig.1). Additional information on magnetic properties of Dy^{3+} ions in trifluorides was obtained from EPR studies of $\text{YF}_3:\text{Dy}^{3+}$ single crystals at liquid helium temperatures. The measured components of the g -tensor in the ground state of Dy^{3+} ions and variations of the magnetization in DyF_3 with temperature, magnetic field strength and direction are described in the frameworks of the crystal field theory and the mean field approximation. Crystal field parameters for concentrated DyF_3 and diluted $\text{YF}_3:\text{Dy}^{3+}$ crystals were estimated by making use of the semi-phenomenological exchange charge model and then corrected by comparing results of calculations with the experimental data. Parameters of the internal dipolar field were calculated by the Ewald method, and the constant of the isotropic antiferromagnetic exchange interaction between the nearest neighbor Dy^{3+} ions was estimated from a comparison of the theoretical and experimental values of the Curie temperature.

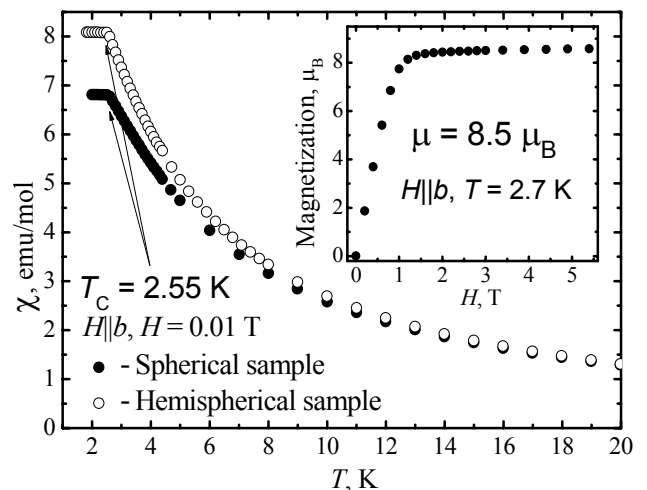


Fig.1. Magnetic susceptibility of DyF_3 samples with different shapes.

[1] L.M. Holmes, F. Hulliger, H.J.Guggenheim, J.P.Maita, *Phys. Lett.*, **50A** (1974) 163.

25PO-13-26

TEMPERATURE EFFECT ON REVERSIBLE AND IRREVERSIBLE PHASE TRANSITIONS BY THE EXAMPLE OF STUDYING MAGNETIC PROPERTIES OF CAST AMORPHOUS MICRO WIRE

Baranov S.A.¹, Karimova G.V.², Lomaev G.V.²

¹Institute of Applied Physics, Academy of Sciences of Moldova, ul. Akademiei 5, Chisinau, MD-2028 Moldova

²Izhevsk State Technical University, Studencheskaj st., 7, 426069, Izhevsk, Russia, lomaev@izhevsk.ru

It is known that the theories of nucleation and magnetic-phase formation have much in common; therefore, the study of magnetic phenomena can be an addition to the solution of problems of nanoparticle crystallization. On the other hand, as is shown further, it is also possible to derive common regularities of the theory of magnetism from the common representations of the nucleation theory.

Cast glass-coated amorphous microwire (CGCAM) with a positive magnetostriction has a rectangular hysteresis loop, which is characterized by a coercive-force stable magnitude H_s . In this case, the coercive force characterizes a new-phase-nucleation switching field and has (as has already been noted) a direct analogy with the nanoparticle nucleation. The coercive-force magnitude (or the nucleation switching field) and the fluctuations of this quantity with the temperature and heat-treatment conditions are of theoretical and practical interest.

The temperature dependence of the switching field in the low-temperature range is defined by the residual stresses considered in detail in [1]. At high temperatures, there are thermal-relaxation processes, which are investigated in this paper. First, we consider the temperature dependence disregarding the structure relaxation but with taking into account the residual-stress change. These changes in the switching field have a reversible character; i.e., after returning to the initial temperature, all the switching-field parameters are restored. It can be relevant both at reasonably low temperatures and for high heating rates. A heat treatment (or annealing), i.e., the sample aging at a particular temperature for a certain time during which the structure relaxes, is an irreversible process. Therefore, the result of the heat treatment can be measured by returning to the initial temperature while also taking into account the reversible temperature processes. In reality, both processes proceed simultaneously in amorphous materials, which we discuss below and in the conclusions.

Let us also note that the principal difficulty in investigating the indicated phenomena arises due to the fact that the amorphous states are metastable and quasi-degenerate. For this reason, in this study, we restrict ourselves only to using the first principles for the possible construction of the theory.

In contrast to magnetic phases, for nucleation phases, we are usually interested only in the irreversible nucleation product. However, as becomes clear below, the irreversibility of these processes can be investigated from unified positions. Dependence of temperature on a field of start in cast amorphous microwire.

We presented the results investigation switching field in cast glass coated amorphous microwires. The theoretical representations about temperature dependence of switching field and its dependence on heat treatment are given.

25PO-13-27

TEMPERATURE DEPENDENCE OF MAGNETIZATION OF $\text{Lu}_2\text{Fe}_{17}$ COMPOUND IN DIFFERENT STRUCTURAL STATES

Korzniakova G.F.¹, Czeppe T.²

¹Institute of Metals Superplasticity Problems, Russian Academy of Sciences, 39 Khalturin st., 450001, Ufa, Russia

²Institute of Metallurgy and Materials Sciences, Polish Academy of Sciences, 25 Reymonta St., 30-059 Krakow, Poland

Intermetallic rare-earth compounds of R-Fe system exhibit high magnetic crystalline anisotropy and sufficient Curie point. As is known, magnetic properties of ferromagnets are sensitive to their structure so it is important to study the influence of the structure on their magnetic properties in order to take advantage of this potential. In the present work we report our studies of temperature dependence of magnetisation and structure analysis of $\text{Lu}_2\text{Fe}_{17}$ samples. The samples revealed various, coarse grained, submicrocrystalline, and nanocrystalline microstructures.

Coarse grained samples, casted by arc melting were initial ones. Submicrocrystalline powder sample was produced by mechanical attrition of coarse grained specimen in protecting environment. Nanocrystalline bulk samples were produced by severe plastic deformation on Bridgman anvils under a pressure of 8 GPa from the initial coarse grained sample at room temperature. Scanning electron microscopy (JSM 840 with EDX system was used) of coarse grained samples revealed homogeneous structure with mean grain sizes about 100 mkm. Phase composition of the samples was checked by X-ray diffraction analysis. X-ray diffractometer Philips PW17/10 was applied. Alongside with main $\text{Lu}_2\text{Fe}_{17}$ phase small amount of $\text{Fe}_{23}\text{Lu}_6$ was revealed as well. Submicrocrystalline powder consists of particles with mean value of diameter about 1 mkm. Microstructure study of nanocrystalline sample was provided on JEM 2000EX transmission electron microscope and revealed crystallite size of about 50 nm.

Thermal analysis was provided by means of differential scanning calorimeters DSC DuPont 910 and SDT Q600. DSC curves revealed exothermal decomposition of $\text{Fe}_{17}\text{Lu}_2$ phase at 1595K and melting at 1615°C, in conformity with equilibrium phase diagram.

The curves of the temperature dependence of magnetization $\sigma(T)$ for samples in different structural states were recorded using the field $H = 250$ kA/m. In all structural states the temperature dependencies of magnetization are of the same nature – a significant drop of magnetization occurs in the vicinity of 305 K corresponding to Curie point of the $\text{Lu}_2\text{Fe}_{17}$ phase. At that, the slope of a curve $\sigma(T)$ depends on structural state – for the coarse grained state it is very steep, while for the nanocrystalline state it is more flat. Curie temperature of the nanocrystalline sample was by 25K higher than that in the coarse grained and submicrocrystalline samples.

The authors thank Dr. S.A. Nikitin, Department of Physics, Moscow State University, for supplying the $\text{Lu}_2\text{Fe}_{17}$ compound sample. Financial support of Russian Foundation for Basic Research (project No. 08-08-99062) is acknowledged.

25PO-13-28

THE LOCAL ELECTRON STRUCTURE AND MAGNETIZATION IN β -Fe₈₆Mn₁₃C

Kveglis L.I.¹, Kazantzeva V.V.¹, Noskov F.M.¹, Nyavro A.V.², Musikhin V.A.³

¹Siberian Federal University, Krasnoyarsk, 660074, Russia

²Tomsk State University, Tomsk, 634050, Russia

³Institute of Physics SB RAS, Krasnoyarsk, 660036, Russia

Importance of Fe-Mn-C alloys researches connecting with their wide use in machine industry as constructional materials. In this work attempt to find out the physical nature of high shock viscosity of Fe-Mn-C alloy, its mechanical and magnetic properties and calculation of intergranular borders electronic structure is made.

In the present report the observation microstructure of region phase transition from FCC austenitic Fe₈₆Mn₁₃C steel to FK12 + FK14 type of Frank-Kasper tetrahedral close packed structure [1] are described. We used the methods of optical microscopy, electron microscopy, electron and X-ray-diffraction to investigate the transformation area.

To explain the magnetization nature of the sample consisting of austenite and intergranular layers, which have FK12+FK14 structure typical to β -Fe-Mn, local electronic structure has been investigated. The local electron structure of FK12 and FK 14 clusters have been studied by the method of self-consistent field [5, 6] to understand the nature of non-zero magnetization of Fe₈₇Mn₁₃ alloy exposed by shock deformation. For this purpose two cluster elements of a β -Fe₈₇Mn₁₃ cell have been chosen. These cells are differ from each other by structure and number of atoms: 13 (FK12) and 15 (FK14).

We found out that the difference in clusters structure and, as consequence, in potentials of their atoms and wave functions - results in the different magnetic moment in local areas of β -phase. The spin-polarized calculation shows the value of magnetic moment $\langle\mu\rangle=1.4\mu_B/\text{at}$ in case of FK12 cluster and $\langle\mu\rangle=0.5\mu_B/\text{at}$ for FK14 cluster.

It is known that strains can trigger chemical reactions. This fact is very important: mechanochemistry is based on strain-induced chemical reactions [4]. The observed phase transition is accompanied by the appearance of non-zero magnetization, whereas austenitic Fe₈₆Mn₁₃C steel is compensated antiferromagnetic.

Conclusions

1. In Fe-Mn-C alloy with invar consistent (Hadfield manganese steel) of bulk and film states was founded the interboundary layers, which have Frank-Kasper structure FK12+FK14 of β -Fe-Mn type.

2. Magnetic characteristics of both bulk and film states of alloys are spontaneously changing under action of dynamic stressing.

3. The local electron structure constructed by scattering waves method, qualitatively explains of magnetic properties at mechanical stressing.

[1] Pearson U. Crystal chemistry and physics of metals and alloys / Transl. From English - M.: Mir, 1977. T.1-2], [Sidhom H., Portier R. An icosahedral phase in annealed austenitic stainless steel // Philosophical Magazine Lett., 1989, V.59, № .3, P.131-139.

[2] Slatter J.C. The self-consistent field for molecules and solids // Mir, Moscow 1978.

[3] V.S.Demidenko, N.L.hare, I.A.Nechaev, A.V.Njavro, T.V.Menshikov, L.F.Skorentsev Change of the Electronic Structure and Energy of 3d-metal Nanoclusters and Linkings TiFe, TiNi at BCC-FCP-transformation // the Siberian Physicotechnical institute, Tomsk, 2006.

[4] Gilman J.J. Mechanochemistry, Science V.274,, 65 (1996).

25PO-13-29

INVESTIGATION OF FERROMAGNETIC AND SUPERPARAMAGNETIC PARTICLES OF BALL MILLED COBALT-COPPER ALLOYS

Iskhakov R.S.¹, Kuzovnikova L.A.², Denisova E.A.¹, Komogortsev S.V.¹

¹Kirensky Institute of Physics, Academgorodok, Krasnoyarsk, 660036, Russia

²Krasnoyarsk Branch of Irkutsk State University of Railway Communications, st. Lado Ketshoveli, 89, Krasnoyarsk, Russia

e-mail: rauf@iph.krasn.ru

Magnetic and structural properties of nanostructured Co-Cu alloy have been investigated. The metastable Co–Cu solid solution was prepared by a new modification of mechanical alloying in the ball mill (the highly disperse powders of composite particles representing a Co–P amorphous alloy core covered with a nanocrystalline copper shell used as the reaction mixture). This alloy is composed of at least two magnetic phases: ferromagnetic solid solution (formed after milling for 2–3 hours) and superparamagnetic particles. New information on magnetic anisotropy, blocking temperature and concentration of superparamagnetic particles formed during the milling process is obtained.

The blocking temperature T_B and the number of superparamagnetic particles were estimated from $M(T)$ curves near liquid helium temperature. The value of volume concentration of superparamagnetic particles n_{sp} is significantly increased in the course of milling. The n_{sp} for $(\text{Co}_{88}\text{P}_{12})_{80}/\text{Cu}_{20}$ composite particle powder both before and after milling is more than n_{sp} for $(\text{Co}_{88}\text{P}_{12})_{50}/\text{Cu}_{50}$. We suppose that it is result from the buffer function of copper what is more plastic than cobalt. The copper makes the grinding process of Co slower and thus more Cu in composite particle powder results in pure grinding of Co clusters. The value of T_B varies slowly in comparison with n_{sp} . This means that during milling process the superparamagnetic clusters with approximately equal size are broke off from the coarse magnetic particles. The local magnetic anisotropy field of superparamagnetic particles H_{sp_a} is twice smaller than magnetic anisotropy in ferromagnetic phase H_{f_a} but it is increased with milling and reached the same value as in ferromagnetic particles.

This work was supported by the RFBR and KRSEF, project no.07-03-96808 and National Science Fund (2008, PhD RAS).

25PO-13-30

TRANSFORMATION OF MAGNETIC PROPERTIES OF $Y_2(Fe,Mn)_{17}$ COMPOUNDS UNDER HYDRIDOGENATION

Pankratov N.Yu.¹, Iwasieczko W.², Skokov K.P.³, Nikitin S.A.³, Drulis H.²

¹Department of Physics, M.V. Lomonosov Moscow State University, 119992, Moscow, Russia

²Trzebiatowski Institute of Low Temperatures and Structure Research, 1410, Wrocław, Poland

³Department of Physics, Tver State University, 170002, Tver, Russia

Intermetallic compounds based on the rare-earth and 3d-transition metals form a large class of materials which are interesting both practical and fundamental points of view. At present there is a great interest to study the effects caused by Mn substitution of Fe that induces anomaly magnetic properties. The substitution varies the occupation of 3d-band and changes the local susceptibility and intensity of spin fluctuation. The increase of Curie temperature caused by the hydrogenation also is narrowly studied. The aim of this work is to investigate the transformation of magnetic properties of $Y_2Fe_{17-x}Mn_x$ under hydrogenation.

The $Y_2Fe_{17-x}Mn_x$ alloys ($x = 0-8$) were prepared by melting the pure elements in an induction furnace in argon atmosphere. The metal hydride syntheses were carried out in a high-pressure reactor chamber. The samples were activated for 4 hours in vacuum at 670 K. The amount of absorbed hydrogen was determined from the hydrogen pressure change in the reactor chamber. The $Y_2Fe_{17-x}Mn_xH_y$ ($y = 1; 2; 3$) hydrides was obtained. X-ray diffraction measurements show that the investigated compounds have hexagonal crystalline structure with space group $P6_3/mmc$. The features of X-ray spectrum show that there are great defects in crystal lattice.

The termomagnetic analyze (TMA) was performed in temperature range 1.77-400 K in magnetic field 100 Oe. A sharp slump of magnetization at Curie temperature was observed. There are sharp distinctions between zero field cooling and field cooling $\mu(T)$ curves at low temperature. Similar phenomena were also observed in the $Pr_2(Fe,Mn)_{17}$ compounds [1], and was ascribed to the presence of narrow Bloch walls at low temperature. It was established that Curie temperature of Y_2Fe_{17} compound is 317 K. It slightly increases with small substitution of Mn for Fe ($T_C = 322$ K of $Y_2Fe_{16}Mn_1$) and then monotonically decreases up to Mn concentration $x = 6$ ($T_C = 83$ K for $Y_2Fe_{11}Mn_6$). The antiferromagnetic ordering with Neel temperature close to 150 K was found for $Y_2Fe_{10}Mn_7H_y$ and $Y_2Fe_9Mn_8H_y$ compounds.

The spontaneous magnetic moment of $Y_2Fe_{17-x}Mn_x$ and their hydrides was determined from the dependences of magnetization vs. field at $T = 1.77$ K. It was shown that there is no saturation on magnetization curves in magnetic field up to 140 kOe. The following conclusion can be reached that the magnetic field suppresses antiferromagnetic ordering of Mn and Fe magnetic moment. The magnetic moment of Mn sublattice was calculated assuming an antiparallel spin arrangement of Fe and Mn sublattice and the Fe ions moment $\mu_{Fe} = 2 \mu_B$. It was found that Mn magnetic moment heavily decreases with Mn concentration increasing: from 4.1 μ_B for $x = 3$ to 2.5 μ_B for $x = 8$. In contrast, the magnetic moment of $Y_2Fe_{17-x}Mn_xH_y$ ($x > 3$) strongly increases under hydrogenation. The increase of magnetic moment of $Y_2Fe_{17-x}Mn_xH_3$ hydrides is caused by strong decreasing of Mn magnetic moment at hydrogen insertion.

The exchange interaction decreases with substitution of Fe by Mn in consequence of the antiferromagnetic contribution to Curie temperature. In the contrary hydrogenation of $Y_2Fe_{17-x}Mn_x$ compounds leads to the increasing of magnetic moment and exchange integral.

[1] Z.-G. Sun, H.-W. Zhang, J.-Y. Wang, B.-G. Shen. J.Appl.Phys. v.86(9) (1999) p.5152-5156.

25PO-13-31

CONVERSION ELECTRON MOSSBAUER SPECTROSCOPY OF SOFT MAGNETIC FILMS FeCoNi

Andrianov V.A.¹, Chechenin N.G.¹, Gorkov V.P.², Khomenko E.V.¹, Rohlov N.I.¹

¹Skobeltsyn Institute of Nuclear Physics, Lomonosov Moscow State University, 119991
Moscow, Russia.

²Faculty of Computational Mathematics and Cybernetics, Lomonosov Moscow State University,
119991 Moscow, Russia;

Electroplated nanocrystalline films FeCoNi are now considered as perspective soft magnetic materials for using in recording heads, magnetic sensors and transformers [1, 2]. These films possess higher saturation magnetization than common permalloy layers and have low coercivity of about 1-2 Oe. Unfortunately properties of these films depend very strongly on the deposition conditions and film microstructure. In this report we present the conversion electron Mossbauer effect on ⁵⁷Fe (CEMS) investigation of electroplated films FeCoNi. The CEMS method permits to study thin films and surfaces without destruction of the samples.

The FeCoNi films of different compositions were produced by electrodeposition at room temperature on Si substrate covered by Cu underlayer. During the deposition the magnetic field of 0.1 T were applied. Thicknesses of the films were about 200 nm. For Mossbauer measurements the films were placed inside the gas proportional counter. Mossbauer spectra were obtained at room temperature.

The Mossbauer spectra consist of the well-resolved magnetic sextet with the mean magnetic hyperfine field H_{hf} in the range 31-33.6 T. The hyperfine fields increase with Fe concentration. The lines of the spectra are broadening due to hyperfine field distribution with the dispersion $\Delta H_{hf}/H_{hf}$ about 10%. ΔH_{hf} increases with Ni concentration. The Mossbauer spectra confirm the high quality of the FeCoNi films and the full orientation of the magnetization in plane of the film.

The most interesting results were obtained for the films with the composition in the range of coexistence of the fcc and bcc phases. In this case the Mossbauer spectra contain an additional singlet with approximately the same isomer shift as the sextet and with the intensity up to 20% of the spectrum area. This singlet could not be related to the oxide phases or to phases of contaminations. The strong transformations of the spectra were observed in the special experiments in the external magnetic field of 0.2 T. The singlet disappeared, and the full spectrum became the typical Mossbauer spectrum of the hyperfine field distribution.

We ascribe the observed effects to the superparamagnetic behavior of the small nanocrystalline grains which are created in the range of concentrations corresponding to the fcc and bcc phases coexistence. The paramagnetic behavior of these nanograins at room temperature means that grains have the weak magnetic bonds with surrounding crystallites. The formation of nanocrystalline grains could be responsible for the soft magnetic properties of the FeCoNi films.

[1] T. Osaka and at. all, Nature **392** (1998) 796

[2] N.G. Chechenin and at. all, J.Magn.Magn. Mater. **316** (2007) 451

25PO-13-32

INFLUENCE OF MAGNETIC FIELD ON CARBON ISOTOPES IN CALCITES

Sadykov S., Osipov A.

Institute of mineralogy UB RAS, 456317, Miass, Chelyabinsk region, Russia

Influence of magnetic field on carbon isotopic composition during calcite formation were experimentally revealed in reaction $\text{Ca(OH)}_2 + \text{CO}_2 \Rightarrow \text{CaCO}_3 + \text{H}_2\text{O}\uparrow$.

A glass plate with uniformly put water suspension Ca(OH)_2 was placed in inductance coil with direct current for 500 – 700 hs. Ca(OH)_2 has been prepared from CaCO_3 (reagent grade). Then, the $^{13}\text{C}/^{12}\text{C}$ ratio was defined in the formed calcite through each 5 mm in direction parallel to the magnetic field of a coil.

Results obtained for two various values of magnetic field intensity in an inductance coil are shown on fig. 1. Here we also present a calculated dependence intensity of magnetic field of the coil along its axis in relative units ($H_x^{\text{coil}}/H_x^{\text{solenoid}}$ ratio, where H_x^{coil} – magnetic field intensity of the inductance coil, H_x^{solenoid} – magnetic field intensity of the ideal solenoid with the same density of coils and values of direct current, as in an inductance coil) are shown. It can be seen from fig. 2 that the $^{13}\text{C}/^{12}\text{C}$ ratio in CaCO_3 depends from of intensity magnetic field. The range of maximum enrichment of calcite in ^{13}C -carbon isotope is approximately on the middle of an inductance coil, where intensity of the magnetic field is maximal. In this area enrichment a heavy carbon isotope is more than 14 ‰, in comparison with calcite grown without magnetic field.

Thus, the magnetic field stimulates a spin-selective chemical reaction of interaction between calcium hydroxide and ^{13}C isotope.

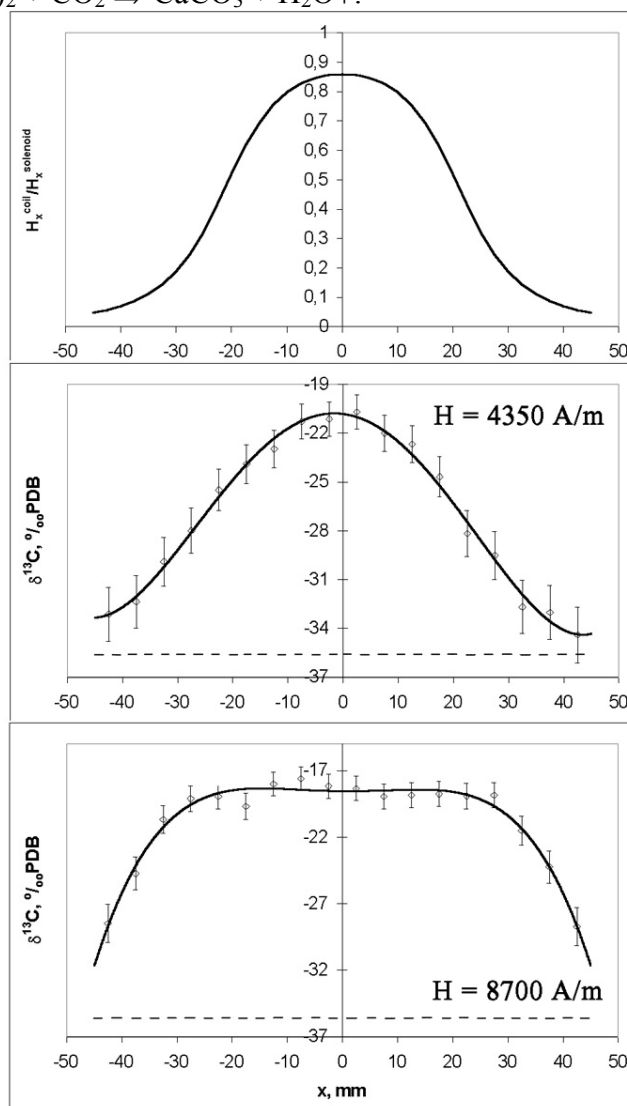


Fig. 1. The values of $\delta^{13}\text{C}$ obtained for two various values of magnetic field intensity in a coil and curve of $H_x^{\text{coil}}/H_x^{\text{solenoid}}$ ratio on an axis of coil. Dashed line – average value $\delta^{13}\text{C}$ in control samples.

25PO-13-33

ONSET OF LONG-RANGE MAGNETIC ORDER IN ITINERANT SUBSYSTEM OF $\text{Er}_{1-x}\text{Y}_x\text{Co}_2$ COMPOUNDS NEAR CRITICAL CONCENTRATION DRIVEN BY EXTERNAL MAGNETIC FIELD

Sherstobitova E.A.¹, Pirogov A.N.¹, Schweizer J.²

¹Institute of Metal Physics, Ural Division, Russian Academy of Sciences, ul. S. Kovalevsko 18, Yekaterinburg, 620219 Russia

²Departement de Recherche Fondamentale sur la Matière Condensée, CEA-Grenoble, F-38054 Grenoble Cedex 9, France

The substitution of R ions in RCO_2 compounds for non-magnetic yttrium leads to the disappearance of the magnetic moment in an itinerant d-electron subsystem at critical Y concentration. In order to study the itinerant metamagnetism in the cubic Laves-phase compounds $\text{R}_{1-x}\text{Y}_x\text{Co}_2$, neutron diffraction measurements of $\text{Er}_{1-x}\text{Y}_x\text{Co}_2$ compounds with yttrium content just below the critical value ($x_c=0.47$) have been performed in an applied magnetic field equal to 1.05 T and in the temperature range from 2 to 24 K.

As is shown in Fig. 1 a, the neutron diffraction pattern measured at 2 K in zero magnetic field exhibits Bragg reflections associated with a long magnetic order and nuclear scattering. Moreover, this pattern includes the broad maxima, which may be ascribed to diffuse scattering caused by the presence of short-range magnetic order coexist in the volume of the sample.

An application of the small magnetic field of 1.05 T (see Fig. 1 b) increases significantly the intensity of Bragg reflections. The magnetic field produces an ordering effect in the partly disordered R-subsystem which is accompanied by an irreversible growth of the magnetization of the R- and Co-subsystems. The moments of the R and Co atoms reach the value of $(5.0 \pm 0.1) \mu_B$ and $(0.6 \pm 0.1) \mu_B$ respectively. An increase of the average Co magnetic moment and an extension of the d-band splitting can be connected with

an increase of the effective molecular field under the application of an external field.

Fig. 1 c presents the neutron-diffraction pattern after removing the magnetic field of 1.05 T at 2 K. The intensity of reflection and the magnitudes of magnetic moments of both subsystems do not return to the itinerant values, that can be associated with the hysteresis of the $\mu_{\text{Co}}(H_{\text{eff}})$ dependence in the vicinity of the critical value of the effective molecular field.

The work was done within RAS Program (Project № 01.2.006 13394), with partial support of the Program for Basic Research OFN RAN "Neutron investigation of the matter structure and the basic behavior of matter", and the Swiss National Science Foundation (SCOPES project no. IB7420-110849).

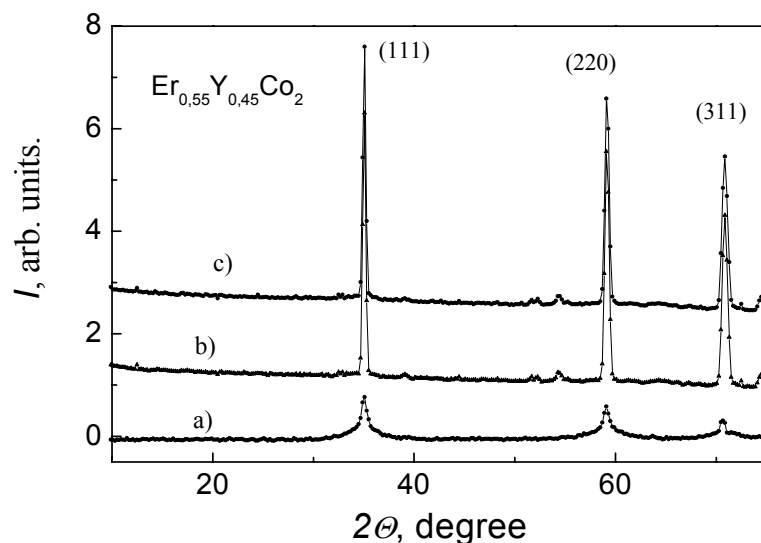


Fig.1 (a,b,c). The neutron-diffraction pattern for the $\text{Er}_{0.55}\text{Y}_{0.45}\text{Co}_2$ compound obtained in: a) zero magnetic field at 2 K, b) a magnetic field of 1.05 T, c) After removing of a magnetic field of 1.05 T.

25PO-13-34

MAGNETIC PROPERTIES OF RFe_9Ti SINGLE CRYSTALS WITH $ThMn_{12}$ STRUCTURE

Skokov K.P.¹, Pastushenkov Yu.G.¹, Semenova E.M.¹, Bartolome J.²

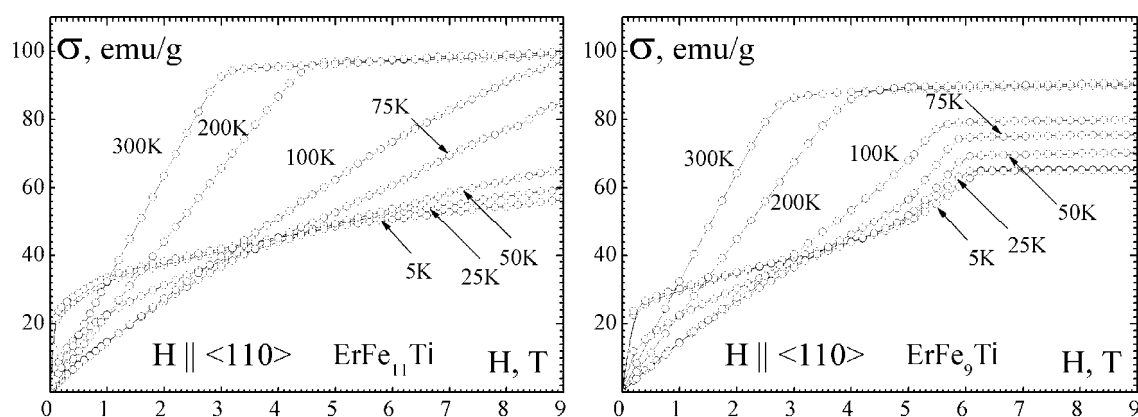
¹Tver State University, 170100 Zheliabova 33, Tver, Russia

²Instituto de Ciencia de Materiales de Aragón, CSIC-Universidad de Zaragoza, 50009 Zaragoza, Spain

Intermetallic compounds R–Fe–Ti with tetragonal crystalline structure $ThMn_{12}$ -type have a wide homogeneity region [1–4]. For R= Gd, Tb, Dy, Ho, Er this structure exists within the interval of Fe concentration from $RFe_{11}Ti$ up to RFe_8Ti . Temperatures of spin-reorientation transitions (SRT) in these compounds depend on Fe concentration.

It is well known that the most important reason for magnetic phase transitions in R–3d ferrimagnetics is the competition between anisotropy energies of R and 3d sublattices. It follows from this that at small changes of Fe concentration it is possible to make a significant change of the parameters of exchange interaction between R and 3d sublattices and shift of spin-reorientation temperature without changes of other important magnetic parameters.

The comparative analysis of the magnetic properties of $RFe_{11}Ti$ and RFe_9Ti single crystals (R = Tb, Dy, Ho, Er) was carried out. It is shown that at the decrease in iron concentration, the magnitude of magnetization saturation steadily decreases (for example, 83 emu/g for $GdFe_9Ti$ and 88 emu/g for $GdFe_{11}Ti$ at RT). Also at the increase in iron concentration in the specimen, Curie temperature steadily increases. The figures below show the magnetisation curves of $ErFe_{11}Ti$ and $ErFe_9Ti$ single crystals. Magnetic field was applied along the $\langle 110 \rangle$ direction. These figures illustrate the dependence of anisotropy type on iron concentration for $RFe_{11-x}Ti$ compounds.



Support by Grant RNP.2.1.1.3674 and MAT05/1272 of the MECD is acknowledged.

- [1] T.I. Ivanova, N.Yu. Pankratov, Yu.G. Pastushenkov, K.P. Skokov. *Acta Physica Polonica A* **97** (2000) 847.
- [2] K. Skokov, A. Grushishev, A. Khokholkov, Yu. Pastushenkov, N. Pankratov, T. Ivanova, S Nikitin. *Journal of Magnetism and Magnetic Materials* **272-276** (2004) 374.
- [3] K. Skokov, A. Grushishev, A. Khokholkov, Yu. Pastushenkov, N. Pankratov, T. Ivanova, S. Nikitin, *Journal of Magnetism and Magnetic Materials* **290-291** (2005) 647
- [4] Yu.G. Pastushenkov, J. Bartolome, A. Larrea, K.P. Skokov, T.I. Ivanova, L. Lebedeva and A. Grushichev *Journal of Magnetism and Magnetic Materials*, **300(1)** (2006), e514.
- [5] Yu. Pastushenkov, J. Bartolome, N. Suponev, K.P. Skokov, T. Ivanova, A. Larrea, M. Lyakhova, E. Semenova, S. Smirnov., *Journal of Alloys and Compounds* **451** (2008) 488.

25PO-13-35

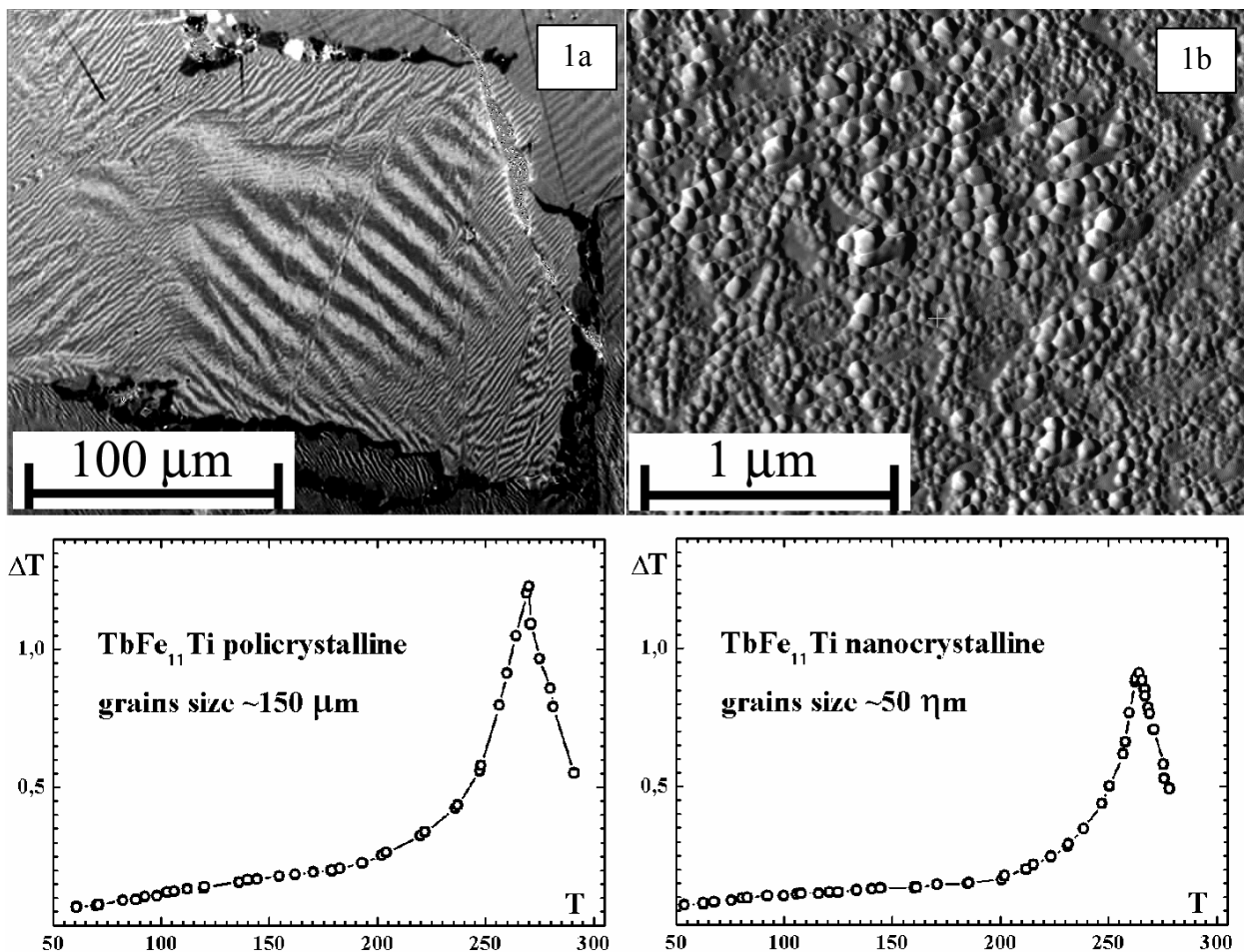
MAGNETOCALORIC EFFECT IN MICRO- AND NANOCRYSTALLINE $RFe_{11-x}Ti$ INTERMETALLIC COMPOUNDS

Skokov K.P., Koshkid'ko Yu.S., Karpenkov D.Yu., Karpenkov A.Yu., Pastushenkov A.G., Pastushenkov Yu.G.

Tver State University, 170100 Zheliabova 33, Tver, Russia

The analysis of magnetocaloric effect in polycrystalline and nanocrystalline $RFe_{11}Ti$ intermetallic compounds was carried out. It was found that with the reduction of grain size below single domain size magnetocaloric effect begins to decrease. Probably, it is connected with the influence of intergrain exchange interaction in nanocrystalline alloys. Figure 1a shows micro- and domain structure of polycrystalline alloy $TbFe_{11}Ti$ received by optical metallography. Atomic force microscopy image of a nanocrystalline alloy is presented on fig. 1b.

Figures below show magnetocaloric effect in micro- and nanocrystalline alloys. It is seen from these figures that the maximum of magnetocaloric effect amounts 1.2 K in the external magnetic field 1.8 T meanwhile for a rapidly quenched alloy this effect does not surpass 0.95K in the same magnetic field.



Support by Grant RNP.2.1.1.3674 is acknowledged

25PO-13-36

MICROMAGNETIC ANALYSIS OF SPIN-REORIENTATION TRANSITIONS. THE ROLE OF MAGNETIC DOMAIN STRUCTURE

Skokov K.P., Pastushenkov Yu.G., Lyakhova M.B., Smirnov S.S.

Tver State University, 170100 Zheliabova 33, Tver, Russia

A method for calculating of micromagnetic state of ferro- or ferrimagnetic single-crystal samples, based on the Néel method of phases [1–3], is proposed. In contrast to the standard Néel technique, which requires different approaches to calculation of micromagnetic state of samples with different anisotropy types and, in addition, cannot be used in calculations of magnetization curves of magnets with the complex type of anisotropy (first-order magnetization process (FOMP) transitions [4]), the proposed technique makes it possible to calculate micromagnetic state of a sample within the unified approach and has no limitations on the anisotropy type.

The proposed technique makes it possible to do the following:

(i) to calculate the volume occupied by the domains with different orientations of magnetization vector, as well as the magnetization directions in each type of magnetic domains;

(ii) to describe in detail the magnetization process for all types of magnetic anisotropy, both in the range of fields corresponding to the domain structure of the sample and for single-domain state;

(iii) to model the process of domain structure transformation at magnetic phase transitions and investigate the degree of domain structure effect on the type and character of spin-reorientation transitions;

(iv) to calculate the field and angular dependences of magnetization for any type of magnetic anisotropy within the unified approach.

Two simulation techniques were used for micromagnetic modeling of magnetization curves: a commonly used vector-moment model (method of calculating of magnetization curves that assumes that the sample is in mono-domain state), and the proposed method. Both simulation methods lead to identical results for the “regular” anisotropy types “easy axis”, “easy cone” and “easy plane”. However, the used methods of calculation cause different results in case of metastable anisotropy energy minimum along c-axis.

It is known, that most of the RE-3d compounds show some degree of anisotropy and some of them also have spin reorientation. We have proposed a way to increase cooling capacity of magnetic refrigerant on the base of RE-3d compounds using magnetic materials with special features, such as large anisotropy and spin reorientation. The nature of that could not be deeply understood without the detailed micromagnetic analyses of magnetic domain structure transformation under the external magnetic field or temperature changes. Our explanation of these effects is based on the proposed technique of calculation of the micromagnetic state of ferro- or ferrimagnetic single-crystalline samples.

This work is supported by grant RNP.2.1.1.3674.

[1] G.Asti. First-order magnetic processes *Ferromagnetic materials.*, **5** (1990) 397.

[2] Neel L.J. *J. de Phys. Radium.*, **5** (1944) 241.

[3] Birss R.R. Martin D.J. *J. Phys. C. Sol. State.*, **8** (1975) 189.

4 Kronmuller H. Traeble H., Seeger A., Boser O. *Mat. Sci. Eng.*, **1** (1966) 91.

25PO-13-37

STABILITY OF MAGNETIC DOMAINS INSIDE THE CORE OF AMORPHOUS WIRE

*Gavriliuk A.A.¹, Mokhovikov A.Yu.¹, Semirov A.V.², Semenov A.L.², Turik N.V.¹,
Kudrewcev V.O.²*

¹Irkutsk State University, 664003, Gagarin bvd., 20, Irkutsk, Russia

²Irkutsk Teachers Training University, 664011, N Naberzhnaya st., 6, Irkutsk, Russia

In work it is carried out the research of conditions of existence of the stable domain in core of amorphous metal wire in case of action of an external magnetic field. For definition of conditions of this existence it is necessary to consider the total energy of the stable domain. It is possible to allocate conditionally two energy components: magnetic W_{magn} energy and dissipative W_{dissp} one at an estimation of a energy condition of the domain in a core of a wire. The magnetostatic energy W_m , domain walls energy W_γ and domain magnetization energy W_H can be carried to magnetic contributions to energy of the domain to the core of amorphous metal wire. It should be noted the dissipative energy component appears at propagation of the domain walls. It is considered following possible forms of the domain inside the core of the wire:

a) The domain which consist of two cone-shaped tops; b) The domain in the form of the cylinder; c) The domain which consist of a cylindrical part and two cone-shaped tops; d) The domain in the form of ellipsoid which strongly extended along length of a wire; e) The domain with zigzag domain walls. Proceeding from the calculations, it is possible to draw a conclusion that all the considered types of the domain inside the core of a wire can receive the stable domain in radius some tens micron, at corresponding values. For realization of this or that domain configuration it is counted up a magnetic part of energy of the considered domain $W_{\text{magn}} = W_\gamma + W_m + W_H$ depending on size of its radius r . According to the results of calculation, the domain possesses the least values of magnetic component energy W_{magn} if it has following forms: cylindrical thing with two domain tops and the domain with zigzag domain walls at the fixed value l . In turn, the domain possesses the greatest values W_{magn} if it has forms: two cone-shaped tops and ellipsoid. Thus, the difference in sizes W_{magn} for domains of the various forms can make two - three orders.

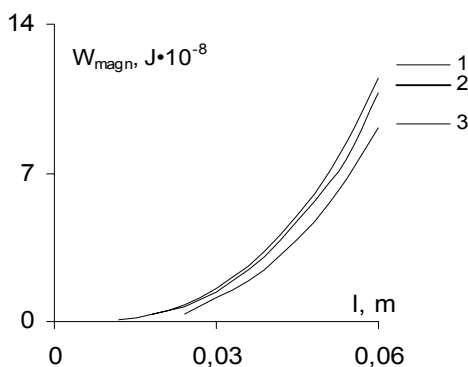


Fig.1 Dependences of the energy of the domain in the form of two cones W_{magn} from l with $H_C^w = 210$ A/m and various H , which is oriented to an opposite direction of magnetization of the domain: 1- $H = 10$ A/m, 2 - $H = 40$ A/m, 3 - $H = 80$ A/m.

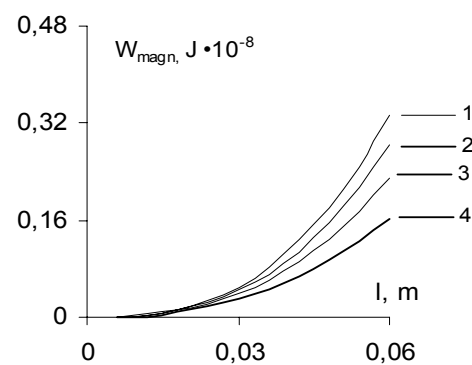


Fig. 2 Dependences of energy W_{magn} of the domain consisting of a cylindrical part and two cone-shaped tops from l with $H_C^w = 10$ A/m and various values of H opposite direction of magnetization of the domain: 1- $H = 2$ A/m, 2 - $H = 5$ A/m, 3 - $H = 7$ A/m, 4- $H = 9$ A/m

The research was supported by RFBR (Project № 05-08-18063)

25PO-13-38

INFLUENCE OF LASER TREATMENT TO THE MAGNETIC PROPERTIES OF AMORPHOUS $\text{Fe}_{64}\text{Co}_{21}\text{B}_{15}$ RIBBON

Gavriliuk A.A.¹, Semirov A.V.², Semenov A.L.¹, Malov S.N.³, Morozov I.L.⁴, Mokhovikov A.Yu.¹,
Turik N.V.³

¹Irkutsk State University, 664003, Irkutsk, Russia

²Irkutsk Teachers Training University, 664011, Irkutsk, Russia

³Irkutsk Institute of Laser Physics of SB RAS, 664007, Irkutsk, Russia

⁴Irkutsk Scientific Research Institute of Chemical Engineering, 664007, Irkutsk, Russia

It was researched the influence of laser treatment to the magnetic and magnetoelastic properties of amorphous $\text{Fe}_{64}\text{Co}_{21}\text{B}_{15}$ ribbon. The ribbons had 25 μm thickness and constant of the magnetostriction $\lambda_s = (25-30) \cdot 10^{-5}$. The samples were narrow ribbons with 0,001-0,0012 m width. All samples were pretreated by the means of the solid neodymium laser. Laser was used in the multimode operation. The frequency of following impulses is 3,5 kHz. The average capacity of target radiation of the laser changed from 2 up to 4 W. Diameter of a bunch of laser radiation was 50-100 microns. Speed of movement of a laser bunch on the sample was 1 m/min. The line of propagation of a laser bunch is perpendicular to length of the ribbon.

The periodic structures are received as a result of carrying out of laser treatment. These structures consist of the sections on the ribbon, which was treated by the laser, with distance between the treated sections was 0,1 mm. According to X-ray analysis, it is certain the conformity with capacity of the target radiation influencing on the sample, and temperature of heating of a section of amorphous ribbon. It is shown the initial stages of crystallization corresponds to the capacity of radiation 3-4 W at the investigated amorphous samples. It should be noted the volume crystallization processes take place at the capacity of the laser more 4 W and they attend with release of the crystal compounds of iron with boron and cobalt with boron.

The quasistatic and dynamic loops of a hysteresis are measured for the treated ribbons. It was also measured the ΔE -effect of these samples. It is shown the growth of capacity of laser treating from 2 up to 4 W leads to increase as quasistatic and dynamic coercitivities and losses on magnetic reversal, and as to reduction of differential magnetic permeability (fig.1). In the treated amorphous ribbons, the positive ΔE -effect was observed at that its magnitude decreases at increase in capacity of laser radiation from 2 up to 4 W only (fig.2). Now the opportunity of purposeful control of the magnetic and magnetoelastic properties of amorphous $\text{Fe}_{64}\text{Co}_{21}\text{B}_{15}$ ribbons is studied by a variation of modes of laser treating.

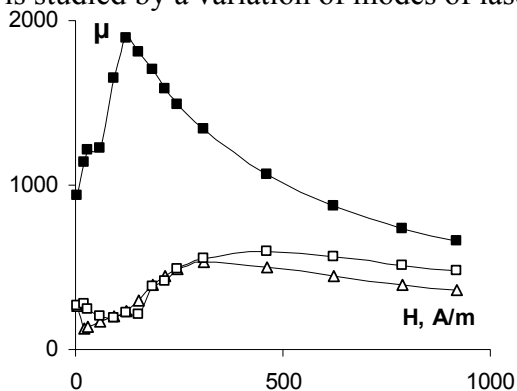


Fig.1 Dependence of $\mu(H)$ for samples with 6 cm length and which treated with different capacities: ■ – P=2W, Δ – P=3W, \square – P=4W

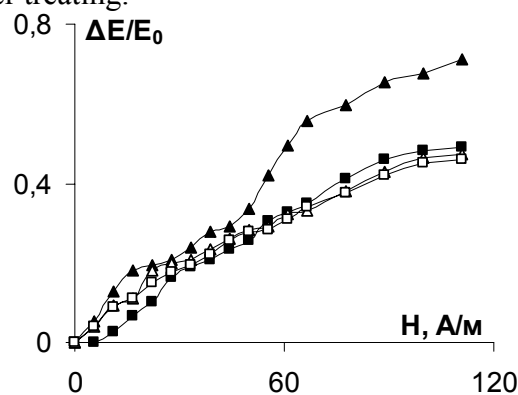


Fig.2 Dependence of $\Delta E/E_0(H)$ for samples which have different length and were treated by capacity 2W: \blacktriangle – l=5cm, \blacksquare – l=4 cm, \triangle – l=3 cm, \square – l=2 cm

The research was supported by RFBR (Project № 08-08-00210)

25PO-13-39

DYNAMICAL DRIFT OF STRIPE MAGNETIC DOMAINS IN FERRITE-GARNET SINGLE CRYSTALS

Lysov M., Pamyatnykh L., Shmatov G., Kandaurova G.
Ural State University, Lenin Av. 51, Ekaterinburg, 620083, Russia

Dislocation mechanism of stripe magnetic domains drift in ferrite-garnet single crystals was proposed in [1]. This work provides comparison of experimental research of stripe magnetic domains dynamical drift in alternating magnetic field with theoretical estimates. Experimentally obtained dependence of domain walls drift speed v from alternating magnetic field frequency f is monotonically increasing. (Frequency f is changing in the interval 10-1000Hz.) This dependence has linear character in the lower part of the frequency band, which is well correlated with theoretical dependence of single domain wall speed from frequency of alternating magnetic field, obtained in [2]. It is established experimentally that the character of dependence $v(f)$ changes with increase of frequency f . Apparently, such deviation from linear dependence is caused by the fact that in real case not a single domain wall, but an ensemble of interacting domain walls is drifting.

The theory of drift of single domain wall in oscillating magnetic field was described in [2]. In particular, it was shown that, if oscillating field is polarized in a plane of a film, dependence $v(f)$ is linear for frequencies of magnetic field $f \ll f_r$, where f_r is a frequency of ferromagnetic resonance. (See [2], expression (40).)

At low frequencies of magnetic field expression (40) that gives single domain wall drift speed can be rewritten as follows:

$$V \sim V_d \frac{\omega}{\omega_r} \frac{k}{\alpha} \frac{H^2}{M_s^2},$$

where $V_d = \pi\gamma\Delta Ms/4\beta$, ω_r – is a ferromagnetic resonance frequency, ω – frequency of alternating magnetic field ($\omega/\omega_r \ll 1$), α – parameter of damping, k – coefficient that depends on anisotropy constants of a sample, H – amplitude of magnetic field, M_s – magnetization of saturation, γ – gyromagnetic ratio, Δ – width of domain wall, β – uniaxial anisotropy constant.

Theoretical estimates, used for comparison with experimental results, were obtained at values of parameters of ferrite-garnet crystal that was experimentally investigated.

[1] L.A. Pamyatnykh, M.S. Lysov, G.S. Kandaurova, *Bulletin of the Russian Academy of Sciences: Physics*, **71** (2007) 1542.

[2] V.G. Bar'yakhtar, Yu.I. Gorobyets, S.I. Denisov, *JETP*, **98** (1990) 1345.

25PO-13-40

DOMAIN STRUCTURE TRANSFORMATION AND MAGNETIC SUSCEPTIBILITY OF $(\text{Er},\text{Ho})_2\text{Fe}_{17}$ SINGLE CRYSTAL

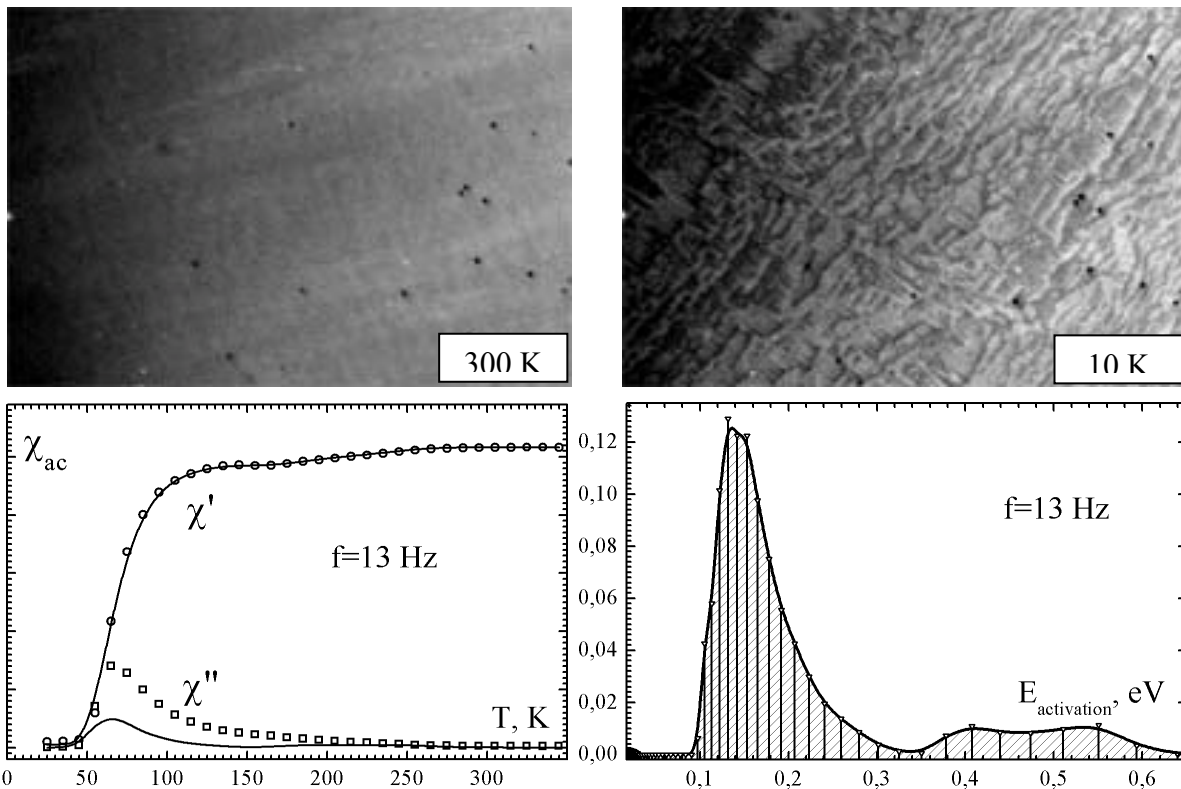
Pastushenkov Yu.G.¹, Skokov K.P.¹, Khokholkov A.G.¹, Bartolome J.³, Albrecht J.², Goll D.², Semenova E.M.¹, Maklygina O.V.¹

¹Tver State University, 170100 Zheliabova 33, Tver, Russia

²Max-Planck-Institut für Metallforschung, Heisenbergstrasse 3, 70569 Stuttgart, Germany

³Instituto de Ciencia de Materiales de Aragon, CSIC-Universidad de Zaragoza, 50009 Zaragoza, Spain

For the first time the investigations of domain structure (DS) of R_2Fe_{17} single crystals ($\text{R}=\text{Ho}, \text{Er}$) in the range of temperatures from 4K to Curie temperature were carried out. In spite of the fact that the R_2Fe_{17} compounds below Curie temperature always have ‘easy plane’ anisotropy and spin reorientations transitions do not occur, there were found considerable DS changes at the temperatures below 110K. Nevertheless, temperature dependences of magnetisation at the given temperature do not have any anomalies.



The measurements of magnetic AC susceptibilities in the field 10 Oe were carried out in a wide interval of temperatures. Below 50K the χ' and χ'' have zero values because of the coercivity of domain walls. Above 100K domain walls of the main domains become movable, this leads to practically invariable value of χ' . The approximation of experimental dependences of magnetic susceptibility allows to determine the distribution of activation energy in the sample. The main maxima in this distribution corresponds to activation energy of the main domains. The additional maximum shows the energy of the processes leading to the occurrence of additional closure domains at the temperatures below 110K.

Support by Grant RNP.2.1.1.3674 and MAT05/1272 of MECD is acknowledged.

25PO-13-41

CRYSTALLINE STRUCTURE AND MAGNETISM OF FeH*Isaev E.I.^{1,2,3}, Skorodumova N.², Ahuja R.², Vekilov Yu.Kh.¹, Johansson B.²*¹Department of Theoretical Physics, Moscow State Institute of Steel and Alloys,
Moscow, Russia²Condensed Matter Theory Group, Uppsala University, S-751 21 Uppsala, Sweden³Department of Physics, Chemistry and Biology (IFM), Linköping University, SE-581 83
Linköping, Sweden

FeH has been synthesized [1] over 25 years ago and its crystalline structure was identified as double hexagonal (DHCP) one with ferromagnetically ordered Fe atoms. But state-of-the-art ab initio methods used to describe FeH phases have shown that ferromagnetic hexagonal close packed (HCP) phase is energetically more favourable compared to DHCP, in contradiction with experimental structure. We have shown [2] that the correct magnetic DHCP structure for FeH can be obtained using the free energy calculations when contribution of vibration of hydrogen atoms is taken into account. Our calculations are based on density functional theory, the linear response method for phonons, and ultrasoft pseudopotentials. We predict also the phases sequence for FeH under high pressure.

Financial support from RFBR (06-02-17542 and 07-02-01266) is acknowledged.

[1] Antonov V.E., Belash I.T., Degtyareva V.F., Ponyatovsky E.G., Shiryayev V.I., *Sov. Phys. - Dokl.*, v. 25, p. 490 (1980).

[2] Eyvaz I. Isaev, Natalia V. Skorodumova, Rajeev Ahuja, Yuri K. Vekilov, and Börje Johansson, "Dynamical stability of Fe-H in the Earth's mantle and core regions", *Proceedings of the National Academy of Sciences of the USA (PNAS)*, v. 104 (22), p.9168 (2007).

25PO-13-42

INFLUENCE OF MAGNETISM ON INTERACTION ENERGY BETWEEN 3D IMPURITIES AND HYDROGEN IN PALLADIUM CRYSTAL IN THE PRESENCE OF VACANCIES*Isaeva L.E.¹, Bazhanov D.I.¹, Ereemeev S.V.², Kulkova S.E.², Abrikosov I.A.³*¹Department of Physics, M.V.Lomonosov Moscow State University, Moscow, Russia²Institute of Strength Physics and Materials Science, Siberian Branch of the Russian Academy of
Sciences, Tomsk, Russia³Institute of Physics, Chemistry and Biology (IFM), Linköping University, Linköping, Sweden

During last years many theoretical and experimental investigations were focused to study the interaction between hydrogen and transition metals as prospective materials for hydrogen storage or membrane separation [1]. The pure palladium and palladium based alloys are the most attractive materials for this research, since palladium is capable to store a plenty amount of hydrogen itself. But it is well known nowadays that hydrogen charging of transition metals and alloys leads to the undesirable changes of their atomic structure, caused by hydrogen-metal interaction, which strongly effect on material durability during technological cycles of hydrogen penetration and extraction [2,3]. To prevent the corruption process of a material and improve its

hydrogen storage performance the various alloying additives of a different degree of affinity for hydrogen are employed. Recent investigations of our group [4] on interaction energies between interstitial hydrogen and 3d-alloying atoms in palladium crystal have shown that this interaction energy is governed by a mechanism similar to Miedema's "reverse stability" rule, i.e., the larger the binding energy of the alloys, the stronger the repulsion between the alloying atom and H. However, the magnetic properties of alloys have been not taken into account during these investigations. The aim of this work is to carry out the first-principles study the effect of magnetism on hydrogen-metal interaction and structural stability of palladium with 3d-alloying atoms in the presence of vacancies, which are induced numerous during hydrogenation process [5]. Our calculations were carried out by means of state of the art *ab initio* method based on density functional theory [6] and all-electron PAW potentials [7]. We analyzed the atomic and electronic structures of palladium crystal with interstitial hydrogen and substitutional 3d-alloying additives in the presence of vacancies. The obtained results have shown that magnetism can strongly affect the hydrogen-metal interaction in palladium based alloys. It has been shown also that the presence of vacancies in palladium matrix enhances the interaction energy between hydrogen and transition metals.

This work was supported by Russian Foundation for Basic Research (grant № 07-02-01452) and The Royal Swedish Academy of Sciences (KVA).

- [1] Morinaga, H. Yukawa. *Materials Sci. Engin. A* 268 (2002), 329
 [2] A. Pundt and R. Kirchheim. *Annu. Rev. Mater. Res.* 36 (2006), 555 .
 [3] Y. Fukai. *The Metal-Hydrogen System, Basic Bulk Properties*. Berlin: Springer-Verlag (1993)
 [4] Y.J.Li, S.E.Kulkova, Q.M.Hu, D.I.Bazhanov, D.S.Xu, Y.L.Hao, R. Yang. *Phys.Rev.B* 76 (2007), 064110 .
 [5] Y. Fukai, N. Okuma. *Phys.Rev.Lett.*, 73 (1994), 1640
 [6] M.C.Payne, M.P.Teter, D.C.Allan, T.A.Arias, J.D.Joannopoulos. *Rev. Mod. Phys.*, 64 (1992), 1045
 [7] P. Blochl. *Phys. Rev. B* 50 (1994), 17953

25PO-13-43

AMORPHOUS MAGNETIC PHASE FORMATION DURING Fe_2O_3 AND Fe MECHANOCHEMICAL INTERACTION

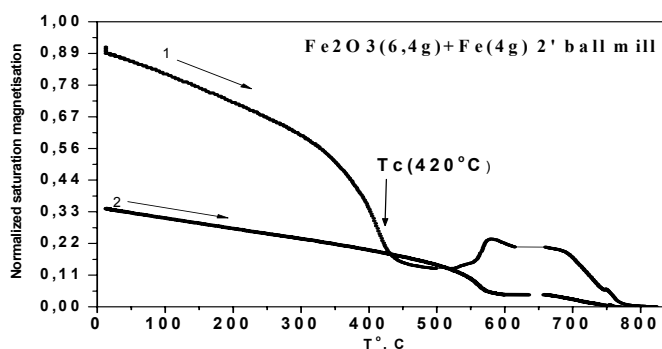
Kiseleva T.Yu.¹, Novakova A.A.¹, Gendler T.S.², Grigor'eva T.F.³, Chistyakova M.¹

¹Moscow M.V.Lomonosov State University, Department of Physics, Vorob'evy Gory, Moscow

²Institute of Physics of the Earth RAS, B.Gruzinskaya 10, Moscow, Russia

³Institute of solid state chemistry and mechanochemistry SO RAS, Novosibirsk, Kutateladze st.

Solid phase mechanochemical $\alpha\text{-Fe}_2\text{O}_3$ reduction as known results in nanocrystalline composite structure consisted of non-stoichiometric oxides forms such as $\text{Fe}_3\text{-VO}_4$, $\gamma\text{-Fe}_2\text{O}_3$ and $\text{Fe}_{1-x}\text{O}_4$ in dependence on the experimental condition (time and mill energy) [1]. In our experiments Fe-powder was applied as additional



reducing agent to α -Fe₂O₃ reduction reaction in high energy ball mill. The formation of disordered or even amorphous magnetic phase in this process was detected by means of Mossbauer spectroscopy. To determine the nature and stability of this amorphous-like phase formation we performed the investigation of mechanochemical interactions in α -Fe₂O₃ + Fe mixtures at constant α -Fe₂O₃ and gradually increased Fe concentrations.

It was carried out by Mossbauer spectroscopy that disordered or even amorphous Fe-based phase formation appeared even at small Fe admixture. Its appearance is accompanied by small amount of defective Fe₃O₄ and decreased α -Fe₂O₃. The quantity of disordered phase rises with Fe concentration increase in a milled powder mixture and accompanies by α -Fe₂O₃ partial destruction. Its Mossbauer spectral shape with hyperfine field distributions and average hyperfine field value of 250 kOe looks like well known spectra of Fe-based amorphous compounds with different surroundings of Fe-atoms. At the same time only Fe-structural peaks drastically decrease and broadening on X-ray diffraction pattern have been determined. The mean crystallite sizes of iron oxides and Fe were about 100-80 nm.

The temperature dependence of saturation magnetization (Fig1) supports the amorphous Fe-based phase formation assumption. Temperature dependence has typical irreversible amorphous-to-crystalline transformation shape [2]. Amorphous phase Curie temperature value determined not only $J_s(T)$ but also $J_{rs}(T)$ dependencies is about 420°C and stable to 550°C. The saturation magnetization increase after $T=550$ C is caused by α -Fe phase crystallisation (as was shown by means of Mossbauer spectroscopy). Magnetic behaviour at repeated heating is evident for Fe₃O₄ / α -Fe composite structure.

We consider observed magnetic amorphous state appearing during α -Fe₂O₃ ball milling in Fe presence as structure associated with oxide/ α -Fe interface.

[1] S.J.Campbell, W.A.Kaczmarek, in: G.J.Long, F.Grandjean (Eds.), Mossbauer Spectroscopy Applied to Materials and Magnetism, Vol. 2, Plenum Press, New York, 1996, p. 273.

[2] A.A.Novakova, T.Yu.Kiseleva, J. Mater. Sci. Forum 1997, V.235-238, p.619-622

25PO-13-44

APPLIED PRESSURE EFFECT ON MAGNETIC STATES IN RARE EARTH-IRON-BASED COMPOUNDS

Medvedeva I.V.

Institute of Metal Physics, Ural Division of the Russian Academy of Sciences,
18 S.Kovalevskaya Str., 620041 Ekaterinburg, Russia

A high sensitivity of magnetic state of intermetallic compounds to external parameters - temperature, magnetic field and applied pressure can be used in magnetic sensors, magnetoresistors, magnetic cooling devices etc. The sources of such sensitivities are different, in particular, they might result from a complex of exchange interactions between magnetic ions or peculiarities of electron bands structure. Such a situation present Fe-rich intermetallic compounds with Rare Earth metals. In the case of iron alloying with R=Y and La which have no magnetic moment of their own the determining contribution to magnetic state comes from 3d-electronic states of iron.

Our experimental studies of applied pressure effect on ferromagnetic transition temperature – a ferromagnet - paramagnet (Curie point) or ferromagnet - antiferromagnet

transition temperature in $Y_2Fe_{17-x}M_x$ ($M = Al, Si$), $Y_2Fe_{14-x}M_xB$ ($M = Mn, Cr$), Ce_2Fe_{17} , $La(Fe_{0.88-x}Co_xAl_{0.12})_{13}$ let us to compare the stability of ferromagnetic state in these R_xFe_y -based compounds with different relative Fe-ions concentration. The pressure derivative of the ferromagnetic transition temperature, dT_C/dP , was regarded as a measure of a stability/sensitivity of ferromagnetic state to applied pressure.

The applied pressure acts to decrease ferromagnetic transition temperature in Fe-rich R_xFe_y -based compounds. The absolute value of the negative pressure derivative of ferromagnetic transition decreases upon the relative Fe-atoms concentration increase in crystalline compounds. However this trend does not hold for the amorphous Fe-based alloys.

The decrease of ferromagnetic transition temperature together with increase of its sensitivity to applied pressure evidence on the progressing instability of ferromagnetic state upon relative Fe atoms concentration increase in the R_xFe_y -based compounds.

For the compounds with a high sensitivity of ferromagnetic state to applied pressure a significant magnetoresistance and baroresistance effects were observed as well, which points to a strong correlation between spin and charge subsystems.

The experimental results are discussed in the framework of localized spin model and band itinerant ferromagnetism model.

Support by Program № 09-03 of the Presidium of the Russian Academy of Sciences is acknowledged.

25PO-13-45

FABRICATION OF FePt FILM FOR PERPENDICULAR MAGNETIC RECORDING MEDIA BY ALTERNATE DEPOSITION

Liu X.¹, Li S.T.¹, Cao J.W.¹, Yang Z.¹, Wei F.L.¹, Kamzin A.S.²

¹Research institute of magnetic materials, Key Lab. on magnetism and magnetic materials, Lanzhou 730000, China

²Ioffe Physical-Technical Institute, Academy of Science, ST. Petersburg 194121, Russia

Magnetic anisotropy is one of the most important technical properties of magnetic materials, particularly for magnetic information storage. Recently, the ordered tetragonal L10 phase FePt alloy thin film have drawn considerable attention as a potential high-density magnetic recording material, due to its large magneto-crystal anisotropy ($K_M=7 \cdot 10^7 \text{ erg/cm}^3$). With the perpendicular magnetic recording becoming main-trend technology, the challenge is perpendicular magnetic anisotropy in the thin films of recording media, in which the easy axis of magnetization is perpendicular to the plane of the film.

The ordered L10 phase FePt alloy is FCT(face central tetragonal) structure. The easy magnetization axis corresponds to the c-axis. For perpendicular magnetic recording film media of FePt alloy, it should show (001) preferential orientation structure. A classical method to obtain (001) is by epitaxially growing on suitable substrate and buffer layer such as Mg or Cr-alloy(CrX) film. On the other hand, we notice that, the ordered FePt alloy has a superlattice structure consisting of Fe and Pt monatomic layers stacked alternately along the c-axis, so it is possible to prepare the ordered FePt film with (001) orientation by alternate deposition.

We prepared ordered FePt alloy films with multilayer structure such as $[Pt/Fe]_n$ on preheated Corning-7059 glass substrate using pure Fe and Pt targets in a magnetron-sputtering system. Investigate the influence of Fe and Pt thickness, substrate temperature and post annealing on orientation(measured by XRD and CEMS methods) and magnetic properties. It is found the L10 ordered FePt alloy film with (001) orientation can be prepared by depositing

[Pt(5.2nm)/Fe(4.8nm)]₁₀ multilayer on preheated glass substrate at 500°C. The orientation of the film depends strongly on the initial layer materials, the total film thickness, the single layer thickness and the substrate temperature.

25PO-13-46

STRESS-INDUCED MAGNETIC ANISOTROPY, ITS THERMAL STABILITY AND STRUCTURE OF NANOCRYSTALLINE Fe-Co-Cu-Nb-Si-B ALLOYS

Lukshina V.A., Dmitrieva N.V., Kleinerman N.M., Serikov V.V., Volkova E.G., Potapov A.P.
Institute of Metal Physics UB RAS, Ekaterinburg, Russia

Subject of the work was a complex research of microstructure, magnetic properties and their thermal stability in Fe_{73.5-x}Co_xCu₁Nb₃Si_{13.5}B₉ ($X = 10, 20, 30$) alloys with the stress-induced magnetic anisotropy (IMA).

Ribbon samples of 20 μm thick, and 1 mm wide were produced in amorphous state by rapid quenching from the melt. They were nanocrystallised in air and subjected simultaneously to stress-annealing (SA) at 520°C for 2 hours with a load of 400 MPa. Mössbauer spectroscopy and electron microscopy were used for structure investigation. Magnetic state was controlled by the form of hysteresis loops measured by ballistic method. Thermal stability of magnetic properties after SA was estimated by changes in the hysteresis-loop shape upon thermal destruction of the IMA during additional annealing at 520° for 6 hours (DA).

It was obtained that the type of anisotropy in the above alloys changed depending on Co content: at $X = 10$ the IMA was induced across to the ribbon axis, as at $X=0$ [1]; at $X = 20$ and 30 it was induced along to one. The hysteresis loops, inclined and linear for alloys with 0 and 10 at%, become rectangular at higher X . For the alloys with the transverse IMA the constant of IMA (K_u) was estimated by formula $K_u = -0.5 \cdot M_s \cdot H_s$, where M_s is the saturation magnetization and H_s is the field at which saturation is reached. For the alloys with the longitudinal IMA the squareness factor (α) was calculated from the hysteresis loops: $\alpha = B_r/B_m$, where B_r is the remanence, B_m is the magnetic induction of technical saturation. Addition of 10% Co reduces the K_u value (by a factor of 2.5) and its thermal stability, compared to the alloy without Co. After the DA K_u decreases to 50 and 70% for alloys with 0 and 10% Co, respectively. The magnetic properties of the alloys with the longitudinal IMA are more thermally stable, compared to alloys with transverse IMA. So, α for the alloy with 30% Co decreases after the DA only to 10%.

The data of structure investigations evidence that no traces of the occurrence of pure Co are present in all the samples. It is shown that the addition of Co results in the decrease of the amount of Fe-Si grains and the formation of some Fe-Co-B containing phases. The IMA is controlled by the volume parts of the structure components, their magnetoelastic properties and coherent bonding of their crystal lattices. So, with increasing Co content to 10% the contribution of the Fe-Si phase with a negative magnetostriction is still sufficient to provide the transverse anisotropy (but with smaller constant and thermal stability). The decrease of the Fe-Si phase and increase of the boron-containing phases with a positive magnetostriction constant in alloys with 20 and 30 % of Co results in the appearance of the longitudinal anisotropy.

Between the alloys with the longitudinal anisotropy the 30% Co composition turns out more stable, which can be related to the changes in the magnetoelastic state gained after SA in such a way that the system of phases retains the coherent bonding, which is favored by both small amount of the Fe-Si phase and the magnetostriction constant of the boron-containing phases with a high Co concentration.

The work was done with a partial support of RFBR (grant no. 06-02-17082).

[1] V.A. Lukshina, N.V. Dmitrieva, N.I. Noskova, E.G. Volkova, N.M. Kleinerman, V.V. Serikov, A.P. Potapov, *Phys. Met. Met.*, **93**(6) (2002) 536.

25PO-13-47

FEATURES OF THE POST-DEFORMATION HARDENING OF Fe-Cr-Co HARD MAGNETIC ALLOYS WITH W AND Ga ADDITIVES

Belozerov E.V., Shchegoleva N.N., Ivanova G.V., Mushnikov N.V.
Institute of Metal Physics, Ural Division of RAS, S Kovalevskaya, 18,
620041 Ekaterinburg, Russia

The Fe-Cr-Co alloys with small additives of tungsten and gallium represent a new class of hard magnetic materials which combine high magnetic and mechanical properties. The strength of this magnetic materials is comparable with that of the maraging structural steels, while the enhanced plasticity prevents brittle fracture, which is especially important for applications as the disk rotors of the power motors with the rotary speeds exceeding 150 thousands rpm.

Our studies showed that these alloys possess the yield strength $\sigma_{0.2} = 1600$ MPa, the tensile elongation $\delta = 6.4$, and simultaneously, high coercive force $H_c = 100-150$ A/cm [1] that is several times higher than that of the early used high-strength steels.

The state with high coercivity and high strength is formed after cold plastic deformation of the alloy with a heterophase structure which is obtained by the quenching from the high-temperature state followed by the precipitation hardening. To achieve the best mechanical and magnetic properties we performed the optimization of the compositions, regimes of deformation and hardening. The morphology of the resultant structures is determined on the level of macroscopic studies. In order to understand the origin of the appearance of high magnetic and strength properties, in this paper we performed X-ray and electron microscopy studies of the formation of the structures of the post-deformation state of these alloys. The studies are performed for different structural states of the alloys with the additives of W and W+Ga in comparison with the Fe-Cr-Co alloy without additives. Special attention is paid to the study of the phase composition in the high-temperature region of the phase diagram, which is mainly responsible for the formation of the post-deformation structures.

For the high-temperature region of the phase diagram we found the phases α , γ and σ , the relative amount of which depends on the annealing temperature. We determined the composition dependence of the lattice parameters of the phases after quenching and after post-deformation hardening. Electron microscopy studies of the alloys for different composition and treatment show a large amount of dislocations, stacking faults and tweed contrast. A monotoneous growth of the coercivity after deformation, and especially, after post-deformation hardening, is accompanied by the growth of strength. These features are indicative of a considerable magnetoelastic energy contribution to the formation of the high-coercive state and a substantial role of the elastic strains in increasing the strength of the alloys.

Support by the RAS Program (project no. 01.2.006 13391) is acknowledged.

[1] E.V. Belozerov, M.A. Uimin, A.E. Ermakov, *Zhurnal funktsionalnykh materialov*, **1** (2007) 36 (in Russian).

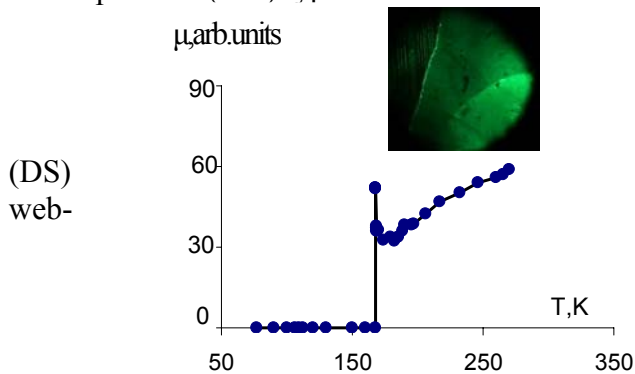
25PO-13-48

RESEARCH OF FEATURES OF DOMAIN STRUCTURES IN $\text{Fe}_2\text{O}_3:\text{Ga}$ CRYSTALS NEAR THE MORIN TRANSITION

Chzhan A.V., Vasiljev V.N., Isaeva T.N., Patrin G.S.

Kirenskii Institute of Physics, the Siberian Branch of RAS, Krasnoyarsk
660036, Krasnoyarsk, Academgorodok, Institute of Physics, Russia

Hematite is weakly ferromagnetic with rhombohedra symmetry. Research of its properties allows revealing the basic features of such magnets. In this paper research results of magnetic, resonance and optical properties of hematite with Ga impurity are represented. Samples have been grown up by a method of spontaneous crystallization from melt solution with a base plane of (111) type.



It is interesting to investigate the behaviour of hematite magnetic system near Morin temperature T_m . For this purpose continuous observing of domain structure was carried near T_m . Specially picked out chamber was used in this experiment. Such chamber allows making visualization in infra-red range. The used method possesses significant sensitivity that enables to find out features of DS formation in wide area of temperatures (the photo of DS hematite is

presented in fig.). Also magnetic permeability μ was investigated. Temperature dependence of initial magnetic permeability at the concentration of gallium 0,076 is illustrated in fig. Such dependences is the same for other Ga concentrations. Thus the increase in maintenance of Ga leads to decrease of Morin temperature. It is revealed that the temperature of abnormal change of μ goes down by application of constant magnetic field. Such behaviour of magnetic permeability has good agreement with behaviour of temperature transition of the first sort, determined in the given crystals by AFMR method [1].

The fact that magnetic permeability increases sharply in a point of transition and then it decreases up to some value attracts attention. A visual observation of magnetic system allows revealing that sharp increase of magnetic permeability at critical temperature is connected with sharp appearance of magnetization in this point. After such process DS formation is observed and magnetic permeability becomes connected with movement of domain walls.

In this work the influence of Ga impurity on optical properties of hematite is researched. It is revealed that addition of such impurity leads to reduction of optical absorption in these crystals.

[1] Vasilev V.N., Matveiko E.N. Physical properties of dielectric. Krasnoyarsk, 1987, p.45-70.

25PO-13-49

MICROSTRUCTURE EVOLUTION UPON THERMOMAGNETIC TREATMENT OF SOFT MAGNETIC ALLOYS

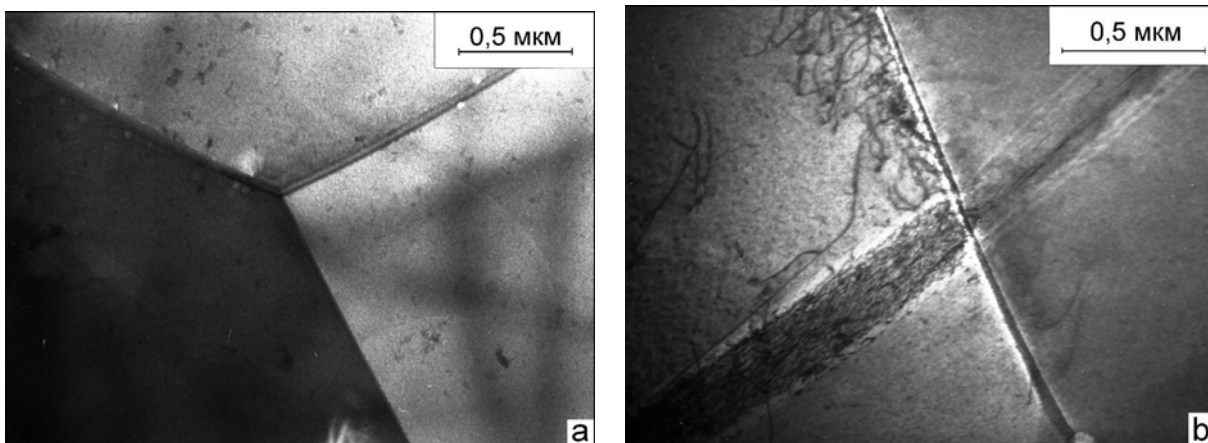
Gubernatorov V.V., Sycheva T.S., Kositsyna I.I.

Institute of Metal Physics, Ural Division, Russian Academy of Sciences, 18 S. Kovalevskaya St., 620041 Ekaterinburg, Russia

Considering results of calculations [1], the change of magnetic properties [2] and X-ray studies [3] of the Fe-3% Si and Fe-70% Ni alloys, we have proposed a new concept explaining effects produced by thermomagnetic treatment (TMT) in soft magnetic alloys.

By this concept, TMT in an alternating magnetic field leads to the magnetoelastic interaction between structural inhomogeneities (clusters with a superstructure, "fresh" defects and impurity atoms) and vibrating boundaries of magnetic domains. Each boundary removes some of the aforementioned inhomogeneities from its vibration range to form a "clean" zone. The inhomogeneities accumulate at extreme positions of the domain boundaries to form narrow "foul" zones extending in the direction of the magnetic field and alternating with "clean" zones. Thus, TMT arranges structural inhomogeneities according to the dynamics of the magnetic domain structure. "Clean" zones add to magnetic permeability and reduce the coercive force and the specific magnetic loss during the magnetization reversal on account of destabilization of the magnetic domain structure. For example, if the ready (with the optimal texture and structure) Fe-70% Ni alloy is loaded with a certain amount of "fresh" (mobile) defects, TMT of this alloy reduces coercive force from 17.8 to 8.4 A/m. After fivefold recurrence of these processings coercive force drops to 7.1 A/m.

Our electron microscope examination of the fine structure of the Fe-70% Ni alloy before and after TMT (figs. a and b, respectively) confirmed the above assumption. It is seen that TMT was followed by formation of narrow "foul" zones – dislocation pileups (DPs), which were located in the {110} planes in the <110> and <111> directions and crossed the crystallite boundaries. The DP width was 100-200 nm and the density of dislocations in these pileups was $\sim 10^9\text{-}10^{12}\text{ cm}^{-2}$. It is not improbable that the DPs were enriched in atoms of alloying and impurity elements.



The work has been done under the RAS Program (project No. 01.2.006 13391) and has been partially supported by RFBR (grant No. 06-02-17082).

[1] V.V. Gubernatorov, A.P. Potapov, A.I. Deryagin, T.S. Sycheva, *PMM*, **92** (2001) 35.

[2] V.V. Gubernatorov, T.S. Sycheva, *JMMM*, **254-255** (2003) 404.

[3] V.V. Gubernatorov, T.S. Sycheva, L.R. Vladimirov, V.M. Gundyrev, *PMM*, **100** (2005) 522.

25PO-13-50

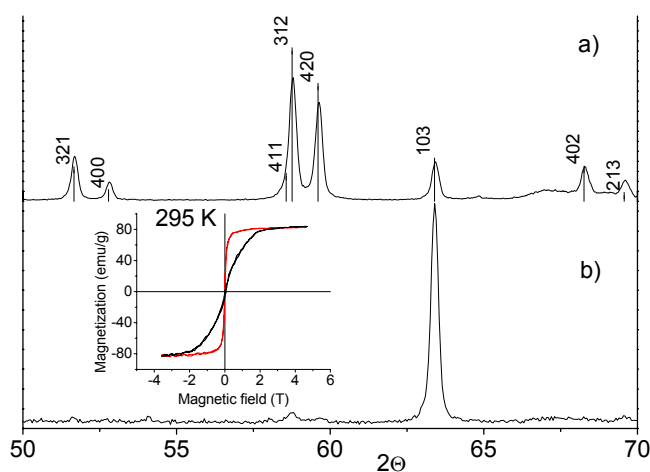
CRYSTAL STRUCTURE AND MAGNETIC PROPERTIES OF NOVEL COMPOUND $\text{PrFe}_8\text{Ga}_3\text{C}$

Gaviko V.S., Popov A.G., Ivanova G.V., Mushnikov N.V., Belozеров Ye.V., Ermolenko A.S., Shreder L.A.

Institute of Metal Physics, Ural Division of RAS, S. Kovalevskaya, 18,
620041 Ekaterinburg, Russia

Numerous studies of iron-rich intermetallic rare-earth - iron compounds are stimulated by the possibility of their application as permanent magnet materials. From this point of view, the most perspective are the compounds with tetragonal or hexagonal symmetry of the lattice, in which a strong uniaxial magnetic anisotropy can be realized. Recently, new ferromagnetic $\text{Pr}(\text{Fe},\text{Si})_{11}\text{C}_x$ compounds have been discovered [1]. They crystallize within a filled variant of the tetragonal BaCd_{11} -type structure (space group $I4_1/amd$), with Pr in the 4(a) position, Fe in the 4(b), 32(i) and 8(d) sites, Si atoms being located in the remaining part of 8(d) sites. Carbon atoms occupy 8(c) octahedral sites surrounded by four Fe and two Pr atoms. In the present paper we showed that compounds with the same structure can crystallize in the Pr-Fe-Ga-C system. We synthesized the compound $\text{PrFe}_8\text{Ga}_3\text{C}$ with the tetragonal BaCd_{11} -type lattice and studied its structure and magnetic properties.

X-ray diffraction studies show that different iron positions are non-uniformly substituted by Ga atoms. Some iron sites are occupied by Ga with great preference. Likely as in [1], the carbon atoms occupy 8(c) sites which are vacant in the BaCd_{11} structure. In order to determine



X-ray diffraction patterns of isotropic (a) and aligned (b) powder samples. The inset shows the hysteresis loops measured for aligned sample in the plane of rotation (1) and normal to it (2).

the type of magnetic anisotropy, the powdered samples were aligned in both steady and rotating magnetic fields. The X-ray diffraction patterns for random powder sample and for the sample aligned in rotating field are shown in figure. A huge increase in the intensity of [103] line, the direction of which is very close to the c -axis of the crystal, indicates that the c -axis is a hard direction. The hysteresis loops given in the inset also clearly show that the compound possesses the easy-plane type magnetocrystalline anisotropy. We studied high-field magnetization curves along the easy and hard direction of the aligned sample for different temperatures between 80 and 300 K in pulsed magnetic fields up to 30 T. From these results we determined temperature dependences of the magnetization, the anisotropy field and the anisotropy constant K_1 of compound. The spontaneous magnetization, anisotropy field and anisotropy constant have the following values: 96.6 emu/g, 12.2 T, -4.19×10^7 erg/cm³ at 80 K and 78 emu/g, 1.8 T, -0.5×10^7 erg/cm³ at 295 K, respectively.

This work was supported by the RAS Program (project no. 01.2.006 13391) and by Russian Foundation for Basic Research (project no 07-02-00219).

[1] V. Klosek, O. Isnard, J. Alloys Comp., **383** (2004) 89.

25PO-13-51

STRUCTURAL AND MAGNETIC PHASE TRANSITIONS IN ErFe_2H_x HYDRIDES

Shreder L.A., Gaviko V.S., Mushnikov N.V.

Institute of Metal Physics, Ural Division of RAS, S. Kovalevskaya, 18,
620041 Ekaterinburg, Russia

The RFe_2 (R is a rare earth) intermetallic compounds display interesting magnetic properties such as giant magnetostriction, highest Curie temperature among the R-Fe compounds, ferrimagnetic compensation. These compounds are of particular interest due to their ability to form RFe_2H_x hydrides with concentrations x ranging from 1.2 to 5. Depending on the hydrogen content, the ErFe_2H_x hydrides at room temperature are characterized by a cubic (C), a rhombohedral (R), or an orthorhombic structures [1,2]. The phase transitions between these phases occur with both hydrogen concentration and temperature changes and are accompanied by the anomalies of magnetic properties. In this work, phase transitions and magnetic properties of ErFe_2H_x ($x = 0, 1.6, 1.8, 3.0, 3.09, 3.1, 3.53, 3.71$) hydrides and $\text{ErFe}_2\text{D}_{3.1}$ deuteride have been studied by X-ray diffraction, magnetization and magnetic susceptibility measurements in temperature range 4–500 K. The hydrides, the composition of which is close to the boundary of the concentration C – R phase transition ($x \sim 3.1$) have been investigated in more details.

The ErFe_2 intermetallic compounds were synthesized by induction melting of the pure elements followed by an annealing over 48 h at 800 C. Hydrogenation was carried out with the Sieverts-type reactor. The required hydrogen content was obtained by varying the hydrogen pressure and temperature. The X-ray diffraction (XRD) patterns were measured in temperature range 80–460 K with a DRON - type diffractometer in monochromatized Cr - K_α radiation using a home-made vacuum X-ray chamber.

At room temperature the XRD patterns of samples with $x \leq 3.0$ were all refined in the cubic structure, for $3.1 \leq x \leq 3.53$ the patterns were refined in a mixture of C and R phases and for $x = 3.71$ only R phase was observed in the sample. The Curie and compensation temperatures both decrease with increasing hydrogen content. For the samples with $x \sim 3.1$, change of temperature initiates the first-order C – R structural phase transition. This transition occurs through a mixture of adjacent phases and is accompanied by a temperature hysteresis and anomalous change of the magnetization.

The low-temperature phase composition of the $\text{ErFe}_2\text{H}_{3.1}$ sample depends on the cooling rate. The amount of the ordered rhombohedral phase after a slow cooling (10 hours) was found to be almost twice of that after an abrupt cooling (5-10 min). Near the transition temperature (~ 290 K) we observe strong magnetic relaxation. These features are indicative of the diffusion nature of hydrogen rearrangement in these hydrides.

Above room temperature, the lattice parameters and cell volume slightly increase with increasing temperature up to 400 K and then sharply drop because of the hydrogen release. For some compositions, a considerable amount of R - phase was found to form again after heating over 420 K. Magnetic susceptibility measurements revealed that, for small hydrogen contents, the Curie temperature of the hydride exceeds that of the parent ErFe_2 . This unusual behavior is likely caused by an increase of the Fe magnetic moment in hydrogen-containing phases.

The study is supported by the RAS Program (project no. 01.2.006 13391), the Priority Program “Hydrogen energy” (grant no. 17-2008) and the Swiss project SCOPES no. IB7420-110849.

- [1] V. Paul-Boncour, S.M. Filipek, I. Marchuk, et al., *J. Phys.: Condens. Matter*, **15** (2003) 4349.
[2] A.V. Andreev, A.V. Deryagin, A.A. Ezov, N.V. Mushnikov, *Phys. Met. Metallogr.*, **58** (1984) 124.

25PO-13-52

MAGNETIC PROPERTIES OF $Tb_{1-x}Y_xMn_6Sn_6$ COMPOUNDS NEAR ANTIFERRO-FERROMAGNETIC PHASE TRANSITION

Terent'ev P.B., Mushnikov N.V., Gerasimov E.G., Gaviko V.S., Rosenfeld E.V., Shreder L.A.
Institute of Metal Physics, Ural Division of RAS, S Kovalevskaya, 18,
620041 Ekaterinburg, Russia

The $TbMn_6Sn_6$ and YMn_6Sn_6 compounds crystallize in the $HfFe_6Ge_6$ -type structure. The lattice has an intrinsic layered structure. The competition between different interlayer exchange interactions results in a variety of magnetic structures. The structure of YMn_6Sn_6 compound is a double flat spiral antiferromagnet. The Neel temperature of YMn_6Sn_6 compound is 333 K. The Mn atoms are arranged ferromagnetically within each layer, and the direction of the magnetic moments rotates from one layer to another. $TbMn_6Sn_6$ is a collinear ferrimagnet with the Curie temperature $T_C = 423$ K. The ferrimagnetic ordering in $TbMn_6Sn_6$ is caused by a strong negative intersublattice Tb–Mn exchange interaction. At low temperatures the “easy-axis”-type uniaxial magnetocrystalline anisotropy is observed in $TbMn_6Sn_6$. At temperatures which are higher than $T_{sr} \approx 310$ K, the “easy-plane”-type anisotropy is observed and a spontaneous spin-reorientation transition occurs. At temperatures which are near to T_{sr} , a first-order magnetization processes (FOMP) occur in the magnetic field applied along the hard direction [1].

The aim of this work is consisted in studies of magnetic properties of the quasi-ternary $Tb_{1-x}Y_xMn_6Sn_6$ ($0 \leq x \leq 1$) compounds in which Tb–Mn exchange interactions can be gradually change. Especial attention was paid to yttrium-rich concentrations where the existence of the antiferromagnetic – ferrimagnetic concentration phase transition was expected.

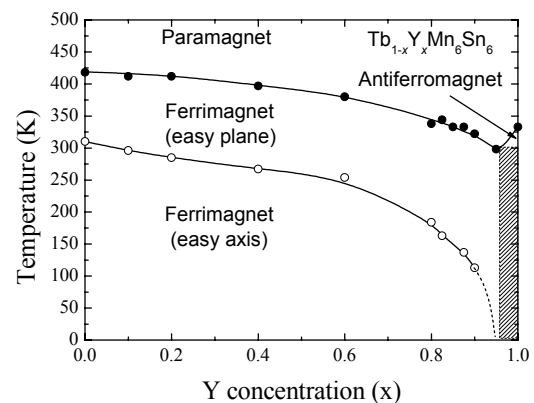
It was shown that the T_{sr} temperature decreases with increasing Y concentration and becomes zero at $x > 0.9$ because of decreasing of Tb contribution to the magnetic anisotropy of the compounds. The Curie temperature slightly decreases with increasing yttrium concentration. At yttrium concentration $x < 0.95$, the antiferromagnet-ferrimagnet phase transition occurs. The x - T magnetic phase diagram was constructed (see Fig.) using measurements of temperature dependences of the AC susceptibility.

The jumps of magnetization were observed in magnetic field applied along the hard direction for all $Tb_{1-x}Y_xMn_6Sn_6$ compounds. For compounds with $x < 0.95$, this jump of magnetization exists at temperatures near T_{sr} and can be explained by FOMP. For compounds with $x \geq 0.95$, the jump of magnetization is due to the field-induced antiferro-ferrimagnetic phase transition.

The obtained results show a significant role of complicate Mn–Mn and Mn–Tb exchange interactions in formation of the magnetic structures of RMn_6Sn_6 compounds.

This study was supported by the RAS Program (project no. 01.2.006 13391), RFBR (grant Nos. 06-02-16951, 05-02-16087), by the Priority Program “Quantum Macrophysics” and by Ural and Siberian Divisions of RAS (grant no. 32-2006).

[1] N.K. Zajkov, N.V. Mushnikov, M.I. Bartashevich, T. Goto, *J. Alloys Comp.*, **309** (2000) 26.



25PO-13-53

POSITIVE MAGNETORESISTANCE AND LARGE MAGNETOSTRICTION AT ANTIFERRO- FERROMAGNETIC PHASE TRANSITION IN RMn_2Si_2 COMPOUNDS

Gerasimov E.G.¹, Mushnikov N.V.¹, Koyama K.², Kanomata T.³, Watanabe T.²

¹Institute of Metal Physics, Ural Division of the Russian Academy of Science, S Kovalevskaya,
18, 620041 Ekaterinburg, Russia

²High Field Laboratory for Superconducting Materials HFLSM, Institute for Materials Research,
Tohoku University, Sendai 980-8577, Japan

³Department of Applied Physics, Faculty of Engineering, Tohoku Gakuin University, Tagajo,
Miyagi 985, Japan

The RMn_2Si_2 (R is a rare-earth metal) compounds crystallize in the layered $ThCr_2Si_2$ -type structure and can be considered as a natural analog of the artificially prepared multilayer structures.

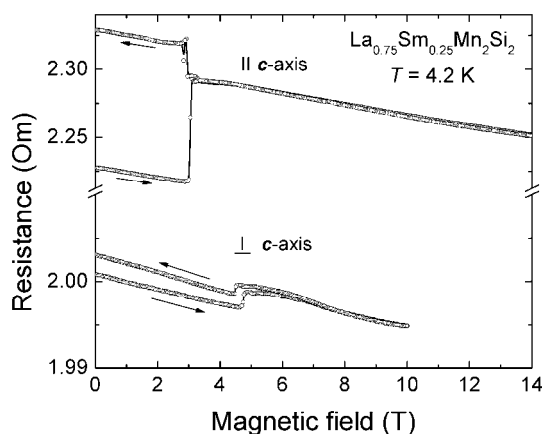
In this work we studied the magnetoresistance and magnetostriction at antiferromagnetic (AF)–ferromagnetic (F) spontaneous and field-induced first order phase transitions in the Mn sublattice of the quasi-single-crystals of $La_{0.25}Sm_{0.75}Mn_2Si_2$, $La_{0.25}Y_{0.75}Mn_2Si_2$ and $La_{0.27}Y_{0.73}Mn_2Si_2$ compounds.

It was shown that the magnetoresistance at AF-F phase transition is positive in these compounds. The value of the electrical resistance in ferromagnetic state is higher than that in the antiferromagnetic state. Maximum magnetoresistance was observed along the c -axis and can reach up to +54%. In the basal plane, the magnetoresistance is about 100 times smaller. In the magnetic field above and below the critical field for the AF-F transition, the magnetoresistance is negative (see figure), which is typical behavior for majority of ferro- and antiferromagnets.

It was also shown that the spontaneous and field-induced AF-F phase transitions are accompanied by a large volume $\Delta V/V \approx 2 \cdot 10^{-3}$ and anisotropic $\Delta a/a \approx 1.6 \cdot 10^{-3}$, $\Delta c/c \approx -0.75 \cdot 10^{-3}$ change of the lattice parameters.

The obtained results allow us to conclude that the magnetoresistance in the RMn_2Si_2 compounds at AF-F phase transition is not connected with the spin-dependent mechanism of the conduction electrons scattering and arises as a result of the electronic band structure changes. The large difference between the magnetoresistance values observed for different samples is due to the large magnetostriction which results in the appearance of microcracks in the samples.

Support by RAS Program (project no. 01.2.006 13391), with partial support of RFBR under grant no. 06-02-16951 and the Ural and Siberian Division of the RAS (project no. 32-2007) is acknowledged.



25PO-13-54

SPONTANEOUS AND FIELD-INDUCED MAGNETIC PHASE TRANSITIONS IN $Tb_{1-x}R_xMn_6Sn_6$ ($R = Gd, Y$) COMPOUNDS

Mushnikov N.V., Terent'ev P.B., Gaviko V.S., Gerasimov E.G., Rosenfeld E.V., Shreder L.A.
Institute of Metal Physics, Ural Division of RAS, S. Kovalevskaya, 18,
620041 Ekaterinburg, Russia

$TbMn_6Sn_6$ belongs to a wide family of RMn_6X_6 compounds (R is a rare earth element, Mg, Sc, Y, Zr, Hf; $X = Sn, Ge$) with hexagonal $HfFe_6Ge_6$ -type crystal structure. The structure is built up of alternating hexagonal planes stacked along the c -axis in the following sequence: Mn-X-X-X-Mn-(R,X)-Mn. The Mn magnetic moments are ferromagnetically coupled within the Mn (001) planes. A much weaker interlayer exchange interaction is responsible for a wide variety of the magnetic structures observed in these compounds. For YMn_6Sn_6 compound, the magnetic structure is a double flat spiral below the Neel temperature 333 K [1]. The compounds with late rare earths contain ferromagnetic R planes which couple antiferromagnetically with the Mn planes giving rise to the stabilization of ferrimagnetic structures. Magnetization curves measured for $TbMn_6Sn_6$ in magnetic fields applied along the hard direction revealed the field-induced first-order magnetic phase transition (FOMP). As a rule, the appearance of the FOMP in the compounds is attributed to the contribution of high-order terms to the magnetic anisotropy. Therefore, these transitions usually appear at low temperatures. Surprisingly, in $TbMn_6Sn_6$ the FOMP is observed near room temperature and in small magnetic fields [2].

In order to reveal the origin of appearance of the FOMP in this compound, we studied the effect of dilution of the anisotropic Tb sublattice by magnetic atoms of Gd with zero orbital momentum and by non-magnetic yttrium atoms. For $Tb_{1-x}Gd_xMn_6Sn_6$ and $Tb_{1-x}Y_xMn_6Sn_6$ systems we measured the magnetic susceptibility and the high-field magnetization curves for aligned powder samples and determined temperature and concentration dependences of the anisotropy constants. The spin-reorientation transition observed at 310 K for $TbMn_6Sn_6$ shifts to the low-temperature region with increasing Gd or Y content and disappears for the compositions with $x \geq 0.9$ [3]. We separate the contributions to the magnetic anisotropy from two magnetic sublattices and show that the FOMP in $TbMn_6Sn_6$ cannot be explained exclusively by a competition of the magnetic anisotropies of Tb and Mn subsystems.

For the compounds $Tb_{1-x}Y_xMn_6Sn_6$ with $x \geq 0.85$ near the transition to the spiral magnetic structure, we studied pressure effect on the magnetization. We found that application of hydrostatic pressure facilitates the ferrimagnetic ordering. This unusual feature is supported by the X-ray diffraction measurements of thermal expansion. Temperature dependences of the lattice parameters reveal large negative spontaneous volume magnetostriction for the compounds with magnetic R sublattice. The obtained results are discussed in a phenomenological model considering three different interlayer Mn-Mn exchange interactions in these compounds.

This study was supported by the RAS Program (project no. 01.2.006 13391), RFBR (grant Nos. 06-02-16951, 05-02-16087), by the Priority Program "Quantum Macrophysics" and by Ural and Siberian Divisions of RAS (grant no. 32-2006).

[1] G. Venturini, D. Fruchart, B. Malaman, *J. Alloys Comp.*, **236** (1996) 102.

[2] N.K. Zajkov, N.V. Mushnikov, M.I. Bartashevich, T. Goto, *J. Alloys Comp.*, **309** (2000) 26.

[3] P.B. Terent'ev, N.V. Mushnikov, V.S. Gaviko, L.A. Shreder, E.V. Rosenfeld, *J. Magn. Mater.*, **320** (2008) 836.

25PO-13-55

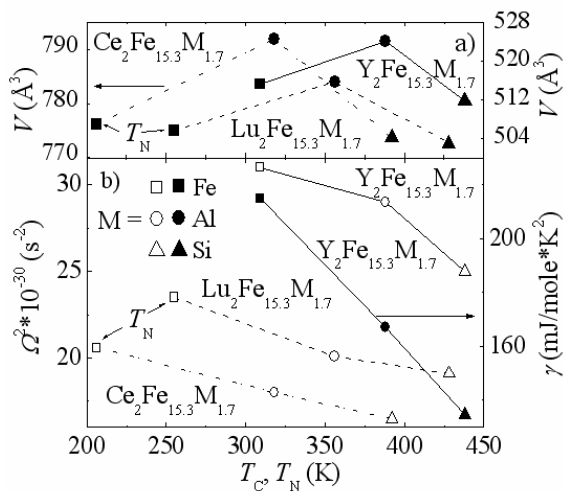
ROLE OF ELECTRONIC BAND STRUCTURE AND LATTICE PARAMETERS IN MAGNETISM OF THE $R_2(Fe,M)_{17}$, $M = Si, Al$ COMPOUNDS

Kuchin A.G.¹, Knyazev Yu.V.¹, Kuz'min Yu.I.¹, Nekrasov I.A.², Anisimov V.I.¹, Kourov N.I.¹, Medvedeva I.V.¹, Voronin V.I.¹

¹Institute of Metal Physics, Ural Division of RAS, Ekaterinburg 620041, Russia

²Institute of Electrophysics, Ural Division of RAS, Ekaterinburg 620049, Russia

Iron-based rare-earth R-Fe intermetallic compounds have attracted attention as promising candidates for permanent magnet developments. The R_2Fe_{17} compounds are rich in iron, an abundant and cheap element which carries a high atomic moment. However, the Curie temperature T_C is low, near room temperature, which is accounted for by too short iron interatomic distances, such as at the so-called “dumbbell” site with two iron atoms in it. In the various pseudobinary $R_2Fe_{17-x}M_x$ solid solutions, the increase of T_C does not result from the only unit cell volume V expansion as has been proposed earlier for the R_2Fe_{17} compounds. We have been found that the helical antiferromagnets Lu_2Fe_{17} and Ce_2Fe_{17} transform to ferromagnets after partial substitution of Si or Al for Fe, but for all that the lattice expands with Al and contracts



with Si atoms (Fig. a). Under high pressure, T_C does not correlate with V in the set of the $Y_2Fe_{15.3}M_{1.7}$, $M = Fe, Si, Al$ compounds: their T_C values can be equal or different for different or equal V values, respectively. Powder X-ray and neutron diffraction data indicate that Si or Al atoms avoid the “dumbbell” sites in the $R_2Fe_{17-x}M_x$, $M = Si, Al$ compounds, i.e. the removal of the iron dumbbell atoms by such speculative substitution cannot explain the increase in T_C . We pioneered in study of electronic band structure parameters to explain the surprising ferromagnetism strengthening in the $R_2Fe_{17-x}M_x$, $M = Si, Al$ systems. Optical

properties and low-temperature heat capacity of the compounds were investigated [1,2]. It was shown that the Curie temperature enhancement for the substitutional alloys of the system R_2Fe_{17} , $R_2Fe_{15.3}Al_{1.7}$ and $R_2Fe_{15.3}Si_{1.7}$, $R = Ce, Lu, Y$ is accompanied by a decrease in the electronic contribution to the specific heat γ or plasma frequency Ω^2 of the conduction electrons (Fig. b), which indicates a decrease in the density of states at the Fermi level $N(E_F)$. In the context of the spin-fluctuation theory of Mohn and Wohlfarth, this T_C rise occurs because of weakening of the spin fluctuations in consequence of the decrease in $N(E_F)$. The small values of Curie temperature in the binary R_2Fe_{17} compounds result from the intense spin fluctuations due to high $N(E_F)$. Self-consistent spin-polarized electronic structure calculations within the LSDA method have been carried out to derive the magnetic and optical properties of the compounds [3,4].

Support by RAS (№ 01.2.006 13391), RFBR (№ 07-02-00259, 08-02-00712) is acknowledged.

- [1] A.G.Kuchin, N.I.Kourov, Yu.V.Knyazev et al., *Phys. Met. Metallogr.*, **79** (1995) 61.
- [2] Yu.V.Knyazev, A.G.Kuchin, Y.I.Kuz'min, *J. Alloys Compd.*, **327** (2001) 34.
- [3] Yu.V. Knyazev, A.V. Lukoyanov, Yu.I. Kuz'min et al., *Phys. Rev. B*, **73** (2006) 094410(6).
- [4] A.V.Lukoyanov, A.S.Shkvarin, Yu.V.Knyazev et al., *Phys. Solid State*, **49** (2007) 99.

25PO-13-56

SPECIFIC HEAT STUDY OF METAMAGNETISM IN Lu₂Fe₁₇-BASED INTERMETALLIC COMPOUNDS

Tereshina E.A.^{1,2}, Andreev A.V.¹

¹Institute of Physics, Academy of Sciences, Na Slovance 2, 18221 Prague, Czech Republic

²Faculty of Mathematics and Physics, Charles University, Ke Karlovu 5, 12116 Prague, Czech Republic

Lu₂Fe₁₇ compound (hexagonal crystal structure of the Th₂Ni₁₇ type) exhibits two types of magnetic ordering. An incommensurate helical magnetic structure with a parallel arrangement of Fe moments in the planes perpendicular to the *c*-axis exists below the Néel temperature $T_N = 274$ K. The propagation vector of the helical structure parallel to the *c*-axis is $\tau = 0.21$ r.l.u. just below T_N (that corresponds to a 60 Å period along the *c*-axis). Upon cooling, it decreases down to zero that results in a transition into a ferromagnetic phase below the Curie temperature $T_C = 130$ K [1,2]. All known substitutions in Lu₂Fe₁₇ compound, such as substitutions of Cr, Ni, Si [3] for Fe and Y, Zr for Lu lead to a total suppression of antiferromagnetism. However, recently we have found that substitution of Ru for Fe and Ce for Lu leads to an opposite effect – stabilization of the antiferromagnetic state in the whole range of magnetic ordering. Magnetization measurements performed for Lu₂Fe_{17-x}Ru_x ($x = 0.5, 1$) and (Lu_{0.8}Ce_{0.2})₂Fe₁₇ single crystals have revealed that (Lu_{0.8}Ce_{0.2})₂Fe₁₇ and Lu₂Fe_{16.5}Ru_{0.5} exhibit metamagnetic transitions in the easy-magnetization direction from the antiferromagnetic state into a ferromagnetic one at fields below 1 T. For a higher Ru content compound, Lu₂Fe₁₆Ru, almost complete suppression of the metamagnetism was observed.

In the present work, a specific heat study of metamagnetism in Lu₂Fe_{17-x}Ru_x ($x = 0.5, 1$) and (Lu_{1-y}Ce_y)₂Fe₁₇ ($y = 0, 0.2$) single crystals was performed. The substitutions enhance the Sommerfeld coefficient γ from 250 mJ mol⁻¹K⁻² in Lu₂Fe₁₇ to 340 mJ mol⁻¹K⁻² in (Lu_{0.8}Ce_{0.2})₂Fe₁₇ and to 340 and 370 mJ mol⁻¹K⁻² in Lu₂Fe_{16.5}Ru_{0.5} and Lu₂Fe₁₆Ru, respectively. This can be due to some atomic disorder as it was observed in many solid solutions among binary compounds. It is known that the magnetic entropy change upon the metamagnetic transition depends on both the value of magnetization jump at the transition and the temperature derivative of the critical field B_c . B_c was found to decrease with increasing temperature in Lu₂Fe_{16.5}Ru_{0.5} as well as in (Lu_{0.8}Ce_{0.2})₂Fe₁₇ at low temperatures which suggests an increase of γ upon the metamagnetic transition. That was indeed observed, $\Delta\gamma$ is about 70 mJ mol⁻¹K⁻² in (Lu_{0.8}Ce_{0.2})₂Fe₁₇ and 40 mJ mol⁻¹K⁻² in Lu₂Fe_{16.5}Ru_{0.5}. The results are compared with the situation in related Ce₂Fe₁₇, where despite the similarity in the low-temperature magnetization curves, B_c increases with increasing temperature and $\Delta\gamma$ is negative [4].

The work is a part of the research project AVOZ10100520 and has been supported by grants GACR 202/06/0185 and GAUK 109-10/257015.

[1] D. Givord, R. Lemaire, *IEEE Trans. Magn.* **MAG-10** (1974) 109.

[2] J. Kamarád, O. Prokhnenko, K. Prokes, Z. Arnold, *J. Phys.: Condens. Matter* **17** (2005) S3069.

[3] J. Kamarád, A.V. Andreev, Z. Machátová, Z. Arnold, *J. Alloys Comp.* **408-412** (2006) 151.

[4] T. Ekino, H. Umeda, H. Fukuda, Y. Janssen, H. Fujii, *J. Phys. Soc. Japan* **23** (1999) 111.

25PO-13-57

LOCAL SPIN CONFIGURATIONS OF Fe ATOMS IN MICROINHOMOGENEOUS PdMn_xFe_{1-x} ALLOYS

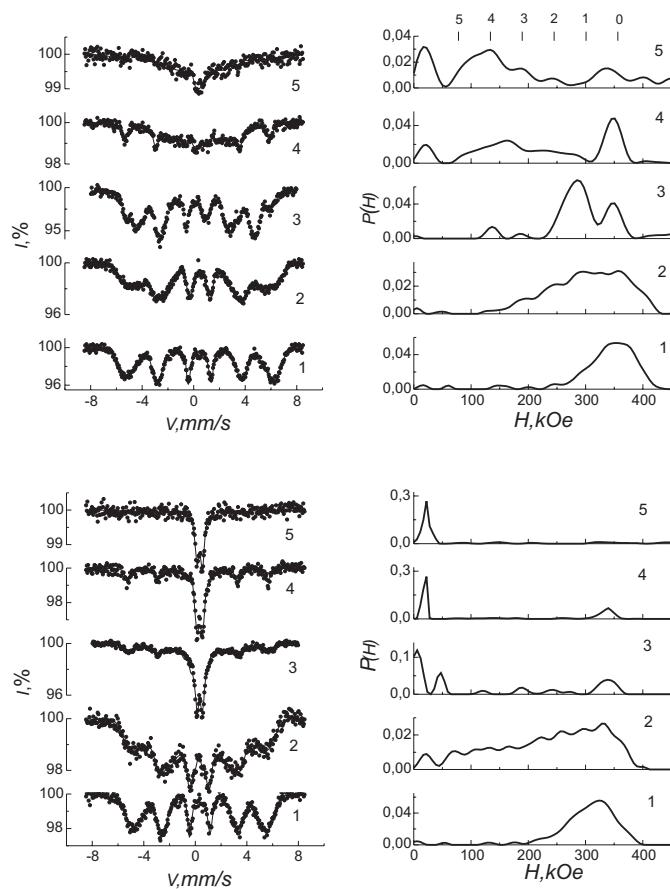
Serikov V.V., Kleinerman N.M., Volkova N.V., Kourov N.I.

Institute of Metal Physics, Russian Acad. of Sci., 18 S.Kovalevskaya str., Ekaterinburg, 620219, Russia

It was previously shown by X-ray diffraction, neutron diffraction and by measurements of magnetic properties of the ternary alloys PdMn_xFe_{1-x} [1] that in the $0.2 < x < 0.8$ concentration range there realizes a microinhomogeneous multiphase medium formed by isostructure phases of constituent compositions: ferromagnetic PdFe ($T_C=730$ K) alloy undergoing atomic ordering and antiferromagnetic PdMn ($T_N=815$ K) intermetallic compound. Structurally, the alloys investigated are two-phase [2].

Microstructure investigations display oblong precipitates of these phases with a characteristic size of (2 - 100) μm . The estimation of relative volumes from theoretical computations of magnetic susceptibility in the mean-field approximation at $x = 0.5$ shows that ferromagnetic-to-antiferromagnetic phase ratio differs significantly from the expected 50% PdFe to 50% PdMn. It makes about 22-30% antiferromagnetic phase to, respectively, 78-70% ferromagnetic phase. Magnetic properties studies evidence the presence of a third presumably noncollinear phase with its own ordering temperature lying below the Curie temperature of the ferromagnetic phase in the $0.2 < x < 0.8$ concentration range. To clarify the nature of this additional phase the Mössbauer spectra studies have been performed. This method allows one to directly detect spin configurations of different types and classify these states by the hyperfine field distribution functions $P(H_{hf})$ analysis.

The figure shows the Mössbauer spectra $I(V)$ obtained at 80 K (top) and at 300 K (bottom) and the calculated hyperfine field distribution functions $P(H_{hf})$ for alloys PdMn_xFe_{1-x}: 1 - $x = 0.1$; 2 - 0.3; 3 - 0.5; 4 - 0.7; 5 - 0.9. In intermediate concentration range several peaks $0 < H_{hf} < 350$ kOe have been observed in the $P(H_{hf})$ curves as a result of microinhomogeneous multiphase state.



[1] N. V. Volkova, Yu. A. Dorofeev, V. A. Kazantsev, N. M. Kleinerman, A. V. Korolyov, N. I. Kourov, V. E. Naish, I. V. Sagaradze, V. V. Serikov, Yu. E. Turkhan, L. N.

Tulenev, Yu. N. Tsiovkin, *Phys. Stat. Sol. (a)*, **188**, No 3 (2001), 1115.

[2] N. V. Volkova, N. M. Kleinerman, N. I. Kourov, V. E. Naish, I. V. Sagaradze, V. V. Serikov, L.N. Tyulenev, *Phys. Met. Metallogr.* **89**, No 3 (2000), 35.

25PO-13-58

THERMAL CONDUCTIVITY OF INTERMEDIATE VALENCE COMPOUNDS $\text{Yb}_{1-x}\text{Ce}_x\text{InCu}_4$

Voloshok T.¹, Pryadun V.¹, Vasiliev A.¹ and Mushnikov N.²

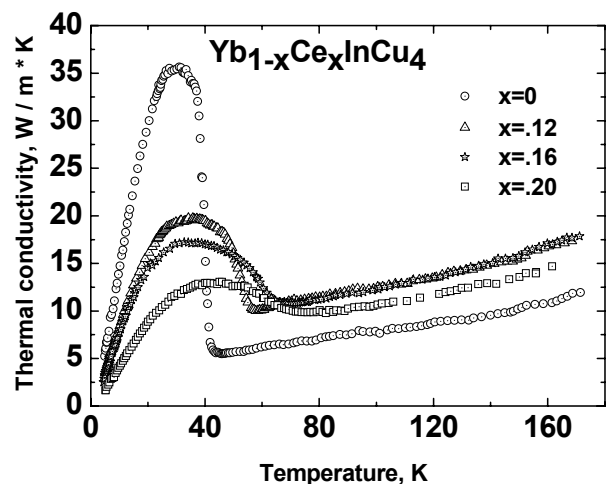
¹Low Temperature Physics Department, Moscow State University,
Moscow 119991, Russia

²Institute of Metal Physics, RAS, Kovalevskaya St. 18, Ekaterinburg 620041, Russia

At $T_V \sim 40$ K, the intermetallic ternary compound YbInCu_4 experiences an isostructural phase transition which is associated with the partial change in the valence state of the Yb ions from $\text{Yb}^{+2.9}$ to $\text{Yb}^{+2.8}$ upon cooling [1]. This change is indicated by sharp anomalies in the thermodynamic and kinetic properties of YbInCu_4 . At T_V , the magnetization drops by an order of magnitude at transformation to low temperature phase. The magnetic susceptibility obeys the Curie - Weiss law above T_V and it is temperature independent below T_V . It was suggested that the phase transition in YbInCu_4 is due to the change in the matrix element of the interaction between the 4f-electrons and the conduction electrons. The substitution of Yb by Ce results in an increase of T_V [2]. It was found that with increasing Ce content the entropy change at phase transition diminishes systematically in $\text{Yb}_{1-x}\text{Ce}_x\text{InCu}_4$ which suggests that the Ce doping affects the valence of the Yb ions [3].

In present work, thermal conductivity in stoichiometric YbInCu_4 and partially Ce-substituted $\text{Yb}_{1-x}\text{Ce}_x\text{InCu}_4$ compounds were studied by the longitudinal steady-state four probe method in wide temperature range. The temperature dependences of thermal conductivity in $\text{Yb}_{1-x}\text{Ce}_x\text{InCu}_4$ are shown in the Figure. At cooling, the thermal conductivity decreases almost linearly, then it grows up T_V and decreases at low temperatures. The anomaly at T_V broadens and diminishes with Ce-content increase. The absolute values of thermal conductivity in the samples studied are significantly higher than the electronic contributions estimated from the

Wiedemann – Franz law. It means that the temperature variation of thermal conductivity is due mostly to phonon contribution. Unusual decrease of thermal conductivity at high temperatures with cooling could be associated with increasing scattering of phonons on Yb ions volume breathing mode. Quantitative analysis of the data presented will be given elsewhere.



[1] J. L. Sarrao, *Physica B* **259-261** (1999) 128 and references therein.

[2] N.V. Mushnikov, T. Goto, A.V. Kolomiets, K. Yoshimura, W. Zhang and H. Kageyama, *J. Phys.: Condens. Matter*, **16** (2004) 2395.

[3] T.N. Voloshok, N.V. Mushnikov, N. Tristan, R. Klingeler, B. Büchner, and A.N. Vasiliev, *Phys. Rev. B*, **76** (2007) 172408.

25PO-13-59

MAGNETIC STRUCTURE AND MAGNETOTRANSPORT PROPERTIES OF THE ORDERED Fe_{100-x}Al_x (25 < x < 35 at. %)

Yelsukov E.P.¹, Voronina E.V.¹, Arzhnikov A.K.¹, Korolyov A.V.², Yelsukova A.E.³, Perov N.S.³,
Granovsky A.B.³, Prudnikov V.N.³

¹Physical-Technical Institute UrB RAS, 132, Kirov Str., 42600 Izhevsk, Russia

²Institute of Metal Physics UrB RAS, 18, S.Kovalevskaya Str., 620041 Ekaterinburg, Russia

³M.V. Lomonosov Moscow State University, Leninskie Gory, 119992 Moscow, Russia

The DO₃ (or B2)-type ordered Fe-Al show unusual behaviour of magnetic properties at x>25 at. %: fast decrease of magnetization at 27<x<35 at. % Al; absence of saturation magnetization up to 50 kOe (in static magnetic field) and up to 150 kOe (pulse magnetic field); anomalous temperature behaviour of magnetization. It was also found in the Fe₇₂Al₂₈ [1] substantial influence of magnetic field (up to 3.5 kOe) on resistance in comparison with that for the disordered ferromagnetic alloys of the same content.

The aim of this work was the study of magnetic structure, its temperature and in-field behaviour, transversal magnetoresistance and anomalous Hall effect in the ordered Fe-Al alloys.

The Fe-Al plates of 10 x 2 x 0.5 mm and powders were used to perform the study. Using various annealing DO₃ -superstructure was obtained in the samples with 26.5 and 30 at. % of Al and B2-superstructure in the samples with 30, 32.6 and 34.1 at. % of Al.

Concerning magnetotransport properties, it has been established:

1) There is no saturation in field dependences of Hall resistance R_H(H) at x > 26.5 at. % and magnetoresistance ΔR/R at x > 25 at. %. The ΔR/R(H) dependences are negative;

2) Concentration dependences of the |ΔR/R|(x) and anomalous Hall constant R_{an}(x) are characterized by maximum at 28-30 at. % Al: |ΔR/R| = 0.8 % (295 K) and 1.6 % (77 K) under H = 16.5 kOe;

3) Absence of a linear dependence R_a versus ρ or ρ² for different x and under H = 16.5 kOe points to the giant character of magnetoresistance.

Magnetotransport properties are explained by the magnetic inhomogeneities on a nanoscale of the ordered Fe-Al alloys with x > 25 at. % Al [2,3] and can be qualitatively understood in the frame of developed theories [4,5]. The magnetic inhomogeneities are due to peculiarities of local Fe magnetic moment dependence on its local atomic surrounding [2,3]. Number of Al atoms determines the sign and magnitude of Fe local magnetic moment.

Support by RFBR (project 06-02-16179).

[1] O. Schneeweiss, T. Zak, M. Vondracek, *JMMM*, **127** (1993) L33.

[2] E.P. Elsukov, E.V. Voronina, A.V. Korolev, A.E. Elsukova, S.K. Godovikov, *Phys. Met. Metallogr.*, **104** (1) (2007) 35

[3] E.V. Voronina, E.P. Elsukov, A.V. Korolev, A.V. Zagainov, A.E. Elsukova, *Phys. Met. Metallogr.*, **104**(4) (2007) 351

[4] Zhang S., Levy P., *J.Appl.Phys.*, **73** (1973) 5312.

[5] A.Granovsky, F.Brouers, A.Kalitsov, M.Chshiev, *JMMM*, **166** (1997) 193.

25PO-13-60

INFLUENCE OF DISSOLUTION OF ALLOYING ELEMENTS IN IRON ON PHYSICAL PROPERTIES OF POWDER MATERIALS OF BINARY SYSTEMS

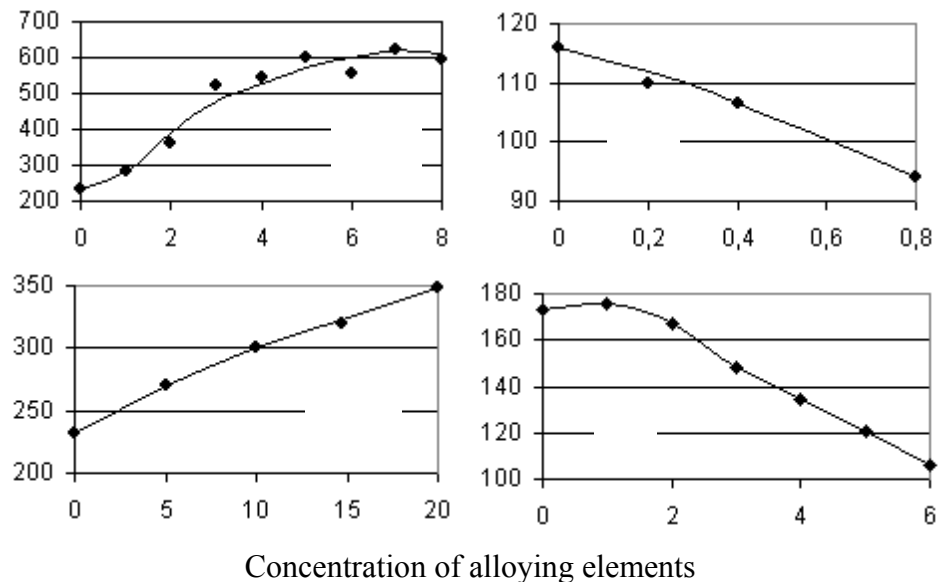
Dorogina G.A.¹, Balakirev V.F.¹, Kuznetsov I.A.²

¹Affiliation nstitut of Metallurgy of Ural Division of Russian Academy of Sciences1, Yekaterinburg, Amundsena st., 1011, Russia1

²Institute of Engineering Science Ural Branch of Russian Academy of Sciences2, Yekaterinburg, Komsomolskaya st., 342, Russia2

When investigated physical properties of powder soft magnets on the basis of iron it was revealed, that in the field of formation of a substitutional solution by alloying elements: metals - Co, Cu and nonmetals - Si, P, coercivity in metal systems increases, and at alloying nonmetals is decreases (fig.).

Silicon, cobalt and phosphorus concern to the elements closing γ -area whereas copper expands area of γ -iron. So area γ , as area α in system iron - copper have the significant breaks in solubility. It is not a ferromagnetic element, has enough the big



Concentration of alloying elements
The increase in H_c for the given system is explained by the theory of strengths.

Cobalt on the contrary is ferromagnetic: the materials in the field of initial dissolution of cobalt before formation of structure Fe_3Co , have the maximal magnetization of saturation. The radius of atom of it is close to the size of atom of iron. Therefore, pressure of a crystal lattice of iron at replacement of atoms of iron by cobalt, should be insignificant.

On the other hand, the nuclear radius of silicon and phosphorus is less in 1,5 - 2 times, than at iron. Besides, both phosphorus and silicon are not ferromagnetics, but coercivity decreases at increase in such soluble elements. The theory of strengths to not explain the received results.

It speaks more trivial reasons: so phosphorus as silicon at heating promote growth of a grain of iron, and also both phosphorus and silicon have refined an effect on a grain of iron, clearing it from carbon or oxygen.

Work is executed at support of the RFBR (grant № 07-03-96093 ural-a).

25PO-13-61

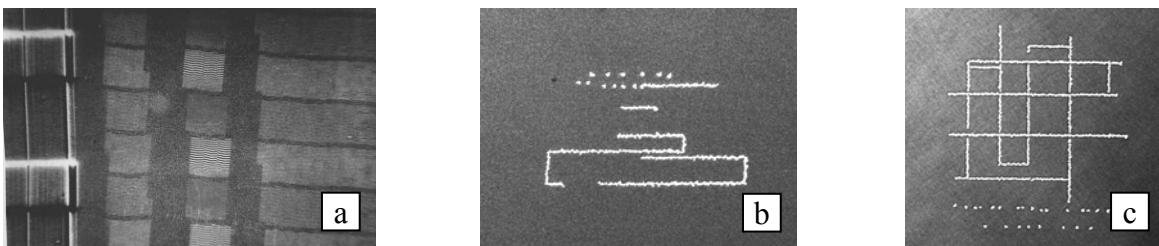
GARNET FILMS FOR THERMO-MAGNETIC RECORDING AND NANOTECHNOLOGY PURPOSES

Berzhansky V.N., Nedviga A.S., Vishnevskii V.G. and Prokopov A.R.
V.I. Vernadsky Taurida National University, Simferopol 95007, Ukraine

It is known that high-coercive garnet films are an optimal media for thermo-magnetic recording by different methods, such as electron or laser beams and by contact printing technique. For example, it was shown by the authors [1] that contact printing magneto-optic (MO) transducers based on the films covered with composite mirror layer can be effectively used in criminalistics (VHS videotape tracks are seen on Fig. a). Recently it has been established that garnet films can appear to be quite promising media for micro-transport or formation of micro-potentials that assist trapping and propagation of neutral atoms. Transparency of garnets in the infrared and visible light and high Faraday effect enable to visualize the routes after thermo-recording, and their magnetic properties ensure the necessary ones of atomic traps. Though the known experiments were successful [2], currently there are some complexities regarding the problem of micro-relief (faceting), since the films are strained and networks of dislocations exist. In this work optimization of properties of MO materials, grown by means of liquid phase epitaxy, for creation of efficient atomic traps and thermo-recording media is provided.

The authors used mono-crystalline gadolinium-gallium garnet (GGG) substrates with (111) crystallographic orientation, positive substrate-film crystalline constants mismatch in a range of 0.04-0.1 Å. As grown films thickness was 4-5 μm and after polishing by abrasives and ion beam 1-3 μm. Saturation magnetization was in a range of 0.7-1.7 kGs. Main compositions of the films were: (Bi, Sm, Lu, Yb, Ca)₃(Fe, Al)₅O₁₂ and (Bi, Sm, Lu)₃(Fe, Al, Sc)₅O₁₂.

The films were characterized by coercivity ~100 Oe, Curie temperature T_C ~200 °C (main difference from contact printing films) and nucleation field more than a half of coercivity value. Period of equilibrium domain structure obtained after heating ($T > T_C$) was 2-4 μm. Specific Faraday rotation was 0.5-1°/μm (633 nm). The films were initially tested in laboratory of Helsinki University of Technology (Finland) [2]. Fig. b and c present 4-5 μm width tracks and dots recorded by focused laser beam (532 nm) according to a standard MO method.



New experiments in the films growth are oriented to provide the atom traps dimensions in sub-micron range. MO, optical, magnetic and morphologic properties of the films are discussed.

Supported by Fundamental Researches State Fund of Ukraine (project F14.1/027).

- [1] V. Vishnevskii, A. Nesteruk, A. Nedviga, S. Dubinko, A. Prokopov, *Sens. Lett.*, **5** (2007) 29.
[2] A. Shevchenko, M. Heilio, T. Lindvall, A. Jaakkola, I. Tittonen, M. Kaivola, *arXiv: Quantum Physics / 0601163* (2006).

25PO-13-62

CALCULATION OF THE TEMPERATURE COEFFICIENT OF INDUCTION Pr-DY-Fe-Co-B MAGNETS BY MOLECULAR FIELD THEORY

Piskorskii V.P., Belousova V.A., Valeev R.A., Chabina E.B., Davidova E.A.
All-Russian Institute of Aviation Materials, 105005, Moscow, Radio, 17, Russia

Alloys Nd-Fe-B have low Curie temperature (T_C) and temperature stability, so their application will be restricted in some cases. Pr-Dy-Fe-Co-B permanent magnets (see the composition in the table) with low temperature coefficients (α) have been studied. The alloys were arc-melted in argon and magnets were prepared by standard powder metallurgy techniques. The temperature coefficients of the samples were measured in open magnet circuit at temperature range 20-100 °C. The observation accuracy was 0,005%/C. The compositions of main tetragonal compounds $(Pr,Dy)_2(Fe,Co)_{14}B$ (phase A) was determined by scanning electron microscope SUPERPROB-733 with energy dispersive x-ray analyzer (EDS) system. We calculated α of phase $(Pr_{1-x}Dy_x)_2(Fe_{1-y}Co_y)_{14}B$ using a three-sublattice molecular field model, which was successfully applied previously to the $(Nd,Dy)_2(Fe,Co)_{14}B$ [1]. Sublattices of Fe and Co were assigned as single F-sublattices. The temperature variation of each moment was described by a Brillouin function:

$$\mu_F(T) = \mu_F(0) B_{J_F} [\mu_F(0) \mu_B H_F(T)/kT],$$

$$\mu_P(T) = \mu_P(0) B_{J_P} [\mu_P(0) \mu_B H_P(T)/kT],$$

$$\mu_D(T) = \mu_D(0) B_{J_D} [\mu_D(0) \mu_B H_D(T)/kT],$$

where $\mu_F(T)$, $\mu_P(T)$, $\mu_D(T)$ - magnetic moment of F, Pr^{3+} , Dy^{3+} ions respectively, $\mu_F(0)$, $\mu_P(0)$, $\mu_D(0)$ - magnetic moment of same ions at $T=0$ K, $H_i(T)$ - molecular fields ($i=F, P, D$). Molecular field coefficient n_{RF} ($R=D, P$) and n_{FF} are determined from:

$$T_C \alpha (T_C \beta - n_{FF}) - n_{RF}^2 = 0,$$

where α, β - coefficients[1] and T_C was taken from literary data in analogy with [1].

The calculated and experimental data are presented in table. The good agreement between the calculated and experimental values of α shows that the three-sublattice molecular field model is fruitful in describing magnets Pr-Dy-Fe-Co-B.

№	Composition of magnets, at. %	α , %/°C (20÷100°C)	
		calculated	experiment
1	$(Pr_{0,49}Dy_{0,51})_{14}(Fe_{0,56}Co_{0,44})_{rem}B_6$	+0,02	+0,02
2	$(Pr_{0,52}Dy_{0,48})_{14}(Fe_{0,59}Co_{0,41})_{rem}B_7$	+0,01	+0,01
3	$(Pr_{0,52}Dy_{0,48})_{14}(Fe_{0,62}Co_{0,38})_{rem}B_7$	+0,01	+0,01
4	$(Pr_{0,40}Dy_{0,60})_{14}(Fe_{0,64}Co_{0,36})_{rem}B_7$	+0,02	+0,03
5	$(Pr_{0,52}Dy_{0,48})_{13}(Fe_{0,65}Co_{0,35})_{rem}B_7$	0,00	0,00
6	$(Pr_{0,50}Dy_{0,50})_{13}(Fe_{0,76}Co_{0,24})_{rem}B_8$	-0,01	-0,01
7	$(Pr_{0,53}Dy_{0,47})_{12}(Fe_{0,77}Co_{0,23})_{rem}B_8$	-0,02	-0,02
8	$(Pr_{0,53}Dy_{0,47})_{15}(Fe_{0,79}Co_{0,21})_{rem}B_{12}$	-0,02	-0,02
9	$(Pr_{0,82}Dy_{0,18})_{12}(Fe_{0,85}Co_{0,15})_{rem}B_8$	-0,08	-0,06

[1] E.N. Kablov, A.F. Petrakov, V.P.Piskorskii and other, *Metallovedenie i termicheskaya obrabotka metallov*, N.4, 2007, C.3-10.

25PO-13-63

MAGNETIC PHASE DIAGRAM AND CHARGE TRANSPORT IN TmB_{12}

*Bogach A.V.¹, Demishev S.V.¹, Flachbart K.², Gabani S.², Glushkov V.V.¹, Levchenko A.V.³,
Shitsevalova N.Yu.³, Sluchanko D.N.¹, Sluchanko N.E.¹*

¹A.M. Prokhorov General Physics Institute of RAS, 38, Vavilov str., Moscow, 119991, Russia

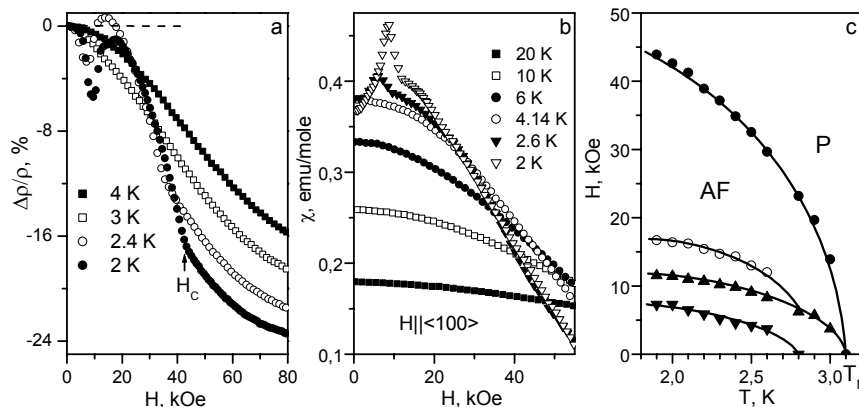
²Center of Low Temperature Physics, IEP SAS, 04001 Košice, Slovakia

³Institute for Problems of Materials Science of NASU, 3, Krzhizhanovsky str.,
Kiev, 03680, Ukraine

In the series of heavy rare earth compounds RB_{12} (R-Tb, Dy, Ho, Er, Tm) with B_{12} clusters thulium dodecaboride is placed just on the boundary of magnetic instability. Indeed, with a filling of the $4f$ shell of rare earth ions along the RB_{12} row the ground state of the dodecaborides changes dramatically between TmB_{12} and YbB_{12} - from antiferromagnetic (AF) metal with small enough Neel temperature ($T_N \sim 3\text{K}$) to paramagnetic insulator YbB_{12} with homogeneous intermediate valence of Yb ion. Moreover, the data of the Hall effect measurements of RB_{12} allowed the authors [1] to conclude in favour of a gradual intensification of spin and charge fluctuations from HoB_{12} to YbB_{12} . As a result, it is natural to expect the magnetic instability effects both to appear in charge carriers scattering and magnetic properties of TmB_{12} .

Thus, the purpose of this study was to investigate in detail the magnetization $M(H, T)$ and magnetoresistance $\Delta\rho/\rho$ of TmB_{12} at helium and intermediate temperatures (1.6-30K). The

measurements were carried out on high quality single crystals of TmB_{12} in magnetic fields up to 80 kOe. The $\Delta\rho/\rho$ experimental results (Fig.a) and magnetic susceptibility dependencies obtained by numerical differentiation of magnetization



$\chi(H, T_0) = dM/dH$ (Fig.b) allowed us to find for the first time some details and reconstruct the magnetic H - T diagram of TmB_{12} (Fig.c).

It was shown that in AF phase of TmB_{12} among a several contributions in $\Delta\rho/\rho$ only small enough (<5%) positive component is observed together with negative ones. As a result, a negative minimum appears on $\Delta\rho/\rho$ curves (Fig.a) and it is accompanied with a small amplitude peak (<25%) on magnetic susceptibility $\chi(H, T_0)$ dependencies at spin-flop transition (Fig.b). The inflection point on $\chi(H, T_0)$ dependence at $H > 20$ kOe (Fig.b) which coincides with a kink on $\Delta\rho/\rho$ curves at H_C (Fig.a) was interpreted in terms of smooth spin-flip transition to the spin polarized paramagnetic state (P) of TmB_{12} . The character of the observed anomalies in combination with a reduced value of the effective magnetic moment $\mu_{\text{eff}} \approx 6.4 \mu_B/\text{Tm}$ detected from Curie-Weiss type behavior of $\chi(T)$ in the interval 3.5-20K are discussed as the arguments in favor of a spin-polaron effect in TmB_{12} .

Support by the RAS Program "Strongly Correlated Electrons" and RFBR is acknowledged.

[1] N.E. Sluchanko et al., phys. stat. sol. (b), **243** (2006) R63.

25PO-13-64

MAGNETIC PROPERTIES AND MAGNITOSTRICTION OF $\text{Fe}_{0.18}\text{Mn}_{0.82}\text{S}$ SINGLE CRYSTAL

Abramova G.^{1,5}, Petrakovskiy G.^{1,5}, Boehm M.², Zuberek R.³, Nabialek A.³, Vorotynov A.¹, Bajukov O.¹, Sokolov V.⁴, Bovina A.¹

¹L.V. Kirensky Institute of Physics SB RAS, Akademgorodok, Krasnoyarsk 660036, Russia

²Institut Laue-Langevin, 6 rue Jules Horowitz, BP 156, 38042 Grenoble, Cedex 9, France

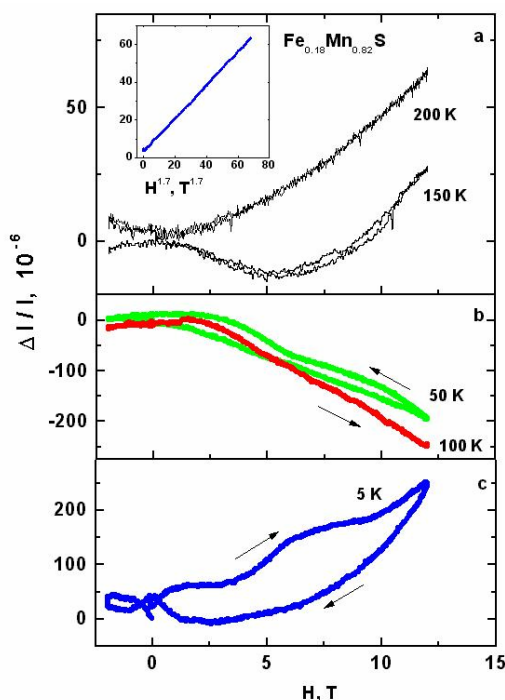
³Institute of Physics, Warszawa, PL-02-668, Poland,

⁴Nikolaev Institute of Inorganic Chemistry SB RAS, Novosibirsk 630090, Russia

⁵Siberia Federal University, Krasnoyarsk 660041, Russia

The interest to manganese-based sulfides with the rock-salt NaCl structure is due to colossal magnetoresistance (CMR) [1] and metal-dielectric transition [2] observed in some $\text{Fe}_x\text{Mn}_{1-x}\text{S}$ compounds and the comparison the mechanism of its magnetic and electrical properties with the classic manganites.

We have synthesized the $\text{Fe}_{0.18}\text{Mn}_{0.82}\text{S}$ single-crystals and investigate the X-ray and magnetic structure by the neutron powder diffraction, the longitudinal magnetostriction $(\Delta l/l)_\parallel$



(at magnetic field up to 12 T), Mossbauer and magnetic spectra. The samples have the fcc NaCl structure at RT. Mossbauer spectra of the $\text{Fe}_x\text{Mn}_{1-x}\text{S}$ single-crystals shown that Fe^{2+} ions are located in the weak distorted octahedron at 300 K. Pure Fe-metal phase is absent with the accuracy better than 1%. Below Neel temperature $\text{Fe}_{0.18}\text{Mn}_{0.82}\text{S}$ ($T=181$ K) has the antiferromagnetic spin-ordered type-II structure (similar to MnS) with the individual atomic moments aligned ferromagnetically in (111) sheets and antiferromagnetically in adjacent sheets. The magnetic transition is accompanied by a weak lattice distortion and jump of the magnetic resonance field. The field dependence of the isothermal magnetostriction for the $\text{Fe}_{0.18}\text{Mn}_{0.82}\text{S}$ single-crystal at selected temperatures is presented in Figure. The magnetostriction value was found of the order of LaMnO_3 one at 200 K and increases up to the colossal value in the magnetoordered state. It can be seen from the Figure the magnetostriction is negative

at temperatures 50-150 K (where the negative magnetoresistance has been found [1]) and it is positive at $T < 50$ K.

We were carried out the present researches due to the partial support of the SB RAS and INTAS funds (N 06-1000013-9002) and Program "Spin-dependent Effects in Solids and Spintronics" of the Division of Physical Sciences of RAS (Project N 2.4.2 SB RAS).

[1] G. A. Petrakovskii, et al. JETP Lett., **72** (2000) 70.

[2] G. M. Abramova, et al. JETP Letters, **86** (2007) 371.

25PO-13-65

SHORT - RANGE ORDER IN AMORPHOUS Fe- B ALLOYS: ¹¹B AND ⁵⁷Fe NMR STUDY

Pokatilov V.S., Pokatilov V.V.

Moscow State Institute of Radioengineering, Electronics and Automation, Moscow, 119454,
pr. Vernadskogo 78, Russia

The determination of the local atomic and magnetic structure of amorphous metal alloys is fundamental in understanding the physical properties of these materials. The radial distribution function obtained from x-ray and neutron scattering provides only the average interatomic distance and coordination number but no detailed information on the probability short-range order (SRO) is obtained. The hyperfine interaction (hyperfine field, isomer shifts and quadrupole splitting) depend sensitively on the nearest neighbor configuration of the atoms. The very local surroundings can be obtained by NMR and Mössbauer methods.

The local atomic and magnetic structure of metallic ferromagnetic amorphous alloys is practically unknown. There are some works (for example, [1,2,3]) where short – range order (SRO) of amorphous Fe-B alloys was studied. It was shown that the local atomic structure of amorphous alloys Fe-(20-25 at.5%B) was defined by the clusters with SRO like tetragonal (t) Fe₃B [1]. The clusters with SRO like orthorhombic (o) Fe₃B could additionally exist when the concentration of B decrease [1, 2]. However some problems of SRO in metallic ferromagnetic amorphous alloys have not been solved yet. These problems in metallic ferromagnetic amorphous alloys Fe –B are: 1) whether the clusters with SRO a – Fe type exist in amorphous Fe-B alloys; 2) how SRO types and their amount dependent on the concentration of B. In this work the near neighbor atomic environments were studied by the ¹¹B and ⁵⁷Fe nuclear magnetic resonance (NMR) in the crystal and amorphous Fe-B alloys in the concentration range Fe – (4 – 25 at. %B). The model samples were combined from the isotopes ¹¹B – ⁵⁶Fe and ¹⁰B – ⁵⁷Fe to separate the NMR signals of ¹¹B and ⁵⁷Fe in the same sample in the frequency range 25 – 50 MHz. Ribbons of these alloys were fabricated by a melt-spinning process. All of the as-quenched samples were controlled by x-ray diffraction at room temperature. X-ray diffraction of the alloys Fe (4 – 12 at. %B) shows that they are crystal and contain the t-, o-Fe₃B and α – Fe lines (a volume of α – Fe phase is more than 94%). NMR study was carried out at 4,2K. The ¹¹B NMR spectra of crystal samples have the peaks at the frequencies 34.5, 36.3 and 41 MHz which are due to the ¹¹B resonance in t-, o-Fe₃B and α – Fe respectively. It was also found the ⁵⁷Fe NMR lines of the Fe sites in the t-, o-Fe₃B and α – Fe phases in the crystal ribbons. When the B concentration increased and the Fe – B alloys transformed into the amorphous state (B > 12 at. %) the resonance positions of the B and Fe peaks did not change but the widths of the resonances increased much. An amount of the clusters with the SRO like t-, o-Fe₃B and α – Fe phases and there dependence from the B concentration was determined in the whole range of amorphous alloys Fe –B. The diagram of the concentration distribution of the various clusters was built. The local structure of the Fe-B amorphous alloys consists of the clusters with the SRO like Fe₃B (t- and o-Fe₃B) in the range 25 – 19 at.% B and of the clusters with the SRO like Fe₃B (t- and o-Fe₃B)and α – Fe phases in the range 18 -12 at% B.

[1] V.S. Pokatilov, *Metallofizika* **5** (1983), 96.

[2] Y. D. Zhang, J.I. Budnick et cet., *J. Appl. Phys.* **61** (1987), 3231.

[3] V.S. Pokatilov et cet., *Hyperfine Interactions*, **59** (1990), 525

25PO-13-66

PECULIARITIES OF HYPERFINE INTERACTION ANISOTROPY OF ^{57}Fe NUCLEI IN $\text{Sc}_{1-x}\text{Zr}_x\text{Fe}_2$ ALLOYS

Rusakov V.S.¹, Pokatilov V.S.², Shkurenko A.V.¹, Pokatilov V.V.²

¹Faculty of Physics M.V. Lomonosov Moscow State University, Leninskie gory, Moscow, 119992, Russia.

²Moscow State Institute of Radioengineering, Automation and Electronics (Technical University), pr. Vernadskogo, 78, Moscow, 119454, Russia.

Search of the experimental methods for extracting of the main contributions in the experimental hyperfine field (HFF) at the nuclei of magnetic atoms is very important for understanding of the local atomic and magnetic states in the various magnetic alloys and compounds. In this work the study of an anisotropy of the ^{57}Fe hyperfine interactions (HFI) has been carried out in the cubic compounds $\text{Sc}_{1-x}\text{Zr}_x\text{Fe}_2$ ($x = 0 - 1$) by the Mössbauer spectroscopy at room temperature and 87 K. Upon using the tensor description of the magnetic HFI the easy magnetization axis and the HFI parameters (the isotropic A_{is} and anisotropic A_{an} HFF (figures 1 and 2), the Mössbauer line shift δ and the quadrupole interaction constant e^2qQ have been determined for each compound.

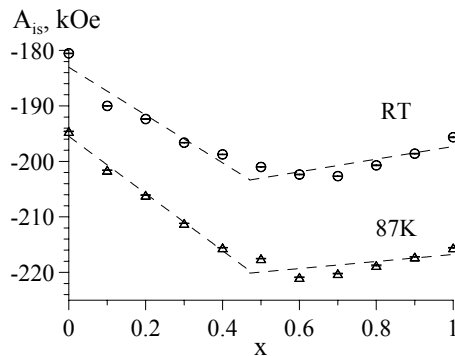


Fig. 1

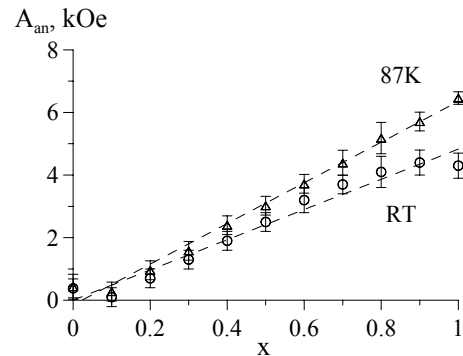


Fig. 2

The alloys were prepared from mixtures of high-purity metals in an argon atmosphere in an arc furnace. The ingots were remelted several times and then annealing at 750C for 50 h. The crystal structure of the alloys was determined by x-ray diffraction. The single alloys were only chosen for measurements. We carried out the investigation selecting samples with the cubic MgCu_2 structure. Chemical analyses showed that the samples had the expected compositions. The saturation magnetization σ was measured at 77 K and room temperature by a vibration magnetometer. The relative error in the determination of σ measured for three and four samples was amounted to 3%.

Our Mössbauer study of the $\text{Sc}_{1-x}\text{Zr}_x\text{Fe}_2$ ($x = 0 - 1$) compounds showed:

- 1) the axis of easy magnetization does not change its direction and the quadrupole constant e^2qQ does not dependent on the Zr content;
- 2) there is an anomaly in the concentration dependence of the Mössbauer line shift δ and the isotropic A_{is} HFF (fig. 1) in the range $x \approx 0.5$;
- 3) the anisotropic A_{an} HFF increases linearly when x increases (fig. 2);
- 4) a correlation between the concentration dependence of the Mössbauer line shift δ and the lattice parameter.

25PO-13-67

FINE DOMAIN WALLS STRUCTURE REVEALED BY MAGNETIC FORCE MICROSCOPY IN SINGLE CRYSTAL FERRITE-GARNET PLATES

Pamyatnykh L.A.¹, Temiryazeva M.P.², Kandaurova G.S.¹

¹Ural State University, 620083, Ekaterinburg, Russia

²Institute of Radioengineering and Electronics RAS, Fryazino, Russia

Results of domain structure (DS) investigation by means of Faraday magneto-optic effect and magnetic force microscopy (MFM) are presented. Sample plates 50mkm thick were cut from ferrite-garnet (TBErGd)₃Fe₅O₁₂ single crystal. Domain structure revealed by means of Faraday effect was typical for cubic crystals [1]. Domain walls looked differently: there was alternation of exact and diffused domain walls.

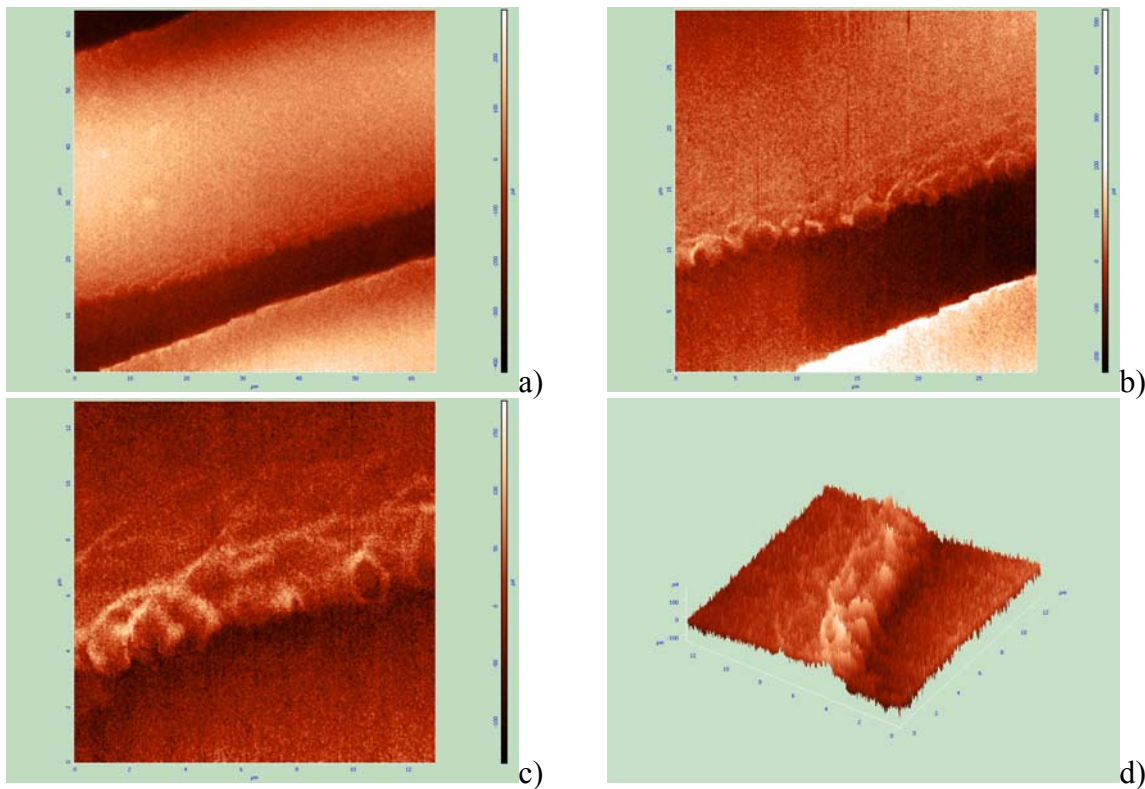


Fig. 1. Magnetic images of the same domain wall, obtained at different resolutions by means of MFM: a – scan size is 65 x 65 mkm, b – 30 x 30 mkm, c – 13 x 13 mkm, d – 3D configuration.

The results of DS observation by means of MFM confirm non-symmetric nature of walls of stripe domains (Fig.1.). Fig. 1 shows that details of fine structure of transitional region between 2 domains are revealed with increase of resolution (Fig. 1a, 1b, 1c.). Diffused domain walls in cubic crystals are excitations of magnetization in the form of “curls”. MFM observations show that the area occupied by these excitations is comparable with the size of the stripe domain.

[1] G.S.Kandaurova, Yu.V. Ivanov, *JETP*, **70**, №2, (1976) 666.

25PO-13-68

MAGNETIC AND MAGNETOSTRICTIVE PROPERTIES OF Tb-Dy-Ho-Fe-Co ALLOYS

*Tereshina I.S.^{1,3}, Nikitin S.A.^{2,3}, Politova G.A.², Opolenko A.A.², Firov A.I.², Burkhanov G.S.^{1,3},
Chistyakov O.D.^{1,3}, Palewski T.³*

¹Baikov Institute of Metallurgy and Material Science RAS, 119991 Moscow, Leninskii pr. 49, Russia

²Faculty of Physics, Lomonosov Moscow State University, Leninskie Gory, Moscow, 119991, Russia

³International Laboratory of High Magnetic Fields and Low Temperatures, 95 Gajowicka str., 53-421 Wroclaw, Poland

The purpose of present work was synthesis of novel magnetostrictive materials $Tb_xDy_yHo_zFe_2$ ($x + y + z = 1$), $Tb_{0.23}Dy_{0.27}Ho_{0.5}Fe_{2-x}Co_x$ and $Tb_{0.37}Dy_{0.5}Ho_{0.13}Fe_{2-x}Co_x$ ($0 \leq x \leq 2$) in high-pure state which possess high values of both: saturation magnetostriction and magnetostrictive susceptibility within the given interval of magnetic fields and temperatures. Complex investigation of the crystal structure, magnetic and magnetostrictive properties, and determination of the main regularities of formation of high magnetostrictive characteristics depending on the composition were done.

Regimes of purification of rare-earth (RE) metals using vacuum sublimation (for Dy and Ho) and distillation (for Tb) have been worked out; certification of the purified metals was performed using laser mass spectrometry. The synthesis of all samples was performed using obtained high-purity rare-earth metals by arc melting in a helium atmosphere. Prepared compounds were certified using metallographic and X-ray fluorescent and X-ray diffraction analyses. A combined analysis of magnetic properties by means of traditional magnetometric methods as well as by ^{57}Fe Mössbauer spectroscopy was also performed. Magnetostriction was measured in magnetic fields of up to 10 kOe and in 80 - 400 K temperature range by means of the strain-gage method.

It was found that the unit cell volume and the value of longitudinal magnetostriction in $Tb_xDy_yHo_zFe_{2-x}Co_x$ decrease monotonously with Co content increase. Concentration dependencies of the magnetostrictive susceptibility $\partial\lambda_{||}/\partial H$, Curie T_C and spin-reorientation transition T_{SR} temperatures, saturation magnetization and a mean value of hyperfine field of Fe atoms demonstrate a non-monotonous behavior. Compounds $Tb_xDy_yHo_zFe_{2-x}Co_x$ with $x = 1.2 - 1.3$ were found to have the maximum value of magnetostrictive susceptibility at room temperature, where the magnetic anisotropy is compensated in both rare-earth and 3d transition metals sublattices.

The work has been supported by RFBR, pr. № 06-03-32850.

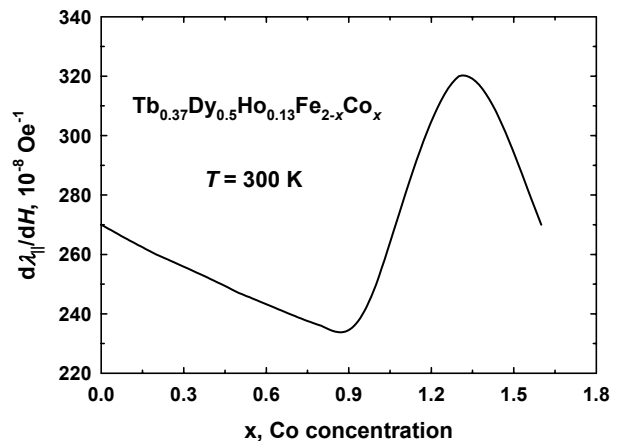


Fig. 1. Concentration dependence of the magnetostrictive susceptibility $\partial\lambda_{||}/\partial H$ for $Tb_{0.37}Dy_{0.5}Ho_{0.13}Fe_{2-x}Co_x$ compounds at $T = 300$ K.

25PO-13-69

DEMAGNETISING FIELD EFFECTS IN HARD MAGNETIC SYSTEMS*Dobrynin A.¹, Barthem V.M.T.S.², Givord D.¹*¹Institut Néel, CNRS/UJF, Grenoble, France²Instituto de Física, Universidade Federal do Rio de Janeiro, Rio de Janeiro, Brazil

It is well known that in ferromagnetic and ferrimagnetic materials, the magnetization variation under an applied magnetic field is affected by the demagnetising field which results from the dipolar interactions existing between the magnetic moments. Although, usual demagnetising field corrections are classically applied in hard magnetic materials (ferrites, Sm-Co, NdFeB, FePt, etc...), a number of experimental results already suggested that these corrections are not directly applicable to these systems. We will show that the demagnetising field slope, higher than in homogeneous ferromagnets, may be simply explained by considering the heterogeneous character of the magnetisation in such systems. Alternative expressions will be proposed to describe the demagnetising field in the various categories of hard materials. These expressions will be shown to be in agreement with numerical modelling. They will be used to describe the experimentally observed magnetisation processes in NdFeB magnets and FePt films

25 June Wednesday

13:30-15:00

poster session

25PO-20

**“Magnetocaloric Effect
and Shape Memory”**

25PO-20-1

EFFECT OF HEAT-TREATMENT ON THE PHASES OF Ni-Mn-Ga MAGNETIC SHAPE MEMORY ALLOYS

Ari-Gur P.¹, Kimmel G.², Richradson J.W.³ [Deceased]

¹Mechanical & Aeronautical Engineering, Western Michigan University, Kalamazoo, MI, USA

²Institute for Applied Research, Ben-Gurion University of the Negev, Beer-Sheva, Israel 84965

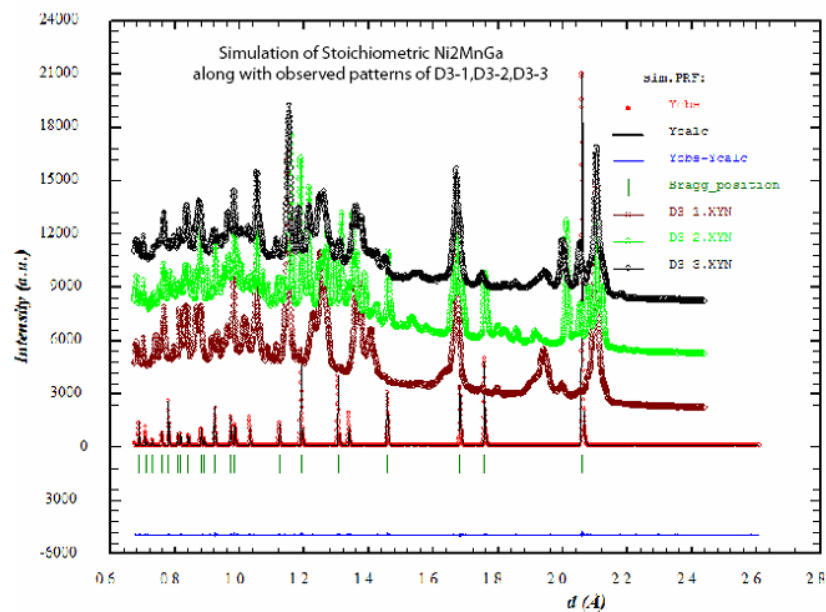
³Intense Pulse Neutron Source, Argonne National Laboratory, Argonne, IL 60439, USA

The Heusler alloys Ni-Mn-Ga display magnetic shape memory effect. The martensitic transformation of stoichiometric Ni₂MnGa is below room temperature [1], and its Curie temperature is 103 °C. Variations from stoichiometry (e.g. Ni_{2-x}Mn_{1+x}Ga or Ni₂Mn_{1+x}Ga_{1-x}) change M_s (saturation magnetization), T_{mart} (martensitic temperature), and T_c (Curie temperature). All are important properties for application at RT and above [2].

The required conditions for a material to demonstrate an isothermal MSM effect are Martensitic structure, a ferromagnetic alloy with high magnetic anisotropy, and twin boundaries (TB) with high mobility [3].

Our studies focused on crystallographic characterization using neutron diffraction of non-stoichiometric Ni-Mn-Ga alloys. Samples of non-stoichiometric Ni-Mn-Ga alloys were cast under protective atmosphere in an arc-melting furnace.

The Figure shows the neutron diffraction results of Ni₅₀Ga₂₆Mn₂₄ at RT. Bottom (1): Simulation of the Heusler diffractogram (cubic); 2: HT @ 900 °C and rapid cooling (mainly martensite). 3: HT @ 900 °C + 700 °C (brief) and rapid cooling; 4: as-cast. Three and four show a mixture of martensite, cubic and extra lines due to segregation of other phases. Hence 900 °C followed by rapid cooling was the best treatment.



[1] Webster, P.J., Ziebeck, K.R.A., Town, S.L., and Peak, M.S., "Magnetic order and phase transformation in Ni₂MnGa", *Philosophical Magazine B (Physics of Condensed Matter, Electronic, Optical and Magnetic Properties)*, 49(1984), pp. 295-310.

[2] Murray, S.J.; Farinelli, M.; Kantner, C.; Huang, J.K.; Allen, S.M.; O'Handley, R.C., "Field-induced strain under load in Ni-Mn-Ga magnetic shape memory materials", *J. Appl. Phys.* 83 (1998), pp.7297-9

[3] Ullakko, K.; Magnetically controlled shape memory alloys: a new class of actuator materials. *J. Mater. Eng. Perform.*, 1996, vol. 5, pp. 405-409.

25PO-20-2

IMPLEMENTATION OF THE MAGNETOCALORIC MATERIALS IN THE FORM OF THE MAGNETIC GLASS COATED MICROWIRES – FEASIBILITY AND NEW OPPORTUNITIES.

Ilyn M., Zhukov A., Zhukova V., Gonzalez J.

Dpto. Física de Materiales, Fac. Químicas, Universidad del País Vasco, 20018 Paseo Manuel de Lardizabal 3, San Sebastian, Spain.

Utilization of the magnetocaloric effect (MCE) for conversion of the work into the heat opens up a way to replace conventional gas-machines by new devices more environmental friendly and having better performance. Magnetocaloric materials displaying the large MCE on the moderate field change are necessary to implement this novel technology.

Since the magnetocaloric effect concerned with the variation of the entropy of the magnetic substance on the field change few different phenomena contributes to its total value. Usually the term originated from the rise of the magnetization saturation with the growth of the magnetic field is responsible to the MCE. It depends on the temperature derivative dI/dT and on the magnitude of the field change. In the so-called giant magnetocaloric materials the large values of the MCE concerned with the release of the latent heat due to the field induced first order phase transitions. In the anisotropic materials term proportional to the temperature derivative of the anisotropy constant dK/dT gives rise to the MCE due to declination of the magnetic moment off the easy magnetization direction.

Magnetic glass coated microwire is a composite material consisted of metallic core enclosed by glass layer. Taylor-Ulitovsky technique allows producing a continuous wire of kilometer length range having an amorphous, nanocrystalline or crystalline metallic thread of various chemical compositions. An intrinsic property of the glass-coated microwires is a large internal stress up to a few GPa, originated from the quenching of the molten alloy and from the difference in the thermal expansion of the metal and glass. This high tension gives rise to the magnetoelastic anisotropy usually exceeding the value of the magnetocrystalline one and have an influence on the saturation magnetization. Variation of the metallic core radius /glass shell width ratio and thermal treatment allows changing of the internal stress and therefore tailoring of the magnetic properties.

The paper is intended to unveil the potential of glass coated magnetic microwire as a magnetocaloric material. Calculation of the rate of heat exchange for different width of glass layer is presented. New opportunities of tuning the magnetocaloric properties of materials concerned with utilization of the glass coated magnetic microwires are discussed.

25PO-20-3

TEMPERATURE DEPENDENCE OF $\text{Ni}_{2.08}\text{Mn}_{0.96}\text{Ga}_{0.96}$ ALLOY MAGNETIZATION IN MAGNETIC FIELDS OF VARIOUS INTENSITIES

Mulyukov Kh. Ya.¹, Musabirov I.I.¹, Shavrov V.G.², Koledov V.V.²

¹Institute for Metals Superplasticity Problems of the Russian Academy of Sciences, Khaturin str.
39, Ufa, 450001, Russia

²Institute of Radio-engineering and Electronics of the Russian Academy of Sciences,
Mokhovaya 11-7, Moscow, 125009, Russia

The interest of researchers to Ni-Mn-Ga base Heusler alloys has been due to the martensite phase transformation that occurs in them at about room temperatures. Both high temperature and low temperature phases of these alloys are ferromagnetic. One more peculiarity of these alloys is that its low temperature phase experiences twinning. The fact that both phases are ferromagnetic leads to the possibility of the magnetic external field influence on the twin structure formation during phase transformation. Such influence may result in the change of the character of temperature dependence of magnetization during measurements in magnetic fields of various intensities.

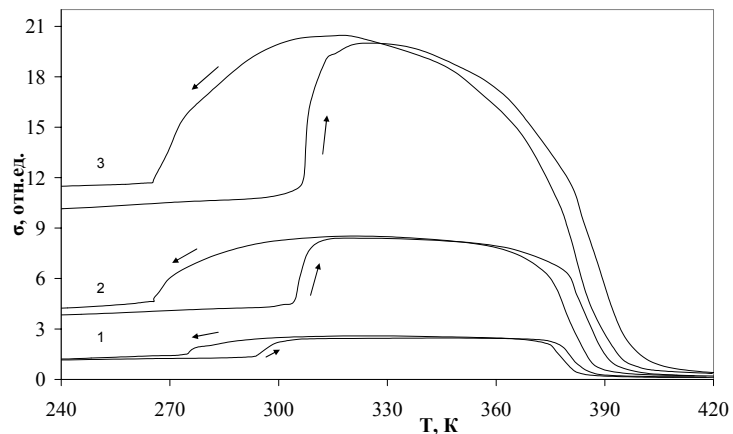
The results of the investigations relating to the magnetization temperature dependence ($\sigma(T)$) of the $\text{Ni}_{2.08}\text{Mn}_{0.96}\text{Ga}_{0.96}$ alloy in magnetic fields of various intensities are reported in this paper. The Figure shows the curves of magnetization temperature dependence recorded during heating and cooling of a specimen within the temperature range from 210 to 390 K. Curve 1 was recorded when the specimen was in the magnetic field of 80 kA/m intensity, while curve 2 – at 128 kA/m and curve 3 – at 240 kA/m.

The character of magnetization temperature dependencies of all three curves has some distinctions.

First, the temperatures A_s and M_f on the second and third curves have 8 K delay as compared with the first curve. Second, the Curie point in the first case is equal to 375 K,

while in the second and third cases it is higher by 5 K and 10 K, respectively. Third, the magnetization values of low temperature phases in the first case is by a factor of 1.5, and in the second and third cases – by a factor of 2 lower than their values in the high temperature phase. And, finally, fourthly, the important point is that in the second and third cycles after specimen's cooling the value of low temperature magnetization is 12% higher than its value before heating.

The differences of low temperature magnetization values before and after heating can be explained by the following. Magnetic moment vectors of domains in twins form a zigzag orientation therefore the value of specimen's magnetization will be lower in the high temperature phase. When the specimen is cooled in a magnetic field, the field, due to magnetic crystalline anisotropy, prevents twinning. Weak magnetic field cannot prevent twinning. In a stronger field the formation of twin structure of some orientations becomes disadvantageous. And the projection of magnetic moment vectors onto external field direction will increase that will result in the difference of magnetization values before and after cooling.



The Russian Foundation for Basic Research sponsored this research under grant RFFI # 06-02-16984.

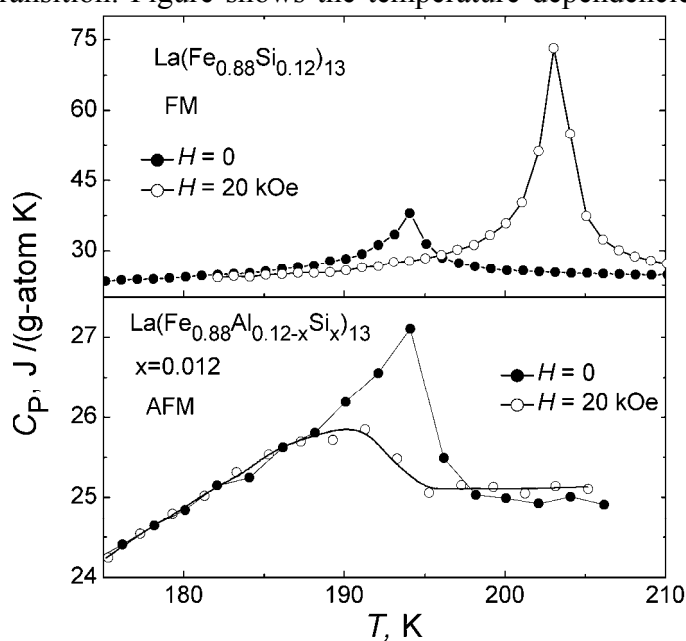
25PO-20-4

HEAT CAPACITY AND THE ENTROPY FOR $\text{La}(\text{Fe}_{0.88}\text{Al}_{0.12-x}\text{Si}_x)_{13}$ FERROMAGNETIC ($x=0.12$) AND ANTIFERROMAGNETIC ($x=0.012$) COMPOUNDS IN VARIOUS MAGNETIC FIELDS

Podgornykh S.M.

Institute of Metal Physics, Ural Division of the Russian Academy of Sciences,
S.Kovalevskya st., 18, 620041, Ekaterinburg, Russia

Recently it was found that for the $\text{La}(\text{Fe}_{0.88}\text{Si}_{0.12})_{13}$ ferromagnetic (FM) compound with the Curie temperature $T_C=194$ K the magnetic heat capacity increased significantly in an external magnetic fields within the technical magnetization range [1]. We feel that the change of the elastic and magnetoelastic energies gives rise to this increase of the heat capacity owing to the spontaneous magnetostriction. To obtain the data for the antiferromagnetic (AFM) we study the $\text{La}(\text{Fe}_{0.88}\text{Al}_{0.108}\text{Si}_{0.012})_{13}$ compound with the Neel temperature $T_N=194$ K and $T_N=T_C$. Magnetic phase diagram of the $\text{La}(\text{Fe}_{0.88}\text{Al}_{0.12-x}\text{Si}_x)_{13}$ compounds was investigated earlier [2]. Now it is found that for the AFM compound the magnetic heat capacity decreases and may completely vanish in an external magnetic field which exceeds the critical field of the metamagnetic transition. Figure shows the temperature dependencies of the heat capacity C_P in zero external magnetic field and in nonzero external magnetic field $H=20$ kOe for the FM and for the AFM compounds. The magnetic field less than 10 kOe has not an influence on the temperature dependence of the magnetic heat capacity of the AFM. Beginning with $H>10$ kOe the metamagnetic phase transition takes place and the magnetic heat capacity decreases. The temperature dependences of the additional entropy are calculated from the data for various external magnetic fields. We believe that the magnetoelastic and magnetovolume parts of the total energy play the essential role in the change of the entropy. Moreover the elastic and magnetostatic parts of the energy give



quite noticeable contributions to the entropy. The external magnetic field of several tens kilooersted is significantly lower than the molecular field of the AFM with the T_N or the FM with T_C about 200 K. With this in mind one may suggest that the observed the excess heat capacity is not associated with the magnetic degrees of freedom. The excess heat capacity reflects the change of the potential energy of the elastic, magnetoelastic and magnetostatic interaction and the magnetic heat capacity originates from the work of the deformation of the specimen.

[1] S.M. Podgornykh, Ye.V. Shcherbakova, *Phys.Rev.* **B 73** (2006) 184421.

[2] S.M. Podgornykh, Ye.V. Shcherbakova, G.M. Makarova, A.A. Yermakov, *EastMag-2007, Abstract book, Kazan 23-26 August, (2007)* 166.

25PO-20-5

MONTE CARLO SIMULATION OF ANTIFERROMAGNETIC CLUSTERS IN Ni-Mn-X (X=In, Sn, Sb) HEUSLER ALLOYS

Taskaev S.V.¹, Buchelnikov V.D.¹, Sokolovsky V.V.¹, and Entel P.²

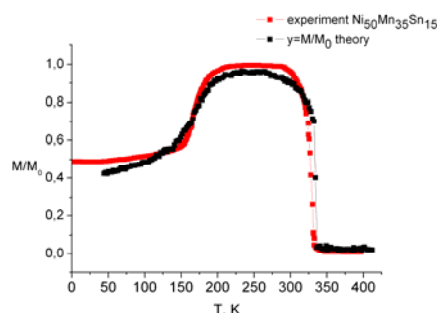
¹Chelyabinsk State University, 454021 Chelyabinsk, Br.Kahirinikh str. 129, Russia

²University of Duisburg-Essen, 47048 Duisburg, Lotharstr. 1, Campus, Germany

From both application and scientific point of view, the ferromagnetic Heusler alloys Ni-Mn-X (X=In, Ga, Sn, Sb) are of great interest due to the shape memory effect resulting from the martensitic transformation. But this is not the only one fundamental effect which is observed in these materials. In some compositions of that alloys the gigantic magnetocaloric effect (comparable with the best magnetocaloric materials, such as Gd-Si-Ge, La-Fe-Si, Mn-As) are observed. The reason of large value of ΔT during the magnetization in the external magnetic field is the coupled magnetostructural phase transition.

The whole lattice of alloy can be representing as two interacting parts – magnetic and structural subsystems. The structural subsystem is described by degenerated Blume-Emery-Griffiths model [1] (DBEG) and the magnetic subsystem is described by “ q -state” Potts model [2]. We consider three dimensional model with 5 spin projections on z axis due to the fact that in Ni-Mn-Ga alloys Mn^{3+} ions have magnetic spin moment $S = 4/2$ and therefore 5 possible spin projections. As far as we know magnetic moment of Ni is much less then magnetic moment of Mn, thus in our investigation we neglect the interaction between them.

For the numerical simulation we used the cubic square lattice with periodic boundary conditions and 6 near-neighbors in each site. The number of sites in lattice was equal to $N=15^3$. The configuration of the antiferromagnetic clusters was random and the clusters concentration was determined from the experimental composition of the Ni-Mn-X (X=In, Sn, Sb) alloys. As the time unit we used one Monte Carlo step, which is consisting in N attempts of change structural σ_i (in our model we have three structural states: +1, -1 and 0) and spin S_i variables. The number of Monte Carlo steps on each site varies from 10^5 to 10^6 . The Monte Carlo simulation starts from ferromagnetic martensite phase with ($\sigma_i=1$ and $S_i=1$). The physical quantities have been averaged over 400 configurations taken every 100 Monte Carlo steps and discarding the first 10^4 Monte Carlo steps for equilibration.



For example, in figure the results of numerical simulations of magnetization are presented (experimental data from [3]). As it seen there are two jumps of magnetization: first jump is connected with the coupled magnetic and structural phase transition from the mixed antiferromagnetic-ferromagnetic martensitic states to the ferromagnetic austenitic state. This transition is accompanied with the jump of strain order parameter and inversion of the sign of exchange interaction. The second jump of magnetization curve is connected with the Curie point.

Support by RFBR 06-02-16266, 07-02-96029-r-ural, 06-02-39030-NNSF, 07-02-13629-OFI_ts, Human Capital is acknowledged.

[1] T. Castán, E. Vives, and P.A. Lindgård. *Phys. Rev. B* **60** (1999) 7071.

[2] F.Y. Wu. *Rev.Mod.Phys.*, **54** (1982) 235.

[3] M.Khan et al. *JAP* **102** (2007) 113914.

25PO-20-6

DIRECT MEASUREMENTS OF ADIABATIC TEMPERATURE CHANGE IN $\text{Ni}_2\text{Mn}_{0.75}\text{Cu}_{0.25}\text{Ga}$ HEUSLER ALLOY

*Khovaylo V.¹, Koledov V.¹, Shavrov V.¹, Karpenkov D.², Koshkid'ko Yu.², Skokov K.², Khan M.³,
Dubenko I.³, Stadler S.³, Ali N.³*

¹Institute of Radioengineering and Electronics, Moscow 125009, Russia

²Physics Faculty, Tver State University, Tver 170000, Russia

³Department of Physics, Southern Illinois University, Illinois 62901, USA

Study of magnetocaloric effect in magnetically ordered substances have attracted growing attention during last years to its potential applicability in room-temperature magnetic refrigeration technology [1]. It has been noticed that materials undergoing a first order magnetic phase transition display, as a rule, giant magnetic entropy change ΔS_m .

Some of Ni-Mn-Ga Heusler alloys undergo a magnetostructural phase transition ferromagnetic martensite \leftrightarrow paramagnetic austenite [2]. Recently, it was shown that partial substitution of Mn for Cu in the stoichiometric Ni_2MnGa decreases Curie temperature T_C and increases martensitic transition temperature T_m thus that they merge in a $\text{Ni}_2\text{Mn}_{0.75}\text{Cu}_{0.25}\text{Ga}$ composition [3]. Studies of magnetocaloric properties of this compound revealed a very large magnetic entropy change ΔS_m at a temperature of the magnetostructural phase transition, reaching - 64 J/kgK in the magnetic field change $\Delta H = 5$ T. Motivated by this results we undertook measurements of the adiabatic temperature change ΔT_{ad} in the $\text{Ni}_2\text{Mn}_{0.75}\text{Cu}_{0.25}\text{Ga}$ alloy.

The adiabatic temperature change was measured, both upon heating and cooling, by a direct method describer in [1]. Contrary to the magnetic entropy change ΔS_m , the adiabatic temperature change in the alloy studied is rather small and in the phase transition region it has a maximal value of about ≈ 0.8 K in the magnetic field change $\Delta H \approx 1.8$ T. We suggest that the small value of ΔT_{ad} can be explained if virtual Curie temperature of the low-temperature martensitic phase is considerably higher than the temperature at which transformation from ferromagnetic martensite to paramagnetic austenite is observed. In this case the magnetic field will have a weak influence on the alignment of the magnetic moments, in contrast with that observed near a second order magnetic phase transition temperature. Other factor which affects values of the directly measured ΔT_{ad} is that in the transition region the $\text{Ni}_2\text{Mn}_{0.75}\text{Cu}_{0.25}\text{Ga}$ alloy is structurally and magnetically inhomogeneous consisting of ferromagnetic low-temperature phase and paramagnetic high-temperature phase. If exchange integral of the high-temperature phase is well below this region, a fraction of the paramagnetic phase will not contribute to ΔT_{ad} and will act as a parasitic load.

This work was partially supported by RFBR (grants Nos. 06-02-16266, 06-02-39030 and 07-02-13629) and by the Office of Basic Energy Sciences, Material Sciences Division of the U.S. Department of Energy (contract No. DE-FG02-06ER46291).

[1] A.M. Tishin and Y.I. Spichkin, *The Magnetocaloric Effect and its Applications* (Institute of Physics Publishing, Bristol, 2003).

[2] A.N. Vasil'ev, V.D. Buchelnikov, T. Takagi, V.V. Khovailo, and E.I. Estrin, *Phys. Usp.*, **46** (2003) 559.

[3] S. Stadler, M. Khan, J. Mitchell, N. Ali, A.M. Gomes, I. Dubenko, A.Y. Takeuchi, and A.P. Guimarres, *Appl. Phys. Lett.*, **88** (2006) 192511.

25PO-20-7

MAGNETOCALORIC EFFECT, MAGNETIC DOMAIN STRUCTURE AND SPIN-REORIENTATION TRANSITIONS IN HoCo_5 SINGLE CRYSTALS

Skokov K.P.¹, Pastushenkov Yu.G.¹, Koshkid'ko Yu.S.¹, Albrecht J.², Goll D.², Ivanova T.I.³, Nikitin S.A.³, Semenova E.M.¹, Petrenko A.V.¹

¹Tver State University, 170100 Zheliabova Str. 33, Tver, Russia

²Max Planck Institut fur Metallforschung, Heisenbergstrasse 3, 70569 Stuttgart, Germany

³Moscow State University, 119992 Leninskie Gory 1, Moscow, Russia

It was shown previously that the competition of RE and 3d contributions to total anisotropy of HoCo_5 compound leads to one or two spin-reorientation transitions (SRT) [1-2]. In this work magnetic domain structure (DS) and magnetocaloric effect (MCE) investigations were used to make the picture of SRT in this compound clear. Magnetic domain structure (DS) on (100)-, (110)-, (001)- and arbitrary oriented planes of HoCo_5 single crystals was investigated in zero magnetic field and in magnetic field up to 0,2 T in the temperature region from RT to 4,2 K. Fig.1-2 show magnetic domain structure on the basal plane of HoCo_5 single crystal in zero magnetic field at different temperatures.

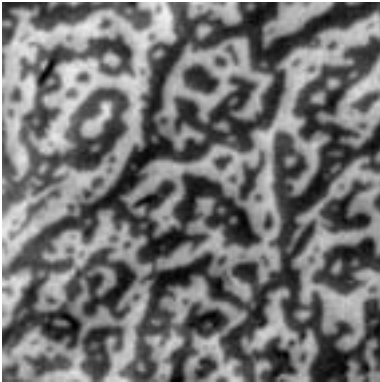


Fig.1. T=100 K

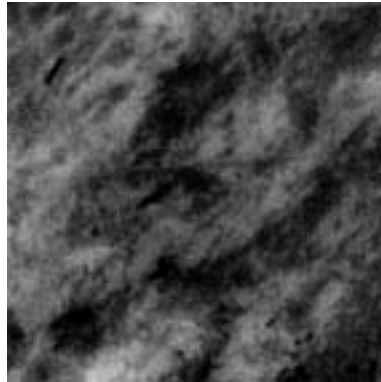


Fig.2. T=20 K

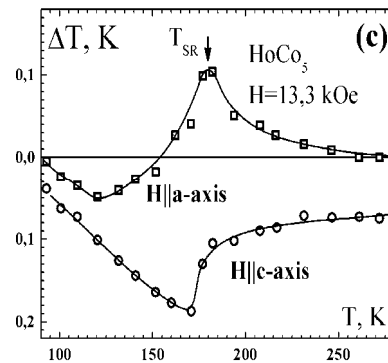


Fig.3.

From fig.1-2 it follows that in zero magnetic field this compound has two SRTs. At RT anisotropy type is “easy axis” with easy [0001]-direction. Fig.1 corresponds to the conical phase and fig.2 corresponds to the planar phase. A continuous deviation of the easy axis from the [001] direction starts at $T_{SR2} \approx 180$ K which constitutes a second-order spin reorientation transition. The second transition occurs at $T_{SR1} = 50$ K and is of the first order. It means that the angle θ between the easy axis and [001] undergoes discontinuous change to 90° . Observation of DS temperature transformation in the magnetic field 0,2 T showed, that magnetic field can change character of spin reorientation in HoCo_5 single crystal.

Magnetocaloric effect (MCE) in HoCo_5 single crystal was measured directly as adiabatic temperature change ΔT . Fig. 3 shows the measured MCE in the magnetic field applied along a-axis and c-axis of HoCo_5 single crystal in the SRT2 temperature region. As it is seen from fig.3, MCE is maximal at $T = T_{SRT2}$ and has different signs for these two directions.

The role of magnetic field and multidomain state in spin reorientation transitions in RCO_5 intermetallic compounds is discussed.

The work was supported by grant RNP.2.1.1.3674.

[1] V.V. Chuev, V.V. Kelarev, S.K. Sidorov et al., Solid State Phys., 23 (1981) 1760.

[2] Zhao Tie-song, Jin Han-min et al., Phys. Rev. B., 43 (1991) 8593.

25PO-20-8

MONTE-CARLO CALCULATIONS OF THE MAGNETOCALORIC EFFECT IN Ni-Mn-Ga ALLOYS

Sokolovsky V., Buchelnikov V., Taskaev S.

Chelyabinsk State University, Br. Kashirinykh Str. 129, 454021 Chelyabinsk, Russia

At present the problem of the research of phase's transformation and the magnetocaloric effect (MCE) in ferromagnetic alloys is topical and actual. The MCE is of some interest both from the point view of fundamental researches and practical application, because materials with a large value of the MCE in relatively low magnetic fields can be used as refrigerants in the technology of the magnetic cooling. Recent researches have shown that ferromagnetic shape memory Heusler alloys such as Ni-Mn-X (such X=Ga, In, Sn, Sb) also seem to be promising materials for investigation and probably application of the MCE in household refrigerators. In non-stoichiometric $\text{Ni}_{2+x}\text{Mn}_{1-x}\text{Ga}$ alloys with x concentrations from 0.18 to 0.27 the coupled magneto-structural first-order phase transition is experimentally observed [1]. In this case the gigantic MCE takes place.

In this the work we use the classical Monte-Carlo method to modeling the coupled first-order magneto-structural phase transformation from the cubic (austenitic) paramagnetic state to the tetragonal (martensitic) ferromagnetic state and the isothermal magnetic entropy change in Heusler alloys $\text{Ni}_{2+x}\text{Mn}_{1-x}\text{Ga}$ (such $x=0.18, 0.20, 0.22, 0.24, 0.27$). In the proposed model whole a three-dimensional cubic lattice included the coupling between the magnetic and structural subsystems. The magnetic subsystem is described by "q-state" Potts model [2]. Here, q is a number of states of spin projections on z axis. Since in Ni-Mn-Ga alloys Mn^{3+} ions have the magnetic spin moment $S=4/2$, therefore 5 possible spin projections on z axis and in our model we consider q equal 5. As far as we know the magnetic moment of Ni ion is much more less then the magnetic moment of Mn ion, thus in our investigation we will neglect the interaction between them. The structural subsystem is described by the degenerated three state Blume-Emery-Griffiths model for martensitic transformations [2]. In the case of martensitic phase transformation the low-temperature martensite phase has a few low-temperature variants or degenerated phases. These variants are described by the lattice distortions (compression or expansion) during phase transitions along x, y and z axes. Therefore it is possible to obtain only six structural variants. At high temperatures the austenite phase with zero distortions along x, y and z axes appears. In the proposed model there are two variants of martensite and the cubic phase will be two times degenerated.

By the help of the theoretical model the temperature dependences of the strain and the magnetic order parameters, susceptibilities associated with fluctuations of the order parameters, the magnetic heat capacity, the internal energy, the magnetic entropy and the magnetic entropy change for the magnetic field variation from 0 to 5 T are obtained. All calculated quantities are in good agreement with the available experimental data [1].

Support by grants RFBR 06-02-16266, 07-02-96029-r-ural, 06-02-39030-NNSF, 07-02-13629-OFI_ts, RF President MK-5658.2006.2, Human Capital is acknowledged.

[1] V.V. Khovailo et al., *2st Int. Conf. on Magnetic Refrigeration at Room Temperature, Portoroz, Slovenia* Apr. 11-13 (2007) 217.

[2] F.Y. Wu, *Reviews of Modern Physics.*, 54 (1982) 235.

[3] T. Castan et al., *Phys. Rev. B.*, 60 (1999) 7071.

25PO-20-9

THERMAL, MAGNETIC AND KINETIC PROPERTIES OF Ni-Mn-Cu-Ga AND Ni-Fe-Ga HEUSLER ALLOYS

Aliev A.M.¹, Batdalov A.B.¹, Khanov L.N.¹, Gamzatov A.G.¹, Buchelnikov V.D.², Taskaev A.S.²,
Bychkov I.V.², Mikhailov G.G.³, D'yachuk V.V.³, Khovailo V.V.⁴, Koledov V.V.⁴, Shavrov V.G.⁴

¹Institute of Physics of Dagestan SC of RAS, Makhachkala, Russia, E-mail: lowtemp@mail.ru

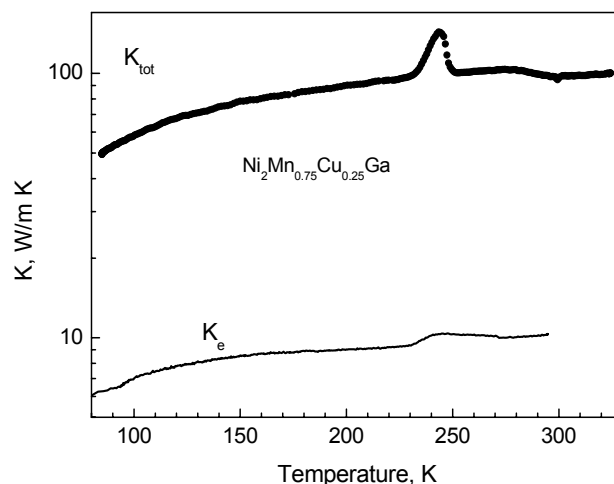
²Chelyabinsk State University, 545021 Chelyabinsk, Russia

³South Ural State University, Chelyabinsk 454080, Russia

⁴Institute of Radioengineering and Electronics of RAS, 125009 Moscow

(Ni-Mn-X (X = In, Sn, Sb) alloys attract attention on account of the effect of giant deformations in external magnetic field (largest of ever observed in solid state physics) and giant magnetocaloric effect (MCE), i.e. the entropy change with magnetic field (highest observed in ferromagnets). This is conditioned by the fact that in Ni-Mn-X two phase transitions may occur together at constant temperature under the action of magnetic field - martensite (structural) transition and transition to the ferromagnetic state. This type of the single transition of the first kind is usually referred as *magnetostructural* one. The giant MCE observed during the magnetostructural transition in Ni-Mn-X as well as in some other ferromagnets, e.g. Gd(GeSi), (MnFe)(AsTe), is regarded promising for the development of economical and ecologically safe solid state coolers working in the region near room temperature.

We present the measurements of specific heat, magnetocaloric effect, as well as thermal conductivity, thermal diffusivity and electrical resistivity of the Ni-Mn-Cu-Ga and Ni-Fe-Ga Heusler alloys from 80 to 380 K and magnetic fields up to 26 kOe. Pronounced anomalous features and significant thermal hysteresis were observed in all measured physical properties near the magnetic and structural martensitic phase transitions. Most attention was paid to the thermal conductivity behavior in the vicinity of phase transitions. Huge peaks were observed in the thermal conductivity near magnetostructural transitions. Y.K. Kuo et al. [1] attribute the giant thermal conductivity peak to the softening of phonon modes that result to the considerable increasing of the heat carried by the soft phonons. Hence, both specific heat and thermal conductivity features around the Peierls like transition could be qualitatively understood in terms of this picture. But our results show that near magnetostructural transitions a considerable peak of thermal diffusivity also is observed. This point out that not only specific heat anomaly is responsible for the thermal conductivity peak, but also a change of mean free path of phonon or (and) sound velocity. Ultrasound measurements are advisable to perform for fundamental understanding of peculiarities of transport properties of Heusler alloys.



This work is supported by Physics Branch of RAS.

[1] Y.K. Kuo, K.M. Sivakumar, and H.C. Chen. Phys. Rev. B 72, 054116 (2005).

25PO-20-10

INFLUENCE OF MAGNETIC FIELD ON PHASE TRANSITIONS IN Ni-Mn-X (X = In, Sn, Sb) HEUSLER ALLOYS

Zagrebin M.A.¹, Buchelnikov V.D.¹, Taskaev S.V.¹, Entel P.²

¹Chelyabinsk State University, Br. Kashirinykh Str. 129, 454021 Chelyabinsk, Russia

²University of Duisburg-Essen, Lotharstr. 1, Campus 47048 Duisburg, Germany

In the Heusler alloys Ni-Mn-X (X=In, Sn, Sb)) the next sequence of phase transitions occurs: paramagnetic (PM) cubic (PC) phase → ferromagnetic (FM) cubic (FC) one → PM tetragonal one → FM tetragonal one [1] or PC phase → FC one → antiferromagnetic (AFM) tetragonal one [2, 3]. Such magnetic behaviors can be explained by the existence in these alloys the inversion of exchange interaction [4]. Experiments shows that in Ni-Mn-X alloys the external magnetic field considerably influence on the magnetization dependence and the shift of magnetostructural phase transition from FM state to AFM one [2]. In this work with the help of Ginzburg-Landau theory the phase transitions in Heusler alloys with inversion of exchange interaction in external magnetic field are theoretically investigated. We used the expression for the Ginzburg-Landau functional [4, 5]

$$F = \alpha m^2 / 2 + \beta m^2 \cos(\varphi) / 2 - \gamma m^4 \cos(\varphi) / 4 + \delta_1 m^4 \cos^2(\varphi) / 4 + \delta_2 m^4 / 4 - \omega_1 m^2 (e_2^2 + e_3^2) - \omega_2 m^2 (e_2^2 + e_3^2) \cos(\varphi) / 2 - 2mM_0H \cos(\varphi / 2) + a(e_2^2 + e_3^2) / 2 + be_3(e_3^2 - 3e_2^2) / 3 + c(e_2^2 + e_3^2)^2 / 4$$

where m is the normalized magnetization; φ is the angle between the magnetizations of two FM sublattices; $e_{2,3}$ are the linear combinations of the strain tensor; $\alpha, \beta, \gamma, \delta_1, \delta_2$ are the exchange parameters; M_0 is the saturation magnetization, H is the magnetic field; ω_1, ω_2 are the magnetoelastic constants; a, b, c are the linear combinations of the elastic moduli. After minimization energy with respect to $m, \varphi, e_{2,3}$ we constructed the phase diagrams. It is shown that at certain values of parameters we obtain on the phase diagram paths which can explain experimentally observed sequences of phase transitions, the temperature dependence of magnetization and the shift of martensitic transition in the magnetic field [1-3]

Work was supported by grants RFBR 06-02-16266, 07-02-96029-r-ural, 06-02-39030-NNSF, 07-02-13629-OFI_ts, RF President MK-5658.2006.2, Human Capital and Dynasty foundations.

[1] T. Krenke et al., *Phys. Rev. B* **72** (2005) 014412.

[2] R. Kainuma et al., *Nature* **439** (2006) 957.

[3] K. Oikava et al. *Appl. Phys. Lett.*, **88** (2006) 122507.

[4] C. Kittel, *Phys. Rev.* **120** (1960) 335.

[5] V.D. Buchelnikov et al. *JETP Lett.* **85** (2007) 560.

25PO-20-11

MAGNETOCALORIC EFFECT IN $Tm_{1-x}Tb_xCo_2$ COMPOUNDS

Proshkin A.V.^{1,2}, Baranov N.V.^{1,2}, Podlesnyak A.³

¹Institute of Metal Physics RAS, 620219 Ekaterinburg, Russia

²Ural State University, 620083 Ekaterinburg, Russia

³Hahn-Meitner-Institut, SF-2, Glienicke Strasse 100, D-14109 Berlin, Germany

Rare earth intermetallic compounds RT_2 ($T = Co, Ni$) are considered as potential candidates for magnetic refrigeration applications [1-3]. Maximal values of the magnetocaloric effect (MCE) are observed for RT_2 ($R = Dy, Ho$ and Er) which display a first-order phase transition (FOT) at the Curie temperature. The presence of FOT in RCO_2 is associated with the itinerant electron metamagnetism of the Co 3d subsystem. The magnetic moment on Co atoms (μ_{Co}) has an induced character and depends on the molecular field acting from the R sublattice. The T_C values in RCO_2 compounds and, consequently, the working temperature intervals may be

changed in a wide range (4 K – 400 K) by the substitutions in the R-sublattice [2]. The aim of the present work is to study the specific heat behavior and the magnetocaloric effect in $Tm_{1-x}Tb_xCo_2$ compounds in the vicinity of a critical Tb- concentration at which the Co magnetic moment reveals instability. According to previous study [4] the Co atoms do not exhibit a magnetic moment in $Tm_{1-x}Tb_xCo_2$ at $x < 0.15$, while μ_{Co} increases abruptly up to a value $\sim 1 \mu_B$ with increasing x up to $x \geq 0.15$. We have measured the specific heat of $Tm_{1-x}Tb_xCo_2$ with the Tb-concentration $x = 0.1$ and $x = 0.15$ at magnetic fields up to 9 T. The measurements were made using a Quantum Design PPMS system.

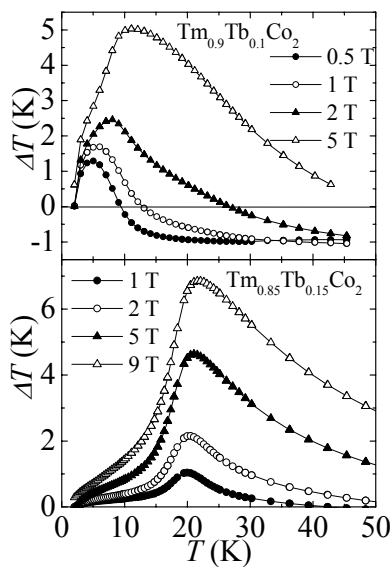


Figure shows the temperature dependences of the adiabatic temperature change ΔT calculated from specific heat data for these compounds. For $Tm_{0.85}Tb_{0.15}Co_2$ which exhibits a long-range ferrimagnetic order at low temperatures, the ΔT value reaches 6.9 K at the field $\mu_0 H = 9$ T around $T_C \approx 19$ K. The magnetic state of the $Tm_{0.9}Tb_{0.1}Co_2$ compound was classified as of

the cluster-glass type, which enters with cooling below the freezing temperature $T_f \approx 9$ K [3]. As seen from Figure, an application of an external field below T_f increases the temperature of a $Tm_{0.9}Tb_{0.1}Co_2$ sample, while reverse MCE is observed at low fields above T_f . Moreover, at $T > T_f$, the ΔT value is observed to change its sign with increasing field. The negative ΔT is associated with the entropy growth under application of a magnetic field. It should be noted, that the increase of the entropy with increasing magnetic field can be observed in some antiferromagnetic compounds as well as in materials with a singlet ground state [5]. The unusual behavior of MCE observed in $Tm_{0.9}Tb_{0.1}Co_2$ may be associated with the itinerant electron metamagnetism of the d-electron subsystem and with non-homogeneous magnetic state of this compound caused by the Tm-Tb substitution.

[1] H. Wada, S. Tomekawa, M. Shiga, *J. Magn. Magn. Mat.*, **196-197** 689(1999)

[2] N.H. Duc, D. T. Kim Anh, P.E. Brommer, *Physica B* **319** 1 (2002)

[3] N.A. de Oliveira, et al., *Phys. Rev. B.*, **55**, 094402 (2002)

[4] N. V. Baranov, et al., *Phys. Rev. B.*, **73**, 104445 (2006)

[5] Y. Aoki, et al., *Phys. Rev. B.*, **62**, 8935 (2000)

25PO-20-12

ELECTRONIC STRUCTURE INVESTIGATION OF Fe₂MnAl HEUSLER ALLOY

Shreder E., Svyazhin A., Yarmoshenko Y., Korotin M., Kuznetsova T.
Institute of Metal Physics, 18 S.Kovalevskaya St., 620041 Ekaterinburg, Russia

We present results of the *ab-initio* electronic structure calculations, magnetic and optical properties, as well as XAS and XPS investigations of Fe₂MnAl compound.

The Heusler alloy Fe₂MnAl is intermetallic compound with L₂₁ crystal structure. General gradient approximation (GGA) in the framework of full-potential linear augmented plane waves (FP-LAPW) method for electronic structure calculation was used. According to the calculation, perfectly ordered Fe₂MnAl alloy is almost half-metallic ferrimagnet (the calculated degree of spin polarization is 92 %). This makes the alloy a promising candidate for spintronic applications. Magnetic moments on Fe (~0,3 μ_B) and Mn (~2,6 μ_B) atoms aligned antiparallely. Magnetic measurements, performed on SQUID-magnetometer, confirm ferrimagnetic ordering below 100 K.

Optical properties in the spectral range (0,1-5) eV were investigated by means of ellipsometric Beattie method. Intensive contribution from interband electron transitions to optical conductivity in the infra-red region is discovered. This is a direct evidence of low-energy gaps existence in the electronic energy spectrum of the alloy.

X-ray photoelectron spectra (XPS) of the valence band and Mn2p core levels, and X-ray photoabsorption spectra (XAS) of the 3d-constituents are discussed. Magnetic exchange splitting of the Mn2p_{3/2} spectra is observed, characteristic for half-metallic Heusler alloys containing Mn. Mn XAS demonstrates shape, typical for Heusler compounds, with clear spectral subbands, peculiar to free atoms [1]. The magnitude of the Mn2p_{3/2}-spectra exchange splitting is proportional to Mn-3d electrons magnetic moment. In this alloy the magnitude is lowest among Mn-based Heusler alloys and in a well agreement with calculated one.

[1]. S. Plogmann, T. Schlathoëlter, J. Braun, M. Neumann et al. Phys.Rev.B, 1999, v.60, N 9, p.6428-6437.

25PO-20-13

ENTROPY AND MAGNETOCALORICAL EFFECT IN FERROMAGNETICS WITH MAGNETIC PHASE TRANSITIONS OF THE FIRST AND SECOND ORDER

Valiev E.Z.

Institute of metal physics, Ural Division, Russian Academy of Science, ul. S. Kovalevskoi 18,
Ekaterinburg, 620041, Russia

With the help of the exchange-striction models an analytical expression is obtained for magnetic entropy of ferromagnetics with magnetic phase transitions of the first and second order. A temperature dependence of ferromagnetics entropy change ΔS_m is calculated at energizing and deenergizing of a magnetic field and pressure (magnetocalorical MCE and barocalorical BCE effects). The behavior of the basic characteristics of the MCE and BCE during a transition

through a tricritical point is analyzed, since the change of the order of magnetic phase transition takes place at this point.

It is shown, that in the region of phase transitions of the second order ΔS_m^{\max} reaches its maximum value at the tricritical point and it increases by of factor of four with a constant of magnetoelastic interactions (MEI) growing from zero up to its critical value. With a further growth of the MEI constant in the region of the magnetic phase transition of the first order ΔS_m^{\max} also grows according to the certain law.

The approximate analytical formulas are obtained for numerical estimations of ΔS_m^{\max} as depending on the magnetic field and pressure in various areas of the phase diagram. The calculation results are compared with the experimental data for ferromagnetics systems $\text{La}(\text{Fe}_x\text{Si}_{1-x})_{13}$, $0.8 < x < 0.9$.

The work was done within RAS Program (Project № 01.2.006 13394), with partial support of Presidium RAS Basic Investigation Program “Effect of the crystal and electron structures on the condensed matter properties” (Project № 21, UD RAS).

25PO-20-14

MAGNETIC PROPERTIES AND STRUCTURAL TRANSITIONS IN $(\text{MnCo})_{1-x}\text{Ge}$

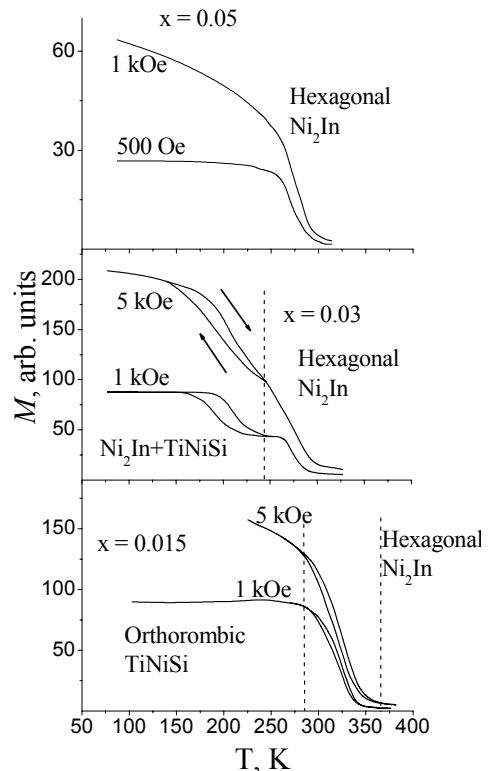
Markin P.E.^{1,2}, Mushnikov N.V.¹, Sosedkov M.A.²

¹Institute of Metal Physics, Ural Division of RAS, S Kovalevskaya, 18, 620041 Ekaterinburg, Russia

²Ural State University, Lenin av. 51, 620083 Ekaterinburg, Russia

During the last period much effort has been devoted to the investigation of the magnetocaloric effect in materials with first-order structural phase transitions near room temperature. Recently, the large entropy change in a relatively small field of 1 T was found in the nonstoichiometric MnCoGe-based alloy in the vicinity of the magnetostructural phase transition, where the transition from the orthorhombic TiNiSi -type to the hexagonal Ni_2In -type structure coincides with the transition from ferromagnetic (FM) to paramagnetic (PM) state [1]. In this work we studied the magnetic properties and crystal structure transformations in the compounds $(\text{MnCo})_{1-x}\text{Ge}$ for $x = 0.05, 0.04, 0.03, 0.025, 0.015, 0$.

It was found that the compound with $x = 0.05$ has the hexagonal Ni_2In structure in the whole temperature range below its melting point. For the compounds with $x = 0.025$ and 0.015 , temperature dependences of the magnetization exhibit a hysteresis at heating and cooling in the temperature regions where the samples undergo the FM - PM transition. The magnetic transition is situated in the two-phase region where the orthorhombic and hexagonal phases coexist. The temperature of the structural transition T_t and the Curie temperature T_C both increase with decreasing x . The compound with $x = 0.03$ has the hexagonal



crystal structure down to $T_i = 220$ K, while below this temperature both orthorhombic and hexagonal phases were found to coexist in the sample.

The entropy changes (ΔS) near T_C were obtained from the field dependences of the magnetization measured at different temperatures for the compounds with $x = 0.05, 0.015$, using the Maxwell relation. It was found that $\Delta S = -1.3$ J/(kg K) for the field change of 1 T in the compound with $x = 0.015$ is nearly twice as large as that for $x = 0.05$ due to the stronger coupling between the magnetic and structural subsystems in the vicinity of the structural phase transition. However, in spite of the hysteresis near T_C , the magnetic phase transition for $x = 0.015$ may be of the second order. Actually, temperature dependence of the spontaneous magnetization for this compound satisfactorily follows the Brillouin function indicating the second-order magnetic transition. The hysteresis of the magnetization near T_C may be associated with the first-order structural phase transition, which leads to the different amounts of orthorhombic and hexagonal phases at heating and cooling. Taking into account the magnetization and X-ray diffraction data, the magnetic and structural x - T phase diagram is obtained for this system.

Support by RFBR (project No.06-02-16951) is acknowledged.

[1] Y.K. Fang, C.C. Yeh, C.W. Chang, et al., *Scripta Materialia*, **57** (2007) 453.

25PO-20-15

EXTENDED SHORT-RANGE ANTIFERROMAGNETIC ORDER AND MAGNETOTHERMAL PROPERTIES OF Tb_3Ni AND Gd_3Ni COMPOUNDS

Baranov N.V.^{1,2}, Gubkin A.F.², Proshkin A.V.^{1,2}, Cervelino A.³, Gerasimov E.G.¹

¹Institute of Metal Physics, Russian Academy of Science, 620041 Ekaterinburg, Russia

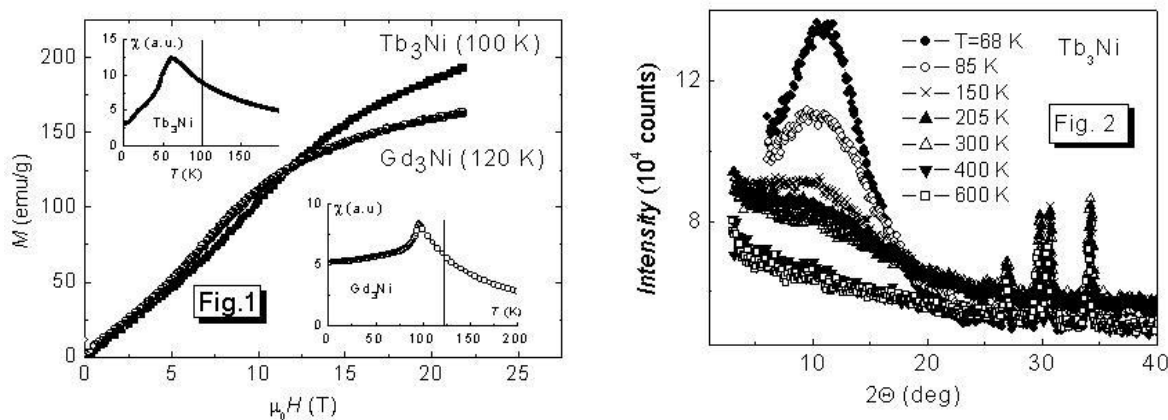
²Ural State University, 620083 Ekaterinburg, Russia

³Paul Scherrer Institut, CH-5232 Villigen PSI, Switzerland

The specific heat studies of rare earth (R) intermetallic compounds R_3M ($M=Co, Ni$) have shown [1–3] that a noticeable magnetic contribution to the specific heat persists well above magnetic ordering temperatures even in antiferromagnetic Gd_3M compounds in which the Gd-ion has zero orbital moment. These results are indicative of the presence of short-range magnetic correlations and spin fluctuations above magnetic ordering temperature. The short-range magnetic order is suggested to influence the behavior of the magnetocaloric effect [4] as well as the electrical resistivity [1, 3] of these compounds. The aim of the present work is to study the peculiarities of the magnetic state of R_3Ni compounds ($R = Tb, Gd$) in paramagnetic region by means of high-field magnetization and neutron diffraction measurements.

Both Gd_3Ni and Tb_3Ni having an orthorhombic crystal structure of the Fe_3C type ($Pnma$ space group) exhibit an antiferromagnetic (AF) behavior below $T_N = 98$ K and 62 K respectively. In Gd_3Ni , application of a magnetic field along the b - or c -axes leads to the phase transitions from AF state to the field induced F-states, while only a gradual increase of the magnetization along the a axis is observed [5]. The Gd magnetic moments are suggested to lie mainly within the bc -plane. The magnetization measurements performed in the present work in pulse fields have revealed that $M(H)$ dependences for both Tb_3Ni and Gd_3Ni exhibit a non-Brillouin shape above T_N and show an inflection point even at $T \sim 1.3 - 1.5 T_N$ (see Fig. 1). Such a behavior may be associated with transformation of the antiferromagnetic structure in regions (clusters) which persist in a wide temperature range above T_N . The presence of a short-range antiferromagnetic

order was indeed revealed by powder neutron diffraction measurements on a Tb_3Ni sample (shown in Fig. 2). The broad diffuse maximum is observed around $2\theta \approx 12^\circ$ at temperatures up to 300 K, which indicates the presence of magnetic correlations well above the magnetic ordering temperature (up to $T \sim 5T_N$). This short-range magnetic order presumably of the two-dimensional nature leads to unusual specific heat and magnetocaloric effect behaviors in R_3M compounds.



- [1] N.V. Baranov et al., *J. Alloys and Comp.*, **329** (2001) 22.
 [2] N.V. Tristan et al., *J. Magn. Magn. Mat.*, **258–259** (2003) 583.
 [3] N.V. Baranov et al., *J. Magn. Magn. Mat.*, **272–276** (2004) 637.
 [4] S.K. Tripathy, K.G. Suresh, A.K. Nigam, *J. Magn. Magn. Mat.*, **306** (2006) 24.
 [5] N.V. Tristan et al., *J. Magn. Magn. Mat.*, **251** (2002) 148.

25PO-20-16

MAGNETIC PROPERTIES AND SHAPE MEMORY EFFECT IN NiMnGaFe AND NiMnIn MELT SPUN RIBBONS

Khovailo V.¹, Koledov V.¹, Kuchin D.¹, Shavrov V.¹, Zolotarev V.¹, Hernando B.²,
 Sánchez Llamazares J.L.², Santos J.D.²

¹Institute of Radioengineering and Electronics of RAS, 125009, Moscow, Russia

²Departamento de Física, Universidad de Oviedo, Calvo Sotelo s/n, 33007 Oviedo, Spain

Since it was discovered that ferromagnetic shape memory alloys (FSMA) may show giant magnetic field strains due to reorientation of martensitic twins [1], and magnetic shape memory effect (SME) due to magnetic field induced martensitic transformation [2], much efforts have been addressed to investigate melt spun ribbons of these materials [3]. Melt spun ribbons of FSMA demonstrating SME are considered promising functional material for sensor and actuator technology. They show some specific properties due to their small thickness and non equilibrium structure. The purpose of the present work was is to study the structure, SME and magnetic properties of NiMnGaFe and NiMnIn rapidly quenched alloys.

Ribbons of $Ni_{2.15}Mn_{0.79}Fe_{0.06}Ga$, $Ni_{2.20}Mn_{0.79}Fe_{0.01}Ga$ and $Mn_{50}Ni_{40}In_{10}$ alloys were produced by melt spinning in argon environment as described in [4]. Microstructure and elemental composition of ribbons were examined by using a JEOL JSM-6100 scanning electron microscope (Fig. 1). Heating and cooling thermomagnetic curves were recorded at $H_{ext} = 1.0$ kOe in a Faraday balance. The thermoelastic properties under bending stress were studied by multipoint technique [5]. The typical strain vs. temperature dependance of ribbon shows pure SME (Fig. 2). Thermoelastic and magnetic properties of ribbons were found to be quite dependant on thermal treatment conditions.

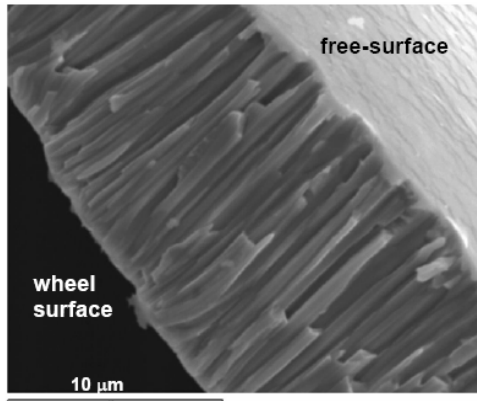


Fig.1. As-spun $\text{Ni}_{2.20}\text{Mn}_{0.79}\text{Fe}_{0.01}\text{Ga}$ ribbons: SEM cross-section image showing their ordered columnar grain microstructure perpendicular to ribbon plane.

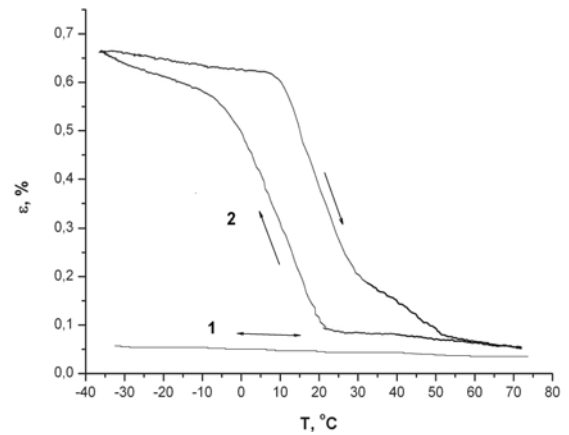


Fig.2. Strain vs. temperature dependence under stress of 14 MPa for $\text{Ni}_{2.15}\text{Mn}_{0.79}\text{Fe}_{0.06}\text{Ga}$ ribbons in as-spun state (curve 1) and after 2 h of annealing at 200 °C (curve 2).

Support by RFBR grants Nos. 06-02-16266, 06-02-39030, 06-02-16984, and Spanish grants Nos. COF07-013, and MAT2006-13925, is acknowledged.

- [1] K. Ullakko, et al. *Appl. Phys. Lett.* **69**, 1966 (1996).
- [2] A. Cherechukin et al. *Phys. Lett. A* **291**, 175 (2001).
- [3] V.A. Chernenko et al. *Smart. Mater. Str.* **3**, 80 (1994).
- [4] J.L. Sánchez Llamazares, et al. *Appl. Phys. Lett.* **92**, 012513 (2008).
- [5] F. Albertini, et al. *J. Communications Technology and Electronics* **50**, 638 (2005).

Author Index

A

Aarts J., 23PO-1-20	429	Ali N., 24RP-D-7	574
Abaloshev A., 24PO-7-14.....	629	Ali N., 25PO-20-6.....	815
Abdulvagidov Sh.B., 24PO-7-30.....	644	Aliev A.M., 24PO-7-30	644
Abe M., 21PL-A-2	11	Aliev A.M., 25PO-20-9	818
Abe S., 25PO-13-25.....	765	Aliev F.G., 24TL-B-7	557
Abramova G., 24PO-6-20.....	608	Alinejad M.R., 23PO-1-32.....	441
Abramova G., 25PO-13-64.....	803	Aliouane N., 24PO-7-65	680
Abrikosov I.A., 23PO-12-19.....	522	Alkaev E.A., 22PO-8-22.....	276
Abrikosov I.A., 23PO-12-21.....	524	Alling B., 24TL-B-1	552
Abrikosov I.A., 24TL-B-1	552	Almukhametov R., 21PO-2-23	95
Abrikosov I.A., 25PO-13-42	781	Alshansky G.A., 24PO-7-58.....	673
Acet M., 23TL-D-1.....	390	Alves F., 25PO-13-2.....	743
Acher O., 24TL-C-1	562	Ambrosch-Draxl C., 25RP-C-7	727
Achkeev A.A., 22RP-A-8.....	194	Ambrosch-Draxl C., 25RP-D-8.....	739
Adamchik D.A., 21PO-16-4	101	Amiens C., 22PO-8-16	270
Adams C.P., 22TL-D-4.....	220	Amirov A.A., 24PO-7-43	658
Ader J-P., 22RP-F-11	251	Amonov B.U., 24PO-7-77	692
Afonina V., 23TL-D-3.....	391	Anashkin O., 21PO-21-10	170
Agafonov Yu.A., 22RP-A-7	193	Anders A.G., 22PO-8-78	330
Agostinelli E., 21TL-B-2.....	27	Ando K., 21TL-C-1	36
Agranat M.B., 21PO-2-13	86	Andre G., 23PO-1-13.....	422
Agzamova P., 24PO-7-35.....	649	Andreev A.V., 21RP-F-4.....	63
Ahuja B.L., 24TL-D-5	573	Andreev A.V., 25PO-13-56.....	795
Ahuja R., 25PO-13-41	781	Andreev B.A., 22RP-A-7.....	193
Akbashev A.R., 24PO-7-62.....	677	Andreev S.V., 22PO-8-24.....	278
Akdoğan N., 22RP-A-8	194	Andreev S.V., 25PO-13-17.....	757
Akinaga H., 21TL-B-7.....	31	Andreeva M., 22PO-8-80	332
Akinaga H., 21TL-C-7.....	41	Andrianov V.A., 25PO-13-31.....	771
Aksenov V.L., 22RP-E-8.....	235	Anferova P.A., 21PO-21-11	171
Aksenov V.L., 23PO-1-9.....	419	Angelakeris M., 22PO-8-66.....	319
Aksenov V.L., 23PO-3-16.....	461	Anisimov M., 23PO-4-22.....	498
Aksenov V.L., 23PO-3-29	474	Anisimov M., 23PO-4-9	486
Aksenov V.L., 23RP-F-4.....	401	Anisimov M., 24PO-6-25	613
Aksoy S., 23TL-D-1	390	Anisimov V.I., 25PO-13-55.....	794
Aktsipetrov O.A., 21PO-2-17.....	89	Anitas E., 23PO-3-17.....	462
Aktsipetrov O.A., 21PO-2-18.....	90	Anitas E.M., 22RP-E-7.....	234
Aktsipetrov O.A., 21PO-2-21	93	Anitas E.M., 23PO-3-9	454
Aktsipetrov O.A., 21TL-A-8	22	Annenkov A.Yu., 21PO-2-11	83
Albrecht J., 25PO-13-40.....	780	Annenkov A.Yu., 21PO-2-12	85
Albrecht J., 25PO-20-7.....	816	Antipov S.D., 22PO-8-15	269
Aleksandrova G.P., 22PO-8-69	321	Antipov S.D., 22PO-8-17	271
Alekseev A.M., 22PO-8-5	260	Antipov S.D., 22PO-8-18	272
Aleshkevych P., 22TL-D-4.....	220	Antonov A.S., 21PO-16-29	126
Alexandrov A.S., 23PO-1-10.....	420	Antonov A.S., 21PO-16-59	155
Alexandrova G.A., 22PO-8-55	307	Antoshina L.G., 24PO-7-46.....	661
Ali Can M., 24PO-6-24	612	Antropov V., 21TL-E-6	57

Anzulevich A., 21PO-16-40	136
Anzulevich A.P., 21PO-16-35	131
Aplesnin S.S., 23PO-12-30	532
Aplesnin S.S., 24PO-6-22	610
Aplesnin S.S., 24RP-F-9	586
Arabi H., 22PO-8-14	268
Arai K.I., 23RP-A-6	363
Arango Y., 22RP-D-8	223
Araujo J.P., 24PO-7-71	686
Arauzo A., 23PO-1-16	425
Arbuzova T., 24PO-7-4	619
Arbuzova T., 24PO-7-67	682
Archer T., 24PO-6-12	601
Arcon D., 21RP-F-2	61
Argyriou D.N., 24PO-7-65	680
Arias J.E., 25TL-A-1	696
Ari-Gur P., 25PO-20-1	810
Armstrong R., 23TL-A-1	356
Aronzon B.A., 23PO-4-11	488
Aronzon B.A., 24PO-6-18	606
Aronzon B.A., 24TL-A-2	540
Aronzon B.A., 25RP-A-11	705
Arzhnikov A.K., 23PO-12-18	522
Arzhnikov A.K., 23PO-12-27	530
Arzhnikov A.K., 24TL-F-4	582
Arzhnikov A.K., 25PO-13-59	798
Asadullin F.F., 21PO-16-1	98
Asadullin F.F., 21PO-16-11	108
Asadullin F.F., 21PO-16-5	102
Asadullina N.S., 21PO-16-1	98
Ashitkov S.I., 21PO-2-13	86
Asker C., 24TL-B-1	552
Askinazi A.Yu., 21PO-16-36	132
Astafurov V.I., 23PO-12-1	506
Astafurov V.I., 23PO-12-10	514
Atake T., 25RP-D-6	738
Atsarkin V., 24PO-7-23	637
Attanasio C., 23PO-1-20	429
Avdeev M., 23PO-1-6	416
Avdeev M.V., 22RP-E-8	235
Avdeev M.V., 23PO-3-16	461
Avdeev M.V., 23PO-3-29	474
Avdeev S.F., 22PO-8-53	305
Avdeeva O.A., 23PO-3-18	462
Averkiev N.S., 24RP-A-4	542
Azamatov Sh., 21PO-16-18	115
Azamatov Sh., 21PO-16-19	116
Aznaurova G.Ya., 23PO-12-24	527

B

Babaev A.B., 23PO-12-24	527
Baberschke K., 21TL-B-4	28
Babushkin A.V., 21PO-16-45	141
Babushkina N.A., 24PO-7-1	616
Babushkina N.A., 24PO-7-8	622
Back Ch., 21TL-B-3	27
Badtalov A.B., 24PO-7-43	658
Baenitz M., 24PO-6-9	598
Bagmut T., 21PO-16-50	146
Bagmut T., 22PO-8-45	298
Bajukov O., 25PO-13-64	803
Bakulina N.B., 21PO-2-8	81
Bakulina N.B., 22PO-8-28	282
Balaev A., 25RP-A-5	700
Balaev A.D., 24PO-6-23	611
Balaev A.D., 24PO-7-60	675
Balaev D.A., 22PO-8-49	302
Balaev D.A., 24PO-6-22	610
Balaev D.A., 24PO-6-23	611
Balaev D.A., 24PO-7-51	666
Balagurov L.A., 22RP-A-7	193
Balakirev V.F., 25PO-13-60	799
Balalae S.Yu., 25PO-13-14	754
Balasoju M., 22RP-E-7	234
Balasoju M., 23PO-3-17	462
Balasoju M., 23PO-3-9	454
Balasoju M., 23RP-F-4	401
Balasoju M., 24PO-7-28	642
Balbashov A., 24PO-7-61	676
Balbashov A.M., 24PO-7-16	631
Balbashov A.M., 24RP-A-9	550
Baldomir D., 24RP-D-9	577
Baldomir D., 25TL-A-1	696
Balkashin O.P., 23PO-4-18	495
Balmashov S.A., 25PO-13-20	760
Balymov K.G., 22PO-8-51	304
Bandurina O.N., 24PO-6-22	610
Banik S., 24TL-D-5	573
Bannikov V.V., 24PO-7-26	640
Bannikova E.M., 24PO-6-19	607
Bannikova N.S., 24PO-7-39	654
Bannikova N.S., 24PO-7-55	670
Bannykh A., 21RP-F-11	71
Bao B., 23TL-D-3	391
Bao Bo, 24RP-D-6	574
Baraduc C., 23PL-A-1	352
Barandiaran J.M., 22PO-8-65	318

Baranov D., 22PO-8-43	296	Bazhanov D., 23PO-4-10.....	487
Baranov N.V., 25PO-20-11	820	Bazhanov D.I., 22PO-8-21	275
Baranov N.V., 25PO-20-15	823	Bazhanov D.I., 22PO-8-96	347
Baranov S.A., 21PO-16-30.....	127	Bazhanov D.I., 25PO-13-42	781
Baranov S.A., 21PO-16-61	157	Bazyliniski D.A., 23RP-A-5	362
Baranov S.A., 21PO-16-62	158	Bea H., 24TL-B-2.....	553
Baranov S.A., 25PO-13-26.....	766	Beale T.A.W., 24PO-7-17	632
Baranovskiy A.E., 23PO-4-23	499	Beale T.A.W., 24TL-A-7.....	548
Baretzky B., 25RP-A-10.....	705	Bebenin N.G., 24PO-7-27	641
Barilo S., 25RP-D-8.....	739	Bebenin N.G., 24PO-7-39	654
Barilo S.N., 22TL-D-4.....	220	Bebenin N.G., 24PO-7-55	670
Barman S.R., 24TL-D-5	573	Bebenin N.G., 24RP-A-8.....	549
Barmin Yu.V., 21PO-21-8.....	168	Bedarev V., 22PO-8-37.....	290
Barmin Yu.V., 25PO-13-14.....	754	Bedarev V.A., 24PO-7-70.....	685
Barnakov Ch.N., 22PO-8-34	287	Belashchenko K.D., 21TL-E-3	55
Barnaš J., 21TL-C-6	40	Beletsky V.V., 25PO-13-22.....	762
Barroy P.R.J., 24PO-6-14.....	602	Bell C., 23PO-1-20	429
Barski A., 22TL-A-2.....	188	Bellet-Amalric E., 22TL-A-2	188
Barsov S.G., 23RP-F-4	401	Belmeguenai M., 22RP-C-8	215
Bartashevich M.I., 22PO-8-24	278	Belodedov M.V., 25PO-13-8.....	748
Bartashevich M.I., 25PO-13-17.....	757	Belosorov D., 22RP-F-4	242
Barthem V.M.T.S., 25PO-13-69.....	808	Belotelov V., 23RP-B-3.....	369
Bartholome A., 24TL-B-2	553	Belotelov V.I., 21PO-2-6.....	79
Bartolome E., 23PO-1-17	426	Belotelov V.I., 21PO-2-7.....	80
Bartolomé F., 22TL-B-3	198	Belotelov V.I., 22RP-F-2.....	240
Bartolome J., 22PO-8-71	323	Belousov V., 23PO-4-17.....	494
Bartolome J., 23PO-1-16.....	425	Belousova V.A., 25PO-13-62.....	801
Bartolome J., 23PO-1-17	426	Belovs M., 22TL-E-1.....	228
Bartolome J., 25PO-13-34.....	774	Belozerov E.V., 25PO-13-47.....	786
Bartolome J., 25PO-13-40.....	780	Belozerov Ye.V., 25PO-13-50.....	789
Baryshev A., 22RP-B-9	205	Ben Youssef J., 23PO-1-34	442
Baryshev A., 23RP-A-3.....	358	Ben Youssef J., 22PO-8-88	339
Baryshev A.V., 21PO-2-10.....	82	Benner H., 21PO-16-9	106
Baryshev A.V., 21PO-2-14.....	86	Berezovets V.A., 24RP-A-4	542
Baryshev A.V., 22RP-B-5	201	Bergman D.J., 24TL-C-6	566
Baryshev A.V., 22RP-B-6	202	Berkov D.V., 23RP-F-3	400
Bassoul P., 24PO-7-2.....	617	Berkov D.V., 25TL-C-6.....	726
Bataronov I.L., 21PO-21-8	168	Berlinsky A.J., 22TL-D-4.....	220
Batdalov A.B., 24PO-7-30.....	644	Bernien M., 21TL-B-4.....	28
Batdalov A.B., 25PO-20-9.....	818	Berret J.-F., 22TL-E-5	232
Battle X., 22TL-B-3.....	198	Berthet P., 23PO-1-15.....	424
Batolomé J., 22TL-B-3	198	Berzhansky V.N., 25PO-13-61	800
Bauer E.D., 23PO-1-4.....	414	Betancourt I., 25TL-B-1	708
Bauykov O., 24PO-7-78	693	Bezmaternikh L.N., 24PO-7-11	625
Baykova E.N., 21PO-21-14	174	Bezmaternikh L.N., 24PO-7-33.....	647
Bayle-Guillemaud P., 22TL-A-2	188	Bezmaternykh L., 24PO-7-29.....	643
Bayreuther G., 22RP-C-8	215	Bezmaternykh L.N., 24PO-7-70.....	685
Bayukov O., 25RP-A-5.....	700	Beznosov A., 24PO-7-3	618
Bayukov O.A., 22PO-8-47	300	Bharat B., 23TL-A-9.....	366
Bayukov O.A., 22PO-8-86	338	Bianconi A., 24TL-A-5.....	546
Bayukov O.A., 23PO-3-4	449	Bibes M., 24TL-B-2	553
Bazarov V., 22RP-A-8.....	194	Bica D., 22RP-E-8	235

Bica D., 23PO-3-16	461	Boulle O., 21TL-C-6	40
Bica D., 23RP-F-4	401	Bouzehouane K., 24TL-B-2	553
Bica I., 22RP-E-7	234	Bouziane K., 22PO-8-36	289
Bica I., 23PO-3-17	462	Bovensiepen U., 21TL-A-4	17
Bica I., 23PO-3-9	454	Bovina A., 24PO-6-20	608
Bichurin M., 24PO-7-68	683	Bovina A., 24PO-7-78	693
Bichurin M.I., 21RP-D-8	52	Bovina A., 25PO-13-64	803
Blanco J.A., 24RP-D-9	577	Bovina A., 25RP-A-5	700
Blanco J.M., 25RP-B-8	715	Boyarsky L.A., 23PO-1-31	440
Blanco J.M., 25TL-B-3	710	Boytsova O.V., 23PO-1-19	428
Blanco-Canosa S., 25TL-A-1	696	Bozhko A.D., 23PO-4-3	480
Bland S.R., 24TL-A-7	548	Bozhko A.A., 23RP-F-12	409
Blinov A.G., 23PO-1-31	440	Brown D.W., 23TL-D-2	390
Blinova E.N., 25PO-13-9	749	Bruk V.V., 23PO-1-14	423
Bludov A.N., 22PO-8-76	328	Bruno P., 22PO-8-96	347
Bobba F., 24PO-7-18	633	Bruno P., 24TL-F-1	580
Bobyl A.V., 22PO-8-88	339	Brusentsov N., 21PO-21-10	170
Boehm M., 25PO-13-64	803	Brusentsov N.A., 23PO-3-6	450
Boehm M., 25RP-A-5	700	Brusentsova T., 21PO-21-10	170
Bogach A., 23PO-4-22	498	Brusentsova T.N., 23PO-3-6	450
Bogach A., 24PO-6-25	613	Bublik V.T., 22RP-A-7	193
Bogach A.V., 21PO-16-57	153	Buchel'nikov V.D., 21PO-16-45	141
Bogach A.V., 21PO-16-58	154	Buchelnikov V., 21PO-16-40	136
Bogach A.V., 23PO-4-7	484	Buchelnikov V., 25PO-20-8	817
Bogach A.V., 25PO-13-63	802	Buchelnikov V.D., 21PO-16-28	125
Bogatkin A.N., 22PO-8-24	278	Buchelnikov V.D., 21PO-16-31	128
Bogatkin A.N., 25PO-13-17	757	Buchelnikov V.D., 21PO-16-32	128
Bolbukh Iu., 22PO-8-10	265	Buchelnikov V.D., 21PO-16-33	129
Boldyrev K.N., 21PO-2-5	78	Buchelnikov V.D., 21PO-16-35	131
Bolsunovskaya O., 24PO-6-21	609	Buchelnikov V.D., 25PO-20-10	819
Boltaev A.P., 22PO-8-89	340	Buchelnikov V.D., 25PO-20-5	814
Bondarenko G., 22PO-8-58	311	Buchelnikov V.D., 25PO-20-9	818
Bondarenko G.N., 22PO-8-86	338	Buchinsky D.I., 23PO-4-26	502
Bondarenko G.V., 22PO-8-60	313	Büchner B., 21PO-2-5	78
Bondarenko N.G., 23PO-12-19	522	Büchner B., 22RP-D-8	223
Bondarev A.V., 21PO-21-8	168	Buchner B., 22TL-D-1	218
Bondarev A.V., 25PO-13-14	754	Buchner B., 23PO-1-15	424
Bondareva N.V., 21PO-21-14	174	Büchner B., 24PO-7-66	681
Boothroyd A.T., 24PO-7-17	632	Buda-Prejbeanu L., 23PL-A-1	352
Borich M.A., 21PO-16-14	111	Bukaemskiy A.A., 22PO-8-31	284
Borin D.Yu., 23RP-F-9	406	Bukhanko F., 24PO-7-64	679
Boris A.V., 23PO-12-8	512	Bukharaev A.A., 22PO-8-72	324
Borisenko I.V., 23PO-1-8	418	Bukreev D.A., 21PO-16-26	123
Borisenko I.V., 24PO-7-19	634	Bukreev D.A., 21PO-16-27	124
Borkar S., 25TL-D-2	733	Bulavin L.A., 23PO-3-16	461
Borshagovskaya L.S., 25PO-13-7	747	Bulavin L.A., 23PO-3-29	474
Botez C., 24PO-7-49	664	Buravtsova V.E., 22PO-8-61	314
Botez C.E., 24PO-7-48	663	Bürgler D.E., 21PO-2-3	76
Bottyan L., 21RP-B-6	30	Bürgler D.E., 23TL-B-7	375
Bou Matar O., 21TL-F-7	67	Burkhanov G.S., 25PO-13-68	807
Bouchaud J.P., 23RP-F-5	401	Burmistrov E., 23PO-3-26	470
Bouchenoir L., 24PO-7-17	632	Burmistrov I., 23PO-1-28	438

Burmistrov I.S., 23PO-1-23	432	Chebotayev N.M., 24PO-7-57	672
Burylov S.V., 23RP-F-11	408	Chechenin N.G., 23PO-4-24	500
Busiello G., 23PO-12-6	510	Chechenin N.G., 22PO-8-73	325
Busiello G., 23PO-12-7	511	Chechenin N.G., 25PO-13-31	771
Butko L.N., 21PO-16-32	128	Chekanova A.E., 22PO-8-3	258
Büttgen N., 22RP-D-10	225	Chekanova L.A., 21PO-16-20	117
Buzdin A.I., 22RP-F-11	251	Chekanova L.A., 22PO-8-31	284
Buznikov N.A., 21PO-16-29	126	Chekanova L.A., 22PO-8-34	287
Buznikov N.A., 21PO-16-59	155	Chekanova L.A., 22PO-8-46	299
Bychkov I., 21PO-16-40	136	Chekanova L.A., 22PO-8-47	300
Bychkov I.V., 21PO-16-28	125	Chekanova L.A., 22PO-8-48	300
Bychkov I.V., 21PO-16-31	128	Chekanova L.A., 22PO-8-49	302
Bychkov I.V., 21PO-16-32	128	Chen Yajie, 25TL-D-3	734
Bychkov I.V., 21PO-16-33	129	Cheong S.W., 25RP-D-7	739
Bychkov I.V., 21PO-16-35	131	Cheong S-W., 22TL-D-5	221
Bychkov I.V., 21PO-16-45	141	Cherepanov V.M., 22PO-8-52	305
Bychkov I.V., 25PO-20-9	818	Cherepanov V.M., 24PO-7-36	650
Bykov I.V., 24RP-C-7	567	Cherhykh P.N., 23PO-4-24	500
Bykova L.E., 22PO-8-86	338	Chérif S.M., 22PO-8-36	289

C

Cabuil V., 22RP-E-6	233	Cherif S., 22TL-A-2	188
Cai W., 21TL-A-5	20	Cherif S., 24TL-B-2	553
Camp P.J., 22RP-E-9	236	Chernenkov Yu.P., 22PO-8-79	331
Canals B., 24TL-F-1	580	Chernenkov Yu.P., 25PO-13-12	752
Cao J.W., 25PO-13-45	784	Chernichenko A., 22PO-8-58	311
Caprara S., 25RP-A-9	704	Chernobrovkin A.L., 22PO-8-85	337
Carbone C., 21TL-D-1	44	Chernovtsev S.V., 22RP-F-4	242
Carmo M.C., 24PO-6-8	597	Cherny A., 24PO-7-64	679
Catalan G., 24TL-B-2	553	Chernykh P., 23PO-4-21	497
Cazzanelli E., 24PO-6-5	594	Chetkin M.V., 25RP-B-5	712
Cēbers A., 22TL-E-1	228	Chevnyuk L.V., 21PO-16-12	109
Celegato F., 25TL-B-2	709	Chevnyuk L.V., 21PO-16-13	110
Cemil Başaran A., 22PO-8-12	267	Chiang R.K., 22PO-8-22	276
Cerdà J.J., 22RP-E-11	238	Chien C.J., 24PO-6-19	607
Cerda J.J., 22RP-E-9	236	Chien C.J., 24PO-6-3	592
Cervelino A., 25PO-20-15	823	Chien C.L., 22PO-8-40	293
Cezar J.C., 22TL-B-3	198	Chien C.L., 25RP-B-6	713
Chabina E.B., 25PO-13-62	801	Chigarev S.G., 24TL-B-5	556
Chaboussant G., 23RP-B-3	369	Chinenkov M.Yu., 23PO-4-14	491
Chakrabarti A., 24TL-D-5	573	Chistyakov O.D., 25PO-13-68	807
Chambers S., 25RP-A-6	701	Chistyakova M., 25PO-13-43	782
Chamor T.G., 21PO-16-12	109	Chistyakova N.I., 21PO-21-17	176
Chamor T.G., 21PO-16-13	110	Chistyakova N.I., 21PO-21-9	169
Chandra Sekar P.V., 25RP-A-4	699	Chizhik A., 25RP-B-8	715
Chang P.C., 24PO-6-19	607	Choi Y.J., 22TL-D-5	221
Chang Yongqin, 24RP-D-6	574	Choi Youn-Seok, 25TL-C-1	720
Chaudret B., 22PO-8-16	270	Christy A.G., 21RP-F-2	61
		Chtchelkatchev N., 23PO-1-28	438
		Chtchelkatchev N.M., 23PO-1-23	432
		Chuang May-Haw, 23TL-A-7	364
		Chuev M.A., 22PO-8-64	317

Chuev M.A., 23PO-4-11	488	Davenport J.W., 24TL-F-2	580
Chukalina E.P., 21PO-2-5	78	Davidova E.A., 25PO-13-62.....	801
Chukalina E.P., 24PO-7-34	648	Davies H.A., 25TL-B-1	708
Chulkina A.A., 21PO-16-24	121	Davies J.J., 25RP-A-2.....	697
Chumakov A.I., 21RP-B-6	30	De Blasi S., 23TL-C-5.....	385
Chzhan A.V., 25PO-13-48	787	Deak L., 21RP-B-6	30
Cibert J., 22TL-A-2	188	Debnath M.C., 21TL-C-1	36
Cirillo C., 23PO-1-20	429	Delaet B., 23PL-A-1	352
Ciuculescu D., 22PO-8-16.....	270	Demidenko O.F., 24PO-6-22.....	610
Clancy J.P., 22TL-D-4.....	220	Demidov A.A., 24PO-7-63.....	678
Clerc J.-P., 24RP-F-7.....	584	Demidov E.S., 22TL-A-6	192
Coisson M., 25TL-B-2.....	709	Demidov V., 24PO-7-23.....	637
Comaniciu E., 21PO-21-18	177	Demidov V.E., 22TL-C-2.....	209
Conde A., 23RP-D-8	395	Demidov V.V., 24PO-7-19.....	634
Conder K., 25RP-D-8	739	Demina P.B., 24PO-6-4.....	593
Constantinian K.Y., 23PO-1-8	418	Demishev S., 23PO-4-22.....	498
Continentino M.A., 22RP-F-10	250	Demishev S., 23PO-4-9.....	486
Cornei N., 24PO-7-28.....	642	Demishev S., 24PO-6-25	613
Cousin F., 22RP-E-6.....	233	Demishev S.V., 21PO-16-57	153
Craus M.L., 22RP-E-7.....	234	Demishev S.V., 21PO-16-58	154
Craus M.L., 23PO-3-9	454	Demishev S.V., 22PO-8-85	337
Craus M.-L., 24PO-7-28	642	Demishev S.V., 23PO-4-23	499
Creanga D.E., 21PO-21-18	177	Demishev S.V., 23PO-4-3	480
Cros V., 21TL-C-6	40	Demishev S.V., 23PO-4-6	483
Cros V., 23PO-4-12	489	Demishev S.V., 23PO-4-7	484
Cros V., 24RP-B-8	558	Demishev S.V., 25PO-13-63	802
Cros V., 24RP-B-9	559	Demokritov S.O., 22TL-C-2.....	209
Cucolo A.M., 24PO-7-18	633	Deng Longjiang, 21PO-16-44	140
Cui Jingjing, 21PO-16-44.....	140	Deng Longjiang, 22TL-C-4	211
Cyrille M.C., 23PL-A-1.....	352	Denisova E.A., 22PO-8-31	284
Czeppe T., 25PO-13-27	767	Denisova E.A., 22PO-8-46.....	299
<hr/>			
D			
D'yachkov A.L., 21PO-16-59	155	Denisova E.A., 22PO-8-47.....	300
D'yachuk V.V., 25PO-20-9.....	818	Denisova E.A., 22PO-8-49.....	302
Dadoenkova N.N., 22RP-F-6	244	Denisova E.A., 25PO-13-29.....	769
Dahlberg E.D., 21TL-B-1.....	26	Deranlot C., 21TL-C-6	40
Dahlberg E.D., 23RP-A-5	362	Deranlot C., 23PO-4-12.....	489
Dalchiele E.A., 22PO-8-12.....	267	Deranlot C., 24TL-B-2	553
Danilin A.N., 21PO-21-2.....	163	Desnenko V., 24PO-7-3.....	618
Danilov V., 22RP-E-10	237	Devillers T., 22TL-A-2.....	188
Danilov Yu.A., 24PO-6-4.....	593	Deych L., 21PO-2-16.....	88
Danilov Yu.A., 24PO-6-8.....	597	Dhalenne G., 23PO-1-15	424
Danilov Yu.A., 24TL-A-2	540	Di Castro C., 25RP-A-9	704
Danilov Yu.A., 25RP-A-11	705	Diebold M., 23TL-D-4	392
Darinskii B., 22PO-8-26.....	280	Dieny B., 23PL-A-1.....	352
Darques M., 21TL-C-6	40	Dietl T., 22PL-A-1.....	184
Darques M., 22RP-C-7	214	Dikansky Yu.I., 23PO-3-13	458
Das I., 24TL-D-1	570	Dikansky Yu.I., 23PO-3-7.....	451
		Ding H.F., 24TL-B-6.....	557
		Dissanayake N., 21TL-A-6.....	20
		Djemia P., 23RP-B-3	369
		Dmitrieva N.V., 25PO-13-46	785
		Dmitrieva T.G., 25PO-13-20.....	760

Dobrowolski V., 25RP-A-3	698
Dobrynin A., 25PO-13-69	808
Dobysheva L.V., 23PO-12-27	530
Dobysheva L.V., 24TL-F-4	582
Doerr M., 24PO-6-3	592
Doerr M., 25PO-13-15	755
Dokukin M.E., 21PO-2-14	86
Dokukin M.E., 22RP-B-5	201
Dolgova T., 21PO-2-4	77
Dong-Hyun Kim, 24PO-7-12	626
Dorofeenko A.B., 24RP-C-7	567
Dorofeenko A.V., 21PO-2-10	82
Dorofeenko A.V., 22RP-F-3	241
Dorogina G.A., 25PO-13-60	799
Dorokhin M.V., 24PO-6-4	593
Doroshenko R.A., 21PO-16-17	114
Doroshenko R.A., 21PO-16-34	130
Doroshev N.N., 22PO-8-53	305
Dorovscoy Yu.V., 21PO-21-8	168
Douadi-Masrouki S., 22RP-E-6	233
Drachev V.P., 21TL-A-5	20
Drechsler S.-L., 24RP-F-8	585
Drew H.D., 25RP-D-7	739
Drewnia J., 23RP-C-7	387
Drichko I.L., 24PO-6-15	603
Drovosekov A., 22PO-8-44	296
Drozdo Yu.N., 24PO-6-8	597
Drulis H., 25PO-13-30	770
Druzhnov D.M., 22TL-A-6	192
Dubenko I., 24RP-D-7	574
Dubenko I., 25PO-20-6	815
Dubina A.I., 23PO-3-6	450
Dubois E., 23RP-F-5	401
Dubov A.L., 22PO-8-3	258
Dubrovina N.V., 21PO-2-17	89
Dudnik M., 23PO-4-27	503
Dufour-Gergam E., 25PO-13-2	743
Dugaev V.K., 24TL-F-1	580
Duginov V.N., 23RP-F-4	401
Dukhnenko A.V., 21PO-16-57	153
Dulov E.N., 24PO-6-1	590
Dunaevsky S., 22PO-8-63	316
Dupuis V., 22RP-E-6	233
Dupuis V., 22TL-E-5	232
Dupuis V., 23RP-F-5	401
Dustmuhammedov Kh., 24PO-7-77	692
Dyakina V.P., 23PO-1-18	427
Dyakonov K.V., 24PO-7-52	667
Dyakonov V.P., 24PO-7-52	667
Džarová A., 23PO-3-3	448
Džarová A., 23RP-F-10	407
Dzyapko O., 22TL-C-2	209

E

Ebels U., 23PL-A-1	352
Éber N., 23RP-F-10	407
Ebert S.V., 21TL-E-4	55
Eckhold Ph., 21TL-B-4	28
Edelman I., 22PO-8-57	310
Edelman I., 22PO-8-58	311
Edelman I., 22PO-8-59	312
Edelman I.S., 21PO-2-19	91
Efetov K.B., 23PO-1-33	442
Efimets Yu.Yu., 21PO-16-3	100
Efimets Yu.Yu., 22PO-8-8	263
Efremova N.N., 23PO-1-27	437
Egelhoff W.F., 22PO-8-27	281
Egolf P.W., 23RP-D-6	393
Egolf P.W., 23TL-D-4	392
Egorov S.V., 23PO-1-3	413
Egov A.A., 22PO-8-15	269
Egov A.A., 22PO-8-17	271
Egov A.A., 22PO-8-18	272
Ekholm M., 24TL-B-1	552
Ekomasov E., 21PO-16-18	115
Ekomasov E., 21PO-16-19	116
Elfimova E.A., 22RP-E-9	236
Elias D., 21RP-F-5	64
Eliseev A.A., 22PO-8-1	256
Eliseev A.A., 22PO-8-2	257
Eliseev A.A., 22PO-8-97	348
Elokhina L.V., 24PO-7-22	636
Elokhina L.V., 24PO-7-39	654
Emelina T.N., 25PO-13-17	757
Endo Y., 22TL-C-1	208
Enss T., 25RP-A-9	704
Entel P., 25PO-20-10	819
Entel P., 25PO-20-5	814
Epshtein E.M., 24TL-B-5	556
Eremeev S., 23PO-4-10	487
Eremeev S.V., 25PO-13-42	781
Eremenko V.V., 23PO-1-13	422
Eremenko V.V., 23PO-1-14	423
Eremenko V.V., 23PO-1-17	426
Eremin E., 24PO-7-47	662
Eremin E.V., 24PO-7-12	626
Eremina E.A., 22PO-8-3	258
Eremina R.M., 22PO-8-19	273
Eremina R.M., 24PO-7-38	653
Ērglis K., 22TL-E-1	228
Erhan R., 22RP-E-7	234

Erhan R., 23PO-3-17	462
Erhan R., 23PO-3-9	454
Eriksson O., 21TL-B-4	28
Ermolenko A.S., 25PO-13-50	789
Erokhin S., 21PO-2-16	88
Ershov N.V., 22PO-8-79	331
Ershov N.V., 25PO-13-12	752
Ershov N.V., 25PO-13-5	746
Escoda Ll., 23TL-D-7	394
Escoda Ll., 24RP-D-8	575
Escoda Ll., 25RP-B-9	716
Eshmirzaeva M., 24PO-7-77	692
Etteger A., 22TL-B-7	203
Ezhov A., 21PO-2-4	77

F

Fähler S., 24PL-A-1	536
Faini G., 21TL-C-6	40
Faizrakhmanov I., 22RP-A-8	194
Falkovskaya L.D., 24PO-7-20	634
Fanciulli M., 23PO-4-21	497
Fannin P.C., 23TL-C-8	388
Farle M., 22TL-B-1	196
Farle M., 22TL-B-2	196
Farle M., 23RP-B-2	369
Farmakovsky B.V., 21PO-16-36	132
Farutin A.M., 22RP-D-9	224
Farzetdinova R., 22PO-8-83	335
Fedy A.A., 21PO-16-28	125
Fedorchenko I.V., 25RP-A-3	698
Fedorenko V.V., 24PO-7-22	636
Fedorov V.I., 22PO-8-79	331
Fedorov V.I., 25PO-13-12	752
Fedyanin A., 21PO-2-4	77
Fedyanin A., 23RP-A-3	358
Fedyanin A.A., 22RP-B-8	204
Feher A., 24PO-7-3	618
Feoktystov A.V., 23PO-3-16	461
Fernández A., 22PO-8-75	327
Fernando G.W., 24TL-F-2	580
Fert A., 21TL-C-6	40
Fert A., 24RP-B-9	559
Fert A., 24TL-B-2	553
Fertman E., 24PO-7-3	618
Fetisov L.Y., 22PO-8-98	349
Fetisov Y.K., 21RP-D-7	51
Fetisov Y.K., 22PO-8-98	349
Fetisov Y.K., 22PO-8-99	350
Fetisov Y.K., 25PO-13-13	753
Fettar F., 22PO-8-39	292
Feyerherm R., 24PO-7-65	680
Feyerherm R., 25PO-13-15	755
Figotin A., 23TL-A-4	359
Filimonov Yu.A., 21PO-16-2	99
Filimonov Yu.A., 21PO-2-2	75
Filippi M., 25RP-D-5	737
Filippov B.N., 23PO-12-4	509
Filippov B.N., 25PO-13-11	751
Fillippov V.B., 21PO-16-57	153
Finkelstein L.D., 23PO-1-27	437
Fink-Finowicki J., 22TL-D-4	220
Fiorani D., 21TL-B-2	27
Firov A.I., 25PO-13-68	807
Firsov I.A., 24PO-7-44	659
Fisun V.V., 23PO-4-18	495
Flachbart K., 23PO-4-7	484
Flachbart K., 24PO-6-25	613
Flachbart K., 25PO-13-63	802
Flerov I., 24PO-7-47	662
Flerov I.N., 24PO-7-25	639
Flevaris N.K., 22PO-8-66	319
Fodor-Csorba K., 23RP-F-10	407
Fomicheva L.N., 22PO-8-7	262
Fomicheva L.N., 23PO-1-22	431
Fomicheva L.N., 23PO-1-4	414
Fominov Ya.V., 23PO-1-33	442
Fontcuberta J., 24TL-B-2	553
Forrester D.M., 21TL-E-5	56
Fors R., 21PO-16-63	159
Fourier S., 21PO-2-18	90
Fraerman A.A., 22PO-8-5	260
Fraerman A.A., 22PO-8-84	336
Fraerman A.A., 25RP-C-2	721
Franco V., 23RP-D-8	395
Franco V., 24RP-D-8	575
Fratini M., 24TL-A-5	546
Freeman A.J., 23PL-A-2	353
Freeman M., 21TL-B-3	27
Fresnais J., 22TL-E-5	232
Frka-Petesic B., 22RP-E-6	233
Frka-Petesic B., 22TL-E-5	232
Fruchart D., 23PO-1-32	441
Fu Bin, 24RP-D-6	574
Fu Chao-Ming, 23TL-A-7	364
Fujicawa R., 25PO-13-9	749
Fujikawa R., 22RP-B-6	202
Fujikawa R., 23RP-A-3	358
Fujikawa T., 25PO-13-19	759
Fukunaga H., 21RP-F-3	62
Fumagalli P., 22PO-8-66	319
Furdyna J.K., 22TL-A-1	188

Fusil S., 24TL-B-2 553

G

Gabani S., 25PO-13-63.....	802	Gavriliuk A.A., 25PO-13-37	777
Gaidukova I.Yu., 24PO-6-19.....	607	Gavriliuk A.A., 25PO-13-38	778
Gaidukova I.Yu., 24PO-6-3.....	592	Gavriliuk A.G., 21RP-F-9	69
Gajek M., 24TL-B-2	553	Gavrilova T.P., 22PO-8-19.....	273
Galakhov V.R., 24PO-7-22.....	636	Gawronski P., 25RP-B-8	715
Galkin V.Yu., 21PO-16-15.....	112	Gazeau F., 22TL-E-2	229
Galkin V.Yu., 21PO-16-39.....	135	Gazeeva E., 23PO-12-6.....	510
Galperin Yu.M., 23PO-1-25	434	Gazeeva E., 23PO-12-7.....	511
Gamzatov A.G., 24PO-7-30	644	Geibel C., 24PO-7-76	691
Gamzatov A.G., 25PO-20-9	818	Geiler A., 25TL-D-3	734
Gan'shina E.A., 22PO-8-61.....	314	Geim A.K., 21RP-F-5.....	64
Gan'shina E., 23RP-A-2	357	Gelin P., 23TL-C-5	385
Gan'shina E., 24PO-7-21.....	635	Gendler T.S., 22PO-8-69.....	321
Gan'shina E.A., 22RP-F-5	243	Gendler T.S., 25PO-13-43.....	782
Gan'shina E.A., 24PO-6-6.....	595	Georges B., 21TL-C-6	40
Ganichev S.D., 22TL-A-4	190	Georges B., 24RP-B-9	559
Ganshina E., 21PO-2-4	77	Georgieva M.I., 23PO-12-1	506
Ganshina E.A., 24PO-7-59.....	674	Georgieva M.I., 23PO-12-10.....	514
Gapontsev A.V., 22PO-8-28.....	282	Gerasimchuk V.S., 24PO-7-69.....	684
Garamus V.M., 22RP-E-8	235	Gerasimov E.G., 25PO-13-52.....	791
Garamus V.M., 23PO-3-16.....	461	Gerasimov E.G., 25PO-13-53.....	792
Garcia C., 23TL-D-7.....	394	Gerasimov E.G., 25PO-13-54.....	793
García C., 25RP-B-9.....	716	Gerasimov E.G., 25PO-20-15.....	823
García K.L., 21PO-16-30.....	127	Gerasimova J., 24PO-6-20.....	608
García L.M., 22TL-B-3	198	Gerus S.V., 21PO-2-11	83
García-Chocano V.M., 21PO-16-60.....	156	Gerus S.V., 21PO-2-12.....	85
García-Miquel H., 21PO-16-60.....	156	Ghoshray K., 22PO-8-77	329
Gardner D.S., 25TL-D-2.....	733	Gierlowski P., 24PO-7-14.....	629
Gareeva Z.V., 21PO-16-34.....	130	Gierlowski P., 24PO-7-52.....	667
Gareyeva Ye.R., 21PO-21-15.....	174	Gignoux D., 23PO-1-32.....	441
Gasparini A., 23PO-1-14	423	Gilyatzidinova N.M., 24PO-7-59	674
Gastev S.V., 22PO-8-11	266	Gippius A.A., 21PO-21-11	171
Gatiyatov R.G., 22PO-8-72	324	Gippius A.A., 22PO-8-20	274
Gatiyatova Ju.I., 25RP-C-4.....	722	Gippius A.A., 24PO-6-9.....	598
Gaulin B.D., 22TL-D-4	220	Giubileo F., 24PO-7-18	633
Gautam B.R., 24RP-D-7.....	574	Givord D., 24PL-A-1	536
Gaviko V.S., 22PO-8-24.....	278	Givord D., 25PO-13-69	808
Gaviko V.S., 24PO-7-59.....	674	Gizhevskii B.A., 24PO-7-22	636
Gaviko V.S., 25PO-13-50.....	789	Gizhevskii B.A., 24PO-7-59.....	674
Gaviko V.S., 25PO-13-51.....	790	Gladkikh D.V., 23PO-3-7	451
Gaviko V.S., 25PO-13-52.....	791	Glasbrenner J.K., 21TL-E-3	55
Gaviko V.S., 25PO-13-54.....	793	Glazkov V.N., 22RP-D-7.....	222
Gavrichkov V., 24PO-7-15	630	Glazkov V.N., 22RP-D-9.....	224
Gavrichkov V.A., 25RP-C-7	727	Glushkov V., 23PO-4-22	498
Gavriliuk A.A., 21PO-16-26	123	Glushkov V., 23PO-4-9	486
Gavriliuk A.A., 21PO-16-27	124	Glushkov V., 24PO-6-25	613
		Glushkov V.V., 21PO-16-57	153
		Glushkov V.V., 22PO-8-85	337
		Glushkov V.V., 23PO-4-23	499
		Glushkov V.V., 23PO-4-3	480
		Glushkov V.V., 23PO-4-6	483
		Glushkov V.V., 23PO-4-7	484

Glushkov V.V., 25PO-13-63	802	Gorelov E., 23PO-12-11	515
Gnatchenko S., 22PO-8-37	290	Gorkov V.P., 25PO-13-31	771
Gnatchenko S.L., 22PO-8-76	328	Gorn N.L., 23RP-F-3	400
Gnatchenko S.L., 24PO-7-70	685	Gornakov V., 22PO-8-41	294
Gnezdilov V., 22PO-8-37	290	Gornakov V.S., 25PO-13-21	761
Gnezdilov V., 25RP-D-8	739	Gornostyrev Yu.N., 25PO-13-12	752
Goering E., 25RP-A-10	705	Gorpyynyuk A.Yu., 21PO-16-13	110
Gofman M.S., 21PO-2-13	86	Gorria P., 24RP-D-9	577
Goikhman A., 23PO-4-21	497	Goryunov G.E., 22PO-8-15	269
Goikhman A., 23PO-4-25	501	Goryunov G.E., 22PO-8-17	271
Goikhman A.Yu., 23PO-4-24	500	Goryunov G.E., 22PO-8-18	272
Goiran M., 21PO-16-43	139	Goto T., 21PO-2-10	82
Golchevsky Yu.V., 21PO-16-1	98	Goto T., 22RP-B-5	201
Goldmann A.I., 25PO-13-15	755	Goulon J., 21TL-D-2	44
Goldobin E., 21RP-F-11	71	Goulon J., 24PO-6-16	604
Golik L.L., 22RP-F-5	243	Gradišek A., 25RP-D-5	737
Golikova T.E., 23PO-1-3	413	Granovskiy A.B., 22RP-F-1	240
Goll D., 25PO-13-40	780	Granovskiy A.B., 22RP-F-4	242
Goll D., 25PO-20-7	816	Granovsky A., 21PO-2-16	88
Gollwitzer C., 23RP-F-8	405	Granovsky A., 22RP-B-9	205
Golov A.V., 21PO-16-6	103	Granovsky A., 23PO-4-17	494
Golovanov A.N., 24PO-6-10	599	Granovsky A.B., 21PO-2-10	82
Golovanov A.Ye., 23PO-4-11	488	Granovsky A.B., 21PO-2-13	86
Golovenchits E.I., 24PO-7-53	668	Granovsky A.B., 21PO-2-20	92
Golovenchits E.I., 24PO-7-54	669	Granovsky A.B., 22RP-A-7	193
Golovenchits E.I., 25RP-D-6	738	Granovsky A.B., 22RP-B-5	201
Golubiatnikov A.N., 23PO-12-14	518	Granovsky A.B., 22RP-F-3	241
Golubov A.A., 22TL-F-14	253	Granovsky A.B., 24PO-6-6	595
Gomonay H., 23PO-4-2	479	Granovsky A.B., 25PO-13-59	798
Gonchar L.E., 24PO-7-45	660	Granovsky S.A., 24PO-6-19	607
Goncharenko I.N., 23PO-1-22	431	Granovsky S.A., 24PO-6-3	592
Gonin C., 23TL-D-4	392	Granovsky S.A., 25PO-13-15	755
Gonkov K.V., 23PO-4-20	496	Gratovsky S.V., 21PO-16-61	157
Gontchar L.E., 24PO-7-44	659	Gratovsky S.V., 21PO-16-62	158
Gonzalez J., 23TL-D-7	394	Grebenkova Yu., 22PO-8-58	311
Gonzalez J., 25PO-20-2	811	Grebennikov A.A., 22PO-8-50	303
Gonzalez J., 25RP-B-8	715	Grebennikov V.I., 23PO-12-22	525
Gonzalez J., 25TL-B-3	710	Grebennikov V.I., 23PO-12-26	529
Goodilin E.A., 22PO-8-3	258	Grebenshchikov Yu.B., 22PO-8-4	259
Goodilin E.A., 22PO-8-85	337	Grechnev G.E., 23PO-4-23	499
Goranov V.A., 23PO-3-1	446	Grechnev G.E., 25PO-13-24	764
Gorbatov O.I., 25PO-13-12	752	Greneche J.-M., 21PO-21-17	176
Gorbenko O., 24PO-7-21	635	Gribkov B.A., 22PO-8-5	260
Gorbenko O., 24PO-7-23	637	Gribkov B.A., 22PO-8-84	336
Gorbenko O.Y., 24PO-7-30	644	Gribkov B.A., 22PO-8-91	342
Gorbenko O.Yu., 23PO-1-19	428	Gribkov B.A., 22TL-A-6	192
Gorbenko O.Yu., 24PO-7-62	677	Gribov I., 24PO-7-14	629
Gorbunov A.I., 23RP-F-9	406	Gridnev V.N., 21RP-A-2	15
Gorbunov Ya.V., 24RP-B-8	558	Gridnev V.N., 21RP-A-3	16
Gorbunov Ya.V., 24RP-B-9	559	Griffin Roberts K., 25RP-A-7	702
Gordeev S.N., 21PO-21-19	178	Grigor'eva T.F., 25PO-13-43	782
Gorelik V.S., 21PO-2-9	82	Grigor'kin A., 22PO-8-63	316

Grigoriev S., 22PO-8-97.....	348	Han J.K., 23RP-B-9.....	376
Grigorieva A.V., 22PO-8-85.....	337	Han Mangui, 22TL-C-4.....	211
Grigorieva N.A., 22PO-8-97.....	348	Hanafin R., 24PO-6-12.....	601
Grigorieva N.Yu., 21PO-16-10.....	107	Handa H., 21PL-A-2.....	11
Grigorieva N.Yu., 23PO-12-2.....	507	Hanyu N., 21PL-A-2.....	11
Grilli M., 25RP-A-9.....	704	Haramus V., 22RP-E-7.....	234
Grishchenko L.A., 22PO-8-69.....	321	Harnsoongnoen S., 21PO-21-23.....	182
Grishin A.M., 21PO-16-63.....	159	Harris V.G., 25TL-D-3.....	734
Grishin A.M., 21PO-2-21.....	93	Harth E., 21RP-B-6.....	30
Grishin A.M., 21TL-A-8.....	22	Hasegawa D., 22TL-C-3.....	210
Grishin A.M., 22PO-8-38.....	291	Hasegawa Y., 21TL-C-5.....	39
Grishin A.M., 23TL-C-2.....	380	Hatakeyama M., 21PL-A-2.....	11
Gritsaj K.I., 23RP-F-4.....	401	Hatsukade Y., 21PO-21-13.....	173
Grollier J., 21TL-C-6.....	40	Hatsukade Y., 21RP-B-8.....	32
Grollier J., 23PO-4-12.....	489	Hatton P.D., 24PO-7-17.....	632
Grollier J., 24RP-B-8.....	558	Hatton P.D., 24TL-A-7.....	548
Grollier J., 24RP-B-9.....	559	Heinrich B., 21TL-B-3.....	27
Groot P.A.J., 21PO-21-19.....	178	Hellmann I., 22RP-D-8.....	223
Grössinger R., 21TL-D-4.....	48	Henner V.K., 22PO-8-68.....	320
Gruner M.E., 21TL-B-5.....	29	Hergert W., 22PO-8-87.....	339
Grunin A., 21PO-2-4.....	77	Hergert W., 22PO-8-96.....	347
Gryasnov V.V., 21PO-2-9.....	82	Hernando B., 23TL-D-7.....	394
Gsell S., 22RP-F-9.....	249	Hernando B., 24RP-D-8.....	575
Guardia P., 22TL-B-3.....	198	Hernando B., 25PO-20-16.....	824
Gubernatorov V.V., 25PO-13-49.....	788	Hernando B., 25RP-B-9.....	716
Gubkin A.F., 25PO-20-15.....	823	Herranz G., 24TL-B-2.....	553
Gudim I., 24PO-7-29.....	643	Hertel R., 23TL-B-7.....	375
Gudin S.A., 22PO-8-28.....	282	Hill E.W., 21RP-F-5.....	64
Gudoshnikov S.A., 25PO-13-7.....	747	Hinov K., 21PO-21-7.....	167
Gudoshnikov S.A., 25RP-B-7.....	714	Hjorvarsson B., 22PO-8-84.....	336
Guennou A., 23TL-C-5.....	385	Hnatowicz V., 22RP-A-8.....	194
Gueorgiev V., 21PO-21-7.....	167	Holm C., 22RP-E-10.....	237
Gulyaev Y.V., 24TL-B-5.....	556	Holm C., 22RP-E-11.....	238
Gumerov A., 21PO-16-19.....	116	Holm C., 22RP-E-9.....	236
Güner S., 22PO-8-12.....	267	Holmes J., 22TL-B-2.....	196
Guo Yu-Feng, 23TL-A-7.....	364	Horn S., 22RP-F-9.....	249
Gupta A., 25PO-13-2.....	743	Houssamedine D., 23PL-A-1.....	352
Gurevich Yu.L., 23PO-3-4.....	449	Hurdequint H., 23PO-1-34.....	442
Gurskii L.I., 24PO-7-41.....	656	Hurdequint H., 23PO-4-12.....	489
Gusev A., 25RP-D-8.....	739	Huynen I., 22RP-C-7.....	214
Gusev S.A., 22PO-8-70.....	322	Hwang Ch., 21RP-F-10.....	70
Gusev S.A., 22PO-8-84.....	336	Hwu S.-J., 22PO-8-37.....	290
Gusev S.N., 22TL-A-6.....	192		
Guslienکو K.Yu., 25TL-C-1.....	720		
Gvasaliya S.N., 25RP-D-6.....	738		

H

Hakioglu T., 24PO-6-24.....	612
Hamid E., 25PO-13-21.....	761

I

Iakubov I.T., 23TL-C-4.....	384
Iatcheva I., 21PO-21-6.....	166
Ibaev J.G., 23PO-12-25.....	528
Ibragimov Sh., 22RP-A-8.....	194
Ibulayev V.V., 23PO-1-13.....	422

Jamet M., 22TL-A-2	188	Kalinin Yu.E., 22PO-8-25	279
Jandl S., 24RP-A-9	550	Kalinin Yu.E., 22PO-8-46	299
Jansen M., 25PO-13-1	742	Kalinin Yu.E., 22PO-8-61	314
Jay J.-Ph., 22PO-8-88	339	Kalinin Yu.E., 22PO-8-8	263
Jeong Hyeon-Seong, 25TL-C-1	720	Kalish A.N., 21PO-2-6	79
Jergel M., 22PO-8-80	332	Kalish A.N., 21PO-2-7	80
Jernenkov K.N., 23PO-1-9	419	Kalish A.N., 22RP-F-2	240
Jiles D.C., 23PO-4-4	481	Kalita V.M., 22PO-8-38	291
Jin X., 21TL-C-4	38	Kalmykov S.A., 23PO-3-30	474
Johansen T.H., 23PO-1-25	434	Kalyakin L.A., 21PO-16-22	119
Johansson B., 23PO-12-19	522	Kalyakin L.A., 21PO-16-23	120
Johansson B., 23PO-12-21	524	Kalyakin L.A., 21PO-16-25	122
Johansson B., 25PO-13-41	781	Kameneva M.Yu., 21PO-16-43	139
Johnson R.D., 24PO-7-17	632	Kamentsev K.E., 21RP-D-7	51
Johnson R.D., 24TL-A-7	548	Kamilov K.I., 24PO-7-16	631
Jolobova N.N., 23PO-12-5	510	Kammermeier T., 25RP-A-6	701
Jouini N., 24PO-6-14	602	Kamzin A.S., 22PO-8-54	306
Jung J.R., 23TL-A-9	366	Kamzin A.S., 22PO-8-56	308
Jungwirth T., 24TL-A-1	540	Kamzin A.S., 22PO-8-93	344
Jutong N., 21PO-21-21	180	Kamzin A.S., 25PO-13-45	784
<hr/>			
K			
Kabanov V.V., 23PO-1-10	420	Kandaurova G., 25PO-13-39	779
Kabanov Yu., 22PO-8-41	294	Kandaurova G.S., 25PO-13-67	806
Kabanov Yu.P., 22PO-8-27	281	Kanomata T., 24TL-D-3	571
Kaczorowski D., 24RP-A-4	542	Kanomata T., 25PO-13-53	792
Kadomtseva A.M., 24PO-7-16	631	Kantorovich S., 22RP-E-10	237
Kadomtseva A.M., 21TL-D-5	48	Kantorovich S., 22RP-E-11	238
Kadomtseva A.M., 24PO-7-11	625	Kantorovich S.S., 23PO-3-12	457
Kadomtseva A.M., 24PO-7-33	647	Kaplan S.F., 22TL-B-4	200
Kagan M.Yu., 24PO-7-5	620	Kapliencko A.N., 22PO-8-78	330
Kainuma R., 24TL-D-3	571	Karakozov A.E., 21TL-E-4	55
Kaiss A., 24RP-F-7	584	Karamat S., 25PO-13-6	747
Kajnakova M., 24PO-7-3	618	Kardasz B., 21TL-B-3	27
Kakáy A., 23TL-B-7	375	Karimova G.V., 25PO-13-26	766
Kakeshita T., 24TL-D-2	570	Karminskaya T.Yu., 22TL-F-14	253
Kalanda N.A., 24PO-7-41	656	Karnik T., 25TL-D-2	733
Kalandadze L., 23PO-3-19	463	Karoutsos V., 22PO-8-66	319
Kalashnikov V., 23TL-D-3	391	Karpenko B.V., 24PO-7-20	634
Kalashnikova A.M., 21RP-A-2	15	Karpenko S.A., 22PO-8-29	283
Kalashnikova A.M., 21TL-A-1	14	Karpenkov A.Yu., 25PO-13-35	775
Kalinikos B.A., 21PO-16-7	104	Karpenkov D., 25PO-20-6	815
Kalinikos B.A., 21PO-16-8	105	Karpenkov D.Yu., 25PO-13-35	775
Kalinikos B.A., 21PO-16-9	106	Kartashev A., 24PO-7-47	662
Kalinikos B.A., 23PO-12-2	507	Kartashev A.V., 24PO-7-25	639
Kalinin Yu., 22PO-8-26	280	Kartavych A.V., 22RP-A-7	193
Kalinin Yu., 23PO-4-15	492	Kartsev A.I., 23PO-12-21	524
Kalinin Yu., 23PO-4-17	494	Karzanov V.V., 22TL-A-6	192
Kalinin Yu.E., 21PO-16-3	100	Kashevsky B.E., 23PO-3-1	446
		Kashevsky B.E., 23RP-F-2	399
		Kashevsky B.E., 23TL-F-1	398
		Kashevsky S.B., 23RP-F-2	399
		Kaspar T., 25RP-A-6	701
		Kassan-Ogly F.A., 23PO-12-4	509

Kataev V., 22RP-D-8	223	Kharisov A.T., 21PO-16-23	120
Kataeva E.A., 23PO-4-3	480	Kharrasov M.Kh., 21PO-21-4	164
Katagiri K., 22RP-E-4	231	Khartsev S.I., 21PO-16-63	159
Katanin A.A., 22PO-8-82	334	Khartsev S.I., 21PO-2-21	93
Katanin A.A., 23PO-12-20	523	Khartsev S.I., 21TL-A-8	22
Katanin A.A., 24RP-F-10	587	Khartsev S.I., 23TL-C-2	380
Kato K., 23RP-A-6	363	Khatsko E., 24PO-7-64	679
Katok K.K., 22PO-8-10	265	Khizenkov P., 23PO-3-24	468
Katsura Sh., 22RP-E-3	230	Khizenkov P., 23PO-3-25	469
Kaul A., 24PO-7-21	635	Khizriev K.Sh., 23PO-12-13	517
Kaul A., 24PO-7-23	637	Khizriev K.Sh., 24PO-7-30	644
Kaul A.R., 23PO-1-19	428	Khlybov E., 23PO-1-7	417
Kaveev A.K., 22PO-8-11	266	Khodzitskiy M., 21PO-16-50	146
Kaviraj B., 25PO-13-2	743	Khodzitskiy M., 22PO-8-45	298
Kawaji H., 25RP-D-6	738	Khodzitskiy M., 22RP-F-4	242
Kazak N.V., 24PO-7-60	675	Khokhlova M.D., 22RP-B-8	204
Kazakov A.P., 23PO-3-10	455	Khokholkov A.G., 25PO-13-40	780
Kazakov A.P., 23RP-F-7	404	Kholin D., 22PO-8-44	296
Kazakova O., 22TL-B-2	196	Kholkin A.L., 24PO-7-71	686
Kazan S., 22PO-8-12	267	Khomchenko A.S., 22PO-8-49	302
Kazan S., 25RP-C-4	722	Khomchenko V.A., 24PO-7-71	686
Kazantzeva V.V., 25PO-13-28	768	Khomenko E.V., 23PO-4-24	500
Kazei Z.A., 21PO-16-43	139	Khomenko E.V., 25PO-13-31	771
Kazhan V.A., 23PO-3-27	472	Khomskii D.I., 24PO-7-50	665
Kazin P.E., 25PO-13-1	742	Khomskii D.I., 25TL-A-1	696
Kehrle J., 22RP-F-9	249	Khovailo V., 23TL-D-3	391
Keimer B., 23PO-12-8	512	Khovailo V., 25PO-20-16	824
Kenjaev A.M., 23PO-12-29	532	Khovailo V.V., 25PO-20-9	818
Kenjaev Z.M., 23PO-12-29	532	Khovaylo V., 25PO-20-6	815
Kettemann S., 23PO-12-11	515	Khripunov D.M., 24PO-6-1	590
Khabarov I., 24PO-7-29	643	Khusainov A.T., 21PO-21-4	164
Khaibullin R., 22PO-8-57	310	Khusainov M., 23PO-1-6	416
Khaibullin R., 22RP-A-8	194	Khusainov M.G., 22RP-F-12	251
Khaibullin R.I., 24PO-6-1	590	Khusainov M.G., 22RP-F-13	252
Khaibullin R.I., 25RP-C-4	722	Khusainov M.G., 23PO-1-1	412
Khaibutdinova I., 23PO-12-6	510	Khusainov M.G., 23PO-1-5	415
Khaibutdinova I., 23PO-12-7	511	Khusainov M.M., 23PO-1-5	415
Khaidukov Yu.N., 21RP-B-6	30	Khvalkovskiy A.V., 23PO-4-14	491
Khaidukov Yu.N., 23PO-1-9	419	Khvalkovskiy A.V., 23PO-4-20	496
Khalfina A.A., 21PO-16-22	119	Khvalkovskiy A.V., 24RP-B-8	558
Khan M., 24RP-D-7	574	Khvalkovskiy A.V., 24RP-B-9	559
Khan M., 25PO-20-6	815	Kikoin K., 22PL-A-2	185
Khanikaev A., 22RP-B-9	205	Kilanski L., 25RP-A-3	698
Khanikaev A.B., 21PO-2-14	86	Kildishev A.V., 21TL-A-5	20
Khanikaev A.B., 22RP-B-5	201	Kim Cheol Gi, 23TL-A-9	366
Khanikaev A.B., 22RP-B-6	202	Kim D.-H., 21TL-B-7	31
Khanin V.V., 23PO-3-26	470	Kim Dojin, 25RP-A-4	699
Khanov L.N., 25PO-20-9	818	Kim J., 22RP-B-6	202
Khapaeva T.M., 23PO-1-21	430	Kim J., 23RP-A-3	358
Khapaeva T.M., 24PO-7-41	656	Kim K.S., 23RP-B-9	376
Khapaeva T.M., 25RP-A-3	698	Kim K.W., 23TL-A-9	366
Kharebov P.V., 22PO-8-68	320	Kim P.D., 22PO-8-29	283

Kim P.D., 24PO-7-12	626	Kohara T., 22RP-F-8	248
Kim Sang-Koog, 25TL-C-1	720	Kohn K., 21TL-D-6	50
Kim Sung-Soo, 21PO-16-52	148	Kokorin V.V., 24TL-D-4	572
Kim Sun-Hong, 21PO-16-52	148	Kokorina E.E., 25RP-C-7	727
Kimel A.V., 21PO-2-1	74	Koksharov Yu.A., 21PO-21-17	176
Kimel A.V., 21RP-A-2	15	Koksharov Yu.A., 21PO-21-9	169
Kimel A.V., 21TL-A-1	14	Koledintseva M., 23RP-C-7	387
Kimel A.V., 22TL-B-4	200	Koledov V., 23TL-D-3	391
Kimmel G., 25PO-20-1	810	Koledov V., 25PO-20-16	824
Kimura H., 21TL-D-6	50	Koledov V., 25PO-20-6	815
Kirik S.D., 22PO-8-49	302	Koledov V.V., 25PO-20-3	812
Kirilyuk A., 21PO-2-1	74	Koledov V.V., 25PO-20-9	818
Kirilyuk A., 21RP-A-2	15	Kolesnik I.V., 22PO-8-97	348
Kirilyuk A., 21TL-A-1	14	Kolesnikov A.A., 23TL-C-3	381
Kirilyuk A., 22TL-B-4	200	Kolezhuk A.K., 22RP-D-7	222
Kirov S.A., 22PO-8-61	314	Kolmakova N.P., 24PO-7-63	678
Kiryukhin V., 22TL-D-5	221	Kolmychek I.A., 21PO-2-18	90
Kisel V., 23TL-C-1	380	Kolotov O.S., 21PO-16-41	137
Kiselev N., 24PO-6-20	608	Kolovos-Vellianitis D., 24RP-A-3	541
Kiseleva T.Yu., 25PO-13-43	782	Komarov E.N., 23RP-F-4	401
Kisielewski M., 22PO-8-62	315	Komarova M.A., 22PO-8-81	333
Kislinskii Y.V., 23PO-1-8	418	Komarova M.A., 25RP-C-5	723
Kitanovski A., 23RP-D-6	393	Komissarova L.Kh., 21PO-21-2	163
Kitanovski A., 23TL-D-4	392	Komissinskiy P.V., 23PO-1-8	418
Kizirgulov I.R., 21PO-21-4	164	Komogortsev S.V., 22PO-8-23	277
Klabukov A.A., 24PO-7-51	666	Komogortsev S.V., 22PO-8-31	284
Klauss H.-H., 22RP-D-8	223	Komogortsev S.V., 22PO-8-34	287
Klauss H.H., 25RP-D-8	739	Komogortsev S.V., 22PO-8-46	299
Klein O., 23PO-4-13	490	Komogortsev S.V., 22PO-8-49	302
Kleiner R., 21RP-F-11	71	Komogortsev S.V., 22PO-8-71	323
Kleinerman N.M., 25PO-13-12	752	Komogortsev S.V., 22PO-8-71	323
Kleinerman N.M., 25PO-13-46	785	Komogortsev S.V., 25PO-13-10	750
Kleinerman N.M., 25PO-13-5	746	Komogortsev S.V., 25PO-13-29	769
Kleinerman N.M., 25PO-13-57	796	Kondrashov A.V., 21PO-16-9	106
Klesheva S.M., 21PO-16-42	138	Koneracká M., 23PO-3-3	448
Klimin S.A., 22PO-8-13	268	Koneracká M., 23RP-F-10	407
Klimin S.A., 22PO-8-95	346	Kong L.B., 22TL-C-6	213
Klimov A.A., 24PO-7-19	634	Konoplyuk S.M., 24TL-D-4	572
Klimov A.Yu., 22PO-8-84	336	Konovalenko A., 23PO-4-18	495
Klimov A.Yu., 22PO-8-91	342	Konygin G.N., 21PO-16-24	121
Klingeler R., 21PO-2-5	78	Kopčanský P., 23PO-3-3	448
Klingeler R., 22RP-D-8	223	Kopčanský P., 23RP-F-10	407
Klingeler R., 23PO-1-15	424	Kopcewicz M., 24PO-7-71	686
Klingeler R., 24PO-7-66	681	Koptev V.P., 23RP-F-4	401
Klyuchnik A.V., 23TL-C-3	381	Korableva S.L., 25PO-13-25	765
Knupfer M., 22RP-D-8	223	Korenivski V., 23PO-4-18	495
Knyazev Yu.V., 25PO-13-55	794	Korolev A., 22PO-8-44	296
Kobyakov A.V., 22PO-8-33	286	Korolev A.V., 24PO-7-57	672
Kocharian A.N., 24TL-F-2	580	Koroleva L.I., 23PO-1-21	430
Kochura A.V., 24PO-6-17	605	Koroleva L.I., 24PO-7-41	656
Koelle D., 21RP-F-11	71	Koroleva L.I., 25RP-A-3	698
Koga M., 23RP-A-3	358	Korolyov A., 25PO-13-19	759
		Korolyov A.V., 25PO-13-59	798

Korotin M., 25PO-20-12	821	Krichevtsov B.B., 21PO-2-3.....	76
Korotkov N.M., 24PO-7-34.....	648	Krichevtsov B.B., 22PO-8-11.....	266
Korovin V.M., 23PO-3-27.....	472	Krikunov A.I., 24TL-B-5	556
Korshak A.B., 24PO-7-46	661	Krinitcina T., 22PO-8-41	294
Korshunov A., 22PO-8-94.....	345	Krishnan K.M., 25RP-A-7.....	702
Korshunov A.S., 24PO-7-42	657	Krivorotov I.N., 21TL-B-1	26
Korshunov M.M., 25RP-C-7	727	Krivoruchko V.N., 23PO-4-4	481
Korzniikova G.F., 25PO-13-27	767	Kruesubthaworn A., 21PO-21-5.....	165
Koshkid'ko Yu., 25PO-20-6.....	815	Krug von Nidda H.-A., 22RP-D-9.....	224
Koshkid'ko Yu.S., 25PO-13-35	775	Krug von Nidda H.-A., 24PO-7-38	653
Koshkid'ko Yu.S., 25PO-20-7	816	Krutikova E.V., 22RP-E-9.....	236
Kositsyna I.I., 25PO-13-49.....	788	Krzymanska B., 25RP-A-3.....	698
Kostenko V.I., 21PO-16-12.....	109	Kuch W., 21TL-B-4.....	28
Kostenko V.I., 21PO-16-13.....	110	Kuchin A.G., 25PO-13-55.....	794
Kostylev M.P., 23RP-B-3.....	369	Kuchin D., 23TL-D-3	391
Kostyuchenko V.V., 22PO-8-35.....	288	Kuchin D., 25PO-20-16	824
Kostyuchenko V.V., 22PO-8-67	319	Kudakov A.D., 21PO-21-20.....	179
Kotov L.N., 21PO-16-1	98	Kudasov Yu., 22PO-8-30	283
Kotov L.N., 21PO-16-11	108	Kudasov Yu., 22PO-8-94	345
Kotov L.N., 21PO-16-3	100	Kudasov Yu.B., 22PO-8-92.....	343
Kotov L.N., 21PO-16-5	102	Kudasov Yu.B., 24PO-7-42.....	657
Kotov L.N., 21PO-16-6.....	103	Kudrevatikh N.V., 22PO-8-24.....	278
Kotov L.N., 22PO-8-8	263	Kudrevatykh N.V., 25PO-13-17.....	757
Kotov L.N., 25PO-13-3	744	Kudrewcev V.O., 25PO-13-37	777
Kotov S.A., 23RP-F-4	401	Kudrin A., 23PO-4-15	492
Kotov V., 21PO-2-15	87	Kudrin A.V., 24PO-6-8	597
Kotov V.A., 21PO-2-22.....	94	Kudryavcev D.N., 23PO-3-10.....	455
Kotov V.A., 22RP-F-2.....	240	Kudryavcev V.O., 21PO-16-26	123
Koudinov A.V., 25RP-A-2	697	Kudryavcev V.O., 21PO-16-27	124
Koumoto K., 22RP-E-4	231	Kuerten K.E., 21TL-E-5.....	56
Kourov N.I., 25PO-13-55.....	794	Kugel K.I., 24PO-7-5.....	620
Kourov N.I., 25PO-13-57	796	Kugel K.I., 24PO-7-50	665
Kováč J., 23PO-3-3	448	Kugel K.I., 24TL-A-6.....	547
Kovacs E., 21TL-E-5.....	56	Kuklin A.I., 22RP-E-7.....	234
Kovalev A.V., 21PO-21-12	172	Kuklin A.I., 23PO-3-17	462
Kovalev B.B., 24PO-6-11	600	Kuklin A.I., 23PO-3-9	454
Kovalev V.I., 22RP-F-5.....	243	Kulagin D., 21PO-2-15.....	87
Kovalev Yu.S., 23PO-3-9.....	454	Kulakovski V.D., 24PO-6-4	593
Kovaleva N.N., 23PO-12-8.....	512	Kulakowski K., 25RP-B-8.....	715
Koyama K., 25PO-13-53	792	Kulatov E., 23PO-4-16	493
Koyama T., 22RP-F-8	248	Kulatov E., 24TL-F-5	583
Kozeeva L.P., 21PO-16-43.....	139	Kulatov E., 25RP-C-8.....	728
Kozhevnikov V.L., 24PO-7-26	640	Kulatov E.T., 23PO-12-23.....	526
Kozlov A.I., 22PO-8-24	278	Kulbachinskii V., 24PO-6-7	596
Kozlov A.I., 25PO-13-17	757	Kulkarni J., 22TL-B-2	196
Kozlova L.E., 24TL-D-4	572	Kulkova S., 23PO-4-10.....	487
Kozlovskii L.V., 22PO-8-81	333	Kulkova S.E., 25PO-13-42.....	781
Krasnikov V., 22TL-D-2	218	Kumal A., 23TL-A-9.....	366
Kreines N., 22PO-8-44	296	Kumar S., 21PO-16-62.....	158
Krekhova M., 23PO-3-8	453	Kunikin S.A., 23PO-3-7	451
Krekhova M., 23RP-F-8.....	405	Kunkova Z.E., 22RP-F-5	243
Kreyssig A., 25PO-13-15	755	Kupriyanov D., 21PO-21-10	170

Kupriyanov D.A., 23PO-3-6.....	450	Lagarkov A.N., 23RP-C-6.....	386
Kupriyanov M.Yu., 22TL-F-14.....	253	Lagarkov A.N., 23TL-C-4.....	384
Kupriyanov M.Yu., 23PO-1-20.....	429	Lagutin A.S., 24PO-6-18.....	606
Kupriyanova G., 23PO-4-25.....	501	Lagutin A.S., 24TL-A-2.....	540
Kurbakov A.I., 24PO-7-7.....	621	Lagutin A.S., 25RP-A-11.....	705
Kurbatova Yu.N., 25RP-B-5.....	712	Lahderanta E., 24PO-6-17.....	605
Kurde J., 21TL-B-4.....	28	Laiho R., 24PO-6-17.....	605
Kurdyukov D.A., 22TL-B-4.....	200	Laiho R., 24TL-A-2.....	540
Kurita H., 22RP-E-3.....	230	Laiho R., 25RP-A-11.....	705
Kurkin I.N., 25PO-13-25.....	765	Laipanov U.M., 21PO-21-3.....	164
Kurkin M.I., 21PO-2-8.....	81	Laletin O.N., 24PO-7-13.....	627
Kurkin M.I., 22PO-8-28.....	282	Lamonova K., 25RP-D-8.....	739
Kurlyandskaya G.V., 21PO-16-56.....	152	Lapsheva E., 24PO-7-66.....	681
Kurlyandskaya G.V., 21PO-16-60.....	156	Laptyeva T.V., 21PO-2-22.....	94
Kurlyandskaya G.V., 22PO-8-65.....	318	Larin V., 25RP-B-4.....	711
Kurlyandskaya G.V., 23TL-A-8.....	365	Lashkul A., 24PO-6-17.....	605
Kurmaev E.Z., 23PO-1-27.....	437	Lashkul A., 24TL-A-2.....	540
Kushnir V.N., 23PO-1-20.....	429	Lashkul A., 25RP-A-11.....	705
Kusmartsev F.V., 21TL-E-5.....	56	Lattermann G., 23PO-3-8.....	453
Kusrayev Yu.G., 25RP-A-2.....	697	Lattermann G., 23RP-F-8.....	405
Kutko K.V., 22PO-8-78.....	330	Laureti S., 21TL-B-2.....	27
Kuvandikov O.K., 24PO-7-77.....	692	Laval J.Y., 24PO-7-2.....	617
Kuz'min Yu.I., 25PO-13-55.....	794	Le Graet C., 23PO-1-34.....	442
Kuzemsky A.L., 23PO-4-1.....	478	Lebedinski Yu., 23PO-4-21.....	497
Kuzmenko A.M., 24PO-7-33.....	647	Lecante P., 22PO-8-16.....	270
Kuzmenko A.M., 24PO-7-11.....	625	Lee C.G., 25PO-13-21.....	761
Kuzmin A., 24PO-6-5.....	594	Lee D.H., 23RP-B-9.....	376
Kuzmin M., 23RP-D-5.....	393	Lee Ki-Suk, 25TL-C-1.....	720
Kuznetsov A., 24PO-6-25.....	613	Lee P., 25PO-13-6.....	747
Kuznetsov A.R., 25PO-13-12.....	752	Lee S., 22TL-D-5.....	221
Kuznetsov A.V., 24PO-7-20.....	634	Lee S.-H., 21TL-B-7.....	31
Kuznetsov E.A., 21PO-16-42.....	138	Lee S.I., 23PO-1-25.....	434
Kuznetsov I.A., 25PO-13-60.....	799	Lee Y.P., 22RP-F-6.....	244
Kuznetsov M., 22TL-B-7.....	203	Lehndorff R., 23TL-B-7.....	375
Kuznetsov N., 24PO-6-7.....	596	Leighton C., 21TL-B-1.....	26
Kuznetsov P.A., 21PO-16-36.....	132	Leiste H., 25TL-D-1.....	732
Kuznetsova T., 25PO-20-12.....	821	Leksikov A., 23PO-4-13.....	490
Kuznetsova T.V., 23PO-1-24.....	433	Lemmens P., 22PO-8-37.....	290
Kuzovnikova L.A., 25PO-13-29.....	769	Lemmens P., 25RP-D-8.....	739
Kvardakov V.V., 23PO-4-11.....	488	Len E.G., 23PO-4-5.....	482
Kveglis L.I., 25PO-13-28.....	768	Leone Ph., 24PO-6-14.....	602
<hr/>			
L		Leonyuk N.I., 21PO-2-5.....	78
Labarta A., 22TL-B-3.....	198	Leskova J.V., 24PO-7-45.....	660
Labrune M., 22PO-8-90.....	341	Leskova Y.V., 24PO-7-44.....	659
Lacroix C., 24TL-F-1.....	580	Lesnikov V.P., 22TL-A-6.....	192
Ladieu F., 23RP-F-5.....	401	Lesnikov V.P., 24PO-6-18.....	606
Ladygina V.P., 23PO-3-4.....	449	Levchenko A., 24PO-6-25.....	613
Lagarkov A., 23TL-C-1.....	380	Levchenko A.V., 25PO-13-63.....	802
		Levchuk S.A., 22TL-A-6.....	192
		Levshin N.L., 21PO-21-20.....	179
		Levy M., 21PO-2-17.....	89
		Levy M., 21TL-A-6.....	20

Maljuk A., 24PO-7-65	680	McMichael R.D., 22PO-8-27.....	281
Malkin B.Z., 25PO-13-25	765	Medvedeva I.V., 25PO-13-44.....	783
Malov S.N., 25PO-13-38.....	778	Medvedeva I.V., 25PO-13-55.....	794
Maltsev V.N., 23PO-12-9.....	513	Mehmood N., 21TL-D-4.....	48
Mamedov T.N., 23RP-F-4.....	401	Meilikhov E., 22PO-8-83	335
Mamin R.F., 24PO-7-10	624	Mel'nikov A.S., 22RP-F-11.....	251
Manchon A., 23PL-A-1	352	Melenev P.V., 23PO-3-23	467
Mankov Yu.I., 21PO-16-16.....	113	Melikhov Y., 23PO-4-4	481
Mankov Yu.I., 24TL-F-3	581	Melkov G.A., 22TL-C-2.....	209
Mañosa L., 23TL-D-1.....	390	Melnikov A., 21TL-A-4	17
Mantovan R., 23PO-4-21.....	497	Melnikov N.B., 23PO-12-26.....	529
Manuilov S.A., 21PO-16-63.....	159	Melnikov O., 24PO-7-21	635
Marcilhac B., 21TL-C-6	40	Melnikov O., 24PO-7-23	637
Marenkin S.F., 24PO-6-17.....	605	Melnikov O.V., 24PO-7-30	644
Marenkin S.F., 25RP-A-3	698	Melnikov V.A., 25RP-C-5.....	723
Marennyy A.M., 23PO-12-1	506	Melnyk I.M., 23PO-4-5	482
Marennyy M.A., 23PO-12-10.....	514	Men'shenin V.V., 24PO-7-74.....	689
Margeat O., 23RP-B-2.....	369	Mennicke R.T., 23TL-A-1.....	356
Mariette H., 23PO-4-16	493	Menshov V.N., 23PO-12-23.....	526
Mariotto G., 24PO-6-5.....	594	Merenkov D.N., 22PO-8-76	328
Markelova M., 24PO-7-23.....	637	Meriakri V.V., 21PO-16-62.....	158
Markin P.E., 22PO-8-24	278	Merkulov A.L., 23TL-C-3	381
Markin P.E., 25PO-13-17	757	Merkulova S.P., 23TL-C-3	381
Markin P.E., 25PO-20-14	822	Mertelj T., 25RP-D-5.....	737
Markina M., 23PO-1-26	436	Merzlikin A.M., 21PO-2-10	82
Markosyan A.S., 24PO-6-19	607	Merzlikin A.M., 22RP-B-5.....	201
Markosyan A.S., 24PO-6-3	592	Merzlikin A.M., 22RP-F-1	240
Martin C., 24PO-7-7	621	Merzlikin A.M., 22RP-F-3	241
Martin I., 23PO-1-30	440	Merzlikin A.M., 22RP-F-4	242
Martin T., 22RP-C-8.....	215	Meshcheryakov V., 22PO-8-39.....	292
Marty A., 24PL-A-1	536	Meshcheryakov V.F., 22PO-8-99.....	350
Martynov S.N., 23PO-12-17.....	521	Meshcheryakov V.F., 25PO-13-13.....	753
Masaki S., 21PO-21-13.....	173	Meshkov G., 24PO-7-31	645
Maslennikov Yu.V., 23PO-3-26.....	470	Mestier N., 23PL-A-1	352
Maslov D., 22PO-8-30.....	283	Mezenkov N.A., 21PO-21-20.....	179
Maslov D., 22PO-8-94.....	345	Michel C.R., 24PO-7-60.....	675
Masquelier C., 22RP-D-8	223	Michel K.H., 24PO-7-6.....	621
Mastin A.A., 21PO-16-37.....	133	Michelini F., 23PO-4-16	493
Masuda Y., 23RP-A-3	358	Miguel J., 21TL-B-4	28
Matsuda A., 22RP-E-4.....	231	Mihailovic D., 25RP-D-5	737
Matsuki H., 21RP-F-8.....	68	Mikhailov F.A., 25RP-C-4	722
Matsumoto K., 25PO-13-25	765	Mikhailov G.G., 25PO-20-9.....	818
Matthew J.A.D., 23TL-A-1	356	Mikhailov S.G., 24PO-6-17.....	605
Matyunin A.V., 21PO-16-41	137	Mikhailova M.P., 24RP-A-4.....	542
Maximova G.V., 22PO-8-81	333	Mikheev M.G., 24PO-6-11	600
Maximova G.V., 25RP-C-5.....	723	Mikirtychyants C.M., 23RP-F-4.....	401
Maydykovskiy A.I., 21PO-2-17	89	Mill B.V., 22PO-8-13	268
Mazalov L., 24PO-6-20	608	Mill B.V., 24PO-6-13	601
Mazilkin A.A., 25RP-A-10.....	705	Milyaev M., 22PO-8-41	294
Mazov L.S., 23PO-1-11.....	421	Milyaev M., 22PO-8-44.....	296
Mazzoli C., 24TL-A-7	548	Milyaev M., 23RP-A-2	357
McCord J., 22TL-C-5	212	Milyaev O.A., 25PO-13-17	757

Napolsky K., 21PO-2-4	77	Nikitushkin D.S., 22PO-8-84.....	336
Narozhnyi V.N., 23PO-1-12.....	422	Nikolaev A., 24PO-7-31	645
Narozhnyy M.V., 22PO-8-13	268	Nikolaev A.V., 24PO-7-6	621
Nasimov Kh.M., 24PO-7-77.....	692	Nikolaev I., 23PO-3-24.....	468
Nateghi S., 22PO-8-14.....	268	Nikolaev I., 23PO-3-25.....	469
Nath R., 24PO-7-76	691	Nikolaev S.N., 24PO-6-18.....	606
Naumov S., 24PO-7-4.....	619	Nikolaeva E., 24PO-7-31	645
Naumov S., 24PO-7-67.....	682	Nikolova E.P., 22PO-8-78	330
Navas D., 23TL-B-1	368	Nikulina V., 23PO-3-24.....	468
Nazarov V.N., 21PO-16-21.....	118	Nikulina V., 23PO-3-25.....	469
Nechaeva O.A., 23PO-3-13	458	Nishihara H., 24TL-D-3	571
Nedukh S., 21PO-16-50.....	146	Nishio N., 21PL-A-2.....	11
Nedviga A.S., 25PO-13-61	800	Nitta J., 21TL-C-5.....	39
Nefedov A., 22RP-A-8	194	Nizhankovskii V., 24RP-A-4.....	542
Nefedov I.M., 21PO-16-4.....	101	Nizola A.A., 22PO-8-24	278
Negulyaev N.N., 22PO-8-87	339	Noda K., 21PO-21-13	173
Nekrasov I.A., 25PO-13-55	794	Noda Y., 21TL-D-6.....	50
Nekrasov I.A., 25RP-C-7.....	727	Nogues J., 21TL-B-1	26
Nekvasil V., 24RP-A-9.....	550	Nomerovannaya L.V., 24PO-7-27.....	641
Netsvetov M., 23PO-3-24.....	468	Noskov F.M., 25PO-13-28	768
Netsvetov M., 23PO-3-25.....	469	Nosov A., 24PO-7-14	629
Neumann K.-U., 24TL-D-3	571	Nosov L.S., 21PO-16-5	102
Neumann M., 24PO-7-22	636	Nosov L.S., 21PO-16-6	103
Ney A., 25RP-A-6	701	Noudem J., 24PO-7-2	617
Ney V., 25RP-A-6	701	Novakova A.A., 22PO-8-69	321
Nguyen Chau, 24PO-7-12	626	Novakova A.A., 25PO-13-43	782
Nicolodi S., 24PO-6-8	597	Novitskii N., 22PO-8-39.....	292
Niedoba H., 22PO-8-90	341	Novitskii N., 22PO-8-45.....	298
Nikanorova I.A., 25PO-13-4	745	Novitskii N.N., 21PO-16-2.....	99
Nikiforov A., 24PO-7-35.....	649	Novitskii N.N., 23RP-B-3	369
Nikiforov A.E., 24PO-7-44	659	Novokshonov S.G., 23PO-4-26.....	502
Nikiforov A.E., 24PO-7-45	660	Novosad V.A., 22PO-8-76.....	328
Nikiforov V.N., 22PO-8-3	258	Novoselov K.S., 21RP-F-5	64
Nikitenko V.I., 22PO-8-27	281	Novotortsev V.M., 25RP-A-3.....	698
Nikitenko V.I., 22PO-8-40.....	293	Nurgazizov N., 22PO-8-62	315
Nikitenko V.I., 25RP-B-6.....	713	Nuzhdin V.I., 24PO-6-1.....	590
Nikitenko Yu.V., 21RP-B-6	30	Nyavro A.V., 25PO-13-28.....	768
Nikitenko Yu.V., 23PO-1-9.....	419		
Nikitin L.V., 23PO-3-10.....	455		
Nikitin L.V., 23RP-F-7.....	404		
Nikitin M., 21PO-21-10.....	170		
Nikitin M.P., 23PO-3-6	450		
Nikitin N.Yu., 23PO-12-19.....	522		
Nikitin P., 21PO-21-10.....	170		
Nikitin P.I., 23PO-3-6.....	450		
Nikitin S.A., 25PO-13-30	770		
Nikitin S.A., 25PO-13-68	807		
Nikitin S.A., 25PO-20-7.....	816		
Nikitov S.A., 21PO-16-2	99		
Nikitov S.A., 21PO-2-2	75		
Nikitov S.A., 24PO-7-19	634		
Nikitushkin D.S., 22PO-8-5.....	260		

O

Obermeier G., 22RP-F-9.....	249
Oboznov V.A., 22PO-8-6	261
Odenbach S., 23RP-F-9	406
Odintsov B., 24PO-7-23	637
Ogarkov S.L., 24PO-7-5	620
Ogawa T., 22TL-C-3	210
Ohta H., 21PO-16-58.....	154
Ohtani T., 21RP-B-8.....	32
Ohtomo Y., 23RP-A-6.....	363
Oikawa K., 24TL-D-3.....	571

Okamoto N., 23PO-4-19.....	495	Pamyatnykh E.A., 24PO-7-58.....	673
Okhotnikov K.S., 21PO-21-11.....	171	Pamyatnykh L., 25PO-13-39.....	779
Okhotnikov K.S., 22PO-8-20.....	274	Pamyatnykh L.A., 25PO-13-67.....	806
Okhotnikov K.S., 24PO-6-9.....	598	Panas A.I., 24TL-B-5.....	556
Okubo S., 21PO-16-58.....	154	Panchmatia P.M., 21TL-B-4.....	28
Okulov V.I., 24PO-7-58.....	673	Panfilov A.S., 25PO-13-24.....	764
Ol'khovik L.P., 22PO-8-54.....	306	Panina L.V., 24TL-C-4.....	564
Ol'khovik L.P., 22PO-8-56.....	308	Pankov V., 22PO-8-39.....	292
Ollefs K., 25RP-A-6.....	701	Pankratov A.L., 21PO-16-4.....	101
Onan A.G., 25RP-C-4.....	722	Pankratov N.Yu., 25PO-13-30.....	770
Ono T., 23TL-B-8.....	376	Pankrats A., 24PO-7-29.....	643
Opolenko A.A., 25PO-13-68.....	807	Pankrats A., 24PO-7-75.....	690
Oppeneer P.M., 21TL-B-4.....	28	Pankrats A.I., 24PO-7-72.....	687
Orlov A.F., 22RP-A-7.....	193	Pantelides S.T., 25RP-A-7.....	702
Orlov A.F., 24PO-6-6.....	595	Papageorgiou T., 24PO-6-3.....	592
Orlova T.S., 24PO-7-2.....	617	Papaioannou E.Th., 22PO-8-66.....	319
Orue I., 22PO-8-65.....	318	Parchinskiy P.B., 25RP-A-4.....	699
Osipov A., 25PO-13-32.....	772	Pardo V., 24RP-D-9.....	577
Osipov A.V., 21PO-16-24.....	121	Pardo V., 25TL-A-1.....	696
Osipov A.V., 21PO-16-47.....	143	Parfeniev R.V., 24RP-A-4.....	542
Osipov A.V., 23RP-C-6.....	386	Parfenova E.L., 23PO-1-1.....	412
Osipov A.V., 23TL-C-4.....	384	Parker D., 23RP-F-5.....	401
Osipov V.A., 23PO-3-17.....	462	Pärs M., 24PO-6-5.....	594
Ostanin S., 24RP-F-6.....	584	Parshin A.S., 22PO-8-55.....	307
Ott F., 23RP-B-3.....	369	Paruch P., 24TL-B-2.....	553
Ottaviano L., 22TL-B-2.....	196	Pashaev E.M., 23PO-4-11.....	488
Otter M., 22TL-D-2.....	218	Pashchenko M., 22PO-8-37.....	290
Ou Yu, 22TL-C-4.....	211	Pashchenko M.I., 24PO-7-70.....	685
Oubensaïd E.-H., 25PO-13-2.....	743	Pashkevich M., 22PO-8-39.....	292
Ovchinnikov S., 24PO-7-15.....	630	Pashkevich Yu., 22PO-8-37.....	290
Ovchinnikov S.G., 22PO-8-55.....	307	Pashkevich Yu., 25RP-D-8.....	739
Ovchinnikov S.G., 22PO-8-71.....	323	Pastushenkov A.G., 25PO-13-35.....	775
Ovchinnikov S.G., 24PO-7-60.....	675	Pastushenkov Yu.G., 25PO-13-34.....	774
Ovchinnikov S.G., 25RP-C-7.....	727	Pastushenkov Yu.G., 25PO-13-35.....	775
Ovsyannikov G.A., 24PO-7-19.....	634	Pastushenkov Yu.G., 25PO-13-36.....	776
Ovysuannikov G.A., 23PO-1-8.....	418	Pastushenkov Yu.G., 25PO-13-40.....	780
Ozawa T., 23RP-A-6.....	363	Pastushenkov Yu.G., 25PO-20-7.....	816
Ozherelyev V.V., 21PO-21-8.....	168	Pathak A.K., 24RP-D-7.....	574
Ozherelyev V.V., 25PO-13-14.....	754	Patrin G., 22PO-8-58.....	311
<hr/>			
P			
Padilha I.T., 22RP-F-10.....	250	Patrin G., 25PO-13-23.....	763
Paduan-Filho A., 22RP-D-7.....	222	Patrin G.S., 22PO-8-33.....	286
Pahari B., 22PO-8-77.....	329	Patrin G.S., 24PO-7-51.....	666
Paille F., 25TL-D-2.....	733	Patrin G.S., 25PO-13-22.....	762
Palandage K., 24TL-F-2.....	580	Patrin G.S., 25PO-13-48.....	787
Palewski T., 25PO-13-68.....	807	Patrin K.G., 22PO-8-33.....	286
Palvanov P.S., 25PO-13-7.....	747	Patrin K.G., 24PO-7-51.....	666
Palvanov P.S., 25RP-B-7.....	714	Patrusheva T.N., 22PO-8-49.....	302
		Patrusheva T.N., 24PO-7-51.....	666
		Pavlov A.I., 21PO-2-2.....	75
		Pavlov E.S., 21PO-16-2.....	99
		Pavlov V., 22PO-8-94.....	345
		Pavlov V.V., 22TL-B-4.....	200

Pchelkina Z.V., 25RP-C-7	727	Pilugin V.P., 24PO-7-59	674
Pchenichnikov M.S., 22TL-D-2	218	Pimenov A.V., 24PO-7-9	623
Pennycook S.J., 25RP-A-7	702	Piñeiro A., 24RP-D-9	577
Peralagu U., 21RP-F-11	71	Piñeiro A., 25TL-A-1	696
Perekos A.E., 24TL-D-4	572	Piroux L., 22RP-C-7	214
Pérez M.J., 24RP-D-8	575	Pirogov A.N., 25PO-13-17	757
Pérez N., 22TL-B-3	198	Pirogov A.N., 25PO-13-33	773
Pernod P., 21TL-F-7	67	Pirogov Y.A., 23PO-3-6	450
Perov N.S., 22PO-8-69	321	Pirogov Yu., 21PO-21-10	170
Perov N.S., 22RP-A-7	193	Pirota K.R., 22PO-8-75	327
Perov N.S., 23PO-1-9	419	Pirota K.R., 23TL-B-1	368
Perov N.S., 24PO-6-18	606	Pisarev R.V., 21PO-2-1	74
Perov N.S., 24PO-6-6	595	Pisarev R.V., 21PO-2-8	81
Perov N.S., 24PO-6-8	597	Pisarev R.V., 21RP-A-2	15
Perov N.S., 25PO-13-10	750	Pisarev R.V., 21TL-A-7	21
Perov N.S., 25PO-13-59	798	Pisarev R.V., 22TL-B-4	200
Perzynski R., 22RP-E-6	233	Piskorskii V.P., 25PO-13-62	801
Perzynski R., 22TL-E-5	232	Piskunova N.I., 23PO-12-30	532
Perzynski R., 23PO-3-23	467	Planes A., 23TL-D-1	390
Perzynski R., 23RP-F-5	401	Platonov V.V., 24PO-7-42	657
Petit S., 23PL-A-1	352	Plestil J., 22RP-E-7	234
Petit S., 24TL-B-2	553	Ploog K.H., 24RP-A-3	541
Petrakov A.P., 21PO-16-3	100	Poccia N., 24TL-A-5	546
Petrakov A.P., 25PO-13-3	744	Podgornykh S.M., 23PO-1-18	427
Petrakovskaya E.A., 23PO-3-4	449	Podgornykh S.M., 25PO-20-4	813
Petrakovskii G., 24PO-6-21	609	Podlesnyak A., 25PO-20-11	820
Petrakovskii G., 24PO-7-29	643	Podlivaev A., 23PO-1-2	412
Petrakovskii G., 24PO-7-75	690	Podolskii V.V., 22TL-A-6	192
Petrakovskii G., 24PO-7-78	693	Podolskii V.V., 24PO-6-18	606
Petrakovskii G., 25RP-A-5	700	Pogorelov Y.G., 24PO-7-71	686
Petrakovskii G.A., 24PO-6-23	611	Pokatilov V.S., 24PO-7-36	650
Petrakovskii G.A., 24RP-F-9	586	Pokatilov V.S., 24PO-7-37	651
Petrakovskiy G., 24PO-6-20	608	Pokatilov V.S., 25PO-13-20	760
Petrakovskiy G., 25PO-13-64	803	Pokatilov V.S., 25PO-13-65	804
Petrenko A.V., 21RP-B-6	30	Pokatilov V.S., 25PO-13-66	805
Petrenko A.V., 25PO-20-7	816	Pokatilov V.V., 24PO-7-37	651
Petrenko V.I., 23PO-3-29	474	Pokatilov V.V., 25PO-13-65	804
Petrov D., 22PO-8-57	310	Pokatilov V.V., 25PO-13-66	805
Petrov D.A., 21PO-16-24	121	Pokrovskii S., 23PO-1-2	412
Petrov D.A., 21PO-16-39	135	Poleshchikov S.M., 21PO-16-1	98
Petrov D.A., 23RP-C-6	386	Polianski V., 21PO-21-10	170
Petrov V., 24PO-7-68	683	Politova G.A., 25PO-13-68	807
Petrov V.M., 21RP-D-8	52	Poljakov P.I., 21PO-21-1	162
Petrov V.N., 21TL-D-3	45	Polochanina S.V., 22PO-8-31	284
Petrova O.S., 22PO-8-3	258	Polukhin D.S., 23PO-12-12	516
Petrusenko Yu.T., 23PO-1-17	426	Polushkin N.P., 25RP-C-3	721
Petrzhik A.M., 24PO-7-19	634	Polyakov P.A., 21PO-16-41	137
Pfeiffer J., 21RP-F-11	71	Polyakov S., 22PO-8-43	296
Piano S., 24PO-7-18	633	Polyakov S.N., 21PO-21-9	169
Piantek M., 21TL-B-4	28	Polyakov V.V., 22PO-8-60	313
Pichugin N.A., 24PO-6-10	599	Polyakova K.P., 22PO-8-60	313
Pichugin N.A., 24PO-6-11	600	Polyakova K.P., 24PO-7-51	666

Randoshkin V.V., 21PO-16-37.....	133	Romanyuk V.F., 21PO-16-12.....	109
Ranno L., 24PO-7-14.....	629	Romashev L., 22PO-8-41.....	294
Rao K.V., 23RP-A-5.....	362	Romashev L., 22PO-8-44.....	296
Rasch J., 24PO-6-20.....	608	Romashev L., 23RP-A-2.....	357
Rashkeev S., 25RP-A-7.....	702	Romensky M., 23PO-3-25.....	469
Rasing Th., 21PL-A-1.....	10	Ronning F., 22PO-8-7.....	262
Rasing Th., 21PO-2-1.....	74	Rosenfeld E.V., 25PO-13-52.....	791
Rasing Th., 21RP-A-2.....	15	Rosenfeld E.V., 25PO-13-54.....	793
Rasing Th., 21TL-A-1.....	14	Roslyakov I.V., 22PO-8-1.....	256
Rasing Th., 22RP-F-6.....	244	Rosner H., 24PO-7-76.....	691
Rasing Th., 22TL-B-4.....	200	Rossolenko A.N., 22PO-8-6.....	261
Rasing Th., 22TL-B-7.....	203	Rosta L., 22RP-E-8.....	235
Rawat R., 24TL-D-5.....	573	Rosta L., 23PO-3-29.....	474
Rawat R.S., 25PO-13-6.....	747	Rousigné Y., 22RP-C-8.....	215
Razdolski I.E., 21PO-2-17.....	89	Roussigné Y., 22PO-8-36.....	289
Razdolski I.E., 21PO-2-21.....	93	Roussigné Y., 23RP-B-3.....	369
Razdolski I.E., 21TL-A-8.....	22	Roy E., 24PO-7-23.....	637
Razumovskaya O.N., 24PO-7-43.....	658	Rozanov K.N., 21PO-16-24.....	121
Rehberg I., 23RP-F-8.....	405	Rozanov K.N., 21PO-16-39.....	135
Ren Y., 23TL-D-2.....	390	Rozanov K.N., 21PO-16-47.....	143
Repetsky S.P., 23PO-4-5.....	482	Rozanov K.N., 23RP-C-6.....	386
Repina N.M., 25PO-13-18.....	758	Rozanov K.N., 23TL-C-4.....	384
Reser B.I., 23PO-12-26.....	529	Rozhkov A.V., 23PO-12-15.....	519
Revcolevschi A., 22TL-D-2.....	218	Ruban A.V., 24TL-B-1.....	552
Revenko I., 23RP-A-5.....	362	Rudnev I., 23PO-1-2.....	412
Revenko Yu.F., 23PO-4-4.....	481	Rueffer R., 21RP-B-6.....	30
Reznichenko L.A., 24PO-7-43.....	658	Rusakov A.E., 21PO-16-41.....	137
Richard V., 24PO-6-14.....	602	Rusakov V.S., 21PO-21-17.....	176
Richradson J.W., 25PO-20-1.....	810	Rusakov V.S., 21PO-21-9.....	169
Richter K., 25RP-B-4.....	711	Rusakov V.S., 25PO-13-4.....	745
Richter R., 23RP-F-8.....	405	Rusakov V.S., 25PO-13-66.....	805
Rillo C., 23PO-1-16.....	425	Rusakov V.V., 23PO-3-23.....	467
Rinkevich A., 24PO-7-14.....	629	Rusanov A.Yu., 23PO-1-3.....	413
Rinkevich A.B., 21PO-16-42.....	138	Ryabchenko S.M., 22PO-8-38.....	291
Ritter C., 25PO-13-15.....	755	Ryabinkina L.I., 24PO-6-22.....	610
Rivadulla F., 25TL-A-1.....	696	Ryabinkina L.I., 24PO-6-23.....	611
Rivas J., 25TL-A-1.....	696	Ryazanov V.V., 22RP-F-9.....	249
Roca A.G., 22TL-B-3.....	198	Ryazanov V.V., 24PL-A-2.....	536
Rode A.V., 21RP-F-2.....	61	Rykova A., 24PO-7-64.....	679
Rodimin V.E., 24PO-6-19.....	607	Rylkov V.V., 23PO-4-11.....	488
Rodionov A.A., 25PO-13-25.....	765	Rylkov V.V., 24PO-6-18.....	606
Rogalev A., 21TL-D-2.....	44	Rylkov V.V., 24TL-A-2.....	540
Rogalev A., 22PO-8-16.....	270	Rylkov V.V., 25RP-A-11.....	705
Rogalev A., 22PO-8-80.....	332	Ryu Gi-Bong, 21PO-16-52.....	148
Rogalev A., 22RP-A-7.....	193	Ryu K.-S., 21TL-B-7.....	31
Rogalev A., 24PO-6-16.....	604	Ryzhikov I.A., 24RP-C-7.....	567
Rogalev A., 25RP-A-6.....	701	Ryzhikov I.A., 23TL-C-4.....	384
Rogov V.V., 22PO-8-84.....	336	Rzhevsky A.A., 21PO-2-3.....	76
Rogov V.V., 22PO-8-91.....	342		
Rohlov N.I., 25PO-13-31.....	771		
Romanova O.B., 24PO-6-22.....	610		
Romanova O.B., 24PO-6-23.....	611		

S

Sablina K., 24PO-7-47	662	Sanvito S., 24PO-6-12	601
Sablina K., 24PO-7-75	690	Sanyal B., 21TL-B-4	28
Sablina K., 24PO-7-78	693	Sapega V.F., 24RP-A-3	541
Sablina K., 25RP-A-5	700	Sapelkin A., 22RP-A-7	193
Sablina K.A., 24PO-7-25	639	Sapozhnikov M.V., 22TL-A-6	192
Sablina K.A., 24PO-7-72	687	Sapozhnikov M.V., 24PO-6-8	597
Saburova R., 23PO-12-6	510	Sapronova N., 24PO-7-78	693
Saburova R., 23PO-12-7	511	Saraikin V.V., 22RP-A-7	193
Sadeghi S., 22PO-8-14	268	Sarkar D., 23PO-4-8	485
Sadykov S., 25PO-13-32	772	Sarychev A.K., 24TL-C-3	563
Saito H., 21TL-C-1	36	Sasage K., 23PO-4-19	495
Saitoh E., 23PO-4-19	495	Sasaki S., 24TL-D-3	571
Sakuma H., 23RP-B-4	370	Sato F., 21RP-F-8	68
Salakhitdinova M.K., 24PO-7-77	692	Sato M., 21PO-16-35	131
Saletsky A.M., 22PO-8-87	339	Sato Turtelli R., 21TL-D-4	48
Saletsky A.M., 22PO-8-96	347	Savchenko A., 21PO-2-15	87
Samarin N., 23PO-4-22	498	Savelieva O.A., 24PO-6-10	599
Samarin N., 23PO-4-9	486	Savina Yu.A., 22PO-8-76	328
Samarin N., 24PO-6-25	613	Savinkov A.V., 25PO-13-25	765
Samarin N.A., 21PO-16-58	154	Savu D., 23PO-3-9	454
Samarin N.A., 22PO-8-85	337	Savu S., 23PO-3-9	454
Samoilenkov S.V., 23PO-1-19	428	Sazanova L.A., 24PO-7-24	638
Samoilovich M.I., 21PO-16-42	138	Sboychakov A.O., 23TL-C-4	384
Samoilovich M.I., 21PO-2-9	82	Sboychakov A.O., 24PO-7-5	620
Samsonova V.V., 21PO-16-59	155	Sboychakov A.O., 24PO-7-50	665
Samsonova V.V., 23TL-C-4	384	Sboychakov A.O., 24TL-A-6	547
Sanchez Llamazares J.L., 23TL-D-7	394	Scarfato A., 24PO-7-18	633
Sánchez Llamazares J.L., 24RP-D-8	575	Scheglov M., 24PO-7-53	668
Sánchez Llamazares J.L., 24RP-D-9	577	Scheglov M., 24PO-7-54	669
Sánchez Llamazares J.L., 25PO-20-16	824	Scherbachev K.D., 22RP-A-7	193
Sánchez Llamazares J.L., 25RP-B-9	716	Schmitz R., 23RP-F-3	400
Sanchez M.L., 23TL-D-7	394	Schneider C.M., 21PO-2-3	76
Sánchez-Marcos J., 24RP-D-9	577	Schneider C.M., 23TL-B-7	375
Sandhu A., 21PL-A-2	11	Schreck M., 22RP-F-9	249
Sandratskii L.M., 21TL-E-7	58	Schreyer A., 22RP-E-7	234
Sandre O., 22RP-E-6	233	Schrom G., 25TL-D-2	733
Sandre O., 22TL-E-5	232	Schuhl A., 23TL-B-6	374
Sa-ngiamsak C., 21PO-21-23	182	Schuller I.K., 21TL-B-1	26
Sanina V.A., 24PO-7-53	668	Schütz G., 25RP-A-10	705
Sanina V.A., 24PO-7-54	669	Schweizer J., 25PO-13-33	773
Sanina V.A., 25RP-D-6	738	Sedova M.V., 24RP-C-7	567
Sannikov D.G., 21PO-16-48	144	Seemann K., 25TL-D-1	732
Santos J.D., 23TL-D-7	394	Seki T., 21TL-C-5	39
Santos J.D., 24RP-D-8	575	Selemir V.D., 24PO-7-42	657
Santos J.D., 25PO-20-16	824	Selivanova E.M., 21PO-16-33	129
Santos J.D., 25RP-B-9	716	Semeno A.V., 21PO-16-57	153
Sanvito S., 21TL-C-2	37	Semeno A.V., 21PO-16-58	154
		Semeno A.V., 22PO-8-85	337
		Semenov A.L., 25PO-13-37	777
		Semenov A.L., 25PO-13-38	778
		Semenova E.M., 25PO-13-34	774
		Semenova E.M., 25PO-13-40	780

Semenova E.M., 25PO-20-7	816	Shavrov V., 25PO-20-6	815
Semenova O.R., 23PO-3-22	466	Shavrov V.G., 21PO-16-11	108
Semenova Yu.S., 24TL-D-4	572	Shavrov V.G., 21PO-2-22	94
Sementsov D.I., 21PO-16-48	144	Shavrov V.G., 25PO-20-3	812
Semin S., 22TL-B-7	203	Shavrov V.G., 25PO-20-9	818
Semirov A.V., 21PO-16-26	123	Shcheglov V.I., 21PO-16-38	134
Semirov A.V., 21PO-16-27	124	Shcheglov V.I., 21PO-16-49	145
Semirov A.V., 25PO-13-37	777	Shcheglov V.I., 21PO-16-53	148
Semirov A.V., 25PO-13-38	778	Shcheglov V.I., 21PO-16-54	150
Semisalova A.S., 22RP-A-7	193	Shchegoleva N.N., 25PO-13-47	786
Semisalova A.S., 24PO-6-8	597	Shcherbakov G.V., 23RP-F-4	401
Senina V.A., 22PO-8-15	269	Shchurova L., 24PO-6-7	596
Senina V.A., 22PO-8-17	271	Sheftel E.N., 25PO-13-10	750
Senina V.A., 22PO-8-18	272	Sheftel E.N., 25PO-13-9	749
Seong-Cho Yu, 24PO-7-12	626	Shcheglov V.I., 21PO-16-11	108
Seredkin V., 22PO-8-57	310	Shein I.R., 24PO-7-26	640
Seredkin V.A., 22PO-8-60	313	Shepeta N.A., 21PO-16-20	117
Sergeeva N., 23PO-1-34	442	Sherstobitova E.A., 25PO-13-33	773
Sergeeva N., 23PO-4-12	489	Shevelkov A.V., 24PO-6-9	598
Serikov V.V., 25PO-13-12	752	Shi Puji, 24RP-D-6	574
Serikov V.V., 25PO-13-46	785	Shilov V.E., 23PO-12-16	520
Serikov V.V., 25PO-13-5	746	Shilova E.V., 23PO-12-16	520
Serikov V.V., 25PO-13-57	796	Shima H., 21TL-C-7	41
Serna C.J., 22TL-B-3	198	Shimada Y., 22TL-C-1	208
Sese J., 22PO-8-71	323	Shin S.-C., 21TL-B-7	31
Shabalin M., 21PO-16-18	115	Shipkova I., 22PO-8-45	298
Shadrin A.V., 23PO-1-8	418	Shirakashi J., 21RP-B-9	33
Shakarov X.O., 24PO-7-77	692	Shiryaev S.V., 22TL-D-4	220
Shakhov M.S., 24PO-6-17	605	Shitov A.A., 24PO-7-69	684
Shalaev V.M., 21TL-A-5	20	Shitsevalova N., 23PO-4-22	498
Shalyapin A.L., 23PO-12-3	508	Shitsevalova N., 23PO-4-9	486
Shalygin A.N., 21PO-16-15	112	Shitsevalova N., 24PO-6-25	613
Shalygin A.N., 21PO-16-39	135	Shitsevalova N.Yu., 21PO-16-57	153
Shalygin A.N., 22PO-8-81	333	Shitsevalova N.Yu., 21PO-16-58	154
Shalygin A.N., 25RP-C-5	723	Shitsevalova N.Yu., 23PO-4-23	499
Shalygina E.E., 22PO-8-81	333	Shitsevalova N.Yu., 23PO-4-6	483
Shalygina E.E., 25RP-C-5	723	Shitsevalova N.Yu., 23PO-4-7	484
Shamonina E., 24RP-C-8	567	Shitsevalova N.Yu., 25PO-13-24	764
Shamonina E., 24TL-C-5	565	Shitsevalova N.Yu., 25PO-13-63	802
Shamsutdinov M.A., 21PO-16-22	119	Shkurenko A.V., 25PO-13-4	745
Shamsutdinov M.A., 21PO-16-23	120	Shkurenko A.V., 25PO-13-66	805
Shamsutdinov M.A., 21PO-16-21	118	Shkvarin A.S., 23PO-1-27	437
Shamsutdinov M.A., 21PO-16-25	122	Shlimak I., 22TL-A-3	189
Shapaeva T.B., 25RP-B-5	712	Shmatov G., 25PO-13-39	779
Shapiro A.J., 22PO-8-27	281	Shneyder E.I., 25RP-C-7	727
Shapiro A.J., 22PO-8-40	293	Shodiyev Z.M., 24PO-7-77	692
Shapiro A.J., 25RP-B-6	713	Shreder E., 25PO-20-12	821
Sharapova V.A., 22PO-8-9	264	Shreder L.A., 22PO-8-24	278
Shashkov I.V., 23PO-3-10	455	Shreder L.A., 25PO-13-50	789
Shavrov V., 21PO-2-15	87	Shreder L.A., 25PO-13-51	790
Shavrov V., 23TL-D-3	391	Shreder L.A., 25PO-13-52	791
Shavrov V., 25PO-20-16	824	Shreder L.A., 25PO-13-54	793

Shul'ga N.V., 21PO-16-17	114	Slavin A .N., 22TL-C-2	209
Shull R.D., 22PO-8-27	281	Slobodchikov V.Yu., 23PO-3-26	470
Shull R.D., 22PO-8-40	293	Sluchanko D.N., 23PO-4-23	499
Shull R.D., 25RP-B-6	713	Sluchanko D.N., 23PO-4-6	483
Shulyatev D.A., 24PO-7-39	654	Sluchanko D.N., 23PO-4-7	484
Shuravin A.S., 21PO-16-24	121	Sluchanko D.N., 25PO-13-63	802
Shurina E.V., 22PO-8-54	306	Sluchanko N., 23PO-4-22	498
Shurina E.V., 22PO-8-56	308	Sluchanko N., 23PO-4-9	486
Shust V.A., 24PO-7-32	646	Sluchanko N., 24PO-6-25	613
Shutov V., 24PO-7-66	681	Sluchanko N.E., 21PO-16-57	153
Shuvaev A.M., 24PO-7-9	623	Sluchanko N.E., 21PO-16-58	154
Shvedun M., 23PO-1-13	422	Sluchanko N.E., 22PO-8-85	337
Sidorenko A., 22RP-F-9	249	Sluchanko N.E., 23PO-4-23	499
Sidorenko P.K., 25PO-13-10	750	Sluchanko N.E., 23PO-4-3	480
Sidorenko P.K., 25PO-13-9	749	Sluchanko N.E., 23PO-4-6	483
Sidorov V.A., 22PO-8-7	262	Sluchanko N.E., 23PO-4-7	484
Sidorov V.A., 23PO-1-4	414	Sluchanko N.E., 25PO-13-63	802
Sildos I., 24PO-6-5	594	Slynko E.I., 24PO-6-11	600
Simonovsky A.Ya., 23PO-3-15	460	Slynko V.E., 24PO-6-11	600
Simonovsky A.Ya., 23PO-3-18	462	Smagin V.V., 21PO-16-14	111
Simonovsky A.Ya., 23PO-3-21	465	Smekhova A., 21TL-D-2	44
Simonovsky A.Ya., 23PO-3-5	449	Smekhova A., 22PO-8-16	270
Sirenko V.A., 23PO-1-13	422	Smekhova A., 22PO-8-80	332
Sirenko V.A., 23PO-1-14	423	Smekhova A., 22RP-A-7	193
Sirenko V.A., 23PO-1-17	426	Smekhova A., 24PO-6-16	604
Siritaratiwat A., 21PO-21-21	180	Smelova K.M., 22PO-8-96	347
Siritaratiwat A., 21PO-21-22	181	Smirnitskaya G.V., 22PO-8-15	269
Siritaratiwat A., 21PO-21-23	182	Smirnitskaya G.V., 22PO-8-17	271
Siritaratiwat A., 21PO-21-5	165	Smirnitskaya G.V., 22PO-8-18	272
Sitnikov A., 22PO-8-26	280	Smirnov A.I., 22RP-D-7	222
Sitnikov A., 23PO-4-15	492	Smirnov I.Yu., 24PO-6-15	603
Sitnikov A., 23PO-4-17	494	Smirnov S.I., 22PO-8-23	277
Sitnikov A.V., 21PO-16-3	100	Smirnov S.S., 25PO-13-36	776
Sitnikov A.V., 22PO-8-25	279	Snegirev V.V., 21PO-16-43	139
Sitnikov A.V., 22PO-8-46	299	Snigirev O., 22PO-8-43	296
Sitnikov A.V., 22PO-8-50	303	Snigirev O.V., 23PO-3-26	470
Sitnikov A.V., 22PO-8-53	305	Sobolev N.A., 24PO-6-8	597
Sitnikov A.V., 22PO-8-61	314	Soboleva I.V., 22RP-B-8	204
Sitnikov A.V., 22PO-8-8	263	Sokolov A.E., 21PO-2-19	91
Sizova Z.I., 22PO-8-54	306	Sokolov N.S., 22PO-8-11	266
Sizova Z.I., 22PO-8-56	308	Sokolov V., 24PO-6-20	608
Skipetrov E.P., 24PO-6-10	599	Sokolov V., 25PO-13-64	803
Skipetrov E.P., 24PO-6-11	600	Sokolovsky V., 25PO-20-8	817
Skipetrova L.A., 24PO-6-11	600	Sokolovsky V.V., 25PO-20-5	814
Skokov K., 25PO-20-6	815	Solin N.I., 24PO-7-57	672
Skokov K.P., 25PO-13-30	770	Solontsov A., 23PO-12-28	531
Skokov K.P., 25PO-13-34	774	Sompongse D., 21PO-21-21	180
Skokov K.P., 25PO-13-35	775	Sompongse D., 21PO-21-22	181
Skokov K.P., 25PO-13-36	776	Sorochak A.M., 21PO-16-12	109
Skokov K.P., 25PO-13-40	780	Sorokin A.N., 22PO-8-51	304
Skokov K.P., 25PO-20-7	816	Sorokin A.N., 22PO-8-65	318
Skorodumova N., 25PO-13-41	781	Sosedkov M.A., 25PO-20-14	822

Sosin S.S., 22RP-D-7.....	222	Straumal B.B., 25RP-A-10	705
Souche Y., 24PL-A-1	536	Straumal P.B., 25RP-A-10.....	705
Spasova M., 23RP-B-2	369	Strelniker Y.M., 24TL-C-6	566
Spiegel J., 22RP-C-7.....	214	Struzhkin V.V., 21RP-F-9	69
Spitaler J., 25RP-C-7.....	727	Stukalov V.I., 23PO-12-3	508
Šprincová A., 23PO-3-3	448	Subbotin I.A., 23PO-4-11	488
Šprincová A., 23RP-F-10	407	Suemasu T., 21TL-C-7	41
Srinivasan G., 21PO-16-8.....	105	Sukhachev A.L., 21PO-2-19.....	91
Srinivasan G., 21RP-D-8.....	52	Sukhonosov A.L., 21PO-16-22	119
Srinivasan G., 22PO-8-98.....	349	Sukhorukov Yu., 23RP-A-2	357
Srinivasan G., 24PO-7-68.....	683	Sukhorukov Yu., 24PO-7-21	635
Srivastava P., 21TL-B-4	28	Sukhorukov Yu., 24PO-7-61	676
Stadler S., 24RP-D-7	574	Sukhorukov Yu.P., 21PO-2-20.....	92
Stadler S., 25PO-20-6.....	815	Sukhorukov Yu.P., 24PO-7-59.....	674
Stancheva R., 21PO-21-6	166	Sun S., 23TL-A-9	366
Stanciu C.D., 21TL-A-1	14	Suñol J.J., 24RP-D-8	575
Stanton T., 23TL-A-1	356	Suñol J.J., 25RP-B-9.....	716
Starostenko S.N., 21PO-16-24.....	121	Suryanarayanan R., 24PO-7-8	622
Starostenko S.N., 21PO-16-39.....	135	Sushkov A.B., 25RP-D-7	739
Starostenko S.N., 21PO-16-47.....	143	Suslov A.V., 24PO-6-15.....	603
Starostenko S.N., 23RP-C-6	386	Suwannata N., 21PO-21-22	181
Stashkevich A.A., 23RP-B-3	369	Suzuki H., 25PO-13-25.....	765
Stashkevitch A., 22PO-8-99	350	Suzuki Sh., 21RP-B-8.....	32
Stemler T., 21PO-16-9.....	106	Sucol J.J., 23TL-D-7.....	394
Stepanov A., 22PO-8-57.....	310	Svalov A.V., 21PO-16-56.....	152
Stepanov G.V., 23RP-F-7	404	Svalov A.V., 22PO-8-51.....	304
Stepanov G.V., 23RP-F-9.....	406	Svalov A.V., 22PO-8-65.....	318
Stepanov S., 22PO-8-59	312	Svechkarev I.V., 25PO-13-24.....	764
Stepanov V.I., 23TL-F-1	398	Svistov L.E., 22RP-D-10.....	225
Stepanyuk O.V., 22PO-8-87.....	339	Svyazhin A., 25PO-20-12.....	821
Stepanyuk V.S., 22PO-8-96.....	347	Sycheva T.S., 25PO-13-49	788
Stepin S.G., 24PO-7-48	663	Sydoruk O., 24RP-C-8.....	567
Stetsenko A.N., 22PO-8-78	330	Sydoruk O., 24TL-C-5.....	565
Stetsenko P.N., 22PO-8-15.....	269	Syromyatnikov A.V., 25RP-C-9.....	729
Stetsenko P.N., 22PO-8-17.....	271	Sysoev N.N., 21PO-16-37	133
Stetsenko P.N., 22PO-8-18.....	272	Szilagyi E., 21RP-B-6.....	30
Stingaciu M., 25RP-D-8	739	Szymanski B., 22PO-8-80	332
Stirk S., 23TL-A-1	356	Szymczak H., 22TL-D-4.....	220
Stobiecki F., 22PO-8-62	315	Szymczak H., 24PO-7-14	629
Stognei O.V., 22PO-8-25.....	279	Szymczak H., 24PO-7-48	663
Stognei O.V., 22PO-8-50.....	303	Szymczak H., 24PO-7-49	664
Stognei O.V., 22PO-8-53.....	305	Szymczak H., 24PO-7-52	667
Stognij A., 22PO-8-39	292	Szymczak R., 22TL-D-4.....	220
Stognij A., 22PO-8-45	298	Szymczak R., 24PO-6-20	608
Stognij A.I., 21PO-16-2.....	99	Szymczak R., 24PO-7-29.....	643
Stognij A.I., 23RP-B-3	369	Szymczak R., 24PO-7-72	687
Stolyar S.V., 21PO-16-20.....	117	Szymczak R., 24PO-7-75	690
Stolyar S.V., 22PO-8-29.....	283	Szymczak R., 25RP-A-3.....	698
Stolyar S.V., 22PO-8-32.....	285		
Stolyar S.V., 23PO-3-4.....	449		
Stolyarov V.S., 23PO-1-3.....	413		
Stoneham A.M., 23PO-12-8.....	512		

T

Tabata Y., 22RP-F-8.....	248	Tatartschuk E., 24TL-C-5.....	565
Tada M., 21PL-A-2.....	11	Telegin A., 23RP-A-2.....	357
Tagirov L., 22PO-8-74.....	326	Telegin A., 24PO-7-21.....	635
Tagirov L., 22RP-A-8.....	194	Telegin A.V., 24PO-7-59.....	674
Tagirov L., 23PO-4-27.....	503	Temerov V.L., 21PO-2-19.....	91
Tagirov L.R., 22RP-F-9.....	249	Temerov V.L., 24PO-7-70.....	685
Tagirov L.R., 24PO-6-1.....	590	Temiryazeva M.P., 21PO-16-38.....	134
Tagirov M.S., 25PO-13-25.....	765	Temiryazeva M.P., 25PO-13-67.....	806
Tahrilov H., 21PO-21-6.....	166	Terent'ev P.B., 25PO-13-52.....	791
Taillefumier M., 24TL-F-1.....	580	Terent'ev P.B., 25PO-13-54.....	793
Tajabor N., 23PO-1-32.....	441	Terentieva L.A., 23PO-1-1.....	412
Takahashi M., 22TL-C-3.....	210	Tereshina E.A., 25PO-13-56.....	795
Takahashi S., 21TL-C-3.....	37	Tereshina I.S., 25PO-13-68.....	807
Takahashi S., 21TL-C-5.....	39	Tertykh V.A., 22PO-8-10.....	265
Takahashi Y., 22RP-F-8.....	248	Testa A.M., 21TL-B-2.....	27
Takanashi K., 21TL-C-5.....	39	Thirion C., 23PL-A-1.....	352
Takano F., 21TL-C-7.....	41	Thompson J.D., 22PO-8-7.....	262
Takashima K., 22RP-E-3.....	230	Thompson J.D., 23PO-1-4.....	414
Takeda H., 21RP-F-3.....	62	Thompson S.M., 23TL-A-1.....	356
Takemura Y., 21RP-B-9.....	33	Tiberto P., 25TL-B-2.....	709
Taldenkov A.N., 24PO-7-1.....	616	Tidecks R., 22RP-F-9.....	249
Taldenkov A.N., 24PO-7-8.....	622	Tikhomirov O.A., 22PO-8-27.....	281
Talipov R.A., 23RP-F-7.....	404	Timirgazin M.A., 23PO-12-18.....	522
Tan T.L., 25PO-13-6.....	747	Timko M., 23PO-3-3.....	448
Tanaka K., 21TL-F-1.....	60	Timko M., 23RP-F-10.....	407
Tanaka S., 21PO-21-13.....	173	Timopheev A.A., 22PO-8-38.....	291
Tanaka S., 21RP-B-8.....	32	Tischenko D.A., 23PO-3-6.....	450
Tanaka S., 22PO-8-43.....	296	Titov A., 23PO-4-16.....	493
Tanaka T., 21PL-A-2.....	11	Tiunov V.F., 25PO-13-11.....	751
Tancziko F., 21RP-B-6.....	30	Tomašovičová N., 23PO-3-3.....	448
Tang Wu, 22TL-C-4.....	211	Tomašovičová N., 23RP-F-10.....	407
Tankeyev A.P., 21PO-16-14.....	111	Tomčo L., 23RP-F-10.....	407
Tarapov S., 21PO-16-50.....	146	Tomilin A.K., 21PO-16-51.....	147
Tarapov S., 22PO-8-45.....	298	Torre J., 22RP-C-7.....	214
Tarapov S.I., 21PO-16-61.....	157	Tóth-Katona T., 23RP-F-10.....	407
Tarapov S.I., 22RP-F-4.....	242	Trampert A., 24RP-A-3.....	541
Tarasenko O.S., 21PO-2-22.....	94	Tran M., 23RP-B-2.....	369
Tarasenko S., 21PO-2-15.....	87	Travkin V.D., 24PO-7-9.....	623
Tarasenko S.A., 22TL-A-5.....	191	Travkina T.V., 23PO-3-5.....	449
Tarasenko S.V., 21PO-2-22.....	94	Treninkov I.A., 21PO-21-9.....	169
Tardif S., 22TL-A-2.....	188	Tretyakov Yu.D., 22PO-8-1.....	256
Täschner C., 22RP-D-8.....	223	Tretyakov Yu.D., 22PO-8-2.....	257
Taskaev A.S., 25PO-20-9.....	818	Tretyakov Yu.D., 22PO-8-3.....	258
Taskaev S., 25PO-20-8.....	817	Tretyakov Yu.D., 22PO-8-97.....	348
Taskaev S.V., 25PO-20-10.....	819	Tripadus V., 22RP-E-7.....	234
Taskaev S.V., 25PO-20-5.....	814	Tripadus V., 23PO-3-9.....	454
Tatarenko V.A., 23PO-4-5.....	482	Tripadus V., 23RP-F-4.....	401
		Triputen L.Yu., 23PO-4-18.....	495
		Tristan N., 21PO-2-5.....	78
		Tristan N., 23PO-1-15.....	424
		Trotsenko P.A., 22PO-8-38.....	291
		Troyanchuk I.O., 24PO-7-40.....	655

Trukhan B.M., 24PO-7-41	656	Ungvichian V., 21PO-21-5	165
Trukhanov A.V., 24PO-7-48	663	Urusova B.I., 21PO-21-3	164
Trukhanov A.V., 24PO-7-49	664	Usachev P.A., 21PO-2-1	74
Trukhanov S.V., 24PO-7-48	663	Usachev P.A., 21RP-A-2	15
Trukhanov S.V., 24PO-7-49	664	Usachev P.A., 22TL-B-4	200
Trusov L.A., 25PO-13-1	742	Useinov A., 23PO-4-27	503
Tsarevskii S., 23PO-1-6	416	Useinov N., 22PO-8-74	326
Tsema B., 21PO-2-4	77	Usmanova G.Sh., 25PO-13-9	749
Tsikalov D.S., 21PO-16-16	113	Usov N.A., 22PO-8-4	259
Tsikalov V.S., 24PO-7-12	626	Usov N.A., 25PO-13-7	747
Tsirlin A.A., 24PO-7-76	691	Usov N.A., 25RP-B-7	714
Tsirlina G., 21PO-2-4	77	Uspenskaya L., 23PO-1-29	439
Tsirlina G., 22TL-B-7	203	Uspenskaya L.S., 25RP-B-6	713
Tsujikawa H., 23PO-4-19	495	Uspenskii Yu., 25RP-C-8	728
Tsukamoto A., 21TL-A-1	14	Uspenskii Yu.A., 23PO-4-16	493
Tsunoda Y., 23RP-A-3	358	Uspenskii Yu.A., 24TL-F-5	583
Tsurkan V., 22RP-D-9	224	Ustinov A.B., 21PO-16-7	104
Tsvjatshenko A.V., 25PO-13-4	745	Ustinov A.B., 21PO-16-8	105
Tsvyashchenko A.V., 22PO-8-7	262	Ustinov A.B., 21PO-16-9	106
Tsvyashchenko A.V., 23PO-1-22	431	Ustinov V., 22PO-8-41	294
Tsvyashchenko A.V., 23PO-1-4	414	Ustinov V., 22PO-8-44	296
Tufescu F.M., 21PO-21-18	177	Ustinov V., 23RP-A-2	357
Tugarinov V., 24PO-7-29	643	Ustinov V.V., 21PO-16-42	138
Tugushev V., 25RP-C-8	728	Ustinov V.V., 22PO-8-28	282
Tugushev V.V., 23PO-12-23	526	Ustinov V.V., 23RP-B-10	377
Tugushev V.V., 23PO-4-16	493	Ustinov V.V., 24PO-7-55	670
Tugushev V.V., 25RP-A-11	705	Ustinov V.V., 24RP-A-8	549
Turik N.V., 25PO-13-37	777	Ustugov V.A., 21PO-16-5	102
Turik N.V., 25PO-13-38	778	Utitskikh S.I., 25PO-13-10	750
Turkov V.A., 23PO-3-30	474	Uzdenova F.A., 21PO-21-3	164
Turkov V.K., 21PO-16-3	100	Uzdin V.M., 23PO-12-13	517
Turpanov I., 22PO-8-58	311		
Turpanov I.A., 22PO-8-29	283		
Turpanov I.A., 22PO-8-33	286		
Tyatyushkin A.N., 21PO-21-16	175		
Tyatyushkin A.N., 23PO-3-2	447		
Tynjälä T., 23RP-F-12	409		

U

Uchevatkin A., 21PO-21-10	170	Vahaplar K., 21TL-A-1	14
Uchevatkin A.A., 23PO-3-6	450	Vajda A., 23RP-F-10	407
Uchida H., 22RP-B-6	202	Vakhitov R.M., 21PO-21-15	174
Uchida H., 23RP-A-3	358	Vakhitova M.M., 21PO-21-15	174
Udalov O.G., 25RP-C-2	721	Valdés Aguilar R., 25RP-D-7	739
Udod L.V., 24PO-7-72	687	Valdner V., 22TL-B-7	203
Ueda Y., 23PO-1-26	436	Valeev I., 21PO-2-23	95
Uimin M.A., 22PO-8-9	264	Valeev R.A., 25PO-13-62	801
Ulmanis U., 24PO-6-5	594	Valeev V., 22PO-8-57	310
Umhaeva Z.S., 25PO-13-4	745	Valeev V.F., 24PO-6-1	590
		Valeev V.F., 25RP-C-4	722
		Valiev E.Z., 25PO-20-13	821
		Valkov V.V., 23PO-12-5	510
		Valkova T.A., 23PO-12-5	510
		Varela M., 25RP-A-7	702
		Varfolomeev A.E., 22PO-8-52	305

V

Varga R., 23TL-D-7	394	Velikanov D.A., 24PO-6-23	611
Varga R., 25RP-B-4	711	Velikanov D.A., 24PO-7-51	666
Varnakov S.N., 22PO-8-55	307	Velikanov D.A., 25PO-13-22	762
Varnakov S.N., 22PO-8-71	323	Verbenko I.A., 24PO-7-43	658
Varnavskii S.A., 25RP-A-3	698	Verbiest T., 21PO-2-18	90
Varvaro G., 21TL-B-2	27	Veshchunov I.S., 22PO-8-6	261
Vas'kovskiy V.O., 22PO-8-51	304	Viau G., 22PO-8-99	350
Vas'kovskiy V.O., 22PO-8-65	318	Viau G., 23RP-B-3	369
Vashkovsky A.V., 21PO-16-38	134	Vieira J.M., 24PO-7-71	686
Vashkovsky A.V., 21PO-16-49	145	Viglin N.A., 23RP-B-10	377
Vashuk M.V., 24PO-6-6	595	Vikhrova O.V., 24PO-6-4	593
Vasilchikova T., 23PO-1-26	436	Vikhrova O.V., 24PO-6-8	597
Vasilchikova T.M., 24PO-7-40	655	Vilkov E., 21PO-16-55	151
Vasiliev A., 23PO-1-26	436	Vinai F., 25TL-B-2	709
Vasiliev A., 24PO-7-66	681	Vincent E., 23RP-F-5	401
Vasiliev A., 25PO-13-58	797	Vinnikov L.Ya., 22PO-8-6	261
Vasiliev A.N., 21PO-21-11	171	Vinogradov A., 24PO-7-21	635
Vasiliev A.N., 23PO-1-15	424	Vinogradov A.N., 22RP-F-5	243
Vasiliev A.N., 24PO-7-40	655	Vinogradov A.P., 21PO-2-10	82
Vasiliev A.N., 24PO-7-63	678	Vinogradov A.P., 22RP-B-5	201
Vasiliev A.N., 21PO-2-5	78	Vinogradov A.P., 22RP-F-1	240
Vasiljev V.N., 25PO-13-48	787	Vinogradov A.P., 22RP-F-3	241
Vassiliev V., 24PO-7-14	629	Vinogradov A.P., 22RP-F-4	242
Vavilova E., 22RP-D-8	223	Vinogradov A.P., 24RP-C-7	567
Vávra I., 23PO-3-3	448	Vinokurov A.A., 24PO-6-10	599
Vazhenina I.G., 22PO-8-48	300	Vishnevskii V.G., 25PO-13-61	800
Vazquez M., 21PO-16-30	127	Visontai D., 21RP-B-6	30
Vázquez M., 22PO-8-75	327	Visser A., 23PO-1-14	423
Vázquez M., 23TL-B-1	368	Vitebskiy I., 23TL-A-4	359
Vdovichev S.N., 21PO-16-4	101	Vittoria C., 25TL-D-3	734
Vdovichev S.N., 22PO-8-5	260	Vittorini-Orgeas A., 24TL-A-5	546
Vdovichev S.N., 22PO-8-84	336	Vladimirova E., 24PO-7-14	629
Vdovichev S.N., 22PO-8-91	342	Vlasenko L.S., 24PO-6-17	605
Vdovin V.I., 22RP-A-7	193	Vlasov V.S., 21PO-16-11	108
Vecchione A., 23PO-1-20	429	Volchkov S.O., 21PO-16-56	152
Vedyaev A., 23PL-A-1	352	Volkov A., 22PO-8-42	295
Vedyaev A.V., 21PO-16-15	112	Volkov A., 22PO-8-43	296
Vedyayev A.V., 21RP-F-12	72	Volkov A.F., 23PO-1-33	442
Vega V., 22PO-8-75	327	Volkov A.N., 22PO-8-10	265
Vega V., 24RP-D-8	575	Volkov A.V., 22PO-8-52	305
Vega V., 25RP-B-9	716	Volkov D.V., 24PO-7-63	678
Vekas L., 22RP-E-8	235	Volkov I., 22PO-8-42	295
Vekas L., 23PO-3-16	461	Volkov I., 22PO-8-43	296
Vekas L., 23RP-F-4	401	Volkov I.A., 22PO-8-52	305
Vekilov Yu.Kh., 23PO-12-19	522	Volkov N., 24PO-7-47	662
Vekilov Yu.Kh., 23PO-12-21	524	Volkov N., 24PO-7-78	693
Vekilov Yu.Kh., 25PO-13-41	781	Volkov N.V., 24PO-7-12	626
Velikanov D., 22PO-8-58	311	Volkov N.V., 24PO-7-25	639
Velikanov D., 24PO-6-20	608	Volkov N.V., 24PO-7-51	666
Velikanov D., 24PO-7-78	693	Volkova E.G., 25PO-13-46	785
Velikanov D., 25PO-13-23	763	Volkova L.M., 24PO-7-56	671
Velikanov D.A., 22PO-8-33	286	Volkova N.V., 25PO-13-57	796

Volkova O., 24PO-7-66	681
Voloshok T., 25PO-13-58.....	797
Volynsky A., 22PO-8-42	295
Vorob'ev G.P., 21TL-D-5	48
Vorob'ev G.P., 24PO-7-11	625
Vorob'ev G.P., 24PO-7-16	631
Vorobyev S.I., 23RP-F-4	401
Voronin V.I., 25PO-13-55	794
Voronina E., 25PO-13-19	759
Voronina E.V., 25PO-13-59	798
Vorotynov A., 24PO-6-20	608
Vorotynov A., 25PO-13-64	803
Vorotynova O., 22PO-8-57.....	310
VorotynovA., 24PO-7-78	693
Vuarnoz D., 23TL-D-4	392
Vyacheslavov A.S., 22PO-8-2.....	257
Vyshivanaya I.G., 23PO-4-5	482
Vysotsky S.L., 21PO-16-2.....	99
Vysotsky S.L., 21PO-2-2.....	75

W

Wan Farong, 24RP-D-6	574
Wang S.Q., 21TL-E-4.....	55
Wang Y.D., 23TL-D-2.....	390
Wang Yuh-Feng, 23TL-A-7	364
Warot-Fonrose B., 24TL-B-2	553
Wassermann E.F., 23TL-D-1.....	390
Watanabe T., 25PO-13-53	792
Watson J.H.P., 21PO-21-19.....	178
Webb N.V., 23PO-12-1	506
Wehling T., 21TL-A-4.....	17
Wei F., 22PO-8-93.....	344
Wei F.L., 25PO-13-45	784
Weides M., 21RP-F-11	71
Weis C., 21TL-B-4	28
Weisheit M., 24PL-A-1	536
Wende H., 21TL-B-4.....	28
Westerholt K., 22RP-C-8.....	215
Westerholt K., 23PO-1-9	419
Wilhelm C., 22TL-E-2.....	229
Wilhelm F., 21TL-D-2.....	44
Wilhelm F., 22PO-8-16	270
Wilhelm F., 22PO-8-80	332
Wilhelm F., 24PO-6-16	604
Wilhelm F., 25RP-A-6.....	701
Wilkins S.B., 24TL-A-7	548
Willumeit R., 22RP-E-8	235
Willumeit R., 23PO-3-16.....	461
Wittborn J., 23RP-A-5.....	362

Wojtowicz T., 25RP-A-2	697
Woltersdorf G., 21TL-B-3	27
Woltersdorf G., 22RP-C-8.....	215
Wolverson D., 25RP-A-2	697
Wosnitza J., 22RP-D-7	222
Wosnitza J., 24PO-6-3	592
Wouters J., 21PO-2-18	90
Wu Hua, 25TL-A-1	696
Wu M., 21PO-16-9	106
Wu Y.P., 22TL-C-6	213
Wu Yen-Wen, 23TL-A-7.....	364
Wurtz G., 23RP-B-3	369
Wysocki A.L., 21TL-E-3.....	55

X

Xu X., 21TL-B-4	28
-----------------------	----

Y

Yabukami S., 23RP-A-6	363
Yakovchuk V.Yu., 21PO-16-20	117
Yakubenya S.M., 24PO-6-2.....	591
Yamaguchi M., 21PO-16-30.....	127
Yamaguchi M., 22TL-C-1	208
Yamani Z., 22TL-D-4.....	220
Yamaoka T., 23PO-4-19.....	495
Yamashita F., 21RP-F-3	62
Yamashita H., 22RP-F-8.....	248
Yanai T., 21RP-F-3.....	62
Yang A., 25TL-D-3	734
Yang Z., 25PO-13-45	784
Yanovsky Yu.G., 21PO-21-2.....	163
Yanson I.K., 23PO-4-18	495
Yanushkevich K.I., 24PO-6-22	610
Yanushkevich K.I., 24PO-6-23	611
Yarmoshenko Y., 25PO-20-12	821
Yartseva E.P., 23PO-3-15.....	460
Yasuda H., 22RP-E-3	230
Yasuda T., 24TL-D-3	571
Yatchev I., 21PO-21-7	167
Yatsyk I.V., 24PO-7-38	653
Ye Rongchang, 24RP-D-6	574
Ye S., 25RP-A-6.....	701
Yelsukov E.P., 21PO-16-24.....	121
Yelsukov E.P., 23RP-C-6	386
Yelsukov E.P., 25PO-13-59.....	798
Yelsukov Eu., 25PO-13-19.....	759

Yelsukova A.E., 25PO-13-59	798	Zashchirinskii D.M., 24PO-7-41	656
Yemets V.N., 21PO-16-31	128	Zashchirinskii D.M., 25RP-A-3	698
Yerin C.V., 23PO-3-14	459	Zavarzina D.G., 21PO-21-17	176
Yermakov A.Ye., 22PO-8-9	264	Zavarzina D.G., 21PO-21-9	169
Yershova E.A., 21PO-2-7	80	Závišová V., 23PO-3-3	448
Yi H.T., 22TL-D-5	221	Závišová V., 23RP-F-10	407
Yoon S.S., 23TL-A-9	366	Zayats A., 23RP-B-3	369
Yoon Soack Dae, 25TL-D-3	734	Zayats A.V., 24TL-C-2	563
Yoshida S., 21PO-21-13	173	Zayets V., 21TL-C-1	36
Yoshikawa N., 21PO-16-35	131	Zdravkov V., 22RP-F-9	249
You Chun-Yeol, 24RP-B-4	554	Zeidis I., 23PO-3-30	474
Yu Fucheng, 25RP-A-4	699	Zekri L., 24RP-F-7	584
Yu Young-Sang, 25TL-C-1	720	Zekri N., 24RP-F-7	584
Yuan H.-K., 21TL-A-5	20	Zenkevich A., 23PO-4-21	497
Yukalov V.I., 22PO-8-68	320	Zenkevich A.V., 23PO-4-24	500
Yumaguzin A.R., 21PO-21-15	174	Zenkov A.V., 24PO-7-24	638
Yurasov A.N., 21PO-2-20	92	Zenkov E.V., 24PO-7-24	638
Yurasov N.I., 21PO-16-46	142	Zenkov E.V., 24PO-7-73	688
Yurasov N.I., 21PO-2-9	82	Zhang Y., 23RP-C-7	387
Yurchenko V.M., 21PO-2-22	94	Zharekeshev I., 23PO-12-11	515
Yurchenko V.V., 23PO-1-25	434	Zharkov S.M., 22PO-8-60	313
Yurkin G., 25PO-13-23	763	Zharkovsky A.E., 22PO-8-52	305
Yurkin G.Yu., 25PO-13-22	762	Zhdan P., 22PO-8-62	315
Yurkov G.Y., 22PO-8-10	265	Zhdanov A., 21PO-2-4	77
Yushkov V.I., 22PO-8-33	286	Zhdanov A.G., 22RP-B-8	204
Yusupov R., 25RP-D-5	737	Zhdanov A.G., 24PO-7-32	646
<hr/>			
Z			
Zabel H., 22PO-8-84	336	Zheludev A., 22TL-D-3	219
Zabel H., 22RP-A-8	194	Zhirnov S.V., 21PO-16-48	144
Zabel H., 23PO-1-9	419	Zhiteytsev E.R., 24PO-6-8	597
Zabluda V., 22PO-8-59	312	Zhitomirsky M.E., 22TL-D-6	221
Zabolotin A.E., 22RP-F-6	244	Zholud A.M., 23PO-3-1	446
Zagrebin M.A., 25PO-20-10	819	Zhou Z., 21TL-A-6	20
Zaikovskiy V., 22PO-8-59	312	Zhu F.Q., 25RP-B-6	713
Zainullina R.I., 24PO-7-39	654	Zhu L.Y., 22PO-8-40	293
Zainullina R.I., 24PO-7-55	670	Zhukov A., 25PO-20-2	811
Zainullina R.I., 24RP-A-8	549	Zhukov A., 25RP-B-4	711
Zaitsev D.D., 25PO-13-1	742	Zhukov A., 25RP-B-8	715
Zaitsev S.V., 24PO-6-4	593	Zhukov A., 25TL-B-3	710
Zakharova G.S., 22RP-D-8	223	Zhukov A.A., 21RP-F-5	64
Zakhlevnykh A.N., 23PO-3-11	456	Zhukov A.V., 23PO-3-28	473
Zakhlevnykh A.N., 23PO-3-22	466	Zhukova V., 25PO-20-2	811
Zakinyan A.R., 23PO-3-13	458	Zhukova V., 25TL-B-3	710
Zalesskii V.G., 24PO-7-53	668	Zhuravlev A.K., 23PO-12-11	515
Zalesskii V.G., 24PO-7-54	669	Zhuravlev M.Ye., 24RP-B-3	554
Zalesskii V.G., 25RP-D-6	738	Ziebeck K.R.A., 24TL-D-3	571
Zapf V.S., 22RP-D-7	222	Ziganshina S.A., 22PO-8-72	324
Zarasky E.I., 21PO-21-2	163	Zigheem F., 22PO-8-36	289
		Zigheem F., 22RP-C-8	215
		Zikanov O., 23PO-3-20	464
		Zilberman P.E., 24TL-B-5	556
		Zimmermann K., 23PO-3-30	474
		Zinenko V.I., 22RP-A-7	193

Zlomanov V.P., 24PO-6-10	599	Zvezdin A.K., 23PO-4-14.....	491
Zolotorev V., 23TL-D-3	391	Zvezdin A.K., 24PO-7-32.....	646
Zolotorev V., 25PO-20-16.....	824	Zvezdin A.K., 24RP-B-8	558
Zorchenko V.V., 22PO-8-78	330	Zvezdin A.K., 24RP-B-9	559
Zrínyi M., 23TL-F-6.....	402	Zvezdin K.A., 23PO-4-14.....	491
Zubenko E.V., 23PO-3-21	465	Zvezdin K.A., 23PO-4-20.....	496
Zuberek R., 25PO-13-64.....	803	Zvezdin K.A., 24RP-B-8	558
Zubkov V.I., 21PO-16-53	148	Zvezdin K.A., 24RP-B-9	559
Zubkov V.I., 21PO-16-54	150	Zvezdin A.K., 24PO-7-11	625
Zubov V.E., 21PO-21-20.....	179	Zvonkov B.N., 22RP-F-5.....	243
Zuo Xu, 25TL-D-3.....	734	Zvonkov B.N., 24PO-6-4.....	593
Zvereva E.A., 24PO-6-10	599	Zvonkov B.N., 24PO-6-8.....	597
Zvezdin A.K., 21PO-2-6.....	79	Zvonkov B.N., 24TL-A-2.....	540
Zvezdin A.K., 21PO-2-7.....	80	Zvonkov B.N., 25RP-A-11	705
Zvezdin A.K., 21TL-D-5	48	Zvyagin S., 22PO-8-37	290
Zvezdin A.K., 22RP-F-2.....	240	Zvyagin S.A., 22RP-D-7	222